

The chemistry of  
**Organomagnesium Compounds**

*The chemistry of organomagnesium compounds*

Edited by Z. Rappoport and I. Marek © 2008 John Wiley & Sons, Ltd. ISBN: 978-0-470-05719-3

## Patai Series: The Chemistry of Functional Groups

*A series of advanced treatises founded by Professor Saul Patai and under the general editorship of Professor Zvi Rappoport*

The **Patai Series** publishes comprehensive reviews on all aspects of specific functional groups. Each volume contains outstanding surveys on theoretical and computational aspects, NMR, MS, other spectroscopic methods and analytical chemistry, structural aspects, thermochemistry, photochemistry, synthetic approaches and strategies, synthetic uses and applications in chemical and pharmaceutical industries, biological, biochemical and environmental aspects.

To date, 118 volumes have been published in the series.

### Recently Published Titles

- The chemistry of the Cyclopropyl Group (Volume 2)
- The chemistry of the Hydrazo, Azo and Azoxy Groups (Volume 2, 2 parts)
- The chemistry of Double-Bonded Functional Groups (Volume 3, 2 parts)
- The chemistry of Organophosphorus Compounds (Volume 4)
- The chemistry of Halides, Pseudo-Halides and Azides (Volume 2, 2 parts)
- The chemistry of the Amino, Nitro and Nitroso Groups (2 volumes, 2 parts)
- The chemistry of Dienes and Polyenes (2 volumes)
- The chemistry of Organic Derivatives of Gold and Silver
- The chemistry of Organic Silicon Compounds (2 volumes, 4 parts)
- The chemistry of Organic Germanium, Tin and Lead Compounds (Volume 2, 2 parts)
- The chemistry of Phenols (2 parts)
- The chemistry of Organolithium Compounds (2 volumes, 3 parts)
- The chemistry of Cyclobutanes (2 parts)
- The chemistry of Peroxides (Volume 2, 2 parts)
- The chemistry of Organozinc Compounds (2 parts)
- The chemistry of Anilines (2 parts)

### Forthcoming Titles

- The Chemistry of Hydroxylamines, Oximes and Hydroxamic Acids
- The Chemistry of Metal Enolates

### The Patai Series Online

Starting in 2003 the **Patai Series** is available in electronic format on Wiley InterScience. All new titles will be published as online books and a growing list of older titles will be added every year. It is the ultimate goal that all titles published in the **Patai Series** will be available in electronic format.

For more information see under **Online Books** on:

[www.interscience.wiley.com](http://www.interscience.wiley.com)

---

---

# The chemistry of **Organomagnesium Compounds**

Part 1

*Edited by*

ZVI RAPPOPORT

*The Hebrew University, Jerusalem*

*and*

ILAN MAREK

*Technion-Israel Institute of Technology, Haifa*

---

2008



John Wiley & Sons, Ltd

*An Interscience<sup>®</sup> Publication*

---

---

---

---

# The chemistry of **Organomagnesium Compounds**

Part 2

*Edited by*

ZVI RAPPOPORT

*The Hebrew University, Jerusalem*

*and*

ILAN MAREK

*Technion-Israel Institute of Technology, Haifa*

---

2008



John Wiley & Sons, Ltd

*An Interscience<sup>®</sup> Publication*

---

---



Copyright © 2008

John Wiley & Sons Ltd, The Atrium, Southern Gate, Chichester,  
West Sussex PO19 8SQ, England

Telephone (+44) 1243 779777

Email (for orders and customer service enquiries): [cs-books@wiley.co.uk](mailto:cs-books@wiley.co.uk)  
Visit our Home Page on [www.wileyeurope.com](http://www.wileyeurope.com) or [www.wiley.com](http://www.wiley.com)

All Rights Reserved. No part of this publication may be reproduced, stored in a retrieval system or transmitted in any form or by any means, electronic, mechanical, photocopying, recording, scanning or otherwise, except under the terms of the Copyright, Designs and Patents Act 1988 or under the terms of a licence issued by the Copyright Licensing Agency Ltd, 90 Tottenham Court Road, London W1T 4LP, UK, without the permission in writing of the Publisher. Requests to the Publisher should be addressed to the Permissions Department, John Wiley & Sons Ltd, The Atrium, Southern Gate, Chichester, West Sussex PO19 8SQ, England, or emailed to [permreq@wiley.co.uk](mailto:permreq@wiley.co.uk), or faxed to (+44) 1243 770620.

Designations used by companies to distinguish their products are often claimed as trademarks. All brand names and product names used in this book are trade names, service marks, trademarks or registered trademarks of their respective owners. The Publisher is not associated with any product or vendor mentioned in this book. This publication is designed to provide accurate and authoritative information in regard to the subject matter covered. It is sold on the understanding that the Publisher is not engaged in rendering professional services. If professional advice or other expert assistance is required, the services of a competent professional should be sought.

#### ***Other Wiley Editorial Offices***

John Wiley & Sons Inc., 111 River Street, Hoboken, NJ 07030, USA

Jossey-Bass, 989 Market Street, San Francisco, CA 94103-1741, USA

Wiley-VCH Verlag GmbH, Boschstr. 12, D-69469 Weinheim, Germany

John Wiley & Sons Australia Ltd, 42 McDougall Street, Milton, Queensland 4064, Australia

John Wiley & Sons (Asia) Pte Ltd, 2 Clementi Loop #02-01, Jin Xing Distripark, Singapore 129809

John Wiley & Sons Canada Ltd, 6045 Freemont Blvd, Mississauga, Ontario, L5R 4J3, Canada

Wiley also publishes its books in a variety of electronic formats. Some content that appears in print may not be available in electronic books.

#### ***British Library Cataloguing in Publication Data***

A catalogue record for this book is available from the British Library

ISBN 978-0-470-05719-3

Typeset in 9/10pt Times by Laserwords Private Limited, Chennai, India

Printed and bound in Great Britain by Biddles Ltd, King's Lynn

This book is printed on acid-free paper responsibly manufactured from sustainable forestry in which at least two trees are planted for each one used for paper production.

Dedicated to the memory of

**Yair Avni**

# Contributing authors

- Jaap Boersma      Chemical Biology & Organic Chemistry, Faculty of Science, Utrecht University, Padualaan 8, 3584 CH Utrecht, The Netherlands
- Katja Brade      Department Chemie und Biochemie, Ludwig-Maximilians-Universität München, Butenandtstr., 5-13, D-81377 München, Germany.  
Fax: +49-89-2180-77680
- Gérard Cahiez      Laboratoire de Synthèse Organique Sélective et de Chimie Organométallique (SOSCO), UMR 8123 CNRS-ESCOM-UCP, 5 Mail Gay Lussac, Neuville <sup>s</sup>/Oise, F-95092 Cergy-Pontoise, France.  
Fax: +3-313-425-7383; e-mail: g.cahiez@escom.fr
- Christophe Duplais      Laboratoire de Synthèse Organique Sélective et de Chimie Organométallique (SOSCO), UMR 8123 CNRS-ESCOM-UCP, 5 Mail Gay Lussac, Neuville <sup>s</sup>/Oise, F-95092 Cergy-Pontoise, France.  
Fax: +3-313-425-7383
- Ben L. Feringa      Stratingh Institute for Chemistry, University of Groningen, Nijenborgh 4, 9747 AG, Groningen, The Netherlands.  
Fax: ++3-150-363-4296; e-mail: B.L.Feringa@rug.nl
- Andrey Gavryushin      Department Chemie und Biochemie, Ludwig-Maximilians-Universität München, Butenandtstr., 5-13, D-81377 München, Germany.  
Fax: +49-89-2180-77680
- Claude Grison      UMR CNRS-Université de Montpellier 2 5032, ENSCM, 8 rue de l'Ecole Normale, F-34296 Montpellier, France.  
Fax: +3-346-714-4342; e-mail: cgrison@univ-montp2.fr
- Peter J. Heard      School of Science and Technology, North East Wales Institute, Mold Road, Wrexham LL112AW, UK;  
e-mail: p.heard@newi.ac.uk
- Kenneth W. Henderson      Department of Chemistry and Biochemistry, 251 Nieuwland Science Hall, University of Notre Dame, Notre Dame, IN 46556, USA. Fax: +1-574-631-6652;  
e-mail: khenders@nd.edu
- Katherine L. Hull      Department of Chemistry and Biochemistry, 251 Nieuwland Science Hall, University of Notre Dame, Notre Dame, IN 46556, USA. Fax: +1-574-631-6652

- Torkil Holm  
Department of Chemistry, Technical University of Denmark, Building 201, DK-2800, Lyngby, Denmark.  
Fax: +45-4-593-3968; e-mail: th@kemi.dtu.dk
- Kenichiro Itami  
Department of Chemistry and Research Center for Materials Science, Nagoya University, Chikusa-ku, Nagoya 464-8602, Japan. Fax: +8-152-788-6098; e-mail: itami@chem.nagoya-u.ac.jp
- Johann T. B. H. Jastrzebski  
Chemical Biology & Organic Chemistry, Faculty of Science, Utrecht University, Padualaan 8, 3584 CH Utrecht, The Netherlands. Fax: +3-130-252-3615; e-mail: j.t.b.h.jastrzebski@uu.nl
- Jan S. Jaworski  
Faculty of Chemistry, Warsaw University, 02-093 Warszawa, Poland. Fax: +4-822-822-5996; e-mail: jaworski@chem.uw.edu.pl
- Gerard van Koten  
Chemical Biology & Organic Chemistry, Faculty of Science, Utrecht University, Padualaan 8, 3584 CH Utrecht, The Netherlands. Fax: +3-130-252-3615; email: g.vankoten@uu.nl
- Paul Knochel  
Department Chemie und Biochemie, Ludwig-Maximilians-Universität München, Butenandtstr., 5-13, D-81377 München, Germany.  
Fax: +49-89-2180-77680; e-mail: paul.knochel@cup.uni-muenchen.de
- Joel F. Liebman  
Department of Chemistry and Biochemistry, University of Maryland, Baltimore County, 1000 Hilltop Circle, Baltimore, Maryland 21250, USA.  
Fax: +1-410-455-2608; e-mail: jliebman@umbc.edu
- Fernando López  
Departamento de Química Orgánica, Facultad de Química, Universidad de Santiago de Compostela, Avda. de las ciencias, s/n, 15782, Santiago de Compostela, Spain; e-mail: qofer@usc.es
- Adriaan J. Minnaard  
Stratingh Institute for Chemistry, University of Groningen, Nijenborgh 4, 9747 AG, Groningen, The Netherlands.  
Fax: ++3-150-363-4296; e-mail: A.J.Minnaard@rug.nl
- Richard A. J. O'Hair  
School of Chemistry, The University of Melbourne, Victoria 3010, Australia; Bio21, Molecular Science and Biotechnology Institute, The University of Melbourne, Victoria, 3010, Australia; ARC Centre of Excellence for Free Radical Chemistry and Biotechnology, Australia.  
Fax: +6-139-347-5180; e-mail: rohair@unimelb.edu.au
- Koichiro Oshima  
Department of Material Chemistry, Graduate School of Engineering, Kyoto University, Kyoto-daigaku Katsura, Nishikyo, Kyoto 615-8510, Japan. Fax: +8-175-383-2438; e-mail: oshima@orgrxn.mbox.media.kyoto-u.ac.jp
- Mathias O. Senge  
School of Chemistry, SFI Tetrapyrrole Laboratory, Trinity College Dublin, Dublin 2, Ireland. Fax: +3-531-896-8536; e-mail: sengem@tcd.ie.

- Natalia N. Sergeeva School of Chemistry, SFI Tetrapyrrole Laboratory, Trinity College Dublin, Dublin 2, Ireland. Fax: +3-531-896-8536
- Tsuyoshi Satoh Department of Chemistry, Faculty of Science, Tokyo University of Science; Ichigayafunagawara-machi 12, Shinjuku-ku, Tokyo 162-0826, Japan.  
Fax: 8-135-261-4631; e-mail: tsatoh@rs.kagu.tus.ac.jp
- Suzanne W. Slayden Department of Chemistry, George Mason University, 4400 University Drive, Fairfax, Virginia 22030, USA.  
Fax: +1-703-993-1055; e-mail: sslayden@gmu.edu
- James Weston Institut für Organische Chemie und Makromolekulare Chemie, Friedrich-Schiller-Universität, Humboldtstraße 10, D-07743 Jena, Germany. Fax: +49(0)-36-419-48212; e-mail: c9weje@uni-jena.de
- Shinichi Yamabe Department of Chemistry, Nara University of Education, Takabatake-cho, Nara, 630-8528, Japan.  
Fax: +81-742-27-9208; e-mail: yamabes@nara-edu.ac.jp
- Shoko Yamazaki Department of Chemistry, Nara University of Education, Takabatake-cho, Nara, 630-8528, Japan.  
Fax: +81-742-27-9289; e-mail: yamazaks@nara-edu.ac.jp
- Hideki Yorimitsu Department of Material Chemistry, Graduate School of Engineering, Kyoto University, Kyoto-daigaku Katsura, Nishikyo, Kyoto 615-8510, Japan.  
Fax: +81-75-383-2438;  
e-mail: yori@orgrxn.mbox.media.kyoto-u.ac.jp
- Jun-Ichi Yoshida Department of Synthetic Chemistry and Biological Chemistry, Graduate School of Engineering, Kyoto University, Nishikyo-ku, Kyoto 615-8510, Japan.  
Fax: +81-75-383-2727;  
e-mail: yoshida@sbchem.kyoto-u.ac.jp
- Jacob Zabicky Department of Chemical Engineering, Ben-Gurion University of the Negev, P. O. Box 653, Beer-Sheva 84105, Israel. Fax: +9-72-8647-2969;  
e-mail: zabicky@bgu.ac.il

# Foreword

The present book, *The Chemistry of Organomagnesium Compounds*, is a continuation of the sub-group of volumes in 'The Chemistry of Functional Groups' series that deals with organometallic derivatives. Closely related to it are the two volumes, *The Chemistry of Organolithium Compounds* (Zvi Rappoport and Ilan Marek, Eds., 2003 and 2005) in three parts and the two parts of *The Chemistry of Organozinc Compounds* (Zvi Rappoport and Ilan Marek, Eds., 2006). Organomagnesium (or Grignard) reagents play a key role in organic chemistry. Although considered as one of the oldest organometallic reagents in synthesis, there have been a complete renaissance of the field in the last decade.

The two parts of the present volume contain 17 chapters written by experts from 11 countries. They include chapters dealing with structural chemistry, thermochemistry and NMR of organomagnesium compounds, formation of organomagnesium compounds in solvent-free environment, photochemistry of magnesium derivatives of porphyrins and phthalocyanines, and electrochemistry, analysis and biochemistry of organomagnesium derivatives. Special chapters are devoted to special families of compounds, such as magnesium enolates, ate-complexes, carbenoids and bonded-complexes with groups 15 and 16 compounds. Processes such as enantioselective copper-catalyzed 1,4-addition of organomagnesium halides, the iron-catalyzed reactions of Grignard reagents, and theoretical aspects of their addition to carbonyl compounds as well as carbomagnesiation reactions are covered in separate chapters. Both synthesis and reactivities of organomagnesium compounds are extensively discussed.

Unfortunately, the planned chapter on 'Theoretical Aspects of Organomagnesium Compounds' was not delivered. However, some theoretical aspects are covered in other chapters, especially Chapter 9. Another chapter on 'Mechanisms of Reactions of Organomagnesium Compounds' was not included after it was found that recent material on the topic was meager as compared with the coverage of the topic in Richey's book *Grignard Reagents, New Developments*, published in 2000. We gratefully acknowledge the contributions of all the authors of these chapters.

The literature coverage is mostly up to and sometimes including 2007.

We will be grateful to readers who draw our attention to any mistakes in the present volume or to omissions, and to new topics which deserve to be included in a future volume on organomagnesium compounds.

Jerusalem and Haifa  
November 2007

Zvi Rappoport  
Ilan Marek

# The Chemistry of Functional Groups

## Preface to the series

The series 'The Chemistry of Functional Groups' was originally planned to cover in each volume all aspects of the chemistry of one of the important functional groups in organic chemistry. The emphasis is laid on the preparation, properties and reactions of the functional group treated and on the effects which it exerts both in the immediate vicinity of the group in question and in the whole molecule.

A voluntary restriction on the treatment of the various functional groups in these volumes is that material included in easily and generally available secondary or tertiary sources, such as Chemical Reviews, Quarterly Reviews, Organic Reactions, various 'Advances' and 'Progress' series and in textbooks (i.e. in books which are usually found in the chemical libraries of most universities and research institutes), should not, as a rule, be repeated in detail, unless it is necessary for the balanced treatment of the topic. Therefore each of the authors is asked not to give an encyclopaedic coverage of his subject, but to concentrate on the most important recent developments and mainly on material that has not been adequately covered by reviews or other secondary sources by the time of writing of the chapter, and to address himself to a reader who is assumed to be at a fairly advanced postgraduate level.

It is realized that no plan can be devised for a volume that would give a complete coverage of the field with no overlap between chapters, while at the same time preserving the readability of the text. The Editors set themselves the goal of attaining reasonable coverage with moderate overlap, with a minimum of cross-references between the chapters. In this manner, sufficient freedom is given to the authors to produce readable quasi-monographic chapters.

The general plan of each volume includes the following main sections:

- (a) An introductory chapter deals with the general and theoretical aspects of the group.
- (b) Chapters discuss the characterization and characteristics of the functional groups, i.e. qualitative and quantitative methods of determination including chemical and physical methods, MS, UV, IR, NMR, ESR and PES—as well as activating and directive effects exerted by the group, and its basicity, acidity and complex-forming ability.
- (c) One or more chapters deal with the formation of the functional group in question, either from other groups already present in the molecule or by introducing the new group directly or indirectly. This is usually followed by a description of the synthetic uses of the group, including its reactions, transformations and rearrangements.
- (d) Additional chapters deal with special topics such as electrochemistry, photochemistry, radiation chemistry, thermochemistry, syntheses and uses of isotopically labeled compounds, as well as with biochemistry, pharmacology and toxicology. Whenever applicable, unique chapters relevant only to single functional groups are also included (e.g. 'Polyethers', 'Tetraaminoethylenes' or 'Siloxanes').

This plan entails that the breadth, depth and thought-provoking nature of each chapter will differ with the views and inclinations of the authors and the presentation will necessarily be somewhat uneven. Moreover, a serious problem is caused by authors who deliver their manuscript late or not at all. In order to overcome this problem at least to some extent, some volumes may be published without giving consideration to the originally planned logical order of the chapters.

Since the beginning of the Series in 1964, two main developments have occurred. The first of these is the publication of supplementary volumes which contain material relating to several kindred functional groups (Supplements A, B, C, D, E, F and S). The second ramification is the publication of a series of 'Updates', which contain in each volume selected and related chapters, reprinted in the original form in which they were published, together with an extensive updating of the subjects, if possible, by the authors of the original chapters. Unfortunately, the publication of the 'Updates' has been discontinued for economic reasons.

Advice or criticism regarding the plan and execution of this series will be welcomed by the Editors.

The publication of this series would never have been started, let alone continued, without the support of many persons in Israel and overseas, including colleagues, friends and family. The efficient and patient co-operation of staff-members of the Publisher also rendered us invaluable aid. Our sincere thanks are due to all of them.

The Hebrew University  
Jerusalem, Israel

SAUL PATAI  
ZVI RAPPOPORT

Sadly, Saul Patai who founded 'The Chemistry of Functional Groups' series died in 1998, just after we started to work on the 100th volume of the series. As a long-term collaborator and co-editor of many volumes of the series, I undertook the editorship and I plan to continue editing the series along the same lines that served for the preceding volumes. I hope that the continuing series will be a living memorial to its founder.

The Hebrew University  
Jerusalem, Israel  
May 2000

ZVI RAPPOPORT



# Contents

1. Structural organomagnesium chemistry <b>Johann T. B. H. Jastrzebski, Jaap Boersma and Gerard van Koten</b>	1
2. The thermochemistry of organomagnesium compounds <b>Joel F. Liebman, Torkil Holm and Suzanne W. Slayden</b>	101
3. NMR of organomagnesium compounds <b>Peter J. Heard</b>	131
4. Formation, chemistry and structure of organomagnesium species in solvent-free environments <b>Richard A. J. O'Hair</b>	155
5. Photochemical transformations involving magnesium porphyrins and phthalocyanines <b>Natalia N. Sergeeva and Mathias O. Senge</b>	189
6. Electrochemistry of organomagnesium compounds <b>Jan S. Jaworski</b>	219
7. Analytical aspects of organomagnesium compounds <b>Jacob Zabicky</b>	265
8. Biochemistry of magnesium <b>James Weston</b>	315
9. Theoretical studies of the addition of RMgX to carbonyl compounds <b>Shinichi Yamabe and Shoko Yamazaki</b>	369
10. Organomagnesium-group 15- and Organomagnesium-group 16-bonded complexes <b>Katherine L. Hull and Kenneth W. Henderson</b>	403
11. Preparation and reactivity of magnesium enolates <b>Claude Grison</b>	437
12. Functionalized organomagnesium compounds: Synthesis and reactivity <b>Paul Knochel, Andrey Gavryushin and Katja Brade</b>	511

13.	Iron-Catalyzed Reactions of Grignard Reagents <b>G�rard Cahiez and Christophe Duplais</b>	595
14.	Carbomagnesiation reactions <b>Kenichiro Itami and Jun-ichi Yoshida</b>	631
15.	The chemistry of organomagnesium ate complexes <b>Hideki Yorimitsu and Koichiro Oshima</b>	681
16.	The chemistry of magnesium carbenoids <b>Tsuyoshi Satoh</b>	717
17.	Catalytic enantioselective conjugate addition and allylic alkylation reactions using Grignard reagents <b>Fernando L�pez, Adriaan J. Minnaard and Ben L. Feringa</b>	771
	Author index	803
	Subject index	855

# List of abbreviations used

Ac	acetyl (MeCO)
acac	acetylacetone
Ad	adamantyl
AIBN	azoisobutyronitrile
Alk	alkyl
All	allyl
An	anisyl
Ar	aryl
Bn	benzyl (PhCH <sub>2</sub> )
Bu	butyl (C <sub>4</sub> H <sub>9</sub> )
Bz	benzoyl (C <sub>6</sub> H <sub>5</sub> CO)
<i>c</i> -	cyclo
CD	circular dichroism
CI	chemical ionization
CIDNP	chemically induced dynamic nuclear polarization
CNDO	complete neglect of differential overlap
Cp	$\eta^5$ -cyclopentadienyl (C <sub>5</sub> H <sub>5</sub> )
Cp*	$\eta^5$ -pentamethylcyclopentadienyl (C <sub>5</sub> Me <sub>5</sub> )
DABCO	1,4-diazabicyclo[2.2.2]octane
DBN	1,5-diazabicyclo[4.3.0]non-5-ene
DBU	1,8-diazabicyclo[5.4.0]undec-7-ene
DIBAH	diisobutylaluminium hydride
DME	1,2-dimethoxyethane
DMF	<i>N,N</i> -dimethylformamide
DMSO	dimethyl sulfoxide
<i>E</i> -	entgegen
ee	enantiomeric excess
EI	electron impact
ESCA	electron spectroscopy for chemical analysis
ESR	electron spin resonance
Et	ethyl (C <sub>2</sub> H <sub>5</sub> )
eV	electron volt

Fc	ferrocenyl
FD	field desorption
FI	field ionization
FT	Fourier transform
Fu	furyl ( $\text{OC}_4\text{H}_3$ )
GLC	gas liquid chromatography
Hex	hexyl ( $\text{C}_6\text{H}_{13}$ )
<i>c</i> -Hex	cyclohexyl ( <i>c</i> - $\text{C}_6\text{H}_{11}$ )
HMPA	hexamethylphosphortriamide
HOMO	highest occupied molecular orbital
HPLC	high performance liquid chromatography
<i>i</i> -	iso
ICR	ion cyclotron resonance
Ip	ionization potential
IR	infrared
LAH	lithium aluminium hydride
LCAO	linear combination of atomic orbitals
LDA	lithium diisopropylamide
LUMO	lowest unoccupied molecular orbital
M	metal
<i>M</i>	parent molecule
MCPBA	<i>m</i> -chloroperbenzoic acid
Me	methyl ( $\text{CH}_3$ )
Mes	mesityl ( $2,4,6\text{-Me}_3\text{C}_6\text{H}_2$ )
MNDO	modified neglect of diatomic overlap
MS	mass spectrum
<i>n</i> -	normal
Naph	naphthyl
NBS	<i>N</i> -bromosuccinimide
NCS	<i>N</i> -chlorosuccinimide
NMR	nuclear magnetic resonance
Pen	pentyl ( $\text{C}_5\text{H}_{11}$ )
Ph	phenyl
Pip	piperidyl ( $\text{C}_5\text{H}_{10}\text{N}$ )
ppm	parts per million
Pr	propyl ( $\text{C}_3\text{H}_7$ )
PTC	phase transfer catalysis or phase transfer conditions
Py	pyridine ( $\text{C}_5\text{H}_5\text{N}$ )
Pyr	pyridyl ( $\text{C}_5\text{H}_4\text{N}$ )

R	any radical
RT	room temperature
<i>s</i> -	secondary
SET	single electron transfer
SOMO	singly occupied molecular orbital
<i>t</i> -	tertiary
TCNE	tetracyanoethylene
TFA	trifluoroacetic acid
TFE	2,2,2-trifluoroethanol
THF	tetrahydrofuran
Thi	thienyl (SC <sub>4</sub> H <sub>3</sub> )
TLC	thin layer chromatography
TMEDA	tetramethylethylene diamine
TMS	trimethylsilyl or tetramethylsilane
Tol	tolyl (MeC <sub>6</sub> H <sub>4</sub> )
Tos or Ts	tosyl ( <i>p</i> -toluenesulphonyl)
Trityl	triphenylmethyl(Ph <sub>3</sub> C)
Vi	vinyl
XRD	X-ray diffraction
Xyl	xylyl (Me <sub>2</sub> C <sub>6</sub> H <sub>3</sub> )
Z-	zusammen

In addition, entries in the 'List of Radical Names' in *IUPAC Nomenclature of Organic Chemistry*, 1979 Edition, Pergamon Press, Oxford, 1979, p. 305–322, will also be used in their unabbreviated forms, both in the text and in formulae instead of explicitly drawn structures.

# The Chemistry of Organomagnesium Compounds

Editors: Professor **Zvi Rappoport, Ilan Marek**

Series Editors: Professor Saul Patai, Professor Zvi Rappoport .

## CONTENTS

Page	
i	Front Matter
c1	Colour Plates
<b>1</b>	<b>Chapter 1:</b> Structural Organomagnesium Chemistry
<b>101</b>	<b>Chapter 2:</b> The Thermochemistry of Organomagnesium Compounds
<b>131</b>	<b>Chapter 3:</b> NMR of Organomagnesium Compounds
<b>155</b>	<b>Chapter 4:</b> Formation, Chemistry and Structure of Organomagnesium Species in Solvent-Free Environments
<b>189</b>	<b>Chapter 5:</b> Photochemical Transformations Involving Magnesium Porphyrins and Phthalocyanines
<b>219</b>	<b>Chapter 6:</b> Electrochemistry of Organomagnesium Compounds
<b>265</b>	<b>Chapter 7:</b> Analytical Aspects of Organomagnesium Compounds
<b>315</b>	<b>Chapter 8:</b> Biochemistry of Magnesium
<b>369</b>	<b>Chapter 9:</b> Theoretical Studies of the Addition of RMgX to Carbonyl Compounds
<b>403</b>	<b>Chapter 10:</b> Organomagnesium-Group 15- and Organomagnesium-Group 16 Bonded Complexes
<b>437</b>	<b>Chapter 11:</b> Preparation and Reactivity of Magnesium Enolates
<b>511</b>	<b>Chapter 12:</b> Functionalized Organomagnesium Compounds: Synthesis and
<b>595</b>	<b>Chapter 13:</b> Iron-Catalyzed Reactions of Grignard Reagents
<b>631</b>	<b>Chapter 14:</b> Carbomagnesiation Reactions
<b>681</b>	<b>Chapter 15:</b> The Chemistry of Organomagnesium Ate Complexes
<b>717</b>	<b>Chapter 16:</b> The Chemistry of Magnesium Carbenoids
<b>771</b>	<b>Chapter 17:</b> Catalytic Enantioselective Conjugate Addition and Allylic Alkylation Reactions Using Grignard Reagents
<b>803</b>	Author Index
<b>855</b>	Subject Index

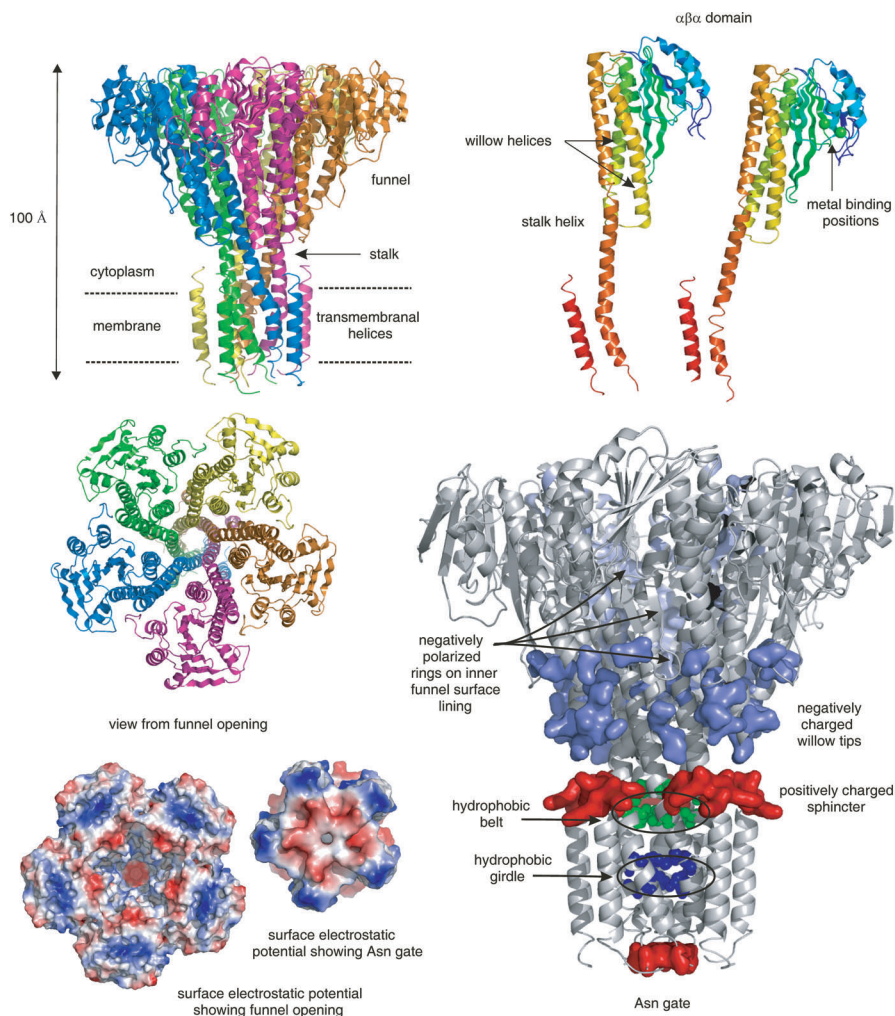


PLATE 1 Top left: Ribbon diagram of the CorA magnesium transporter (PDB 2BBJ). Top right: Monomeric subunit. Middle and bottom left: Various views of the funnel and membrane openings. Bottom right: Illustration of critical structural features

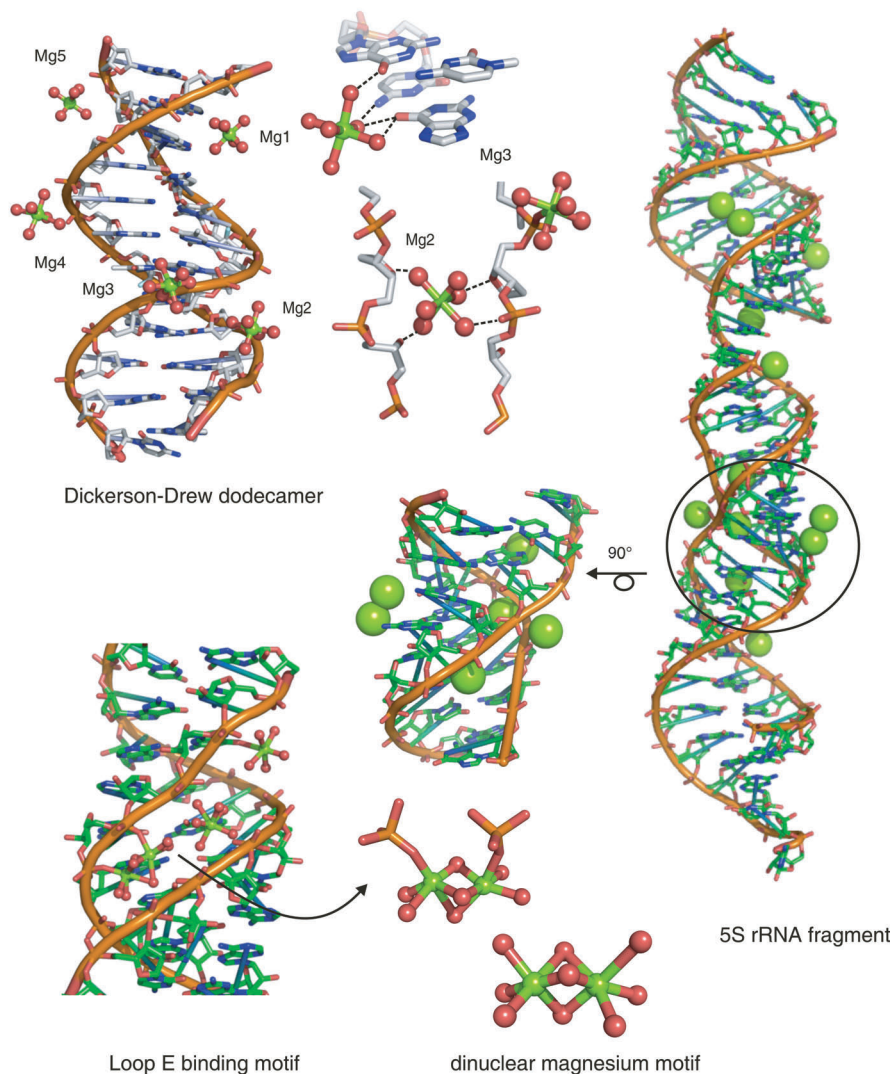


PLATE 2 Examples of specific  $Mg^{2+}$  interactions with DNA and RNA. Upper left: the Dickerson-Drew DNA fragment CGCCAATTCGCG (NDB BD0007). Lower left: the RNA loop E backbone zipper motif containing a dinuclear magnesium cluster (NDB URL064). Right: the 5S rRNA fragment from ribosomal *E. coli* (NDB file URL065) containing two dinuclear magnesium clusters and a twisted loop E motif (blow-up)



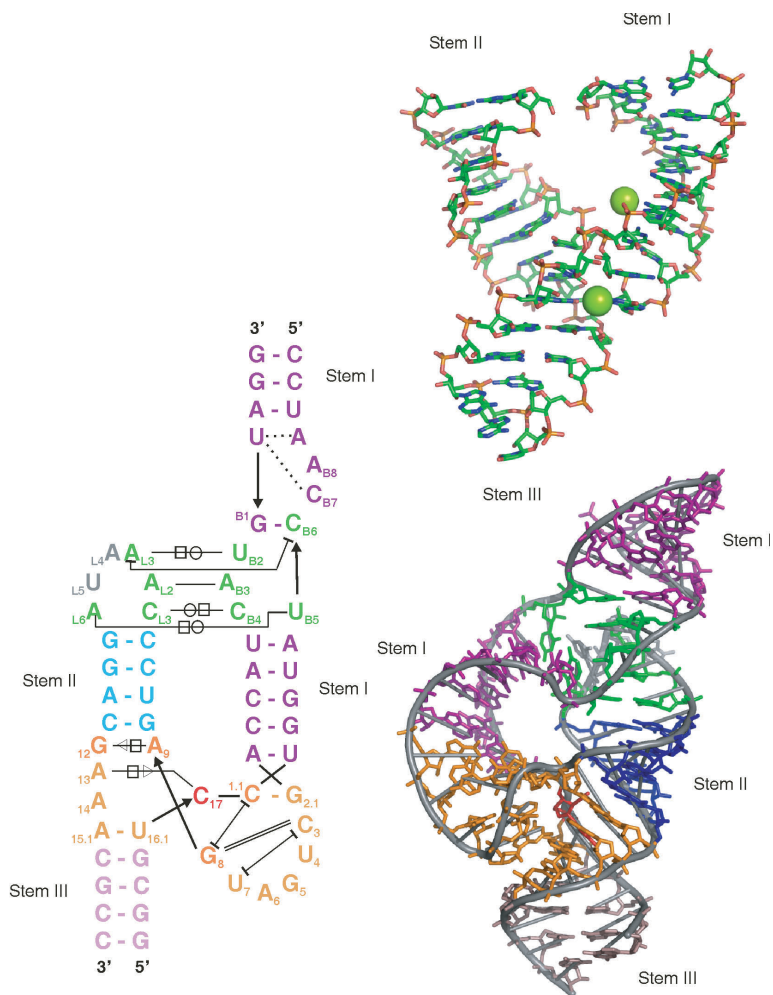


PLATE 3 Top right: The Y-structure of a minimal hammerhead construct (PDB 301D). Left: Sequence, secondary structure and tertiary interactions of the *Schistosoma mansoni* ribozyme. Stems I, II, and II are purple, blue and lilac, respectively. Nucleotides involved in tertiary interactions are green. The catalytic core is orange and the cleavage site is red. Thick black arrowed lines denote backbone continuity and thin lines show tertiary interactions; T-termini represent stacking interactions and  $\square\square/\square\square$  denotes a Watson-Crick/Hoogsteen interaction and  $\square\square/\triangle\square$  is a Hoogsteen/sugar edge interaction. Reproduced with permission from reference 190 © Wiley-VCH Verlag GmbH & Co. KGaA. Bottom right: Solid state structure drawn with the color notation indicated above (PDB 2goz)

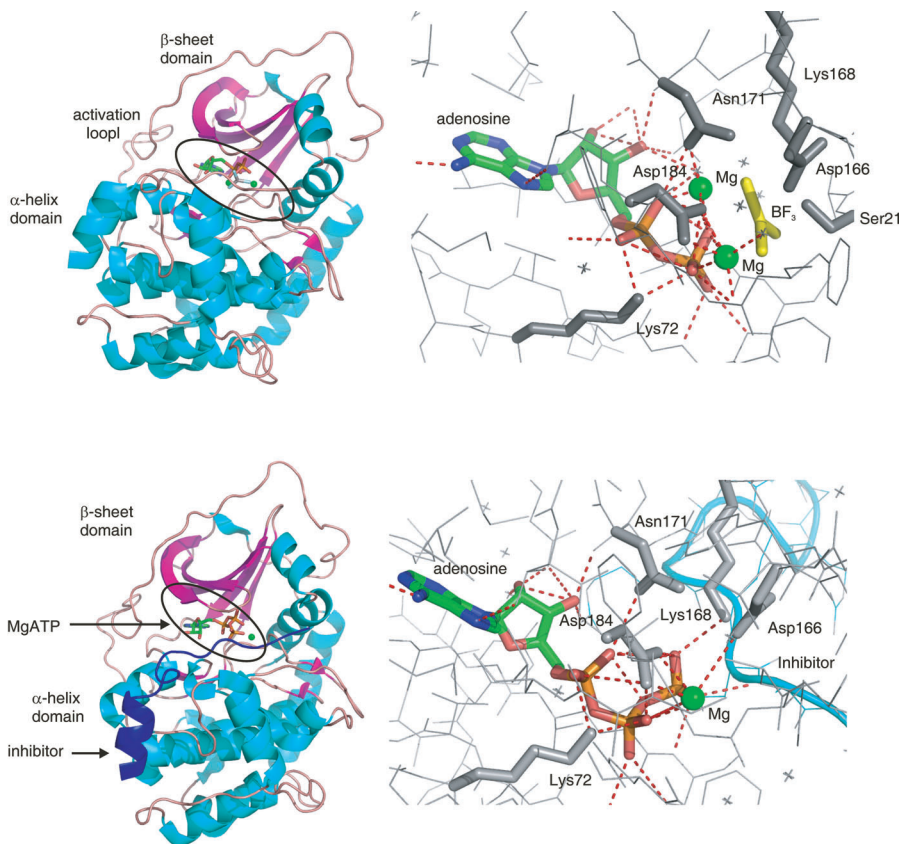


PLATE 4 Top: Transition state analog of cAMP dependent protein kinase complexed with ADP, two  $\text{Mg}^{2+}$  ions and  $\text{BF}_3$  (left) as well as a blowup of the active center (right) showing polar interactions with essential side chains (PDB 1L3R). Bottom: An engineered variant of cAMP dependent protein kinase complexed with  $\text{MgATP}^{2-}$  and the inhibitor peptide fragment 5–24 (left) and a blowup of the active site (right). Drawn from the PDB file 1Q24

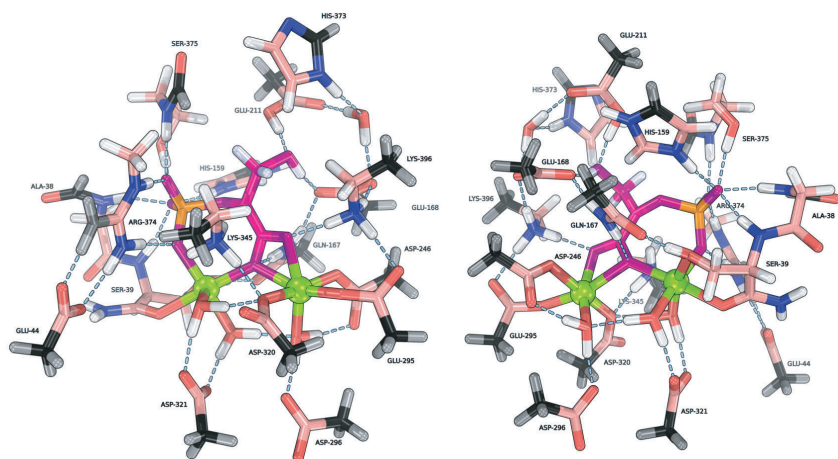
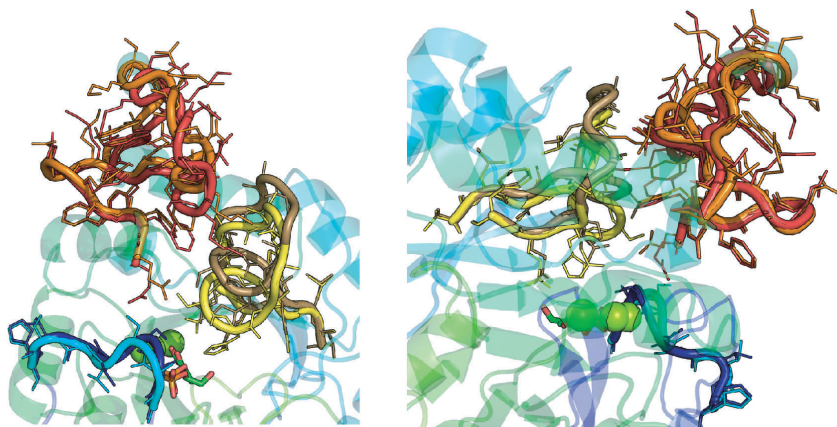


PLATE 5 Loop movement in the active site of yeast enolase. Upper left: 'closed' conformation (PDB 2AL1) superimposed upon the 'open' conformation (PDB 1P43). Upper right: view from the back. Lower left: A quantum chemical 'soccer ball' model for yeast enolase illustrated on the enol-intermediate and calculated at the TPSS(MARI-J;COSMO)/SV(P) level of theory. Lower right: view from the back

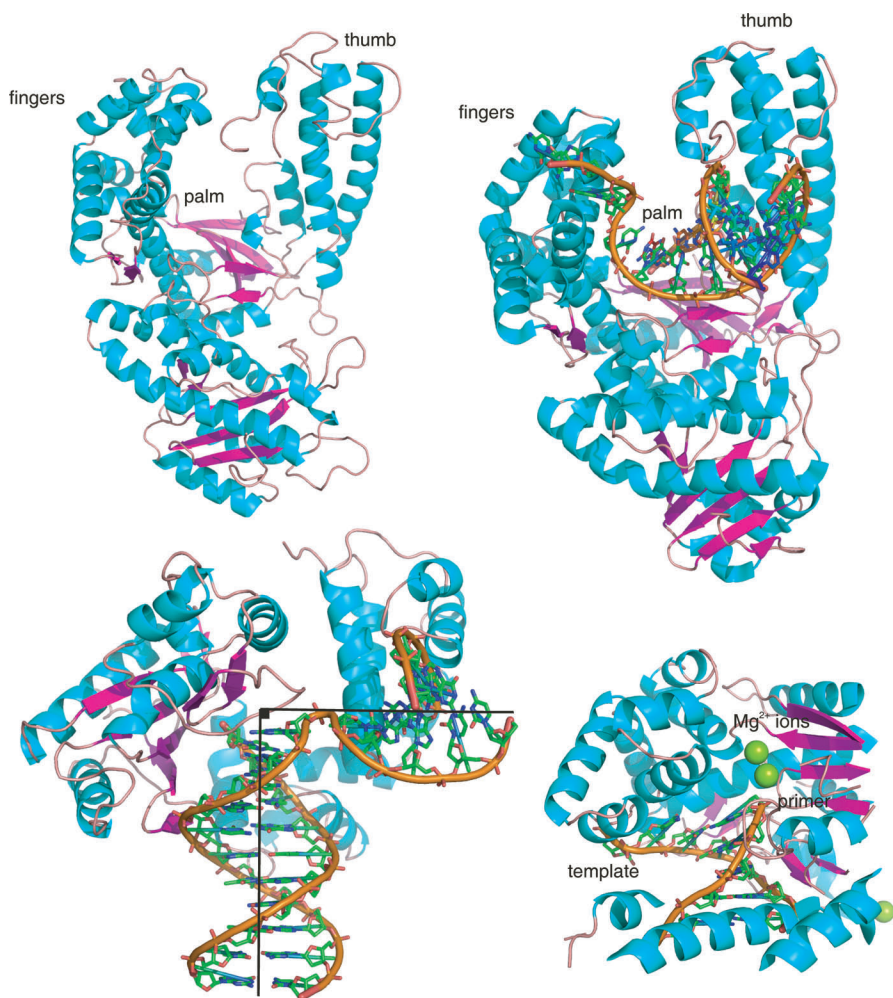


PLATE 6 Top left: Klenow fragment (engineered) showing the typical “hand” structure of polymerases (PDB 2KZZ). Top right: Klenow fragment of *E. coli* polymerase I (*Bacillus stearothermophilus*) complexed with 9 base pairs of duplex DNA (PDB 1L3S). Bottom left: Human DNA polymerase  $\beta$  complexed with a gapped DNA inhibitor showing the typical  $90^\circ$  orientation of the template to the growing replicant (PDB 1BPX). Bottom right: Active site of T7 DNA demonstrating the position of the metal ions with respect to the primer and template (PDB 1T7P)

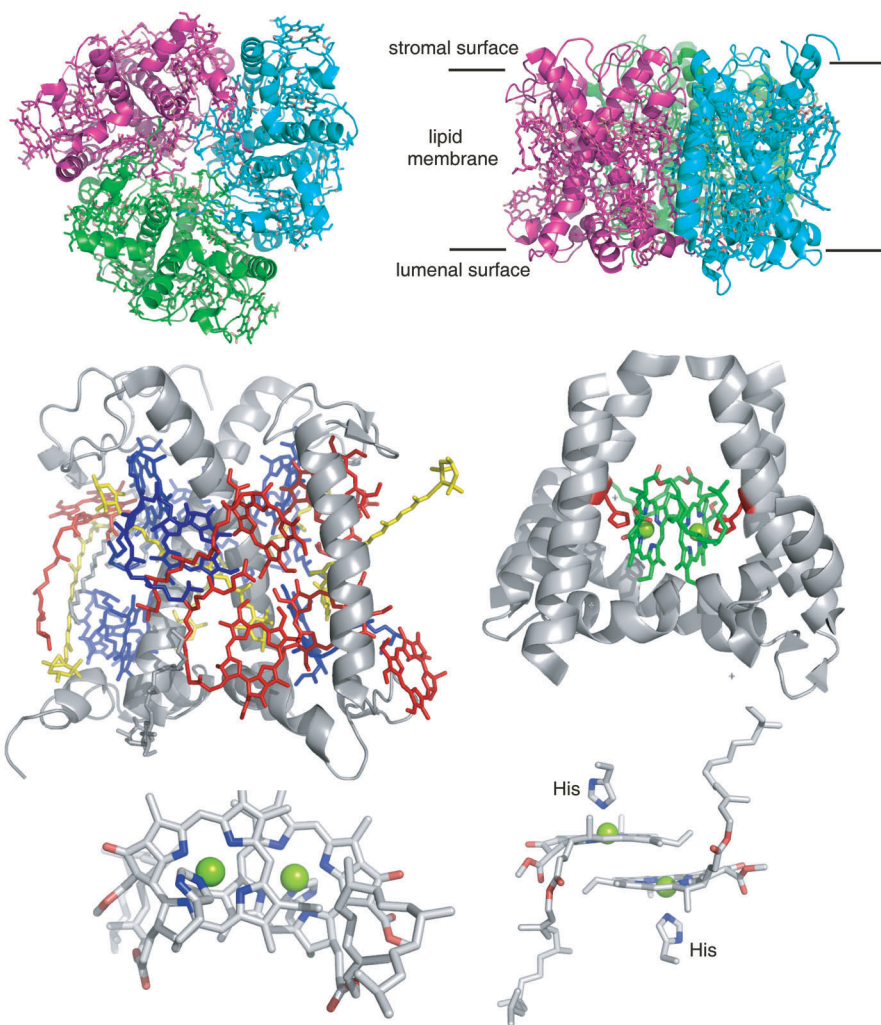


PLATE 7 Top left: Plant (pea) light harvesting complex LHC-II—view from the luminal membrane surface (PDB 2BHW). Top right: View from the side. Middle left: One sub unit of LHC-II showing the placement of chlorophyll a (blue), chlorophyll b (red) and carotenoid cofactors (yellow). Middle right: The primary electron donor P700 and its protein environment in the photosystem I of *Synechococcus elongates* (PDB 1JB0). Bottom left: A closer view (from the top) of P700. Bottom right: View from the side



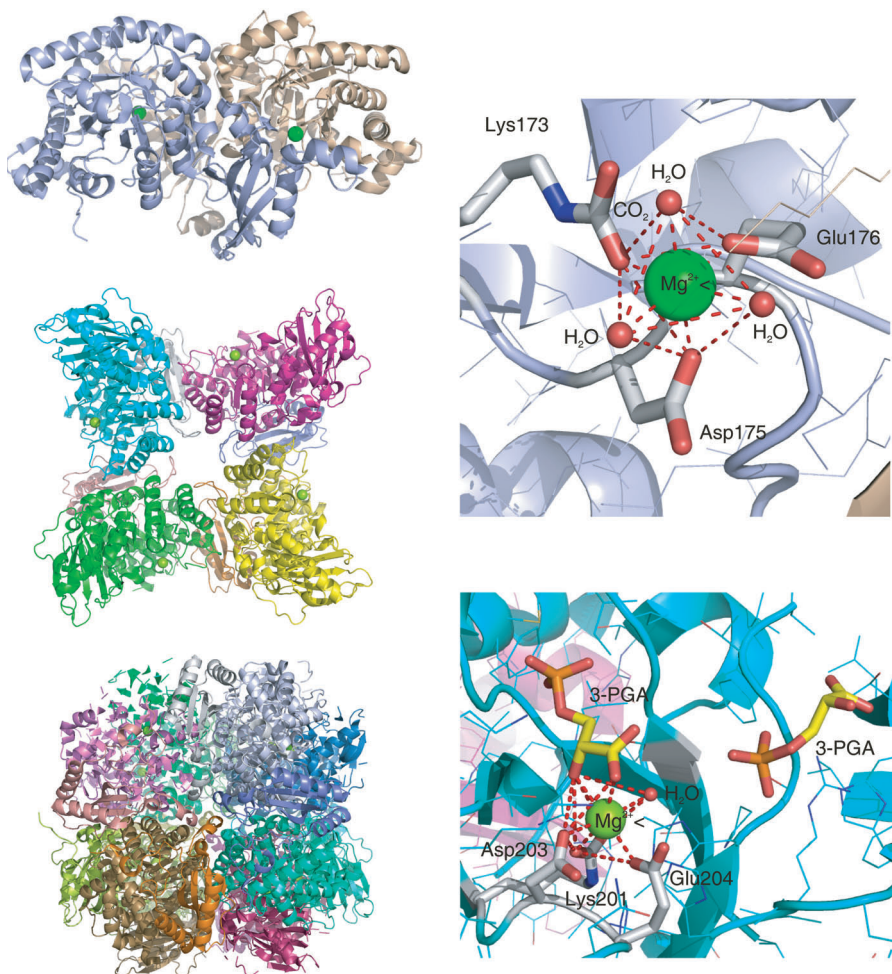


PLATE 8 Top left: Structure of a rubisco-like protein showing the basic dimeric unit (PDB 2OEK). Top right: Active site of this rubisco-like protein showing conserved residues and the coordination sphere of  $\text{Mg}^{2+}$ . Middle left: Structure (dimer of dimers) of activated spinach rubisco complexed with product (PDB 1AA1). Bottom right: Active site of this spinach rubisco product complex. Bottom left: Structure of activated green algae rubisco (tetramer of dimers)

## CHAPTER 1

# Structural organomagnesium chemistry

JOHANN T. B. H. JASTRZEBSKI, JAAP BOERSMA and  
GERARD VAN KOTEN

*Chemical Biology & Organic Chemistry, Faculty of Science Utrecht University,  
Padualaan 8, 3584 CH Utrecht, The Netherlands*  
Fax: +31-30-2523615; e-mail: j.t.b.h.jastrzebski@uu.nl

---

I. INTRODUCTION . . . . .	2
II. ORGANOMAGNESIATES . . . . .	4
A. Introduction . . . . .	4
B. Tetraorganomagnesiates $M_2[R_4Mg]$ . . . . .	5
C. Triorganomagnesiates $M[R_3Mg]$ . . . . .	12
D. Heteroleptic Organomagnesiates $M[R_2YMg]$ and $M[RY_2Mg]$ . . . . .	14
III. DIORGANOMAGNESIUM COMPOUNDS . . . . .	23
A. Donor-base-free Diorganomagnesium Compounds . . . . .	23
B. Diorganomagnesium Compounds Containing Multi-hapto-bonded Groups . . . . .	25
C. Diorganomagnesium Compounds Containing Intramolecularly Coordinating Substituents . . . . .	30
D. Donor–Acceptor Complexes of $\sigma$ -Bonded Diorganomagnesium Compounds . . . . .	36
E. Magnesium Anthracene Compounds . . . . .	44
F. Donor–Acceptor Complexes of Diorganomagnesium Compounds with Multi-hapto-bonded Groups . . . . .	47
IV. HETEROLEPTIC $RMgY$ COMPOUNDS . . . . .	54
A. Introduction . . . . .	54
B. Monoorganomagnesium Cations . . . . .	56
C. Monoorganomagnesium Compounds $RMgY$ with $Y = \text{halogen}$ (Grignard Reagents) . . . . .	58
D. Monoorganomagnesium Compounds $RMgY$ with $Y = OR$ . . . . .	69
E. Monoorganomagnesium Compounds $RMgY$ with $Y = NR_2$ . . . . .	71
F. Monoorganomagnesium Compounds $RMgY$ with $Y = SR$ or $PR_2$ . . . . .	83
V. MIXED ORGANOMAGNESIUM TRANSITION-METAL COMPOUNDS . . . . .	85

---

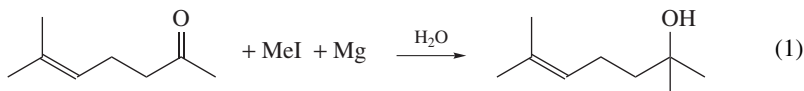
*The chemistry of organomagnesium compounds*

Edited by Z. Rappoport and I. Marek © 2008 John Wiley & Sons, Ltd. ISBN: 978-0-470-05719-3

VI. CONCLUSIONS . . . . .	91
VII. REFERENCES . . . . .	92

## I. INTRODUCTION

Although organomagnesium compounds are among the earliest reported organometallic compounds they were regarded as curiosities until 1900. At that time Victor Grignard, then a graduate student, worked in the laboratory of Professor Barbier at the University of Lyon in France. His task was to optimize conditions for what is now known as the Barbier reaction (equation 1)<sup>1</sup>.



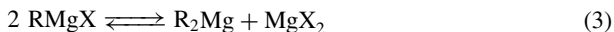
Grignard proposed the intermediate in this reaction to be a RMgI species and concluded that yields might be improved by preparing this compound first and then adding it to the ketone. He found that alkyl halides indeed react readily with magnesium in diethyl ether as solvent to give compounds formulated as RMgX (equation 2). Addition of these reaction mixtures to a ketone or an aldehyde affords the corresponding alcohols in higher yields than when the Barbier procedure is used<sup>2</sup>.



Immediately, the synthetic potential of the Grignard reagents was recognized, resulting in an ever increasing number of investigations towards their preparation and application<sup>3-5</sup>, and nowadays the Grignard reagent is one of the most powerful synthetic tools in chemistry. For Grignard's discovery and subsequent development of this finding, he was awarded the Nobel Prize in Chemistry in 1912.

Soon after its discovery an onium-type structure (1) for methylmagnesium iodide in ether was proposed by Baeyer and Villiger<sup>6</sup>, while a somewhat different onium-type structure (2) was proposed by Grignard (Figure 1)<sup>7</sup>.

Although it seemed that Standnikov had evidence to support Grignard's proposal<sup>8</sup>, investigations by Thorp and Kamm demonstrated conclusively that Grignard reagents could not be represented by an onium type of structure<sup>9</sup>. A polar composition of the Grignard reagent  $\text{R}^- (\text{MgX})^+$  was proposed by Abegg<sup>10</sup> and he suggested the possibility of an equilibrium (equation 3), which nowadays is known as the Schlenk equilibrium.



With these proposals a debate started about the constitution of Grignard reagents in solution which lasted for about sixty years. This topic has been reviewed by Ashby<sup>11</sup>.

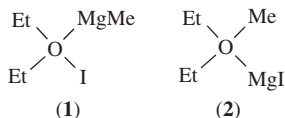


FIGURE 1. The earliest proposed structures for methylmagnesium iodide in diethyl ether solution



Nowadays it has been well-established that the simple representation of Grignard reagents as  $\text{RMgX}$ , used in most organic text books, is far beyond the truth. Instead, in coordinating solvents like diethyl ether Grignard reagents exist as complicated mixtures of various aggregated species, in which the Schlenk equilibrium (equation 3) plays an important role<sup>12</sup>. The actual structures of the species present in solution depend on the nature of R, the nature of X, the properties of the coordinating solvent, concentration and temperature<sup>3–5, 11, 13–15</sup>.

Modern techniques like X-ray absorption spectroscopy and large-angle X-ray scattering, which have been reviewed recently<sup>16</sup>, have provided detailed information about the actual species present in solutions of organomagnesium compounds. Such studies are a prerequisite for a better understanding of the structure–activity relationships of organomagnesium compounds and in particular Grignard reagents, and the mechanisms involved in the reactions thereof<sup>17, 18</sup>.

Elucidation of the structures of organomagnesium compounds in the solid state started in the early sixties of the previous century when modern X-ray crystallographic techniques became available. Single-crystal X-ray structure determinations of both the diethyl etherate of phenylmagnesium bromide and the diethyl etherate of ethylmagnesium bromide unambiguously showed that in the solid state these compounds exist as discrete monomers. In these structures the magnesium atom has a distorted tetrahedral coordination geometry as a result of the bonding of both the carbon atom and the bromine atom to magnesium and the coordination of two additional diethyl ether molecules to magnesium<sup>19, 20</sup>. Until then it was thought that Grignard reagents exist as asymmetric dimers in the solid state (Figure 2).

At the same time the structures in the solid state of  $\text{Me}_2\text{Mg}$  and  $\text{Et}_2\text{Mg}$  were determined by X-ray powder diffraction studies<sup>21, 22</sup>. Both compounds form polymeric chains as the result of the bridging of two methyl groups between two magnesium atoms, rendering the magnesium atoms almost perfectly tetrahedrally coordinated.

These early studies started a renaissance in the structural investigations of organomagnesium compounds in the solid state and nowadays hundreds of structures are known. In fact, in the January 2007 version of the CSD database<sup>23</sup> 423 structures containing at least one direct magnesium–carbon interaction have been found. The present chapter gives an overview of the structural investigations on organomagnesium compounds in the solid state, a topic that has been reviewed earlier by others<sup>15, 24–28</sup>. It should be noted that the structures of organomagnesium compounds obtained from X-ray crystallographic studies do not necessarily represent the structure as present in solution. Nowadays it is well known that organomagnesium compounds in solution are involved in complicated redistribution and aggregation equilibria. Such equilibria are driven by thermodynamics and therefore often the thermodynamic most stable species crystallize from such solutions. However, solubility properties and crystal packing effects also determine which particular organomagnesium compound crystallizes from solution.

According to its position in the Periodic Table of the Elements, magnesium is divalent and therefore should form organomagnesium compounds with two groups attached to it. However, because magnesium has only four electrons in its valence shell, this bonding

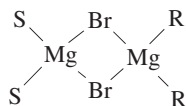


FIGURE 2. Proposed structure in the solid state for Grignard reagents before X-ray crystallography became available, S =  $\text{Et}_2\text{O}$  or THF

situation violates the octet rule. Therefore such a (linear) dicoordinate state, as e.g. found in simple diorganozinc compounds<sup>29</sup>, is very rare. Organomagnesium compounds escape from such bonding situations by the additional coordination of donor molecules and/or by aggregation via bridging multi-center bonds or agostic interactions, resulting in most cases in a (distorted) tetrahedral coordination geometry at magnesium, which is the preferred one.

From a structural point of view, three classes of organomagnesium compounds can be distinguished, according to the number of carbon atoms directly bound to magnesium. These classes are: (i) ionic organomagnesium compounds in which the number of carbon atoms (three or four) bound to magnesium exceeds the valence number of magnesium, the so-called organomagnesiates, (ii) diorganomagnesium compounds and their coordination complexes and (iii) heteroleptic RMgX compounds in which X is an electronegative substituent like a halogen atom (Grignard Reagents) or a monoanionic group bound to magnesium via an electronegative atom like oxygen or nitrogen. Depending on the nature of X the latter class of compounds may be further divided into sub-classes. In the following sections the structures of these classes of compounds will be discussed.

## II. ORGANOMAGNESIATES

### A. Introduction

Alkali-metal ate compounds are among the first organometallic compounds reported. Already in 1858 the formation of a crystalline material formulated as 'Na[Et<sub>3</sub>Zn]', obtained from the reaction of metallic sodium with Et<sub>2</sub>Zn, was reported by Wanklyn<sup>30</sup>. It then took almost a century before the first organomagnesiate was reported. In 1951 Wittig and coworkers realized that organometallic compounds with anionic formulations, for which he coined the term 'ate', could be made<sup>31</sup>. In this paper the formation of Li[Ph<sub>3</sub>Mg] and other 'ate'-type compounds from its homometallic components was described (equation 4).



The special and unique reactivities associated with this class of compounds were rapidly recognized. For example, the reaction of Li[Ph<sub>3</sub>Mg] with benzalacetophenone yields mainly the 1,4-addition product while the same reaction with PhLi affords the 1,2-addition product. Wittig rationalized the chemistry of 'ate-complexes' in terms of anionic activation by which all of the ligands surrounding the metal were activated through an inductive effect<sup>32</sup>. In an early review of 'structures and reactions of organic ate-complexes' by Tochtermann this idea was emphasized<sup>33</sup>.

When a diorganomagnesium compound and an alkali metal organic compound are mixed, an enhanced solubility of the resulting species in organic solvents is often observed, which is an indication of the formation of a mixed metal ate compound. This observation was reported by Coates and Heslop, who observed that Me<sub>2</sub>Mg dissolves better in diethyl ether solutions that contain butyllithium than in the neat diethyl ether solvent. In this case the formation of a compound having the stoichiometry [Li(OEt<sub>2</sub>)] [Me<sub>2</sub>BuMg] had been suggested<sup>34</sup>. A special feature of these 'ate' species with M[R<sub>3</sub>Mg] and also M<sub>2</sub>[R<sub>4</sub>Mg] stoichiometry is that they exist in solution as an equilibrium mixture of various species with different metal-to-ligand molar ratios. For example, NMR studies of solutions containing a diorganomagnesium compound and an organolithium compound in various molar ratios established the presence in solution of at least three distinct different ate compounds in a rapid exchange equilibrium<sup>35-37</sup>.

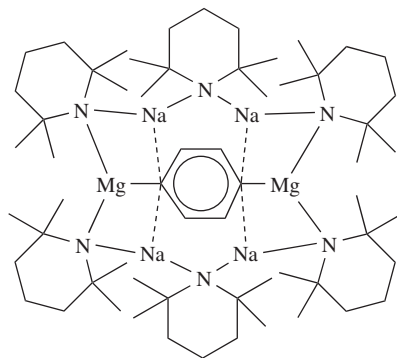


FIGURE 3. Example of an inverse crown containing a 1,4-phenylene dianion

The elucidation of the structures of organomagnesiates in the solid state started with the groundbreaking X-ray crystallographic studies by Weiss on the structures of organoalkalimetal compounds including a series of organomagnesiates and organozincate compounds<sup>38</sup>.

So far only organomagnesiates in which all the organic ligands are identical, i.e. the homoleptic organomagnesiates, have been considered. It should be noted, however, that this is not a prerequisite and organomagnesiates also exist having different organic groups. Another important class of organomagnesiates is that in which one or two of the monoanionic organic ligands are replaced by either a halide anion, or by an amido or alkoxide anion, the so-called heteroleptic organomagnesiates. During structural investigations of the latter type of compounds the concept of ‘inverse crown’ was discovered<sup>39,40</sup>. These are aggregated compounds, usually built-up from magnesium amides or alkoxides and alkali metal amides or alkoxides, that have a very strong affinity to anionic species. Some of these are even capable of abstracting one or even two protons from an arene in a very regioselective way, forming heteroleptic organomagnesiates. Figure 3 shows an inverse crown containing bis-magnesiated benzene.

Examples of the application of organomagnesiates in organic synthesis are: (i) halogen–magnesium exchange reactions of (functionalized) aryl and alkenyl halides<sup>41–43</sup>, (ii) the direct deprotonation of furans<sup>44</sup> and (iii) in highly selective addition reactions to ketones<sup>45</sup>. Another application of organomagnesiates is their use as a catalyst in the polymerization of butadiene to highly crystalline *trans*-1,4-polybutadiene<sup>46</sup>.

## B. Tetraorganomagnesiates $M_2[R_4Mg]$

Before discussing the structural features of tetraorganomagnesiates in the solid state it should be noted that structures in which the presence of separated anionic and cationic moieties can be distinguished are rare. In most cases such units are linked via electron-deficient bonds, i.e. two-electron three-center bridge-bonded carbon atoms between magnesium and the counter cation.

The first structure, unambiguously established by an X-ray crystal-structure determination, is  $Me_8Al_2Mg$  (**3**), that has the structural motif of four monoanionic carbon ligands bound to magnesium in a distorted tetrahedral coordination geometry (Figure 4)<sup>47</sup>.

The molecular geometry of **3** comprises a central magnesium atom pairwise linked via four two-electron three-center bonded methyl groups to the two dimethylaluminium units. The four carbon-to-magnesium bonds (2.20, 2.22, 2.19 and 2.22 Å) are slightly elongated compared to the C–Mg distances observed in linear bis(neopentyl)magnesium

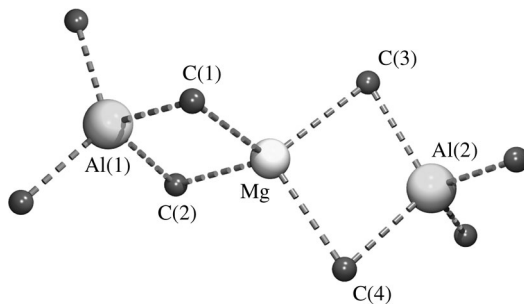


FIGURE 4. Molecular geometry of  $\text{Me}_8\text{Al}_2\text{Mg}$  (**3**) in the solid state

(2.13 Å) and  $[2,4,6\text{-}(t\text{-Bu})_3\text{C}_6\text{H}_2]_2\text{Mg}$  (2.12 Å). Such an elongation is not unexpected for bridging methyl groups. The  $\text{C}(1)\text{--Mg--C}(2)$  and  $\text{C}(3)\text{--Mg--C}(4)$  bond angles ( $98.4^\circ$  and  $99.1^\circ$ , respectively) are smaller than expected for the ideal tetrahedral value, but are compensated by larger values for the other  $\text{C--Mg--C}$  bond angles (average  $115^\circ$ ). The acute  $\text{Mg--C--Al}$  bond angles of approximately  $77^\circ$  are in the range expected for bridging methyl groups. Arguably, this compound may be described as a true tetraorganomagnesiate comprising a central  $\text{Me}_4\text{Mg}^{2-}$  dianion linked to two  $\text{Me}_2\text{Al}^+$  cations.

Crystalline  $[\text{Li}(\text{TMEDA})_2]_2[\text{Me}_4\text{Mg}]$  (**4**) was obtained from the reaction of  $\text{Me}_2\text{Mg}$ ,  $[\text{MeLi}]_4(\text{TMEDA})_2$  and TMEDA in diethyl ether as a solvent. Its X-ray crystal structure determination<sup>48</sup> revealed a molecular geometry (Figure 5) comprising a central  $\text{Me}_4\text{Mg}$  unit with average  $\text{C--Mg}$  distances of 2.260(8) Å. All  $\text{C--Mg--C}$  angles deviate less than  $1^\circ$  from the ideal tetrahedral value of  $109.5^\circ$ , pointing to an almost perfect tetrahedral coordination geometry around the magnesium atom. The four methyl groups interact pairwise with the lithium atoms of two  $\text{Li}(\text{TMEDA})$  units. The relatively short  $\text{C--Li}$  distances range from 2.26(1) to 2.30(1) Å, values that are very close to the  $\text{C--Mg}$  distances, indicating that the methyl groups are symmetrically bridge-bonded between the magnesium and lithium atoms.

The solid-state structure of  $[\text{Na}(\text{PMDTA})_2]_2[\text{Ph}_4\text{Mg}]$  (**5**)<sup>49</sup> shows a great similarity with that of **4**. Four aryl groups are bonded to the magnesium atom ( $\text{C--Mg}$  2.29 Å, average) in an almost perfect tetrahedral arrangement (Figure 6). Two  $\text{Na}(\text{PMDTA})$  units are linked to the central  $\text{Ph}_4\text{Mg}$  unit via bridge-bonding of two phenyl groups to each sodium atom,

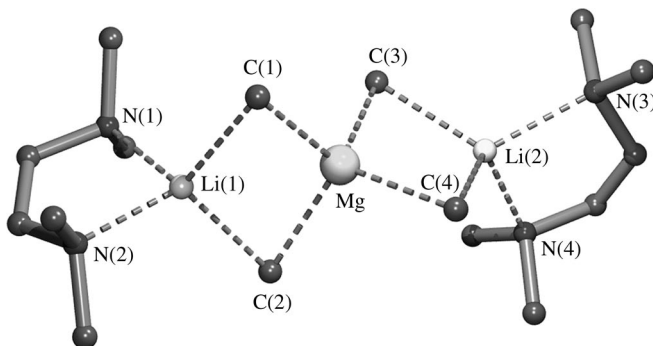


FIGURE 5. Molecular geometry of  $[\text{Li}(\text{TMEDA})_2]_2[\text{Me}_4\text{Mg}]$  (**4**) in the solid state

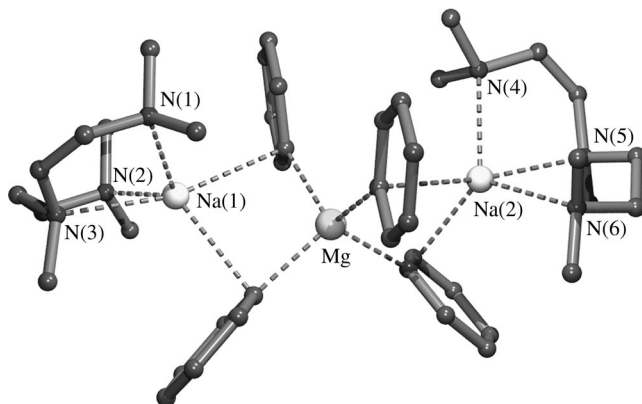
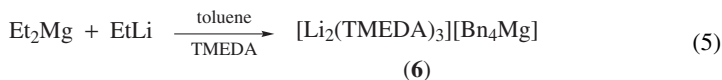


FIGURE 6. Molecular geometry of  $[\text{Na}(\text{PMDTA})]_2[\text{Ph}_4\text{Mg}]$  (**5**) in the solid state

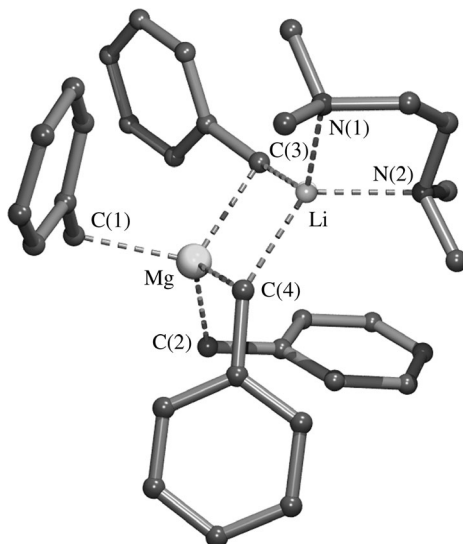
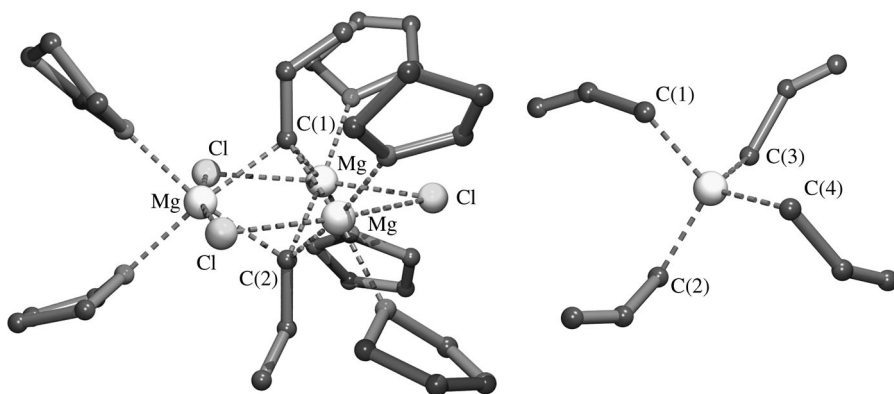
rendering these sodium atoms penta-coordinate. However, the bridging phenyl groups are less symmetrically bonded between magnesium and sodium than the bridging methyl groups between magnesium and lithium in **4**. This is shown by the longer  $C_{ipso}-\text{Na}$  bond lengths, ranging from 2.73 to 2.89 Å, compared to the  $\text{C}-\text{Mg}$  bond lengths of 2.29 Å. Furthermore, the  $C_{ipso}-\text{Na}$  vectors are orientated perpendicular to the planes of the aryl groups, pointing to a  $\pi$ -type interaction between  $C_{ipso}$  and sodium.

During the attempted preparation of an ethylmagnesiato from  $\text{Et}_2\text{Mg}$  and  $\text{EtLi}$  in a hexane/toluene solvent mixture it appeared that an unexpected metallation of toluene had occurred resulting in a compound with the formulation  $\text{Li}_2[\text{Bn}_4\text{Mg}]$ . According to a similar procedure,  $[\text{Li}_2(\text{TMEDA})_3][\text{Bn}_4\text{Mg}]$  (**6**) was obtained from the reaction of  $\text{Et}_2\text{Mg}$  with  $\text{EtLi}$  in the presence of toluene and TMEDA (equation 5)<sup>50</sup>.



An X-ray crystal-structure determination of **6** revealed a solid-state structure consisting of  $[\text{Li}(\text{TMEDA})][\text{Bn}_4\text{Mg}]$  anionic and  $\text{Li}(\text{TMEDA})_2$  cationic units. The molecular geometry of the anion comprises a  $\text{Bn}_4\text{Mg}$  unit linked to the  $\text{Li}(\text{TMEDA})$  moiety via two bridging benzyl groups (Figure 7). The  $\text{C}-\text{Mg}$  bond lengths of the bridge-bonding benzyl groups  $[\text{C}(3)-\text{Mg}$  2.313(9) and  $\text{C}(4)-\text{Mg}$  2.322(9) Å] are slightly elongated compared to those of the terminally bonded benzyl groups  $[\text{C}(1)-\text{Mg}$  2.22(1) and  $\text{C}(2)-\text{Mg}$  2.26(1) Å]. The observed  $\text{C}-\text{Li}$  bond lengths  $[\text{C}(3)-\text{Li}$  2.27(1) and  $\text{C}(4)-\text{Li}$  2.23(2) Å] point to a slightly asymmetric bridge-bonding of the benzyl groups between magnesium and lithium. The  $\text{C}(3)-\text{Mg}-\text{C}(4)$  bond angle of  $104.7(4)^\circ$  is smaller than the ideal tetrahedral value, but is compensated by a value of  $111.1(5)^\circ$  for the  $\text{C}(1)-\text{Mg}-\text{C}(2)$  bond angle. These deviations point to a slightly distorted tetrahedral coordination geometry at the magnesium atom. Finally, coordination saturation at the lithium atom is reached by a  $N,N'$ -chelate bonded TMEDA molecule.

The reaction of allylmagnesium chloride with methylaluminium dichloride affords, after workup of the reaction mixture and recrystallization from THF, a rather unexpected compound (**7**), which, according to its crystal-structure determination, appears to consist of  $[(\text{allyl})_2\text{Mg}_3\text{Cl}_3(\text{THF})_6]^+$  cations and  $[(\text{allyl})_4\text{Mg}]^{2-}$  anions in a 2:1 molar ratio (Figure 8)<sup>51</sup>.

FIGURE 7. Molecular geometry of the  $[\text{Li}(\text{TMEDA})][\text{Bn}_4\text{Mg}]$  anion of **6**FIGURE 8. Cationic (left) and anionic (right) units of compound **7**

This compound is one of the few examples of tetraorganomagnesiates that contains isolated tetraorganomagnesium dianions in the crystal lattice. Due to the location of the magnesium atom at a special position (inversion center in space group *Ibam*) the four allyl groups in the anion are symmetry related. The C–Mg distances of 1.996(8) Å are relatively short. The C–Mg–C bond angles range from 108.4(6) to 110.6(6)°, indicating an almost perfect tetrahedral geometry around this magnesium atom.

The structure of the cationic part of **7** consists of a  $[\text{Mg}_3\text{C}_2]$  trigonal bipyramidal arrangement (Figure 8) with the magnesium atoms in the equatorial plane and the carbon atoms at the apical positions. The two allyl groups are  $\mu_3$ -bonded (one above and one

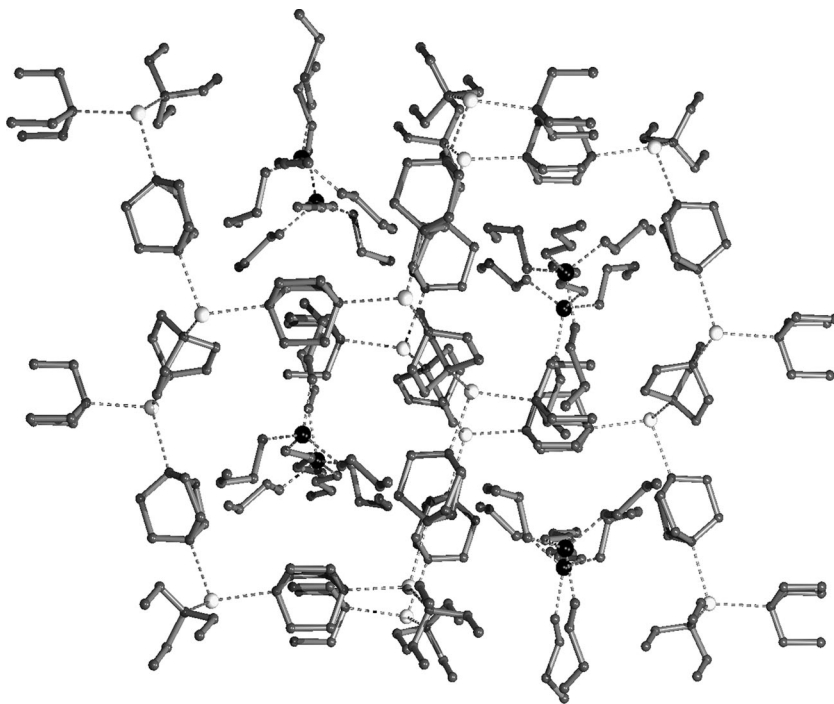


FIGURE 9. Part of the polymeric network of **8**. Disorder components and hydrogen atoms are omitted for clarity

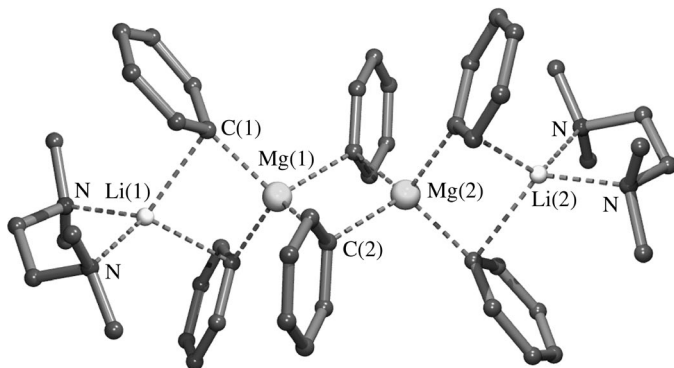
below the trigonal plane) with their terminal carbon atoms to the three magnesium atoms. Each of the three chlorine atoms are bridge-bonded between two magnesium atoms in the equatorial plane.

The only other example of a tetraorganomagnesiates that contains isolated anions in its solid-state structure is  $[\text{Na}_2(\text{DABCO})_3(\text{toluene})][\text{Bu}_4\text{Mg}]$  (**8**). Each DABCO and toluene molecule bridges two sodium atoms, forming a polycationic three-dimensional coordination network, in which isolated  $\text{Bu}_4\text{Mg}^{2-}$  anions are embedded (Figure 9)<sup>52</sup>.

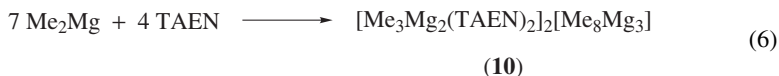
Like in **7** the Mg–C distances in the tetrabutylmagnesium dianion in **8** are relatively short [2.009(6), 2.010(7), 2.042(7) and 2.041(7) Å]. All C–Mg–C bond angles are close to  $109^\circ$ , indicating tetrahedral coordination geometry at the magnesium atoms.

Although the solid-state structure of  $[\text{Li}(\text{TMEDA})]_2[\text{Ph}_6\text{Mg}_2]$  (**9**) reveals that to each of the magnesium atoms four carbon atoms are bonded, this compound is best described as consisting of a central  $\text{Ph}_6\text{Mg}_2$  dianion in which the magnesium atoms are linked via two symmetrically bridging phenyl groups [C(2)–Mg(1) 2.329(3) and C(2)–Mg(2) 2.286(3) Å] (Figure 10)<sup>53</sup>. Furthermore, to each of the magnesium atoms two phenyl groups are bridging between magnesium and lithium in an asymmetric way [C(1)–Mg(1) 2.186(3), C(1)–Li(1) 2.419(9) Å]. Coordination saturation at lithium is reached by a *N,N'*-chelate bonded TMEDA molecule.

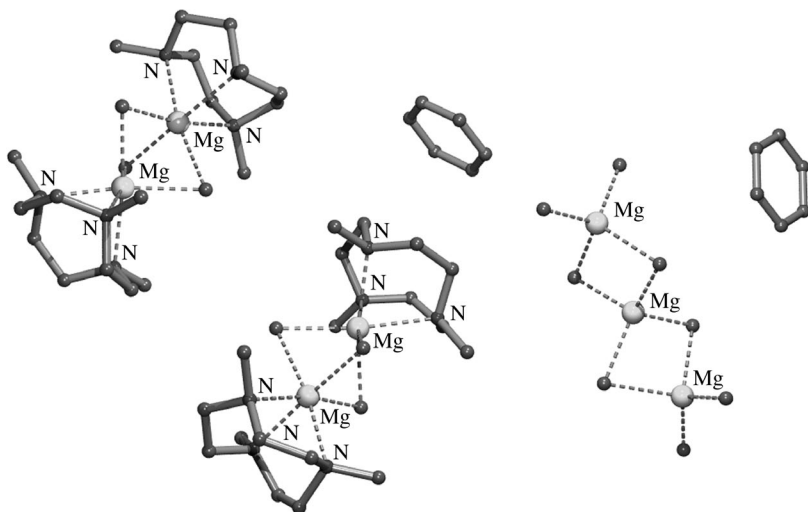
During a study in which the cyclic tripod amine *N,N',N''*-trimethyltriazacyclononane (TAEN) was used as a solvent for  $\text{Me}_2\text{Mg}$ , a rather unexpected product was obtained

FIGURE 10. Molecular geometry of **9** in the solid state

which, according to its X-ray structural analysis, appeared to be  $[\{\text{Me}_3\text{Mg}_2(\text{TAEN})_2\}^+]_2 [\text{Me}_8\text{Mg}_3]^{2-}$  (**10**)<sup>54</sup>. This product is the result of a disproportionation reaction (equation 6).



An X-ray crystal-structure determination of **10** revealed an asymmetric unit that contains two ‘triple-decker’ dimagnesium cations, a  $\text{Me}_8\text{Mg}_3$  dianion and two benzene molecules (Figure 11). The two cations differ slightly with respect to bond distances and bond angles, but are chemically identical. In the cation the three methyl groups are symmetrically bridge-bonded (C–Mg average 2.354 Å) between the two magnesium atoms. To each magnesium atom a TAEN molecule is tridentate facially-coordinated with its

FIGURE 11. The asymmetric unit of **10**



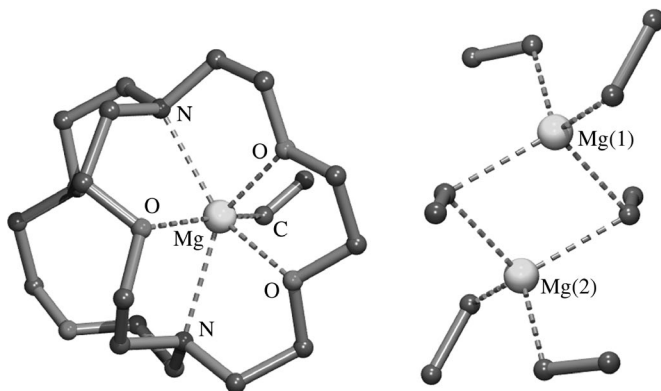


FIGURE 12. Molecular geometry of the cationic (left) and anionic (right) parts of **11**

three nitrogen atoms, resulting in a slightly distorted octahedral coordination geometry at each magnesium atom. The  $[\text{Me}_8\text{Mg}_3]$  dianion consists of a linear arrangement of three magnesium atoms with two symmetrically bridging methyl groups between each of the two magnesium atoms. To each of the two terminal magnesium atoms two further methyl groups are bonded, resulting in a tetrahedral coordination geometry at each of the magnesium atoms. As might be expected, the C–Mg bond distances of the terminal methyl groups (C–Mg average 2.161 Å) are slightly shorter than those of the bridging methyl groups (C–Mg average 2.294 Å).

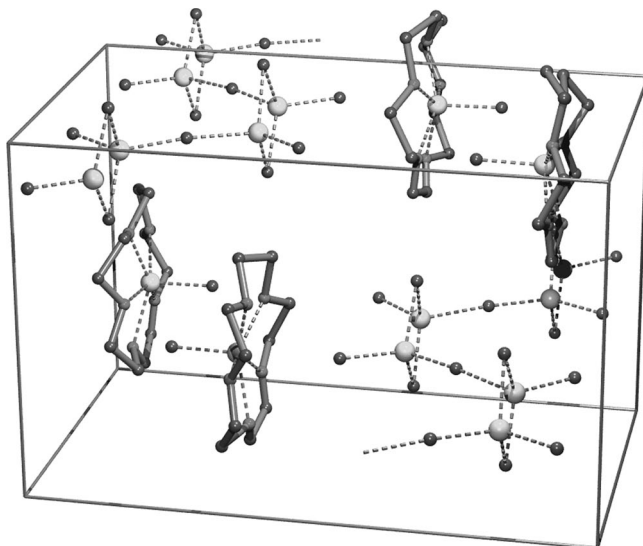
Like TAEN also cryptands are capable of initiating a disproportionation reaction in diorganomagnesium compounds. From the reaction of  $\text{Et}_2\text{Mg}$  with 2,1,1-cryptand a crystalline product (**11**) was obtained. According to its X-ray crystal-structure determination **11** consists of isolated  $[\text{EtMg}(2,1,1\text{-cryptand})]^+$  cations and  $[\text{Et}_6\text{Mg}_2]^{2-}$  anions in the crystal lattice (Figure 12)<sup>55</sup>. The dianion in fact is a dimer formed from two  $[\text{Et}_3\text{Mg}]^-$  anions via two bridging ethyl groups between the two magnesium atoms. The two halves of the dimer are symmetry related via a crystallographic inversion center. The C–Mg bond distances, 2.336 Å for the bridging ethyl group and 2.223 Å for the terminal ethyl groups, are in the range as expected.

The cation contains a  $[\text{EtMg}]^+$  moiety (C–Mg 2.157(9) Å) to which three oxygen atoms and two nitrogen atoms of the cryptand are coordinated.

It has been suggested that the formation of organomagnesiate anions from equilibria of dialkylmagnesium compounds with crown ethers, although in concentrations too low to be detectable by e.g. NMR spectroscopy, are responsible for the specific chemical behavior of such solutions (equation 7)<sup>56</sup>.

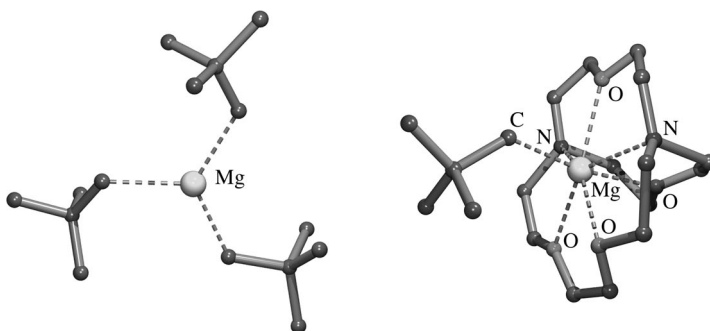


A crystalline product with the formulation  $[\text{MeMg}(15\text{-C-5})][\text{Me}_5\text{Mg}_2]$  (**12**) was obtained from a solution of  $\text{Me}_2\text{Mg}$  and 15-C-5, making use of special crystallization techniques. An X-ray crystal-structure determination revealed the presence of isolated  $[\text{MeMg}(15\text{-C-5})]^+$  cations. The anionic counter part consists of  $[\text{Me}_5\text{Mg}_2]^-$  units in which two methyl groups are bridge-bonded between the magnesium atoms while one of the other methyl groups forms a bridge bond to a next  $[\text{Me}_5\text{Mg}_2]^-$  unit, thus forming a polymeric chain (Figure 13)<sup>57</sup>.

FIGURE 13. Unit cell contents of **12**

### C. Triorganomagnesiates $M[R_3Mg]$

In contrast to their zinc congeners<sup>29</sup> only a very few compounds are known that contain a  $[R_3Mg]^-$  structural unit in the solid state. The only compound having isolated anions and cations in its crystal lattice is  $[neo-PentMg(2,1,1-cryptand)][neo-Pent_3Mg]$  (**13**) obtained from a disproportionation reaction of  $neo-Pent_2Mg$  in the presence of 2,1,1-cryptand<sup>55</sup>. An X-ray crystal-structure determination (Figure 14) of **13** shows that the closest approach between the magnesium atom in the anion and a heteroatom in the cryptand is 5.71 Å, indicating the presence of isolated cations and anions in the crystal lattice. Although the C–Mg bond distances in the anionic  $[neo-Pent_3Mg]^-$  moiety vary slightly [C–Mg 2.125(12), 2.240(12) and 2.296(16) Å], the sum of the C–Mg–C bond angles around magnesium is 360° within experimental error, indicating a planar trigonal coordination

FIGURE 14. Molecular geometry of the anionic (left) and cationic (right) moieties of **13** in the solid state

geometry at the magnesium atom. In the  $[\text{neo-PentMg}(2,1,1\text{-cryptand})]^+$  cationic part all heteroatoms of the cryptand are involved in coordination to magnesium, resulting in an essentially pentagonal bipyramidal geometry at magnesium. Five of the heteroatoms of the cryptand and the magnesium atom lie approximately in a plane while one of the oxygen atoms of the cryptand and the bonding carbon atom of the neopentyl group occupy the apical sites.

A triarylmagnesiates  $[\text{Li}(\text{THF})][\{2,4,6\text{-}(i\text{-Pr})_3\text{C}_6\text{H}_2\}_3\text{Mg}]$  (**14**) was obtained from the stoichiometric reaction of the parent organometallic compounds. An X-ray crystal-structure determination of **14** revealed a molecular geometry in which the triarylmagnesiates and lithium are associated via bridging aryl groups (Figure 15)<sup>58</sup>. Both the magnesium atom and the lithium atom in **14** are three-coordinate, the magnesium atom as the result of the bonding of two bridging and one terminal carbon atom, and the lithium atom as the result of the bonding of two bridging carbon atoms and an oxygen atom of an additional coordinating THF molecule. The sum of the bond angles around both the magnesium atom and the lithium atom is close to  $360^\circ$ , indicating for both metals a trigonal planar coordination geometry. As expected, the  $\text{Mg}-\text{C}$  bond distances of the bridging carbon atoms  $[\text{Mg}-\text{C}(2)$  2.249(4) and  $\text{Mg}-\text{C}(3)$  2.206(4) Å] are somewhat longer than the terminal  $\text{Mg}-\text{C}$  bond  $[\text{Mg}-\text{C}(1)$  2.147(4) Å]. The  $\text{C}-\text{Li}$  bond distances are relatively short  $[\text{Li}-\text{C}(2)$  2.195(9) and  $\text{Li}-\text{C}(3)$  2.251(9) Å] but not unexpected due to the bonding to a three-coordinate lithium atom. For the same reason also the bond distance of the coordinating oxygen atom of the THF molecule to magnesium is extremely short  $[\text{Li}-\text{O}$  1.858(8) Å].

The mixed metal alkyl-amido base  $[\text{BuNa}(\text{TMEDA})][\text{TMP}_2\text{Mg}]$  ( $\text{TMP} = 2,2,6,6\text{-tetramethylpiperidine}$ ) is capable of deprotonating furan selectively at its 2-position in THF as a solvent. The product obtained is a complex tris-furylmagnesiates, with the empirical formula  $[\text{Na}_2(\text{THF})_3][2\text{-furyl}_6\text{Mg}_2(\text{TMEDA})]$  (**15**)<sup>59</sup>. An X-ray crystal-structure determination showed that in the solid state this compound exists as a coordination polymer of  $[\text{Na}_2(\text{THF})_3][2\text{-furyl}_6\text{Mg}_2]$  units linked by bridging TMEDA molecules (Figure 16).

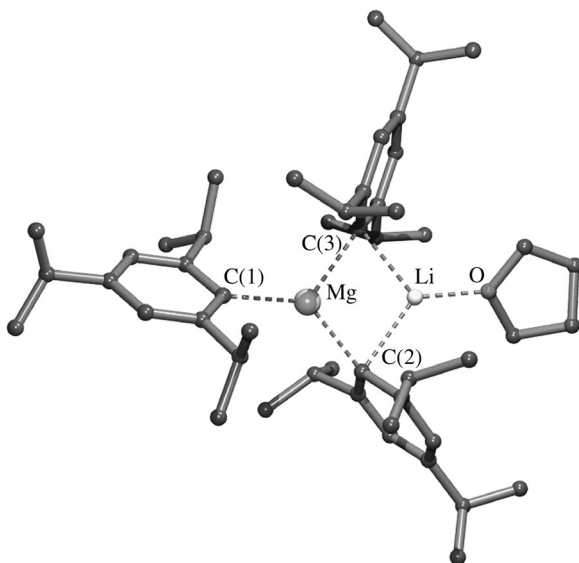
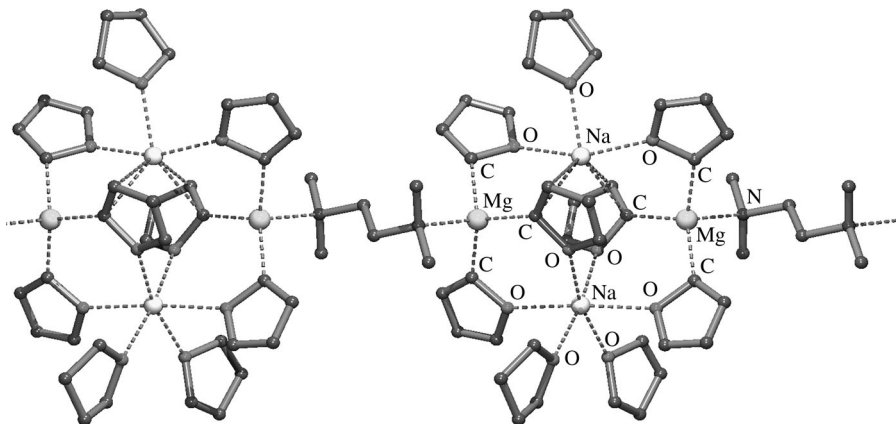


FIGURE 15. Molecular geometry of **14** in the solid state

FIGURE 16. Part of the polymeric chain of inverse crown ether structure **15**

This compound represents an example of an inverse crown ether structure (Lewis acidic host–Lewis basic guest macrocyclic heterometallic alkoxides or amides)<sup>45,46</sup>.

The repeating unit in **15** contains two  $[(2\text{-furyl})_3\text{Mg}]^-$  anionic moieties and two sodium cations assembled in a cyclic structure (Figure 16). Four of the furyl groups are pointing to the outside of this cycle and are coordinating pairwise to the sodium atoms with their furyl oxygen atoms. Two furyl groups are located inside the cycle and are coordinating with their oxygen atoms to the same sodium atom to which also two additional THF molecules are coordinated. These furyl groups also have a  $\pi$ -interaction with the other sodium atom to which one additional THF molecule is also coordinated.

Also aggregated magnesiates, containing acetylenic organic groups,  $[\text{Li}_2(\text{TMEDA})_2][(\text{PhC}\equiv\text{C})_6\text{Mg}_2]^{50}$  (**16**),  $[\text{Na}_2(\text{TMEDA})_2][(t\text{-BuC}\equiv\text{C})_6\text{Mg}_2]^{49}$  (**17**) and  $[\text{Na}_2(\text{PMDTA})_2][(t\text{-BuC}\equiv\text{C})_6\text{Mg}_2]^{49}$  (**18**), have been structurally characterized.

#### D. Heteroleptic Organomagnesiates $\text{M}[\text{R}_2\text{YMg}]$ and $\text{M}[\text{RY}_2\text{Mg}]$

So far, only organomagnesiates have been considered consisting of an anionic moiety in which three or four carbon atoms are directly bound to the magnesium atom. However, also organomagnesiates exist in which the anionic moiety contains only one or two carbon atoms as well as one or two anions bound to the magnesium atom via a N- or O-heteroatom.

In particular, studies of the constitution of Grignard reagents in the solid state revealed that in addition to neutral organomagnesium species, also ionic structures exist that in fact are heteroleptic organomagnesiates. Three different types of species were observed in the solid state. The first are ionic  $[\text{Mg}_2(\mu\text{-Cl})_3(\text{THF})_6][\text{RMgCl}_2(\text{THF})]$  ones [ $\text{R} = t\text{-Bu}$  (**19**) and  $\text{R} = \text{Ph}$  (**20**)], which were obtained from THF solutions of  $t\text{-BuMgCl}$  and  $\text{PhMgCl}$ , respectively<sup>60</sup>. The second are neutral  $\text{R}_2\text{Mg}_4\text{Cl}_6(\text{THF})_6$  species [ $\text{R} = \text{Me}$  (**21**),  $\text{R} = t\text{-Bu}$  (**22**) and  $\text{R} = \text{benzyl}$  (**23**)], isolated from THF solutions of  $\text{MeMgCl}$ ,  $t\text{-BuMgCl}$  and  $\text{BnMgCl}$ , respectively<sup>60</sup>. The last is ionic  $[\text{Mg}_2(\mu\text{-Cl})_3(\text{THF})_3]_2[\text{Ph}_4\text{Mg}_2(\mu\text{-Cl})_2]$  (**24**), obtained from a THF solution of  $\text{PhMgCl}$ <sup>60</sup>. As the ratio of organic group to magnesium to chloride in these compounds is not 1:1:1, it is obvious that formation of these particular compounds can never be quantitative and that the remaining solutions must contain magnesium compounds having other stoichiometries.

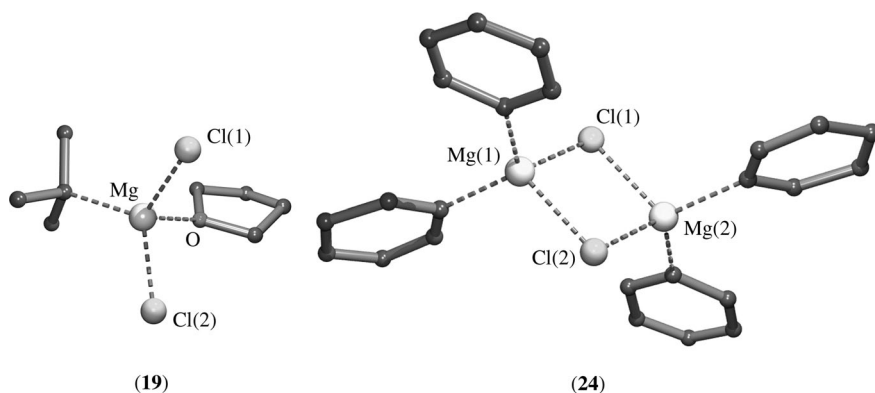


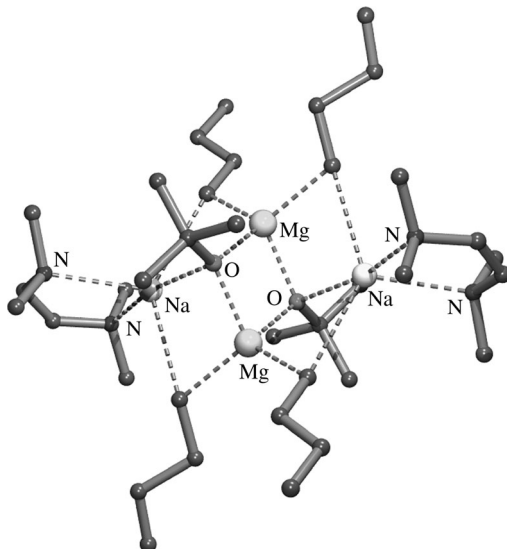
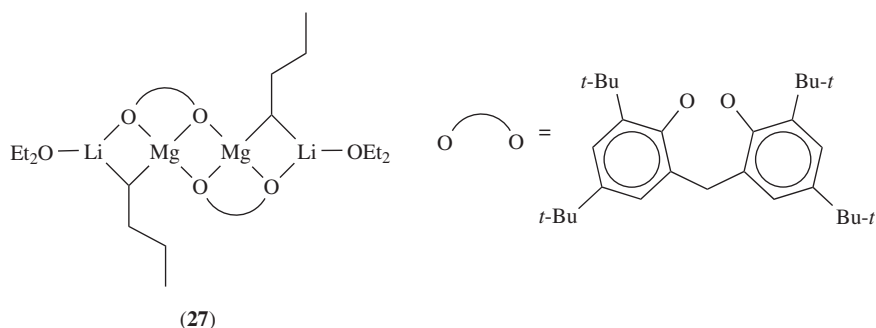
FIGURE 17. Monoanionic part of magnesiate **19** and bis-anionic part of magnesiate **24**

The magnesium atoms in the monoanionic moieties of **19** (Figure 17) and **20** have, as expected, a slightly distorted tetrahedral geometry. In **19** the Cl(1)–Mg–Cl(2) and C–Mg–O bond angles of  $109.2(1)^\circ$  and  $110.9(1)^\circ$ , respectively, are very close to the ideal tetrahedral value. The bis-anion  $[\text{Ph}_4\text{Mg}_2\text{Cl}_2]^{2-}$  (Figure 17) in **24** may be regarded as being formed from the dimerization of two hypothetical  $[\text{Ph}_2\text{MgCl}]^-$  moieties via chloride bridges. The almost equal Mg–Cl bond distances [Mg(1)–Cl(1) 2.432(1) and Mg(2)–Cl(1) 2.464(2) Å] indicate that the chlorides are symmetrically bridging. These bond distances are somewhat elongated compared to the terminal Mg–Cl bonds in **19** [both 2.232(2) Å], but this is not unexpected for bridging halogens. The ionic compounds, **19**, **20** and **24**, have in common that charge compensation is reached by the same cation, i.e.  $[\text{Mg}_2\text{Cl}_3(\text{THF})_6]^+$  in which the three chlorides are bridge-bonded between the two magnesium atoms while the three THF molecules provide to each of the magnesium atoms an octahedral coordination geometry.

The actual aggregate that crystallizes from a solution of a Grignard reagent is largely influenced by the nature of the solvent used. This became evident by the crystals obtained from a solution of  $\text{MeMgBr}$  in triglyme having stoichiometry  $[\text{Mg}_2\text{Br}_2(\text{triglyme})_2][\text{Me}_2\text{MgBr}_4]$  (**25**). The crystal structure determination of **25** revealed that the crystal lattice contains isolated  $[(\mu\text{-Me})_2\text{Mg}_2\text{Br}_4]^{2-}$  magnesiate anions and  $[\text{Mg}_2(\mu\text{-Br})_2(\text{triglyme})_2]^+$  cations<sup>61</sup>. It is surprising that in the magnesiate anion of **25** the methyl groups rather than the bromide act as bridges between the two magnesium atoms. Usually, the softer halogen atoms have a stronger tendency to form bridges than the harder carbon atom.

Solutions of mixtures of alkali alkoxides and diorganomagnesium compounds have been studied in solution because of their relevance as initiators for styrene polymerization. From such solutions crystalline  $[\text{Bu}_2\text{MgNaOBu-}t(\text{TMEDA})]_2$  (**26**) and  $[\text{Bu}_2\text{MgKOBu-}t(\text{TMEDA})]_2$  (**27**) were isolated and structurally characterized<sup>62</sup>. They are aggregated species and may be regarded as heteroleptic organomagnesiates. Because **26** and **27** are isostructural, only the overall structural geometry (Figure 18) of **26** is discussed in more detail.

The central core of **26** is a flat four-membered O–Mg–O–Mg ring. One of the *t*-Bu groups is located above, and the other below this plane. To each of the oxygen atoms a sodium atom is bonded [Na–O 2.533(5) Å] while the four butyl groups are bridge-bonded between the sodium and magnesium atoms in a rather asymmetric way [C–Mg 2.190(6) and C–Na 2.852(7) Å]. Penta-coordination at each sodium atom is reached by the additional *N,N'*-chelate bonding of a TMEDA molecule.

FIGURE 18. Molecular geometry of **26** in the solid stateFIGURE 19. Schematic structure of heteroleptic magnesiate **27**

Reaction of 2,2'-ethyldienebis(2,4-di-*tert*-butylphenol) (EDBP- $H_2$ ) with butyllithium and dibutylmagnesium in a 1:1:1 molar ratio in diethyl ether as a solvent affords the heteroleptic organomagnesiate  $[BuMgLi(EDBP)(OEt_2)]_2$  (**27**) of which the structure is shown schematically (Figure 19)<sup>63</sup>.

The butyl groups are slightly asymmetric bridge-bonded between lithium and magnesium [C–Li 2.263(7) and C–Mg 2.175(4) Å]. The bis-anionic EDBP ligands are *O,O'*-chelate bonded, with one of the oxygen atoms bridging between the two magnesium atoms, giving rise to a central O–Mg–O–Mg four-membered ring while the other oxygen atom is bridging between a magnesium atom and a lithium atom. To each of the lithium atoms an additional diethyl ether molecule is coordinated, affording a distorted trigonal coordination geometry at lithium. It is interesting to note that **27** is an efficient initiator for methyl methacrylate polymerization.

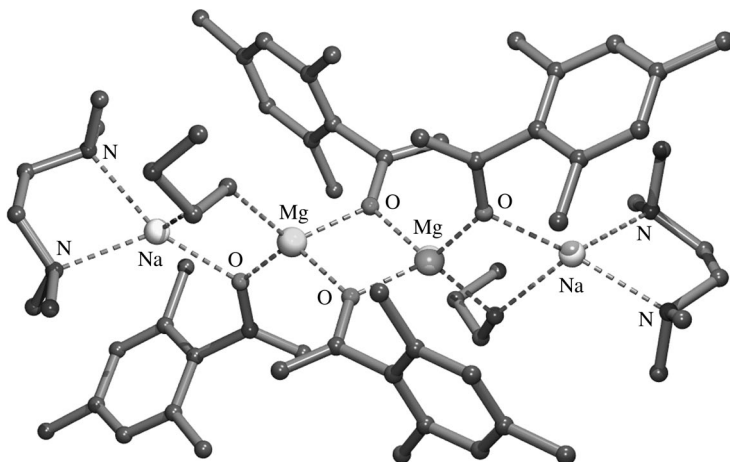


FIGURE 20. Molecular geometry of **28** in the solid state

Reaction of *in situ* prepared  $\text{Na}[\text{Bu}_3\text{Mg}]$  with 2,4,6-trimethylacetophenone and crystallization of the product from toluene in the presence of TMEDA afforded the heteroleptic organomagnesiate  $[\text{BuMgNa}\{\text{OC}(=\text{CH}_2)\text{Mes}\}_2(\text{TMEDA})]_2$  (**28**)<sup>64</sup>. It appeared that instead of deprotonation of the 2,4,6-trimethylacetophenone to give an enolate moiety, 1,2-addition had occurred. The X-ray crystal-structure determination of **28** (Figure 20) showed an almost linear  $\text{Na} \cdots \text{Mg} \cdots \text{Mg} \cdots \text{Na}$  arrangement. The two magnesium atoms in this arrangement are linked by two bridging oxygen atoms of two enolate moieties while each of the sodium atoms is linked by one bridging carbon atom of the butyl group and one bridging oxygen atom of an enolate group. Coordination saturation at each of the sodium atoms is reached by the additional coordination of a TMEDA molecule.

During studies of the synthesis and structural characterization of mixed magnesium–lithium secondary amide aggregates, a heteroleptic organomagnesiate,  $[\text{BuMgLi}\{\text{N}(\text{SiMe}_3)_2(\text{Py})\}]$  (**29**), crystallized as a by-product from a reaction mixture of *n*-BuLi, *sec*-Bu<sub>2</sub>Mg and  $\text{HN}(\text{SiMe}_3)_2$  in the presence of pyridine<sup>65</sup>. An X-ray crystal-structure determination of **29** revealed a monomolecular structure (Figure 21) in which two  $(\text{Me}_3\text{Si})_2\text{N}$  amido groups are symmetrically bridge-bonded [ $\text{N}–\text{Li}$  2.066(5) and  $\text{N}–\text{Mg}$  2.090(3) Å] between magnesium and lithium while the butyl group is  $\eta^1$ -bonded to magnesium. An additional pyridine molecule is coordinated to the lithium atom. The sum of the bond angles around both lithium and magnesium is  $360^\circ$  within experimental error, indicating a trigonal planar coordination geometry around these metals. It should be noted that in the crystal lattice of **29** the  $\eta^1$ -bonded butyl group is chemically disordered with *n*-butyl and *sec*-butyl groups, indicating that prior to the amide-formation step scrambling of *n*-butyl and *sec*-butyl groups has occurred, most probably via a  $[(\text{sec}\text{-Bu})_2(\text{n-Bu})\text{Mg}]^-$  magnesiate-type species.

The reaction of *t*-BuLi with  $[(\text{Me}_3\text{Si})_2\text{N}]_2\text{Mg}$  in a 1:1 molar ratio in hydrocarbon solvents affords a crystalline product that appears to be the heteroleptic organomagnesiate  $[\text{t-BuMgLi}\{\text{N}(\text{SiMe}_3)_2\}]_2$  (**30**). Its X-ray crystal-structure determination revealed a structure (Figure 22) that shows similarities with that of **29**<sup>66</sup>. In **30** the two amide nitrogen atoms are symmetrically bridge-bonded between magnesium and lithium [ $\text{N}–\text{Mg}$  2.079(1) and  $\text{N}–\text{Li}$  2.055(2) Å] while the *t*-Bu group is  $\sigma$ -bonded to magnesium [ $\text{C}–\text{Mg}$  2.174(1) Å]. The coordination unsaturation at lithium is released by an agostic interaction with the carbon atom [ $\text{C}–\text{Li}$  2.563(3) Å] of a *t*-Bu group of a neighboring molecule,

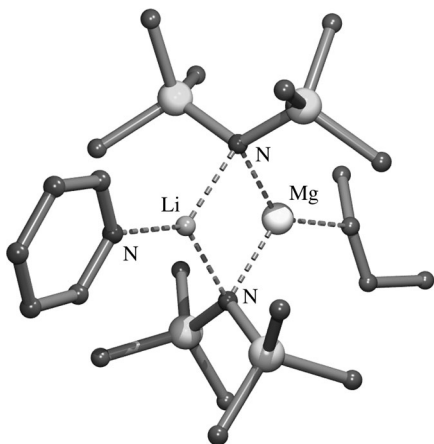


FIGURE 21. Molecular geometry of **29** in the solid state. (The minor *n*-butyl disorder component is omitted for clarity.)

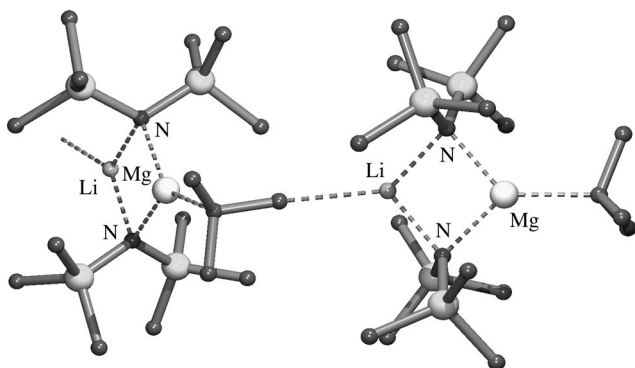


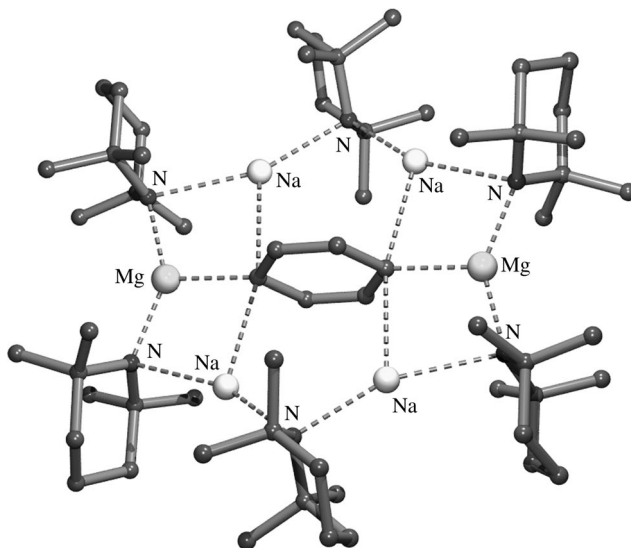
FIGURE 22. Two units of the polymeric structure of **30** in the solid state

resulting in polymeric chains (Figure 22). Like in **29** both the magnesium atom and the lithium atom have a trigonal planar coordination geometry.

The sodium analog of **30** was prepared from *t*-BuMgCl and two equivalents of  $[(\text{Me}_3\text{Si})_2\text{N}]_2\text{Na}$  in diethyl ether as a solvent. The structure of the resulting heteroleptic organomagnesiates  $[t\text{-BuMgNa}\{\text{N}(\text{SiMe}_3)_2\}_2(\text{OEt}_2)]$  (**31**) shows great similarities with that of the repeating unit of **30**, but now with a diethyl ether molecule coordinated to the sodium atom instead of an agostic interaction, thus preventing the formation of polymeric chains.

It has been well-established that deprotonative metallation is one of the most widely studied and utilized tools in chemical synthesis. Selective di-metallation of arenes has been observed using mixed metal reagents. Reaction of a mixture of BuNa, Bu<sub>2</sub>Mg and TMPH (2,2,6,6-tetramethylpiperidine) in 1:1:3 molar ratio in the presence of toluene or benzene affords the aggregated compounds  $[(\text{MeC}_6\text{H}_3)\text{Mg}_2\text{Na}_4(\text{TMP})_6]$  (**32**) and  $[(\text{C}_6\text{H}_4)\text{Mg}_2\text{Na}_4(\text{TMP})_6]$  (**33**), respectively, formed in a self-assembly process<sup>67</sup>. X-ray crystal-structure determinations of **32** and **33** (Figure 23) revealed macrocyclic structures with



FIGURE 23. Molecular geometry of **33** in the solid state

six metal atoms (four sodium and two magnesium) alternating with six bridging amido nitrogen atoms in a twelve-membered ring, while a  $[\text{MeC}_6\text{H}_3]^{2-}$  (in **32**) or  $[\text{C}_6\text{H}_4]^{2-}$  (in **33**) dianion is located inside the ring. Each of the deprotonated carbon atoms has a relatively short C–Mg interaction [2.200(2) Å] and two longer C–Na bonds [2.691(2) and 2.682(2) Å]. Such structures represent examples of inverse crowns (Lewis acidic host–Lewis basic guest macrocyclic heterometallic amides)<sup>45,46</sup>. It is noteworthy that in **32** the deprotonation of toluene is regioselective at its 2- and 5-position.

That small variations can have large influence on the ultimate structures of the aggregates formed during arene deprotonating and aggregation steps became evident when the same reaction under identical reaction conditions as for **33** was carried out using BuK instead of BuNa. Instead of the expected potassium analog of **33** an unprecedented twenty-four-membered  $[(\text{KNMgN})_6]^{6+}$  ring system was formed, which acts as a polymetallic host to which six mono-deprotonated arene anions are bonded. The X-ray crystal structures of  $[(\text{C}_6\text{H}_5)\text{Mg}_6\text{K}_6(\text{TMP})_{12}]$  (**34**) (Figure 24) containing six mono-deprotonated benzene molecules and of  $[(\text{MeC}_6\text{H}_4)\text{Mg}_6\text{K}_6(\text{TMP})_{12}]$  (**35**) containing six mono-deprotonated toluene molecules have been elucidated<sup>68</sup>. The twenty-four-membered ring is built up of six sequences of a potassium atom, a bridging amido nitrogen atom, a magnesium atom and again a bridging amido nitrogen atom. The deprotonated arene carbon atom is  $\sigma$ -bonded to magnesium [C–Mg 2.196(6) Å], while the other interatomic distances suggest that the hapticity of the aryl rings with respect to the potassium atoms is  $\mu\text{-}\eta^3\text{:}\eta^2$ , i.e. three carbon atoms (one *ipso* and two *ortho*) on one face and two carbon atoms (one *ipso* and one *ortho*) on the opposing face.

When, under the reaction conditions outlined above for the preparation of **33**, ferrocene was added as the arene to be deprotonated, it appeared that 1,1'-di-deprotonation occurs resulting in an aggregated species  $[(\text{C}_5\text{H}_4)_2\text{Fe}]_3\text{Mg}_3\text{Na}_2(\text{TMP})_2(\text{TMPH})_2$  (**36**)<sup>69</sup>. Unfortunately, its X-ray structure determination showed disordered moieties especially with respect to the coordinated TMPH molecules. Its lithium analog  $[(\text{C}_5\text{H}_4)_2\text{Fe}]_3\text{Mg}_3\text{Li}_2(\text{TMP})_2(\text{TMPH})_2$  (**37**) was prepared in a similar way and, after treatment with pyridine (to

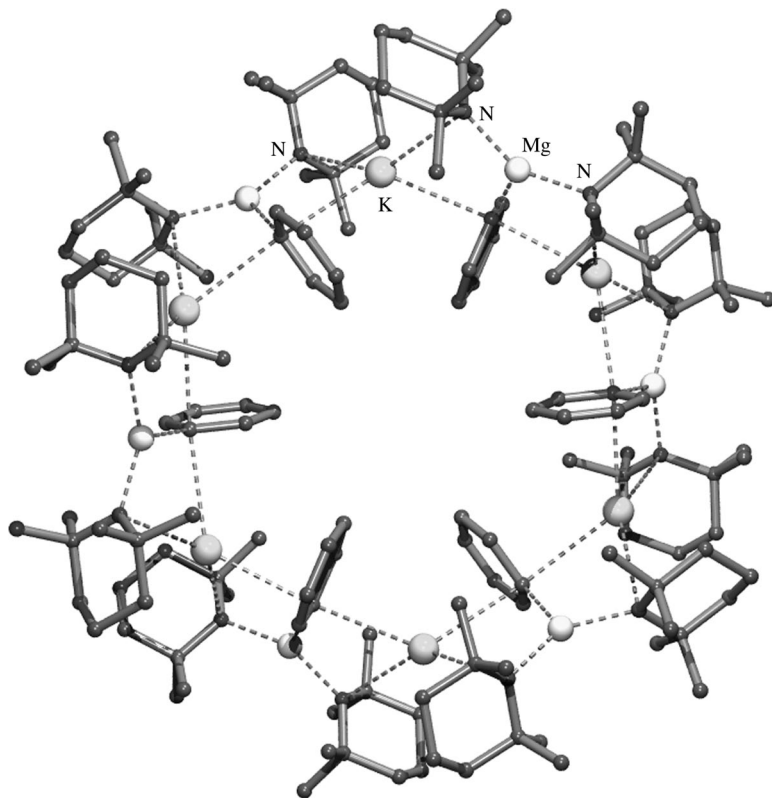
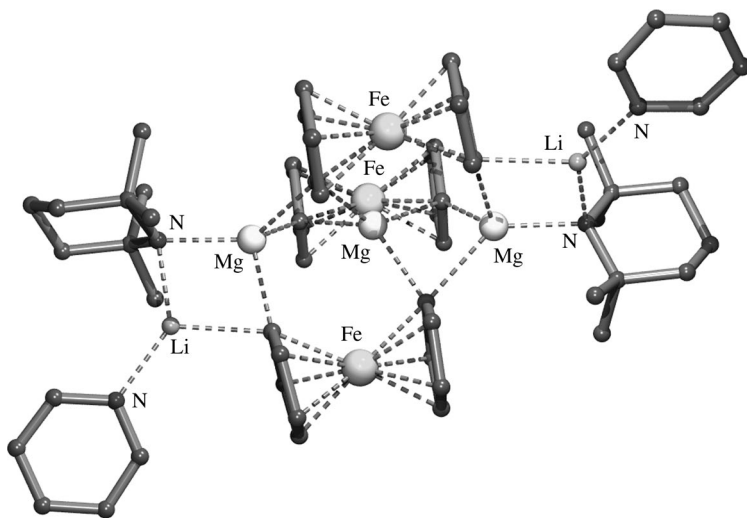
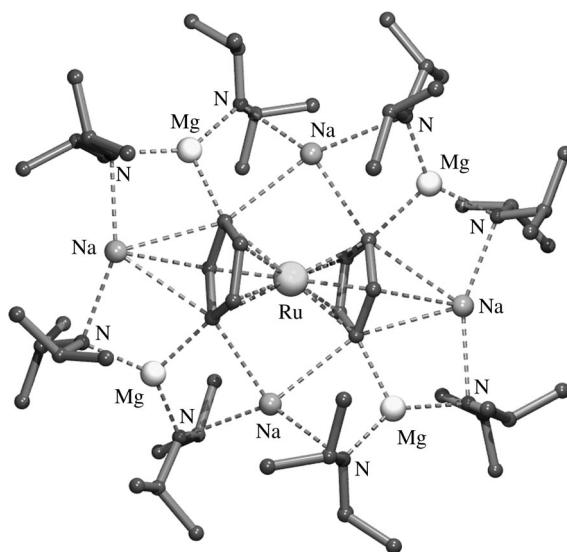


FIGURE 24. Molecular geometry of **34** in the solid state

effect substitution of the coordinated TMPH molecules by pyridine), crystalline  $[(C_5H_4)_2Fe]_3Mg_3Li_2(TMP)_2(py)_2$  (**38**) was obtained suitable for X-ray structural analysis. Its structure comprises a bent Li–Mg–Mg–Mg–Li arrangement to which two ferrocenyl dianions with one deprotonated carbon atom are bridge-bonded between lithium and magnesium, while the other deprotonated carbon atom is bridge-bonded between two magnesium atoms (Figure 25). The two deprotonated carbon atoms of the third ferrocenyl group are both bridge-bonded between two magnesium atoms. The two TMP groups are each bridge-bonded with their amide nitrogen atom between magnesium and lithium. Finally, a pyridine molecule is coordinated to each lithium atom, resulting in a trigonal planar coordination geometry of the lithium atoms.

Surprisingly, changing the secondary amine from TMPH to diisopropylamine results in the formation of entirely different structures. When three equivalents of diisopropylamine are added to *in situ* prepared  $Na[Bu_3Mg]$  and the resulting reaction mixture is used for deprotonating the metallocenes  $Cp_2Fe$ ,  $Cp_2Ru$  or  $Cp_2Os$ , unprecedented inverse-crown architectures are obtained. For all three metallocenes isostructural architectures were obtained, consisting of a sixteen-membered  $[(NaNMgN)_4]^{4+}$  host and a tetra deprotonated metallocene guest<sup>70</sup>. For all three compounds  $[(C_5H_3)_2Fe]Mg_4Na_4(i-Pr_2N)_8$  (**39**),  $[(C_5H_3)_2Ru]Mg_4Na_4(i-Pr_2N)_8$  (**40**) and  $[(C_5H_3)_2Os]Mg_4Na_4(i-Pr_2N)_8$  (**41**) the structures were elucidated by X-ray crystallography. That of **40** is shown (Figure 26).

FIGURE 25. Molecular geometry of **38** in the solid stateFIGURE 26. Molecular geometry of inverse crown architecture **40** in the solid state

The sixteen-membered ring consists of alternating magnesium and sodium atoms (four of each) with bridging amide nitrogen atoms between magnesium and sodium. The metallocene is selectively 1,3-1',3'-tetra-deprotonated and each of the deprotonated carbon atoms forms a bridge-bond between magnesium and sodium while the 2- and 2'-carbon atoms have an additional interaction with a sodium atom (Figure 26).

In order to gain insight into the mechanism and species involved in the metallation of the arenes described above, the reaction steps prior to the metallation were studied in more detail<sup>71</sup>. The first step is the formation of  $\text{Na}[\text{Bu}_3\text{Mg}]$  from its parent organometallic compounds in a 1:1 molar ratio. The second step is the addition of three equivalents of TMPH. A detailed NMR spectroscopic study of this reaction mixture showed the presence of metal-bonded butyl groups and TMPH. From this observation it was concluded that not the anticipated  $\text{Na}[\text{TMP}_3\text{Mg}]$  but instead  $[\text{BuMgNa}(\text{TMP})_2(\text{TMPH})]$  had been formed. Most likely this latter compound is the actual intermediate that is active in the arene metallation step. Unfortunately, this compound was isolated as an oil and therefore its structural characterization by X-ray crystallography was impossible. However, addition of TMEDA afforded a crystalline compound with the formula  $[\text{BuMgNa}(\text{TMP})_2(\text{TMEDA})]$  (**42**). The X-ray crystal-structure determination of **42** reveals a structure with a central four-membered ring formed by a magnesium atom and a sodium atom with a butyl group bridge-bonded  $[\text{C}-\text{Mg}$  2.200(2) and  $\text{C}-\text{Na}$  2.669(2) Å] and an amido-nitrogen atom of one of the TMP groups bridge-bonded  $[\text{N}-\text{Mg}$  2.079(1) and  $\text{N}-\text{Na}$  2.452(1) Å] between these atoms (Figure 27). The other TMP group is  $\sigma$ -bonded  $[\text{N}-\text{Mg}$  2.001(1) Å] to magnesium and the TMEDA molecule is chelate-bonded to sodium, giving this atom a tetrahedral coordination geometry.

Compound **42** is active in the deprotonation/metallation of arenes. When a solution of **42** is boiled under reflux in benzene,  $[\text{PhMgNa}(\text{TMP})_2(\text{TMEDA})]$  (**43**) is obtained which, according to its X-ray crystal-structure determination, is isostructural (bridging butyl group replaced by a bridging phenyl group) with **42**. In a similar way, using toluene, bis(benzene)chromium or bis(toluene)chromium, successful metallations to  $[\text{3-(MeC}_6\text{H}_4)\text{MgNa}(\text{TMP})_2(\text{TMEDA})]$  (**44**)<sup>72</sup>,  $[\{(\text{C}_6\text{H}_6)\text{Cr}(\text{C}_6\text{H}_5)\}\text{MgNa}(\text{TMP})_2(\text{TMEDA})]$  (**45**)<sup>73</sup> and  $[\{(\text{MeC}_6\text{H}_5)\text{Cr}(4\text{-MeC}_6\text{H}_4)\}\text{MgNa}(\text{TMP})_2(\text{TMEDA})]$  (**46**)<sup>74</sup> were achieved. All three compounds were structurally characterized by X-ray crystal-structure determinations and are isostructural with **42** and **43**. It is noteworthy that toluene is selectively metallated at its 3-position, while the  $\eta^6$ -toluene group in bis(toluene)chromium is selectively metallated at its 4-position.

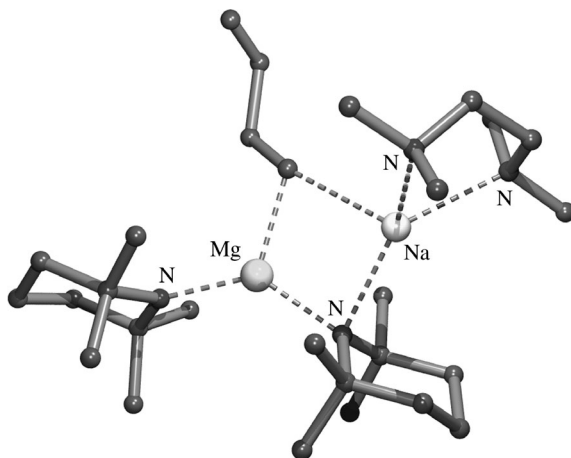


FIGURE 27. Molecular geometry of **42** in the solid state

### III. DIORGANOMAGNESIUM COMPOUNDS

#### A. Donor-base-free Diorganomagnesium Compounds

As outlined before, diorganomagnesium compounds with two linear  $\sigma$ -bonded alkyl or aryl groups are very rare due to coordination unsaturation at magnesium. Usually, magnesium avoids such bonding situations by binding additional Lewis bases, by aggregating via three-center two-electron bonding or by forming agostic interactions. So far, the structures of only three diorganomagnesium compounds are known in which magnesium is two-coordinate.

Bis(neopentyl)magnesium (**47**) occurs in benzene solution as a trimer, for which both a linear structure **I** and a cyclic structure **II** (Figure 28) have been proposed<sup>75</sup>.

Due to the high volatility of **47**, its structure in the gas phase could be determined by gas-phase electron diffraction<sup>76</sup>. This study showed that **47** exists as discrete monomers with a linear C–Mg–C arrangement with Mg–C bond distances of 2.126(6) Å in the gas phase.

The only two diorganomagnesium compounds with di-coordinated magnesium of which the structure in the solid state has been determined by X-ray crystallography are bis[(trimethylsilyl)methyl]magnesium (**48**)<sup>77,78</sup> and bis[(2,4,6-tri-*t*-butylphenyl)magnesium (**49**)<sup>79</sup>. Like observed in the gas phase for **47**, the magnesium atom of **48** in the solid state (Figure 29) has a perfect linear coordination geometry (C–Mg–C 180°). The observed Mg–C bond distance of 2.116(2) Å is also very close to the value observed for this bond in **47** in the gas phase.

In contrast to the linear structure of **47** and **48**, the X-ray crystal structure determination of **49** shows that in the solid state the di-coordinate magnesium atom has a bent structure [C–Mg–C 158.4(1)°]. This bending may be a consequence of the steric requirements of

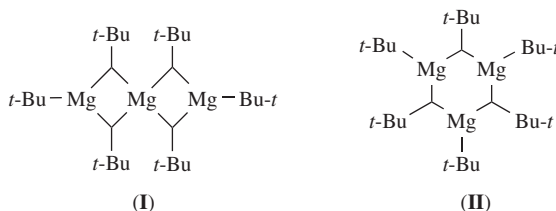


FIGURE 28. Proposed structures for bis(neopentyl)magnesium **47** in solution

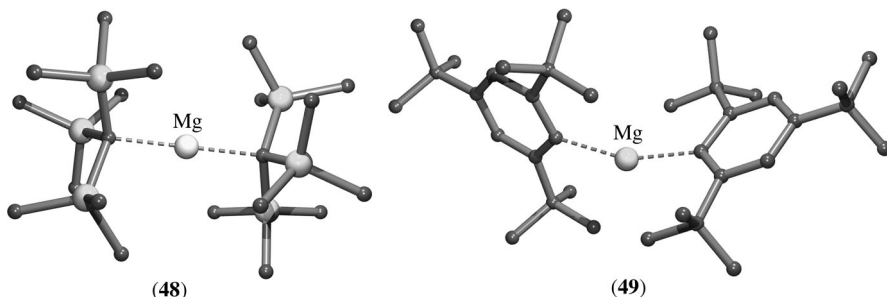


FIGURE 29. Molecular geometries of diorganomagnesium compounds **48** and **49** in the solid state

the bulky *t*-Bu groups, but also secondary (agostic) interactions of hydrogen atoms of the *ortho-tert*-butyl groups, two of which are in close proximity (2.28 Å) to the magnesium atom, might play a role. It was observed that **49** does not form donor complexes with Lewis bases like diethyl ether or THF, which is a striking difference with the 2,4,6-trimethyl- or 2,4,6-tri-isopropyl analogs of **49**<sup>58</sup>.

When the bulky (Me<sub>3</sub>Si)<sub>3</sub>C groups in compound **48** are replaced by less sterically demanding (Me<sub>3</sub>Si)<sub>2</sub>CH groups, the structure of the resulting diorganomagnesium compound [(Me<sub>3</sub>Si)<sub>2</sub>CH]<sub>2</sub>Mg (**50**) in the solid state is entirely different. Its structure was determined both by X-ray and by neutron diffraction data and revealed a polymeric network of [(Me<sub>3</sub>Si)<sub>2</sub>CH]<sub>2</sub>Mg molecules linked via intermolecular agostic interactions with methyl groups of neighboring [(Me<sub>3</sub>Si)<sub>2</sub>CH]<sub>2</sub>Mg molecules (Figure 30)<sup>80</sup>. The intramolecular Mg–C distances are 2.117(4) and 2.105(4) Å, respectively, while the intermolecular (agostic) Mg–C interaction is 2.535 Å. This latter distance is considerably shorter than the sum of the Van der Waals radii (3.4 Å). Although the individual C–Mg–C bond angles deviate from 120°, the intramolecular C–Mg–C bond angle being 140.0(2)°, the sum of these bond angles is 360°, pointing to a distorted trigonal planar coordination geometry at magnesium.

When the steric congestion in **49** is slightly released, i.e. by replacement of the *t*-Bu groups by Et groups, again an entirely different structure for the corresponding diorganomagnesium compound in the solid state is observed. The X-ray crystal-structure determination of bis[2,6-diethylphenyl]magnesium (**51**) revealed a dimeric structure in which two of the four aryl groups are bridge-bonded [C–Mg 2.259(7) and 2.263(7) Å] between two magnesium atoms forming a central flat C–Mg–C–Mg four-membered ring (Figure 31)<sup>81</sup>. Furthermore, to each of the magnesium atoms an aryl group is terminal-bonded (C–Mg 2.121 Å) resulting in trigonal planar coordination at the magnesium atoms. The aryl groups are rotated out of the central C–Mg–C–Mg plane in a propeller-like fashion by angles in the range of 42.7 to 74.6°.

Bis-*tert*-butylmagnesium (**52**) also forms dimeric aggregates in the solid state. Its molecular geometry comprises two *t*-Bu groups each bridging between two magnesium atoms [C(1)–Mg(1) 2.3044(9), C(1)–Mg(2) 2.2978(8), C(2)–Mg(1) 2.3057(8) and

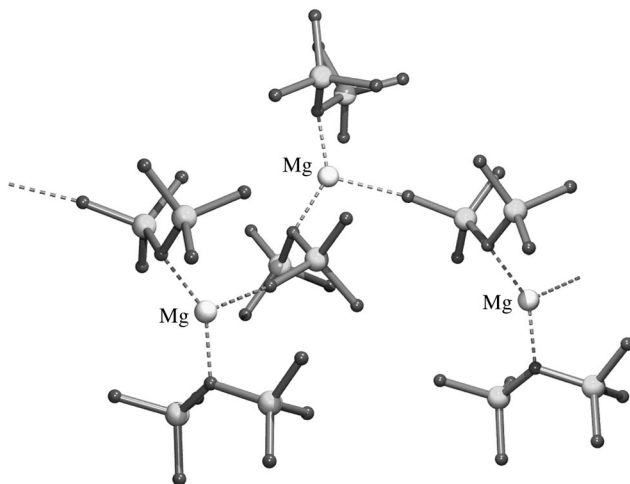


FIGURE 30. Part of the polymeric network of **50** in the solid state

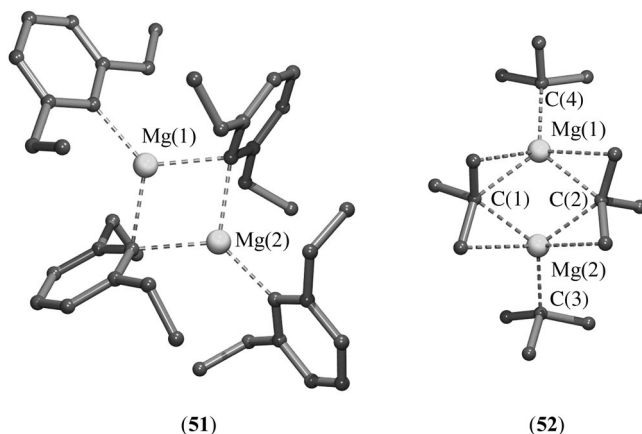


FIGURE 31. Molecular geometries of the dimeric diorganomagnesium compounds **51** and **52** in the solid state

C(2)–Mg(2) 2.2987(8) Å] as well as two *t*-Bu groups each terminally bonded to one magnesium atom [C(3)–Mg(2) 2.1483(8) and C(4)–Mg(1) 2.1424(9) Å] (Figure 31)<sup>82</sup>. The central four-membered C(1)–Mg(1)–C(2)–Mg(2) ring is folded, as is indicated by a C(1)–Mg(2)–Mg(1)–C(2) torsion angle of 140.45(4)°. Two methyl groups of each of the bridging *t*-Bu groups are rather close to a magnesium atom (Mg–C 2.489–2.542 Å). This distance is considerably less than the sum of the Van der Waals radii (3.4 Å) and points to agostic interactions with these methyl groups. It has been proposed that these agostic interactions promote  $\beta$ -hydrogen elimination and thus are responsible for the low thermal stability of **52**<sup>82</sup>.

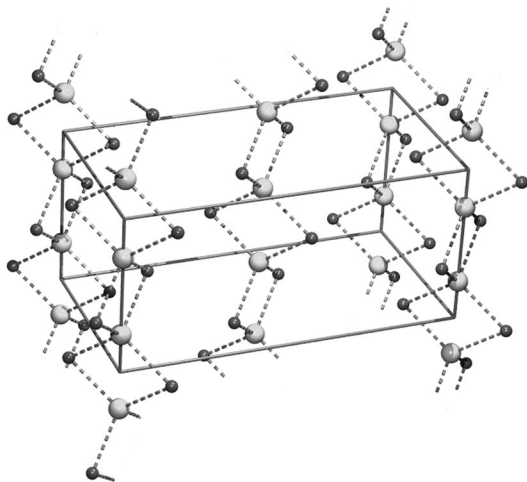
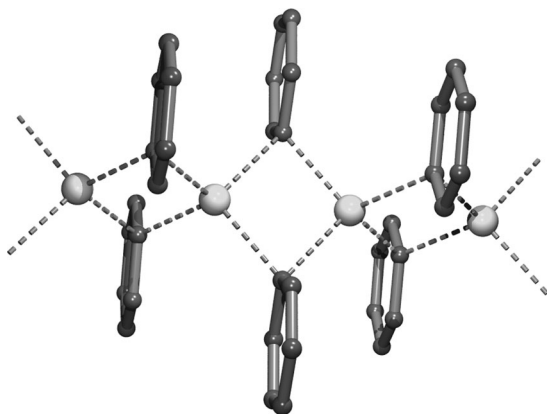
The simple diorganomagnesium compounds Me<sub>2</sub>Mg (**53**) and Et<sub>2</sub>Mg (**54**) are non-volatile solids, in strong contrast to their zinc analogs, which are low boiling liquids<sup>29</sup>. The structures of **53** and **54** in the solid state have been determined from X-ray powder diffraction data<sup>21,22</sup>. Both compounds form polymeric chains in the solid state (Figure 32) comprising a chain of magnesium atoms which are mutually connected by two bridging alkyl groups. As a consequence, each of the magnesium atoms has a tetrahedral coordination geometry. The observed Mg–C bond distances are 2.24(3) and 2.2(1) Å for **53** and **54**, respectively.

The structure of Ph<sub>2</sub>Mg (**55**) in the solid state has been determined by a single-crystal X-ray diffraction study<sup>83</sup>. Like **53** and **54**, Ph<sub>2</sub>Mg exists in the solid state as polymeric chains (Figure 33) in which two phenyl groups are symmetrically bridge-bonded [C–Mg 2.261(2) Å] between two magnesium atoms.

## B. Diorganomagnesium Compounds Containing Multi-hapto-bonded Groups

The discovery and structural elucidation of ferrocene in 1951 and the subsequent development of metal-cyclopentadienyl chemistry started a new era in organometallic chemistry<sup>84–86</sup>.

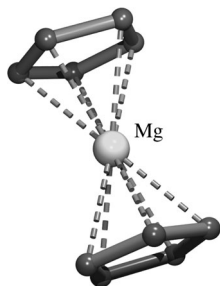
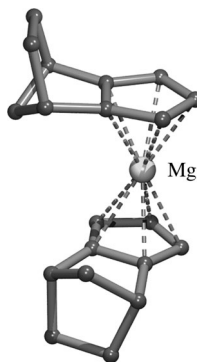
Soon after the first synthesis of bis(cyclopentadienyl)magnesium<sup>87,88</sup> (**56**), its structure in the solid state, based on X-ray powder diffraction data, was reported<sup>89</sup>. A more refined structure based on a single-crystal X-ray diffraction study was reported later<sup>90</sup>. The structure in the solid state is isostructural with that of ferrocene. The two parallel

FIGURE 32. Unit cell content of **53** (space group *Ibam*)FIGURE 33. Part of the polymeric structure of **55** in the solid state

cyclopentadienyl rings each are  $\eta^5$ -bonded to the magnesium atom (Figure 34) with almost identical bond distances [average C–Mg 2.304(8) Å]. The two cyclopentadienyl rings adopt a staggered conformation, in contrast to the eclipsed conformation found for the structure of **56** in the gas phase, obtained from a gas-phase electron diffraction study<sup>91</sup>.

Various substituted cyclopentadienylmagnesium compounds,  $(t\text{-BuC}_5\text{H}_4)_2\text{Mg}^{92}$  (**56**),  $[1,2,4\text{-(Me}_3\text{Si)}_3\text{C}_5\text{H}_2]_2\text{Mg}^{93}$  (**57**),  $[1,2,4\text{-(}t\text{-Bu)}_3\text{C}_5\text{H}_2]_2\text{Mg}^{94}$  (**58**),  $(\text{Me}_4\text{C}_5\text{H})_2\text{Mg}^{95}$  (**59**),  $(t\text{-BuMe}_4\text{C}_5)_2\text{Mg}^{95}$  (**60**),  $[(3\text{-butenyl})\text{Me}_4\text{C}_5]_2\text{Mg}^{96}$  (**61**) and  $(\text{Me}_5\text{C}_5)_2\text{Mg}^{97}$  (**62**), have been prepared and were structurally characterized by X-ray crystallography. All compounds have a basic structural motif that is identical to **56**, but the conformation of the cyclopentadienyl rings is such that steric interference is minimal. A slight deviation from

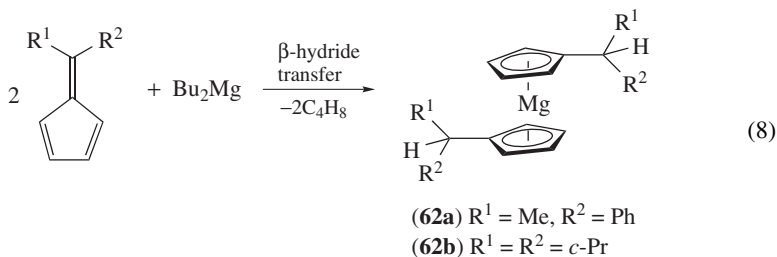


FIGURE 34. Molecular geometry of **56** in the solid stateFIGURE 35. Molecular geometry of **61** in the solid state

the linear structure to a slightly bent structure is observed for **57**, **58** and **60**, due to the presence of bulky substituents.

The *exo,exo*-bis(iso-dicyclopentadienyl)magnesium metallocene (**61**) has been prepared by reacting  $\text{Bu}_2\text{Mg}$  with iso-dicyclopentadiene. Its structure in the solid state has been determined by X-ray crystallography (Figure 35)<sup>98</sup>. The two cyclopentadienyl rings are  $\eta^5$ -bonded to magnesium with bond distances that range from 2.314(1) to 2.347(1) Å and adopt a staggered conformation.

The substituted cyclopentadienylmagnesium compounds **62a** and **62b** have been prepared from the corresponding fulvenes (equation 8) and were structurally characterized in the solid state by X-ray crystallography<sup>99</sup>. The structures are, as expected, ( $\eta^5$ -bonded cyclopentadienyl groups) for bis(cyclopentadienyl)magnesium compounds.



The magnesium atom of compound **62a** lies on a crystallographic inversion center, and consequently the substituents are in *anti*-configuration. The structure of **62b** shows an eclipsed conformation and leads to steric repulsion between the dicyclopropylmethyl groups (Figure 36). As a consequence a slight deviation from linear structure is observed.

Bis(indenyl)magnesium (**63**) has been prepared by the thermal decomposition of indenylmagnesium bromide, and its structure in the solid state has been established by X-ray crystallography<sup>100</sup>. Instead of the expected sandwich-type compound, a structure was found consisting of an infinite polymeric arrangement of which the repeating unit contains two magnesium atoms and four indenyl anions with two types of bonding modes (Figure 37). To each of the magnesium atoms an indenyl anion is  $\eta^5$ -bonded with its five-membered ring. The bond distances Mg(1)–C range from 2.31(1) to 2.54(1) Å and

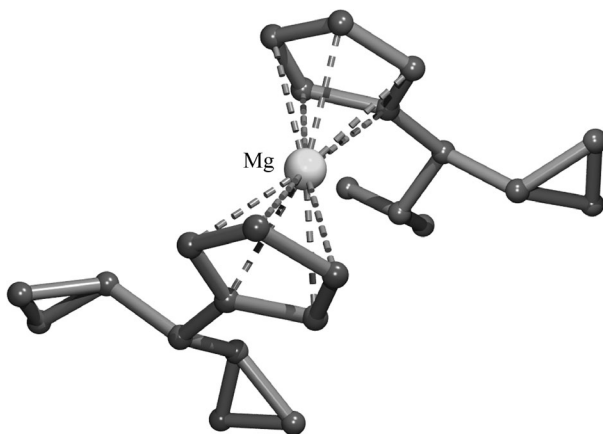


FIGURE 36. Molecular geometry of **62b** in the solid state

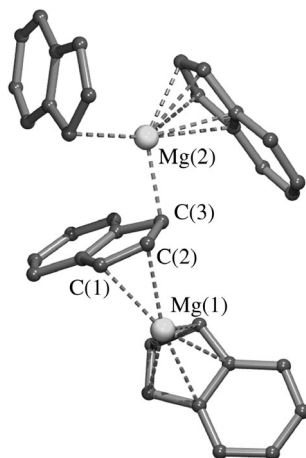
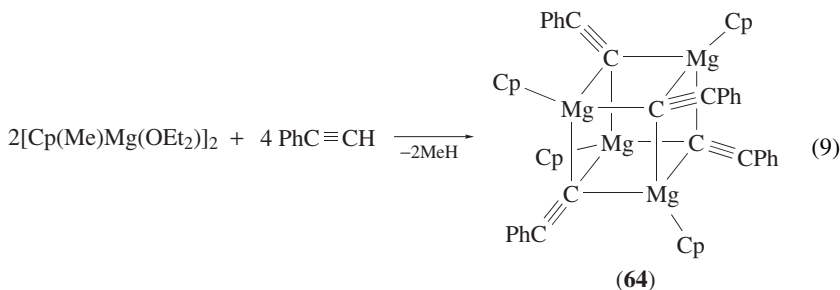


FIGURE 37. Molecular geometry of the repeating unit in polymeric **63**

Mg(2)–C range from 2.26(1) to 2.60(1) Å. One of the indenyl anions acts as bridge between the two magnesium atoms and is  $\eta^2$ -bonded to Mg(1) [Mg(1)–C(1) 2.40(1) and Mg(1)–C(2) 2.44(1) Å] and  $\eta^1$ -bonded to Mg(2) [Mg(2)–C(3) 2.26(1) Å]. In a similar bridging mode an indenyl anion is linking the repeating units.

Reaction of  $[\text{Cp}(\text{Me})\text{Mg}(\text{OEt}_2)]_2$  with phenylacetylene affords tetrameric  $[\text{CpMgC}\equiv\text{CPh}]_4$  (**64**) (equation 9). Its structure in the solid state has been established by X-ray crystallography<sup>101</sup> and it is the only example of a heteroleptic diorganomagnesium compound for which the structure in the solid state is known. The structure of **64** has a heterocubane structure with alternating four magnesium atoms and four terminal carbon atoms of the acetylenic group at the corners of the cube. To each of the magnesium atoms a Cp group is  $\eta^5$ -bonded. The structure is shown schematically in equation 9. The bond distances between the terminal acetylenic carbon atoms and the magnesium atoms vary in a small range from 2.249(2) to 2.348(2) Å, resulting in an almost perfect cube.



The structure of cyclopentadienyl(neopentyl)magnesium (**65**) in the gas phase has been determined by gas-phase electron diffraction<sup>102</sup>. The Mg–C bond distances of the  $\eta^5$ -bonded cyclopentadienyl group are 2.328(7) Å while the Mg–C bond distance of the neopentyl group was found to be 2.12(2) Å.

The structures in the solid state of bis(1-methylboratabenzene)magnesium (**66a**) and bis[3,5-dimethyl-1-(dimethylamino)boratabenzene]magnesium (**66b**) were determined by X-ray crystallography<sup>103</sup>. Both **66a** (Figure 38) and **66b** are typical sandwich structures and have common structural features. The magnesium atoms are located at crystallographic inversion centers, which implies coplanarity of the rings and an antiperiplanar arrangement with respect to the exocyclic substituents. The bond distances of the  $\eta^6$ -bonded boratabenzene ring to magnesium are Mg–C(1) 2.359(2), Mg–C(2) 2.422(2), Mg–C(3) 2.453(2), Mg–C(4) 2.420(2), Mg–C(5) 2.361(2) and Mg–B 2.436(2) Å.

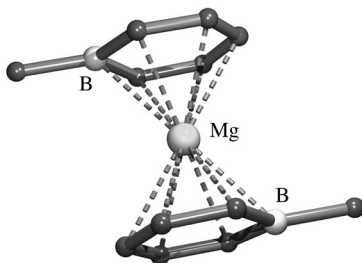


FIGURE 38. Molecular geometry of **66a** in the solid state

### C. Diorganomagnesium Compounds Containing Intramolecularly Coordinating Substituents

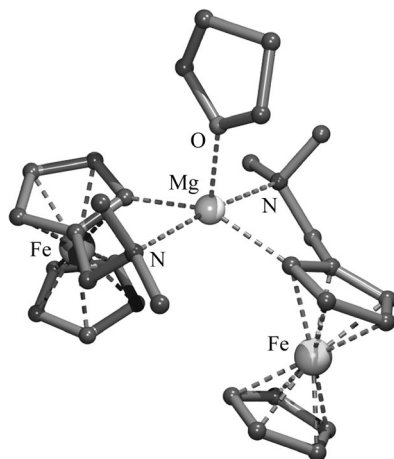
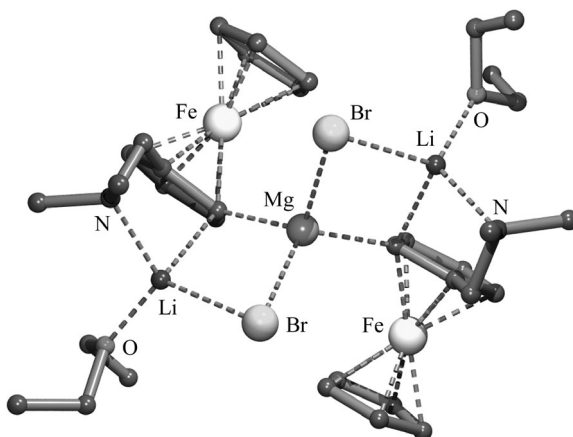
In the early days of the development of organometallic chemistry it was thought that in many cases the metal- $\sigma$ -carbon bond would be intrinsically unstable, especially in transition-metal organic compounds. Thermally induced homolytic cleavage of the metal-carbon bond and  $\beta$ -hydrogen elimination are the two most important pathways by which decomposition of organometallic compounds may occur. Several approaches have been put forward to suppress such decomposition pathways, e.g. the use of organic groups lacking  $\beta$ -hydrogen atoms, the introduction of bulky (often trimethylsilyl-containing) substituents and the use of organic groups containing a functionalized substituent capable of coordinating to the metal. The isolation and structural characterization of  $(\text{Me}_3\text{SiCH}_2)_4\text{Cu}_4$ <sup>104</sup> and  $(2\text{-Me}_2\text{NCH}_2\text{C}_6\text{H}_4)_4\text{Cu}_4$ <sup>105</sup> are clear examples of these approaches and represent the first examples of organocopper compounds sufficiently stable to allow their structural characterization by X-ray crystallography. In  $(2\text{-Me}_2\text{NCH}_2\text{C}_6\text{H}_4)_4\text{Cu}_4$  the monoanionic, potentially bidentate  $2\text{-Me}_2\text{NCH}_2\text{C}_6\text{H}_4$  ligand stabilizes the organocopper compound via intramolecular coordination of the nitrogen to copper. This particular ligand has been used in the early days to stabilize a variety of organometallic compounds. When other ligand skeletons and also other heteroatom-functionalized substituents capable of intramolecular coordination are included, several thousands of these organometallic derivatives, covering almost the whole periodic system of the elements, have been structurally characterized<sup>23</sup>.

It is rather surprising that only a few diorganomagnesium compounds have been reported in which intramolecular coordination of a heteroatom-containing substituent is present. The synthesis of  $(2\text{-Me}_2\text{NCH}_2\text{C}_6\text{H}_4)_2\text{Mg}$  (**67**) was reported. It has been used in a study on the influence of the presence of potentially intramolecular coordinating substituents on Schlenk equilibria<sup>106</sup>. However, it has never been structurally characterized.

The monoanionic potentially bidentate 2-[(dimethylamino)methyl]ferrocenyl ligand has coordinating properties similar to that of the 2-[(dimethylamino)methyl]phenyl ligand, and has also been used to stabilize a variety of organometallic derivatives. Bis{[(2-dimethylamino)methyl]ferrocenyl}magnesium (**68**) has been synthesized and was structurally characterized in the solid state by X-ray crystallography.

The molecular structure of **68**, crystallized from a solution containing THF and  $\text{Et}_2\text{O}$ , comprises two *C,N*-chelate bonded 2-[(dimethylamino)methyl]ferrocenyl groups [ $\text{Mg}-\text{C}$  2.151(2) and 2.160(2) Å, and  $\text{Mg}-\text{N}$  2.421(2) and 2.419(2) Å] (Figure 39). In addition, a THF molecule is coordinated [ $\text{Mg}-\text{O}$  2.077(2) Å] to the magnesium atom resulting in five-coordinate magnesium. Based on the bond angles around magnesium the coordination geometry shows a 63% distortion from a trigonal bipyramid (with the carbon atoms and the oxygen atom in the equatorial plane) towards a square pyramid along the Berry pseudorotation coordinate<sup>107</sup>. When crystallization was performed in the absence of THF, the diethyl ether adduct was isolated, having structural features that are very similar to those of **68**.

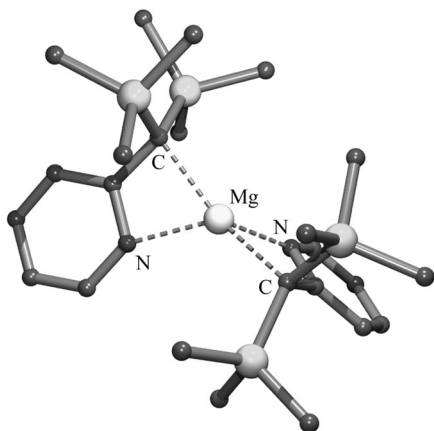
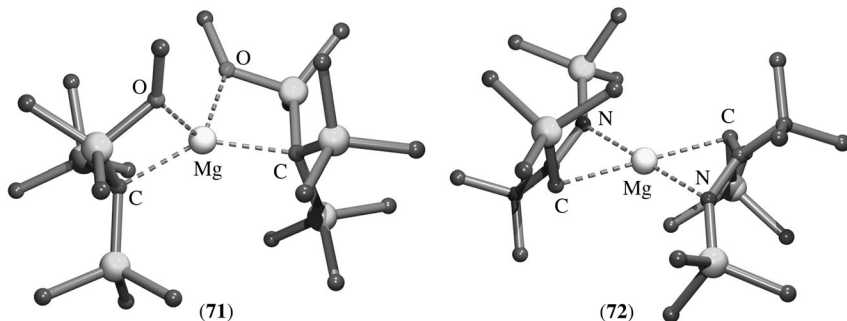
An aggregate of bis{[(2-dimethylamino)methyl]ferrocenyl}magnesium with two molecules of LiBr (**69**) has been isolated and structurally characterized (Figure 40)<sup>108</sup>. This compound is a nice illustration of the capability of diorganomagnesium compounds to aggregate with other metal salts. In **69**, each of the 2-[(dimethylamino)methyl]ferrocenyl groups is slightly asymmetrically bridge-bonded with its carbon atom between magnesium and lithium [ $\text{Mg}-\text{C}$  2.169(4) and 2.167(4) Å, and  $\text{Li}-\text{C}$  2.390(8) and 2.311(8) Å]. Also, the bromine atoms are bridge-bonded between magnesium and lithium [ $\text{Mg}-\text{Br}$  2.600(1) and 2.605(1), and  $\text{Li}-\text{Br}$  2.508(7) and 2.493(7) Å] leading to a distorted tetrahedral coordination geometry at magnesium. The nitrogen atoms of the (dimethylamino)methyl substituents are each coordinating to a lithium atom [ $\text{Li}-\text{N}$  2.074(8) and 2.065(7) Å]

FIGURE 39. Molecular geometry of **68** in the solid stateFIGURE 40. Molecular geometry of **69** in the solid state

while coordination saturation at each lithium atom is reached by the coordination of an additional diethyl ether molecule.

The potentially bidentate  $\alpha$ -(2-pyridyl)- $\alpha,\alpha$ -bis(trimethylsilyl)methyl monoanionic ligand also has been used in a variety of organometallic derivatives. Its magnesium derivative bis[ $\alpha$ -(2-pyridyl)- $\alpha,\alpha$ -bis(trimethylsilyl)methyl]magnesium (**70**) has been structurally characterized by X-ray crystallography (Figure 41)<sup>109</sup>.

In **70**, the two  $\alpha$ -(2-pyridyl)- $\alpha,\alpha$ -bis(trimethylsilyl)methyl ligands are *C,N*-chelate bonded to magnesium [Mg–C 2.21(9), Mg–N 2.13(1) Å]. As a consequence of the four-membered chelate rings the coordination geometry at magnesium is distorted from tetrahedral, as is indicated by the large C–Mg–C and N–Mg–N bond angles of 157.0(7)° and 117(4)° respectively, and the acute C–Mg–N angle of 67.3(2)°.

FIGURE 41. Molecular geometry of **70** in the solid stateFIGURE 42. Molecular geometries of **71** and **72** in the solid state

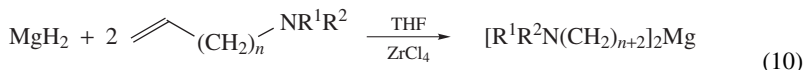
A similar distortion of the tetrahedral coordination geometry at magnesium was observed in  $[\text{MeOSi}(\text{Me})_2\text{C}(\text{SiMe}_3)_2\text{C}]_2\text{Mg}$  (**71**) in which two *C,O*-chelating ligands are forming four-membered chelate rings (Figure 42)<sup>110</sup>.

An unusual planar coordination geometry at magnesium has been observed in  $[\text{Me}_3\text{SiN}=\text{C}(t\text{-Bu})\text{CHSiMe}_3]_2\text{Mg}$  (**72**) in which two *C,N*-chelating ligands are present (Figure 42)<sup>111</sup>. However, the observed bond distances [ $\text{Mg}-\text{C}(1)$  2.284(4),  $\text{Mg}-\text{C}(2)$  2.408(4) and  $\text{Mg}-\text{N}$  2.084(3) Å] suggest that the ligand binds rather in an aza-allyl type of manner than in a *C,N*-chelate bonding mode.

A heteroleptic diorganomagnesium compound  $[(\text{Me}_2\text{N}(\text{Me})_2\text{Si})(\text{Me}_3\text{Si})_2\text{C}](n\text{-Bu})\text{Mg}$  (THF) (**73**) has been synthesized and characterized by X-ray crystallography<sup>112</sup>. Its structure comprises one *C,N*-chelate bonded  $(\text{Me}_2\text{N}(\text{Me})_2\text{Si})(\text{Me}_3\text{Si})_2\text{C}$  group [ $\text{Mg}-\text{C}$  2.241(2) and  $\text{Mg}-\text{N}$  2.203(2) Å], one  $\sigma$ -bonded *n*-butyl group [ $\text{Mg}-\text{C}$  2.130(3) Å] and an additional coordinating THF molecule [ $\text{Mg}-\text{O}$  2.069(2) Å] to complete a distorted tetrahedral coordination geometry at magnesium.

An elegant synthetic pathway to bis[(3-(dialkyl)aminobutyl)magnesium and bis[4-(dialkylamino)butyl]magnesium compounds was developed involving the addition reaction of dialkylallyl amines and 1-dialkylamino-3-alkenes to highly reactive  $\text{MgH}_2$ <sup>113</sup> in

the presence of catalytic amounts (1mol%) of  $\text{ZrCl}_4$ <sup>114</sup>. According to this procedure, compounds **74a–74i** and **75a–75g** have been prepared (equation 10).  $^1\text{H}$  and  $^{13}\text{C}$  NMR spectroscopic studies in solutions indicated that in all these compounds the nitrogen atoms are involved in intramolecular coordination.



(74a)  $n = 1$ ,  $\text{R}^1 = \text{R}^2 = \text{Me}$

(74b)  $n = 1$ ,  $\text{R}^1 = \text{R}^2 = \text{Et}$

(74c)  $n = 1$ ,  $\text{R}^1 = \text{R}^2 = n\text{-Pr}$

(74d)  $n = 1$ ,  $\text{R}^1 = \text{R}^2 = i\text{-Pr}$

(74e)  $n = 1$ ,  $\text{R}^1 = \text{R}^2 = n\text{-Bu}$

(74f)  $n = 1$ ,  $\text{R}^1 = \text{Me}$ ,  $\text{R}^2 = \text{Et}$

(74g)  $n = 1$ ,  $\text{R}^1 = \text{Me}$ ,  $\text{R}^2 = n\text{-Bu}$

(74h)  $n = 1$ ,  $\text{R}^1 = \text{Me}$ ,  $\text{R}^2 = c\text{-Hex}$

(74i)  $n = 1$ ,  $\text{R}^1 = \text{Me}$ ,  $\text{R}^2 = \text{Ph}$

(75a)  $n = 2$ ,  $\text{R}^1 = \text{R}^2 = \text{Me}$

(75b)  $n = 2$ ,  $\text{R}^1 = \text{R}^2 = \text{Et}$

(75c)  $n = 2$ ,  $\text{R}^1 = \text{R}^2 = n\text{-Pr}$

(75d)  $n = 2$ ,  $\text{R}^1 = \text{R}^2 = n\text{-Bu}$

(75e)  $n = 2$ ,  $\text{R}^1 = \text{Me}$ ,  $\text{R}^2 = \text{Et}$

(75f)  $n = 2$ ,  $\text{R}^1 = \text{Me}$ ,  $\text{R}^2 = n\text{-Bu}$

(75g)  $n = 2$ ,  $\text{R}^1 = \text{Me}$ ,  $\text{R}^2 = c\text{-Hex}$

Making use of the same procedure, the ether-functionalized diorganomagnesium compounds **76a–76f** were prepared from 3-butenyl ethers and  $\text{MgH}_2$  (equation 11)<sup>114</sup>. It should be noted that the addition reaction of allyl ethers to  $\text{MgH}_2$  failed because in that case ether cleavage by  $\text{MgH}_2$  becomes a competing reaction. Also, for these compounds intramolecular O–Mg coordination in solution was established by NMR spectroscopic studies.



(76a)  $\text{R} = \text{Me}$

(76b)  $\text{R} = \text{Et}$

(76c)  $\text{R} = n\text{-Pr}$

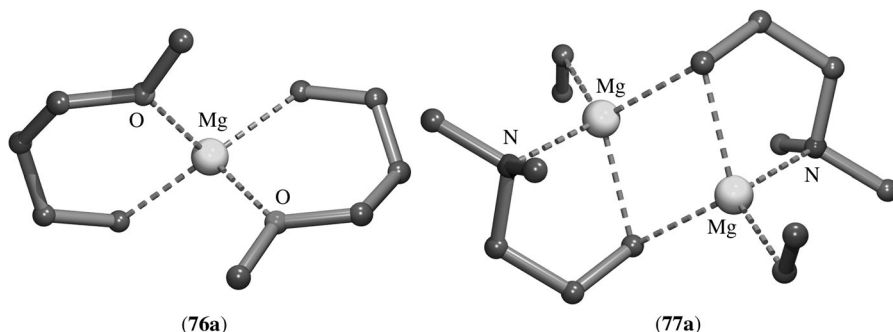
(76d)  $\text{R} = n\text{-Bu}$

(76e)  $\text{R} = n\text{-Pent}$

(76f)  $\text{R} = n\text{-Hex}$

An X-ray crystal-structure determination of **76a** confirmed that intramolecular O–Mg coordination is present in the solid state (Figure 43). Both 4-methoxybutyl ligands are *C,O*-chelate bonded to magnesium [ $\text{Mg}-\text{C}$  2.144(4) and  $\text{Mg}-\text{O}$  2.071(3) Å]. The bond angles around magnesium [ $\text{C}-\text{Mg}-\text{C}'$  140.2(2)°,  $\text{O}-\text{Mg}-\text{O}'$  96.4(1)°,  $\text{C}-\text{Mg}-\text{O}$  95.7(1)° and  $\text{C}-\text{Mg}-\text{O}'$  110.8(1)°] indicate that the coordination geometry at magnesium is distorted from the ideal tetrahedral geometry.

The above-mentioned functionalized diorganomagnesium compounds undergo clean redistribution reactions with  $\text{Et}_2\text{Mg}$  to form the heteroleptic diorganomagnesium compounds. For example, reaction of  $[\text{Me}_2\text{N}(\text{CH}_2)_3]_2\text{Mg}$  (**74a**) with  $\text{Et}_2\text{Mg}$  gives  $\text{Me}_2\text{N}(\text{CH}_2)_3\text{MgEt}$  (**77**) in quantitative yield<sup>115</sup>. An X-ray crystal-structure determination of **77a** showed this compound to exist as a centrosymmetric dimer in the solid state (Figure 43). The two dimethylaminopropyl groups are  $\eta^2\text{-C}$  bridge-bonded between two magnesium atoms [ $\text{Mg}-\text{C}$  2.294(2) and 2.273(2) Å] while both nitrogen atoms are coordinated to the magnesium atoms [ $\text{Mg}-\text{N}$  2.181(2) Å]. To each of the magnesium atoms an ethyl group is  $\sigma$ -bonded [ $\text{Mg}-\text{C}$  2.142(3) Å]. Also, the structure of heteroleptic  $\text{MePhN}(\text{CH}_2)_3\text{MgEt}$

FIGURE 43. Molecular geometries of **76a** and **77a** in the solid state

(**77b**) in the solid state was established by X-ray crystallography. Its structural features are similar to those of **77a**.

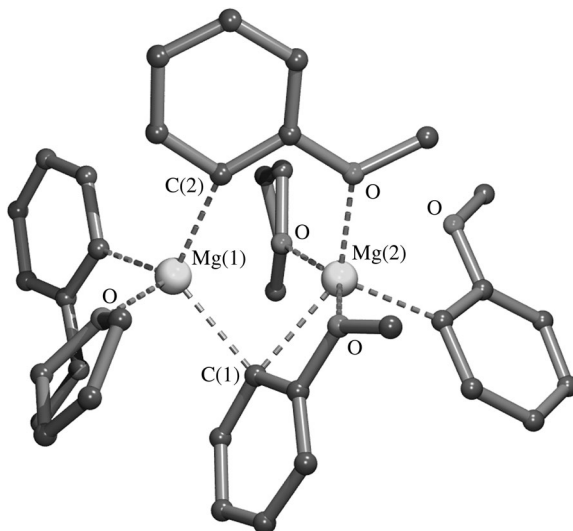
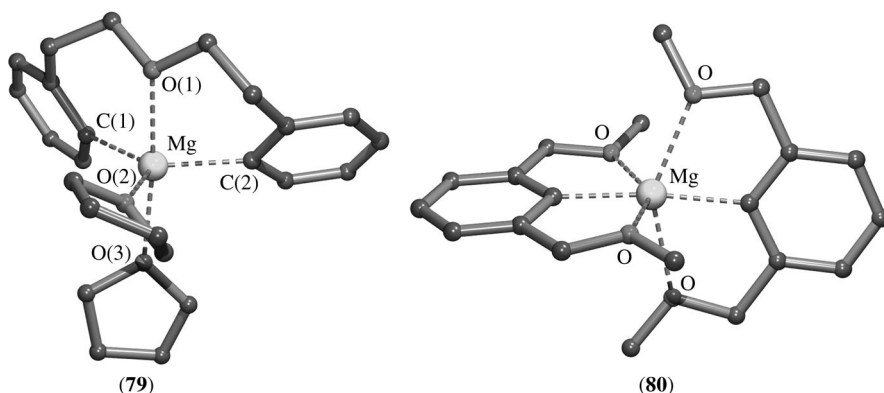
A remarkable structure was found for bis(*ortho*-anisyl)magnesium which crystallizes from THF as a dimeric bis-THF adduct (**78**) (Figure 44)<sup>116</sup>. This aggregate contains four *ortho*-anisyl groups with three different bonding modes. One anisyl group is  $\mu^2$ -bridge-bonded between the two magnesium atoms [C(1)–Mg(1) 2.327(6) and C(1)–Mg(2) 2.305(6) Å] while the oxygen substituent is intramolecularly coordinated to one of these magnesiums [O–Mg(2) 2.166(4) Å]. A second anisyl group is  $\sigma$ -bonded to Mg(1) [C(2)–Mg(1) 2.199(7) Å] and the oxygen of the anisyl functionality coordinates to Mg(2) [O–Mg(2) 2.056(5) Å]. The two other *ortho*-anisyl groups are  $\sigma$ -bonded via  $C_{ipso}$  to different magnesium atoms [C–Mg(1) 2.147(7) and C–Mg(2) 2.132(6) Å] while the oxygen substituents are not involved in coordination to magnesium. Finally, to each of the magnesium atoms a THF molecule is coordinated, resulting in one four-coordinate magnesium atom [Mg(1)] and one five-coordinate magnesium atom [Mg(2)]. The rather strange structural motif present in **78** has been explained in terms of an intramolecular ‘ate’-type of structure in which Mg(2) has a formally partial negative charge and Mg(1) has a formally partial positive charge.

A pseudo-trigonal-bipyramidal arrangement at magnesium was observed in the crystal structure of magnesacycle (**79**) (Figure 45)<sup>106</sup>. The two carbon atoms [C(1) and C(2)] of the  $\sigma$ -bonded aryl groups and the oxygen atom [O(2)] of one of the coordinating THF molecules lie in the equatorial plane. The intramolecular coordinating ether functionality and the oxygen atom of the other coordinating THF molecule are at the axial positions. As expected, the C–O distances of the axially bonded oxygen atoms [Mg–O(1) 2.242(4) and Mg–O(3) 2.221(4) Å] are significantly longer than of the equatorial one [Mg–O(2) 2.095(3) Å].

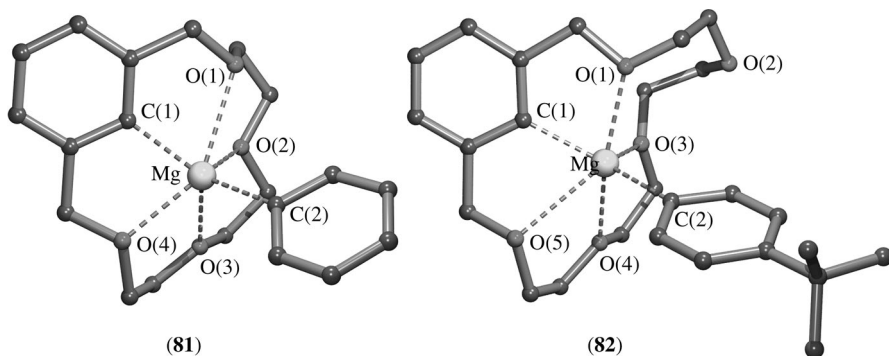
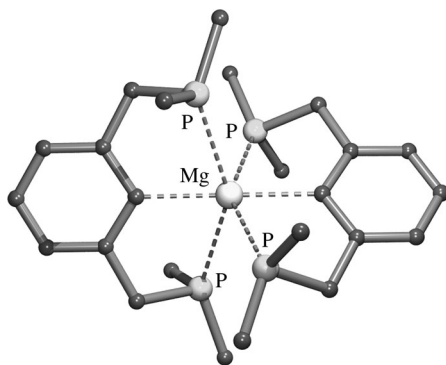
An X-ray crystal-structure determination of bis[1,3-bis-((dimethoxy)methyl)phenyl]magnesium (**80**) revealed a distorted octahedral coordination geometry at magnesium because all four methoxy substituents are involved in intramolecular Mg–O coordination (Figure 45)<sup>106</sup>. The Mg–C bond distances are very short [Mg–C 2.093(4) and 2.105(4) Å], but are compensated for by relatively long Mg–O bond distances (average 2.315 Å). The C–Mg–C bond angle [173.4(2)°] deviates only slightly from linear.

An unprecedented metallation was observed when 1,3-xylyl crown ethers are reacted with diarylmagnesium compounds. Reaction of 1,3-xylylene-15-crown-4 with diphenylmagnesium gives in quantitative yield 2-(phenylmagnesium)-1,3-xylylene-15-crown-4 (**81**), the structure of which was established by an X-ray crystal-structure determination



FIGURE 44. Molecular geometry of **78** in the solid stateFIGURE 45. Molecular geometries of **79** and **80** in the solid state

(Figure 46)<sup>117</sup>. The Mg–C distances [Mg–C(1) 2.127(4) and Mg–C(2) 2.154(4) Å] are as expected for aryl groups  $\sigma$ -bonded to magnesium. All four oxygen atoms of the crown are involved in intramolecular coordination with Mg–O bond distances ranging from 2.183(3) to 2.619(3) Å, leading to a six-coordinate magnesium atom. Similarly, 2-[(4-*tert*-butylphenyl)magnesium]-1,3-xylylene-18-crown-5 (**82**) has been prepared and structurally characterized in the solid state (Figure 46)<sup>118</sup>. Compound **82** has structural features similar to those of **81**, but only four of the five oxygen atoms of the crown are involved in intramolecular coordination to magnesium. The formation of compounds **81** and **82** has been explained by a mechanism involving arylmagnesium cations encapsulated in the crown and tris[aryl]magnesium anions<sup>118</sup>.

FIGURE 46. Molecular geometries of **81** and **82** in the solid stateFIGURE 47. Molecular geometry of **83** in the solid state

Bis[1,3-bis{((dimethylphosphino)methyl)phenyl}magnesium (**83**) is the only example of a diorganomagnesium compound in which phosphorus to magnesium coordination in the solid state is established unambiguously by X-ray crystallography. The molecular geometry of **83** in the solid state comprises a centrosymmetric molecule in which the two aryl groups are  $\sigma$ -bonded to magnesium [Mg–C 2.216(1) Å] and all four phosphorus atoms are involved in intramolecular coordination [Mg–P 2.770(1) and 2.761(1) Å] (Figure 47)<sup>119</sup>. The coordination geometry at magnesium is a distorted octahedral one, with only a slight deviation of the C–Mg–C bond angle [178.10(8)°] from linear.

#### D. Donor–Acceptor Complexes of $\sigma$ -Bonded Diorganomagnesium Compounds

As has been outlined before, the preferred coordination geometry at magnesium in organomagnesium compounds is tetrahedral, although also organomagnesium compounds are known with either lower or higher coordination numbers.

The only diorganomagnesium compound with three-coordination at magnesium, for which the structure was established by X-ray crystallography, is [(Me<sub>3</sub>Si)<sub>2</sub>CH]<sub>2</sub>Mg(OEt<sub>2</sub>) (**84**) (Figure 48)<sup>120</sup>. Probably, the combination of two sterically demanding (Me<sub>3</sub>Si)<sub>2</sub>CH groups and a rather bulky diethyl ether molecule in proximity to the magnesium atom

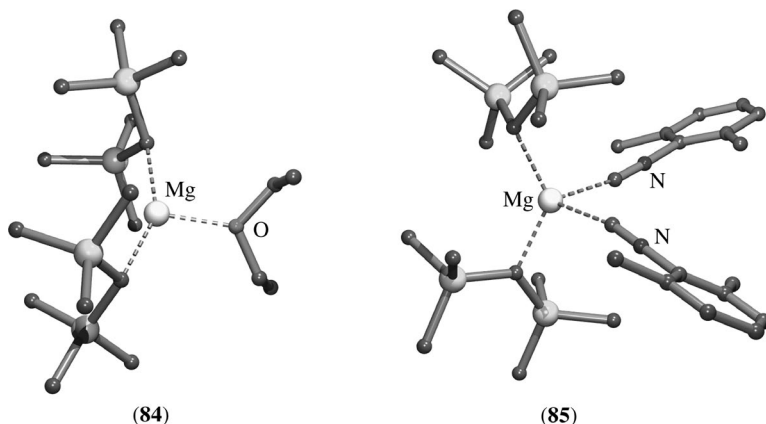


FIGURE 48. Molecular geometry of the diorganomagnesium complexes **84** and **85** in the solid state

prevents the coordination of a second diethyl ether molecule. Although in **84** the C–Mg–C bond angle is rather large ( $148.45^\circ$ ), the sum of the bond angles around magnesium is within experimental error  $360^\circ$ , indicating a planar trigonal coordination geometry.

The same diorganomagnesium compound is capable of coordinating two 2,6-xylylisocyanide molecules, thus forming  $[(\text{Me}_3\text{Si})_2\text{CH}]_2\text{Mg}(\text{CNC}_6\text{H}_3\text{Me}_2-2,6)_2$  (**85**) with a distorted tetrahedral coordination geometry at magnesium (Figure 48)<sup>121</sup>. The C–Mg–C bond angle of the bonding carbon atoms [Mg–C 2.148(7) and 2.138(9) Å] of the  $(\text{Me}_3\text{Si})_2\text{CH}$  groups in **85** has narrowed to  $128.40(7)^\circ$  compared to that in **84**. However, the C–Mg–C bond angle of carbon atoms of the coordinating isocyanide groups [Mg–C 2.306(9) and 2.307(10) Å] is extremely acute with  $88.79(2)^\circ$ .

The usual, distorted, tetrahedral coordination geometry at magnesium has been established by X-ray crystallographic studies for a series of diorganomagnesium complexes **86–92** containing amine ligands. The relevant structural features of these complexes are summarized in Table 1. Notable are the acute N–Mg–N angles in the TMEDA complexes **86–91**; probably this is a consequence of the small bite angle of the chelating TMEDA ligand.

Like amines, ethers like THF and diethyl ether are also capable of coordinating to the magnesium atom of diorganomagnesium compounds to form 1:2 adducts causing a tetrahedral coordination geometry at magnesium. The structures in the solid state of a series of these adducts (**93–99**) have been unambiguously determined by X-ray crystallography. The relevant structural data of these compounds are compiled in Table 2. With the exception of the THF adduct of bis(*p*-tolyl)magnesium (**94**), *vide infra*, these compounds are discrete monomeric species. Notable are the relatively large C–Mg–C bond angles, which are compensated by acute O–Mg–O angles.

The X-ray crystal-structure determination of the THF adduct of bis(*p*-tolyl)magnesium showed that the unit cell contains two different molecules, a monomer  $(4\text{-MeC}_6\text{H}_4)_2\text{Mg}(\text{THF})_2$  (**94a**) and a dimeric molecule  $(4\text{-MeC}_6\text{H}_4)_4\text{Mg}_2(\text{THF})_2$  (**94b**) (Figure 49)<sup>83</sup>.

The structure of monomer **94a** is straightforward and isostructural with those of **93** and **95–97**. In dimer **94b** two *p*-tolyl groups are bridge-bonded with the  $\text{C}_{\text{ipso}}$  atoms between two magnesium atoms [Mg–C 2.245(7) and 2.313(7) Å]. To each of the magnesium atoms a *p*-tolyl group is  $\sigma$ -bonded [Mg–C 2.130(7) Å] and an additional THF molecule is coordinate bonded [Mg–O 2.020(5) Å], to give four-coordinate magnesium atoms. The

TABLE 1. Relevant structural features of diorganomagnesium complexes **86–92**

Compound	Mg–C (Å)	Mg–N (Å)	C–Mg–C (°)	N–Mg–N (°)	Reference
Me <sub>2</sub> Mg(TMEDA) ( <b>86</b> )	2.166(6) 2.166(6)	2.257(6) 2.227(6)	130.0(4)	81.5(3)	122
Ph <sub>2</sub> Mg(TMEDA) ( <b>87</b> )	2.167(5) 2.167(5)	2.205(5) 2.199(5)	119.2(1)	82.5(1)	123
Bn <sub>2</sub> Mg(TMEDA) ( <b>88</b> )	2.169(2) 2.169(2)	2.192(2) 2.207(2)	117.12(7)	83.36(5)	124
Et <sub>2</sub> Mg(TMEDA) ( <b>89</b> )	2.163(6) 2.137(6)	2.236(5) 2.237(7)	127.7(3)	82.7(2)	125
<i>s</i> -Bu <sub>2</sub> Mg(TMEDA) ( <b>90</b> )	2.181(3) 2.181(3)	2.252(3) 2.252(3)	133.6(3)	81.0(2)	126
(Ph <sub>2</sub> PCH <sub>2</sub> ) <sub>2</sub> Mg(TMEDA) ( <b>91</b> )	2.171(4) 2.171(4)	2.226(4) 2.226(4)	130.0(2)	82.3(2)	127
Me <sub>2</sub> Mg(quin) <sub>2</sub> <sup>a</sup> ( <b>92</b> )	2.163(9) 2.224(8)	2.231(6) 2.247(6)	129.0(3)	108.2(2)	128

<sup>a</sup> Quinuclidine (1-azabicyclo[2.2.2]octane).TABLE 2. Relevant structural features of diorganomagnesium ether complexes **93–99**

Compound	Mg–C (Å)	Mg–O (Å)	C–Mg–C (°)	O–Mg–O (°)	Reference
Ph <sub>2</sub> Mg(THF) <sub>2</sub> ( <b>93</b> )	2.132(8) 2.126(7)	2.050(5) 2.031(6)	124.4(3)	96.7(2)	83
(4-MeC <sub>6</sub> H <sub>4</sub> ) <sub>2</sub> Mg(THF) <sub>2</sub> ( <b>94a</b> )	2.181(3) 2.181(3)	2.252(3) 2.252(3)	133.6(3)	81.0(2)	83
(2,4,6-Me <sub>3</sub> C <sub>6</sub> H <sub>2</sub> ) <sub>2</sub> Mg(THF) <sub>2</sub> ( <b>95</b> )	2.182(3) 2.165(3)	2.067(3) 2.079(3)	118.8(1)	88.4(1)	58
(2,4,6- <i>i</i> -Pr <sub>3</sub> C <sub>6</sub> H <sub>2</sub> ) <sub>2</sub> Mg(THF) <sub>2</sub> ( <b>96</b> )	2.179(3) 2.177(3)	2.107(2) 2.110(2)	123.1(1)	87.1(1)	58
(2-C <sub>2</sub> H <sub>3</sub> C <sub>6</sub> H <sub>4</sub> ) <sub>2</sub> Mg(THF) <sub>2</sub> ( <b>97</b> )	2.14(1) 2.14(1)	2.044(8) 2.027(8)	127.8(5)	91.2(4)	129
Ph[(Me <sub>3</sub> Si) <sub>3</sub> Si]Mg(THF) <sub>2</sub> ( <b>98</b> )	2.150(4) 2.650(1) <sup>a</sup>	2.051(3) 2.059(3)	128.2(1) <sup>b</sup>	95.4(1)	130
[Ph(Me)HC] <sub>2</sub> Mg(OEt <sub>2</sub> ) <sub>2</sub> ( <b>99</b> )	2.195(1) 2.195(1)	2.058(1) 2.058(1)	122.2(1)	93.8(1)	131

<sup>a</sup> Mg–Si bond length.<sup>b</sup> C–Mg–Si bond angle.

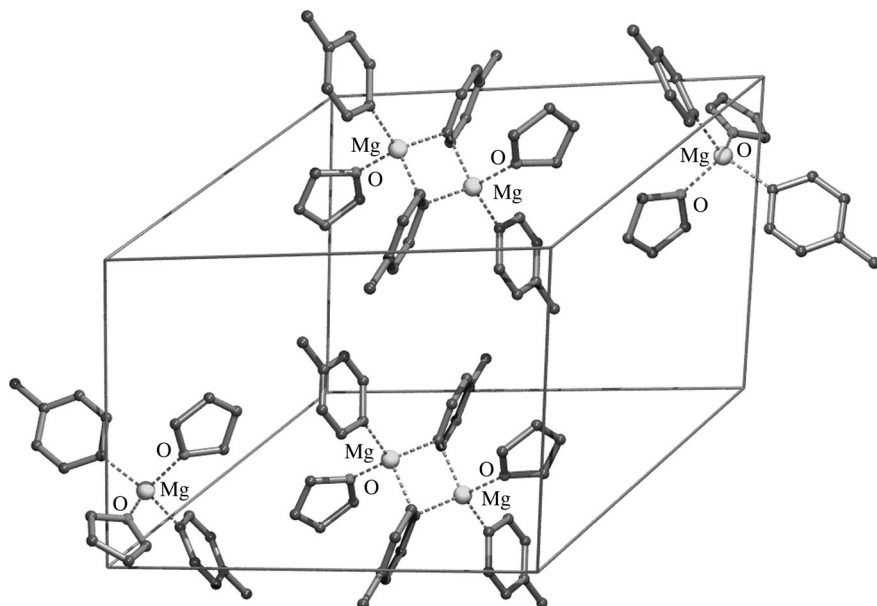


FIGURE 49. Unit-cell contents of **94** in space-group  $P\bar{1}$

acute Mg–C–Mg bond angle of  $77.5(2)^\circ$  is in the range expected for bridging three-center two-electron bonded aryl groups.

It should be noted that in the solid-state structure of **99** the two chiral centers within an individual molecule have identical configurations, either both *R* or both *S*, although **99** was prepared from racemic starting material<sup>131</sup>. However, as a requirement of the space-group symmetry ( $C2/c$ ) both enantiomers are present in 1:1 molar ratio in the crystal lattice.

Diorganomagnesium compounds also form complexes with bis-donor-atom ligands that are not capable of forming chelates. When dimethylmagnesium is crystallized from a THF solution that contains DABCO, a complex  $(\text{Me}_2\text{Mg})_2(\text{DABCO})(\text{THF})_2$  (**100**) is obtained. An X-ray crystal-structure determination showed that this complex consists of two  $\text{Me}_2\text{Mg}(\text{THF})$  moieties between which a DABCO molecule is *N,N'*-bridge bonded [ $\text{Mg}–\text{N}$  (2.208(3) Å) (Figure 50)]<sup>132</sup>. As a result the magnesium atoms have a slightly distorted tetrahedral coordination geometry.

In many cases diorganomagnesium dioxane complexes,  $\text{R}_2\text{Mg}(\text{dioxane})$ , have been obtained as unwanted side-products. Only for two of these,  $\text{Et}_2\text{Mg}(\text{dioxane})$ <sup>133</sup> (**101**) and *neo*- $\text{Pent}_2\text{Mg}(\text{dioxane})$ <sup>134</sup> (**102**), were the structures in the solid state determined by X-ray crystallography. Both compounds exist in the solid state as polymeric chains in which dioxane molecules are *O,O'*-bridge bonded between the  $\text{Et}_2\text{Mg}$  units in **101** [ $\text{Mg}–\text{O}$  2.077(2) and 2.084(2) Å], and the *neo*- $\text{Pent}_2\text{Mg}$  units in **102** [ $\text{Mg}–\text{O}$  2.132(1) Å], resulting in tetrahedral coordinate magnesium atoms. The structure of **101** is shown in Figure 50.

During studies on bifunctional organomagnesium compounds<sup>135, 136</sup>, the structures in the solid state of several such compounds were determined. Association measurements of magnesiacyclohexane in THF solution indicated that this compound is in equilibrium with a dimer. An X-ray crystal-structure determination of the product that crystallizes from

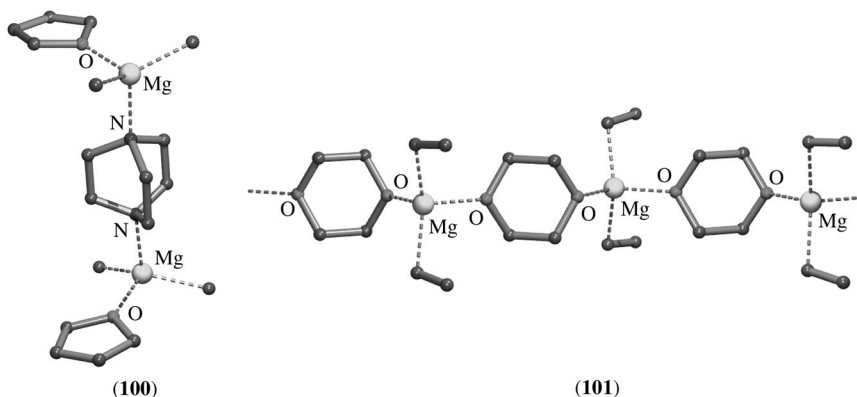


FIGURE 50. Molecular geometry of **100** in the solid state and part of the polymeric chain of **101** in the solid state

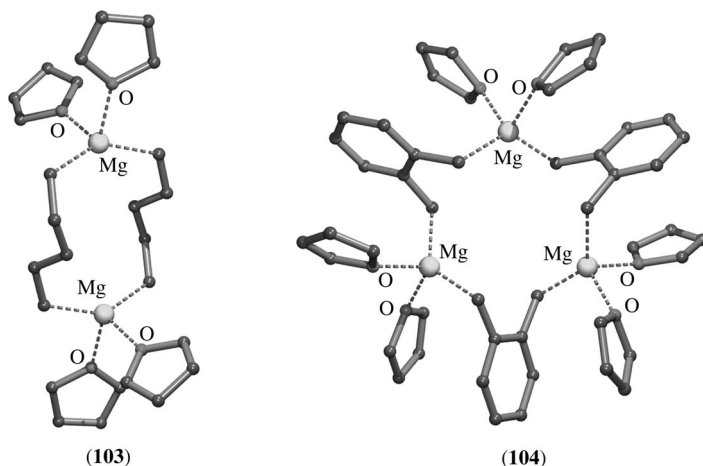


FIGURE 51. Bifunctional cyclic organomagnesium compounds **103** and **104** in the solid state

such solutions indicated the presence of a cyclic dimer, the 1,7-dimagnesiocyclododecane tetra THF complex (**103**) in the solid state (Figure 51)<sup>137,138</sup>. To each of the magnesium atoms in the twelve-membered ring two additional THF molecules are coordinated to complete a tetrahedral coordination geometry at the magnesium atoms.

The *o*-xylidenemagnesium bis THF complex (**104**) exists in the solid state as a cyclic trimer (Figure 51)<sup>139</sup>. Each of the benzylic carbon atoms of the xylidene moieties is  $\sigma$ -bonded to a magnesium atom, thus forming a nine-membered ring. To each of the magnesium atoms two THF molecules are coordinated to give a tetrahedral coordination geometry.

The structures in the solid state of the 1,2-phenylenemagnesium THF complex (**105**), the 1,8-naphthalenediylmagnesium THF complex (**106**) and the *cis*-diphenylvinylmagnesium THF complex (**107**) were determined by X-ray crystallography<sup>140</sup>. All three

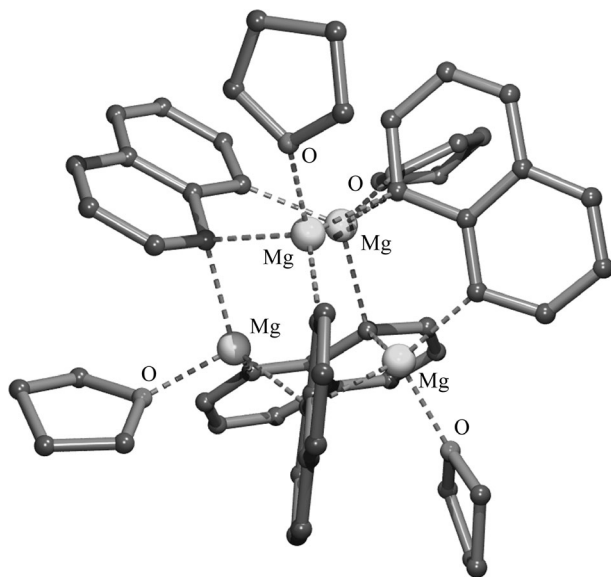


FIGURE 52. Molecular geometry of the tetrameric aggregate **106**

compounds are tetrameric aggregates with similar structural features. The core of these compounds consists of a tetrahedron of four magnesium atoms, arranged in a similar fashion as the  $\text{Li}_4$  core of many tetrameric organolithium compounds<sup>141</sup>. Above each face of the tetrahedron an organic fragment is positioned that is bonded with two carbon atoms to three magnesium atoms. One of the carbon atoms is  $\sigma$ -bonded to one magnesium atom and the other carbon atom bridges two magnesium atoms via a three-center two-electron bond. To the top positions of each of the magnesium atoms a THF molecule is coordinated to complete a distorted tetrahedral coordination geometry at each of the magnesium atoms. As an illustrative example the structure of **106** is shown in Figure 52.

Tridentate nitrogen- or oxygen-containing ligands form complexes with diorganomagnesium compounds in which the magnesium atom is five-coordinate. The X-ray crystal-structure determination of  $\text{Me}_2\text{Mg}(\text{PMDTA})$  (**108**)<sup>125, 132</sup> shows that in the solid state the magnesium atom exhibits a trigonal bipyramidal coordination geometry with the methyl groups [ $\text{Mg}-\text{C}$  2.173(4) and 2.191(4) Å] and the central nitrogen atom [ $\text{Mg}-\text{N}$  2.381(3) Å] at equatorial positions (Figure 53). The terminal nitrogen atoms occupy the axial positions. The sum of the bond angles in the equatorial plane is  $360^\circ$  within experimental error, but the  $\text{N}-\text{Mg}-\text{N}$  bond angle [ $138.3(1)^\circ$ ] between the axial nitrogen atoms deviates considerably from linear as a consequence of the presence of two five-membered chelate rings.

Bis(4-*tert*-butylphenyl)magnesium forms a complex with diglyme, complex **109**, in which all three oxygen atoms of the diglyme ligand are involved in coordination to magnesium. Like in **108**, in **109** the magnesium atom has a trigonal bipyramidal coordination geometry with the bonding carbon atoms and the central oxygen atom of the diglyme ligand in equatorial positions (Figure 53)<sup>142</sup>. Also, in this complex the bond angles in the equatorial plane add up to  $360^\circ$ . The terminal oxygen atoms of the diglyme ligand are at the axial sites, but as a consequence of the presence of the two five-membered chelate rings the  $\text{O}-\text{Mg}-\text{O}$  bond angle [ $141.97(9)^\circ$ ] deviates considerably from linear.

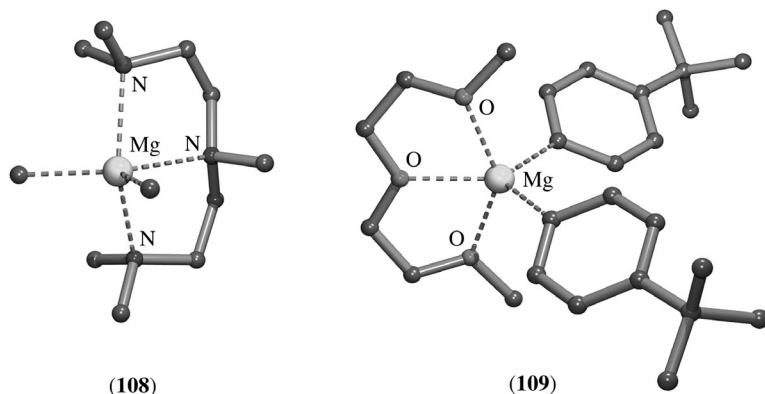


FIGURE 53. Molecular geometry of five-coordinate organomagnesium complexes **108** and **109** in the solid state

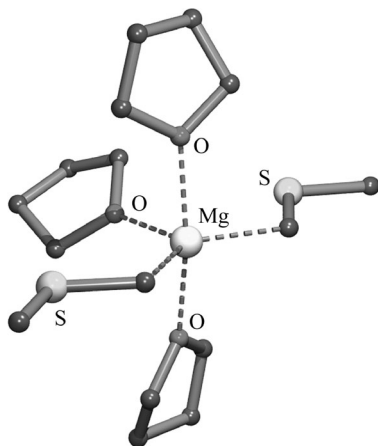
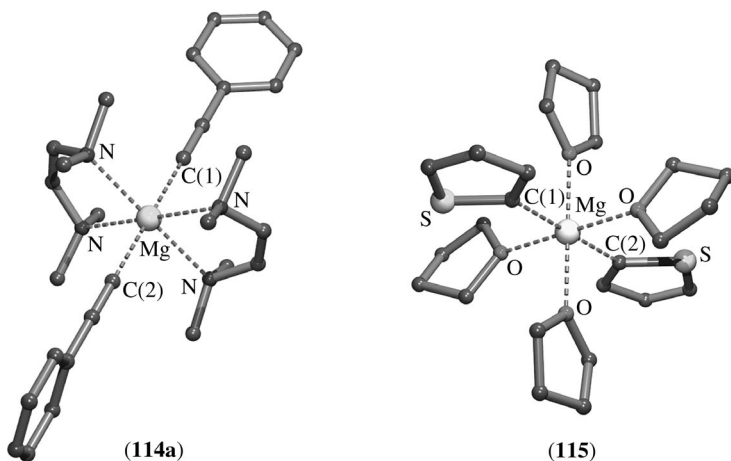
The structure of bis(4-*tert*-butylphenyl)magnesium tetraglyme (**110**) in the solid state has also been determined by X-ray crystallography<sup>142</sup>. Only the terminal and the next two oxygen atoms of the tetraglyme ligand are involved in coordination to magnesium. The asymmetric unit of **110** contains three crystallographically independent molecules in which the environments around the magnesium atoms are similar to that observed in **109** but differ in the orientation of the uncomplexed tail.

The crown ether 1,3,16,18-dioxylene-30-crown-8 is capable of forming a complex (**111**) with two molecules of bis(4-*tert*-butylphenyl)magnesium of which the structure in the solid state was determined by X-ray crystallography<sup>142</sup>. To each of the magnesium atoms three oxygen atoms of the crown ether are coordinated. Also, in this compound the environment around the magnesium atoms is similar to that observed in **109**. It has been suggested that the formation of complexes like **111** is the initial step in the formation of diorganomagnesium–rotaxane-type compounds, *vide infra*.

The structures in the solid state of the bis(thiomethyl)magnesium compounds (MeSCH<sub>2</sub>)<sub>2</sub>Mg(THF)<sub>3</sub> (**112**) and (PhSCH<sub>2</sub>)<sub>2</sub>Mg(THF)<sub>3</sub> (**113**) have been determined by X-ray crystallography<sup>143</sup>. Because these compounds are isostructural, only details of **112** are given here. The overall structural geometry comprises a trigonal bipyramidal coordination geometry of the magnesium atom (Figure 54). The two bonding carbon atoms [Mg–C 2.178(3) and 2.191(3) Å] and an oxygen atom of one of the coordinating THF molecules [Mg–O 2.095(2) Å] are at the equatorial positions. The oxygen atoms of the two other coordinating THF molecules [Mg–O 2.178(2) and 2.185(2) Å] are at the axial sites. The sum of the bond angles in the equatorial plane is 360°, but the O–Mg–O bond angle [163.40(8)°] between the axial oxygen atoms slightly deviates from linear.

An octahedral coordination geometry at magnesium was observed in the solid-state structures of the magnesium acetylides (PhC≡C)<sub>2</sub>Mg(TMEDA)<sub>2</sub> (**114a**)<sup>144</sup> (Figure 55) and (*t*-BuC≡C)<sub>2</sub>Mg(TMEDA)<sub>2</sub> (**114b**)<sup>49</sup>. In **114a** the bonding carbon atoms [Mg–C 2.176(6) and 2.200(6) Å] are *trans* positioned in a perfect linear arrangement (C–Mg–C 180°). Also, the C(1)–Mg–N [89.4(2)°] and C(2)–Mg–N [90.6(2)°] bond angles are in agreement with an almost perfect octahedral coordination geometry. Only the N–Mg–N bond angle [80.4(2)°] of the nitrogen atoms in one TMEDA molecule is less than 90° as a consequence of the bite angle of the TMEDA ligand, but that is compensated by a larger N–Mg–N bond angle between the nitrogen atoms of the two TMEDA molecules. The structural features of **114b** are closely related to those of **114a**.



FIGURE 54. Molecular geometry of **112** in the solid stateFIGURE 55. Molecular geometry of six-coordinate organomagnesium complexes **114a** and **115** in the solid state

Bis(2-thienyl)magnesium crystallizes from THF as a complex  $(2\text{-thienyl})_2\text{Mg}(\text{THF})_4$  (**115**) containing four-coordinated THF molecules. An X-ray crystal-structure determination showed that the bonded thienyl groups, like the acetylenic groups in **114a**, are *trans* positioned [ $\text{C}(1)\text{--Mg--C}(2)$   $180^\circ$ ] (Figure 55)<sup>145</sup>. Also, the other bond angles around magnesium deviate less than  $0.2^\circ$  from the ideal octahedral values.

When diphenylmagnesium is crystallized from a solution containing 1,3-xylyl-18-crown-5, an X-ray crystal-structure determination showed the formation of rotaxane **116** (Figure 56)<sup>146</sup>. Only four of the five oxygen atoms of the crown are involved in coordination to magnesium, two with a relatively short bond distance [2.204(3) and 2.222(4) Å] and two with a longer bond distance [2.516(4) and 2.520(4) Å]. The  $\text{C}(1)\text{--Mg--C}(2)$

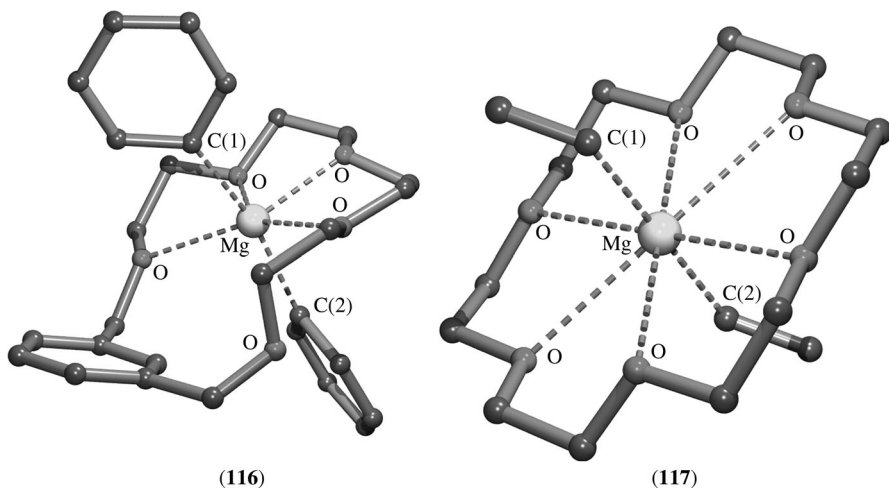


FIGURE 56. Molecular geometries in the solid state of the rotaxane complexes **116** and **117**

angle [ $163.8(2)^\circ$ ] deviates considerably from linear, pointing to a distorted octahedral coordination geometry at magnesium. An isostructural rotaxane was obtained from bis(*p*-*tert*-butylphenyl)magnesium and 1,3-xylyl-18-crown-5<sup>142</sup>.

Diethylmagnesium and 18-crown-6 form a complex  $\text{Et}_2\text{Mg}(18\text{-C-6})$  (**117**) that, according to an X-ray crystal-structure determination, also has a rotaxane structure (Figure 56)<sup>147</sup>. The C(1)–Mg–C(2) arrangement is perfectly linear. At first sight it seems that all six oxygen atoms are involved in bonding to magnesium, although with extreme long bond lengths ranging from 2.767(1) to 2.792(2) Å. As an extreme, **117** might be regarded as a clathrate, having a linear  $\text{Et}_2\text{Mg}$  encapsulated within a crown ether, but bonded weakly to its oxygen atoms.

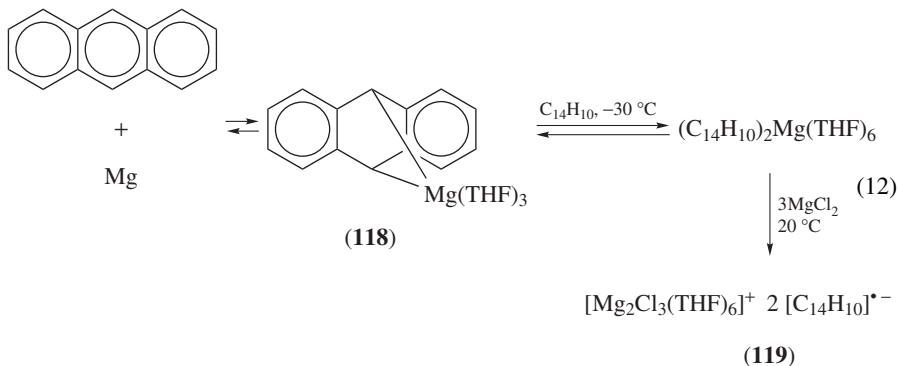
### E. Magnesium Anthracene Compounds

Although the formation of magnesium anthracene was discovered in 1965 and mentioned in a patent<sup>148</sup>, the chemistry of magnesium anthracene systems began to develop thirteen years later, triggered by the discovery of a catalyst system for the hydrogenation of magnesium under mild conditions<sup>113</sup>.

Magnesium anthracene compounds attracted broad interest because of their versatile applications in synthesis and their ability to catalyze reactions of metallic magnesium. In the presence of a catalytic amount of anthracene, magnesium can be hydrogenated to a highly reactive form of magnesium hydride. This magnesium hydride is an excellent reducing agent for transition-metal salts, and can be used for the preparation of Grignard compounds that are inaccessible otherwise. Another application involves a  $\text{MgH}_2\text{--Mg}$  system, available via phase-transfer catalysis of magnesium, that can be used for chemical synthesis and is, moreover, an outstanding medium for hydrogen storage. These, and other topics of the magnesium anthracene system, have been reviewed<sup>149–152</sup>.

Magnesium anthracene  $\text{C}_{14}\text{H}_{10}\text{Mg}(\text{THF})_3$  (**118**) can be prepared in high yield from the reaction of metallic magnesium and anthracene in THF (equation 12)<sup>153</sup>. Kinetic measurements showed that a reversible temperature-dependent equilibrium exists between anthracene, magnesium and **118**, the latter being favored at lower temperatures. This equilibrium opened a way to the preparation of elemental magnesium in a finely dispersed,

very active form, by raising the temperature of a solution of **118**. Another method for the preparation of highly active magnesium involves heating of solid **118** to 200 °C in high vacuum to remove the THF and anthracene, leaving the highly active elemental magnesium as a black pyrophoric powder with a specific surface area of 60–110 m<sup>2</sup> g<sup>-1</sup><sup>154</sup>.



The molecular structures in the solid state of **118**<sup>155</sup> and its 1,4-dimethyl derivative<sup>156</sup> were determined by X-ray crystallography and appeared to be isostructural. In **118** the magnesium atom is bound to C(9) and C(10) with rather long bond distances [2.25(1) and 2.33(1) Å] (Figure 57). Due to the loss of aromaticity in the central ring of the anthracene skeleton, the molecule is folded (26.6°). As the result of three additional coordinating THF molecules [Mg–O 2.059(7), 2.028(8) and 2.091(8) Å], the magnesium atom is five-coordinate.

At  $-30\text{ }^\circ\text{C}$  in THF, in the presence of anthracene a single-electron transfer from **118** to anthracene occurs, with the formation of insoluble  $(\text{C}_{14}\text{H}_{10})_2\text{Mg}(\text{THF})_6$  (equation 12)<sup>156</sup>. A further reaction with  $\text{MgCl}_2$  affords the radical anion complex  $[\text{Mg}_2\text{Cl}_3(\text{THF})_6]^+ [\text{C}_{14}\text{H}_{10}]^{\bullet-}$  (**119**). An X-ray crystal-structure determination of **119** clearly shows the presence of anthracene radical anions as distinct species in the crystal lattice (Figure 58)<sup>156</sup>. The bond lengths and the deformation of the electron density of the anthracene radical anion clearly show that in **119** the LUMO is occupied by one electron<sup>156</sup>.

Also, the structure in the solid state of 9,10-bis(trimethylsilyl)anthracene magnesium was determined by X-ray crystallography<sup>157</sup>. Its structural features are similar to those of

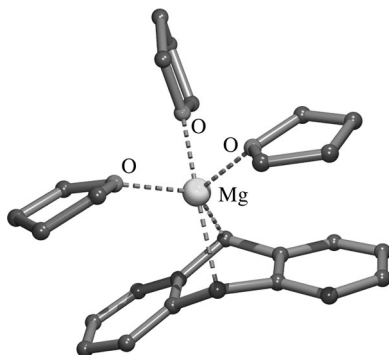


FIGURE 57. Molecular geometry of **118** in the solid state

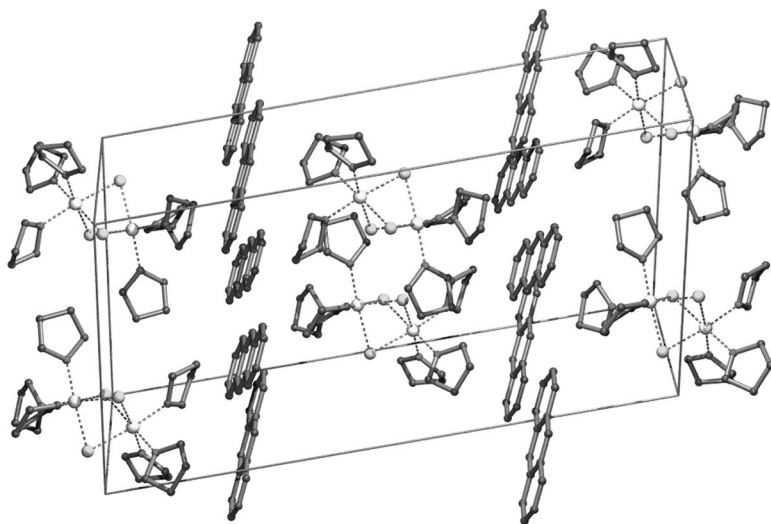


FIGURE 58. Unit-cell contents of crystalline **119** showing the separated anthracene radical anions and  $[\text{Mg}_2\text{Cl}_3(\text{THF})_6]^+$  cations

**118**, but, probably as a result of the sterically demanding  $\text{Me}_3\text{Si}$  groups, only two THF molecules are coordinated to magnesium, giving a tetrahedral coordinated magnesium atom. When this compound is crystallized from THF in the presence of TMEDA, an X-ray crystal-structure determination of the crystalline material (**120**) revealed an asymmetric unit that contains two molecules, one with two coordinating THF molecules and one with a chelate-bonded TMEDA molecule (Figure 59)<sup>158</sup>.

Reaction of **118** with ethylene under a pressure of 60 bar gives a new magnesiacyclic product (**121**) of which the structure in the solid state was established by X-ray

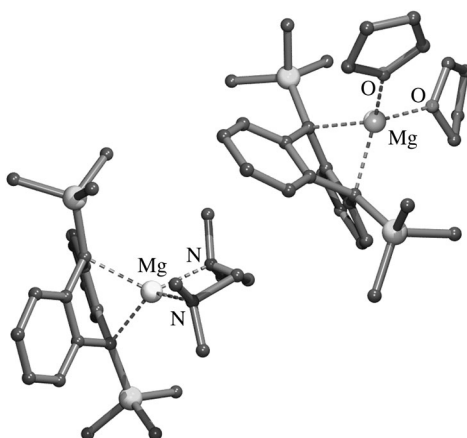
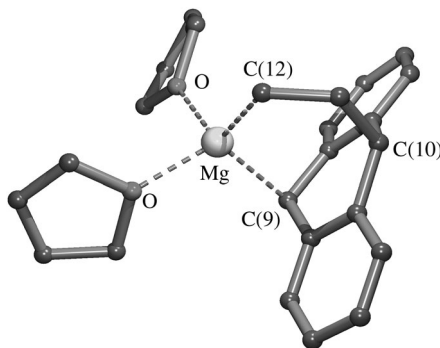


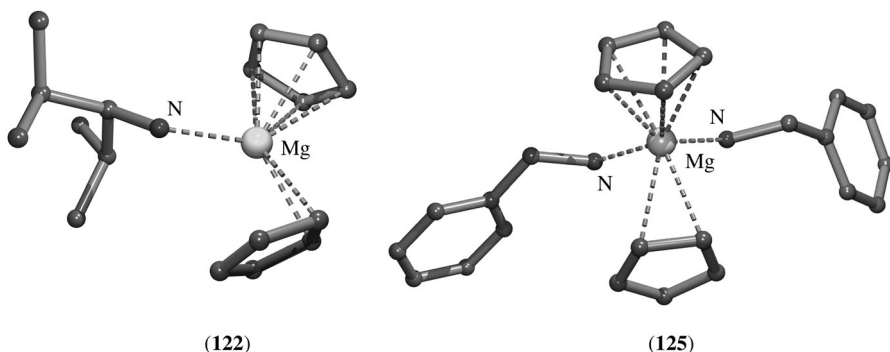
FIGURE 59. The asymmetric unit of **120**

FIGURE 60. Molecular geometry of **121** in the solid state

crystallography (Figure 60)<sup>159</sup>. In **121**, the magnesium atom is bound to an anthracene carbon atom C(9) [Mg–C(9) 2.204(5) Å] and to the terminal carbon atom of the inserted ethylene molecule [Mg–C(12) 2.110(6) Å]. Two THF molecules are coordinated to magnesium, giving it a distorted tetrahedral coordination geometry.

#### F. Donor–Acceptor Complexes of Diorganomagnesium Compounds with Multi-hapto-bonded Groups

Bis(cyclopentadienyl)magnesium reacts with a variety of primary and secondary alkylamines to give the corresponding 1:1 adducts in high yields<sup>160,161</sup>. The structures in the solid state of three of these, i.e.  $\text{Cp}_2\text{Mg}[\text{H}_2\text{NCH}(\text{CHMe}_2)_2]$  (**122**),  $\text{Cp}_2\text{Mg}[\text{H}_2\text{N}(c\text{-C}_6\text{H}_{11})]$  (**123**) and  $\text{Cp}_2\text{Mg}[\text{HN}(i\text{-Pr})(\text{CH}_2\text{Ph})]$  (**124**), were determined by X-ray crystallography. In **122** (Figure 61), one of the cyclopentadienyl groups is  $\eta^5$ -bonded to magnesium with Mg–C bond distances ranging from 2.407(4) to 2.414(4) Å while the other cyclopentadienyl group is  $\eta^2$ -bonded [Mg–C 2.380(4) and 2.301(3) Å]. The nitrogen–magnesium bond length [2.112(3) Å] is in the range as expected for nitrogen-to-magnesium coordination bonds. Likewise, adduct **123** contains a  $\eta^5$ -bonded and a  $\eta^2$ -bonded cyclopentadienyl group, but in **124** both cyclopentadienyl groups are  $\eta^5$ -bonded to magnesium. In the latter compound, a somewhat longer N–Mg distance was found [Mg–N 2.210(4) Å]. Molecular

FIGURE 61. Molecular geometries of amine complexes **122** and **125** in the solid state

orbital calculations and infrared spectroscopic studies of these compounds suggest that a NH–hydrogen–(C<sub>5</sub>H<sub>5</sub>)<sup>−</sup> interaction is involved in the stabilization of these complexes.

In contrast to the other Cp<sub>2</sub>Mg amine complexes, which were purified by sublimation (110 °C/0.05 Torr), the benzylamine complex appeared to be thermally unstable under these conditions and disproportionates into Cp<sub>2</sub>Mg and the bis-benzylamine complex Cp<sub>2</sub>Mg(H<sub>2</sub>NCH<sub>2</sub>Ph)<sub>2</sub> (**125**). The structure of **125** in the solid state was established by an X-ray crystal-structure determination (Figure 61). Its molecular geometry comprises one cyclopentadienyl group  $\eta^5$ -bonded and one cyclopentadienyl group  $\eta^2$ -bonded to magnesium as well as two coordinating benzylamine molecules [Mg–N 2.146(3) and 2.156(2) Å].

When Cp<sub>2</sub>Mg is reacted with *t*-BuNH<sub>2</sub> and the product subsequently recrystallized from THF, complex Cp<sub>2</sub>Mg(H<sub>2</sub>NBu-*t*)(THF) (**126**) is obtained which contains *N*-coordinated *t*-BuNH<sub>2</sub> and *O*-coordinated THF molecules<sup>162</sup>. An X-ray crystal-structure determination clearly showed the presence of one  $\eta^5$ -bonded- and one  $\eta^2$ -bonded cyclopentadienyl group, a coordinating *t*-BuNH<sub>2</sub> molecule [Mg–N 2.140(2) Å] and a coordinating THF molecule [Mg–O 2.067(2) Å].

When Cp<sub>2</sub>Mg is crystallized from neat THF, its bis-THF adduct Cp<sub>2</sub>Mg(THF)<sub>2</sub> (**127**) is obtained<sup>163</sup>. Its X-ray crystal-structure determination shows, apart from the two coordinated THF molecules [Mg–O 2.088(2) and 2.098(2) Å], one cyclopentadienyl group which is  $\eta^5$ -bonded to magnesium. The distances between magnesium and the carbon atoms of the other cyclopentadienyl group, one being 2.282(2) Å and the next closest one 2.736(2) Å, suggest that this cyclopentadienyl group is  $\eta^1$ -bonded to magnesium.

Bis(indenyl)magnesium has a polymeric structure in the solid state, the details of which have been discussed in a previous section. When it is recrystallized from THF, a discrete monomeric bis-THF adduct, indenyl<sub>2</sub>Mg(THF)<sub>2</sub> (**128**), is obtained<sup>164</sup>. An X-ray crystal-structure determination shows that the magnesium atom has one relatively short bond [2.256(3) Å] with C(1) of each of the indenyl groups, but also interactions with the two adjacent carbon atoms at a much longer distance [Mg–C 2.723(3) and 2.738(3)]. This bonding mode was described as intermediate between  $\eta^1$  and  $\eta^3$ .

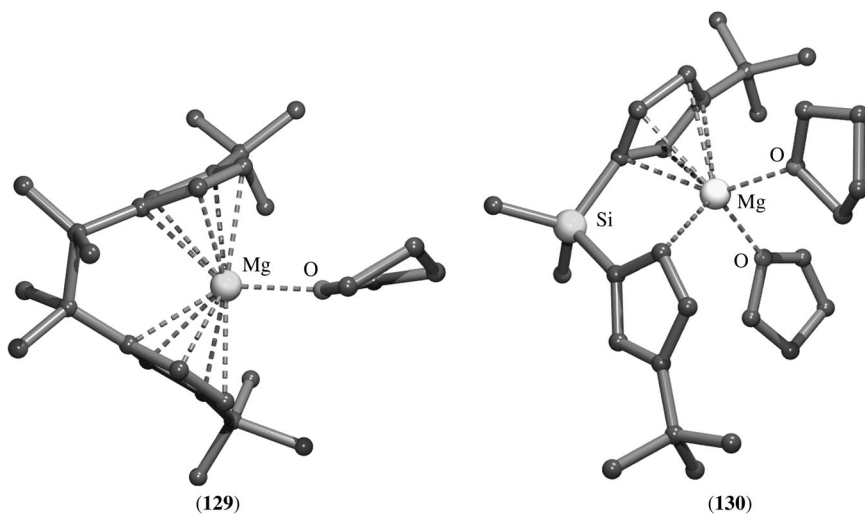
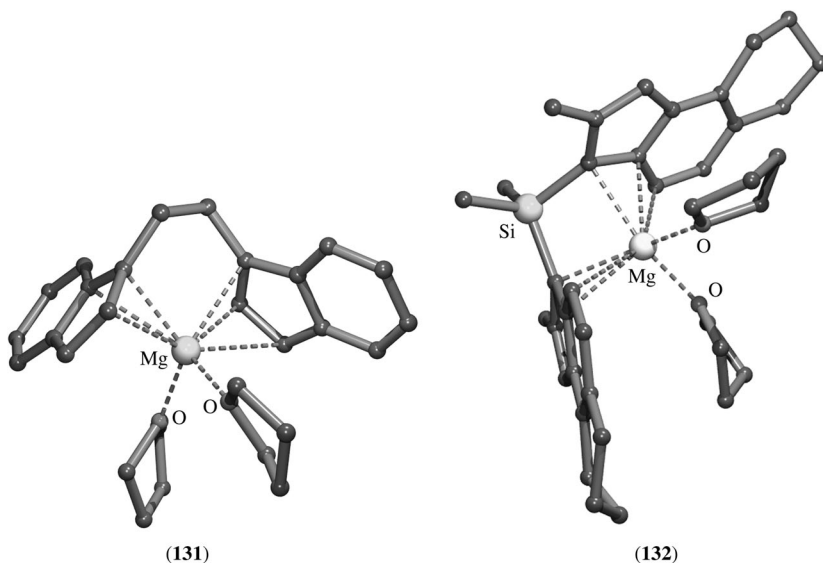
Several *ansa*-magnesocene complexes have been prepared and structurally characterized by X-ray diffraction<sup>165</sup>.

The tetramethylethanediy-bridged, *t*-butyl-substituted bis-cyclopentadienyl complex Me<sub>4</sub>C<sub>2</sub>(3-*t*-BuC<sub>5</sub>H<sub>3</sub>)<sub>2</sub>Mg(THF) (**129**) is present in the solid state as a *meso*-diastereoisomer. It has a structure in which both cyclopentadienyl groups are  $\eta^5$ -bonded to magnesium while only one THF molecule is coordinated to magnesium (Figure 62)<sup>165</sup>.

For the Me<sub>2</sub>Si-bridged analog Me<sub>2</sub>Si(3-*t*-BuC<sub>5</sub>H<sub>3</sub>)<sub>2</sub>Mg(THF)<sub>2</sub> (**130**) a different bonding situation is observed at magnesium (Figure 62). One of the cyclopentadienyl groups is  $\eta^5$ -bonded to magnesium with three relatively short Mg–C bond distances (2.34–2.41 Å) and two longer ones (2.64–2.68 Å). The other cyclopentadienyl group is  $\eta^1$ -bonded to magnesium (Mg–C 2.36 Å). The different bonding modes of the cyclopentadienyl rings result in a large dihedral angle of 77° between the planes of both cyclopentadienyl rings. As a result of the widened coordination gap two THF molecules are coordinated to the magnesium atom.

In the *ansa*-C<sub>2</sub>H<sub>4</sub>-bridged bis-indenyl complex C<sub>2</sub>H<sub>4</sub>(indenyl)<sub>2</sub>Mg(THF)<sub>2</sub> (**131**)<sup>165</sup> (Figure 63), the bonding of the five-membered rings to magnesium is similar to that observed in (indenyl)<sub>2</sub>Mg(THF)<sub>2</sub> (**128**), *vide supra*. Based on the observed bond distances to magnesium of the carbon atoms in the five-membered rings, the bonding mode is regarded to be intermediate between  $\eta^1$  and  $\eta^3$ . Like in (indenyl)<sub>2</sub>Mg(THF)<sub>2</sub>, two THF molecules are coordinated to magnesium.

Because no crystals suitable for an X-ray crystal-structure determination could be obtained for the Me<sub>2</sub>Si-bridged analog of **131**, the structure of its alkyl-substituted

FIGURE 62. Structures of *ansa*-magnesocene complexes **129** and **130** in the solid stateFIGURE 63. Structures of *ansa*-magnesocene complexes **131** and **132** in the solid state

derivative  $\text{Me}_2\text{Si}(2\text{-Me-6,7,8,9-tetrahydro-benz[e]indenyl})_2\text{Mg}(\text{THF})_2$  (**132**)<sup>165</sup> (Figure 63) was investigated. The indenyl–magnesium binding in the latter differs substantially from that observed in **131**. In **132** both indenyl groups are bound in an exocyclic  $\eta^3$ -geometry to magnesium. The magnesium atom is closest to a  $\text{C}_3$ -fragment comprising the bridgehead and the adjacent angular position as well as the neighboring carbon atom in

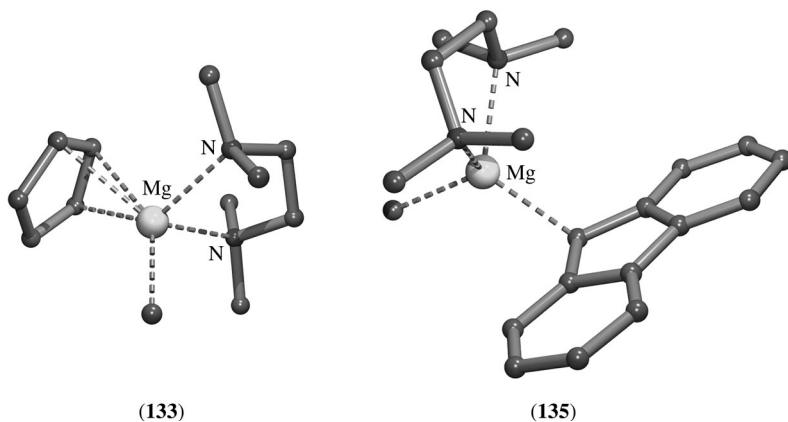


FIGURE 64. Molecular geometries of the heteroleptic organomagnesium TMEDA complexes **133** and **135** in the solid state

the aromatic six-membered ring. Coordination saturation at magnesium is reached by the additional coordination of two THF molecules.

A straightforward protonolysis reaction of  $\text{Me}_2\text{Mg}(\text{TMEDA})$  with the carbon-acids cyclopentadiene, indene and fluorene affords the corresponding heteroleptic organomagnesium TMEDA complexes  $\text{Me}(\text{Cp})\text{Mg}(\text{TMEDA})$  (**133**),  $\text{Me}(\text{indenyl})\text{Mg}(\text{TMEDA})$  (**134**) and  $\text{Me}(\text{fluorenyl})\text{Mg}(\text{TMEDA})$  (**135**), respectively, in quantitative yield. The structures in the solid state of these complexes have been determined by X-ray crystallography<sup>166</sup>. In **133** the cyclopentadienyl group is  $\eta^3$ -bonded to magnesium [ $\text{Mg}-\text{C}$  2.351(3), 2.488(3) and 2.488(3) Å] while the methyl group is  $\sigma$ -bonded to magnesium (Figure 64). The TMEDA molecule is  $N,N'$ -chelate bonded to magnesium [ $\text{Mg}-\text{N}$  2.256(2) and 2.290(2) Å].

The structure in the solid state of **134** is closely related to that of **133**. Likewise, in **134** the indenyl group is  $\eta^3$ -bonded to magnesium.

In the fluorenyl derivative **135** the methyl group is  $\sigma$ -bonded and the TMEDA molecule  $N,N'$ -chelate bonded to magnesium (Figure 64). The fluorenyl group, however, is  $\eta^1$ -bonded to magnesium [ $\text{Mg}-\text{C}$  2.273(2) Å], resulting in a distorted tetrahedral coordination geometry at the magnesium atom.

Heteroleptic (isodicyclopentadienyl)(butyl)magnesium TMEDA complex (**136**) was prepared via a quantitative redistribution reaction from its parent magnesocene, *exo,exo*-bis(isodicyclopentadienyl)magnesium (**61**) (*vide supra*) and  $\text{Bu}_2\text{Mg}$  in the presence of TMEDA<sup>98</sup>. An X-ray crystal-structure determination of **136** showed that the magnesium atom is positioned on the *exo* face and interacts in a  $\eta^5$ -manner with the cyclopentadienyl ring with  $\text{Mg}-\text{C}$  bond distances ranging from 2.439(4) to 2.545(4) Å (Figure 65). The butyl group is  $\sigma$ -bonded to magnesium [ $\text{Mg}-\text{C}$  2.145(4) Å] and the two nitrogen atoms of the chelate-bonded TMEDA molecule complete the coordination sphere of magnesium.

Tetrameric  $[\text{CpMgC}\equiv\text{CPh}]_4$  (**64**) (*vide supra*) has a heterocubane structure and deaggregates in THF solution to a dimeric THF complex  $[\text{Cp}(\text{PhC}\equiv\text{C})\text{Mg}(\text{THF})_2]_2$  (**137**)<sup>101</sup>. The overall structural geometry of **137** comprises two magnesium atoms between which two terminal acetylenic carbon atoms are bridge-bonded in a slightly asymmetric manner [ $\text{Mg}-\text{C}$  2.185(3) and 2.266(3) Å] (Figure 65). To each of the magnesium atoms a cyclopentadienyl ring is  $\eta^5$ -bonded and coordination saturation at magnesium is reached by the coordination of a THF molecule.



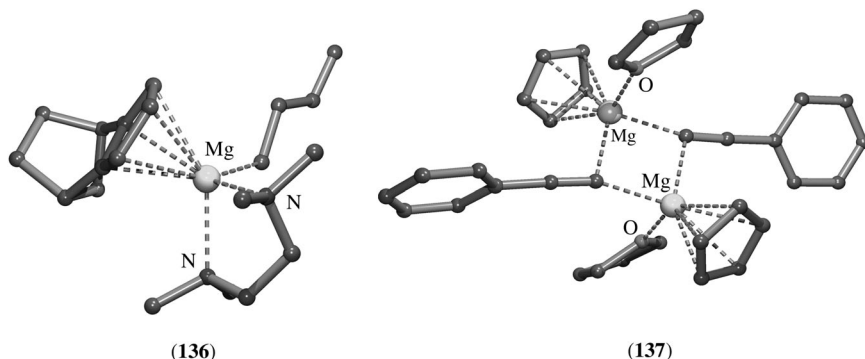


FIGURE 65. Molecular geometries of the heteroleptic organomagnesium complexes **136** and **137**

So far, only multi-hapto-bonded groups have been considered that contain a cyclic unsaturated functionality. It appeared that linear conjugated unsaturated functionalities are also capable of being involved in such multi-hapto interactions.

The 1,4-bis(phenyl)-2-butene-1,4-diylmagnesium tris-THF complex (**138**) has been prepared from activated magnesium and 1,4-diphenyl-1,3-butadiene, and its structure in the solid state was determined by X-ray crystallography<sup>167</sup>. Its molecular geometry comprises a  $\text{Mg}(\text{THF})_3$  unit (average  $\text{Mg}-\text{O}$  2.12 Å) that has a  $\eta^4$ -interaction with the butene skeleton. The butene skeleton adopts a *s-cis* geometry in which the four central carbon atoms lie in one plane, with the magnesium atom positioned 1.71 Å above this plane (Figure 66). The bond distances between magnesium and the C(1) and C(4) atoms of the butene moiety, 2.32 and 2.26 Å, respectively, are shorter than the  $\text{Mg}-\text{C}(2)$  and  $\text{Mg}-\text{C}(3)$  interactions of 2.56 and 2.52 Å.

The structure in the solid state of the 1,4-bis(trimethylsilyl)-2-butene-1,4-diylmagnesium TMEDA complex (**139**) shows similarities with that of **138** (Figure 66)<sup>168</sup>. Also, in **139** the butene skeleton has a  $\eta^4$ -interaction with magnesium with shorter  $\text{Mg}-\text{C}(1)$  and  $\text{Mg}-\text{C}(4)$  bonds [2.200(9) and 2.191(9) Å, respectively] and longer  $\text{Mg}-\text{C}(2)$  and  $\text{Mg}-\text{C}(3)$  bonds [2.381(8) and 2.399(8) Å, respectively]. Instead of the three coordinating THF molecules in **138**, in **139** a *N,N'*-chelate bonded TMEDA molecule is present.

Another type of ligand, capable of forming multi-hapto interactions with metals, are boron and boron-carbon cage compounds of which in particular the carboranes have been used extensively in organometallic chemistry<sup>169</sup>. The structures in the solid state of a few magnesacarboranes have been determined by X-ray crystallographic studies.

An X-ray crystal-structure determination of the magnesacarborane, *closo*-1- $\text{Mg}(\text{THF})_3$ -2,4-( $\text{Me}_3\text{Si}$ )<sub>2</sub>-2,4- $\text{C}_2\text{B}_4\text{H}_4$  (**140**), showed that this compound exists in the solid state as a discrete monomer<sup>170</sup>. The molecular geometry of **140** comprises a  $\text{Mg}(\text{THF})_3$  moiety, of which the magnesium atom is located at an apical position above an open pentagonal face of the  $\text{C}_2\text{B}_4$  cage (Figure 67). The observed  $\text{Mg}-\text{C}$  and  $\text{Mg}-\text{B}$  bond distances [ $\text{Mg}-\text{C}$  2.390(3) and 2.429(3) Å,  $\text{Mg}-\text{B}$  2.452(3), 2.404(3) and 2.381(4) Å] are indicative for  $\eta^5$ -bonding to magnesium.

The molecular geometry of the magnesacarborane *closo*-1- $\text{Mg}(\text{TMEDA})$ -2,3-( $\text{Me}_3\text{Si}$ )<sub>2</sub>-2,3- $\text{C}_2\text{B}_4\text{H}_4$  (**141**) in the solid state shows some similarities with that of **140**. In this case, a  $\text{Mg}(\text{TMEDA})$  moiety is  $\eta^5$ -bonded to the open pentagonal face of the  $\text{C}_2\text{B}_4$  cage (Figure 67)<sup>171,172</sup>. However, in contrast to **140**, here the molecule is dimeric via an interaction of the magnesium atoms with the unique boron atoms of the neighboring  $\text{C}_2\text{B}_4\text{H}_4$  cage involving two  $\text{Mg}-\text{H}-\text{B}$  bridges.

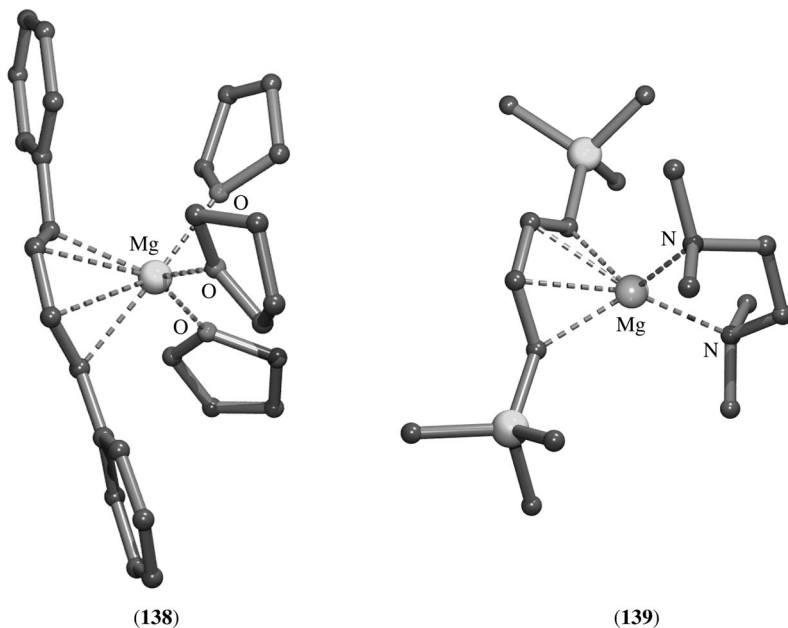


FIGURE 66. Molecular geometries of the 2-butene-1,4-diylmagnesium complexes **138** and **139**

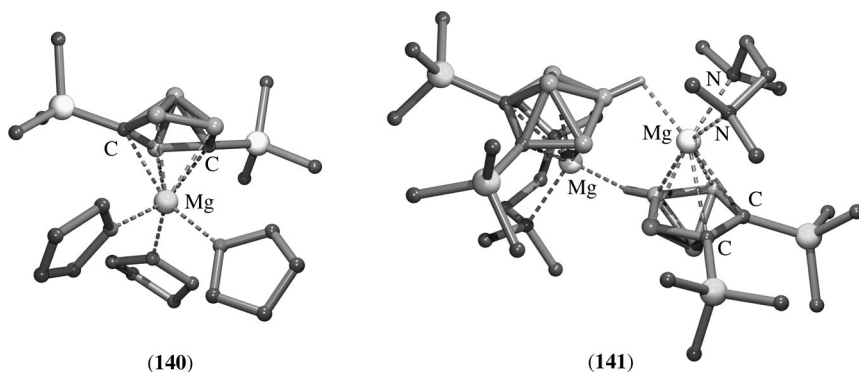
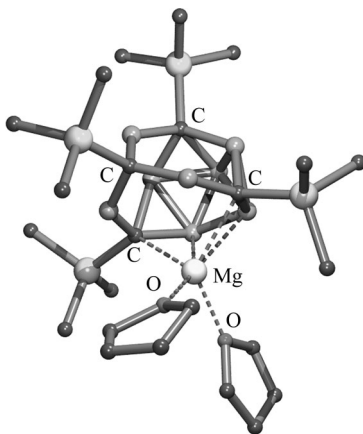


FIGURE 67. Molecular geometry of the magnesium C<sub>2</sub>B<sub>4</sub>H<sub>4</sub> carboranes **140** and **141**

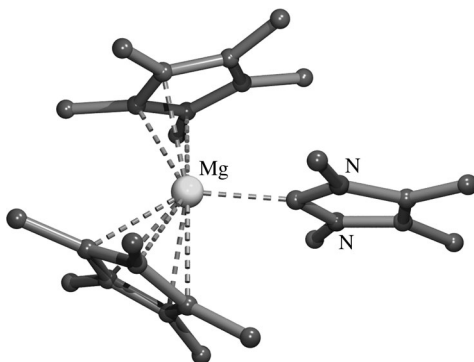
Also, magnesacarboranes with a C<sub>4</sub>B<sub>8</sub>H<sub>8</sub> cage have been prepared and were structurally characterized in the solid state by X-ray diffraction studies. The magnesacarborane (THF)<sub>2</sub>Mg(Me<sub>3</sub>Si)<sub>4</sub>C<sub>4</sub>B<sub>8</sub>H<sub>8</sub> (**142**) has been prepared from *nido*-2,4,6,12-(Me<sub>3</sub>Si)<sub>4</sub>-2,4,6,12-C<sub>4</sub>B<sub>8</sub>H<sub>8</sub> and metallic magnesium in THF. Its molecular geometry in the solid state comprises a Mg(THF)<sub>2</sub> unit that is η<sup>4</sup>-bonded to four adjacent atoms, two carbon [Mg–C 2.315(10) and 2.326(9) Å] and two boron atoms [Mg–B 2.393(12) and 2.402(11)], of a seven-membered open face of the carborane cage (Figure 68)<sup>173</sup>.

FIGURE 68. Molecular geometry of magnesacarborane **142**

The boron-substituted analogs  $(\text{THF})_2\text{Mg}(\text{Me}_3\text{Si})_4(t\text{-BuB})\text{C}_4\text{B}_7\text{H}_7$  (**143**) and  $(\text{THF})_2\text{Mg}(\text{Me}_3\text{Si})_4(\text{MeB})\text{C}_4\text{B}_7\text{H}_7$  (**144**) have also been prepared and structurally characterized in the solid state<sup>174</sup>. Their structures are essentially the same as that of **142**, except that one of the borons in **143** and **144** is alkylated.

So far, only diorganomagnesium complexes have been considered in which the heteroatom involved in coordination to magnesium is either nitrogen or oxygen. The only other functional group forming a coordination bond to magnesium in organomagnesium compounds that have been structurally characterized are carbenes.

Bis(pentamethylcyclopentadienyl)magnesium reacts smoothly with 1,3,4,5-tetramethylimidazol-2-ylidene to form carbene complex **145**<sup>175</sup>. An X-ray crystal-structure determination unambiguously showed that the ligand is bound to magnesium via its carbene carbon atom [ $\text{Mg}-\text{C}$  2.194(2) Å] (Figure 69). Compared to  $(\text{Me}_5\text{C}_5)_2\text{Mg}$  itself, in which both cyclopentadienyl groups are  $\eta^5$ -bonded to magnesium, the bonding mode of the cyclopentadienyl groups in **145** has changed. One of these is still  $\eta^5$ -bonded to magnesium with average  $\text{Mg}-\text{C}$  distances of 2.46(8) Å, but the other one exhibits a ‘slipped’

FIGURE 69. Molecular geometry of carbene complex **145**

geometry with three carbon atoms closest to magnesium at distances of 2.309(3), 2.465(2) and 2.605(2) Å. Together with the observed C–C bond distances in this ring, these values suggest a bonding mode of this cyclopentadienyl ring with magnesium that is intermediate between  $\eta^3$  and  $\eta^1$  ( $\sigma$ -bonded).

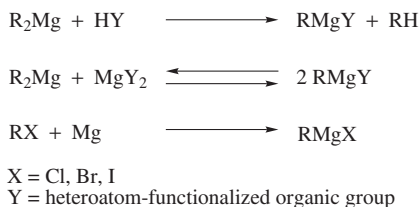
A similar carbene complex was obtained from the reaction of  $(\text{Me}_4\text{C}_5\text{H})_2\text{Mg}$  with 1,3-di-isopropyl-4,5-dimethylimidazol-2-ylidene, with a structure in the solid state that is closely related to that of **145**<sup>95</sup>.

## IV. HETEROLEPTIC $\text{RMgY}$ COMPOUNDS

### A. Introduction

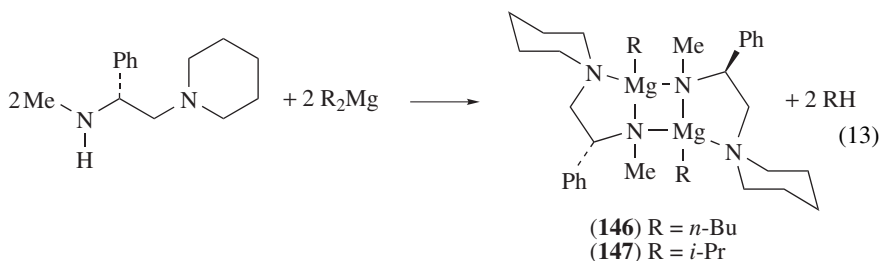
In heteroleptic monoorganomagnesium compounds  $\text{RMgY}$  an organic group is  $\sigma$ -bonded or, in some particular cases, multi-hapto bonded to magnesium via several carbon atoms. The other group, Y, is bound to magnesium via a heteroatom. Examples of the latter groups are: halogen atoms, oxygen-containing groups like alkoxides, nitrogen-containing groups like primary and secondary amides, and other groups functionalized with heteroatoms like sulfur and phosphorus.

For the synthesis of heteroleptic monoorganomagnesium compounds, three major pathways are available (Scheme 1).



SCHEME 1. The pathways for the synthesis of heteroleptic organomagnesium compounds

The first route involves the protonolysis of one of the alkyl or aryl groups of dialkyl- or diarylmagnesium compounds by an organic molecule containing an acidic proton bound to a heteroatom. Examples of such acidic compounds are alcohols and primary and secondary amines. A nice illustration of this first route is the formation of organomagnesium amides from the reaction of enantiomerically pure *N*-(2-methylamino-2-phenylethyl)piperidine with  $\text{Bu}_2\text{Mg}$  or  $i\text{-Pr}_2\text{Mg}$  (equation 13). The *n*-butylmagnesium derivative (**146**) has been successfully applied in the enantioselective addition of butyl groups to aldehydes<sup>176</sup>, and the iso-propylmagnesium compound (**147**) has been used for the enantioselective reduction of ketones<sup>177</sup>.



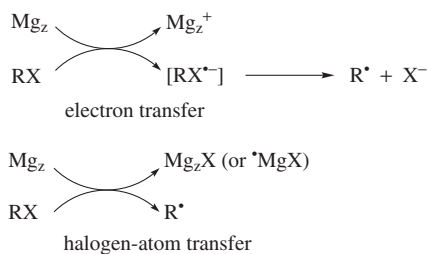
The second route (Scheme 1) is a redistribution reaction, in fact the Schlenk equilibrium. This route may be used in the reverse direction for the preparation of pure diorganomagnesium compounds from organomagnesium halides. Addition of a ligand, usually dioxane, that forms an insoluble complex with magnesium dihalide, shifts the Schlenk equilibrium completely to the left side and allows isolation of pure diorganomagnesium compounds from the remaining solution<sup>178</sup>.

The third pathway (Scheme 1) for the preparation of heteroleptic monoorganomagnesium compounds, especially monoorganomagnesium halides, involves the reaction of an organic halide with metallic magnesium, the classical Grignard reaction (equation 14).



The reaction of the organic halide with magnesium is carried out in a non-protic polar solvent, usually diethyl ether or THF. Typical by-products are  $\text{RR}$ ,  $\text{RH}$  and  $\text{R}(\text{-H})$  (alkene), resulting from coupling and disproportionation reactions of the organic moiety. Also, by-products resulting from solvent attack are sometimes formed, but usually to a lesser extent.

Although the formation of Grignard reagents at first looks simple (equation 14), the mechanisms involved are still speculative despite about a hundred years of work and have been the subject of several reviews<sup>179–182</sup>. The mechanisms of the formation of Grignard reagents can be divided into two parts, an organic and an inorganic one. The organic mechanism traces the organic fragment  $\text{R}$  from  $\text{RX}$  to  $\text{RMgX}$  and by-products containing residues from  $\text{R}$  and occasionally the solvent. The inorganic part of the mechanism traces the  $\text{Mg}$  from metallic magnesium to  $\text{RMgX}$  and deals with surface films, inhibition, initiation and activation. It should be noted that the organic part of the mechanism has received far more attention than the inorganic part. Nowadays, there is overwhelming evidence that radicals play a major role in the formation of Grignard reagents. In the initial step, in which  $[\text{RX}^{\bullet-}]$  may be an intermediate or transition structure, both electron transfer and halogen-atom transfer may play a role (Scheme 2). For further details of these mechanistic studies, the reader is urged to consult the references cited.



SCHEME 2. The initial step in the formation of Grignard reagents

Due to the presence of an electronegative group directly bound to magnesium, the Lewis acidity of magnesium is enhanced and therefore heteroleptic monoorganomagnesium compounds readily form complexes with donor molecules. Moreover, these directly bound heteroatoms can act as multi-electron pair donors which facilitates aggregate formation in which these heteroatoms form four-electron three-center bridge-bonds between two or more magnesium atoms. The presence of the unavoidable Schlenk equilibrium in solutions of heteroleptic monoorganomagnesium compounds should also be taken into account. When crystalline material is harvested from such solutions for structural studies,

the structures found in the solid state do not necessarily represent structures that actually are present (in a majority) in solution. Which particular compound, aggregated or not, crystallizes from solution is determined by several factors like thermodynamic stability, solubility and packing effects in the crystal lattice.

Based on the nature of the heteroatom directly bound to magnesium, the structures of heteroleptic monoorganomagnesium compounds can be divided into several sub-classes that will be discussed separately below. These sub-classes are: (i) monoorganomagnesium cations (i.e. compounds consisting of ion pairs), (ii) monoorganomagnesium halides, the Grignard reagents, (iii) monoorganomagnesium compounds with an oxygen atom  $\sigma$ -bonded to magnesium, (iv) monoorganomagnesium compounds with a nitrogen atom  $\sigma$ -bonded to magnesium and (v) monoorganomagnesium compounds containing anions  $\sigma$ -bonded to magnesium via other heteroatoms.

## B. Monoorganomagnesium Cations

As has been outlined in the section on organomagnesiates (*vide supra*), in the presence of a 2,1,1-cryptand diorganomagnesium compounds undergo a disproportionation reaction, forming an organomagnesiates anion and a monoorganomagnesiates cation encapsulated in the 2,1,1-cryptand<sup>55</sup>. Likewise, a crystalline material containing  $[\text{MeMg}(\text{15-C-5})]^+$  cations and a linear polymeric chain in which the  $[\text{Me}_5\text{Mg}_2]^-$  anion is the repeating unit has been isolated from a solution of  $\text{Me}_2\text{Mg}$  and 15-crown-5<sup>57</sup>.

When a solution of heteroleptic  $\text{MeMgCp}$  is crystallized in the presence of the azacrown 1,4,8,11-tetramethyl-1,4,8,11-tetraazacyclotetradecane (14-N-4) a crystalline material is obtained (**148a**) that, according to its X-ray crystal-structure determination, consists of isolated  $\text{MeMg}(\text{14-N-4})$  cations and cyclopentadienyl anions in the crystal lattice (Figure 70)<sup>183</sup>. In the cationic  $\text{MeMg}(\text{14-N-4})^+$  fragment  $[\text{Mg}-\text{C} \ 2.136(7) \text{ \AA}]$  all four nitrogen atoms are involved in coordination to magnesium  $[\text{Mg}-\text{N} \text{ ranging from } 2.208(6) \text{ to } 2.252(5) \text{ \AA}]$  resulting in a penta-coordinate magnesium atom.

Similarly, crystallization of a solution containing  $\text{Me}_2\text{Mg}$ ,  $\text{Me}_2\text{Cd}$  and 14-N-4 affords a crystalline product  $[\text{MeMg}(\text{14-N-4})]^+ [\text{Me}_3\text{Cd}]^-$  (**148b**)<sup>184</sup>. The cationic  $[\text{MeMg}(\text{14-N-4})]^+$  fragment is chemically identical with that of **148a** and shows only small differences in bond distances and angles.

When  $\text{MeMgI}$  is prepared in THF/DME as a solvent, a crystalline material  $[\text{MeMg}(\text{DME})_2(\text{THF})]^+ \text{I}^-$  (**149**) was isolated in high yield. An X-ray crystal-structure deter-

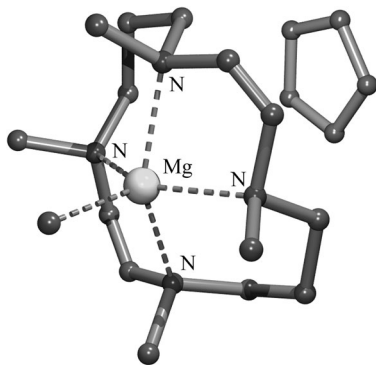


FIGURE 70. Molecular geometry of the  $\text{MeMg}(\text{14-N-4})$  cation and the cyclopentadienyl anion **148a**

mination showed that in the solid state **149** consists of isolated  $[\text{MeMg}(\text{DME})_2(\text{THF})]^+$  cations and iodide anions. In the cation two DME molecules are *O,O*-chelate bonded to magnesium and an additional coordinating THF molecule makes the magnesium atom octahedral coordinate (Figure 71)<sup>185</sup>. It should be noted that such octahedral arrangements are chiral. In fact, **149** crystallizes at  $-20^\circ\text{C}$  as conglomerates in space group  $P2_12_12_1$ , i.e. the crystals are chiral. When crystallization is performed at much lower temperature ( $-60^\circ\text{C}$ ) a racemic phase crystallizes in space group  $Pbca$  in which as a requirement of space group symmetry both enantiomers,  $\Delta$ -*cis* and  $\Lambda$ -*cis*, are present.

The only organomagnesium cation, containing a multi-hapto-bonded organic group, for which the structure in the solid state has been elucidated by X-ray crystallography, is  $[\text{CpMg}(\text{PMDTA})]^+ [\text{Cp}_2\text{Ti}]^-$  (**150**). This compound was obtained from the reaction of  $\text{Cp}_2\text{Mg}$  with  $\text{CpTiI}$  in the presence of PMDTA. Its solid-state structure comprises isolated  $[\text{CpMg}(\text{PMDTA})]^+$  cations and  $[\text{Cp}_2\text{Ti}]^-$  anions in the crystal lattice<sup>186</sup>.

In the cation of **150** (Figure 72) the cyclopentadienyl group is  $\eta^5$ -bonded to magnesium with  $\text{Mg}-\text{C}$  distances of 2.40(3), 2.38(2), 2.44(3), 2.41(2) and 2.40(2) Å. The PMDTA molecule is chelate-bonded with its three nitrogen atoms to magnesium [ $\text{Mg}-\text{N}$  2.21(2), 2.16(2) and 2.25(2) Å].

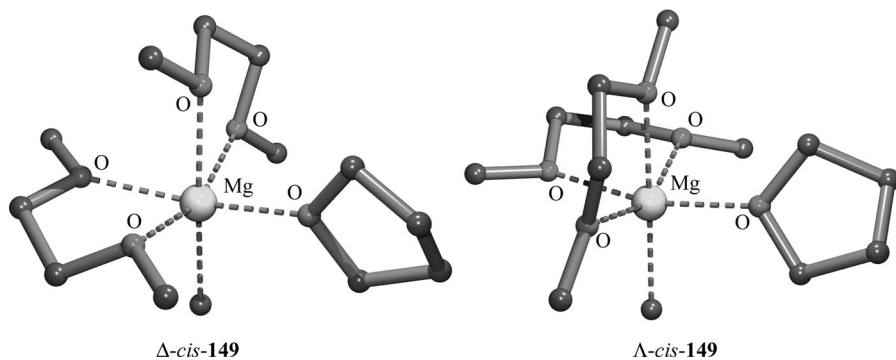


FIGURE 71. The two enantiomers of the chiral cation  $\text{cis}-[\text{MeMg}(\text{DME})_2(\text{THF})]^+$

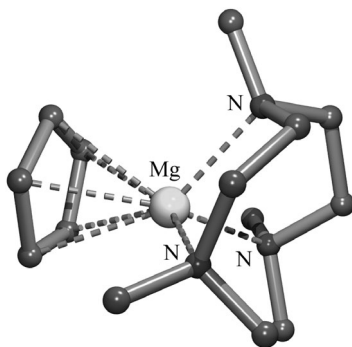


FIGURE 72. Molecular geometry of the  $[\text{CpMg}(\text{PMDTA})]^+$  cation of **150** in the solid state

### C. Monoorganomagnesium Compounds $\text{RMgY}$ with $\text{Y} = \text{halogen}$ (Grignard Reagents)

One of the most fascinating and fundamental problems in organic chemistry concerns the constitution of Grignard reagents in ethereal solution. A closely related problem involves the mechanism of formation of Grignard reagents and the mechanism or mechanisms involved in the reaction of Grignard reagents with organic functional groups<sup>3–5, 11, 13, 14, 187</sup>. Structures in the solid state, obtained by X-ray crystallography from crystals grown from Grignard solutions, have helped to partly solve these problems. However, as mentioned before, the obtained structures are not necessarily representative for the bulk of the solution but only give an indication of what types of structures might be present in solution. Various structural motifs for Grignard reagents in the solid state have been observed: monomers, dimers and higher aggregates, with coordination numbers at magnesium varying from four to six. A particular type of Grignard reagents are those containing a heteroatom-functionalized group, which is capable of coordinating intramolecularly to magnesium. Those compounds can be regarded as containing a built-in coordinating solvent molecule.

The first Grignard compound that was structurally characterized in the solid state by X-ray crystallography was  $\text{PhMgBr}(\text{OEt}_2)_2$  (**151**)<sup>19, 188</sup>. It was unambiguously established that **151** exists in the solid state as a monomer with the phenyl group  $\sigma$ -bonded to magnesium. Furthermore, the bromine atom [ $\text{Mg}-\text{Br}$  2.44(2) Å] and two oxygen atoms [ $\text{Mg}-\text{O}$  2.01(4) and 2.06(4) Å] of two coordinating diethyl ether molecules are bonded to magnesium, giving it a distorted tetrahedral coordination geometry. Due to poor reflection data the location of the phenyl-carbon atoms could not be obtained exactly. Similarly,  $\text{PhMgBr}(\text{THF})_2$  (**152**) exists in the solid state as a discrete monomer, but also in this case reflection data were poor<sup>189</sup>. For  $\text{EtMgBr}(\text{OEt}_2)_2$  (**153**) a more reliable data set was obtained, allowing a more detailed discussion of its structure in the solid state<sup>20, 190</sup>. Compound **153** exists in the solid state as a monomer with four-coordinate magnesium as a result of bonding of the ethyl group [ $\text{Mg}-\text{C}$  2.15(2) Å], the bromine atom [ $\text{Mg}-\text{Br}$  2.48(1) Å] and two oxygen atoms [ $\text{Mg}-\text{O}$  2.03(2) and 2.05(2) Å] of two coordinating diethyl ether molecules (Figure 73). With the exception of the  $\text{C}-\text{Mg}-\text{Br}$  bond angle [ $125.0(5)^\circ$ ] the bond angles around the magnesium atom are close to the ideal tetrahedral value, indicating an only slightly distorted tetrahedral coordination geometry at magnesium.

So far, the two other Grignard compounds known as having a monomeric structure in the solid state with four-coordinate magnesium are  $(\text{Ph}_3\text{C})\text{MgBr}(\text{OEt}_2)_2$  (**154**)<sup>155</sup>

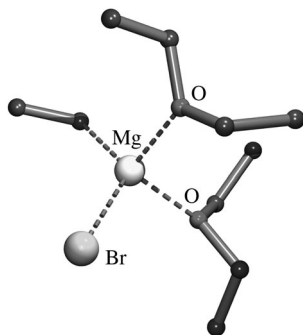


FIGURE 73. Molecular geometry of **153** in the solid state



and 2,6-Tip<sub>2</sub>C<sub>6</sub>H<sub>3</sub>MgBr(THF)<sub>2</sub> (**155**)<sup>191</sup> (Tip = 2,4,6-*i*-Pr<sub>3</sub>C<sub>6</sub>H<sub>2</sub>). The overall structural geometries of **154** and **155** with respect to the magnesium environment are closely related to that of **153**.

The structures of three monomeric organomagnesium bromides in which the magnesium center is penta-coordinate have been established in the solid state. These compounds are: MeMgBr(THF)(TMEDA) (**156**)<sup>132</sup>, 9-bromo-9-[(bromomagnesium)methylene]fluorene tris-THF complex (**157**)<sup>192</sup> and MeMgBr(THF)<sub>3</sub> (**158**)<sup>193</sup>.

The structure of **156** comprises a magnesium atom to which the methyl group and the bromine atom are  $\sigma$ -bonded [Mg–C 2.25(1) Å, Mg–Br 2.485(1) Å], the TMEDA ligand is *N,N'*-chelate bonded [Mg–N 2.246(2) and 2.334(3) Å] and an additional coordinating THF molecule [Mg–O 2.204(9) Å] completes five-coordination at magnesium (Figure 74). The magnesium atom has a trigonal bipyramidal coordination geometry with the carbon atom, the bromine atom and one of the nitrogen atoms of the TMEDA molecule at the equatorial sites. The other nitrogen atom and the oxygen atom of the coordinating THF molecule reside at the apical positions. The sum of the bond angles in the equatorial plane is 360°. The bond angle between magnesium and the apical bonded nitrogen and oxygen atom [N–Mg–O 166.5(5)°] deviates considerably from linear, but most probably is a consequence of the small bite angle of the TMEDA ligand.

In **157**, which represents a magnesium carbenoid compound, the magnesium atom has a trigonal bipyramidal coordination geometry with the carbon atom bound to magnesium [Mg–C 2.19(1) Å], the bromine atom [Mg–Br 2.517(3) Å] and an oxygen atom [Mg–O 2.045(7) Å] of one of the coordinating THF molecules at the equatorial positions (Figure 74).

Also, the magnesium atom in **158** has a trigonal bipyramidal geometry. However, due to disorder in the structure, details cannot be given.

A series of Grignard reagents has been recrystallized from neat dimethoxyethane (DME) resulting in compounds in which, according to X-ray crystal-structure determinations, the magnesium atoms have an octahedral coordination environment, due to the *O,O'*-chelate bonding of both DME molecules. The following compounds have been isolated and structurally characterized: *n*-PrMgBr(DME)<sub>2</sub> (**159**)<sup>61</sup>, (allyl)MgBr(DME)<sub>2</sub> (**160**)<sup>61</sup>, *i*-PrMgBr(DME)<sub>2</sub> (**161**)<sup>61</sup>, (vinyl)MgBr(DME)<sub>2</sub> (**162**)<sup>145</sup>, (2-thienyl)MgBr(DME)<sub>2</sub> (**163**)<sup>145</sup>

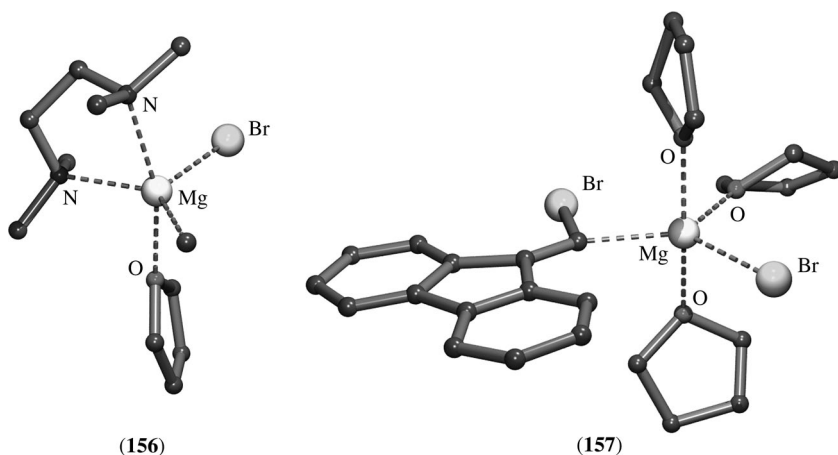


FIGURE 74. Molecular geometries of **156** and **157** in the solid state

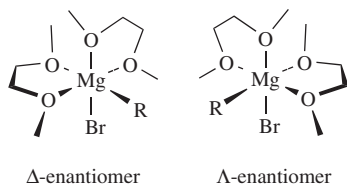


FIGURE 75. The  $\Delta$ - and  $\Lambda$ -enantiomers of *cis*-octahedral Grignard compounds

and *p*-TolMgBr(DME)<sub>2</sub> (**164**)<sup>185</sup>. In all compounds the organic group and the bromine atom are in *cis*-position. It should be noted that in such *cis*-octahedral arrangements the magnesium atom is chiral and thus a  $\Delta$ - and  $\Lambda$ -enantiomer of the Grignard compound exists (Figure 75).

Upon crystallization of such chiral compounds two things might happen: (i) the material crystallizes as a racemate, i.e. the crystal contains both the  $\Delta$ - and  $\Lambda$ -enantiomer, and (ii), the material crystallizes as a conglomerate, i.e. the crystals are chiral, one particular crystal contains only one of the enantiomers. X-ray crystal-structure determinations of **159–163** revealed centrosymmetric space groups, and thus these solid-state materials are by definition racemic. Surprisingly, crystallization of **164** at  $-20^\circ\text{C}$  yielded crystals which, according to an X-ray crystal-structure determination, have the a-centric spacegroup  $P2_12_12_1$ , and moreover, the asymmetric unit contains one molecule. This observation is a proof that **164** crystallizes as a conglomerate. Making use of special seeding techniques, both enantiomers of crystalline **164** could be isolated enantiomerically pure. Reaction of this enantiopure Grignard reagent, at  $-70^\circ\text{C}$  in DME as the solvent, with butyraldehyde afforded the corresponding alcohol with e.e. values of up to 22%.

Another approach to induce enantioselectivity during reactions with Grignard reagents is the use of chiral additives, usually chiral compounds that form a complex with the Grignard reagent. The structures in the solid state of the following complexes containing a chiral ligand have been determined: *t*-BuMgCl[(–)-sparteine] (**165**)<sup>194</sup>, EtMgBr[(–)-sparteine] (**166**)<sup>195</sup>, EtMgBr[(–)- $\alpha$ -isosparteine] (**167**)<sup>196</sup> and EtMgBr[(+)-6-benzylsparteine] (**168**)<sup>197</sup>. These four compounds are discrete monomers with the organic group and the halogen atom  $\sigma$ -bonded to magnesium and the sparteine ligand *N,N'*-chelate bonded to magnesium resulting in a tetrahedral coordination geometry at magnesium. As an example

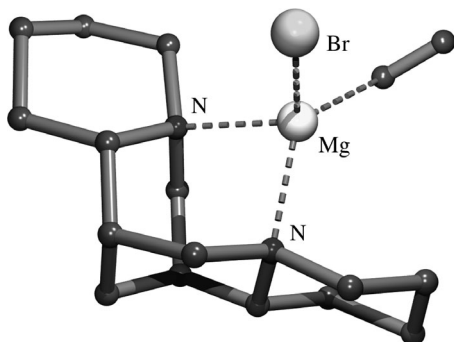


FIGURE 76. Molecular geometry of **166** in the solid state

the structure of **166** is shown (Figure 76). Complex **165** has been successfully applied as a catalyst for the selective asymmetric polymerization of racemic methacrylates<sup>197</sup>.

1,1-Di-Grignard reagents are valuable synthons in both organic and organometallic chemistry<sup>136</sup>. The only 1,1-di-Grignard reagent for which the structure in the solid state was unambiguously established by X-ray crystallography is  $(\text{Me}_3\text{Si})_2\text{C}[\text{MgBr}(\text{THF})_2]_2$  (**169**)<sup>198</sup>. Its structure comprises two almost identical  $\text{MgBr}(\text{THF})_2$  units  $\sigma$ -bonded  $[\text{Mg}-\text{C}$  2.10(4) and 2.14(4) Å] to the central carbon atom (Figure 77). Each of the magnesium atoms has a slightly distorted tetrahedral coordination geometry. Its relative unreactivity was explained in terms of an effective shielding of the central carbon atom from attack by electrophiles by the two bulky  $\text{Me}_3\text{Si}$  groups and two bulky  $\text{MgBr}(\text{THF})_2$  units.

In the solid state, the Grignard complexes **170–177** (Table 3) all have a dimeric structural motif, via two bridging halogen atoms between the two magnesium atoms, as shown schematically in Figure 78.

The basic structure of these compounds consists of a central flat, four-membered  $\text{Mg}-\text{X}-\text{Mg}-\text{X}$  ring in which the halogen atoms are symmetrically bridge-bonded between the magnesium atoms. To each of the magnesium atoms is  $\sigma$ -bonded one organic group and a donor molecule which is coordinated via its heteroatom, resulting in a tetrahedral coordination geometry at the magnesium atoms. In principle two geometrically different isomers are possible, one with the organic groups approaching the four-membered ring from opposite sides, and one approaching the four-membered ring from the same side. So far only structures are known in which the organic groups, and consequently the coordinating donor molecules, are at opposite sides.

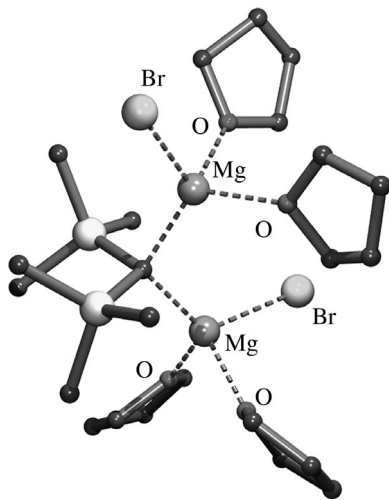


FIGURE 77. Molecular geometry of the 1,1-di-Grignard reagent **169** in the solid state

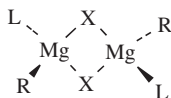


FIGURE 78. Schematic structural motif of the Grignard complexes **170–177** in the solid state

TABLE 3. Dimeric Grignard complexes **170–177**

Compound	R	X	L	Reference
<b>170</b>	Et	Br	<i>i</i> -Pr <sub>2</sub> O	199
<b>171</b>	Et	Br	Et <sub>3</sub> N	200
<b>172</b>	(Me <sub>3</sub> Si) <sub>2</sub> CH	Br	Et <sub>2</sub> O	120
<b>173</b>	(Me <sub>3</sub> Si) <sub>3</sub> C	I	Et <sub>2</sub> O	112
<b>174</b>	(PhMe <sub>2</sub> Si)(Me <sub>3</sub> Si) <sub>2</sub> C	I	Et <sub>2</sub> O	112
<b>175</b>	(PhMe <sub>2</sub> Si)(Me <sub>3</sub> Si)CH	Br	Et <sub>2</sub> O	201
<b>176</b>	2,6-Mes <sub>2</sub> C <sub>6</sub> H <sub>3</sub>	Br	THF	202
<b>177</b>	9-Anthryl	Br	<i>n</i> -Bu <sub>2</sub> O	203

When allylmagnesium chloride is crystallized from THF in the presence of TMEDA, a dimeric complex [(allyl)MgCl(TMEDA)]<sub>2</sub> (**178**) is obtained. Its X-ray crystal-structure determination showed that in this complex two chlorine atoms are bridging between two magnesium atoms in a rather asymmetric way [Mg–Cl 2.400(1) and 2.694(1) Å]<sup>204</sup>. To each of the magnesium atoms one allyl group is  $\eta^1$ -bonded via its terminal carbon atom [Mg–C 2.179(3) Å] and one TMEDA molecule *N,N'*-chelate bonded [Mg–N 2.211(2) and 2.285(2) Å], resulting in penta-coordinate magnesium atoms.

Crystallization of a series of monoorganomagnesium chlorides afforded crystalline materials with the formulation R<sub>2</sub>Mg<sub>4</sub>Cl<sub>6</sub>(THF)<sub>6</sub>; R = Et (**179**)<sup>205</sup>, R = Me (**180**)<sup>60</sup>, R = *t*-Bu (**181**)<sup>60</sup> and R = benzyl (**182**)<sup>60</sup>. X-ray structure determinations of these compounds show that they exist as complex aggregates shown schematically in Figure 79. The four magnesium atoms are linked via chloride bridges, four of which are bridge-bonded between two magnesium atoms and two are bridging between three magnesium atoms (Figure 79). The central two magnesium atoms have an octahedral coordination geometry, due to interaction with four chlorine atoms and two coordinating THF molecules in *cis*-position. The other two magnesium atoms have trigonal bipyramidal coordination geometry with the organic group and two chlorine atoms at equatorial positions and one chlorine atom and one coordinating THF molecule at the apical sites.

It should be noted that the ratio of organic group to magnesium to halide is not 1:1:1 as in the general formulation of Grignard reagents RMgX. In fact these aggregates contain an additional MgCl<sub>2</sub> molecule, which is always present in solutions of Grignard reagents due to the Schlenk equilibrium. This implies that if such a type of structures is present in solution, also other (aggregated) species having different stoichiometries must be present.

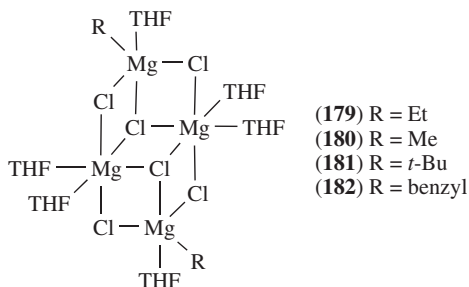


FIGURE 79. Schematic representation of the structure in the solid state of the aggregated Grignard complexes **179–182**

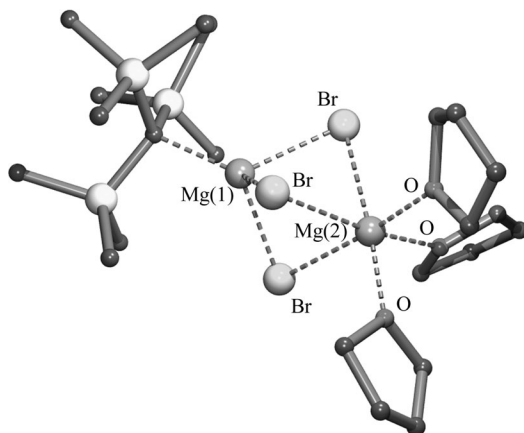


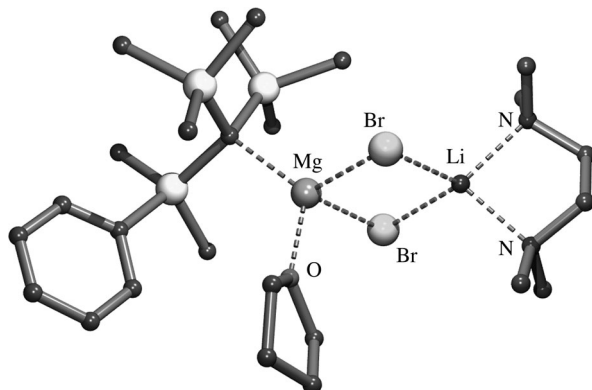
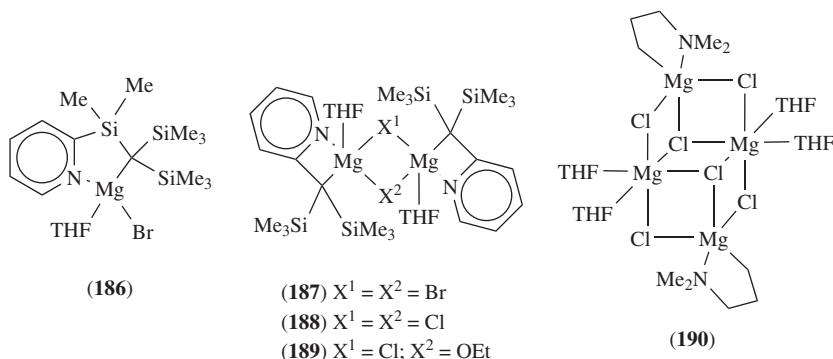
FIGURE 80. Molecular geometry of **183** in the solid state

According to an X-ray crystal-structure determination the crystalline material obtained from a solution of  $[(\text{Me}_3\text{Si})_3\text{C}]\text{MgBr}$  in THF appeared to be  $[(\text{Me}_3\text{Si})_3\text{C}]\text{Mg}_2\text{Br}_3(\text{THF})_3$  (**183**)<sup>206</sup>. Its molecular geometry comprises two magnesium atoms between which three bromine atoms are bridge-bonded. To one of the magnesium atoms the  $(\text{Me}_3\text{Si})_3\text{C}$  group is  $\sigma$ -bonded [ $\text{Mg}-\text{C}$  2.16(3) Å] while to the other magnesium atom three additional THF molecules are coordinated [ $\text{Mg}-\text{O}$  2.09(2), 2.06(2) and 2.04(2) Å]. Consequently, one of the magnesium atoms is four-coordinate whereas the other one is six-coordinate (Figure 80). It is notable that the  $\text{Br}-\text{Mg}$  distances to the four-coordinate magnesium atom [average  $\text{Mg}(1)-\text{Br}$  2.571(9) Å] are considerably shorter than those to the six-coordinate magnesium atom [ $\text{Mg}(2)-\text{Br}$  2.741(9) Å]. It has been suggested, based on cold-spray ionization mass spectroscopy, that species having a structure similar to that of **183** are the predominant ones in THF solutions of Grignard reagents<sup>60</sup>.

Grignard reagents are also capable of aggregating with other metal salts like LiBr. The structure of  $[(\text{PhMe}_2\text{Si})(\text{Me}_3\text{Si})_2\text{C}]\text{MgBr}_2\text{Li}(\text{THF})(\text{TMEDA})$  (**184**) was elucidated by X-ray crystallography<sup>112</sup>. In the structure of **184** two bromine atoms are symmetrically bridge-bonded between magnesium and lithium [ $\text{Mg}-\text{Br}$  2.530(3) Å and  $\text{Li}-\text{Br}$  2.507(13) Å] (Figure 81). The  $(\text{PhMe}_2\text{Si})(\text{Me}_3\text{Si})_2\text{C}$  group is  $\sigma$ -bonded [ $\text{Mg}-\text{C}$  2.186(8) Å] to magnesium and a THF molecule is coordinating to magnesium [ $\text{Mg}-\text{O}$  2.056(5) Å]. To attain a tetrahedral coordination geometry at lithium a TMEDA molecule is  $N,N'$ -chelated bonded to this lithium atom. A similar structure has been found in the solid state for  $[(\text{Me}_3\text{Si})_3\text{C}]\text{MgBr}_2\text{Li}(\text{THF})_3$  (**185**). In **185**, instead of the chelate-bonded TMEDA molecule two THF molecules are coordinate to the lithium atom<sup>207</sup>.

A few organomagnesium halides containing a monoanionic,  $C,N$ -chelating ligand have been structurally characterized by X-ray crystallographic studies. A discrete monomeric structure was found for  $(2\text{-PySiMe}_2)(\text{Me}_3\text{Si})_2\text{CMgBr}(\text{THF})$  (**186**)<sup>208</sup> (Figure 82). The  $(2\text{-PySiMe}_2)(\text{Me}_3\text{Si})_2\text{C}$  monoanionic ligand forms a five-membered chelate ring with magnesium via a  $\sigma$ -carbon-magnesium bond [ $\text{Mg}-\text{C}$  2.189(9) Å] and a coordinate bond of the pyridyl nitrogen atom with magnesium [ $\text{Mg}-\text{N}$  2.097(9) Å]. A tetrahedral coordination geometry at magnesium is reached by a  $\text{Mg}-\text{Br}$  bond and an additional coordinating THF molecule.

The dimeric organomagnesium halide complexes **187–189** (Figure 82) were obtained from the reaction of  $(2\text{-Py})(\text{SiMe}_2)_2\text{C}-\text{Sb}=\text{C}(\text{SiMe}_3)(2\text{-Py})$  with  $\text{Et}_2\text{Mg}$  in THF in the

FIGURE 81. Molecular geometry of **184** in the solid stateFIGURE 82. Schematic structures of organomagnesium halides containing monoanionic *C,N*-chelating ligands

presence of  $\text{Br}^-$ ,  $\text{Cl}^-$  and  $\text{EtO}^-$ , respectively<sup>209</sup>. These three complexes have closely related structures consisting of two  $(2\text{-Py})(\text{Me}_3\text{Si})_2\text{CMg}(\text{THF})$  moieties linked via two bridging halogen atoms in **187** and **188**, or a chloride and an ethoxy bridge in **189**. The  $(2\text{-Py})(\text{Me}_3\text{Si})_2\text{C}$  monoanionic, *C,N*-chelating ligand forms a four-membered chelate ring with magnesium. Dimerization occurs via two symmetrically bridge-bonded halogen atoms in **187** and **188** and one bridge-bonded chlorine atom and one bridging ethoxy group in **189**. As a consequence the magnesium atoms are penta-coordinate, in **187** and **188** close to square pyramidal and in **188** distorted trigonal bipyramidal with the  $\sigma$ -bonded carbon atom, the oxygen atom of the ethoxy group and the oxygen atom of the coordinating THF molecule at the equatorial positions.

In the solid state the Grignard reagent  $\text{Me}_2\text{N}(\text{CH}_2)_3\text{MgCl}$  aggregates with  $\text{MgCl}_2$  to a complex structure  $[\text{Me}_2\text{N}(\text{CH}_2)_3\text{Mg}_2\text{Cl}_3(\text{THF})_2]_2$  (**190**) (Figure 82)<sup>210</sup>. A similar overall structural motif has been found for monoorganomagnesium halides **179–182**, *vide supra*. In **190** the monoanionic, *C,N*-chelating  $\text{Me}_2\text{N}(\text{CH}_2)_3$  group forms a five-membered chelate ring with magnesium via a  $\sigma$ -bonded carbon atom [ $\text{Mg}-\text{C}$  2.146(9) Å] and a coordination bond with nitrogen [ $\text{Mg}-\text{N}$  2.23(1) Å].

The Grignard reagent 2-pyridylmagnesium bromide crystallizes from THF as a dimeric complex  $(2\text{-Py})_2\text{Mg}_2\text{Br}_2(\text{THF})_3$  (**191**). Its structure in the solid state comprises two magnesium atoms between which two 2-pyridyl groups are bridge-bonded via a  $\sigma$ -carbon–magnesium bond [ $\text{Mg}-\text{C}$  2.149(3) Å] and a nitrogen–magnesium coordination bond [2.129(3) Å] (Figure 83)<sup>211</sup>. To each of the magnesium atoms one bromine atom is bonded [ $\text{Mg}-\text{Br}$  2.4887(9) Å] and one THF molecule is coordinated. Finally, one additional THF molecule is bridge-bonded via its oxygen atom [ $\text{Mg}-\text{O}$  both 2.374(2) Å] between the two magnesium atoms. It here probably acts as a four-electron donor.

The structures of some Grignard reagents containing monoanionic,  $C,O$ -chelating ligands have been established in the solid state by X-ray crystallography. The 1-bromo-magnesium-tris-THF derivative (**192**) of *N*-pivaloyl-tetrahydroisoquinoline crystallizes as a discrete monomer (Figure 84)<sup>212</sup>. Coordination of the carbonyl oxygen atom to magnesium [ $\text{Mg}-\text{O}$  2.049(8) Å] results in the formation of a five-membered chelate ring. Three additional THF molecules are coordinate-bonded to the magnesium, resulting in an octahedral coordination geometry. Due to the geometry of the  $C,O$ -chelating ligand

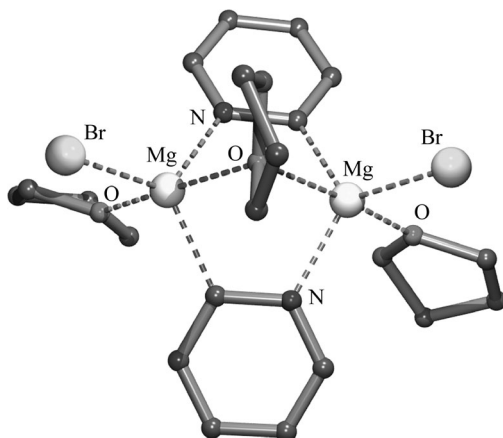


FIGURE 83. Molecular geometry of **191** in the solid state

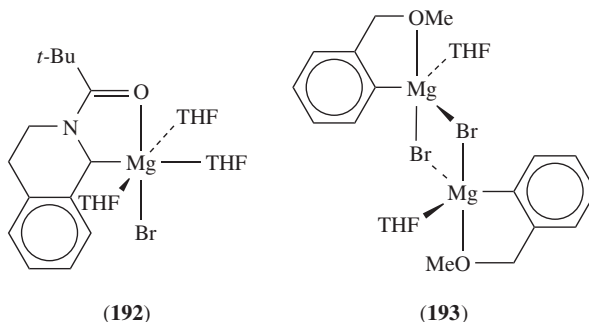


FIGURE 84. Schematic representation of the molecular structures of **192** and **193** in the solid state

the magnesium-bonded carbon atom and the coordinating carbonyl-oxygen atom are in *cis*-position while the bromine atom is in *trans*-position with respect to this oxygen atom.

A systematic study of the structures in the solid state of 2-CH<sub>2</sub>(OCH<sub>2</sub>CH<sub>2</sub>)<sub>*n*</sub>OMe-substituted phenylmagnesium bromides (*n* = 0–3) has been carried out<sup>213</sup>. For the most simple compound (*n* = 0), i.e. 2-(methoxymethyl)phenylmagnesium bromide (**193**), a dimeric structure via two bridge-bonded bromine atoms in the solid state was found (Figure 84). The coordination geometry at the magnesium atoms is trigonal bipyramidal, with the magnesium-bonded carbon atom of the *C,O*-chelating ligand, a bromine atom and an additional coordinating THF molecule at the equatorial positions and the intramolecular coordinating oxygen atom and the other bromine atom at the axial sites. The bridge-bonding of the bromine atoms is such that an equatorial-bonded bromine atom in one half of the dimer occupies an axial site of the magnesium in the other half of the dimer, and *vice versa*. As might be expected the Mg–Br bond distance of equatorially-bonded bromine [Mg–Br 2.509(3) Å] is considerably shorter than that of an axially bonded one [Mg–Br 2.705(3) Å].

The 2-CH<sub>2</sub>(OCH<sub>2</sub>CH<sub>2</sub>)<sub>*n*</sub>OMe-substituted phenylmagnesium bromides with *n* = 1 (**194**), *n* = 2 (**195**) and *n* = 3 (**196**) are all discrete monomers in the solid state (Figure 85). In all three compounds the magnesium atom has an octahedral coordination geometry with the magnesium-bonded carbon atom and the coordinating benzylic oxygen atom in *cis*-position with respect to each other and the bromine atom in *trans*-position with respect to the coordinating benzylic oxygen atom. In **194**–**196** all the oxygen atoms of the substituents are involved in intramolecular coordination, but to complete six-coordination at magnesium in **194** two additional coordinating THF molecules are present, while in **195** only one additional THF molecule is required for that purpose.

In continuation of this study, the same authors investigated the structures in the solid state of crown-ether Grignard reagents. The structures of 2-(bromomagnesium)-1,3-xylyl-15-crown-4 (**197**)<sup>214</sup>, 2-(bromomagnesium)-1,3-phenylene-16-crown-5 (**198**)<sup>215</sup> and 2-(bromomagnesium)-1,3-xylyl-18-crown-5 (**199**)<sup>216</sup> were determined by X-ray crystallography (Figure 86). In **197** all oxygen atoms of the crown are involved in coordination to magnesium, two with a relatively short Mg–O bond distance [Mg–O 2.12(1) and 2.13(1) Å] and two with a longer bond distance [Mg–O 2.33(1) and 2.49(1) Å]. The coordination sphere of magnesium may be considered as pentagonal-bipyramidal, with the bromine atom at the apex<sup>214</sup>.

In **198** (Figure 86) the two phenolic oxygen atoms are not involved in coordination to magnesium, most probably because this would require the formation of two highly unfavorable four-membered chelate rings. Instead, an additional THF molecule is coordinating to the magnesium atom, giving it a distorted octahedral coordination geometry with the bromine atom *cis*-positioned with respect to the  $\sigma$ -bonded carbon atom and the coordinating THF molecule in a *trans*-position to the bromine atom.

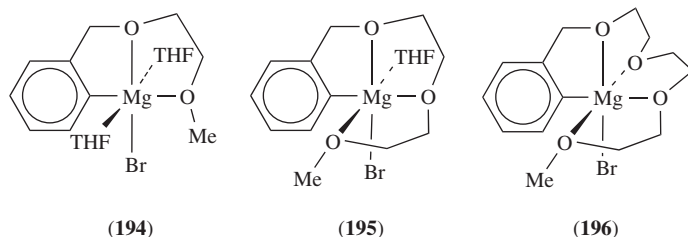


FIGURE 85. Schematic representation of the molecular structures of **194**–**196** in the solid state



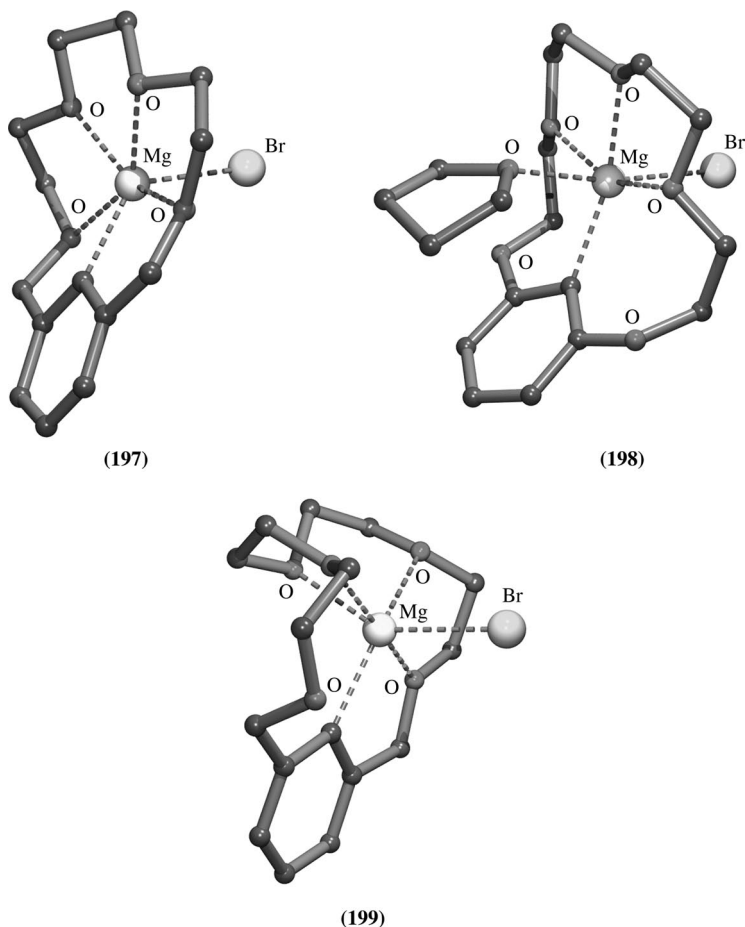
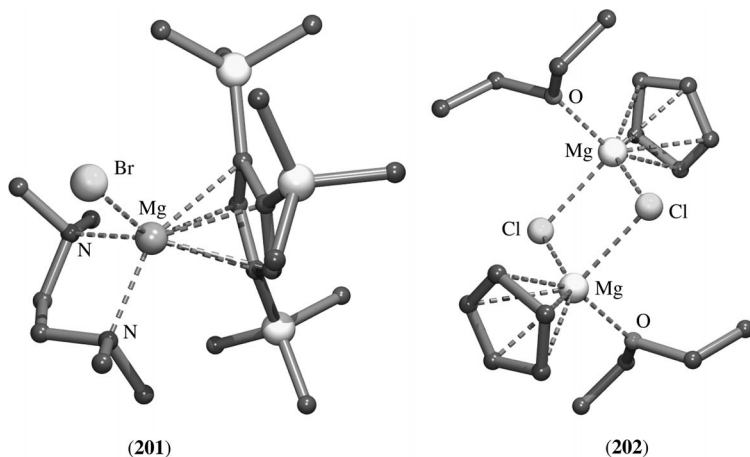


FIGURE 86. Molecular geometries of the crown-ether Grignard compounds **197**–**199** in the solid state

In the 18-crown-5 derivative **199** four of the five oxygen atoms of the crown-ether are involved in coordination to magnesium (Figure 86). Together with the  $\sigma$ -bonded carbon atom and the bromine atom this leads to a distorted octahedral coordination geometry at magnesium. Like in **198** the bromine atom is *cis*-positioned with respect to the  $\sigma$ -bonded carbon atom.

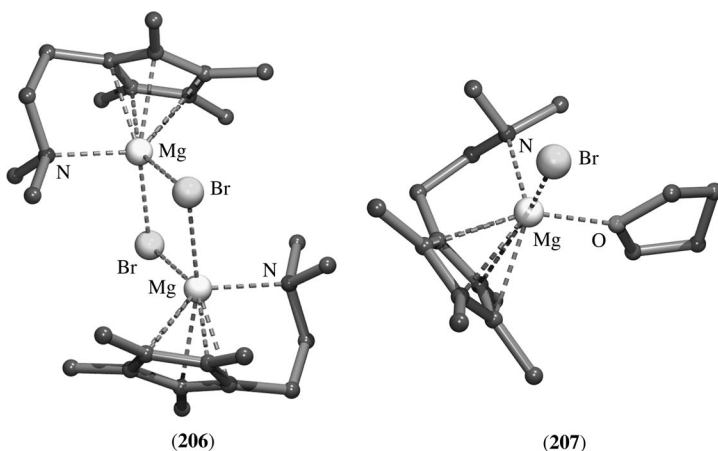
The structures in the solid state of a few cyclopentadienylmagnesium halide complexes have been determined by X-ray crystallography. The structures of  $\text{CpMgBr}(\text{tetraethylethylenediamine})$  (**200**)<sup>217</sup> and  $1,2,4\text{-(Me}_3\text{Si)}_3\text{C}_5\text{H}_2\text{MgBr(TMEDA)}$  (**201**)<sup>93</sup> show large similarities. The structure of **201** is shown (Figure 87). Both compounds are discrete monomers in which the cyclopentadienyl group is  $\eta^5$ -bonded to magnesium and the diamine ligand is *N,N'*-chelate bonded.

In the solid state cyclopentadienylmagnesium chloride exists as a dimer  $[\text{CpMgCl}(\text{OEt}_2)]_2$  (**202**)<sup>218</sup> (Figure 87). The dimeric structure is caused by two symmetrically

FIGURE 87. Molecular geometries of **201** and **202** in the solid state

bridge-bonded chlorine atoms between the two magnesium atoms [Mg–Cl 2.419(2) and 2.432(2) Å]. To each of the magnesium atoms one cyclopentadienyl group is  $\eta^5$ -bonded and one coordinating diethyl ether molecule completes the coordination sphere of magnesium. Also, the structures of [Cp\* $\text{MgCl}(\text{OEt}_2)_2$ ] (**203**)<sup>218</sup>, [Cp\* $\text{MgCl}(\text{THF})_2$ ] (**204**)<sup>219</sup> and [Cp\* $\text{MgBr}(\text{THF})_2$ ] (**205**)<sup>220</sup> in the solid state were determined by X-ray crystallography. They have a similar dimeric structural motif as observed for **202**.

A cyclopentadienylmagnesium bromide containing a heteroatom-functionalized substituent at the cyclopentadienyl group has also been structurally characterized. When 1-[2-(dimethylamino)ethyl]-2,3,4,5-tetramethylcyclopentadienylmagnesium bromide is recrystallized from dichloromethane, dimeric [(Me<sub>2</sub>N(CH<sub>2</sub>)<sub>2</sub>)Me<sub>4</sub>C<sub>5</sub>MgBr]<sub>2</sub> (**206**) (Figure 88) is obtained<sup>221</sup>. Its X-ray crystal-structure determination reveals a structure in the solid state

FIGURE 88. Molecular geometries of **206** and **207** in the solid state

that is closely related to the dimeric structure observed for **202**. However, instead of the coordinating diethyl ether molecule in **202**, in **206** the nitrogen atom of the  $\text{Me}_2\text{NCH}_2\text{CH}_2$  substituent is coordinating intramolecularly to the magnesium atom.

When **206** is recrystallized from THF the dimeric structure is broken down to a discrete monomeric one  $(\text{Me}_2\text{N}(\text{CH}_2)_2)\text{Me}_4\text{C}_5\text{MgBr}(\text{THF})$  (**207**), as was shown by an X-ray crystal-structure determination. In **207**, the substituted cyclopentadienyl group is  $\eta^5$ -bonded to magnesium while the nitrogen atom of the functional substituent is intramolecularly coordinated to magnesium. The bromine atom and an additional coordinating THF molecule complete the coordination at magnesium.

#### D. Monoorganomagnesium Compounds $\text{RMgY}$ with $\text{Y} = \text{OR}$

The number of heteroleptic organomagnesium compounds  $\text{RMgOR}$  for which the structure in the solid state was established unambiguously by X-ray crystallography is rather limited, in contrast to the large number of structures known for the corresponding heteroleptic  $\text{RZnOR}$  congeners<sup>29</sup>.

The structures of only two monomeric  $\text{RMgOR}$  complexes are known. The reaction of  $\text{Et}_2\text{Mg}$  with one equivalent of 2,6-di-*tert*-butylphenol in the presence of TMEDA affords a crystalline product with composition  $\text{EtMgOC}_6\text{H}_3\text{Bu-}t\text{-}2,6(\text{TMEDA})$  (**208**)<sup>189</sup>. Its X-ray crystal-structure determination reveals a monomeric molecule with the ethyl group  $\sigma$ -bonded to magnesium [ $\text{Mg}-\text{C}$  2.147(10) Å] and the phenoxy group also  $\sigma$ -bonded with a very short bond distance [ $\text{Mg}-\text{O}$  1.888(5) Å] (Figure 89). A  $N,N'$ -chelate-bonded TMEDA molecule completes a tetrahedral coordination geometry at magnesium.

A similar reaction of *i*- $\text{Bu}_2\text{Mg}$  with 2,6-di-*tert*-butylphenol in the presence of 18-crown-6 affords *i*- $\text{BuMgOC}_6\text{H}_3\text{Bu-}t\text{-}2,6(18\text{-crown-}6)$  (**209**) as a crystalline solid<sup>183</sup>. An X-ray crystal-structure determination showed that this compound in the solid state also exists as a monomer with a  $\sigma$ -bonded *i*-butyl group and a  $\sigma$ -bonded phenoxy oxygen atom. Three adjacent oxygen atoms of the crown-ether are involved in coordination to magnesium, resulting in penta-coordination.

A dimeric structural motif, formed by bridge-bonding of two oxygen atoms between two magnesium atoms, has been observed in the solid-state structures of  $[\textit{s}\text{-BuMgOC}_6\text{H}_3(\text{Bu-}t\text{-}2,6)]_2$  (**210**)<sup>222</sup> and  $[\textit{n}\text{-HexMgOC}_6\text{H}_2(\text{Bu-}t\text{-}2,6\text{-Me-}4)]_2$  (**211**)<sup>223</sup> (Figure 90). In both compounds two phenoxy groups are symmetrically bridge-bonded between two magnesium atoms, while the organic group is  $\sigma$ -bonded to magnesium. As a result the magnesium atoms in **210** and **211** have a trigonal planar coordination geometry.

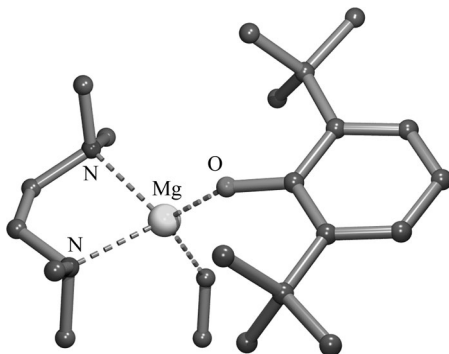
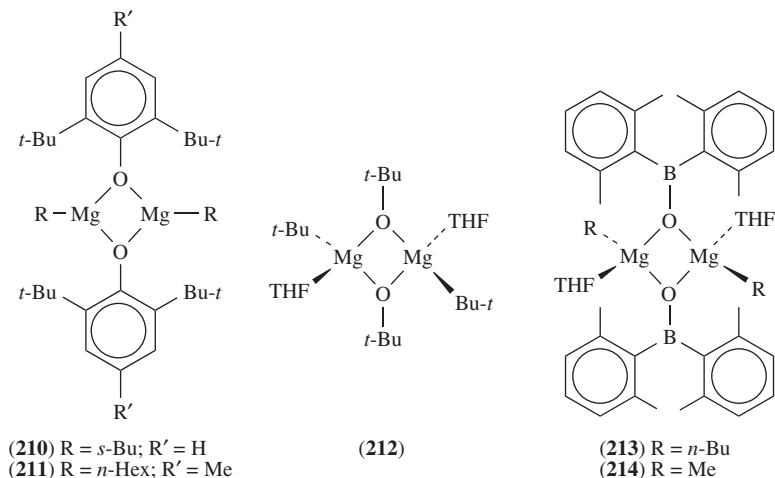


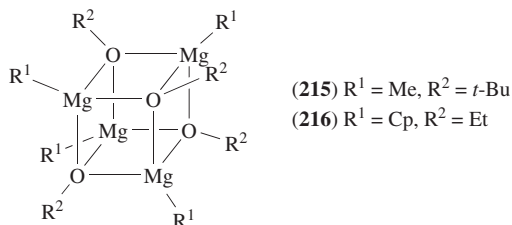
FIGURE 89. Molecular geometry of **208** in the solid state

FIGURE 90. Schematic representation of the structures of **210–214** in the solid state

Also,  $t\text{-BuMgOBu-}t$  exists in the solid state as a dimeric complex  $[t\text{-BuMgOBu-}t(\text{THF})]_2$  (**212**)<sup>224</sup>. Two  $t\text{-BuO}$  groups are symmetrically bridge-bonded between two magnesium atoms forming a flat four-membered  $\text{Mg-O-Mg-O}$  ring (Figure 90). To each of the magnesium atoms a  $t\text{-Bu}$  group is  $\sigma$ -bonded while a coordinating THF molecule completes a tetrahedral coordination geometry at magnesium.

Crystalline  $[n\text{-BuMgOB}(\text{Mes})_2(\text{THF})]_2$  (**213**) was obtained from the reaction of  $n\text{-Bu}_2\text{Mg}$  with dimesityl boronic acid in THF. The corresponding methyl derivative  $[\text{MeMgOB}(\text{Mes})_2(\text{THF})]_2$  (**214**) was prepared via a transmetalation reaction of the lithium salt of dimesityl boronic acid with  $\text{MeMgCl}$  in THF. For both compounds the structure in the solid state was determined by X-ray crystallography<sup>225</sup>. The basic structural motif of these compounds is identical to that of **212**; both are dimers, via bridge-bonding of the oxygen atoms of two dimesityl boronic acid anions between two magnesium atoms. An additional coordinating THF molecule completes a tetrahedral geometry at magnesium (Figure 90).

Methylmagnesium *tert*-butoxide exists in the solid state as a tetrameric aggregate  $[\text{MeMgOBu-}t]_4$  (**215**). Its X-ray crystal-structure determination reveals a heterocubane structure with alternating magnesium and oxygen atoms at the corners of the cube (Figure 91)<sup>226</sup>. To each of the magnesium atoms one methyl group is  $\sigma$ -bonded.

FIGURE 91. Schematic representation of the structures of **215** and **216** in the solid state

Like **215**, cyclopentadienylmagnesium ethoxide exists in the solid state as tetrameric  $[\text{CpMgOEt}]_4$  (**216**) with a heterocubane structure (Figure 91)<sup>227</sup>. In **216** the cyclopentadienyl groups are  $\eta^5$ -bonded to the magnesium atoms.

### E. Monoorganomagnesium Compounds $\text{RMgY}$ with $\text{Y} = \text{NR}_2$

Despite the capability of anionic amide groups to form aggregates with metals via bridging nitrogen atoms, most of the monoorganomagnesium amides that have been structurally characterized in the solid state have a discrete monomeric structure.

The monoorganomagnesium amides **217**<sup>228</sup>, **218**<sup>228</sup>, **219**<sup>229</sup>, **220**<sup>224</sup> and **221**<sup>230</sup> (Figure 92), derived from substituted anilines, have comparable structures in the solid state. They are all monomers with a tetrahedrally coordinated magnesium center formed by one  $\sigma$ -bonded organic group, one  $\sigma$ -bonded amido nitrogen atom and two coordinating heteroatoms. In **217**–**219** these are two THF molecules and in **220** a  $N,N'$ -chelate-bonded TMEDA molecule. In **217**–**220** the sum of the bond angles around the nitrogen atoms is  $360^\circ$  within experimental error, indicating that these nitrogen atoms are  $\text{sp}^2$ -hybridized. In **221** the carbazole skeleton is essentially flat, but the carbazole carbon  $\text{C}-\text{N}-\text{Mg}$  bond angles [both  $108.2(2)^\circ$ ] indicate that the magnesium atom is bonded to a  $\text{sp}^3$ -hybridized nitrogen atom. In the latter compound the  $\text{Mg}-\text{N}$  bond distance [ $\text{Mg}-\text{N}$  2.087(3) Å] is slightly longer than the  $\text{Mg}-\text{N}$  bond distances in **217**–**220** [2.040(3), 2.037(3), 2.027(4) and 2.004(2) Å, respectively].

Reaction of dialkylmagnesium compounds with 2,6-bis(imino)pyridines results in quantitative  $N$ -alkylation of the pyridine skeleton (equation 15).

The structures in the solid state of three of the initially formed organomagnesium amides, **222**, **223** and **224**, were determined by X-ray crystallography<sup>231</sup>. All three compounds are discrete monomers and have comparable structures of which that of **222** is shown (Figure 93). In **222** the ethyl group is  $\sigma$ -bonded to magnesium and interacts with the three nitrogen atoms of the  $N$ -alkylated 2,6-bis(imino)pyridine in a 'pincer-type'<sup>232</sup>

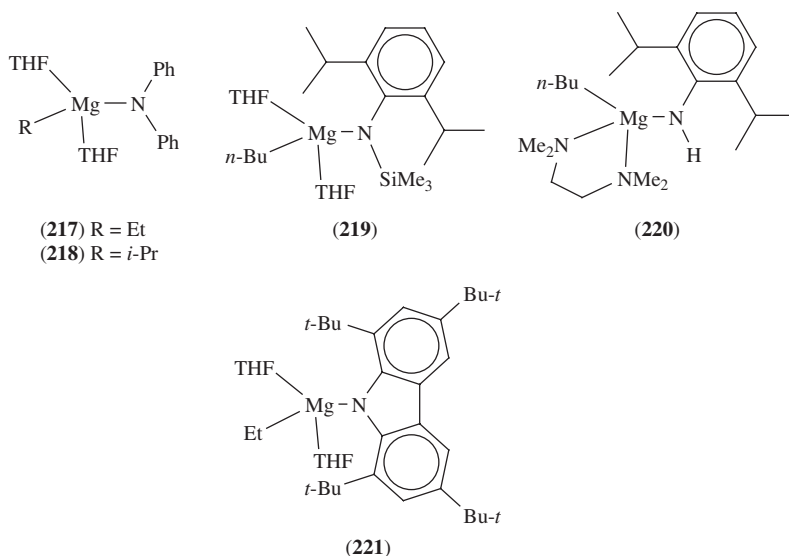
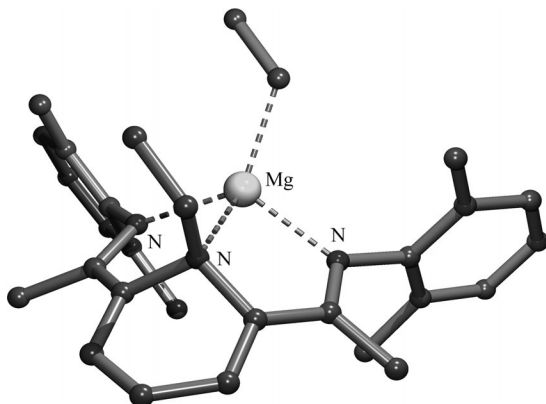
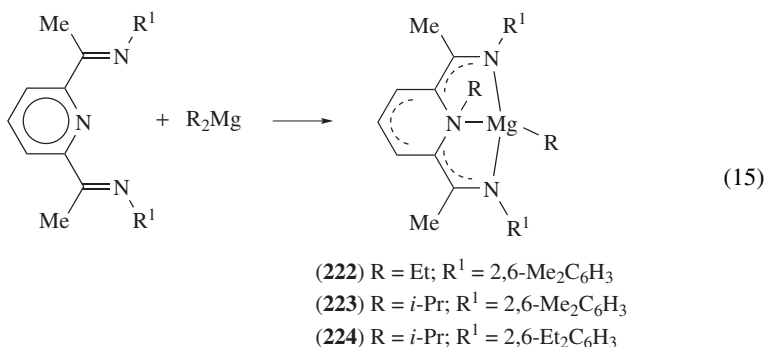


FIGURE 92. Schematic representation of the structures of **217**–**221** in the solid state

FIGURE 93. Molecular geometry of **222** in the solid state

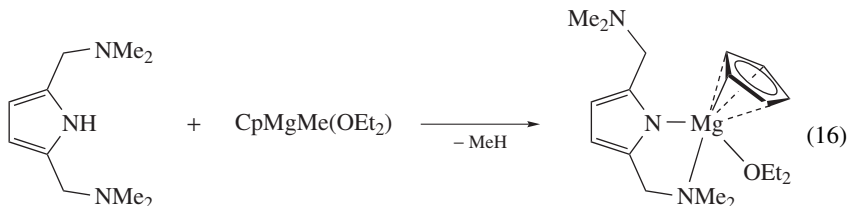
fashion. Due to the rigidity of the monoanionic, tridentate ligand system the geometry around magnesium is severely distorted from tetrahedral.



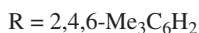
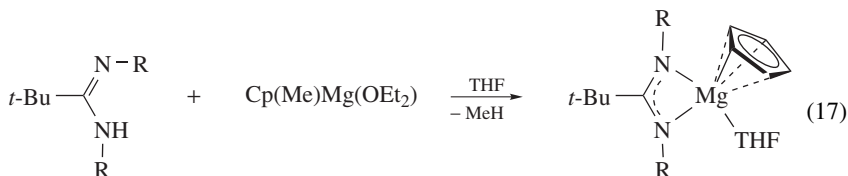
Reaction of  $\text{Cp}(\text{Me})\text{Mg}(\text{OEt}_2)$  with 2,5-bis[(dimethylamino)methyl]pyrrole in diethyl ether results in selective protonolysis of the magnesium-bonded methyl group and results in the formation of the corresponding  $\text{CpMg}$  amide (**225**) (equation 16). An X-ray crystal-structure determination showed that **225**, of which the structure is shown schematically (equation 16), exists in the solid state as a monomer.<sup>233</sup> The cyclopentadienyl group is  $\eta^5$ -bonded to magnesium, while the pyrrole amido-nitrogen atom is  $\sigma$ -bonded to magnesium [ $\text{Mg}-\text{N}$  2.043(1) Å]. Only one of the (dimethylamino)methyl substituents forms an intramolecular coordination bond to magnesium [ $\text{Mg}-\text{N}$  2.225(2) Å]. An additional diethyl ether molecule coordinates to magnesium to complete the coordination saturation.

In a similar way  $\text{Cp}(\text{Me})\text{Mg}(\text{OEt}_2)$  is capable of deprotonating  $N,N'$ -bis(2,4,6-trimethylphenyl)(*tert*-butyl)amidine to form the corresponding cyclopentadienylmagnesium amidinate complex (**226**) (equation 17). An X-ray crystal-structure determination of **226**, of which the structure is shown schematically (equation 17), showed that this compound also exists as a monomer in the solid state<sup>234</sup>. Like in **225** the cyclopentadienyl group is  $\eta^5$ -bonded to magnesium while the amidinate anion is  $N,N'$ -chelate bonded with almost equal  $\text{Mg}-\text{N}$  bond distances [ $\text{Mg}-\text{N}$  2.090(2) and 2.097(2) Å]. Furthermore, an additional

THF molecule is coordinate-bonded to magnesium. Due to the small bite angle of the amidinate anion the N–Mg–N bond angle is very acute [N–Mg–N 63.3(1)°].



(225)



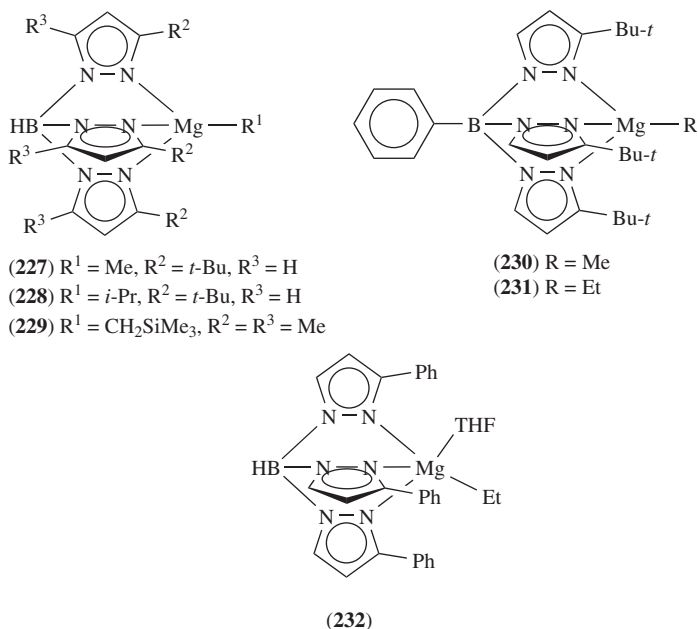
(226)

Various tris(pyrazolyl)borato alkylmagnesium derivatives have been prepared and were structurally characterized in the solid state. X-ray crystal-structure determinations of methylmagnesium tris(3-*tert*-butylpyrazolyl)hydroborate (**227**)<sup>235, 236</sup>, isopropylmagnesium tris(3-*tert*-butylpyrazolyl)hydroborate (**228**)<sup>236, 237</sup> and trimethylsilylmethylmagnesium tris(3,5-dimethylpyrazolyl)hydroborate (**229**)<sup>236, 238</sup> show that they have comparable structures in the solid state (Figure 94). In these compounds the tris(pyrazolyl)hydroborate moiety acts as a monoanionic, tridentate ligand which is bonded with almost equal Mg–N bond distances to the alkylmagnesium moiety. Due to the small bite angle of the tripodal ligand, all N–Mg–N bond angles are close to 90°, and differ significantly from the ideal tetrahedral value. As a consequence the coordination geometry at magnesium is considerably distorted from tetrahedral.

The structures of methylmagnesium tris(3-*tert*-butylpyrazolyl)phenylborate (**230**) and ethylmagnesium tris(3-*tert*-butylpyrazolyl)phenylborate (**231**) have been determined by X-ray crystallography and are shown schematically (Figure 94)<sup>239</sup>. Their structures show large similarities with that of **227** and **228** and only differ in the presence of a boron-bonded phenyl group in **230** and **231**.

The X-ray crystal-structure determination of ethylmagnesium tris(3-phenylpyrazolyl)hydroborate (**232**)<sup>240</sup> (Figure 94) shows that the magnesium atom is penta-coordinate as the result of one  $\sigma$ -bonded ethyl group, three magnesium–nitrogen bonds with the tris(3-phenylpyrazolyl)hydroborate moiety and one additional, coordinating THF molecule.

Reaction of  $\beta$ -diketimines with dialkylmagnesium compounds in a 1:1 molar ratio affords the corresponding monoorganomagnesium  $\beta$ -diketimines in high yield (Scheme 3). An alternative synthetic route involves deprotonation of the  $\beta$ -diketimine with *n*-BuLi and subsequent transmetalation of the initially formed lithium  $\beta$ -diketiminato with a suitable Grignard reagent. Extensive X-ray diffraction studies of the compounds obtained from these reactions have showed that, depending on the nature of the organic group bound to magnesium and the nature of the solvent used for the synthesis, three basic structural motifs, **A**, **B** and **C** (Scheme 3), are observed in the solid state for monoorganomagnesium  $\beta$ -diketimines. These motifs are: (i), monomers in which the  $\beta$ -diketiminato anion is

FIGURE 94. Schematic structures of the alkylmagnesium tris(pyrazolyl)borates **227–232**

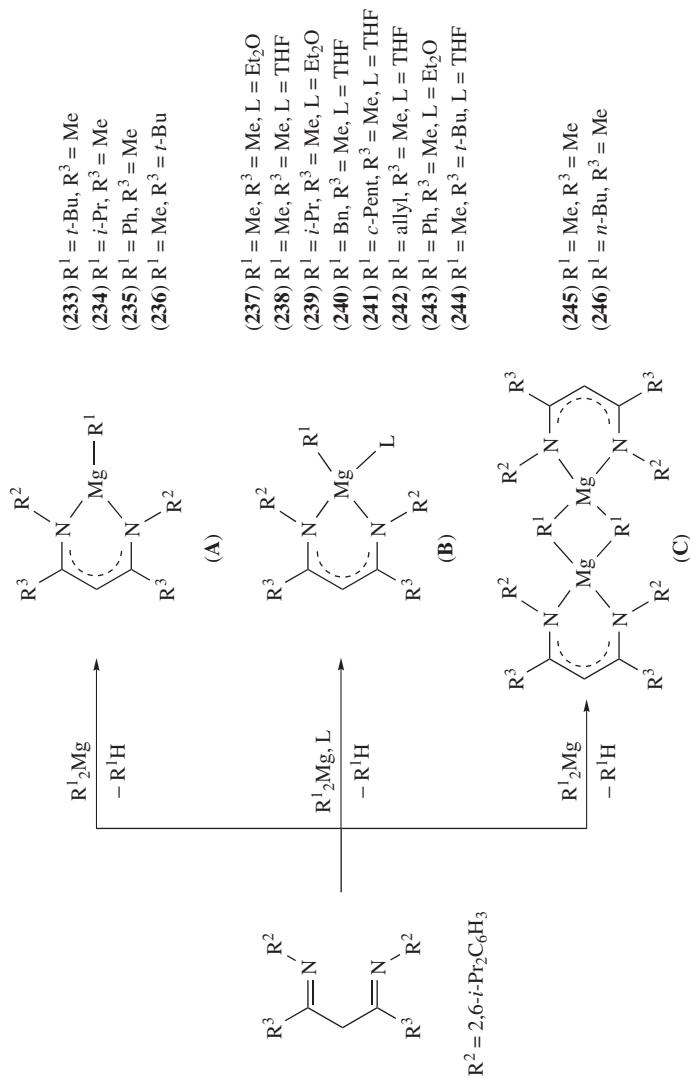
$N,N'$ -chelate bonded to the alkylmagnesium moiety, with trigonal planar coordination geometry at magnesium, (ii) monomers in which the  $\beta$ -diketiminato anion is  $N,N'$ -chelate bonded to the alkylmagnesium moiety and an additional ligand is coordinating to the magnesium atom, giving it a tetrahedral coordination geometry, and (iii) dimers formed via bridging of two two-electron three-center bonded alkyl groups between two magnesium atoms, while a  $\beta$ -diketiminato anion is  $N,N'$ -chelate bonded to each magnesium atom.

The structures of the monoorganomagnesium  $\beta$ -diketiminates **233**<sup>241</sup>, **234**<sup>242</sup>, **235**<sup>242</sup> and **236**<sup>243</sup> are comparable. The  $N,N'$ -chelate bonding of the  $\beta$ -diketiminato anion with almost equal  $\text{Mg}-\text{N}$  bond distances to magnesium results in a six-membered  $\text{MgN}_2\text{C}_3$  ring with all atoms located in one plane. The  $\text{Mg}-\text{C}$  bond of the  $\sigma$ -bonded alkyl group also lies in this plane. As a representative example the structure of **233** is shown (Figure 95).

The structures of the monoorganomagnesium  $\beta$ -diketiminates **237**<sup>241</sup>, **238**<sup>244</sup>, **239**<sup>245</sup>, **240**<sup>124</sup>, **241**<sup>246</sup>, **242**<sup>247</sup>, **243**<sup>242</sup> and **244**<sup>242</sup> show similar structural features. A distorted tetrahedral coordination geometry at magnesium is reached by a  $N,N'$ -chelate bonded  $\beta$ -ketiminato anion, a  $\sigma$ -bonded organic group and an additional coordinating solvent molecule, either THF or diethyl ether. In contrast to the flat six-membered  $\text{MgN}_2\text{C}_3$  ring in **233–236**, this ring in **237–244** deviates considerably from planar and can best be described as having a distorted boat conformation with the magnesium atom at the front and the opposing carbon atom at the back. As an example the structure of **238** is shown (Figure 95).

The structures of the dimers **245**<sup>244</sup> (Figure 95) and **246**<sup>248</sup> show large similarities. The two halves of the dimers are linked via two symmetrically bridging two-electron three-center bonded alkyl groups. A  $\beta$ -diketiminato anion is  $N,N'$ -chelate bonded to each of the magnesium atoms giving them distorted tetrahedral coordination geometries. Also, in **245** and **246** the  $\text{MgN}_2\text{C}_3$  ring deviates considerably from planar.



SCHEME 3. Synthesis of organomagnesium  $\beta$ -diketiminates

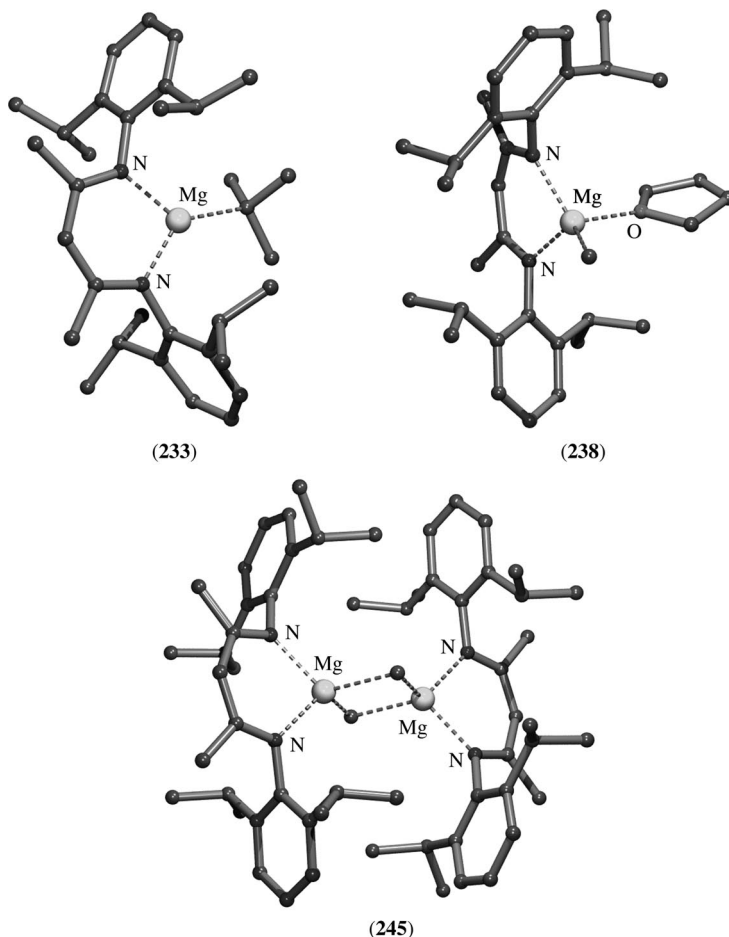


FIGURE 95. Molecular geometries of the monoorganomagnesium  $\beta$ -diketiminates **233**, **238** and **245** in the solid state

In some of the monoorganomagnesium  $\beta$ -diketiminates having structural motif **B**, i.e. complexes **237**–**244**, the coordinating solvent molecule is relatively weakly bound and can be removed at reduced pressure. For example, when **243** is dried for a few hours in high vacuum and the residue is recrystallized from a non-coordinating solvent like toluene, crystalline **235** is obtained<sup>242</sup>. However, when the allylmagnesium  $\beta$ -diketimate THF complex **242** is dried in vacuo it loses its coordinated THF molecule. An X-ray crystal-structure determination of the resulting product shows that instead of the anticipated monomeric structural motif **A**, this THF-free allylmagnesium  $\beta$ -diketimate is a cyclic hexameric aggregate (**247**) in the solid state (Figure 96)<sup>249</sup>. In the twenty-four-membered ring structure the magnesium atoms are linked by bridging allyl groups in a very rare  $trans\text{-}\mu\text{-}\eta^1 : \eta^1$  bonding mode. A  $\beta$ -diketimate anion is  $N,N'$ -chelate bonded to each of the magnesium atoms to complete its coordination sphere.

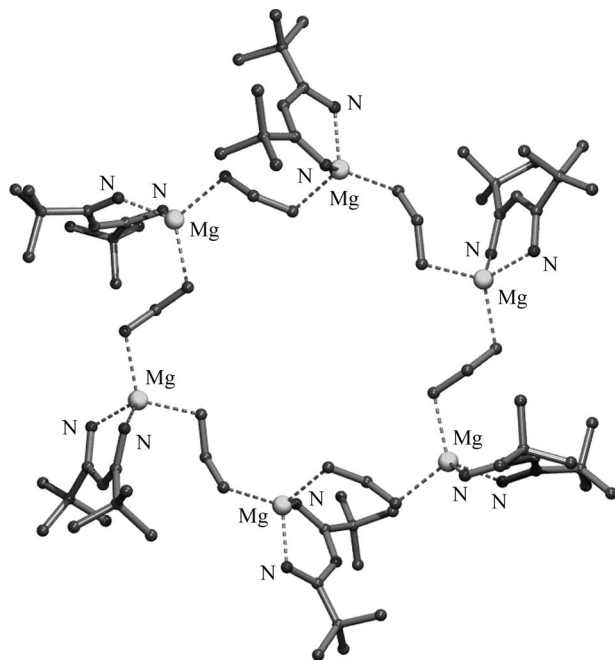
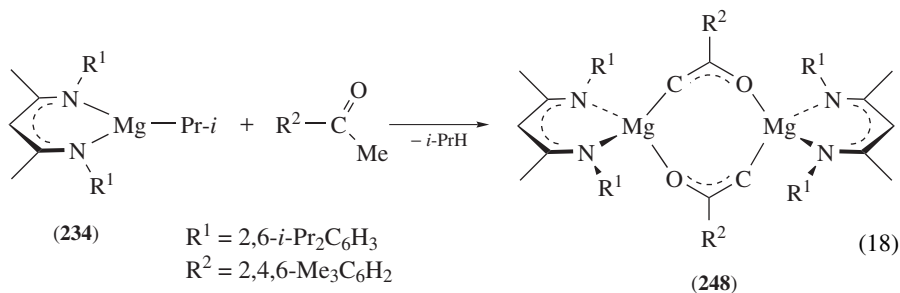


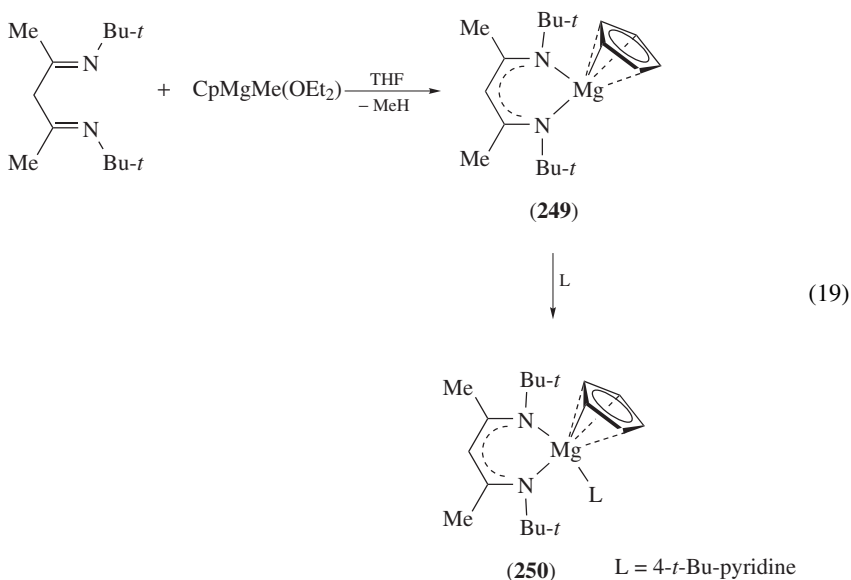
FIGURE 96. Molecular geometry of **247** in the solid state. The 2,6-*i*-Pr<sub>2</sub>C<sub>6</sub>H<sub>3</sub> substituents at the nitrogen atoms of the  $\beta$ -diketiminato anions are omitted for clarity

The reaction of isopropylmagnesium  $\beta$ -diketiminato **234** with 2',4',6'-trimethylacetophenone in an apolar solvent like toluene results in deprotonation of the ketone with the formation of an enolate (equation 18).



An X-ray crystal-structure determination showed that this enolate exists in the solid state as a dimer (**248**) in which two enolate moieties are *C,O*-bridge-bonded [Mg–O 1.908(2) Å and Mg–C 2.318(3) Å] between two magnesium  $\beta$ -diketiminato units, resulting in distorted tetrahedral coordination geometries at the magnesium atoms<sup>250</sup>. The structure of **248** is shown schematically (equation 18). Such a *C,O*-bridge bonding mode for enolates is rather rare, but has also been observed in the Reformatski reagent [*t*-BuO<sub>2</sub>CCH<sub>2</sub>ZnBr(THF)]<sub>2</sub><sup>251</sup>.

The cyclopentadienyl  $\beta$ -diketiminate **249** and its 4-*tert*-butylpyridine adduct **250** have been prepared and structurally characterized (equation 19)<sup>252</sup>. An X-ray crystal-structure determination of **249** showed that the cyclopentadienyl group is  $\eta^5$ -bonded to magnesium. On the basis of the observed bonding parameters of magnesium with the  $\beta$ -diketiminate skeleton [Mg–N 2.006(2) and 2.021(2) Å, Mg–C $_{\alpha}$  2.729(3) and 2.826(3) Å and Mg–C $_{\beta}$  2.689(3) Å] this bonding is described in terms of a  $\pi$ -interaction. However, in **250** the  $\beta$ -diketiminate is  $N,N'$ -chelate bonded to magnesium.



The hybrid boroamidinate/amidinate ligand as present in the methylmagnesium complex **251** (Figure 97) is isoelectronic with the  $\beta$ -diketiminate skeleton<sup>253</sup>. The X-ray crystal-structure determination of **251** shows that the boroamidinate/amidinate anion adopts a similar  $N,N'$ -chelate bonding as observed in organomagnesium  $\beta$ -diketimines. The structure of **251** is shown schematically (Figure 97).

However, in the donor-ligand-free *tert*-butylmagnesium derivative (**252**), the same boroamidinate/amidinate ligand system adopts an entirely different bonding mode. An X-ray crystal-structure determination of **252** showed that all three nitrogen atoms of

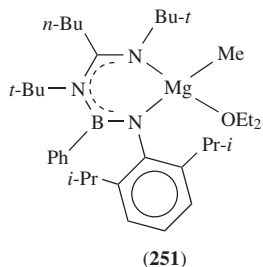
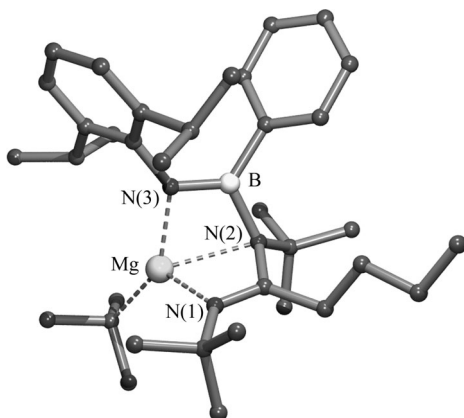
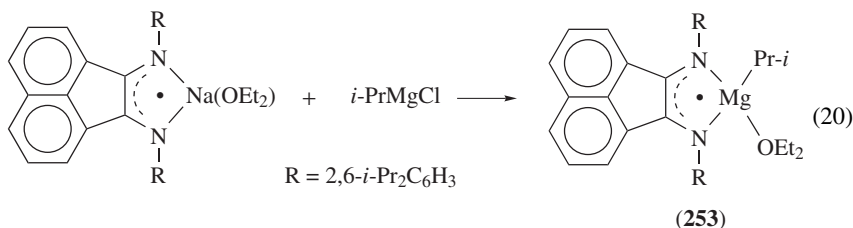


FIGURE 97. Schematic representation of the structure of **251** in the solid state

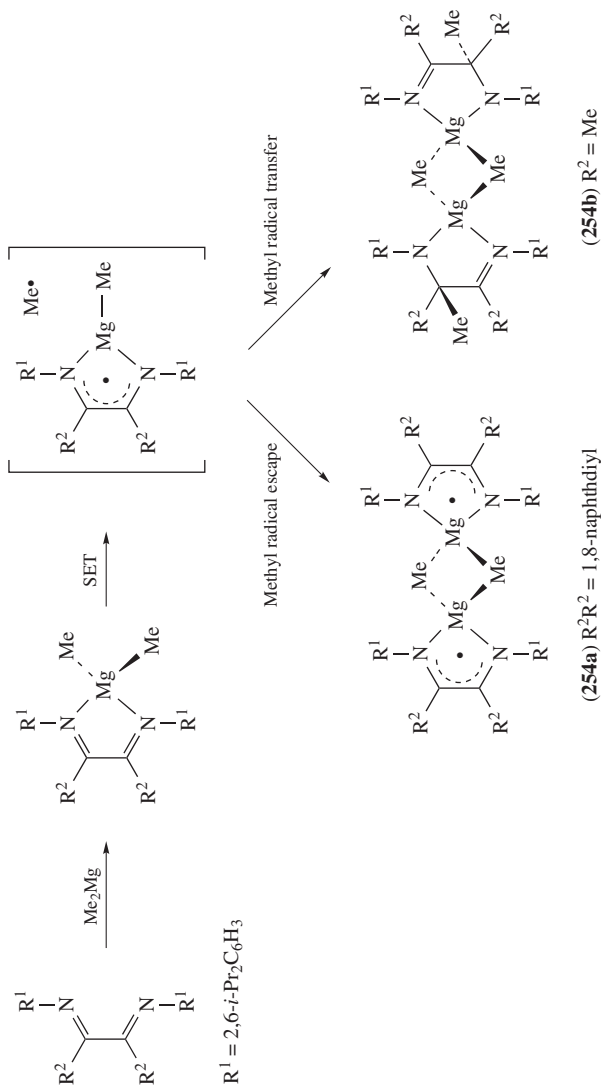
FIGURE 98. Molecular geometry of **252** in the solid state

the boroamidinate/amidinate anion are involved in bonding to magnesium [Mg–N(1) 2.004(2) Å, Mg–N(2) 2.390(2) Å and Mg–N(3) 2.080(2) Å]. Together with the  $\sigma$ -bonded *tert*-butyl group this leads to a distorted tetrahedral coordination geometry at magnesium (Figure 98).

From the reaction of the radical anion of 1,2-bis[(2,6-diisopropylphenyl)imino]acene-aphthene (dpp-bian) with *i*-PrMgCl, the persistent radical complex isopropylmagnesium dpp-bian (**253**) was isolated in yields up to 60% (equation 20)<sup>254</sup>. An X-ray crystal-structure determination of **253** showed that the magnesium atom has distorted tetrahedral coordination geometry as the result of the  $\sigma$ -bonded isopropyl group, one coordinate-bonded diethyl ether molecule and *N,N'*-chelate bonding of the dpp-bian radical anion. The radical anionic character of the dpp-bian moiety is indicated by the relatively long Mg–N bond distances [Mg–N 2.120(2) and 2.103(2) Å].



The first step in the reaction of  $\text{Me}_2\text{Mg}$  with bulky  $\alpha$ -diimine ligands is the formation of a complex in which the  $\alpha$ -diimine is *N,N'*-chelate bonded to  $\text{Me}_2\text{Mg}$  (Scheme 4)<sup>255, 256</sup>. The second step is a single electron transfer (SET) resulting in radical-pair formation. From this point two pathways are possible. The first pathway involves escape of a methyl radical from the solvent cage resulting in a methylmagnesium diimine radical that subsequently dimerizes to **254a**. The second pathway involves transfer of a methyl radical to the diimine skeleton resulting in an imino-amide ligand bonded to magnesium which subsequently dimerizes to **254b**. At low temperature the methyl radical-transfer reaction predominates while at room temperature the dimerized radical is the major product. It should be noted that similar radical processes have been observed in the reaction of dialkylzinc compounds with  $\alpha$ -diimines<sup>257, 258</sup>.



SCHEME 4. The radical mediated processes in the reaction of  $\text{Me}_2\text{Mg}$  with  $\alpha$ -dimines

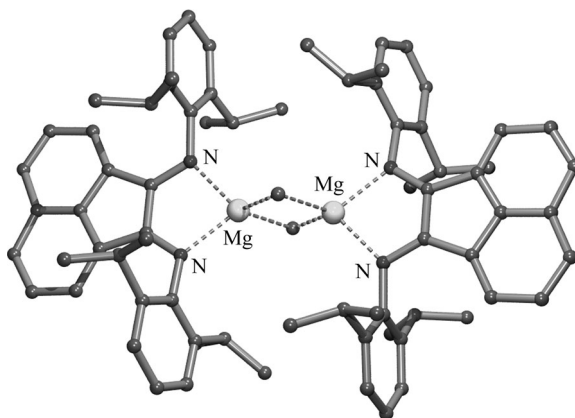


FIGURE 99. Molecular geometry of **254a** in the solid state

The structures of **254a** and **254b** in the solid state were established by X-ray crystal-structure determinations<sup>255,256</sup>. The structure of **254a** (Figure 99) comprises a symmetric dimer in which two methyl groups are two-electron three-center bonded between two magnesium atoms [Mg–C 2.263(5) Å] and a reduced dpp-bian ligand *N,N'*-chelate bonded to each magnesium atom [Mg–N 2.066(5) and 2.065(4) Å]. As a result both magnesium atoms have a tetrahedral coordination geometry. An X-ray crystal-structure determination of **254b** clearly shows its dimeric structure via two bridging two-electron three-center bonded methyl groups between the magnesium atoms. However, the methyl groups at the diimine skeleton are crystallographically disordered.

The structures of a series of organomagnesium amides, derived from secondary amines, have been determined. These compounds, [*n*-BuMg(TMP)]<sub>2</sub> (**255**)<sup>259</sup>, [*t*-BuMg(TMP)]<sub>2</sub> (**256**)<sup>224</sup>, [*t*-BuMgN(Bn)]<sub>2</sub> (**257**)<sup>224</sup>, [*t*-BuMgN(*Pr-i*)]<sub>2</sub> (**258**)<sup>224</sup>, [*t*-BuMgN(*c*-Hex)]<sub>2</sub> (**259**)<sup>224</sup>, [*t*-BuMgN(SiMe<sub>3</sub>)]<sub>2</sub> (**260**)<sup>224</sup> and [*s*-BuMgN(SiMe<sub>3</sub>)]<sub>2</sub> (**261**)<sup>260</sup>, have in common that they exist as dimers in the solid state. The amido nitrogen atoms are bridging in a symmetric way between the two magnesium atoms, forming a flat four-membered N–Mg–N–Mg ring. An organic group is  $\sigma$ -bonded to each of the magnesium atoms giving them a trigonal planar coordination geometry. The structures of these compounds are shown schematically (Figure 100).

The acetylenic organomagnesium amides [Me<sub>3</sub>SiC≡CMgN(*Pr-i*)]<sub>2</sub>(THF)]<sub>2</sub> (**262**)<sup>228</sup> and [PhC≡CMgN(*Pr-i*)]<sub>2</sub>(THF)]<sub>2</sub> (**263**)<sup>228</sup> (Figure 100) exist in the solid state as dimers. Their structures comprise a central flat N–Mg–N–Mg four-membered ring as the result of two bridging amide nitrogen atoms between the two magnesium atoms. To each of the magnesium atoms an acetylenic group is  $\sigma$ -bonded and an additional THF molecule is coordinate-bonded, giving the magnesium atoms a tetrahedral coordination geometry. The magnesium-bonded acetylenic groups and the oxygen atoms of the coordinating THF molecules are pairwise located in *anti*-position with respect to the N–Mg–N–Mg plane.

The structures of the organomagnesium amides [*t*-BuMgNHBu-*t*](THF)]<sub>2</sub> (**264**)<sup>162</sup> and [MeMgNHSi(*Pr-i*)]<sub>2</sub>(THF)]<sub>2</sub> (**265**)<sup>261</sup>, derived from primary amines, were determined by X-ray crystallography. The structure of **264** is closely related to those of **262** and **263**. The two amide nitrogen atoms are symmetrically bridge-bonded between the two magnesium atoms, resulting in a central flat, four-membered N–Mg–N–Mg ring (Figure 101). Like in **263** and **264**, the magnesium-bonded *tert*-butyl groups and the oxygen atoms of the coordinating THF molecules are pairwise located in *anti*-position with respect to the

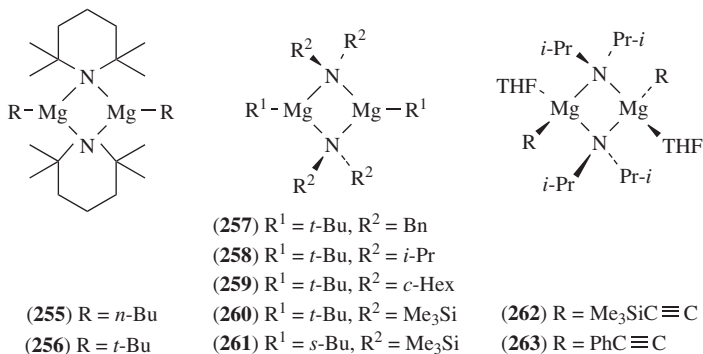


FIGURE 100. Schematic representation of the structures of organomagnesium amides **255–263** derived from secondary amines

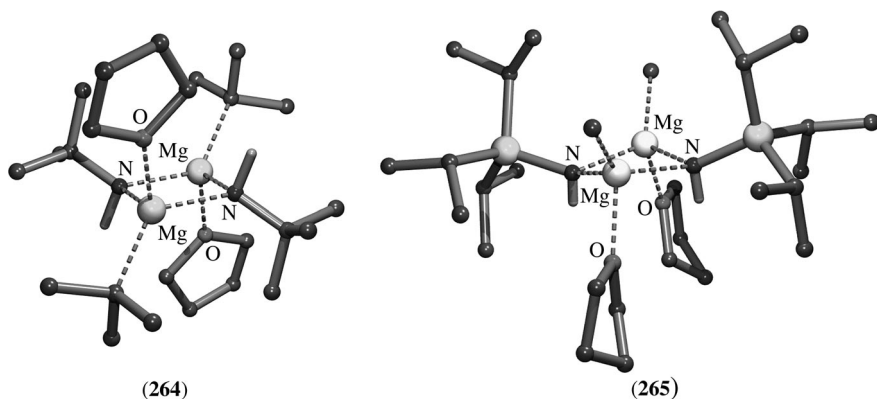


FIGURE 101. Molecular geometries of **264** and **265** in the solid state

N–Mg–N–Mg plane. A similar pairwise *anti*-position is observed for the nitrogen-bonded *tert*-butyl groups and the amide-hydrogen atoms.

The structure of **265** also comprises a central four-membered N–Mg–N–Mg ring as the result of bridging amide nitrogen atoms between the magnesium atoms. However, this ring is slightly folded ( $14.8^\circ$ ). The magnesium-bonded methyl groups and the oxygen atoms of the coordinating THF molecules show a pairwise *syn*-arrangement, as is also observed for the triethylsilyl substituent and the amide hydrogen atoms (Figure 101).

A remarkable structure in the solid state was found for the ethylmagnesium amide derived from the primary amine 2,6-diisopropylaniline. An X-ray crystal-structure determination showed that this compound exists as a cyclic dodecamer  $[\text{EtMgN}(\text{H})\text{C}_6\text{H}_3(\text{Pr-}i)_2\text{-}2,6]_{12}$  (**266**) in the solid state<sup>162</sup>. The cycle consists of twelve magnesium atoms between each of which one amide nitrogen atom is bridge-bonded and one ethyl group is two-electron three-center bridge-bonded resulting in a local N–Mg–N–Mg four-membered ring (Figure 102). The average Mg–C distance is  $2.21(2)$  Å, and the average Mg–N distance is  $2.086(10)$  Å. The ethyl groups are all disposed toward the interior of the cycle and the bulkier 2,6-*i*-Pr<sub>2</sub>C<sub>6</sub>H<sub>3</sub> substituents are all pointing outward.



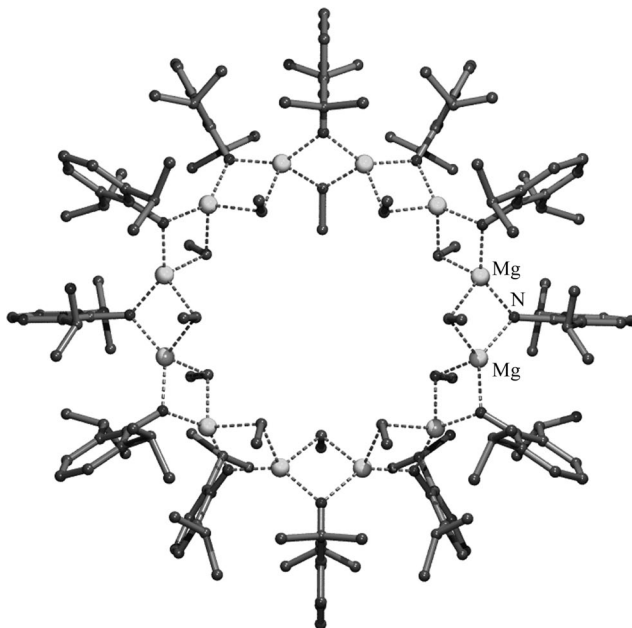


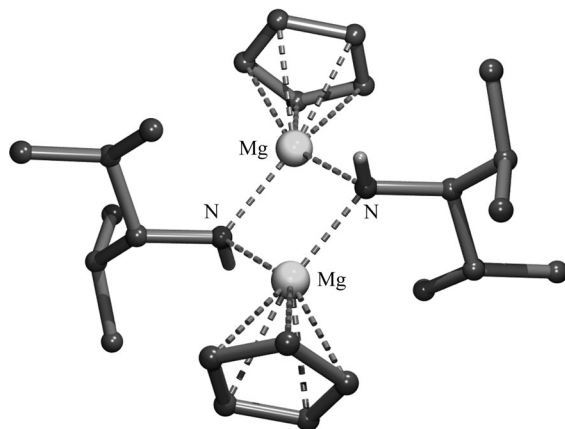
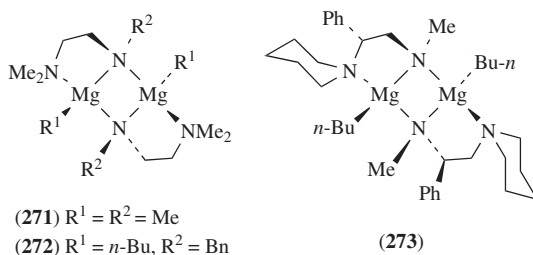
FIGURE 102. Molecular geometry of dodecameric **266** in the solid state

The solid-state structures of four cyclopentadienylmagnesium amides,  $[\text{CpMgNPh}_2]_2$  (**267**),  $[\text{CpMgN(H)CH}(i\text{-Pr})_2]_2$  (**268**),  $[\text{CpMgN(H)C}_6\text{H}_3(\text{Pr-}i)_2\text{-2,6}]_2$  (**269**) and  $[\text{CpMgNBn}(i\text{-Pr})]_2$  (**270**), have been determined<sup>233</sup>. The structures of these compounds are closely related and consist of a central flat four-membered N–Mg–N–Mg ring as the result of two bridging amide-nitrogen atoms between two magnesium atoms. In all compounds the cyclopentadienyl group is bonded in a  $\eta^5$ -fashion to magnesium. In **268** and **269** the nitrogen substituents and the amide-hydrogen atoms adopt an *anti*-configuration with respect to the N–Mg–N–Mg plane, like the benzyl-nitrogen and isopropyl-nitrogen substituents in **270**. As an example the structure of **268** is shown (Figure 103).

The monoorganomagnesium amides  $[\text{MeMgN(Me)CH}_2\text{CH}_2\text{NMe}_2]_2$  (**271**)<sup>262</sup>,  $[n\text{-BuMgN(Bn)CH}_2\text{CH}_2\text{NMe}_2]_2$  (**272**)<sup>263</sup> and  $[n\text{-BuMgN(Me)CH}_2\text{CH(Ph)N(CH}_2)_5]_2$  (**273**)<sup>176</sup> derived from *N,N',N'*-trisubstituted ethylenediamines have closely related structures in the solid state, of which the structures are shown schematically (Figure 104). These structures comprise a flat four-membered N–Mg–N–Mg ring formed via two bridging amide-nitrogen atoms between two magnesium atoms. The tertiary nitrogen atoms are intramolecularly coordinate-bonded to the magnesium atoms, one lying above the N–Mg–N–Mg plane and the other one below that plane. Consequently, the magnesium-bonded organic groups are in *anti*-position with respect to this plane. The chiral derivative **273** has been successfully applied in the enantioselective alkylation of aldehydes<sup>176</sup>.

#### F. Monoorganomagnesium Compounds $\text{RMgY}$ with $\text{Y} = \text{SR}$ or $\text{PR}_2$

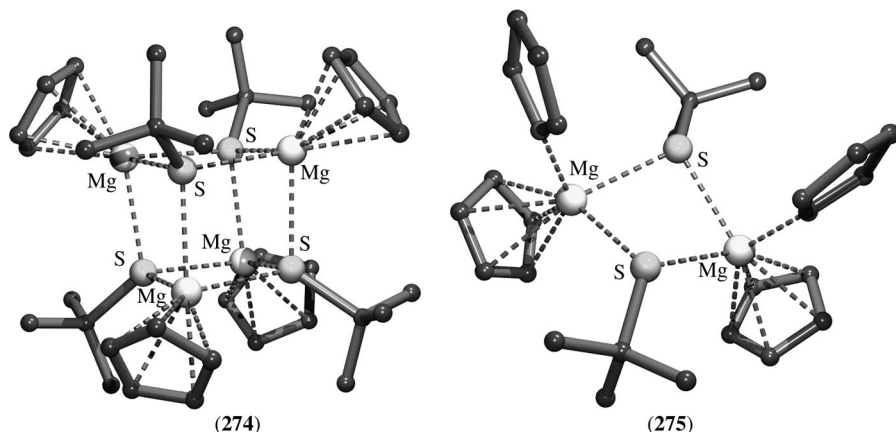
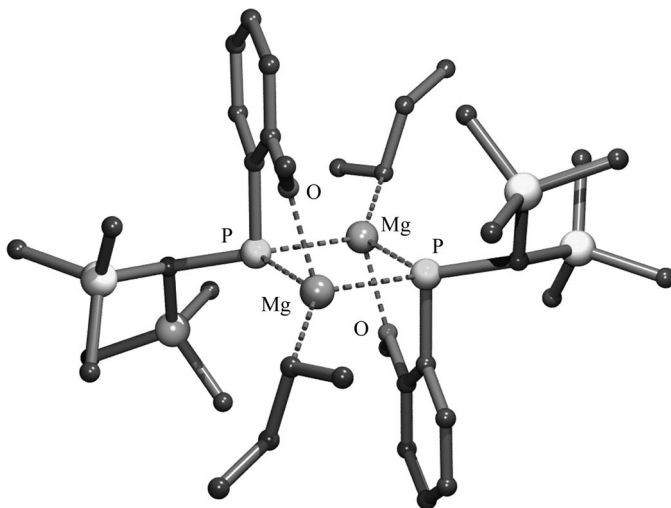
The structures of only a very few heteroleptic monoorganomagnesium compounds with a magnesium–heteroatom bond with heteroatoms other than halogen, oxygen or nitrogen have been determined.

FIGURE 103. Molecular geometry of **268** in the solid stateFIGURE 104. Schematic representation of the structures of **271–273** in the solid state

Cyclopentadienylmagnesium *tert*-butylthiolate exists as a tetrameric aggregate  $[\text{CpMgSBU-}t]_4$  (**274**) in the solid state. An X-ray crystal-structure determination revealed a heterocubane structure with magnesium and sulfur atoms at the corners (Figure 105)<sup>264</sup>. The Mg–S bond distances within the cube vary in a narrow range of 2.584(2) to 2.602(2) Å, indicating that the shape of the cube is close to perfect. To each of the magnesium atoms a cyclopentadienyl group is bonded in a  $\eta^5$ -fashion.

THF effectively breaks down tetrameric **274** to a dimeric THF complex  $[\text{CpMgSBU-}t(\text{THF})]_2$  (**275**). An X-ray crystal-structure determination of **275** showed a central four-membered S–Mg–S–Mg ring as the result of two symmetrically bridging sulfur atoms [Mg–S 2.503(1) and 2.504(1) Å] between two magnesium atoms (Figure 105)<sup>264</sup>. This four-membered ring is slightly folded, as indicated by the sum of the bond angles within this ring ( $243.93^\circ$ ). The cyclopentadienyl groups are  $\eta^5$ -bonded to magnesium and an additional THF molecule is coordinate-bonded to each magnesium atom.

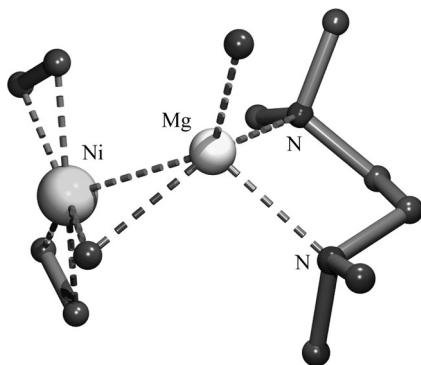
The reaction of the secondary phosphine 2-MeOC<sub>6</sub>H<sub>4</sub>PHCH(SiMe<sub>3</sub>)<sub>2</sub> with *s*-Bu<sub>2</sub>Mg gives heteroleptic  $[s\text{-BuMgP}(\text{C}_6\text{H}_4\text{OMe-2})(\text{CH}(\text{SiMe}_3)_2)]_2$  (**276**). An X-ray crystal-structure determination revealed a dimeric complex with a flat four-membered P–Mg–P–Mg ring as the result of two slightly asymmetric bridging phosphido groups between the magnesium atoms [Mg–P 2.5760(8) and 2.5978(8) Å] (Figure 106)<sup>265</sup>. To each of

FIGURE 105. Molecular geometries of **274** and **275** in the solid stateFIGURE 106. Molecular geometry of **276** in the solid state

the magnesium atoms a *s*-butyl group is  $\sigma$ -bonded. The magnesium atoms are four-coordinate as the result of intramolecular coordination of the oxygen atoms of methoxy substituents, one approaching a magnesium atom from above the P–Mg–P–Mg plane and the other approaching the other magnesium atom from below that plane. The resulting five-membered chelate rings are almost planar.

## V. MIXED ORGANOMAGNESIUM TRANSITION-METAL COMPOUNDS

In this section, structures of compounds are described that contain both an organomagnesium moiety and a transition-metal-containing part. These moieties are linked via either

FIGURE 107. Molecular geometry of **277** in the solid state

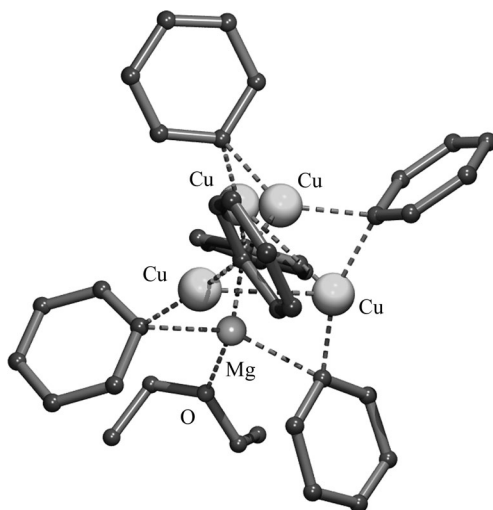
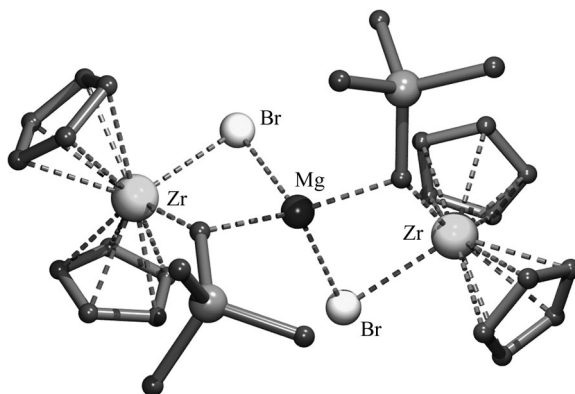
a direct magnesium to transition-metal bond or via bridge-bonded atoms, like hydrogen, carbon and halogen, between magnesium and the transition metal.

The reaction of tris(ethylene)nickel(0) with  $R_2Mg$  in the presence of donor molecules like  $Et_2O$ , THF, dioxane and TMEDA, at  $-10^\circ C$ , gives crystalline materials with the formulation  $R_2MgL_2Ni(C_2H_4)_2$ <sup>266, 267</sup>. The structure of one of these complexes,  $Me_2Mg(TMEDA)Ni(C_2H_4)_2$  (**277**), was determined by X-ray crystallography (Figure 107)<sup>266</sup>. In **277** one methyl group is two-electron three-center bridge-bonded between magnesium and nickel [Mg–C 2.294(3) Å and Ni–C 2.031(3) Å]. The other methyl group is  $\sigma$ -bonded to magnesium [Mg–C 2.150(3) Å]. A  $N,N'$ -chelate bonded TMEDA molecule [Mg–N 2.252(2) and 2.264(2) Å] completes the coordination sphere of magnesium. Two ethylene molecules are  $\pi$ -bonded to nickel. The Mg–Ni bond distance of 2.615(1) Å indicates that a bonding interaction exists between these metals.

An X-ray crystal-structure determination of the copper–magnesium cluster compound  $Ph_6Cu_4Mg(OEt_2)$  (**278**) shows that it comprises a central core of five metal atoms in a trigonal bipyramidal arrangement, with the magnesium atom at the axial position (Figure 108)<sup>268</sup>. The six phenyl groups bridge across the equatorial–axial edges of the trigonal bipyramid via two-electron three-center bonds. Coordination saturation at magnesium is reached by the additional coordination of a diethyl ether molecule.

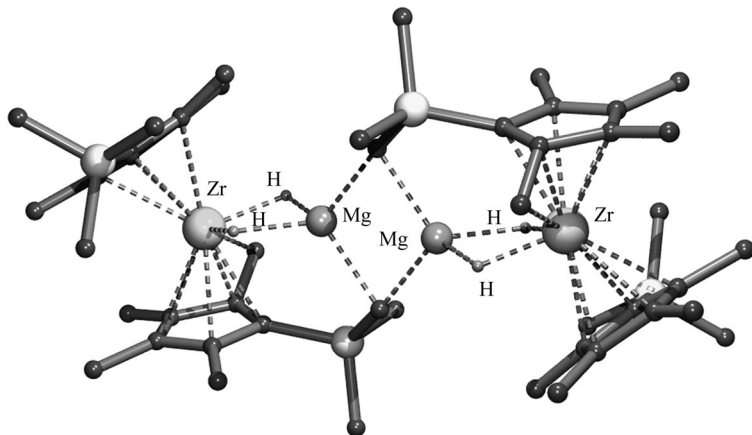
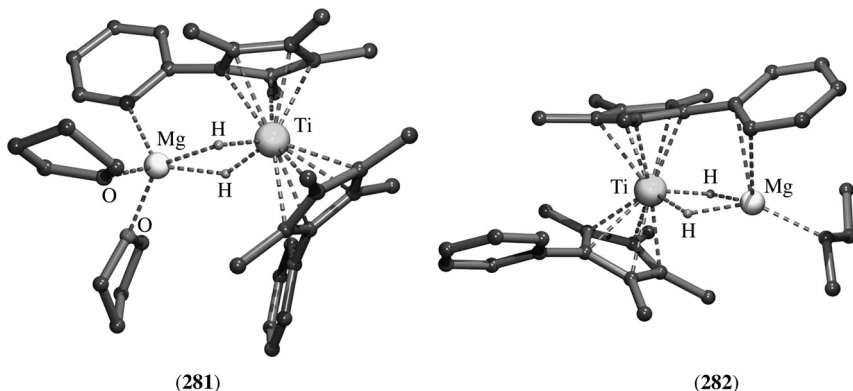
Instead of the anticipated metalla-cyclobutane, reaction of the 1,1-di-Grignard reagent  $Me_3SiCH(MgBr)_2$  with  $Cp_2ZrCl_2$  gives an unexpected product. An X-ray structure determination showed the formation of a Tebbe-type spiro-organomagnesium compound  $[Cp_2(Me_3SiCH)ZrBr]_2Mg$  (**279**)<sup>269</sup>. Its structure (Figure 109) comprises two  $Cp_2Zr$  moieties, each linked to a central magnesium atom via a bridging  $Me_3SiCH$  group [Mg–C 2.188(8) Å and Mg–Zr 2.147(7) Å] and a bridging bromine atom [Mg–Br 2.672(3) Å and Zr–Br 2.723(1) Å]. The coordination geometry at magnesium is distorted tetrahedral with the smallest angle being C–Mg–Br [ $92.2(2)^\circ$ ], which is a consequence of the four-membered C–Mg–Br–Zr ring.

Reduction of  $(Me_3Si(Me)_4C_5)_2ZrCl_2$  with metallic magnesium in THF affords as the major product a mixed zirconium–magnesium hydride  $[(Me_3Si(Me)_4C_5)(CH_2Me_2Si(Me)_3C_5(CH_2))ZrH_2Mg]_2$  (**280**) in which one of the substituted cyclopentadienyl groups at zirconium became doubly activated by abstraction of one hydrogen atom from the trimethylsilyl group and one hydrogen atom from the adjacent methyl group<sup>270</sup>. An X-ray crystal-structure determination showed that **280** is a centrosymmetric dimer as the result of two-electron three-center bridge-bonding of two methylene groups, generated from the

FIGURE 108. Molecular geometry of **278** in the solid stateFIGURE 109. Molecular geometry of **279** in the solid state

trimethylsilyl substituents, between two magnesium atoms [Mg–C 2.218(9) and 2.255(9) Å] (Figure 110). Between each of the magnesium atoms and its adjacent zirconium atom two hydrogen atoms are bridge-bonded [Mg–H 1.81(5) and 1.86(4) Å and Zr–H 1.89(6) and 1.92(4) Å] resulting in a tetrahedral coordination geometry at magnesium. EPR studies showed that **280** is contaminated with a product having a structure that is closely related to that of **280**, but lacks the activation of the methyl group adjacent to the activated trimethylsilyl substituent. Consequently, in this complex the zirconium atoms have a trivalent oxidation state. In fact, the only isolable product from the reaction with the titanium analog is such a dimeric complex with trivalent titanium<sup>271</sup>.

When (PhMe<sub>4</sub>C<sub>5</sub>)<sub>2</sub>TiCl<sub>2</sub> is reduced with magnesium in THF three main products are formed. They are the diamagnetic doubly ‘tucked-in’ titanocene complex (PhMe<sub>4</sub>C<sub>5</sub>)

FIGURE 110. Molecular geometry of **280** in the solid stateFIGURE 111. Molecular geometries of **281** and **282** in the solid state

( $\text{PhMe}_2(\text{CH}_2)_2\text{C}_5\text{Ti}$ , the paramagnetic trinuclear  $\text{Ti-Mg-Ti}$  hydride-bridged complex  $[(\text{PhMe}_4\text{C}_5)_2\text{Ti}(\mu\text{-H})_2]_2\text{Mg}$  and the paramagnetic binuclear titanocene hydride-magnesium hydride complex  $(\text{PhMe}_4\text{C}_5)[(2\text{-C}_6\text{H}_4)\text{Me}_4\text{PhC}_5]\text{Ti}(\mu\text{-H})_2\text{Mg}(\text{THF})_2$  (**281**). Of the latter complex the structure was determined by X-ray crystallography (Figure 111)<sup>272, 273</sup>. Its structure comprises a  $(\text{PhMe}_4\text{C}_5)_2\text{Ti}$  moiety in which both cyclopentadienyl groups are  $\eta^5$ -bonded to titanium. The magnesium atom is linked to titanium via two bridge-bonded hydrogen atoms [ $\text{Ti-H}$  1.72(3) and 1.78(3) Å,  $\text{Mg-H}$  1.97(3) and 1.99(3) Å]. It appears that one of the phenyl groups was metallated in its 2-position by forming a  $\sigma$ -bond with magnesium [ $\text{Mg-C}$  2.144(2) Å], resulting in an additional bridge between titanium and magnesium. The coordination sphere at magnesium is completed by two additional coordinating THF molecules, resulting in penta-coordinate magnesium.

When the same reaction was performed using an excess of  $n\text{-Bu}_2\text{Mg}$  as the reducing agent, essentially the same products are formed as from the reduction with metallic magnesium, *vide supra*. However, from this reaction mixture a by-product  $(\text{PhMe}_4\text{C}_5)_2\text{Ti}$

$(\mu\text{-H})_2\text{Mg}(\text{2-buten-2-yl})$  (**282**) was isolated in low yield. Its X-ray crystal-structure determination showed a similar titanocene-type structure as observed for **281** with two bridge-bonded hydrogen atoms between titanium and magnesium [ $\text{Ti-H}$  1.87(3) and 1.77(3) Å,  $\text{Mg-H}$  1.85(3) and 1.85(3) Å] (Figure 111)<sup>273</sup>. One of the phenyl groups has a  $\pi$ -type interaction with magnesium, as is indicated by the distances between its  $\text{C}_{ipso}$  and the adjacent carbon atom and the magnesium atom of 2.657(4) and 2.644(4) Å, respectively. The presence of a  $\sigma$ -bonded 2-buten-2-yl group at magnesium [ $\text{Mg-C}$  2.123(4) Å] implies a hydrogen transfer from the butyl group into the titanium–magnesium bond.

When  $\text{Cp}_2\text{TiCl}_2$  or its methyl-substituted derivative  $(\text{MeH}_4\text{C}_5)_2\text{TiCl}_2$  are reduced with magnesium in THF, in the presence of bis(trimethylsilyl)acetylene, a mixture of products is obtained. Two of these appeared to be the mixed titanium–magnesium complexes  $\text{CpTiMgCp}(\text{Me}_3\text{SiCCSiMe}_3)_2$  (**283**)<sup>274</sup> and its methyl-substituted derivative (**284**). X-ray crystal-structure determinations of **283** and **284** showed that they have similar structures, of which that of **284** is shown (Figure 112)<sup>274, 275</sup>. In **284** two  $\text{Me}_3\text{SiCCSiMe}_3$  moieties are bridge-bonded in a  $\mu\text{-}\eta^2\text{-}\eta^2$  fashion between magnesium and titanium, while to both titanium and magnesium a methylcyclopentadienyl group is  $\eta^5$ -bonded. The C–C bond lengths of 1.31(1) Å in the  $\text{Me}_3\text{SiCCSiMe}_3$  moiety and C–C–Si bond angles of average  $140^\circ$  indicate a change of the hybridization from  $\text{sp}$  to  $\text{sp}^2$  of these carbon atoms. The observed Mg–Ti distance of 2.776(2) Å indicates the presence of a bonding interaction between these metals.

Another product isolated from the above-mentioned reaction mixture is  $(\text{MeH}_4\text{C}_5)\text{TiMgCl}_2\text{Mg}(\text{C}_5\text{H}_4\text{Me})(\text{Me}_3\text{SiCCSiMe}_3)_2$  (**285**)<sup>275</sup>. An X-ray crystal-structure determination showed an almost perfect linear Ti–Mg–Mg arrangement with two  $\text{Me}_3\text{SiCCSiMe}_3$  moieties bridge-bonded in a  $\mu\text{-}\eta^2\text{-}\eta^2$  fashion between magnesium and titanium while a methylcyclopentadienyl group is  $\eta^5$ -bonded to titanium (Figure 112). Between the two magnesium atoms two chlorides are bridge-bonded in a slightly asymmetric way. The Mg–Cl bond distances to the terminal magnesium atom [ $\text{Mg-Cl}$  2.440(5) and 2.439(5) Å]

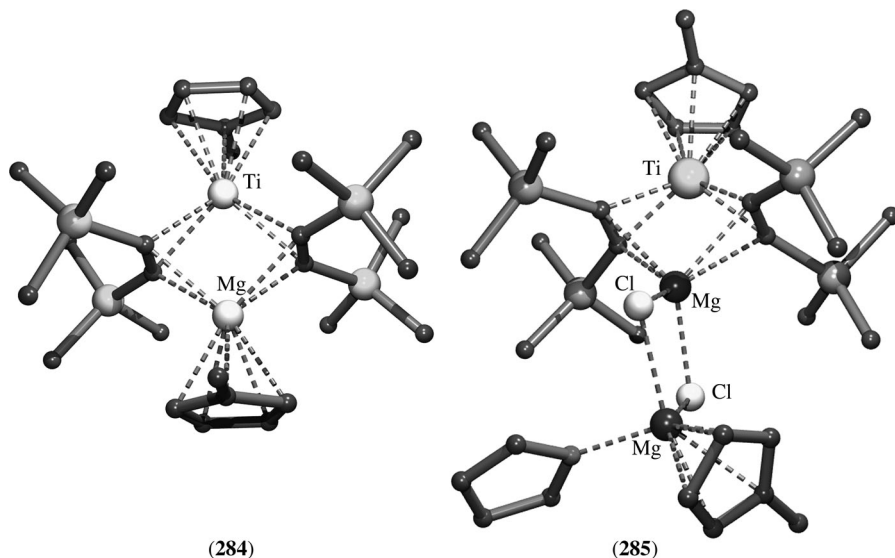


FIGURE 112. Molecular geometries of **284** and **285** in the solid state

are slightly longer than those to the central magnesium atom [Mg–Cl 2.340(4) and 2.352(4) Å]. To the terminal magnesium atom a methylcyclopentadienyl group is  $\eta^5$ -bonded and coordination saturation is completed by an additional coordinating THF molecule. Also, in this compound the observed Mg–Ti distance of 2.763(4) Å indicates a bonding interaction between these two metals.

It has been shown that one of the  $\mu^3$ -bridging hydrogen atoms in the  $\text{Cp}^*_3\text{Ru}_3\text{H}_5$  cluster can be easily replaced by a main group organometallic fragment like MeGa, EtAl *i*-PrMg or EtZn<sup>276</sup>. The X-ray crystal-structure determination of the product  $\text{Cp}^*_3\text{Ru}_3\text{Mg}(i\text{-Pr})\text{H}_4$  (**286**) obtained from the reaction of  $\text{Cp}^*_3\text{Ru}_3\text{H}_5$  with *i*-Pr<sub>2</sub>Mg shows that the main

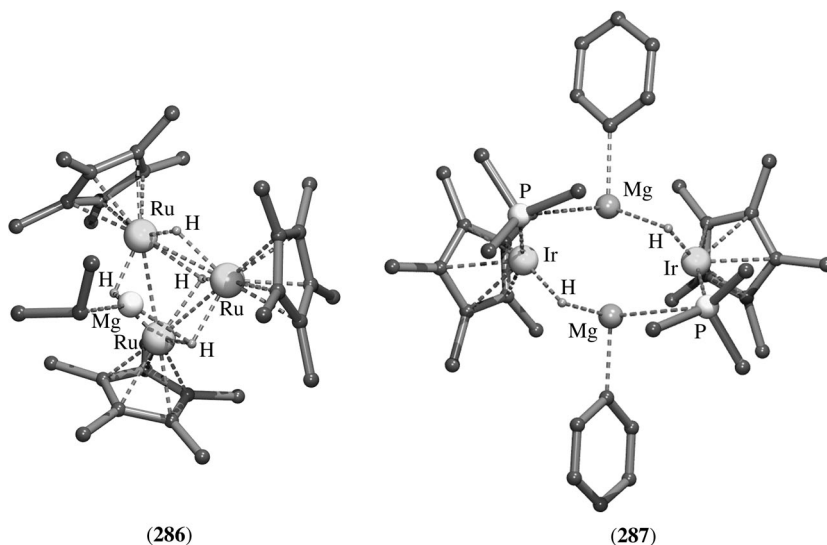


FIGURE 113. Molecular geometries of **286** and **287** in the solid state

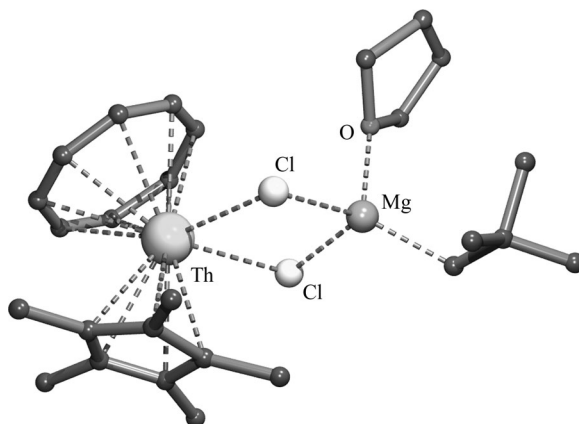


FIGURE 114. Molecular geometry of **288** in the solid state



structural features of the originating  $\text{Cp}^*_3\text{Ru}_3\text{H}_5$  cluster are retained, but one of the  $\mu^3$ -bridging hydrogen atoms is replaced by a  $\mu^3$ -bridging *i*-PrMg group (Figure 113), with almost equal Mg–Ru distances of 2.7487(13), 2.8007(12) and 2.7715(13) Å.

The reaction of  $\text{Cp}^*\text{IrH}_2(\text{PMe}_3)$  with  $\text{Ph}_2\text{Mg}$  gives a product formulated as  $\text{Cp}^*\text{IrH}(\text{PMe}_3)\text{MgPh}$ . An X-ray crystal-structure determination showed this compound to be a dimer  $[\text{Cp}^*\text{IrH}(\text{PMe}_3)\text{MgPh}]_2$  (**287**) in which two  $\text{Cp}^*\text{IrH}(\text{PMe}_3)$  moieties are connected by the two PhMg groups, on one side to the phosphorus atom and on the other side to the hydride (Figure 113)<sup>277</sup>. The geometry at the magnesium atoms is trigonal planar, and the distances to iridium are slightly different [Mg–Ir 2.669(2) and 2.748(2) Å].

Instead of the anticipated transmetallation product, the reaction of  $\text{Cp}^*(\text{C}_8\text{H}_8)\text{ThCl}$  with *t*-BuCH<sub>2</sub>MgCl in THF gives a complex  $\text{Cp}^*(\text{C}_8\text{H}_8)\text{ThCl}_2\text{Mg}(\text{CH}_2\text{Bu-}t)(\text{THF})$  (**288**). An X-ray crystal-structure determination showed that **288** contains a  $\text{Cp}^*(\text{C}_8\text{H}_8)\text{Th}$  moiety with a  $\eta^8$ -bonded cyclooctatetraenyl group and a  $\eta^5$ -bonded pentamethylcyclopentadienyl group (Figure 114)<sup>278</sup>. Two chlorides are bridge-bonded between thorium and magnesium while a neopentyl group is  $\sigma$ -bonded to magnesium and an additional THF molecule completes the coordination sphere at magnesium.

## VI. CONCLUSIONS

In this chapter it has become clear that knowledge about the structures of organomagnesium compounds both in the solid state and in solution is often a pre-requisite for a better understanding of the reaction pathways involved in reactions of organomagnesium compounds. For the design of new synthetic pathways for the synthesis of new organic products this knowledge is of particular importance.

In contrast to their zinc analogs, simple dialkyl- and diaryl-magnesium compounds are, with a very few exceptions, not simple monomeric molecules. Due to the strong tendency of magnesium to extend its coordination number to usually four or even higher, these compounds form aggregates via multi-center, usually two-electron three-center, bonded organic groups. The only exceptions are a few diorganomagnesium compounds bearing very bulky substituents that prevent multi-center bonding for steric reasons. An example is  $[(\text{Me}_3\text{Si})_3\text{C}]_2\text{Mg}$  that has a linear monomeric structure in the solid state.

In the presence of Lewis bases, diorganomagnesium compounds form complexes with one or two donor molecules. The usually observed coordination number for magnesium is four in complexes where magnesium has a tetrahedral coordination geometry. When a diorganomagnesium compound and/or ligand contains sterically demanding groups, complexes with one donor molecule are formed in which the magnesium is trigonal planar coordinate. However, higher coordination numbers are also observed, especially in complexes with multidentate donor ligands.

Various structural motifs are observed in the solid-state structures of heteroleptic organomagnesium compounds  $\text{RMgY}$ . In these compounds Y is either a halide or a heteroatom-containing group. In a few exceptional cases this group is  $\sigma$ -bonded to magnesium, resulting in monomeric heteroleptic organomagnesium compounds. Usually, such groups form multi-center bonds in which the group Y is either  $\mu^2$ - or  $\mu^3$ -bridge-bonded between two and three magnesium centers, respectively. Consequently, such bridge-bonding gives rise to the formation of aggregated structures.

In solutions containing  $\text{RMgY}$  species, the possible existence of a Schlenk equilibrium between  $\text{RMgY}$  and both  $\text{R}_2\text{Mg}$  and  $\text{MgY}_2$  should always be considered. Moreover, equilibria between various aggregated species cannot be excluded. It should be noted that the formation of crystalline material, e.g. for structural studies in the solid state, may well be influenced by factors such as differences in solubilities of the various aggregates in solution and packing effects in the crystal lattice. As a consequence, care should be taken

in drawing conclusions about structures in solution from data obtained from solid-state structural investigations (e.g. X-ray crystallography). It is perhaps prudent to regard these solid-state structures as resting states and to realize that they may represent only one of many structural forms present in solution.

## VII. REFERENCES

1. P. Barbier, *Compt. Rend. Acad. Sci.*, **128**, 111 (1899).
2. V. Grignard, *Compt. Rend. Acad. Sci.*, **130**, 1322 (1900).
3. W. E. Lindsell, in *Comprehensive Organometallic Chemistry* (Eds. G. Wilkinson, F. G. A. Stone and E. W. Abel), Vol. 1, Pergamon, Oxford, 1982, pp. 155–252.
4. W. E. Lindsell, in *Comprehensive Organometallic Chemistry II* (Eds. E. W. Abel, F. G. A. Stone and G. Wilkinson), Vol. 1, Pergamon/Elsevier, Oxford, 1995, pp. 57–127.
5. T. P. Hanusa, in *Comprehensive Organometallic Chemistry III* (Eds. R. H. Crabtree and M. D. P. Mingos), Vol. 2, Elsevier, Oxford, 2006, pp. 67–152.
6. A. Baeyer and V. Villiger, *Chem. Ber.*, **35**, 1201 (1902).
7. V. Grignard, *Compt. Rend. Acad. Sci.*, **136**, 1260 (1903).
8. G. L. Stadnikov, *J. Russ. Phys.-Chem. Soc.*, **43**, 1235 (1912); *Chem. Abstr.*, **6**, 5482 (1912).
9. L. Thorp and O. Kamm, *J. Am. Chem. Soc.*, **36**, 1022 (1914).
10. R. Abegg, *Chem. Ber.*, **38**, 4112 (1905).
11. E. C. Ashby, *Q. Rev.*, **21**, 259 (1967).
12. W. Schlenk and W. Schlenk, Jr., *Chem. Ber.*, **62**, 920 (1929).
13. G. S. Silverman and P. E. Rakita (Eds.), *Handbook of Grignard Reagents*, Marcel Dekker, New York, 1996.
14. H. G. Richey, Jr. (Ed.), *Grignard Reagents, New Developments*, Wiley, Chichester, 2000.
15. P. R. Markies, O. S. Akkerman, F. Bickelhaupt, W. J. J. Smeets and A. L. Spek, *Adv. Organomet. Chem.*, **32**, 147 (1991).
16. T. S. Ertel and H. Bertagnolli, in *Grignard Reagents, New Developments* (Ed. H. G. Richey, Jr.), Wiley, Chichester, 2000, p. 329.
17. T. Holm and I. Crossland, in *Grignard Reagents, New Developments* (Ed. H. G. Richey, Jr.), Wiley, Chichester, 2000, p. 1.
18. C. Blomberg, in *Handbook of Grignard Reagents* (Eds. G. S. Silverman and P. E. Rakita), Marcel Dekker, New York, 1996, p. 249.
19. G. D. Stucky and R. E. Rundle, *J. Am. Chem. Soc.*, **85**, 1002 (1963).
20. L. J. Guggenberger and R. E. Rundle, *J. Am. Chem. Soc.*, **86**, 5344 (1964).
21. E. Weiss, *J. Organomet. Chem.*, **2**, 314 (1964).
22. E. Weiss, *J. Organomet. Chem.*, **4**, 101 (1965).
23. Cambridge Structural Database, release 5.28, January 2007.
24. N. S. Poonia and A. V. Bajaj, *Chem. Rev.*, **79**, 389 (1979).
25. C. E. Holloway and M. Melnik, *J. Organomet. Chem.*, **465**, 1 (1994).
26. C. E. Holloway and M. Melnik, *Coord. Chem. Rev.*, **135/136**, 287 (1994).
27. H. L. Uhm, in *Handbook of Grignard Reagents* (Eds. G. S. Silverman and P. E. Rakita), Marcel Dekker, New York, 1996, p. 117.
28. F. Bickelhaupt, in *Grignard Reagents, New Developments* (Ed. H. G. Richey, Jr.), Wiley, Chichester, 2000, p. 299.
29. J. T. B. H. Jastrzebski, J. Boersma and G. van Koten, in *The Chemistry of Organozinc Compounds*, Part 1 (Eds. Z. Rappoport and I. Marek), Chap. 2, Wiley, Chichester, 2006, pp. 31–135.
30. J. A. Wanklyn, *Liebigs Ann. Chem.*, **108**, 67 (1858).
31. G. Wittig, F. J. Meyer and G. Lange, *Liebigs Ann. Chem.*, **571**, 167 (1951).
32. G. Wittig, *Angew. Chem.*, **70**, 65 (1958).
33. W. Tochtermann, *Angew. Chem., Int. Ed. Engl.*, **5**, 351 (1966).
34. G. E. Coates and J. A. Heslop, *J. Chem. Soc. A*, 514 (1968).
35. L. M. Seitz and T. L. Brown, *J. Am. Chem. Soc.*, **88**, 4140 (1966).
36. L. M. Seitz and T. L. Brown, *J. Am. Chem. Soc.*, **89**, 1602 (1967).
37. L. M. Seitz and B. F. Little, *J. Organomet. Chem.*, **18**, 227 (1969).
38. E. Weiss, *Angew. Chem., Int. Ed. Engl.*, **32**, 1501 (1993).

39. R. E. Mulvey, *Chem. Commun.*, 1049 (2001).
40. R. E. Mulvey, *Organometallics*, **25**, 1060 (2006).
41. K. Kitagawa, A. Inoue, H. Shinokubo and K. Oshima, *Angew. Chem., Int. Ed.*, **39**, 2481 (2000).
42. A. Inoue, K. Kitagawa, H. Shinokubo and K. Oshima, *J. Org. Chem.*, **66**, 4333 (2001).
43. S. Y. W. Lau, G. Hughes, P. D. O'Shea and I. W. Davies, *Org. Lett.*, **9**, 2239 (2007).
44. F. Mongin, A. Bucher, J. P. Bazureau, O. Bayh, H. Awad and F. Trécourt, *Tetrahedron Lett.*, **46**, 7989 (2005).
45. M. Hatano, T. Matsumura and K. Ishihara, *Org. Lett.*, **7**, 573 (2005).
46. D. B. Patterson and A. F. Halasa, *Macromolecules*, **24**, 1583 (1991).
47. J. L. Atwood and G. D. Stucky, *J. Am. Chem. Soc.*, **91**, 2538 (1969).
48. T. Greiser, J. Kopf, D. Thoennes and E. Weiss, *Chem. Ber.*, **114**, 209 (1981).
49. T. Greiser, J. Kopf and E. Weiss, *Chem. Ber.*, **122**, 1395 (1989).
50. B. Schubert and E. Weiss, *Chem. Ber.*, **117**, 366 (1984).
51. R. A. Layfield, T. H. Bullock, F. García, S. M. Humphrey and P. Schüler, *Chem. Commun.*, 2039 (2006).
52. P. C. Andrikopoulos, D. R. Armstrong, E. Hevia, A. L. Kennedy, R. E. Mulvey and C. T. O'Hara, *Chem. Commun.*, 1131 (2005).
53. D. Thoennes and E. Weiss, *Chem. Ber.*, **111**, 3726 (1978).
54. H. Viebrock, U. Behrens and E. Weiss, *Angew. Chem., Int. Ed. Engl.*, **33**, 1257 (1994).
55. E. P. Squiller, R. R. Whittle and H. G. Richey Jr., *J. Am. Chem. Soc.*, **107**, 432 (1985).
56. H. G. Richey Jr. and B. A. King, *J. Am. Chem. Soc.*, **104**, 4672 (1982).
57. A. D. Pajerski, M. Parvez and H. G. Richey Jr., *J. Am. Chem. Soc.*, **110**, 2660 (1988).
58. K. M. Waggoner and P. P. Power, *Organometallics*, **11**, 3209 (1992).
59. D. V. Graham, E. Hevia, A. R. Kennedy, R. E. Mulvey, C. T. O'Hara and C. Talmard, *Chem. Commun.*, 417 (2006).
60. S. Sakamoto, T. Imamoto and K. Yamaguchi, *Org. Lett.*, **3**, 1793 (2001).
61. M. Vestergren, J. Eriksson and M. Håkansson, *J. Organomet. Chem.*, **681**, 215 (2003).
62. N. D. R. Barnett, W. Clegg, A. R. Kennedy, R. E. Mulvey and S. Weatherstone, *Chem. Commun.*, 375 (2005).
63. M.-L. Hsueh, B.-T. Ko, T. Athar, C.-C. Lin, T.-M. Wu and S.-F. Hsu, *Organometallics*, **25**, 4144 (2006).
64. E. Hevia, K. W. Henderson, A. R. Kennedy and R. E. Mulvey, *Organometallics*, **25**, 1778 (2006).
65. G. C. Forbes, A. R. Kennedy, R. E. Mulvey, P. J. A. Rodger and R. B. Rowlings, *J. Chem. Soc., Dalton Trans.*, 1477 (2001).
66. P. C. Andrikopoulos, D. R. Armstrong, A. R. Kennedy, R. E. Mulvey, C. T. O'Hara, R. B. Rowlings and S. Weatherstone, *Inorg. Chim. Acta*, **360**, 1370 (2007).
67. D. R. Armstrong, A. R. Kennedy, R. E. Mulvey and R. B. Rowlings, *Angew. Chem., Int. Ed.*, **38**, 131 (1999).
68. P. C. Andrews, A. R. Kennedy, R. E. Mulvey, C. L. Raston, B. A. Roberts and R. B. Rowlings, *Angew. Chem., Int. Ed.*, **39**, 1960 (2000).
69. K. W. Henderson, A. R. Kennedy, R. E. Mulvey, C. T. O'Hara and R. B. Rowlings, *Chem. Commun.*, 1678 (2001).
70. P. C. Andrikopoulos, D. R. Armstrong, W. Clegg, C. J. Gilfillan, E. Hevia, A. R. Kennedy, R. E. Mulvey, C. T. O'Hara, J. A. Parkinson and D. M. Tooke, *J. Am. Chem. Soc.*, **126**, 11612 (2004).
71. E. Hevia, D. J. Gallagher, A. R. Kennedy, R. E. Mulvey, C. T. O'Hara and C. Talmard, *Chem. Commun.*, 2422 (2004).
72. P. C. Andrikopoulos, D. R. Armstrong, D. V. Graham, E. Hevia, A. R. Kennedy, R. E. Mulvey, C. T. O'Hara and C. Talmard, *Angew. Chem., Int. Ed.*, **44**, 3459 (2005).
73. E. Hevia, G. W. Honeymann, A. R. Kennedy, R. E. Mulvey and D. C. Sherrington, *Angew. Chem., Int. Ed.*, **44**, 68 (2005).
74. P. C. Andrikopoulos, D. R. Armstrong, E. Hevia, A. R. Kennedy and R. E. Mulvey, *Organometallics*, **25**, 2415 (2006).
75. R. A. Anderson and G. Wilkinson, *J. Chem. Soc., Dalton Trans.*, 809 (1977).
76. E. C. Ashby, L. Fernholt, A. Haaland, R. Seip and R. S. Smith, *Acta Chem. Scand.*, **A 34**, 213 (1980).

77. S. S. Al-Juaid, C. Eaborn, P. B. Hitchcock, C. A. McGeary and J. D. Smith, *J. Chem. Soc., Chem. Commun.*, 273 (1989).
78. S. S. Al-Juaid, C. Eaborn, P. B. Hitchcock, C. A. McGeary, K. Kundu and J. D. Smith, *J. Organomet. Chem.*, **480**, 199 (1994).
79. R. J. Wehmschulte and P. P. Power, *Organometallics*, **14**, 3264 (1995).
80. P. B. Hitchcock, J. A. K. Howard, M. F. Lappert, W.-P. Leung and S. A. Mason, *J. Chem. Soc., Chem. Commun.*, 847 (1990).
81. R. J. Wehmschulte, B. Twamley and M. A. Khan, *Inorg. Chem.*, **40**, 6004 (2001).
82. K. B. Starowieyski, J. Lewinski, R. Wozniak, J. Lipkowski and A. Chrost, *Organometallics*, **22**, 2458 (2003).
83. P. R. Markies, G. Schat, O. S. Akkerman, F. Bickelhaupt, W. J. J. Smeets, P. van der Sluis and A. L. Spek, *J. Organomet. Chem.*, **393**, 315 (1990).
84. T. J. Kealy and P. L. Pauson, *Nature*, **168**, 1039 (1951).
85. S. A. Miller, J. A. Tebboth and J. F. Tremaine, *J. Chem. Soc.*, 632 (1952).
86. P. Laszlo and R. Hoffman, *Angew. Chem., Int. Ed.*, **39**, 123 (2000).
87. F. Cotton and G. Wilkinson, *Chem. Ind.*, 307 (1954).
88. E. O. Fischer and W. Hafner, *Z. Naturforsch.*, **B9**, 503 (1954).
89. E. Weiss and E. O. Fischer, *Z. Anorg. Allg. Chem.*, **278**, 219 (1955).
90. W. Bünder and E. Weiss, *J. Organomet. Chem.*, **92**, 1 (1975).
91. A. Haaland, J. Luszyk and D. P. Novak, *J. Chem. Soc., Chem. Commun.*, 54 (1974).
92. M. G. Gardiner, C. L. Raston and C. H. L. Kennard, *Organometallics*, **10**, 3680 (1991).
93. C. P. Morley, P. Jutzi, C. Krüger and J. M. Wallis, *Organometallics*, **6**, 1084 (1987).
94. F. Weber, H. Sitzmann, M. Schultz, C. D. Soffield and R. A. Andersen, *Organometallics*, **21**, 3139 (2002).
95. H. Schumann, J. Gottfriedsen, M. Glanz, S. Dechert and J. Demtschuk, *J. Organomet. Chem.*, **616–618**, 588 (2001).
96. H. Schumann, S. Schutte, H. J. Kroth and D. Lentz, *Angew. Chem., Int. Ed.*, **43**, 6208 (2004).
97. J. Vollet, E. Baum and H. Schnöckel, *Organometallics*, **22**, 2525 (2003).
98. O. Gobley, S. Gentil, J. D. Schloss, R. D. Rogers, J. C. Gallucci, P. Meunier, B. Gautheron and L. A. Paquette, *Organometallics*, **18**, 2531 (1999).
99. M. Westerhausen, N. Makropoulos, B. Wieneke, K. Karaghiosoff, H. Nöth, H. Schwenk-Kircher, J. Knizek and T. Seifert, *Eur. J. Inorg. Chem.*, 965 (1998).
100. J. L. Atwood and K. D. Smith, *J. Am. Chem. Soc.*, **96**, 994 (1974).
101. A. Xia, J. Heeg and C. H. Winter, *Organometallics*, **22**, 1793 (2003).
102. R. A. Andersen, R. Blom, A. Haaland, B. E. R. Schilling and H. Volden, *Acta Chem. Scand.*, **A39**, 563 (1985).
103. X. Zheng, U. Englert, G. E. Herberich and J. Rosenplänter, *Inorg. Chem.*, **39**, 5579 (2000).
104. J. A. J. Jarvis, B. T. Kilbourn, R. Pearce and M. F. Lappert, *J. Chem. Soc., Chem. Commun.*, 475 (1973).
105. J. M. Guss, R. Mason, I. Sjøtofte, G. van Koten and J. G. Noltes, *J. Chem. Soc., Chem. Commun.*, 446 (1972).
106. P. R. Markies, R. M. Altink, A. Villena, O. S. Akkerman, F. Bickelhaupt, W. J. J. Smeets and A. L. Spek, *J. Organomet. Chem.*, **402**, 289 (1991).
107. R. R. Holmes, *Prog. Inorg. Chem.*, **32**, 119 (1984).
108. N. Seidel, K. Jacob, A. K. Fischer, C. Pietzsch, P. Zanello and M. Fontani, *Eur. J. Inorg. Chem.*, 145 (2001).
109. M. J. Henderson, R. I. Papasergio, C. L. Raston, A. H. White and M. F. Lappert, *J. Chem. Soc., Chem. Commun.*, 672 (1986).
110. C. Eaborn, P. B. Hitchcock, A. Kowalewska, Z.-R. Lu, J. D. Smith and W. A. Stańczyk, *J. Organomet. Chem.*, **521**, 113 (1996).
111. C. F. Caro, P. B. Hitchcock and M. F. Lappert, *Chem. Commun.*, 1433 (1999).
112. S. S. Al-Juaid, A. G. Avent, C. Eaborn, S. M. El-Hamruni, S. A. Hawkes, M. S. Hill, M. Hopman, P. B. Hitchcock and J. D. Smith, *J. Organomet. Chem.*, **631**, 76 (2001).
113. B. Bogdanović, S. Liao, M. Schwickardi, P. Sikorsky and B. Spliethoff, *Angew. Chem., Int. Ed. Engl.*, **19**, 818 (1980).
114. K. Angermund, B. Bogdanović, G. Koppetsch, C. Krüger, R. Mynott, M. Schwickardi and Y.-H. Tsay, *Z. Naturforsch.*, **B41**, 455 (1986).
115. B. Bogdanović, G. Koppetsch, C. Krüger and R. Mynott, *Z. Naturforsch.*, **B41**, 617 (1986).

116. P. R. Markies, G. Schat, A. Villena, O. S. Akkerman, F. Bickelhaupt, W. J. J. Smeets and A. L. Spek, *J. Organomet. Chem.*, **411**, 291 (1991).
117. P. R. Markies, T. Nomoto, O. S. Akkerman, F. Bickelhaupt, W. J. J. Smeets and A. L. Spek, *Angew. Chem., Int. Ed. Engl.*, **27**, 1084 (1988).
118. P. R. Markies, T. Nomoto, G. Schat, O. S. Akkerman, F. Bickelhaupt, W. J. J. Smeets and A. L. Spek, *Organometallics*, **10**, 3826 (1991).
119. A. Pape, M. Lutz and G. Müller, *Angew. Chem., Int. Ed. Engl.*, **33**, 2281 (1994).
120. A. G. Avent, C. F. Caro, P. B. Hitchcock, M. F. Lappert, Z. Li and X.-H. Wei, *Dalton Trans.*, 1567 (2004).
121. C. F. Caro, P. B. Hitchcock, M. F. Lappert and M. Layh, *Chem. Commun.*, 1297 (1998).
122. T. Greiser, J. Kopf, D. Thoenes and E. Weiss, *J. Organomet. Chem.*, **191**, 1 (1980).
123. D. Thoenes and E. Weiss, *Chem. Ber.*, **111**, 3381 (1978).
124. P. J. Bailey, R. A. Coxall, C. M. Dick, S. Fabre, L. C. Henderson, C. Herber, S. T. Liddle, D. Loroño-González, A. Parkin and S. Parsons, *Chem. Eur. J.*, **9**, 4820 (2003).
125. H. Viebrock and E. Weiss, *J. Organomet. Chem.*, **464**, 121 (1994).
126. N. D. R. Barnett, W. Clegg, R. E. Mulvey, P. A. O'Neil and D. Reed, *J. Organomet. Chem.*, **510**, 297 (1996).
127. T. Rüffer, C. Bruhn and D. Steinborn, *Main Group Met. Chem.*, **24**, 369 (2001).
128. J. Toney and G. D. Stuckey, *J. Organomet. Chem.*, **22**, 241 (1970).
129. H. Erikson, M. Örtendahl and M. Håkansson, *Organometallics*, **15**, 4823 (1996).
130. W. Gaderbauer, M. Zirngast, J. Baumgartner, C. Marschner and T. D. Tilley, *Organometallics*, **25**, 2599 (2006).
131. U. Nagel and G. Nedden, *Chem. Ber./Recueil*, **130**, 535 (1997).
132. R. I. Yousef, B. Walfort, T. Rüffer, C. Wagner, H. Schmidt, R. Herzog and D. Steinborn, *J. Organomet. Chem.*, **690**, 1178 (2005).
133. R. Fischer, D. Walther, P. Gerhardt and H. Görls, *Organometallics*, **19**, 2532 (2000).
134. M. Parvez, A. D. Pajerski and H. G. Richey Jr., *Acta Cryst.*, **C44**, 1212 (1988).
135. F. Bickelhaupt, *Angew. Chem., Int. Ed. Engl.*, **26**, 990 (1987).
136. F. Bickelhaupt, *Pure Appl. Chem.*, **62**, 699 (1990).
137. H. C. Holtkamp, C. Blomberg and F. Bickelhaupt, *J. Organomet. Chem.*, **19**, 279 (1969).
138. A. L. Spek, G. Schat, H. C. Holtkamp, C. Blomberg and F. Bickelhaupt, *J. Organomet. Chem.*, **131**, 331 (1977).
139. M. F. Lappert, T. R. Martin, C. L. Raston, B. W. Skelton and A. H. White, *J. Chem. Soc., Dalton Trans.*, 1959 (1982).
140. M. A. G. M. Tinga, G. Schat, O. S. Akkerman, F. Bickelhaupt, E. Horn, H. Kooijman, W. J. J. Smeets and A. L. Spek, *J. Am. Chem. Soc.*, **115**, 2808 (1993).
141. T. Stey and D. Stalke, in *The Chemistry of Organolithium Compounds*, Part 1 (Eds. Z. Rappoport and I. Marek), Chap. 2, Wiley, Chichester, 2004, pp. 47–120.
142. P. R. Markies, O. S. Akkerman, F. Bickelhaupt, W. J. J. Smeets and A. L. Spek, *Organometallics*, **13**, 2616 (1994).
143. D. Steinborn, T. Rüffer, C. Bruhn and W. Heinemann, *Polyhedron*, **17**, 3275 (1998).
144. B. Schubert, U. Behrens and E. Weiss, *Chem. Ber.*, **114**, 2640 (1981).
145. M. Vestergren, B. Gustafsson, Ö. Davidsson and M. Håkansson, *Angew. Chem., Int. Ed.*, **39**, 3435 (2000).
146. P. R. Markies, T. Nomoto, O. S. Akkerman, F. Bickelhaupt, W. J. J. Smeets and A. L. Spek, *J. Am. Chem. Soc.*, **110**, 4845 (1988).
147. A. D. Pajerski, G. L. BergStresser, M. Parves and H. G. Richey Jr., *J. Am. Chem. Soc.*, **110**, 4844 (1988).
148. H. E. Ramsden, U.S. Patent 3354190 (1967); *Chem. Abstr.*, **68**, 114744 (1968).
149. B. Bogdanović, *Angew. Chem., Int. Ed. Engl.*, **24**, 262 (1985).
150. B. Bogdanović, *Acc. Chem. Res.*, **21**, 261 (1988).
151. C. L. Raston, in *Grignard Reagents, New Developments* (Ed. H. G. Richey, Jr.), Wiley, Chichester, 2000, pp. 278–298.
152. B. Bogdanović, N. Janke, H.-G. Kinzelmann and U. Westeppe, *Chem. Ber.*, **121**, 33 (1988).
153. B. Bogdanović, S. Liao, R. Mynott, K. Schlichte and U. Westeppe, *Chem. Ber.*, **117**, 1378 (1984).
154. E. Bartmann, B. Bogdanović, N. Janke, S. Liao, K. Schlichte, B. Spliethoff, J. Treber, U. Westeppe and U. Wilczok, *Chem. Ber.*, **123**, 1517 (1990).

155. L. M. Engelhardt, S. Harvey, C. L. Raston and A. H. White, *J. Organomet. Chem.*, **341**, 39 (1988).
156. B. Bogdanović, N. Janke, C. Krüger, R. Mynott, K. Schlichte and U. Westeppe, *Angew. Chem., Int. Ed. Engl.*, **24**, 960 (1985).
157. H. Lehmkuhl, A. Shakoor, K. Mehler, C. Krüger, K. Angermund and Y.-H. Tsay, *Chem. Ber.*, **118**, 4239 (1985).
158. T. Alonso, S. Harvey, P. C. Junk, C. L. Raston, B. W. Skelton and A. H. White, *Organometallics*, **6**, 2110 (1987).
159. B. Bogdanović, N. Janke, C. Krüger, K. Schlichte and J. Treber, *Angew. Chem., Int. Ed. Engl.*, **26**, 1025 (1987).
160. A. Xia, M. J. Heeg and C. H. Winter, *J. Am. Chem. Soc.*, **124**, 11264 (2002).
161. A. Xia, J. E. Knox, M. J. Heeg, H. B. Schlegel and C. H. Winter, *Organometallics*, **22**, 4060 (2003).
162. M. M. Olmstead, W. J. Grigsby, D. R. Chacon, T. Hascall and P. P. Power, *Inorg. Chim. Acta*, **251**, 273 (1996).
163. A. Jaenschke, J. Paap and U. Behrens, *Organometallics*, **22**, 1167 (2003).
164. H. Gritz, F. Schaper and H.-H. Brintzinger, *Acta Cryst.*, **E60**, m1108 (2004).
165. H.-R. Damrau, A. Geyer, M.-H. Prosenc, A. Weeber, F. Schaper and H.-H. Brintzinger, *J. Organomet. Chem.*, **553**, 331 (1998).
166. H. Viebrock, D. Abeln and E. Weiss, *Z. Naturforsch.*, **49**, 89 (1994).
167. Y. Kai, N. Kanehisa, K. Miki, N. Kasai, K. Mashima, H. Yasuda and A. Nakamura, *Chem. Lett.*, 1277 (1982).
168. M. G. Gardiner, C. L. Raston, F. G. N. Cloke and P. B. Hitchcock, *Organometallics*, **14**, 1339 (1995).
169. R. N. Grimes, *Chem. Rev.*, **92**, 251 (1992).
170. C. Zheng, J.-Q. Wang, J. A. Maguire and N. S. Hosmane, *Main Group Met. Chem.*, **22**, 361 (1999).
171. N. S. Hosmane, D. Zhu, J. E. McDonald, H. Zhang, J. A. Maguire, T. G. Gray and S. C. Helfert, *J. Am. Chem. Soc.*, **117**, 12362 (1995).
172. N. S. Hosmane, D. Zhu, J. E. McDonald, H. Zhang, J. A. Maguire, T. G. Gray and S. C. Helfert, *Organometallics*, **17**, 1426 (1998).
173. N. S. Hosmane, H. Zhang, Y. Wang, K.-J. Lu, C. J. Thomas, M. B. Ezhova, S. C. Helfert, J. D. Collins, J. A. Maguire, T. C. Gray, F. Baumann and W. Kaim, *Organometallics*, **15**, 2425 (1996).
174. N. S. Hosmane, H. Zhang, J. A. Maguire, Y. Wang, T. Demissie, T. J. Colacot, M. B. Ezhova, K.-J. Lu, D. Zhu, T. C. Gray, S. C. Helfert, S. N. Hosmane, J. D. Collins, F. Baumann, W. Kaim and W. N. Lipscomb, *Organometallics*, **19**, 497 (2000).
175. A. J. Arduengo III, F. Davidson, R. Krafczyk, W. J. Marshall and M. Tamm, *Organometallics*, **17**, 3375 (1998).
176. K. H. Yong, N. J. Taylor and J. M. Chong, *Org. Lett.*, **4**, 3553 (2002).
177. K. H. Yong and J. M. Chong, *Org. Lett.*, **4**, 4139 (2002).
178. K. C. Cannon and G. R. Krow, in *Handbook of Grignard Reagents* (Eds. G. S. Silverman and P. E. Rakita), Marcel Dekker, New York, 1996, p. 271.
179. H. M. Walborsky, *Acc. Chem. Res.*, **23**, 286 (1990).
180. J. F. Garst, *Acc. Chem. Res.*, **24**, 95 (1991).
181. C. Walling, *Acc. Chem. Res.*, **24**, 255 (1991).
182. J. F. Garst and F. Ungváry, in *Grignard Reagents, New Developments* (Ed. H. G. Richey, Jr.), Wiley, Chichester, 2000, p. 185.
183. A. D. Pajerski, E. P. Squiller, M. Parvez, R. R. Whittle and H. G. Richey Jr., *Organometallics*, **24**, 809 (2005).
184. H. Tang, M. Parvez and H. G. Richey Jr., *Organometallics*, **15**, 5281 (1996).
185. M. Vestergren, J. Eriksson and M. Håkansson, *Chem. Eur. J.*, **9**, 4678 (2003).
186. D. R. Armstrong, R. Herbst-Irmer, A. Kuhn, D. Moncrieff, M. A. Paver, C. A. Russell, D. Stalke, A. Steiner and D. S. Wright, *Angew. Chem., Int. Ed. Engl.*, **32**, 1774 (1993).
187. F. Bickelhaupt, *J. Organomet. Chem.*, **475**, 1 (1994).
188. G. Stucky and R. E. Rundle, *J. Am. Chem. Soc.*, **86**, 4825 (1964).
189. F. A. Schröder, *Chem. Ber.*, **102**, 2035 (1969).
190. L. J. Guggenberger and R. E. Rundle, *J. Am. Chem. Soc.*, **90**, 5375 (1968).

191. C.-S. Hwang and P. P. Power, *Bull. Korean Chem. Soc.*, **24**, 605 (2003).
192. G. Boche, K. Harms, M. Marsch and A. Müller, *J. Chem. Soc., Chem. Commun.*, 1393 (1994).
193. M. Vallino, *J. Organomet. Chem.*, **20**, 1 (1969).
194. H. Kageyama, K. Miki, Y. Kai, N. Kasai, Y. Okamoto and H. Yuki, *Bull. Chem. Soc. Jpn.*, **56**, 2411 (1983).
195. H. Kageyama, K. Miki, N. Tanaka, N. Kasai, Y. Okamoto and H. Yuki, *Bull. Chem. Soc. Jpn.*, **56**, 1319 (1983).
196. H. Kageyama, K. Miki, Y. Kai, N. Kasai, Y. Okamoto and H. Yuki, *Acta Cryst.*, **B38**, 2264 (1982).
197. H. Kageyama, K. Miki, Y. Kai, N. Kasai, Y. Okamoto and H. Yuki, *Bull. Chem. Soc. Jpn.*, **57**, 1189 (1984).
198. M. Hogenbirk, G. Schat, O. S. Akkerman and F. Bickelhaupt, *J. Am. Chem. Soc.*, **114**, 7302 (1992).
199. A. L. Spek, P. Voorbergen, G. Schat, C. Blomberg and F. Bickelhaupt, *J. Organomet. Chem.*, **77**, 147 (1974).
200. J. Toney and D. Stucky, *J. Chem. Soc., Chem. Commun.*, 1168 (1967).
201. F. Antolini, P. B. Hitchcock, M. F. Lappert and X.-H. Wei, *Organometallics*, **22**, 2505 (2003).
202. J. J. Ellison and P. P. Power, *J. Organomet. Chem.*, **526**, 263 (1996).
203. H. Bock, K. Ziemer and C. Näther, *J. Organomet. Chem.*, **511**, 29 (1996).
204. M. Marsch, K. Harms, W. Massa and G. Boche, *Angew. Chem., Int. Ed. Engl.*, **26**, 696 (1987).
205. J. Toney and G. D. Stucky, *J. Organomet. Chem.*, **28**, 5 (1971).
206. S. S. Al-Juaid, C. Eaborn, P. B. Hitchcock, A. J. Jaggar and J. D. Smith, *J. Organomet. Chem.*, **469**, 129 (1994).
207. N. H. Buttrus, C. A. Eaborn, M. N. A. El-Kheli, P. B. Hitchcock, J. D. Smith, A. C. Sullivan and K. Tavakkoli, *J. Chem. Soc., Dalton Trans.*, 381 (1988).
208. S. S. Al-Juaid, C. Eaborn, P. B. Hitchcock, M. S. Hill and J. D. Smith, *Organometallics*, **19**, 3224 (2000).
209. P. C. Andrews, M. Brym, C. Jones, P. C. Junk and M. Kloth, *Inorg. Chim. Acta*, **359**, 355 (2006).
210. U. Castellato and F. Ossola, *Organometallics*, **13**, 4105 (1994).
211. A. V. Churakov, D. P. Krut'ko, M. V. Borzov, R. S. Krisanov, S. A. Belov and J. A. K. Howard, *Acta Cryst.*, **E62**, m1094 (2006).
212. D. Seebach, J. Hansen, P. Seiler and J. M. Gromek, *J. Organomet. Chem.*, **285**, 1 (1985).
213. P. R. Markies, G. Schat, S. Griffioen, A. Villena, O. S. Akkerman, F. Bickelhaupt, W. J. J. Smeets and A. L. Spek, *Organometallics*, **10**, 1531 (1991).
214. P. R. Markies, O. S. Akkerman, F. Bickelhaupt, W. J. J. Smeets and A. L. Spek, *J. Am. Chem. Soc.*, **110**, 4284 (1988).
215. I. D. Kostas, G.-J. M. Gruter, O. S. Akkerman, F. Bickelhaupt, H. Kooijman, W. J. J. Smeets and A. L. Spek, *Organometallics*, **15**, 4450 (1996).
216. P. R. Markies, A. Villena, O. S. Akkerman, F. Bickelhaupt, W. J. J. Smeets and A. L. Spek, *J. Organomet. Chem.*, **463**, 7 (1993).
217. C. Johnson, J. Toney and G. D. Stucky, *J. Organomet. Chem.*, **40**, C11 (1972).
218. C. Dohmeier, D. Loos, C. Robl and H. Schnöckel, *J. Organomet. Chem.*, **448**, 5 (1993).
219. R. E. Cramer, P. N. Richmann and J. W. Gilje, *J. Organomet. Chem.*, **408**, 131 (1991).
220. J. Vollet, J. R. Hartig and H. Schnöckel, *Angew. Chem., Int. Ed.*, **43**, 3186 (2004).
221. P. Jutzi, J. Kleimeier, T. Redeker, H.-G. Stammer and B. Neumann, *J. Organomet. Chem.*, **498**, 85 (1995).
222. K. W. Henderson, G. W. Honeyman, A. R. Kennedy, R. E. Mulvey, J. A. Parkinson and D. C. Sherrington, *Dalton Trans.*, 1365 (2003).
223. J. Gromada, A. Montreux, T. Chenal, J. W. Ziller, F. Leising and J.-F. Carpentier, *Chem. Eur. J.*, **8**, 3773 (2002).
224. B. Conway, E. Hevia, A. R. Kennedy, R. E. Mulvey and S. Weatherstone, *Dalton Trans.*, 1532 (2005).
225. S. C. Cole, M. P. Coles and P. B. Hitchcock, *Organometallics*, **23**, 5159 (2004).
226. M. M. Sung, C. G. Kim, J. Kim and Y. Kim, *Chem. Mater.*, **14**, 826 (2002).
227. H. Lehmkuhl, K. Mehler, R. Benn, A. Ruffńska and C. Krüger, *Chem. Ber.*, **119**, 1054 (1986).

228. K.-C. Yang, C.-C. Chang, J.-Y. Huang, C.-C. Lin, G.-H. Lee, Y. Wang and M. Y. Chiang, *J. Organomet. Chem.*, **648**, 176 (2002).
229. W. Vargas, U. Englisch and K. Ruhlandt-Senge, *Inorg. Chem.*, **41**, 5602 (2002).
230. N. Kuhn, M. Schulten, R. Boese and D. Bläser, *J. Organomet. Chem.*, **421**, 1 (1991).
231. I. J. Blackmore, V. C. Gibson, P. B. Hitchcock, C. W. Rees, D. J. Williams and A. J. P. White, *J. Am. Chem. Soc.*, **127**, 6012 (2005).
232. D. Morales-Morales and C. M. Jensen (Eds.), *The Chemistry of Pincer Compounds*, Elsevier, Amsterdam, 2007.
233. A. Xia, M. J. Heeg and C. H. Winter, *Organometallics*, **21**, 4718 (2002).
234. A. Xia, M. El-Kaderi, M. J. Heeg and C. H. Winter, *J. Organomet. Chem.*, **682**, 224 (2003).
235. R. Han, A. Looney and G. Parkin, *J. Am. Chem. Soc.*, **111**, 7276 (1989).
236. R. Han and G. Parkin, *Organometallics*, **10**, 1010 (1991).
237. R. Han and G. Parkin, *J. Am. Chem. Soc.*, **112**, 3662 (1990).
238. R. Han and G. Parkin, *Polyhedron*, **9**, 2655 (1990).
239. J. L. Kisko, T. Fillebeen, T. Hascall and G. Parkin, *J. Organomet. Chem.*, **596**, 22 (2000).
240. M. H. Chisholm, N. W. Eilerts, J. C. Huffman, S. S. Iyer, M. Pacold and K. Phomphrai, *J. Am. Chem. Soc.*, **122**, 11845 (2000).
241. V. C. Gibson, J. A. Segal, A. J. P. White and D. J. Williams, *J. Am. Chem. Soc.*, **122**, 7120 (2000).
242. A. P. Dove, V. C. Gibson, P. Hornmairun, E. L. Marshall, J. A. Segal, A. J. P. White and D. J. Williams, *Dalton Trans.*, 3088 (2003).
243. P. J. Bailey, R. A. Coxall, C. M. Dick, S. Fabre and S. Parsons, *Organometallics*, **20**, 798 (2001).
244. P. J. Bailey, C. M. E. Dick, S. Fabre and S. Parsons, *J. Chem. Soc., Dalton Trans.*, 1655 (2000).
245. J. Prust, K. Most, I. Müller, E. Alexopoulos, A. Stasch, I. Usón and H. Roesky, *Z. Anorg. Allg. Chem.*, **627**, 2032 (2001).
246. K. H. D. Ballem, K. M. Smith and B. O. Patrick, *Acta Cryst.*, **E60**, m408 (2004).
247. L. F. Sánchez-Barbara, D. L. Hughes, S. M. Humphrey and M. Bochman, *Organometallics*, **25**, 1012 (2006).
248. H. Hao, H. W. Roesky, Y. Ding, C. Cui, M. Schormann, H.-G. Schmidt, M. Noltemeyer and B. Žemva, *J. Fluorine Chem.*, **115**, 143 (2002).
249. P. J. Bailey, S. T. Liddle, C. A. Morrison and S. Parsons, *Angew. Chem., Int. Ed.*, **40**, 4463 (2001).
250. A. P. Dove, V. C. Gibson, E. L. Marshall, A. J. P. White and D. J. Williams, *Chem. Commun.*, 1208 (2002).
251. J. Dekker, P. H. M. Budzelaar, J. Boersma, G. J. M. van der Kerk and A. L. Spek, *Organometallics*, **3**, 1403 (1984).
252. H. M. El-Kaderi, A. Xia, M. J. Heeg and C. H. Winter, *Organometallics*, **23**, 3488 (2004).
253. T. Chivers, C. Fedorchuk and M. Parvez, *Organometallics*, **24**, 580 (2005).
254. I. L. Fedushkin, A. A. Skatova, M. Hummert and H. Schumann, *Eur. J. Inorg. Chem.*, 1601 (2005).
255. P. J. Baily, R. A. Coxall, C. M. Dick, S. Fabre, S. Parsons and L. J. Yellowlees, *Chem. Commun.*, 4563 (2005).
256. P. J. Baily, C. M. Dick, S. Fabre, S. Parsons and L. J. Yellowlees, *Dalton Trans.*, 1602 (2006).
257. G. van Koten, J. T. B. H. Jastrzebski and C. Vrieze, *J. Organomet. Chem.*, **250**, 49 (1983).
258. M. Kaupp, H. Stoll, H. Preuss, W. Kaim, T. Stahl, G. van Koten, E. Wissing, W. J. J. Smeets and A. L. Spek, *J. Am. Chem. Soc.*, **113**, 5606 (1991).
259. E. Hevia, A. R. Kennedy, R. E. Mulvey and S. Weatherstone, *Angew. Chem., Int. Ed.*, **43**, 1709 (2004).
260. L. M. Engelhardt, B. S. Jolly, P. C. Junk, C. L. Raston, B. W. Skelton and A. H. White, *Aust. J. Chem.*, **39**, 1337 (1986).
261. M. Westerhausen, T. Bollewein, N. Makropoulos and H. Piotroski, *Inorg. Chem.*, **44**, 6439 (2005).
262. V. R. Magnuson and G. D. Stucky, *Inorg. Chem.*, **8**, 1427 (1969).
263. K. W. Henderson, R. E. Mulvey, W. Clegg and P. O'Neil, *J. Organomet. Chem.*, **439**, 237 (1992).
264. A. Xia, M. J. Heeg and C. H. Winter, *J. Organomet. Chem.*, **669**, 37 (2003).



265. S. Blair, K. Izod, W. Clegg and R. W. Harrington, *Eur. J. Inorg. Chem.*, 3319 (2003).
266. W. Kaschube, K.-R. Pörschke, K. Angermund, C. Krüger and G. Wilke, *Chem. Ber.*, **121**, 1921 (1988).
267. G. Wilke, *Angew. Chem., Int. Ed. Engl.*, **27**, 185 (1988).
268. S. I. Khan, P. G. Edwards, H. S. H. Yuan and R. Bau, *J. Am. Chem. Soc.*, **107**, 1682 (1985).
269. M. Hogenbirk, G. Schat, F. J. J. de Kanter, O. S. Akkerman, F. Bickelhaupt, H. Kooijman and A. L. Spek, *Eur. J. Inorg. Chem.*, 2045 (2004).
270. M. Horáček, P. Štěpnička, J. Kubišta, K. Fejfarová, R. Gyepes and K. Mach, *Organometallics*, **22**, 861 (2003).
271. M. Horáček, J. Hiller, Y. Thewalt, M. Polášek and K. Mach, *Organometallics*, **16**, 4185 (1997).
272. V. Kupfer, U. Thewalt, M. Horáček, L. Petrusová and K. Mach, *Inorg. Chem. Commun.*, **2**, 540 (1999).
273. K. Mach, R. Gyepes, M. Horáček, L. Petrusová and J. Kubišta, *Collect. Czech. Chem. Commun.*, **68**, 1877 (2003).
274. V. Varga, K. Mach, G. Schmid and U. Thewalt, *J. Organomet. Chem.*, **454**, C1 (1993).
275. V. Varga, K. Mach, G. Schmid and U. Thewalt, *J. Organomet. Chem.*, **475**, 127 (1994).
276. M. Ohashi, K. Matsubara, T. Iizuka and H. Suzuki, *Angew. Chem., Int. Ed.*, **42**, 937 (2003).
277. J. T. Golden, T. H. Peterson, P. L. Holland, R. G. Bergman and R. A. Andersen, *J. Am. Chem. Soc.*, **120**, 223 (1998).
278. T. M. Gilbert, R. R. Ryan and A. P. Sattelberger, *Organometallics*, **8**, 857 (1989).

## CHAPTER 2

# The thermochemistry of organomagnesium compounds

JOEL F. LIEBMAN

*Department of Chemistry and Biochemistry, University of Maryland, Baltimore County,  
1000 Hilltop Circle, Baltimore, Maryland 21250, USA  
Fax: +1 410 455 2608; e-mail: jliebman@umbc.edu*

TORKIL HOLM

*Department of Chemistry, Technical University of Denmark, Building 201, DK-2800  
Lyngby, Denmark  
Fax: +45 45933968; e-mail: th@kemi.dtu.dk*

and

SUZANNE W. SLAYDEN

*Department of Chemistry, George Mason University, 4400 University Drive, Fairfax,  
Virginia 22030, USA  
Fax: +1 703 993 1055; e-mail: sslayden@gmu.edu*

---

I. INTRODUCTION: SCOPE AND DEFINITIONS . . . . .	102
A. Thermochemistry . . . . .	102
B. Sources of Data . . . . .	102
C. Magnesium: A Metal Among Metals . . . . .	102
D. Calorimetry of Organomagnesium Compounds . . . . .	104
II. COMPOUNDS COMPOSED SOLELY OF MAGNESIUM AND CARBON . . . . .	106
III. THE SCHLENK EQUILIBRIUM . . . . .	107
IV. ORGANOMAGNESIUM HALIDES . . . . .	109
A. Isomers and Homologous Series . . . . .	110
B. Unsaturated Compounds . . . . .	112
1. Formal protonation reactions . . . . .	112
2. Enthalpies of hydrogenation . . . . .	113
C. Organomagnesium Bromides Containing Heteroatoms . . . . .	113

---

*The chemistry of organomagnesium compounds*

Edited by Z. Rappoport and I. Marek © 2008 John Wiley & Sons, Ltd. ISBN: 978-0-470-05719-3

V. DIORGANOMAGNESIUM COMPOUNDS . . . . .	116
VI. ORGANOMAGNESIA AND RINGS . . . . .	117
A. Cycloalkylmagnesium Halides . . . . .	117
B. Magnesacycloalkanes and Their Dimers (Dimagnesacycloalkanes) . . . .	120
C. Other Magnesacycles . . . . .	121
VII. MAGNESIUM SANDWICH SPECIES . . . . .	122
A. Magnesocene (Bis(cyclopentadienyl) magnesium) . . . . .	122
B. Neutral Magnesium Half-Sandwiches . . . . .	123
C. Triple Decker (Club) Sandwiches . . . . .	123
D. Cationic Sandwiches and Half-Sandwiches . . . . .	124
VIII. MAGNESIUM COMPLEXES WITH CARBON MONOXIDE . . . . .	125
IX. REFERENCES AND NOTES . . . . .	126

---

## I. INTRODUCTION: SCOPE AND DEFINITIONS

### A. Thermochemistry

The current chapter is primarily devoted to the thermochemical properties of molar standard enthalpies of formation and of reaction,  $\Delta_f H_m^\circ$  and  $\Delta_r H_m^\circ$ , often called the ‘heat of formation’,  $\Delta H_f$  and ‘heat of reaction’,  $\Delta H_r$ . We will only briefly discuss bond dissociation energies, Gibbs energy and complexation energies. This chapter foregoes discussion of other thermochemical properties such as entropy, heat capacity or excess enthalpy. Temperature and pressure are assumed to be 25 °C (‘298 K’) and 1 atmosphere or the nearly equal 1 bar (101,325 or 100,000 Pa) respectively. The energy units are  $\text{kJ mol}^{-1}$  where 4.184 kJ is defined to equal 1 kcal. Although our thermochemical preference is for the gas phase, we find that for many of the species discussed here, only solution phase data are available. We interpret the ‘organomagnesium’ in the title of this work to mean that the minimum requirement for a species to be included is that it have at least one magnesium atom and one carbon atom. And so there is a section on compounds consisting solely of magnesium and carbon. The remaining sections consider the traditional CHONS atom combinations in several manifestations as they are bonded to magnesium.

### B. Sources of Data

Unreferenced enthalpies of formation for any organic species in the current chapter are taken from the now ‘classic’ thermochemical archives by Pedley and his coauthors<sup>1</sup>. Likewise, unreferenced enthalpies of formation for inorganic compounds come from the compilation of Wagman and his coworkers<sup>2</sup>. These thermochemical numbers are usually for comparatively simple and well-understood species where we benefit from the data evaluation performed by these authors rather than using the raw, but much more complete, set of data found in the recent, evolving, on-line NIST WebBook database<sup>3</sup>. All other thermochemical quantities come from sources explicitly cited in the chapter.

### C. Magnesium: A Metal Among Metals

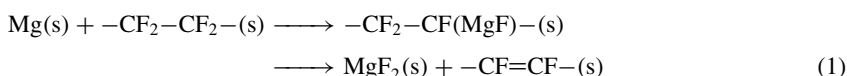
That magnesium is by far the most useful metal for preparing organometallic reagents to be used in syntheses is due to several factors. Although a highly electropositive metal, it is easily handled and stable in the atmosphere since it is protected by an invisible coating of oxide-hydroxide. It is non-toxic and presents no problems for the environment. Of the Group II metals, Ba, Sr, Ca, Mg, Be, Zn, Cd and Hg, the most electropositive Ba, Sr

and Ca have been little studied and the free metals and their alkyl compounds are rather inaccessible. Their reactions are similar to those of sodium but they are less reactive. Magnesium forms rather polar bonds to carbon which consequently possesses significant carbanionic character. Grignard reagents combine the virtues of being at the same time very reactive and very easy to prepare from metallic magnesium, which is unique among electropositive metals in being readily available and requiring little or no cleaning before use. Beryllium and its compounds are exceptionally toxic, and so discussion as useful reagents logically ends there.

Among hydrocarbylmetals formed from alkali metals, only hydrocarbyllithium compounds match the Grignard reagents in utility and reactivity. A choice will often exist between magnesium and lithium compounds for a given reaction, but magnesium is much easier and safer to handle and organomagnesium compounds furthermore have the advantage of being stable in ether solution while organic alkali compounds all attack ether and are handled in hydrocarbon solvents.

Metals more electronegative than magnesium, like beryllium, zinc, cadmium and mercury, form useful reagents for specific purposes, but the metals themselves are not sufficiently active to form organic derivatives under normal laboratory conditions and are unwanted in the environment since they are toxic. Aluminum compounds are useful for industrial purposes, but their use in the laboratory is insignificant in comparison with Grignard reagents.

Lest one forget and be complacent, organomagnesium species are high energy compounds as expressed in terms of the considerable exothermicity of many of their spontaneous reactions—those with water and/or air are perhaps best known. Almost all laboratory investigations of the chemistry of organomagnesium compounds have been with the homoleptic species  $R_2Mg$ , or with the classical Grignard reagents  $RMgX$  with one hydrocarbyl (alkyl or aryl) R group and either chlorine, bromine or iodine attached as an X to the metal. Organomagnesium fluorides have been relatively ignored as they are more difficult to prepare than the related compounds with the other halogens<sup>4</sup>. These are plausible species in mixed metal fluorocarbon ‘pyrolants’, chemical sources of high temperatures (multi-thousand K) resulting from solid phase reactions of magnesium and fluorinated organic polymers.<sup>5</sup> That is, mechanically combined Mg and polymer are induced to chemically react presumably via the following schematic reactions (equations 1 and 2), shown here for polytetrafluoroethylene.



While the C–F bond is recognized as strong, the Mg–F bond is stronger. From enthalpy of formation data<sup>2</sup> per monomeric unit of  $C_2F_4$ , this reaction is exothermic by over 1400 kJ mol<sup>-1</sup>.

Numerous other reactions are occasionally problematic because of unexpected heat evolution and temperature increase. Although not widely publicized, trifluoromethylphenyl chlorides and bromides are prone to explode during preparation of the Grignard reagent<sup>6</sup>. It was hypothesized that phenylethylene intermediates can polymerize in a runaway exothermic reaction<sup>7</sup>, while loss of solvent contact and an excess of highly activated magnesium were shown to favor violent reactivity.<sup>8</sup> Fluorine-containing aryl Grignards are not the only culprits.<sup>9</sup> As such, there has been active industrial interest in safety hazards surrounding Grignard formation during scale-up, initiation and reagent addition<sup>10</sup>.

### D. Calorimetry of Organomagnesium Compounds

As with so many other classes of compounds, calorimetric measurements and derived thermochemical concepts were important in the early era of the study of organomagnesium compounds—and then largely ignored once the field gained maturity. For example, 100 years ago the interaction of amines with propylmagnesium iodide was discussed in terms of measured solvation energies, and the energies compared with those from the interaction of ethers with the same organometallic<sup>11</sup>. That ethers are less basic than amines and that oxonium ions and related salts are less stable than their ammonium counterparts, was used to suggest the solvation of Grignard reagents in terms of  $[\text{Solvent-Mg-R}]^+ \text{I}^-$  ion pairs. These suggested structures presaged our modern understanding of solvent-stabilized molecular, rather than ionic complexes, in solution. Our current knowledge is that the C-Mg bond energy is very much the same for all primary alkyl groups attached to the magnesium—from observations on an extensive variety of other alkyl derivatives, we may now ask first how could it be otherwise, and then ask how could this entirely plausible result be experimentally demonstrated. Century-old experiments are relevant here as well. Direct calorimetric measurements<sup>12</sup> of the enthalpy of hydrolysis were made on three sets of isomeric pairs of  $\text{R}_2\text{O}\cdot\text{R}' \text{MgI}$  and  $\text{RR}'\text{O}\cdot\text{RMgI}$  species in which the groups now recognized to be on oxygen and magnesium were interchanged. The reaction exothermicities were found to be nearly the same for the cases where  $\text{R} = \text{Et}$ ,  $\text{R}' = \text{Pr}$ ;  $\text{R} = \text{Et}$ ,  $\text{R}' = \text{Bu}$  and  $\text{R} = \text{Et}$ ,  $\text{R}' = \text{Pen}$ .

Calorimetry is a discipline demanding exquisite experimental care, and is an art as well as a science: compared to many other areas of the chemical sciences, there are comparatively few new apprentices of this study. To aid future researchers interested in performing new experiments on the energetics of organomagnesium compounds, as well as historians of our science, we describe in considerable detail the earlier experiments performed by one of the authors (T.H.) but not included in the original publication.

Because of the high reactivity of Grignard reagents, calorimetric measurements require total exclusion of air and moisture and vacuum tight equipment must be used. The following three reactions (equations 3–5) have usually been studied: formation, protonation and reaction with bromine.



Protonation reagents such as water and alcohol have been used, but HBr is the preferred reagent because the reaction leads to well defined, ether-soluble products.

The use of a normal adiabatic calorimeter is not ideal when the reaction studied has an induction period as in reaction 3 or when a reaction has to be initiated by breaking an ampoule as in reaction 4 or 5. Much more convenient and reliable is the use of a steady-state heat flow calorimeter. The method used in References 13 and 14 is described here.

The calorimeter consisted of a 500-mL flask with an air-filled jacket, a magnetic stirrer and a manganin heating coil (Figure 1). The calorimeter was closed with a B 29 standard taper rubber sealed adapter which fitted a Beckman thermometer (8), the leads (9) for the heating coil (4) and a glass capillary inlet (x) for the liquid or gaseous reactant. Internally, the inlet capillary had a 1.5-mm polyethylene tube leading to the bottom of the flask. Externally, this capillary was connected by a glass capillary either to a hydrogen bromide supply or to a Metrohm piston burette driven by a synchronous motor which delivered 20 mL/180 min.

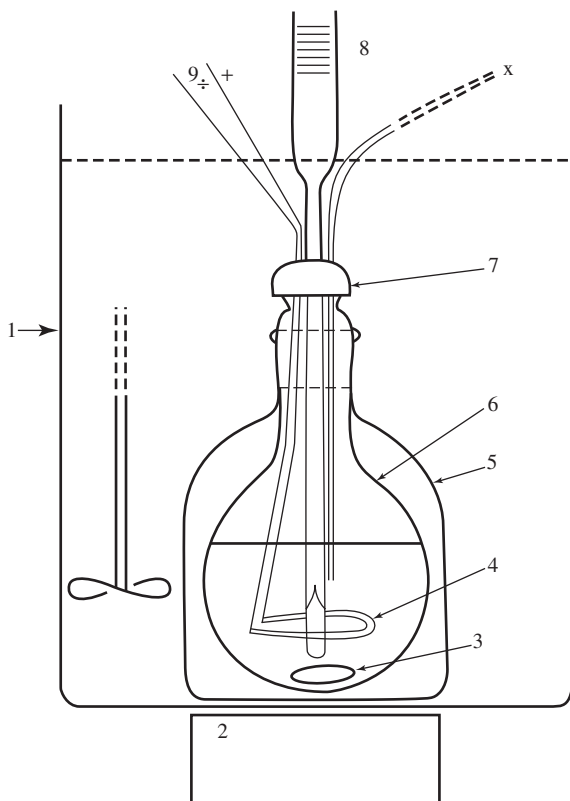


FIGURE 1. The steady-state heat flow calorimeter

For measurement of reaction 3 the calorimeter was filled with 15 g magnesium turnings and 400 mL of ether distilled from  $\text{LiAlH}_4$ . The calorimeter was mounted in a precision water thermostat (1) and the magnetic stirrer (2) was started. Pure alkyl bromide was pumped from the motorburette at the constant rate of  $1.8517 \mu\text{L s}^{-1}$ . After the start of the reaction the addition was continued for 30–60 min. By adjusting the thermostat a steady state was obtained with a temperature in the calorimeter about  $10^\circ\text{C}$  higher than in the thermostat, so that the reading of the Beckman thermometer was constant within  $\pm 0.002^\circ\text{C}$ . The addition of  $\text{RBr}$  was then stopped and the temperature was kept constant by leading an electric current through the heating coil using a precision constant current generator, 'Fluke 382 A' (not shown). The enthalpy of reaction is equal to the substituted electrical effect and, knowing the molarity of the pure alkyl bromide, the molar reaction enthalpy could be calculated.

Methyl bromide was kept in an ampoule at  $0^\circ\text{C}$  and was displaced by the introduction of  $1.8517 \mu\text{s}^{-1}$  of mercury from the motorburette. The methyl bromide was passed through a 2-m stainless steel capillary heating coil which was placed in the thermostat water. In order to derive the enthalpy of reaction of liquid methyl bromide, the enthalpy of vaporization ( $23.0 \text{ kJ mol}^{-1}$ ) was subtracted from the value obtained for gaseous methyl bromide.

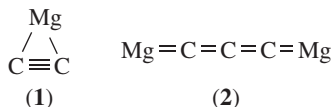
Measurement of the enthalpy of reaction 4 required a constant stream of HBr. This was obtained by placing an HBr cylinder in an ice bath and connecting the outlet to a glass capillary which allowed a stream of  $18\text{--}20\ \mu\text{mol}^{-1}$ . The exact value was found by leading the HBr stream into water for 100 s and titrating with sodium hydroxide. This determination was made before and after each experiment.

For addition of liquid bromine, a 5-mL piston burette was used delivering  $0.4629\ \mu\text{L s}^{-1}$ . In the calorimeter was placed 400 mL of a 0.4 M alkylmagnesium bromide in diethyl ether. The measuring procedure followed the same principles as used for HBr addition.

It was found that in the study of reaction 4, the most important source of error when using this calorimetry procedure was the change of vapor pressure in the calorimeter caused by the formation of gases. This resulted in a significant change in the heat transfer coefficient for the heat transfer for the calorimeter due to a change in the rate of reflux of the ether solvent from the uncovered walls. The error was almost eliminated by filling the calorimeter with ether leaving only 10% empty space. Errors were introduced also by assuming that gaseous alkanes dissolve in ether with evolution of the full enthalpy of vaporization. By measurements this was found to be true within experimental uncertainty for  $\text{C}_5$  alkanes and higher, but incorrect for the lower alkanes. Corrections were made for  $\text{C}_1\text{--C}_4$  alkanes. The results were usually reproducible to within  $\pm 1\ \text{kJ mol}^{-1}$  when using liquid alkanes, and  $\pm 2.2\ \text{kJ mol}^{-1}$  when using gaseous alkanes. The purity and the density of the alkyl bromides were the data given by the manufacturer and are estimated to be within  $\pm 0.5\%$ .

## II. COMPOUNDS COMPOSED SOLELY OF MAGNESIUM AND CARBON

In principle, there are many binary species that are composed solely of divalent Mg and C. Admittedly, such species characterized by carbon bonded to only magnesium or another carbon appear quite strange. Two such species would thus be the magnesium-containing 'too small' cyclopropyne,  $\text{MgC}_2$  (**1**), and the cumulene,  $\text{Mg}_2\text{C}_3$  (**2**), which is a bimetallic carbon suboxide mimic.



However, these compounds, or, more properly, those species with the same Mg:C ratios and resulting stoichiometries are not fanciful. They are two of the best known magnesium carbides and more often written in an ionic dialect, as  $\text{Mg}^{2+} (\text{C}_2)^{2-}$  and  $(\text{Mg}^{2+}) (\text{C}_3)^{4-}$ , i.e. they are the magnesium salts of totally deprotonated acetylene and propyne (or alternatively allene), respectively. It is clear that these species are not the covalent metallocycle and metallo-olefin drawn above. It is clear also that the totally ionic carbides also are inadequate representations since the isolated anions lie far above the corresponding neutrals and free electrons in energy<sup>15</sup>.

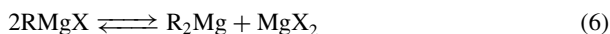
These representations—essentially covalent molecule and totally ionized salt—presage the conflicting descriptions of the alternatives that can be drawn for the more conventional organomagnesium compounds that fill this chapter and the current volume. Indeed, the relative stability of the cycloalkyne ring description compared to the less-bonded (hypovalent) chain cumulene  $\text{Mg}=\text{C}=\text{C}$  recurs in the question of the general  $\text{C}_2\text{X}$  species with X chosen among other third row elements. For  $\text{X} = \text{Na} - \text{Si}$ , the ring is seemingly preferred over the chain and the opposite is found for  $\text{X} = \text{P} - \text{Cl}$ <sup>16</sup>. (For  $\text{X} = \text{CH}_2$  the chain is seemingly the more stable, but not by so much that  $\text{CH}_2\text{CC}$  facily automerizes into  $\text{CCCH}_2$  by way of the parent cyclopropyne<sup>17</sup>.) Additionally, crystalline  $\text{MgC}_2$

has been described as having 'MgCCMgCCMg... chains ... [with] a weak interaction [2.510(1) Å] between Mg and the triple bond of the crossing chains above and below'<sup>18</sup>. Indeed, a crystallographic investigation of Mg<sub>2</sub>C<sub>3</sub> described this species in terms of 'bridging of the C–C bonds by Mg ... reminiscent of polycenter, electron-deficient bonds'<sup>19</sup> and corresponding low ionicity.

However exotic are these species and however quixotic appear the attempts at a unique simple description, MgC<sub>2</sub> and Mg<sub>2</sub>C<sub>3</sub> are well-known solids (see References 18 and 19 and citations therein) for which the enthalpies of formation of 84 and 71 kJ mol<sup>–1</sup> are well-chronicled<sup>2</sup>. As no sublimation data are available from experiment or estimate, we are seemingly thwarted in any attempt to derive Mg–C bond energies from these data<sup>20</sup>. We remain optimistic in our understanding because, besides organic and organometallic chemists, materials scientists<sup>18,21</sup> and astrochemists<sup>22</sup> have joined the hunt for new magnesium–carbon species and their understanding.

### III. THE SCHLENK EQUILIBRIUM

In 1900, Victor Grignard<sup>23</sup> presented the reaction product from an alkyl halide, RX, and magnesium in ether as simply RMgX. He and contemporary workers were aware that ethyl ether was somehow built into the molecule and for a time an oxonium structure was suggested<sup>24</sup> that had no bond between carbon and magnesium. The modern concept of bonding between an anionic alkyl and a cationic magnesium was presented in 1905 by Abegg<sup>25</sup> and at the same time the possibility of alkyl–halogen exchange was suggested. In a footnote this author was the first to suggest an equilibrium as shown in equation 6.



The equilibrium was 25 years later named after Schlenk and Schlenk<sup>26</sup>, who found that magnesium halide precipitates from an ethereal Grignard reagent solution by addition of dioxane. They thought that by filtering and weighing the crystalline dioxanate precipitate it would be possible to determine the position of the equilibrium. This was not possible, however, because removal of magnesium halide led to an immediate readjustment of the equilibrium so that after addition of a sufficient amount of dioxane (>3 moles), all halide was removed leaving a solution of pure dialkylmagnesium.

For many years the equilibrium was formulated as in equation 7 and the monomer RMgBr was thought not to exist<sup>27</sup>.



Clarification of the problem was delayed several years after it was concluded by the use of isotopically labelled magnesium that magnesium–halogen exchange did not take place in the solution<sup>28</sup>. That this was incorrect was reported in 1963 when it was shown by the use of osmometric measurements that the monomeric EtMgBr is present in dilute solutions (<0.1 M) in THF<sup>29</sup> and diethyl ether<sup>30</sup>, respectively. The osmometric measurements showed that at higher concentrations various loose aggregates form<sup>31</sup>. Aggregates are more apt to form in less polar solvents like diethyl ether than in more polar solvents like THF. Only alkylmagnesium fluorides are dimeric in THF<sup>32</sup>. The R group of the Grignard reagent likewise influences the degree of association. Organomagnesium molecules associate by halogen or/and alkyl bridges between magnesium atoms. Chlorine and fluorine are a better bridging ligands than either bromine and iodine, so alkyl magnesium chlorides and fluorides are dimeric over a wide concentration range.

Thermochemically, the association is not a major factor since the enthalpies of dilution of Grignard reagents are very small in diethyl ether as well as in THF<sup>33,34</sup>. An explanation



may be that bonding between molecules by means of halogen or alkyl bridging replace the coordinating ether molecules and that the enthalpies of coordination of the two types of bonding are nearly equivalent. Likewise, the association of Grignard reagents does not seem to have much influence on the position of the Schlenk equilibrium<sup>33</sup>. This is in accord with an equilibrium with the same number of entities on the two sides as in equation 6. Equation 7 represents an equilibrium that will be shifted to the right with higher dilution. The fact that the Schlenk equilibrium is almost independent of dilution must mean that equation 6 is a better description than equation 7 and that the tendency for association with solvent is, on an average, the same on both sides of equation 6.

Just as the association equilibria have little effect on the position of the Schlenk equilibrium, there has been no clear demonstration of a correlation between the association equilibria and the reactivity of the reagents. Plots of reaction rates versus concentration of Grignard reagents for various substrates often deviate from a straight line so that the reaction order is below 1 and even may approach zero<sup>35</sup>. This phenomenon has been shown not to correlate with an association of the reagent itself but rather with a complexation of the Grignard reagent with the substrate which occurs if the substrate has a Lewis basicity greater than that of the ether solvent<sup>36</sup>. With substrates of low basicity like methyl trifluoroacetate or benzonitrile the reaction order with respect to Grignard reagent is close to 1<sup>37</sup>.

Although the position of equation 6 could not be determined by dioxane precipitation of magnesium halide, it was found that the position could be determined by thermometric titration<sup>33, 34, 36, 38</sup>. Adding  $R_2Mg$  to a solution of  $MgBr_2$  in ether led to an increase in temperature. The plot of added  $R_2Mg$  versus temperature gave both the enthalpy for complete reaction as well as the composition of the mixture and the equilibrium constant for equation 6. The  $\Delta t$  was positive in ether but was shown<sup>34, 36</sup> to be negative in THF. Thermometric titration of dialkylmagnesium–magnesium bromide has been published for alkyl = methyl, ethyl, butyl and phenyl in both ether and THF as shown in Table 1.

The position of the Schlenk equilibrium has alternatively, and less accurately, been estimated by means of IR<sup>39</sup> and NMR spectra<sup>40, 41</sup>. The latter method has confirmed the extreme rate of alkyl–halide exchange for alkyl = methyl and ethyl. Separate signals for dialkylmagnesium and alkylmagnesium halide were not discernable at room temperature, but for methyl separate signals appeared at  $-80^\circ C$  when the alkyl–halide exchange process was slowed down. For dimethylmagnesium, which is associated by bridging methyl

TABLE 1. Equilibrium constants ( $K_{Schlenk}$ ) and enthalpies of reaction for the Schlenk reaction  $R_2Mg + MgBr_2 \rightleftharpoons 2RMgBr$

RMgBr	Solvent	$K_{Schlenk}$	$\Delta H_{rxn}$ (kJ mol <sup>-1</sup> )	Method <sup>a</sup>	Reference
MeMgBr	THF	3.5		IR	39
		4.0		NMR	40
	Et <sub>2</sub> O	320		T	43
		455		C	32
EtMgBr	THF	5.09	25.5	C	34
	Et <sub>2</sub> O	480, 484	-15.5	T	33
BuMgBr	THF	ca 9	14.2	T	36
	Et <sub>2</sub> O	ca 1000	-13.4	T	36
		ca 1400		K	31
PhMgBr	THF	3.8	11.8	C	34
		4.0	13.4	NMR	41
	Et <sub>2</sub> O	55, 62	-8.5	C	33

<sup>a</sup> T = thermometric titration; C = calorimetry; K = kinetics.

TABLE 2. Enthalpy of solvation of components of the Schlenk equilibrium in Et<sub>2</sub>O and THF (kJ mol<sup>-1</sup>)<sup>44</sup>

Solvent	Et <sub>2</sub> Mg	EtMgBr	MgBr <sub>2</sub>
Et <sub>2</sub> O	-24	-31	-32
THF	-36.6	-68.3	-109

groups, separate signals for terminal and for bridging methyl groups could be observed. Because crystallization took place, the signals were not useful for quantitative measurements. It was found that the alkyl exchange rate depended on both the solvent and on the alkyl group. The signals for di-*t*-butylmagnesium and *t*-butylmagnesium bromide in THF could be discerned at room temperature because of a slow alkyl exchange.

An estimate of the equilibrium may also be obtained by kinetic measurements since dialkylmagnesium is often 50–100 times more reactive than alkylmagnesium bromide<sup>42</sup>. Addition of MgBr<sub>2</sub> to a Grignard reagent converts R<sub>2</sub>Mg to RMgBr. When comparing the reactivity of this manipulated Grignard reagent with the reactivity of both R<sub>2</sub>Mg and 'normal' RMgBr, the content of R<sub>2</sub>Mg and  $K_{\text{Schlenk}}$  may be found. The non-basic methyl trifluoroacetate has a negligible reactivity toward BuMgBr and has been used for this type of estimation of the position of the Schlenk equilibrium<sup>37</sup>. The content of dibutylmagnesium in nominally 0.5 M butylmagnesium X was found to be 5%. This corresponds to an equilibrium constant of 1400 (not 400 as given in Reference 37). The reaction between methylmagnesium bromide and benzophenone has likewise been used to determine  $K_{\text{Schlenk}}$  and the value found was in reasonable agreement with the value obtained by thermometric titration<sup>43</sup>.

Of the three components of the Schlenk equilibrium, the electrophilicity decreases in the order MgBr<sub>2</sub> > RMgBr > R<sub>2</sub>Mg. In diethyl ether the total bonding in 2 mol RMgBr is stronger than the total bonding in 1 mol each of R<sub>2</sub>Mg and MgBr<sub>2</sub>. For this reason, equilibrium 6 lies to the left in diethyl ether. The stronger solvation of especially MgBr<sub>2</sub> favors the right side of equilibrium 6 in a more solvating donor solvent like THF. The endothermic reaction between R<sub>2</sub>Mg and MgBr<sub>2</sub> in THF is the result of an entropy-driven reaction leading to an almost statistical distribution of the three components. Approximate values of the enthalpy of solvation of the components of the Schlenk equilibrium are given in Table 2<sup>44</sup>.

#### IV. ORGANOMAGNESIUM HALIDES

Holm determined the enthalpies of formation of a collection of hydrocarbylmagnesium bromides by reaction calorimetry with HBr in diethyl ether<sup>13,14</sup>. He also determined the enthalpies of formation in ethereal solution of the magnesium bromide salts of 20 Bronsted acids, HB, by measuring the enthalpies of reaction of the acid with pentylmagnesium bromide<sup>45</sup>. For those species that were reported in both studies (hydrocarbyl = phenylethynyl, phenyl, methyl, cyclopropyl, cyclopentyl, cyclohexyl), the enthalpies of formation were identical. The values are listed in Tables 3 and 4.

There is one other report in the literature of a measurement of the enthalpy of formation of an organomagnesium halide. The enthalpy of reaction of magnesium with methyl iodide in ether was calorimetrically determined as  $-273.6 \pm 0.8$  kJ mol<sup>-1</sup><sup>46</sup>. Using a recent enthalpy of formation for liquid methyl iodide of  $-13.6 \pm 0.5$  kJ mol<sup>-1</sup><sup>47</sup>, the enthalpy of formation of methylmagnesium iodide is  $-287.2$  kJ mol<sup>-1</sup>. The exchange (equation 8) is thus 11.2 kJ mol<sup>-1</sup> endothermic.

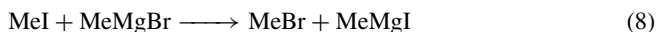


TABLE 3. Enthalpies of reaction and enthalpies of formation of hydrocarbylmagnesium bromides (RMgBr) in ether solution ( $\text{kJ mol}^{-1}$ )

R	$\Delta H_r$ RMgBr (soln) <sup>a,b</sup>	$\Delta H_f$ RMgBr(soln) <sup>b</sup>
Methyl	-274.5	-331.8
Vinyl	-294.1 <sup>c</sup>	-264.4 <sup>c</sup>
Ethyl	-299.2	-323.0
Allyl	-259.4	-265.7
<i>n</i> -Propyl		-360.7
<i>i</i> -Propyl	-305.9	-339.7
<i>n</i> -Butyl	-292.5	-378.2
<i>i</i> -Butyl	-289.1	-391.6
<i>sec</i> -Butyl	-305.9	-368.2
<i>tert</i> -Butyl	-306.7	-370.7
<i>n</i> -Pentyl		-406.7
1-Ethylpropyl	-306.3	-389.9
Neopentyl	-286.6	-430.1
<i>n</i> -Hexyl		-427.6
<i>n</i> -Heptyl		-452.3
<i>n</i> -Octyl		-478.6
Cyclopropyl	-282.8	-211.3
Cyclobutyl	-289.1	-229.7
Cyclopentyl	-291.6	-336.8
Cyclohexyl	-298.7	-380.3
Cycloheptyl	-299.6	-379.5
Cyclooctyl	-295.0	-395.4
Phenyl	-263.2	-208.4
Benzyl	-256.5	-252.3
4-Methylphenyl	-262.3	-244.8
4-Chlorophenyl	-260.2	-251.5
Phenylethynyl	-169.9	-69.5
Triphenylmethyl	-231.0	-120.5

<sup>a</sup> Enthalpies of reaction were determined for  $\text{RMgBr(soln)} + \text{HBr(g)} \rightarrow \text{RH(soln)} + \text{MgBr}_2(\text{soln})$ .

<sup>b</sup> All values are from References 13 and 14. The experimental uncertainties are  $\pm 2.2 \text{ kJ mol}^{-1}$ .

<sup>c</sup> In THF. It is expected that less heat would be evolved in ether solution.

There is one additional study on the enthalpy of hydrolysis of solid butylmagnesium chloride<sup>48</sup>. Additional calculations<sup>3</sup> result in a solid phase enthalpy of formation of  $-455.7 \pm 2.0 \text{ kJ mol}^{-1}$ .

## A. Isomers and Homologous Series

We briefly discussed in an earlier volume the behavior of the isomeric and homologous organomagnesium bromides compared to the organolithium compounds as a means of furthering our understanding of the thermochemistry of the latter species<sup>49</sup>. Here, we will discuss only the magnesium compounds. Discussion of the cycloalkylmagnesium bromides is deferred to a later section in this chapter.

The linear correlation of enthalpies of formation with the number of carbon atoms is a useful and well-known feature of homologous series of functionalized organic compounds. The slope of the regression line for the gaseous *n*-alkanes ( $\text{CH}_3-(\text{CH}_2)_x-\text{H}$ ),  $-20.6 \text{ kJ mol}^{-1}$ , and the similar values of the slopes for other  $\text{CH}_3-(\text{CH}_2)_x-\text{Z}$  series is often called the 'universal methylene increment'<sup>50</sup>. In the liquid phase, the increment for the *n*-alkanes is  $-25.6 \pm 0.1 \text{ kJ mol}^{-1}$ . The most accurate determination of the increment

TABLE 4. Enthalpies of reaction and enthalpies of formation of organomagnesium bromides in ether solution ( $\text{kJ mol}^{-1}$ )

HB	$\Delta H_r$ BMgBr <sup>a,b</sup>	$\Delta H_f$ BMgBr <sup>c</sup>
Methane	-15.1	-331.0
Cyclopropane	-6.7	-204.7
Cyclopentane	2.1	-336.2
Cyclohexane	9.2	-380.4
1,3-Cyclopentadiene	-148.5	-275.8
C <sub>6</sub> H <sub>6</sub>	-26.4	-210.6
PhCH <sub>3</sub>	-33.1	-253.9
PhC≡CH	-125.9	-75.6
CH <sub>2</sub> (CN) <sub>2</sub>	-203.3	-59.7 <sup>b</sup>
CH <sub>3</sub> NH <sub>2</sub>	-130.5	-411.0
<i>c</i> -C <sub>6</sub> H <sub>11</sub> NH <sub>2</sub>	-133.1	-514.0
PhNH <sub>2</sub>	-153.1	-355.0
(C <sub>2</sub> H <sub>5</sub> ) <sub>2</sub> NH	-111.3	-448.2
<i>c</i> -C <sub>6</sub> H <sub>11</sub> NHCH <sub>3</sub>	-122.6	-501.2
<i>c</i> -(CH <sub>2</sub> ) <sub>5</sub> NH	-116.7	-436.4
Ph <sub>2</sub> NH	-118.8	-192.0
C <sub>11</sub> H <sub>23</sub> CONHCH <sub>3</sub>	-186.2	
CH <sub>3</sub> OH	-219.7	-692.0
C <sub>2</sub> H <sub>5</sub> OH	-199.6	-721.0
(CH <sub>3</sub> ) <sub>2</sub> CHOH	-193.3	-744.6
(CH <sub>3</sub> ) <sub>3</sub> COH	-177.8	-770.2
CF <sub>3</sub> CH <sub>2</sub> OH	-199.6	-1365.2
PhOH	-202.5	-589.3
C <sub>6</sub> F <sub>5</sub> OH	-233.9	-1474.8
C <sub>2</sub> H <sub>5</sub> CO <sub>2</sub> H	-251.0	-994.9
C <sub>11</sub> H <sub>23</sub> CO <sub>2</sub> H	-243.1	-1214.2
CF <sub>3</sub> CO <sub>2</sub> H	-273.6	-1576.7
C <sub>12</sub> H <sub>25</sub> SH	-183.3	-744.6
PhSH	-178.2	-347.7

<sup>a</sup> Enthalpies of reaction are for C<sub>5</sub>H<sub>11</sub>MgBr + B-H → C<sub>5</sub>H<sub>12</sub> + B-MgBr.<sup>b</sup> Values are from Reference 45. The experimental uncertainties are *ca* 2–3%.<sup>c</sup> Values calculated in this work unless otherwise noted. See text.

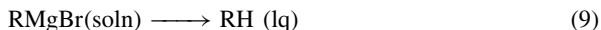
is from a dataset consisting of homologs of four or more carbons. The methyl derivative in most series deviates from the otherwise linear relationship.

There are seven *n*-alkylmagnesium bromides for which there are solution phase enthalpy of formation data, C<sub>2</sub>–C<sub>8</sub>. The methylene increment is  $-25.0 \pm 0.8 \text{ kJ mol}^{-1}$ , which is nearly identical to both the *n*-alkane series and the *n*-alkyl bromide series ( $-25.3 \pm 0.4 \text{ kJ mol}^{-1}$ ). The methylmagnesium bromide enthalpy of formation is *ca*  $9 \text{ kJ mol}^{-1}$  more negative than that for ethylmagnesium bromide, even though MeMgBr has the smaller molecular weight. This is typical of a methyl group bonded to more electropositive atoms such as lithium, boron and aluminum. The enthalpies of formation of methyl derivatives bonded to atoms more electronegative than carbon also deviate from the correlation but in the opposite direction: they are typically less negative than for the ethyl derivatives. The magnitude of the gaseous methyl deviations can be correlated to the electronegativity of Z<sup>51</sup>. For the three *sec*-alkylmagnesium bromides, the methylene increment is  $-25.1 \pm 2.0 \text{ kJ mol}^{-1}$ . There are only two *sec*-alkyl bromides to compare, isopropyl and *sec*-butyl, and the difference between their enthalpies of formation, and thus the methylene increment, is  $-24.3 \text{ kJ mol}^{-1}$ .

In isomeric alkanes substituted with an electronegative atom, alkyl group branching at the carbon bonded to the substituent atom increases the thermodynamic stability in both the liquid and gaseous phases. For example, the stability order of the butyl bromides is *t*-Bu > *sec*-Bu > *n*-Bu. The increasing stability parallels the alkyl group carbocation stability. For alkyl groups bonded to metals, the alkyl group is more electronegative, and it might be expected that the stability order would be the opposite and thus parallel the alkyl group carbanion stability. Indeed, the enthalpy of formation of *n*-propylmagnesium bromide shows it to be more stable than the isomeric isopropylmagnesium bromide by *ca* 21 kJ mol<sup>-1</sup>. Non-calorimetric corroboration of the relative stabilities is provided by the observation that in the presence of small amounts of TiCl<sub>4</sub>, isopropylmagnesium bromide rearranges to *n*-propylmagnesium bromide<sup>52</sup>. Organomagnesium enthalpies of formation cannot track those of the parent hydrocarbon—after all, isopropyl hydride and *n*-propyl hydride must have the same enthalpy of formation since they are both propane, *n*- and *sec*-butyl hydrides must have the same enthalpy of formation since they are both *n*-butane, and isobutyl and *tert*-butyl hydride must have the same enthalpy of formation as they are both isobutane.

In the isomeric butyl series, the secondary butyl derivative is less stable than either of the primary butylmagnesium bromides. The carbon-branched isobutylmagnesium bromide is more stable than the *n*-butyl isomer in keeping with the usual observation that alkyl branching remote from the carbon bonded to the heteroatom increases the thermodynamic stability. Within the experimental uncertainties, *sec*-butyl- and *t*-butylmagnesium bromide have the same enthalpies of formation, which is the same as that observed for the corresponding alkyl lithiums. The explanation may be that there is a fortuitous cancellation of the stabilizing effects of carbon-branching in the tertiary group and of secondary-carbon bonded to metal.

A useful comparison is between the alkylmagnesium bromide and its corresponding hydrocarbon, as for the formal protonation reaction (equation 9). The average enthalpy of formation difference,  $\delta\Delta H_f$ , for primary R is  $233.5 \pm 5.1$  kJ mol<sup>-1</sup> and for secondary R it is  $214.7 \pm 3.3$  kJ mol<sup>-1</sup>. For the lone example of the tertiary butyl group,  $\delta\Delta H$  is 217.2 kJ mol<sup>-1</sup>, which is similar to that for secondary R, as expected. The larger endothermicity of the formal reaction is associated with the group of relatively more stable Grignard reagents.



## B. Unsaturated Compounds

### 1. Formal protonation reactions

Just as there is a nearly constant  $\delta\Delta H_f$  value for the enthalpy of the formal protonation reaction (equation 9) for Grignard reagents of similar structural type (primary vs. secondary, tertiary), we expect there to be a nearly constant (but different)  $\delta\Delta H_f$  also for the various groups of unsaturated species. The enthalpies of formal reaction for the three aromatic Grignards are quite consistent,  $259.0 \pm 3.0$  kJ mol<sup>-1</sup>. The enthalpy of protonation of vinylmagnesium bromide is 304 kJ mol<sup>-1</sup>. Considering that phenyl and vinyl species often exhibit similar thermochemistry, this latter value seems much too high. However, the reaction for vinylmagnesium bromide in THF is expected to be more exothermic than the same reaction in ether. The allyl- and benzylmagnesium bromides have nearly identical enthalpies of protonation: 267.4 and 264.7 kJ mol<sup>-1</sup>, respectively. Using a liquid phase enthalpy of formation for triphenylmethane of 192.2 kJ mol<sup>-1</sup><sup>53</sup>, the  $\delta\Delta H_f$  is *ca* 314 kJ mol<sup>-1</sup>. The enthalpy of reaction of the lone example of triple bond unsaturation, phenylethynylmagnesium bromide, is 353.0 kJ mol<sup>-1</sup>. Again, the stable phenylethynyl and triphenylmethide carbanions have the most endothermic reaction enthalpies.

## 2. Enthalpies of hydrogenation

There are enthalpies of formation for several unsaturated organomagnesium bromides as well as for species that are their saturated counterparts. How do the enthalpies of the formal hydrogenation reaction (equation 10) of the organomagnesium bromides compare with those for the corresponding hydrocarbons?



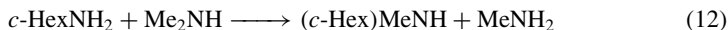
The unsaturated Grignard reagents are phenyl-, allyl- and vinylmagnesium bromide and their hydrogenated products are cyclohexyl-, *n*-propyl- and ethylmagnesium bromide. The calculated formal hydrogenation reaction enthalpies are  $-171.9$ ,  $-95.0$  and  $-58.6$  kJ mol $^{-1}$ , respectively. However, the last value for hydrogenation of vinylmagnesium bromide in THF rather than ether solution, must be corrected to *ca*  $-90$  kJ mol $^{-1}$  to account for the extremely high enthalpy of solution of MgBr $_2$  in THF. For the hydrocarbon counterparts, benzene/cyclohexane, propene/propane and ethene/ethane, the reaction enthalpies are  $-205.4$ ,  $-123.4$  and  $-136.2$  kJ mol $^{-1}$ , respectively. All of the Grignard reagents' reactions are less exothermic than those of the corresponding hydrocarbons. The lower exothermicity of hydrogenation of the phenyl and vinyl Grignard reagents indicates that there is a stabilizing interaction between the double bond electrons and the magnesium bonded to carbon. In the allyl case, stabilization takes place by resonance. In the phenyl and vinyl cases the carbon bonded to magnesium changes hybridization from  $sp^2$  to  $sp^3$ . By this change, we go from a rather stable to a rather unstable Grignard reagent.

## C. Organomagnesium Bromides Containing Heteroatoms

Enthalpies of formation of the magnesium bromide salts of the Bronsted acids are calculated from the measured enthalpies of the reaction of the Bronsted acid, HB, with pentylmagnesium bromide and the known enthalpies of formation of pentylmagnesium bromide and pentane according to equation 11. Because some of the HB enthalpies of formation have been revised and others newly measured since the original publication, the BMgBr enthalpies of formation have been recalculated and appear in Table 4<sup>54</sup>.



There remain three Bronsted acids that have no liquid phase enthalpy of formation data that we know of: dodecanethiol, cyclohexyl methyl amine and *N*-methyl dodecanamide. Although the enthalpy of formation of 1-dodecanethiol has not been measured, there are experimental values available for other members of its homologous series, C $_2$ –C $_7$ , C $_{10}$ . From a weighted least-squares analysis of the data from which a slope,  $-25.4$ , and an intercept,  $-23.3$ , are derived, the enthalpy of formation of dodecanethiol is  $-328.1$  kJ mol $^{-1}$ <sup>55</sup>. The enthalpy of formation of dodecanethiolate magnesium bromide is thus estimated as  $-744.6$  kJ mol $^{-1}$ . We can estimate the enthalpy of formation of cyclohexyl methyl amine by assuming equation 12 is thermoneutral.



From the archival enthalpies of formation of the other species, the enthalpy of formation of cyclohexyl methyl amine is  $-145.4$  kJ mol $^{-1}$ . From equation 11, the enthalpy of formation of the corresponding salt is  $-501.2$  kJ mol $^{-1}$ . Attempts to estimate an enthalpy of formation for *N*-methyldodecanamide reveals a paucity of data to work with, primarily for unsubstituted and *N*-methylamides<sup>56</sup>. There is much enthalpy of formation data for *n*-alkyl carboxylic acids, including dodecanoic acid. The methylene increment

is  $-25.4 \text{ kJ mol}^{-1}$ , typical of liquid phase enthalpies of formation. There are only two liquid enthalpies of formation for *n*-alkyl amides, butanamide and hexanamide, and the difference between them is  $-25.5 \text{ kJ mol}^{-1}$  per  $-\text{CH}_2-$  group. A fairly accurate enthalpy of formation for dodecanamide of  $-550.9 \text{ kJ mol}^{-1}$  could be derived from these data. However, for the only two enthalpies of formation for *N*-methyl-*n*-alkylamides in the liquid phase, *N*-methylacetamide and *N*-methylpropanamide, the difference is  $6.9 \text{ kJ mol}^{-1}$  which is extremely atypical for a methylene increment. However, the acetamide is the methyl derivative and so is expected to deviate from the other *N*-methylalkylamides. Furthermore, there is no liquid enthalpy of formation for either acetamide or propanamide upon which to base an estimate for *N*-methylation of any amide.

Earlier it was stated that within the set of hydrocarbylmagnesium bromides the enthalpy of formation difference,  $\delta\Delta H_f$ , for the magnesium compound and its corresponding hydrocarbon was slightly larger for the primary alkyl groups compared to the secondary and tertiary groups. This differentiation by  $\delta\Delta H_f$  with respect to structure and stability would likewise be expected for sets of compounds with C-Mg, N-Mg, O-Mg and S-Mg bonds. Figure 2 shows a plot of the enthalpies of formation of the organomagnesium bromide species in Tables 3 and 4 vs. the enthalpies of formation of the corresponding protonated species. The data points for each bond type fall on separate straight lines, the slopes of which are close to 1 (C-Mg, 0.78; N-Mg, 0.98; O-Mg, 1.1; S-Mg, 1.0). Even though there are differences in structure within each set, the correlations ( $r^2$ ) are quite good: C-MgBr, 0.98; N-MgBr, 0.98; O-MgBr, 0.99. There are only two data points for S-MgBr.

Within each bond-type group, further distinctions can be made, as mentioned earlier for the alkylmagnesium bromides. In Figure 2, the points corresponding to mono- and polyunsaturated hydrocarbyl groups all appear to the right of the points belonging to the saturated groups. Said differently, the  $\delta\Delta H_f$  values are substantially larger for the species with unsaturated substituents,  $257\text{--}359 \text{ kJ mol}^{-1}$  vs.  $211\text{--}248 \text{ kJ mol}^{-1}$ . This difference indicates an extra stabilization for the Grignard reagent which is absent in the hydrocarbon. The negative charge can be better accommodated in such compounds by  $\text{sp}^2$ -inductive and/or resonance effects.

Within the O-MgBr group are at least three subcategories: the alkoxy and phenoxy, the carboxy and the fluorinated species. Within the alkoxy subgroup, the endothermic

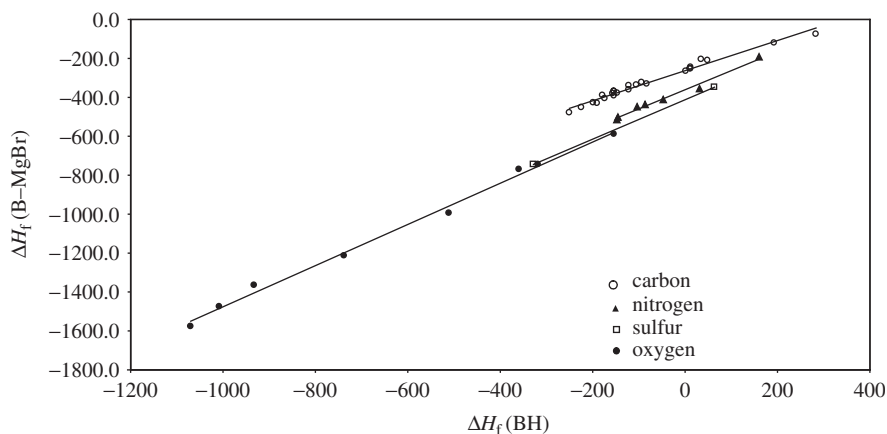


FIGURE 2. Enthalpies of formation of BMgBr vs. those of BH ( $\text{kJ mol}^{-1}$ )

$\delta\Delta H_f$  from equation 9 is in the order  $t\text{-BuO} < i\text{-PrO} < \text{EtO} < \text{MeO}$ , which is the order of increasing stability of the alkoxides in solution. The two carboxy species are more endothermic than the alkoxy, and the trifluoroacetoxy is the most endothermic. While pentafluorophenoxy is more endothermic than phenoxy, trifluoroethoxy and ethoxy have identical endothermicities.

The N—MgBr group does not show much variation in  $\delta\Delta H_f$  except for PhNHMgBr, which is comparatively endothermic. By comparison, Ph<sub>2</sub>NMgBr is about the same as the saturated amine species.

The vertical distance between the lines may crudely be taken as the difference in bond energy between the B—H/B—MgBr bond types, at least for B atoms in the same row of the periodic table. From the plot, the bond strength increases in the order C—MgBr, N—MgBr, S—MgBr and O—MgBr, which is also expected from electronegativity differences. The bond strength to hydrogen increases in the order S—H, C—H, N—H and O—H. It has been suggested<sup>45</sup> that the very strong bond between oxygen and magnesium is due to back-donation of lone pairs on oxygen into empty orbitals on magnesium. This may be the case also with sulfur and less obviously with nitrogen. This is consistent from a consideration of the atomization energies of solid MgO, MgS and Mg<sub>3</sub>N<sub>2</sub>. From the enthalpies of formation of solid MgO, MgS and Mg<sub>3</sub>N<sub>2</sub> and those of the gaseous atoms Mg, O, S and N, one can derive the enthalpies of atomization of the binary magnesium 'salts' to be 852, 773 and 1378 kJ mol<sup>-1</sup>. Dividing these numbers by 2, 2 and 6, respectively (the number of 'bonds' per formula unit), results in 426, 382 and 230 kJ mol<sup>-1</sup> for effective Mg—O, Mg—S and Mg—N bond strengths. Unfortunately, the enthalpy of formation of solid Mg<sub>2</sub>C is not available from the literature—indeed, this seemingly simple binary species is still unknown—and so the remaining Mg—C bond strength cannot be derived for the final comparison.

One of the original goals in the determination of the enthalpy of reaction of Brønsted acids with pentylmagnesium bromide was to explain the relationship between the enthalpy and the  $pK_a$  of the acid<sup>13,14,45</sup>. For a set of hydrocarbons having disparate structures, the correlation coefficient,  $r^2$ , is 0.98. For the nitrogen-containing acids, again a group with disparate structures, there is an excellent correlation ( $r^2 = >0.99$ ) if the aromatic aniline (phenylamine) and diphenylamine data are ignored. The oxygen-containing acid data show much scatter. For acids of the same acidity, the oxygen and nitrogen acid reactions are more exothermic than those for the carbon acids and the author assumes the cause is back-donation of lone pairs on the heteroatoms to empty orbitals on magnesium<sup>45</sup>.

The only data omitted in this analysis are those for vinyl- (determined in THF) and cyclopentadienylmagnesium bromide. Including the data point for cyclopentadienyl in the analysis worsens the correlation. This may be caused by a difference in carbon bonding to the magnesium for cyclopentadienide compared to the other carbon–magnesium bonds. This bonding will be mentioned in a later section on magnesium sandwich compounds.

There is a report of calorimetrically-determined enthalpies of reaction of methyl- and ethylmagnesium bromides with some ketones in ether solution at 15 °C<sup>57</sup>. The reaction shown in equation 13, which results in an exotherm of  $-202.3 \text{ kJ mol}^{-1}$ , produces an alkoxymagnesium bromide that also appears as a product of a different reaction in Table 4. Using the enthalpy of formation of MeMgBr<sup>13,14</sup> and the liquid phase enthalpy of formation of acetone, the enthalpy of formation of the *t*-butoxymagnesium bromide is calculated as  $-783.5 \text{ kJ mol}^{-1}$ . This is within 10 kJ mol<sup>-1</sup> of the value reported in Table 4.



All the experimental enthalpies of the Grignard reaction appear in Table 5 along with the enthalpies of formation calculated using the same method as illustrated above. Unfortunately there are no liquid enthalpy of formation data for the halogenated ketones, nor are



TABLE 5. Enthalpies of reaction between ketones and Grignard reagents and calculated enthalpies of formation of alkoxy magnesium bromides ( $\text{kJ mol}^{-1}$ )

Ketone	RMgBr	$\Delta H_{\text{rxn}}^a$	$\Delta H_f(\text{R'OMgBr})^b$
$\text{Me}_2\text{CO}$	$\text{MeMgBr}$	-202.3	-782.2
$\text{MeCOEt}$	$\text{MeMgBr}$	-188.1	-793.2
$\text{Me}_3\text{CCOMe}$	$\text{MeMgBr}$	-162.1	-822.5
$\text{ClCH}_2\text{COMe}$	$\text{MeMgBr}$	-226.6	
$\text{BrCH}_2\text{COMe}$	$\text{MeMgBr}$	-233.7	
$\text{MeCOPh}$	$\text{MeMgBr}$	-184.9	-659.2
$\text{Me}_2\text{CO}$	$\text{EtMgBr}$	-222.6	-802.5
$\text{MeCOEt}$	$\text{EtMgBr}$	-209.2	-814.3
$\text{Me}_3\text{CCOMe}$	$\text{EtMgBr}$	-161.7	-822.1
$\text{ClCH}_2\text{COMe}$	$\text{EtMgBr}$	-240.2	
$\text{BrCH}_2\text{COMe}$	$\text{EtMgBr}$	-262.7	
$\text{MeCOPh}$	$\text{EtMgBr}$	-210.5	-684.8

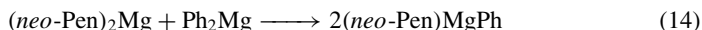
<sup>a</sup> Enthalpies of reaction are from Reference 57.<sup>b</sup> Enthalpies of formation of the alkoxy magnesium bromides are calculated from enthalpies of formation of the ketones from References 1 and 3 and of methyl and ethylmagnesium bromide from References 13 and 14. See text for discussion.

they easily estimated. The error in experimental measurements and assumptions can be understood by inspecting the two entries that both give the same alkoxy magnesium bromide product, although their calculated enthalpies of formation differ by *ca* 10  $\text{kJ mol}^{-1}$ :  $\text{Me}_2\text{CO} + \text{EtMgBr}$  and  $\text{MeEtCO} + \text{MeMgBr}$ .

## V. DIORGANOMAGNESIUM COMPOUNDS

The only dialkylmagnesium compound whose enthalpy of formation has been measured is dineopentyl magnesium<sup>58</sup>: (s)  $-236.8 \pm 7.2 \text{ kJ mol}^{-1}$  and (g)  $-74.3 \pm 7.6 \text{ kJ mol}^{-1}$ . Unfortunately there are no enthalpies of formation for any of its isomers or homologs. We cannot even calculate the enthalpy of the Schlenk equilibrium because, although the enthalpy of formation of neopentylmagnesium bromide is for the ether solution, that for dineopentylmagnesium is not, and there is no experimental value for the enthalpy of solution.

Organomagnesium compounds undergo fast intermolecular carbon–magnesium bond exchange in solution. One such process in THF solution, (equation 14) was studied by NMR line-shape analysis<sup>59</sup>:



The thermodynamic quantities for the reaction were found to be  $\Delta H = 10.0 \text{ kJ mol}^{-1}$ ,  $\Delta S = 57.7 \text{ eu}$  and  $\Delta G = -7.24 \text{ kJ mol}^{-1}$  at 298 K.

With knowledge of the enthalpies of formation of magnesium bromide and an alkylmagnesium bromide, and by using the data for the Schlenk reaction from Table 1, the enthalpy of formation of a dialkylmagnesium compound in ether solution may be calculated. In diethyl ether, the equilibrium equation 6 may be considered to be shifted to the side of the unsymmetrically substituted magnesium compound. Subtraction of the enthalpy of solution<sup>44</sup> gives the enthalpy of formation of the solvent-free components of the Schlenk equilibrium. The enthalpy of formation of  $\text{MgBr}_2$  in diethyl ether is  $-559 \pm 4 \text{ kJ mol}^{-1}$ <sup>13,14</sup>. Only for ethyl- and butylmagnesium bromide in ether are all the enthalpy values available. The enthalpies of formation of diethylmagnesium

and dibutylmagnesium in diethyl ether are accordingly calculated to be  $-71.4 \text{ kJ mol}^{-1}$  and  $-184.4 \text{ kJ mol}^{-1}$ , respectively. Using the enthalpy of solvation for diethylmagnesium (the only solvation enthalpy available), its solid-phase enthalpy of formation is  $-47.4 \text{ kJ mol}^{-1}$ . Is this a reasonable value? If we assume the methylene increment for the solid  $n\text{-R}_2\text{Mg}$  homologous series is at least  $-25 \text{ kJ mol}^{-1}$ , then the enthalpy of formation of di- $n$ -pentylmagnesium derived from the aforementioned value for diethylmagnesium is *ca*  $-197 \text{ kJ mol}^{-1}$ . The stabilizing isomerization of  $n$ -pentylmagnesium bromide to neopentylmagnesium bromide is  $-23.4 \text{ kJ mol}^{-1}$  and should be about the same as for isomerization of dipentylmagnesium. Twice that value yields an estimate of *ca*  $-244 \text{ kJ mol}^{-1}$ , less than  $10 \text{ kJ mol}^{-1}$  different from the experimental measurement of the enthalpy of formation of dineopentylmagnesium.

## VI. ORGANOMAGNESIA AND RINGS

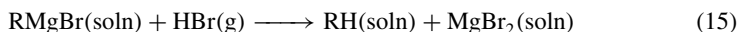
Magnesium can be incorporated in cyclic compounds in two ways. The first is as an exocyclic divalent substituent, i.e. part of a species of the type  $\text{RMgZ}$  where R is a carbocyclic ring and Z is some univalent substituent. As discussed for acyclic organomagnesia, Z can be halide or hydrocarbyl (either cyclic or acyclic), and so again we consider Grignard reagents and diorganomagnesium compounds.

Alternatively, magnesium may be an endocyclic component of a ring, as found in a magnesacycle (or magnesiacycle). Recall that dicoordinate, divalent oxygen forms diverse, indeed nearly ubiquitous, heterocycles ranging from simple ethers such as the reactive oxiranes and the Grignard-‘friendly’ solvent THF, to biologically relevant sugars and nucleosides/tides. Dicoordinate oxygen with an unstrained bond angle of *ca*  $105^\circ$  is a natural ring component in that it mimics the tetracoordinate carbon that necessarily dominates the chemistry of organic rings. From simple models of molecular structure, dicoordinate, divalent magnesium is expected to be linear and so rings with  $\text{-Mg-}$  might appear to mimic the generally highly strained cycloalkynes and cycloallenes with their linear multiple bond components rather than the saturated and considerably less strained cycloalkanes.

Perhaps, surprisingly, there are other structural types found for magnesium-containing rings. These, too, will be discussed. So, we now ask—what is found from the experimental literature, especially that which is of thermochemical consequence and direct interest in this chapter.

### A. Cycloalkylmagnesium Halides

The enthalpies of formation of the cycloalkylmagnesium bromides that have been determined by reaction calorimetry are listed in Table 3<sup>14</sup>. As with other functionalized cycloalkanes and the cycloalkanes themselves, there is no regularity to these values with respect to carbon number as there are for their acyclic analogs because of the influence of ring strain on the enthalpies. Unfortunately, there are no enthalpies of formation for the bromocycloalkanes with which to compare these values; there are, however, enthalpies of formation for liquid phase cycloalkanes. Figure 3 is a plot of the enthalpies of formation for the cycloalkyl-MgBr vs. those for cycloalkyl-H. There is a linear relationship with  $r^2 < 0.99$ . Indeed, the enthalpies of formation of the cycloalkylmagnesium bromides were calculated from the enthalpies of formation of the cycloalkanes themselves by way of the protonation reaction (equation 15).



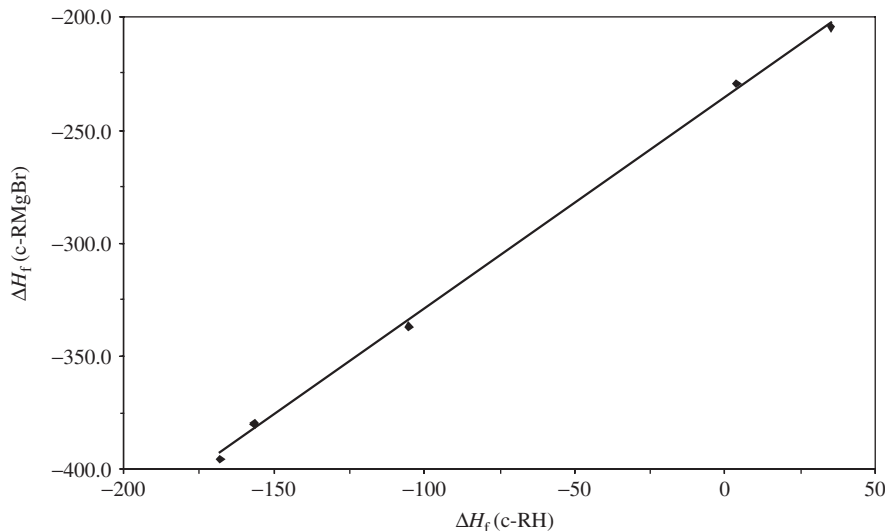


FIGURE 3. Enthalpies of formation of cycloalkylmagnesium bromides vs. those of cycloalkanes (kJ mol<sup>-1</sup>)

The linear relationship thus demonstrates the near-constancy of the enthalpies of the protonation reaction of the secondary cycloalkylmagnesium bromides ( $-292.8 \pm 6.3$  kJ mol<sup>-1</sup>).

Not surprisingly, the enthalpy of reaction for cyclopropylmagnesium bromide,  $-282.8$  kJ mol<sup>-1</sup>, is somewhat of an outlier, given the numerous anomalies associated with this small ring<sup>60</sup>. For example, cyclopropane is the most olefinic and most acidic of the cycloalkanes—which correctly suggests that cyclopropyl forms the most polar C–Mg bond and, accordingly, is the thermodynamically most stable cycloalkylmagnesium species.

Despite our earlier enunciated electronegativity and bond polarity logic, we must forego nearly all comparison with the free (uncomplexed) carbanions R<sup>-</sup>. Unlike the rather stable cyclopropyl anion, the cyclobutyl and cyclopentyl ions<sup>61</sup> are unbound with regard to loss of their ‘extra’ electron. That is, the gas phase ionization process to form the radical from the carbanion,  $R:^- \rightarrow R^\bullet + e^-$ , is energetically favorable.

Nonetheless, it is telling that while allylMgBr is some 60 kJ mol<sup>-1</sup> more stable than its isomer cyclopropylMgBr (value from Table 3), at least in diethyl ether solution, the difference between liquid phase formation of the corresponding hydrocarbons, propene and cyclopropane, is only some 30 kJ mol<sup>-1</sup>, favoring the former. This is consistent with allyl anion being more stable than cyclopropyl anion, a phenomenon generally ascribed to the significant resonance stabilization in the former. Presumably, at least some of that anionic resonance stabilization is still present—indeed, some 30 kJ mol<sup>-1</sup>—in the derived organometallic, i.e. in the formally carbanionic part of the Grignard. However, despite their thermochemical proclivity, cyclopropyl Grignards seemingly do not rearrange, at least on the time scale of calorimetric investigations.

As shown by their reaction chemistry, cyclobutyl Grignards likewise do not rearrange to either their 3-butenyl or cyclopropylmethyl isomers; reaction of cyclobutylmagnesium chloride with benzoic acid results in almost quantitative yield of cyclobutane accompanied by only 1% 1-butene. In contrast, the cyclopropylmethylmagnesium chloride is *ca*

17 kJ mol<sup>-1</sup> less stable than the 3-butenyl species at equilibrium (in refluxing ether) in terms of their free energies (and presumably, at least roughly in terms of enthalpies), while the corresponding bromides favor the acyclic species by *ca* 29 kJ mol<sup>-1</sup>. There was no cyclobutane found with the isomeric butene and methylcyclopropane in the product mixture<sup>62</sup>. The average of these two differences is 23 kJ mol<sup>-1</sup>. Applying an entropy correction of 16 eu at 298 K based on cyclopropane/propene, the enthalpy differences for the chloride and bromide are *ca* 1 and 13 kJ mol<sup>-1</sup>, respectively. The enthalpy of formation difference between the corresponding liquid phase hydrocarbons, 1-butene and methylcyclopropane, is 22 kJ mol<sup>-1</sup>.

An estimate of the enthalpies of formation of the magnesium species above is made as follows. The  $\delta\Delta H_f$  introduced in an earlier section for the enthalpy of formation difference for equation 9 for the set of primary alkyl magnesium bromides in Table 3 (except allyl and benzyl) is 233.5  $\pm$  5.1 kJ mol<sup>-1</sup>. From the enthalpy of formation of liquid 1-butene (-20.5 kJ mol<sup>-1</sup>), the enthalpy of formation of 3-butenylmagnesium bromide is thus -254 kJ mol<sup>-1</sup>. The formal enthalpy of hydrogenation of 3-butenylmagnesium bromide to *n*-butylmagnesium bromide (equation 10) is then calculated as -124 kJ mol<sup>-1</sup>, virtually identical to that for its butene/butane hydrocarbon counterpart, -126.1 kJ mol<sup>-1</sup>. Since the double bond is remote from the C-Mg bond and there is no special stabilization of the Grignard, the hydrogenation enthalpies should be about the same. From the approximate difference between the equilibrium enthalpies for the cyclopropylmethyl-/3-butenylmagnesium bromide, 13 kJ mol<sup>-1</sup>, the enthalpy of formation of cyclopropylmethylmagnesium bromide is -241 kJ mol<sup>-1</sup>.

The enthalpies of formation of liquid methylcyclopropane and cyclobutane are quite close, -1.7  $\pm$  0.6 and 3.7  $\pm$  0.5 kJ mol<sup>-1</sup>. How do the enthalpies of formation of their corresponding Grignards compare? The enthalpy of formation from Table 3 for cyclobutyl MgBr is -230 kJ mol<sup>-1</sup>. The enthalpy difference between the cyclic C<sub>4</sub>H<sub>7</sub>MgBr isomers is thus *ca* 11 kJ mol<sup>-1</sup>, which is not too different from that for the hydrocarbon counterparts, especially considering the uncertainties of the estimates used in this derivation.

Reaction chemistry and associated product analysis shows the free-energy difference between cyclobutylmethyl magnesium chloride and its more stable 4-pentenyl isomer to be *ca* 27 kJ mol<sup>-1</sup><sup>63</sup>. Using an unspecified entropic correction, the authors determined the difference in enthalpies of the isomers to be *ca* 9 kJ mol<sup>-1</sup>. Again using the  $\delta\Delta H_f$ , above, the enthalpy of formation of 4-pentenylmagnesium bromide is -280.4 kJ mol<sup>-1</sup>. The enthalpy of formation of cyclobutylmethylmagnesium bromide is accordingly -271.4 kJ mol<sup>-1</sup>. The enthalpy difference between their hydrocarbon counterparts is 2.4 kJ mol<sup>-1</sup>.

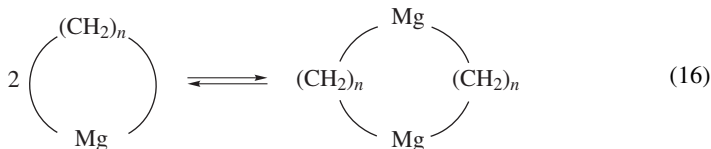
The experimental enthalpies of protonation<sup>14</sup> and the formal enthalpies of protonation, RMgBr  $\rightarrow$  RH, are fairly constant for structurally similar species (R = cycloalkyl, primary alkyl) and would be expected to be constant also for the primary cycloalkylmethylmagnesium bromides. For the two examples just discussed, the formal enthalpies of protonation that are calculated using the derived enthalpies of formation for the cyclopropyl- and cyclobutylmethylmagnesium bromides are 262 and 235 kJ mol<sup>-1</sup>, respectively. The mean value is thus 248 kJ mol<sup>-1</sup>, which is very close to that expected for the formal protonation of other primary R groups.

Cyclopentylmethyl- and norbornylmethyl organometallic compounds are reportedly stable to ring cleavage<sup>64</sup>. Evidently, the ring strain associated with the small 3- and 4-membered rings is required for the reaction. However, *endo*- and *exo*-norbornenyl-5-methylmagnesium chlorides thermally interconvert with each other and with that of the ring-opened 4-allylcyclopentenylmagnesium chloride which is stabilized by allylic anion resonance<sup>64</sup>. These species apparently have comparable Gibbs energies. Now, how does this compare with the enthalpies of formation of corresponding hydrocarbons? The liquid phase enthalpy of formation of (*endo*)-5-methylnorborn-2-ene is 15.8  $\pm$  1.1 kJ mol<sup>-1</sup>.

The enthalpy of formation of allylcyclopentene is unknown, but accepting the value for allylcyclopentane ( $-66.1 \pm 1.0 \text{ kJ mol}^{-1}$ , from Reference 65) and assuming the same dehydrogenation enthalpy as for the parent carbocycles, cyclopentane/cyclopentene, of  $109.5 \pm 1.0 \text{ kJ mol}^{-1}$ , we derive an enthalpy of formation of either allylcyclopentene isomer of *ca*  $43 \text{ kJ mol}^{-1}$ . This is a difference of  $27 \text{ kJ mol}^{-1}$  favoring the norbornene. However, correcting by *ca*  $30 \text{ kJ mol}^{-1}$  for the earlier enunciated resonance stabilization of an allyl anion results in the allylcyclopentene and norbornenyl Grignards having very nearly the same enthalpy of formation. This is consistent with the above putative thermoneutrality suggested for the two Grignards from their experimentally observed interconversion, although it must be acknowledged we have completely ignored entropic considerations in our analysis.

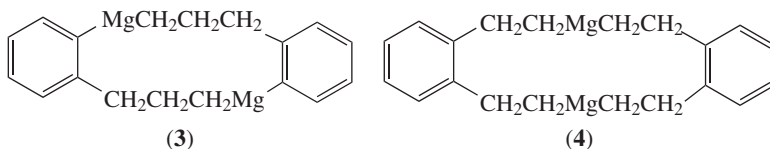
## B. Magnesacycloalkanes and Their Dimers (Dimagnesacycloalkanes)

The magnesacycloalkanes,  $(\text{CH}_2)_n\text{Mg}$  where  $n = 4-6, 9$ , have a strong tendency to dimerize in THF solution, as shown in equation 16<sup>66,67</sup>. It would seem that relief of angle strain caused by the large C–Mg–C bond angle incorporated into the ring is the driving force for the dimerization of the smaller rings. However, magnesacyclodecane, which dimerizes to a 20-membered ring, should not be unduly strained<sup>68</sup>.

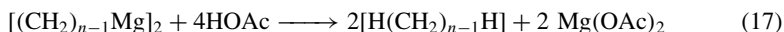


Magnesacyclopentane, -heptane and -decane all completely dimerize, while magnesacyclohexane exists to a small extent as the monomer. The authors assert that the magnesacyclohexane monomer is only observable because of the highly dilute solution that shifts the equilibrium toward the monomer<sup>67</sup>. The enthalpy and entropy of the dimerization reaction for  $n = 5$  were determined to be  $-48.0 \pm 3 \text{ kJ mol}^{-1}$  and  $106.0 \pm 10.0 \text{ J mol}^{-1} \text{ deg}^{-1}$ , respectively. The dimerization enthalpies for reactions when  $n = 6, 9$  are more exothermic than  $65 \text{ kJ mol}^{-1}$ . This thermodynamic (and kinetic) proclivity to dimerization obviously is not shared by the corresponding carbocycles.

While no thermochemical data exist for any magnesacycloalkenes, there are some relevant data for their benzo analogs. It is interesting that 2,3-benzomagnesacyclohexene exists almost totally as a dimer, **3** (similar to its non-benzo analog, magnesacyclohexane), and 4,5-benzomagnesacycloheptene exists totally as monomer (shown as the dimer, **4**). While there is a mix of  $\text{sp}^2$  and  $\text{sp}^3$  carbon bonding to magnesium in the former, there can be only  $\text{sp}^3$  bonding in the latter, and so this species would be expected to behave similarly to the other magnesacycles that also are  $\text{sp}^3$ -bonded and thus dimerize.



The reaction enthalpies<sup>67</sup> for the acetolysis reaction given in equation 17 are discussed as a measure of ring strain as compared to the strainless and monomeric diethylmagnesium.

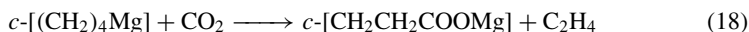


The dimers of magnesacycloheptane and -decane are shown to be strain-free. Unlike the original authors (also, see Reference 69) we will not try to estimate strain energies for the various magnesacycles nor to interpret them. Besides the normal complications of medium-sized rings such as transannular repulsions of hydrogens, there are also electrostatic effects arising from the positively charged magnesium atoms and adjoining negative carbons. This may be compared to the enthalpy of formation of cyclic ethers, with negative oxygens and adjoining positive carbons, for which the dimerization and trimerization of dioxane to form 12-crown-4 (1,4,8,11-tetraoxacyclododecane) and 18-crown-6 (1,4,8,11,14-hexaoxacyclooctadecane) are essentially thermoneutral<sup>70</sup>.

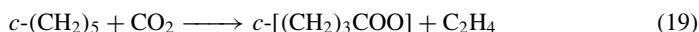
Having just mentioned negative oxygen and positive magnesium invites the question of rings containing both of these elements. We may expect strong dative, coordinate bonding between them. Indeed, this is found<sup>71</sup>: both 1-oxa-5-magnesacyclooctane and 1-oxa-6-magnesacyclodecane are found as monomers and have acetolysis enthalpies of  $-210.8 \pm 3.8$  and  $-212.6 \pm 2.0$  kJ mol<sup>-1</sup>. The difference between these values and those for the rings with only magnesium is not that large—then it is to be remembered that these species also have interactions with the solvent THF which are weakened, if not replaced, upon intramolecular complexation.

### C. Other Magnesacycles

Atomic magnesium has been shown to react with carbon dioxide and with ethylene to form small ring-containing products<sup>72</sup>. With CO<sub>2</sub> alone, a metastable 1:1 four-membered ring product MgCO<sub>2</sub> is found with magnesium bonded to both oxygens. With ethylene only, the monomeric (and unsolvated) 1:2 product, magnesacyclopentane is found. With the addition of both gaseous organics, a magnesalactone is formed suggesting that equation 18 is exothermic.

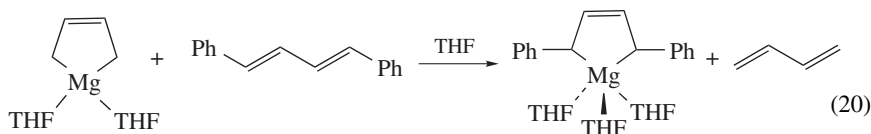


We note, however, that this is not the case for the corresponding carbocyclic reaction 19.



Indeed, it is endothermic by over 130 kJ mol<sup>-1</sup>! This documents that the polar/ionic bond between magnesium and oxygen is exceptionally strong, a fact we already surmised by the vigor of the reaction of Grignard reagents with air and water.

Within the general description of ligand exchange<sup>73</sup>, the relative stability of a variety of magnesium–olefin complexes/magnesacycles has been studied. For example, 1,4-diphenylbutadiene replaces the parent butadiene in equation 20 to form the penta-coordinated magnesium compound<sup>74</sup>.



A variety of other olefins were studied: 1,6-diphenylhexatriene, anthracene and cyclooctatetraene also displace butadiene from its polymeric magnesium complex. Now should these olefin–magnesium species be viewed as magnesacycles? Or as contact ion pairs with olefin dianions? In any case, no enthalpies of hydrolysis are available, nor quantitation of stabilities by even equilibrium constants. We welcome this information.

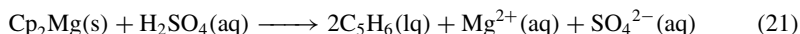
## VII. MAGNESIUM SANDWICH SPECIES

By the description “magnesium sandwich species” are meant compounds with the general structural formula  $[(CH)_m]_nMg_p$  (and their substituted and/or ionized derivatives) where  $m \geq 3$ ,  $n \geq 2$  and  $p \geq 1$ . In addition, it is tacitly assumed that the  $(CH)_m$  rings are attached to the metal by at least three carbons, i.e., that they are  $\eta^k$  species with  $k \geq 3$ .

### A. Magnesocene (Bis(cyclopentadienyl) magnesium)

The classic (if not classical) metal sandwich species bis(cyclopentadienyl)iron has the formula  $[(CH)_5]_2Fe$  ( $Cp_2Fe$ ) and the semisystematic name ferrocene, and so the related magnesium-containing species  $[(CH)_5]_2Mg$  ( $Cp_2Mg$ ) is often accompanied by the name magnesocene. We commence our discussion with this species.

There are two independent determinations of the solid-phase enthalpy of formation of magnesocene. The first measurement<sup>75</sup> of  $66.9 \pm 3.3 \text{ kJ mol}^{-1}$  results from analysis of the hydrolytic reaction of magnesocene with aqueous  $H_2SO_4$  (equation 21).



From the solid-phase enthalpy of formation and the enthalpy of sublimation from the same source, the gas-phase enthalpy of formation is  $135.1 \pm 3.8 \text{ kJ mol}^{-1}$ . By contrast, static bomb calorimetry<sup>76</sup> resulted in a value of  $77 \pm 3 \text{ kJ mol}^{-1}$  for the enthalpy of formation value of the solid. The discrepancy of *ca*  $10 \text{ kJ mol}^{-1}$  may be ascribed to differences in the enthalpy of formation of the inorganic ancillary reference state species in the hydrolysis reaction (1N  $H_2SO_4$  and 1:200  $MgSO_4$ ), the enthalpy of formation of the  $C_5H_6$  product and ‘foibles’ of static as opposed to rotating bomb calorimetry. Let us accept a consensus value of *ca*  $72 \pm 5 \text{ kJ mol}^{-1}$ . We note that the value of the sublimation enthalpy (uncontested from Reference 75) for magnesocene,  $68.2 \pm 1.3 \text{ kJ mol}^{-1}$ , is very similar to that of other ‘ocenes’. This is despite the considerable difference in their behavior otherwise, e.g. the ease of hydrolysis of magnesocene derivatives relative to the difficulty for those of ferrocene corroborates rather ionic ring–metal interactions in the former, and considerable covalency for the latter. Unfortunately, there are no data for the enthalpies of formation of correspondingly substituted magnesocenes and ferrocenes<sup>77</sup> with which one can further compare these at least formally related sandwich species.

Magnesocene does not appear to form a stable carbonyl complex. By contrast, there are seemingly stable 1:1 and 1:2  $NH_3$  complexes of magnesocene<sup>78</sup> with  $Mg-N$  bond energies of *ca*  $25 \text{ kJ mol}^{-1}$ , and indeed stable complexes of magnesocene with aliphatic (primary and secondary) amines have been crystallographically characterized<sup>79</sup>. There seems to be bonding between the N and the Mg and between the hydrogen of the ammonia or amines and the ring. There is also loss of hapticity of one of the cyclopentadienyl rings, i.e. one of the rings is coordinated by only two carbons as opposed to five for the other ring and in the uncomplexed magnesocene. Magnesocene is also complexed by a variety of other N and O (and P)—centered bases: NMR studies<sup>80</sup> suggest the order of increasing strength of complexation of di-isopropyl ether  $\sim$  anisole  $\sim$  triethylamine  $<$  diethyl ether  $<$  trimethylphosphine  $<$  1,4-dioxane  $<$  1,2-dimethoxyethane  $<$  THF  $<$  N, N, N', N'-tetramethylethylenediamine. It is quite clear that the cyclopentadienyl rings are rather weakly attached to the magnesium core. For example, magnesocene reacts with DMSO and THF to form the totally dissociated salt  $Mg(DMSO)_6^{2+} (Cp^-)_2$  while THF forms the mixed  $\eta^5\eta^1$  complex dicoordinated by this ether<sup>81</sup>.

There are few studies that address relative isomer stability of substituted magnesocenes. For example, the acid-catalyzed transalkylation (alkyl scrambling) studies of disubstituted benzenes<sup>82</sup> would destroy the organometallic of interest. One suggestive

investigation—although it may reflect kinetic as opposed to thermodynamic effects—is the reaction of isodicyclopentadiene (4,5,6,7-tetrahydro-4,7-methano-2*H*-indene) with di-*n*-butylmagnesium to form the bis isodicyclopentadienyl complex in which both ligands are ‘exo’, i.e. it is the CH<sub>2</sub>, and not the CH<sub>2</sub>CH<sub>2</sub> bridge, that faces the Mg<sup>83</sup>.

## B. Neutral Magnesium Half-Sandwiches

By the description ‘half-sandwich’ we mean species of the type [(CH)<sub>*m*</sub>]<sub>*n*</sub>Mg<sub>*p*</sub> where *n* now equals 1. While there are no thermochemical data available for neutral cyclopentadienyl magnesium, CpMg, the lowest excited electronic state is known to be *ca* 242 kJ mol<sup>−1</sup> above the ground state<sup>84</sup>, which tells us that the Cp–Mg bond energy must be at least 242 kJ mol<sup>−1</sup>. This value is within 1 kJ mol<sup>−1</sup> (*ca* 100 cm<sup>−1</sup>) for the excitation energy, and thus lower bound to the bond energies in the corresponding substituted methylcyclopentadienylmagnesium and nitrogen-containing pyrrolylmagnesium species. In that bond strength is often taken to relate to bond stretching frequencies and not bond energies, we note that the ring-Mg force constants are nearly the same as well: 112.6, 112.4 and 115.3 N m<sup>−1</sup>. By contrast, that of magnesocene itself is 173 N m<sup>−1</sup>, suggestive of stronger Cp–Mg bonding in the sandwich than half-sandwich compound. No spectroscopic or excitation data are available for the bisaza species, bis(pyrrolyl)magnesium for comparison, nor are there any enthalpy of formation or reaction measurements.

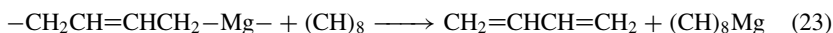
Affixing an R group to the Mg of our half-sandwiches results in the second class of species, e.g. CpMgR. It is quite clear that the reaction in equation 22



readily proceeds as written, e.g. for R = allyl<sup>80</sup> and neopentyl<sup>85</sup>. No relevant reaction or formation enthalpies are available, however, except for the solution phase difference of the  $\eta^1$  and  $\eta^3$ -allyl (actually methallyl) derivative favoring the former by 54.4 kJ mol<sup>−1</sup><sup>86</sup>. Other CpMg derivatives are known but the associated thermochemistry is not available.

The species (CH)<sub>8</sub>Mg, or we should say its THF 2.5-solvate<sup>73,87,88</sup>, is readily formed from cyclooctatetraene and Mg<sup>88</sup>. The NMR spectrum shows eight equivalent ring atoms<sup>87</sup> and so suggests either the cyclooctatetraene dianion and Mg<sup>2+</sup> salt<sup>88</sup> or a putative (and highly fluxional) solvated ‘magnesacyclopentene’ (or more properly magnesabicyclononatriene). However, there is no structural data for the  $\eta^8$  open sandwich species and the enthalpy of formation of this simple and sensible half-sandwich, or tight ion pair, cannot even be estimated.

We note that both of the reactions (equations 23 and 24) (without additional solvating ligands explicitly being shown) proceed facilely<sup>73,89</sup>.



However, lacking thermochemical data on the other two butadiene and anthracene-related organomagnesias does not even allow us to deduce a bound for the enthalpy of formation of (CH)<sub>8</sub>Mg<sup>90</sup>.

## C. Triple Decker (Club) Sandwiches

We know of no example wherein any (Cp)<sub>3</sub>Mg<sub>2</sub> derivative or related species is known. Indeed, as documented crystallographically, magnesocene reacts with CpTl (thallocene) to form the (Cp<sub>2</sub>Tl)<sup>−</sup> ion accompanied by a solvent-complexed CpMg<sup>+</sup> cation rather than

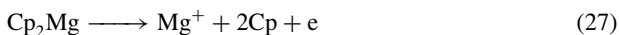
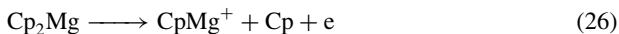


a CpTiCpMgCp complex. (By contrast, CpLi produces a complexed 4-layer CpTiCpLi species<sup>91</sup>.)

#### D. Cationic Sandwiches and Half-Sandwiches

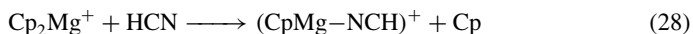
We have already mentioned the formation of solvated CpMg<sup>+</sup> in the context of the solution phase reaction of magnesocene and thallocene. In this section are discussed aspects of the experimental gas-phase ion energetics of CpMg<sup>+</sup>, Cp<sub>2</sub>Mg<sup>+</sup> and related species.

The two ring-Mg bond energies in Cp<sub>2</sub>Mg and CpMg have been determined from electron impact measurements<sup>92</sup> for reactions 25–27.

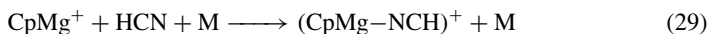


The energy thresholds (enthalpy of reactions) are roughly 8.0, 11.0 and 13.9 eV (772, 1061 and 1341 kJ mol<sup>-1</sup>), respectively. From these values<sup>93</sup>, the CpMg<sup>+</sup>–Cp and Cp–Mg<sup>+</sup> bond dissociation energy values are very nearly the same, 289 and 280 kJ mol<sup>-1</sup>. By contrast, there is the observation that the bond energy for CpMg<sup>+</sup>–RH is meaningfully larger than that of Mg<sup>+</sup>–RH and is consistent with the formal description of CpMg<sup>+</sup> as Cp<sup>-</sup>Mg<sup>2+</sup><sup>94</sup>.

Although Cp<sub>2</sub>Mg<sup>+</sup> does not undergo further ligation or reaction with RH, it does undergo a ligand exchange with HCN (equation 28)<sup>95</sup>.



The half-sandwich ion is also formed by direct clustering (with a third body M required) as in equation 29.



With additional HCN molecules, additional clustering of CpMg<sup>+</sup> with this ligand is observed as opposed to proton transfer according to equations 30 and 31.



Analogous processes (some proceeding, some not) to the above ion–molecule reactions have been discussed for other ligands<sup>96</sup>.

The Mg<sup>+</sup>–C<sub>6</sub>H<sub>6</sub> dissociation energy at 0 K was determined to be 134 ± 4 kJ mol<sup>-1</sup> (1.39 ± 0.10 eV) using collision induced dissociation<sup>97</sup> and 112 kJ mol<sup>-1</sup> by laser photo-dissociation<sup>98</sup>. Using the radiative association kinetics approach to ion cyclotron resonance spectrometry, the value was shown<sup>99</sup> to be the comparable 1.61 eV (155 kJ mol<sup>-1</sup>). It was also shown that the binding of the second benzene to Mg<sup>+</sup>, i.e. the Mg<sup>+</sup> (C<sub>6</sub>H<sub>6</sub>)–C<sub>6</sub>H<sub>6</sub> bond energy, is less than 1.4 eV (135 kJ mol<sup>-1</sup>).

The binding energy of MgCl<sup>+</sup> to a benzene was shown<sup>99</sup> to be >2.5 eV (*ca* 240 kJ mol<sup>-1</sup>) and to a second benzene by less than 1.4 eV (*ca* 135 kJ mol<sup>-1</sup>). Mesitylene might be expected to bind more strongly than benzene because of the electron donation from the three methyl groups; we are told<sup>99</sup> that the first and second bond energies to magnesium

are greater than 2 eV (*ca* 190 kJ mol<sup>-1</sup>). Based on these results and related ones for other alkaline earth species, the following rule was enunciated<sup>99</sup>: 'The qualitative picture is presented that MX<sup>+</sup> behaves as a metal ion center with the charge of a monovalent ion but the electronic character of a divalent alkaline earth cation.'

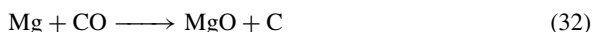
We close by noting that Mg<sup>+</sup> combines with multiple molecules of cyanoacetylene sequentially to form complexes of the generic formula Mg(HCCCN)<sub>*n*</sub><sup>+</sup><sup>95</sup>. Of particular relevance to our discussion is the anomalous stability of the *n* = 4 species, suggested by the original authors to possibly be the Mg<sup>+</sup> complex of 1,3,5,7-tetracyanocyclooctatetraene. If so, this is the sole complex of the type (CH)<sub>*n*</sub>Mg<sup>+</sup> with *n* > 6 or, more precisely, a tetracyano derivative thereof. We know of no experimental evidence for any *n* = 7 species with or without any additional ligands or any charge. Tropylium salts are reduced by Mg powder to form the radical dimer (C<sub>7</sub>H<sub>7</sub>)<sub>2</sub><sup>100</sup>. The sole species with the small *n* = 3 is C<sub>3</sub>H<sub>3</sub>Mg<sup>+</sup>, seen experimentally as a product of the fragmentation of (CH)<sub>5</sub>Mg<sup>+</sup> and quantum chemically suggested to be CH<sub>3</sub>C≡CMg<sup>+</sup> and not a cyclopropenyl derivative<sup>101</sup>.

### VIII. MAGNESIUM COMPLEXES WITH CARBON MONOXIDE

Iron, as found in the porphyrin derivative hemoglobin, complexes CO to form a stable metal carbonyl. Iron also forms a variety of metal carbon monoxide derivatives such as the homoleptic Fe(CO)<sub>5</sub>, Fe<sub>2</sub>(CO)<sub>9</sub> and Fe<sub>3</sub>(CO)<sub>12</sub>, the anionic [Fe(CO)<sub>4</sub>]<sup>2-</sup> and its covalent derivative Fe(CO)<sub>4</sub>Br<sub>2</sub>, [CpFe(CO)<sub>2</sub>]<sup>-</sup> and its alkylated covalent derivatives CpFe(CO)<sub>2</sub>-R with its readily distinguished π (and η<sup>5</sup>) and σ (and η<sup>1</sup>) iron carbon bonds. By contrast, Mg in its chlorin derivative chlorophyll, which very much resembles porphyrin, forms no such bonds with CO nor is there a rich magnesium carbonyl chemistry (if indeed, there is any at all).

This is not surprising—there are many textbook discussions of the difference between transition and main group elements. Consonant with this is the finding that (Cp\*)<sub>2</sub>Mg (the sandwich species alternatively called bis(pentamethylcyclopentadienyl)magnesium and dexamethylmagnesium) does not react with CO, unlike the corresponding species with Ca and some other metals and metalloids<sup>102</sup>. Indeed, in (Cp\*)<sub>2</sub>Mg, there is little room for another ligand around the central metal and Mg seems electronically satisfied.

Let us return to simple compounds and simple reactions involving Mg and CO. To begin with, consider the reaction 32.



For solid Mg, MgO and C (and gaseous CO), this reaction is significantly exothermic: the reaction enthalpy is *ca* -491 kJ mol<sup>-1</sup>. This is not surprising—Mg is more electropositive than C and so oxygen combines with the more metallic element. Indeed, combustion results from the aforementioned reaction (e.g. Reference 103). By contrast, this reaction is endothermic by an even more spectacular 697 kJ mol<sup>-1</sup> when all of the species are in their gaseous phase<sup>104</sup>. The Mg—O bond in MgO, in any phase, is strong; the C—O bond in gaseous CO is stronger than any other bond in a gaseous molecule.

We know of no evidence for any discrete molecular species of the type Mg<sub>*x*</sub>(CO)<sub>*y*</sub> that parallels mostly transition metal carbonyls. However, the related cations MgCO<sup>+</sup> and Mg(CO)<sub>2</sub><sup>+</sup> have been studied experimentally and quantum-chemically by gas phase ion chemists for which binding energies of *ca* 0.43 ± 0.06<sup>105, 106</sup> and 0.40 ± 0.03 eV<sup>105</sup> (41.5 ± 5.8 and 38.6 ± 2.9 kJ mol<sup>-1</sup>) were found. By contrast, Mg(CO)<sub>2</sub><sup>2+</sup> has a calculated binding energy<sup>107</sup> of *ca* 200 kJ mol<sup>-1</sup> as befits the considerably stronger Lewis acidity of Mg<sup>2+</sup> over that of Mg<sup>+</sup><sup>108</sup>. Although there is an absence of neutral Mg<sub>*x*</sub>(CO)<sub>*y*</sub> species, it is only for the 'ground state species' in that the excited state (involving the s<sup>1</sup>π<sup>1</sup> Mg instead of s<sup>2</sup>) of neutral Mg(CO)<sub>2</sub> has been calculated to be bound<sup>109</sup>.

## IX. REFERENCES AND NOTES

1. J. B. Pedley, R. D. Naylor and S. P. Kirby, *Thermochemical Data of Organic Compounds* (2nd edn.), Chapman & Hall, New York, 1986; J. B. Pedley, *Thermochemical Data and Structures of Organic Compounds*, Volume 1, Thermodynamics Research Center, College Station, 1994.
2. D. D. Wagman, W. H. Evans, V. B. Parker, R. H. Schumm, I. Halow, S. M. Bailey, K. L. Churney and R. L. Nuttall, 'The NBS tables of chemical thermodynamic properties: Selected values for inorganic and C<sub>1</sub> and C<sub>2</sub> organic substances in SI units', *J. Phys. Chem. Ref. Data*, **11** (Supplement No. 2) (1982).
3. P. J. Linstrom and W. G. Mallard (Eds.) *NIST Chemistry WebBook, NIST Standard Reference Database Number 69*, June 2005, National Institute of Standards and Technology, Gaithersburg MD, 20899 (<http://webbook.nist.gov>).
4. (a) E. C. Ashby and S. Yu, *J. Organomet. Chem.*, **29**, 339 (1971).  
(b) S. Yu and E. C. Ashby, *J. Org. Chem.*, **36**, 2123 (1971).  
(c) E. C. Ashby and J. Nackashi, *J. Organomet. Chem.*, **72**, 11 (1974).
5. (a) S. Cudzilo and W. A. Trzcinski, *Polish J. Appl. Chem.*, **45**, 25 (2001); *Chem. Abstr.*, **137**, 171930 (2001).  
(b) E-C. Koch, *Propellants, Explosives, Pyrotechnics*, **27**, 340 (2002).
6. I. C. Appleby, *Chem. Ind. (London)*, 120 (1971).
7. E. C. Ashby and D. M. Al-Fekri, *J. Organomet. Chem.*, **390**, 275 (1990).
8. J. L. Leazer Jr., R. Cvetovich, F-R. Tsay, U. Dolling, T. Vickery and D. Bachert, *J. Org. Chem.*, **68**, 3695 (2003).
9. T. Reeves, M. Sarvestani, J. J. Song, Z. Tan, L. J. Nummy, H. Lee, N. K. Yee and C. H. Senanayake, *Org. Proc. Res. Dev.*, **10**, 1258 (2006).
10. (a) D. J. Ende, P. J. Clifford, D. M. DeAntonis, C. SantaMaria and S. J. Brenek, *Org. Proc. Res. Dev.*, **3**, 319 (1999).  
(b) H. D. Ferguson and Y. M. Puga, *J. Therm. Anal.*, **49**, 1625 (1997).
11. W. Tschelinzeff, *Ber. Dtsch. Chem. Ges.*, **40**, 1487 (1907); *Chem. Abstr.*, **1**, 8288 (1907).
12. (a) W. Tschelinzeff, *Compte Rendu*, **144**, 88 (1907).  
(b) V. Tshelintsev, *J. Russ. Phys.-Chem. Soc.*, **39**, 1019 (1908); *Chem. Abstr.*, **2**, 4832 (1908).
13. T. Holm, *J. Organomet. Chem.*, **56**, 87 (1973).
14. T. Holm, *J. Chem. Soc., Perkin Trans. 2*, 484 (1981).
15. H. D. B. Jenkins, *Z. Phys. Chem. (Munich)*, **194**, 165 (1996). This paper discusses the energetics of (C<sub>2</sub>)<sup>2-</sup> and also that of C<sup>4-</sup>. This study offers no reason to assume any particular stabilization for (C<sub>3</sub>)<sup>4-</sup>.
16. A. Largo, P. Redondo and C. Barrientos, *J. Am. Chem. Soc.*, **126**, 14611 (2004).
17. R. A. Seburg, E. V. Patterson, J. F. Stanton and R. J. McMahon, *J. Am. Chem. Soc.*, **119**, 5847 (1997).
18. P. Karen, Å. Kjekshus, Q. Huang and V. L. Karen, *J. Alloys Compd.*, **282**, 72 (1999); *Chem. Abstr.*, **130**, 176622 (1999).
19. H. Fjellvaag and P. Karen, *Inorg. Chem.*, **31**, 3260 (1992).
20. (a) The formal carbon-containing anions of MgC<sub>2</sub> and Mg<sub>2</sub>C<sub>3</sub>, the aforementioned C<sub>2</sub><sup>2-</sup> and C<sub>3</sub><sup>4-</sup>, are isoelectronic to CO and CO<sub>2</sub> and thereby to other 10 and 16 valence electron neutral and singly charged triatomics such as NO<sup>+</sup> and AlO<sup>-</sup>, NO<sub>2</sub><sup>+</sup> and AlO<sub>2</sub><sup>-</sup>. The atomization energies of these latter sets of diatomics and triatomics are simply related by E(triatomic)/E(diatomic) ≈ constant, cf. I. Tomaszewicz, G. A. Hope and P. A. G. O'Hare, *J. Chem. Thermodyn.*, **29**, 1031 (1997).  
(b) C. A. Deakyne, L. Li, W. Zheng, D. Xu and J. F. Liebman, *J. Chem. Thermodyn.*, **34**, 185 (2002).  
(c) C. A. Deakyne, L. Li, W. Zheng, D. Xu and J. F. Liebman, *Int. J. Quantum Chem.*, **95**, 713 (2003). However, we are convinced that none of this prepares us for the relevant multiply charged anionic species and/or extensive multicenter bonding.
21. K. Kobayashi and M. Arai, *Physica C: Superconductivity and Its Applications* (Amsterdam, Netherlands), **388–389**, 201 (2003).
22. See, for example:  
(a) D. E. Woon, *Astrophys. J.*, **456** (2 Pt 1), 602 (1996); *Chem. Abstr.*, **124**, 188082 (1996).

- (b) S. Itono, K. Takano, T. Hirano and U. Nagashima, *Astrophys J.*, **538** (2 Pt. 2), L163-5-(2000); *Chem. Abstr.*, **133**, 288140 (2000).
23. V. Grignard, *Compte Rendu*, **130**, 1322 (1900).
24. A. Baeyer and V. Villiger, *Ber.*, **35**, 1201 (1902).
25. R. Abegg, *Ber.*, **38**, 4112 (1905).
26. W. Schlenk and W. Schlenk Jr., *Ber.*, **62**, 920 (1929).
27. P. Jolibois, *Compte Rendu*, **155**, 353 (1912).
28. R. E. Dessy, G. S. Handler, H. Wotiz and C. Hollingsworth *J. Am. Chem. Soc.*, **79**, 3476 (1957).
29. E. C. Ashby and W. E. Becker, *J. Am. Chem. Soc.*, **85**, 118 (1963).
30. A. D. Vreugdenhill and C. Blomberg, *Recl. Trav. Chim. Pays-Bas*, **82**, 453 (1963).
31. E. C. Ashby and W. B. Smith, *J. Am. Chem. Soc.*, **86**, 4363 (1964).
32. E. C. Ashby, J. Laemmle and H. M. Neumann, *Acc. Chem. Res.*, **7**, 272 (1974).
33. M. B. Smith and W. F. Becker, *Tetrahedron*, **22**, 3027 (1966).
34. M. B. Smith and W. F. Becker, *Tetrahedron*, **23**, 4215 (1967).
35. S. G. Smith and G. Su, *J. Am. Chem. Soc.*, **86**, 2750 (1964).
36. T. Holm, *Acta Chem. Scand.*, **20**, 2821 (1966).
37. T. Holm, *Acta Chem. Scand.*, **21**, 2753 (1967).
38. M. B. Smith and W. F. Becker, *Tetrahedron Lett.*, 3843 (1965).
39. R. M. Salinger and H. S. Mosher, *J. Am. Chem. Soc.*, **86**, 1782 (1964).
40. G. E. Parris and E. C. Ashby, *J. Am. Chem. Soc.*, **93**, 1206 (1971).
41. (a) D. E. Evans and G. V. Fazakerley, *J. Chem. Soc. A*, 184 (1971).  
(b) D. E. Evans and G. V. Fazakerley, *Chem. Commun.*, 974 (1968).
42. T. Holm, *Tetrahedron Lett.*, 3329 (1966).
43. T. Holm, *Acta Chem. Scand.*, **23**, 579 (1969).
44. G. van der Wal, Thesis, Vrije Universiteit, Amsterdam, 1979.
45. T. Holm, *Acta Chem. Scand., Ser. B*, **37**, 797 (1983).
46. A. S. Carson and H. A. Skinner, *Nature*, **165**, 484 (1950).
47. A. S. Carson, P. G. Laye, J. B. Pedley and A. M. Welsby, *J. Chem. Thermodyn.*, **25**, 261 (1993).
48. V. G. Genchel, E. V. Evstigneeva and N. V. Petrova, *Zh. Fiz. Khim.*, **50**, 1909 (1976); *Chem. Abstr.*, **85**, 176675 (1976).
49. S. W. Slayden and J. F. Liebman, 'Thermochemistry of organolithium compounds', Chap. 3 in *The Chemistry of Organolithium Compounds* (Eds. Z. Rappoport and I. Marek), Wiley, Chichester, 2004.
50. J. D. Cox and G. Pilcher, *Thermochemistry of Organic and Organometallic Compounds*, Academic Press, London, 1970.
51. J. F. Liebman, J. A. Martinho Simões and S. W. Slayden, *Struct. Chem.*, **6**, 65 (1995).
52. G. D. Cooper and H. L. Finkbeiner *J. Org. Chem.*, **27**, 1493 (1962).
53. The enthalpy of formation for the solid triphenylmethane is from Reference 5. The enthalpy of fusion, 22.0 kJ mol<sup>-1</sup> at 365 K, is taken from Reference 8.
54. The enthalpy of formation values for the liquid phase compounds are taken from Reference 1 when they are available. For the remaining compounds, data were obtained from Reference 3. The liquid phase enthalpy of formation of diphenyl amine of 132 kJ mol<sup>-1</sup>, derived from combustion of the liquid, as reported in Reference 3 is seemingly incorrect with a too-small enthalpy of fusion, if the enthalpy of formation of the solid is accepted. The enthalpy of formation of the solid given by Reference 1, 130.2 ± 1.7 kJ mol<sup>-1</sup>, is the average of two selected determinations. It is virtually the same as the average value of all known seven determinations in the 20<sup>th</sup> century, 129.8 ± 10 kJ mol<sup>-1</sup>, as given in Reference 3. There are two enthalpies of sublimation: 89.1 as found in Reference 1 and 96.7 as found in Reference 3. Using the average value for both the above quantities, the enthalpy of formation of gaseous diphenyl amine is 222.6 kJ mol<sup>-1</sup>. Finally, using the average of the two enthalpies of vaporization found in Reference 3, 62.6 kJ mol<sup>-1</sup>, the enthalpy of formation for the liquid diphenyl amine is 160.0 kJ mol<sup>-1</sup>. This value is used in the analysis.
55. J. F. Liebman, K. S. K. Crawford and S. W. Slayden, 'Thermochemistry of Organosulphur Compounds', Chap. 4 in *The Chemistry of Groups, Supplement S: The Chemistry of Sulphur-containing Functional Groups* (Eds. S. Patai and Z. Rappoport), Wiley, Chichester, 1993.

56. J. F. Liebman, H. Y. Afeefy and S. W. Slayden, 'The thermochemistry of amides', Chap. 4 in *The Amide Linkage: Structural Significance in Chemistry, Biochemistry, and Materials Science* (Eds. A. Greenberg, C. M. Breneman and J. F. Liebman), Wiley, New York, 2000.
57. A. V. Tuulmets, E. O. Parts and L. R. Ploom, *Zh. Obshch. Khim.*, **33**, 3124 (1963); *Chem. Abstr.*, **60**, 6714 (1964).
58. O. S. Akkerman, G. Schat, E. A. I. M. Evers and F. Bickelhaupt, *Recl. Trav. Chim. Pays-Bas*, **102**, 109 (1983).
59. G. Fraenkel and S. H. Yu, *J. Am. Chem. Soc.*, **96**, 6658 (1974).
60. See, for example, Z. Rappoport (Ed.), *The Chemistry of the Cyclopropyl Group*, Wiley, Chichester, 1987 and Vol. 2, Wiley, Chichester, 1995.
61. C. H. DePuy, S. Gronert, S. E. Barlow, V. M. Bierbaum and R. Damrauer, *J. Am. Chem. Soc.*, **111**, 1968 (1989).
62. D. J. Patel, C. L. Hamilton and J. D. Roberts, *J. Am. Chem. Soc.*, **87**, 5144 (1965).
63. E. A. Hill and H.-R. Ni, *J. Org. Chem.*, **36**, 4133 (1971).
64. E. A. Hill, K. Hsieh, K. Conroski, H. Sonnentag, D. Skalitzy and D. Gagas, *J. Org. Chem.*, **54**, 5286 (1989).
65. A. Labbauf and F. D. Rossini, *J. Phys. Chem.*, **65**, 476 (1961).
66. H. C. Holtkamp, G. Schat, C. Blomberg and F. Bickelhaupt, *J. Organomet. Chem.*, **240**, 1 (1982).
67. F. J. M. Freijee, G. Schat, O. S. Akkerman and F. Bickelhaupt, *J. Organomet. Chem.*, **240**, 217 (1982).
68. The bond angles in crystalline 1,6-dimagnesacyclododecane and 1,7-dimagnesacyclododecane, where each magnesium atom is coordinated with two THF molecules, are 128° and 142°, respectively. A. L. Spek, G. Schat, H. C. Holtkamp, C. Blomberg and F. Bickelhaupt, *J. Organomet. Chem.*, **131**, 331 (1977).
69. F. Bickelhaupt, *Pure Appl. Chem.*, **58**, 537 (1986).
70. The thermochemical data for 1,4-dioxane and 12-crown-4 come from our archival source; that for 18-crown 6 come from summing those from V. P. Vasil'ev, V. A. Borodin and S. B. Kopnyshev, *Russ. J. Phys. Chem. (Engl. Transl.)*, **66**, 585 (1992) (enthalpy of formation, solid) and G. Nichols, J. Orf, S. M. Reiter, J. Chickos and G. W. Gokel, *Thermochim. Acta*, **346**, 15 (2000) (enthalpy of sublimation).
71. F. J. M. Freijee, G. Van der Wal, G. Schat, O. S. Akkerman and F. Bickelhaupt, *J. Organomet. Chem.*, **240**, 229 (1982).
72. V. N. Solov'ev, E. V. Polikarpov, A. V. Nemukhin and G. B. Sergeev, *J. Phys. Chem. A*, **103**, 6721 (1999).
73. K. Mashima, Y. Matsuo, H. Fukumoto, K. Tani, H. Yasuda and A. Nakamura, *J. Organomet. Chem.*, **545–546**, 549 (1997).
74. Y. Kai, N. Kanehisa, K. Miki, N. Kasai, K. Mashima, H. Yasuda and A. Nakamura, *Chem. Lett.* 1277 (1982).
75. H. S. Hull, A. F. Reid and A. G. Turnbull, *Inorg. Chem.*, **6**, 805 (1967).
76. J. R. Chipperfield, J. C. R. Sneyd and D. E. Webster, *J. Organomet. Chem.*, **178**, 177 (1979).
77. In fact, we know of no enthalpy of formation data at all for substituted magnesocenes and only the following references for phase change enthalpies thereof: A. K. Baev, *Zh. Fiz. Khim.*, **78**, 1519 (2004); *Chem. Abstr.*, **142**, 392494 (2004) and A. I. Podkovyrov and A. K. Baev, *Izv. Vys. Ucheb. Zaved., Khim. Khim. Tekhn.*, **37**, 108 (1994); *Chem. Abstr.*, **122**, 239772 (1995). It has also been suggested that the monocyclopentadienyl amidinate species CpMg(HC(C(Me)(NBu-t))<sub>2</sub>) has a comparable 'ease' of sublimation as magnesocene, H. M. El-Kaderi, A. Xia, M. Je. Heeg and C. H. Winter, *Organometallics*, **23**, 3488 (2004), suggestive of a comparable enthalpy of sublimation as well.
78. G. T. Wang and J. R. Creighton, *J. Phys. Chem. A*, **108**, 4873 (2004).
79. A. Xia, J. E. Knox, M. J. Heeg, H. Schlegel and C. H. Winter, *Organometallics*, **22**, 4060 (2003).
80. H. Lehmkuhl, K. Mehler, R. Benn, A. Rufinska and C. Krueger, *Chem. Ber.*, **119**, 1054 (1986).
81. A. Jaenschke, J. Paap and U. Behrens, *Organometallics*, **22**, 1167 (2003).
82. See, for example, the isomerization of 2- and 3-pentyl benzene and related dialkylated species, A. A. Pimerzin, T. N. Nesterova and A. M. Rozhnov, *J. Chem. Thermodyn.*, **17**, 641 (1985).

83. O. Gobley, S. Gentil, J. D. Schloss, R. D. Rogers, J. C. Gallucci, P. Meunier, B. Gautheron and L. A. Paquette, *Organometallics*, **18**, 2531 (1999).
84. E. S. J. Robles, A. M. Ellis and T. A. Miller, *J. Phys. Chem.*, **96**, 8791 (1992).
85. R. A. Andersen, R. Blom, A. Haaland, B. E. R. Schilling and H. Volden, *Acta Chem. Scand., Ser. A*, **39**, 563 (1985).
86. R. Benn, H. Lehmkuhl, K. Mehler and A. Rufinska, *J. Organomet. Chem.*, **293**, 1 (1985).
87. R. S. Muslukhov, L. M. Khalilov, A. A. Ibragimov, U. M. Dzhemilev and A. A. Panasenko, *Metalloorganicheskaya Khimiya*, **1**, 680 (1988); *Chem. Abstr.*, **110**, 95299 (1989).
88. H. Lehmkuhl, S. Kintopf and K. Mehler, *J. Organomet. Chem.*, **46**, C1 (1972).
89. T. Alonso, S. Harvey, P. C. Junk, C. L. Raston, B. Skelton and A. H. White, *Organometallics*, **6**, 2110 (1987).
90. Quantum chemical calculations on the valence isoelectronically related COT Ca, Sr and Ba complexes for which bonding energies of 89.8, 63.5 and 51.2 kcal mol<sup>-1</sup> (376, 266 and 214 kJ mol<sup>-1</sup>) were determined. Z. Gong, H. Shen, W. Zhu, X. Luo, K. Chen and H. Jiang, *Chem. Phys. Lett.*, **423**, 339 (2006).
91. D. R. Armstrong, R. Herbst-Irmer, A. Kuhn, D. Moncrieff, M. A. Paver, C. A. Russel, D. Stalke, A. Steiner and D. S. Wright, *Angew. Chem., Int. Ed. Engl.*, **32**, 1774 (1993).
92. G. M. Begun and R. N. Compton, *J. Chem. Phys.*, **58**, 2271 (1973).
93. We are encouraged in the use of this number because the photoelectron derived (vertical) ionization potential, nominally the same number as the first of the three electron impact derived values, is in fact very much the same value, namely 8.11 eV (783 kJ mol<sup>-1</sup>), as the above value of 772 kJ mol<sup>-1</sup>. See S. Evans, M. L. H. Green, B. Jewitt, A. F. Orchard and C. F. Pygall, *J. Chem. Soc., Faraday Trans. 2*, **68**, 1847 (1972).
94. R. K. Milburn, M. V. Frash, A. C. Hopkinson and D. K. Bohme, *J. Phys. Chem. A*, **104**, 3926 (2000).
95. R. K. Milburn, A. C. Hopkinson, and D. K. Bohme, *J. Am. Chem. Soc.*, **127**, 13070 (2005).
96. R. K. Milburn, V. Baranov, A. C. Hopkinson and D. K. Bohme, *J. Phys. Chem. A*, **103**, 6373 (1999).
97. A. Andersen, F. Muntean, D. Walter, C. Rue and P. B. Armentrout, *J. Phys. Chem. A*, **104**, 692 (2000).
98. K. F. Willey, C. S. Yeh, D. L. Robbins and M. A. Duncan, *J. Phys. Chem.*, **96**, 9106 (1992).
99. A. Gapeev and R. C. Dunbar, *J. Phys. Chem. A*, **104**, 4084 (2000).
100. K. Okamoto, K. Komatsu and H. Shingu, *Bull. Chem. Soc. Jpn.*, **42**, 3249 (1969).
101. J. Berthelot, A. Luna and J. Tortajada, *J. Phys. Chem. A*, **102**, 6025 (1998).
102. P. Selg, H. H. Brintzinger, M. Schultz and R. A. Andersen, *Organometallics*, **21**, 3100 (2002).
103. U. I. Gol'dshleger and E. Ya. Shafirovich, *Fizika Goreniya i Vzryva*, **36**, 67 (2000); *Chem. Abstr.*, **133**, 19400 (1985).
104. The enthalpy of formation of MgO(g) remains seriously contentious, cf. A. Lesar, S. Prebil and M. J. Hodoscek, *Chem. Inf. Comp. Sci.*, **42**, 853 (2002). However, our qualitative conclusions including our suggested adjectives remain unchanged.
105. A. Andersen, F. Muntean, D. Walter, C. Rue and P. B. Armentrout, *J. Phys. Chem. A*, **104**, 692 (2000).
106. R. C. Dunbar and S. Petrie, *J. Phys. Chem. A*, **109**, 1411 (2005).
107. S. Petrie, *J. Phys. Chem. A*, **106**, 7034 (2002).
108. When the Mg is suitably complexed, or, should we say, coordinated, such as found in 'polycrystalline MgO smoke', the binding of CO is much reduced, cf. the 11 kJ mol<sup>-1</sup> suggested for this binding by G. Spoto, E. Gribov, A. Damin, G. Ricchiardi and A. Zecchina, *Surf. Sci.*, **540**, L605 (2003).
109. S. Sakai and S. Inagaki, *J. Am. Chem. Soc.*, **112**, 7961 (1990).

## CHAPTER 3

# NMR of organomagnesium compounds

PETER J. HEARD

*School of Biological and Chemical Sciences, Birkbeck University of London, Malet Street, London, WC1E 7HX, UK*  
*Fax: +0207 6316246; e-mail: p.heard@bbk.ac.uk*

---

I. INTRODUCTION .....	131
II. CONCENTRATION OF REAGENT SOLUTIONS .....	132
III. ALKYL AND ARYL COMPOUNDS .....	133
A. Alkyl Compounds .....	133
B. Aryl Compounds .....	138
C. The Schlenk Equilibrium .....	140
IV. ALLYLIC AND VINYLIC COMPOUNDS .....	141
V. ALKOXIDE AND PEROXIDE COMPOUNDS .....	145
VI. CO-ORDINATION COMPLEXES .....	148
VII. <sup>25</sup> Mg NMR STUDIES .....	151
VIII. REFERENCES .....	153

---

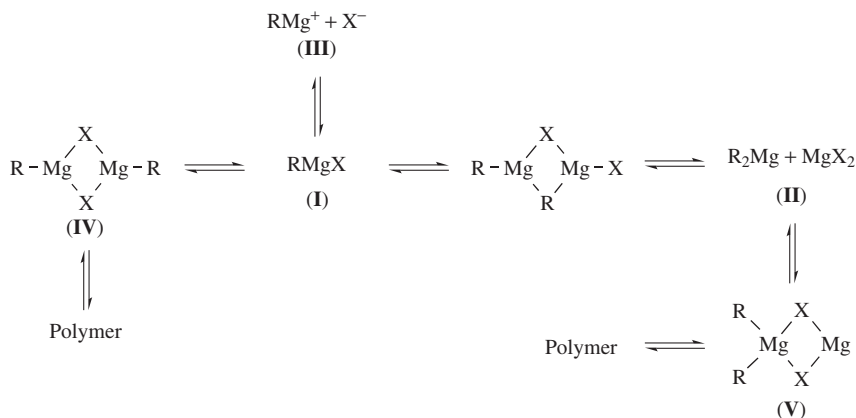
### I. INTRODUCTION

Since their discovery, the exact solution composition of Grignard compounds has been the subject of considerable debate, and given the power of NMR in elucidating chemical structure it is unsurprising that it was applied to the study of Grignard and other organomagnesium compounds from its earliest days. However, the complex nature of the solution behaviour of such compounds and the low magnetic field strengths then available often frustrated proper analysis of the data, and the first reported NMR studies were generally inconclusive<sup>1</sup>. Worse, the interpretation of early NMR spectra was often based on preconceived (and as it is now realized incorrect) notions as to the nature of the compounds in solution, so caution must be exercised when considering much of the pre-1970's data.

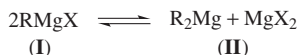
Although the advent of higher field NMR instruments and our increasing understanding of the solution behaviour of organomagnesium reagents have greatly improved the veracity of NMR studies, detailed NMR reports on such compounds remain relatively sparse. The

bulk of the literature that has been published was done so prior to the 1980's. The reasons for the paucity of reported NMR studies are probably three-fold: (i) organomagnesium reagents are generally highly sensitive, making the isolation of sufficiently pure samples problematic; (ii) different preparations can apparently give quite different NMR spectra; (iii) the exact solution behaviour depends on a number of factors, making it difficult to draw any general conclusions.

The weight of evidence, accumulated over many years of detailed studies using a combination of physicochemical techniques, including NMR, reveals that the solution composition of Grignard reagents is best represented by extended Schlenk equilibria (Scheme 1)<sup>1,2</sup>. However, because of the complexity of the solution behaviour, the vast majority of their NMR spectra are analysed on the basis of the basic equilibrium first proposed by Schlenk and Schlenk<sup>3</sup> (Scheme 2).



SCHEME 1. Extended Schlenk equilibria. Co-ordinated solvent molecules are omitted for clarity



SCHEME 2. Basic Schlenk equilibrium

In Et<sub>2</sub>O, the fluorides and chlorides, RMgF and RMgCl, exist predominately as the halide-bridged symmetrical dimers RMgX<sub>2</sub>MgR (IV) (Scheme 1), whereas the Br and I analogues are best described as the monomeric RMgX species (I) at low concentrations (<0.1 mol dm<sup>-3</sup>) and as linear, singly halide-bridged polymers at higher concentration.

In THF, monomeric RMgX (I) and R<sub>2</sub>Mg (II) co-exist over a wide concentration range for the chlorides, bromides and iodides. The fluorides are present as the F-bridged dimers across the whole concentration range. Similarly, the alkoxide and aryloxide compounds, RMgOR', are present as the R<sub>2</sub>Mg(μ-OR')<sub>2</sub>Mg species in THF.

The predominate solution-state species in Et<sub>2</sub>O and THF are summarized in Scheme 3.

## II. CONCENTRATION OF REAGENT SOLUTIONS

The concentrations of organomagnesium reagent solutions have traditionally been determined by acid titration, but this method suffers from the disadvantage that it only provides



Solvent	X	Composition
Et <sub>2</sub> O	F, Cl	$  \begin{array}{c}  \text{R} \quad \text{X} \quad \text{OEt}_2 \\  \diagdown \quad \diagup \\  \text{Mg} \quad \text{Mg} \\  \diagup \quad \diagdown \\  \text{Et}_2\text{O} \quad \text{X} \quad \text{R}  \end{array}  $
	Br, I	$  \begin{array}{c}  \text{R} \quad \text{OEt}_2 \\  \diagdown \quad \diagup \\  \text{Mg} \\  \diagup \quad \diagdown \\  \text{Et}_2\text{O} \quad \text{X}  \end{array}  $ <p>&lt; 0.1 mol dm<sup>-3</sup></p>
		$  \begin{array}{c}  \text{R} \\    \\  \left[ \text{Mg} - \text{X} \right]_n \\    \\  \text{OEt}_2  \end{array}  $ <p>&gt; 0.1 mol dm<sup>-3</sup></p>
THF	F, OR	$  \begin{array}{c}  \text{R} \quad \text{X} \quad \text{THF} \\  \diagdown \quad \diagup \\  \text{Mg} \quad \text{Mg} \\  \diagup \quad \diagdown \\  \text{THF} \quad \text{X} \quad \text{R}  \end{array}  $
	Cl, Br, I	$2\text{RMgX} \rightleftharpoons \text{MgX}_2 + \text{R}_2\text{Mg}$

SCHEME 3. Composition of Grignard compounds in solution

an estimation of the total basic content, which is also likely to include non-metal species. NMR, on the other hand, can provide a quick and convenient method for the direct determination of the concentration of organomagnesium species present, without the need to eliminate non-magnesium-containing bases. The NMR methodology relies on comparing the integrals of the reagent resonances with those of a suitable reference compound, of precisely known concentration. The accuracy of the method is limited only by the accuracy of the integration process, *ca*  $\pm$  5%. It is interesting to note that in the comparison of the two methods reported, the molarities determined by NMR were generally slightly higher than those estimated volumetrically<sup>4</sup>. Rather than NMR giving an overestimation, it seems more likely that the volumetric method slightly underestimates the concentration due to unavoidable decomposition of the reagents during the analysis.

### III. ALKYL AND ARYL COMPOUNDS

#### A. Alkyl Compounds

At ambient temperature, most alkylmagnesium compounds display a single set of signals in their NMR spectra indicating that, if there is more than one solution-state species present, the organic groups are equivalent on the NMR time-scale. Although the positions of the NMR signals were shown to be both concentration and temperature dependent, early NMR studies failed to provide any direct evidence for the presence of more than a single species. However, with the development of higher field instruments, it has become

possible to distinguish between  $R_2Mg$  and  $RMgX$  species, and even between terminal and bridging groups in some associated species.

$^1H$  and  $^{13}C$  NMR chemical shift data for alkylmagnesium compounds are collected in Table 1<sup>5-17</sup>, together with those for other selected organomagnesium compounds. The data presented in Table 1 should be interpreted with some caution. The chemical shifts are generally solvent, concentration and temperature dependent and different authors often quote different data for the same compounds because of the irreproducibility of the conditions. Unless otherwise noted in Table 1, the data are quoted at ambient temperature, under which conditions the compounds are generally undergoing rapid structural rearrangements: such data are therefore a weighted time-average of the various species present.

Despite the inherent limitations of the data, examination of Table 1 reveals several key features. The resonances of the  $\alpha$ -hydrogen and  $\alpha$ -carbon atoms are shifted significantly to lower frequency than those of the corresponding hydrocarbons<sup>8</sup>. The magnitude of the low frequency shift is generally greater in THF than in diethyl ether, in line with the relative strengths of the  $Mg-O(THF)$  and  $Mg-O(Et_2O)$  bonds (see below). Similar, though less marked trends are observed for the  $\beta$ -environments.

The first simultaneous observation by NMR of both  $RMgX$  and  $R_2Mg$  species in solutions of Grignard reagents was made by Ashby and coworkers in 1969<sup>18</sup>. They showed that on cooling a diethyl ether solution of methylmagnesium bromide to *ca*  $-100^\circ C$ , the  $^1H$  NMR spectrum displayed signals due to both  $Me_2Mg$  and  $MeMgBr$ . The relative intensity of the signal due to  $Me_2Mg$  increased significantly on standing at low temperature, concomitant with the precipitation of  $MgBr_2$ , consistent with a gradual shift in the position of the Schlenk equilibrium. This first preliminary report was followed by a detailed NMR study of methylmagnesium compounds in both THF and diethyl ether solutions<sup>5</sup>.

In diethyl ether at *ca*  $-100^\circ C$ ,  $Me_2Mg$  displays three signals in the  $^1H$  NMR spectrum. The signal at  $-1.32$  was assigned to bridging methyl groups of associated species (Scheme 1), while those at  $-1.74$  and  $-1.70$  were assigned to terminal methyl groups of the same associated species and to the methyl groups of solvated monomers, respectively. At the same temperature, the  $^1H$  NMR spectrum of  $MeMgBr$  displays signals at  $-1.55$  ppm, which gradually disappears on standing, and at  $-1.70$  ppm, assigned to  $MeMgBr$  and  $Me_2Mg$ , respectively. Since the  $RMgX$  species are known to be associated in diethyl ether solution, even at quite low concentrations, the observation of just a single ' $RMgX$ ' species in the  $^1H$  NMR spectrum indicates that the associated species are either indistinguishable from each other and/or that there is rapid exchange between them, even at low temperatures. Rapid halide exchange might certainly be expected and, although caution should be exercised when attempting to draw any inferences on the general nature of organomagnesium compounds, it is noteworthy in this context that NMR studies on aryl Grignard compounds (see below) indicate that halide exchange is significantly more rapid than aryl group exchange.

In THF solvent at  $-76^\circ C$ ,  $Me_2Mg$  displays two signals of widely different intensities at  $-1.83$  (major) and  $-1.70$  (minor) ppm, assignable to monomeric  $Me_2Mg(thf)_n$  and to the terminal methyl groups of associated species, respectively. In the corresponding solution of the Grignard compound,  $MeMgBr$ , only signals due to  $Me_2Mg$  are observed, indicating that the Schlenk equilibrium is shifted much further towards  $Me_2Mg$  in THF than in diethyl ether.

On warming the solutions of both  $Me_2Mg$  and  $MeMgBr$ , the signals broaden and then coalesce giving a single, time-averaged signal at ambient temperature. In both cases the dynamic process involves alkyl group exchange. In  $Me_2Mg$ , exchange occurs between terminal and bridging methyl groups as a consequence of the reversible disassociation of associated species, while in the Grignard compound, the dynamic process also involves

TABLE 1.  $^1\text{H}$  and  $^{13}\text{C}$  NMR chemical shift data <sup>a</sup> for selected organomagnesium compounds

Compound	Solvent	$\delta^1\text{H}$	$\delta^{13}\text{C}$	Reference
$\text{Me}_2\text{Mg}$	$\text{Et}_2\text{O}$	-1.46 -1.74 <sup>b,c</sup>		5
	THF	-1.76	-16.9	5
		-1.81 <sup>d</sup>		6
$\text{MeMgCl}$	THF	-1.72		5
		-1.83 <sup>c</sup>		5
$\text{MeMgBr}$	$\text{Et}_2\text{O}$	-1.55 <sup>c</sup>		5
	THF	-1.70	-16.3	5
		-1.85 <sup>c</sup>		6
$\text{MeMgI}$	$\text{Et}_2\text{O}$	-1.53	-14.5	7, 8
$\text{MeMgH}$	THF	-1.80 ( $-\text{CH}_3$ )		9
$\text{Et}_2\text{Mg}$	THF	<i>ca</i> -1.80 ( $-\text{CH}_2-$ )		9
		<i>ca</i> 1.15 ( $-\text{CH}_3$ )		
$\text{EtMgBr}$	$\text{Et}_2\text{O}$		-2.9 ( $-\text{CH}_2-$ )	8
			12.2 ( $-\text{CH}_3$ )	
$\text{EtMgH}$	THF	-1.79 ( $-\text{CH}_2-$ )		9
		1.15 ( $-\text{CH}_3$ )		
<i>n</i> -PrMgBr	$\text{Et}_2\text{O}$		11.3 ( $\text{MgCH}_2-$ )	8
			22.1 ( $-\text{CH}_2\text{CH}_3$ )	
			22.1 ( $-\text{CH}_3$ )	
<i>i</i> -Pr <sub>2</sub> Mg	THF	-0.75 ( $-\text{CH}-$ )	9.6 ( $-\text{CH}-$ )	10, 11
		1.13 ( $-\text{CH}_3$ )	26.3 ( $-\text{CH}_3$ )	
<i>i</i> -PrMgCl	THF	-0.44 ( $-\text{CH}-$ )	9.6 ( $-\text{CH}-$ )	11
		1.20 ( $-\text{CH}_3$ )	26.3 ( $-\text{CH}_3$ )	
<i>i</i> -PrMgBr			8.9 ( $-\text{CH}-$ )	8
			22.9 ( $-\text{CH}_3$ )	
<i>n</i> -BuMgBr	$\text{Et}_2\text{O}$		5.9 ( $\text{MgCH}_2-$ )	8
			31.6 ( $\text{MgCH}_2\text{CH}_2-$ )	
			30.6 ( $-\text{CH}_2\text{CH}_3$ )	
			13.2 ( $-\text{CH}_3$ )	
$(t\text{-BuCH}_2)_2\text{Mg}$	benzene	0.4 ( $-\text{CH}_3$ )		12
		1.3 ( $-\text{CH}_2-$ )		
<i>n</i> -BuCH(Cl)MgPr- <i>i</i>	THF <sup>e</sup>		68.8 ( $-\text{CHCl}-$ )	10
$[n\text{-BuCH(Cl)}]_2\text{Mg}$	THF <sup>e</sup>		69.4, 69.6 ( $-\text{CHCl}-$ )	10
$\text{EtCH(Me)CH}_2\text{MgBr}$	$\text{Et}_2\text{O}$	0.17 ( $\text{Mg}-\text{CH}_2-$ )		13
$[\text{EtCH(Me)CH}_2]_2\text{Mg}$	$\text{Et}_2\text{O}$	0.23 ( $\text{Mg}-\text{CH}_2-$ )		13
	THF	0.17 ( $\text{Mg}-\text{CH}_2-$ )		
$(\text{PhCH}_2)_2\text{Mg}$	$\text{Et}_2\text{O}$		21.9 ( $-\text{CH}_2-$ )	8
			115.9 ( <i>para</i> -C)	
			123.2 ( <i>ortho</i> -C)	

(continued overleaf)

TABLE 1. (continued)

Compound	Solvent	$\delta^1\text{H}$	$\delta^{13}\text{C}$	Reference
PhCH <sub>2</sub> MgCl	Et <sub>2</sub> O		127.4 ( <i>meta</i> -C)	8
			155.2 ( <i>ipso</i> -C)	
			22.2 (-CH <sub>2</sub> -)	
			116.1 ( <i>para</i> -C)	
			123.4 ( <i>ortho</i> -C)	
			127.3 ( <i>meta</i> -C)	
PhCH <sub>2</sub> CH(Br)MgPr- <i>i</i>	THF <sup><i>e</i></sup>		155.1 ( <i>ipso</i> -C)	10
			63.7 (-CHBr-)	
[PhCH <sub>2</sub> CH(Br)] <sub>2</sub> Mg	THF <sup><i>e</i></sup>		145.6 ( <i>ipso</i> -C)	10
			66.7, 67.0 (-CHBr-)	
PhCH <sub>2</sub> CH(I) MgPr- <i>i</i>	THF <sup><i>e</i></sup>		145.8, 146.2 ( <i>ipso</i> -C)	10
			9.0 (-CHMe <sub>2</sub> )	
			26.5, 26.6 (-CH <sub>3</sub> )	
			41.4 (-CHI-)	
			48.3 (PhCH <sub>2</sub> -)	
			146.3 ( <i>ipso</i> -C)	
[PhCH <sub>2</sub> CH(I)] <sub>2</sub> Mg	THF <sup><i>e</i></sup>		44.1, 46.7 (-CHI-)	10
			46.9, 47.3 (PhCH <sub>2</sub> -)	
			145.8, 146.2 ( <i>ipso</i> -C)	
Cp <sub>2</sub> Mg	toluene	<i>ca</i> 5.75	103.8 107.7	14, 15
CpMgMe	THF	2.11 (CH <sub>3</sub> ) 5.09 (Cp- <i>H</i> )		7
CpMgCl	THF	<i>ca</i> 6.02		14
(1-MeC <sub>5</sub> H <sub>4</sub> )MgCl	THF		11.1 (-CH <sub>3</sub> ) 101.6 (Cp-C) 104.1 (Cp-C) 116.1 (Cp-C)	14
(1,3-Me <sub>2</sub> C <sub>5</sub> H <sub>3</sub> )MgCl	THF		11.2 (-CH <sub>3</sub> ) 101.4 (Cp-C) 105.2 (Cp-C) 114.4 (Cp-C)	14
CpMgBr	THF		105.7	15
(MeSCH <sub>2</sub> ) <sub>2</sub> Mg	THF	0.66 (-CH <sub>2</sub> -)	12.9 (-CH <sub>2</sub> -)	16
(PhSCH <sub>2</sub> ) <sub>2</sub> Mg	THF	0.86 (-CH <sub>2</sub> -)	4.9 (-CH <sub>2</sub> -)	16
LMg <sup>13</sup> CH <sub>3</sub> <sup><i>f</i></sup>	benzene	-0.05 ( <sup>1</sup> <i>J</i> <sub>CH</sub> = 108Hz)		17
LMgC≡CPh <sup><i>f</i></sup>	benzene	7.78 ( <i>ortho</i> ) 7.15 ( <i>meta</i> ) 7.03 ( <i>para</i> )	113.6 (Mg-CC) <sup><i>g</i></sup> 121.8 (Mg-CC) <sup><i>g</i></sup> 126.2 ( <i>para</i> -C) 128.3 ( <i>ortho</i> -C) 128.6 ( <i>ipso</i> -C) 131.9 ( <i>meta</i> -C)	17

TABLE 1. (continued)

Compound	Solvent	$\delta^1\text{H}$	$\delta^{13}\text{C}$	Reference
$\text{LMgC}\equiv\text{CSi}(\text{Me})_3^f$	benzene	0.40 (Si- $\text{CH}_3$ )	1.35 (Si- $\text{CH}_3$ ) 120.0 (Mg-CC) <sup>g</sup> 146.7 (Mg-CC) <sup>g</sup>	17

<sup>a</sup> Data quoted in ppm relative to TMS. Spectra recorded at ambient temperature unless otherwise stated.

<sup>b</sup> Monomer (see text).

<sup>c</sup> Spectrum acquired at  $-100^\circ\text{C}$ .

<sup>d</sup> Spectrum acquired at  $-60^\circ\text{C}$ .

<sup>e</sup> Spectrum acquired at  $-78^\circ\text{C}$ .

<sup>f</sup> Ligand abbreviation: L =  $\eta^3$ -tris(3-*tert*-butylpyrazolyl)borate.

<sup>g</sup> Assignment may be reversed.

exchange between  $\text{MeMgBr}$  and  $\text{Me}_2\text{Mg}$ , i.e. the Schlenk equilibrium (Scheme 2). The rate of alkyl group exchange depends primarily on the nature of the organic group and the solvent.

Dynamic NMR studies have been used to probe organic group exchange in diorganomagnesium compounds<sup>7</sup>. Generally, rates of exchange are enhanced when the organic group is a good bridging ligand and reduced when bulky groups are present. The effect of the size of the alkyl group is particularly evident in  $\text{PhCH}_2\text{CH}(\text{I})\text{MgPr}$ , which shows no tendency to disproportionate into  $(\text{PhCH}_2\text{CHI})_2\text{Mg}$  and  $(i\text{-Pr})_2\text{Mg}$  even in THF<sup>10</sup>. The exchange of the organic groups that takes place on mixing bis(3,3-dimethylbutyl)magnesium with bis(cyclopentadienyl)magnesium occurs with retention of configuration at the  $\alpha$ -carbon atoms of bis(3,3-dimethylbutyl)magnesium: the rate of exchange is greater than the rate of inversion by a factor of  $10^4$ – $10^5$ <sup>7</sup>. Such observations are consistent with a concerted exchange mechanism, with an alkyl-bridged intermediate (Figure 1). This mechanism is supported by the fact that rates of exchange are retarded in the presence of strongly co-ordinating solvents or chelating ligands, such as  $N,N,N',N'$ -tetramethylethylenediamine: binding of the donor groups inhibits association of the magnesium species.

In Grignard compounds, the halide exerts a secondary effect on the rate of alkyl group transfer. The rates are in the order  $\text{RMgCl} > \text{RMgBr} > \text{RMgI}$ , in accord with the relative ease of formation of halide bridges<sup>19</sup>, suggesting that a mixed alkyl/halide bridged intermediate is involved in the exchange process.

Exchange between Mg-alkyl groups and the alkyl group of alkyl halides has also been long-suspected. The first direct evidence of such an exchange was demonstrated by  $^1\text{H}$  NMR spectroscopy using  $^{13}\text{C}$ -labelled methyl iodide. Han and Parkin<sup>17</sup> observed the appearance of a doublet at  $-0.05$  ppm ( $^1J_{\text{CH}} = 108$  Hz) due to the  $\text{Mg}-^{13}\text{CH}_3$  group of  $\{\eta^3\text{-HB}(3\text{-}i\text{-Bupz})_3\}\text{Mg}^{13}\text{CH}_3$  (3-*tert*-Bupz = 3-*tert*-butylpyrazolyl) on mixing  $\{\eta^3\text{-HB}(3\text{-}i\text{-Bupz})_3\}\text{MgCH}_3$  and  $^{13}\text{CH}_3\text{I}$ . Alkyl group exchange was also observed on mixing  $\{\eta^3\text{-HB}(3\text{-}i\text{-Bupz})_3\}\text{MgCH}_2\text{CH}_3$  with methyl iodide. Although no alkyl exchange was observed directly on mixing  $n\text{-BuMgBr}$  and  $t\text{-BuBr}$ , the NMR spectra of the reaction

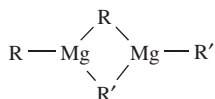


FIGURE 1. Proposed intermediate in alkyl group exchange. Co-ordinated solvent molecules are omitted for clarity

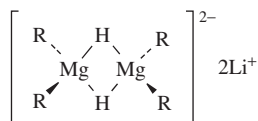


FIGURE 2. Proposed *ate* structure of the  $\text{LiMgR}_2\text{H}$  compounds

mixture showed radical enhancement of signals assignable to isobutylene<sup>20</sup>, formed from the disproportionation of *tert*-butyl radicals. The *tert*-butyl radicals are presumably formed as the result of a one-electron transfer from Mg, suggesting alkyl group exchange does indeed occur.

Reaction of  $\text{R}_2\text{Mg}$  ( $\text{R} = \text{Me}, \text{Et}, i\text{-Pr}, \text{Bu}$ ) with activated  $\text{MgH}_2$  yields the corresponding alkylmagnesium hydrides,  $\text{RMgH}$ , which display  $^1\text{H}$  NMR spectra very similar to those of the dialkylmagnesium starting materials. Although no  $\text{Mg-H}$  signals are observed in the NMR,  $\text{Mg-H}$  stretching bands are observed in the IR spectra, clearly indicating the formation of the hydrides<sup>9,21</sup>. Compounds of empirical formula  $\text{LiMgR}_2\text{H}$  are obtained on addition of  $\text{RLi}$  to the alkylmagnesium hydrides, but their ambient-temperature  $^1\text{H}$  NMR spectra in THF solution are indistinguishable from those of the alkylmagnesium hydrides from which they are derived and, importantly, their spectra are temperature independent. Taken together with molecular weight measurements, which suggest them to be strictly dimeric over a wide concentration range, the NMR data have been interpreted in terms of the hydrogen-bridged *ate* species shown in Figure 2<sup>9</sup>.

The configurational stability of the metal-bonded carbon atom in organomagnesium compounds is of significant interest in terms of both our understanding of the structure and reactivity of such compounds, and more generally in gaining insights on the nature of the bonding of organic moieties to metals. If the  $\beta$ -carbon atom of the organic moiety is asymmetric or possesses a bulky substituent, the equivalence (chemical or magnetic) of the  $\alpha$ -hydrogen atoms is broken and the NMR spectra become sensitive to the configuration at the  $\alpha$ -carbon atom<sup>13, 22–25</sup>.

Both the  $\alpha$ -hydrogen atoms of 3,3-dimethylbutylmagnesium chloride and bis(3,3-dimethylbutyl)magnesium, for example<sup>23</sup>, give rise to an  $\text{AA}'$  sub-spectrum of an  $\text{AA}'\text{BB}'$  spin system at *ca*  $-55^\circ\text{C}$  in diethyl ether solution. On warming, the signals collapse to an  $\text{A}_2$  sub-spectrum of an  $\text{A}_2\text{B}_2$  spin system. In these particular compounds the rate of inversion is much higher in the Grignard species, which reaches the fast exchange limit just above ambient temperature, than in the diorganomagnesium compound, which reaches the fast exchange regime only above  $100^\circ\text{C}$ . This large difference in rate is not consistently observed, and in other organomagnesium compounds the rates of inversion are similar in the  $\text{RMgX}$  and  $\text{R}_2\text{Mg}$  species<sup>13</sup>. Rates of inversion also appear to vary for the same species, depending on the method of preparation, the solvent and concentration. This variation presumably reflects changes in the exact composition of the solution under investigation, and frustrates attempts to draw any general conclusions, for example on the mechanism of inversion, from the data.

## B. Aryl Compounds

As with the alkyl Grignard compounds, most aryl Grignards display only a single set of NMR resonances due to the organic group at ambient temperature but, on cooling, signals assignable to  $\text{RMgX}$  and  $\text{R}_2\text{Mg}$  become apparent as aryl group exchange becomes slow on the NMR time-scale. Appreciable chemical shift differences are observed between the *ortho*-group  $^1\text{H}$  NMR signals of the aryl Grignards and their corresponding diarylmagnesium compounds, enabling them to be distinguished unambiguously<sup>19</sup>. At  $-65^\circ\text{C}$  in THF

TABLE 2.  $^{19}\text{F}$  chemical shift data<sup>a</sup> for the *p*-F in fluoroaryl-magnesium compounds

Compound	$\delta^{19}\text{F}$
$(\text{C}_6\text{F}_5)_2\text{Mg}$	97.8 95.5 <sup>b</sup>
$\text{C}_6\text{F}_5\text{MgBr}$	97.97 <sup>c</sup> , 98.12 <sup>c</sup> 95.64 <sup>c,d</sup> , 96.313 <sup>c,d</sup>
$\text{C}_6\text{F}_5\text{MgI}$	95.30 <sup>c,e</sup> , 95.95 <sup>c,e</sup>
$\text{C}_6\text{F}_5\text{MgCl}$	96.33 <sup>c,f</sup> , 96.97 <sup>c,f</sup>
$(p\text{-FC}_6\text{H}_4)_2\text{Mg}$	56.42 <sup>d</sup>
$p\text{-FC}_6\text{H}_4\text{MgBr}$	57.78 55.77 <sup>c,d</sup>
$p\text{-FC}_6\text{H}_4\text{MgI}$	55.62 <sup>c,f</sup>

<sup>a</sup> Chemical shifts reported relative to benzotrifluoride in THF solvent at ambient temperature, unless otherwise stated. Data from Reference 26.

<sup>b</sup> In  $\text{Et}_2\text{O}$ .

<sup>c</sup> Shifts are concentration dependent. Data quoted at a concentration of *ca* 1.0 mol dm<sup>-3</sup>.

<sup>d</sup> Shifts are concentration dependent. Data quoted at a concentration of *ca* 0.8 mol dm<sup>-3</sup>.

<sup>e</sup> Shifts are concentration dependent. Data quoted at a concentration of *ca* 0.7 mol dm<sup>-3</sup>.

<sup>f</sup> In toluene.

[3,5- $^2\text{H}_2$ ]-phenylmagnesium bromide, for example, displays two sets of *ortho*-hydrogen doublets of unequal intensity due to  $\text{ArMgBr}$  and  $\text{Ar}_2\text{Mg}$ . The chemical shift difference between the signals of the two species is *ca* 0.13 ppm, which compares with shift differences of <0.05 ppm between the alkyl signals in the corresponding alkylmagnesium compounds (Table 1).

The  $^{19}\text{F}$  NMR spectra of fluoroarylmagnesium compounds have been studied in some detail<sup>26</sup>. The wider chemical shift range of  $^{19}\text{F}$ , compared to that of  $^1\text{H}$ , allows the various possible solution-state species to be distinguished readily. The *para*-fluorine resonances were found to be most sensitive to the chemical structure: *p*-F  $^{19}\text{F}$  NMR data for selected fluoroarylmagnesium compounds are given in Table 2.

The presence of fluorine atoms on the phenyl ring reduces the rate of aryl group exchange and two sets of signals, due to  $\text{ArMgX}$  and  $\text{Ar}_2\text{Mg}$  species, are observed at ambient temperature in these compounds. However, these signals do undergo reversible broadening and coalesce at higher temperature giving a single, time-averaged signal. The same factors that govern the alkyl group exchange in alkylmagnesium compounds similarly govern rates of aryl group exchange, and an analogous (aryl-bridged) intermediate to that depicted in Figure 1 is presumed to be involved.

Despite the much greater range of chemical shifts and the slower rates of aryl group exchange (see below) only one set of signals assignable to 'ArMgX' species is observed in the  $^{19}\text{F}$  NMR spectra of the Grignard compounds in diethyl ether, indicating a rapid equilibrium between associated species. The  $^{19}\text{F}$  NMR spectrum of a mixture of  $\text{C}_6\text{F}_5\text{MgBr}$  and  $\text{C}_6\text{F}_5\text{MgI}$  at ambient temperature gives a single set of fluorine resonances at intermediate positions between those of the individual species. Since aryl group exchange is clearly slow at ambient temperature in these compounds, the observation of a single species is clearly indicative of rapid halide exchange.

In contrast to  $\text{LiMgMe}_3$ , which appears to dissociate to a mixture of  $\text{MeLi}$  and  $\text{Me}_2\text{Mg}$  in solution, NMR evidence suggests  $\text{LiMgPh}_3$  remains intact<sup>9</sup>. The chemical shift difference between the centres of the *ortho* and *meta/para* multiplets (the latter being unresolved

from each other) is 0.99 and 0.68 ppm for PhLi and Ph<sub>2</sub>Mg, respectively, but is found to be 0.73 ppm in LiMgPh<sub>3</sub>. That the chemical shift difference in LiMgPh<sub>3</sub> is not the weighted average of that found in PhLi and Ph<sub>2</sub>Mg discounts the possibility that LiMgPh<sub>3</sub> exists as a dynamic equilibrium mixture of PhLi and Ph<sub>2</sub>Mg, and rather points towards a discrete species.

### C. The Schlenk Equilibrium

Determining the position of the Schlenk equilibrium is clearly of key importance in understanding the reactivity of Grignard compounds and, provided the exchange rate can be slowed sufficiently, NMR can be used to determine populations of the various species present and the rates of exchange between them. Most data on the Schlenk equilibrium have been obtained in diethyl ether or THF, as Grignard reactions are generally performed in these solvents. Although the degree of aggregation of species is concentration dependent, particularly in diethyl ether, NMR spectra are usually analysed assuming only a basic Schlenk equilibrium (Scheme 2). The approximate equilibrium constants for selected Grignard compounds, determined by integration of their *static* NMR signals, are given in Table 3.

Since diorganomagnesium species are stronger Lewis acids than the corresponding Grignards, the Schlenk equilibrium generally lies further towards R<sub>2</sub>Mg in stronger basic media. Thus diorganomagnesium species are generally more favoured in THF solution

TABLE 3. Schlenk equilibrium constants (*K*) for selected Grignard compounds

Compound <sup>a</sup>	Solvent	Temperature (°C)	<i>K</i> <sup>b</sup>	Reference
MeMgBr	THF	−85	1.1	19
MeMgBr(thf)	THF	−80	<i>ca</i> 0.1–0.2	6
MeMgBr(diglyme)	THF	−80	<i>ca</i> 0.1–0.2	6
MeMgBr(NEt <sub>3</sub> )	THF	−80	<i>ca</i> 0.1–0.2	6
MeMgBr(tmeda)	THF	−80	<i>ca</i> 4	6
EtMgBr	THF	−60	<i>ca</i> 0.5	19
[3,5- <sup>2</sup> H <sub>2</sub> ]C <sub>6</sub> H <sub>3</sub> MgBr	THF	−80	0.3	19
<i>t</i> -BuMgCl	THF (0.6 mol dm <sup>−3</sup> )	33	1.12	5
2-MeC <sub>6</sub> H <sub>4</sub> MgBr	THF	−50	2.3	19
( <i>t</i> -Bu-allyl)MgCl	THF		<i>ca</i> 50	27
(1,3-Me <sub>2</sub> -allyl)MgCl	THF		<i>ca</i> 50	27
2-EtC <sub>6</sub> H <sub>4</sub> MgBr	THF	−40	4.0	19
2,6-Me <sub>2</sub> C <sub>6</sub> H <sub>3</sub> MgBr	THF	−60	7.8	19
	Et <sub>2</sub> O (0.3 mol dm <sup>−3</sup> )	−60	>400	19
2,6-Me <sub>2</sub> C <sub>6</sub> H <sub>3</sub> MgCl	THF	−30	30.3	19
2,4,6-Me <sub>3</sub> C <sub>6</sub> H <sub>2</sub> MgBr	THF	−40	12.3	19
2-CF <sub>3</sub> C <sub>6</sub> H <sub>4</sub> MgBr	THF	−60	15.2	19
	Et <sub>2</sub> O	−50	324	19
C <sub>6</sub> F <sub>5</sub> MgCl	Et <sub>2</sub> O (0.7 mol dm <sup>−3</sup> )	22	16.0	19
C <sub>6</sub> F <sub>5</sub> MgBr	THF	22	2.0	19
	Et <sub>2</sub> O (0.1–1.0 mol dm <sup>−3</sup> )	−55	4.0	19
C <sub>6</sub> F <sub>5</sub> MgI	Et <sub>2</sub> O (0.85 mol dm <sup>−3</sup> )	22	7.8	19
4-FC <sub>6</sub> H <sub>4</sub> MgBr	Et <sub>2</sub> O	−75	>1600	19
4-FC <sub>6</sub> H <sub>4</sub> MgI	Et <sub>2</sub> O	−75	>1600	19
CpMgCl	THF (0.09 mol dm <sup>−3</sup> )	−75	54	14
CpMgBr	THF (0.20 mol dm <sup>−3</sup> )	−75	74	14

<sup>a</sup> Ligand abbreviations: diglyme = bis(2-methoxyethyl)ether; tmeda = tetramethylethylenediamine.

<sup>b</sup> The equilibrium constants given are for the formation of the Grignard species, i.e. R<sub>2</sub>Mg + MgX<sub>2</sub> ⇌ 2RMgX.



than in Et<sub>2</sub>O, irrespective of the nature of the R group or the halogen. Bulky organic groups, however, can restrict solvent co-ordination more in R<sub>2</sub>Mg than in RMgX, thereby favouring RMgX.

Given the effect of the relative solvent basicity on the position of the Schlenk equilibrium, the affinity of particular solvents towards Mg is of importance, and has been investigated by NMR<sup>28</sup>. The chemical shifts of the organic moiety, particularly those on the  $\alpha$ -carbon, have been shown to correlate with the co-ordinating ability of the solvent. Thus in more strongly basic solvents the NMR signals are generally shifted to lower frequency, consistent with a greater degree of charge separation between the Mg and  $\alpha$ -carbon as a result of stronger Mg-solvent interactions. Based on <sup>1</sup>H NMR studies of EtMgBr and Et<sub>2</sub>Mg, the preference for solvent co-ordination is in the order DME > THF > Et<sub>2</sub>O > *n*-Bu<sub>2</sub>O > Et<sub>3</sub>N > *i*-Pr<sub>2</sub>O. This trend is governed by both steric and electronic factors.

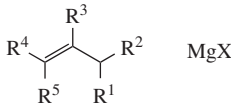
The number of co-ordinated solvent molecules is also of considerable interest. The magnesium atom has been shown typically to display co-ordination numbers of four or five in the solid state (see below) in organomagnesium compounds, depending on the nature of the magnesium moiety (i.e. organic group and/or halide atoms) and the donor groups. Although the situation is less clear in solution, the magnesium atom is probably co-ordinated by at least two or three solvent molecules. In many instances, the co-ordinated solvent molecules will be in rapid exchange with those in the bulk solution.

#### IV. ALLYLIC AND VINYLIC COMPOUNDS

The question of the solution structure of allylmagnesium compounds is an intriguing one and such compounds have been studied in more detail by NMR than any other organomagnesium species. <sup>1</sup>H and <sup>13</sup>C NMR data for selected allylmagnesium compounds are given in Tables 4 and 5, respectively.

Asymmetrically substituted allyl magnesium compounds often react to yield products derived from both the parent allyl halide and the corresponding allylic isomer, in varying relative yields<sup>33,34</sup>. Depending on the arrangement of the substituents, *cis* and *trans*

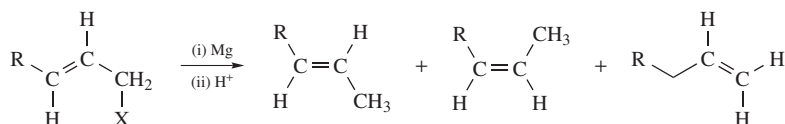
TABLE 4. <sup>1</sup>H NMR data<sup>a</sup> for allylmagnesium Grignards in Et<sub>2</sub>O at ambient temperature

<div style="text-align: center;">  </div>											
X	R <sup>1</sup>	R <sup>2</sup>	R <sup>3</sup>	R <sup>4</sup>	R <sup>5</sup>	R <sup>1</sup>	R <sup>2</sup>	R <sup>3</sup>	R <sup>4</sup>	R <sup>5</sup>	Reference
Cl	H	H	H	H	H	2.50	2.50	6.38	2.50	2.50	27
Cl	H	H	H	H	Me	ca 0.8	ca 0.8	ca 5.9	ca 4.5	ca 1.5	27
Cl	H	H	H	H	Et	0.79	0.79	5.94	4.56	2.09 (−CH <sub>2</sub> −) 0.97 (−CH <sub>3</sub> )	27
Cl	H	H	H	H	<i>i</i> -Pr	0.78	0.78	5.91	4.57	2.26 (−CH−) 0.96 (−CH <sub>3</sub> )	27
Cl	H	H	H	H	<i>t</i> -Bu	0.71	0.71	5.95	4.73	0.98	27
Cl	H	H	H	Me	Me	0.57	0.57	5.58	1.55	1.55	27
Cl	Me	H	H	H	Me	1.76	2.82	6.20	2.82	1.76	27
Br	H	H	H	H	H	2.69	2.69	6.54	2.69	2.69	29
Br	H	H	Me	H	H	2.41	2.41	1.76	2.41	2.41	29

<sup>a</sup> Chemical shifts reported in ppm relative to TMS.

TABLE 5.  $^{13}\text{C}$  NMR chemical shift data<sup>a</sup> for allylmagnesium compounds

$  \begin{array}{c}  \text{R}^2 \\    \\  \text{R}^3 - \text{C}^2 = \text{C}^1 - \text{H} \\    \quad   \\  \text{R}^4 \quad \text{R}^1  \end{array}  \quad \text{MgX}  $												Reference
X	R <sup>1</sup>	R <sup>2</sup>	R <sup>3</sup>	R <sup>4</sup>	C <sup>1</sup>	C <sup>2</sup>	C <sup>3</sup>	R <sup>1</sup>	R <sup>2</sup>	R <sup>3</sup>	R <sup>4</sup>	
Cl	H	H	H	H	57.8	149.8	57.8					29
Cl	H	Me	H	H	26.7 <sup>b</sup>	156.8 <sup>b</sup>	57.8 <sup>b</sup>					30
Cl	Me	H	Me	H	62.8	147.6	62.8	18.15		18.15		29
Br	H	H	H	H	57.5	149.5	57.5					31
Br	H	H	H	H	58.0	149.5	56.5					31
					57.3	137.3	57.3					32
Br	H	H	Me	H	<sup>c</sup>	141	102			15		31
					17.6 <sup>b</sup>	141.5 <sup>b</sup>	97.2 <sup>b</sup>			12.5 <sup>b</sup>		30
Br	H	Me	H	H	59.5	156.9	59.5		27.2			29
Br	H	H	Me	Me	ca 22	150	ca 92			<sup>c</sup>	<sup>c</sup>	31
					25.4 <sup>b,d</sup>	131.8 <sup>b,d</sup>	108.4 <sup>b,d</sup>			16.7 <sup>b,d,e</sup>	16.4 <sup>b,d,e</sup>	30
allyl	H	H	H	H	57.2	149.4	57.2					29
					57.9 <sup>d</sup>	148.7 <sup>d</sup>	57.9 <sup>d</sup>					29

<sup>a</sup> Chemical shifts reported in ppm relative to TMS. Spectra acquired at ambient temperature in THF except<sup>b</sup> and<sup>d</sup>.<sup>b</sup> Spectra recorded at  $-78^\circ\text{C}$ .<sup>c</sup> Not observed because of dynamic line broadening.<sup>d</sup> In  $\text{Et}_2\text{O}$ .<sup>e</sup> Assignment of R<sup>3</sup> and R<sup>4</sup> is arbitrary.

SCHEME 4. Possible stereochemistries of products from reactions proceeding via substituted allyl Grignard intermediates

isomers may also be observed (Scheme 4). Thus, besides the question of the position of the Schlenk equilibrium and the degree of aggregation, it is necessary to account for the observed patterns in reactivity.

The  $^1\text{H}$  NMR spectra of allylmagnesium compounds display simple  $\text{AX}_4$  patterns at temperatures as low as  $-80$  to  $-120^\circ\text{C}$ <sup>35,36</sup>. Such simple spectra can be interpreted in terms of either rapidly interconverting  $\sigma$ -bonded allylmagnesium species or an essentially ionic species, with rapid rotation about the C—C partial double bonds.

It is possible to distinguish indirectly between rapidly interconverting  $\sigma$ -bonded allylic and ionic species using the isotopic perturbation technique<sup>31</sup>. If allylmagnesium compounds exist as a pair of allylic isomers then, in the corresponding  $[1\text{-}^2\text{H}]$ allylmagnesium species (Figure 3), the concentration of **a** will be greater than that of **b**, irrespective of any exchange, because of the lower zero-point energy. Thus in the fast exchange regime, the average shift of C(1) will be moved towards that of the static shift of C(1) in isomer **a**, i.e. the exchange-averaged signal of C(1) will be shifted to higher frequency in the deuterium labelled analogue. Although the signal due to C(1) would also be expected to be shifted if the compounds existed as ionic species, any shift would be quite small. The

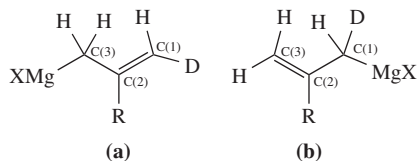


FIGURE 3. The two allylic isomers of  $[1\text{-}^2\text{H}]$ allylmagnesium compounds. **a** is favoured because of the lower zero-point energy

TABLE 6. Eyring activation parameters<sup>a</sup> for allylic exchange in allyl Grignards

Compound	$\Delta H^\ddagger$ (kcal mol <sup>-1</sup> )	$\Delta S^\ddagger$ (cal mol <sup>-1</sup> K <sup>-1</sup> )	$\Delta G^\ddagger$ (298K) (kcal mol <sup>-1</sup> )
C <sub>3</sub> H <sub>5</sub> MgCl	5.5 (0.3)	-6.0 (1.3)	7.29
C <sub>3</sub> H <sub>5</sub> MgBr	5.88 (0.11)	-7.3 (0.5)	8.06
2-MeC <sub>3</sub> H <sub>4</sub> MgBr	9.7 (0.6)	7.0 (2.3)	7.61
1,3-Me <sub>2</sub> C <sub>3</sub> H <sub>3</sub> MgCl <sup>b</sup>	6.6 (0.4)	-4.7 (1.3)	8.00

<sup>a</sup> Data from Reference 29. Obtained by <sup>13</sup>C NMR in Et<sub>2</sub>O except for the last entry. Standard deviations are given in parentheses.

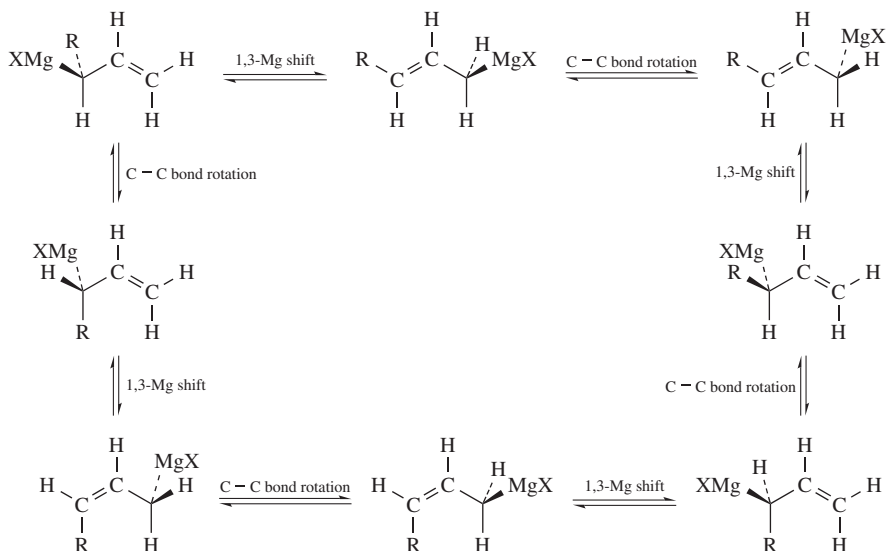
<sup>b</sup> In THF solvent.

actual change in the shift of C(1) in allylmagnesium bromide observed on deuteration is *ca* 1.4–1.9 ppm in both diethyl ether and tetrahydrofuran solution, consistent with a dynamic equilibrium between the allylic isomers.

The advent of higher field NMR instruments, together with the larger chemical shift range of <sup>13</sup>C, has subsequently enabled the direct observation of  $\sigma$ -bonded allylic isomers<sup>29,32</sup>, allowing an estimation of the activation barrier to allylic exchange to be obtained<sup>29</sup> in allyl Grignards: activation parameters are given in Table 6. In contrast to the Grignard compounds, the <sup>13</sup>C spectra of bis(allyl)magnesium remain essentially temperature independent down to at least -95 °C, indicating that either (i) the barrier is significantly lower or (ii) a more ionic-type structure is preferred. Conversely, the barrier to the allyl rearrangement is significantly higher in (cyclopentadienyl)(2-methylallyl)magnesium and, at moderately low temperatures, their NMR spectra clearly show the allyl ligand to be  $\sigma$ -bonded<sup>37</sup>. <sup>25</sup>Mg NMR data (see below) are also in accord with  $\sigma$ -bonded species.

The dynamic equilibrium between allylic isomers accounts for the observation of *cis* and *trans* product isomers in reactions of substituted allylmagnesium compounds. Rapid rotation about the C–C single bonds in each allylic isomer gives rise to both *cis* and *trans* magnesium species (Scheme 5) that can go on to yield *cis* and/or *trans* products. This rapid rotation is clearly evidenced in the <sup>1</sup>H NMR spectra by the equivalence of the methylene hydrogens, i.e. both isomer interconversion and rapid C–C is necessary to account for the observation of an AX<sub>4</sub> spin pattern in the fast exchange regime. The exact constitution of the product mixture resulting from reaction of allylmagnesium compounds thus depends on the equilibrium populations of the various species and the relative kinetics for the reaction of each isomer. It is therefore difficult to make any generalizations regarding the likely composition of products. However, it is noteworthy that, in the absence of steric hindrance, allylmagnesium reagents have been shown to favour the *cis* configuration, while in the presence of bulky substituents this gives way to a *trans* preference<sup>27</sup>.

The <sup>3</sup>J<sub>HH</sub> spin coupling constants (Table 7) also provide valuable insight into the structure of allylmagnesium compounds<sup>27</sup>. Assuming the Karplus relationship holds, the magnitude of the coupling between the unique hydrogen, H<sup>2</sup>, and the two equivalent



SCHEME 5. Dynamic equilibria in allylmagnesium compounds

TABLE 7. <sup>n</sup> J<sub>HH</sub> coupling constants<sup>a</sup> for allylmagnesium chlorides

$  \begin{array}{c}  \text{H}^2 \\    \\  \text{R}^2 - \text{C} = \text{C} - \text{CH} - \text{H}^1 \\    \quad   \\  \text{R}^3 \quad \text{R}^1  \end{array}  \quad \text{MgCl}  $							
R <sup>1</sup>	R <sup>2</sup>	R <sup>3</sup>	J <sub>H(1)H(2)</sub> <sup>b</sup>	J <sub>H(1)R(2)</sub> <sup>c</sup>	J <sub>H(2)R(2)</sub>	J <sub>H(2)R(3)</sub>	J <sub>R(2)R(3)</sub>
H	H	Me	9.6	1.2	11.7	1.5	6.4
H	H	Et	9.5	1.5	12.4	1.25	6.5
H	H	<i>i</i> -Pr	9.4	1.3	13.6	1.1	7.3(CH)
H	H	<i>t</i> -Bu	9.1	1.3	15.1		
Me	H	Me	11.0		11.0	ca 0.8	7.0

<sup>a</sup> Data from Reference 29. Recorded at 32 °C in Et<sub>2</sub>O solvent.<sup>b</sup> Where R<sup>1</sup> = H, J<sub>R(1)H(2)</sub> = J<sub>H(1)H(2)</sub>.<sup>c</sup> Where R<sup>1</sup> = H, J<sub>R(1)R(2)</sub> = J<sub>H(1)R(2)</sub>.

allylic (–CH<sub>2</sub>–) hydrogens suggests the presence of two rapidly exchanging, energetically equivalent conformers with dihedral angles of approximately 30° (Figure 4). Thus the <sup>3</sup>J<sub>HH</sub> couplings are consistent with the magnesium being σ-bonded to an sp<sup>3</sup>-hybridized carbon atom.

Although the interconversion of the allylic isomers remains rapid at temperatures as low as –80 °C, the Schlenk equilibrium is slowed sufficiently to enable signals due to both the allyl Grignard and bis(allyl)magnesium compounds to be observed at such temperatures in their <sup>1</sup>H NMR spectra. The NMR parameters for the bis(allyl)magnesium compounds are not very different from those of the Grignards, suggesting that they possess essentially

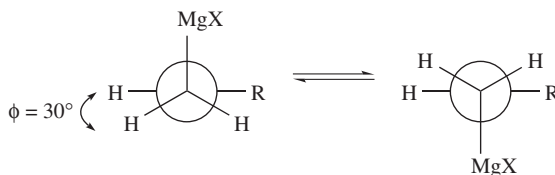


FIGURE 4. The magnitudes of  $^n J_{\text{HH}}$  coupling constants found in allylmagnesium compounds are consistent with the presence of two rapidly interconverting, equivalent conformers with dihedral angles of *ca*  $30^\circ$

the same structural features. Substantial overlap of the signals due to the  $\text{RMgX}$  and  $\text{R}_2\text{Mg}$  species frustrates the evaluation of a good quantitative estimate of the Schlenk equilibrium constant, but a value of *ca* 50 (Table 3) has been estimated for both *tert*-butyllallylmagnesium chloride and 1,3-dimethylallylmagnesium chloride<sup>27</sup>.

Few NMR studies have been carried out on vinylmagnesium compounds. However, NMR has been used to probe the stereospecificity of vinyl Grignard formation, as this has important consequences on product stereochemistry<sup>38,39</sup>. Reaction of *cis*- $\beta$ -bromostyrene with Mg in THF, followed by the addition of  $\text{D}_2\text{O}$  gave a 10:1 *cis:trans* ratio of  $\beta$ -[1- $^2\text{H}$ ]-styrene, indicating the reaction proceeds, essentially, with overall retention of configuration<sup>38</sup>. A similar result is obtained when the Grignard reagent is formed by the magnesium-halogen exchange reaction of *cis*- $\beta$ -bromostyrene with butylmagnesium bromide<sup>39</sup>. Retention of stereochemistry is also generally observed when starting from *trans*- $\beta$ -bromostyrene, although to a significantly lesser extent. The degree of retention is solvent dependent: retention is greater in THF than in  $\text{Et}_2\text{O}$ . The solvent effect has been shown clearly to exert itself in the formation of the Grignard, rather than in the subsequent reaction with  $\text{D}_2\text{O}$ .

## V. ALKOXIDE AND PEROXIDE COMPOUNDS

The solution compositions of a number of methylmagnesium alkoxides have been studied in some detail by Ashby and coworkers using a variety of physicochemical methods, including  $^1\text{H}$  NMR spectroscopy<sup>40</sup>. The NMR spectra displayed broad signals due to the  $\text{Mg}-\text{CH}_3$  groups in the region  $-1$  to  $-2$  ppm (Table 8), which are strongly solvent, concentration and time dependent.

The solvent and concentration dependence of the spectra arises from changes in the degree of molecular association. Time-dependent NMR studies have shown that, in more strongly co-ordinating solvents such as THF,  $\mu^2$ -alkoxide bridged dimers are favoured, but in weakly co-ordinating solvents such as diethyl ether, linear oligomers or  $\mu^3$ -alkoxide bridged cubane-like tetramers (Figure 5) gradually form on standing. The nature of the alkoxide also affects the degree of association: bulky groups hinder association.

Variable temperature NMR studies on 1:1 mixtures of the alkoxides,  $\text{RMgOR}'$ , and  $\text{Me}_2\text{Mg}$  reveals methyl group exchange between the magnesium atoms. Exchange is rapid in the dimeric species, but slow in the tetrameric species, suggesting that there is no convenient mechanism in the latter case. Mixed alkyl/alkoxide bridged dimeric species are thus assumed to be intermediate in the exchange process: in the tetrameric species formation of such dimers first requires dissociation of the *cube*. Although there is no evidence of alkoxide group exchange in these compounds, the  $^{13}\text{C}$  NMR spectrum of  $[\textit{n}\text{-BuMg}(\mu\text{-OAr})_2\{\text{Ar} = 2,6\text{-}(t\text{-Bu})_2\text{C}_6\text{H}_3\}]$  in THF solution displays two distinct

TABLE 8. Selected  $^1\text{H}$  and  $^{13}\text{C}$  NMR data <sup>a</sup> for magnesium alkoxide and aryloxy compounds

Compound <sup>b</sup>	Structure <sup>c</sup>	Solvent	$\delta$ ( $^1\text{H}$ ) (ppm)	$\delta$ ( $^{13}\text{C}$ ) (ppm)	Reference
MeMgO <i>Bu-t</i>	cubane	C <sub>6</sub> D <sub>6</sub>	1.47 [C(CH <sub>3</sub> ) <sub>3</sub> ] −0.66[MgCH <sub>3</sub> ]		40
		Et <sub>2</sub> O	1.55 [C(CH <sub>3</sub> ) <sub>3</sub> ] −1.11[MgCH <sub>3</sub> ]		
		THF	1.55 [C(CH <sub>3</sub> ) <sub>3</sub> ] −1.12[MgCH <sub>3</sub> ]		
	oligomer	Et <sub>2</sub> O	1.2 [C(CH <sub>3</sub> ) <sub>3</sub> ] −1.20[MgCH <sub>3</sub> ] −1.45[MgCH <sub>3</sub> ]		
	dimer	THF	1.20 [C(CH <sub>3</sub> ) <sub>3</sub> ] −1.60[MgCH <sub>3</sub> ]		
MeMgO <i>Pr-i</i>	cubane	C <sub>6</sub> D <sub>6</sub>	1.30 [CH(CH <sub>3</sub> ) <sub>2</sub> ] −0.76[MgCH <sub>3</sub> ]		40
	cubane/ oligomer dimer	Et <sub>2</sub> O	1.44 [CH(CH <sub>3</sub> ) <sub>2</sub> ] −1.30[MgCH <sub>3</sub> ]		
		THF	1.12 [CH(CH <sub>3</sub> ) <sub>2</sub> ] −1.66[MgCH <sub>3</sub> ]		
MeMgO <i>Pr-n</i>	oligomer <sup>d</sup> cubane/ oligomer dimer	C <sub>6</sub> D <sub>6</sub>	−0.82[MgCH <sub>3</sub> ]		40
		Et <sub>2</sub> O	−1.33[MgCH <sub>3</sub> ]		
		THF	−1.70[MgCH <sub>3</sub> ]		
BuMgOAr <sup>1</sup>	dimer	C <sub>6</sub> D <sub>5</sub> CD <sub>3</sub>	−0.10[MgCH <sub>2</sub> −] 1.37 [OArC(CH <sub>3</sub> ) <sub>3</sub> ]	7.06 [MgCH <sub>2</sub> −] 32.80 [OArC(CH <sub>3</sub> ) <sub>3</sub> ] 35.14 [OArC(CH <sub>3</sub> ) <sub>3</sub> ]	41
				8.67 [MgCH <sub>2</sub> −]	
		THF	−1.70[MgCH <sub>2</sub> −] 1.53 [OArC(CH <sub>3</sub> ) <sub>3</sub> ]	31.12 [OArC(CH <sub>3</sub> ) <sub>3</sub> ] 35.64 [OArC(CH <sub>3</sub> ) <sub>3</sub> ]	
Mg(OAr <sup>1</sup> ) <sub>2</sub> (thf) <sub>2</sub>	monomer	C <sub>6</sub> D <sub>5</sub> CD <sub>3</sub>	1.25 [−CH <sub>2</sub> (thf)] 1.55 [OArC(CH <sub>3</sub> ) <sub>3</sub> ] 3.64 [−OCH <sub>2</sub> (thf)]	24.86 [−CH <sub>2</sub> (thf)] 31.88 [OArC(CH <sub>3</sub> ) <sub>3</sub> ] 35.53 [OArC(CH <sub>3</sub> ) <sub>3</sub> ] 70.75 [−OCH <sub>2</sub> (thf)]	41
				26.59 [−CH <sub>2</sub> (thf)]	
				32.24 [OArC(CH <sub>3</sub> ) <sub>3</sub> ] 36.01 [OArC(CH <sub>3</sub> ) <sub>3</sub> ] 68.44 [−OCH <sub>2</sub> (thf)]	
		THF	1.37 [OArC(CH <sub>3</sub> ) <sub>3</sub> ] 1.77 [−CH <sub>2</sub> (thf)] 3.62 [−OCH <sub>2</sub> (thf)]	32.24 [OArC(CH <sub>3</sub> ) <sub>3</sub> ] 36.01 [OArC(CH <sub>3</sub> ) <sub>3</sub> ] 68.44 [−OCH <sub>2</sub> (thf)]	
Mg(OAr <sup>1</sup> ) <sub>2</sub>	dimer	C <sub>6</sub> D <sub>5</sub> CD <sub>3</sub>	1.20 [OArC(CH <sub>3</sub> ) <sub>3</sub> ] 1.58 [OArC(CH <sub>3</sub> ) <sub>3</sub> ]	31.92 [OArC(CH <sub>3</sub> ) <sub>3</sub> ] 34.13 [OArC(CH <sub>3</sub> ) <sub>3</sub> ] 35.07 [OArC(CH <sub>3</sub> ) <sub>3</sub> ] 36.06 [OArC(CH <sub>3</sub> ) <sub>3</sub> ]	41
				32.17 [OArC(CH <sub>3</sub> ) <sub>3</sub> ] 32.22 [OArC(CH <sub>3</sub> ) <sub>3</sub> ] 32.37 [OArC(CH <sub>3</sub> ) <sub>3</sub> ] 35.94 [OArC(CH <sub>3</sub> ) <sub>3</sub> ] 36.00 [OArC(CH <sub>3</sub> ) <sub>3</sub> ]	
		THF	1.37 [OArC(CH <sub>3</sub> ) <sub>3</sub> ] 1.40 [OArC(CH <sub>3</sub> ) <sub>3</sub> ] 1.41 [OArC(CH <sub>3</sub> ) <sub>3</sub> ]		
	dimer	THF	1.19 [ <i>i</i> -Pr−CH <sub>3</sub> ] 6.79 [ <i>meta</i> -H] 6.92 [ <i>para</i> -H]		
HMgOAr <sup>3</sup>	dimer	THF	1.39 [ <i>t</i> -Bu−CH <sub>3</sub> ] 2.12 [Ph−CH <sub>3</sub> ]		42
HMgOCH <sub>2</sub> CH <sub>2</sub> Ph	dimer	THF	1.26 [−CH <sub>2</sub> Ph] 6.92–7.36 [Ph−H]		42

TABLE 8. (continued)

Compound <sup>b</sup>	Structure <sup>c</sup>	Solvent	$\delta$ ( <sup>1</sup> H) (ppm)	$\delta$ ( <sup>13</sup> C) (ppm)	Ref- erence
HMgOCPh <sub>3</sub>	dimer	THF	7.19–7.36 [Ph–H]		42
L <sup>1</sup> MgOEt	monomer	C <sub>6</sub> D <sub>6</sub>	1.72 [–OCH <sub>2</sub> CH <sub>3</sub> ] 4.93 [–OCH <sub>2</sub> CH <sub>3</sub> ]	35.7 [–OCH <sub>2</sub> CH <sub>3</sub> ] 64.2 [–OCH <sub>2</sub> CH <sub>3</sub> ]	17
L <sup>1</sup> MgOPr- <i>i</i>	monomer	C <sub>6</sub> D <sub>6</sub>	1.65 [–OCH(CH <sub>3</sub> ) <sub>2</sub> ] 4.84 [–OCH(CH <sub>3</sub> ) <sub>2</sub> ]	30.2 [–OCH(CH <sub>3</sub> ) <sub>2</sub> ] 64.2 [–OCH(CH <sub>3</sub> ) <sub>2</sub> ]	17
L <sup>1</sup> MgOBu- <i>t</i>	monomer	C <sub>6</sub> D <sub>6</sub>	1.75 [–OC(CH <sub>3</sub> ) <sub>3</sub> ]	35.7 [–OC(CH <sub>3</sub> ) <sub>3</sub> ] 68.1 [–OC(CH <sub>3</sub> ) <sub>3</sub> ]	17
L <sup>1</sup> MgOPh	monomer	C <sub>6</sub> D <sub>6</sub>	6.96 [ <i>para</i> -H] 7.28 [ <i>ortho</i> -H] 7.52 [ <i>meta</i> -H]	114.5 [ <i>para</i> -C] 120.2 [ <i>meta</i> -C] 129.0 [ <i>ortho</i> -C] 163.3 [ <i>ipso</i> -C]	17

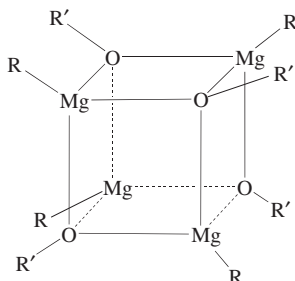
<sup>a</sup> Data acquired at ambient temperature.<sup>b</sup> Ligand abbreviations: OAr<sup>1</sup> = 2,6-di-*tert*-butylphenoxy; OAr<sup>2</sup> = 2,6-diisopropylbenzyl; OAr<sup>3</sup> = 2,6-di-*tert*-butyl-4-methylbenzyl; L<sup>1</sup> =  $\eta^3$ -tris(3-*tert*-butylpyrazolyl)borate.<sup>c</sup> See text.<sup>d</sup> Unsolvated.

FIGURE 5. Cubane structure of the tetrameric compounds RMgOR'. The tetramers are thermodynamically favoured when the alkyl groups are small and the solvent is only weakly co-ordinating

(CH<sub>3</sub>)<sub>3</sub>C–resonances of widely different intensities at 31.1 (major) and 32.24 (minor) ppm, respectively<sup>41</sup>. The latter signal coincides with the (CH<sub>3</sub>)<sub>3</sub>C–resonance of Mg( $\mu$ -OAr)<sub>2</sub>, indicating at least some disproportionation of [*n*-BuMg( $\mu$ -OAr)]<sub>2</sub> and implying slow alkoxide group exchange on the NMR chemical shift time-scale.

Dimeric alkoxy- and aryloxy-magnesium hydrides, HMgOR, are prepared by the reaction of activated MgH<sub>2</sub> with the appropriate Mg(OR)<sub>2</sub> compounds in THF<sup>42</sup>. Their NMR spectra display a single set of signals due to the alkoxide/aryloxy group (Table 8) but, as with the alkylmagnesium hydrides, no Mg–H resonance is observed. An Mg–H stretching band is, however, observed in the IR spectra. The complexes are dimeric and presumed to possess bridging hydrides, rather than bridging alkoxide groups, on steric grounds.

The oxidation of Grignard reagents with dioxygen, yielding alcohols, has long been known. The reaction is presumed to proceed via an alkylperoxide intermediate, ROOMgX. The first magnesium alkylperoxides reported, { $\eta^3$ -HB(3-*t*-Bupz)<sub>3</sub>}MgOOR (R=Me, Et, *i*-Pr, *t*-Bu), were prepared by the insertion of dioxygen into the Mg–C bond in { $\eta^3$ -HB(3-*t*-Bupz)<sub>3</sub>}MgR and characterized by <sup>1</sup>H and <sup>17</sup>O NMR spectra<sup>17</sup>. The <sup>17</sup>O NMR

TABLE 9.  $^{17}\text{O}$  NMR data<sup>a</sup> for magnesium peroxide complexes

Compound <sup>b</sup>	$\delta(\text{MgOOR})$	$\delta(\text{MgOOR})$
LMgOOMe	427	102
LMgOOEt	407	130
LMgOOPr- <i>i</i>	373	159
LMgOOBu- <i>t</i>	323	183

<sup>a</sup> Data from Reference 17. Chemical shifts reported relative to  $\text{H}_2\text{O}$ .

<sup>b</sup> L =  $\eta^3$ -tris(3-*tert*-butylpyrazolyl)borate.

spectra display two well-separated signals in the regions 102—183 and 323—427 ppm (Table 9), assigned to the  $\beta$ - and  $\alpha$ -oxygen atoms, respectively. Interestingly, the oxygen chemical shifts vary almost linearly with increasing steric bulk of the alkyl group. More recently, Bailey and coworkers reported the structure of the benzylperoxide complex  $\text{HC}\{\text{C}(\text{CH}_3)\text{NAr}\}_2\text{MgOOCH}_2\text{Ph}$  {Ar=2,6-(*i*-Pr) $_2\text{C}_6\text{H}_3$ }, in which the peroxybenzyl moiety binds in an unusual  $\mu$ - $\eta^2$  :  $\eta^1$ -O,O fashion in the solid state<sup>43</sup>. No  $^{17}\text{O}$  NMR data were reported for the complex, so it is not possible to compare data with those for  $\{\eta^3\text{-HB}(3\text{-}t\text{-Bupz})_3\}\text{MgOOR}$  complexes, in which the bonding mode of the alkylperoxide was not established.

## VI. CO-ORDINATION COMPLEXES

The co-ordination complexes of organomagnesium reagents have been studied quite extensively, primarily with the aim of obtaining sufficiently stable adducts to permit their structural characterization. X-ray studies have revealed a range of co-ordination numbers from two to eleven for the magnesium atom in the solid state: unsurprisingly, the most commonly occurring co-ordination number is four<sup>44</sup>. The higher co-ordination numbers are found in  $\eta^5$ -cyclopentadienyl complexes, in which each carbon is considered to occupy a separate co-ordination site.

It is difficult to ascertain if the same co-ordination numbers are retained in solution. Solution NMR studies indicate small co-ordination shifts for the ligand resonances, suggesting relatively weak, and hence labile, metal–ligand bonds<sup>6,45</sup>. The lability of the ligands, particularly monodentate ones, is further illustrated by the fact that adducts of different ligands often give identical NMR spectra (Table 10): the ligands are presumably substituted by solvent molecules, yielding identical solution species. The degree of solvation is clearly a matter of conjecture in most instances, but it is not unreasonable to expect co-ordination numbers of four or five to predominate in solution as they do in the solid state.

Despite the greater Lewis acidity of  $\text{R}_2\text{Mg}$  species, the co-ordination induced ligand shifts are smaller in the diorganomagnesium compounds than in the analogous Grignards, indicating that they have a lower affinity for complex formation. A particularly interesting exception to the low propensity of  $\text{R}_2\text{Mg}$  compounds for complex formation is that when sparteine, which is used to treat arrhythmic heart disorders, is the ligand in question. Sparteine forms a stable 1:1 adduct with bis(2-methylbutyl)magnesium in which the ligand has been shown by  $^1\text{H}$  NMR to adopt a *cisoid* configuration (Figure 6), even at elevated temperatures<sup>48</sup>.



TABLE 10. NMR data <sup>a</sup> for selected organomagnesium adducts

Complex	Solvent	$\delta^1\text{H}$		$\delta^{13}\text{C}$		Reference
		Mg–R	ligand	Mg–R	ligand	
MeMgBr(OEt <sub>2</sub> )	THF	–1.71	1.10 3.38	–16.4	15.7 66.3	6
MeMgBr(thf)	THF	–1.70		–16.3		6
MeMgBr(diglyme)	THF	–1.73	3.33 3.52 3.61	–16.0	59.1 71.0 72.5	6
MeMgBr(NEt <sub>3</sub> )	THF	–1.72	0.96 2.43	–16.5	12.6 47.3	6
MeMgBr(tmeda)	THF	–1.67	2.32 2.48	–15.5	47.0 57.7	6
MeMgBr(pmdta)	THF	–1.68	2.31 2.43 2.54 2.70	–13.2	44.2 45.8 57.4 57.6	6
Me <sub>2</sub> Mg(pmdta)	THF	–1.80	2.25 2.46 2.57	–14.1	42.6 46.7 57.6	6
EtMgBr(teed)	benzene		0.76 <i>ca</i> 2.05 2.12			45
EtMgNPh <sub>2</sub> (thf) <sub>2</sub>	benzene	0.51 1.82	1.11 3.34 6.76– 7.19	1.39 14.32	25.59 69.39 117.7 121.68 130.6 157.02	46
<i>i</i> -PrMgNPh <sub>2</sub> (thf) <sub>2</sub>	benzene	0.26 1.81	1.17 3.38 6.77– 7.27	9.63 26.39	26.39 69.53 116.99 117.66 121.27 121.61 129.99 130.10 156.99 157.45	46
<i>s</i> -Bu <sub>2</sub> Mg(tmeda)	benzene	0.05 1.44 1.75	1.53 2.36			47
<i>p</i> -FC <sub>6</sub> H <sub>4</sub> MgBr(teed)	benzene		0.82 <i>ca</i> 2.26 2.33			45
(PhCH <sub>2</sub> ) <sub>2</sub> Mg(thf) <sub>2</sub>	benzene	1.9 6.83 7.18 7.25	1.28 3.34	22.8 115.4 123.2 127.7 157.2	25.8 67.7	43

(continued overleaf)

TABLE 10. (continued)

Complex	Solvent	$\delta^1\text{H}$		$\delta^{13}\text{C}$		Reference
		Mg–R	ligand	Mg–R	ligand	
$(\text{PhCH}_2)_2\text{Mg}(\text{tmeda})$	benzene	1.33	2.15	21.0	43.9	43
		6.30	2.33	113.6	56.0	
		6.67		121.6		
		6.75		125.9		
				155.2		
$\text{Mg}(t\text{-BuCH}_2)_2(\text{OEt}_2)_2$	benzene	0.30	0.97			12
		1.45	3.46			
$\text{Mg}(t\text{-BuCH}_2)_2(\text{tmeda})$	benzene	0.07	1.74			12
		1.59	1.97			
$\text{Mg}(\text{PhCMe}_2\text{CH}_2)_2(\text{tmeda})$	benzene	−0.08	1.06			12
		1.08	1.32			
		7.3				
		6.8				
$\text{CpMgBr}(\text{teed})$	benzene		0.81			45
			ca 2.20			
			2.26			
$\text{Mg}(\text{OAr})_2(\text{thf})_2$	toluene	1.55	1.25	31.88	24.64	41
		6.73	3.64	35.53	70.75	
		7.33		114.22		
				125.25		
				137.57		
$\text{Mg}(\text{OAr})_2(\text{tmeda})$	toluene	1.55	1.55	32.53	32.53	41
		6.71	2.05	35.83	57.18	
		7.33		114.28		
				125.57		
				137.48		
				163.05		

<sup>a</sup> Data acquired at ambient temperature. Ligand abbreviations: diglyme = bis(2-methoxyethyl) ether; tmeda = tetramethylethylenediamine; pmdta = pentamethyldiethylenetriamine; teed = tetraethylethylenediamine; OAr = 2,6-di-*tert*-butylphenoxy.

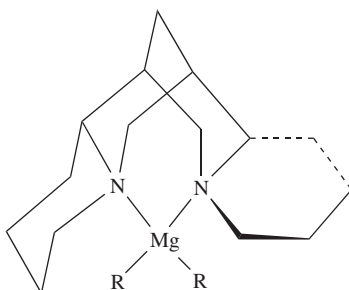


FIGURE 6. Dialkylmagnesium compounds form unusually strong adducts with sparteine. NMR data indicate that sparteine adopts *cisoid* configuration on co-ordination

### VII. <sup>25</sup>Mg NMR STUDIES

Magnesium possesses a single NMR active nuclide, <sup>25</sup>Mg, which is only of limited utility owing to its low natural abundance and high quadrupole moment (Table 11)<sup>49</sup>. The large quadrupole moment (and small magnetic moment) also gives rise to efficient quadrupolar relaxation effects in solution resulting in broad spectral lines which, coupled with the relatively narrow chemical shift range, further limit the utility of <sup>25</sup>Mg NMR studies on organomagnesium complexes.

Despite the obvious difficulties associated with the acquisition of good quality spectra, <sup>25</sup>Mg NMR has been usefully applied to the study of organomagnesium compounds<sup>15, 50, 51</sup>. The <sup>25</sup>Mg NMR parameters reported for organomagnesium complexes are listed in Table 12. Examination of Table 12 shows that the total solution chemical shift range is relatively narrow: -85 to +110 ppm. The  $\eta^5$ -cyclopentadienyl complexes resonate at significantly lower frequency than the  $\sigma$ -bonded alkyl and aryl compounds, the latter occurring between 56–110 ppm. Comparison of the chemical shift data for these compounds can provide useful additional information on the bonding between the organic moiety and the metal centre. The relatively high <sup>25</sup>Mg chemical shift (*ca* 70 ppm) observed for bis(allyl)magnesium, for example, is similar to that found in alkylmagnesium compounds, suggesting that the allyl moiety is indeed  $\sigma$ -bonding to magnesium, in agreement with more recent <sup>1</sup>H and <sup>13</sup>C variable-temperature NMR measurements.

Unsurprisingly, the <sup>25</sup>Mg chemical shifts of Grignard compounds are solvent, temperature and concentration dependent, in keeping with the effect of these variables on the position of the Schlenk equilibrium. Although the chemical shifts of MgCl<sub>2</sub> and MgBr<sub>2</sub> (Table 12) lie within the range found for organomagnesium compounds, they are sufficiently separated from those of the RMgX and R<sub>2</sub>Mg (R=alkyl) compounds to allow the simultaneous observation of all three species. The <sup>25</sup>Mg NMR spectrum of EtMgBr (0.36 mol dm<sup>-3</sup>; THF solution), for example, reveals the presence of three non-exchanging species, namely Et<sub>2</sub>MgBr, Et<sub>2</sub>Mg and MgBr<sub>2</sub>. On warming, the spectra broaden and coalesce, and at 340 K a single exchange averaged signal is observed at *ca* 54 ppm<sup>15</sup>.

Although often a hindrance to the acquisition of good quality spectra, the half-height line widths of the <sup>25</sup>Mg resonances are of diagnostic use. The degree of covalency in (cyclopentadienyl)magnesium compounds has been the subject of considerable conjecture, but the very narrow half-height line width (105 Hz) of the <sup>25</sup>Mg NMR signal of Cp<sub>2</sub>Mg in non-polar solvents clearly suggests significant covalent character<sup>50</sup>, despite the

TABLE 11. Magnesium-25 NMR parameters

Spin	5/2
Natural abundance (%)	10.13
Magnetogyric ratio (10 <sup>7</sup> rad T <sup>-1</sup> s <sup>-1</sup> )	-1.6370
Frequency <sup>a</sup> (MHz)	6.120
Quadrupole moment (10 <sup>-28</sup> m <sup>-2</sup> )	0.22
Relative sensitivity <sup>b</sup>	2.71 × 10 <sup>-4</sup>
Standard reference	Mg <sub>aq</sub> <sup>2+</sup>
Chemical shift range <sup>c</sup>	<i>ca</i> 180 ppm

<sup>a</sup> Relative to <sup>1</sup>H = 100 MHz.

<sup>b</sup> Relative to <sup>1</sup>H.

<sup>c</sup> Total range reported for organomagnesium complexes<sup>50</sup>.

TABLE 12. Magnesium-25 NMR data <sup>a</sup> for organomagnesium compounds

Compound	$\delta^{25}\text{Mg}$	$W_{1/2}$ (Hz)
MeMgBr	67.8	1900
EtMgBr	56.2	1100
allylMgBr	29.7	1000
CpMgBr	-26.8	60
<sup>R</sup> CpMgBr(tmeda) <sup>b</sup>	-15.0	300
Et <sub>2</sub> Mg	99.2	3200
<i>n</i> -Pr <sub>2</sub> Mg(tmeda) <sup>c</sup>	110.0	1700
{CH <sub>2</sub> CH(Me)CH <sub>2</sub> } <sub>2</sub> Mg	70.4	2000
Ph <sub>2</sub> Mg·dioxane <sup>c</sup>	108	2800
Cp <sub>2</sub> Mg <sup>b</sup>	-85.4	105
Cp <sub>2</sub> Mg(thf) <sub><i>n</i></sub>	-33.8	90
Cp* <sub>2</sub> Mg	-78.3	350
<sup>R</sup> Cp <sub>2</sub> Mg	-82.0	550
<sup>R</sup> Cp <sub>2</sub> Mg(thf) <sub><i>n</i></sub>	-36.7	250
CpMgEt	-4.0	1500
CpMg{CH <sub>2</sub> CH(Me)CH <sub>2</sub> }	-14.7	710
Cp* <sub>2</sub> MgEt	-10.0	1300
(indenyl)MgEt <sup>d</sup>	26.6	900
<sup>R</sup> CpMgMe(tmeda)	15.0	1100
CpMg·OEt <sub>2</sub>	-34.1	160
MgCl <sub>2</sub>	16.4	350
MgBr <sub>2</sub>	14.1	36

<sup>a</sup> Data from Reference 50. Data acquired in THF solvent at ambient temperature, unless otherwise stated. Ligand abbreviations: <sup>R</sup>Cp = 1, 2, 4-tris(trimethylsilyl)cyclopentadienyl; tmeda = tetramethylethylenediamine. Data for MgCl<sub>2</sub> and MgBr<sub>2</sub> are given for comparison.

<sup>b</sup> In toluene solvent.

<sup>c</sup> At 353 K.

<sup>d</sup> At 340 K.

relatively long C—Mg distances observed in the solid state<sup>52</sup>. The narrow line widths displayed by (cyclopentadienyl)magnesium compounds has also permitted their co-ordination chemistry with a variety of N, O and P Lewis bases to be explored by <sup>25</sup>Mg NMR. Cp<sub>2</sub>Mg forms tetrahedral co-ordination complexes of the type Cp<sub>2</sub>MgB<sub>2</sub> which, in some cases, have been isolated from toluene solution. The <sup>25</sup>Mg chemical shifts of these adducts (Table 12) correlate closely with the <sup>13</sup>C chemical shifts of the cyclopentadienyl ring carbons (Figure 7). Although, as expected, the <sup>25</sup>Mg signals are the more sensitive, both the <sup>25</sup>Mg and <sup>13</sup>C chemical shifts move to higher frequency as the stability of the adduct increases<sup>51</sup>. The comparatively high <sup>25</sup>Mg shift of the THF adduct, [Cp<sub>2</sub>Mg·(thf)<sub>*n*</sub>], is presumed to arise from the formation of a penta-coordinate species, rather than an unusually stable adduct.

The acquisition of solid-state NMR spectra of half-integer quadrupolar nuclei, such as <sup>25</sup>Mg, is particularly challenging and the first <sup>25</sup>Mg SSNMR study of an organomagnesium compound, Cp<sub>2</sub>Mg, has only been reported within the last few years<sup>52</sup>. The <sup>25</sup>Mg MAS QCPMG NMR spectrum of Cp<sub>2</sub>Mg displays a single second-order quadrupolar pattern with an isotropic shift of -91 ppm. The chemical shielding anisotropy is estimated to be less than 60 ppm. The spectrum is consistent with Cp<sub>2</sub>Mg possessing local C<sub>*i*</sub> symmetry, with the two cyclopentadienyl rings undergoing rapid rotation about the Cp(centroid)—Mg axis at ambient temperature.

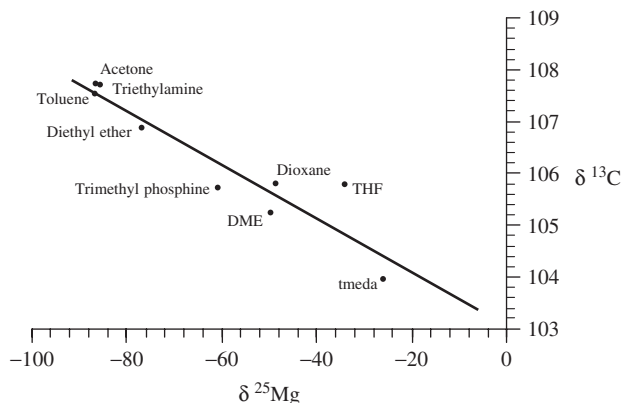


FIGURE 7. Correlation of the  $^{25}\text{Mg}$  and  $^{13}\text{C}$  NMR chemical shifts in bis(cyclopentadienyl) magnesium adducts. The  $^{13}\text{C}$  shifts are those of the cyclopentadienyl ring carbons. The points on the line are the co-ordinating ligands

## VIII. REFERENCES

1. E. C. Ashby, *Q. Rev.*, **21**, 259 (1967).
2. E. C. Ashby, *Pure Appl. Chem.*, **52**, 545 (1980).
3. W. Schlenk and W. Schlenk Jr., *Ber.*, **61B**, 720 (1928).
4. R. Jones, *J. Organomet. Chem.*, **18**, 15 (1969).
5. G. E. Paris and E. C. Ashby, *J. Am. Chem. Soc.*, **93**, 1206 (1971).
6. R. I. Yousef, B. Walford, T. Ruffer, C. Wagner, H. Schmidt, R. Herzog and D. Steinborn, *J. Organomet. Chem.*, **690**, 1178 (2005).
7. H. O. House, R. L. Latham and G. M. Whitesides, *J. Org. Chem.*, **32**, 2481 (1967).
8. D. Leibfritz, B. O. Wagner and J. D. Roberts, *Liebigs Ann. Chem.*, **763**, 173 (1972).
9. E. C. Ashby and A. B. Goel, *Inorg. Chem.*, **17**, 322 (1978).
10. V. Schulze, R. Lowe, S. Fau and R. W. Hoffmann, *J. Chem. Soc., Perkin Trans. 2*, 463 (1998).
11. V. P. W. Bohm, V. Schulze, M. Bronstrup, M. Muller and R. W. Hoffmann, *Organometallics*, **22**, 2925 (2003).
12. R. A. Anderson and G. Wilkinson, *J. Chem. Soc., Dalton Trans.*, 809 (1977).
13. G. Fraenkel and D. T. Dix, *J. Am. Chem. Soc.*, **88**, 979 (1966).
14. W. T. Ford and J. B. Grutzner, *J. Org. Chem.*, **37**, 2561 (1972).
15. R. Benn, H. Lehmkuhl, K. Mehler and A. Rufinska, *Angew. Chem., Int. Ed. Engl.*, **23**, 534 (1984).
16. D. Steinborn, T. Ruffer, C. Bruhn and F. W. Heinemann, *Polyhedron*, **17**, 3275 (1998).
17. R. Han and G. Parkin, *J. Am. Chem. Soc.*, **114**, 748 (1992).
18. E. C. Ashby, G. Paris and F. Walker, *Chem. Commun.*, 1464 (1969).
19. D. F. Evans and G. V. Fazakerley, *J. Chem. Soc., A*, 184 (1971).
20. H. R. Ward, R. G. Lawler and T. A. Marzilli, *Tetrahedron Lett.*, 521 (1970).
21. E. C. Ashby and A. B. Goel, *Chem. Commun.*, 169 (1977).
22. G. M. Whitesides, F. Kaplan and J. D. Roberts, *J. Am. Chem. Soc.*, **85**, 2167 (1963).
23. G. M. Whitesides, M. Witanowski and J. D. Roberts, *J. Am. Chem. Soc.*, **87**, 2854 (1965).
24. G. M. Whitesides and J. D. Roberts, *J. Am. Chem. Soc.*, **87**, 4878 (1965).
25. M. Witanowski and J. D. Roberts, *J. Am. Chem. Soc.*, **88**, 737 (1966).
26. D. F. Evans and M. S. Khan, *J. Chem. Soc., A*, 1643 (1967).
27. G. Westera, C. Blomberg and F. Bickelhaupt, *J. Organomet. Chem.*, **155**, C55 (1978).
28. D. A. Hutchison, K. R. Beck, R. A. Benkeser and J. B. Grutzner, *J. Am. Chem. Soc.*, **95**, 7075 (1973).
29. E. A. Hill, W. A. Boyd, H. Desai, A. Darki and L. Bivens, *J. Organomet. Chem.*, **514**, 1 (1996).

30. B. H. Lipshutz and C. Hackmann, *J. Org. Chem.*, **59**, 7437 (1994).
31. M. Schlosser and M. Stahle, *Angew. Chem., Int. Ed. Engl.*, **19**, 487 (1980).
32. R. Benn and A. Rufinska, *Organometallics*, **4**, 209 (1985).
33. R. H. DeWolfe and W. G. Young, *Chem. Rev.*, **56**, 753 (1956).
34. G. M. Whitesides, J. E. Nordlander and J. D. Roberts, *Discuss. Faraday Soc.*, **34**, 185 (1962).
35. J. E. Nordlander and J. D. Roberts, *J. Am. Chem. Soc.*, **81**, 1769 (1959).
36. H. E. Zieger and J. D. Roberts, *J. Org. Chem.*, **34**, 1976 (1969).
37. R. Benn, H. Lehmkuhl, K. Mehler and A. Rufinska, *J. Organomet. Chem.*, **293**, 1 (1985).
38. T. Yoshino and Y. Manabe, *J. Am. Chem. Soc.*, **85**, 2860 (1963).
39. T. Sugita, Y. Sakabe, T. Sasahara, M. Tsukada and K. Ichikawa, *Bull. Chem. Soc. Jpn.*, **57**, 2319 (1984).
40. E. C. Ashby, J. Nackashi and G. E. Parris, *J. Am. Chem. Soc.*, **97**, 3162 (1975).
41. K. W. Henderson, G. W. Honeyman, A. R. Kennedy, R. E. Mulvey, J. A. Parkinson and D. C. Sherrington, *J. Chem. Soc., Dalton Trans.*, 1365 (2003).
42. E. C. Ashby and B. Goel, *Inorg. Chem.*, **18**, 1306 (1979).
43. P. J. Bailey, R. A. Coxhall, C. M. Dick, S. Fabre, L. C. Henderson, C. Herber, S. T. Liddle, D. Lorono-Gonzalez, A. Parkin and S. Parsons, *Chem. Eur. J.*, **9**, 4820 (2003).
44. Cambridge Crystallographic Database.
45. D. F. Evans and M. S. Khan, *J. Chem. Soc., A*, 1648 (1967).
46. K.-C. Yang, C.-C. Chang, J.-Y. Huang, C.-C. Lin, G.-H. Lee, Y. Wang and M. Y. Chiang, *J. Organomet. Chem.*, **648**, 176 (2002).
47. N. D. R. Barnett, W. Clegg, R. E. Mulvey, P. A. O'Neil and D. Reed, *J. Organomet. Chem.*, **510**, 297 (1996).
48. G. Fraenkel, C. Cotterell, J. Ray and J. Russell, *Chem. Commun.*, 273 (1971).
49. R. K. Harris and B. E. Mann (Eds.), *NMR and the Periodic Table*, Academic Press, New York, 1978.
50. R. Benn and A. Rufinska, *Angew. Chem., Int. Ed. Engl.*, **25**, 861 (1986) and references cited therein.
51. H. Lehmkuhl, K. Mehler, R. Benn, A. Rufinska and C. Kruger, *Chem. Ber.*, **119**, 1054 (1986).
52. I. Hung and R. W. Schurko, *Solid State Nucl. Magn. Reson.*, **24**, 78 (2003).

## CHAPTER 4

# Formation, chemistry and structure of organomagnesium species in solvent-free environments

RICHARD A. J. O'HAIR

*School of Chemistry, The University of Melbourne, Victoria 3010, Australia; Bio21 Molecular Science and Biotechnology Institute, The University of Melbourne, Victoria 3010, Australia; ARC Centre of Excellence in Free Radical Chemistry and Biotechnology*  
Fax: +61 3 9347-5180; e-mail: rohair@unimelb.edu.au

---

I. INTRODUCTION . . . . .	156
II. FORMATION OF ORGANOMAGNESIUM SPECIES IN SOLVENT-FREE ENVIRONMENTS . . . . .	156
A. Reactions of Magnesium Atoms with Organic Substrates . . . . .	157
1. Reactions of Mg with alkanes . . . . .	157
2. Reactions of Mg with alkyl halides . . . . .	157
3. Reactions of Mg with unsaturated organic substrates . . . . .	158
4. Reactions of Mg with other organic substrates . . . . .	159
B. Reactions of Magnesium Cations with Organic Substrates . . . . .	160
1. Adduct-forming reactions of $Mg^{+\bullet}$ with alkanes, alkenes and other unsaturated species . . . . .	160
2. Reactions of $Mg^{+\bullet}$ with alkyl halides . . . . .	160
3. Reactions of $Mg^{+\bullet}$ with alcohols . . . . .	161
4. Reactions of $MgX^+$ ( $X = Cl, O, OH$ ) . . . . .	162
5. Photoactivation reactions of complexes $Mg(L)^{+\bullet}$ , where L = an alkane . . . . .	162
6. Photoactivation reactions of complexes $Mg(L)^{+\bullet}$ , where L = an organohalogen . . . . .	163
7. Photoactivation reactions of complexes $Mg(L)^{+\bullet}$ , where L = an alcohol or ether . . . . .	165
8. Photoactivation reactions of complexes $Mg(L)^{+\bullet}$ , where L = an amine . . . . .	167

---

*The chemistry of organomagnesium compounds*

Edited by Z. Rapoport and I. Marek © 2008 John Wiley & Sons, Ltd. ISBN: 978-0-470-05719-3

9. Photoactivation reactions of complexes $\text{Mg(L)}^{+\bullet}$ , where L contains a C=X bond (X = O or S) . . . . .	169
C. Reactions of Magnesium Clusters with Organic Substrates . . . . .	171
D. Reactions of Magnesium Surfaces and Films with Organic Substrates . . . . .	172
E. Gas-phase Fragmentation of Ligated Magnesium Ions to Yield Organomagnesium Ions . . . . .	174
1. Fragmentation reactions of $\text{Mg(L)}_n^{2+}$ complexes . . . . .	175
2. Fragmentation reactions of $\text{XMg(L)}_n^+$ complexes (where X = an anionic ligand) . . . . .	176
3. Fragmentation reactions of $\text{Mg(X)}_3^-$ complexes . . . . .	178
III. BIMOLECULAR REACTIONS OF ORGANOMAGNESIUM IONS IN THE GAS PHASE . . . . .	179
IV. UNIMOLECULAR REACTIONS OF ORGANOMAGNESIUM IONS IN THE GAS PHASE . . . . .	182
V. STRUCTURES OF ORGANOMAGNESIUMS AND MAGNESIUM HALIDES IN THE GAS PHASE . . . . .	183
VI. CONCLUDING REMARKS . . . . .	184
VII. ACKNOWLEDGMENTS . . . . .	184
VIII. REFERENCES . . . . .	184

## I. INTRODUCTION

Unlike other stable organoelement compounds (e.g. organosilicon<sup>1</sup> and organophosphorus<sup>2</sup>), which have been widely studied by mass-spectrometry-based techniques, only a handful of studies have examined organomagnesium species using mass spectrometry<sup>3–6</sup>. This may be due to the challenges of introducing these water- and oxygen-sensitive compounds into traditional EI sources of mass spectrometers. Recent studies using coldspray ionization<sup>6,7</sup> and matrix assisted laser desorption ionization (MALDI)<sup>5</sup> show promise for the analysis of organomagnesium compounds. Thus, unlike previous chapters in 'The Chemistry of Functional Groups' series that were solely devoted to mass spectrometry of organoelement species<sup>1,2</sup>, a wider net is cast in this review to include studies relevant to the formation, chemistry, structure and mass spectrometry of organomagnesium species in the gas phase and related solvent-free environments (e.g. matrix conditions). These studies highlight the broad scientific interest in the interaction of magnesium species with organic molecules, which span the range from traditional organic and organometallic chemistry through to the role of magnesium in planetary atmospheres<sup>8–11</sup> and interstellar science<sup>12–14</sup>. Although the heavier congeners of magnesium are not reviewed here, some comparison of their reactivity is made where appropriate. Theoretical studies are not reviewed here, unless they are directly related to experimental work. Finally, experimental techniques are not reviewed in this chapter.

## II. FORMATION OF ORGANOMAGNESIUM SPECIES IN SOLVENT-FREE ENVIRONMENTS

The formation of organomagnesium species such as Grignard reagents typically involves activating C–X bonds by magnesium metal. Since it is difficult to theoretically model in detail the interactions of an organic substrate with bulk magnesium metal, there is considerable interest in C–X bond activation in solvent-free environments using simpler magnesium species (e.g. magnesium atoms and ions; magnesium clusters or well-defined magnesium surfaces). In fact it has been argued that 'the active sites of a Mg surface are constituted by sets of clusters of highly variable reactivity rather than by a unique entity



called metallic Mg<sup>15</sup>. Key experimental and theoretical work on these ‘idealized’ systems are described in the next sections. Note that reactivity of a wide range of organic substrates is considered, including those that do not ultimately yield organomagnesium species.

## A. Reactions of Magnesium Atoms with Organic Substrates

Magnesium atoms are readily formed via vaporization of magnesium metal using either thermal techniques or laser ablation. The reactions of magnesium atoms with a range of compounds have been the subject of several studies in both the gas phase<sup>16</sup> and using matrix isolation techniques<sup>17</sup>. Since both areas have been nicely reviewed<sup>16, 17</sup>, here the focus is on key aspects of reactivity of Mg with organic substrates. Magnesium atoms in the <sup>1</sup>S ground state are generally unreactive towards organic substrates such as CH<sub>4</sub> due to repulsive interactions with bonding orbitals. In order to activate a bond in the organic substrate, photoactivation of one of the valence 3s electrons of Mg is required to generate the <sup>3</sup>P<sub>1</sub> or <sup>1</sup>P<sub>1</sub> excited-state. The outcome of reactions of excited-state Mg atoms with organic substrates is dependent on the medium. For example, gas-phase reactions with alkanes, RH, tend to produce R• + MgH•<sup>16</sup>, while the insertion product, RMgH, can be observed in matrix environments<sup>17</sup>. In the next sections, the reactions of Mg atoms are described with alkanes, alkyl halides and other substrates.

### 1. Reactions of Mg with alkanes

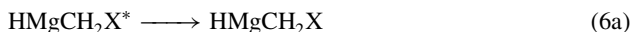
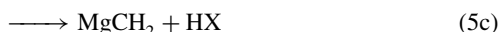
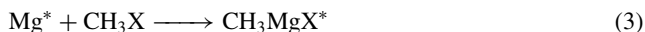
Excited-state Mg atoms react with methane and other alkanes via H atom abstraction in the gas phase (equation 1). By studying the vibrational states of the MgH• product, information on the mechanism has been inferred<sup>18</sup>. It has been found that regardless of the alkane, RH (and thus the C–H bond strength), the vibrational state distributions are essentially identical. This suggests that long-lived vibrationally excited [RMgH]\* complexes are not intermediates for equation 1 in the gas phase. The situation is quite different for excited-state Mg atoms reacting with methane under matrix conditions, where the insertion product (equation 2) is sufficiently stable for analysis via infrared spectroscopy<sup>19, 20</sup>. Calcium atoms have been shown to insert into the C–H bonds of cycloalkanes<sup>21</sup>.



### 2. Reactions of Mg with alkyl halides

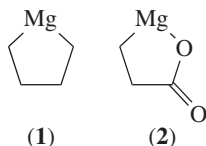
Skell and Girard appear to have been the first to report on the formation of solvent-free Grignard reagents via the codeposition of alkyl halides and magnesium atoms under matrix conditions over 30 years ago<sup>22</sup>. They noted that these solvent-free Grignards reacted differently compared to solution-phase Grignard reagents. For example, the solvent-free Grignard formed from *n*-propyl iodide reacted with acetone via enolization rather than addition. For some time the precise nature and mechanism of formation of these solvent-free Grignards formed under matrix conditions was obscure. Although Skell and Girard claimed they were observing ground-state reactivity of Mg atoms and Ault later confirmed that Mg atoms could react with methyl halides under matrix conditions to form monomeric reagents, CH<sub>3</sub>MgX<sup>23</sup>, subsequent work by Klabunde and coworkers suggested that the reactivity was due to the presence of Mg clusters<sup>24, 25</sup>. Thus Imizu and Klabunde found that Mg atoms were ‘totally inert’ towards CH<sub>3</sub>Br<sup>24</sup>. This is consistent with early theoretical calculations, which predicted a substantial activation barrier to form CH<sub>3</sub>MgX

from reaction of Mg with  $\text{CH}_3\text{X}$  ( $31.3 \text{ kcal mol}^{-1}$  for  $\text{X} = \text{F}$ ; and  $39.4 \text{ kcal mol}^{-1}$  for  $\text{X} = \text{Cl}$ )<sup>26</sup>. In 1997, Solov'ev and coworkers revisited the formation of  $\text{CH}_3\text{MgX}$  ( $\text{X} = \text{Cl}$  and  $\text{Br}$ ) using matrix isolation of reactions between evaporated Mg atoms and the methyl halide<sup>27</sup>. They concluded that the products were monomeric reagents. A year later Bare and Andrews examined the reactivity of laser-ablated Mg atoms with  $\text{CH}_3\text{X}$  ( $\text{X} = \text{F}$ ,  $\text{Cl}$ ,  $\text{Br}$  and  $\text{I}$ )<sup>28</sup>. Using a combination of IR spectroscopy, C, H and Mg isotopic labeling and DFT calculations, they identified the isolated monomeric  $\text{CH}_3\text{MgX}$  species as the primary product together with the following other products:  $\text{MgX}^\bullet$ ,  $\text{MgX}_2$ ,  $\text{MgH}^\bullet$ ,  $\text{MgH}_2$ ,  $\text{CH}_4$ ,  $\text{C}_2\text{H}_6$ ,  $\text{CH}_2\text{X}^\bullet$ ,  $\text{CH}_3\text{MgCH}_3$ ,  $\text{XMgCH}_2^\bullet$ ,  $\text{MgCH}_2$ ,  $\text{CH}_3\text{MgH}$  and  $\text{HMgCH}_2\text{X}$ . A key difference in their experiments is that laser ablation produces a portion of excited-triplet-state Mg atoms. They suggested that these excited-state atoms react with the methyl halide to form two different excited-state monomeric species, which arise from the expected C–X bond activation pathway (equation 3) as well as an unusual C–H bond activation pathway (equation 4). These may either relax to form the monomeric Grignard  $\text{CH}_3\text{MgX}$  (equation 5a) and C–H insertion product  $\text{HMgCH}_2\text{X}$  (equation 6a), or can decompose via a range of pathways (equations 5b–e and 6b–c). The most recent theoretical calculations confirm the role of triplet states in the insertion reaction of Mg with  $\text{CH}_3\text{Cl}$ <sup>29,30</sup>. Finally, the magnesium carbene product,  $\text{MgCH}_2$ , has been examined in more detail<sup>31</sup>.

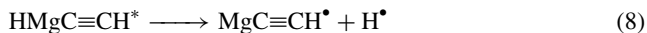


### 3. Reactions of Mg with unsaturated organic substrates

The reactions of Mg atoms and clusters with  $\text{CO}_2$ , ethylene and their mixtures have been examined using a combination of matrix isolation and theoretical calculations<sup>32</sup>. Products were characterized by IR and UV-visible techniques. One of the most interesting findings is that Mg appears to promote the formation of bonds between two ligands, thereby forming the five-membered rings **1** (between two ethylene ligands) and **2** (between one ethylene ligand and one  $\text{CO}_2$  ligand).



The only identified reaction product of laser-ablated Mg atoms and acetylene under matrix isolation conditions is  $\text{MgC}\equiv\text{CH}^\bullet$ <sup>33</sup>. It was suggested that this reaction involves the insertion of excited-state Mg into the H–C bond to form an excited complex (equation 7), which then decomposes via H atom loss (equation 8).



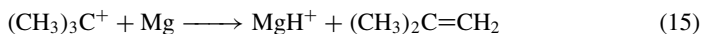
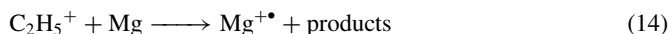
Mg atoms formed via laser ablation react with  $\text{H}\equiv\text{CN}$  to form  $\text{MgN}\equiv\text{C}^\bullet$  rather than  $\text{MgC}\equiv\text{N}^\bullet$ <sup>34</sup>. This suggests coordination at N to form an excited-state intermediate (equation 9) which decomposes via H atom loss (equation 10) rather than via a C–H insertion reaction (cf equations 7 and 8). Finally, the monomethyl magnesium radical,  $\text{MgCH}_3^\bullet$ , has been formed via reaction of laser-ablated magnesium metal reacting with either  $\text{CH}_3\text{I}$  or acetone<sup>35</sup>. Although the emphasis of this study was on an examination of the radical via ESR spectroscopy, a possible mechanism may involve C–X bond insertion via excited-state magnesium atoms to form an excited organomagnesium intermediate (cf equation 3) which then decomposes (cf equation 5d).



#### 4. Reactions of Mg with other organic substrates

Much less is known about the reactions of Mg atoms with other organic substrates. In fact it appears that there is only one gas-phase study in which the reactions of neutral organic substrates other than alkanes were studied. Thus as part of a systematic study of C–H bond activation by excited-state Mg atoms, Breckenridge and Umemoto studied a range of organic substrates including  $\text{CH}_3\text{OH}$ ,  $(\text{CH}_3)_2\text{O}$ ,  $(\text{CH}_3\text{CH}_2)_2\text{O}$ ,  $\text{CH}_3\text{NH}_2$  and  $(\text{CH}_3)_4\text{Si}$ <sup>18</sup>. All reacted via H atom abstraction (equation 1). In contrast, reaction of Mg atoms with  $\text{CH}_3\text{OH}$  under matrix conditions yields a  $\text{Mg}(\text{CH}_3\text{OH})$  complex, which undergoes C–O bond activation to yield  $\text{CH}_3\text{MgOH}$  under conditions of UV-Vis irradiation (cf equation 5a)<sup>36</sup>. Interestingly,  $\text{CH}_3\text{MgOH}$  undergoes further reaction with Mg to yield  $\text{CH}_3\text{MgOMgH}$  arising from O–H bond activation.

Finally, two studies have reported on the reactions of carbocations with Mg atoms using mass spectrometry<sup>37,38</sup>. The types of products formed depend on the nature of the carbocation. The labeled methanium ion,  $\text{CH}_4\text{D}^+$ , reacts via proton transfer (equation 11), deutron transfer (equation 12) and charge transfer (equation 13)<sup>37</sup>. The ethyl cation reacts via charge transfer (equation 14)<sup>38</sup> while the *tert*-butyl cation reacts via proton transfer (equation 15)<sup>37</sup>. In all cases there was no evidence for formation of an organomagnesium species.



## B. Reactions of Magnesium Cations with Organic Substrates

The bond activation reactions of monoatomic main group and transition metal cations have been widely studied for decades and have been the subject of several reviews<sup>39–44</sup>. Gas-phase monoatomic magnesium cations can readily be formed via a range of processes including electron impact on magnesium vapors<sup>45</sup> and magnesium organometallics<sup>46</sup> and laser ablation on magnesium metal<sup>47</sup>. The reactivity of  $\text{Mg}^{+\bullet}$  is first described, followed by a discussion on the reactions of ligated magnesium ions and finally on the photoactivation of magnesium adduct ions.

### 1. Adduct-forming reactions of $\text{Mg}^{+\bullet}$ with alkanes, alkenes and other unsaturated species

Using the selected ion flow tube technique (SIFT), Bohme and coworkers have shown that thermalized  $\text{Mg}^{+\bullet}$  reacts with alkanes (L) via simple adduct formation without bond activation (equation 16)<sup>46</sup>. Only single ligation was observed, and the efficiency of this reaction depends on the size of the alkane (L). Methane and ethane are unreactive. Larger alkanes become more reactive, with *n*-heptane reacting at the collision rate. DFT calculations reveal that while the binding energies can be strong (around 12–16 kcal mol<sup>−1</sup> for *n*-pentane), interconversion of different  $\text{MgL}^{+\bullet}$  isomers should be facile.



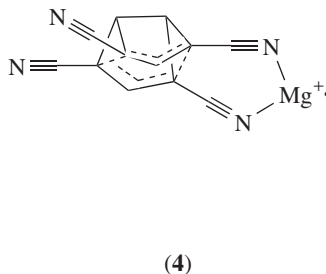
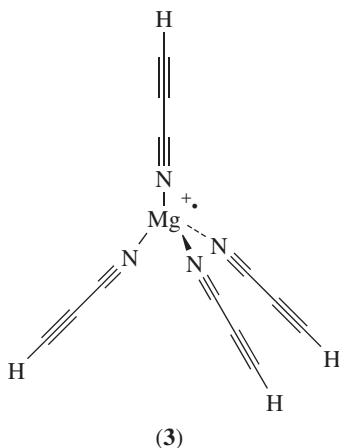
Several studies have examined the reactions of  $\text{Mg}^{+\bullet}$  with unsaturated molecules. Under the lower pressure conditions of FT-ICR mass spectrometry,  $\text{Mg}^{+\bullet}$  reacts with the polycyclic aromatic hydrocarbon, coronene, via a combination of radiative associative adduct formation (equation 16) and electron transfer (equation 17)<sup>48</sup>. The latter reaction is 8 times faster, consistent with it being exothermic. Adduct formation (equation 16) also readily occurs in reactions with  $\text{C}_{60}$ <sup>49–51</sup>. Theoretical calculations suggest that related radiative associative adduct formation of  $\text{Mg}^{+\bullet}$  with cyanopolyenes and polyenes should be highly efficient<sup>52,53</sup>.



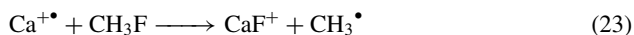
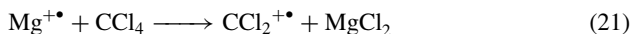
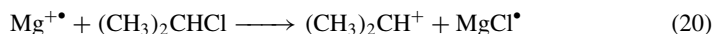
The reactions of  $\text{Mg}^{+\bullet}$  with cyanoacetylene are remarkable in that while  $\text{Mg}^{+\bullet}$  is unreactive towards HCN, multiple ligation occurs for cyanoacetylene<sup>54</sup>. Furthermore, there is evidence from collision induced dissociation (CID) studies that ligand–ligand interactions occur. In fact, the  $\text{Mg}(\text{NC}_3\text{H})_4^{+\bullet}$  is especially stable, being resistant to CID. DFT calculations suggest that the semibulvalene-type structure, **4**, is around 12 kcal mol<sup>−1</sup> more stable than the tetrahedral structure, **3**. These are reminiscent of the reactions of Mg atoms with ethylene to form **1**<sup>32</sup>.

### 2. Reactions of $\text{Mg}^{+\bullet}$ with alkyl halides

$\text{Mg}^{+\bullet}$  reacts with alkyl halides in the gas phase via a range of substrate-dependent pathways<sup>45,47</sup>. Not all halides are reactive—examples of unreactive substrates include methyl chloride, vinyl chloride, trichloro and tetrachloro ethylene. Reaction with ethyl chloride proceeds via an elimination reaction (equation 18) followed by a displacement reaction (equation 19). For larger alkyl halides, such as isopropyl chloride, chloride abstraction also occurs (equation 20). For multiply halogenated substrates such as carbon tetrachloride, oxidative reactions occur (equations 21 and 22), although organometallic

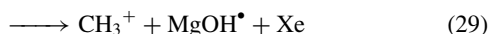
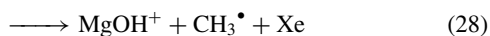
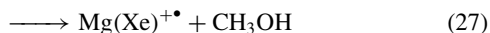
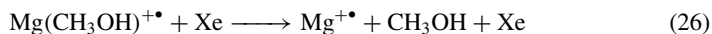
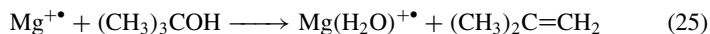


species are not found. Finally, the related calcium cation reacts with methyl fluoride via oxidation (equation 23)<sup>55</sup>.



### 3. Reactions of $\text{Mg}^{+\bullet}$ with alcohols

$\text{Mg}^{+\bullet}$  reacts with alcohols via either condensation or via elimination. The outcome is substrate dependent. Thus while *n*-BuOH reacts via condensation (equation 24), *t*-BuOH reacts via elimination (equation 25). No oxidative reactions (cf equations 21–23) are observed. Armentrout and coworkers<sup>56</sup> have examined the CID reactions of methanol adducts of  $\text{Mg}^{+\bullet}$  using Xe as the collision gas and found competition between ligand loss (equation 26), ligand switching (equation 27) and C–O bond activation (equations 28 and 29).

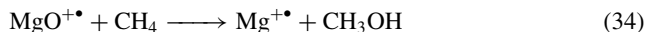
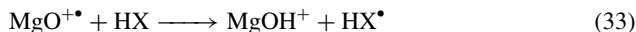
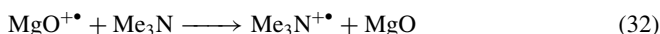


#### 4. Reactions of $\text{MgX}^+$ ( $X = \text{Cl}, \text{O}, \text{OH}$ )

$\text{MgCl}^+$  ions undergo anion abstraction reactions with organic halides (equation 30)<sup>42,44</sup> and nitric acid (equation 31).



The  $\text{MgO}^{+\bullet}$  ion has significant radical character and reacts via electron transfer (equation 32)<sup>57</sup>. It is also a potent H atom acceptor, readily reacting with water via H atom abstraction (equation 33,  $X = \text{HO}$ )<sup>53</sup>. A recent combined experimental and theoretical study reveals that the  $\text{MgO}^{+\bullet}$  ion readily activates the C–H bond of methane to yield  $\text{MgOH}^+$  as the major product ion (equation 33,  $X = \text{CH}_3$ ) as well as  $\text{Mg}^{+\bullet}$  as a minor product ion via O atom insertion into the C–H bond (equation 34)<sup>58</sup>.



The  $\text{MgOH}^+$  ion is a weak acid, failing to react via proton transfer (equation 35) with even a strong base such as *N,N,N',N'*-tetramethyl-1,8-naphthalenediamine<sup>53</sup>. Although its reactions with organic reagents are largely unexplored,  $\text{MgOH}^+$  reacts with nitric acid via  $\text{HO}^-$  abstraction (cf equation 31)<sup>42</sup>.



#### 5. Photoactivation reactions of complexes $\text{Mg(L)}^{+\bullet}$ , where $L = \text{an alkane}$

Intracomplex reactions in  $\text{Mg(L)}^{+\bullet}$  complexes (where  $L = \text{an organic molecule}$ ) have been studied for a wide range of organic molecules using gas-phase photodissociation spectroscopy experiments. These experiments offer a number of advantages since: (a) they start from a well-defined complex; (b) chemical reactivity is triggered by exciting  $\text{Mg}^{+\bullet}$  electronically (the  $\text{Mg}^{+\bullet} \ 3P \leftarrow 3S$  transition) via absorption of a photon in the UV-Vis region; (c) the presence of a positive charge means that ionic products can readily be detected via mass spectrometry; (d) the systems are often sufficiently small so that they are amenable to high-level theoretical calculations. While this area was reviewed in 1998<sup>59</sup>, progress has been rapid and so in the next sections the C–X bond activation observed in these studies is described by class of organic molecule.

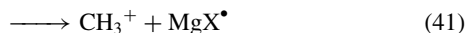
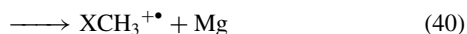
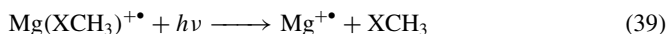
Cheng and coworkers have examined the photodissociation spectroscopy of  $\text{MgCH}_4^{+\bullet}$  in detail<sup>60</sup>. The photofragmentation action spectrum has a broad featureless continuum ranging from 310 to 342 nm, with a maximum at 325 nm. In this region the channels observed are nonreactive (equation 36, *ca* 60%), H abstraction (equation 37, *ca* 7%) and  $\text{CH}_3$  abstraction (equation 38, *ca* 33%). Recent theoretical calculations on the C–H bond activation in  $\text{MgCH}_4^{+\bullet}$  reveal that the formation of the insertion intermediate,  $\text{CH}_3\text{MgH}^{+\bullet}$ , proceeds via a three-centered transition state<sup>61</sup>.



The photodissociation spectroscopy of  $\text{CaCH}_4^{+\bullet}$  contrasts that of  $\text{MgCH}_4^{+\bullet}$ , with complex rovibrational structure in the spectrum, but with no evidence for C–H bond activation<sup>62</sup>. Although not relevant to C–H bond activation, the photodissociation spectroscopy of the prototypical alkene complex,  $\text{MgC}_2\text{H}_4^{+\bullet}$ , exhibits a rich photochemistry arising from metal-centered transitions, ligand-centered transitions, and from charge transfer processes (which give rise to electron transfer to yield Mg and  $\text{C}_2\text{H}_4^{+\bullet}$ )<sup>63</sup>.

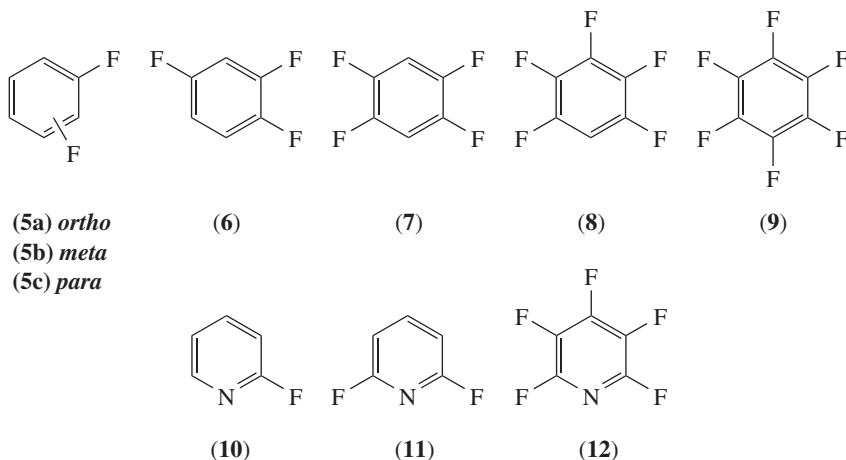
#### 6. Photoactivation reactions of complexes $\text{Mg}(\text{L})^{+\bullet}$ , where $\text{L}$ = an organohalogen

The photoactivation of  $\text{Mg}(\text{L})^{+\bullet}$  complexes of organohalogens has been widely studied<sup>64–74</sup>. The photodissociation spectra of the methyl halide complexes,  $\text{Mg}(\text{XCH}_3)^{+\bullet}$  (where  $\text{X} = \text{F}, \text{Cl}, \text{Br}$  and  $\text{I}$ ), have been studied in great detail by Furuya and coworkers in two publications<sup>66,67</sup>. Each of the four halides exhibits spectra with three absorption bands at the red and blue sides of the free  $\text{Mg}^{+\bullet} \text{ } ^2P \leftarrow ^2S$  transition. These three absorption bands were assigned to the splitting of the  $\text{Mg}^{+\bullet} \text{ } 3p$  orbitals as a result of interaction with the methyl halide molecules. Six different fragment ions were produced including intermolecular bond breaking (evaporation) without (equation 39) and with charge transfer (equation 40), anion abstraction (equations 41 and 42) and oxidation (equations 43 and 44). Equations 39, 41 and 43 were observed for all four halides, equation 40 was observed for  $\text{X} = \text{Cl}, \text{Br}$  and  $\text{I}$ , equation 42 was only observed for the iodide, while equation 44 was observed when  $\text{X} = \text{Cl}$  and  $\text{Br}$ . The yields of each product channel depend on which of the three absorption bands was excited. Detailed theoretical calculations were carried out to explain the experimental data. Of interest is that the complex with connectivity  $\text{MgXCH}_3^{+\bullet}$  is predicted to be more stable than the organomagnesium ion,  $\text{CH}_3\text{MgX}^{+\bullet}$ , in all cases (for  $\text{X} = \text{F}$ , by  $12.4 \text{ kcal mol}^{-1}$ ;  $\text{X} = \text{Cl}$ , by  $4.8 \text{ kcal mol}^{-1}$ ;  $\text{X} = \text{Br}$ , by  $3.7 \text{ kcal mol}^{-1}$ ;  $\text{X} = \text{I}$ , by  $3.9 \text{ kcal mol}^{-1}$ ). The photodissociation spectra of  $\text{Mg}(\text{FCH}_3)^{+\bullet}$  complexes ‘solvated’ by up to three other methyl fluoride molecules are dominated by the formation of bare and solvated  $\text{MgF}^+$  (cf equation 43)<sup>68</sup>.

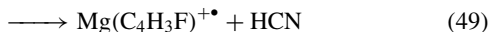
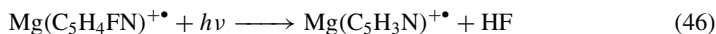


The photodissociation spectra of benzene and halobenzene complexes,  $\text{Mg}(\text{C}_6\text{H}_5\text{X})^{+\bullet}$  (where  $\text{X} = \text{H}, \text{F}, \text{Cl}$  and  $\text{Br}$ ), are dominated by the formation of  $\text{Mg}^{+\bullet}$  (cf equation 39), although charge transfer (cf equation 40) is observed for all cases<sup>69</sup>. Fluorobenzene gives  $\text{MgF}^+$  as a unique product (cf equation 43). New fragmentation channels open up in the photodissociation spectra of polyfluorinated benzenes,  $\text{C}_6\text{H}_{4-n}\text{F}_{2+n}$ , **5–9**<sup>70,71,73</sup>. Apart from formation of  $\text{Mg}^{+\bullet}$  (cf equation 39) and  $\text{MgF}^+$  (cf equation 43), benzyne radical cations,  $\text{C}_6\text{H}_{4-n}\text{F}_n^{+\bullet}$ , are formed (equation 45). These benzyne radical cations undergo further fragmentation reactions, the nature of which depends on the number of fluorines present. The  $\text{C}_6\text{H}_{4-n}\text{F}_n^{+\bullet}$  ions of **5** and **7** fragment via loss of  $\text{C}_2\text{H}_2$  and  $\text{C}_2\text{HF}$  respectively, while **6** fragments via competitive loss of  $\text{C}_2\text{H}_2$  and  $\text{C}_2\text{HF}$ . Instead of fragmenting via  $\text{C}_2\text{HX}$  loss (where  $\text{X} = \text{H}$  or  $\text{F}$ ), **8** yields  $\text{CF}^+$ ,  $\text{C}_5\text{H}^+$  and  $\text{C}_5\text{HF}^{+\bullet}$  fragment ions, while

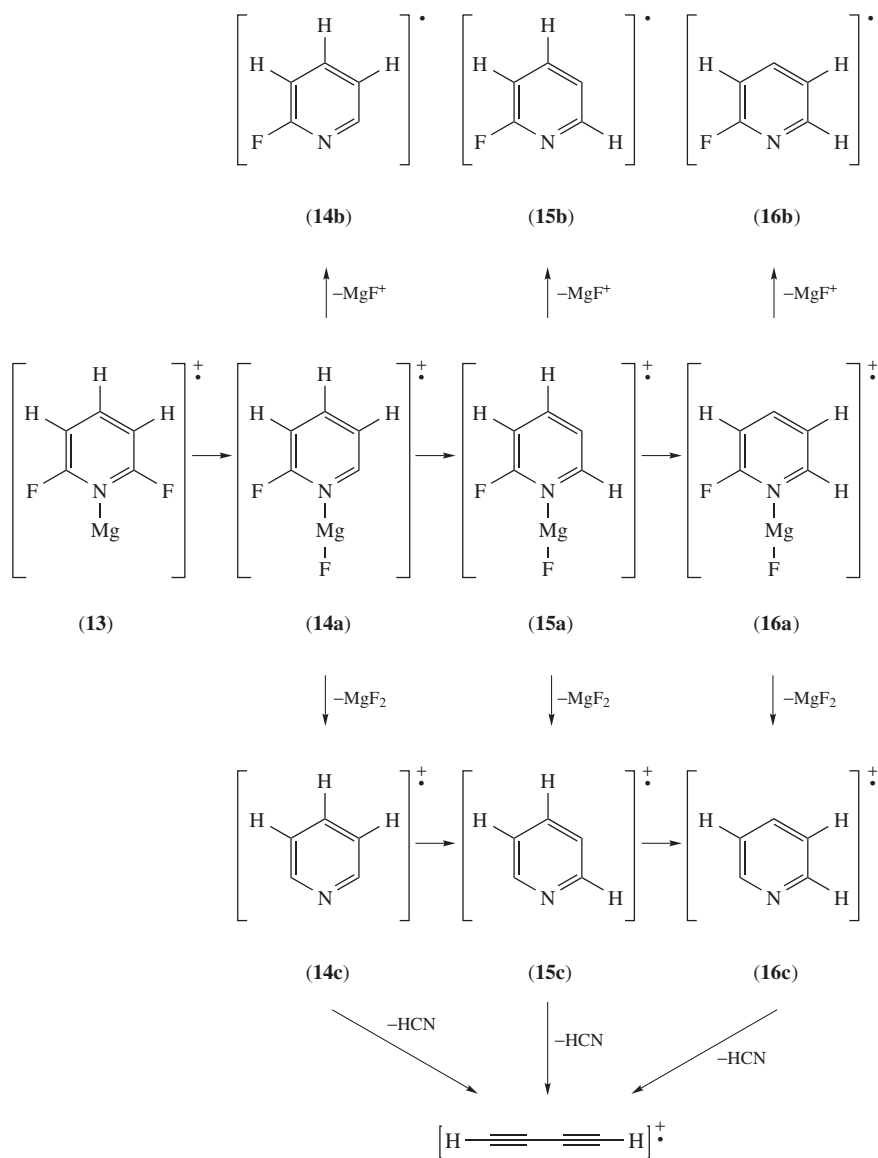
**9** yields  $\text{CF}^+$ ,  $\text{C}_5\text{F}^+$ ,  $\text{C}_5\text{F}_2^{+\bullet}$  and  $\text{C}_5\text{F}_3^+$ .



The same group has studied the photodissociation spectra of  $\text{Mg}^{+\bullet}$  complexes of 2-fluoropyridine **10**<sup>63</sup> and the polyfluorinated pyridines **11** and **12**<sup>64</sup>. The photodissociation chemistry of the  $\text{Mg}^{+\bullet}$  complexes of **10** is rich. Aside from  $\text{Mg}^{+\bullet}$  formation (equation 39), anion abstraction (equation 41) and oxidation (equation 43), HF extrusion (equation 46) and reactions which result in the destruction of the aromatic ring are also observed. The latter include  $\text{FMgNC}^{+\bullet}$  (equation 47) and  $\text{FMgNC}$  (equation 48) formation and extrusion of HCN (equation 49). Further substitution of fluorine onto the pyridine ring results in changes in the photodissociation chemistry. Thus the polyfluorinated pyridines **11** and **12** react via  $\text{Mg}^{+\bullet}$  formation (equation 39), oxidation (equation 43) and dehydropyridine radical cation formation (cf equation 45)<sup>64</sup>. In the case of **11**, the resultant dehydropyridine radical cation undergoes further fragmentation via loss of HCN to give  $\text{C}_4\text{H}_2^{+\bullet}$ . Although the structures of some of these product ions and neutrals are not known from experiment, DFT calculations were preformed to suggest possible mechanisms. For example, all the fragments for the complex of **11** were rationalized as potentially arising from the initial N bound adduct **13** reacting via the processes shown in Scheme 1. Note that the radical cation structures,  $\text{C}_5\text{H}_3\text{N}^{+\bullet}$ , can include the dehydropyridines **14c**, **15c** and **16c** as well as open-chain isomers. Structures **14c**, **15c** and **16c** can arise from H atom migrations either within the initial Mg complex (e.g. processes **14a**  $\rightarrow$  **15a**  $\rightarrow$  **16a** in Scheme 1), or from subsequent H atom migrations within the  $\text{C}_5\text{H}_3\text{N}^{+\bullet}$  product ion (e.g. processes **14c**  $\rightarrow$  **15c**  $\rightarrow$  **16c** in Scheme 1). The DFT calculations suggest that the experiments are likely to produce a mixture of  $\text{C}_5\text{H}_3\text{N}^{+\bullet}$  isomers, but that extrusion of HCN is energetically preferred from **16c**.







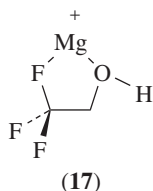
SCHEME 1

### 7. Photoactivation reactions of complexes $\text{Mg}(\text{L})^+ \bullet$ , where $\text{L}$ = an alcohol or ether

The photodissociation spectra of  $\text{Mg}(\text{CH}_3\text{OH})_n^+ \bullet$  complexes has been studied as a function of cluster size,  $n^{75}$ . For  $n = 1$ , the main reaction channels involve formation of  $\text{Mg}^+ \bullet$  (cf equation 39) and  $\text{MgOH}^+$  (cf equation 43). Small amounts of  $\text{CH}_3^+$  (cf equation 41)

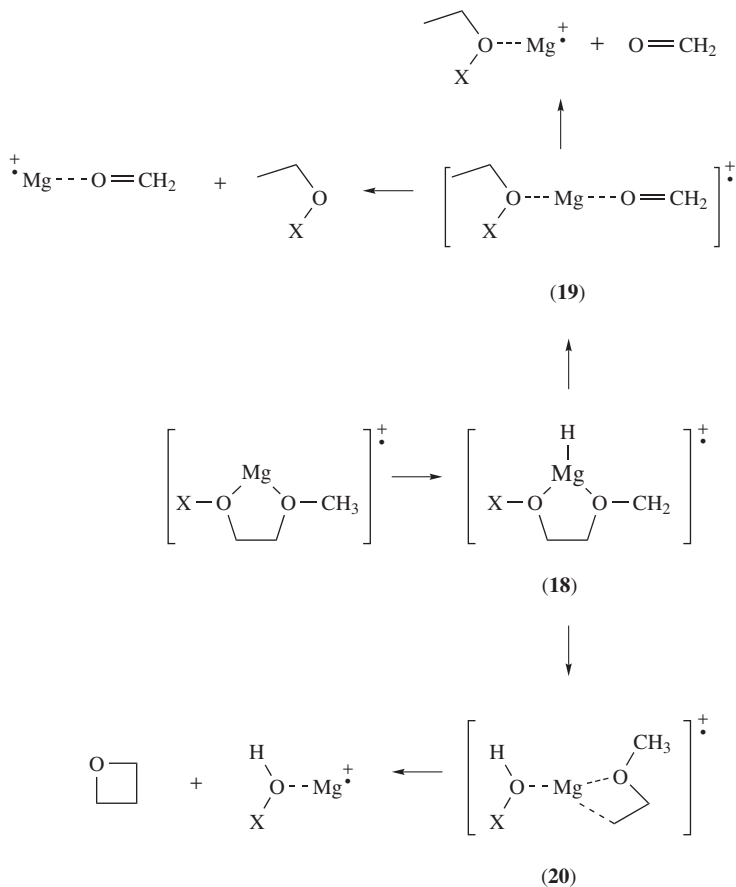
and  $\text{MgO}^{+\bullet}$  are also observed. Although the neutral product(s) and mechanism associated with the formation of the latter ion are unknown, they may represent the reverse of the reaction involving C–H bond activation of methane by  $\text{MgO}^{+\bullet}$  (equation 34). Larger clusters ( $2 \leq n \leq 6$ ) undergo efficient dissociation at 350 nm to yield products arising from two competing pathways: (i) elimination of solvent, and (ii) an excited-state photoinduced reaction to yield  $\text{MgOH}(\text{CH}_3\text{OH})_m^+$  (the solvated equivalent of equation 43, where  $m < n$ ). When  $n \geq 6$ , photodissociation is no longer efficient, suggesting the loss of the  $\text{Mg}^{+\bullet}$  chromophore. Similar results were observed in the photodissociation spectra of  $\text{Mg}(\text{CH}_3\text{OD})_n^{+\bullet}$  complexes, although a unique loss of  $\text{CH}_3\text{D}$  was observed when  $n = 2$ <sup>76</sup>.

The photoproducts of the  $\text{Mg}(\text{CF}_3\text{CH}_2\text{OH})^{+\bullet}$  complex have been examined using a combination of experiment and theory<sup>77</sup>. Apart from non-reactive formation of  $\text{Mg}^{+\bullet}$  (cf equation 39), ionic products arise from the scission of the C–F bond (to yield  $\text{MgF}^+$ ), as well as from the simultaneous rupture of two bonds. The latter include  $\text{MgOH}_2^{+\bullet}$ ,  $\text{CHF}_2\text{CO}^+$  and  $\text{CF}_2\text{CH}_2^{+\bullet}$ . The observed products are consistent with those arising from structure **17**, which was predicted to be the minimum energy structure based on *ab initio* calculations.

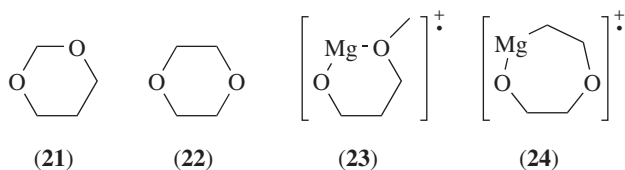


A similar formation of five-membered rings involving bidentate coordination to  $\text{Mg}^{+\bullet}$  appears to be at the heart of the photofragmentation of the  $\text{Mg}^{+\bullet}$  complexes of 2-methoxyethanol and 1,2-dimethoxyethane<sup>78</sup>. Aside from  $\text{Mg}^{+\bullet}$  formation (cf equation 39), a range of photoproducts were identified. Interestingly, a significant number of the photoproducts are complexes of  $\text{Mg}^{+\bullet}$  with neutral molecules such as  $\text{H}_2\text{O}$ ,  $\text{CH}_2\text{O}$  and  $\text{CH}_3\text{OH}$ . Based on *ab initio* calculations, a key hydrogen shift mechanism is proposed to form intermediate **18** (Scheme 2, where  $\text{X} = \text{H}$  or  $\text{CH}_3$ ). This carbon-centered radical intermediate then undergoes a range of competing fragmentation reactions. Two decomposition pathways of **18** which are common to the complexes of 2-methoxyethanol and 1,2-dimethoxyethane are shown in Scheme 2. The first involves H attack onto a carbon atom to yield **19**, which can then fragment via either loss of  $\text{CH}_2\text{O}$  or  $\text{CH}_3\text{CH}_2\text{OX}$ . The second involves H attack onto an oxygen atom to yield **20**, which can then fragment via loss of the cyclic ether.

The photoinduced reactions of the  $\text{Mg}(\text{CF}_3\text{OC}_6\text{H}_5)^{+\bullet}$  complex have been examined using a combination of experiments and theory<sup>79</sup>. Four ionic products are observed:  $\text{Mg}^{+\bullet}$  (cf equation 39),  $\text{MgF}^+$  (cf equation 43),  $\text{C}_6\text{H}_5^+$  (cf equation 41) and  $\text{CF}_3\text{OC}_6\text{H}_5^{+\bullet}$  (cf equation 40). Other  $\text{Mg}^{+\bullet}$  complexes of ethers that have been examined using photodissociation spectroscopy are those of 2-methoxyethanol and 1,2-dimethoxyethane described above (Scheme 2) and those of 1,3- (**21**) and 1,4- (**22**) dioxane<sup>80</sup>. The main ionic photoproduct of the complexes of **21** and **22** is  $\text{Mg}^{+\bullet}$  (cf equation 39). While the complex of **21** gives only one other product,  $\text{Mg}(\text{O}=\text{CH}_2)^{+\bullet}$ , the complex of **22** gives a much richer range of ionic fragments including  $\text{MgOH}^+$ ,  $\text{Mg}(\text{O}=\text{CH}_2)^{+\bullet}$ ,  $\text{Mg}(\text{OCH}=\text{CH}_2)^{+\bullet}$ ,  $\text{Mg}(\text{OCH}_2\text{CH}_3)^{+\bullet}$ ,  $\text{C}_2\text{H}_4^{+\bullet}$  and  $\text{C}_3\text{H}_6\text{O}^{+\bullet}$ . Based on theoretical calculations, the insertion complex **23** is the first key intermediate in the formation of  $\text{Mg}(\text{O}=\text{CH}_2)^{+\bullet}$  from the complex of **21**. In a similar fashion, the insertion complex **24** is a key intermediate for



SCHEME 2



the formation of many of the products of the complex of **22**. Photoionization of neutral  $\text{Mg}(\text{O}(\text{CH}_3)_2)_n$  clusters results in the formation of  $\text{Mg}(\text{O}(\text{CH}_3)_2)_n^{\bullet+}$  clusters as well as  $\text{Mg}(\text{OCH}_3)(\text{O}(\text{CH}_3)_2)_n^+$  ions arising from C–O bond activation<sup>81</sup>.

#### 8. Photoactivation reactions of complexes $\text{Mg}(\text{L})^{\bullet+}$ , where $\text{L}$ = an amine

Photoactivation of  $\text{Mg}(\text{amine})^{\bullet+}$  complexes has been the subject of several studies<sup>82–85</sup>. The photofragmentation pathways are dependent on the structure of the amine. For

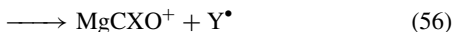
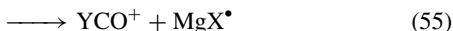
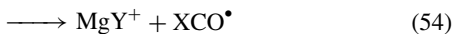
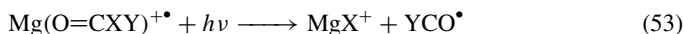


studied as a function of cluster size,  $n^{87}$ . For  $n = 1$ , there are two products:  $\text{Mg}^{+\bullet}$  as the major product (cf equation 39) and  $\text{MgNC}^+$  as the minor product (cf equation 43). Solvent evaporation is the sole reaction channel observed for all the other clusters,  $n = 2-4$  (equation 52).

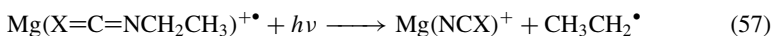


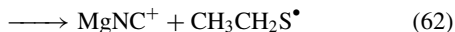
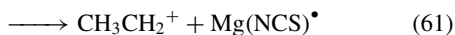
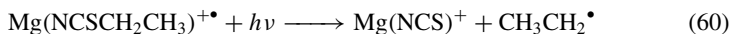
9. Photoactivation reactions of complexes  $\text{Mg}(\text{L})^{+\bullet}$ , where L contains a C=X bond ( $\text{X} = \text{O}$  or S)

The photodissociation spectra of the  $\text{Mg}(\text{L})^{+\bullet}$  complexes containing substrates with a C=O moiety have been studied for formaldehyde<sup>88,89</sup>, acetaldehyde<sup>90,91</sup>, acetic acid<sup>92</sup> and *N,N*-dimethylformamide<sup>93</sup>. Apart from  $\text{Mg}^{+\bullet}$  formation (cf equation 39), these complexes share some common reactive channels (equations 53–56). Formaldehyde undergoes a significant amount of H abstraction (equation 53,  $\text{X} = \text{Y} = \text{H}$ ) for the magnesium complex<sup>78</sup>, which contrasts with the calcium complex<sup>79</sup>. For the acetaldehyde complex, the Mg attacks both the C–H bond (equations 53, where  $\text{X} = \text{H}$  and  $\text{Y} = \text{CH}_3$ ) as well as the C–C bond (equations 54 and 56, where  $\text{X} = \text{H}$  and  $\text{Y} = \text{CH}_3$ )<sup>80,81</sup>. Deuterium labeling confirms that the C–H bond attacked is the aldehydic C–H bond rather than the methyl C–H bond. The adduct of acetic acid fragments via formation of the following ions:  $\text{Mg}^{+\bullet}$  (cf equation 39),  $\text{MgCH}_3^+$  (equation 53 where  $\text{X} = \text{CH}_3$  and  $\text{Y} = \text{OH}$ ),  $\text{MgOH}^+$  (equation 53) and  $\text{CH}_3\text{CO}^+$  (equation 55). In addition, dehydration of acetic acid to form ketene and  $\text{MgOH}_2^{+\bullet}$  is observed. When  $\text{CH}_3\text{CO}_2\text{D}$  is used, a minor yield of  $\text{MgOH}^+$  is observed, suggesting activation of the C–H bond. When  $\text{L} = \text{N,N}$ -dimethylformamide the following photoproducts are observed:  $\text{Mg}^{+\bullet}$  (cf equation 39),  $\text{MgH}^+$  [equation 53 where  $\text{X} = \text{H}$  and  $\text{Y} = (\text{CH}_3)_2\text{N}$ ] and  $(\text{CH}_3)_2\text{NCO}^+$  (equation 55). Once again, deuterium labeling was used to confirm that the C–H bond attacked is the formyl C–H bond rather than the methyl C–H bond. The dimer complex,  $\text{Mg}(\text{HCON}(\text{CH}_3)_2)_2^{+\bullet}$ , simply undergoes solvent evaporation (cf equation 52)<sup>93</sup>.

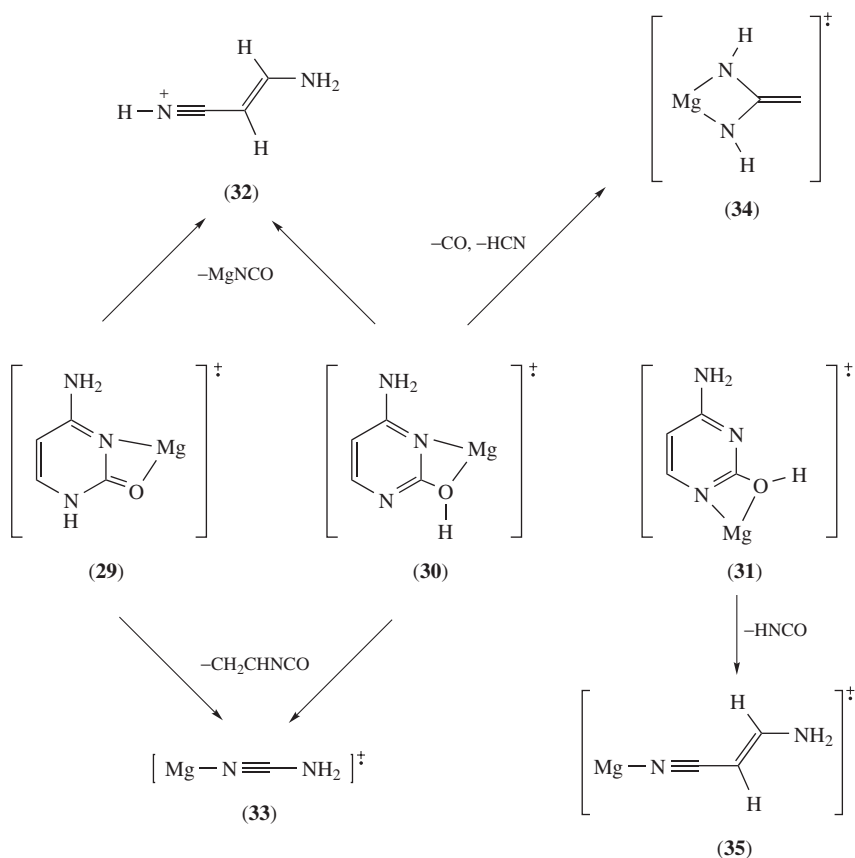


The photodissociation spectra of the  $\text{Mg}(\text{L})^{+\bullet}$  complexes of ethyl isocyanate<sup>94,95</sup> and ethyl isothiocyanate<sup>96</sup> show some common photofragments. Aside from the ubiquitous formation of  $\text{Mg}^{+\bullet}$  (cf equation 39), both ethyl isocyanate and ethyl isothiocyanate yield products from attack of the N–C single bond (equations 57 and 58). The ethyl isothiocyanate complex also yields  $\text{MgS}$  via equation 59. The photodissociation spectrum of the ethyl thiocyanate isomer was also examined and gave the products shown in equations 60–62. Thus each isomer gives a unique ionic product [ $\text{MgS}^{+\bullet}$  for ethyl isothiocyanate (equation 59) vs  $\text{MgNC}^+$  for ethyl thiocyanate (equation 62)] which allows their distinction. Finally, the  $\text{Mg}(\text{ethyl isocyanate})_n^{+\bullet}$  complexes simply undergo solvent evaporation for  $n = 2$  and 3 (cf equation 52).





The  $\text{Mg}^{+\bullet}$  complexes of cytosine, thymine and uracil are the most complex system studied via photodissociation spectroscopy to date<sup>97,98</sup>. A complication for these systems is that these nucleobases can exist in various tautomeric forms and that complexation of a metal can change the stability order of the tautomers. DFT calculations located four tautomeric  $\text{Mg}(\text{cytosine})^{+\bullet}$  complexes, and three of these (**29**, **30**, and **31**) were suggested to be responsible for the four reactive photofragment ions **32**–**35** observed at a wavelength of 360 nm (Scheme 4)<sup>97</sup>. Related photofragmentation reactions were observed for the  $\text{Mg}(\text{thymine})^{+\bullet}$  and  $\text{Mg}(\text{uracil})^{+\bullet}$  complexes<sup>98</sup>.



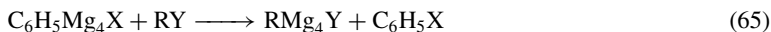
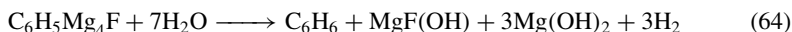
SCHEME 4

### C. Reactions of Magnesium Clusters with Organic Substrates

Klabunde and coworkers compared the reactivity of metal atoms with metal clusters (metal = magnesium and calcium) with  $\text{CH}_3\text{X}$  ( $\text{X} = \text{F}, \text{Cl}, \text{Br}$  and  $\text{I}$ ) under conditions of matrix isolation (Ar matrix)<sup>24, 25</sup>. UV-Vis spectroscopy was used to monitor the reactivity of the metal clusters to form organometallic cluster reagents (equation 63). The general metal reactivity trends were:  $\text{Ca}_x$  ( $x > 2$ )  $\approx \text{Ca}_2 > \text{Mg}_x$  ( $x > 4$ )  $\approx \text{Mg}_4 > \text{Mg}_3 \approx \text{Mg}_2 > \text{Ca} > \text{Mg}$ . The substrates reacted in the order:  $\text{CH}_3\text{I} > \text{CH}_3\text{F} > \text{CH}_3\text{Br} > \text{CH}_3\text{Cl}$ . The enhanced reactivity of the clusters is consistent with the early theoretical calculations, which predicted a greater stability of  $\text{CH}_3\text{Mg}_2\text{X}$  relative to the formation of  $\text{CH}_3\text{MgX}$  and an isolated Mg atom<sup>99</sup>.

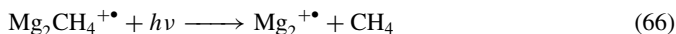


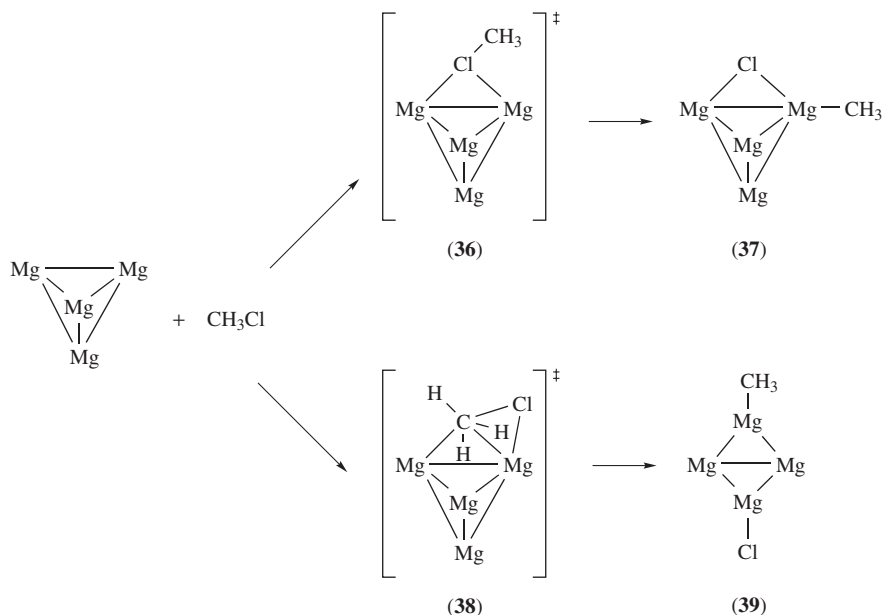
Although cluster Grignard reagents are the proposed products of equation 63 (where Metal = Mg), the first spectroscopic evidence for the formation of the  $\text{PhMg}_4\text{X}$  cluster Grignard reagents ( $\text{X} = \text{F}, \text{Cl}$  and  $\text{Br}$ ) involved the assignment of their molecular weights via the formation of their protonated ions under conditions of MALDI MS<sup>5</sup>. These assignments were consistent with the stoichiometries of the hydrolysis reaction (equation 64). The cluster Grignard reagents undergo a number of interesting reactions including transmetalation (equation 65)<sup>100, 101</sup> and catalysis of the isomerization of allylbenzene to  $\beta$ -methylstyrene<sup>102</sup>.



Two studies have examined the formation of  $\text{CH}_3\text{Mg}_n\text{Cl}$  cluster Grignard reagents via the use of theoretical methods<sup>103, 104</sup>. Two different competing pathways were located for the reaction of the tetrahedral  $\text{Mg}_4$  cluster with  $\text{CH}_3\text{Cl}$  (Scheme 5). The first involves formation of the transition state **36**, which yields the cluster **37**, in which the tetrahedral  $\text{Mg}_4$  framework is maintained. The second involves the formation of the transition state **38**, which yields the cluster **39**, in which the  $\text{Mg}_4$  framework is rhombic instead. Interestingly, while the activation energy for the first pathway is lower (18.4 kcal mol<sup>-1</sup> for **36** versus 24.8 kcal mol<sup>-1</sup> for **38**) the most stable product is that for the second pathway (−48.2 kcal mol<sup>-1</sup> for **37** versus −51.5 kcal mol<sup>-1</sup> for **39**)<sup>92</sup>. Jasien and Abbondondola found that the activation energy for transition states related to **38** decrease as the size of the magnesium cluster increases, with the lowest activation energy being 9.8 kcal mol<sup>-1</sup> for the  $\text{Mg}_{21}$  cluster<sup>103</sup>.

The sole gas-phase study on a cationic magnesium cluster examined the photodissociation spectrum of the  $\text{Mg}_2(\text{CH}_4)^{+\bullet}$  complex<sup>105</sup>.  $\text{Mg}_2^{+\bullet}$  is only a minor product (equation 66) while  $\text{Mg}^{+\bullet}$  is the main ionic fragment and may arise via either of the processes shown in equations 67 and 68. The latter reaction is predicted to only be slightly more endothermic.





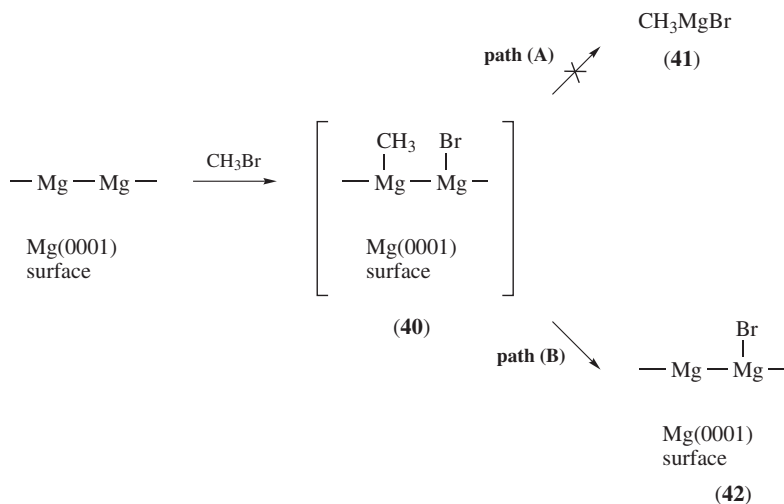
SCHEME 5

#### D. Reactions of Magnesium Surfaces and Films with Organic Substrates

The formation of Grignard reagents is a complex heterogeneous process that involves surface chemistry, interfacial chemistry and solution-phase chemistry. Since this topic has been comprehensively reviewed<sup>106,107</sup>, here the chemistry of well-defined, clean Mg surfaces and Mg thin films is briefly discussed. Using X-ray photoelectron spectroscopy, Abreu and coworkers have examined the nature of the surface film formed when a clean Mg metal surface is subjected to pretreatments that simulate exposure to ambient environments<sup>108</sup>. They noted that as-received Mg metal contains a surface covered by a film mainly composed of magnesium hydroxide with smaller quantities of magnesium bicarbonate. These surface films slow down Grignard formation since the alkyl halide must bypass the surface hydroxide and bicarbonate sites to interact with Mg metal site(s). Nuzzo and Dubois used a Mg(0001) single-crystal surface to examine the chemisorption and subsequent decomposition of MeBr<sup>109</sup>. They found evidence for the formation of a surface bromide and gas-phase ethane. Although stable surface methyls were not observed even at  $-150^\circ\text{C}$ , they suggested the mechanistic picture in Scheme 6, in which cleavage of the C–Br bond yields **40**. Rather than form the Grignard, **41**, the surface bromide **42** is formed. The role of surface modification was also examined. For example, while co-adsorbed dimethyl ether does not perturb the reactivity pattern, formation of either a thin surface bromide or a surface oxide passivates the surface to further reaction under the ultra-high-vacuum conditions of the experiments.

Gault and coworkers have used a specially constructed chamber interfaced to a mass spectrometer to examine the reactions of organic substrates with magnesium films<sup>110–114</sup>. In contrast to the chemistry of the pristine Mg(0001) surface, Gault found that alkyl halides were adsorbed irreversibly on Mg films to ultimately yield solid dull films of the organomagnesium 'RMgX' (R = Et, Me<sub>2</sub>CH, *n*-Pr, *n*-Bu; X = Br, Cl)<sup>110</sup>. These





SCHEME 6

films were soluble in diethyl ether and underwent all the reactions of solvated Grignard reagents. For example, the 'EtMgBr' film liberated  $\text{C}_2\text{H}_6$  on treatment with water or alcohols and underwent the Grignard reaction with adsorbed carbonyl compounds. In separate experiments, Gault<sup>110</sup> and Lefrancois and Gault<sup>111</sup> examined the decomposition of the organomagnesium films at high temperature. For example, 'EtMgBr' decomposed at  $180^\circ\text{C}$  with liberation of a mixture of saturated and unsaturated hydrocarbons. Ethylene was the main constituent of the unsaturated fraction along with butenes and hexenes. All hydrocarbons were formed initially, thus ruling out a chain reaction mechanism involving  $\text{CH}_2=\text{CH}_2$ . Decomposition of the 'EtMgBr' film in the presence of propene gave appreciable amounts of pentenes and some heptenes as immediate products, suggesting reactions between olefins and 'RMgX' or radicals produced during decomposition.

In a series of three papers, Gault<sup>112,113</sup> and Choplin and Gault<sup>114</sup> used the same apparatus to examine the self-hydrogenation of alkynes and dienes of Mg films. In the first report, Gault noted that when either 1-alkynes, 2-alkynes or 1,2-dienes are allowed to interact with a magnesium film in the absence of co-adsorbed hydrogen, the gaseous reaction products consisted of alkenes as well as isomers of the starting material<sup>112</sup>. In follow-up studies, the species which remained adsorbed on the Mg during the reaction were desorbed by quenching reactions with  $\text{D}_2\text{O}$  and characterized as the deuteriated hydrocarbons. The structures of these hydrocarbons and the variation in their D distribution with temperature and reaction time are consistent with a mechanism consisting of two parallel processes:

(i) The dehydrogenation to the metallated species **43** which is stable at 373 K but is further dehydrogenated to the carbide, **44**, at 423 K. Indirect evidence for these intermediates was gained via reaction with  $\text{D}_2\text{O}$ , which yielded  $\text{d}_1$  and  $\text{d}_4$  propyne (Scheme 7).

(ii) The two-step hydrogenation of the reactant to propene. A possible mechanism to rationalize the experimental data is shown in Scheme 8. Reaction with a portion of the film containing magnesium hydride moieties, **45** (formed via processes related to Scheme 7), yields intermediate **46**. The desorption of propene can occur via either heating of **46** (which presumably involves a reductive elimination) or via reaction of **46** with  $\text{D}_2\text{O}$ . By



### 1. Fragmentation reactions of $\text{Mg}(\text{L})_n^{2+}$ complexes

Kebarle and coworkers carried out some of the pioneering studies in this area by subjecting metal salts to ESI conditions using various solvents/ligands,  $\text{L}^{115}$ . In addition, Stace and coworkers have developed an alternative technique whereby solvated/ligated Mg atoms are subject to electron impact<sup>116–122</sup>. Both these techniques provide fundamental information on the inherent kinetic stability of  $\text{Mg}(\text{L})_n^{2+}$  complexes with respect to fragmentation. In addition, Kebarle and coworkers have determined the sequential binding energies of water, acetone and *N*-methylacetamide to  $\text{Mg}^{2+}$ <sup>123</sup>. Table 1 lists the stability of a range of  $\text{Mg}(\text{L})_n^{2+}$  complexes as a function of the ionization energy of the ligand. The criterion for stability is a kinetic one and relates to the smallest cluster number ( $n$ ) for which a stable doubly charged cluster,  $\text{Mg}(\text{L})_n^{2+}$ , is observed (defined as  $n_{\min}$ ). Since the second ionization energy of Mg is 15.03 eV, it is not surprising that  $n_{\min} > 1$  for most ligands.

Several studies have not only examined  $n_{\min}$ , but have also identified the key fragmentation channels of  $\text{Mg}(\text{L})_n^{2+}$  complexes as a function of both the ligand structure as well as the number of ligands,  $n$ . The fragmentation channels can be divided into 5 main classes of reactions: loss of a neutral ligand (equation 69); metal charge reduction via electron transfer which yields the two complementary ions  $\text{Mg}(\text{L})_{n-1}^{+\bullet}$  and  $\text{L}^{+\bullet}$  (equation 70); charge reduction via interligand proton transfer which yields the two complementary ions  $\text{Mg}(\text{L})_{n-2}(\text{L} - \text{H})^+$  and  $[\text{L} + \text{H}]^+$  (equation 71); ligand fragmentation via neutral loss (equation 72); and ligand fragmentation via loss of a cation (equation 73). Which fragmentation channel dominates depends upon both the type of ligand and its properties (such as ionization energy, which influences reaction 70) as well as the number of ligands<sup>101</sup>. A key difference in the stability and fragmentation reactions of the related  $\text{Ca}(\text{L})_n^{2+}$  complexes is that the lower second ionization energy of Ca allows ions with

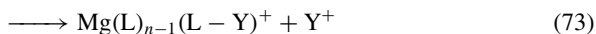
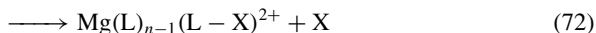
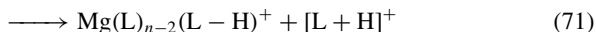
TABLE 1. Stability of  $\text{Mg}(\text{L})_n^{2+}$  complexes in the gas phase as a function of ligand ionization energy (IE)

Ligand, L =	IE (eV) <sup>a,b</sup>	$n_{\min}$	Reference
CO <sub>2</sub>	13.78	2	122
H <sub>2</sub> O	12.62	2	122
CH <sub>3</sub> CN	12.20	1	122
Methanol	10.84	2	122
Ethanol	10.48	3	122
<i>n</i> -Propanol	10.22	3	122
Ammonia	10.07	2	122
Acetone	9.70	3	122
Acetamide	9.69	2	129
2-Butanone	9.52	2	122
Diethyl ether	9.51	2	122
Tetrahydrofuran	9.40	2	122
2-Pentanone	9.38	2	122
Pyridine	9.26	2	122
Dimethyl sulfoxide	9.10	1	126
<i>n</i> -Butylamine	8.73	2	122
Pyrrole	8.21	2	122
Pentan-2,4-dione	8.85	1	122
4-Hydroxy-4-methylpentan-2-one	unknown	1	128
Ethylene diamine	8.6	—	122

<sup>a</sup> IE is defined as:  $\text{M} \rightarrow \text{M}^{+\bullet} + e^-$ ;  $\Delta H = \text{IE}$ .

<sup>b</sup> All IEs are taken from <http://webbook.nist.gov>.

low  $n$  to become more kinetically stable with respect to electron transfer (equation 70).



Under conditions of CID,  $\text{Mg}(\text{L})_n^{2+}$ , where  $\text{L}$  = methanol, fragment via several different pathways<sup>120</sup>. For larger clusters (e.g.  $n = 10$ ), methanol loss dominates (equation 69). At  $n = 4$ , charge transfer products appear (equation 70) together with products from other fragment channels. The  $n = 3$  cluster fragments via reactions that reduce the overall charge state to +1: charge transfer (equation 70), proton transfer (equation 71) and two ligand fragmentation channels [equation 71, where  $(\text{L}-\text{Y}) = \text{OH}$  and  $\text{HJ}$ ].  $\text{Mg}(\text{L})_n^{2+}$  clusters from larger alcohols such as  $n$ -propanol are less stable and undergo charge transfer more readily<sup>121</sup>. Recent theoretical calculations on  $\text{Mg}(\text{CH}_3\text{OH})^{2+}$  suggest that while there are three exothermic reaction channels (charge transfer, equation 70, and ligand fragmentation, equation 73, to form  $\text{MgOH}^+$  and  $\text{MgH}^+$ ), this cluster ion should be kinetically stable due to significant barriers to all three reaction channels<sup>124</sup>.

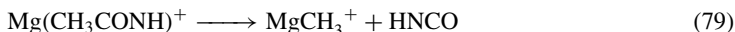
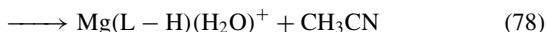
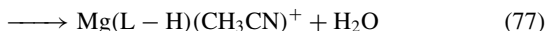
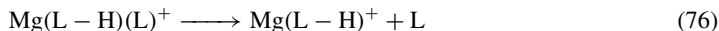
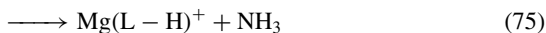
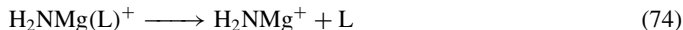
When  $\text{L}$  is the commonly used solvent THF, a particularly stable  $\text{Mg}(\text{THF})_4^{2+}$  ion is formed in the gas phase.  $\text{Mg}(\text{THF})_3^{2+}$  undergoes ligand fragmentation via neutral loss (equation 72,  $\text{X} = \text{C}_3\text{H}_6$ ) to yield  $\text{Mg}(\text{THF})_2(\text{CH}_2\text{O})^{2+}$ <sup>119</sup>. There are interesting differences in the fragmentation of the  $\text{CH}_3-\text{X}$  bonds in the  $\text{Mg}(\text{L})_n^{2+}$  complexes of acetonitrile and dimethyl sulfoxide. Thus while the acetonitrile clusters tend to fragment via heterolytic cleavage to yield  $\text{MgCN}(\text{L})_{n-1}^+$  and  $\text{CH}_3^+$  (equation 73)<sup>125</sup>, the dimethyl sulfoxide fragment via  $\text{CH}_3$  and  $\text{CH}_4$  loss (equation 72)<sup>126</sup>. Destruction of the aromatic ring is observed for the  $\text{Mg}(\text{L})_n^{2+}$  complexes of pyridine<sup>127</sup>. For example,  $\text{MgCN}(\text{L})_{n-1}^+$  and  $\text{C}_4\text{H}_5^+$  formation is observed (equation 73). The  $\text{Mg}(\text{L})_n^{2+}$  complexes of 4-hydroxy-4-methylpentan-2-one undergo a range of ligand fragmentation including C–C bond cleavage via a retro-aldol reaction<sup>128</sup>.

One of the few studies to have combined experiment and theory has provided detailed mechanistic insights into the fragmentation reactions of the  $\text{Mg}(\text{L})_n^{2+}$  complexes of acetamide<sup>129</sup>. The  $\text{Mg}(\text{L})_3^{2+}$  complex fragments via neutral ligand loss (equation 69) in competition with interligand deprotonation (equation 71). The chemistry of the latter product,  $\text{Mg}(\text{L}-\text{H})(\text{L})^+$ , is described further below. The  $\text{Mg}(\text{L})_2^{2+}$  complex fragments solely via heterolytic amide bond cleavage (equation 71) to yield  $\text{Mg}(\text{NH}_2)(\text{L})^+$  and  $\text{CH}_3\text{CO}^+$ . DFT calculations on the  $\text{Mg}(\text{L})_2^{2+}$  complex reveal that neutral ligand loss (equation 69) is much more endothermic than interligand deprotonation (equation 71).

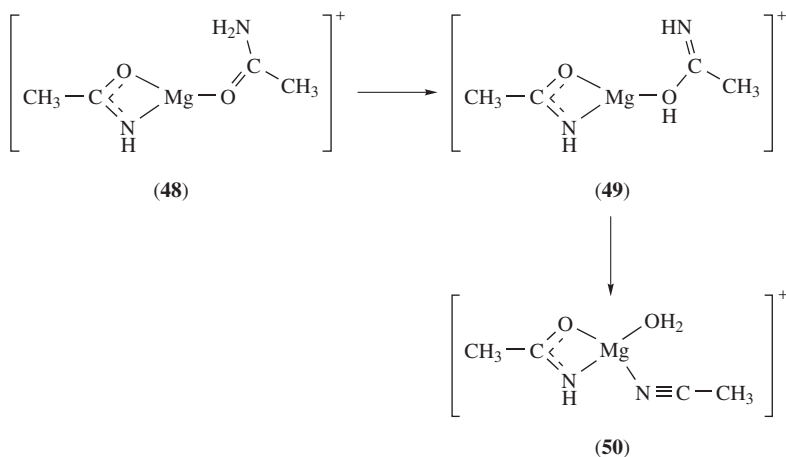
## 2. Fragmentation reactions of $\text{XMg}(\text{L})_n^+$ complexes (where $\text{X} = \text{an anionic ligand}$ )

Surprisingly few studies have thoroughly investigated the gas-phase chemistry of  $\text{XMg}(\text{L})_n^+$  complexes. An exception is the combined experimental and theoretical study on the fragmentation reactions of the  $\text{XMg}(\text{L})^+$  (where  $\text{X} = \text{L}-\text{H}$  and  $\text{NH}_2$ ) and  $\text{Mg}(\text{L}-\text{H})^+$  complexes of acetamide ( $\text{L} = \text{CH}_3\text{CONH}_2$ )<sup>129</sup>. The  $\text{H}_2\text{NMg}(\text{L})^+$  complex fragments via ligand loss (equation 74) and  $\text{NH}_3$  loss (equation 75). The  $\text{Mg}(\text{L}-\text{H})(\text{L})^+$  complex fragments via ligand loss (equation 76), water (equation 77) and acetonitrile loss

(equation 78). Finally, the  $\text{Mg}(\text{L}-\text{H})^+$  complex fragments via losses of  $\text{HNCO}$  (equation 79),  $\text{MgO}$  (equation 80) and acetonitrile loss (equation 81).

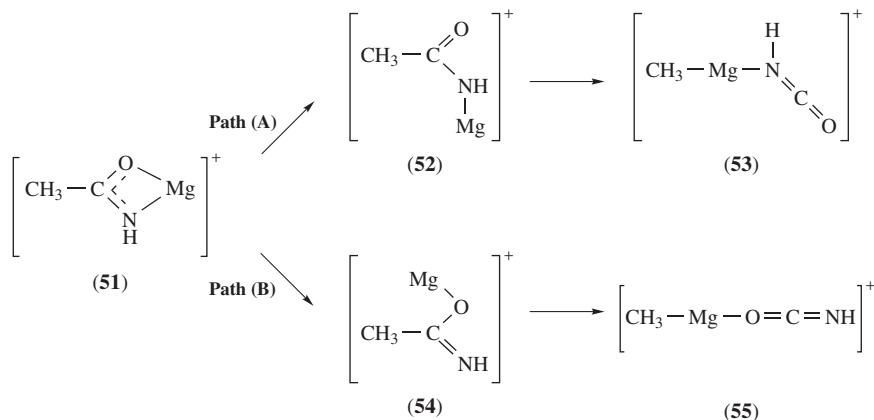


DFT calculations on the  $\text{Mg}(\text{L}-\text{H})(\text{L})^+$  complex reveal how water and acetonitrile can be lost (Scheme 9). Thus intramolecular proton transfer tautomerizes the neutral acetamide ligand in **48** into the hydroxyimine form in **49**, which can then dissociate via another intramolecular proton transfer to yield the four-coordinate adduct **50**, which now contains both water and acetonitrile ligands. It is this complex that is the direct precursor to water and acetonitrile loss. Note that the reaction shown in Scheme 9 is a retro-Ritter reaction and involves fragmentation of the neutral rather than the anionic acetamide ligand, which is a bidentate spectator ligand.



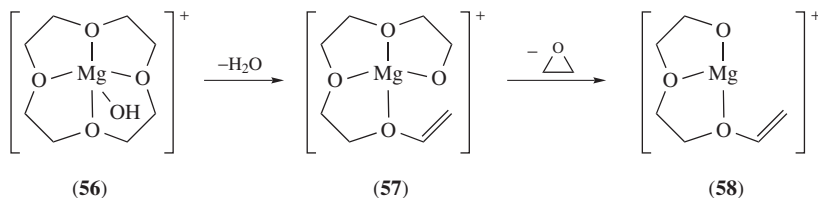
SCHEME 9

DFT calculations on the  $\text{Mg}(\text{L}-\text{H})^+$  complex also reveal how  $\text{HNCO}$  might be lost (Scheme 10). Thus the bidentate interaction of the acetamide ligand with  $\text{Mg}$  in **51** must be disrupted to yield either of the monodentate structures **52** or **54**. These intermediates can insert into the  $\text{CH}_3-\text{C}$  bond via four-centered transition states to yield the organometallic ions **53** or **55**, which can then lose  $\text{HNCO}$  to form  $\text{MgCH}_3^+$ . The DFT calculations reveal that path (A) of Scheme 10 is kinetically favored.



SCHEME 10

Wu and Brodbelt have studied the gas-phase fragmentation reactions of  $\text{HOMg(L)}^+$  complexes of crown ethers and glymes<sup>130</sup>. A common loss involves units of  $\text{C}_2\text{H}_4\text{O}$ , which can either directly occur from the precursor ion, or can be triggered by an initial interligand reaction between  $\text{HO}^-$  and L. This latter reaction is illustrated in Scheme 11 for the complex of 12-Crown-4. Thus loss of  $\text{H}_2\text{O}$  from the initial adduct **56** yields the ring-opened complex **57**, which contains a coordinated alkoxide moiety, which can then lose an epoxide to form the related complex **58**.

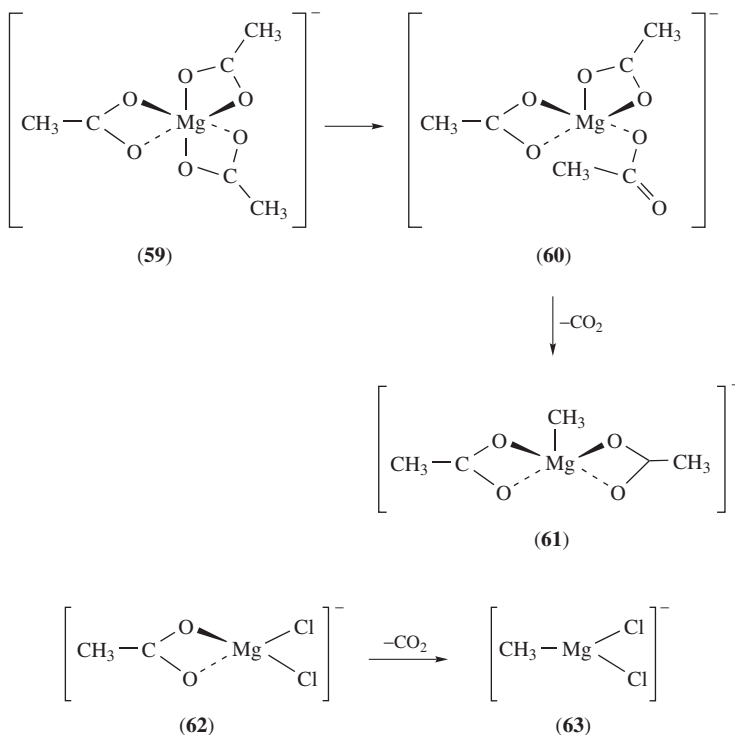
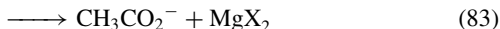
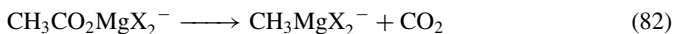


SCHEME 11

### 3. Fragmentation reactions of $\text{Mg(X)}_3^-$ complexes

The final class of  $\text{Mg(II)}$  ions which can readily be formed via ESI MS involves magnesate anions, which are formed by coordinating an anion to a  $\text{Mg(II)}$  salt. The gas-phase fragmentation reactions of  $\text{CH}_3\text{CO}_2\text{MgX}_2^-$  (where  $\text{X} = \text{Cl}$  and  $\text{CH}_3\text{CO}_2$ ) have been studied using a combination of CID experiments in a quadrupole ion trap in conjunction with DFT calculations<sup>131</sup>. Decarboxylation (equation 82) is the main reaction channel, with some acetate loss (equation 83) also being observed. DFT calculations reveal that the former reaction is less endothermic. The decarboxylation reactions yield the organomagnesates,  $\text{CH}_3\text{MgX}_2^-$ , and are reminiscent of the  $\text{HNCO}$  loss described above (equation 79 and Scheme 10). The DFT calculations also provide insights into the coordination modes of reactants and products for the decarboxylation reactions (Scheme 12). Generally, the carboxylate ligands bind in a bidentate fashion, while the chloride ions are monodentate.

When  $X = \text{CH}_3\text{CO}_2$ , the ground-state reactant structure is six-coordinate, **59**. The 'reactive' geometry for decarboxylation, **60**, requires cleavage of one of the  $\text{Mg}-\text{O}$  bonds. The product, **61**, is five-coordinate. In contrast, when  $X = \text{Cl}$ , the three-coordinate product, **63**, is directly formed via decarboxylation of the four-coordinate reactant **62**.



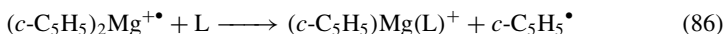
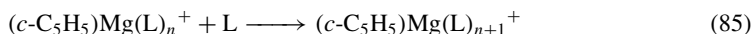
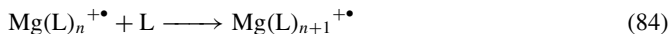
SCHEME 12

Related decarboxylation reactions have been used to synthesize magnesium hydride anions from formate anions<sup>132</sup> and organocalcium, organobarium and organostrontium metallates<sup>133</sup>.

### III. BIMOLECULAR REACTIONS OF ORGANOMAGNESIUM IONS IN THE GAS PHASE

Relatively few studies have examined the bimolecular reactivity of organomagnesium species in the gas phase. In terms of organomagnesium ions, this has largely been due to the fact that it has been difficult to generate organomagnesium cations via traditional electron ionization (EI). Not surprisingly, the bimolecular chemistry of organomagnesium cations has focused on the chemistry of  $(\textit{c}\text{-C}_5\text{H}_5)\text{Mg}^+$  and  $(\textit{c}\text{-C}_5\text{H}_5)_2\text{Mg}^{+\bullet}$ , which are

readily formed via EI on magnesocene. Bohme and coworkers have compared the reactivity of  $\text{Mg}^{+\bullet}$ ,  $(c\text{-C}_5\text{H}_5)\text{Mg}^+$  and  $(c\text{-C}_5\text{H}_5)_2\text{Mg}^{+\bullet}$  towards alkanes<sup>46</sup> and a range of small inorganic ligands ( $\text{H}_2$ ,  $\text{NH}_3$ ,  $\text{H}_2\text{O}$ ,  $\text{N}_2$ ,  $\text{CO}$ ,  $\text{NO}$ ,  $\text{O}_2$ ,  $\text{CO}_2$ ,  $\text{N}_2\text{O}$  and  $\text{NO}_2$ )<sup>134,135</sup>. As noted in Section II.B.1,  $\text{Mg}^{+\bullet}$  reacts with alkanes via ligand addition (equation 16). Single ligation of  $\text{Mg}^{+\bullet}$  with  $(c\text{-C}_5\text{H}_5)^{\bullet}$  substantially enhances the efficiency of subsequent ligation. Thus ligation is rapid with all the hydrocarbons investigated. In contrast, no reaction was observed between the alkanes and the full-sandwich magnesocene cation,  $(c\text{-C}_5\text{H}_5)_2\text{Mg}^{+\bullet}$ .  $\text{Mg}^{+\bullet}$  was unreactive towards all the inorganic ligands except with ammonia, which was found to sequentially add up to 5 ligands (equation 84). The structures of the  $\text{Mg}(\text{NH}_3)_n^{+\bullet}$  ions ( $n = 1\text{--}4$ ) were probed via DFT calculations. In all cases, structures in which the  $\text{NH}_3$  ligands are directly coordinated to the  $\text{Mg}^{+\bullet}$  were more stable than other structures (such as those in which one  $\text{NH}_3$  ligand is hydrogen bonded to a coordinated  $\text{NH}_3$  ligand). Once again, the singly ligated  $(c\text{-C}_5\text{H}_5)\text{Mg}^+$  complex substantially enhances the efficiency of ligation by inorganic ligands (equation 85). Thus initial ligation is rapid with all ligands except  $\text{H}_2$ ,  $\text{N}_2$  and  $\text{O}_2$ . The 'full-sandwich' magnesocene radical cation,  $(c\text{-C}_5\text{H}_5)_2\text{Mg}^{+\bullet}$ , does not undergo ligation. Instead, fast bimolecular ligand-switching reactions occur with  $\text{NH}_3$  and  $\text{H}_2\text{O}$ , suggesting that these two ligands bind more strongly to  $(c\text{-C}_5\text{H}_5)\text{Mg}^+$  than does  $c\text{-C}_5\text{H}_5^{\bullet}$  itself (equation 86).

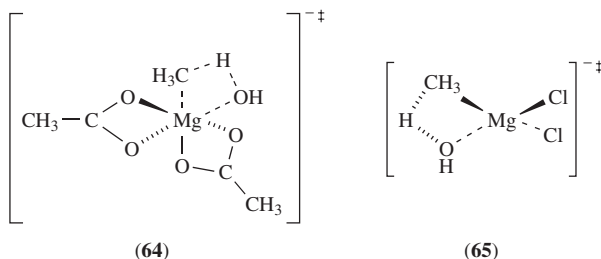


As noted in a previous review<sup>136</sup>, one of the benefits of the quadrupole ion trap mass spectrometer is that ions are stored in the quadrupole ion trap and can be manipulated to undergo multiple stages of mass spectrometry associated with different types of reactions. Thus CID can be used to 'synthesize' organometallic ions via CID and their gas-phase reactivity can then be examined via subsequent ion-molecule reactions. We have used the decarboxylation reaction (equation 82) to synthesize organoalkaline earths,  $[\text{CH}_3\text{MetalX}_2]^-$ , and have studied their acid-base reactions with neutral acids,  $\text{AH}$  (equation 87), to establish how reactivity is controlled by the auxiliary ligand<sup>131</sup>, the nature of the metal<sup>133</sup> and the substrate,  $\text{AH}$ <sup>131</sup>. In our first study on the organomagnesates  $\text{CH}_3\text{MgX}_2^-$  ( $\text{X} = \text{Cl}$  and  $\text{O}_2\text{CCH}_3$ ) we examined the influence of the auxiliary ligand and the substrate on reactivity<sup>131</sup>. We found that these  $\text{CH}_3\text{MgX}_2^-$  ions exhibit some of the reactivity of Grignard reagents, reacting with acids,  $\text{AH}$ , via addition with concomitant elimination of methane to form  $\text{AMgX}_2^-$  ions (equation 87,  $\text{Metal} = \text{Mg}$ ), in direct analogy to the acid-base reactions of Grignard reagents. Kinetic measurements, combined with DFT calculations, provided clear evidence for an influence of the auxiliary ligand on reactivity of the organomagnesates  $[\text{CH}_3\text{MgX}_2]^-$ . Thus when  $\text{X} = \text{O}_2\text{CCH}_3$ , reduced reactivity towards water was observed. The DFT calculations suggest that this may arise from the bidentate binding mode of acetate, which induces overcrowding of the  $\text{Mg}$  coordination sphere in the transition state relative to the chloride organomagnesate (compare **64** and **65** of Scheme 13). Interestingly, there is a report in the literature on the enhanced selectivity (i.e. reduced reactivity) of solution-phase Grignard reagents processing carboxylate ligands instead of the traditional halides<sup>137</sup>.



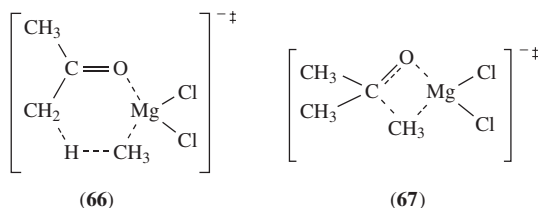
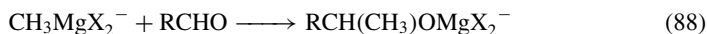
The substrate also plays a key role in the reactivity of the  $[\text{CH}_3\text{MgX}_2]^-$  ions. This is illustrated dramatically for the reaction of aldehydes containing enolisable protons, which reacted via enolisation (equation 87), rather than via the Grignard reaction (equation 88).





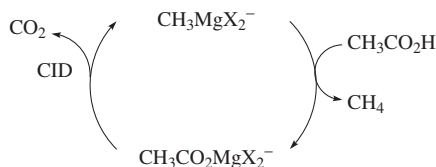
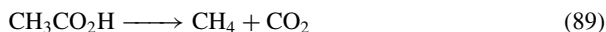
SCHEME 13

This is consistent with DFT calculations on  $[\text{CH}_3\text{MgCl}_2]^-$ , which reveal that the six-centered transition state for the enolisation reaction **66** is entropically favored over the four-centered transition state for the Grignard reaction **67** (Scheme 14).



SCHEME 14

Interestingly, when acetic acid is the substrate, the  $\text{CH}_3\text{MgX}_2^-$  ions (where  $\text{X} = \text{Cl}$  or  $\text{CH}_3\text{CO}_2$ ) complete a catalytic cycle for the decarboxylation of acetic acid (equation 89, Scheme 15)<sup>131</sup>. The first step is a metathesis reaction, in which a  $\text{CH}_3$  ligand is switched for a carboxylato ligand (equation 87, Scheme 15). The second step is the rate-determining step (equation 82, Scheme 15) as it requires activation (under CID conditions) to induce decarboxylation of the magnesium acetate anion  $\text{CH}_3\text{CO}_2\text{MgX}_2^-$ , to reform the organometallic catalyst  $\text{CH}_3\text{MgX}_2^-$ . A similar catalytic cycle has been observed for decarboxylation of formic acid<sup>132</sup>.



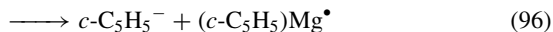
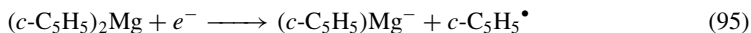
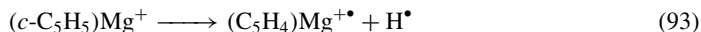
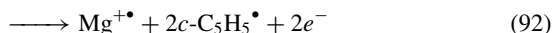
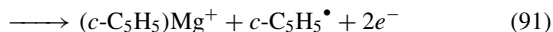
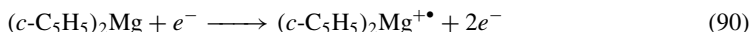
SCHEME 15

Each of the organoalkaline earths  $[\text{CH}_3\text{Metal}(\text{O}_2\text{CCH}_3)_2]^-$  reacts with water via addition with concomitant elimination of methane to form the metal hydroxide  $[\text{HOMetal}(\text{O}_2$

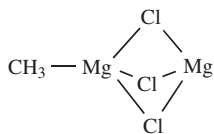
$\text{CCH}_3)_2]^-$  ions (equation 87), with a relative reactivity order of:  $[\text{CH}_3\text{Ba}(\text{O}_2\text{CCH}_3)_2]^- \approx [\text{CH}_3\text{Sr}(\text{O}_2\text{CCH}_3)_2]^- > [\text{CH}_3\text{Ca}(\text{O}_2\text{CCH}_3)_2]^- > [\text{CH}_3\text{Mg}(\text{O}_2\text{CCH}_3)_2]^-$ <sup>133</sup>. DFT calculations on the reaction exothermicities for these reactions generally supported the reaction trends observed experimentally, with  $[\text{CH}_3\text{Mg}(\text{O}_2\text{CCH}_3)_2]^-$  being the least reactive.

#### IV. UNIMOLECULAR REACTIONS OF ORGANOMAGNESIUM IONS IN THE GAS PHASE

As noted in the introduction, few studies have examined the mass spectra of organomagnesium compounds. Of these, there are only three that have examined the unimolecular fragmentation reactions of organomagnesium ions. Under conditions of electron ionization, magnesocene yields the following ions in the positive ionization mode: the parent radical cation (equation 90), the monoligated ('half-sandwich') cation (equation 91) and the bare magnesium ion (equation 92)<sup>4</sup>. Note that Bohme and coworkers have studied the bimolecular reactivity of all these ions as described in Sections II and III above. The gas-phase fragmentation reactions of  $(c\text{-C}_5\text{H}_5)\text{Mg}^+$  have been studied using a combination of metastable and CID experiments as well as DFT calculations<sup>138</sup>. Under metastable conditions,  $(c\text{-C}_5\text{H}_5)\text{Mg}^+$  fragments via loss of a H atom (equation 93) and  $c\text{-C}_5\text{H}_5^\bullet$  (equation 94). Collisional activation induces further fragmentation, resulting in the formation of  $(\text{C}_3\text{H}_3)\text{Mg}^+$  and  $(\text{C}_3\text{H}_2)\text{Mg}^+$ . Electron ionization of magnesocene in the negative ionization mode yields the monoligated ('half-sandwich') anion (equation 95) and the cyclopentadienyl anion (equation 96)<sup>4</sup>.



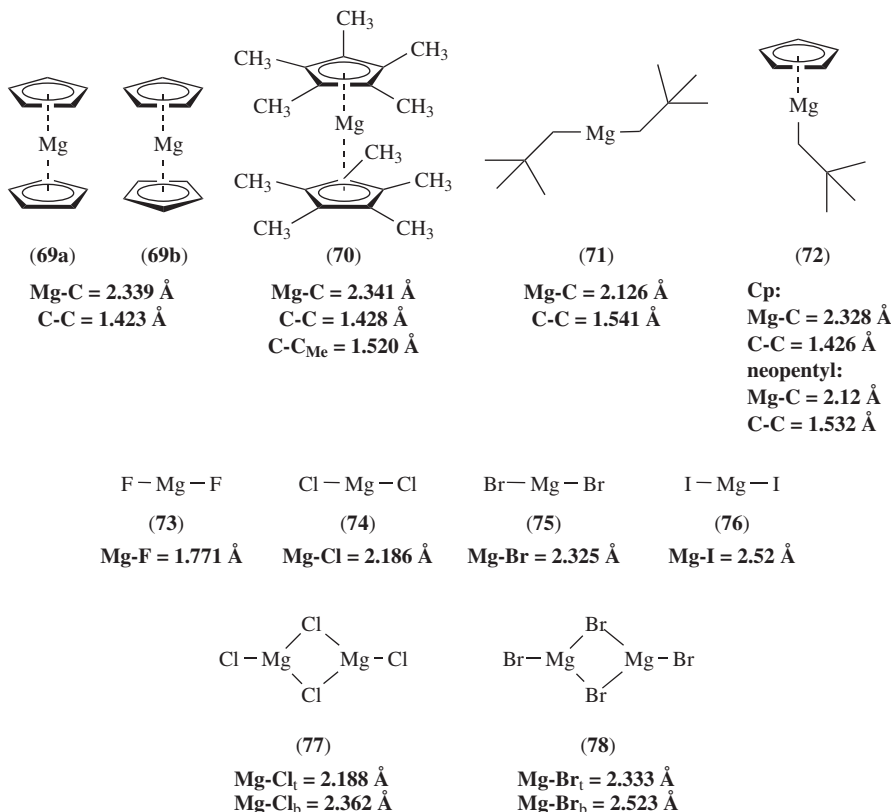
The only study to have examined the composition and fragmentation reactions of a Grignard reagent via MS is that of Sakamoto and coworkers, who used a combination of coldspray ionization in conjunction with tandem mass spectrometry to evaluate the types of ions formed from a THF solution of ' $\text{CH}_3\text{MgCl}$ '<sup>6</sup>. They noted the formation of  $[\text{CH}_3\text{Mg}_2\text{Cl}_3(\text{THF})_n\text{-H}]^+$  (where  $n = 4\text{--}6$ ) under coldspray ionization. When  $[\text{CH}_3\text{Mg}_2\text{Cl}_3(\text{THF})_6\text{-H}]^+$  was subjected to CID, an envelope of  $[\text{CH}_3\text{Mg}_2\text{Cl}_3(\text{THF})_n\text{-H}]^+$  product ions was observed arising from sequential losses of up to 4 THF solvent molecules. Based on these results in conjunction with considerations of X-ray crystal structures of a range of organomagnesiums, structure **68** was suggested to be the core of the ' $\text{CH}_3\text{MgCl}$ ' Grignard in THF solution.



(68)

## V. STRUCTURES OF ORGANOMAGNESIUMS AND MAGNESIUM HALIDES IN THE GAS PHASE

Gas-phase electron diffraction (GED) has been used to gain insights into the gas-phase structures of a range of inorganic and organometallic compounds. Since the area has been reviewed on several occasions<sup>139–145</sup>, here the structures of key organomagnesiums<sup>146–149</sup> and magnesium halides<sup>150–155</sup> are briefly described. Scheme 16 shows the structures of all organomagnesium and magnesium halides studied via gas-phase electron diffraction to date, and includes key bond lengths. A key feature is that all monomers (**71**, **73–76**) are linear. The GED data require modeling of the structure to determine the best fit. For magnesocene, the best fit is for the eclipsed structure **69a** rather than the staggered structure, **69b**<sup>146</sup>. Permethylation of magnesocene results in a slight elongation of the Mg–C and ring C–C bonds (compare **69** and **70**) while replacement of a Cp ring with a neopentyl group decreases the Mg–Cp bond (compare **69** and **72**). The GED of the halides **73–76** were first studied 50 years ago<sup>152, 154</sup>, and their structures have been refined over the years by further experimental and theoretical work. The most recent studies of Hargittai and coworkers on  $\text{MgCl}_2$  (**74**)<sup>150</sup> and  $\text{MgBr}_2$  (**75**)<sup>151</sup> were carried out on a GED instrument interfaced with a mass spectrometer, which allowed the vapor constitution to



SCHEME 16

be analyzed via MS. It was found that the vapor consisted of over 10% of the dimers, **77** and **78**. By carefully modeling the GED data, the structures of both the monomers and dimers were determined. The latter are interesting structures, directly relevant to the Schlenk equilibrium. Note that in both cases, the terminal Mg–X bond lengths (Mg–X<sub>t</sub>) are shorter than the bridging Mg–X bond lengths (Mg–X<sub>b</sub>). If the GED data do not take into account the presence of dimers, the Mg–X bond is overestimated. Thus the bond lengths for MgF<sub>2</sub> (**73**)<sup>155</sup> and MgI<sub>2</sub> (**76**)<sup>152</sup> shown in Scheme 16, which are derived from early data that were not modeled using dimer contributions, may be overestimates.

## VI. CONCLUDING REMARKS

An attempt has been made to bring together a seemingly disparate set of studies on the formation, reactions and structures of organomagnesium species in solvent-free environments. Although the spectroscopy of such species has not been discussed, there have been several studies on the ESR, IR, UV-Vis and laser-induced fluorescence of organomagnesium species in the gas-phase, in matrices and in helium nanodroplets. Interested readers are referred to a number of recent reviews and articles<sup>156–162</sup>. Finally, given the advances in mass spectrometry, further studies on the gas-phase reactivity of organomagnesium ions are eagerly anticipated.

## VII. ACKNOWLEDGMENTS

R.A.J.O thanks the Australian Research Council for financial support for studies on metal-mediated chemistry (Grant# DP0558430) and via the ARC Centres of Excellence program (ARC Centre of Excellence in Free Radical Chemistry and Biotechnology).

## VIII. REFERENCES

1. N. Goldberg and H. Schwarz, in *The Chemistry of Organic Silicon Compounds*, Vol. 2, Part 2, (Eds. Z. Rappoport and Y. Apeloig), Wiley, Chichester, 1998, pp. 1105–1142.
2. R. A. J. O'Hair, in *The Chemistry of Organophosphorus Compounds*, Vol. 4, (Ed. F. R. Hartley), Wiley, Chichester, 1996, pp. 731–765.
3. H. O. House, R. A. Latham and G. M. Whitesides, *J. Org. Chem.*, **32**, 2481 (1967).
4. G. M. Bejun and R. N. Compton, *J. Chem. Phys.*, **58**, 2271 (1973).
5. L. A. Tjurina, V. V. Smirnov, G. B. Barkovskii, E. N. Nikolaev, S. E. Esipov and I. P. Beletskaya, *Organometallics*, **20**, 2449 (2001).
6. S. Sakamoto, T. Imamoto and K. Yamaguchi, *Org. Lett.*, **3**, 1793 (2001).
7. K. Yamaguchi, *J. Mass Spectrom.*, **38**, 473 (2003).
8. E. E. Ferguson, B. R. Rowe, D. W. Fahey and F. C. Fehsenfeld, *Planet. Space. Sci.*, **29**, 479 (1981).
9. S. Petrie, *Icarus*, **171**, 199 (2004).
10. S. Petrie, *Environ. Chem.*, **2**, 25 (2005).
11. S. Petrie and R. C. Dunbar, *AIP Conf. Proc.*, **855**, 272 (2006).
12. S. Petrie, *Aust. J. Chem.*, **56**, 259 (2003).
13. S. Petrie and D. K. Bohme, *Top. Curr. Chem.*, **225**, 37 (2003).
14. R. C. Dunbar and S. Petrie, *AIP Conf. Proc.*, **855**, 281 (2006).
15. E. Peralez, J.-C. Negrel, A. Goursot and M. Chanon, *Main Group Met. Chem.*, **21**, 69 (1998).
16. W. H. Breckenridge, *J. Phys. Chem.*, **100**, 14840 (1996).
17. H.-J. Himmel, A. J. Downs and T. M. Greene, *Chem. Rev.*, **102**, 4191 (2002).
18. W. H. Breckenridge and H. Umemoto, *J. Chem. Phys.*, **81**, 3852 (1984).
19. J. G. McCaffrey, J. M. Parnis, G. A. Ozin and W. H. Breckenridge, *J. Phys. Chem.*, **89**, 4945 (1985).
20. T. M. Greene, D. V. Lanzisera, L. Andrews and A. J. Downs, *J. Am. Chem. Soc.*, **120**, 6097 (1998).

21. K. Mochida, K. Kojima and Y. Yoshida, *Bull. Chem. Soc. Jpn.*, **60**, 2255 (1987).
22. P. S. Skell and J. E. Girard, *J. Am. Chem. Soc.*, **94**, 5518 (1972).
23. B. S. Ault, *J. Am. Chem. Soc.*, **102**, 3480 (1980).
24. Y. Imizu and K. J. Klabunde, *Inorg. Chem.*, **23**, 3602 (1984).
25. K. J. Klabunde and A. Whetten, *J. Am. Chem. Soc.*, **108**, 6529 (1986).
26. S. R. Davis, *J. Am. Chem. Soc.*, **113**, 4145 (1991).
27. V. N. Solov'ev, G. B. Sergeev, A. V. Nemukhin, S. K. Burt and I. A. Topol, *J. Phys. Chem. A*, **101**, 8625 (1997).
28. W. D. Bare and L. Andrews, *J. Am. Chem. Soc.*, **120**, 7293 (1998).
29. A. A. Tulub, *Russ. J. Gen. Chem.*, **72**, 886 (2002).
30. A. V. Tulub, V. V. Porsev and A. A. Tulub, *Dokl. Phys. Chem.*, **398**, 241 (2004).
31. W. D. Bare, A. Citra, C. Trindle and L. Andrews, *Inorg. Chem.*, **39**, 1204 (2000).
32. V. N. Solov'ev, E. V. Polikarpov, A. V. Nemukhin and G. B. Sergeev, *J. Phys. Chem. A*, **103**, 6721 (1999).
33. C. A. Thompson and L. Andrews, *J. Am. Chem. Soc.*, **118**, 10242 (1996).
34. D. V. Lanzisera and L. Andrews, *J. Phys. Chem. A*, **101**, 9666 (1997).
35. A. J. McKinley and E. Karakyriakos, *J. Phys. Chem. A*, **104**, 8872 (2000).
36. Z. Huang, M. Chen, Q. Liu and M. Zhou, *J. Phys. Chem. A*, **107**, 11380 (2003).
37. P. L. Po and R. F. Porter, *J. Am. Chem. Soc.*, **99**, 4922 (1977).
38. G. I. Gellene, N. S. Kleinrock and R. F. Porter, *J. Chem. Phys.*, **78**, 1795 (1983).
39. P. B. Armentrout, *Top. Organomet. Chem.*, **4**, 1 (1999).
40. K. Eller and H. Schwarz, *Chem. Rev.*, **91**, 1121 (1991).
41. K. Eller, *Coord. Chem. Rev.*, **126**, 93 (1993).
42. B. S. Freiser, *Acc. Chem. Res.*, **27**, 353 (1994).
43. B. S. Freiser, *J. Mass Spectrom.*, **31**, 703 (1996).
44. L. Operti and R. Rabezzana, *Mass Spectrom. Rev.*, **25**, 483 (2006).
45. B. R. Rowe, D. W. Fahey, E. E. Ferguson and F. C. Fehsenfeld, *J. Chem. Phys.*, **75**, 3325 (1981).
46. R. K. Milburn, M. V. Frash, A. C. Hopkinson and D. K. Bohme, *J. Phys. Chem. A*, **104**, 3926 (2000).
47. J. S. Uppal and R. H. Staley, *J. Am. Chem. Soc.*, **104**, 1229 (1982).
48. B. P. Pozniak and R. C. Dunbar, *J. Am. Chem. Soc.*, **119**, 10439 (1997).
49. M. Welling, R. I. Thompson and H. Walther, *Chem. Phys. Lett.*, **253**, 37 (1996).
50. M. Welling, H. A. Schuessler, R. I. Thompson and H. Walther, *Int. J. Mass Spectrom. Ion Proc.*, **172**, 95 (1998).
51. R. I. Thompson, M. Welling, H. A. Schuessler and H. Walther, *J. Chem. Phys.*, **116**, 10201 (2002).
52. S. Petrie and R. C. Dunbar, *J. Phys. Chem. A*, **104**, 4480 (2000).
53. R. C. Dunbar and S. Petrie, *Astrophys. J.*, **564**, 792 (2002).
54. R. K. Milburn, A. C. Hopkinson and D. K. Bohme, *J. Am. Chem. Soc.*, **127**, 13070 (2005).
55. X. Zhao, G. K. Koyanagi and D. K. Bohme, *J. Phys. Chem. A*, **110**, 10607 (2006).
56. A. Andersen, F. Muntean, D. Walter, C. Rue and P. B. Armentrout, *J. Phys. Chem. A*, **104**, 692 (2000).
57. L. Operti, E. C. Tews, T. J. MacMahon and B. S. Freiser, *J. Am. Chem. Soc.*, **111**, 9152 (1989).
58. D. Schroeder and J. Roithova, *Angew. Chem., Int. Ed.*, **45**, 5705 (2006).
59. P. D. Kleiber and J. Chen, *Int. Rev. Phys. Chem.*, **17**, 1 (1998).
60. Y. C. Cheng, J. Chen, L. N. Ding, T. H. Wong, P. D. Kleiber and D.-K. Liu, *J. Chem. Phys.*, **104**, 6452 (1996).
61. W. Guo, T. Yuan, X. Chen, L. Zhao, X. Lu and S. Wu, *J. Mol. Struct. (THEOCHEM)*, **764**, 177 (2006).
62. J. Chen, Y. C. Cheng and P. D. Kleiber, *J. Chem. Phys.*, **106**, 3884 (1997).
63. J. Chen, T. H. Wong and P. D. Kleiber, *Chem. Phys. Lett.*, **279**, 185 (1997).
64. X. Yang, Y. Hu and S. Yang, *J. Phys. Chem. A*, **104**, 8496 (2000).
65. X. Yang, Y. Hu and S. Yang, *Chem. Phys. Lett.*, **322**, 491 (2000).
66. A. Furuya, F. Misaizu and K. Ohno, *J. Chem. Phys.*, **125**, 094309/1 (2006).
67. A. Furuya, F. Misaizu and K. Ohno, *J. Chem. Phys.*, **125**, 094310/1 (2006).
68. X. Yang, H. Liu and S. Yang, *J. Chem. Phys.*, **113**, 3111 (2000).

69. X. Yang, K. Gao, H. Liu and S. Yang, *J. Chem. Phys.*, **112**, 10236 (2000).
70. H.-C. Liu, X.-H. Zhang, Y.-D. Wu and S. Yang, *Phys. Chem. Chem. Phys.*, **7**, 826 (2005).
71. H.-C. Liu, C.-S. Wang, W. Guo, Y.-D. Wu and S. Yang, *J. Am. Chem. Soc.*, **124**, 3794 (2002).
72. H.-C. Liu, S. Yang, X.-H. Zhang and Y.-D. Wu, *J. Am. Chem. Soc.*, **125**, 12351 (2003).
73. H. Liu, X. Zhang, C. Wang, W. Guo, Y. Wu and S. Yang, *J. Phys. Chem. A*, **108**, 3356 (2004).
74. H.-C. Liu, X.-H. Zhang, C. Wang, Y.-D. Wu and S. Yang, *Phys. Chem. Chem. Phys.*, **9**, 607 (2007).
75. M. R. France, S. H. Pullins and M. A. Duncan, *Chem. Phys.*, **239**, 447 (1998).
76. J. I. Lee, D. C. Sperry and J. M. Farrar, *J. Chem. Phys.*, **114**, 6180 (2001).
77. W. Guo, H. Liu and S. Yang, *J. Chem. Phys.*, **116**, 9690 (2002).
78. H. Liu, J. Sun and S. Yang, *J. Phys. Chem. A*, **107**, 5681 (2003).
79. Y. Hu, H. Liu and S. Yang, *Chem. Phys.*, **332**, 66 (2007).
80. H. Liu, Y. Hu, S. Yang, W. Guo, Q. Fu and L. Wang, *J. Phys. Chem. A*, **110**, 4389 (2006).
81. B. Soep, M. Elhanine and C. P. Schulz, *Chem. Phys. Lett.*, **327**, 365 (2000).
82. W. Guo, H. Liu and S. Yang, *J. Chem. Phys.*, **117**, 6061 (2002).
83. H. Liu, Y. Hu, S. Yang, W. Guo, X. Lu and L. Zhao, *Chem. Eur. J.*, **11**, 6392 (2005).
84. W. Guo, X. Lu, S. Hu and S. Yang, *Chem. Phys. Lett.*, **381**, 109 (2003).
85. W. Guo, H. Liu and S. Yang, *J. Chem. Phys.*, **116**, 2896 (2002).
86. W. Guo, H. Liu and S. Yang, *Int. J. Mass Spectrom.*, **226**, 291 (2003).
87. H. Liu, W. Guo and S. Yang, *J. Chem. Phys.*, **115**, 4612 (2001).
88. W. Y. Lu, T. H. Wong, Y. Sheng and P. D. Kleiber, *J. Chem. Phys.*, **117**, 6970 (2002).
89. W. Y. Lu, T. H. Wong, Y. Sheng and P. D. Kleiber, *J. Chem. Phys.*, **118**, 6905 (2003).
90. W. Y. Lu and P. D. Kleiber, *Chem. Phys. Lett.*, **338**, 291 (2001).
91. W. Y. Lu and P. D. Kleiber, *J. Chem. Phys.*, **114**, 10288 (2001).
92. Y. Abate and P. D. Kleiber, *J. Chem. Phys.*, **125**, 184310 (2006).
93. H. Liu, Y. Hu and S. Yang, *J. Phys. Chem. A*, **107**, 10026 (2003).
94. J.-L. Sun, H. Liu, K.-L. Han and S. Yang, *J. Chem. Phys.*, **118**, 10455 (2003).
95. J.-L. Sun, H. Liu, H.-M. Yin, K.-L. Han and S. Yang, *J. Phys. Chem. A*, **108**, 3947 (2004).
96. Y. Hu, H. Liu and S. Yang, *J. Chem. Phys.*, **120**, 2759 (2004).
97. J.-L. Sun, H. Liu, H.-M. Wang, K.-L. Han and S. Yang, *Chem. Phys. Lett.*, **392**, 285 (2004).
98. H. Liu, J.-L. Sun, Y. Hu, K.-L. Han and S. Yang, *Chem. Phys. Lett.*, **389**, 342 (2004).
99. P. G. Jasien and C. E. Dykstra, *J. Am. Chem. Soc.*, **105**, 2089 (1983).
100. L. A. Tjurina, V. V. Smirnov and I. P. Beletskaya, *J. Mol. Catal. A*, **182–183**, 395 (2002).
101. L. A. Tjurina, V. V. Smirnov, D. A. Potapov, S. A. Nikolaev, S. E. Esipov and I. P. Beletskaya, *Organometallics*, **23**, 1349 (2004).
102. D. A. Potapov, L. A. Tjurina and V. V. Smirnov, *Russ. Chem. Bull.*, **54**, 1185 (2005).
103. P. G. Jasien and J. A. Abbondondola, *J. Mol. Struct. (THEOCHEM)*, **671**, 111 (2004).
104. V. V. Porsev and A. V. Tulub, *Dokl. Phys. Chem.*, **409**, 237 (2006).
105. Y. C. Cheng, J. Chen, P. D. Kleiber and M. A. Young, *J. Chem. Phys.*, **107**, 3758 (1997).
106. J. F. Garst and M. P. Soriaga, *Coord. Chem. Rev.*, **248**, 623 (2004).
107. J. F. Garst and F. Ungvary, 'Mechanisms of Grignard reagent formation', in *Grignard Reagents: New Developments*; (Ed. G. H. Richey, Jr.), Wiley, Chichester, 2000, p. 185.
108. J. B. Abreu, J. E. Soto, A. Ashley-Facey, M. P. Soriaga, J. F. Garst and J. L. Stickney, *J. Colloid Interface Chem.*, **206**, 247 (1998).
109. R. G. Nuzzo and L. H. Dubois, *J. Am. Chem. Soc.*, **108**, 2881 (1986).
110. Y. Gault, *Tetrahedron Lett.*, **67** (1966); *Chem. Abstr.*, **64**, 75247 (1966).
111. M. Lefrancois and Y. Gault, *J. Organomet. Chem.*, **16**, 7 (1969); *Chem. Abstr.*, **70**, 68449 (1969).
112. Y. Gault, *J. Chem. Soc., Chem. Commun.*, 478 (1973).
113. Y. Gault, *J. Chem. Soc., Faraday Trans.*, **74**, 2678 (1978).
114. A. Choplin and Y. Gault, *J. Organomet. Chem.*, **179**, C1 (1979).
115. A. T. Blades, P. Jayaweera, M. G. Ikononou and P. Kebarle, *J. Chem. Phys.*, **92**, 5900 (1990).
116. A. J. Stace, *J. Phys. Chem. A*, **106**, 7993 (2002).
117. A. Stace, *Science*, **294**, 1292 (2001).
118. A. J. Stace, *Phys. Chem. Chem. Phys.*, **3**, 1935 (2001).
119. M. P. Dobson and A. J. Stace, *Chem. Commun.*, 1533 (1996).
120. C. A. Woodward, M. P. Dobson and A. J. Stace, *J. Phys. Chem. A*, **101**, 2279 (1997).
121. C. A. Woodward, M. P. Dobson and A. J. Stace, *J. Phys. Chem.*, **100**, 5605 (1996).

122. N. Walker, M. P. Dobson, R. R. Wright, P. E. Barran, J. N. Murrell and A. J. Stace, *J. Am. Chem. Soc.*, **122**, 11138 (2000).
123. M. Peschke, A. T. Blades and P. Kebarle, *J. Am. Chem. Soc.*, **122**, 10440 (2000).
124. A. M. El-Nahas, S. H. El-Demerdash and E.-S. E. El-Shereefy, *Int. J. Mass Spectrom.*, **263**, 267 (2007).
125. A. A. Shvartsburg, J. G. Wilkes, J. O. Lay and K. W. M. Siu, *Chem. Phys. Lett.*, **350**, 216 (2001).
126. A. A. Shvartsburg and J. G. Wilkes, *J. Phys. Chem. A*, **106**, 4543 (2002).
127. A. A. Shvartsburg, *Chem. Phys. Lett.*, **376**, 6 (2003).
128. A. A. Shvartsburg and J. G. Wilkes, *Int. J. Mass Spectrom.*, **225**, 155 (2003).
129. T. Shi, K. W. M. Siu and A. C. Hopkinson, *Int. J. Mass Spectrom.*, **255–256**, 251 (2006).
130. H.-F. Wu and J. S. Brodbelt, *J. Am. Chem. Soc.*, **116**, 6418 (1994).
131. R. A. J. O'Hair, A. K. Vrkic and P. F. James, *J. Am. Chem. Soc.*, **126**, 12173 (2004).
132. G. N. Khairallah and R. A. J. O'Hair, *Int. J. Mass Spectrom.*, **254**, 145 (2006).
133. A. P. Jacob, P. F. James and R. A. J. O'Hair, *Int. J. Mass Spectrom.*, **255–256**, 45 (2006).
134. R. K. Milburn, V. Baranov, A. C. Hopkinson and D. K. Bohme, *J. Phys. Chem. A*, **103**, 6373 (1999).
135. R. K. Milburn, V. I. Baranov, A. C. Hopkinson and D. K. Bohme, *J. Phys. Chem. A*, **102**, 9803 (1998).
136. R. A. J. O'Hair, *Chem. Commun.*, 1469 (2006).
137. M. T. Reetz, N. Harmat and R. Mahrwald, *Angew. Chem.*, **104**, 333 (1992).
138. J. Berthelot, A. Luna and J. Tortajada, *J. Phys. Chem. A*, **102**, 6025 (1998).
139. A. Haaland, *Top. Curr. Chem.*, **1** (1975).
140. P. R. Markies, O. S. Akkerman, F. Bickelhaupt, W. J. J. Smeets and A. L. Spek, *Adv. Organomet. Chem.*, **32**, 147 (1991).
141. D. W. H. Rankin and H. E. Robertson, *Spect. Prop. Inorg. Organomet. Compd.*, **38**, 348 (2006).
142. I. Hargittai, *Struct. Chem.*, **16**, 1 (2005).
143. M. Hargittai, *Struct. Chem.*, **16**, 33 (2005).
144. M. Hargittai, *Chem. Rev.*, **100**, 2233 (2000).
145. M. Hargittai, *Coord. Chem. Rev.*, **91**, 35 (1988).
146. A. Haaland, J. Luszyk, D. P. Novak, J. Brunvoll and K. B. Starowieyski, *J. Chem. Soc., Chem. Commun.*, 54 (1974).
147. R. A. Andersen, R. Blom, J. M. Boncella, C. J. Burns and H. V. Volden, *Acta Chem. Scand., Ser. A*, **A41**, 24 (1987).
148. E. C. Ashby, L. Fernholt, A. Haaland, R. Seip and R. S. Smith, *Acta Chem. Scand., Ser. A*, **A34**, 213 (1980).
149. R. A. Andersen, R. Blom, A. Haaland, B. E. R. Schilling and H. V. Volden, *Acta Chem. Scand., Ser. A*, **A39**, 563 (1985).
150. J. Molnar, C. J. Marsden and M. Hargittai, *J. Phys. Chem.*, **99**, 9062 (1995).
151. B. Reffy, M. Kolonits and M. Hargittai, *J. Phys. Chem. A*, **109**, 8379 (2005).
152. P. A. Akishin and V. P. Spiridonov, *Zh. Fiz. Khim.*, **32**, 1682 (1958); *Chem. Abstr.*, **53**, 4621 (1959).
153. V. V. Kasparov, Y. S. Ezhov and N. G. Rambidi, *Zh. Strukt. Khim.*, **20**, 260 (1979); *Chem. Abstr.*, **91**, 30922 (1979).
154. P. A. Akishin, V. P. Spiridonov, G. A. Sobolev and V. A. Naumov, *Zh. Fiz. Khim.*, **31**, 461 (1957); *Chem. Abstr.*, **51**, 84261 (1957).
155. V. V. Kasparov, Y. S. Ezhov and N. G. Rambidi, *Zh. Strukt. Khim.*, **21**, 41 (1980). *Chem. Abstr.*, **93**, 86015 (1980).
156. M. S. Beardah and A. M. Ellis, *J. Chem. Tech. Biotech.*, **74**, 863 (1999).
157. A. M. Ellis, *Int. Rev. Phys. Chem.*, **20**, 551 (2001).
158. M. A. Duncan, *Ann. Rev. Phys. Chem.*, **48**, 69 (1997).
159. N. R. Walker, R. S. Walters and M. A. Duncan, *New J. Chem.*, **29**, 1495 (2005).
160. F. Dong and R. E. Miller, *J. Phys. Chem. A*, **108**, 2181 (2004).
161. D. T. Moore and R. E. Miller, *J. Phys. Chem. A*, **108**, 9908 (2004).
162. P. L. Stiles, D. T. Moore and R. E. Miller, *J. Chem. Phys.*, **121**, 3130 (2004).

## CHAPTER 5

# Photochemical transformations involving magnesium porphyrins and phthalocyanines

NATALIA N. SERGEEVA and MATHIAS O. SENGE

*School of Chemistry, SFI Tetrapyrrole Laboratory, Trinity College Dublin,  
Dublin 2, Ireland*

*Fax: +353-1-608-8536; e-mail: sengem@tcd.ie*

---

I. INTRODUCTION	190
A. Abbreviations	190
B. General Introduction	190
II. BASIC PHOTOCHEMISTRY OF PORPHYRINS	192
A. General Concepts and Theoretical Background	192
B. Stability	193
III. PHOTOSYNTHESIS	194
IV. ELECTRON TRANSFER SYSTEMS	196
A. Introduction	196
B. Donor–Acceptor Electron Transfer Compounds	196
C. Heteroligand Systems	201
V. PHOTOCHEMICAL REACTIONS	206
A. Porphyrins	206
B. Photoinduced Ring-opening Reactions	207
C. Reactions of Chlorophyll	209
VI. APPLIED PHOTOCHEMISTRY	212
VII. ACKNOWLEDGMENT	214
VIII. REFERENCES	214

---



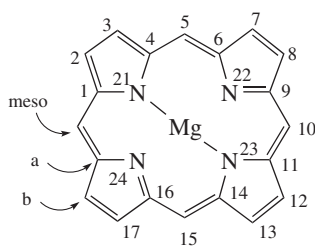
## I. INTRODUCTION

### A. Abbreviations

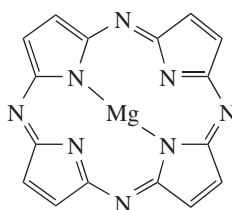
bchl	bacteriochlorophyll	OEP	2,3,7,8,12,13,17,18-octaethylporphyrinato
chl	chlorophyll	P	porphyrin
D-B-A	donor-bridge-acceptor systems	PET	photoinduced electron transfer
ET	electron transfer	PS	photosensitizer
MV	methyl viologen	TPP	5,10,15,20-tetraphenylporphyrinato

### B. General Introduction

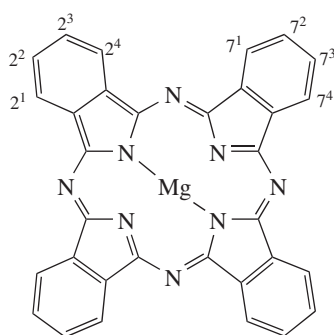
The photochemistry of true organomagnesium compounds remains almost completely unexplored. A literature search in preparation of this work found only a few scattered examples of photochemical studies, mostly in relation to Grignard reactions<sup>1</sup> and 1,3-diketonate chelates<sup>2,3</sup>. Similar to the situation with organozinc compounds<sup>4</sup> magnesium tetrapyrrole chelates, i.e. magnesium porphyrins **1**, 5,10,15,20-tetraazaporphyrins (porphyrazines) **2** and phthalocyanines **3** have found more interest. This is primarily related



(1)



(2)

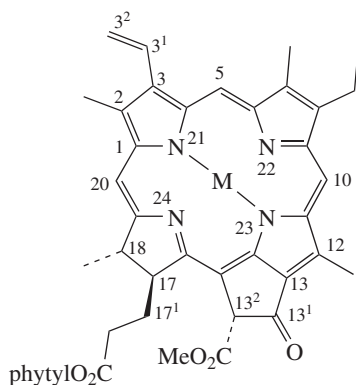


(3)

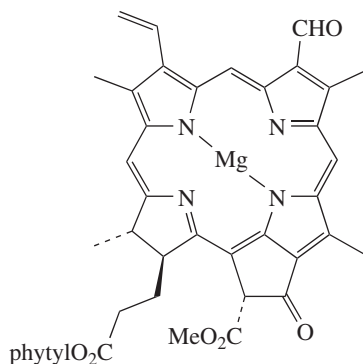
to the biological relevance of magnesium porphyrins in nature, notably in photosynthesis and electron transfer, and we will focus on this aspect in this review. Outside this area not many 'true' photochemical studies have been performed with magnesium tetrapyrroles. Nevertheless, even in this area the body of available literature is limited and we only use selected examples to highlight the state of the art of this field. A description of syntheses, methodology or electron transfer reactions is outside the purview of this work and the present work can only give a broad overview and selected examples of studies in this area.

Chlorophylls (chl) and the related bacteriochlorophylls (bchl) are the ubiquitous pigments of photosynthetic organisms and the predominant class of magnesium tetrapyrroles in nature. As such they share common structural principles and functions. They are either involved in light harvesting (exciton transfer) as antenna pigments or charge separation (electron transfer) as reaction center pigments. The best-known pigment is chl a, **4**, which occurs in all organisms with oxygenic photosynthesis. In higher plants it is accompanied in a 3:1 ratio by chl b, **6**, where the 7-methyl group has been oxidized to a formyl group. Both compounds typically consist of the tetrapyrrole moiety and a C-20 terpenoid alcohol, phytol. Most compounds are magnesium chelates, but the free base of chl a, pheo a **5**, is also active in electron transfer. Chl a and b can be obtained easily from plants or algae and their synthetic chemistry has mainly targeted total syntheses and medicinal application in photodynamic therapy (PDT)<sup>5,6</sup>.

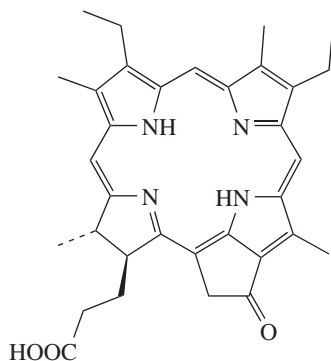
However, many other similar photosynthetic pigments occur in nature<sup>4-7</sup>. All share either a phytychlorin **7** or a 7,8-dihydrophytychlorin framework and by now about one hundred related pigments have been isolated<sup>8</sup>. For example, such compounds include chl d **8** from Rhodophytes, the bchls c (**9**), d and e (which are chlorins **12** and show significant variability in their peripheral groups) from Chlorobiaceae and Chloroflexaceae, and bchl a (**10**) and b (true bacteriochlorins **13**) found in Rhodospirillales. Other natural pigments are chl c, bchl g and many of these are esterified with different isoprenoid alcohols. Chemically related chlorins have also been found in many oxidoreductases, marine sponges, tunicates and in *Bonella viridis*. The deep-sea dragon fish *Malacosteus niger* even utilizes a chl derivative as a visual pigment<sup>9</sup>. Most of these are believed to be derived from chl and then processed by the plant or animal.



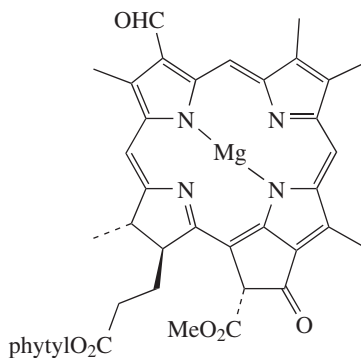
(**4**) M = Mg, chl a  
(**5**) M = 2H, pheo a



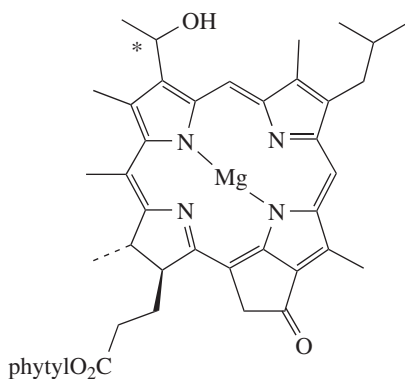
(**6**) chl b



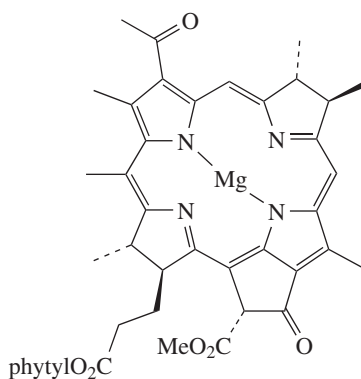
(7) phytylchlorin



(8) chl d



(9) bchl c



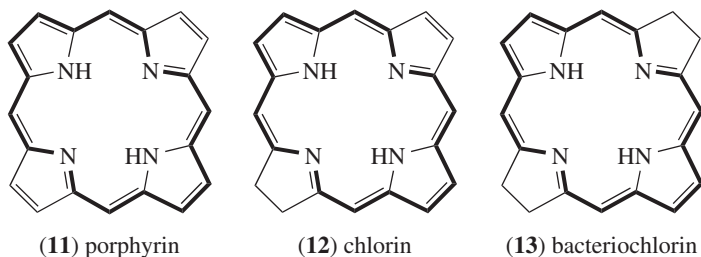
(10) bchl a

## II. BASIC PHOTOCHEMISTRY OF PORPHYRINS

### A. General Concepts and Theoretical Background

Chls and all tetrapyrroles are heteroaromatic compounds and the aromatic character of the underlying tetrapyrrole moiety and the reactivity of the functional groups in the side chains govern their chemistry. Three different classes of tetrapyrroles, differentiated by their oxidation level, occur in nature: porphyrins (**11**, e.g. hemes), chlorins (**12**, e.g. chls) and bacteriochlorins (**13**, e.g. bchls). As a cyclic tetrapyrrole with a fused five-membered ring, the overall reactivity of chl is that of a standard phytylchlorin **7**. Such compounds are capable of coordinating almost any known metal with the core nitrogen atoms. Together with the conformational flexibility of the macrocycle and the variability of its side chains, this accounts for their unique role in photosynthesis and applications<sup>10,11</sup>.

Tetrapyrroles contain an extended  $\pi$ -conjugated system which is responsible for their use in a wide range of applications ranging from technical (pigments, catalysts, photoconductors) to medicinal (photodynamic therapy) uses. The electronic absorption spectra are governed by the aromatic 18  $\pi$ -electron system and typically consist of two main bands. In phthalocyanines the Q band around 660–680 nm is the most intense one accompanied by a weaker Soret band near 340 nm<sup>12</sup>. In porphyrins the situation is reversed with an



intense Soret band around 380–410 nm and weaker Q bands in the 550–650 nm region. The position and intensity of the absorption bands are affected by the central metal, axial ligands, solvation, substituents and their regiochemical arrangement, and aggregation. The theoretical background has been widely reviewed and established<sup>13</sup> in pioneering works by Gouterman<sup>14</sup> and Mack and Stillman<sup>15</sup>. The spectral characteristics depend strongly on the substituent pattern. By now almost all possible combinations of electron-donating, electron-withdrawing or sterically demanding groups have been prepared<sup>11</sup>.

Magnesium(II) tetrapyrroles behave like most other organic chromophores. Absorption of light will lead to the rapid formation of the lowest excited singlet state by promotion of an electron from the HOMO to the LUMO. The excited state can then either relax to the ground state via radiative (fluorescence) or nonradiative processes (internal conversion of vibrational relaxation). Another possibility is intersystem crossing to form a triplet state which again can relax either via radiative (phosphorescence) or nonradiative processes. In our context, both excited-state types can take part in photochemical reactions and, in the presence of donor or acceptor units, energy transfer or electron transfer between the chromophores, can compete with these processes<sup>16</sup>. In addition, metallo(II) porphyrins and phthalocyanines may form ions upon illumination. These are either anion or  $\pi$ -cation radicals that undergo further photochemical reactions<sup>17,18</sup>.

## B. Stability

Although porphyrins and especially phthalocyanines are stable compounds, both will undergo photooxidative degradation or photoexcited ET reactions<sup>19–21</sup>. An additional problem with magnesium complexes is their low stability in aqueous solution, as they demetallate quite easily. This is one of the main reasons that many photochemical studies targeted at modeling the natural situation use the more stable zinc(II) complexes. In addition, past years have seen increasing evidence that both Mg(II) and Zn(II) chlorophylls do exist in nature.

Photosynthetic organisms that utilize chls or bchls containing metals other than Mg were unknown for a long time<sup>22</sup>. By now it has been satisfactorily demonstrated that a novel purple pigment occurring in a group of obligatory aerobic bacteria is in fact a zinc-chelated bchl (Zn-bchl)<sup>23–25</sup>. The natural occurrence of Zn-bchl *a* has been proven for a limited group of aerobic acidophilic proteobacteria, including species of the genus *Acidiphilium*. The major photopigment in *Acidiphilium* was first identified tentatively as Mg-bchl *a* on the basis of preliminary spectral analyses<sup>26,27</sup>. However, more detailed studies revealed that all previously known species of *Acidiphilium* contained Zn-bchl *a* as the major photopigment and showed *Acidiphilium* to be a photosynthetic organism<sup>23,25</sup>.

The naturally occurring Zn-bchl *a* and Mg-bchl *a* show large structural similarities and have very similar physicochemical characteristics<sup>28</sup>. Likewise, Zn-chl *a* exhibits features similar to Mg-chl *a* with regard to redox potential and absorption maxima in organic solvents. The light-harvesting efficiency of Zn-chl *a* and Mg-chl *a* are very similar although

the fluorescence quantum yield of the former is lower than that of the latter. Compared to other chlorophyll-type pigments Zn-bchl *a* is much more stable towards acid. For example, the rate of pheophytinization for Zn-bchl *a* is  $10^6$ -fold slower than for Mg-bchl *a*<sup>29</sup>. In fact, it is difficult to fully demetallate Zn-bchl *a* to bacteriopheophytin (bPhe) by treatment with 1N HCl, which is commonly used for pheophytinization of Mg-bchl and Mg-chl. Due to the chemical stability of Zn-(b)chl *a* and their photo- and electrochemical similarities with Mg-(b)chl *a*, Zn-(b)chls are an alternative pigment for photosynthesis. Thus, it is not surprising that they have been used along with magnesium porphyrins in studies of artificial photosynthetic systems<sup>30,31</sup>.

### III. PHOTOSYNTHESIS

The natural photosynthetic process is a rather complex biochemical system that primarily relies on the light absorption by organic chromophores, followed by generation of reduction equivalents and ATP. The main photosynthetic pigments are chlorophylls that have very strong absorption bands in the visible region of the spectrum. Together with accessory pigments (carotenoids and open-chain tetrapyrroles) the various photosynthetic pigments complement each other in absorbing sunlight. Photosynthetic bacteria mostly contain bacteriochlorophylls with absorption maxima shifted towards the bathochromic region compared to chlorin-based pigments.

In its simplest form photosynthesis can be envisaged as the absorption of light through pigments arranged in a light-harvesting complex. These antenna systems permit an organism to increase greatly the absorption cross section for light and the use of light harvesting complexes with different pigments allows for a more efficient process through absorption of more photons and a more efficient use of the visible spectrum. The antenna pigments funnel the excitation energy through exciton transfer to a closely coupled pair of (b)chl molecules in the photochemical reaction center (Figure 1). The reaction center is an integral membrane pigment-protein that carries out light-driven electron transfer reactions. The excited (bacterio)chlorophyll molecule transfers an electron to a nearby acceptor molecule, thereby creating a charge separated state consisting of the oxidized chlorophyll and reduced acceptor.

After the initial electron transfer event, a series of electron transfer reactions takes place that eventually stabilizes the stored energy in reduction equivalents and ATP. Higher plants have two different reaction center complexes that work together in sequence, with the reduced acceptors of one photoreaction (photosystem II) serving as the electron donor for photosystem I. Here, the ultimate electron donor is water, liberating molecular oxygen, and the ultimate electron acceptor is carbon dioxide, which is reduced to carbohydrates. More simple and evolutionary older types of photosynthetic organisms contain only a single photosystem, either similar to photosystem II or photosystem I<sup>32–35</sup>. A simplified scheme of the complex photosynthetic apparatus is shown in an adaptation of the Z-scheme in Figure 2. The Z-scheme illustrates the two light-dependent reactions in photosynthetic systems of higher plants and exemplifies that two photosystems function in sequence to convert solar energy into chemical energy.

In chemical terms the photoinduced electron transfer results in transfer of an electron across the photosynthetic membrane in a complex sequence that involves several donor–acceptor molecules. Finally, a quinone acceptor is reduced to a semiquinone and subsequently to a hydroquinone. This process is accompanied by the uptake of two protons from the cytoplasm. The hydroquinone then migrates to a cytochrome bc complex, a proton pump, where the hydroquinone is reoxidized and a proton gradient is established via transmembrane proton translocation. Finally, an ATP synthase utilizes the proton gradient to generate chemical energy. Due to the function of tetrapyrrole-based pigments as electron donors and quinones as electron acceptors, most biomimetic systems utilize some

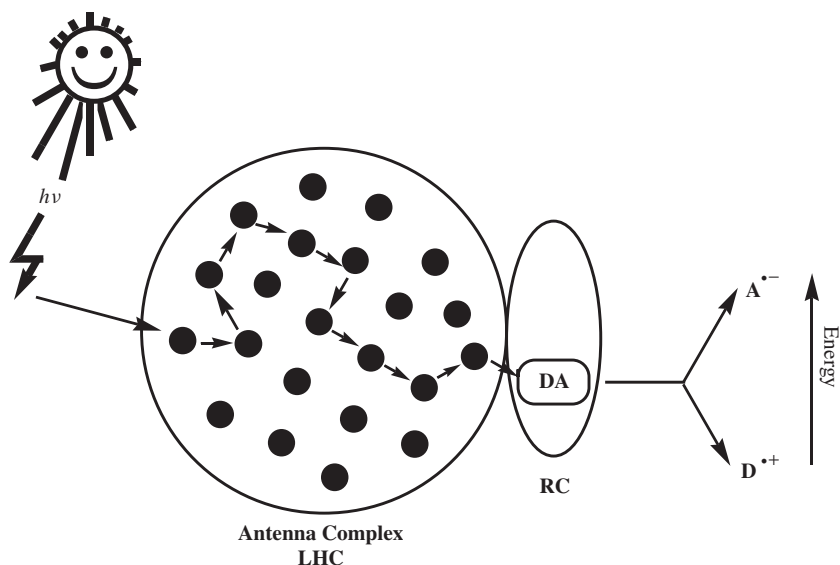


FIGURE 1. General scheme of a photosynthetic system (RC = reaction center, DA = donor-acceptor complex, LHC = light-harvesting complex)

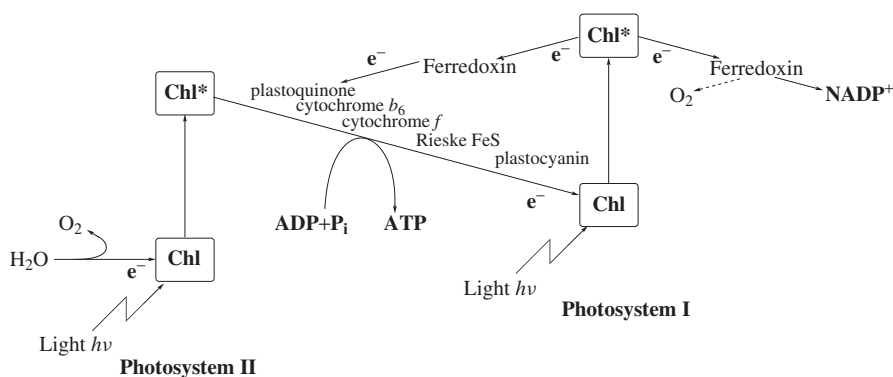


FIGURE 2. Simplified Z-scheme of the photosynthetic apparatus in higher plants

kind of donor-acceptor construct to model the natural photosynthetic process (Figure 3). Variation of the components (donor, bridge, linking group, acceptor), their spatial relationship, solvents and environmental factors then serves to modulate and optimize the physicochemical properties. Several thousand systems of this general type have been prepared and used for investigation of the photoinduced electron transfer (PET) and numerous reviews have been published in this area<sup>16,36</sup>. Most of the available literature on ET studies in donor-acceptor compounds focuses on porphyrins. Phthalocyanine building blocks have been used less often, a result of their low solubility and the lack of appropriate synthetic methodologies to selectively introduce functional groups or for the synthesis

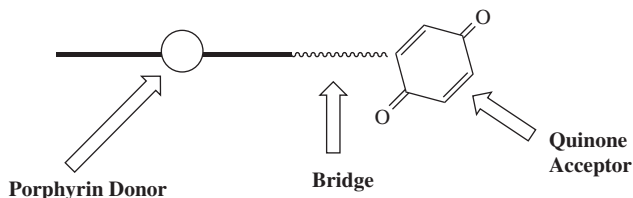


FIGURE 3. Schematic view of a biomimetic electron transfer compound

of unsymmetrically substituted derivatives. An overview of the various synthetic and structural principles to model the components of the photosynthetic apparatus has been given in the relevant chapter on zinc(II) porphyrins<sup>4</sup>.

## IV. ELECTRON TRANSFER SYSTEMS

### A. Introduction

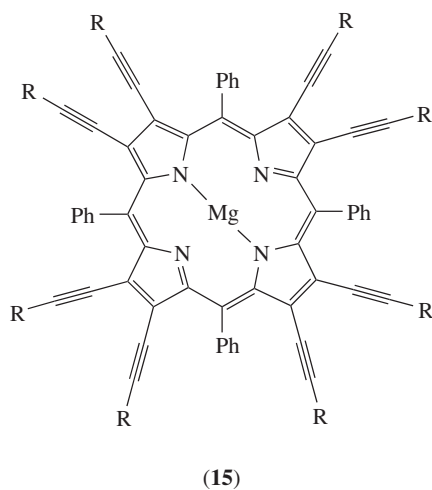
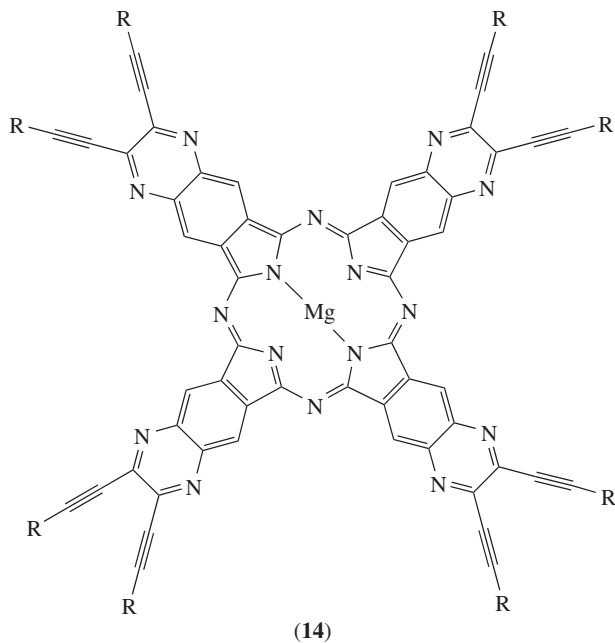
Studies on photoinduced energy and electron transfer in supramolecular assemblies have witnessed a rapid growth in the past decade. These studies were focused on the mechanistic details of light-induced chemical processes. One of these aims of photoinduced electron transfer studies in molecular systems is to produce a long-lived charge-separated state to mimic photosynthesis. Recently, the development of novel photochemically active systems has focused on polychromophoric, dendritic, supramolecular systems and novel materials. Researchers attempt to generate systems with ultrafast charge transfer and charge recombination applicable as light-induced switches or with a long-lived charge-separated state for solar energy generation<sup>37</sup>. These studies have yielded an expanding body of information on porphyrin/phthalocyanine dyads, their design and energy, exciton and charge transfer properties. Incorporation of these systems into larger architectures now offers the possibility for applications in molecular photonics, electronics, solar energy conversion and quantum optics.

The simplest covalently linked systems consist of porphyrin linked to electron acceptor or donor moiety with appropriate redox properties as outlined in Figure 1. Most of these studies have employed free base, zinc and magnesium tetrapyrroles because the first excited singlet state is relatively long-lived (typically 1–10 ns), so that electron transfer can compete with other decay pathways. Additionally, these pigments have relatively high fluorescence quantum yields. These tetrapyrroles are typically linked to electron acceptors such as quinones, perylenes<sup>38–40</sup>, fullerenes<sup>41,42</sup>, acetylenic fragments (**14**, **15**) and aromatic spacers<sup>43–46</sup> and other tetrapyrroles (e.g. boxes and arrays).

The basic photochemistry of magnesium tetrapyrroles is similar to other tetrapyrroles. Magnesium porphyrins<sup>47–49</sup> and phthalocyanines<sup>50–53</sup> may form cation radicals and ions via the triplet state upon illumination. For (phthalocyaninato)magnesium both photochemical oxidations and reductions have been shown. In the presence of carbon tetrabromide as an irreversible electron acceptor the mechanism proceeds via the radical cation<sup>54</sup>. The suggested mechanism for the photochemical oxidation is through the lowest lying triplet state of the phthalocyanine and is thought to be similar to that of porphyrins such as (2,3,7,8,12,13,17,18-octaethylporphyrinato)magnesium and (5,10,15,20-tetraphenylporphyrinato)magnesium.

### B. Donor–Acceptor Electron Transfer Compounds

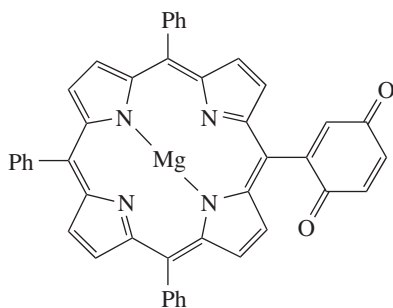
Biomimetic systems comprised of porphyrins and quinones have been studied extensively with regard to their electron transfer and charge transfer properties. Porphyrin–



quinone (PQ) model systems, in which the quinone is fused directly to the porphyrin periphery, therefore have a special relevance for the fundamental understanding of rapid biological electron transfer reactions. Although the importance of these compounds as structurally simple models with large electronic donor–acceptor coupling has long been recognized, only few examples of magnesium-containing systems have been reported so far.



Many spectroscopic methods have been employed for the investigation of such systems<sup>55–59</sup>. For example, wide-band, time-resolved, pulsed photoacoustic spectroscopy was employed to study the electron transfer reaction between a triplet magnesium porphyrin and various quinones in polar and nonpolar solvents<sup>55</sup>. Likewise, ultrafast time-resolved anisotropy experiments with [5-(1,4-benzoquinonyl)-10,15,20-triphenylporphyrinato]magnesium **16** showed that the photoinduced electron transfer process involving the locally-excited  $\text{MgP}^*\text{Q}$  state is solvent-independent, while the thermal charge recombination reaction is solvent-dependent<sup>56,57</sup>. Recently, several examples of quinone–phthalocyanine systems have also been reported<sup>58,59</sup>.

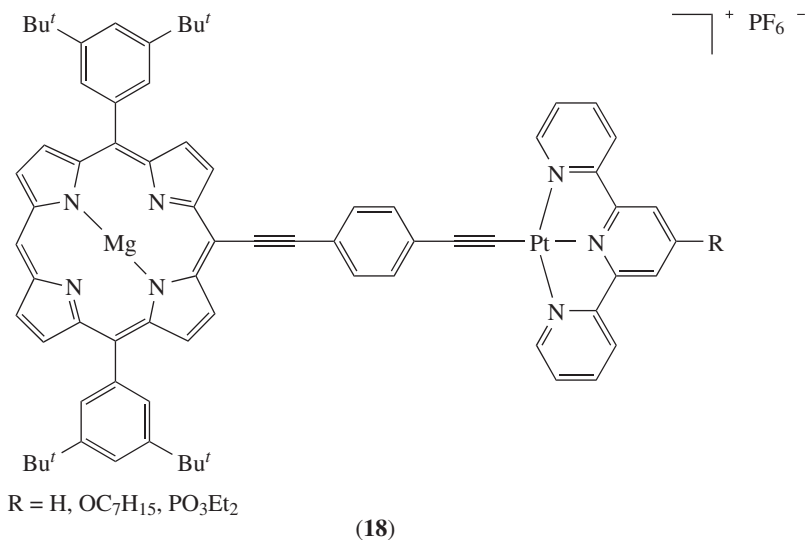
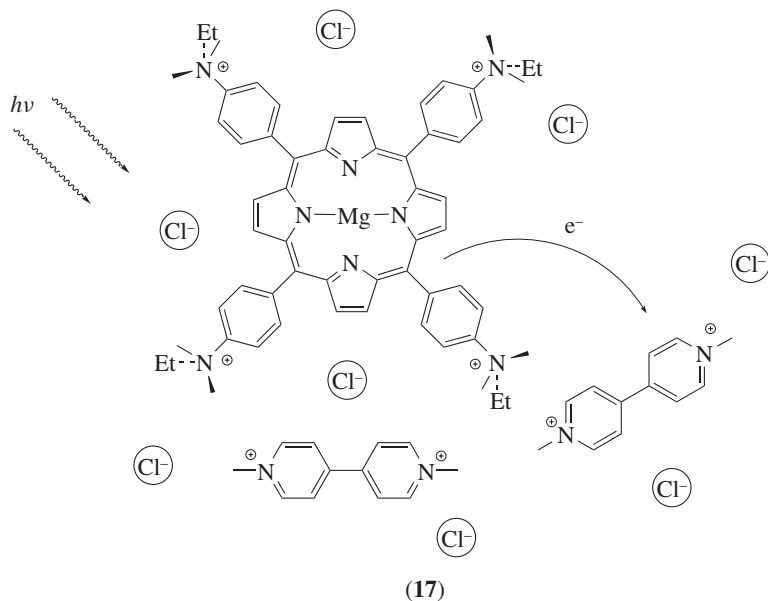


(16)

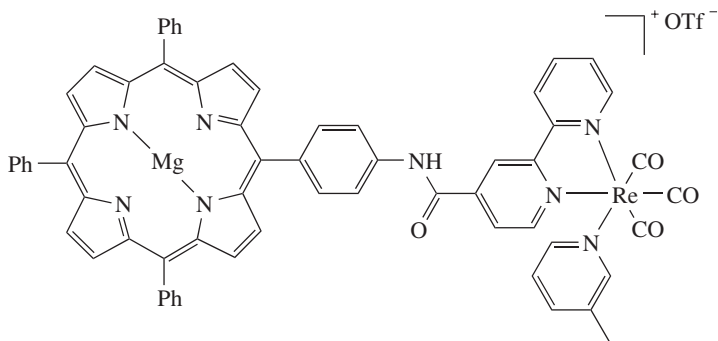
Viologen (4,4'-bipyridyl) derivatives are attractive electron-accepting units for tetrapyrrole-containing dyads and more complex donor–acceptor systems as they can be easily reduced, conveniently linked to other molecules via *N*-alkylation of precursors, and can be used to vary the solubility in polar solvents by virtue of their charged nature. Based on the fact that the viologen radical monocation absorbs in the visible region, they can be used as convenient charge-separation indicators. As a result, a number of magnesium porphyrin<sup>60,61</sup>/phthalocyanine<sup>62–64</sup>–viologen systems have been studied. Typically, excitation of a porphyrin–viologen dyad **17** leads to the porphyrin first excited singlet state, which can then induce photoelectron transfer to the viologen or undergo intersystem crossing to yield the porphyrin triplet state. As viologen is easily reduced, the porphyrin triplet state may also act as an electron donor in these systems.

A different strategy involves using a transition metal center linked to an organic chromophore. This greatly expands the number of electron/energy transfer reactions that can take place within the assembly compared to pure organic or inorganic-organometallic systems. Covalently linking metal complexes to porphyrins yields a cornucopia of candidates for photosynthesis-related studies. Again, only a few examples of photoinduced processes based on magnesium phthalocyanine<sup>65</sup> and porphyrins<sup>66,67</sup> have been reported so far (e.g. **18**, **19**).

For example, in 1963 the photochemistry of magnesium phthalocyanine with coordinated uranium cations was studied in pyridine and ethanol and indicated the occurrence of PET to the uranium complex<sup>65</sup>. A rapid photoinduced electron transfer (2–20 ps) followed by an ultrafast charge recombination was shown for various zinc and magnesium porphyrins linked to a platinum terpyridine acetylide complex<sup>66</sup>. The results indicated the electronic interactions between the porphyrin subunit and the platinum complex, and underscored the potential of the linking *para*-phenylene bisacetylene bridge to mediate a rapid electron transfer over a long donor–acceptor distance.



Complexes of rhenium(bipyridine)(tricarbonyl)(picoline) units linked covalently to magnesium tetraphenylporphyrins via an amide bond between the bipyridine and one phenyl substituent of the porphyrin **19** exhibited no signs of electronic interaction between the  $\text{Re}(\text{CO})_3(\text{bpy})$  units and the metalloporphyrin units in their ground states. However, emission spectroscopy revealed a solvent-dependent quenching of porphyrin emission upon irradiation into the long-wavelength absorption bands localized on the porphyrin.

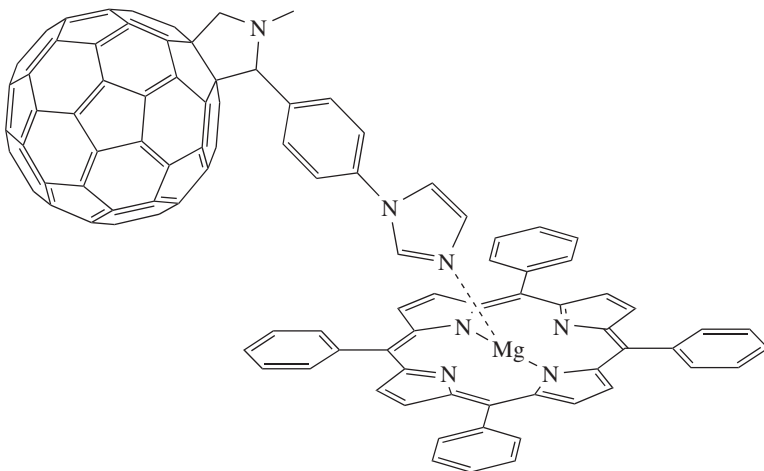


(19)

The presence of the charge-separated state involving electron transfer from Mg(II)TPP to Re(bpy) was shown by time-resolved IR spectroscopy<sup>67</sup>.

The system is reversible in the absence of an added electron donor but undergoes irreversible reaction at the reduced rhenium bipyridine center in the presence of added triethylamine. The observation of reaction at the rhenium site upon excitation in the absorption band of the metalloporphyrin site is compatible with an ultrafast back electron transfer, provided that the triethylamine coordinated to the magnesium prior to absorption and that the electron transfer from the metalloporphyrin to the bipyridine was followed rapidly by irreversible electron transfer from the triethylamine to the metalloporphyrin. The experiments graphically demonstrated the benefits of the incorporation of carbonyl ligands at the electron acceptor as they allowed a tracking of the sequence of charge separation and back electron transfer via time-resolved IR data<sup>67</sup>.

Fullerenes are currently enjoying considerable attention as acceptor groups in ET compounds<sup>68,69</sup>. Fullerenes can accept up to six electrons, exhibit small reorganization



(20)

energies while photoinduced charge separation is accelerated and charge recombination is slowed. Thus, relatively long-lived charge-separated states are obtained without a special environment such as an apoprotein<sup>70</sup>. A recently described system consisting of a ferrocene, two porphyrins and one C<sub>60</sub> unit exhibited a lifetime of 1.6 s (!), comparable to bacterial photosynthetic reaction centers. The quantum yields for charge separation in complex biomimetic systems can reach unity. Recent advances in their synthetic methodologies allow one to functionalize fullerenes and link them to other pigments.

Several self-assembled donor–acceptor systems containing fullerenes as three-dimensional electron acceptors and porphyrins as electron donors have been described. Noncovalently and covalently linked Mg porphyrin–fullerene dyads have been synthesized and investigated spectroscopically<sup>41,42</sup>. For example, a covalently linked magnesium porphyrin–fullerene (MgP–C<sub>60</sub>) dyad with a flexible ethylene dioxide bridge<sup>41</sup> was compared to a self-assembled noncovalently linked dyad (MgP•••C<sub>60</sub>Im, **20**). In the latter, axial coordination of an imidazole (Im) functionalized fullerene<sup>42</sup> to the magnesium porphyrin was used for bonding. Significant increases in the lifetime of the charge-separated states were observed upon coordinating nitrogenous axial ligands to the latter.

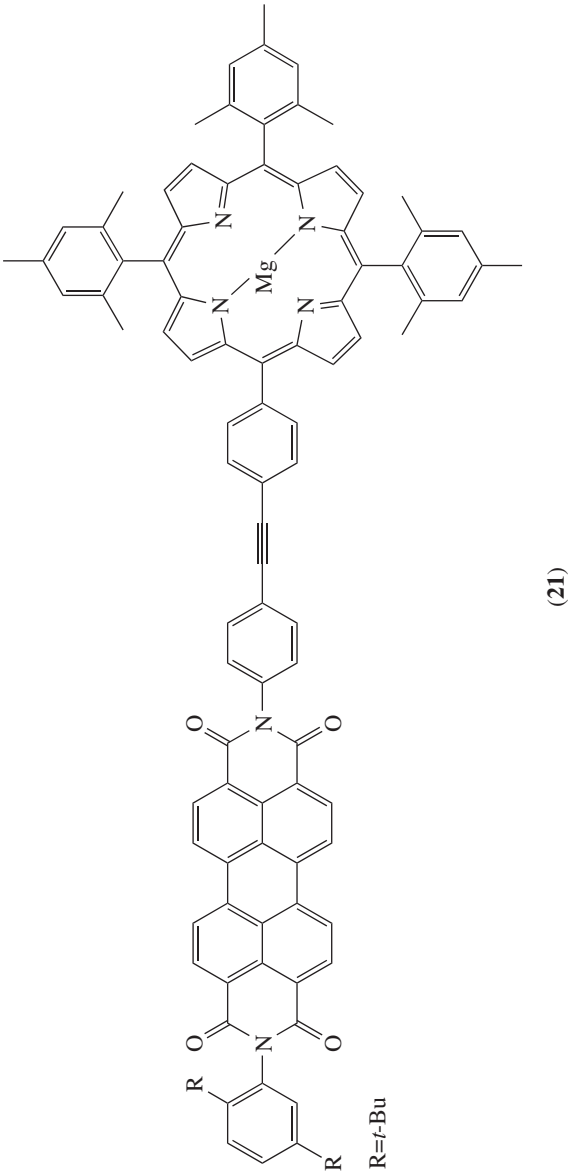
Perylene-linked systems represent another class of useful compounds for PET studies. Classic cases are **21** and **22**. They represent a family of closely related bichromophoric systems with properties designed to utilize PET strategies<sup>38–40</sup>.

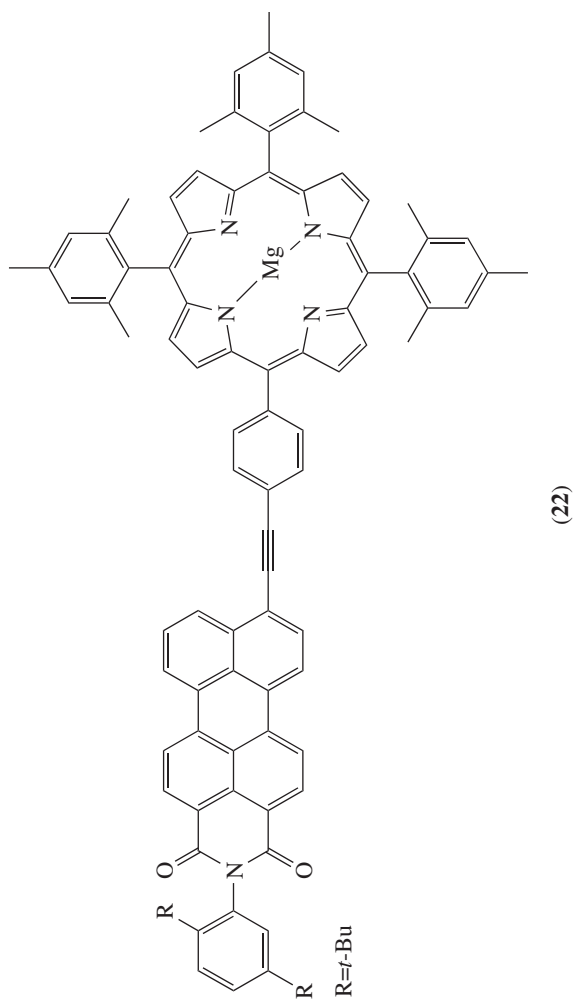
### C. Heteroligand Systems

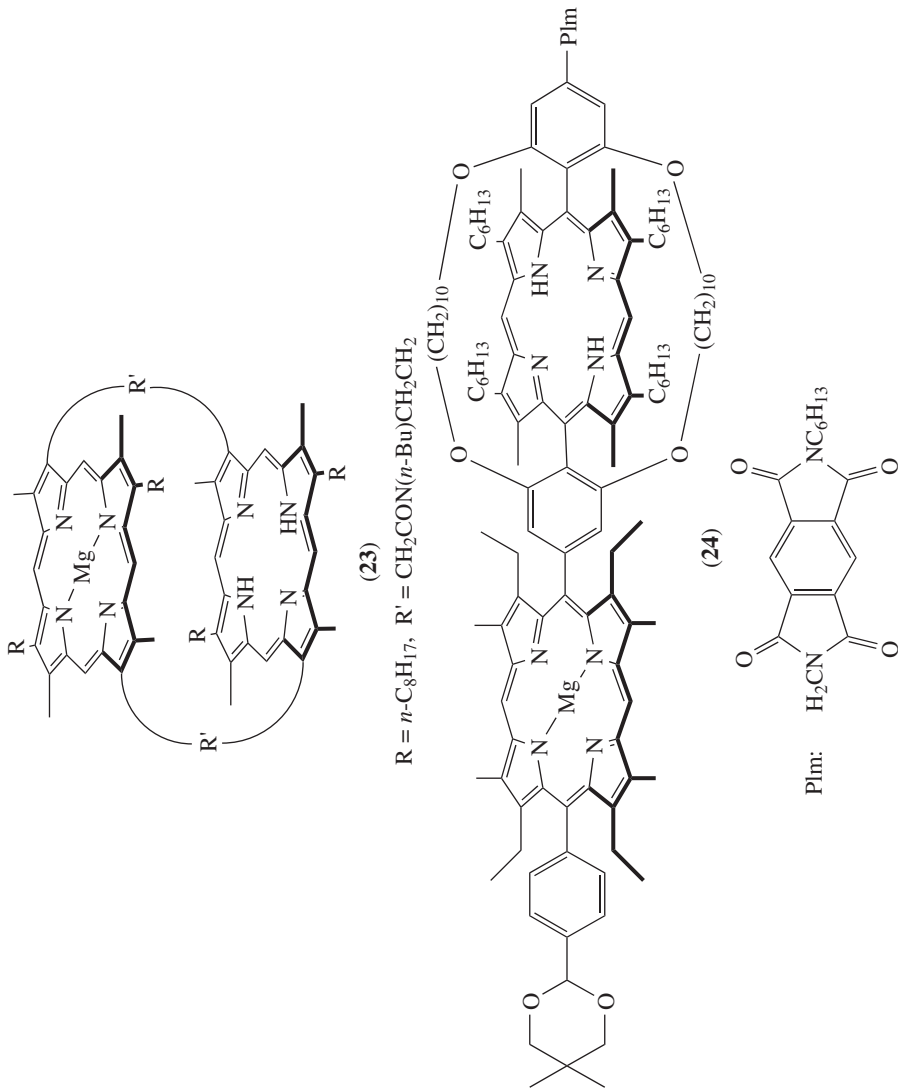
Photoinduced ET between metalloporphyrins and free bases in dimeric, trimeric and oligomeric porphyrin systems has been studied extensively. Depending on the choice of the donor and acceptor unit, electron transfer from either the singlet or triplet states can be observed. Electron transfer studies in systems based on heterodimers with covalent or electrostatic bonds is of particular interest as it relates directly to the special pair of the reaction center chlorophylls. For systems such as the magnesium–free-base porphyrin, heterodimer **23** EPR spectroscopy has been shown to be an essential analytical tool that provides information not available from optical studies. It provides details on the magnetic interactions and spin dynamics of states with different multiplicities, such as doublets, triplets and charge-transfer states. The communication between these states strongly depends on the temperature and the solvent, and the EPR results established the existence of the radical species deduced in ps optical experiments and the corresponding theoretical calculations<sup>71–73</sup>.

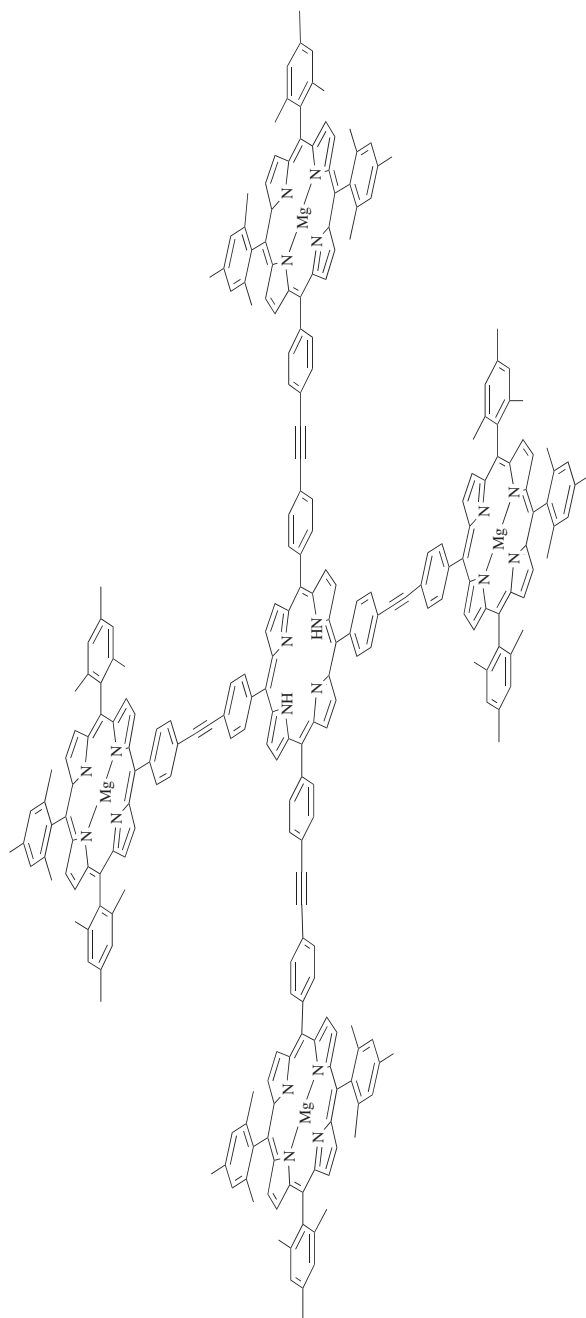
Using series of conformationally restricted magnesium–free-base hybrid arrays bridged linearly via aryl-spacers to form di- (**24**) or trimeric porphyrins, the intramolecular electron-transfer reactions from the singlet excited state of the distal doubly strapped free-base porphyrin to the pyromellitimide acceptor (Plm) was studied by time-resolved ps fluorescence and transient absorption spectroscopy<sup>74–76</sup>. The electron transfer was more effective in magnesium–porphyrin bridged models than in the related zinc–porphyrin bridged ones, indicating that the past reliance on the use of zinc-based biomimetic models is not always sufficient. Remarkably, the electron transfer over two porphyrins proceeded with rates almost similar to those for the ET over one porphyrin regardless of the bridging metalloporphyrin.

A simple method has been developed to construct a variety of molecular architectures containing free base–magnesium or magnesium–metalloporphyrin systems consisting of two to nine porphyrin units. Compound **25** is a typical example for such a compound that are important for studying the electronic communication in multichromophoric systems.<sup>45,46</sup>









(25)



An example for a study involving dimeric systems linked through noncovalent bonds used (5,10,15,20-tetrakis(4-sulfonatophenyl)porphyrinato)zinc(II) and (5,10,15,20-tetrakis(4-*N,N,N*-trimethylanilinium)porphyrinato)magnesium(II) with complementary charge and results in dimerization in solution. Continuous-wave time-resolved EPR spectroscopy demonstrated that intramolecular electron and/or energy transfer in electrostatically bound metalloporphyrin dimers can be controlled via simple metal and substituent effects. Although the metal constituents are identical in these two dimers, it was the peripheral charged substituents that governed the fate of the electron transfer, whereas the energy transfer is controlled via the metal substituents<sup>77,78</sup>.

## V. PHOTOCHEMICAL REACTIONS

### A. Porphyrins

As lipophilic pigments where the (b)chls are embedded in natural systems in apoproteins, photosynthesis in general is a transmembrane process. Thus, PET reactions in lipid membranes have been investigated extensively. Many reports have been published on photoinitiated (where the photoinitiated species acts as a catalysts to mediate thermodynamically favored reactions) and photodriven (where some of the light energy is converted into the products) processes<sup>79</sup>. A typical example are Mg(II)OEP-sensitized electron transfer reactions across lipid bilayer membranes<sup>80</sup>. The reaction mechanism involved a reduction of photoexcited Mg(II)OEP at the reducing (ascorbate) side of the bilayer with the charge carrier most likely being a neutral protonated Mg(II)OEP anion. Thus, the magnesium porphyrin participated as a sensitizer and a transmembrane redox mediator.

More detailed data are available on Mg-substituted horseradish peroxidases. This system can form stable porphyrin  $\pi$ -cation radicals in the presence of oxidants<sup>81,82</sup> and photooxidation and reduction occur through direct reaction of the excited-state porphyrins with oxidants and reductants, respectively. In general, porphyrins appear to be photooxidized both via electron transfer and  $^1\text{O}_2$  mechanisms. Thus, photoirradiation of the Mg-substituted horseradish peroxidase under aerobic conditions results in two simultaneously occurring reactions. A porphyrin  $\pi$ -cation radical is generated through electron transfer from excited porphyrin to  $\text{O}_2$  and a so-called 448-nm compound via a singlet oxygen mechanism. A species with an absorption band at 448 nm was first formed upon irradiation and was then converted in the dark to a final product with a band at 489 nm (Figure 4). The conversion of the 448 nm compound to the 489 nm compound seems

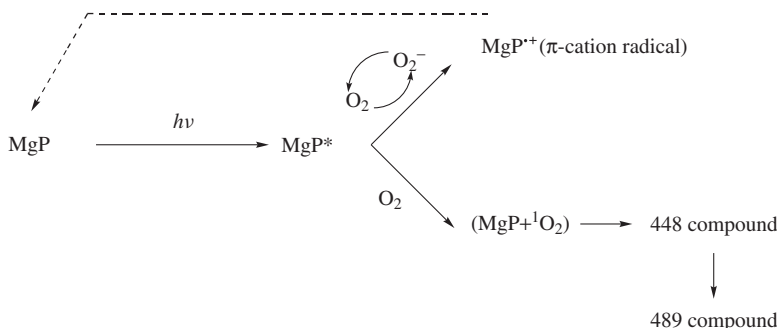


FIGURE 4. Scheme for the photooxidation of porphyrin (P) by Mg horseradish peroxidase

to be an isomerization reaction which requires a high activation energy, probably due to structural restrictions in the heme crevice. Noteworthy is that the 448 and 489 nm compounds both form the same chlorine-type hydroporphyrin with an intense band at 712 nm upon the addition of ascorbate.

## B. Photoinduced Ring-opening Reactions

The formation of long-lived excited states of chlorophyll and its function as energy-storage and catalytic material in photosensitization reactions has been postulated for some time on the basis of indirect evidence. For example, in the 1930s Rabinowitch and Weiss performed spectrophotoelectrochemical studies on the reversible oxidation and reduction of chl<sup>83,84</sup>. An ethylchlorophyllide solution was reversibly oxidized by FeCl<sub>3</sub> to a yellow, unstable intermediate from which the green solution was regenerated by reduction with FeCl<sub>2</sub>. The oxidation was greatly favored by illumination and the equilibrium was shifted by light towards the yellow form. The nature of the reversible reaction with Fe<sup>3+</sup> was considered to be an oxidation in which Fe<sup>3+</sup> was reduced to Fe<sup>2+</sup> and chlorophyll was oxidized to a chl cation or a dehydrochlorophyll species.

About a decade later Calvin and coworkers<sup>85–87</sup> reported that the photochemical reactions of simple chlorins in the presence of either oxygen or various *ortho/para* quinones led to the corresponding porphyrins and unidentified products. Based on kinetic experiments, they proposed a mechanism for the photochemical oxidation of 5,10,15,20-tetraphenylchlorin (H<sub>2</sub>TPC) and  $\beta$ -naphthoquinone involving the triplet state of the chlorin molecule as an intermediate<sup>85</sup>. The production of ions P<sup>+</sup> and P<sup>–</sup> from the first excited triplet state (**T**) of Mg(II)OEP (**P**) predominantly involves triplet–triplet annihilation. Evidence was obtained indicating that the reaction of **T** with ground-state **P** is not a significant source of ions. On the other hand, the two triplets initially can combine to form an excited charge-transfer complex. The relationship between the multiplicity of this charge-transfer complex and triplet quenching, delayed fluorescence and ion formation is illustrated in Figure 5. Less extensive experiments were carried out with Mg(II)TPC due to its instability. However, the data obtained confirmed the existence of a phosphorescence state<sup>86</sup>. The photooxidation rates for the magnesium chlorins were significantly lower (almost 8 times) than for the corresponding zinc complexes.

The magnesium and zinc complexes of TPC can be photooxidized using quinones as hydrogen acceptors. More detailed studies showed that the reaction between quinones and Zn(II)TPC resulted in the formation of Zn(II)TPP<sup>86</sup>. Subsequent work showed that Mg(II)TPC and Zn(II)TPC can be photooxidized by molecular oxygen and *o/p*-quinones. Oxygen is reduced to hydrogen peroxide with a concomitant reduction of quinones to hydroquinones. However, oxygen differs from quinones, as the primary formation of oxidation to porphyrins here is followed by secondary reactions<sup>87</sup>. This second reaction involves H<sub>2</sub>O<sub>2</sub> that can react either directly or as an initiator of Haber–Weiss processes and resulted in the formation of unidentified products<sup>87</sup> similar to those obtained by ‘bleaching’ of chlorophyll in the presence of oxygen<sup>83,84</sup>.

Subsequent work in this area clarified some aspects of the photooxidation of magnesium porphyrins. Barrett found no alteration in the spectral and chromatographic properties of nonfluorescent protoporphyrin complexes of Fe, Ni, Co, Cu and Ag upon irradiation<sup>88</sup>. However, irradiation of (protoporphyrinato dimethyl ester)magnesium(II) **26** in various organic solvents resulted in rapid photooxygenation to green-brown products that did not contain magnesium. Moreover, spectroscopic data indicated an interruption of the aromatic ring system, showed no fluorescence and the appearance of a strong band at 1680 cm<sup>–1</sup>

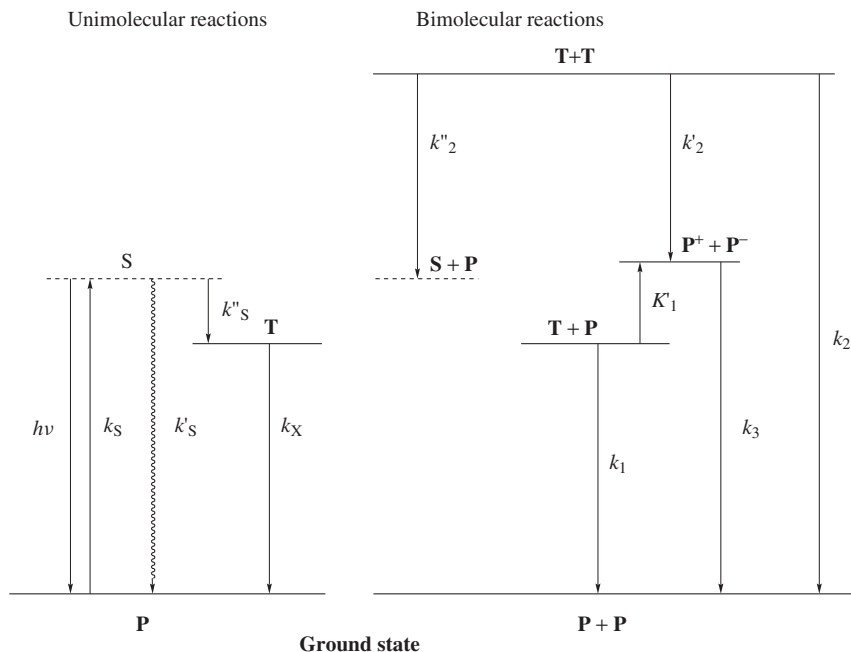
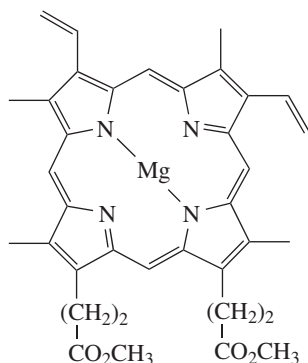


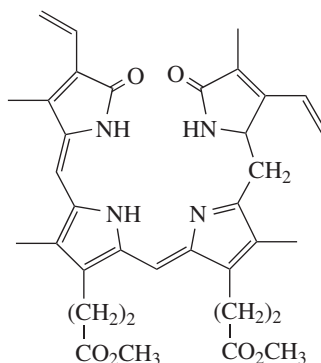
FIGURE 5. Diagram of the triplet decay mechanism

(CCl<sub>4</sub>) in the IR spectrum of the newly formed compound. This green pigment was very photolabile and quickly decomposed to yield 15,16-hydrobiliverdin **27**. Magnesium porphyrins without vinyl side-chains were photooxidized to similar green compounds with the band at 1680 cm<sup>-1</sup>, confirming no oxidation of the vinyl group. The UV/vis spectra of these green products were similar to those of the phlorins obtained by photoreduction of uro-, copro- and hematoporphyrins<sup>89</sup>. Thus, photooxidation of magnesium protoporphyrins resulted in the formation of 15,16-hydrobiliverdins upon ring cleavage. This is in contrast to the enzymatic breakdown of heme which proceeds through biochemical transformations via biliverdin **28** towards the phycobilins<sup>90-92</sup>.

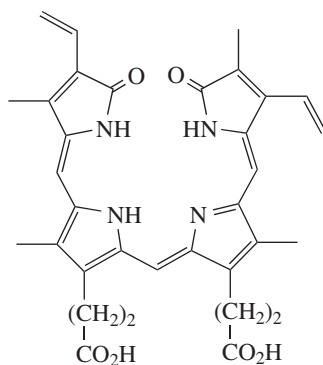
The reaction of porphyrin ligands with molecular oxygen is related to catabolic processes of naturally occurring porphyrins and drugs and is of great importance. Various metalloporphyrins, particularly the chlorophylls present in photosynthetic organisms, can be rapidly destroyed by light and oxygen. In fact, without the presence of photoprotective pigments such as carotenes, no natural chlorophyll-based photosynthetic system would be stable. First studies on the photooxygenation of Mg(II)OEP (**29**),<sup>93-95</sup> Mg(II)TPP<sup>96,97</sup> and Mg(II)protoporphyrin<sup>88</sup> and Mg(II)(tetrabenzoporphyrin)<sup>98,99</sup> were reported in the 1970s and 1980s. For example, when Mg(II)OEP was exposed to visible light in the presence of air in benzene solution, spectroscopic examinations showed that the porphyrin was quantitatively converted into a chromophore with an intense absorption band above 800 nm<sup>88,93,94</sup>. This reaction proceeded uniformly and no intermediates with lifetimes of more than 10 s occurred. The primary product was an open-chain magnesium



(26)



(27)



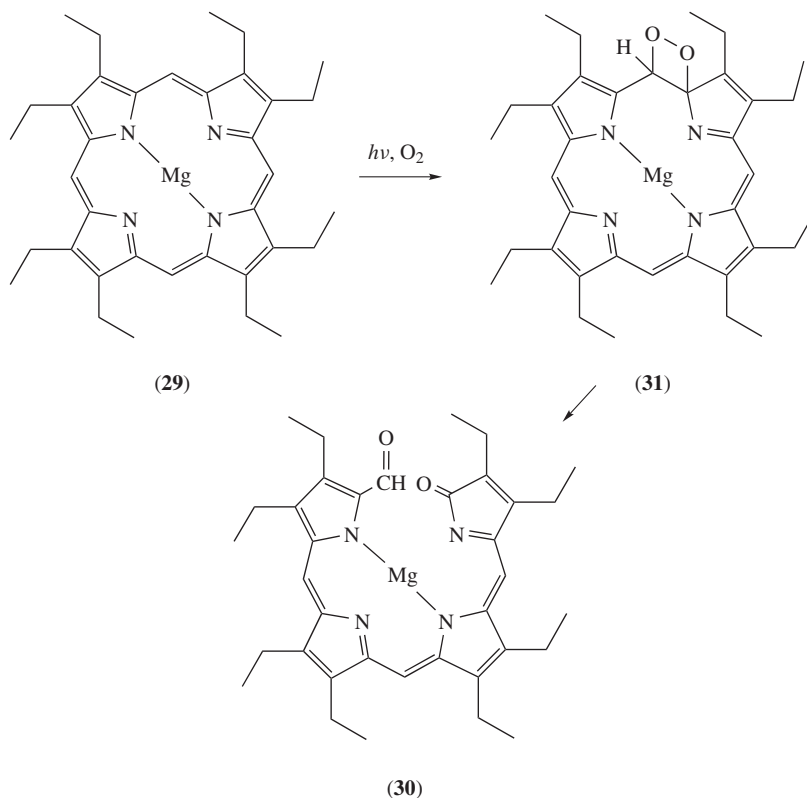
(28)

formylbiliverdin complex **30** that can be easily demetallated to the formylbiliverdin (Scheme 1).

A similar photooxidation pathway was found for Mg(II)TPP. It reacted readily with molecular oxygen to give the corresponding 15,16-dihydrobiliverdin, similar to the one shown for Mg(II)OEP in Scheme 1. Further studies have proposed that the photooxygenation of metallo-*meso*-tetrasubstituted porphyrins proceeds via a one-molecule mechanism involving only one oxygen molecule. Most likely, the first intermediates formed upon photooxygenation are short-lived peroxides. Such compounds are very unstable and a possible dioxetane structure is shown in formula **31**.

### C. Reactions of Chlorophyll

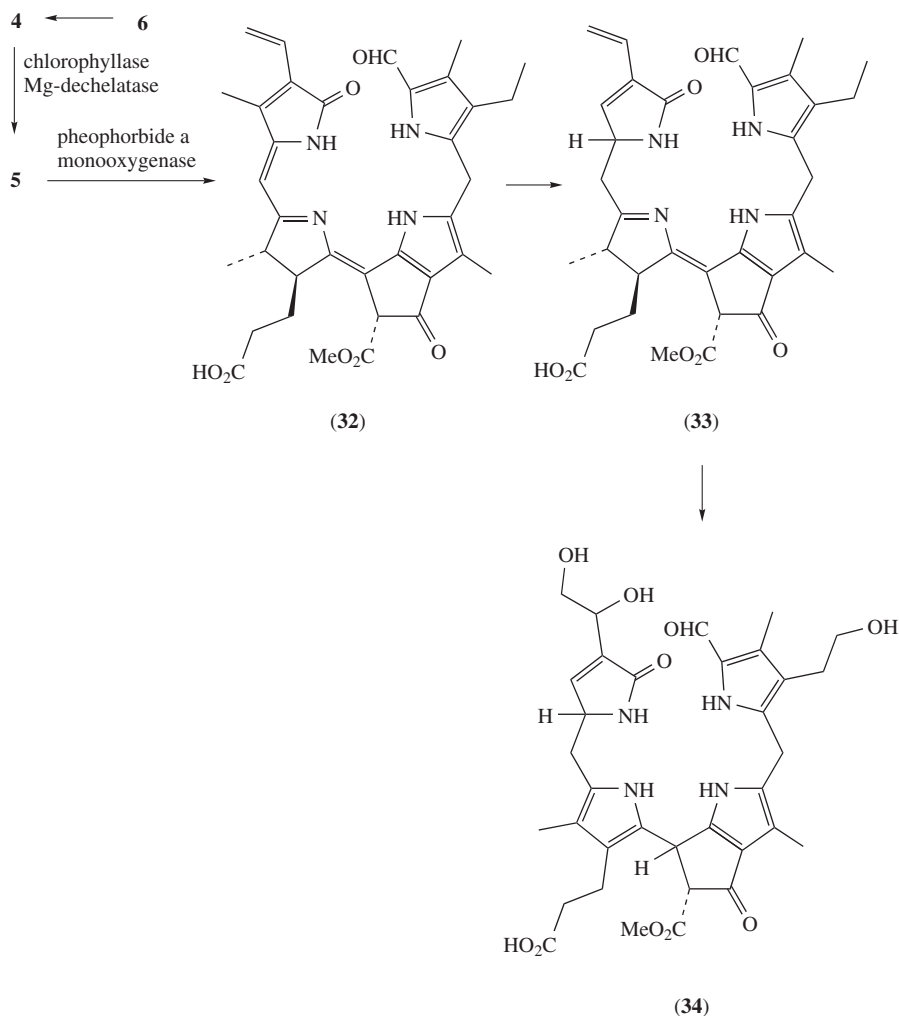
The most obvious chemical reaction involving chlorophyll is the chlorophyll breakdown in fall and during senescence. This process involves annually more than  $10^9$  tons of chlorophyll and, despite its obvious prominence in the natural beauty of the fall season,



SCHEME 1. Photooxygenation of Mg(II)OEP

and its mechanism remained unknown until about 20 years ago<sup>100</sup>. Work by the groups of Kräutler, Matile and Gossauer showed that the central step is a ring-opening reaction at the 5-position<sup>101–103</sup>. This is in contrast to the situation encountered for heme, which is oxidatively cleaved at the 20-position. As shown in Scheme 2, the crucial steps during chl degradation are the conversion of chl a into pheophorbide a (**5**), followed by enzymatic transformation into the bilinone **32**. During this step the macrocycle undergoes oxidative C5 ring-opening, incorporates two oxygen atoms (the CHO one from O<sub>2</sub>) and is saturated at the 10-position. This reaction is catalyzed by a monooxygenase and the red compound **32** is further converted to the still fluorescing compound **33** and finally into the nonfluorescing derivative **34**, along with some changes in the side chains directed to increase the hydrophilicity of the breakdown products. Chl b **6** is first converted into chl a **4** and then subjected to the same reactions. Note that this is an enzymatic process, not a simple photochemical reaction, and should not be confused with the photooxidative ring-opening reactions.

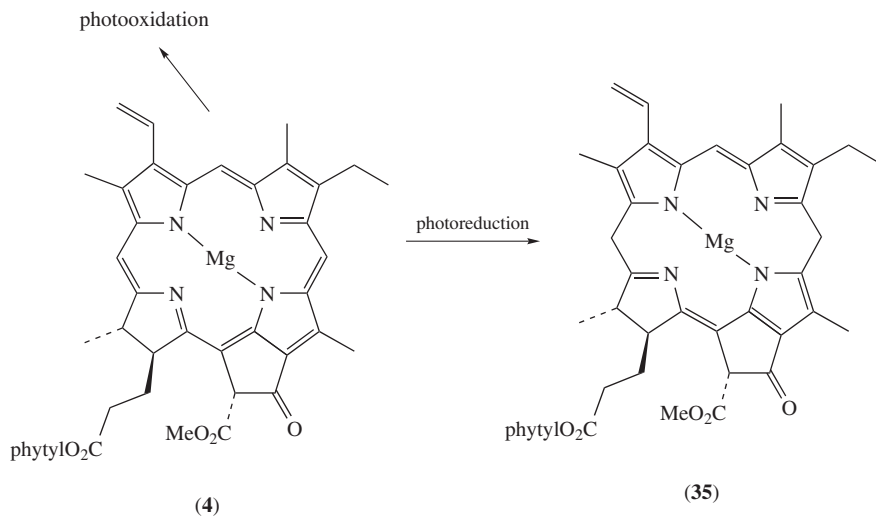
A second reaction involves the chlorin-to-porphyrin conversion. Any chlorin which has hydrogen atoms at the sp<sup>3</sup>-hybridized centers of the reduced ring can be oxidized to the respective porphyrin. Oxidation may be achieved by various oxidants including oxygen<sup>104</sup>. Likewise, reductions to hydroporphyrins and other reactions of the macrocycle are possible. However, most of these are of interest only for the specialist. Under



SCHEME 2. Chlorophyll breakdown during senescence

appropriate conditions photochemical reductions, notably the Krasnovskii reduction to **35**, can occur<sup>105</sup>.

Like porphyrins, chls undergo photooxygenation<sup>106, 107</sup>. Chlorophylls are potent photosensitizers and will produce singlet oxygen in the presence of air or triplet oxygen<sup>104</sup>. Thus, chls can undergo self-destruction (Figure 6). The chemistry of this photooxygenation is very involved and differs somewhat for individual types of (b)chls<sup>103, 105, 108, 109</sup>. While being partially responsible for the low stability of chls in solution<sup>110</sup>, and for unwanted side reactions in food stuff<sup>111</sup>, the same reaction also offers potential for future applications. Chl and derivatives thereof may be used as photosensitizers to affect desired chemical transformations and they have been utilized for applications in photodynamic therapy (PDT)<sup>112</sup>.



SCHEME 3. Formation of the Krasnovski photoproduct of chl

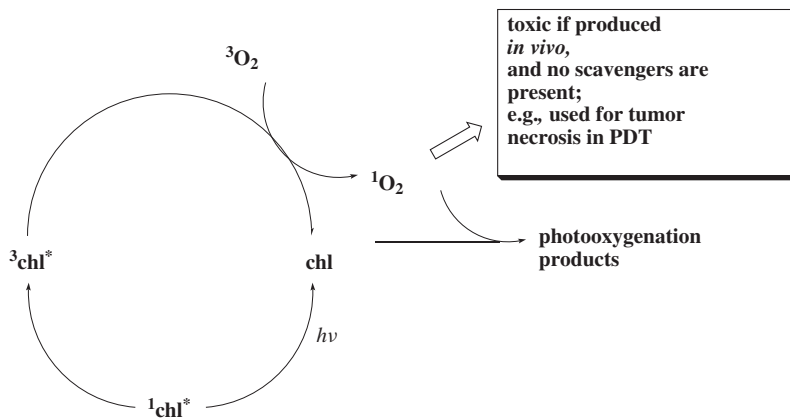
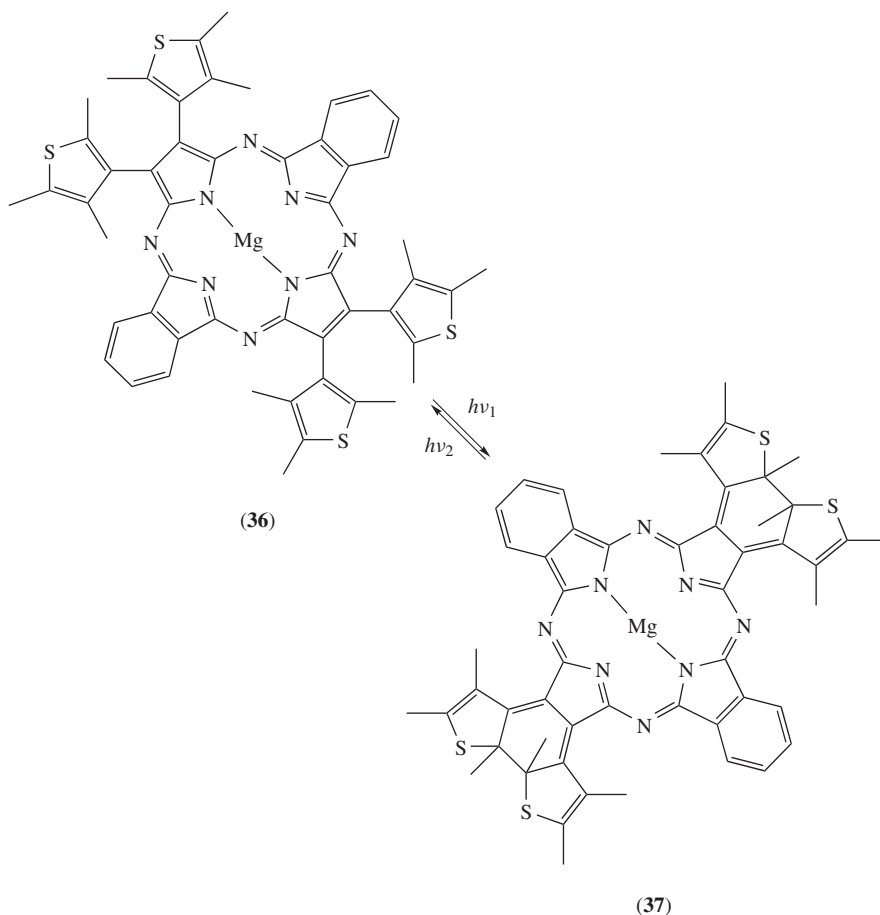


FIGURE 6. Photooxidation reactions of chl

## VI. APPLIED PHOTOCHEMISTRY

The low stability of the magnesium porphyrins has precluded most potential applications. Other metallotetrapyrroles have found industrial uses for oil desulfurization, as photoconducting agents in photocopiers, deodorants, germicides, optical computer disks, semiconductor devices, photovoltaic cells, optical and electrochemical sensing, and molecular electronic materials. A few scattered examples of the use of Mg porphyrins in nonlinear optical studies have appeared<sup>113, 114</sup>, and magnesium phthalocyanines have been used in a few studies as semiconductor or photovoltaic materials<sup>115–117</sup>. One of the few



SCHEME 4. Photochemical interconversion of a magnesium(II) phthalocyanine

true photochemical reactions described for Mg(II) phthalocyanines involved a wavelength-dependent photocyclization of **36** to **37**. Together with the back reaction, the system shown in Scheme 4 was developed to act as a photochromic readout system.<sup>118</sup>

Like the porphyrins, the phthalocyanines can undergo photooxidation and act as photosensitizers for the production of singlet oxygen<sup>119–122</sup>. One of the few chemical synthetic applications was the acceleration of the autoxidation of cumene and photooxidation of pinenes<sup>123</sup>.

Despite their low (photo)stability, chlorophylls, or rather their derivatives, have found some applications, especially in the nutrition industry. In Europe the food additive E140 is chl, and E141 is chlorophyllin (a semisynthetic sodium/copper derivative of chlorophyll), and they are used in cakes, beverages, sweets, icecream etc. As color No 125 they find applications in toothpaste, as a soap pigment and in shampoos. The older literature also



describes its use in candles<sup>124</sup> and as a lipophilic oil bleaching additive (to neutralize the yellow color of oils in food stuff or giving them a greener touch)<sup>125</sup>.

Nevertheless, this is a somewhat misleading statement as in most cases chl is used in the form of chlorophyllin and metal complexes thereof. Chlorophyllin is an inhomogeneous water-soluble material. It is prepared by saponification of the phytol side chain with NaOH and exchange of the central magnesium atom against copper (or other metals). The harsh reaction conditions (and the use of the natural chl a/b mix) results in the formation of a mixture of chemical compounds. Most prominent constituents are derivatives 3<sup>1</sup>,3<sup>2</sup>-didehydrorhodochlorin, pheophorbide salts and the typical allomerization products<sup>126, 127</sup>. Chlorophyllin is a stable pigment with intense light green to dark blue-green color. Related formulations are sodium zinc chlorophyllin, chlorophyll paste, oil-soluble chlorophyll and sodium magnesium chlorophyllin.

Besides the traditional use of chlorophyll and its derivatives as pigments, early investigations on the medicinal use of chlorophyllin in the 1940s led to a first boom in chlorophyll use and initiated more serious investigation of medicinal applications. During those times it was used in bathroom tissue, diapers, chewing gum, bed sheets, shoe liners, toothpaste<sup>128</sup> and other daily products, mostly as an antiodorant. Chlorophyll preparations are still available as over-the-counter (OTC) medicine to reduce fecal odor due to incontinence or to reduce odor from a colostomy or ileostomy. Other applications involved use in wound healing, germ killing and the treatment of infections and inflammations (use of bandages, antiseptic ointments, surgical dressings). Despite these sometime dubious applications all outside the area of photochemistry, there is growing evidence for a medicinal use of chlorophylls. Antimutagenic effects, both *in vitro* and in animal models, have been proven, notably against aflatoxins. Likewise, there are indications for an anticarcinogenic role<sup>128, 129</sup>. For example, an animal study showed inhibition of dioxin absorption and increased fecal excretion of dioxin<sup>130</sup>. At the very least, these results indicate the need for further research and offer the promise of some future chl applications<sup>131, 132</sup>.

Photodynamic therapy presents the one clearly established medicinal application of chlorophyll derivatives to date<sup>133, 134</sup>. This method relies on the selective accumulation of a tetrapyrrole photosensitizer in target tissue where it can be activated with light to produce toxic singlet oxygen resulting in, e.g., tumor necrosis as outlined in Figure 6. Several porphyrin-based compounds have been approved for medicinal applications and others are in Phase-2 trials. Among these tetrapyrroles, chlorophyll derivatives are currently under active investigation and show great promise<sup>112</sup>. Due to the low stability, most cases of chlorin-type hydroporphyrins used in clinical studies and applications are free-base tetrapyrroles. The use of chlorophyll derivatives in technical applications is still in the early developmental stage. Topics of current interest are both solar energy conversion and hydrogen production<sup>135</sup>. As in the case of the PET model compounds, most studies in these cases do use the zinc(II) and not the magnesium(II) derivatives<sup>136, 137</sup>. More specialized works have treated emerging trends and contemporary approaches and a number of reviews dealt with chlorophyll chemistry and related chromophore systems<sup>138, 139</sup>.

## VII. ACKNOWLEDGMENT

Writing of this chapter was made possible by generous funding from Science Foundation Ireland (Research Professorship—SFI 04/RP1/B482).

## VIII. REFERENCES

1. P. C. Harvey, C. L. Junk, C. L. Colin and G. Salem, *J. Org. Chem.*, **53**, 3134 (1988).
2. B. Marciniak and G. L. Hug, *J. Photochem. Photobiol. A: Chem.*, **78**, 7 (1994).
3. B. Marciniak and G. L. Hug, *Coord. Chem. Rev.*, **159**, 55 (1997).

4. M. O. Senge and N. N. Sergeeva, in *The Chemistry of Organozinc Compounds* (Eds. Z. Rappoport and I. Marek), Wiley, Chichester, 2006, pp. 395–419.
5. H. Scheer, in *Chlorophylls* (Ed. H. Scheer), CRC Press, Boca Raton, 1991, pp. 3–30.
6. M. O. Senge, *Chem. Unserer Zeit*, **26**, 86 (1992).
7. M. O. Senge and J. Richter, in *Biorefineries-Industrial Processes and Products* (Eds. B. Kamm, P. R. Gruber and M. Kamm), Vol. 2, Wiley-VCH, Weinheim, 2006, pp. 325–343.
8. M. O. Senge, A. Wiehe and C. Ryppa, in *Chlorophylls and Bacteriochlorophylls* (Eds. B. Grimm, R. J. Porra, W. Rüdiger and H. Scheer), Springer, Berlin, 2006, pp. 27–37.
9. R. H. Douglas, J. C. Partridge, K. Dulai, D. Hunt, C. W. Mullineaux, A. Y. Tauber and P. H. Hynninen, *Nature*, **393**, 423 (1998).
10. M. O. Senge, *J. Photochem. Photobiol. B: Biol.*, **16**, 3 (1992).
11. K. M. Kadish, K. M. Smith and R. Guilard, *The Porphyrin Handbook*, Vol. 1–20, Academic Press, San Diego, CA, 2000.
12. T. Nyokong and H. Isago, *J. Porphyrins Phthalocyanines*, **8**, 1083 (2004).
13. K. M. Kadish, K. M. Smith and R. Guilard, *The Porphyrin Handbook*, Vol. 17, Vol. 19, Academic Press, San Diego, CA, 2000.
14. M. Gouterman, in *The Porphyrins* (Ed. D. Dolphin), Vol. 3, Academic Press, New York, 1978, p. 1.
15. J. Mack and M. J. Stillman, in *The Porphyrin Handbook* (Eds. K. M. Kadish, K. M. Smith and R. Guilard), Vol. 16, Academic Press, San Diego, CA, 2003, pp. 43–116.
16. D. Gust and T. A. Moore, in *The Porphyrin Handbook* (Eds. K. M. Kadish, K. M. Smith and R. Guilard), Vol. 8, Academic Press, San Diego, CA, 2000, pp. 153–190.
17. S. G. Ballard and D. Mauzerall, *Biophys. J.*, **24**, 335 (1978).
18. J. Mack and M. J. Stillman, *J. Am. Chem. Soc.*, **116**, 1292 (1994).
19. S. P. Keizer, W. Han and M. J. Stillman, *Inorg. Chem.*, **41**, 353 (2002).
20. K. Lang, D. M. Wagnerova and J. Brodilova, *J. Photochem. Photobiol. A: Chem.*, **72**, 9 (1993).
21. J. D. Spikes, J. E. van Lier and J. C. Bommer, *J. Photochem. Photobiol. A: Chem.*, **91**, 193 (1995).
22. A. Hiraishi and K. Shimada, *J. Gen. Appl. Microbiol.*, **47**, 161 (2001).
23. A. Hiraishi, K. V. P. Nagashima, K. Matsuura, K. Shimada, S. Takaichi, N. Wakao and Y. Katayama, *Int. J. Syst. Bacteriol.*, **48**, 1389 (1998).
24. N. Wakao, A. Hiraishi, K. Shimada, M. Kobayashi, S. Takaichi, M. Iwaki and S. Itoh, in *The Phototrophic Prokaryotes* (Ed. G. A. Peschek), Kluwer Academic/Plenum Publishers, New York, 1999, p. 745–753.
25. N. Wakao, N. Yokoi, N. Ioyama, A. Hiraishi, K. Shimada, M. Kobayashi, H. Kise, S. Iwaki, S. Itoh, S. Takaichi and Y. Sakurai, *Plant Cell Physiol.*, **37**, 889 (1996).
26. N. Wakao, T. Shiba, A. Hiraishi, M. Ito and Y. Sakurai, *Curr. Microbiol.*, **27**, 277 (1993).
27. N. Kishimoto, F. Fukaya, K. Inagaki, T. Sugio, H. Tanaka and T. Tano, *FEMS Microbiol. Ecol.*, **16**, 291 (1995).
28. H. Scheer and G. Hartwich, in *Anoxygenic Photosynthetic Bacteria* (Eds. R. E. Blankenship, M. T. Madigan and C. E. Bauer), Kluwer Academic Publishers, Dordrecht, 1995, pp. 649–663.
29. M. Kobayashi, M. Yamamura, M. Akiyama, H. Kise, K. Inoue, M. Hara, S. Takaichi, N. Wakao, K. Yahara and T. Watanabe, *Anal. Sci.*, **14**, 1149 (1998).
30. A. Osuka, S. Nakajima, K. Maruyama, N. Mataga, T. Asahi, I. Yamazaki, Y. Nishimura, T. Ohno and K. Nozaki, *J. Am. Chem. Soc.*, **115**, 4577 (1993).
31. M. R. Wasielewski and M. P. Niemczyk, *J. Am. Chem. Soc.*, **106**, 5043 (1984).
32. K. M. Kadish, K. M. Smith and R. Guilard, *The Porphyrin Handbook*, Vol. 13, Academic Press, San Diego, CA, 2000.
33. A. S. Raghavendra, *Photosynthesis*, Cambridge University Press, Cambridge, 1998.
34. R. van Grondelle and V. I. Novoderezhkin, *Phys. Chem. Chem. Phys.*, **8**, 793 (2006).
35. D. Gust, T. A. Moore and A. L. Moore, *Acc. Chem. Res.*, **34**, 40 (2001).
36. M. R. Wasielewski, *Chem. Rev.*, **92**, 435 (1992).
37. Y. Iseki and S. Inoue, *J. Chem. Soc., Chem. Commun.*, 2577 (1994).
38. S. I. Yang, S. Prathapan, M. A. Miller, J. Seth, D. F. Bocian, J. S. Lindsey and D. Holten, *J. Phys. Chem. B*, **105**, 8249 (2001).
39. S. I. Yang, R. K. Lammi, S. Prathapan, M. A. Miller, J. Seth, J. R. Diers, D. F. Bocian, J. S. Lindsey and D. Holten, *J. Mater. Chem.*, **11**, 2420 (2001).

40. S. Fukuzumi, K. Ohkubo, J. Ortiz, A. M. Gutierrez, F. Fernandez-Lazaro and A. Sastre-Santos, *J. Chem. Soc., Chem. Commun.*, 3814 (2005).
41. M. E. El-Khouly, Y. Araki, O. Ito, S. Gadde, A. L. McCarty, P. A. Karr, M. E. Zandler and F. D'Souza, *Phys. Chem. Chem. Phys.*, **7**, 3163 (2005).
42. F. D'Souza, M. E. El-Khouly, S. Gadde, A. L. McCarty, P. A. Karr, M. E. Zandler, Y. Araki and O. Ito, *J. Phys. Chem. B*, **109**, 10107 (2005).
43. F. Mitzel, S. FitzGerald, A. Beeby and R. Faust, *Chem. Eur. J.*, **9**, 1233 (2003).
44. T. Chandra, B. J. Kraft, J. C. Huffman and J. M. Zaleski, *Inorg. Chem.*, **42**, 5158 (2003).
45. W. J. Youngblood, D. T. Gryko, R. K. Lammi, D. F. Bocian, D. Holten and J. S. Lindsey, *J. Org. Chem.*, **67**, 2111 (2002).
46. F. Li, S. Gentemann, W. A. Kalsbeck, J. Seth, J. S. Lindsey, D. Holten and D. F. Bocian, *J. Mater. Chem.*, **7**, 1245 (1997).
47. J. Fajer, D. C. Borg, A. Forman, D. Dolphin and R. H. Felton, *J. Am. Chem. Soc.*, **92**, 3451 (1970).
48. J. F. Smalley, S. W. Feldberg and B. S. Brunschwig, *J. Phys. Chem.*, **87**, 1757 (1983).
49. R. Slota and G. Dyrda, *Inorg. Chem.*, **42**, 5743 (2003).
50. H. van Willigen and M. H. Ebersole, *J. Am. Chem. Soc.*, **109**, 2299 (1987).
51. A. P. Bobrovskii and V. E. Kholmogorov, *Russ. J. Phys. Chem.*, **47**, 983 (1973).
52. E. Ough, Z. Gasyna and M. J. Stillman, *Inorg. Chem.*, **30**, 2301 (1991).
53. D. Kim, *Bull. Korean Chem. Soc.*, **7**, 416 (1986).
54. H. Stiel, K. Teuchner, A. Paul, W. Freyer and D. Leupold, *J. Photochem. Photobiol. A: Chem.*, **80**, 289 (1994).
55. J. Feitelson and D. C. Mauzerall, *J. Phys. Chem.*, **97**, 8410 (1993).
56. K. Wynne, S. M. LeCours, C. Galli, M. J. Therien and R. M. Hochstrasser, *J. Am. Chem. Soc.*, **117**, 3749 (1995).
57. T. L. Netzel, M. A. Bergkamp, C. K. Chang and J. Dalton, *J. Photochem.*, **17**, 451 (1981).
58. V. B. Evstigneev and V. A. Gavrilova, *Biofizika*, **14**, 43 (1969); *Chem. Abstr.*, **70**, 93263w (1969).
59. A. V. Barmasov, V. I. Korotkov and V. Ye. Kholmogorov, *Biofizika*, **39**, 263 (1994); *Chem. Abstr.*, **121**, 267490g (1994).
60. J. M. Furois, P. Brochette and M. P. Pileni, *J. Colloid Interface Sci.*, **97**, 552 (1984).
61. W. S. Szulbinski, *Inorg. Chim. Acta*, **228**, 243 (1995).
62. J. Zakrzewski and C. Giannotti, *Inorg. Chim. Acta*, **232**, 63 (1995).
63. A. Harriman, G. Poter and M.-C. Richoux, *J. Chem. Soc., Faraday Trans.*, **77**, 1175 (1981).
64. H. Ohtani, T. Kobayashi, T. Ono, S. Kato, T. Tanno and A. Yamada, *J. Phys. Chem.*, **88**, 4431 (1984).
65. G. I. Kobyshev, G. N. Lyalin and A. N. Terenin, *Dokl. Akad. Nauk SSSR*, **153**, 865 (1963); *Chem. Abstr.*, **60**, 14357e (1963).
66. C. Monnereau, J. Gomez, E. Blart and F. Odobel, *Inorg. Chem.*, **44**, 4806 (2005).
67. A. Gabrielsson, F. Hartl, H. Zhang, J. R. Lindsay Smith, M. Towrie, A. Vlcek Jr. and R. N. Perutz, *J. Am. Chem. Soc.*, **128**, 4253 (2006).
68. H. Imahori, *Org. Biomol. Chem.*, **2**, 1425 (2004).
69. H. Imahori and S. Fukuzumi, *Adv. Funct. Mater.*, **14**, 525 (2004).
70. H. Imahori, K. Tamaki, Y. Araki, T. Hasobe, O. Ito, A. Shimomura, S. Kundu, T. Okada, Y. Sakata and S. Fukuzumi, *J. Phys. Chem. A*, **106**, 2803 (2002).
71. H. Levanon, A. Regev, T. Galili, M. Hugerat, C. K. Chang and J. Fajert, *J. Phys. Chem.*, **97**, 13198 (1993).
72. H. Zhang, E. Schmidt, W. Wu, C. K. Chang and G. T. Babcock, *Chem. Phys. Lett.*, **234**, 133 (1995).
73. J. M. Zaleski, W. Wu, C. K. Chang, G. E. Leroi, R. I. Cukier and D. G. Nocera, *Chem. Phys.*, **176**, 483 (1993).
74. A. Osuka, S. Marumo, S. Taniguchi, T. Okada and N. Mataga, *Chem. Phys. Lett.*, **230**, 144 (1994).
75. A. Osuka, S. Marumo, K. Maruyama, N. Mataga, M. Ohkohchi, S. Taniguchi, T. Okada, I. Yamazaki and Y. Nishimura, *Chem. Phys. Lett.*, **225**, 140 (1994).
76. A. Osuka, F. Kobayashi, K. Maruyama, N. Mataga, T. Asahi, T. Okada, I. Yamazaki and Y. Nishimura, *Chem. Phys. Lett.*, **201**, 223 (1993).

77. S. Murov, I. Carmichael and G. Hug, *Handbook of Photochemistry*, Marcel Dekker, New York, 1993.
78. A. Berg, M. Rachamim, T. Galili and H. Levanon, *J. Phys. Chem.*, **100**, 8791 (1996).
79. S. Tunuli and J. H. Fendler, *J. Am. Chem. Soc.*, **103**, 2507 (1981).
80. A. Ilani, M. Woodle and D. Mauzerall, *Photochem Photobiol.*, **49**, 673 (1989).
81. Y. Kuwahara, M. Tamura and I. Yamazaki, *J. Biol. Chem.*, **257**, 11517 (1982).
82. J. Deguchi, M. Tamura and I. Yamazaki, *J. Biol. Chem.*, **260**, 15542 (1985).
83. E. Rabinowitch and J. Weiss, *Nature*, **138**, 1098 (1936).
84. E. Rabinowitch and J. Weiss, *Proc. Roy. Soc. London*, **A162**, 251 (1937).
85. M. Calvin and G. D. Dorough, *J. Am. Chem. Soc.*, **70**, 699 (1948).
86. F. M. Huennekens and M. Calvin, *J. Am. Chem. Soc.*, **71**, 4024 (1949).
87. F. M. Huennekens and M. Calvin, *J. Am. Chem. Soc.*, **71**, 4031 (1949).
88. J. Barrett, *Nature*, **215**, 733 (1967).
89. D. Mauzerall, *J. Am. Chem. Soc.*, **84**, 2437 (1962).
90. S. I. Beale and J. Cornejo, *J. Biol. Chem.*, **266**, 22341 (1991).
91. S. I. Beale and J. Cornejo, *J. Biol. Chem.*, **266**, 22333 (1991).
92. S. I. Beale and J. Cornejo, *J. Biol. Chem.*, **266**, 22328 (1991).
93. J.-H. Fuhrhop and D. Mauzerall, *Photochem. Photobiol.*, **13**, 453 (1971).
94. J.-H. Fuhrhop, *Angew. Chem., Int. Ed. Engl.*, **13**, 321 (1974).
95. J.-H. Fuhrhop, P. K. W. Wasser, J. Subramanian and U. Schrader, *Justus Liebig's Ann. Chem.*, 1450 (1974).
96. T. Matsuura, K. Inoue, C. R. Ranade and I. Saito, *Photochem. Photobiol.*, **31**, 23 (1980).
97. K. M. Smith, S. B. Brown, R. E. Troxler and J.-J. Lai, *Tetrahedron Lett.*, **21**, 2763 (1980).
98. J. C. Goedheer and J. P. J. Siero, *Photochem. Photobiol.*, **6**, 509 (1967).
99. J. C. Goedheer, *Photochem. Photobiol.*, **6**, 521 (1967).
100. G. A. Hendry, J. D. Houghton and S. B. Brown, *New Phytol.*, **107**, 25 (1987).
101. B. Kräutler and P. Matile, *Acc. Chem. Res.*, **32**, 35 (1999).
102. A. Gossauer and N. Engel, *J. Photochem. Photobiol. B: Biol.*, **32**, 141 (1996).
103. J. Iturraspe, N. Moyano and B. Frydman, *J. Org. Chem.*, **60**, 6664 (1995).
104. H. H. Inhoffen, *Pure Appl. Chem.*, **17**, 443 (1968).
105. H. Scheer and J. J. Katz, *Proc. Natl. Acad. Sci. USA*, **71**, 1626 (1974).
106. P. H. Hynninen, in *Chlorophylls* (Ed. H. Scheer), CRC Press, Boca Raton, 1991, pp. 145–209.
107. V. V. Gurinovich and M. P. Tsvirko, *J. Appl. Spectrosc.*, **68**, 110 (2001).
108. R. F. Troxler, K. M. Smith and S. B. Brown, *Tetrahedron Lett.*, **21**, 491 (1980).
109. C. A. Llewellyn, R. F. C. Mantoura and R. G. Brereton, *Photochem. Photobiol.*, **52**, 1037 (1990); *Photochem. Photobiol.*, **52**, 1043 (1990).
110. A. Peled, Y. Dror, I. Baal-Zedaka, A. Porat, N. Michrin and I. Lapsker, *Synth. Metals*, **115**, 167 (2000).
111. D. B. Min and J. M. Boff, *Compr. Rev. Food Sci. Food Saf.*, **1**, 58 (2002).
112. E. S. Nyman and P. H. Hynninen, *J. Photochem. Photobiol. B: Biol.*, **73**, 1 (2004).
113. M. O. Senge, M. Fazekas, E. G. A. Notaras, W. J. Blau, M. Zawadzka, O. B. Locos and E. M. Ni Mhuircheartaigh, *Adv. Mater.*, **19**, 2737 (2007).
114. S. Yamada, K. Kuwata, H. Yonemura and T. Matsuo, *J. Photochem. Photobiol. A: Chem.*, **87**, 115 (1995).
115. C. Ingrosso, A. Petrella, P. Cosma, M. L. Curri, M. Striccoli and A. Agostiano, *J. Phys. Chem. B*, **110**, 24424 (2006).
116. Y. Osada, A. Mizumoto and H. Tsuruta, *J. Macromol. Sci., Chem.*, **A24**, 403 (1987).
117. Y. S. Shumov, V. I. Kromov, P. F. Sidorskih and V. I. Mityaev, *Russ. J. Phys. Chem.*, **52**, 886 (1978).
118. Q. Luo, H. Tian, B. Chen and W. Huang, *Dyes Pigments*, **73**, 118 (2007).
119. M. Kobayashi, M. Yamamura, M. Akiyama, H. Kise, K. Inoue, M. Hara, S. Takaichi, N. Wakao, K. Yahara and T. Watanabe, *Anal. Sci.*, **14**, 1149 (1998).
120. N. A. Kuznetsova, N. S. Gretsova, V. M. Derkacheva, O. L. Kaliya and E. A. Lukyanets, *J. Porphyrins Phthalocyanines*, **7**, 147 (2003).
121. W. Maqanda, T. Nyokong and M. D. Maree, *J. Porphyrins Phthalocyanines*, **9**, 343 (2005).
122. N. A. Kuznetsova, V. V. Okunchikov, V. M. Derkacheva, O. L. Kaliya and E. A. Lukyanets, *J. Porphyrins Phthalocyanines*, **9**, 393 (2005).
123. H. Kropf and B. Kasper, *Justus Liebig's Ann. Chem.*, 2232 (1975).

124. H. J. Arpe, *Ullmann's Encyclopedia of Industrial Chemistry*, 5th Edition, Wiley-VCH, Weinheim, 1997.
125. J. C. Kephart, *Econ. Bot.*, **9**, 3 (1955).
126. M. Strell, A. Kalojanoff and F. Zuther, *Arzneimittel-Forsch.*, **5**, 640 (1955); *Chem. Abstr.*, **50**, 3712h (1955).
127. M. Strell, A. Kalojanoff and F. Zuther, *Arzneimittel-Forsch.*, **6**, 8 (1956); *Chem. Abstr.*, **50**, 5993f (1956).
128. J. W. Hein, *J. Am. Dent. Assoc.* **48**, 14 (1954).
129. D. L. Sudakin, *J. Toxicol. Clin. Toxicol.*, **41**, 195 (2003).
130. A. R. Waladkhani and M. R. Clemens, *Int. J. Mol. Med.*, **1**, 747 (1998).
131. S. Chernomorsky, A. Segelmann and R. D. Poretz, *Teratogen. Carcin. Mut.*, **19**, 313 (1999).
132. K. Morita, M. Ogata and T. Hasegawa, *Environ. Health Perspect.*, **109**, 289 (2001).
133. J. D. Spikes and J. C. Bommer, in *Chlorophylls* (Ed. H. Scheer), CRC Press, Boca Raton, 1991, pp. 1181–1204.
134. R. Bonnett, *Chemical Aspects of Photodynamic Therapy*; Gordon and Breach Sci. Publ., Amsterdam, 2000.
135. N. Himeshima and Y. Amao, *Energ. Fuel.*, 1641 (2003).
136. J. Woodward, M. Orr, K. Cordray and E. Greenbaum, *Nature*, **405**, 1014 (2000).
137. T. Inoue, S. N. Kumar, T. Karnachi and I. Okura, *Chem. Lett.*, 147 (1999).
138. B. D. Berezin, S. V. Rumyantseva, A. P. Moryganov and M. B. Berezin, *Russ. Chem. Rev.*, **73**, 185 (2004).
139. M. O. Senge and K. M. Smith, in *Anoxygenic Photosynthetic Bacteria* (Eds. R. E. Blankenship, M. T. Madigan and C. E. Bauer), Kluwer, Dordrecht, 1995, pp. 137–151.

## CHAPTER 6

# Electrochemistry of organomagnesium compounds

JAN S. JAWORSKI

*Faculty of Chemistry, University of Warsaw, 02-093 Warszawa, Poland*  
*Fax: +48-22-822-5996; e-mail: jaworski@chem.uw.edu.pl*

I. INTRODUCTION .....	219
II. ELECTROCHEMICAL SYNTHESIS OF ORGANOMAGNESIUM COMPOUNDS .....	221
III. CONDUCTIVITY OF SOLUTIONS OF ORGANOMAGNESIUM COMPOUNDS .....	224
IV. ANODIC OXIDATION OF ORGANOMAGNESIUM COMPOUNDS ...	227
A. Simple Diorganomagnesium Compounds .....	227
B. Grignard Reagents .....	228
1. Oxidation at inert electrodes .....	229
2. Anodic addition to olefins .....	237
3. Oxidation on sacrificial anodes .....	237
4. Processes at semiconductor anodes .....	241
C. Other Compounds .....	243
V. CATHODIC REDUCTION OF ORGANOMAGNESIUM COMPOUNDS .	244
A. General Mechanism of the Reduction .....	244
B. Deposition of the Metallic Magnesium and the Reverse Process .....	245
VI. ORGANOMAGNESIUM COMPOUNDS AS INTERMEDIATES IN ELECTRODE REACTIONS .....	253
VII. CONCLUDING REMARKS: ELECTROCHEMICAL DATA IN THE ELUCIDATION OF REACTIVITY OF GRIGNARD REAGENTS .....	258
VIII. REFERENCES .....	260

### I. INTRODUCTION

In the last 37 years a number of chapters and reviews have been published on electrochemistry of organoelemental and organometallic compounds<sup>1-9</sup> discussing electrode reactions of organomagnesium compounds, in particular Grignard reagents, the most important ones

---

*The chemistry of organomagnesium compounds*

Edited by Z. Rappoport and I. Marek © 2008 John Wiley & Sons, Ltd. ISBN: 978-0-470-05719-3

in organic chemistry among the title compounds. However, so far no separate monograph has been devoted to that specific topic. Nevertheless, the investigations into electrochemical behavior of Grignard reagents have a rich and long history, going back to 1912 with the unsuccessful attempt of Jolibois<sup>10,11</sup> to isolate the expected gaseous hydrocarbons during the electrolysis of their ethereal solutions, and the report of Nelson and Evans in 1917 on the conductivity of such solutions<sup>12</sup>. Kondyrew verified in 1925 that the loss of a magnesium anode in the electrolysis of these reagents fulfills Faraday laws and magnesium is deposited at a cathode<sup>13</sup>. Dimeric hydrocarbons as the main products of electrolysis were found by Gaddum and French in 1927<sup>14</sup>. The earliest research on the conductivity and electrolysis was continued and it helped to explain the nature of Grignard reagents in ethereal solutions<sup>15</sup>. A general mechanism of electrode processes in these solutions was established around 1940 by Evans and coworkers after a couple of years of investigations<sup>15–23</sup>. It was progressively found that the following reactions of alkyl or aryl radicals formed at electrodes are strongly dependent on the conditions of the electrolysis: the nature of the radical and the halide as well as on the electrode material. This behavior opened up a wide area of synthetic applications. It is one of the most characteristic and fascinating trends in the electrochemistry of organomagnesium compounds: most investigations were strongly directed to applications in industry and laboratory practice. A large amount of the results was patented. As a result, large-scale industrial production of tetraalkyl lead from Grignard reagents by the Nalco process started in 1964 (followed by the production of adiponitrile by the Monsanto process in the next year). This stimulated a rapid development of organic electrochemistry as a separate field with wide potential applications in industry. Although the next decades brought about a significant decrease in the production of  $R_4Pb$  because of environmental constraints, yet electroorganic methods are still thought to be particularly safe and valuable for ‘green chemistry’. In this Chapter references to important, mostly US, patents are given; however, our attention is focused only on the reaction mechanisms and products distribution under the given conditions, which is the essential topic of interest for organic chemists. More details can be found in original documents easily available (using the given patent number) from websites, e.g. European Patent Office: [ep.espacenet.com](http://ep.espacenet.com).

On the other hand, because of this strong interest in the practical use of organomagnesium compounds, as well as the beginnings of electrochemical studies in the early decades of the 20th century, many details of mechanisms of their heterogeneous reactions were not investigated later by modern and powerful electroanalytical and spectroscopic techniques. There is still a lack of such data, with the exception perhaps of some very recent studies which focus their interest on applications in rechargeable magnesium batteries (Section V.B) and a grafting of a silicon surface by anodic reactions of Grignard reagents for use in electronics (Section IV.B.4). It may also be interesting to note that these last investigations are strictly related to the ‘modern face’ of electrochemistry, which increasingly becomes the surface science investigating electrochemical reactions at well-defined solid surfaces, using different *in situ* spectroscopic techniques to determine the nature, structure and reactivity of the adsorbed species and open new directions, like material science and nanotechnology.

In this Chapter, first of all in Section II, the synthesis of diorganomagnesium compounds is reviewed, including the use of direct electrochemical reactions and combined methods with electrochemical and homogeneous steps. A brief review on the conductivity of solutions of organomagnesium compounds indicating a complex nature and dynamic behavior of ionic species present in solutions is given in Section III. The discussion of electrochemical behavior of the title compounds is divided into two parts. First, in Section IV, the anodic oxidation is given involving the reactions of organic radicals that are probably more interesting for the readers of this book. Then, in Section V the cathodic reduction is described, accompanied by the deposition of metallic magnesium.

Such a division should make the discussion clearer for readers, although it should be remembered that many investigations, in particular the research of Grignard reagents, were often performed in undivided electrochemical cells, where both kinds of processes occur at the same time. For anodic processes, consecutively the oxidation of simple diorganomagnesium compounds (Section IV.A) and Grignard reagents at various kinds of anodes (Section IV.B) are discussed. The example of the oxidation of other groups in organomagnesium compounds is mentioned in Section IV.C. For cathodic processes the general mechanism is presented in Section V.A, but the following reactions of organic radicals are the same as in anodic processes, discussed earlier. However, the deposition of metallic magnesium and the reverse process, important in recent years because of applications in rechargeable batteries, but also giving some interesting explanations of the nature of electroactive organomagnesium species, are discussed in Section V.B.

The use of sacrificial magnesium anodes in the electrochemical preparation of a number of organic compounds with high selectivity has been popular for decades. In most of the reported mechanisms magnesium cations produced from an anode form salts or complexes with organic anions. However, in a few cases the organomagnesium compounds are formed as intermediates and these processes are discussed in Section VI. Finally, the concluding remarks in Section VII focus on the use of some electrochemical data in order to elucidate the nature of Grignard reagents in solutions and to explain the most probable mechanism of homogeneous Grignard reactions.

In this Chapter the following common abbreviations are used, beside those used in this book:  $n_e$ , the number of electrons in a given reaction; CV, cycling voltammetry; OCP, open circuit potential; rds, rate-determining step; EDAX, elemental analysis by dispersive X-rays; SEM, scanning electron microscopy; STM, scanning tunneling microscopy; ATR, attenuated total reflection; XPS, X-ray photoelectron spectroscopy; EQCM, electrochemical quartz crystal microbalance; ECL, electrochemiluminescence; ACN, acetonitrile; TBAP, tetrabutylammonium perchlorate; TBAPF<sub>6</sub>, tetrabutylammonium hexafluorophosphate; TBABF<sub>4</sub>, tetrabutylammonium tetrafluoroborate; GC, glassy carbon; and M, mole dm<sup>-3</sup>.

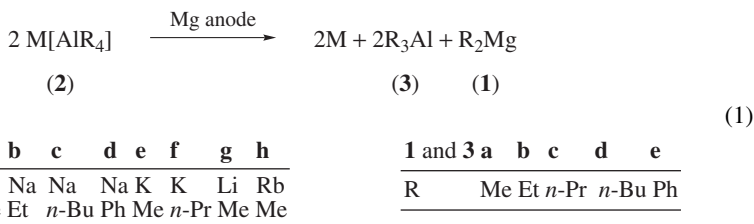
The quoted potentials are rarely expressed versus standard hydrogen electrode (SHE) but mainly versus an aqueous saturated calomel electrode (SCE) or versus Ag/Ag<sup>+</sup> couple in ACN or in a solvent used in particular experiments. However, in some cases the Mg/Mg<sup>2+</sup> couple in THF or other solvents is used as the reference electrode.

## II. ELECTROCHEMICAL SYNTHESIS OF ORGANOMAGNESIUM COMPOUNDS

In general, it is possible to obtain diorganomagnesium compounds R<sub>2</sub>Mg (**1**) by the anodic oxidation of organoelemental complexes, such as Na[ZnR<sub>3</sub>], Na[AlR<sub>4</sub>] or Na[BR<sub>4</sub>], using the sacrificial magnesium anode. For example, Et<sub>2</sub>Mg (**1b**) can be obtained with 73% yield in the electrolysis at 150 °C of melted Na[BEt<sub>4</sub>] using a Mg anode and a Hg cathode<sup>24</sup>; the second product Et<sub>3</sub>B can be used to regenerate the electrolyte. The use of alkylaluminates (**2**) for this purpose was reviewed by Lehmkuhl<sup>2</sup>. R<sub>2</sub>Mg•2AlR<sub>3</sub> formed at the magnesium anode and liquid alkali metal or its amalgam, depending on the metal of the cathode, are the products of electrolysis. In particular, from the electrolysis of a 1:1 mixture of Na[AlEt<sub>4</sub>] (**2b**) and K[AlEt<sub>4</sub>] using a mercury cathode it is possible to obtain Mg[AlEt<sub>4</sub>]<sub>2</sub>, which formally corresponds to Et<sub>2</sub>Mg•2Et<sub>3</sub>Al. In the method patented by Ziegler and Lehmkuhl<sup>25</sup> the electrolysis was performed in an inert gas atmosphere (e.g. nitrogen or argon) using melted NaF•2Et<sub>3</sub>Al (m.p. 35 °C) as an electrolyte and the final product **1b** could be continuously extracted by Et<sub>3</sub>Al (**3b**) with which it forms Et<sub>2</sub>Mg•2Et<sub>3</sub>Al. Volatile **3** is easily removed by heating at about 120 °C in vacuum and **1b** remains in the solid state. The anodic and cathodic spaces should be separated by



a diaphragm, because otherwise magnesium is deposited at the iron cathode, instead of aluminium, which can be converted to **3b** and reused. Kobetz and Pinkerton patented a method<sup>26</sup> based on the electrolysis according to reaction 1 using a steel cathode and a magnesium anode in melted electrolytes, containing a mixture of two alkylaluminates (**2**) with methyl groups in at least one of them. The addition of a second component, with other alkyl or phenyl groups, results in lowering of the melting point and increasing the electrical conductivity of the mixture in comparison with the values characteristic of each component alone. However, then the product is the mixture of molecules of **1** with different R's, as is shown in Table 1 for the first entry. The yield of the main product is increased by the proper ratio of both components of the electrolyte and some results reported<sup>26</sup> are shown in Table 1. The original electrolysis product  $R_2Mg \cdot 2R_3Al$  is floating on the electrolyte adjacent to the anode and the vacuum distillation of **3** (at 300 mm Hg) releases crystalline **1**. The distillation can be performed continuously during vacuum electrolysis or the electrolysis is carried out in the atmosphere of an inert gas, to avoid any contact with oxygen and moisture (**3** is flammable on air). Compound **3** is next used to regenerate the electrolyte in the reaction with  $M[BR_4]$ .



The improved electrolytic production of magnesium dialkyls **1** with R containing from 2 to 6 carbon atoms using melted **2** as an electrolyte (with M = Na or a mixture of Na with up to 80% of K), a copper cathode and a magnesium anode, separated by a diaphragm in an originally designed apparatus was also patented by Ziegler and Lehmkuhl<sup>27</sup> and the example of their electrolysis is given in Table 1 in the last entry.

Versatile electrochemical generation of diorganomagnesium compounds **1** corresponding to unusual Grignard reagents, containing electrophilic groups, such as halogen, carbonyl and cyano, was proposed by Lund and coworkers<sup>28</sup>. Those substituents are reduced by magnesium and thus such reagents cannot be obtained by the classical reduction of

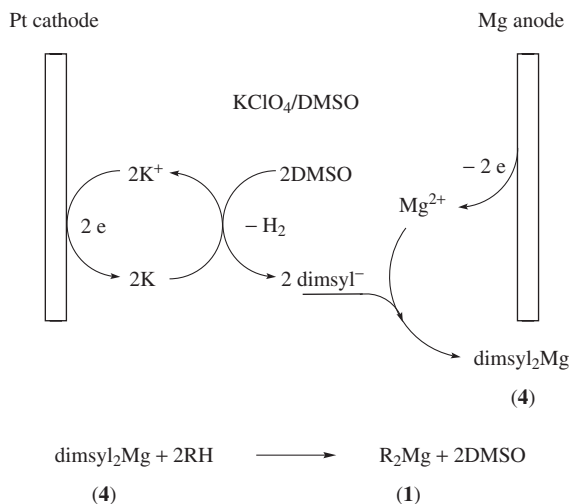
TABLE 1. Main products (after distillation of **3**) and temperatures of the electrolysis of **2** at the Mg anode<sup>26,27</sup>

Electrolyte		Temperature (°C)	Main product	Reference
components	mole ratio			
<b>2a:2b</b>	1:1	<i>ca</i> 100	<b>1b</b> <sup>a</sup>	26
<b>2a:2b</b>	1:3	<i>ca</i> 100	<b>1b</b> <sup>b</sup>	26
<b>2e:2f</b>	1:8	150	<b>1c</b>	26
<b>2a:2d</b>	2:3	175	<b>1a + 1e</b>	26
<b>2h:2a</b>	1:5	140	<b>1a</b>	26
<b>2g:2c</b>	1:3	not specified	<b>1d</b>	26
<b>2b</b>	—	120	<b>1b</b> <sup>c</sup>	27

<sup>a</sup>The electrolysis at 7.4 V and 0.25 A cm<sup>-2</sup>; other products are **1a** and MeEtMg.

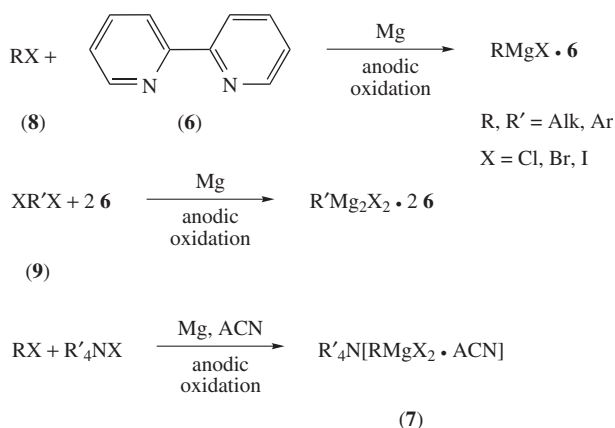
<sup>b</sup>Ethyl groups in  $R_2Mg \cdot 2R_3Al$  approach 90%.

<sup>c</sup>95% yield; the electrolysis at 5 V.



SCHEME 1

organic halide by Mg. The method proposed consists of the electrolysis of potassium perchlorate in dry and deaerated DMSO in an undivided cell with a platinum cathode and a sacrificial magnesium anode. The overall process<sup>28</sup>, shown in Scheme 1, results in the formation of strong dimsylvan base (i.e. the conjugate base of DMSO) in the reaction of potassium, formed at the cathode, with the solvent. Simultaneously, magnesium cations generated at an anode stabilize dimsylvan anions through the interaction viewed as ion association (ion-pairs<sup>28</sup> or rather triple ion formation) in a magnesium salt  $\text{dimsylvan}_2\text{Mg}$  (**4**). In a second nonelectrochemical step, the added weakly acidic substrate, RH, with  $\text{p}K_{\text{a}} < 26$  (all  $\text{p}K_{\text{a}}$  values cited<sup>28</sup> refer to DMSO), is deprotonated by **4**, resulting in the formation of **1**.



SCHEME 2

The effective deprotonation of fluorene ( $pK_a = 22.6$ ), 2-bromofluorene ( $pK_a = 20.0$ ), 2,7-dibromofluorene ( $pK_a \leq 20.0$ ), acetophenone ( $pK_a = 24.7$ ) and phenylacetonitrile ( $pK_a = 21.9$ ) was shown<sup>28</sup>, but not for weaker acids such as 4-benzylpyridine ( $pK_a = 26.7$ ). The usefulness of generated reagents **1** was illustrated<sup>28</sup> in reactions of nucleophilic addition to electrophiles, characteristic of the ordinary Grignard reagents (**5**, Tables 2 and 3), as will be reviewed in Section VI.

The direct electrochemical synthesis (Scheme 2) of the adducts of organomagnesium halides with 2,2'-bipyridine (**6**) and salts of organodihalogenomagnesium(II) anions (**7**) was reported by Hayes and coworkers<sup>29</sup>. Adducts of different stoichiometry and **7** were obtained in the electrochemical oxidation of magnesium in ACN solutions containing organic halides RX (**8**),  $\alpha,\omega$ -dihalides  $XR'X$  (**9**) and **8** with ammonium salts  $R'_4NX$ , respectively. All new products showed none of the typical reactions of Grignard reagents.

### III. CONDUCTIVITY OF SOLUTIONS OF ORGANOMAGNESIUM COMPOUNDS

Ethereal solutions of organomagnesium compounds at room temperature show weak electric conductivity<sup>15,16,30–35</sup>, as is evident from data collected in Tables 2 and 3. This behavior indicates the existence of ionic species at relatively low concentrations,  $c$ .

The conductivity (or the specific conductance in earlier literature),  $\kappa$ , of Grignard reagents EtMgBr (**5b**) and PhMgBr (**5e**) in Et<sub>2</sub>O solutions of  $c = 0.5$  M (Table 2) lies between those of MgBr<sub>2</sub> and the corresponding R<sub>2</sub>Mg, **1b** and **1e**, respectively<sup>15</sup>. Thus, for some electrochemical measurements, in particular for **1**, the addition of a supporting electrolyte is necessary<sup>36–38</sup>. For higher concentration of **5** ( $c = 1$  M) their conductivity in Et<sub>2</sub>O (Table 3) is even higher than for MgBr<sub>2</sub>. The values of  $\kappa$  for **5** in Et<sub>2</sub>O solutions are not strongly dependent on the nature of R and in general they are higher for Et than for *n*-Bu, and higher for Bn than for Ph. However, for **5c**,  $\kappa$  is lower than for **5d** at room temperature (Table 3) but it is higher at lower temperatures<sup>16</sup>. Conductivities of *n*-PrMgBr (**5h**) and *i*-PrMgBr (**5i**) are similar for the same concentrations and temperatures<sup>32</sup> ( $\kappa$  is only 1.3 times higher for **5h**). On the other hand, the molar conductivity,  $\lambda = \kappa/c$ , of **5b** and **5e** in Et<sub>2</sub>O decreases with dilution between 2 M and 0.5 M<sup>16</sup>, but for **5b** it increases at much higher concentrations<sup>30</sup>. Similarly, the plot of molar conductivity of EtMgI (**5j**) solutions against  $c$  shows a maximum<sup>15,31</sup>; it was observed<sup>15</sup> at  $c = 1.5$  M

TABLE 2. Conductivity,  $\kappa$ , at 20 °C of 0.5 M solutions of organomagnesium compounds and MgBr<sub>2</sub> in Et<sub>2</sub>O

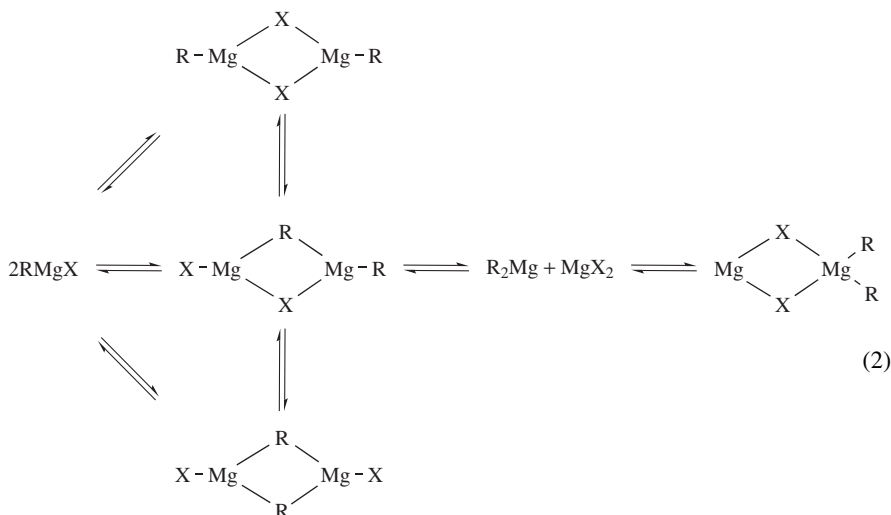
Compound	R = Et		R = Ph	
	$10^3 \kappa \text{ (}\Omega^{-1} \text{ m}^{-1}\text{)}$	Reference	$10^3 \kappa \text{ (}\Omega^{-1} \text{ m}^{-1}\text{)}$	Reference
R <sub>2</sub> Mg ( <b>1</b> )	1	15	0.9	33
RMgBr ( <b>5</b> )	1.6	15	1.2	16
MgBr <sub>2</sub>	2	15	2	15

TABLE 3. Conductivity,  $\kappa$ , of 1.0 M solutions of RMgX (**5**) and MgBr<sub>2</sub> in Et<sub>2</sub>O at 20 °C<sup>16</sup> and in THF at 22 °C<sup>35</sup>

Compound	<b>5a</b>	<b>5b</b>	<b>5c</b>	<b>5d</b>	<b>5e</b>	<b>5f</b>	<b>5g</b>	MgBr <sub>2</sub>
R	Me	Et	<i>n</i> -Bu	Bn	Ph	Et	<i>n</i> -Bu	—
X	Br	Br	Br	Br	Br	Cl	Cl	—
Et <sub>2</sub> O $10^3 \kappa \text{ (}\Omega^{-1} \text{ m}^{-1}\text{)}$	—	6.16	—	5.88	4.74	—	—	<i>ca</i> 1.9
THF $10^3 \kappa \text{ (}\Omega^{-1} \text{ m}^{-1}\text{)}$	30.5	23.7	21.8	—	—	40.3	34.9	—

and was interpreted as a manifestation of the formation of ion associates higher than ion pairs. Moreover, the temperature coefficient of  $\kappa$  for solutions of **5** in Et<sub>2</sub>O is often negative<sup>16</sup> but it depends on  $c$  and can change sign, as found for **5b**<sup>30</sup> and **5e**<sup>16</sup>. All the above observations show that there are complex and dynamic equilibria existing in various solutions.

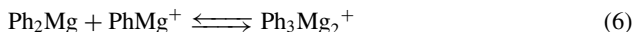
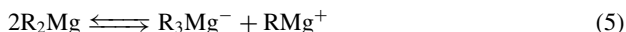
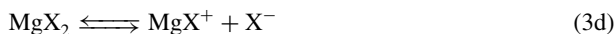
The constitution of Grignard reagents in solutions depends first of all on the Schlenk equilibrium<sup>39</sup> (equation 2) including molecular association of R<sub>2</sub>Mg, MgX<sub>2</sub> and RMgX. However, the association with solvent molecules is also important. A comprehensive view<sup>40</sup> on the Schlenk equilibrium is shown in Scheme 3. In general, the equilibria under consideration depend on the solvent, the R group and, to a lesser extent, on the halide, as well as on the temperature and concentration. Dimers are more favorable in Et<sub>2</sub>O than THF (most probably because MgX<sub>2</sub> is solvated by four THF molecules but only by two Et<sub>2</sub>O molecules) and more favorable for Alk, in particular Bu, than for Ar groups. Temperature effect on the composition of **5** in solutions can be either kinetic or thermodynamic in nature, and for the latter it should be remembered that the enthalpy changes for the Schlenk equilibrium in Et<sub>2</sub>O and in THF have opposite signs<sup>40</sup>.



SCHEME 3

The details of the above equilibria are beyond the scope of this Chapter. However, for further understanding of the electrode processes it is important to recognize the nature of ions present in solutions. Thus, different ionization reactions (equations 3–6) postulated on the basis of conductivity measurements and other experimental data are listed below. Evans and coworkers considered<sup>15, 19, 21</sup> that the cations, RMg<sup>+</sup> and MgX<sup>+</sup>, formed in simple ionization reactions 3a–3d, are coordinated with the Et<sub>2</sub>O molecules and are relatively small, whereas the anions are large in size due to a coordination with **1**, **5** and MgBr<sub>2</sub>. These processes can be summarized by a simplified equilibrium (equation 4) for Grignard reagents **5**<sup>19, 21</sup> and by the equilibrium in equation 5 for **1**<sup>33, 34</sup>, but the participation of anions R<sub>2</sub>MgX<sup>−</sup> was also considered<sup>17</sup> as well as the equilibrium (equation 6) for **1e**<sup>33</sup>. Moreover, a nonlinear increase in the logarithm of the equivalent conductivity of **1e** solutions in 1,4-dioxane with log  $c$  found by Strohmeier<sup>33</sup> (in contrast to linear dependencies for Ph<sub>2</sub>Cd and Ph<sub>2</sub>Zn) supported the opinion that in solutions of **1e** there

is no domination of a simple equilibrium. However, it should be added here that the molecules of 1,4-dioxane irreversibly coordinate to  $\text{MgX}_2$ , forming insoluble complexes; this ability is commonly used in the course of preparation of **1** from solutions of **5**.



On the other hand, a strong effect of the nature of the solvent on the conductivity of **1b** and **1e** was reported<sup>33,34</sup>. It was explained only qualitatively in terms of two phenomena. One of them, previously suggested by Evans and Pearson<sup>15</sup>, are donor–acceptor interactions between solvent molecules acting as donors and organomagnesium cations which have acceptor properties due to unoccupied orbitals. The other one is an ion association which increases with the decrease in the solvent electric permittivity,  $\epsilon$ . Fortunately, nowadays Gutmann's donor number,  $\text{DN}^{41}$ , can be used as a quantitative measure of Lewis basicity for solvent molecules. A reasonable relationship between  $\log \kappa$  and DN for solutions of **1e** is shown in Figure 1. The values of  $\kappa$  for **1b** solutions were measured<sup>34</sup> in solvents with greater variation of  $\epsilon$  and thus a correlation (equation 7) with two explanatory parameters, DN and  $1/\epsilon$ , must be applied. It holds with a correlation coefficient of  $r = 0.9853$  and the addition of the second parameter is statistically significant with probability 78.7%; standard deviations are given in parentheses. The plot of the experimental  $\log \kappa$  against the calculated value is shown in Figure 2.

$$\log \kappa = 0.11(\pm 0.03)\text{DN} - 10(\pm 2)/\epsilon - 6(\pm 1) \quad (7)$$

Solvent effects on the conductivity of **5** also play a significant role in electrochemical applications. For example, the observation of a remarkable increase in the conductivity of **5f** solutions in  $(n\text{-BuOCH}_2)_2$  caused by the addition of THF was patented<sup>42</sup> for

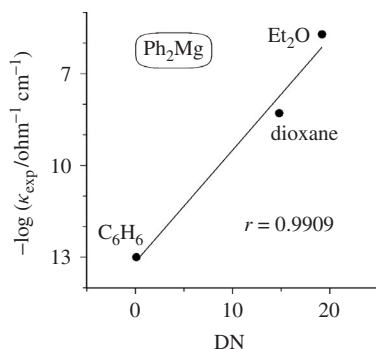


FIGURE 1. Dependence of the log of conductivity of 0.1 M solutions of **1e** measured<sup>33</sup> at 20 °C on the solvent donor number DN. The correlation coefficient is given

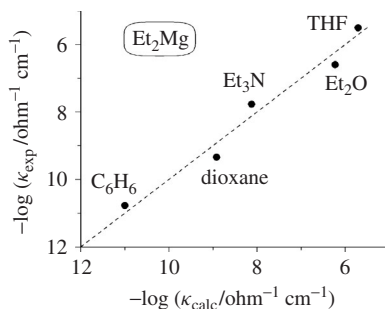


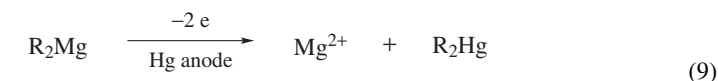
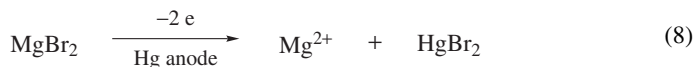
FIGURE 2. Relationship between experimental<sup>34</sup>  $\log \kappa$  for 0.1 M solutions of **1b** at 20 °C and the calculated values from equation 7. The theoretical line with unit slope is shown

use in electrolytic preparation of organolead compounds. The above summary of complicated ionization phenomena in Grignard solutions can point to difficulties in detailed understanding and control of their electrochemical reactions.

#### IV. ANODIC OXIDATION OF ORGANOMAGNESIUM COMPOUNDS

##### A. Simple Diorganomagnesium Compounds

The polarographic behavior of simple diorganomagnesium compounds **1** in DME solutions (containing 1 mM of **1** and 0.1 M TBAP) was investigated by Psarras and Dessy<sup>36</sup>. For each compound the irreversible oxidation wave at a mercury electrode corresponding to the diffusion-controlled two-electron process was observed. The same half-wave potential for all the compounds was equal to  $E_{1/2} = -1.2$  V vs. 1 mM  $\text{AgClO}_4/\text{Ag}$  electrode. However, this value is very uncertain because of pronounced maxima observed on the waves. Exhaustive controlled-potential oxidation of **1b** and **1e** confirmed that  $n_e = 2$  and indicated two main products. One was the same for all the compounds under study and was identified as  $\text{Mg}(\text{ClO}_4)_2$  by a comparison of its reduction potential  $E_{1/2}$  with the potential found for the original compound ( $E_{1/2} = -2.30$  V vs.  $\text{Ag}^+/\text{Ag}$ ). The second product was assumed to be an organomercury compound  $\text{R}_2\text{Hg}$  (**10**) but only **10e**, the oxidation product of diphenylmagnesium (**1e**), could be identified by the reduction at the potential of  $E_{1/2} = -3.34$  V vs.  $\text{Ag}^+/\text{Ag}$ . Reduction of other compounds **10** had to be beyond the discharge of the supporting electrolyte. However, it was also possible to identify  $\text{HgBr}_2$  as the product formed in the oxidation reaction of  $\text{MgBr}_2$  ( $E_{1/2} = -0.6$  V vs.  $\text{Ag}^+/\text{Ag}$ ) (equation 8). Then, for the other compounds a similar oxidation reaction (equation 9) was proposed<sup>36</sup>.

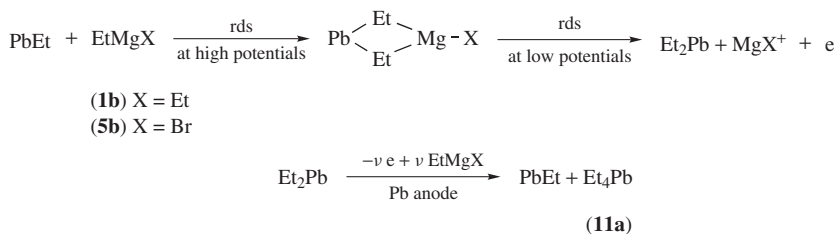


(**1b**) R = Et  
(**1e**) R = Ph

(**10b**) R = Et  
(**10e**) R = Ph

The oxidation of **1** in solutions is much easier at mercury and lead electrodes which form organometallic compounds<sup>37</sup> than at inert electrodes. For example, the oxidation of **1b** in THF containing 0.25 M TBAP at a lead electrode gives<sup>37</sup> a CV peak at a scan rate of 0.3 V s<sup>-1</sup> with the half-peak potential equal to  $E_{p/2} = -1.72$  V vs. 0.01 M Ag<sup>+</sup>/Ag, whereas at a platinum electrode the process needs potentials over 1.5 V more positive. Thus, the formation of a carbon–lead bond during the electrode process was suggested<sup>37</sup>. Steady-state current/potential curves showed, after the first oxidation wave, a plateau with limiting current 1.0 mA cm<sup>-2</sup> in 0.05 M **1b** solutions, i.e. much lower than expected for the diffusion-controlled process. This behavior indicates a slow chemical process. Moreover, the Tafel slope, equal to 60 mV<sup>-1</sup>, corresponds to the reversible electron transfer, contrary to the behavior found for Grignard reagent **5b**. However, the chemical reactions determining the overall rate of the oxidation of **1b** and **5b** are probably the same<sup>37</sup> and they are shown in Scheme 4.

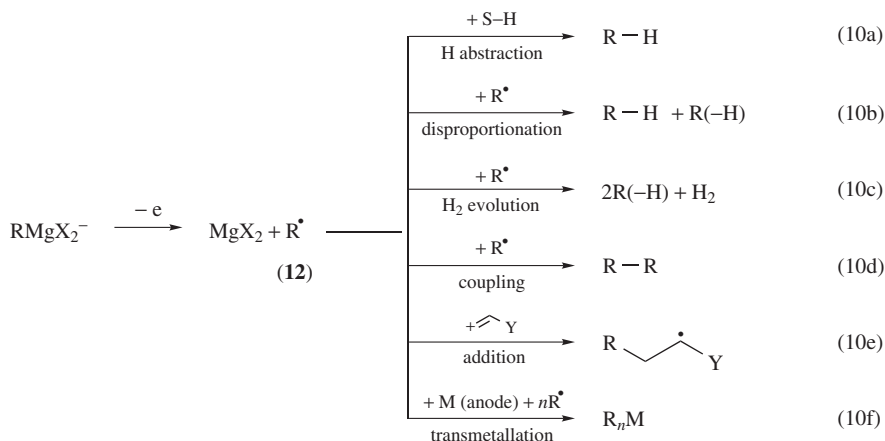
Thus, the oxidation of **1**, as well as of **5**, using sacrificial anodes, yields the corresponding new organometallic compounds. For example, bis(indenyl) manganese was obtained with a good yield<sup>43</sup> by the electrolysis at 200 °C of bis(indenyl) magnesium in a saturated solution of Me<sub>2</sub>O containing indene. A method of purifying organometallic complexes, in particular **1b** with NaF, by extraction with **11a** at 60 °C in order to remove EtMgOEt and (EtO)<sub>2</sub>Mg contaminants, and further electrolysis of the above complex at 30 °C using a Pb anode and a Cu cathode, was patented<sup>44</sup> as a convenient procedure for the preparation of **11a**.



SCHEME 4

## B. Grignard Reagents

For the electrolysis of Grignard reagents **5**, it is well documented in numerous experiments<sup>15–23</sup> that the electroactive species at anodes contains the R group as well as magnesium. Thus, they can be represented by the anion RMgX<sub>2</sub><sup>-</sup> formed in equation 4. In general, its anodic oxidation involves an electron transfer and a bond cleavage with the formation of free radicals, R<sup>•</sup> (**12**), which follow a number of competitive chemical reactions depending on the nature of **12**, the solvent and the anode material. For inert anodes, made most often from platinum, the following reactions of **12**, shown in Scheme 5, can involve a hydrogen atom abstraction from solvent molecules (equation 10a) or an attack on another molecule of **5**, the disproportionation reaction between two radicals (equation 10b) yielding saturated, RH, and unsaturated, R(–H), hydrocarbons, the formation of unsaturated hydrocarbon accompanied by hydrogen evolution (equation 10c), or a coupling of two radicals (equation 10d). Moreover, an addition reaction (equation 10e) can occur with specially added reactants. On the other hand, metals from active anodes react with radicals **12**, in the reaction shown in equation 10f, called ‘anodic transmetalation’. Examples discussed below show how the main products depend on the nature of the reactants and reaction conditions.



SCHEME 5

### 1. Oxidation at inert electrodes

Methane (**13**) and ethane (**14**) are the main organic products at Pt anodes of the electrolysis at a constant current density of methyl Grignard reagents MeMgX in Et<sub>2</sub>O solutions (Table 4)<sup>17</sup>. However, the relative yields of these products depend strongly on the concentration as is shown in Figure 3 for **5a**. At a lower concentration **13** is mainly produced but also ethene (**15**), *i*-butene (**16**) and traces of *n*-butene (**17**) and *n*-propene (**18**). On the other hand, the yield of **14** increases with increase in the concentration of **5a** and finally **14** becomes the only product at *c* = 3 M. Thus, it is evident that the coupling reaction (equation 10d) dominates at higher concentrations. In that case the electrochemical yield of the electrolysis, given as moles of **14** per 1 Faraday, is equal to 43.8% (Table 4), close to the theoretical value of 50%. The formation of **13** at lower concentrations was explained<sup>19</sup> by the H atom abstraction from Et<sub>2</sub>O molecules in equation 10a. The above reaction can also explain the formation of **15**, ethanol (**19**) and *i*-propanol (**20**), which were determined experimentally in small amounts, because on the basis of a pyrolysis of ethers, the formation of EtOMgX and Me<sub>2</sub>CHOMgX were predicted<sup>19</sup>. The decomposition of ether was also supported by the formation of CO<sub>2</sub> (cf. Table 4). Moreover, Evans and Field found<sup>19</sup> that the fraction, Φ, of methyl radicals Me<sup>•</sup> (**12a**), which couple to form **14** (equation 11),

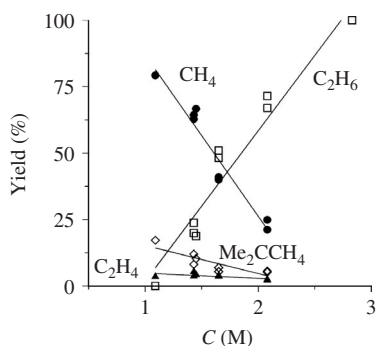
$$\Phi = [2n_{\text{ethane}} / (2n_{\text{ethane}} + n_{\text{methane}})]100\% \quad (11)$$

is independent of the concentration of **5** but increases with increase in the current density during the electrolysis, as is shown in Figure 4 for MeMgI (**5k**). The relationships shown in Figure 4 can be explained taking into account that an increase in current density results<sup>19</sup> in an increase in the concentration of **12a** radicals at the electrode; hence their coupling (equation 10d) to **14** is more favored than the reaction with solvent molecules (equation 10a). The relationships shown in Figure 3 can be explained by a similar reasoning. Electrochemical efficiency, calculated as the number of methyl groups per Faraday, decreases in the order Cl > Br > I and also decreases linearly with increasing concentration (the formation of MeX at an anode followed by a regeneration of **5** at a cathode was suggested<sup>19</sup> to explain the last observation). A decrease in electrochemical efficiency



TABLE 4. Distribution of anodic products after the electrolysis of MeMgX solutions in Et<sub>2</sub>O and *n*-Bu<sub>2</sub>O on bright Pt electrodes<sup>a</sup>

5	X	C (M) <sup>b</sup>	I (A dm <sup>-2</sup> ) <sup>c</sup>	Yield of gaseous products (%)				Y <sub>el</sub> (%) <sup>d</sup>	Reference
Et <sub>2</sub> O				<b>13</b>	<b>14</b>	<b>15</b>	<b>16</b>		
<b>5a<sup>e</sup></b>	Br	1.09	1	79.3	0	3.5	17.2	56.6	17
		2.08	2	23.1	69.2	2.3	5.4	48.5	17
		2.83	2	0	100	0	0	43.8	17
<b>5k</b>	I	2.10	2	64.3	13.2	5.9	16.7	35.8	17
		4.11	2	56.6	27.8	6.9	8.5	46.3	17
				<b>13</b>	<b>14</b>	<b>15</b>	CO <sub>2</sub>		
<b>5k<sup>f</sup></b>	I	0.91	0.02	78.8	19.5	1.7	0	52	19
		0.91	0.545	30.7	68.2	0.5	0.6	43	19
		0.91	1.13	17.8	81.0	0.3	0.9	40	19
		0.91	2.62	14.9	84.2	0.3	0.6	38	19
<i>n</i> -Bu <sub>2</sub> O				<b>13</b>	<b>14</b>	<b>21</b>	<b>22</b>		
<b>5k<sup>g,h</sup></b>	I	0.95	0.2	75.4	23.2	0.45	0.95	34.3	20
<b>5k<sup>i</sup></b>	I	0.95	0.04	88.5	5.8	1.9	3.8	34.3	20
<b>5k<sup>i,h</sup></b>	I	0.95	1.60 <sup>j</sup>	59.3	23.1	5.8	11.5	34.3	20

<sup>a</sup>In each case MgX<sub>2</sub> is also formed at the anode.<sup>b</sup>Initial concentration of **5**.<sup>c</sup>Current density during electrolysis.<sup>d</sup>Electrochemical efficiency equal to the number of moles of gaseous products per Faraday.<sup>e</sup>Traces of **17** and **18** were also found.<sup>f</sup>Electrolysis in refluxing solutions. **19** and traces of **20** were found but no **16** and H<sub>2</sub>.<sup>g</sup>Electrolysis at 90 °C. No **15** and CO<sub>2</sub> were found.<sup>h</sup>Average yield from two measurements.<sup>i</sup>Electrolysis at 143 °C. No **15** was found.<sup>j</sup>0.3% of CO<sub>2</sub> was found.FIGURE 3. Dependence of product yields for the anodic oxidation of MeMgBr (**5a**) in Et<sub>2</sub>O solutions on its concentration<sup>17</sup>. Constant current density 1 or 2 A dm<sup>-2</sup>

at the same current density after increasing the effective anode area by the platinization was found<sup>20</sup>, in agreement with the proposed explanation by the regeneration of **5**.

The reaction of radicals **12a** with solvent molecules was supported by the electrolysis of **5k** performed in *n*-Bu<sub>2</sub>O solutions. This process produced mainly<sup>20</sup> **13** and **14**, but also

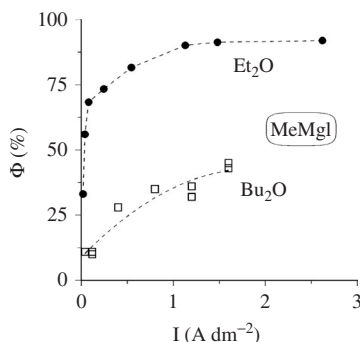
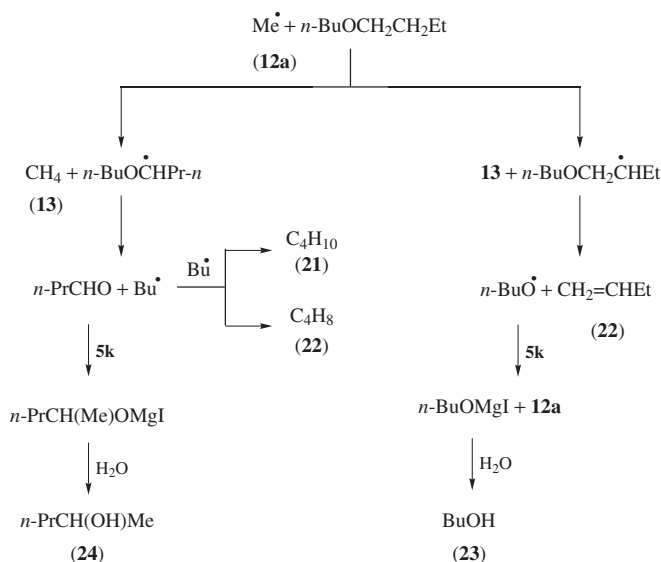


FIGURE 4. Effect of the current density on the fraction of  $\text{Me}^\bullet$  radicals coupled to ethane,  $\Phi$ , for **5k** in refluxing  $\text{Et}_2\text{O}$ <sup>19</sup> and in  $n\text{-Bu}_2\text{O}$ <sup>20</sup> at  $143^\circ\text{C}$ . Adapted with permission from Reference 20. Copyright 1936 American Chemical Society

butane (**21**) and butene-1 (**22**), whereas **15** was absent (cf. Table 4). It is evident from the data collected in Table 4 and Figure 4 that the hydrogen atom abstraction from  $n\text{-Bu}_2\text{O}$  molecules in reaction 10a is more favored than a similar reaction with  $\text{Et}_2\text{O}$ ; moreover, a higher temperature favors reaction 10a as well. Small amounts of 1-butanol (**23**) and 2-pentanol (**24**) were also determined<sup>20</sup> after hydrolysis under nitrogen atmosphere of the solution remaining when the electrolysis was completed. The formation of all the products found was explained<sup>20</sup> by the reactions shown in Scheme 6; however, Evans and Field were not sure if the mechanism was radical or ionic. Gaseous products were also found<sup>45</sup> for the electrolysis of  $\text{MeMgX}$  solutions in pyridine.



SCHEME 6

For higher alkyl radicals formed in the anodic oxidation of  $\text{AlkMgX}$  in  $\text{Et}_2\text{O}$  solutions, the participation of competitive reactions given in Scheme 5 is different and thus the products distribution is also different<sup>17,21,22</sup> than that found for  $\text{MeMgX}$  (cf. Tables 4 and 5). The corresponding alkane and alkene formed in an approximately equivalent amount are the main gaseous products, e.g. **14** and **15**, propane (**25**) and propene (**26**), **21** and **22** for  $\text{Alk} = \text{Et}$ ,  $\text{Pr}$  and  $n\text{-Bu}$ , respectively. However, a small amount of hydrogen was also determined. The products distribution is independent of the concentration and current density. The above results indicate that the main route of the decay of  $\text{Et}^\bullet$  (**12b**),  $n\text{-Pr}^\bullet$  (**12c**) and  $i\text{-Pr}^\bullet$  (**12d**) radicals is the disproportionation in equation 10b but a secondary competitive reaction (equation 10c) also occurs. The high electrochemical efficiency for the above alkyls ( $>86\%$ ) supports the conclusion that reactions other than that in equation 10b take place to only a very small extent. The efficiency increases in the order of  $\text{X}$  of  $\text{I} < \text{Br} < \text{Cl}$ . The formation of small amounts of  $\text{CO}_2$  and alcohols [**19** and **20** for **12d** and **19**,  $n\text{-PrOH}$  (**27**) and  $s\text{-PenOH}$  (**28**) for **12c**] was explained by reactions of alkyl radicals with  $\text{Et}_2\text{O}$ , similar to those proposed for **12a** in Scheme 6.

For higher alkyls the competition between disproportionation (equation 10b) and coupling (equation 10d) reactions is of particular interest. First of all, a tendency toward radical coupling increases for straight-chain radicals with their length, and for radicals with four or more carbon atoms the coupling approaches 100%. For example, for radicals **12b** the dimer **21** was not detected but its formation was suggested<sup>17</sup> on the basis of a determined number of carbon atoms in product molecules, equal to 2.15, i.e. higher than for pure **14**. **12c** has a 50% tendency to couple forming  $n\text{-hexane}$  (**29**)<sup>21</sup>. On the other hand, for  $n\text{-Hex}^\bullet$  (**12e**),  $n\text{-Bu}^\bullet$  (**12f**) (in experiments with a higher distance between the electrodes) and  $s\text{-Bu}^\bullet$  (**12g**) only the products of coupling were detected, although their isolation, in particular for the last radical, was poor. Second, the tendency toward coupling

TABLE 5. Products distribution after the anodic oxidation on Pt electrodes of solutions of  $\text{AlkMgX}$  (**5**) in  $\text{Et}_2\text{O}^a$

5	Alk	X	Yield of gaseous products (%) <sup>b</sup>				Y <sub>el</sub> (%) <sup>c</sup>	Reference
			14	15	H <sub>2</sub>			
5j	Et	I	51.8	47.3	0.97		88.1	17
5b	Et	Br	48.7	50.3	1.1		89.8	17
5f	Et	Cl	50.9	48.0	1.1		95.1	17
			25	26	15	H <sub>2</sub>		
5h	<i>n</i> -Pr	Br	50.5	48.5	—	1.0	96.3	17
5h	<i>n</i> -Pr	Br	46.8	46.7	1.4	1.5 <sup>d</sup>	~91 <sup>e</sup>	21
5i	<i>i</i> -Pr	Br	44.4	50.7	0.8	1.9 <sup>f</sup>	>90 <sup>g</sup>	21
			21	22	H <sub>2</sub>			
5c <sup>h</sup>	<i>n</i> -Bu	Br	52.3	41.7	0.3–2.5		~65 <sup>i</sup>	22

<sup>a</sup>Current density in the range 0.4–2  $\text{A dm}^{-2}$ . In each case  $\text{MgX}_2$  is also formed at the anode.

<sup>b</sup>Average values from two to seven measurements.

<sup>c</sup>Electrochemical efficiency (moles of gaseous products per Faraday).

<sup>d</sup>Other gaseous products:  $\text{CO}_2$  0.6% and  $\text{O}_2$  1.5% (probably formed at cathode).

<sup>e</sup>Liquid products: **19**, **27**, **28** and **29**.

<sup>f</sup>Other gaseous products:  $\text{CO}_2$  0.3% and  $\text{O}_2$  1.4% (probably formed at cathode).

<sup>g</sup>Liquid products: **19** and **20**.

<sup>h</sup>Gas was liberated only when the electrodes were nearly closed; other gaseous products: unsaturated hydrocarbons 1.2–2.1%,  $\text{CO}_2$  0.8–2.0% and  $\text{O}_2$  1.5–2.0%.

<sup>i</sup>**26** is the main liquid product.

is reduced for branched-chain compounds. Finally, Evans and coworkers suggested<sup>22</sup> that the tendency to couple increases as the Et• radical (**12b**) becomes substituted with methyl groups, i.e. in the order of: Et < *i*-Pr < *t*-Bu < *n*-Pr < *s*-Bu < *i*-Bu. Similar trends were found later by Martinot<sup>46</sup> for the electrolysis under similar conditions and the results of both reports are given in Table 6. Radical dimerization in the electrolysis of **5** with various R's in Et<sub>2</sub>O solutions at a Pt anode and a Hg cathode was also investigated by Morgat and Pallaud<sup>47,48</sup>. However, the yields of dimers were low, in the range of 35–60% even for long-chain radicals, e.g. for R = C<sub>18</sub>H<sub>37</sub> it was 54%; a list of results was also reported in the review<sup>2</sup>.

The behavior of BnMgBr (**5d**) is similar to that observed for compounds with higher alkyl groups, i.e. only the coupling product was detected<sup>23</sup> and the earlier report on the additional formation of benzyl alcohol<sup>14</sup> was not confirmed<sup>23</sup>. On the other hand, reactions of Ar• radicals formed in the anodic oxidation of aryl Grignard reagents are different from those established for Alk•, as is evident from the percent distribution of parent radicals in major products given in Table 7.

Reactions of Ph• radicals (**12h**) formed at anodes yield<sup>23</sup> styrene (**30**), biphenyl (**31**), *p*-terphenyl (**32**), insoluble hydrocarbon of high molecular weight and, in smaller amounts, benzene (**33**) as well as ethanol (**19**). **30** was the main product for substituted reagents **5q** and **5r** but for unsubstituted **5e** only if the current efficiency, *Y*<sub>el</sub>, was low. For higher *Y*<sub>el</sub> values **31** became the chief organic product. However, in contrast to aliphatic Grignard reagents, except methyl, the current efficiency was always much below 100%. In order to explain the above results the possibility of another route of anodic oxidation, different

TABLE 6. Percent participation of alkyl radicals which couple in the oxidation of AlkMgBr in Et<sub>2</sub>O solutions at Pt anodes

AlkMgBr	<b>5b</b>	<b>5h</b>	<b>5c</b>	<b>5l</b>	<b>5m</b>	<b>5n</b>	<b>5o</b>	<b>5p</b>	Reference
Alk	Et	<i>n</i> -Pr	<i>n</i> -Bu	<i>i</i> -Bu	<i>s</i> -Bu	<i>t</i> -Bu	<i>n</i> -Hex	<i>n</i> -C <sub>7</sub> H <sub>15</sub>	
Alk <sub>2</sub> (%)	<sup>a</sup>	50	>85	96	43–49	<sup>b</sup>	82.5	<sup>c</sup>	22
	50	<sup>c</sup>	91	85	<sup>c</sup>	25	<sup>c</sup>	100	46

<sup>a</sup> Only traces.

<sup>b</sup> A slight amount.

<sup>c</sup> Not investigated.

TABLE 7. Products distribution<sup>a</sup> after the anodic oxidation<sup>b</sup> of solutions of ArMgBr in Et<sub>2</sub>O at Pt electrodes<sup>23</sup>

Reagent	Ar	<i>Y</i> <sub>el</sub> (%) <sup>c</sup>	Distribution of Ar• in major products (%) <sup>d</sup>			
			<b>30</b>	Ar <sub>2</sub>	<b>32</b>	Polymer <sup>e</sup>
<b>5e</b>	Ph	14	49.7	5.5	11.0	5.5
		18	42.0	0	14.0	7.0
		41	18.0	29.9	3.5	2.0
		66	0	67.4	11.2	5.6
<b>5q</b>	<i>p</i> -Tol	31	72.5	0	—	<sup>f</sup>
<b>5r</b>	<i>p</i> -ClC <sub>6</sub> H <sub>4</sub>	20	27.5	0	—	<sup>f</sup>

<sup>a</sup> MgX<sub>2</sub> is also formed at the anode. Other minor products: **19** and **33**.

<sup>b</sup> Current density in the range 0.16–0.48 A dm<sup>-2</sup>.

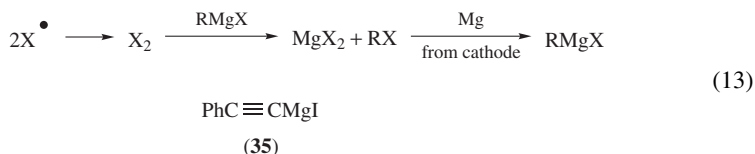
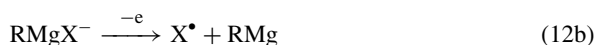
<sup>c</sup> Electrochemical efficiency given as the number of moles of **5** decomposed per Faraday.

<sup>d</sup> The ratio of moles of Ar• radicals to moles of **5**.

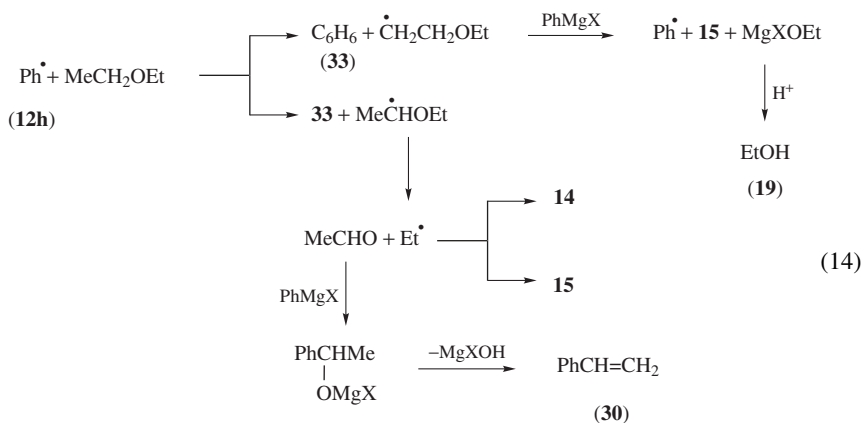
<sup>e</sup> Insoluble polymeric hydrocarbon formed on the anode.

<sup>f</sup> A small amount.

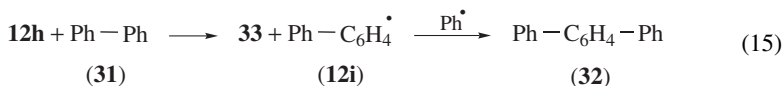
from that discussed in Scheme 5, was suggested<sup>15,23</sup>. This route includes the formation of halogen atom (equations 12a, 12b or 12c) and a sequence of further reactions (equation 13) producing  $X_2$  and  $ArX$ , which react with magnesium at the cathode yielding again **5**. The formation of bromobenzene (**34**) at the anode during the electrolysis conducted in a transference cell, where diffusion was avoided, supported<sup>23</sup> the last suggestion. It was also shown<sup>15</sup> that iodine, not aryl radicals, are formed during the electrolysis of **35** because crystalline iodine was collected upon the anode. The discharge of halogen instead of R is favored<sup>15</sup> by the high electronegativity of R and low electronegativity of X, as well as by high voltage and high current density. In full accordance with the above reasoning the current efficiency was lower for Ar than for Alk, and it was changing in the order of  $I < Br < Cl$ .



Two series of reactions were considered by Evans and coworkers<sup>23</sup> in order to explain the products given in Table 7. The reactions in equations 14 of **12h** with solvent molecules (Scheme 7) produce progressively **33**, **30** and **19**. However, gaseous **14** and **15** shown in Scheme 7 were not detected. On the other hand, the radical coupling (equation 10d) yields **31**, which next gives **33** and **32** (equation 15), including the hydrogen atom abstraction from **31** by **12h** and the coupling of **12h** and **12i** radicals<sup>23</sup>.



SCHEME 7



The formation of dimers was also observed<sup>47,48</sup> in the electrolysis of RMgBr solutions in Et<sub>2</sub>O with R =  $\alpha$ -Naph (the yield of 1,1'-binaphthyl was 43%) and a number of Grignard reagents with R being the derivatives of terpenes.

It is interesting that a very marked anodic luminescence was observed during the electrolysis of ethereal solutions of **5e**<sup>14</sup> and thirteen other ArMgX, in particular those produced from *p*-MeC<sub>6</sub>H<sub>4</sub>I and 1,4-chlorobromonaphthalene<sup>49</sup>. For a number of compounds **5** a similar electron transfer step in an electrochemiluminescence (ECL) and a chemiluminescence caused by oxygen was suggested<sup>14</sup>. However, it was shown later<sup>50</sup> that the anodic emission of light during the electrolysis of **5e** could be caused by oxygen contaminations in solutions. The ECL mechanism of **5** still looked unclear in 1985<sup>51</sup>. A photovoltaic effect in the cell containing a solution of 1 M **5e** in Et<sub>2</sub>O with gold and silver electrodes was also reported<sup>49</sup>.

The effect of various R's on the anodic reactivity of **5** was investigated by Evans and coworkers<sup>18</sup> and Holm<sup>52,53</sup> for solutions in Et<sub>2</sub>O and by Martinot<sup>46</sup> for solutions in THF. The decomposition potentials, *E*<sub>d</sub>, corresponding to the beginning of the oxidation process in Et<sub>2</sub>O solutions<sup>18</sup> are collected in Table 8. The back electromotoric forces determined for a Pt anode at the current density 0.06 A cm<sup>-2</sup>,  $\eta_{0.06}$ , i.e. when the slopes of Tafel plots for each compound are identical<sup>52</sup> and the tentative standard oxidation potentials, *E*<sub>o</sub><sup>53</sup>, recalculated from  $\eta_{0.06}$  values, are also collected in Table 8. The corresponding bond dissociation energies, *D*(R–MgBr), for a C–Mg bond obtained from thermochemical measurements<sup>54</sup> are given in Table 8 as well. A linear plot of *E*<sub>o</sub> against *D*(R–MgBr) was reported by Holm<sup>55</sup> and a plot of *E*<sub>o</sub> against *E*<sub>d</sub> was reported by Ebersson<sup>56</sup>, but they did not use these relationships to elucidate the electrochemical process.

However, standard oxidation potentials for the dissociative electron transfer, *E*<sup>o</sup>(RMgX/R<sup>•</sup>+MgX<sup>+</sup>), described by the Savèant theory<sup>57,58</sup>, can be expressed by the sum of the

TABLE 8. Decomposition potentials, *E*<sub>d</sub><sup>18</sup>, anodic overvoltage for a current density 0.06 A cm<sup>-2</sup>,  $\eta_{0.06}$ <sup>52</sup>, standard oxidation potentials *E*<sub>o</sub><sup>53</sup> for the oxidation of RMgBr in Et<sub>2</sub>O solutions and the bond dissociation energy, *D*(R–MgBr), of the C–Mg bond<sup>54</sup> in RMgBr

RMgBr	R	<i>E</i> <sub>d</sub> (V) <sup>a</sup>	$\eta_{0.06}$ (V) <sup>b</sup>	– <i>E</i> <sub>o</sub> (V vs. SHE)	<i>D</i> (R–MgBr) (kJ mol <sup>-1</sup> ) <sup>c</sup>
<b>5e</b>	Ph	2.17	—	0.0 <sup>d</sup>	289
<b>5a</b>	Me	1.94	1.98	0.25	255
<b>5c</b>	<i>n</i> -Bu	1.32	1.70	0.53	213
<b>5l</b>	<i>i</i> -Bu	—	—	0.63	213 <sup>e</sup>
<b>5h</b>	<i>n</i> -Pr	1.42	—	—	209
<b>5b</b>	Et	1.28	1.57	0.66	205
<b>5d</b>	Bn	—	1.50	0.73	201
<b>5s</b>	All	0.86	1.07	1.16	201
<b>5t</b>	<i>c</i> -C <sub>5</sub> H <sub>9</sub>	—	1.35	0.88	201
<b>5i</b>	<i>i</i> -Pr	1.07	1.28	0.95	184
<b>5m</b>	<i>s</i> -Bu	1.24	1.36	0.87	184
<b>5n</b>	<i>t</i> -Bu	0.97	1.16	1.07	172

<sup>a</sup> Measured at 22 °C for *ca* 1 M solutions.

<sup>b</sup> Anodic overvoltage at a Pt anode relative to a Pt | Mg | MgBr<sub>2</sub> cathode at 20 °C for *ca* 0.8 M solutions.

<sup>c</sup> Obtained for the reaction: RMgBr<sub>(soln)</sub> + HBr<sub>(g)</sub> → RH<sub>(soln)</sub> + MgBr<sub>2(soln)</sub> in Et<sub>2</sub>O.

<sup>d</sup> Value estimated in Reference 56 from the correlation between *E*<sub>d</sub> and *E*<sub>o</sub>.

<sup>e</sup> Obtained for the reaction: RBr<sub>(l)</sub> + Mg<sub>(s)</sub> → RMgBr<sub>(soln)</sub> in Et<sub>2</sub>O.

homolytic bond dissociation energy  $D(\text{R}-\text{MgBr})$  and the standard potential for the oxidation of  $\text{MgX}^\bullet$  radicals (equation 16)

$$E^\circ(\text{RMgX}/\text{R}^\bullet + \text{MgX}^+) = D(\text{R}-\text{MgBr}) - T\Delta S^\circ + E^\circ(\text{MgX}^\bullet/\text{MgX}^+) \quad (16)$$

where  $\Delta S^\circ$  is the entropy change for the homolytic cleavage. For the series under consideration the last potential is constant and, if  $\Delta S^\circ$  is not strongly dependent on R, the linear correlation between standard potential and bond dissociation energy with a unit slope is expected. The expected relationship holds for  $E^\circ$  potentials originally determined by Holm<sup>53</sup> for 9 compounds (one point for R = All strongly deviates) and  $D(\text{R}-\text{MgBr})$  expressed in the same units, i.e. eV, with a correlation coefficient of  $r = 0.963$  and the Snedecor F test 89.41 indicating statistical importance at the level of 99.997% (equation 17)

$$E^\circ = 0.96(\pm 0.12)D(\text{R}-\text{MgBr}) - 2.75(\pm 0.51) \quad (17)$$

where 95% errors are given in parentheses. In our opinion, equation 17 shows that the anodic process represents a concerted electron transfer and bond breaking. Thus, equation 17 also explains the order of electrochemical reactivity of compounds **5**: the lower the bond dissociation energy the easier the oxidation and the anodic potential become less positive.

The products of anodic oxidation of  $\text{AlkMgX}$  in THF and  $\text{Et}_2\text{O}$  solutions at bright Pt anodes are the same<sup>46,59</sup>. Using rotating electrodes in THF solutions containing 0.2–0.6 M  $\text{RMgCl}$ , Chevrot and coworkers found<sup>60</sup> that the anodic oxidation depends on the anode material (the easiest oxidation occurs at platinized Pt, next at Au and the most difficult one at bright Pt anodes) and it also decreases in the order  $t\text{-Bu} > \text{Et} > i\text{-Pr}$ ,  $\text{CH}=\text{CH}_2 > n\text{-Bu} > \text{Me} > \text{Ph}$ . Thus, general trends for the reactivity of **5** with both halogens (Br and Cl) and in both solvents are similar and can be understood in terms of changes in the C–Mg bond dissociation energy.

On the other hand, details of the electrochemical steps are more complex. For the oxidation of  $\text{AlkMgX}$  (Alk = Et,  $n\text{-Bu}$ ,  $i\text{-Bu}$  and  $t\text{-Bu}$ ) Martinot found<sup>46,59</sup> that the potential of Pt electrodes depends linearly on  $\log I$  (where  $I$  is the current density) according to the Tafel plot and the slope is equal to 0.2 V and 0.3 V in  $\text{Et}_2\text{O}$  and THF solutions, respectively. On the basis of polarization curves, reaction orders and capacity data, the ionic mechanism of the oxidation was proposed<sup>59</sup> with an initial electron transfer to anions  $\text{RMgX}_2^-$  or  $\text{R}_3\text{Mg}^-$  as the rds, yielding the radical  $\text{R}^\bullet$  (**12**), which is further oxidized at the electrode to the carbocation  $\text{R}^+$ . However, the electrochemical oxidation of **12** looks unlikely unless very positive potentials are applied; provisional standard potentials of the  $\text{R}^+/\text{R}^\bullet$  couple in acetonitrile estimated by Eberson<sup>61</sup> are 1.91 V and 1.47 V more positive than  $E^\circ$  from Table 8 for R = Et and  $t\text{-Bu}$ , respectively. Moreover, for the electrolysis of a wider series of  $\text{RMgBr}$  in  $\text{Et}_2\text{O}$  solutions and using a wider range of  $I$  values ( $10^{-5}$  to  $0.1 \text{ A cm}^{-2}$ ) Holm found<sup>52,53</sup> different slopes of Tafel plots. They were equal (after corrections for ohmic drops and concentrations) to 0.15 for **5d**, **5n** and **5s**, but ca 0.30 for **5a**, whereas for **5b**, **5c** and **5i** the slope was 0.30 at low  $I$  (ca  $1 \text{ mA cm}^{-2}$ ), but it changes toward 0.15 at high  $I$  values. The reported behavior indicates beyond doubt that there exist two different mechanisms of the oxidation. Holm proposed<sup>52</sup> that surface-bonded radicals **12** act as catalysts for a further electron transfer at a ‘radical saturated’ platinum, decreasing the activation barrier and resulting in a lower Tafel slope. The surface saturation occurs for stable  $\text{All}^\bullet$ ,  $\text{Bn}^\bullet$  and  $t\text{-Bu}^\bullet$  radicals at low  $I$  values, but for less stable radicals only at higher current densities, whereas for the least stable radical **12a** no saturation was reached at all. However, there is not enough experimental data to decide about the kinetics details.

## 2. Anodic addition to olefins

Anodic oxidation of Grignard reagents (**5**) in the presence of styrene (**30**), butadiene (**36**) or vinyl ethyl ether (**37**) was investigated by Schäfer and Küntzel<sup>62</sup> as an interesting (for preparative use) extension of other anodic reactions with olefins. The electrolysis was carried out at constant current density at Pt, Cu or graphite electrodes. It was found that the products obtained depend on the electrode material, as is seen from the data presented in Table 9.

The scheme of reactions proposed<sup>62</sup> to explain the products obtained is shown, after small modifications, in Scheme 8. Primary radicals **12** formed at the anodes produce with added **30** or **36** (equation 10e) the substituted benzyl or allyl radicals **38**, which can dimerize to **39** or can couple with the added olefin to form radicals **40** or **41**. For allyl radical (**38**) a 1,1'- or 1,3'-coupling is possible yielding **41** and **40**, respectively. Further couplings of **40** and **41** with the primary radical **12** produce **39** and head-to-tail dimer **42**, respectively. It was evident from the products obtained<sup>62</sup> that the coupling of **38** in the 1-position occurs 5 to 11 times faster than in the 3-position. However, for readily polymerizable olefins, rather polymerization occurs, in particular at graphite electrodes. At Pt electrodes both dimers **39** and **42** are formed, but for Cu electrodes exclusively dimers **39** were obtained with moderate yields. Thus, an indirect electrolysis including the oxidation of copper to Cu<sup>+</sup> ions and their further reaction with **5** yielding intermediate RCu was considered, but not proved<sup>62</sup>.

On the other hand, the formation of unsaturated hydrocarbons **45**, **46** and **48** (Table 9) can be illustrated by the reactions shown in Scheme 9, with radicals **44** and **47** as intermediates.

## 3. Oxidation on sacrificial anodes

The electrooxidation of Grignard reagents (**5**) on reactive metal anodes produces the corresponding organometallic compounds, or more generally organoelemental compounds,

TABLE 9. Products of anodic oxidation of 0.2 M RMgBr in Et<sub>2</sub>O solutions containing 0.1 M LiClO<sub>4</sub> in the presence of olefins<sup>a</sup>

RMgBr	Olefin	C (M)	Anode	Products	Yield (%) <sup>b</sup>
<b>5c</b>	<b>30</b>	0.7	Pt	6,8-diphenyldodecane <b>42a</b> 6,7-diphenyldodecane <b>39a</b>	10 5
<b>5c</b>	<b>30</b>	2.0	Pt	polymer <sup>c</sup> <b>43</b>	2.6 <sup>d</sup>
<b>5c</b>	<b>30</b>	0.7	Cu	6,7-diphenyldodecane <b>39a</b>	29
<b>5n</b>	<b>30</b>	0.7	Cu	4,5-diphenyl-2,2,7,7-tetramethyloctane <b>39b</b>	14
<b>5c</b>	<b>36</b>	2.0	Cu	6,7-divinyldodecane <b>39c</b> 6-vinyl-8-tetradecaene <b>48a</b> 6,10-hexadecadiene <b>46a</b> 6-dodecene <b>45a</b>	3 15 15 7
<b>5o</b>	<b>36</b>	2.0	Cu	8-vinyl-10-octadecaene <b>48b</b> 8,12-eicosadiene <b>46b</b> 8-hexadecaene <b>45b</b>	8 11 6
<b>5e</b>	<b>37</b>	4.2	Pt	polymer <sup>c</sup> <b>43</b>	11 <sup>d</sup>

<sup>a</sup>This Table was published in *Tetrahedron Letters*, H. Schäfer and H. Küntzel, 'Anodic addition of Grignard-reagents to olefins', 3333–3336, Copyright Elsevier, 1970.

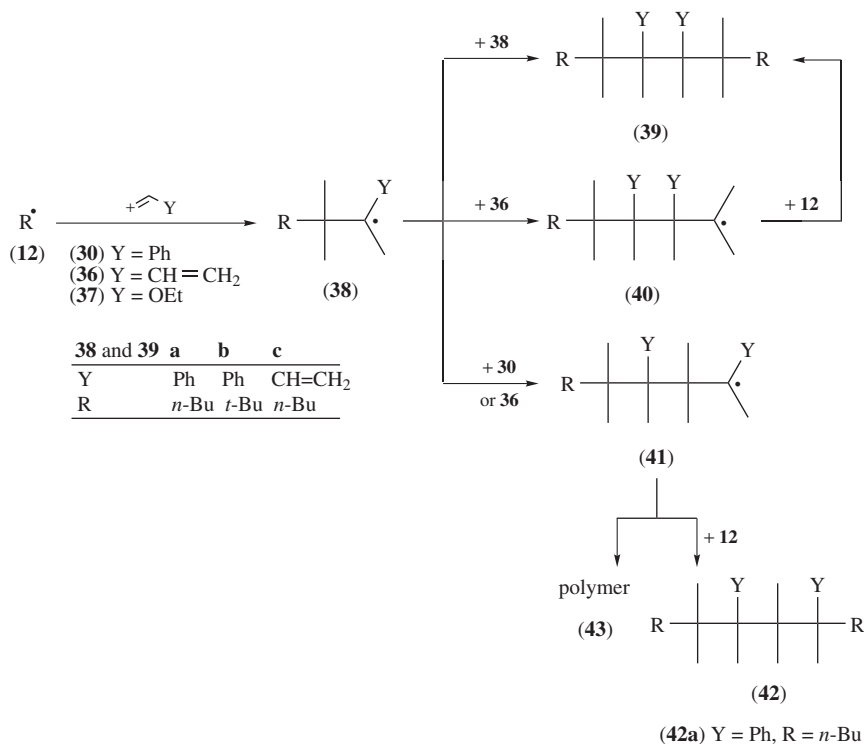
<sup>b</sup>Current yield. Electrolysis at  $I = 10 \text{ mA cm}^{-2}$  in a flow cell without diaphragm.

<sup>c</sup>Average molecular weight 2500.

<sup>d</sup>Yield in g Ah<sup>-1</sup>.

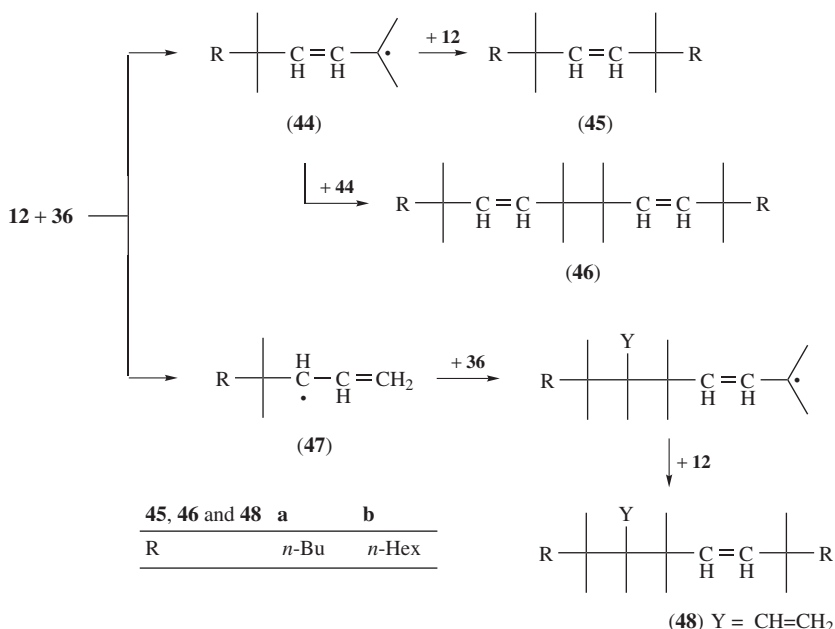
<sup>e</sup>Average molecular weight 1040.





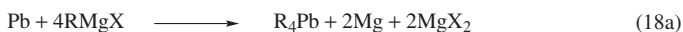
SCHEME 8

in the so-called 'anodic transmetallation' shown in Scheme 4 (equation 10f). The first observations on the dissolution of Mg, Al and Zn anodes, in amounts described by Faraday laws, during the electrolysis of **5b** solutions in Et<sub>2</sub>O was reported in 1925 by Kondyrew<sup>13</sup>. French and Drane<sup>63</sup> supported the reactivity of Al, Zn and Cd anodes in the electrolysis of ethereal solutions of *i*-PenMgCl and suggested that 'metallic alkyls' are formed. The formation of Et<sub>3</sub>Al was also suggested by Evans and Lee<sup>17</sup>. In further research the list of sacrificial anodes was extended to Pb, Bi, Mn, B, P and a number of industrial processes were patented<sup>42, 64–76</sup>. Most of the investigations were devoted to the production of R<sub>4</sub>Pb (**11**) and the yields of tetraalkyllead obtained in electrochemical processes increased from *ca* 73% in the first patent<sup>64</sup>, when Et<sub>2</sub>O was used as a solvent and the electrolysis needed the high voltage of 100 V, to 80–90% or even more in the Nalco process after finding better solvents and, above all, after the addition of extraneous organic halide (**8**) to the solutions of **5** in a molar ratio of *ca* 1:1 for **11a**<sup>65</sup> and up to 0.5:1 for Me<sub>4</sub>Pb (**11b**)<sup>67</sup>. The added **8** reacts with the magnesium deposited on the cathode (equation 18b) recovering **5** and changing the overall process (Scheme 10) from the reactions in equations 18a to 18c. It should be added here that reaction 18a can occur in nonelectrochemical conditions<sup>77</sup> and this can explain<sup>6</sup> why current efficiencies of the electrolysis extend to 100%<sup>66–69, 75</sup> (cf. data given in Table 10). The best media developed for the commercial production of **11** were anhydrous mixtures of organic solvents containing diethers of glycols [e.g. (MeOCH<sub>2</sub>)<sub>2</sub> (**49**)<sup>65</sup>, (*n*-BuOCH<sub>2</sub>)<sub>2</sub> (**50**)<sup>42, 69</sup>, *n*-HexOC<sub>2</sub>H<sub>4</sub>OEt (**51**), Bz(OC<sub>2</sub>H<sub>4</sub>)<sub>3</sub>OEt (**52**), (EtOC<sub>2</sub>H<sub>4</sub>)<sub>2</sub> (**53**) or others] with THF<sup>42, 66–68, 75</sup>, which increases the conductivity (cf.



SCHEME 9

Section III), thus increasing the efficiency of the electrolysis. Small amounts of aromatic hydrocarbons, like toluene or benzene (**33**)<sup>66–70,75</sup>, were also added to the mixtures used. A number of typical examples described in patents are illustrated in Table 10, including the products and conditions of equation 10f.



5	b	e	f	o	u	v
R	Et	Ph	Et	<i>n</i> -Hex	Me	CH=CH <sub>2</sub>
X	Br	Br	Cl	Br	Cl	Cl

8	a	b	c	d	e	f	g
R	Ph	Ph	<i>n</i> -Hex	Me	Et	<i>t</i> -Bu	<i>c</i> -Hex
X	Br	Cl	Br	Cl	Cl	Cl	Cl

SCHEME 10

The industrial Nalco process for the production of **11a** and **11b** was conducted<sup>78</sup> in mixtures of **53** with THF, at 35–40 °C or 40–50 °C and about 2 kg cm<sup>–2</sup> pressure, in a cell divided by porous diaphragms and with current densities of 1.5–3.0 A dm<sup>–2</sup> at 15–30 V. However, production details are beyond the scope of this Chapter. Effective methods of recovery of **11** from mixtures after or during the electrolysis were elaborated<sup>73,74</sup>. Of

TABLE 10. Organoelemental compounds produced by electro-oxidation of Grignard reagents **5** on sacrificial anodes

Reactants (mole ratio)	Anode	Solvent	Conditions	Product (yield <sup>a</sup> /%) $I_{\text{eff}}^b$ (%)	Reference
<b>5b</b>	Pb <sup>c</sup>	Et <sub>2</sub> O	100 V	Et <sub>4</sub> Pb (73)	64
<b>5f</b> + <b>8e</b> (1:1)	Pb <sup>d</sup>	<b>49</b>	50–65 °C, 12–26 V	Et <sub>4</sub> Pb (81)	65
<b>5u</b> + <b>8d</b> (1:0.29)	Pb <sup>d</sup>	THF, <b>33</b> , <b>50</b>	29.9 °C, 27.2 V	Me <sub>4</sub> Pb (92.1, 81.2 <sup>e</sup> ) ( <b>9</b> + <b>10</b> 1.26%) 149	67
<b>5u</b> + <b>8d</b>	Pb <sup>d</sup>	<b>52</b> , THF	46 °C, 28 V	Me <sub>4</sub> Pb (100, 82.5 <sup>e</sup> ) 174	68
<b>5e</b> + <b>8a</b>	Pb <sup>d</sup>	<b>50</b>	55 °C, 25.6–26.8 V	Ph <sub>4</sub> Pb	69
<b>5u</b> + <b>8b</b> (2:1)	Pb <sup>d</sup>	<b>50</b>	38 °C, 30 V	R <sub>4</sub> Pb <sup>f</sup>	69
<b>5u</b> + <b>8d</b>	Pb <sup>d</sup>	12% THF, 28% <b>33</b> , 60% <b>50</b>	30 °C, 27 V	Me <sub>4</sub> Pb (89.6, 71 <sup>e</sup> ) 164	75
<b>5u</b> + <b>8d</b>	Pb <sup>d</sup>	10% THF, 45% <b>33</b> , 45% <b>51</b>	40 °C, 22 V	Me <sub>4</sub> Pb (99.1, 94 <sup>e</sup> ) 161	75
<b>5v</b>	Pb <sup>d</sup>	THF	1.7–3.9 V	(CH <sub>2</sub> =CH) <sub>4</sub> Pb	76
<b>5o</b> + <b>8c</b>	Al <sup>c</sup>	<b>51</b>	35–45 °C, 26.5–27 V	( <i>n</i> -Hex) <sub>3</sub> Al 134.2	69
<b>5e</b> + <b>8a</b>	Al <sup>c</sup>	<b>51</b>	55 °C	Ph <sub>3</sub> Al	69
<b>5o</b> + <b>8c</b>	Zn, Cd Mn, Bi <sup>c</sup>	<b>51</b>	35–45 °C, 26.5–27 V	( <i>n</i> -Hex) <sub>x</sub> M	69
<b>5f</b>	Pt <sup>g</sup> (black)	Et <sub>2</sub> O		Et <sub>3</sub> P	72
<b>5f</b>	B <sup>d,h</sup>	Et <sub>2</sub> O		Et <sub>3</sub> B	71

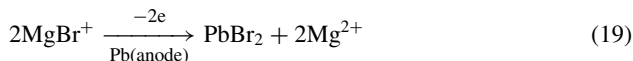
<sup>a</sup>Yield based on **5**.<sup>b</sup>Current efficiency.<sup>c</sup>Cathode from the same metal as the anode.<sup>d</sup>Cathode: stainless steel.<sup>e</sup>Yield based on Mg.<sup>f</sup>A mixture of compounds with different R's.<sup>g</sup>Pt cathode.<sup>h</sup>Boron-coated tantalum.

course, equation 10f is general and products with various alkyl or aryl groups can be obtained; the list of R's in molecules **5** and **8** given in Scheme 10 includes only some compounds reported in patents<sup>42, 66–68, 75</sup> and mentioned in Table 10. For example, the production of R<sub>3</sub>P with R being Ph, Bn, Tol and Alk from Me to C<sub>8</sub>H<sub>17</sub> was described<sup>72</sup>, as well as of R<sub>3</sub>B with R being Ph and Alk groups from Me to Hex<sup>71</sup>. In equation 18c, the use of **5** with R from Me to *n*-Hex and *c*-Hex, as well as Ph and Bn, was suggested<sup>66, 69</sup>. Moreover, by using different groups in **5** and **8** all possible molecules with mixed R's were produced.

The use of other sacrificial anodes, such as Ca, La, Hg, Tl, As, Te and Se, was also mentioned in patents<sup>65, 68, 69</sup>, but no experimental evidence of their use was described.

As concerns the mechanism of anodic oxidation of **5** at sacrificial anodes, it can be noted that the process occurs at potentials close to those of the oxidation of the corresponding diorganomagnesium compounds (**1**). For example, half-peak potentials for the oxidation of **5b** and **1b** in THF containing 0.25 M TBAP at a lead electrode measured<sup>37</sup> at a scan rate of 0.3 V s<sup>-1</sup> are equal to  $E_{p/2} = -1.73$  and  $-1.72$  V vs. 0.01 M Ag<sup>+</sup>/Ag, respectively. However, the oxidation mechanism for both compounds is different, as shown

by different Tafel slopes: 0.12 and 0.06 V for **5b** and **1b**, respectively<sup>37</sup>. The high Tafel slope for **5b** means that the electron transfer is slow. Nevertheless, chemical reactions following the formation of the first Pb–Et bond and controlling the overall rate constants are the same for both kinds of compounds, as proposed by Fleischmann and coworkers<sup>37</sup> in Scheme 4 (Section IV.A). The second oxidation process (equation 19) observed at a potential of –1.2 V corresponds to the formation of the insoluble PbBr<sub>2</sub> layer on the electrode surface.



Moreover, the oxidation process is strongly dependent on the state of the electrode surface<sup>37</sup>. At a freshly cleaned and polished lead the oxidation of **5b** occurs at  $E_{p/2} = -1.52$  V on the first sweep, but on subsequent cycles the potential shifts in the cathodic direction approaching  $E_{p/2} = -1.72$  V.

#### 4. Processes at semiconductor anodes

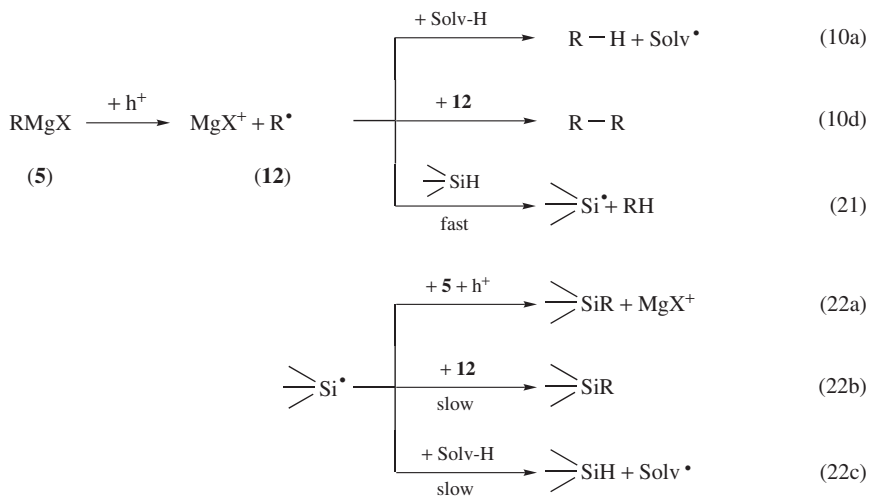
In recent years there has been great interest in the derivatization of silicon surfaces and, beside other methods, electrochemical oxidations of **5** at silicon anodes were successfully used for this purpose<sup>79–84</sup>. Although a perfect electronic passivation toward electron–hole recombination of the (111)-oriented silicon surface can be obtained by hydrogen termination, yet its chemical stability toward oxidation is limited, in particular when it comes into contact with air or moisture. Molecular grafting of silicon surfaces by organic groups, first of all alkyl but in perspectives also biochemical, provides a promising approach to improve the stability of silicon interfaces and to develop silicon-based molecular electronic, biochip and sensing devices. In the electrochemical approach, the oxidation of **5** produces radicals **12** which form covalent C–Si bonds with anode atoms. Thus, there is some similarity to the oxidation of **5** on sacrificial metal anodes. However, the process is different because new bonds are formed only with surface atoms and there is no loss of the anode material. Moreover, oxidation processes at metal and semiconductor electrodes are different because of their different electronic properties.

Electrochemical grafting of methyl groups on the porous<sup>79</sup> as well as the atomically flat (111) Si surface<sup>80</sup> was reported. Fast methylation of the hydrogenated (111) surface of p-type silicon wafer, used as the anode, with the Cu counter electrode was performed<sup>80</sup> in 3 M solution of **5k** in Et<sub>2</sub>O in a glove box under purified nitrogen by passing the anodic current from 0.1 to 5 mA cm<sup>–2</sup> from 1 to 30 min. Differential attenuated total reflection (ATR) FTIR spectra, obtained with the electrode shaped as an ATR prism, allowing multiple reflections of the IR beam inside the plate and avoiding propagation across the electrolyte, supported substitution of the hydrogen atoms by methyl groups. Namely, a narrow single  $\nu\text{SiH}$  line at 2083 cm<sup>–1</sup> in p polarization, characteristic of the stretching mode of Si–H bonds perpendicular to the surface, was not observed. On the other hand, lines of methyl groups appeared according to predictions<sup>80</sup>: the symmetric deformation  $\delta_{\text{S}}$  mode at 1255 cm<sup>–1</sup> in p polarization and the asymmetric  $\delta_{\text{AS}}$  mode at 1410 cm<sup>–1</sup> in s and p polarization. The presence of additional carbon on Si surfaces after grafting was evidently confirmed by high-resolution XPS spectra<sup>83</sup> which also confirmed the practical absence of surface oxidation. The *in situ* IR spectroscopy with a current-pulse method allowed researchers to investigate<sup>81,83</sup> the kinetics of the electrochemical grafting. With the increase of the cumulated charge the integrated band intensities showed the loss of  $\nu\text{SiH}$  accompanied by a simultaneous gain of  $\delta_{\text{Me}}$  (for methyls covalently bonded to Si), supporting the electrochemical character of the process. Independent *ex situ* IR

measurements showed that the fraction of substituted hydrogens was of the order of 90%. There was no effect of concentration and solvent ( $\text{Et}_2\text{O}$  or THF) on the kinetics, but a larger current density caused faster variations in IR signals and increased the yield of surface modification. The overall grafting process (equation 20), including the transfer of positively charged holes,  $h^+$ , is fast and irreversible<sup>81</sup>, with the participation of very short-lived intermediates, most probably radicals.

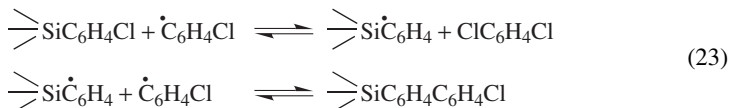


The necessary breaking of SiH bonds may be realized either through direct potential activation, or more often through anodic generation of **12** at the first step of the oxidation of **5** at semiconductor electrodes<sup>82</sup>. However, for higher current densities a competition between reactions with silicon (equation 20) and other following reactions of **12**, similar to those accompanying the anodic oxidation of **5** at metal electrodes (cf. Scheme 5 in Section IV.B), was pointed out. Thus, a more detailed mechanism of grafting was proposed<sup>83</sup> as is shown in Scheme 11. **12** can abstract a hydrogen atom from the hydrogenated silicon surface (equation 21) and the dangling bond, then created at the Si surface, may react with **5** (equation 22a), or with another **12** (equation 22b) or may abstract a hydrogen atom from the solvent (equation 22c). The last competing step was confirmed by the observation of a weak reincrease in the SiH band after turning off the anodic current. The reactions in Scheme 11 as well as equation 20 correspond to two elementary charges per one attached R group, which is in best agreement with experimental data. Moreover, a detailed kinetic model was proposed<sup>83</sup> reproducing the shapes of kinetic curves and their dependence on experimental conditions. In conclusion, it was shown<sup>83</sup> that anodic alkylation of the Si surface by **5** is less favorable for attaining maximum coverage than chemical techniques, but it is much faster because the Faradaic efficiency may be close to unity, although the concentration of radicals **12** at the surface remains very low. Thus, grafting of a full monolayer requires only a charge of several hundred  $\mu\text{C cm}^{-2}$ , which can be completed in one second<sup>82, 83</sup>.



SCHEME 11

Investigations of **5** with different R groups showed<sup>82</sup> that fast grafting can be obtained for the most inert radicals, R = Alk (from Me to C<sub>18</sub>H<sub>37</sub>) and ethynyl, whereas for more reactive **12**, e.g. Ar•, side reactions were observed<sup>82</sup>, in particular electropolymerization on the silicon surface. For example, such behavior was found for **5r** and the first steps of the formation of a polymeric layer can be described by equations 23.

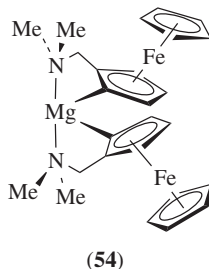


However, if the molecules of **5** had R alkyl chains longer than Me, the steric hindrance prevented 100% substitution<sup>83</sup> and IR examinations indicated a 50% less derivatization. Moreover, XPS analysis showed that the surface is partly modified by substitution of hydrogen by halogen<sup>83</sup>. In the case of **5** with X = I and to some extent X = Br, the formation of X• radicals (besides **12**) in a secondary reaction was reported<sup>81,83</sup>. They participate in reactions analogous to equations 21 and 22b, but with X• instead of **12**, and attach to the Si surface improving the electronic passivation of the surface at defect sites, sterically inaccessible to **12**. A possibility that surface dangling bonds may also appear in the charged states was discussed as well<sup>83</sup>.

On the other hand, alkylation of silicon surfaces using **5** can be achieved by chemical methods: chlorination with PCl<sub>5</sub> or Cl<sub>2</sub> followed by alkylation with **5**. A comparison of the electrical properties and chemical stability of (111) silicon surfaces alkylated by different chemical and electrochemical methods was reported by Webb and Lewis<sup>84</sup>. They found that the surfaces prepared by anodization of Si in 3 M solutions of **5k** in Et<sub>2</sub>O displayed extensive oxidation in air and higher initial charge-carrier surface recombination velocities than those observed for the samples prepared by chemical methods. However, it should be added here that even in the thermal grafting of hydrogenated silicon surfaces using **5**, some electrochemistry is hidden<sup>85</sup>. Namely, a zero-current electrochemical step was proposed<sup>85</sup> in order to explain the following experimental results: (i) the addition of **8** to **5** significantly increased the grafting efficiency of alkyl chains, (ii) the grafting is also possible in solutions containing only **8** and, moreover, (iii) the process in 1 M C<sub>10</sub>H<sub>21</sub>MgBr solution in Et<sub>2</sub>O is much faster on n-type than on p-type silicon. The last result indicates that the rds is of electrochemical nature. A reaction model containing simultaneous oxidation of **5** and reduction of **8** at the silicon surface, with the second step acting as rds, was proposed<sup>83</sup> on the basis of electrochemical thermodynamic considerations.

### C. Other Compounds

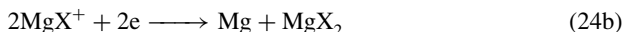
Basically, it is possible to obtain organomagnesium compounds with electroactive groups oxidized without the cleavage of the Mg–C bond. They are formally beyond the scope of this Chapter, and thus only one example is mentioned. **54** (written as the *S, S* diastereomer), having a dimethylaminomethylferrocenyl unit, which is (*C, N*)-bidentate ligand with the α-carbon atom from the substituted Cp ring and the amine nitrogen atom as donors, was investigated<sup>86</sup> at a platinum electrode in CH<sub>2</sub>Cl<sub>2</sub> containing 0.2 M TBAPF<sub>6</sub> electrolyte. Reversible oxidation of both ferrocene moieties was found with a two-electron CV peak at *E*<sub>pa</sub> = 0.41 V vs. SCE at any scan rate, which indicates no electronic communication between the two ferrocene units. A yellow-to-blue color change, typical of the formation of the ferrocenium cation, corroborated the nature of the electrochemical process.



## V. CATHODIC REDUCTION OF ORGANOMAGNESIUM COMPOUNDS

### A. General Mechanism of the Reduction

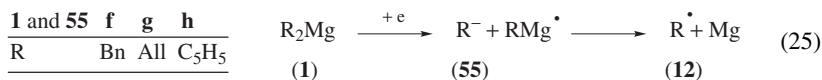
The earliest investigations on the electrode reduction of organomagnesium compounds already indicated the magnesium deposition on the cathode. It was found in 1927 for solutions of **5** in Et<sub>2</sub>O using a Pt cathode<sup>14</sup> and later evidently supported<sup>187</sup> by the formation of a magnesium amalgam on a Hg electrode. Evans and coworkers excluded<sup>19,21</sup> the existence of magnesium(II) ions in Et<sub>2</sub>O solutions (considered earlier<sup>14</sup>) and suggested<sup>15</sup>, on the basis of conductivity measurements and transference study of solutions of **5c**, the formation of RMg<sup>+</sup> and MgX<sup>+</sup> ions (equations 3a–3c in Section III). The overall equations 24 proposed<sup>15</sup> indicated the final products of the reduction, but details were unclear, although the participation of free radicals RMg<sup>•</sup> and MgX<sup>•</sup>, as intermediates formed in the one-electron transfer from the electrode, was postulated.



Dessy and Handler supported<sup>88</sup> earlier findings of Evans and Pearson<sup>15</sup> on the mass balance during the electrolysis of **5b** solutions in Et<sub>2</sub>O, which indicated the magnesium migration to both Pt electrodes, the loss of Et in preference to Br in the cathode compartment (separated by a stopcock bore) and the existence of large aggregates of ions. The most interesting result was obtained<sup>88</sup> from a study of radioactivity balance in the cell containing the Grignard reagent prepared by mixing **1b** and labeled <sup>28</sup>MgBr<sub>2</sub>. After the exchange two different types of magnesium were found in the solution, indicating not only that **5b** should be represented by Et<sub>2</sub>Mg•MgBr<sub>2</sub>, in accordance with the Schlenk equilibrium (equation 2), but also that the magnesium deposited at the cathode has its origin in **1b**, whereas MgBr<sub>2</sub> migrates to the anode compartment. Thus, it was postulated that the cathodic reaction (equation 24b) is not involved in the electrochemical process and the RMg<sup>+</sup> ion plays the main role in the reduction. It should be noted that **1b** was reduced at high voltage equal to 160 V<sup>88</sup>. However, the nature of the intermediates and the detailed mechanism was not explained until recent years (see next Section).

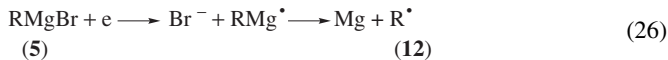
On the other hand, the polarographic behavior of organomagnesium compounds in DME solutions containing 0.1 M TBAP, reported by Psarras and Dessy<sup>36</sup>, was quite different. Compounds **1** with R = Alk and Ph were not reducible before a supporting electrolyte discharge. However, solutions of **1f**, **1g** and **1h**, with R = Bn, All and C<sub>5</sub>H<sub>5</sub>, respectively, i.e. containing groups capable of forming in DME fairly stable carbanions (**55**) (they are formed if the pK values of the parent hydrocarbons are lower than 44)<sup>89</sup>, were easily reduced (equation 25). The polarographic waves observed were irreversible, diffusion-controlled and corresponded to n<sub>e</sub> = 1, as proved by the controlled-potential electrolysis at –3 V. Their half-wave potentials are given in Table 11. Radicals RMg<sup>•</sup>, formed in the

first step, decomposed with the deposition of Mg on the cathode and formation of radicals **12**. Their further reactions were the same as for **12** formed during the oxidation at anodes, including mainly equations 10a, 10b and 10d<sup>36</sup>, as was discussed in Section IV.B.



Furthermore, the polarographic reduction of RMgBr under the same conditions gave two waves<sup>36</sup> (with the exception of **5a**, when only the first wave was observed). The first one had half-wave potentials,  $E_{1/2}^I$ , given in Table 11, close to the value  $E_{1/2} = -2.47$  V characteristic of the reduction of MgBr<sub>2</sub> (which is different than  $E_{1/2} = -2.3$  V for the reduction of Mg<sup>2+</sup> ions). However, the reduction of MgBr<sub>2</sub> was the two-electron process yielding Mg and 2Br<sup>−</sup>, but the coulombic analysis of the reduction of **5** showed the total number of electrons for both waves of  $n_e = 1$ . This behavior was explained by taking into account the Schlenk equilibrium (equation 2)<sup>36</sup>. In full accordance with the equilibrium 2, the addition of MgBr<sub>2</sub> to a solution of **5i** caused an increase in the height of both waves and the addition of *i*-Pr<sub>2</sub>Mg (**1i**) caused an increase in the second wave at the expense of the first one. It should be remembered that compounds **1**, participating in the Schlenk equilibrium, were not reducible<sup>36</sup>. Moreover,  $E_{1/2}$  values found for **5** and for mixtures of MgBr<sub>2</sub> and the corresponding **1** are practically the same (Table 11).

On the other hand, the values for  $E_{1/2}^{II}$  for the second reduction wave of **5** (Table 11) are dependent on the nature of R. It is evident that the reduction becomes more difficult with the increase in the size of R in the order of Et < *i*-Pr < *i*-Bu < Ph. All the observations above indicated<sup>36</sup> that the second polarographic waves correspond to the reduction of **5** themselves (equation 26). Thus, for both types of compounds, **1** and **5**, the unstable radicals RMg<sup>•</sup> formed in the reduction of parent, neutral molecules are responsible for the magnesium deposition<sup>36</sup> and radicals **12** are involved in further reactions, already discussed in Section IV.B.



## B. Deposition of the Metallic Magnesium and the Reverse Process

Although the electrochemical deposition of magnesium from Grignard reagents is not interesting for organic chemists, yet the investigations into such processes undertaken

TABLE 11. Half-wave potentials for the polarographic reduction of 2 mM solutions of **1** and **5** in DME + 0.1 M TBAP<sup>a</sup>

Compound	$-E_{1/2}^I$ (V) <sup>b</sup>	Compound	$-E_{1/2}^I$ (V) <sup>b</sup>	$-E_{1/2}^{II}$ (V) <sup>b</sup>	Mixture <sup>c</sup> of MgBr <sub>2</sub> + <b>1</b>	$-E_{1/2}^I$ (V) <sup>b</sup>	$-E_{1/2}^{II}$ (V) <sup>b</sup>
<b>1f</b>	2.74	<b>5a</b>	2.49	—	<b>1a</b>	2.49	—
<b>1g</b>	2.65	<b>5b</b>	2.44	2.70	<b>1b</b>	2.43	2.66
<b>1h</b>	2.54	<b>5i</b>	2.44	2.75	<b>1i</b>	2.46	2.74
		<b>5l</b>	2.46	2.75	<b>1j</b>	2.50	2.78
MgBr <sub>2</sub>	2.47	<b>5e</b>	2.46	2.80	<b>1e</b>	2.50	2.83

<sup>a</sup> Adapted with permission from Reference 36. Copyright 1966 American Chemical Society.

<sup>b</sup> Expressed vs. Ag/1 mM AgClO<sub>4</sub>. Precision of  $E_{1/2}$  values is  $\pm 0.04$  V.

<sup>c</sup> Corresponding to **5** given in 3<sup>rd</sup> column.

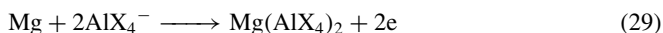
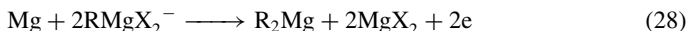


in recent years should be mentioned here because they shed new light on the nature of organomagnesium cations active at electrodes and on the details of electrochemical processes, in particular the reasons of their reversibility, observed only in specific electrolytes. It also resulted in the synthesis and electrochemical investigations of organomagnesium complexes with organoaluminum compounds.

Preparation of a relatively thick, uniform and coherent microcrystalline layer of magnesium is important for some galvanotechnique applications, like the production of parabolic reflectors used for solar collectors and antennas. Aqueous solutions as well as those of the most common organic solvents cannot be used for this purpose. On the other hand, exceptionally good results were obtained using ethereal solutions of **5**, following evidence of magnesium deposition from these solutions reported in early studies<sup>13, 14, 30, 90</sup>. Patented methods<sup>91–93</sup> preferably used THF solutions of **5b**, if **8g** was added after starting electrodeposition at a rate sufficient to dissolve sponge-like magnesium deposits but low enough to avoid corrosion of the magnesium compact layer<sup>91</sup>. Other methods used electrolytes containing among others **1** and **3** in, e.g., toluene<sup>93, 94</sup>.

Even more important in recent years were continuous efforts<sup>95</sup> to develop rechargeable batteries with magnesium anodes, which would be cheap, environment-friendly and safe to handle, and would substitute for the commonly used lead–acid and nickel–cadmium systems for heavy load applications<sup>96</sup>. In such devices the metallic magnesium could be applied as a rechargeable negative electrode if reversible cycling of the magnesium occurred in organic electrolytes, i.e. the  $\text{Mg}^{2+}$  ions were released from the electrode during discharge and a redeposition of  $\text{Mg}^0$  would occur during recharge. The electrodisolution of magnesium in most organic solutions is also difficult, similarly to the electrodeposition, due to the dense passivation layer formed on the magnesium surface by reduction products of the solution species. The electrochemical Mg dissolution can only occur via breakdown of the surface films at relatively high overpotentials, whereas the electrochemical Mg deposition on electrodes covered by a passivating layer is impossible. In the review given below our attention is focused on the nature of species existing in solutions and the mechanism of processes at electrodes, but many electrochemical problems discussed in the cited references are omitted.

Cathodic deposition and anodic dissolution of magnesium from ethereal solutions of **5** have been repeatedly reported<sup>46, 59, 97, 98</sup>. For example, in 0.5 M solutions of **5b** in THF at 293 K using a Cu electrode both processes were reversible<sup>98</sup>, with an exchange current density of  $1 \text{ mA cm}^{-2}$ . Moreover, the addition of magnesium bromide etherate in refluxing THF at 338 K enhances the rate of Mg deposition; however, no deposition was observed from solutions of  $\text{MgBr}_2$  alone. A good magnesium deposition from organoboron complexes with **5** in ethers was found<sup>99</sup>. However, better crystalline deposits with purities of 99.99+% can be obtained<sup>100</sup> from mixtures of less expensive and toxic  $\text{AlCl}_3$  (0.1 M solution in THF) with 0.8–1.5 M solutions of **5**, in particular organomagnesium chlorides, but not bromides or iodides. In the cathodic deposition (equation 24a) mainly a participation of  $\text{RMg}^+$  ions, formed in reactions 4 and 27, were considered<sup>100</sup>. For the dissolution of the Mg anode equations 28 and 29 were proposed<sup>100</sup> followed by further dissociation of  $\text{Mg}(\text{AlX}_4)_2$ .



However, the solutions of **5** were found to be unsuitable as electrolytes for rechargeable batteries. The deposition of Mg at high current efficiency is possible<sup>100</sup> from solutions in

THF of aminomagnesium halides, like (*N*-methylaniline)MgCl, but much better was the solution of magnesium dibutylidiphenylborate,  $\text{Mg}(\text{BBu}_2\text{Ph}_2)_2$  (**56**) in THF, even without the addition of other organomagnesium compounds. By using a solution of **56** in a mixture of THF and DME it was possible to construct<sup>100</sup> and patent<sup>101</sup> the first cell with a magnesium anode which could be discharged and recharged, but only in four cycles. It was noted<sup>100</sup> that a few magnesium compounds which appear to be capable of Mg deposition from organic solvents have a relatively covalent nature of bonds to the Mg atom.

The rate of the reoxidation of Mg deposits is controlled by their morphology<sup>102</sup>, which in turn depends on the substrate material. Smooth and compact deposits were obtained using silver or gold, but not nickel or copper. It was also established<sup>103</sup> that the open circuit potential (OCP) of magnesium electrode (a fresh deposit on a Pt) in concentrated solutions of **5** depends strongly on the solvent used. In THF solutions with *c* around 1 M at 22 °C under argon atmosphere, the values of OCP for **5a**, **5b** and **5f** were equal to  $-2.8$ ,  $-2.73$  and  $-2.77$  V vs.  $\text{Ag}^+/\text{Ag}$ , respectively<sup>35</sup>.

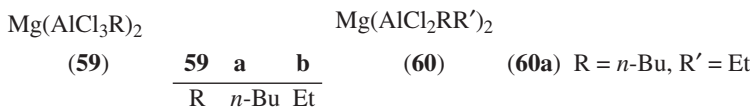
The electrodeposition of magnesium from THF solutions containing **5**, amidomagnesium halides or magnesium organoborates was compared by Liebenow and coworkers<sup>35</sup>. Conductivity of solutions of **5** in THF (cf. Table 3 in Section II) is lower than that for a solution of bis(trimethylsilyl) magnesium chloride (**57**), but the highest value ( $0.31 \Omega^{-1} \text{cm}^{-1}$  at a concentration of 0.4 M) was found for solutions of  $\text{Mg}(\text{B}(s\text{-Bu})(n\text{-Bu})_3)_2$  (**58**). The reversibility of the magnesium deposition in solutions of **5** was high and the reoxidation efficiency of magnesium deposit on silver in 10 cycles was 100%, much better than for solutions of **58**. However, the last electrolyte was found to be the most stable for irreversible oxidation, which is favorable in energy storage devices. The best result at that time for a complete cell was obtained<sup>35, 104</sup> with a solution of the magnesium salt **56**. Conducting polymer electrolytes were also proposed<sup>104–106</sup> in order to construct all solid-state magnesium rechargeable batteries.

Significant progress in understanding the mechanism of the processes discussed was recently reached by the group of Aurbach<sup>96, 107–117</sup>. The results obtained, little known by organic chemists, can also be interesting for understanding the processes of classical preparation of **5** by the reaction with magnesium, most often used in organic chemistry. A comparison of Mg electrochemistry in solutions of **5b**, **5f** and **5g** in THF and different magnesium salts in dipolar aprotic solvents was performed<sup>107</sup> under a very pure argon atmosphere at room temperature using a number of modern techniques: CV, impedance spectroscopy, surface sensitive FTIR spectroscopy, elemental analysis by dispersive X-rays (EDAX), scanning and tunneling electron microscopy (SEM and STM) and electrochemical quartz crystal microbalance (EQCM). FTIR spectra showed evidently that the surface chemistry of magnesium electrode in THF solutions (without **5**) is dominated primarily by possible reactions of the salt anions and atmospheric contaminants, such as trace water. The electrochemical examinations supported the conclusion that in solutions of all the solvents used, magnesium electrodes are covered by surface films formed spontaneously even if the surface is freshly prepared in solutions. Organic or inorganic magnesium salts, MgO and  $\text{Mg}(\text{OH})_2$ , as well as some hydrated forms of the two last compounds, formed at the surface do not conduct Mg ions and this passivation of the electrode makes the Mg deposition impossible. It was believed<sup>96, 114</sup> that magnesium ions are located at a specific site in the lattice and their mobility is close to zero. On the other hand, those layers also prevent a spontaneous reaction of the metal with the solvent and/or solution components. In THF, which was the least polar solvent under examination, the pristine surface films are very stable but thick passivation layers are not formed. Those films must be confined to a monolayer scale as was supported<sup>115</sup> by X-ray photoelectron spectroscopy (XPS). Moreover, THF and other ethers are not reactive with Mg.

Thus, the Mg electrode in a solution of the supporting electrolyte [0.1 M (CH<sub>3</sub>COO)<sub>2</sub>Mg and 1 M TBAP] in THF was blocked and did not show any voltammetric activity in the potential range from -3.5 to +0.5 V vs. Ag/Ag<sup>+</sup>. However, after the addition of **8g** to that solution, the Mg dissolution and deposition was obtained at relatively low overpotentials and the oxidation and reduction peaks appear in voltammetric curves. This means that the presence of alkyl halides leads to a breakdown of 'native' films (some electron tunneling through the surface films was assumed<sup>107</sup>) and the formation of soluble **5** with unreactive anions toward magnesium metal. Thus, a reversible electrochemical behavior was observed only in passivating surface-film free conditions. It was also emphasized<sup>117</sup> that the molecules of **1** as Lewis bases are effective scavengers for trace atmospheric contaminants and react with them in the bulk of solution, preventing the magnesium surface from the passivation. The CV-EQCM experiments supported the conclusion that stable passivating surface films were not formed on Mg electrodes in THF solutions of **5** and that the magnesium deposited does not react with THF but remains electrochemically active. Moreover, the anodic process around the 1.5 V vs. Mg/Mg<sup>2+</sup> reference electrode was considered<sup>107</sup> as related to the oxidation of Alk groups. On the other hand, there were indications of some adsorption/desorption processes and it was evidently shown that the electroreduction corresponds to equation 24a as well as the reduction of Alk<sub>2</sub>Mg but not Mg<sup>2+</sup> ion.

Most important for practical application as electrolytes for rechargeable batteries were the solutions in THF or polyethers of some of the complexes synthesized<sup>96</sup> by Aurbach and coworkers. These complexes are based on Mg organohaloaluminate salts, such as Mg(AlCl<sub>3</sub>R)<sub>2</sub> (**59**) and Mg(AlCl<sub>2</sub>RR')<sub>2</sub> (**60**), preferably **59a**, **59b** and **60a**. The electrochemical deposition–dissolution of magnesium in these solutions is reversible with almost 100% efficiency, as is illustrated in Figure 5 for **60a** in THF. Moreover, it is evident from Figure 5 that the electrolyte decomposition of **60a** solution occurs at the most negative potential in comparison with other electrolytes, i.e. the anodic stability is the best, giving a potential range of more than 2.5 V in which the solution is inactive. Using these electrolytes, a magnesium anode and a Mg<sub>x</sub>Mo<sub>3</sub>S<sub>4</sub> cathode with intercalated Mg ions, it was possible to develop the Mg battery system with promise for applications<sup>96,113</sup>.

In subsequent papers<sup>109–111</sup> Aurbach and coworkers extended an examination of the mechanism to the ethereal solutions of complexes of general formula Mg(AX<sub>4-n</sub>R<sub>n'</sub>R'<sub>n''</sub>)<sub>2</sub> (A = Al or B, X = halide, R, R' = Alk or Ar and n' + n'' = n), which can be considered as products of the interaction between R'RMg Lewis bases and AX<sub>3-n</sub>R<sub>n'</sub>R'<sub>n''</sub> Lewis acids. The order of anodic stability found<sup>110,114</sup> is **59a** > **60a** > **56** > **5g**.



The morphology of Mg deposition on a gold electrode is strongly dependent on the composition of solutions, as indicated by *in situ* imaging using the STM method and by the high impedance measured. That behavior is caused by the adsorption of different species present in each solution in the course of deposition. Surface residuals of carbon, aluminium and chlorine were detected<sup>115</sup> by the XPS technique in THF solutions containing **60a**, but they are restricted to the outermost part of the surface, as physically adsorbed species. The mass balance of the Mg deposition–dissolution process is zero, whereas the cycling efficiency, describing the charge balance, depends on the solution composition and is

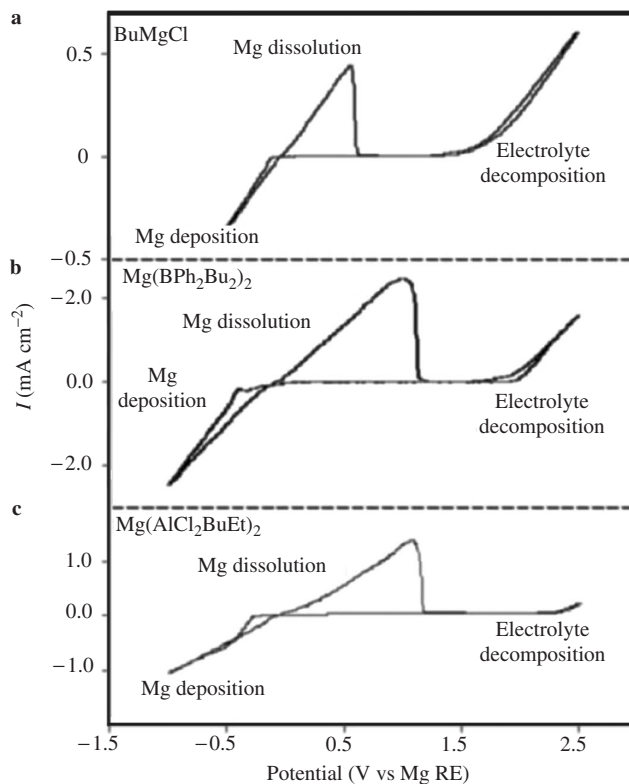
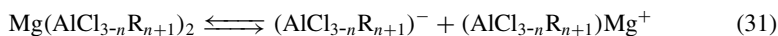
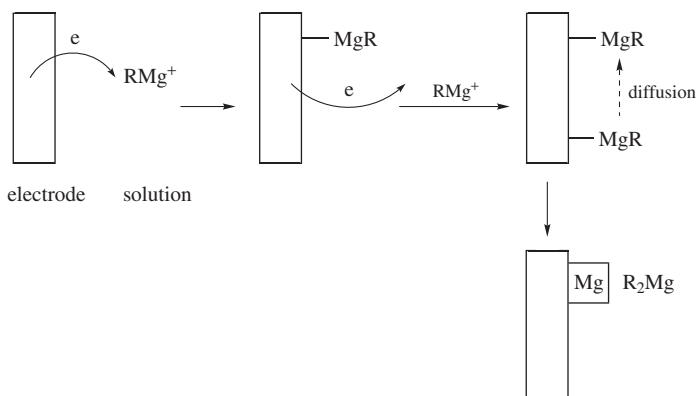


FIGURE 5. Cycling voltammograms recorded at  $5 \text{ mV s}^{-1}$  using a Pt working and Mg counter and reference electrodes in THF solutions containing: (a) 2 M *n*-BuMgCl (**5g**), (b) 0.25 M  $\text{Mg}(\text{BPh}_2\text{Bu}_2)_2$  (**56**), (c) 0.25 M  $\text{Mg}(\text{AlCl}_2\text{BuEt})_2$  (**60a**). Reprinted by permission from Macmillan Publishers Ltd: *Nature*, **407**, 724, copyright 2000

higher in THF solutions of **5g** and **60a**. Taking into account the complicated structures of **5** as well as organomagnesium chloroaluminate complexes in THF solutions, it was assumed<sup>110</sup> that the electrochemical processes of **5** occur via electron transfer to cations such as  $\text{RMg}^+$  or  $\text{MgX}^+$  adsorbed at the electrode surface, as shown in Scheme 12 for the case of  $\text{RMg}^+$  ions. For chloroaluminate complexes the equilibria (equations 30 and 31) were considered<sup>110</sup>, but also the adsorption of other species, like  $\text{Mg}_2\text{Cl}_3(n\text{THF})^+$  and  $\text{Mg}_x\text{Cl}_y\text{R}_z(n\text{THF})^+$ .



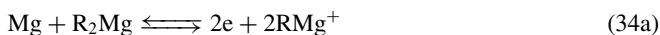
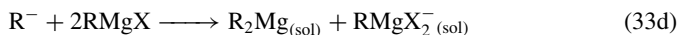
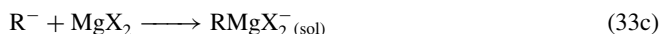
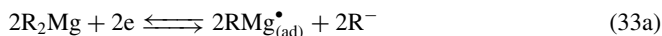
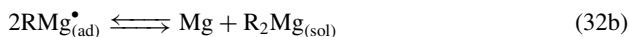
In order to explain the results of EQCM and microscopy, it was postulated that in all the solutions studied the deposition occurs as a two-stage process. Initially, when the amount of charge involved is small ( $< 0.4 \text{ C cm}^{-2}$ ), a porous and irregular-in-shape magnesium deposit is formed. EDAX spectra of the electrode in a solution of **5g** revealed that this initial deposit contains, in addition to magnesium, also carbon and chlorine. This means



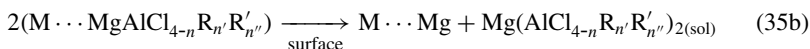
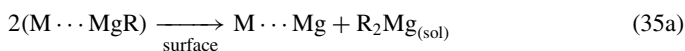
SCHEME 12

that traces of the electrolyte are trapped in the porous structure of the initial deposit. However, while the Mg deposition proceeds further from all kinds of solutions<sup>110</sup>, **5g**, **60a** or **56**, the Mg layer becomes compact and crystalline, mostly composed of distorted, pyramid-shaped magnesium crystals. The pure magnesium deposition from the THF solution of **60a** was supported by XPS measurements<sup>115</sup>. The mass per mole of the electrons for this step is close to 12 g mol<sup>-1</sup>, reflecting the deposition of pure magnesium from solutions of **5**<sup>110</sup>. The nature of the species adsorbed at electrodes was investigated *in situ* by FTIR spectroscopy, using an internal reflectance mode<sup>111</sup>. In those experiments the working electrode was prepared by plating first a platinum layer and next a gold layer on the spectroelectrochemical KBr window. FTIR spectra measured at open circuit voltage for gold electrodes on which magnesium was earlier deposited at -0.5 V vs. Mg/Mg<sup>2+</sup>, in solutions containing **5g**, **5u** or BnMgCl (**5v**), showed new peaks around 550 cm<sup>-1</sup> and 600–650 cm<sup>-1</sup> which were attributed to Mg–C and Mg–Cl bonds, respectively. This was supported by a comparison with FTIR spectra obtained in transmittance mode for **5** and MgX<sub>2</sub> salts pelletized with KBr. Similar spectra obtained after deposition from **60a** and **59a** solutions also revealed bands in that range attributed to Mg–Cl and Mg–C bonds; for the last solution an additional peak at 466 cm<sup>-1</sup> was attributed to Al–Cl bonds. For the solution of **56**, new peaks at 3000 cm<sup>-1</sup> found after a deposition have higher wave numbers than those attributed to the  $\nu_{C-H}$  mode of the phenyl groups. In conclusion, the adsorption of the following species on the Mg electrode surface was suggested<sup>111</sup>: RMg<sup>+</sup> or RMg<sup>•</sup> for solutions of **5**, Mg<sub>x</sub>Cl<sub>y</sub><sup>+</sup>, e.g. Mg<sub>2</sub>Cl<sub>3</sub><sup>+</sup> (*n*THF), as well as the species with Al–Cl bonds [e.g. (AlCl<sub>4-n</sub>R<sub>n</sub>'R<sub>n</sub>'')Mg<sup>+</sup> (*n*THF) etc.] and Mg–C bonds for complex solutions of Mg(Al<sub>4-n</sub>R<sub>n</sub>) and probably PhMg<sup>+</sup> and B(Ph<sub>2</sub>Bu<sub>2</sub>)Mg<sup>+</sup> for the solutions of **56**. All of the above species are stabilized by THF molecules coordinated to the Mg ions [i.e. RMg<sup>+</sup> (*n*THF) exists instead of RMg<sup>+</sup>], as was supported by bipolar IR peaks, similar but shifted to a lower wave number as compared with the peaks of the bulk THF molecules. Thus, a general mechanism of Mg deposition involves an adsorption of the cationic species to the electrode surface during the polarization to low potentials and then charge transfer to them followed by disproportionation of the adsorbed species in the radical state to form Mg deposits and solution species. The proposed mechanism for solutions of **5** is shown<sup>110</sup> in Scheme 12 (similar processes for RX<sup>+</sup> cations also take place<sup>110</sup>) and is described<sup>111</sup> by equations 32 or 33. On the other hand, the magnesium dissolution is represented<sup>111</sup> by equations 34. However, for some species in solutions the Schlenk equilibrium (equation 2) and the ionization equilibrium (equation 4) should be

taken into account in the overall mechanism.



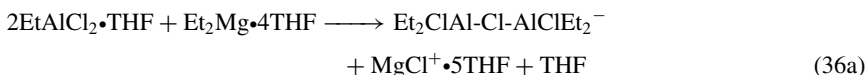
The adsorbed cationic species are next transformed to the adsorbed radical species by the electron transfer. Finally, the Mg deposition may occur via the adsorbed radicals that disproportionate laterally on the electrode surface to form Mg metal and solution species, as represented, for example, by equations 35<sup>111</sup>.



Very high impedance ( $>10 \text{ k}\Omega \text{ cm}^2$ ) of reversible Mg electrode systems studied also indicated<sup>112</sup> adsorption processes. However, overpotentials of only several tens of millivolts are sufficient to break down the adsorbed layers, resulting in a much lower impedance ( $<100 \Omega \text{ cm}^2$ ) during the electrochemical processes.

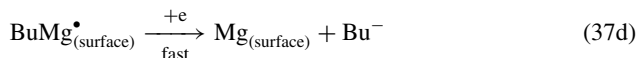
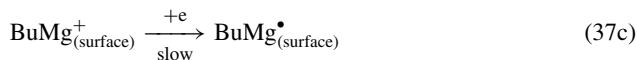
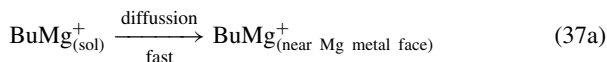
The electrochemical behavior of a number of complexes with formal formulae  $\text{Mg}(\text{AX}_{4-n}\text{R}_n)_2$  (where A = Al, B, Sb, P, As, Fe and Ta; X = Cl, Br and F; R = Bu, Et, Ph and Bn) in several solvents, including THF, Et<sub>2</sub>O, diglyme and tetraglyme, was also investigated<sup>114</sup>. It was found that a highest decomposition potential  $>2.1 \text{ V}$  vs.  $\text{Mg}/\text{Mg}^{2+}$  couple and a cycling efficiency close to 100% can be obtained for  $(\text{Bu}_2\text{Mg})_x(\text{EtAlCl}_2)_y$  complexes (considered as products of the reaction between a **1d** base and the  $\text{EtAlCl}_2$  (**61**) Lewis acid) in THF or tetraglyme solutions. It was clearly demonstrated that electrochemical processes are influenced by both the nature of the Lewis acid–base systems and the solvent molecules. A series of experiments with precipitation of crystals and their redissolution in THF indicated that the structures of the solution species and of the crystals are different. The structure of the solution species is undefinable and should be described as a series of complicated equilibria, depending on the acid–base ratio, the nature of the solvent and other molecules in the solution, and temperature, in the same manner as in the solutions of **5**. The most interesting conclusion of Aurbach and coworkers<sup>114</sup> for this Chapter is that the electrochemically active cation includes more than one Mg ion and may have a general structure of  $\text{Mg}_2\text{R}_{3-n}\text{Cl}_n^+$  solv, while the anion probably has the structure of  $\text{AlCl}_{4-n}\text{R}_n$ . In any case, the presence of the R group in the cation is crucial for reversible magnesium deposition. However, the concentration of **61** cannot be too high because a sufficient content of R groups is necessary for a reversible behavior. Thus, the optimal ratio of **61** to **1d** in solutions of interest was found<sup>114</sup> to be close to 2:1. Moreover, the determination of the anodic stability in THF solutions without  $\text{Mg}^{2+}$  ions, but containing  $0.25 \text{ M AlEt}_3\text{Cl}^-$ ,  $\text{AlEt}_2\text{Cl}_2^-$ ,  $\text{AlEtCl}_3^-$  and  $\text{AlCl}_4^-$ , showed

oxidation potentials equal to 2.0, 2.2, 2.5 and 2.6 V vs.  $\text{Mg}/\text{Mg}^{2+}$ , respectively<sup>116</sup>. The above result means that the anodic stability is mainly determined by the weakest Al–C bond, and not, as thought previously<sup>114</sup>, by C–Mg bonds, as in **5**. The existence of different species in solutions, depending on the components ratio, was also suggested by nonmonotonous changes in the conductivity,  $\kappa$ , of 0.25 M solutions in THF against the acid-to-base ratio. The highest  $\kappa$  ( $1.6 \text{ mS cm}^{-1}$  for  $\text{R} = \text{Bu}$  and  $0.8 \text{ mS cm}^{-1}$  for  $\text{R} = \text{Et}$ ) was obtained for ratios of **1:61** equal to 0.5:1 and 2:1, whereas for a ratio of 1:1 a lowest  $\kappa = 0.4 \text{ mS cm}^{-1}$  was observed<sup>116</sup> for both R groups. On the basis of  $^1\text{H}$ ,  $^{13}\text{C}$ ,  $^{27}\text{Al}$  and  $^{25}\text{Mg}$  NMR measurements (for **1d**) and in agreement with the above-mentioned conductivity data, the existence of major components in each solution was identified<sup>116</sup>, as shown by equations 36a–c for complexes with acid-to-base ratio of 2:1, 1:1 and 1:2, respectively, hexacoordination of magnesium species was assumed in equations 36. However, it was not clear if the same species are responsible for magnesium electrodeposition and the authors rather suggested<sup>116</sup> that other, possibly organomagnesium, species undetected by NMR play a major role in the Mg deposition and dissolution from 2:1 complex solutions<sup>116</sup>. The last suggestion is in line with the observed increase in the rates of magnesium electrochemical processes after the addition of **1d** to 2:1 complex solutions.



The kinetics of the Mg deposition on Pt microelectrodes in THF solutions of different compositions, starting from a complex containing only Cl ligands ( $\text{MgCl}_2 + \text{AlCl}_3$ ) to the all-organic electrolyte **1d**, was analyzed<sup>117</sup> in detail on the basis of Tafel and Allen & Hickling plots. The exchange current density increased considerably as the ratio of organic ligand to Cl ligand increased and this acceleration of the Mg deposition was attributed to the change in proportions of the electroactive  $\text{BuMg}^+$  and  $\text{MgCl}^+$  species in solutions. However, the Faradaic efficiency is much higher for electrolytes containing chloride anions. For all the solution compositions studied, the transfer coefficients for the cathodic and anodic reactions at overpotentials close to 0 were 0.5 and 1.5, respectively, indicating two one-electron steps with the first one being the rds. On the other hand, Tafel slopes increase remarkably at higher overvoltages, giving finally the cathodic transfer coefficient of 0.09, which indicates a more complex reaction mechanism. The results obtained were interpreted in terms of a three-stage electrocrystallization mechanism, which describes the growth of the metallic deposits on the faces, steps and kinks of the substrate metal. The first stage, which is the formation of ad-atoms on the metallic faces, is the most interesting for the present Chapter. For the case of  $\text{BuMg}^+$  as electroactive species in a solution, this stage involves fast diffusion to the metal face (equation 37a), slow adsorption (equation 37b), followed by a slow first electron transfer (equation 37c) yielding a radical  $\text{BuMg}^\bullet$  on the metal surface and a fast electron transfer to it with the formation of magnesium ad-atom on the metal face (equation 37d). Note the difference in the second electron transfer from the electrode instead of the disproportionation between the adsorbed radicals (equation 32b), as considered previously<sup>110,111</sup>. However, at higher overvoltage the rate of electron transfer (equation 37c) increases and the adsorption of  $\text{BuMg}^+$  becomes the rds, resulting in unusually high Tafel slopes. Finally, the reaction of  $\text{Bu}^-$  with  $\text{BuMg}^+$  yields **1d**, which is highly soluble in THF, contrary to insoluble  $\text{MgCl}_2$ . This may explain the acceleration of Mg deposition in all-organic electrolyte in comparison with the process in solutions containing only  $\text{MgCl}_2$  and  $\text{AlCl}_3$ . In the last

solutions, the overall mechanism is similar but with  $\text{MgCl}^+$  ions instead of  $\text{BuMg}^+$  as the electroactive species. On the other hand, for the magnesium dissolution at small positive overpotentials the same steps in the opposite direction, from the process in equation 37d to 37a, was suggested<sup>117</sup> and the same electron transfer as the rds. However, at higher positive overpotentials the nonelectrochemical step in which the magnesium atom from the metallic lattice is placed near the kink, before the formation of Mg ad-atom, becomes the rds.



It should be added that nonaqueous electrolytes for high-energy rechargeable electrochemical cells developed by Aurbach and coworkers were patented for use as solutions in organic solvents<sup>118</sup> or as gel-type solids<sup>119</sup>.

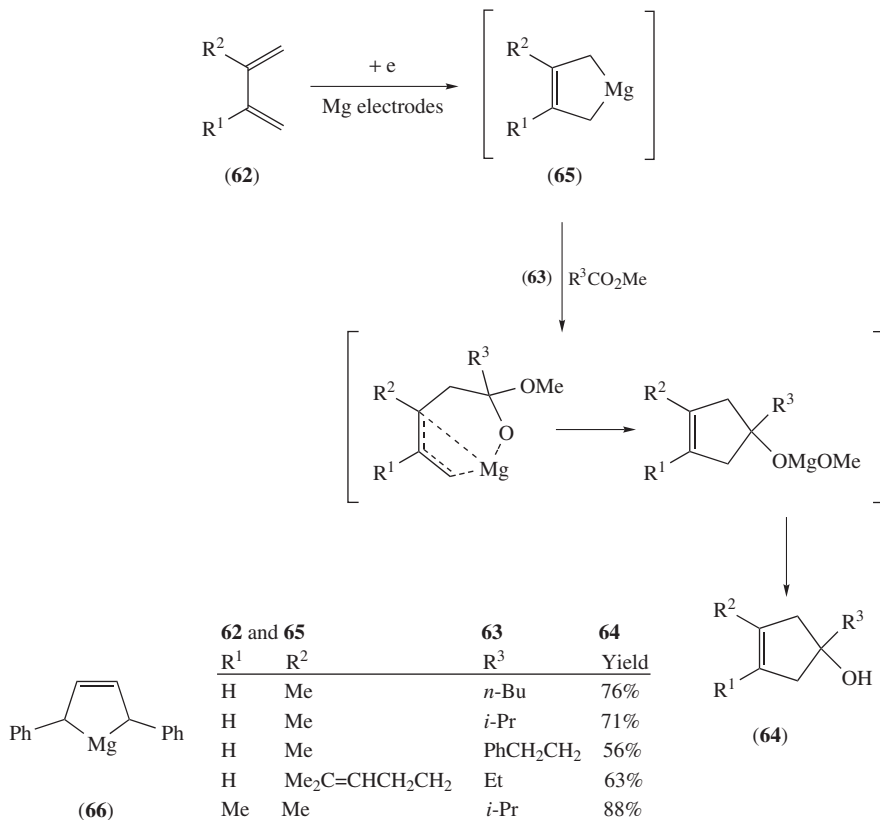
Moreover, the magnesium deposition on silver substrate from 0.25 M solution of **60a** in THF is accompanied<sup>120</sup> by the formation of silver–magnesium alloy, which decreases the overpotential of deposition–dissolution processes and promotes the cycling efficiency.

## VI. ORGANOMAGNESIUM COMPOUNDS AS INTERMEDIATES IN ELECTRODE REACTIONS

A number of electroorganic syntheses based on the use of sacrificial magnesium anodes have been described. However, in only a few reactions, listed below, was the formation of intermediate organomagnesium compounds postulated or documented.

Shono and coworkers<sup>121</sup> reported that magnesium electrodes promote cyclocoupling reactions of 1,3-dienes (**62**) with aliphatic carboxylic esters (**63**) resulting (Scheme 13) in the formation of cyclic products **64** with a five-membered ring. The electrode process was carried out in a single-compartment cell with a magnesium rod cathode and the same anode, which were alternated at an interval of 15 s. The electrolysis was carried out under nitrogen atmosphere in dry THF containing  $\text{LiClO}_4$  and 5 Å molecular sieves. The electrodes from other metals (Pt, Al, Zn, Cu, Ni or Pb) did not yield **64**. The role of a sacrificial magnesium anode in the synthesis based on electrogenerated reagents was well recognized as the source of  $\text{Mg}^{2+}$  ions which stabilize intermediate organic anions (often called electrogenerated bases) forming with them coordination complexes or magnesium organic salts, like carboxylates or enolates; references can be found in reviews<sup>122, 123</sup> and in a more recent paper<sup>124</sup>. However, Shono and coworkers<sup>121</sup> found the same product **64** if a solution of a diene (**62**) was reduced electrochemically at the Mg electrode and an ester (**63**) then added, after the current was terminated. The above result led the authors to suggest that a magnesium–diene compound (**65**) is formed during the electroreduction and not the Mg complex with an ester. It is known that organomagnesium compounds can be obtained in the reaction of 1,3-dienes with metallic magnesium, in particular, when highly reactive magnesium, prepared by the reduction of  $\text{MgCl}_2$  in THF,





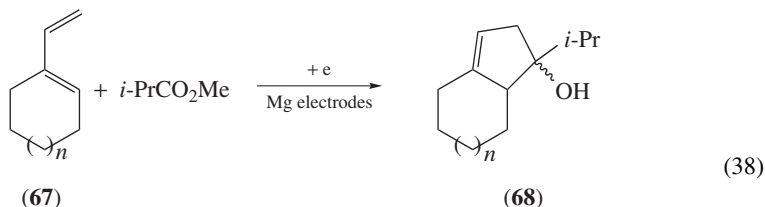
SCHEME 13

is used<sup>125</sup>. A cyclic structure for **65** was proposed<sup>121</sup> by analogy to (1,4-diphenyl-2-butene-1,4-diyl)magnesium (**66**), the crystal structure of which was shown<sup>126</sup> to be a five-membered ring.

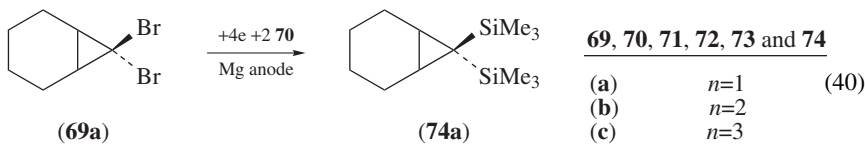
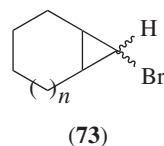
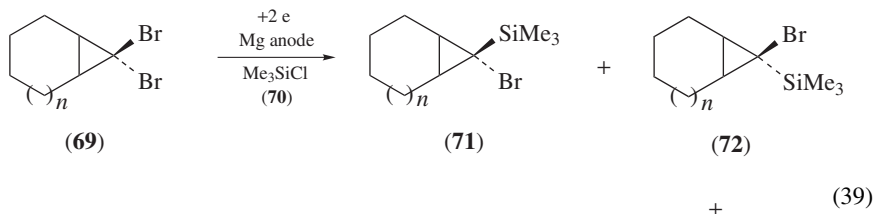
The cathodic cyclocoupling reaction (equation 38) with a diene under similar conditions was also observed<sup>121</sup> for 1-vinylcyclohexene (**67a**) and 1-vinylcycloheptene (**67b**), giving **68** as the final product with satisfactory yields. Thus, similar intermediate metalocycles can be expected for this reaction. On the other hand, for the cathodic coupling of styrenes the formation of a Mg compound was not proved<sup>121</sup>, although a magnesium electrode was necessary in order to obtain a 2-phenylcyclopropanol-type product.

During electrochemical reduction of bicyclic 1,1-dibromocyclopropanes (**69a–69c**) in DMF or THF in the presence of chlorotrimethylsilane (**70**), using a stainless steel cathode and a sacrificial magnesium anode in an undivided cell, the replacement of one or both bromine atoms (depending on the amount of current passed) by a trimethylsilyl group was observed<sup>127</sup>. The reaction (equation 39) was stereoselective giving **71**, the *exo*-silyl bromide with the trialkylsilyl group in the *cis* position to hydrogen atoms at the ring junction, as the major product (and the *endo*-silyl compound **72** as the second product), in contrast to the reaction of **69** with *n*-BuLi and **70** which yield **72** as the major product. The by-product **73** was formed by a hydrogen atom abstraction from a solvent molecule.

A detailed mechanism was proposed for **69a** as an example<sup>127</sup>. The overall reaction (equation 40) finally produced the disilyl compound **74a** with a yield not much higher than 50%. However, unexpected results were obtained using ultrasonic irradiation during the electrolysis. The apparent current efficiency increased up to 200% giving, for example, 71% of disilane **74b** (and by-products) but no monosilane **71b** or **72b** after passage of 2.5 Faradays per mole of **69b**.



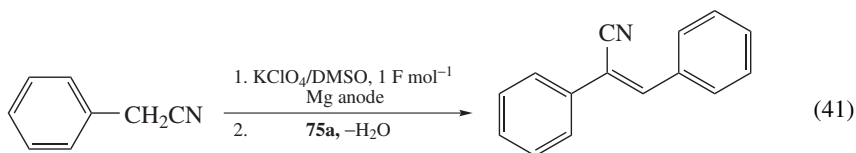
67 and 68		Yield
(a)	$n = 1$	62%
(b)	$n = 2$	72%



Moreover, in the divided cell the *exo:endo* ratio of bromosilanes was 91:9 in the anode compartment but only 52:48 in the cathode compartment. Thus, the nature of the ultrasonic effect was explained assuming that beside the electrochemical silylation at the cathode, a parallel silylation process occurs at a magnesium anode, namely the silylation by **70** of an intermediate Grignard reagent produced from dibromide **69**. It appears as a rare example of the 'anodic reduction'<sup>127</sup>. However, the increase in the current density during electrolysis caused a decrease in the apparent current efficiency. This observation indicates a chemical nature of the anodic process. Of course, the ultrasonic irradiation facilitates the formation of the organomagnesium intermediate at the sacrificial anode<sup>127</sup> and the authors reported<sup>128</sup> a similar ultrasonic effect for the nonelectrochemical but purely sonochemical

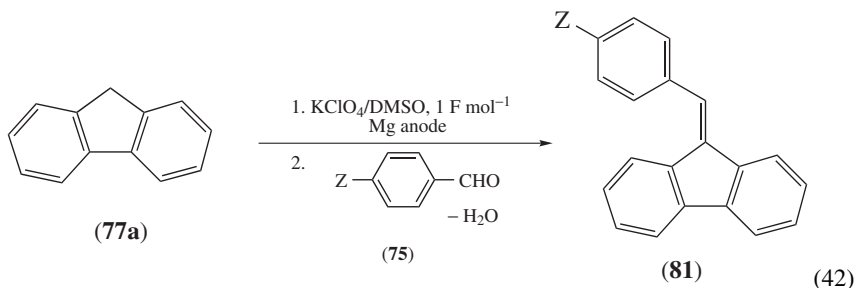
reaction in THF in the presence of a bulk magnesium rod; the latter reaction had given even higher yields and stereoselectivity.

Nucleophilic addition of diorganomagnesium compounds **1** with unusual substituents, generated by an indirect electrochemical method according to Scheme 1 in Section II, to the electrophiles benzaldehyde and its 4-substituted derivatives (**75**) or 2,2,2-trifluoroacetophenone (**76**) was reported by Lund and coworkers<sup>28</sup>. We recall that the electrochemical step involves only the formation of the magnesium salt,  $\text{dimethyl}_2\text{Mg}$  (**4**), and **1** is formed in the nonelectrochemical reaction of **4** with fluorene or its derivatives (**77**), acetophenone (**78**) and phenylacetonitrile (**79**). Nevertheless, overall reactions are carried out without isolation of intermediate compounds from the electrochemical cell. The overall processes<sup>28</sup> and isolated yields of the main products are shown in equations 41 and 42 and in Scheme 14. It should be emphasized that, in general, these products cannot be obtained in classical reactions. For example, the Grignard reagent with a cyano group,  $\alpha$  to acidic hydrogens, necessary for the preparation of (*Z*)-2,3-diphenylacrylonitrile (**80**), cannot be generated in a direct reaction with magnesium. However, **80** was obtained with an isolated yield of 92% (equation 41). Similarly, 9-benzylidene fluorene (**81a**) was obtained via magnesium fluorenyl (equation 42) with 89% yield, whereas the Grignard reagent, 9-fluorenylmagnesium bromide (**82**), cannot be obtained directly from Mg and 9-bromofluorene. If **82** was obtained indirectly, it gave **81a** as a by-product only<sup>28</sup>.



(79)

(80)



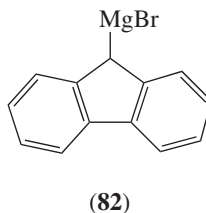
(77a)

(75)

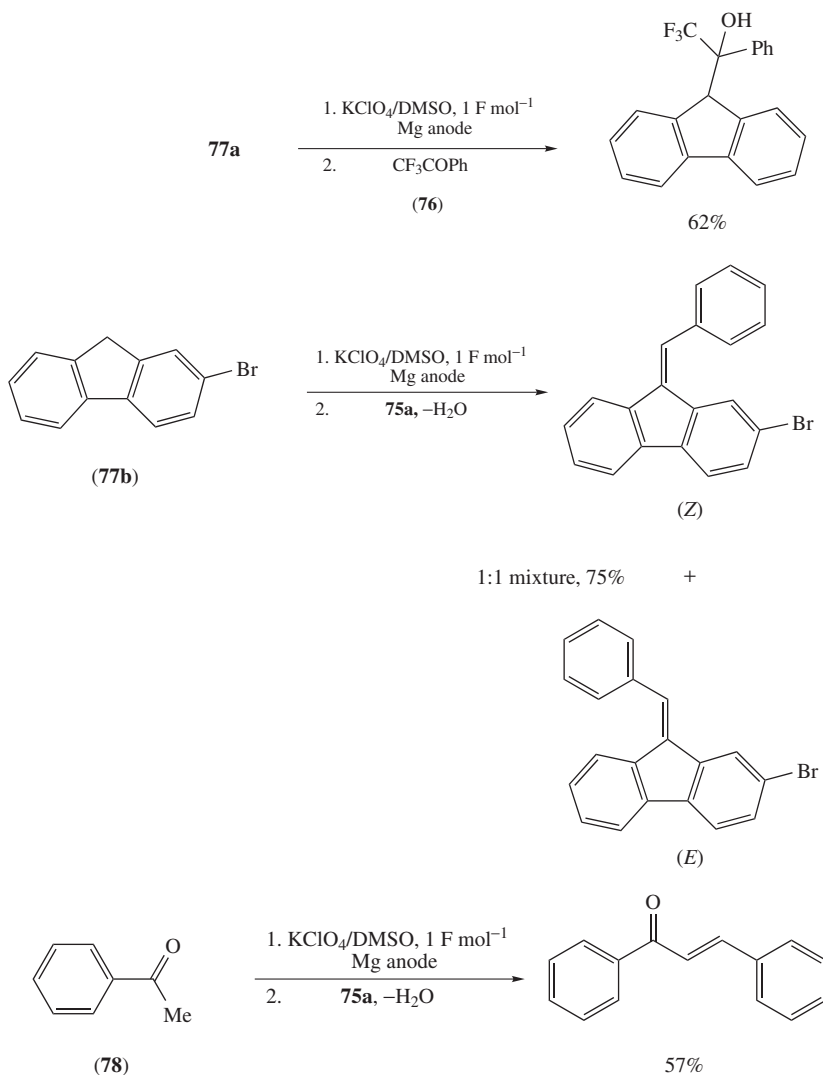
(81)

(42)

<b>75 and 81</b>	<b>a</b>	<b>b</b>	<b>c</b>	<b>d</b>	<b>e</b>	<b>f</b>
Z	H	CN	OMe	NMe <sub>2</sub>	NO <sub>2</sub>	Br
Yield (%)	89	87	61	42	51	61



(82)



SCHEME 14

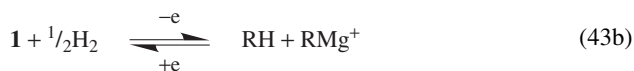
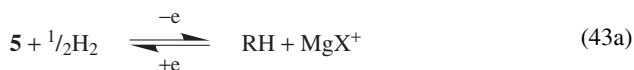
The electrochemical method of conversion *in situ* halogenated organic contaminants  $\text{RX}_n$  in wet soil formations or groundwaters to intermediate Grignard reagents, followed by their hydrolysis to  $\text{RH}_n$  and  $\text{HOMgX}$  [or  $\text{Mg}(\text{OH})_2$  produced in a competing reaction] was patented<sup>129</sup>. The electrical potential applied between magnesium and counter electrodes allows enhanced reactions between  $\text{RX}_n$  and magnesium metal and also allows one to clean magnesium surfaces from oxidation products after periodical reversal of the polarity of the potential.

## VII. CONCLUDING REMARKS: ELECTROCHEMICAL DATA IN THE ELUCIDATION OF REACTIVITY OF GRIGNARD REAGENTS

It is evident from the review presented above that the most recent electrochemical investigations of organomagnesium compounds, like magnesium deposition or grafting on silicon surfaces, are far removed from the main topics of organic chemistry. On the other hand, progress in contemporary synthetic use of Grignard reagents does not include electrochemical methods. Nevertheless, for a detailed elucidation of the mechanisms of Grignard reactions and the formation of Grignard reagents by classical methods, the electrochemical approach can be helpful. A brief review of some of the problems in which electrochemical data were used in the chemistry of organomagnesium compounds is given below.

As was already mentioned, the constitution of reagents **5** in ethereal solutions and of the complexes formed by them with a number of Lewis acids was investigated by electrochemical methods<sup>15, 88, 109–111</sup> and the nature of existing ions and electroactive species was elucidated. It was also possible to evaluate the equilibrium constant for the Schlenk equilibrium for **5b**, **5e** and **5i** in DME solutions from polarographic measurements<sup>36</sup>.

The basicity of a number of reagents **1**, **5** and related compounds in THF solutions was determined voltammetrically by Chevrot and coworkers<sup>38, 130</sup>. Using platinized platinum and hydrogen electrodes, they measured the cathodic–anodic current as a function of potential for overall electrode reactions (equations 43a and 43b)



and found that zero current potentials of the hydrogen electrode are equilibrium potentials, and thus the corresponding pH is a measure of the  $\text{p}K_a$  of organomagnesium compounds. A summary of  $\text{p}K_a$  values reported by Chevrot and coworkers in a number of papers and typical trends for different compounds were recently reviewed<sup>131</sup>.

The reaction mechanisms of Grignard reactions, in particular those with ketones, were the subject of a long debate as a result of which a reactivity spectrum was ascertained between the radical mechanism with the single electron transfer (SET) from **5** to ketone, the classic polar mechanism and the concerted mechanism. A history of these findings was reviewed in 1996 by Blomberg<sup>132</sup>. Linear correlations between logarithms of homogeneous rate constants,  $\log k$ , and oxidation potentials of **5**, obtained from electrochemical measurements, were used as a strong support of the SET step or at least of ‘a significant amount of radical character of the transition state’<sup>52</sup>. Such correlations were found, for example, for pseudo-first-order rate constants for the reaction of **5a**, **5b**, **5e**, **5i** and **5n** with di-*tert*-butyl peroxide in  $\text{Et}_2\text{O}$ <sup>133</sup> and for the reaction of  $\text{AlkMgBr}$  (cf. Table 8) with benzophenone (**83**)<sup>52, 53</sup> and azobenzene (**84**)<sup>53</sup> in  $\text{Et}_2\text{O}$ . Moreover, the kinetic data for Grignard reactions were also analyzed<sup>53</sup> in terms of the Marcus theory of electron transfer kinetics, assuming that SET is the rds and using the oxidation potentials of **5**,  $E_{\text{ox}}$ , in order to calculate the thermodynamic driving force. Marcus nonlinear plots of the activation barrier against the reaction free-energy change were reported<sup>53</sup> for reactions of a series of **5** with **83** and **84**. It was also found on the basis of the Marcus approach that the SET steps are feasible for the reaction of 5-hexenylmagnesium bromide with 3-phenylimido-2-phenyl-3*H*-indole and with 2-methoxy-1-nitronaphthalene in THF but are not feasible for the reaction of **5b** with pyrazine in ethers<sup>56</sup>. However, later investigations<sup>134</sup> on kinetic isotope effects in reactions of **83** with a series of reagents **5**

showed different rds steps for different reagents **5**, although all the reactions followed the SET mechanism (a different mechanism for **5s** was invoked recently<sup>135</sup>). In conclusion, the correlations of  $\log k$  and  $E_{\text{ox}}$  reported earlier were explained<sup>134</sup> rather as an indication of an electron transfer preequilibrium before the rds.

Nevertheless, redox potentials (evaluated in part by electrochemical methods) can be useful for support of the SET step and for predicting the formation of radical products. For example, it was reported<sup>136, 137</sup> that when the oxidation potentials of carbanions ( $E^{\circ}_{\text{R}\bullet/\text{R}^-}$ , obtained in DMF+TBABF<sub>4</sub> and expressed vs. SCE) are compared with the reduction potentials of ketones, they may be helpful in predicting the reaction path of the Grignard reaction. For example, in reactions of **83** ( $E^{\circ} = -1.72$  V) with *t*-BuMgCl ( $E^{\circ}_{\text{R}\bullet/\text{R}^-} = -1.77$  V) and *s*-BuMgCl ( $E^{\circ}_{\text{R}\bullet/\text{R}^-} = -1.72$  V), radical products were obtained, whereas with **5k** ( $E^{\circ}_{\text{R}\bullet/\text{R}^-} = -1.19$  V) and **5v** ( $E^{\circ}_{\text{R}\bullet/\text{R}^-} = -1.40$  V) no radical products were found. On the other hand, in the reaction with fluorenone ( $E^{\circ} = -1.19$  V) all of the **5** mentioned above give the same products ratio as was found for reactions of the corresponding **8** with the electrogenerated radical anion of fluorenone.

In general, it is evident<sup>61</sup> that a SET process is governed by the difference in the oxidation potential of a nucleophile and the reduction potential of a partner reactant. The difference between these two potentials,  $\Delta E = E_{\text{ox}} - E_{\text{red}}$ , was used by Okubo and coworkers<sup>138–142</sup> to estimate the relative efficiency of SET (the so-called ‘ $\Delta E$  approach’). The distribution of products obtained in polar and radical routes for reactions between magnesium compounds, including ArMgBr, as well as ArSMgBr, ArNHMgBr, ArN(MgBr)<sub>2</sub> and ArOMgBr, with a number of carbonyl, nitro and cyano compounds, was correlated with  $\Delta E$  even for multistep reactions.

Irreversible oxidation peaks of **5u**, PhMgCl and *n*-HexMgCl recorded at a Pt electrode in THF containing 0.1 M LiBr were found<sup>143</sup> in the same potential range ( $-2.5$  to  $-1.5$  V vs. Ag<sup>+</sup>/Ag) as for the irreversible reduction peak of the Cl-terminated Si(111) surface ( $-2.5$  V). This result evidently shows that **5** can reduce chlorine bonds on the surface, and thus a SET step participates in the alkylation, as included in the mechanism proposed<sup>143</sup>.

For the unusual reactivity of ferrocenylsilanes toward **5u** in THF, affording ketones instead of the expected tertiary alcohols, a mechanism was proposed<sup>144</sup> including the inner-sphere electron transfer from **5u** within a reactant complex. The proposition was based on an electrochemical CV examination, which indicated that the outer-sphere process is thermodynamically unfavorable.

Finally, it may be noted that the formation of Grignard reagents from organic halides (**8**) and metallic magnesium is a heterogeneous reaction and starts by a SET from magnesium to **8**, as is now commonly accepted<sup>145</sup>. However, many aspects of this reaction are not clear, in particular those connected with its surface nature<sup>146, 147</sup>. Similarities to electrochemical reduction of **8** were considered in order to explain the reaction mechanism. Logarithms of relative rate constants for reactions of Mg with a series of substituted bromobenzenes in Et<sub>2</sub>O and Bu<sub>2</sub>O–C<sub>6</sub>H<sub>12</sub> mixture<sup>148</sup> and with a series of alkyl chlorides in Et<sub>2</sub>O<sup>149</sup> were correlated with electrochemical  $E_{1/2}$  values obtained in DMF for the reduction of the corresponding **8** at a Hg or a glassy carbon (GC) electrode. However, the real sense of these correlations is not straightforward, taking into account the different electrode mechanisms for both series under examination, as is now well documented<sup>58</sup>. Moreover, the absolute rate constants for the formation of **5** reported recently<sup>146</sup> showed much smaller variations with the nature of **8** and the lack of correlations with  $E_{1/2}$  values, indicating that the SET step is not the rds. The last conclusion was also supported<sup>146</sup> by free energies of activation, determined for the same reactions, which were substantially smaller than the literature intrinsic activation barriers for the dissociative electron transfer to **8**.

The electrochemical reduction at GC electrodes in ACN of a number of organic bromides (mainly with cyclopropyl systems), used as radical clocks in reactions of the

formation of **5**, was applied to support the concerted electron transfer and cleavage of a carbon–halogen bond in both types of processes<sup>150</sup> and this conclusion looks quite justified.

On the other hand, the results concerning the heterogeneous nature of the formation of **5** should be interpreted with special care, in particular, in comparison with rearranged products obtained from the radical clock reactions under homogeneous conditions. Recent experiments<sup>147</sup> comparing the behavior of potassium and magnesium in THF and Et<sub>2</sub>O solutions containing the precursor of the aryl radical clock, 1-bromo-2-(3-butenyl)benzene, evidently indicate that the reactions with both metals are comparable to the heterogeneous electron transfer occurring at a cathode, whereas a similar reaction of potassium in the presence of crown ethers corresponds to homogeneous SET processes observed in redox catalysis. In conclusion, it was emphasized<sup>147</sup> that certain unclear problems in the formation of **5**, like a hypothesis of the participation of dianions, can be most probably resolved by treating the dissolution of a metal in these reactions in a similar approach to the one recently developed for elementary steps occurring at electrodes.

### VIII. REFERENCES

1. C. K. Mann and K. Barnes, *Electrochemical Reactions in Nonaqueous Systems*, Chap. 13.1, Dekker, New York, 1970.
2. H. Lehmkuhl, in *Organic Electrochemistry. An Introduction and a Guide* (Ed. M. M. Baizer), Chap. 18, Dekker, New York, 1973, pp. 621–678.
3. M. D. Morris, in *Electroanalytical Chemistry* (Ed. A. J. Bard), Vol. VII, Dekker, New York, 1974, pp. 79–160.
4. S. G. Mairanovskii, *Russ. Chem. Rev.*, **45**, 298 (1976).
5. M. D. Morris and G. L. Kok, in *Encyclopedia of Electrochemistry of the Elements* (Eds. A. J. Bard and H. Lund), Vol. XIII, Chap. XIII-1, Dekker, New York, 1979, pp. 41–76.
6. D. A. White, in *Organic Electrochemistry. An Introduction and a Guide* (Eds. M. M. Baizer and H. Lund), 2<sup>nd</sup> ed., Chap. 19, Dekker, New York, 1983, pp. 591–636.
7. A. P. Tomilov, I. N. Chernyh and Yu. M. Kargin, *Elektrokhimiya elementoorganicheskikh soedinenij*, Nauka, Moscow, 1985.
8. L. Walder, in *Organic Electrochemistry. An Introduction and a Guide* (Eds. H. Lund and M. M. Baizer), 3<sup>rd</sup> ed., Dekker, New York, 1991, pp. 809–875.
9. J. Yoshida and S. Suga, in *Organic Electrochemistry* (Eds. H. Lund and O. Hammerich), 4<sup>th</sup> ed., Chap. 20, Dekker, New York, 2002, pp. 765–794.
10. P. Jolibois, *Compt. Rend.*, **155**, 353 (1912).
11. P. Jolibois, *Compt. Rend.*, **156**, 712 (1913).
12. J. M. Nelson and W. V. Evans, *J. Am. Chem. Soc.*, **39**, 82 (1917).
13. N. W. Kondyrew, *Chem. Ber.*, **58**, 459 (1925).
14. L. W. Gaddum and H. E. French, *J. Am. Chem. Soc.*, **49**, 1295 (1927).
15. W. V. Evans and R. Pearson, *J. Am. Chem. Soc.*, **64**, 2865 (1942).
16. W. V. Evans and F. H. Lee, *J. Am. Chem. Soc.*, **55**, 1474 (1933).
17. W. V. Evans and F. H. Lee, *J. Am. Chem. Soc.*, **56**, 654 (1934).
18. W. V. Evans, F. H. Lee and C. H. Lee, *J. Am. Chem. Soc.*, **57**, 489 (1935).
19. W. V. Evans and E. Field, *J. Am. Chem. Soc.*, **58**, 720 (1936).
20. W. V. Evans and E. Field, *J. Am. Chem. Soc.*, **58**, 2284 (1936).
21. W. V. Evans and D. Braithwaite, *J. Am. Chem. Soc.*, **61**, 898 (1939).
22. W. V. Evans, D. Braithwaite and E. Field, *J. Am. Chem. Soc.*, **62**, 534 (1940).
23. W. V. Evans, R. Pearson and D. Braithwaite, *J. Am. Chem. Soc.*, **63**, 2574 (1941).
24. K. Ziegler and H. Lehmkuhl, German Patent to Ziegler, DE1212085 (1966).
25. K. Ziegler and H. Lehmkuhl, US Patent to Ziegler, US2985568 (1961).
26. P. Kobetz and R. C. Pinkerton, US Patent to Ethyl Corp, US3028319 (1962).
27. K. Ziegler and H. Lehmkuhl, US Patent to Ziegler, US3306836 (1967).
28. H. Lund, H. Svith, S. U. Pedersen and K. Daasbjerg, *Electrochim. Acta*, **51**, 655 (2005).
29. P. C. Hayes, A. Osman, N. Seudeal and D. G. Tuck, *J. Organomet. Chem.*, **291**, 1 (1985).

30. N. W. Kondyrew and D. P. Manojew, *Chem. Ber.*, **58**, 464 (1925).
31. N. W. Kondyrew and A. K. Ssusi, *Chem. Ber.*, **62B**, 1856 (1929).
32. N. W. Kondyrew and A. I. Zhel'vis, *J. Gen. Chem. USSR.*, **4**, 203 (1934); *Chem. Abstr.*, **29**, 25 (1935).
33. W. Strohmeier, *Z. Elektrochem.*, **60**, 396 (1956).
34. W. Strohmeier and F. Seifert, *Z. Elektrochem.*, **63**, 683 (1959).
35. C. Liebenow, Z. Yang and P. Lobitz, *Electrochem. Comm.*, **2**, 641 (2000).
36. T. Psarras and R. E. Dessy, *J. Am. Chem. Soc.*, **88**, 5132 (1966).
37. M. Fleischmann, D. Pletcher and C. J. Vance, *J. Organomet. Chem.*, **40**, 1 (1972).
38. C. Chevrot, J. C. Folest, M. Troupel and J. Périchon, *J. Electroanal. Chem.*, **54**, 135 (1974).
39. W. Schlenk and W. Schlenk, Jr., *Chem. Ber.*, **62B**, 920 (1929).
40. K. C. Cannon and G. R. Krow, in *Handbook of Grignard Reagents* (Eds. G. S. Silverman and P. E. Rakita), Chap. 13, Dekker, New York, 1996, pp. 271–290.
41. V. Gutmann, *The Donor–Acceptor Approach to Molecular Interactions*, Plenum Press, New York, 1978.
42. J. Linsk and E. A. Mayerle, US Patent to Standard Oil Co, US3155602 (1964).
43. A. P. Giraitis, T. H. Pearson and R. C. Pinkerton, US Patent to Ethyl Corp, US2960450 (1960).
44. A. P. Giraitis, US Patent to Ethyl Corp, US2944948 (1960).
45. C. E. Thurston and K. A. Kobe, *Philippine J. Sci.*, **65**, 139 (1938); *Chem. Abstr.*, **32**, 6956 (1938).
46. L. Martinot, *Bull. Soc. Chim. Belg.*, **75**, 711 (1966).
47. J. L. Morgat and R. Pallaud, *C. R. Acad. Sci. C (Paris)*, **260**, 574 (1965).
48. J. L. Morgat and R. Pallaud, *C. R. Acad. Sci. C (Paris)*, **260**, 5579 (1965).
49. R. T. Dufford, D. Nightingale and L. W. Gaddum, *J. Am. Chem. Soc.*, **49**, 1858 (1927).
50. T. H. Bremer and H. Friedman, *Bull. Soc. Chim. Belg.*, **63**, 415 (1954).
51. G. A. Tolstikov, R. G. Bulgakov and V. P. Kazakov, *Russ. Chem. Rev.*, **54**, 1058 (1985).
52. T. Holm, *Acta Chem. Scand.*, **B28**, 809 (1974).
53. T. Holm, *Acta Chem. Scand.*, **B37**, 567 (1983).
54. T. Holm, *J. Chem. Soc., Perkin Trans. 2*, 464 (1981).
55. T. Holm, *Acta Chem. Scand.*, **B42**, 685 (1988).
56. L. Eberson, *Acta Chem. Scand.*, **B38**, 439 (1984).
57. J. M. Savéant, *J. Am. Chem. Soc.*, **109**, 6788 (1987).
58. J. M. Savéant, *Elements of Molecular and Biomolecular Electrochemistry*, Chap. 3, Wiley-Interscience, Hoboken, 2006, pp. 182–250.
59. L. Martinot, *Bull. Soc. Chim. Belg.*, **76**, 617 (1967).
60. C. Chevrot, M. Troupel, J. C. Folest and J. Périchon, *C. R. Acad. Sci. C (Paris)*, **273**, 493 (1971).
61. L. Eberson, *Electron Transfer Reactions in Organic Chemistry*, Chap. IV, Springer-Verlag, Berlin, 1987, pp. 39–66.
62. H. Schäfer and H. Küntzel, *Tetrahedron Lett.*, 3333 (1970).
63. H. E. French and M. Drane, *J. Am. Chem. Soc.*, **52**, 4904 (1930).
64. D. G. Braithwaite, US Patent to Nalco Chemical Co, US3007857 (1961).
65. D. G. Braithwaite, US Patent to Nalco Chemical Co, US3007858 (1961).
66. D. G. Braithwaite, US Patent to Nalco Chemical Co, US3234112 (1966).
67. D. G. Braithwaite, US Patent to Nalco Chemical Co, US3256161 (1966).
68. D. G. Braithwaite, US Patent to Nalco Chemical Co, US3312605 (1967).
69. D. G. Braithwaite, US Patent to Nalco Chemical Co, US3391066 (1968).
70. D. G. Braithwaite, US Patent to Nalco Chemical Co, US3391067 (1968).
71. J. W. Ryznar and J. G. Premo, US Patent to Nalco Chemical Co, US3100181 (1963).
72. W. P. Hettinger, Jr., US Patent to Nalco Chemical Co, US3079311 (1963).
73. J. Linsk, US Patent to Standard Oil Co, US3118825 (1964).
74. J. Linsk, W. C. Ralph and E. Field, US Patent to Standard Oil Co, US3164537 (1965).
75. J. Linsk, US Patent to Standard Oil Co, US3298939 (1967).
76. G. C. Robinson, US Patent to Ethyl Corp, US3522156 (1970).
77. G. Calingaert and H. Shapiro, US Patent to Ethyl Corp, US2535193 (1950).
78. D. E. Danly, in *Organic Electrochemistry. An Introduction and a Guide* (Eds. M. M. Baizer and H. Lund), 2<sup>nd</sup> ed., Chap. 30, Dekker, New York, 1983, pp. 959–994.



79. T. Dubois, F. Ozanam and J.-N. Chazalviel, *Electrochem. Soc. Proc.*, **97**–7, 296 (1997).
80. A. Fidélis, F. Ozanam and J.-N. Chazalviel, *Surf. Sci.*, **444**, L7 (2000).
81. J.-N. Chazalviel, S. Fellah and F. Ozanam, *J. Electroanal. Chem.*, **524**–525, 137 (2002).
82. A. Teyssot, A. Fidélis, S. Fellah, F. Ozanam and J.-N. Chazalviel, *Electrochim. Acta*, **47**, 2565 (2002).
83. S. Fellah, A. Teyssot, F. Ozanam, J.-N. Chazalviel, J. Vigneron and A. Etcheberry, *Langmuir*, **18**, 5851 (2002).
84. L. J. Webb and N. S. Lewis, *J. Phys. Chem. B*, **107**, 5404 (2003).
85. S. Fellah, R. Boukherroub, F. Ozanam and J.-N. Chazalviel, *Langmuir*, **20**, 6359 (2004).
86. N. Seidel, K. Jacob, A. K. Fischer, C. Pietzsch, P. Zanello and M. Fontani, *Eur. J. Inorg. Chem.*, 145 (2001).
87. N. W. Kondyrew, *J. Russ. Phys. Chem. Soc.*, **60**, 545 (1928); *Chem. Abstr.*, **23**, 1321 (1929).
88. R. E. Dessy and G. S. Handler, *J. Am. Chem. Soc.*, **80**, 5824 (1958).
89. R. E. Dessy, W. Kitching, T. Psarras, R. Salinger, A. Chen and T. Chivers, *J. Am. Chem. Soc.*, **88**, 460 (1966).
90. D. M. Overcash and F. C. Mathers, *Trans. Electrochem. Soc.*, **64**, 305 (1933).
91. E. Findl, M. A. Ahmadi and K. Lui, US Patent to Xerox Corp., US3520780 (1970).
92. J. Eckert and K. Gneupel, GDR Patent to Technische Hochschule 'C. Schorlemmer', DD 243722 (1987).
93. A. Mayer, US Patent to US Dept. of Energy, US4778575 (1988).
94. A. Mayer, *J. Electrochem. Soc.*, **137**, 2806 (1990).
95. P. Novák, R. Imhof and O. Haas, *Electrochim. Acta*, **45**, 351 (1999).
96. D. Aurbach, Z. Lu, A. Schechter, Y. Gofer, H. Gizbar, R. Turgeman, Y. Cohen, M. Moshkovich and E. Levi, *Nature*, **407**, 724 (2000).
97. H. Göhr and A. Seiler, *Chem.-Ing.-Tech.*, **42**, 196 (1970).
98. J. D. Genders and D. Pletcher, *J. Electroanal. Chem.*, **199**, 93 (1986).
99. A. Brenner, *J. Electrochem. Soc.*, **118**, 99 (1971).
100. T. D. Gregory, R. J. Hoffman and R. C. Winterton, *J. Electrochem. Soc.*, **137**, 775 (1990).
101. R. J. Hoffman, R. C. Winterton and T. D. Gregory, US Patent to Dow Chemical Company, US4894302 (1990).
102. C. Liebenow, *J. Appl. Electrochem.*, **27**, 221 (1997).
103. C. Liebenow, Z. Yang and P. Lobitz, *Bull. Electrochem.*, **15**, 424 (1999).
104. C. Liebenow, *Electrochim. Acta*, **43**, 1253 (1998).
105. C. Liebenow, *Solid State Ionics*, **136**–137, 1211 (2000).
106. O. Chusid, Y. Gofer, H. Gizbar, Y. Vestfrid, E. Levi, D. Aurbach and I. Riech, *Adv. Mater.*, **15**, 627 (2003).
107. Z. Lu, A. Schechter, M. Moshkovich and D. Aurbach, *J. Electroanal. Chem.*, **466**, 203 (1999).
108. D. Aurbach, M. Moshkovich, A. Schechter and R. Turgeman, *Electrochem. Solid State Lett.*, **3**, 31 (2000).
109. D. Aurbach, Y. Cohen and M. Moshkovich, *Electrochem. Solid State Lett.*, **4**, A113 (2001).
110. D. Aurbach, A. Schechter, M. Moshkovich and Y. Cohen, *J. Electrochem. Soc.*, **148**, A1004 (2001).
111. D. Aurbach, R. Turgeman, O. Chusid and Y. Gofer, *Electrochem. Comm.*, **3**, 252 (2001).
112. D. Aurbach, Y. Gofer, A. Schechter, O. Chusid, H. Gizbar, Y. Cohen, M. Moshkovich and R. Turgeman, *J. Power Sources*, **97**–98, 269 (2001).
113. D. Aurbach, Y. Gofer, Z. Lu, A. Schechter, O. Chusid, H. Gizbar, Y. Cohen, V. Ashkenazi, M. Moshkovich, R. Turgeman and E. Levi, *J. Power Sources*, **97**–98, 28 (2001).
114. D. Aurbach, H. Gizbar, A. Schechter, O. Chusid, H. E. Gottlieb, Y. Gofer and I. Goldberg, *J. Electrochem. Soc.*, **149**, A115 (2002).
115. Y. Gofer, R. Turgeman, H. Cohen and D. Aurbach, *Langmuir*, **19**, 2344 (2003).
116. H. Gizbar, Y. Vestfrid, O. Chusid, Y. Gofer, H. E. Gottlieb, V. Marks and D. Aurbach, *Organometallics*, **23**, 3826 (2004).
117. Yu. Vestfrid, M. D. Levi, Y. Gofer and D. Aurbach, *J. Electroanal. Chem.*, **576**, 183 (2005).
118. D. Aurbach, Y. Gofer, A. Schechter, L. Zhonghua and C. Gizbar, US Patent to Bar Ilan University, US6316141 (2001).
119. D. Aurbach, O. Chasid, Y. Gofer and C. Gizbar, US Patent to Bar Ilan University, US6713212 (2004).
120. Z. Feng, Y. NuLi, J. Wang and J. Yang, *J. Electrochem. Soc.*, **153**, C689 (2006).

121. T. Shono, M. Ishifune, H. Kinugasa and S. Kashimura, *J. Org. Chem.*, **57**, 5561 (1992).
122. J. Simonet and J.-F. Pilard, in *Organic Electrochemistry* (Eds. H. Lund and O. Hammerich), 4<sup>th</sup> ed., Chap. 29, Dekker, New York, 2002, pp. 1163–1225.
123. J. H. P. Utley and M. F. Nielsen, in *Organic Electrochemistry* (Eds. H. Lund and O. Hammerich), 4<sup>th</sup> ed., Chap. 30, Dekker, New York, 2002, pp. 1227–1257.
124. R. Yee, J. Mallory, J. D. Parrish, G. L. Carroll and R. D. Little, *J. Electroanal. Chem.*, **593**, 69 (2006).
125. R. D. Rieke and H. Xiong, *J. Org. Chem.*, **56**, 3109 (1991).
126. Y. Kai, N. Kanehisa, K. Miki, N. Kasai, K. Mashima, H. Yasuda and A. Nakamura, *Chem. Lett.*, 1277 (1982).
127. A. J. Fry and J. Touster, *Electrochim. Acta*, **42**, 2057 (1997).
128. J. Touster and A. J. Fry, *Tetrahedron Lett.*, **38**, 6553 (1997).
129. P. A. Rock, W. H. Casey and R. B. Miller, US Patent to Regents of the University of California, US6004451 (1999).
130. C. Chevrot, K. Kham, J. Périchon and J. F. Fauvarque, *J. Organomet. Chem.*, **161**, 139 (1978).
131. W. Kosar, in *Handbook of Grignard Reagents* (Eds. G. S. Silverman and P. E. Rakita), Chap. 23, Dekker, New York, 1996, pp. 441–453.
132. C. Blomberg, in *Handbook of Grignard Reagents* (Eds. G. S. Silverman and P. E. Rakita), Chap. 11, Dekker, New York, 1996, pp. 219–248.
133. W. A. Nugent, F. Bertini and J. K. Kochi, *J. Am. Chem. Soc.*, **96**, 4945 (1974).
134. H. Yamataka, T. Matsuyama and T. Hanafusa, *J. Am. Chem. Soc.*, **111**, 4912 (1989).
135. T. Holm, *J. Org. Chem.*, **65**, 1188 (2000).
136. H. Lund, K. Daasbjerg, T. Lund, D. Occhialini and S. U. Pedersen, *Acta Chem. Scand.*, **51**, 135 (1997).
137. H. Lund, K. Skov, S. U. Pedersen, T. Lund and K. Daasbjerg, *Collect. Czech. Chem. Commun.*, **65**, 829 (2000).
138. M. Okubo, T. Tsutsumi, A. Ichimura and T. Kitagawa, *Bull. Chem. Soc. Jpn.*, **57**, 2679 (1984).
139. M. Okubo, T. Tsutsumi and K. Matsuo, *Bull. Chem. Soc. Jpn.*, **60**, 2085 (1987).
140. M. Okubo, K. Matsuo, N. Tsurusaki, K. Niwaki and M. Tanaka, *J. Phys. Org. Chem.*, **6**, 509 (1993).
141. K. Matsuo, R. Shiraki and M. Okubo, *J. Phys. Org. Chem.*, **7**, 567 (1994).
142. M. Okubo and K. Matsuo, *Nippon Kagaku Kaishi*, 1 (2000); *Chem. Abstr.*, **132**, 200217 (2000).
143. E. J. Nemanick, P. T. Hurley, B. S. Brunschwig and N. S. Lewis, *J. Phys. Chem. B*, **110**, 14800 (2006).
144. A. Alberti, M. Benaglia, B. F. Bonini, M. Fochi, D. Macciantelli, M. Marcaccio, F. Paolucci and S. Roffia, *J. Phys. Org. Chem.*, **17**, 1084 (2004).
145. C. Hamdouchi and H. M. Walborsky, in *Handbook of Grignard Reagents* (Eds. G. S. Silverman and P. E. Rakita), Chap. 10, Dekker, New York, 1996, pp. 145–218.
146. B. J. Beals, Z. I. Bello, K. P. Cuddihy, E. M. Healy, S. E. Koon-Church, J. M. Owens, C. E. Teerlinck and W. J. Bowyer, *J. Phys. Chem. A*, **106**, 498 (2002).
147. H. Hazimeh, J.-M. Mattalia, C. Marchi-Delapierre, R. Barone, N. S. Nudelman and M. Chanon, *J. Phys. Org. Chem.*, **18**, 1145 (2005).
148. H. R. Rogers, R. J. Rogers, H. L. Mitchell and G. M. Whitesides, *J. Am. Chem. Soc.*, **102**, 231 (1980).
149. J. J. Barber and G. M. Whitesides, *J. Am. Chem. Soc.*, **102**, 239 (1980).
150. H. M. Walborsky and C. Hamdouchi, *J. Am. Chem. Soc.*, **115**, 6406 (1993).

## CHAPTER 7

# Analytical aspects of organomagnesium compounds

JACOB ZABICKY

*Department of Chemical Engineering, Ben-Gurion University of the Negev, P. O. Box 653, Beer-Sheva 84105, Israel*  
*Fax: +972 8 6472969; e-mail: zabicky@bgu.ac.il*

---

I. ACRONYMS . . . . .	266
II. INTRODUCTION AND SCOPE OF THE CHAPTER . . . . .	267
III. ELEMENTAL ANALYSIS OF MAGNESIUM . . . . .	269
A. Introduction . . . . .	269
B. Sample Preparation . . . . .	271
1. Matrix obliteration . . . . .	271
2. Preconcentration . . . . .	272
C. Column Separation Methods . . . . .	273
1. Ion chromatography . . . . .	273
2. High-performance liquid chromatography . . . . .	274
3. Electrophoresis . . . . .	274
D. Electrochemical Methods . . . . .	275
1. Ion-selective electrodes . . . . .	275
2. Electroanalytical determination . . . . .	276
E. Spectral Methods . . . . .	277
1. Atomic absorption spectrometry . . . . .	277
2. Atomic emission spectrometry . . . . .	278
3. Ultraviolet-visible spectrophotometry and colorimetry . . . . .	279
4. Ultraviolet-visible fluorometry . . . . .	283
5. Chromatic chemosensors . . . . .	285
6. Nuclear magnetic resonance spectroscopy . . . . .	286
7. Mass spectrometry . . . . .	287
IV. SPECIATION ANALYSIS OF ORGANOMAGNESIUM COMPOUNDS . . . . .	288
A. Titration Methods . . . . .	288
1. Visual endpoint . . . . .	288
2. Potentiometric and other instrumental titrations . . . . .	291
B. Chromatographic Methods . . . . .	292

---

*The chemistry of organomagnesium compounds*

Edited by Z. Rappoport and I. Marek © 2008 John Wiley & Sons, Ltd. ISBN: 978-0-470-05719-3

1. Liquid chromatography . . . . .	292
2. Gas chromatography . . . . .	293
C. Spectral Methods . . . . .	295
1. Infrared spectroscopy . . . . .	295
2. Gilman's color tests . . . . .	295
3. Nuclear magnetic resonance spectroscopy . . . . .	296
4. Electron spin resonance spectroscopy . . . . .	299
D. Cryoscopy . . . . .	299
V. GRIGNARD REAGENTS AS ANALYTICAL REAGENTS AND AIDS . . . . .	299
A. Active Hydrogen . . . . .	299
B. Derivatization Reagents . . . . .	300
1. Gas chromatography of organometallic compounds . . . . .	300
2. Analysis of glycerides and waxes . . . . .	301
C. Ancillary Applications . . . . .	301
1. Surface conditioning . . . . .	301
2. Electrochemical behavior . . . . .	305
VI. REFERENCES . . . . .	306

---

## I. ACRONYMS

AAS	atomic absorption spectroscopy/spectrometry
AED	atomic emission detection/detector
AES	atomic emission spectroscopy/spectrometry
ANN	artificial neural network
AOAC	Association of Official Analytical Chemists
ASTM	American Society for Testing and Materials
CE	capillary electrophoresis
CPE	carbon paste electrode
CRM	certified reference material
CZE	capillary zone electrophoresis
DA	diode array
DCTA	1,2-diaminocyclohexylenetetraacetic acid
DIN	direct injection nebulizer
DRIFTS	diffuse reflectance infrared Fourier transform spectroscopy
EDTA	ethylenediaminetetraacetic acid
EGTA	ethylene glycol bis( $\beta$ -aminoethyl ether)- <i>N,N,N',N'</i> -tetraacetic acid
EI	electron impact
ESR	electron spin resonance
ETAAS	electrothermal AAS
EXSY	2D $^1\text{H}$ — $^1\text{H}$ exchange spectroscopy
FAAS	flame AAS
FAES	flame AES
FFGD	fast flow glow discharge
FIA	flow injection analysis
FLD	fluorescence detection/detector
FPD	flame photometric detection/detector
GCE	glassy carbon electrode
GFAAS	graphite furnace AAS
GPC	gel permeation chromatography
HMPT	hexamethylphosphoric triamide
IC	ion chromatography

ICP	inductively coupled plasma
ISE	ion-selective electrode(s)
LLE	liquid-liquid extraction
LOD	limit(s) of detection
LOQ	limit(s) of quantitation
LSCSV	linear sweep cathodic strip voltametry
LTA	low temperature ashing
MIP	microwave-induced plasma
MSD	mass spectrometric detection/detector
NCI	negative-ion chemical ionization
NMR	nuclear magnetic resonance
PCI	positive-ion chemical ionization
PDVB	polystyrene-divinylbenzene
PEBBLE	probe encapsulated by biologically localized embedding
PEO	poly(ethylene oxide)
PLS	partial least squares
PQCD	piezoelectric quartz crystal detection/detector
RP	reversed phase
RSD	relative standard deviation
SDS	sodium dodecylsulfate
SEFT	spin-echo Fourier transform
SFE	supercritical fluid extraction
SIA	sequential injection analysis
SIM	selected ion monitoring
SNR	signal to noise ratio
SSCE	silver-silver chloride electrode
SWAdSV	square wave adsorptive stripping voltametry
TAG	triacylglycerol
TCD	thermal conductivity detection/detector
THF	tetrahydrofuran
TPPI	time proportional phase increment
UVD	UVV detection/detector
UVV	ultraviolet-visible

## II. INTRODUCTION AND SCOPE OF THE CHAPTER

Research related to magnesium belongs to various groups of substances: (i) The metal, its alloys and its intermetallic compounds, all outside the scope of this chapter; (ii) combinations of Mg(II) cations with inorganic and organic anions, without or with additional ligands, to which reference will be made in Section III; and (iii) the organomagnesium compounds, containing at least one C-Mg  $\sigma$ -bond, dealt with in Sections IV and V. Minor types of Mg compounds may be incorporated into one of these main groups.

The earlier research period of the inorganic and metallorganic compounds of group (ii), extending from the 18th century to the first quarter of the 20th century, consists mainly of the development of chemical and pharmacological knowledge. The most relevant research efforts on Mg compounds in the modern period, extending from 1926 to the present, relate to biological and biomedical subjects; they began with recognition of the essential character of this element and were followed with development of our knowledge of the physiological, epidemiological and clinical aspects<sup>1</sup>. The bibliography mentioned in Table 1 will help to appreciate the enormous research effort invested in this field; it is a small selection of reviews published in the last quarter of a century, dealing with biological and biomedical subjects related to magnesium. As for the organomagnesium compounds

TABLE 1. Selection of reviews on biological and biomedical subjects related to magnesium<sup>a</sup>

General subjects	Specialized areas and bibliography
Analytical issues	(i) X-ray elemental microanalysis <sup>12,13</sup> . (ii) Ion-selective electrodes for clinical use <sup>14–21</sup> . (iii) Electron probe and electron energy loss analysis <sup>22</sup> . (iv) Intracellular measurements <sup>21,23–27</sup> . (v) Determination of Mg in human tissues and fluids <sup>21,25,28–34</sup> . (vi) Trace elements in hair <sup>35</sup> . (vii) Determination of Ca and Mg in wines <sup>36</sup> .
Biological issues	(i) Mg bioavailability, metabolism and physiology <sup>21,37–57</sup> . (ii) Cell proliferation and differentiation <sup>21,58</sup> . (iii) Animal husbandry <sup>59</sup> . (iv) Magnesium in blood <sup>60–63</sup> . (v) Genetic regulation <sup>61,64–67</sup> . (vi) Mineral phase composition of bone and teeth <sup>68–70</sup> . (vii) Brain and nervous system <sup>21,71–73</sup> . (viii) Renal handling of magnesium <sup>21,74,75</sup> .
Biomedical issues	(i) General clinical analysis <sup>b 3,20,21,31,38,39,41,49,54,76–90</sup> . (ii) Blood conditions <sup>c 21,63,91–96</sup> . (iii) Cardiovascular diseases <sup>21,62,84,97–111</sup> . (iv) Kidney diseases <sup>b 13,64–66,112–117</sup> . (v) Lung diseases <sup>118</sup> . (vi) Mental diseases <sup>119</sup> . (vii) Nutrition <sup>b 21,57,70,112,120–130</sup> . (viii) Gynecology and obstetrics <sup>131,132</sup> . (ix) Pediatrics <sup>42,67,70,116,124,133–135</sup> . (x) Geriatrics <sup>136–139</sup> .
Pharmacological issues	(i) Renal handling of magnesium <sup>74,140,141</sup> . (ii) Metabolic effects of diuretics <sup>142</sup> . (iii) Myocardial infarction <sup>143</sup> . (iv) Hypomagnesemia <sup>144</sup> . (v) Central nervous system injury <sup>145</sup> .

<sup>a</sup> References were picked up among more than 700 reviews and belong to the period from 1980 to 2006.

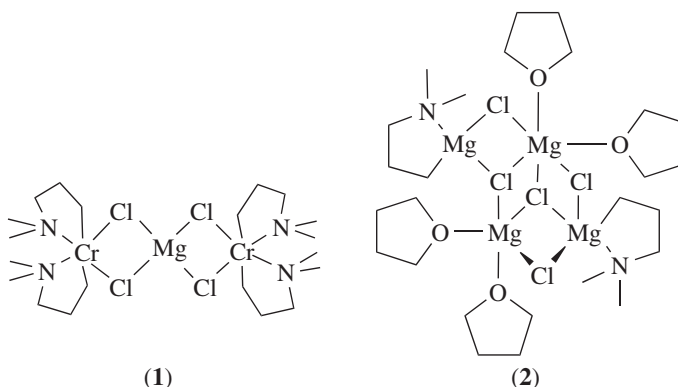
<sup>b</sup> References 85, 112 and 126 belong to veterinary medicine.

<sup>c</sup> Reference 93 is about short-term space flights in Shuttle and Skylab.

of group (iii), their study began in the second half of the 19th century. However, the most significant research started after 1900, when Victor Grignard synthesized the alkyl-magnesium halides (the Grignard reagents), of utmost importance in synthetic organic chemistry<sup>2</sup>. Chemical research of organomagnesium compounds continues to the present in the direction of multinuclear or functionalized Grignard reagents, mainly to extend their capabilities as synthons, as shown in many reviews<sup>3–11</sup>.

Elemental analysis is an important feature of organic analysis. In the case of organometallics, determination of Mg usually involves a mineralization step, by which an inorganic salt of Mg(II) is obtained before proceeding to the end analysis. Methods for determination of Mg(II) have long been established. However, advancements in analytical science of Mg are still made for determination of Mg(II) related to the subjects listed in Table 1, because of the low LOD required and the difficulties of speciation of this ion in complex biological matrices. Methods for Mg(II) analysis are presented in Section III.

The classical methods for the analysis of organomagnesium compounds in general and of Grignard reagents in particular were developed in the first half of the 20th century<sup>146</sup>. However, some advances took place more recently, with the appearance of new instrumentation, especially for the various chromatographic modalities. The analytical speciation and quantitative analysis of organomagnesium compounds are discussed in Section IV. The compounds addressed in that section are mostly uninuclear. Although analytical speciation of multinuclear compounds such as the dinuclear MeMgMgF and MeMgFMg, the trinuclear MeMgFMg<sub>2</sub><sup>147</sup> and **1** or the tetranuclear **2**<sup>148</sup> is usually outside the scope of the chapter, brief consideration is given to some multinuclear compounds to illustrate the application of various analytical techniques.



Grignard reagents may be used in the determination of other analytes and as ancillary agents for various analytical applications. The use of Grignard reagents in analysis is presented in Section V.

### III. ELEMENTAL ANALYSIS OF MAGNESIUM

#### A. Introduction

The most characteristic element of organomagnesium compounds usually is magnesium and its analysis may afford important information about the identity and the quality of the sampled material. In contrast to speciation analysis, which may require delicate handling and involves sample preparation procedures to preserve the analyte or its identity features, elemental analysis of Mg frequently requires destructive processes leading to mineralization of the element to form a salt. Although Mg elemental analysis for quality control usually requires sample dilution before the end analysis, the present section will also deal with methods for trace and ultratrace analysis, as sometimes required for samples of biological and environmental origin. The sample preparation processes will preferably refer to this type of materials, as they are more akin to those required for organometallic compounds. Reviews appeared on the various steps of determination of Mg in biological materials, from sampling to end analysis<sup>149,150</sup>.

Speciation of Mg in certain complex matrices refers to distinguishing among Mg bound to different fractions of the matrix, as opposed to identification of definite magnesium compounds; according to IUPAC's recommendations, the latter distinction should be referred to as speciation analysis<sup>151</sup>. An important speciation case is that of Mg in plasma, for which various values may be distinguished: (i) total Mg, (ii) Mg strongly bound in metalloproteins, (iii) Mg weakly bound to proteins, (iv) Mg bound to low molecular mass anions, such as amino acids, carboxylates, carbonate, ascorbate, salicylate, etc., and (v) free hydrated Mg ions. The set of these values is controlled by the pH, temperature, ionic strength and concentration of other metal ions. All or part of these values are of clinical relevance and pertinent analytical methods will be discussed below. It was proposed to save the labor and expense involved in such speciation analyses, making instead estimations by applying the artificial neural network (ANN) methodology. During the ANN training phase pH,  $[Mg]_{total}$  and  $[Mg(II)]_{free}$  data were used, which were determined for the plasma of patients. Cross-validation of the ANN method for a given set of pH and  $[Mg(II)]_{total}$  values showed an average error of 8% for estimated  $[Mg(II)]_{free}$

values<sup>152</sup>. A method was proposed for determination of classes (ii) to (v) in plasma and serum, combining ISE determination of  $[\text{Mg(II)}]_{\text{free}}$  (Section III.D.1), AAS determination of  $[\text{Mg(II)}]_{\text{total}}$  (Section III.E.1) and, after controlled ultrafiltration, AAS determinations of  $[\text{Mg(II)}]_{\text{protein}}$  retained on the filter and of  $([\text{Mg(II)}]_{\text{free}} + [\text{Mg(II)}]_{\text{complexed}})$  in the filtrate<sup>153</sup>. Reviews appeared on the determination of the total contents and activity of Ca(II) and Mg(II) in serum<sup>154</sup> and on the physiological and clinical aspects of magnesium in human beings, paying attention to the principal analytical methods applied for determining the various magnesium species<sup>153,155</sup>. See also pertinent reviews listed among the analytical issues in Table 1.

Approximately 1 mol of Mg is found in the adult human body, equally distributed among bones and soft tissues. Only about 0.3% of the total body Mg is present in serum, yet most of the analytical results are for this body fluid. Speciation of Mg for an individual is difficult, for the lack of fast and accurate assays for intracellular magnesium, but determination of total and free magnesium in tissues and physiological tests may give helpful information<sup>29,77</sup>. Mg(II) is the most abundant divalent cation within cells, followed by Ca(II) by far; it is the fourth most abundant cation in the body, after Na(I), K(I) and Ca(II), and is the second most common cation in the intracellular free fluid, after Na(I). Magnesium alone or bound to proteins is essential for many cellular functions, for example, acting as cofactor for hundreds of enzymatic reactions, and being required for protein and nucleic acid synthesis, signal transduction, energy metabolism, maintenance of cytoskeletal and mitochondrial integrity, and the modulation of various ion transport pumps, carriers and channels<sup>156</sup>. In plasma Mg(II), as well as Ca(II), is found in three forms: (i) an ultrafiltrable fraction consisting of free Mg(II) (70 to 80%), (ii) complex-bound Mg(II) (1 to 2%) and (iii) a protein-bound non-ultrafiltrable fraction (20 to 30%). Free Mg(II) is an important parameter in clinical analysis. The reference range for total Mg concentration in adult blood plasma is 0.65 to 1.05 mM and 0.55 to 0.75 mM for free Mg (usually determined with ISE, Section III.D.1); the range for total Mg in erythrocytes is 1.65 to 2.65 mM<sup>155</sup>. The Mg content in the food intake affects the level of certain trace (e.g. Pb, Rb, Sr) and ultratrace (e.g. As, Au, Ba, Ir, Mo, Se, Ta) elements in plasma, of which As, Mo, Rb, Pb and Se have already been shown to be essential. The concentration of As, Au, Ir, Rb, Sr and Ta was significantly higher in the plasma of rats fed with a low-Mg diet than in the control group fed with normal Mg levels<sup>157</sup>.

Methods for determining magnesium in body fluids fall into several major categories: (i) complexometric titration, (ii) atomic absorption spectrometry, (iii) atomic emission spectrometry, (iv) fluorometry and (v) various spectrophotometric techniques, which include enzymatic and dye binding methods<sup>158</sup>. The presence of heparin solution in sampling syringes, used to avoid coagulation of blood, may introduce a significant negative bias in the determination of Ca(II) and Mg(II)<sup>159</sup>.

Another important speciation refers to Mg bound to RNA, which is essential to the folding and function of this macromolecule. A computational approach to this analysis was presented for site-bound and diffusively bound Mg(II) ions in RNA. This method confirmed the locations of experimentally determined sites and pointed to potentially important sites not currently annotated as Mg binding sites but deserving experimental follow-up in that direction<sup>160</sup>.

Mg speciation can also be applied to olives and olive oil: (i) Total Mg can be determined by AAS, after mineralization of a sample by nitric acid digestion; (ii) covalently bound Mg is extracted with  $\text{CCl}_4$  from homogenized olives and is determined after evaporating the solvent and dissolving the residue in AcBu-*i*; (iii) extraction of homogenized olives with  $\text{CHCl}_3$  leads to chlorophyll-bound Mg; and (iv) extraction of homogenized olives with water is also performed. Four fractions can be defined for Mg in the water extract, which are obtained following a definite experimental procedure: (iv-a) Mg in particulate



matter, passing a paper filter but not a 0.45  $\mu\text{m}$  polymeric filter; (iv-b) polyphenol-bound Mg; (iv-c) polysaccharide-bound Mg; and (iv-d) free cationic Mg. End analysis of Mg in all these fractions is carried out by FAAS or ETAAS, after dissolving in an adequate solvent<sup>161</sup>.

## B. Sample Preparation

### 1. Matrix obliteration

An easy method for eliminating the organic and volatile components of the matrix is dry ashing. The sample should be initially dried in air or in an oven to avoid losses by sputtering, and be placed in a furnace at temperatures sufficiently high to burn the organic matter and sufficiently low to avoid volatilizing of analytes. Heating to the final calcination temperature should be gradual to avoid losses by kindling the sample. The ashes are dissolved in dilute HCl or  $\text{HNO}_3$  and submitted to end analysis. Sometimes the ashes contain remnants of the organic matrix, appearing as carbonate, sulfate, phosphate or silicate anions, which may interfere with the analysis of Mg by certain methods. For example, milk fermentation samples were dried, calcined in a furnace at 600 °C, the ash was dissolved in 0.03 M HCl, the solution was centrifuged and the supernatant was analyzed<sup>162</sup>. Determination of Ca, Cu, Fe, K, Mg, Mn, Na and Zn in foodstuffs involves placing the oven-dried sample in a furnace at 200 °C and raising the temperature in 50 °C steps every time the sample stops fuming, and finally it is left for 16 h at 450 °C. End analysis of Ca and Mg was by FAAS, after dissolving the ashes in dilute HCl and adding  $\text{LaCl}_3$ <sup>163</sup>.

Dry ashing is unfit for volatile analytes or when it is necessary to preserve the mineral matter structure. In such cases the organic parts of the matrix can be eliminated by low temperature ashing (LTA), the main variant of which consists of exposing the sample to a MIP in a low-pressure atmosphere of pure oxygen. The slow combustion of the organic matter develops temperatures below 200 °C and possibly below 150 °C. For example, LTA followed by microwave-aided extraction of the analytes with aqua regia was applied for determination of As and Hg in coal, coal fly ash and slag<sup>164</sup>. Lower ashing temperatures (60 to 70 °C) may be achieved on developing the MIP in oxygen diluted with helium<sup>165</sup>.

Wet mineralization is also frequently applied for elimination of organic matter present in the matrix and is recommended in many official methods<sup>166</sup>. It is mainly based on the oxidizing action of  $\text{HNO}_3$  alone or with additives aiming at reinforcing the oxidative action, such as  $\text{H}_2\text{O}_2$ , increasing the temperature of the process, such as  $\text{H}_2\text{SO}_4$  and  $\text{HClO}_4$ , or achieving special effects, such as HF for volatilization of Si. Various examples follow of wet mineralization prior to end analysis.

The details for the mineralization of infant milk formulas with  $\text{HNO}_3$ – $\text{HClO}_4$  for the analysis of major and trace elements are given in AOAC Official Method 984.27<sup>166a</sup>. A household microwave oven on-line with a flow system was proposed for mineralization of urine in the presence of 1 M  $\text{HNO}_3$ . The off-line end analysis of Ca and Mg was by FAAS with good results<sup>167</sup>. Mineralization of milk samples for Mg analysis by FAAS was carried out by three methods: (i) wet digestion of a sample after adding thrice the volume of a 4:1 mixture of concentrated  $\text{HNO}_3$  and  $\text{HClO}_4$ , heating for 65 min at 120 °C, cooling and adding water to a 25-fold dilution of the sample; (ii) placing in an acid digestion bomb 0.2 mL of sample and 2.5 mL of 1 N  $\text{HNO}_3$  and digesting for 90 s in a microwave oven at full power, cooling to room temperature for 1 h and adding water to 125-fold dilution of the sample; and (iii) drying of the sample at 80 to 100 °C for 4 h, calcinating at 550 °C for 5 h, dissolving the white ash in some 1 N  $\text{HNO}_3$  and adding water to a 25-fold dilution of the sample and end analysis by FAAS<sup>168</sup>. Total hair digestion with  $\text{HNO}_3$ – $\text{H}_2\text{O}_2$  is hard to accomplish. When reaching a pale brown stage any fatty residue

can be emulsified on addition of a surfactant. After adding La(III) in agar solution the end analysis of Ca and Mg by FAAS was consistent with that obtained by the dry ashing method<sup>169</sup>.

A comparison study was made of ultrasonic extraction and microwave digestion of plant material for FAAS determination of Mg, Mn and Zn. The optimal conditions for recovery of these elements by ultrasound assisted extraction were: 3 min sonication, at 30% ultrasonic amplitude, of 0.1 g of material milled to  $<50\ \mu\text{m}$  particle size, dispersed in 5 mL of 0.3% (m/v) HCl solution; after 4 min of centrifugation at 4500 rpm, the supernatant was used for FAAS end analysis. For the microwave digestion, 0.1 g of sample was placed in 5 mL of 69.5% (m/m)  $\text{HNO}_3$  and 0.5 mL of 48% (m/m) HF; the mixture was heated in the microwave oven for 1 min at 40 psi, 1 min at 80 psi and 5 min at 120 psi; after cooling the digestion vessel with ice, the solution was evaporated to dryness, the residue was dissolved in 37% (m/m) HCl and diluted with water to 5 mL for end analysis. Analytical results for both methods were similar. The advantages of ultrasound-assisted extraction over microwave-assisted digestion are: (i) much shorter processing time, (ii) simpler proceedings, (iii) lower consumption of reagents and (iv) better safety as no harsh acids, heating or high pressure operations are involved. Some disadvantages are: (i) lower amounts of sample can be processed, (ii) milling to  $<50\ \mu\text{m}$  particle size is required and (iii) aging of the ultrasonic probe surface may reduce the extraction efficiency<sup>170</sup>.

Determination of Mg(II) in a cellulose matrix requires dissolution of the matrix in 70%  $\text{H}_2\text{SO}_4$ , dilution, neutralization with NaOH, and addition of  $\text{CaCl}_2$  and  $\text{K}_2\text{CO}_3$  solutions in that order. A quantitative coprecipitation of Mg(II) takes place with Ca(II) and  $\text{CO}_3^{2-}$  ions. The double salt is filtered, washed with water and dissolved in dilute HCl for end analysis by FAAS<sup>171</sup>. A comparison was made of methods for mineralization of plant material. Dry ashing in a furnace at  $470^\circ\text{C}$  followed by ash dissolution in 5 M HCl is preferable to digestion in a 9:2:1 by volume mixture of  $\text{HNO}_3$ – $\text{H}_2\text{SO}_4$ – $\text{HClO}_4$ , followed by dilution. The wet method seems to be problematic because of  $\text{CaSO}_4$  formation; however, this may be corrected by leaving the dilute digest overnight, when slow dissolution takes place. End analysis of the metallic elements is by AAS<sup>172</sup>. If N and P also are to be determined from the mineralized sample, then digestion in the Kjeldahl fashion is called for, using concentrated  $\text{H}_2\text{SO}_4$  containing *ca* 1% w/v Se<sup>173</sup>.

Sometimes the nature of the solid matrix allows sample preparation without mineralization. In the determination of Cu and Mg in polyethylene, the sample was milled to a fine powder and suspended in a solution of a detergent (Triton X-100) in EtOH. A reference solution of the same viscosity was prepared by adding ethylene glycol instead of polymer to the supporting solution. The end analysis by FAAS was carried out using Sr(II) as releasing agent and *n*-BuOH as enhancement reagent<sup>174</sup>.

## 2. Preconcentration

Problems attaining the GFAAS determination of ppb levels of Ca, Mg, Sr and Si in saturated NaCl brines for electrolytic chloroalkali cells were discussed; Mg is the most problematic among these analytes because the boiling points of  $\text{MgCl}_2$  and NaCl are very near to each other and special handling procedures are needed for improving the analytical quality. A general problem concerning analysis at ppb levels is avoiding contamination of the sample and instrumentation and some recommendations were given in this regard<sup>175</sup>. Traces of Ca(II) and Mg(II) present in salt were concentrated by passing a solution of the sample through an ion-exchange resin containing chelating groups. End analysis after elution was by FAAS<sup>176, 177</sup>.

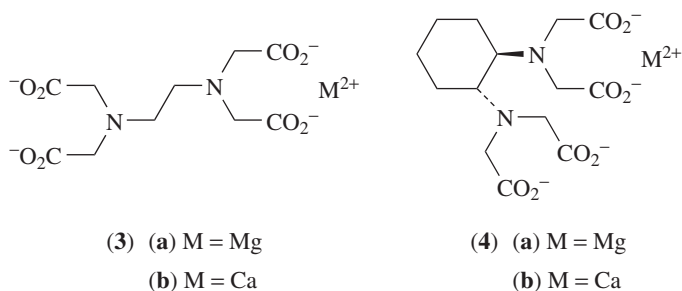
An interesting method for preconcentration of ultratrace amounts of Mg(II) in water consists of treating a PTFE tube with 2 M NaOH solution, at  $70^\circ\text{C}$  for 3 h. On passing

the weakly alkaline sample of water through the tube, Mg(II) is adsorbed on the wall. The analyte is recovered with dilute HCl for end analysis, e.g. by fluorometry (Section III.E.4)<sup>178</sup>.

### C. Column Separation Methods

#### 1. Ion chromatography

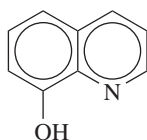
Modern techniques for ion chromatography (IC) allow simultaneous determination of anions and cations in the same run and with a unique detector. One possibility for attaining such results is introducing into the eluting solution chelating agents such as EDTA or DCTA, which are totally ionized at the high pH of the solution (e.g. NaHCO<sub>3</sub>–Na<sub>2</sub>CO<sub>3</sub> buffer), and form negatively charged chelated ions with the cationic analytes, such as **3a**, **3b**, **4a** and **4b**, respectively. The concentration of the chelates may be determined by UVD. A frequently used detection method in IC is conductivity measurement (CND); however, certain eluting solutions are not appropriate for this. Such solutions can be simplified by the use of suppression membranes, allowing easier determination by CND. If the suppression membrane is a cation exchanger in acidic form, it collects Na(I) ions and transfers them to a regenerating solution supplying H<sup>+</sup> ions to the analysis solution<sup>179</sup>. Some technical problems and their solutions were discussed regarding the use of suppression membranes in the determination of the four major cations found in human plasma<sup>180</sup>. Also, the **3a** and **3b** chelates are decomposed and the conductivity of the free EDTA is measured together with that of other anions present in the analytical sample. LOD in the ppb range were achieved for Ca(II) and Mg(II), with precisions better than 1%<sup>181</sup>. This approach varied from another separation technique where gradient elution was applied to accelerate the analysis<sup>182</sup>. An alternative to CND is piezoelectric detection with a PQCD, which is responsive to conductivity and permittivity of a solution; however, one of its advantages is being free from errors stemming from a double electric layer or Faraday impedance. IC-PQCD was applied for determination of Ca(II) and Mg(II) in saliva and urine, which were passed through a 0.45 μm filter membrane. The chromatographic column was a cation exchange resin on PDVB copolymer support and the mobile phase was an aqueous solution at pH 4.0 of 4.0 mM tartaric acid and 2.0 mM ethylenediamine. The LOD (SNR = 3) were 0.4 and 0.2 ppm, with linear behavior in the ranges from 0.8 to 500 ppm and from 1.0 to 500 ppm for Ca(II) and Mg(II), respectively<sup>183</sup>.



Magnesium speciation (Section III.A) in serum was carried out using an anion exchange column for protein separation, with mobile phase at pH 7.4; the effluent was collected in an automatic fraction collector. On-line quantitation of the protein fractions was carried out by DA-UVD, and Mg determination was carried out from the automatic sampler in a GFAAS apparatus, measuring at 202.8 nm<sup>184</sup>.

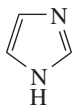
## 2. High-performance liquid chromatography

Oxine (**5**) forms complexes of analytical applicability with various metal ions<sup>185</sup>. A RP-HPLC-FLD method ( $\lambda_{\text{ex}} = 370 \text{ nm}$ ,  $\lambda_{\text{fl}} = 516 \text{ nm}$ ) was proposed for simultaneous determination of Al(III) and Mg(II), using a C<sub>18</sub> column. Various details of the method are noteworthy: Optimization of the method showed that for both ions it is best to have also precolumn and in-column complex formation, caused by the presence of **5** in the injection loop and in the carrier solution; FLD detection is preferable to simple UVD because it avoids the background of **5** and interference of various ions forming nonfluorescent chromogenic complexes, e.g. Ca(II) and Zn(II); the intensity of the fluorescence can be increased by micelle formation on addition of SDS and neutralized *N,N*-bis(2-hydroxyethyl)-2-aminoethanesulfonic acid (**6**). The LOD (SNR = 3) were  $0.74 \mu\text{M}$  (18 ppb) Mg(II) and  $0.60 \mu\text{M}$  (16 ppb) Al(III); the latter was attributed in part to residual impurities in the purified water<sup>186, 187</sup>.

**(5)****(6)**

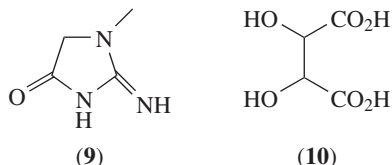
## 3. Electrophoresis

After denaturation of the protein in plasma with trichloroacetic acid and centrifugation, the concentration of Na(I), K(I), Mg(II) and Ca(II) in the supernatant was determined by CZE with DA-UVD. The background electrolyte was an aqueous solution containing 20 mM imidazole (**7**), 0.5 mM oxalic acid (**8**) and 5% (v/v) MeOH, brought to pH 2.8 with 0.1 M HCl; Cd(II) served as internal standard. Separations were carried out by hydrodynamic injection at the anodic side, on a 50  $\mu\text{m}$  capillary coated with polyvinyl alcohol, in positive mode, applying a constant 30 kV potential. The cations were detected at 214 nm ( $\lambda_{\text{max}}$  of **7**). The LOD (SNR = 3), LOQ (SNR = 10) and linearity range, in ppm, for the ions in their order of emergence were: K(I) 0.25, 0.75, 0.75–50, Ca(II) 0.50, 0.90, 0.9–50, Na(I) 1.00, 4.00, 4–400 and Mg(II) 0.20, 0.50, 0.5–50<sup>188</sup>.

**(7)****(8)**

At slightly acidic pH values weak dibasic acids H<sub>2</sub>L give on dissociation anions HL<sup>−</sup>, forming ion pairs MHL with metal ions. These ion pairs are neutral for M(I), which is the case of Na(I), K(I) and ammonium ions, and electrophoretically mobile for M(II), such as Ca(II) and Mg(II). A chromophore BH/B consisting of a weak base B, which at slightly acidic pH values is in equilibrium with its conjugate acid BH, also has electrophoretic mobility due to the latter ion and may serve for indirect UVD of the M(II) ions. These principles have been applied as a CE method for determination of trace concentrations of Ca(II) and Mg(II) in aqueous solutions containing more than 5000-fold concentrations

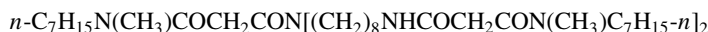
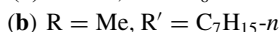
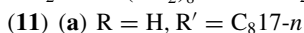
of Na(I). Two systems of weak acid ligand/weak base chromophore proved especially efficient under the particular conditions of a developed CE assay: 2 mM oxalic acid (**8**)/10 mM creatinine (**9**) at pH 4.6 and 8 mM tartaric acid (**10**)/14.4 mM benzylamine at pH 4.8; in both cases UVD was carried out at 214 nm. A LOD of 4  $\mu$ M was achieved for a simulated matrix containing 500 ppm Na(I)<sup>189</sup>.



## D. Electrochemical Methods

### 1. Ion-selective electrodes

Electrically neutral magnesium ionophores should fulfill the following requirements for their use in ISE: (i) Ionophores should be lipophilic to assure their longevity and stable response on the electrode. (ii) The complex formed with the main analyte cation should be stable, however, not too stable to avoid emulation of classical anion exchangers; a lipophilic anion should be present on the membrane to induce cation permeability and to reduce anion interference. (iii) The electromotive force developed by the ion-selective electrode depends on the selectivity coefficients of the analyte *vs* the other cations present and the activity of all the cations present in the sample. Most Mg-selective electrodes are designed for analysis of biological fluids, where the most abundant cations are Na(I), K(I), Ca(II) and Mg(II) (Section III.A). Selectivity toward the univalent cations is usually high, however Ca(II) may interfere in the determination of Mg(II). The following were found among ionophores with a selectivity for Mg(II) over Ca(II) of at least one order of magnitude: ETH 5220 (**11a**), ETH 4030 (**11b**), ETH 7025 (**12**) and ETH 3832 (**13**)<sup>190</sup>. Ion-selective electrodes incorporating in the membrane **11a**<sup>191,192</sup> or **12**<sup>193</sup> can be used for potentiometric determination of Mg(II); these electrodes are used in clinical ionic analyzers, for determination of free Mg(II) in blood and its derived fractions.



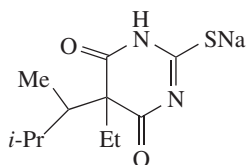
Instruments are offered in the market for clinical determination of electrolytes in blood, plasma or serum. One of them, for example, carries out simultaneous determinations of Na, K, Ca, Mg, hematocrit and pH. The cations are of the free type (see Section III.A) and are measured with specific ion-selective electrodes. In complex matrices such as blood or its derived fractions the concentration of free Ca and Mg is affected by the pH of the solution, for example, a slight change of pH will produce or neutralize anionic sites in the proteins, binding or releasing these cations; furthermore, the response of the Mg-selective electrode is also affected by the concentration of free Ca(II). The correction

for the concentration of cation M determined at pH  $x$ , is made for pH 7.4, a standard value for blood, applying equation 1, and the correction for the interference of Ca(II) on the Mg-selective electrode is made using the selectivity constant  $K_{\text{MgCa}}$ , based on calibration measurements<sup>194–196</sup>. Application of Mg ISE in clinical practice and research has been reviewed<sup>9, 14–18</sup>.

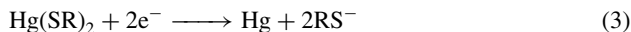
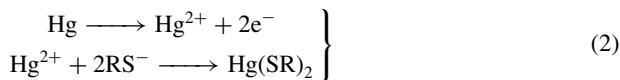
$$\log[M]_{\text{pH } 7.4} = \log[M]_{\text{pH } x} - 0.24(7.4 - x) \quad (1)$$

## 2. Electroanalytical determination

Direct electroanalytical determination of Mg(II) ions is of little practical value because of the interference by hydrogen, aluminum and alkali earth metal ions<sup>197</sup>. To avoid these and other difficulties, an indirect method was proposed based on the voltametric determination of sodium pentothal (**14**). The voltametric (LSCSV) determination of **14** is carried out in two steps in a phosphate buffer solution at pH *ca* 10.5, using a hanging mercury drop electrode and an auxiliary Pt wire electrode. In the preconcentration (deposition) step at  $-0.1$  V the thiolate ion of **14** is attached to mercury cations generated *in situ* according to equation 2, whereas in the stripping step ending at  $-0.8$  V the Hg(II) ions are reduced to  $\text{Hg}^0$ , according to equation 3. The LOD is about 10 ppb for 180 s deposition time, and no interference is observed for equimolar concentrations of Ca(II), Cr(VI), Cu(II), Fe(III), Ni(II), Pb(II) or Zn(II). On the other hand, addition of  $2 \mu\text{M}$  of Mg(II) to the same concentration of **14** caused about a fourfold peak current increase<sup>198</sup>. The latter behavior of Mg(II) was the basis for another method for determination of this cation, after introducing some modifications in the method used for **14**. Thus, instead of a hanging Hg drop, a mercury film was developed on a CPE, and the electroanalytical technique was SWAdSV, using sodium phosphate buffer at pH 10.75. A calibration is necessary for the increment in the peak cathodic current,  $\Delta I_p$ , measured on adding Mg(II) to the solution of **14**, which is a function of the cation concentration and the deposition time. The LOD is 0.14 ppb Mg(II) for 60 s deposition time, with RSD 0.5% ( $n = 5$ ). The method was applied to analysis of urine and tap water, and the results were in good agreement with FAAS determinations<sup>199</sup>.



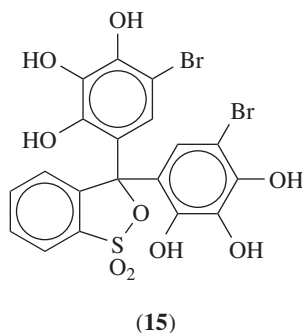
(RSNa, **14**)



A setup proposed for simultaneous determination of Al(III) and Mg(II) included a working GCE, a reference SSCE and a Pt auxiliary electrode, operating under  $\text{N}_2$  atmosphere, at pH 5.0, in the presence of 0.01M  $\text{KNO}_3$  and 0.02 M  $\text{Me}_4\text{NCl}$ , according to the Osteryoung square wave stripping voltametric technique. After 120 s deposition time at  $-0.8$  V the scan proceeds in the positive direction, with the peaks of Mg(II) and Al(III) appearing at *ca*  $-0.42$  and  $+0.20$  V, respectively. The LOD are as low as 0.4 nM Mg(II)

and 0.05 nM Al(III); no interference is observed for Ba(II), Ca(II), Cd(II), Co(II), Fe(III), K(I), Mn(II), Na(I), Pb(II), Sr(II), Ti(IV), Zn(II) or  $\text{UO}_2^{2+}$ ; however, Cu(II) can be determined as it shows a peak at *ca*  $-0.05$  V. The method was applied to the analysis of a Portland cement CRM after HCl digestion<sup>200</sup>. A catalytic polarographic method for determination of water hardness (Ca + Mg) was proposed. The method is based on reduction of Mg(II) which has been displaced from its complex with EDTA (**3a**) by an added metal ion, such as Cu(II), which forms a much stronger complex with EDTA. The catalytic signal current shows about 100-fold amplification relative to the diffusion signal. The method was claimed to be of the same precision as the EDTA complexometric titration (Section III.E.3) but less cumbersome<sup>201</sup>.

An alkaline solution of the complex formed by Mg(II) and Bromopyrogallol Red (**15**) shows a polarographic wave at  $-1.30$  V, the intensity of which is linear with the Mg(II) concentration in the 0.05 to 2 ppm range. The LOD is 0.01 ppm Mg(II). The method is sensitive and selective; it was applied to determination of Mg(II) in food and the results corresponded to those obtained by AAS<sup>202</sup>.



## E. Spectral Methods

### 1. Atomic absorption spectrometry

For various mineralization methods prior to FAAS determination of Mg in many materials, see Section III.B.1. Analysis of the four major elements (Na, K, Ca and Mg) in drinking and other types of water by the FAAS method is well established and is the subject of several national and international standards. Nevertheless, there is a continuous discussion about the improvement of analytical quality and efficiency. A comparison was made of certain details of Polish standards with other national or international ones (ASTM, USEPA, ISO) and published research; of special concern were the presence of interfering ions and the effect of avoiding sample dilution on the analytical results. The latter consideration affords considerable savings in time and solvent expenses<sup>203,204</sup>. Both Ca and Mg can be determined in solutions by FAAS with air-acetylene, measuring at 422.8 and 285.2 nm, respectively. When applying the method to analysis of urine<sup>205</sup>, minor nutrients in fertilizers (AOAC Official Method 965.09<sup>166b</sup>), in water (AOAC Official Method 974.27<sup>166c</sup>) or cheese after dry ashing (AOAC Official Method 991.25<sup>166d</sup>),  $\text{LaCl}_3$  can be used as releasing reagent, to avoid possible interference by phosphate, sulfate or silicate ions present in the matrix. Analysis of some toxic and essential elements in eggs of various origins was carried out after drying and mineralizing with a  $\text{HNO}_3\text{--HClO}_4\text{--H}_2\text{O}_2$  mixture. Ca, Fe and Mg were determined by FAAS (LOD 20 to 70 ppb), whereas Cu, Pb and Zn by GFAAS, after adding a modifier containing palladium nitrate, yttrium nitrate and citric acid (LOD 1 to 0.03 ppb)<sup>206</sup>. The serum of patients

receiving total parental nutrition was analyzed for trace elements after 10-fold dilution with Triton X-100 solution. Mg was determined by FAAS using an air-acetylene flame and measuring at 258.2 nm from a deuterium lamp; Cu, Mn, Pb and Zn were determined by GFAAS<sup>207</sup>. A procedure for FAAS analysis of Mg in a water-soluble multivitamin pharmaceutical preparation was validated and found adequate for the purpose<sup>208</sup>.

Mg concentration in plasma was determined by FAAS, after centrifuging whole blood samples, acidifying and centrifuging again. A rise to 130% of the baseline levels took place during cerebral ischemia (stopping blood supply) in gerbils, which gradually returned to normal after reperfusion<sup>209</sup>. Blood fractions were analyzed for Cu, Fe, Mg, Se and Zn by FAAS, after suitable sample preparation. Blood with added EDTA was separated by centrifugation into plasma and erythrocytes; the latter were hemolyzed by freezing and thawing and further treated with HCl, before determination of Cu, Fe and Zn. In each of these fractions the protein was precipitated by  $\text{CF}_3\text{CO}_2\text{H}$  and centrifugation, taking the supernatant for analysis; determination of selenium required digestion with  $\text{HNO}_3\text{--HClO}_4\text{--H}_2\text{SO}_4$  mixture and reduction of Se(VI) to Se(IV)<sup>210</sup>. A device for determining Mg in the extracellular fluids of the gerbil brain consisted of an on-line microdialysis unit implanted in the organ; the collected fluids are passed by a microinjection pump together with a diluent to a sample collector, from which an automatic sampler injects the solution into a GFAAS device. The mean Mg after on-line dilution of the basal dialysate was  $1.50\text{ }\mu\text{g L}^{-1}$ , and it significantly decreased to about 40% during cerebral ischemia, gradually returning to the basal value on reperfusion<sup>209, 211</sup>. Implanting more than one microdialysis unit for sample collection and ETAAS may afford important information on changes taking place simultaneously in an organism<sup>212</sup>.

A multiparametric flow system was devised for the automated determination of Na(I) and K(I) by FAES and Ca(II) and Mg(II) by FAAS, to be applied in the quality control of large-volume parental solutions and concentrated hemodialysis solutions. The latter are rather concentrated pharmaceutical solutions whereas the determination methods operate at trace concentrations, thus requiring dilution and addition of reagents such as a La salt as releasing agent. The automated system allows a sampling frequency of nearly  $60\text{ h}^{-1}$  for Mg and  $70\text{ h}^{-1}$  for the other ions<sup>213</sup>. The same spectrophotometric methods were applied for determination of these elements in surgically excised cataractous lenses after  $\text{HNO}_3\text{--H}_2\text{O}_2$  digestion<sup>214</sup>.

Research is carried out to find noninvasive pathogenesis indicators for cancer. Trace elements in scalp hair have been investigated. As the morphology and other characteristics of this material drastically change with age, sex and ethnic group, proper healthy control groups are needed to evaluate the results. The hair samples of a group of stage III breast cancer patients and a corresponding healthy control group were digested in hot concentrated  $\text{HNO}_3$ , properly diluted and Cu, Mg and Zn were determined by FAAS with Zeeman-effect background correction. Significant differences were found in the patients for Cu (nearly doubled) and Zn (nearly halved), whereas a 4% average decrease in Mg was not considered significantly different (Student's test). Other reported behavior of these trace elements is as follows: Zn was higher with malignant breast tumors as compared with benign tumors or healthy persons; it was lower in cases of prostatic carcinoma, nasopharyngeal and lung cancers. No significant difference was found for Cu in hair for lung cancer (it increased in plasma). Trace Mg in hair was significantly lower for esophageal cancer, acute lymphoblastic leukemia and malignant lymphoma<sup>215</sup>.

## 2. Atomic emission spectrometry

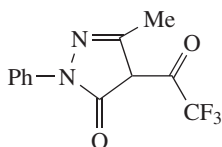
Tracking local variations of trace element concentration in body fluids requires sensitive methods capable of returning sufficiently accurate and precise results with small samples.



The analytical quality in such cases can be better assessed when CRMs of similar nature are available. For example, samples of arterial blood weighing 5 to 15 mg were withdrawn from different parts of a rabbit and were subjected to mineralization with hot 50% (v/v)  $\text{HNO}_3$  in a closed vessel microwave device. After adequate dilution end analysis of Ca, Mg and Fe was carried out by ICP/AES<sup>216</sup>.

A method for determination of various elements in infant milk formulas consists of mineralization by wet digestion with  $\text{HNO}_3$ – $\text{HClO}_4$ , and end analysis by ICP-AES. In the AOAC Official Method 984.27 the following measuring wavelengths in nm units are recommended, where \* denotes the need for background correction: Ca (317.9), Cu (324.7\*), Fe (259.9), K (766.5), Mg (383.2), Mn (257.6), Na (589.0), P (214.9) and Zn (213.8\*)<sup>166a</sup>. The ICP-AES determination of Na, K, Ca and Mg in urine shows quantitative recovery for the alkali elements; however, the analysis of Ca and Mg is affected by the presence of the other cations and the anions in the matrix. The problem was solved by 10-fold dilution of the sample with water<sup>217</sup>.

Determination of Mg in the hard tissues (shell and pearl) of shellfish by the ICP-AES method involves dissolution of the sample by hot concentrated nitric acid, hydrochloric acid and perchloric acid. However, the large excess of Ca in the matrix strongly interferes with the end analysis and causes damage to the torch. After adjusting the pH to 4.5, the Mg ions were extracted by a 0.01 M solution of 3-methyl-1-phenyl-4-trifluoroacetylpyrazol-5-one (**16**) in dibutyl ether and the ICP-AES analysis was carried out by direct injection of the organic solution<sup>218</sup>.



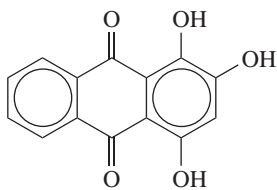
(16)

A method was described for simultaneous determination of Ca, Mg, Fe, Cu, Zn and P in blood serum by spark AES using DA-UVD. For this modality of AES, a few milligrams of dry sample are placed in the hollow graphite anode and a spark is produced between the anode and the tapered cathode for a few seconds. The method development took into account various sources of systematic error and means of correcting them. Preconcentration and mineralization was carried out by dry ashing for 2 h in an oven at 450 °C; this avoids evaporative losses of analytes and reduces organic matter to a level where it ceases to interfere. The elements in serum can be classified for their abundance into macroelements (Na, Ca, Mg, K), which are easily ionized elements, and microelements. By far the most abundant metallic element in serum is Na, which at low concentrations causes a significant intensity enhancement of the emission lines of certain analytes; however, at higher concentration (4% was used) this effect is minor. The presence of Ca, Mg and K in the matrix causes underestimation of the microelements, and this can be corrected with a concentration-dependent factor, if the Na concentration is kept constant<sup>219</sup>.

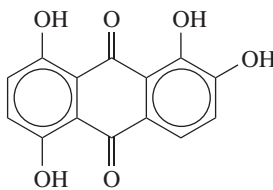
### 3. Ultraviolet-visible spectrophotometry and colorimetry

The formation of complexes of various metal ions with oxine (**5**) and some of its derivatives, their extraction into  $\text{CHCl}_3$  and their  $\lambda_{\text{max}}$  and  $\epsilon$  values have been reviewed<sup>185</sup>. Purpurin ( $\text{LH}_3$ , **17**) forms with  $\text{Mg(II)}$  colored complexes of varied composition. However, at pH 9.5 the complex  $\text{MgLH}$  is formed and can be measured at 540 nm ( $\epsilon =$

9200 L mol<sup>-1</sup> cm<sup>-1</sup>); first derivative spectra are of advantage over direct absorption spectra. For a 0.1 mM Mg(II) solution no interference was observed from alkali metal cations, about 25-fold excess of Al(III), Cu(II), Fe(II), Hg(II), Mn(II), Mo(VI), Ti(IV) and V(V), about 50-fold excess of Ba(II), Ca(II), Cd(II), Ni(II), Pb(II), Sr(II) and Zn(II) or about 100-fold excess of Br<sup>-</sup>, Cl<sup>-</sup>, ClO<sub>4</sub><sup>-</sup>, NO<sub>3</sub><sup>-</sup>, PO<sub>4</sub><sup>3-</sup> and SO<sub>4</sub><sup>2-</sup>. The strong interference of Fe(III) can be avoided on adding ascorbic acid to the sample solution which reduces the ion to Fe(II). The LOD for normal spectrophotometry is 75 ppb Mg(II) and 34 ppb for first derivative measurements. The method was applied for analysis of Mg in cement clinker<sup>220</sup>. A spot test for Mg(II) is based on formation of a blue lake with quinalizarin (**18**) in alkaline solution, in contrast to a violet color obtained for a blank test. The LOD is 0.25 µg Mg, with interference by Be, Ce, La, Nd, Pt, Th and Zr<sup>221</sup>.

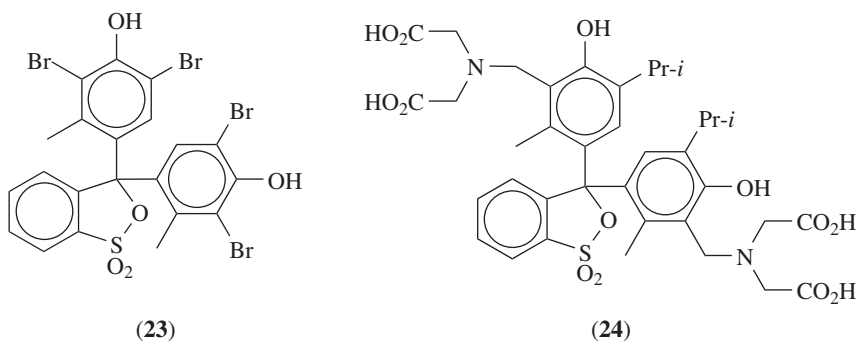
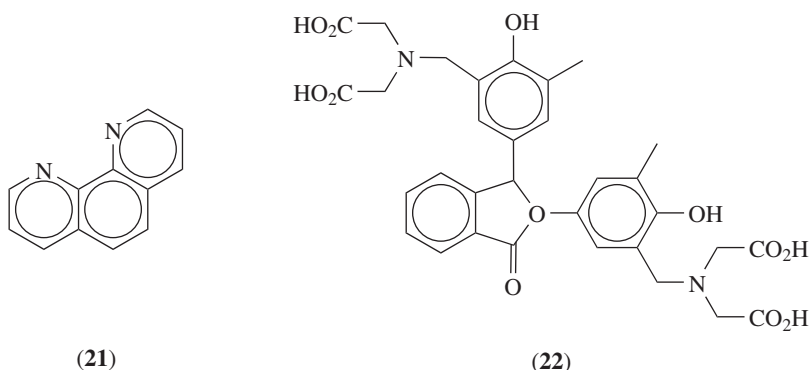
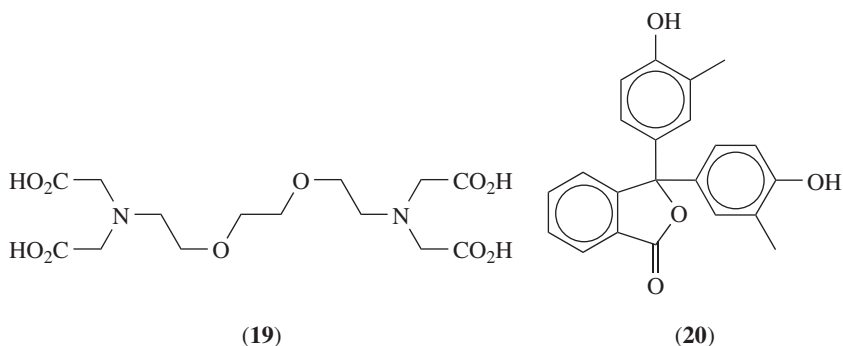


(17)



(18)

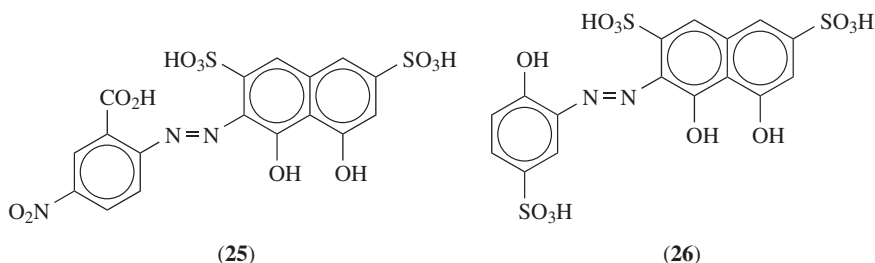
FIA systems have the disadvantage of employing one manifold per determination; if more than one determination has to be carried out on the same manifold, the reagents have to be changed. This limitation is avoided in SIA systems, where the sample and reagents are sequentially introduced into a holding coil by means of a selection valve; on reversing the flow the stacked zones mix on their way to the detector. Additional manifolds can be easily added to the computer-controlled SIA systems<sup>222</sup>. This subject has been reviewed<sup>223</sup>. A SIA method was proposed for the digestion of food samples and subsequent colorimetric determination of Ca(II), Mg(II) and Fe(III), including an in-line microwave digestion unit, from which the analytical samples are withdrawn. The sequential operation for end analysis is as follows: (1) For Mg(II) determination, an aliquot of the digested sample is mixed with aliquots of solutions of EGTA (**19**), serving as masking reagent for Ca(II), and *o*-cresolphthalein (**20**), the chromogenic reagent for Mg(II); in the detector a transient signal is measured at 535 nm, the intensity of which is proportional to the analyte concentration. (2) An aliquot of the digested sample is mixed with one of **20**, serving as chromogenic reagent for both Ca(II) and Mg(II) and the intensity of the color is similarly measured. (3) An aliquot of digested sample is mixed with one of reagent solution of *o*-phenanthroline (**21**), forming a colored complex with Fe(II), which is obtained by reduction of Fe(III) with ascorbic acid present in the reagent solution, and further measured in the detector. Each reagent carries its own buffer and other additives<sup>224</sup>. A SIA procedure was used for determination of hardness (Ca + Mg) and alkalinity of water. A common complexing agent was used for Ca and Mg, Cresolphthalein Complexone (**22**), measuring at 572 nm. However, to distinguish between the two ions EGTA (**19**) served to mask Ca(II) in the Mg(II) determination and oxine (**5**) to mask Mg(II) in the Ca(II) determination. Bromocresol Green (**23**) was used for determination of alkalinity, measuring at 611 nm<sup>225</sup>. An analogous SIA protocol was applied for determination of Mg in pharmaceutical preparations, based on complexation with **22**, masking with EGTA (**19**) and UVD at 570 nm<sup>226</sup>. A FIA system was designed for the simultaneous determination of Ca(II) and Mg(II) ions, by which the complexes of both ions with Methylthymol Blue (**24**) were measured simultaneously at  $\lambda_{\text{max}} = 610$  nm. On application of the zone sampling technique, part of the solution in the first loop was mixed with a solution of oxine



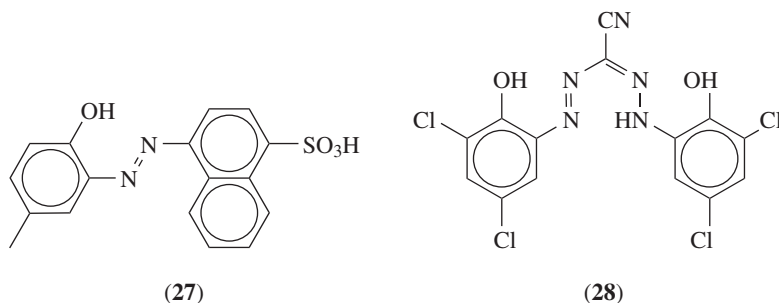
(5), to mask the Mg(II) ions, and a second measurement was made for Ca(II) alone. The method was applied for analysis of white, rose and red wines<sup>227</sup>.

3-(2-Carboxy-4-nitrophenylazo)-4,5-dihydroxy-2,7-naphthalenedisulfonic acid (**25**) at pH 10.4 forms a colored complex with Mg(II) ions with high selectivity in the presence of Ca(II) and minor elements such as Al(III), Cd(II), Co(II), Cr(III), Cu(II), Fe(II), Hg(II), In(III), Mn(II), Mo(II), Ni(II), Sn(II), Ti(II) and Zn(II). Application of the spectrophotometric method for determination of Mg with this reagent requires measurement at 582 nm, because at the maximum for the complex ( $\lambda_{\text{max}} = 560 \text{ nm}$ ) there is considerable interference of **25** itself. To correct for this interference a second measurement is taken at

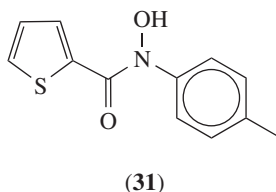
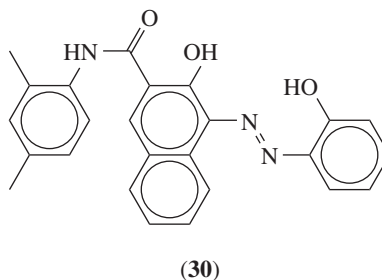
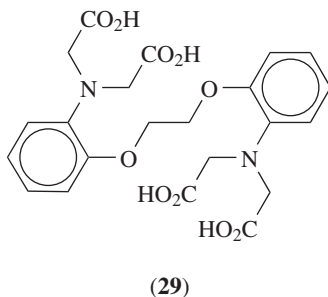
505 nm. The complex has  $\text{Mg}_2(\mathbf{25})$  composition, with stability constant  $K = 1.92 \times 10^4$  and  $\varepsilon = 2.25 \times 10^4 \text{ L mol}^{-1} \text{ cm}^{-1}$  at 582 nm<sup>228</sup>. A kinetic method was proposed for determination of ultratrace concentrations of  $\text{Mg}(\text{II})$ , based on the inhibition that this ion causes to the  $\text{Mn}(\text{II})$ -catalyzed decoloration of Acid Chome Blue K (**26**) by  $\text{KIO}_4$ , in Britton–Robinson buffer at pH 11.9. The LOD was 7.6 ppb, with linearity up to 0.48 ppm. The method was applied for analysis of soybean and human serum<sup>229</sup>.



A commercial kit consists of two solutions, one containing calmagite (**27**) serving as chromogenic complexant for  $\text{Mg}(\text{II})$  and the second one containing EDTA, as chelating agent for  $\text{Ca}(\text{II})$ . Measurements are carried out at 500 nm. The kit is recommended for serum, urine, water and soil analysis<sup>230</sup>. Another kit, recommended for biological fluids, is based on the action of 1,5-bis(3,5-dichloro-2-hydroxyphenyl)-3-cyanoformazan (**28**) as chromogenic complexant for  $\text{Mg}(\text{II})$ , with 1,2-bis(2-aminophenoxy)ethane- $N,N,N',N'$ -tetraacetic acid (**29**) as  $\text{Ca}(\text{II})$  masking agent, both on a dry slide. After contact with the sample, quantitation is carried out by colorimetric measurements<sup>231</sup>. Magon (**30**) forms a red complex with  $\text{Mg}(\text{II})$ , which is measured spectrophotometrically at 520 and 600 nm, with no significant interference from  $\text{Ca}(\text{II})$ , phosphate, albumin or bilirubin. The method was applied in clinical analysis for  $\text{Mg}(\text{II})$  determination in serum<sup>158,232</sup>. Aqueous  $\text{Mg}(\text{II})$  at pH 9.5 can be extracted by a solution of  $N$ - $p$ -tolyl-2-thenohydroxamic acid (**31**) in chloroform. A colored complex is formed on addition of quinalizarin (**18**) to the extract ( $\lambda_{\text{max}} = 590 \text{ nm}$ ,  $\varepsilon = 2800 \text{ L mol}^{-1} \text{ cm}^{-1}$ ). No interference was observed by most common ions<sup>233</sup>.



The complexometric method for determination of  $\text{Ca}(\text{II})$  and  $\text{Mg}(\text{II})$  is based on two titrations with EDTA in alkaline solution, one where both ions are determined together and the second after one of them has been masked with a specific complexing agent. The effect of interfering heavy metals such as Cu, Fe, Mn or Zn can be avoided by adding cyanide. The AOAC Official Method 964.01 for determination of acid-soluble

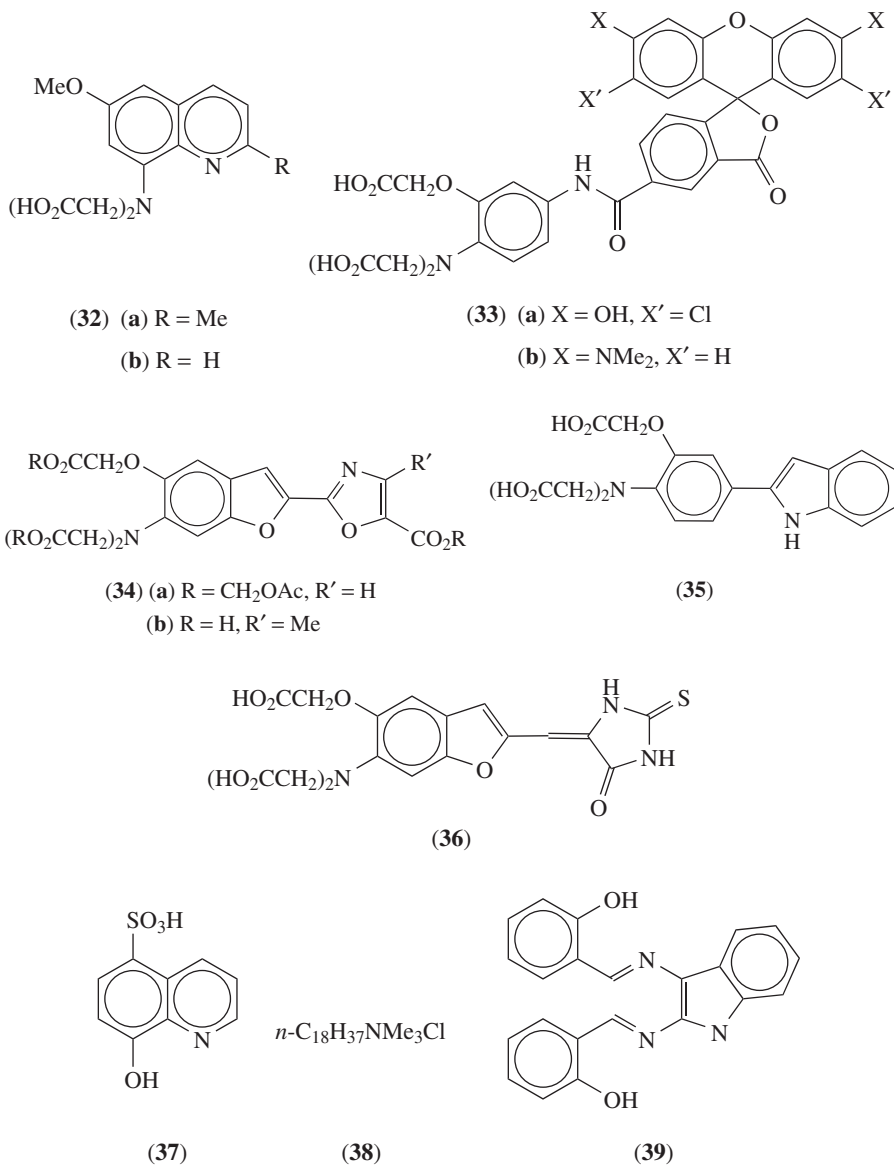


Mg in fertilizers is based on such proceedings<sup>166e</sup>. This standard method or variation thereof has been applied on multiple occasions. In a recent publication it was used for milk fermentation, where the samples were dried, calcined in a furnace at 600 °C, the ash was dissolved in 0.03 M HCl, the solution was centrifuged and the supernatant was thus analyzed<sup>162</sup>. The complexometric method for determination of Ca(II) and Mg(II) can be carried out in a single titration with EDTA in alkaline solution, using a Ca-ISE for potentiometric determination of two endpoints. This is accomplished on digitally plotting pCa values measured by the ISE as a function of the volume *V* of titrant added to the aliquot of analyte; the first and second inflection points of the curve mark the Ca(II) and Mg(II) equivalences, respectively<sup>234</sup>.

#### 4. Ultraviolet-visible fluorometry

A spectrophotometric and photochemical study was carried out on Mg(II)-selective fluorophores in their free and complexed form. The lifetimes of the excited state of Mag-quin-1 (**32a**), Mag-quin-2 (**32b**), Magnesium Green (**33a**) and Magnesium Orange (**33b**) increased two- to ten-fold on Mg(II) binding, whereas the presence of this cation did not affect those of Mag-fura-2 (**34a**), Mag-fura-5 (**34b**), Mag-indo-1 (**35**) and Mag-fura Red (**36**). On applying phase modulation fluorometry, it was found for **32b** and **33a** that a much wider Mg(II) sensitivity range is available than from intensity measurements. These two dyes undergo significant photochemical change under intense and prolonged illumination<sup>235</sup>.

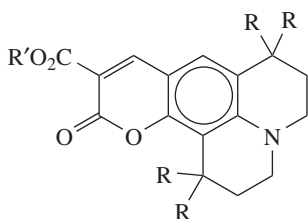
Mg(II) forms a complex with 8-hydroxyquinoline-5-sulfonic acid (**37**) at pH 9.0 with Tris-HCl buffer, which can be determined by FLD ( $\lambda_{\text{ex}} = 388$  nm,  $\lambda_{\text{fl}} = 495$  nm) with micellar enhancement by cetyltrimethylammonium chloride (**38**). Masking of Ca(II) is achieved by EGTA (**19**). The method was applied in a SIA system for analysis of natural waters<sup>236</sup>. After elution of the Mg(II) ions adsorbed on an alkali-activated PTFE tube with 0.1 M HCl and addition of *N,N'*-bis(salicylidene)-2,3-diaminobenzofuran (**39**), the end analysis was by fluorometric determination of the Mg(II) complex ( $\lambda_{\text{ex}} = 475$  nm,  $\lambda_{\text{fl}} = 545$  nm). Possible interference of Ca(II) is masked on addition of the chelating agent



**29.** LOD is 82 ppt. A sample of distilled water showed 3.1 ppb Mg(II), in good agreement with the result obtained by ICP-AES<sup>178</sup>.

Fluorescent probes for microscopic evaluation of free intracellular Mg(II) should fulfil requirements such as adequate photochemical properties (excitation with laser-based instrumentation, high extinction coefficient and quantum yield, reduced interference from autofluorescence), low toxicity and low photochemical damage. Several Mg(II) microfluorescent probes are in the market, for example, Mag-fura-2 (**34a**), Mag-indo-1 (**35**) and

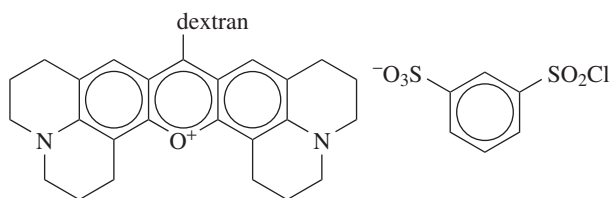
Magnesium Green (**33a**). Although the formation constant,  $K_{Ca}$ , of the Ca(II) complex with **33a**, **34a** and **35** is about two orders of magnitude larger than the corresponding  $K_{Mg}$ , the method takes advantage of the much reduced intracellular concentration of free Ca(II) as compared to that of free Mg(II). Nevertheless, it would be of advantage to have probes with higher Mg(II) selectivity, such as Coumarin 343 (**40a**), which, however, does not penetrate the cell membrane. This is overcome by esterification with an acetyloxymethyl group which yields fluorophores such as KMG-20-AM (**40b**) and KMG-27-AM (**40c**), with  $K_{Mg}/K_{Ca}$  ca 3.0, by which the presence of intracellular free Ca(II) cannot interfere with free Mg(II)<sup>237</sup>. An alternative to this approach is the PEBBLE technique, by which a Mg(II) complexant, such as **40a** with  $K_{Mg}/K_{Ca}$  of ca 2.0, and an unreactive reference fluorophore, such as Texas Red–dextran (**41**), are encapsulated in biocompatible polyacrylamide nanospheres. The PEBBLES are introduced into the cell by gene gun injection and do not interfere with the cell normal functions. Fluorometric measurements are carried out by exciting the sample at 445 nm and recording the resulting emission from 460 (for the Mg(II) complex) to 640 nm (for the reference). The LOD was 340  $\mu$ M for a dynamic range of 0 to 30 mM<sup>156</sup>.



(40) (a)  $R = R' = H$

(b)  $R = H, R' = CH_2OAc$

(c)  $R = Me, R' = CH_2OAc$

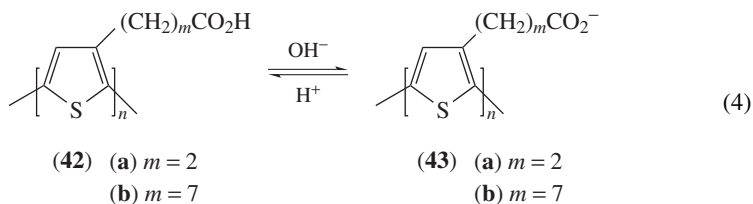


(41)

## 5. Chromatic chemosensors

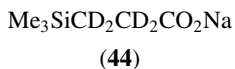
A potentially useful group of polymers changes coloration mainly due to their state of aggregation and may serve as sensors in solid state or solution for various ions. An example for this functionality is afforded by regioregular head-to-tail poly(thiophene-3-alkanoic acid)s (**42**), which are electrically conducting with low band gaps due to their ability for self-assembling into planar  $\pi$ -stacked aggregates. Polythiophene derivatives are also known for chromatic response to various stimuli, showing properties such as affinity chromism<sup>238</sup>, biochromism<sup>239,240</sup>, electrochromism<sup>241</sup>, ionochromism<sup>242</sup>, photochromism<sup>239,243</sup>, piezochromism and thermochromism<sup>239</sup>. Polymers **42a** and **42b** are not very

soluble in ordinary organic solvents and appear as violet crystals. On the other hand, they are soluble in water yielding the corresponding polycarboxylate ions **43a** and **43b**, on addition of an equivalent amount of a base, according to equation 4. The solutions show ionochromism from violet to yellow, depending on the length of the pending carboxylic acid chain and the size of the univalent base cation (ammonium and alkali metal) used to produce the carboxylate. The mechanism responsible for the ionochromism in solution seems to be self-assembly of  $\pi$ -stacked regions with color shift to violet; however, if the cations are too large (e.g.  $\text{Bu}_4\text{N}^+$  or  $\text{Cs}^+$ ), ion pair formation with the carboxylate groups of **43a** causes unzipping of the chains and shift to yellow color; in the case of **43b**, with longer pending chains, color is only slightly affected by cation size. Polymers such as **42a** may serve for detection of divalent cations. Addition of divalent cations to a red solution of **43a** with  $\text{Et}_4\text{N}^+$  counterions causes color changes and precipitate formation, probably by interchain ion pairing taking place with the divalent cations. Thus, solutions turn purple and purple precipitates form on adding small amounts of  $\text{Fe(II)}$ ,  $\text{Mg(II)}$  or  $\text{Mn(II)}$  salts; more stable red to purple solutions can be attained with  $\text{Cd(II)}$ ,  $\text{Co(II)}$ ,  $\text{Cu(II)}$ ,  $\text{Hg(II)}$ ,  $\text{Ni(II)}$  or  $\text{Zn(II)}$ , however, magenta to brown solids are formed much before the equivalent concentration is reached<sup>244</sup>.



## 6. Nuclear magnetic resonance spectroscopy

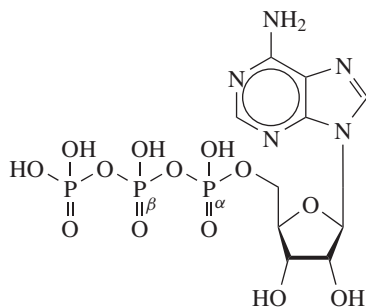
EDTA forms stable chelate complexes with  $\text{Mg(II)}$  and  $\text{Ca(II)}$  ions (**3**) at high pH, when the dissociation of the organic ligand is total<sup>245</sup>. This allows application of SEFT<sup>246</sup> or single pulse<sup>247</sup>  $^1\text{H}$  NMR techniques for determination of these ions in mM concentrations. For quantitative analysis of magnesium and calcium, a reusable sealed capillary containing a solution of sodium salt of 3-(trimethylsilyl)propionic acid- $d_4$  (**44**) in  $\text{D}_2\text{O}$  is inserted coaxially; the **44** signal serves as a chemical shift and quantitation reference while deuterium oxide provides the field-frequency deuterium lock. Two types of proton can be distinguished, an AB multiplet for acetate and a singlet for ethylene which is easier to handle in quantitative analysis. As the chemical shifts of both proton types are slightly different for **3a** and **3b**, simultaneous analysis of  $\text{Mg}$  and  $\text{Ca}$  is enabled. Application of the EXSY and TPPI techniques demonstrated that a slow exchange takes place between the free tetravalent anion and the complexed anions **3a** and **3b**. The method was proposed for clinical determination of these ions and various organic analytes in plasma and erythrocytes, as it requires no separation or mineralization steps<sup>247</sup>.



$\text{Mg(II)}$  forms a complex with adenosine triphosphate (ATP, **45**), which at pH 7.2 and  $37^\circ\text{C}$  has dissociation constant  $K_d = 3.8 \times 10^{-5} \text{ mol L}^{-1}$ . The fraction of the total ATP which did not undergo complexation present in a cell,  $\phi$ , can be estimated on the basis of  $^{31}\text{P}$  NMR spectra by means of equation 5, where the subscripts  $\alpha\beta$  denote the chemical shift of  $\text{P}_\beta$  relative to that of  $\text{P}_\alpha$  and the superscripts denote the value measured for



the cell, pure ATP and the Mg complex under similar pH and temperature conditions. The concentration of free Mg(II) in the cell is calculated by equation 6. This method was applied to determine the concentration of free Mg(II) in erythrocytes and was in accord with values determined by other methods<sup>192,248,249</sup>. Although ATP hydrolysis *in vivo* releases Mg(II), certain muscle conditions may minimize this<sup>250</sup>.



(45)

$$\varphi = \frac{\delta_{\alpha\beta}^{\text{cell}} - \delta_{\alpha\beta}^{\text{MgATP}}}{\delta_{\alpha\beta}^{\text{ATP}} - \delta_{\alpha\beta}^{\text{MgATP}}} \quad (5)$$

$$[\text{Mg(II)}]_{\text{free}} = K_d[(1/\varphi) - 1] \quad (6)$$

### 7. Mass spectrometry

Short reviews appeared on the various MS techniques for quantitation of stable isotopes and long-lived radioisotopes<sup>251</sup> and the application of Mg stable isotopes as tracers in biology and medicine<sup>252</sup>. The radioactive isotope <sup>28</sup>Mg is not usually available and has a short half-life (21.3 h), hence its limited usefulness as a tracer<sup>252</sup>. The sensitivities and interference problems encountered in activation analysis for Al, Mg, Mo, P, Si and Zr were discussed. Much higher sensitivities were found for cyclotron-produced than for reactor-produced fast neutrons or 14 MeV neutrons<sup>253</sup>.

The reverse isotope dilution technique can be applied for accurate determination of the Mg contents in a sample,  $Q_{\text{sample}}$ , on applying equation 7, by measuring the isotope ratio of a selected pair of stable isotopes,  $R_{\text{mix}}$ , in a weighed mixture of the sample with an isotopically enriched CRM. The average atomic masses  $m$  and the isotopic ratios  $R$  of Mg in the enriched CRM and in nature are known. The method was applied for determination of Mg in plant material using a CRM isotopically enriched with <sup>26</sup>Mg, measuring with an ICP/MS instrument<sup>251</sup>.

$$Q_{\text{sample}} = Q_{\text{CRM}} \left( \frac{R_{\text{CRM}} - R_{\text{mix}}}{R_{\text{mix}} - R_{\text{nature}}} \right) \left( \frac{m_{\text{nature}}}{m_{\text{CRM}}} \right) \quad (7)$$

More than 300 enzyme systems of the human being are dependent on the presence of magnesium, hence the clinical importance of determining the input–output balance and homeostatic levels of this element. For estimation of Mg absorption two possible input avenues are considered, oral and intravenous injection, two output avenues, feces and urine, and the general pool in plasma. The input amounts are known by design;

determination of the output and plasma amounts requires digestion of the samples and final analysis by FAAS after dilution with 0.5%  $\text{LaCl}_3$  to a Mg concentration of 0.1 to 0.4 ppm. The Mg absorption calculated from the oral input and feces output is undervalued because of the fecal endogenous excretion (FEE), by which Mg is transferred from the blood to the digestive tract. The FEE cannot be estimated from the FAAS analyses. Additional information is obtained on labeling the inputs with different stable Mg isotopes,  $^{26}\text{Mg}$  for the oral intake and  $^{25}\text{Mg}$  for the intravenous injection. The end analysis of the digested plasma, urine and feces samples is carried out by the ICP-MS method, measuring the abundance of the  $^{24}\text{Mg}$ ,  $^{25}\text{Mg}$  and  $^{26}\text{Mg}$  isotopes. Following the development of the  $^{25}\text{Mg}$ : $^{24}\text{Mg}$  and  $^{26}\text{Mg}$ : $^{24}\text{Mg}$  isotope ratios in the samples, it is possible to evaluate the FEE and to correct the fecal Mg balance and the Mg absorption. In fact, following the double isotope labeling of the Mg inputs, one can save the labor and expense involved in the feces analysis, leaving only plasma and urine analyses for clinical purposes<sup>254, 255</sup>. The fractional absorption of Mg in the intestine of rats was studied on applying a dietary intake enriched with  $^{25}\text{Mg}$ . Solid samples (feces and bone) were mineralized by calcination in a furnace at 500 °C and dissolution of the ashes in  $\text{HNO}_3/\text{H}_2\text{O}_2$ ; liquid samples (urine, plasma and red blood cells) were diluted to the appropriate Mg concentration before end analysis by FAAS for total Mg and ICP/MS for isotope ratios<sup>256</sup>.

A study of the exchange taking place between Mg pool masses was based on measurement of stable isotope ratios after administration of  $^{25}\text{Mg}$  or  $^{26}\text{Mg}$  doses, and analysis of plasma by ICP-MS<sup>257, 258</sup>. In a study of Mg transport in epithelial cells the isotope ratios were determined by MS for intracellular free Mg(II) after cell dissolution, as obtained from a feed enriched with  $^{25}\text{Mg}$ , whereas the total free Mg(II) in the cell was determined by a microfluorimetric method using the complex of Mag-fura-2 (**34a**) with Mg(II) (Section III.E.4)<sup>252</sup>.

## IV. SPECIATION ANALYSIS OF ORGANOMAGNESIUM COMPOUNDS

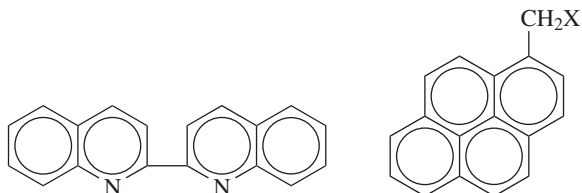
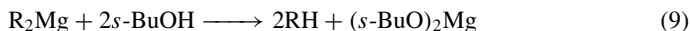
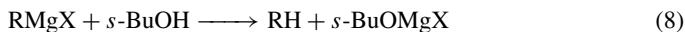
### A. Titration Methods

Many of the titration methods for organomagnesium compounds are similar to those for organolithium compounds, which have been reviewed elsewhere<sup>146, 259, 260</sup>.

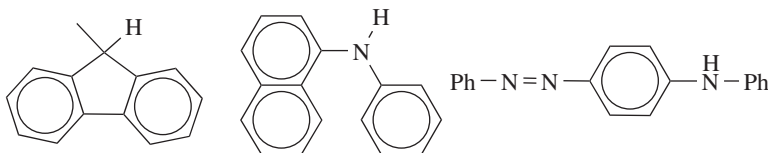
#### 1. Visual endpoint

Titrations of organomagnesium or organolithium compounds take advantage of two characteristic properties of these compounds: they may act as strong Lewis bases forming salts with acids, e.g. butanol, as in equations 8 and 9, or forming charge-transfer complexes, usually with aromatic bases. The latter property affords good indicators for titration; for example, 1,10-phenanthroline (**21**) or 2,2'-biquinoline (**46**) form deeply colored complexes with alkyl Grignard reagents or with dialkylmagnesium compounds, which persist until the titrant is in excess<sup>261, 262</sup>; the same titration method may be applied to assess the quality of  $\text{LiAlH}_4$ <sup>262</sup>. 1-Pyreneacetic acid (**47a**) and 1-pyrenemethanol (**47b**) were proposed as titrant/indicator for Grignard reagents. On dropwise addition of the analyte to an aliquot of **47a**, the endpoint is marked by a turn to intense red due to formation of a dianion. The titrant can be recovered<sup>263</sup>. Not all indicators suitable for titration of organolithium compounds are fit for titration of organomagnesium compounds, probably due to the lesser reactivity of the latter. Thus, 9-methylfluorene (**48**) and *N*-phenyl-1-naphthylamine (**49**) were successfully used for titration of various organolithium compounds with a solution of *s*-BuOH in THF according to equation 8, by virtue of the red discoloration obtained on losing their active proton in the presence of the

organometallic analyte. Neither MeMgCl nor *t*-BuMgCl could be titrated with either indicator, PhMgCl responded only to **49**, and only with vinylmagnesium chloride could both indicators be used<sup>264</sup>. The requirement for compounds such as **49** to serve as indicator in this type of titration is that their basicity be lower than that of the Grignard reagent<sup>265</sup>. However, the analytical quality of the titration of this compound according to equation 8 with *o*-phenanthroline (**21**) as indicator is uncertain when the vinylmagnesium halide has deteriorated (see Section IV.B.1)<sup>266</sup>. Arylmagnesium halides were dissolved in xylene and titrated with *s*-BuOH using **49** as endpoint indicator, turning to a colorless solution. These titrations served for validation of two chromatographic methods for speciation analysis of the Grignard reagents and their impurities (Section IV.B)<sup>267</sup>. 4-(Phenylazo)diphenylamine (**50**) was used as indicator for the titration of MeMgI with PrOH, the color turning from pink to yellow<sup>268</sup>.



(46)

(47) (a) X = CO<sub>2</sub>H  
(b) X = OH

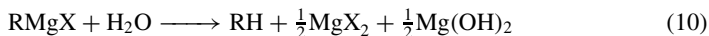
(48)

(49)

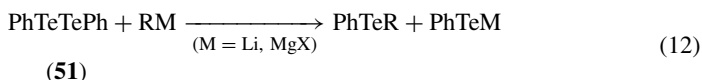
(50)

Gilman and coworkers<sup>269,270</sup> pointed out that titration of the alkalinity produced by hydrolysis of the sample according to equations 10 and 11 can yield high values. Organomagnesium compounds may undergo deterioration on being exposed to oxygen, moisture or carbon dioxide in the environment; also, long storage at room temperature may cause condensation, elimination or rearrangement reactions. Various titration methods have been proposed for the quality assessment of organomagnesium compounds in general and Grignard reagents in particular. The double titration method has been often applied for organolithium compounds. One aliquot of the compound is hydrolyzed and the alkalinity produced by RLi, ROLi and LiOH present in the sample is determined by titration with acid. A second aliquot is treated with a specific reagent for the organolithium compound, e.g. BnCl, and titrated for the alkalinity of ROLi and LiOH. The difference between these values is the content of organometallic compound. The ASTM E233-90 standard method for assay of *n*-butyllithium solutions is an example of such proceedings<sup>271</sup>. The subject was briefly reviewed<sup>260a</sup> and is of applicability to other organometallics, such as Grignard reagents, for which CCl<sub>4</sub> has been proposed as reagent for the second titration<sup>272</sup>.

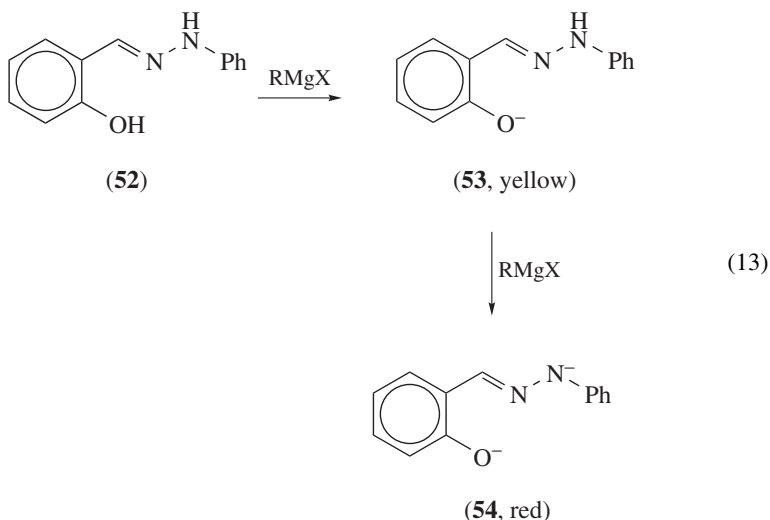
Titration with water, based on equations 10 and 11, have been of wide application, and are appropriate for concentrations as low as about 2 mM<sup>273</sup>.



Diphenyl ditelluride (**51**) serves both as titrant and indicator for organometallic compounds as shown in equation 12. Reagent **51** imparts a deep red discoloration when dissolved in THF or other solvents used in carbene chemistry; on reaching the endpoint the color turns to yellow. The chemical process is more complicated than in equation 12 when dealing with analytes of basicity stronger than that of Grignard reagents or alkynyllithium compounds; however, the stoichiometry of the overall titration is not disturbed. No interference was observed by alkoxide impurities present in organometallic compounds<sup>274</sup>.

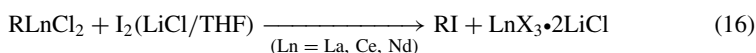
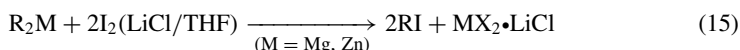
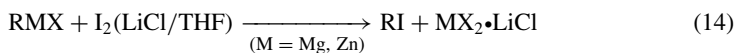


Salicylaldehyde phenylhydrazone (**52**) is an easily prepared and inexpensive titrant/indicator for organometallics such as Grignard reagents (equation 13) and organolithium compounds and for hydride species such as lithium aluminum hydride and sodium bis(2-methoxyethoxy)aluminum hydride. A solution of the analyte is added to THF containing a weighed amount of **52**; a yellow color appears due to the presence of the phenolate ion **53**. On reaching the endpoint the solution turns bright orange due to formation of the **54** dianion<sup>275</sup>.

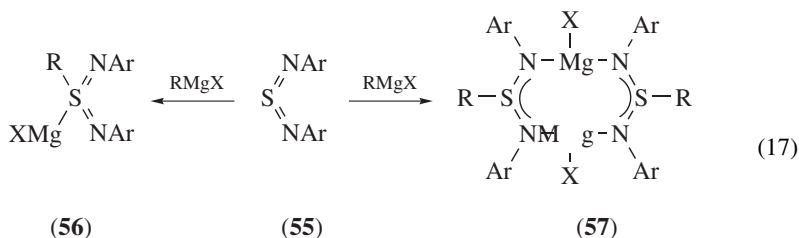


A titration method for organomagnesium, organozinc or organolanthanides is based on the reaction of these compounds with iodine dissolved in a saturated solution of LiCl in THF. The analyte solution is added to an aliquot of I<sub>2</sub> solution until the brown color disappears. The chemical process for organozinc or organomagnesium is as shown in equations 14 and 15<sup>276</sup>. In the case of the organolanthanides, conveniently prepared

from a Grignard reagent<sup>277</sup>, the titration proceeds as shown in equation 16<sup>276</sup>. Note in equations 14 to 16 that the equivalence is one mol of I<sub>2</sub> per mol of organo group; the X on the right hand side are halide ions present in the solution.



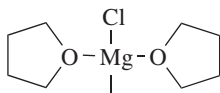
In a typical titration of Grignard reagents with substituted diimidosulfur compounds (55) the analyte is added dropwise to the red-orange solution of 55 until it becomes colorless, yielding monomeric (56) or dimeric adducts (57), as shown in equation 17. Dialkyl magnesium and alkyllithium compounds undergo a similar reaction. No interference occurs by alkoxides, hydroxides and other products stemming from degradation of the analytes on storing<sup>278</sup>.



## 2. Potentiometric and other instrumental titrations

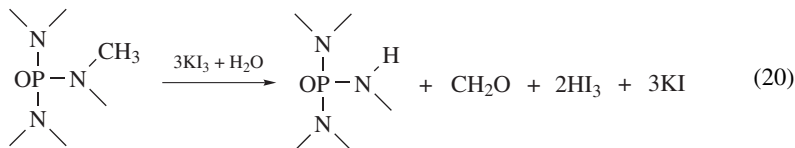
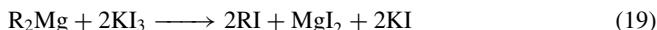
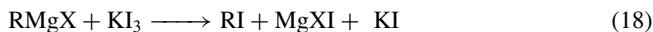
Determination of organomagnesium compounds with various titrants can be carried out with a potentiometric endpoint, using a Ag working electrode and a Ag/AgClO<sub>4</sub>/Bu<sub>4</sub>NClO<sub>4</sub>/THF reference electrode. Thus, MeMgCl and EtMgCl could be titrated with THF solutions of AgClO<sub>4</sub>, BuOH or PhNH<sub>2</sub>, and PhMgCl with the latter two titrants<sup>279</sup>. A combined Pt-Ag/AgCl electrode for use in nonaqueous titrations has to be prepared from an ordinary electrode of this type, by changing the KCl electrolyte solution with a saturated solution of LiCl in THF, to which a few drops of AgNO<sub>3</sub> solution were added. The endpoint is chosen at the inflexion point of the potential vs titrant curve, or more clearly from the first derivative of this curve. This method is suitable for automatic titration of Grignard reagents with BuOH, according to equation 8. An alternative method for determining the titration endpoint is based on in-line FTIR. Spectra of the titration solution are collected at a rate of 2 min<sup>-1</sup>, over the 4000 to 600 cm<sup>-1</sup> range, with a 4 cm<sup>-1</sup> resolution. For example, in the case of MeMgCl, calculated difference spectra, where the spectrum of the solvent alone is subtracted from the collected spectra, show peaks at 1070 and 911 cm<sup>-1</sup>, due to C-O-C stretching and ring breathing in complex 58; the corresponding strong peaks of the THF solvent are at 1037 and 884 cm<sup>-1</sup>. Disappearance of the peaks of 58 in the difference spectra marks the titration endpoint. The potentiometric and FTIR methods for determining the endpoint were in good agreement<sup>280</sup>.

Potentiometric titration with KI<sub>3</sub> dissolved in HMPT, according to equations 18 and 19, was proposed. The method is limited by the relatively low shelf stability of the titrant

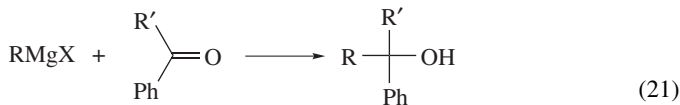


(58)

solution; for example, the oxidation shown in equation 20 can take place in the presence of moisture<sup>281</sup>.



Various methods have been proposed for avoiding interference by the usual degradation products of Grignard reagents. Thus, a sample of the analyte on treatment with excess of an aromatic ketone followed by dilution with an alcohol is converted to a tertiary alcohol, as shown in equation 21. The excess of benzophenone (**59a**) is measured at 333 nm; however, the method is limited to primary alkyl groups  $\text{R}^{282}$ . The method is of more general applicability when the titrating reagent is acetophenone (**59b**), the excess of which is determined at 243 nm<sup>283</sup>.



(59) (a)  $\text{R}' = \text{Ph}$

(b)  $\text{R}' = \text{Me}$

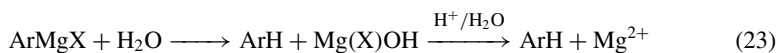
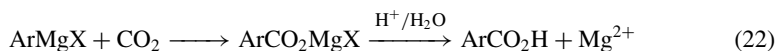
Thermometric titrations were applied for determination of organometallic compounds and, in particular, of Grignard reagents. The method takes advantage of the negative enthalpy of reaction with an alcohol (e.g. equation 8), which causes heating of the reaction mixtures as the titrant solution is added. A typical run consists of measuring the sample temperature while adding the titrant solution at a constant rate. A gradual temperature rise (reaction in progress) is observed until the curve starts bending down (reaction approaching the equivalence point) and then decreasing (reaction finished and mixture cooling down). The endpoint is determined by the intersection of the tangents to the increasing and decreasing parts of the curve. This titration was applied for determination of  $\text{MeMgBr}$ ,  $\text{MeMgI}$ ,  $\text{EtMgI}$  and  $\text{PhMgBr}$  with *i*-PrOH<sup>284</sup>.

## B. Chromatographic Methods

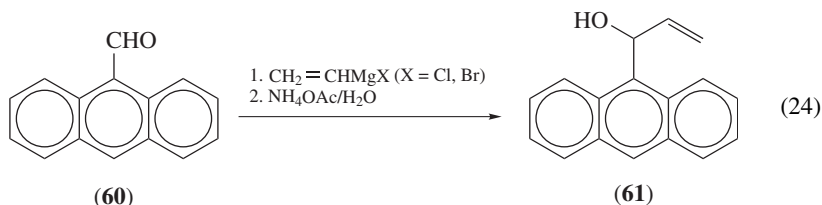
### 1. Liquid chromatography

The titration methods of Section IV.A do not allow detection and quantitation of the impurities accompanying the organomagnesium compound analytes. A method was proposed for fast derivatization (less than 1 min) of aromatic organomagnesium compounds

with carbon dioxide, according to equation 22, followed by dilution with aqueous MeOH. End analysis was by RP-HPLC on a C<sub>8</sub> column, with a mobile phase of aqueous acetonitrile containing 0.05% formic acid to ensure that the analyte derivative is an arenecarboxylic acid. An alternative to CO<sub>2</sub> derivatization was quenching with water to get the arene, according to equation 23. Detection was by EI-MS, in the full scan negative ion mode. For example, titer determination of a *ca* 1 M 4-fluorophenylmagnesium bromide sample with CO<sub>2</sub> showed in the order of emergence from the column 4-fluorophenol, 4-fluorobenzoic acid, fluorobenzene, 4'-fluorobiphenyl-3-carboxylic acid, 4'-fluorobiphenyl-4-carboxylic acid, 4-fluorobiphenyl and 4,4'-difluorobiphenyl; except for 4-fluorobenzoic acid all were in trace amounts. The same sample did not show 4-fluorobenzoic acid by the water quenching method and fluorobenzene was a strong peak<sup>267</sup>.



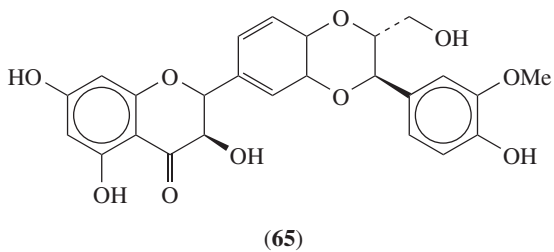
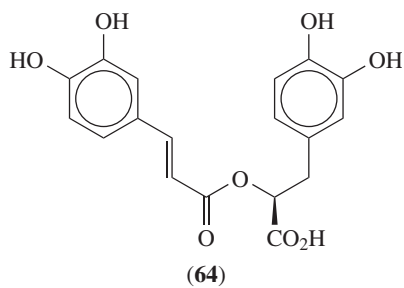
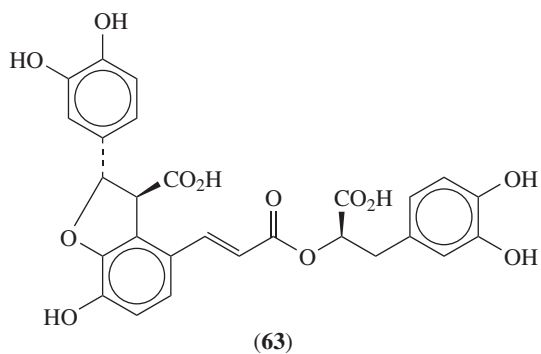
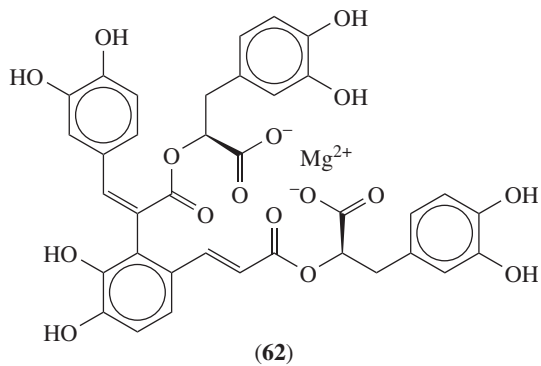
A precolumn derivative recommended for vinylmagnesium halide and alkyl Grignard reagents is a secondary alcohol (**61**) derived from 9-anthraldehyde (**60**), as shown in equation 24. End analysis after appropriate dilution is by RP-HPLC-UV, measuring at 227 nm and using PhAc as internal standard. Although the chromatographic method is more involved than direct titration with *s*-butanol, according to equation 8, wrong results were obtained by titration for the titer of a reagent that partially decomposed on storage<sup>266</sup>.



Separation and quantitation of mixtures of analytes in complex matrices is possible with a combination of sample preparation, column, eluent and detection method. Thus, magnesium lithospermate B (**62**), lithospermic acid (**63**) and rosmarinic acid (**64**), present in *Salvia miltiorrhiza* Bge (*Labiatae*), used in traditional Chinese medicine, were determined in dog serum by LC/tandem MSD. The serum samples, either spiked with the analytes or obtained after intravenous infusion, were spiked with silibinin (**65**), serving as internal standard, treated with formic acid, subjected to LLE with AcOEt and centrifuged to separate the protein. The supernatant extract was evaporated to dryness, dissolved in aqueous 25% acetone, centrifuged and 10  $\mu\text{L}$  of the supernatant were injected into the LC/MS/MS instrument, equipped with a C<sub>18</sub> column, in isocratic regime, using as mobile phase water–MeCN (6:4), containing 0.5% formic acid. The highest sensitivity was attained for negative ion operation, optimized for  $[\text{M} - \text{H}]^-$  ions. Analytical runs of about 3 min were carried out. Analytical figures of merit for **62**, **63** and **64** were, respectively, as follows: LOD 1.0, 1.5 and 1.0  $\text{ng mL}^{-1}$ ; LOQ 8, 4 and 4  $\text{ng mL}^{-1}$ ; linearity ranges 8 to 2048, 4 to 1024 and 4 to 1024  $\text{ng mL}^{-1}$ <sup>285</sup>.

## 2. Gas chromatography

Dialkylmagnesium compounds R<sub>2</sub>Mg and Grignard reagents RMgX can be derivatized to yield volatile compounds containing the R group, and the products may be subjected to





end analysis by GC. Although reaction with active hydrogen compounds such as butanol and water (equations 8 to 11 and 23) is fast and quantitative, the lower members of the R series may produce hydrocarbons that are too volatile and require stringent analytical conditions to avoid losses. Derivatization with carbonyl compounds such as CO<sub>2</sub> (equation 22), esters, ketones (equation 21) or aldehydes (equation 24) requires a hydrolysis step of the R'O-MgX intermediate to obtain the volatile derivatives; furthermore, the R'OH compounds may need further derivatization to assure good chromatographic behavior.

Coupling of Grignard reagents RMgX with reactive halides R'X has the advantage of directly yielding volatile compounds RR' which may be analyzed by GC. This method was applied for determination of vinyl chloride by coupling with Bu<sub>3</sub>SnCl, using dodecane as internal standard<sup>286</sup>, and of methyllithium and methylmagnesium compounds by coupling with Me<sub>2</sub>PhSiCl, using cumene as internal standard<sup>287</sup>. In Section V.B analytical methods are discussed for various organometallic and inorganic compounds based on the coupling reaction with Grignard reagents acting as derivatization agents.

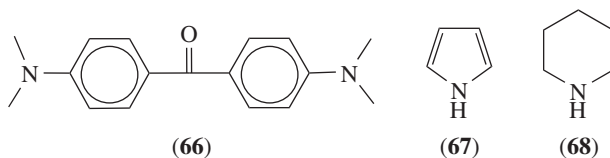
## C. Spectral Methods

### 1. Infrared spectroscopy

The course of development of a process in the solid state usually poses difficult analytical problems. A nondestructive, noninvasive method for determination of multicomponent mixtures uses an IR reflectance technique such as DRIFTS, with data processing by procedures such as the multivariate PLS regression and the RMSEP parameter. A practical advantage of the DRIFTS method is the simplicity of the analytical procedure, with no sample preparation other than proper placement in the instrument, and no post-analytical procedures, as no reagents are used. The method requires previous knowledge of the spectra of the individual components of interest, and it was applied to follow the composition of rocks containing calcium carbonate, magnesium carbonate and magnesium oxide in a process aiming at separation of these components<sup>288</sup>.

### 2. Gilman's color tests

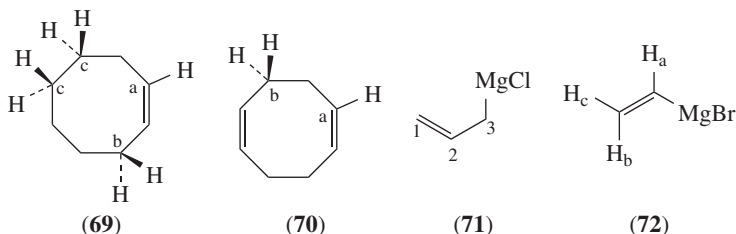
Gilman and coworkers developed color tests for identifying classes of organometallic compounds, including those containing magnesium and lithium. The methods for organomagnesium compounds are easy to perform and may be helpful to assess the development of processes involving Grignard reagents. The first such test consists of treating the sample solution with a 1% solution of Michler's ketone (**66**) in C<sub>6</sub>H<sub>6</sub>, followed by addition of H<sub>2</sub>O and subsequent acidifying with dilute AcOH. A characteristic greenish blue color develops for compounds containing the C-MgX moiety. A deep blue or purple color develops in the presence of metallic Mg, therefore the solution where a Grignard reagent was synthesized should be filtered before carrying out the test<sup>289,290</sup>. The mechanism can be explained as formation of a tertiary alcohol derived from **66**, which forms a colored carbonium ion on acidification<sup>291</sup>. The color test was used for assessing the rate of formation of Grignard reagents in Et<sub>2</sub>O for various alkyl and aryl halides in the presence of Mg turnings, with or without addition of I<sub>2</sub> as catalyst<sup>292</sup>, and for monitoring the progress of the reaction of various Grignard reagents with azobenzene<sup>293</sup>. However, when tracking reaction mixtures interference with the color test was observed for certain halogen compounds, such as BzBr, Cl<sub>2</sub>CO, ClCOCOC and PCl<sub>5</sub> and amino compounds such as pyrrole (**67**), PhNHMe, Bu<sub>2</sub>NH, Al<sub>2</sub>NH, PhNAlkyl<sub>2</sub>, but none was observed for Et<sub>2</sub>NH, Ph<sub>2</sub>NH, BnNHPh or piperidine (**68**)<sup>294-296</sup>. Two color tests using less sensitive



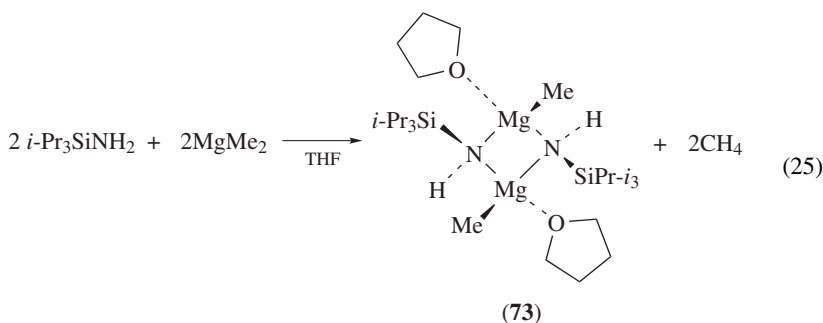
reagents were developed for alkyllithium and aryllithium compounds are ineffective for Grignard reagents<sup>297</sup>. Solutions of various amino compounds develop a discoloration in the presence of alkyllithium compounds but not of Grignard reagents<sup>298</sup>.

### 3. Nuclear magnetic resonance spectroscopy

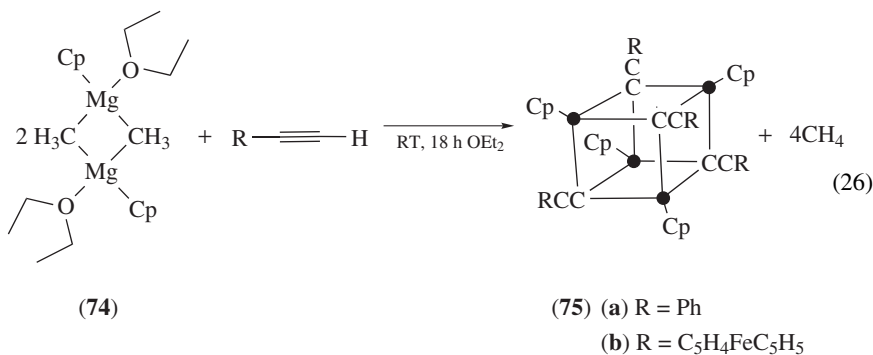
The titer of organolithium compounds, Grignard reagents and lithium diisopropylamide solutions in ordinary (nondeuteriated) organic solvents can be easily determined by the so-called No-D NMR spectroscopy, based on  $^1\text{H}$  NMR spectra, taking advantage of the power, signal stability and operational capabilities of modern instrumentation. Typical concentrations of commercially acquired reagents are in the 1 to 2 M range while those of the solvents are about 10 M, thus the solutes can be clearly seen in the presence of the solvent; furthermore, the analytical quality of the measurements can be improved with various provisions, allowing good quantitation of the solutes. A precisely measured amount of an adequate standard should be added to the solution; cyclooctene (**69**), with three multiplets at  $\delta$ 5.615, 2.14 and 1.49 ppm, in 1:2:4 ratio<sup>299a</sup>, or 1,5-cyclooctadiene (**70**), with two peaks at  $\delta$ 5.558 and 2.36 ppm in 1:2 ratio<sup>299b</sup> (data for  $\text{CDCl}_3$  solution), were used in the following examples. A commercial sample of allylmagnesium chloride (**71**) in THF using **69** as reference compound showed the peaks of solvent and reference, a quintuplet at  $\delta$ 6.0 and a doublet at  $\delta$ 2.1. The latter peaks correspond to H<sub>2</sub> and H<sub>1,3</sub> of **71**, respectively; in this compound the protons at positions 1 and 3 are equivalent by virtue of a fast  $1 \rightleftharpoons 3$  rearrangement of  $\text{MgCl}$  taking place at 25 °C. Integration of the peaks of **69** and **71** pointed to a 1.2 M concentration of the acquired product. The No-D NMR method may also be helpful to assess the quality of an organometallic sample. Thus, a solution of vinylmagnesium bromide (**72**) in THF, using **70** as reference, showed that it contained substantial amounts of vinyl bromide ( $\text{CH}_2=\text{CHBr}$ ) and 1,3-butadiene ( $\text{CH}_2=\text{CHCH}=\text{CH}_2$ ), as all the protons of these compounds appeared in the spectrum, besides the quadruplets of H<sub>a</sub>, H<sub>b</sub> and H<sub>c</sub> of **72**<sup>300</sup>. An earlier version of the No-D NMR method was proposed for titer determination of Grignard reagents and other alkylmetal solutions in  $\text{Et}_2\text{O}$ , THF or hexane, using  $\text{CH}_2\text{Cl}_2$  or  $\text{C}_6\text{H}_6$  as internal standard. Most frequently the peaks used for integration were those of the  $\alpha$ -C protons, as they stood apart from those of solvent or standard. No coupling was observed for these protons with the  $^{25}\text{Mg}$  nucleide (10% natural abundance and  $I = \frac{5}{2}$ )<sup>301</sup>.



$^1\text{H}$  and  $^{13}\text{C}$  NMR spectroscopies afford a means of following the development of complex processes in solution. Equation 25 illustrates the power of this instrumental method, which allows identification and relative quantitation of the various species present. Triisopropylsilylamine reacts with dimethylmagnesium to yield methane by reaction of  $\text{Me}_2\text{Mg}$  with an active hydrogen compound (see Section V.A) and a dimeric heteroleptic organomagnesium compound (**73**), which is further stabilized by coordination with the THF solvent. No equilibrium involving **73** with a homoleptic compound was observed. Furthermore, two sets of chemical shifts (relative to TMS) were obtained for the protons at the secondary and primary positions of the isopropyl groups, pointing to the existence of two diastereoisomers of **73**, with the *N*-triisopropylsilyl groups being at the same or opposite sides of the plane determined by the  $\text{N}_2\text{Mg}_2$  cycle<sup>302</sup>.

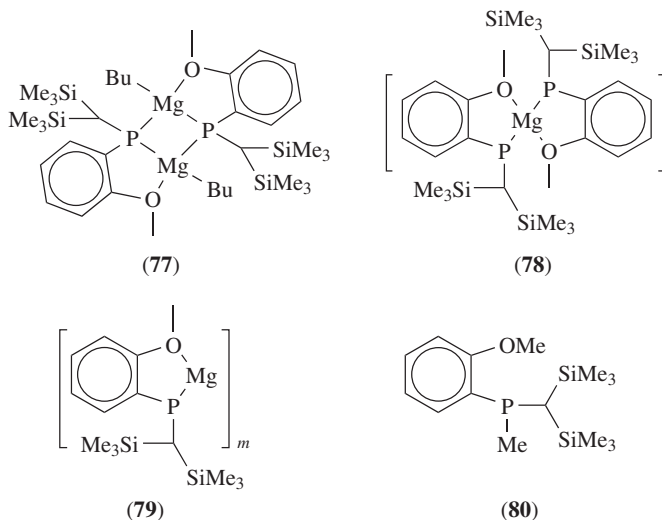
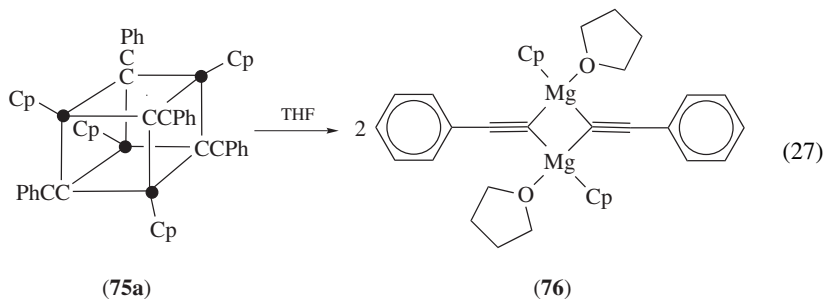


The dimeric complex **74** reacts with phenylacetylene or ferrocenylacetylene to yield the tetrameric complexes **75a** and **75b**, respectively, according to equation 26. These complexes are stable in  $\text{CDCl}_3$  solution in the absence of air and can be characterized by  $^1\text{H}$  and  $^{13}\text{C}$  NMR spectroscopies. The low solubility of **75a** in unreactive organic solvents precludes detailed studies of the solution structure; in reactive solvents it decomposes to a dimeric complex, **76**, according to equation 27<sup>303</sup>. The association behavior of these complexes resembles that of analogous organolithium compounds<sup>260b, 303</sup>.

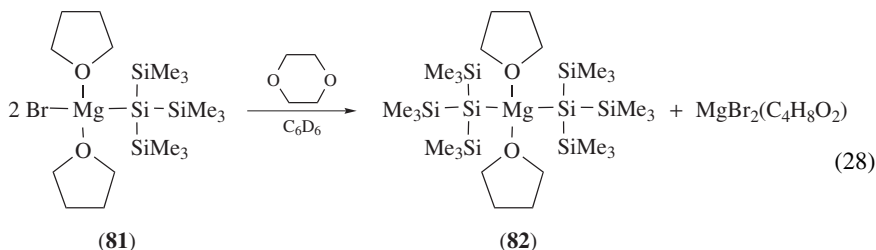


The degradation of a compound in  $\text{THF-}d_8$  solution could be followed by  $^{31}\text{P}\{^1\text{H}\}$  NMR spectroscopy. Thus, for example, the heteroleptic dimeric phosphanide Grignard analogue **77** does not dissolve well in nondonor solvents; the fresh solution in THF shows two main peaks A and B, at  $\delta$ —107.0 and —103.1 ppm, respectively; peak B is tentatively attributed to the homoleptic compound **78**, obtained on loss of  $\text{MgBu}_2$ . After 1 h, peak A is markedly

decreased and peaks C and D appear at  $\delta$ −104.4 and −31.8 ppm, respectively. Peak C possibly corresponds to an oligomeric alkoxophosphanide complex such as **79** while D belongs to the tertiary phosphane **80**. After 36 h, peaks A and B have almost disappeared, leaving fully developed peaks C and D. The fate of the Mg compounds lost on forming **80** is unknown<sup>304</sup>.

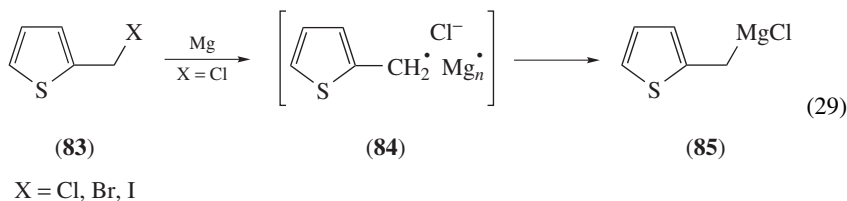


The transformation of a silyl Grignard reagent (**81**,  $\delta$  0.457 ppm) into a disilylmagnesium compound (**82**,  $\delta$  0.465 ppm) by the action of dioxan in  $C_6D_6$  solution, according to equation 28, could be followed in time by  $^1H$  NMR spectroscopy. It should be noted that the THF ligands are strongly coordinated to the Mg atom<sup>305</sup>.



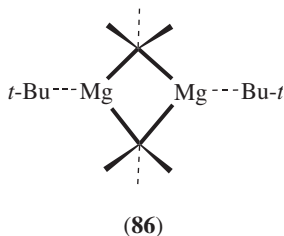
#### 4. Electron spin resonance spectroscopy

The ESR spectrum of the 2-thenyl free radical can be observed at 77 K when preparing a Grignard reagent (**85**), according to equation 29. When thenyl bromide (**83**, X = Br) is in the presence of metallic Mg, a quadruplet with full width of *ca* 55 G is shown, due to the spin interaction of the protons of the methylene group and at positions 3, 4 and 5 of the ring; the ESR spectrum of the free radical observed for 2-thenyl iodide (**83**, X = I) is poorly resolved, however its width corresponds to that of X = Br. In the particular case of **83** (X = Cl), that multiplet is superimposed on a singlet with half width  $9 \pm 2$  G, attributed to the free radical pair **84**, including a Mg cluster. The difference in spectral behavior was correlated with the dissociation energy of the C–X bond in **83**<sup>306</sup>.



#### D. Cryoscopy

Cryoscopic determination of the molecular weight of *t*-Bu<sub>2</sub>Mg in benzene solution pointed to a dimer (**86**), the structure of which was confirmed by <sup>1</sup>H and <sup>13</sup>C NMR spectroscopy and ultimately determined by XRD crystallographic analysis<sup>307</sup>.



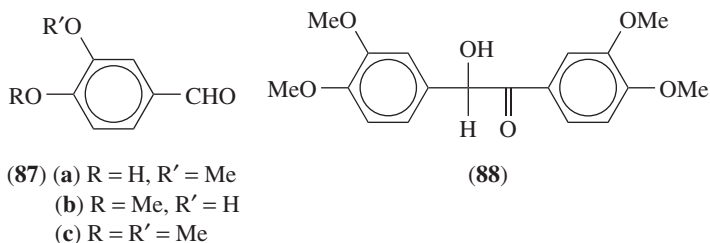
### V. GRIGNARD REAGENTS AS ANALYTICAL REAGENTS AND AIDS

#### A. Active Hydrogen

Since Zerevitinov's publication in 1913<sup>308</sup>, his method underwent analytical refinements and has been applied on multiple occasions. Alcohols (e.g. equation 10, R = Me) and amines evolve at room temperature 1 mol of methane per mol of functional group. Certain compounds containing 'active' CH groups  $\alpha$  to aromatic rings are less reactive and require warming. Compounds achieving only partial evolution of methane after warming were considered to be tautomeric. An apparatus was described for processes involving MeMgI, by which both the volume of CH<sub>4</sub> evolved and the excess Grignard reagent can be determined. Such processes need not necessarily be reaction with active hydrogen<sup>309, 310</sup>. Volumetric determination of MeMgI was proposed instead of the Karl Fischer reagent, for determination of water in metal powders, such as Pb, Sn, Ag and Mg, by volumetric measurement of the evolved methane<sup>311</sup>. A method for selective determination of active hydrogen consists of analyzing the sample by GC-TCD and collecting the emerging fractions in a MeMgI/Bu<sub>2</sub>O solution, which is analyzed for the formation of CH<sub>4</sub> by GC on

a short silica gel column, using a second TCD. The method was verified with a mixture of EtOH, AcOEt, AcEt, PhH and BuOH<sup>312</sup>.

Care should be taken when developing analytical processes using Grignard reagents, choosing the right solvents and conditions of reaction, lest the analytical results will be affected by spurious factors. An example is the simultaneous determination of active hydrogen and carbonyl group in certain aromatic aldehydes, as deduced from methane evolution and total consumption of MeMgI. Vanillin (**87a**) and isovanillin (**87b**) show incomplete reaction in dioxan and the presence of one active hydrogen and one carbonyl group in pyridine solution. Veratraldehyde (**87c**), on the other hand, shows one carbonyl group in xylene, whereas in dioxan or pyridine the analysis shows less than one carbonyl group and the presence of active hydrogen. Indeed, it happens that **87c** undergoes an equilibrium dimerization in the latter solvents to yield **88**, which explains the results<sup>313</sup>.



The concentration of silanol groups in porous borosilicate glass could be determined by the Grignard titration method. The value found ( $1.945 \text{ mmol g}^{-1}$ ) for a sample with mesopores of 10.0 nm diameter and  $0.938 \text{ mL g}^{-1}$  volume was significantly larger than that ( $0.681 \text{ mmol g}^{-1}$ ) found for a sample with micropores of 2.0 nm diameter and  $0.263 \text{ mL g}^{-1}$  volume. On the other hand, the values obtained for these samples by thermogravimetric analysis, due to weight loss by condensation of the silanol groups, were similar to each other. The analytical discrepancy was attributed to restricted access of the Grignard reagent to the silanol groups in the sample with the micropores<sup>314</sup>.

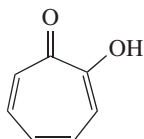
The detection and determination of active hydrogen have been reviewed<sup>315–317</sup>.

## B. Derivatization Reagents

### 1. Gas chromatography of organometallic compounds

Cost-effective methods of good analytical quality are needed for detection and speciation of organometallic compounds, for research, quality control, forensic analysis and environmental pollution control. Of special interest are organotin compounds, for their widespread commercial application as additives in many materials. Frequently, sample preparation includes extraction of organotin compounds with tropolone (**89**) solutions, of organolead compounds with dithizone (**90**) or sodium *N,N*-diethyldithiocarbamate (**91**) solutions<sup>318</sup> and of organoantimony with ammonium pyrrolidinedithiocarbamate (**92**) solutions<sup>319</sup>. A widespread procedure for the analysis of organometallics bearing halogen atoms on the metallic atom consists of treating the sample with a Grignard compound, destroying the excess of reagent, extracting the products and carrying out the end analysis by GC using various detection methods. The synthesis of volatile derivatives of organometallic compounds for GC speciation analysis has been reviewed<sup>320, 321</sup>. The partially alkylated analytes exchange the halogen atoms with the group of the Grignard compound, therefore the latter should bear an organic group different from those of the analyte, and the nature of this group should vary according to the effect to be achieved. For

example, added volatility is attained with small alkyl groups, diminished volatility with large alkyl groups or fingerprinting with perfluoroalkyl groups. Although MSD is probably the most informative detection method, other less expensive detectors can give satisfactory results, especially in routine analysis. Applications of GC in speciation analysis of organometallic compounds after derivatization with Grignard reagents are summarized in Table 2.



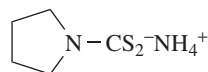
(89)



(90)



(91)



(92)

## 2. Analysis of glycerides and waxes

The abundance of fatty acids in triacylglycerols (TAG) can be determined by conversion of the acyl groups into tertiary alcohols on reaction with an alkyl Grignard reagent, followed by chromatographic separation. The method was found to be of advantage over saponification and conversion to a methyl ester, especially in the determination of short-chain fatty acids, which suffer losses by volatilization<sup>355</sup>.

A standard procedure for identifying the fatty acid at the  $\beta$ -position of TAG is carrying out a pancreatic lipase hydrolysis. Analysis of the acyl groups at  $\alpha$ -positions, however, is affected by isomerization taking place in the diacylglycerols<sup>356</sup>. An alternative approach was proposed based on partial conversion of the acyl groups to tertiary alcohols with MeMgBr or EtMgBr. The process lasts a few seconds, resulting in a mixture of  $\alpha$ - and  $\beta$ -monoacylglycerols,  $\alpha,\alpha'$ - and  $\alpha,\beta$ -diacylglycerols, unreacted TAG and tertiary alcohols<sup>357,358</sup>. After separation by preparative TLC on silicic acid impregnated with boric acid to prevent isomerization, each fraction can be further analyzed for identification (besides that indicated by the  $R_f$  values) and quantitation. For example, the glycerol esters can be converted to methyl esters by direct addition on the TLC spot of MeOH containing  $\text{BF}_3$ , followed by extraction and GC. The method was demonstrated by the regiodistribution analysis of tuna oil and milk fat<sup>358</sup>. Derivatization of TAG with EtMgBr for determination of the distribution of fatty acids in TAG was part of extensive analytical investigations of the oil extracted from *Rhodococcus opacus* strain PD630<sup>359</sup> or from evening primrose oil<sup>360</sup>.

The fatty acid/fatty alcohol distribution of jojoba wax was determined after derivatization with EtMgBr, leaving a mixture of tertiary alcohols stemming from the fatty acid and the primary alcohols which were present as esters in the wax. The progress of wax disappearance due to the Grignard reaction could be assessed by TLC, with only traces left after 10 min. MeMgBr was even faster; however, reaction with *n*-BuMgBr or BnMgBr was complete only after 2 h. End analysis was by GC-FID<sup>361</sup>.

## C. Ancillary Applications

### 1. Surface conditioning

Fused silica capillary tubes were variously coated for capillary electrophoresis. The chemical process involving a Grignard reaction is shown in equation 30. The silanol groups on the silica surface are treated with alkali, dried, converted to chlorosilanes with thionyl chloride and vinylmagnesium bromide replaces the chlorine atoms with vinyl

TABLE 2. Derivatization of organometallic compounds with Grignard reagents for GC analysis

Analytes and comments	Grignard reagent	Detection method
<i>Organotin compounds</i>		
Bu <sub>3</sub> SnCl. Study of SPE effectiveness in environmental samples. After dipping the SPE extraction tube in the sample extract, it was eluted with AcOEt, the eluate evaporated and the residue derivatized, extracted and subjected to end analysis <sup>322</sup> . Better results are obtained for derivatization with <i>n</i> -PenMgBr <sup>323</sup> .	MeMgBr	MSD <sup>322</sup> FPD <sup>323</sup>
BuSnCl <sub>3</sub> , Bu <sub>2</sub> SnCl <sub>2</sub> , Bu <sub>3</sub> SnCl, PhSnCl <sub>3</sub> , Ph <sub>2</sub> SnCl <sub>2</sub> , Ph <sub>3</sub> SnCl, cyhexatin ( <b>93</b> ), fenbutatin oxide ( <b>94</b> ). Determination of butyltin and phenyltin pollutants in mussels, after tissue destruction with NMe <sub>4</sub> OH, extraction with tropolone ( <b>89</b> ) solution and derivatization. Almost similar results were obtained for <i>in situ</i> ethylation with NaBEt <sub>4</sub> in acetate buffer at pH 4 <sup>323,324</sup> . Elution of pesticide residues <b>93</b> and <b>94</b> in food with AcOH/Et <sub>2</sub> O, derivatization, cleaning by GPC. LOD were 0.02 ppm <b>93</b> and 0.05 ppm <b>94</b> . Better results are obtained for derivatization with <i>n</i> -PenMgBr <sup>323</sup> .	EtMgBr	AED <sup>324</sup> FPD <sup>323, 325, 326</sup>
Et <sub>3</sub> SnBr, Bu <sub>3</sub> SnBr, Me <sub>4</sub> Sn, Et <sub>4</sub> Sn, cyhexatin ( <b>93</b> ), fenbutatin oxide ( <b>94</b> ). General procedure <sup>327, 328</sup> . Elution of pesticide residues <b>93</b> and <b>94</b> in crops with HCl/Me <sub>2</sub> CO, transfer to CH <sub>2</sub> Cl <sub>2</sub> , cleaning by GPC <sup>329</sup> . Better results are obtained for derivatization with <i>n</i> -PenMgBr <sup>323</sup> .	<i>n</i> -PrMgCl	FFGD-MSD <sup>328</sup> FPD <sup>323, 329</sup>
MeSnCl <sub>3</sub> , Me <sub>2</sub> SnCl <sub>2</sub> , Me <sub>3</sub> SnCl, BuSnCl <sub>3</sub> , Bu <sub>2</sub> SnCl <sub>2</sub> , Bu <sub>3</sub> SnCl, PhSnCl <sub>3</sub> , Ph <sub>2</sub> SnCl <sub>2</sub> , Ph <sub>3</sub> SnCl. General review <sup>330</sup> . Simultaneous determination of Sn, Pb and Hg organometallics <sup>331</sup> . Contamination analysis of various items: (i) Antarctic bivalve <i>Adamussium colbecki</i> <sup>332</sup> ; (ii) water <sup>333</sup> ; (iii) fish and marine sediments, digestion with concentrated HCl, LLE with <b>89</b> /PenH <sup>334</sup> ; (iv) mussels and marine sediments; higher sensitivity for the <i>n</i> -pentyl than for the <i>n</i> -propyl derivatives; better recoveries for the <i>n</i> -pentyl than for the methyl or <i>n</i> -propyl derivatives <sup>335</sup> ; (v) lard, MeSn(Pr- <i>n</i> ) <sub>3</sub> as internal standard for FPD <sup>336</sup> ; (vi) sediments after LLE with <b>91</b> <sup>318</sup> ; (vii) sediments after SFE <sup>337</sup> ; (viii) occupational exposure to organotin compounds in particulates or as vapors <sup>338</sup> ; (ix) water and sediments. No difference was observed for the FPD <sup>339</sup> , AAS or AES <sup>340</sup> results after pentylation of the alkyltin compounds with <i>n</i> -PenMgBr or ethylation with NaBEt <sub>4</sub> ; however, slightly better results were reported for the Grignard reagent <sup>323</sup> .	<i>n</i> -PenMgBr	EI-MSD <sup>330, 332, 333</sup> PCI-MSD <sup>330</sup> EI-MS-MSD <sup>335</sup> FPD <sup>323, 330, 336, 339</sup> AED <sup>318, 331, 337, 338, 340, 341</sup> ETAAS <sup>340</sup> FAAS <sup>334</sup>
MeSnCl <sub>3</sub> , Me <sub>2</sub> SnCl <sub>2</sub> , Me <sub>3</sub> SnCl. (i) Determination in wastewaters includes LLE with CH <sub>2</sub> Cl <sub>2</sub> , and	<i>n</i> -HexMgBr	FPD



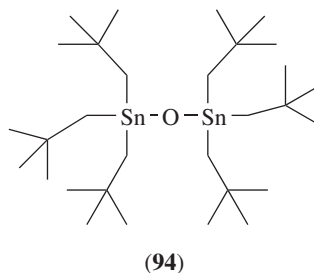
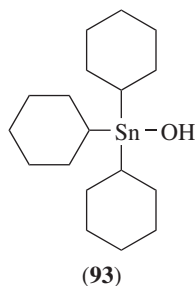
TABLE 2. (continued)

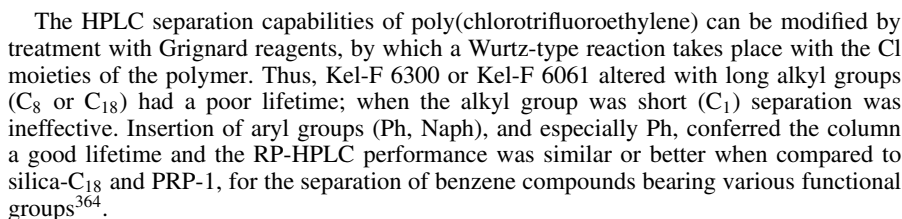
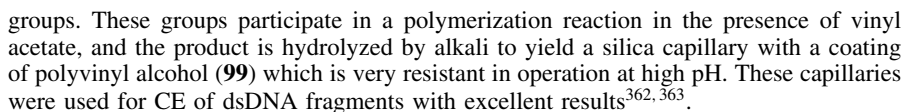
Analytes and comments	Grignard reagent	Detection method
evaluation of an efficiency factor for the extraction <sup>342</sup> ; (ii) ppb levels in seawater, tissues and marine sediments, homogenization in acid, LLE with CH <sub>2</sub> Cl <sub>2</sub> ; LOD in tissues and sediments were 0.29, 0.12 and 0.1 ng for mono-, di- and tributyltin, respectively <sup>343</sup> .		
<i>Arsenic compounds</i>		
As(III) and As(V) compounds. Comparison with derivatization with <i>N</i> - <i>t</i> -butyldimethylsilyl- <i>N</i> -methyltrifluoroacetamide with 1% <i>t</i> -butyldimethylchlorosilane <sup>344</sup> .	4-FC <sub>6</sub> H <sub>4</sub> MgBr	EI-MSD PCI-MSD NCI-MSD
<i>Lead compounds</i>		
Me <sub>2</sub> PbCl <sub>2</sub> , Et <sub>2</sub> PbCl <sub>2</sub> , Me <sub>3</sub> PbCl, Et <sub>3</sub> PbCl, Me <sub>4</sub> Pb, Et <sub>4</sub> Pb. LLE from water with <b>91</b> /HexH, derivatization with <i>n</i> -Pr groups gave better resolution than with <i>n</i> -Bu groups <sup>345</sup> .	<i>n</i> -PrMgCl	AAS <sup>345</sup>
Pb(II), Me <sub>2</sub> PbCl <sub>2</sub> , Me <sub>3</sub> PbCl, Et <sub>2</sub> PbCl <sub>2</sub> , Et <sub>3</sub> PbCl, Et <sub>4</sub> Pb, Bu <sub>4</sub> Pb. Determination of organolead compounds in airborne particulates; Et <sub>4</sub> Pb as internal standard <sup>346</sup> . Derivatization was performed after preconcentration of water pollutants on polymer beads functionalized with dithizone ( <b>90</b> ) groups <sup>347</sup> . LLE from water with <b>91</b> /HexH, derivatization with <i>n</i> -Pr groups gave better resolution than with <i>n</i> -Bu groups <sup>345</sup> . Determination of Pb(II) and organolead compounds in human urine, after LLE of the complexes with <b>91</b> and derivatization; Et <sub>4</sub> Pb as internal standard <sup>348</sup> . The aqueous solution is evaporated to dryness, the solid residue is derivatized and the alkylated Pb was evaporated into an ETAAS instrument; the LOD (SNR 2) was 7 ppb <sup>349</sup> .	<i>n</i> -BuMgCl	ICP-MSD <sup>346</sup> SIM-MSD <sup>348</sup> AAS <sup>345, 347</sup> ETAAS <i>a</i> <sup>349</sup>
Me <sub>3</sub> PbCl, Me <sub>3</sub> PbAc, Et <sub>3</sub> PbAc, Pr <sub>3</sub> PbAc, Me <sub>2</sub> PbAc <sub>2</sub> , Et <sub>2</sub> PbAc <sub>2</sub> , Pr <sub>2</sub> PbAc <sub>2</sub> . Simultaneous determination of Sn, Pb and Hg organometallics <sup>331</sup> . Determination of organotin and organolead pollutants in environmental sediments after LLE with <b>91</b> solution and derivatization <sup>318</sup> .	<i>n</i> -PenMgBr	AED <sup>318, 331</sup>
Pb. Determination in urine and whole blood by isotope dilution. An aliquot of <sup>204</sup> Pb is added to a urine or blood sample and digested with HNO <sub>3</sub> /H <sub>2</sub> O <sub>2</sub> , the residue is dissolved with lithium bis(trifluoroethyl)dithiocarbamate ( <b>95</b> ) to give chelate <b>96a</b> , which yields the volatile <b>97a</b> after derivatization with the Grignard reagent. Total Pb by AAS; <sup>204</sup> Pb/ <sup>206</sup> Pb, <sup>204</sup> Pb/ <sup>207</sup> Pb and <sup>204</sup> Pb/ <sup>208</sup> Pb isotope ratios by MSD (see equation 7R718) <sup>350</sup> .	4-FC <sub>6</sub> H <sub>4</sub> MgBr	EI-SIM-MSD TE-AAS

(continued overleaf)

TABLE 2. (continued)

Analytes and comments	Grignard reagent	Detection method
<i>Antimony compounds</i>		
Sb(III) compounds, Ph <sub>3</sub> Sb. After extraction with <b>92</b> solution, evaporation to dryness and derivatization.	PhMgBr	TE-AAS <sup>319</sup>
<i>Mercury compounds</i>		
MeHgCl, inorganic Hg(II). Extraction of MeHgCl from sediments by SFE or steam distillation, derivatization and end analysis <sup>351</sup> .	<i>n</i> -BuMgCl	DIN-ICP-MSD MIP-AED
MeHgCl, EtHgCl, PhHgOAc, C <sub>7</sub> H <sub>15</sub> HgCl, (Me <sub>3</sub> SiCH <sub>2</sub> ) <sub>2</sub> Hg, Ph <sub>2</sub> Hg. Simultaneous determination of Sn, Pb and Hg organometallics <sup>331</sup> .	<i>n</i> -PenMgBr	AED
<i>Cadmium compounds</i>		
Cd(II). The aqueous solution is evaporated to dryness, the solid residue is derivatized and the alkylated Cd is evaporated and carried into an ICP-AES instrument; the LOD was 11 pg <sup>352</sup> .	EtMgCl	ICP-AES <sup>a</sup>
<i>Gallium compounds</i>		
Ga(III). The aqueous solution is evaporated to dryness, the solid residue is derivatized and the alkylated Ga is evaporated and carried into an ICP-AES instrument; the LOD was 1.9 ng <sup>353</sup> .	EtMgCl	ICP-AES <sup>a</sup>
<i>Tellurium compounds</i>		
Te(IV) and other forms. Determination of Te in urine by isotope dilution after intake of the antitumor drug AS 101 ( <b>98</b> ). An aliquot of <sup>120</sup> Te is added to a urine sample and digested with HNO <sub>3</sub> /H <sub>2</sub> O <sub>2</sub> , the residue is dissolved with a solution of <b>95</b> to give chelate <b>96b</b> , which yields the volatile <b>97b</b> after derivatization with the Grignard reagent. End analysis of total Te by AAS and <sup>120</sup> Te/ <sup>130</sup> Te isotope ratio by MSD (see equation 7R718) <sup>354</sup> .	4-FC <sub>6</sub> H <sub>4</sub> MgBr	EI-SIM-MSD TE-AAS

<sup>a</sup> End analysis without GC separation.



## 2. Electrochemical behavior

EtMgBr solutions in poly(ethylene oxide) containing a small amount of THF or Et<sub>2</sub>O are electrically conducting. Best conductivity is achieved for an ethylene oxide–Mg ratio of 4, e.g. 0.1 mS cm<sup>−1</sup> at 40 °C was found. In contrast, PEO solutions of MgCl<sub>2</sub>, Mg(ClO<sub>4</sub>)<sub>2</sub> or Mg(SCN)<sub>2</sub> show only low electrical conduction below 100 °C. Furthermore, in the presence of EtMgBr solutions Mg can be deposited by cathodic reduction or dissolved by anodic oxidation. Practical application of these solutions are limited by their low thermal and electrochemical stability<sup>365</sup>.

## VI. REFERENCES

1. J. Durlach, N. Pages, P. Bac, M. Bara and A. Guet-Bara, *Magnesium Res.*, **17**, 163 (2004).
2. V. Grignard, *Ann. Chim.*, **24**, 433 (1901); V. Grignard, *Notice sur les Titres et Travaux Scientifiques de M. V. Grignard*, Imprimerie J. Marlhens, Lyon, 1926; (<http://gallica.bnf.fr/ark:/12148/bpt6k90654d>); J. J. Eisch, *Organometallics*, **21**, 5439 (2002).
3. F. Bickelhaupt, *Chem. Soc. Rev.*, **28**, 17 (1999).
4. F. Bickelhaupt, in *Grignard Reagents* (Ed. H. G. Richey, Jr.), Wiley, Chichester, 2000, pp. 367–393.
5. V. V. Smirnov, L. A. Tjurina and I. P. Beletskaya, in *Grignard Reagents* (Ed. H. G. Richey, Jr.), Wiley, Chichester, 2000, pp. 395–410.
6. O. G. Kulinkovich, *Pure Appl. Chem.*, **72**, 1715 (2000).
7. P. Knochel, E. Hupe and H. Houté, *Actualite Chim.*, **12** (2003).
8. P. Knochel, W. Dohle, N. Gommermann, F. F. Kneisel, F. Kopp, T. Korn, I. Sapountzis and V. A. Vu, *Angew. Chem. Int. Ed.*, **42**, 4302 (2003).
9. H. Shinokubo and K. Oshima, *Eur. J. Org. Chem.*, 2081 (2004).
10. H. Ila, O. Baron, A. J. Wagner and P. Knochel, *Chem. Lett.*, **35**, 2 (2006).
11. H. Ila, O. Baron, A. J. Wagner and P. Knochel, *Chem. Commun.*, 583 (2006).
12. I. L. Cameron and N. K. Smith, *Scanning Electron Microsc. Pt. 2*, 463 (1980).
13. K. M. Kim, H. B. Alpaugh and F. B. Johnson, *Scanning Electron Microsc. Pt. 3*, 1239 (1985).
14. U. Oesch, D. Ammann and W. Simon, *Clin. Chem.*, **32**, 1448 (1986).
15. G. J. Kost, *Crit. Rev. Clin. Lab. Sci.*, **30**, 153 (1993).
16. N. Fogh-Andersen and O. Siggaard-Andersen, *Scand. J. Clin. Lab. Invest. Suppl.*, **217**, 89 (1994).
17. M. A. Olerich and R. K. Rude, *New Horiz.*, **2**, 186 (1994).
18. B. T. Altura, *Scand. J. Clin. Lab. Invest. Suppl.*, **217**, 5 (1994).
19. B. T. Altura, J. L. Burack, R. Q. Cracco, L. Galland, S. M. Handwerker, M. S. Markell, A. Mauskop, Z. S. Memon, L. M. Resnick, Z. Zisbrod *et al.*, *Scand. J. Clin. Lab. Invest. Suppl.*, **217**, 53 (1994).
20. B. M. Altura and B. T. Altura, *Scand. J. Clin. Lab. Invest. Suppl.*, **224**, 211 (1996).
21. N. E. Saris, E. Mervaala, H. Karppanen, J. A. Khawaja and A. Lewenstam, *Clin. Chim. Acta*, **294**, 1 (2000).
22. A. P. Somlyo and H. Shuman, *Ultramicroscopy*, **8**, 219 (1982).
23. R. Y. Tsien, *Ann. Rev. Biophys. Bioeng.*, **12**, 91 (1983).
24. R. K. Gupta, P. Gupta and R. D. Moore, *Ann. Rev. Biophys. Bioeng.*, **13**, 221 (1984).
25. R. E. London, *Ann. Rev. Physiol.*, **53**, 241 (1991).
26. H. Koppel, R. Gasser and U. Spichiger, *Wien. Med. Wochenschr.*, **150**, 321 (2000).
27. B. B. Silver, *J. Am. Coll. Nutr.*, **23**, 732S (2004).
28. W. E. Wacker, *Magnesium*, **6**, 61 (1987).
29. R. J. Elin, *Magnesium Trace Elem.*, **10**, 172 (1991–1992).
30. W. R. Kulpmann, *Wien. Klin. Wochenschr., Suppl.*, **192**, 37 (1992).
31. G. A. Quamme, *Clin. Lab. Med.*, **13**, 209 (1993).
32. E. Murphy, *Miner. Electrolyte Metab.*, **19**, 250 (1993).
33. H. Millart, V. Durlach and J. Durlach, *Magnesium Res.*, **8**, 65 (1995).
34. C. Ritter, M. Ghahramani and H. J. Marsoner, *Scand. J. Clin. Lab. Invest. Suppl.*, **224**, 275 (1996).
35. G. Chittleborough, *Sci. Total Environ.*, **14**, 53 (1980).
36. C. Baluja-Santos, A. Gonzalez-Portal and F. Bermejo-Martinez, *Analyst*, **109**, 797 (1984).
37. W. Merlevede, J. R. Vandenheede, J. Goris and S. D. Yang, *Curr. Top. Cell. Regul.*, **23**, 177 (1984).
38. R. A. Reinhart, *Arch. Intern. Med.*, **148**, 2415 (1988).
39. G. Baltzer, *Med. Klin. (Munich)*, **83**, 370 (1988).
40. O. Ferment and Y. Touitou, *Presse Med.*, **17**, 584 (1988).
41. R. J. Elin, *Dis.-Mon.*, **34**, 161 (1988).
42. L. Paunier, *Monatsschr. Kinderheilkd.*, **140** (Suppl. 1), S17 (1992).
43. H. Benech and J. M. Grognet, *Magnesium Res.*, **8**, 277 (1995).
44. R. Mehrotra, K. D. Nolph, P. Kathuria and L. Dotson, *Am. J. Kidney Dis.*, **29**, 106 (1997).
45. R. Whang, *Comp. Ther.*, **23**, 168 (1997).

46. W. Vierling, *Herz*, **22** (Suppl 1), 3 (1997).
47. A. M. Romani and A. Scarpa, *Front. Biosci.*, **5**, D720 (2000).
48. M. D. Yago, M. Manas and J. Singh, *Front. Biosci.*, **5**, D602 (2000).
49. S. Iannello and F. Belfiore, *Panminerva Med.*, **43**, 177 (2001).
50. J. Durlach, N. Pages, P. Bac, M. Bara and A. Guiet-Bara, *Magnesium Res.*, **15**, 49 (2002).
51. M. E. Maguire and J. A. Cowan, *Biometals*, **15**, 203 (2002).
52. R. D. Grubbs, *Biometals*, **15**, 251 (2002).
53. A. M. P. Romani and M. E. Maguire, *Biometals*, **15**, 271 (2002).
54. J. Durlach, N. Pages, P. Bac, M. Bara and A. Guiet-Bara, *Magnesium Res.*, **15**, 203 (2002).
55. K. P. Schlingmann and T. Gudermann, *J. Physiol.*, **566** (Pt. 2), 301 (2005).
56. V. Chubakov, T. Gudermann and K. P. Schlingmann, *Eur. J. Physiol.*, **451**, 228 (2005).
57. F. H. Nielsen and H. C. Lukaski, *Magnesium Res.*, **19**, 180 (2006).
58. F. I. Wolf and A. Cittadini, *Front. Biosci.*, **4**, D607 (1999).
59. T. L. Barton, *Poultry Sci.*, **75**, 854 (1996).
60. P. W. Flatman, *Magnesium Res.*, **1**, 5 (1988).
61. J. G. Henrotte, *Magnesium*, **7**, 306 (1988).
62. M. Gawaz, *Fortschr. Med.*, **114**, 329 (1996).
63. T. Gunther, *Magnesium Res.*, **19**, 190 (2006).
64. S. J. Scheinman, L. M. Guay-Woodford, R. V. Thakker and D. G. Warnock, *New Eng. J. Med.*, **340**, 1177 (1999).
65. I. C. Meij, L. P. van den Heuvel and N. V. Knoers, *Adv. Nephrol. Necker Hosp.*, **30**, 163 (2000).
66. N. V. A. M. Knoers, J. C. de Jong, I. C. Meij, L. P. W. J. van den Heuvel and R. J. M. Bindels, *J. Nephrol.*, **16**, 293 (2003).
67. K. P. Schlingmann, M. Konrad and H. W. Seyberth, *Pediatr. Nephrol.*, **19**, 13 (2004).
68. F. C. Driessens, *Z. Naturforsch. C*, **35**, 357 (1980).
69. R. A. Terpstra and F. C. Driessens, *Calcif. Tissue Int.*, **39**, 348 (1986).
70. J. J. Steichen and W. W. Koo, *Monatsschr. Kinderheilkd.*, **140** (Suppl. 1), S21 (1992).
71. M. E. Morris, *Magnesium Res.*, **5**, 303 (1992).
72. Y. Liu and J. Zhang, *Chin. Med. J.*, **113**, 948 (2000).
73. M. J. Cevette, J. Vormann and K. Franz, *J. Am. Acad. Audiol.*, **14**, 202 (2003).
74. G. A. Quamme, *Magnesium*, **5**, 248 (1986).
75. G. A. Quamme, *Kidney Int.*, **52**, 1180 (1997).
76. D. Juan, *Surgery*, **91**, 510 (1982).
77. R. J. Elin, *Clin. Chem.*, **33**, 1965 (1987).
78. E. Ryzén, K. L. Servis and R. K. Rude, *J. Am. Coll. Nutr.*, **9**, 114 (1990).
79. R. Whang, D. D. Whang, K. W. Ryde and T. O. Oei, *Magnesium Res.*, **3**, 267 (1990).
80. J. W. Van Hook, *Crit. Care Clin.*, **7**, 215 (1991).
81. M. Salem, R. Munoz and B. Chernow, *Crit. Care Clin.*, **7**, 225 (1991).
82. M. F. Ryan, *Ann. Clin. Biochem.*, **28** (Pt. 1), 19 (1991).
83. E. L. Tso and R. A. Barish, *J. Emergency Med.*, **10**, 735 (1992).
84. R. Whang, E. M. Hampton and D. D. Whang, *Ann. Pharmacother.*, **28**, 220 (1994).
85. N. Dhupa and J. Proulx, *Vet. Clin. North Am.*, **28**, 587 (1998).
86. M. F. Ryan and H. Barbour, *Ann. Clin. Biochem.*, **35** (Pt. 4), 449 (1998).
87. Z. S. Agus, *J. Am. Soc. Nephrol.*, **10**, 1616 (1999).
88. G. T. Sanders, H. J. Huijgen and R. Sanders, *Clin. Chem. Lab. Med.*, **37**, 1011 (1999).
89. J. M. Topf and P. T. Murray, *Rev. Endocr. Metab. Disorders*, **4**, 195 (2003).
90. D.-H. Liebscher and D.-E. Liebscher, *J. Am. Coll. Nutr.*, **23**, 730S (2004).
91. M. Gonella and G. Calabrese, *Magnesium Res.*, **2**, 259 (1989).
92. H. O. Garland, *Magnesium Res.*, **5**, 193 (1992).
93. C. S. Leach, *Microgravity Q.*, **2**, 69 (1992).
94. L. Tosiello, *Arch. Intern. Med.*, **156**, 1143 (1996).
95. H. W. de Valk, *Neth. J. Med.*, **5**, 139 (1999).
96. C. Hermes Sales and L. de F. Campos Pedrosa, *Clin. Nutr.*, **25**, 554 (2006).
97. B. M. Altura and B. T. Altura, *Magnesium*, **4**, 226 (1985).
98. B. M. Altura and B. T. Altura, *Magnesium*, **4**, 245 (1985).
99. R. Whang, *Magnesium*, **5**, 127 (1986).
100. L. T. Iseri, *Magnesium*, **5**, 111 (1986).

101. L. M. Resnick, *Am. J. Med.*, **93** (A), 11S (1992).
102. J. Durlach, V. Durlach, Y. Rayssiguier, M. Bara and A. Guiet-Bara, *Magnesium Res.*, **5**, 147 (1992).
103. M. A. Arsenian, *Prog. Cardiovasc. Dis.*, **35**, 271 (1993).
104. H. S. Rasmussen, *Dan. Med. Bull.*, **40**, 84 (1993).
105. C. V. Leier, L. Dei Cas and M. Metra, *Am. Heart J.*, **128**, 564 (1994).
106. J. McCord and S. Borzak, *Hosp. Pract.*, **29**, 47, 53, 57 (1994).
107. C. G. Osborne, R. B. McTyre, J. Dudek, K. E. Roche, R. Scheuplein, B. Silverstein, M. S. Weinberg and A. A. Salkeld, *Nutr. Rev.*, **54**, 365 (1996).
108. T. L. Shirey, *J. Anesth.*, **18**, 118 (2004).
109. A. Hordyjewska and K. Pasternak, *Ann. Univ. Mariae Curie-Sklodowska, Sect. D*, **59**, 108 (2004).
110. W. Bobkowski, A. Nowak and J. Durlach, *Magnesium Res.*, **18**, 35 (2005).
111. R. Rylander, *Clin. Calcium*, **15**, 11 (2005).
112. L. D. Lewis and M. L. Morris, Jr., *Vet. Clin. North Am.*, **14**, 513 (1984).
113. J. J. Pahira, *Urol. Radiol.*, **6**, 74 (1984).
114. M. Labeeuw and N. Pozet, *Magnesium Res.*, **1**, 187 (1988).
115. T. D. Mountokalakis, *Magnesium Res.*, **3**, 121 (1990).
116. O. Richard and M. T. Freycon, *Pediatric*, **47**, 557 (1992).
117. S. Ekane, T. Wildschutz, J. Simon and C. C. Schulman, *Acta Urol. Belg.*, **65**, 1 (1997).
118. G. B. Fedoseev, A. B. Emel'ianov, V. A. Goncharova, K. K. Malakauskas, V. L. Emanuel' and T. M. Sinitsyna, *Klin. Med. (Moscow)*, **72**, 13 (1994).
119. A. Castillo and L. A. Ordóñez, *Acta Cient. Venez.*, **32**, 123 (1981).
120. R. Masironi and A. G. Shaper., *Ann. Rev. Nutr.*, **1**, 375 (1981).
121. T. Hazell, *World Rev. Nutr. Diet.*, **46**, 1 (1985).
122. J. R. Marier, *Magnesium*, **5**, 1 (1986).
123. I. E. Dreosti, *Nutr. Rev.*, **53** (Pt. 2), S23 (1995).
124. B. Lonnerdal, *Physiol. Rev.*, **77**, 643 (1997).
125. T. Clausen and I. Dorup, *Bibl. Nutr. Dieta*, [54], 84 (1998).
126. J. P. Goff, *Food Animal Pract.*, **15**, 619 (1999).
127. J. G. Dorea, *J. Am. Coll. Nutr.*, **19**, 210 (2000).
128. L. K. Massey, *J. Nutr.*, **131**, 1875 (2001).
129. F. Gaucheron, *Reprod. Nutr. Dev.*, **45**, 473 (2005).
130. S. Monarca, F. Donato, I. Zerbini, R. L. Calderon and F. F. Craun, *Eur. J. Cardiovasc. Prev. Rehabil.*, **13**, 495 (2006).
131. M. S. Seelig, *Magnesium Res.*, **3**, 197 (1990).
132. L. Spatling, *Gynakol.-geburtshilfliche Rundschau*, **33**, 85 (1993).
133. F. Mimouni and R. C. Tsang, *Magnesium Res.*, **4**, 109 (1991).
134. G. L. Klein and D. N. Herndon, *Magnesium Res.*, **11**, 103 (1998).
135. R. Mittendorf, P. G. Pryde, R. J. Elin, J. G. Gianopoulos and K.-S. Lee, *Magnesium Res.*, **15**, 253 (2002).
136. R. B. Costello and P. B. Moser-Veillon, *Magnesium Res.*, **5**, 61 (1992).
137. M. P. Vaquero, *J. Nutr. Health Aging*, **6**, 147 (2002).
138. X. Boman, T. Guillaume and J. M. Krzesinski, *Rev. Med. Liege*, **58**, 104 (2003).
139. S. Onishi and S. Yoshino, *Intern. Med.*, **45**, 207 (2006).
140. M. P. Ryan, *Magnesium*, **5**, 282 (1986).
141. H. Lajer and G. Daugaard, *Cancer Treat. Rev.*, **25**, 47 (1999).
142. L. E. Ramsay, W. W. Yeo and P. R. Jackson, *Cardiology*, **84** (Suppl. 2), 48 (1994).
143. K. L. Woods, *Br. J. Clin. Pharmacol.*, **32**, 3 (1991).
144. J. Atsmon and E. Dolev, *Drug Safety*, **28**, 763 (2005).
145. R. Vink and I. Cernak, *Front. Biosci.*, **5**, D656 (2000).
146. M. S. Kharasch and O. Reimuth, *Grignard Reactions of Nonmetallic Substances*, Prentice Hall, New York, 1954, p. 91.
147. A. V. Nemukhin, I. A. Topol and F. Weinhold, *Inorg. Chem.*, **34**, 2980 (1995).
148. U. Casellato and F. Ossola, *Organometallics*, **13**, 4105 (1994).
149. R. G. Martinek, *J. Am. Med. Technol.*, **36**, 241 (1974).
150. H. G. Seiler, *Met. Ions Biol. Syst.*, **26**, 611 (1990).

151. D. M. Templeton, F. Ariese, R. Cornelis, L.-G. Danielsson, H. Muntau, H. P. van Leeuwen and R. Łoibiński, *Pure Appl. Chem.*, **72**, 1453 (2000).
152. A. Liparini, S. Carvalho and J. C. Belchior, *Clin. Chem. Lab. Med.*, **43**, 939 (2005).
153. B. T. Altura and B. M. Altura, *Scand. J. Clin. Lab. Invest. Suppl.*, **217**, 83 (1994).
154. A. Jensen and E. Riber, *Metal Ions Biol. Syst.*, **16**, 151 (1983).
155. N.-E. L. Saris, E. Mervaala, H. Karppanen, J. A. Khawaja and A. Lewenstam, *Clin. Chim. Acta*, **294**, 1 (2000).
156. E. J. Park, M. Brasuel, C. Behrend, M. A. Philbert and R. Kopelman, *Anal. Chem.*, **75**, 3784 (2003).
157. M. Kimura, K. Honda, A. Takeda, M. Imanishi and T. Takeda, *J. Am. Coll. Nutr.*, **23**, 748S (2004).
158. H. M. Barbour and W. Davidson, *Clin. Chem.*, **34**, 2103 (1988).
159. C. S. Shin, C. H. Chang and J.-H. Kim, *Yonsei Med. J.*, **47**, 191 (2006).
160. D. R. Banatao, R. B. Altman and T. E. Klein, *Nucleic Acids Res.*, **31**, 4450 (2003).
161. S. B. Yasar and Ş. Güçer, *Anal. Chim. Acta*, **505**, 43 (2004).
162. C. Jiwoua Ngounou, R. Ndjouenkeu, C. M. F. Mbofung and L. Noubi, *J. Food Eng.*, **57**, 301 (2003).
163. *Compendium of Methods for Chemical Analysis of Foods*, Bureau of Chemical Safety, Health Products and Food Branch, Health Canada, Ottawa, Ont., Canada, Method LPFC-137 (1985). ([http://www.hc-sc.gc.ca/fn-an/res-rech/analy-meth/chem/reg\\_prep\\_dry\\_ashing-reg\\_prep\\_echantillons\\_calcination\\_e.html](http://www.hc-sc.gc.ca/fn-an/res-rech/analy-meth/chem/reg_prep_dry_ashing-reg_prep_echantillons_calcination_e.html)).
164. J. Moreda-Piñeiro, E. Beceiro-González, E. Alonso-Rodríguez, E. González-Soto, P. López-Mahía, S. Muniategui-Lorenzo and D. Prada-Rodríguez, *At. Spectrosc.*, **22**, 422 (2001).
165. A. R. Shirazi and O. Lindqvist, *Fuel*, **72**, 125 (1993).
166. P. Cunniff (Ed.), *Official Methods of Analysis of AOAC International*, AOAC International, Gaithersburg, MD, USA, 1996, (a) Chap. 50, pp. 15–16; (b) Chap. 2, pp. 25–26; (c) Chap. 11, pp. 15–16; (d) Chap. 33, pp. 60–61; (e) Chap. 2, pp. 30–31.
167. L. M. Coelho, E. R. Pereira-Filho and M. A. Z. Arruda, *Quim. Anal.*, **20**, 243 (2002); *Chem. Abstr.*, **137**, 43744 (2002).
168. R. Moreno-Torres, M. Navarro, M. D. Ruiz-López, R. Artacho and C. López, *Lebens. Wiss. Technol.*, **33**, 397 (2000).
169. L. Liu, P. Li, Y. Li and L. Sun, *Guangpuxue Yu Guangpu Fenxi*, **21**, 560 (2001); *Chem. Abstr.*, **135**, 315474 (2001).
170. A. V. Filgueiras, J. L. Capelo, I. Lavilla and C. Bendicho, *Talanta*, **53**, 433 (2000).
171. F. Sugimoto, *Sen'i Gakkaishi*, **59**, 304 (2003); *Chem. Abstr.*, **140**, 340647 (2004).
172. K. L. Sahrawat, G. Ravi Kumar and J. K. Rao, *Commun. Soil Sci. Plant Anal.*, **33**, 95 (2002).
173. K. L. Sahrawat, G. Ravi Kumar and K. V. S. Murthy, *Commun. Soil Sci. Plant Anal.*, **33**, 3757 (2002).
174. L. Lin and L. Zhu, *Fenxi Huaxue*, **30**, 819 (2002); *Chem. Abstr.*, **137**, 311443 (2002).
175. L. A. Powell and R. L. Tease, *Anal. Chem.*, **54**, 2154 (1982).
176. X. Ou, T. Lin, P. Wang, L. Jiang and L. Li, *Guang pu xue yu guang pu fen xi*, **20**, 79 (2000); *PubMed ID*, 12953457.
177. J. Chang, *Yejin Fenxi*, **21**, 65 (2001); *Chem. Abstr.*, **136**, 111798 (2002).
178. K. Watanabe, T. Okada and M. Itagaki, *Bunseki Kagaku*, **52**, 55 (2003); *Chem. Abstr.*, **138**, 146813 (2003).
179. Dionex, *Anion Micromembrane Suppressor<sup>®</sup> III—Cation Micromembrane Suppressor<sup>®</sup> III*, Product Manual, Document No. 031727, Dionex Corporation, 2004. ([http://www1.dionex.com/en-us/webdocs/4366\\_31727-03\\_MMS\\_Combined\\_V21.pdf](http://www1.dionex.com/en-us/webdocs/4366_31727-03_MMS_Combined_V21.pdf)).
180. J. E. Van Nuwenborg, D. Stöckl and L. M. Thienpont, *J. Chromatogr. A*, **770**, 137 (1997).
181. R. García-Fernández, J. I. García-Alonso and A. Sanz-Medel, *J. Chromatogr. A*, **1033**, 127 (2004).
182. M. C. Bruzzoniti, E. Mentasti and C. Sarzanini, *Anal. Chim. Acta*, **382**, 291 (1999).
183. B.-S. Yu, Q.-G. Yuan, L.-H. Nie and S.-Z. Yao, *J. Pharm. Biomed. Anal.*, **25**, 1027 (2001); erratum, *J. Pharm. Biomed. Anal.*, **29**, 969 (2002).
184. B. Godlewska-Żyłkiewicz, B. Leśniowska and A. Hulanicki, *Anal. Chim. Acta*, **358**, 185 (1998).
185. F. Umland, *Fresenius Z. Anal. Chem.*, **190**, 186 (1962).
186. T. Takeuchi, S. Inoue and T. Miwa, *J. Microcolumn Sep.*, **12**, 450 (2000).

187. T. Takeuchi, S. Inoue, M. Yamamoto, M. Tsuji and T. Miwa, *J. Chromatogr. A*, **910**, 373 (2001).
188. E. Nemutlu and N. Özaltın, *Anal. Bioanal. Chem.*, **383**, 833 (2005).
189. S. Motellier, S. Petit and P. Decambox, *Anal. Chim. Acta*, **410**, 11 (2000).
190. M. Maj-Żurawska, *Chem. Anal. (Warsaw)*, **42**, 187 (1997).
191. H. E. van Ingen, H. J. Hutjgen, W. T. Kok and G. T. B. Sanders, *Clin. Chem.*, **40**, 52 (1994).
192. A. Malon, B. Wagner, E. Bulska and M. Maj-Żurawska, *Anal. Biochem.*, **302**, 220 (2002).
193. Z. Cao, C. Tongate and R. J. Elin, *Scand. J. Clin. Lab. Invest.*, **61**, 389 (2001).
194. Nova Biomedical, *Nova Electrolyte/Chemistry Analyzers*, Nova Biomedical Corporation, Waltham, MA, USA. (<http://www.novabiomedical.com/clinical/electrolyte.html#top>).
195. S. Unterer, H. Lutz, B. Gerber, T. M. Glaus, M. Hässig and C. E. Reusch, *Am. J. Vet. Res.*, **65**, 183 (2004).
196. S. Unterer, B. Gerber, T. M. Glaus, M. Hässig and C. E. Reusch, *Vet. Res. Commun.*, **29**, 647 (2005).
197. J. Wang, P. A. M. Farias and J. S. Mahmoud, *Anal. Chim. Acta*, **172**, 57 (1985).
198. A. M. M. Ali, O. A. Farghaly and M. A. Ghandour, *Anal. Chim. Acta*, **412**, 99 (2000).
199. O. A. Farghaly, *Talanta*, **63**, 497 (2004).
200. N. Abo El-Maali, D. Abd El-Hady, M. Abd El-Hamid and M. M. Seliem, *Anal. Chim. Acta*, **417**, 67 (2000).
201. M. C. Cheney, D. J. Curran and K. S. Fletcher III, *Anal. Chem.*, **52**, 942 (1980).
202. X. Zhou, L. Wang, Y. Zeng, G. Lu and P. Zhen, *J. AOAC Int.*, **89**, 782 (2006).
203. Z. Jońca and W. Lewandowski, *Pol. J. Environ. Stud.*, **13**, 275 (2004).
204. Z. Jońca and W. Lewandowski, *Pol. J. Environ. Stud.*, **13**, 281 (2004).
205. Y. Bai, J. M. Ouyang, Y. Bai and M. L. Chen, *Guangpuxue Yu Guangpu Fenxi*, **24**, 1016 (2004); *Chem. Abstr.*, **142**, 193656 (2005).
206. Z. Kiliç, O. Acar, M. Ulaşan and M. İlim, *Food Chem.*, **76**, 107 (2002).
207. T. Papageorgiou, D. Zacharoulis, D. Xenos and G. Androulakis, *Nutrition*, **18**, 32 (2002).
208. A. Abarca, E. Canfranc, I. Sierra and M. L. Marina, *J. Pharm. Biomed. Anal.*, **25**, 941 (2001).
209. M.-C. Lin, Y.-L. Huang, H.-W. Liu, D.-Y. Yang, J.-B. Lee and F.-C. Cheng, *J. Am. Coll. Nutr.*, **23**, 556S (2004).
210. L. E. Walther, K. Winnefeld and O. Sölch, *J. Trace Elements Med. Biol.*, **14**, 92 (2000).
211. M.-C. Lin, Y.-L. Huang, H.-W. Liu, D.-Y. Yang, C.-P. Lee, L.-L. Yang and F.-C. Cheng, *J. Am. Coll. Nutr.*, **23**, 561S (2004).
212. D.-Y. Yang, J.-B. Lee, M.-C. Lin, Y.-L. Huang, H.-W. Liu, Y.-J. Liang and F.-C. Cheng, *J. Am. Coll. Nutr.*, **23**, 552S (2004).
213. M. Pistón, I. Dol and M. Knochen, *J. Autom. Methods Manage. Chem.*, Article ID 47627 (2006). (<http://www.hindawi.com/GetArticle.aspx?doi=10.1155/JAMMC/2006/47627>).
214. N. Dilsiz, A. Olcucu and M. Atas, *Cell Biochem. Funct.*, **18**, 259 (2000).
215. E. Kilic, A. Demiroglu, R. Saraymen and E. Ok, *J. Trace Elem. Exp. Med.*, **17**, 175 (2004).
216. Z. Yang, X. Hou, B. T. Jones, D. C. Sane, M. J. Thomas and D. C. Schwenke, *Microchem. J.*, **72**, 49 (2002).
217. A. Krejčová, T. Černohorský and E. Čurdová, *J. Anal. At. Spectrom.*, **16**, 1002 (2001).
218. H. Fukui, O. Fujino and S. Umetani, *Bunseki Kagaku*, **53**, 1329 (2004); *Chem. Abstr.*, **142**, 351615 (2005).
219. E. V. Polyakova and O. V. Shuvaeva, *J. Anal. Chem.*, **60**, 937 (2005).
220. K. A. Idriss, H. Sedaira and H. M. Ahmed, *Talanta*, **54**, 369 (2001).
221. E. Jungreis, in *Encyclopedia of Analytical Chemistry* (Ed. R. A. Meyers), Vol. 15, Wiley, Chichester, 2000, p. 13609.
222. J. Ruzicka and G. D. Marshall, *Anal. Chim. Acta*, **237**, 329 (1990).
223. G. D. Christian, *Analyst*, **119**, 2309 (1994).
224. C. C. Oliveira, R. P. Sartini and E. A. G. Zagatto, *Anal. Chim. Acta*, **413**, 41 (2000).
225. R. B. R. Mesquita and A. O. S. S. Rangel, *Anal. Sci.*, **20**, 1205 (2004).
226. Z. O. Tesfaldet, J. F. van Staden and R. I. Stefan, *Talanta*, **64**, 981 (2004).
227. D. G. Themelis, P. D. Tzanavaras, A. V. Trellopoulos and M. C. Sofoniou, *J. Agric. Food Chem.*, **49**, 5152 (2001).
228. H.-W. Gao, J.-X. Yang, Z.-Z. Zhou and J.-F. Zhao, *Phytochem. Anal.*, **14**, 91 (2003).
229. C. Liu and C. Han, *Fenxi Huaxue*, **28**, 594 (2000); *Chem. Abstr.*, **133**, 37409 (2000).



230. BioAssay Systems, *QuantiChrom Magnesium Assay Kit (DIMG-250)*, BioAssay Systems, Hayward, CA, USA. (<http://www.bioassaysys.com/DIMG.pdf>).
231. Ortho-Clinical Diagnostics, *Vitros Mg Slide*, Johnson & Johnson Co, Rochester, NY, USA. (<http://www.fda.gov/cdrh/pdf2/k023876.pdf>).
232. I. M. Papazachariou, A. Martinez-Isla, E. Efthimiou, R. C. N. Williamson and S. I. Girgis, *Clin. Chim. Acta*, **302**, 145 (2000).
233. D. Nasser and Y. K. Agrawal, *Iran. J. Chem. Chem. Eng., Int. Eng. Ed.*, **23**, 65 (2004).
234. T. F. Christiansen, J. E. Bush and S. C. Krogh, *Anal. Chem.*, **48**, 1051 (1976).
235. H. Szmazinski and J. R. Lakowicz, *J. Fluoresc.*, **6**, 83 (1996).
236. G. de Armas, A. Cladera, E. Becerra, J. M. Estela and V. Cerdà, *Talanta*, **52**, 77 (2000).
237. Y. Suzuki, H. Komatsu, T. Ikeda, N. Saito, S. Araki, D. Citterio, H. Hisamoto, Y. Kitamura, T. Kubota, J. Nakagawa, K. Oka and K. Suzuki, *Anal. Chem.*, **74**, 1423 (2002).
238. K. Faid and M. Leclerc, *J. Am. Chem. Soc.*, **120**, 5274 (1998).
239. M. Leclerc, *Adv. Mater.*, **11**, 1491 (1999).
240. K. Peter, R. Nilsson and O. Inganäs, *Nature Mater.*, **2**, 419 (2003).
241. K. Faid, R. Cloutier and M. Leclerc, *Macromolecules*, **26**, 2501 (1993).
242. A. Boldea, I. Levesque and M. Leclerc, *J. Mater. Chem.*, **9**, 2133 (1999).
243. H. Mochizuki, Y. Nabeshima, T. Kitsunai, A. Kanazawa, T. Shiono, T. Ikeda, T. Hiyama, T. Maruyama, T. Yamamoto and N. Koide, *J. Mater. Chem.*, **9**, 2215 (1999).
244. P. C. Ewbank, R. S. Loewe, L. Zhai, J. Reddinger, G. Sauvé and R. D. McCullough, *Tetrahedron*, **60**, 11269 (2004).
245. L. G. Sillen (Ed.), *Stability Constants of Metal-Ion Complexes*, **25**, Suppl. 1, The Chemical Society, London, 1971.
246. J. K. Nicholson, M. J. Buckingham and P. J. Sadler, *Biochem. J.*, **211**, 605 (1983).
247. B. S. Somashekar, O. B. Ijare, G. A. Nagana Gowda, V. Ramesh, S. Gupta and C. L. Khetrapala, *Spectrochim. Acta Part A*, **65**, 254 (2006).
248. W. B. Geven, G. M. Vogels-Mentink, J. L. Willems, C. W. v. Os, C. W. Hilbers, J. J. M. Joordens, G. Rijkssen and L. A. H. Monnens, *Clin. Chem.*, **37**, 2076 (1991).
249. A. Malon and M. Maj-Zurawska, *Anal. Chim. Acta*, **448**, 251 (2001).
250. R. F. Burton, *Comp. Biochem. Phys.*, **65A**, 1 (1980).
251. J. Dombóvári, J. S. Becker and H.-J. Dietze, *Int. J. Mass Spectrom.*, **202**, 231 (2000).
252. W. Stegmann and G. A. Quamme, *J. Pharmacol. Toxicol. Meth.*, **43**, 177 (2000).
253. W. Bäuerle, V. Krivan and H. Münzel, *Anal. Chem.*, **48**, 1434 (1976).
254. M. Sabatier, W. R. Keyes, F. Pont, M. J. Arnaud and J. R. Turnlund, *Am. J. Clin. Nutr.*, **77**, 1206 (2003).
255. M. Sabatier, F. Pont, M. J. Arnaud and J. R. Turnlund, *Am. J. Physiol., Regulatory Integrative Comp. Physiol.*, **285**, R656 (2003).
256. C. Coudray, C. Feillet-Coudray, D. Grizard, J. C. Tressol, E. Gueux and Y. Rayssiguier, *J. Nutr.*, **132**, 2043 (2002).
257. C. Feillet-Coudray, C. Coudray, E. Gueux, V. Ducros, A. Mazur, S. Abrams and Y. Rayssiguier, *Metabolism*, **40**, 1326 (2000).
258. C. Feillet-Coudray, C. Coudray, E. Gueux, A. Mazur and Y. Rayssiguier, *Magnesium Res.*, **15**, 191 (2002).
259. T. R. Compton, *Chemical Analysis of Organometallic Compounds*, Vol. 1, Academic Press, New York, 1973.
260. J. Zabicky, in *The Chemistry of Organolithium Compounds* (Eds. Z. Rappoport and I. Marek), Wiley, Chichester, 2004; (a) p. 336; (b) pp. 355 ff.
261. S. C. Watson and J. F. Eastham, *J. Organomet. Chem.*, **9**, 165 (1967).
262. J. Villieras, M. Rambaud and B. Kirschleger, *J. Organomet. Chem.*, **249**, 315 (1983).
263. H. Kiljunen and T. A. Hase, *J. Org. Chem.*, **56**, 6950 (1991).
264. M. E. Bowen, B. R. Aavula and E. A. Mash, *J. Org. Chem.*, **67**, 9087 (2002).
265. D. E. Bergbreiter and E. Pendergrass, *J. Org. Chem.*, **46**, 219 (1981).
266. J. O. Egekeze, H. J. Perpall, C. W. Moeder, G. R. Bicker, J. D. Carroll, A. O. King and R. D. Larsen, *Analyst*, **122**, 1353 (1997).
267. J. Kelly, L. Wright, T. Novak, M. Huffman and V. Antonucci, *J. Liq. Chromatogr. Relat. Technol.*, **24**, 15 (2001).
268. B. J. Magerlein and W. P. Schneider, *J. Org. Chem.*, **34**, 1179 (1969).

269. H. Gilman, P. D. Wilkinson, W. P. Fishel and C. H. Meyers, *J. Am. Chem. Soc.*, **45**, 150 (1923).
270. H. Gilman, E. A. Zoellner and J. B. Dickey, *J. Am. Chem. Soc.*, **51**, 1576 (1929).
271. L. Bernhard, N. C. Furcola, E. L. Gutman, S. L. Kauffman, J. G. Kramer, C. M. Leinweber and V. A. Mayer (Eds.), *1995 Annual Book of ASTM Standards*, Vol. 15.01, American Society for Standards and Materials, Philadelphia, PA, USA, 1995, pp. 311–313.
272. T. Vlismas and R. D. Parker, *J. Organomet. Chem.*, **10**, 193 (1967).
273. J.-Y. Gal, O. Perrier and T. Yvernault, *C. R. Acad. Sci. Paris Ser. C*, **271**, 1561 (1970).
274. Y. Aso, H. Yamashita, T. Otsubo and F. Ogura, *J. Org. Chem.*, **54**, 5627 (1989).
275. B. E. Love and E. G. Jones, *J. Org. Chem.*, **64**, 3755 (1999).
276. A. Krasovskiy and P. Knochel, *Synthesis*, 890 (2006).
277. A. Krasovskiy, F. Kopp and P. Knochel, *Angew. Chem. Int. Ed.*, **45**, 497 (2006).
278. J. Kuyper and K. Vrieze, *Chem. Commun.*, 64 (1976).
279. K. Kham, C. Chevrot, J. C. Folest, M. Troupel and J. Perichon, *Bull. Soc. Chim. Fr. (Pt. 1)*, 243 (1977).
280. Y. Chen, T. Wang, R. Helmy, G. X. Zhou and R. LoBrutto, *J. Pharm. Biomed. Anal.*, **29**, 393 (2002).
281. J.-Y. Gal, O. Mertinat-Perrier and T. Yvernault, *C. R. Acad. Sci. Paris Ser. C*, **277**, 1343 (1973).
282. R. D'Hollander and M. Anteunis, *Bull. Soc. Chim. Belg.*, **72**, 77 (1963).
283. S. Görög and G. Szepesi, *Analyst*, **95**, 727 (1970).
284. R. D. Parker and T. Vlismas, *Analyst*, **93**, 330 (1968).
285. X. Li, C. Yu, W. Sun, G. Liu, J. Jia and Y. Wang, *Rapid Commun. Mass Spectrom.*, **18**, 2878 (2004).
286. A. Wovk and S. Digiovanni, *Anal. Chem.*, **38**, 742 (1966).
287. H. O. House and W. L. Respass, *J. Organomet. Chem.*, **4**, 95 (1965).
288. L. Marder, P. Tomedi, M. F. Ferrão, A. Jablonski and C. U. Davanzo, *J. Braz. Chem. Soc.*, **17**, 594 (2006).
289. H. Gilman and F. Schulze, *J. Am. Chem. Soc.*, **47**, 2002 (1925).
290. H. Gilman and F. Schulze, *Bull. Soc. Chim. Fr.*, **41**, 1479 (1927).
291. H. Gilman and R. G. Jones, *J. Am. Chem. Soc.*, **62**, 1243 (1940).
292. H. Gilman and R. J. Vander Wal, *Bull. Soc. Chim. Fr.*, **45**, 344 (1929).
293. H. Gilman, L. L. Heck and N. B. St. John, *Recl. Trav. Chim. Pays-Bas*, **49**, 212 (1930).
294. H. Gilman and L. L. Heck, *J. Am. Chem. Soc.*, **52**, 4949 (1930).
295. H. Gilman and L. L. Heck, *Recl. Trav. Chim. Pays-Bas*, **49**, 218 (1930).
296. H. Gilman, O. R. Sweeney and L. L. Heck, *J. Am. Chem. Soc.*, **52**, 1604 (1930).
297. H. Gilman and J. Swiss, *J. Am. Chem. Soc.*, **62**, 1847 (1940).
298. H. Gilman and L. A. Woods, *J. Am. Chem. Soc.*, **65**, 33 (1943).
299. AIST, *Spectral Database for Organic Compounds (SDBS)*, National Institute of Advanced Industrial Science and Technology (AIST), Japan, (a) SDBS No. 2051, (b) SDBS No. 2054. ([http://www.aist.go.jp/RIODB/SDBS/cgi-bin/display\\_frame\\_disp.cgi?sdbno=2051](http://www.aist.go.jp/RIODB/SDBS/cgi-bin/display_frame_disp.cgi?sdbno=2051)).
300. T. R. Hoye, B. M. Eklov and M. Voloshin, *Org. Lett.*, **6**, 2567 (2004).
301. R. Jones, *J. Organomet. Chem.*, **18**, 15 (1969).
302. M. Westerhausen, T. Bollwein, N. Makropoulos and H. Piotrowski, *Inorg. Chem.*, **44**, 6439 (2005).
303. A. Xia, M. J. Heeg and C. H. Winter, *Organometallics*, **22**, 1793 (2003).
304. S. Blair, K. Izod, W. Clegg and R. W. Harrington, *Eur. J. Inorg. Chem.*, 3319 (2003).
305. J. D. Farwell, M. F. Lappert, C. Marschner, C. Strissel and T. D. Tilley, *J. Organomet. Chem.*, **603**, 185 (2000).
306. A. M. Egorov, S. V. Kuznetsova and A. V. Anisimov, *Russ. Chem. Bull., Int. Ed.*, **49**, 1544 (2000).
307. K. B. Starowieyski, J. Lewinski, R. Wozniak, J. Lipkowski and A. Chrost, *Organometallics*, **22**, 2458 (2003).
308. T. Zerevitinov, *Ber. Dtsch. Chem. Ges.*, **45**, 2384 (1913).
309. E. P. Kohler, J. F. Stone, Jr. and R. C. Fuson, *J. Am. Chem. Soc.*, **49**, 3181 (1927).
310. E. P. Kohler and N. K. Richtmyer, *J. Am. Chem. Soc.*, **52**, 3736 (1930).
311. K. Banas and M. Rachtan, *Rudy Met. Niezelaz.*, **26**, 557 (1981); *Chem. Abstr.*, **96**, 173541 (1982).

312. D. Ishii, T. Tsuda and N. Tokoro, *Bunseki Kagaku*, **21**, 367 (1972); *Chem. Abstr.*, **77**, 42920 (1972).
313. M. Lieff, G. F. Wright and H. Hibbert, *J. Am. Chem. Soc.*, **61**, 865 (1939).
314. T. Yazawa, H. Tanaka and K. Eguchi, *Nippon Kagaku Kaishi*, 1338 (1984); *Chem. Abstr.*, **101**, 135658 (1984).
315. F. T. Weiss, in *Treatise on Analytical Chemistry* (Eds. I. M. Kolthoff and P. J. Elving), Part 2, Vol. 13, Interscience, New York, 1966, pp. 33–94.
316. G. R. Leader, *Appl. Spectrosc. Rev.*, **11**, 287 (1976).
317. M. A. Williams and J. E. Ladbury, 'Protein-ligand interactions from molecular recognition to drug design', in *Methods and Principles in Medicinal Chemistry* (Eds. H.-J. Böhm and G. Schneider), Vol. 19, Wiley-VCH, Weinheim, 2003, pp. 137–161.
318. Y. K. Chau and F. Yang, *Appl. Organomet. Chem.*, **11**, 851 (1997).
319. M. B. de la Calle-Gutiñas and F. C. Adams, *J. Chromatogr. A*, **764**, 169 (1997).
320. Y. K. Chau and P. T. S. Wong, in *Analysis of Trace Organics in the Aquatic Environment* (Eds. B. K. Afghan and A. S. Y. Chau), CRC Press, Boca Raton, 1989, pp. 283–312.
321. Y. K. Chau, *Analyst*, **117**, 571 (1992).
322. J. M. F. Nogueira, P. Teixeira and M. H. Florencio, *J. Microcolumn Sep.*, **13**, 48 (2001).
323. M. B. de la Calle-Gutiñas, R. Scerbo, S. Chiavarini, P. Quevauviller and R. Morabito, *Appl. Organomet. Chem.*, **11**, 693 (1997).
324. Y. K. Chau, F. Yang and M. Brown, *Anal. Chim. Acta*, **338**, 51 (1997).
325. M. D. Müller, *Anal. Chem.*, **59**, 617 (1987).
326. C. Yamamoto, M. Nakamura, N. Kibune and Y. Maekawa, *Shokuhin Eiseigaku Zasshi*, **37**, 288 (1996); *Chem. Abstr.*, **126**, 59025 (1997).
327. Q. Zhou, G. Jiang and D. Qi, *Fenxi Huaxue*, **27**, 1197 (1999); *Chem. Abstr.*, **132**, 30085 (2000).
328. K. Newman and R. S. Mason, *J. Anal. At. Spectrom.*, **20**, 830 (2005).
329. K. Tonami, C. Sasaki and F. Sakamoto, *Ishikawa-ken Hoken Kankyo Senta Nenpo*, **33**, 95 (1995, publ. 1997); *Chem. Abstr.*, **127**, 46396 (1997).
330. M. A. Unger, J. Greaves and R. J. Huggett, in *Organotin* (Eds. M. A. Champ and P. F. Seligman), Chapman & Hall, London, 1996, pp. 124–134.
331. Y. Liu, V. Lopez-Avila and M. Alcaraz, *J. High Resolut. Chromatogr.*, **17**, 527 (1994).
332. E. Magi, M. Di Carro and P. Rivaro, *Appl. Organometal. Chem.*, **18**, 646 (2004).
333. S. Tsunoi, T. Matoba, H. Shioji, L. T. Huong Giang, H. Harino and M. Tanaka, *J. Chromatogr. A*, **962**, 196 (2002).
334. I. Martin-Landa, F. de Pablos and I. L. Marr, *Anal. Proc.*, **26**, 16 (1989).
335. J. L. Martínez Vidal, A. Belmonte Vega, F. J. Arrebola, M. J. González-Rodríguez, M. C. Morales Sánchez and A. Garrido Frenich, *Rapid Commun. Mass Spectrom.*, **17**, 2099 (2003).
336. G.-b. Jiang and Q.-f. Zhou, *J. Chromatogr. A*, **886**, 197 (2000).
337. Y. Liu, V. Lopez-Avila and M. Alcaraz, *Anal. Chem.*, **66**, 3788 (1994).
338. L. M. Allan, D. K. Verma, F. Yang, Y. K. Chau and R. J. Maguire, *Am. Ind. Hyg. Assoc. J.*, **61**, 820 (2000).
339. L. A. Uzal Barbeito and J. L. Wardell, *Quim. Anal.*, **14**, 158 (1995).
340. M. Ceulemans and F. C. Adams, *Anal. Chim. Acta*, **317**, 161 (1995).
341. R. Łobiński, W. M. R. Dirkx, M. Ceulemans and F. C. Adams, *Anal. Chem.*, **64**, 159 (1992).
342. F. Rodigari, *Proc. Moving toward the 21st Century*, Philadelphia, Aug. 3–6, 1997; *Chem. Abstr.*, **129**, 305920 (1998).
343. M. O. Stallard, S. Y. Cola and C. A. Dooley, *Appl. Organomet. Chem.*, **3**, 105 (1989).
344. S. K. Aggarwal, R. Fitzgerald and D. A. Herold, *BARC News.*, **201**, 95 (2000); *Chem. Abstr.*, **134**, 157030 (2001).
345. M. Radojević, A. Allen, S. Rapsomanikis and R. M. Harrison, *Anal. Chem.*, **58**, 658 (1986).
346. I. A. Leal-Granadillo, J. I. García Alonso and A. Sanz-Medel, *Anal. Chim. Acta*, **423**, 21 (2000).
347. B. Salih, *Spectrochim. Acta, Part B*, **55**, 1117 (2000).
348. B. Pons, A. Carrera and C. Nerín, *J. Chromatogr. B*, **716**, 139 (1998).
349. K. Fujiwara, Y. Okamoto, M. Ohno and T. Kumamaru, *Anal. Sci.*, **11**, 829 (1995).
350. S. K. Aggarwal, M. Kinter and D. A. Herold, *Clin. Chem.*, **40**, 1494 (1994).
351. H. Emteborg, E. Björklund, F. Ödman, L. Karlson, L. Mathiasson, W. Frech and D. C. Baxter, *Analyst*, **121**, 19 (1996).

- 352. S. Tao and T. Kumamaru, *Anal. Chim. Acta*, **310**, 369 (1995).
- 353. T. Kumamaru, S. Tao, M. Uchida and Y. Okamoto, *Anal. Lett.*, **27**, 2331 (1994).
- 354. S. K. Aggarwal, M. Kinter, J. Nicholson and D. A. Herold, *Anal. Chem.*, **66**, 1316 (1994).
- 355. M. Pina, D. Montet, J. Graille, C. Ozenne and G. Lamberet, *Rev. Fr. Corps Gras*, **38**, 213 (1991).
- 356. M. Yurkowski and H. Brockerhoff, *Biochim. Biophys. Acta*, **125**, 55 (1966).
- 357. C. Franzke, E. Hollstein, J. Kroll and H. J. Noske, *Fette, Seifen, Anstrichmittel*, **75**, 365 (1973).
- 358. F. Turon, P. Bachain, Y. Caro, M. Pina and J. Graille, *Lipids*, **37**, 817 (2002).
- 359. M. Wältermann, H. Luftmann, D. Baumeister, R. Kalscheuer and A. Steinbüchel, *Microbiology*, **146**, 1143 (2000).
- 360. P. R. Redden, X. Lin and D. F. Horrobin, *Chem. Phys. Lipids*, **79**, 9 (1996).
- 361. M. Pina, D. Ploch and J. Graille, *Lipids*, **22**, 358 (1987).
- 362. T. Moritani, K. Yoon, M. Rafailovich and B. Chu, *Electrophoresis*, **24**, 2764 (2003).
- 363. T. Moritani, K. Yoon and B. Chu, *Electrophoresis*, **24**, 2772 (2003).
- 364. N. D. Danielson, S. Ahmed, J. A. Huth and M. A. Targrove, *J. Liq. Chromatogr.*, **9**, 727 (1986).
- 365. C. Liebenow, *Solid State Ionics*, **136–137**, 1211 (2000).

## CHAPTER 8

# Biochemistry of magnesium

JAMES WESTON

*Institut für Organische Chemie und Makromolekulare Chemie, Friedrich-Schiller-Universität, Humboldtstraße 10, D-07743 Jena, Germany*  
Fax: +49(0)3641-9-48212; e-mail: c9weje@uni-jena.de

---

I. MAGNESIUM IN BIOLOGICAL SYSTEMS . . . . .	316
II. MAGNESIUM AS AN ESSENTIAL COFACTOR . . . . .	316
III. BASIC COORDINATION SPHERE . . . . .	318
IV. FUNDAMENTAL BINDING MODES . . . . .	320
A. Carboxylate Ligands . . . . .	321
B. Phosphate Functionalities . . . . .	322
C. Nitrogen Ligands . . . . .	324
V. MAGNESIUM TRANSPORT SYSTEMS . . . . .	324
VI. UNIVERSAL ENERGY CURRENCY OF LIFE . . . . .	327
A. $\text{MgATP}^{2-}$ . . . . .	328
B. Biosynthesis of ATP . . . . .	329
C. Hydrolysis of ATP . . . . .	331
VII. INTERACTIONS WITH DNA AND RNA . . . . .	333
A. Magnesium and Structural Stability . . . . .	334
B. Ribozymes . . . . .	335
1. Self-splicing in group I introns . . . . .	337
2. Hammerhead ribozymes . . . . .	339
VIII. PROTEIN-BASED ENZYMES . . . . .	342
A. General Enzymatic Modes of Action . . . . .	342
1. Template enzymes . . . . .	342
2. Sequential systems . . . . .	343
3. Allosteric systems . . . . .	343
B. Metabolic Enzymes . . . . .	345
1. Protein kinases . . . . .	345
2. Enolases . . . . .	348
C. DNA Replication and Repair . . . . .	350
1. DNA replicases . . . . .	351
2. Base excision repair . . . . .	353
3. Generic two-ion mechanism . . . . .	354

---

*The chemistry of organomagnesium compounds*

Edited by Z. Rappoport and I. Marek © 2008 John Wiley & Sons, Ltd. ISBN: 978-0-470-05719-3

D. Magnesium and Photosynthesis . . . . .	355
1. Chlorophyll . . . . .	356
2. Rubisco—a photosynthetic CO <sub>2</sub> fixing enzyme . . . . .	357
IX. REFERENCES . . . . .	359

---

## I. MAGNESIUM IN BIOLOGICAL SYSTEMS

Although most of the magnesium found on earth is tied up in mineral deposits, many magnesium salts are highly soluble in water. Continual leaching processes lead to a constant and relatively high concentration of Mg<sup>2+</sup> both in the soil and in the hydrosphere (for example, the concentration of Mg<sup>2+</sup> in the ocean is *ca* 55 mM<sup>1</sup>) which guarantees a high bioavailability. This together with its unique physico-chemical properties has ensured that Mg<sup>2+</sup> is an indispensable cofactor in countless life processes. One of the distinctive characteristics of Mg<sup>2+</sup> is that it is typically an *intracellular* metal cation. Similar to K<sup>+</sup>, the concentration of Mg<sup>2+</sup> is generally an order of magnitude higher inside cells than in extracellular milieu (in contrast to this, Ca<sup>2+</sup> and Na<sup>+</sup> are extracellular cations and tend to accumulate outside the cells)<sup>1</sup>. Magnesium is present in every cell type in every known organism and is the fourth most common metal cation found in biological systems (Ca<sup>2+</sup> > K<sup>+</sup> > Na<sup>+</sup> > Mg<sup>2+</sup>)<sup>2</sup>. For example, the human body contains a steady-state concentration of *ca* 25 g of magnesium which has to be replenished at a rate of about 1/2 g per day<sup>2</sup>.

For quite some time, the biochemistry of magnesium has been neglected in favor of studying transition metal ions such as iron or copper—mostly because the latter are much easier to study. Magnesium is spectroscopically silent and notoriously difficult to detect and/or monitor<sup>1</sup>. Even solid-state X-ray analysis proves rather difficult due to the extremely low electron density and small size of the Mg<sup>2+</sup> cation. As progress in methodological and spectroscopic approaches has been realized and now that theoretical approaches (especially DFT theory and MM/MD modeling techniques) can be applied to larger biomolecules, more and more mechanistic details for magnesium-containing biomolecules are becoming available. However, we are far from being able to summarize the biochemistry of magnesium in its entirety. The intent of this chapter is thus not that of a comprehensive review but rather an illustrative article in which selected systems are discussed in order that a reader with a general chemical background may gain an overview of the versatility and fascinatingly complex mechanistic biochemistry of magnesium.

## II. MAGNESIUM AS AN ESSENTIAL COFACTOR

Magnesium is perhaps the most versatile metal cation found in living systems. It can and does interact with an extremely wide variety of biomolecules, thus giving rise to multiple biological roles of fundamental importance in life processes. A comprehensive discussion of all biosystems that have an absolute dependency on Mg<sup>2+</sup> as a cofactor would currently have to include hundreds of unrelated examples and more are being discovered all the time.

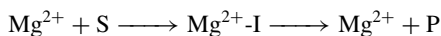
The biochemistry of Mg<sup>2+</sup> begins with cell membranes where metal cations, especially Na<sup>+</sup> and Mg<sup>2+</sup>, are needed to help reduce the strong repulsions between negatively charged phosphates in the densely packed lipids that make up cellular membranes<sup>2</sup>. Since the concentration of Mg<sup>2+</sup> is higher inside cells than outside, nature has to have a way to move it across cell membranes and then keep it there—a task accomplished by magnesium-specific transport proteins<sup>3</sup>. All cationic membrane transport systems (Na<sup>+</sup>, K<sup>+</sup>, Mg<sup>2+</sup> and Ca<sup>2+</sup>) face certain challenges. They must be able to specifically recognize and interact with a hydrated cation. Next, they must strip away most, if not all, of the

water ligands and then move the cation across the membrane. However,  $\text{Mg}^{2+}$  is the most challenging of all to transport due to its very small ionic radius and the fact that its hydration radius and transport number is larger than those of the others<sup>1,4</sup>. In addition, it has the slowest exchange rate (3 orders of magnitude lower) of solvent waters<sup>1</sup>. As a result,  $\text{Mg}^{2+}$  transporters are generally quite unusual members of the transport family<sup>3</sup>.

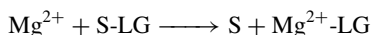
Once in the cell, the most common physiological role of a  $\text{Mg}^{2+}$  cation is to bind ATP or other nucleoside triphosphates (NTP). Differing estimates of the total amount of intracellular  $\text{Mg}^{2+}$  that directly interacts with ATP are available in the literature. These vary from 50%<sup>1</sup> to 75%<sup>5</sup>. Since ATP is the fundamental biochemical unit of energy in life processes, the importance of this function cannot be underestimated. It is believed that one of the purposes of  $\text{Mg}^{2+}$  binding to ATP is to activate it towards specific phosphate hydrolysis. Of significance in this task is the high Lewis acidity of  $\text{Mg}^{2+}$ , i.e. its general ability to polarize functional groups (such as a carbonyl group in a peptide backbone), stabilize anions (carboxylates or phosphates, for example) and polarize water molecules so that they can be more easily deprotonated to provide active nucleophiles for general phosphate or peptide bond hydrolysis.

Magnesium is an intrinsic component of cellular signaling processes in higher organisms<sup>6</sup>. As such,  $\text{Mg}^{2+}$ -dependent enzymes are found in virtually every known metabolic pathway where they often function as key mediators. The well-known glycolytic pathway is no exception to this. In addition to metabolic pathways, magnesium is often an essential cofactor in enzymatic and ribozymatic DNA and RNA replication, repair and transcription. As a consequence, numerous unrelated enzymatic families, both protein and ribozyme based that, in addition, may or may not depend on ATP, have an absolute dependency upon magnesium<sup>7,8</sup>. In the active site of enzymes, magnesium can play several different mechanistic roles, the more important probably being the following<sup>2</sup>:

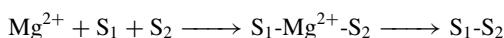
Stabilization of an intermediate, I:



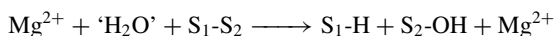
Stabilization of a leaving group, LG (or product P):



Bring two substrates S together for reaction:



Provide an activated, water-based nucleophile for hydrolysis:



Moving away from enzymatic activity, it is a well-known fact that both the structure (conformation as well as topology) and the function of DNA and RNA depend strongly on specific interactions with divalent cations, especially  $\text{Ca}^{2+}$  and  $\text{Mg}^{2+}$ <sup>9,10</sup>. These cations stabilize base pairing and stacking by relieving electrostatic repulsion between phosphates<sup>11</sup>. Among other things,  $\text{Mg}^{2+}$  stimulates the formation of, as well as stabilizes DNA/RNA helices and other structural motifs<sup>11,12</sup>.

Finally, a very unusual binding situation of magnesium, namely its interaction with the porphyrin ring in chlorophyll, plays an essential role in the most thermodynamically demanding reaction to be found in biology—the synthesis of carbohydrates from  $\text{CO}_2$  in plants and cyanobacteria using light energy from the sun. This extremely complex process of photosynthesis is considered to be fundamental for sustaining essentially all life on our planet<sup>13</sup>.

### III. BASIC COORDINATION SPHERE

Before one can study the biochemistry of magnesium in detail, one first needs to understand its structure and behavior under physiological conditions—which basically means understanding the interaction of a single  $\text{Mg}^{2+}$  cation first with water and then with a few selected organic functionalities. It is a well-known fact that, in aqueous solutions,  $\text{Mg}^{2+}$  binds six water molecules in an octahedral arrangement to generate a hexa-aquomagnesium  $[\text{Mg}(\text{H}_2\text{O})_6]^{2+}$  ion—a species which has been the subject of numerous experimental and theoretical studies<sup>14</sup>. The existence of  $[\text{Mg}(\text{H}_2\text{O})_6]^{2+}$  as an independent structural unit is also corroborated by countless solid-state structures of inorganic and bioinorganic compounds in structural data banks worldwide<sup>15</sup>. As compared to other metal cations, the low electronic density of  $\text{Mg}^{2+}$  makes resolving the solid-state structures of large biomolecules in the region of the magnesium ion quite difficult. Although there is continual progress in this field, there are still relatively few solid-state structures of magnesium-containing biomolecules available. Of the known structures, most, but (significantly) not all, possess an octahedral coordination sphere.

The interaction of a single  $\text{Mg}^{2+}$  cation with water is fundamentally electrostatic in nature and is traditionally considered to be quite 'rigid'. An older (1984) analysis of solid-state structures, for example, reported that a hexacoordinated  $\text{Ca}^{2+}$  ion has a much greater angular flexibility with deviations of up to  $40^\circ$  from the ideal  $90^\circ$  whereas the variation in comparable  $\text{Mg}^{2+}$  complexes is no more than  $5\text{--}10^\circ$ <sup>16</sup>. The octahedral arrangement allows for ligand exchange; the water molecules in the first coordination sphere of  $\text{Mg}^{2+}$  are in dynamic equilibrium with individual waters in the looser second coordination sphere (transition region between bulk water and the 'ionic cavity' generated by  $[\text{Mg}(\text{H}_2\text{O})_6]^{2+}$ ). However, this exchange is significantly slower—3 to 4 orders of magnitude—than the other common biologically relevant metal cations ( $\text{Na}^+$ ,  $\text{K}^+$  and  $\text{Ca}^{2+}$ ) and approaches that found for transition metal ions<sup>1</sup>. It is generally accepted that a maximum of 12 water molecules can be accommodated in the second coordination sphere of  $\text{Mg}^{2+}$ <sup>4, 17, 18</sup>. The size of a hydrated  $\text{Mg}^{2+}$  ion is surprisingly large and its volume is *ca* 400-fold larger than its dehydrated ionic form<sup>1</sup>. For comparison, the hydrated volume of the intrinsically much larger  $\text{Ca}^{2+}$  is only 25-fold larger than its ionic volume<sup>1</sup>.

Experiments on isolated  $[\text{Mg}(\text{H}_2\text{O})_6]^{2+}$  ions in the gas phase indicate that the coordination number of the central  $\text{Mg}^{2+}$  is principally somewhat more flexible than is generally assumed. Two different isomers are present—the expected octahedral  $[\text{Mg}(\text{H}_2\text{O})_6]^{2+}$  ion and a previously unknown pentacoordinated  $[\text{Mg}(\text{H}_2\text{O})_5]^{2+} \cdot \text{H}_2\text{O}$  species with the sixth water in the second coordination sphere<sup>19, 20</sup>. The metal binding site of magnesium-containing biomolecules which contain a variable number of organic ligands presents a problematic situation with an environment intermediate between that of bulk water where a hexacoordinated magnesium ion is clearly preferred and the gas phase where the coordination number of  $\text{Mg}^{2+}$  is unusually flexible. Although quite a few theoretical studies of ligand exchange processes ( $\text{H}_2\text{O}$  against  $\text{HCO}_2^-$ ,  $\text{HCO}_2\text{H}$ , formamide, methanol etc.) have been published, all of these studies have *assumed* an octahedral geometry at the central  $\text{Mg}^{2+}$  ion<sup>14</sup>. Only very recently has the possibility of alternative coordination modes begun to be considered. The fact that this is necessary is illustrated by a solid-state structure of a  $\text{Mg}^{2+}$ –GDP complex<sup>21</sup>. This biomolecule crystallizes with two different central coordination geometries for  $\text{Mg}^{2+}$ —the expected hexacoordination observed in all other known members of the GTPase family and an 'unusual' pentacoordinated structure (Figure 1)<sup>21</sup>. Moving away from simple aqueous solutions, organomagnesium compounds, especially those containing aprotic organic ligands such as THF, often exhibit a coordination number of four (tetrahedral geometry)<sup>22, 23</sup>.



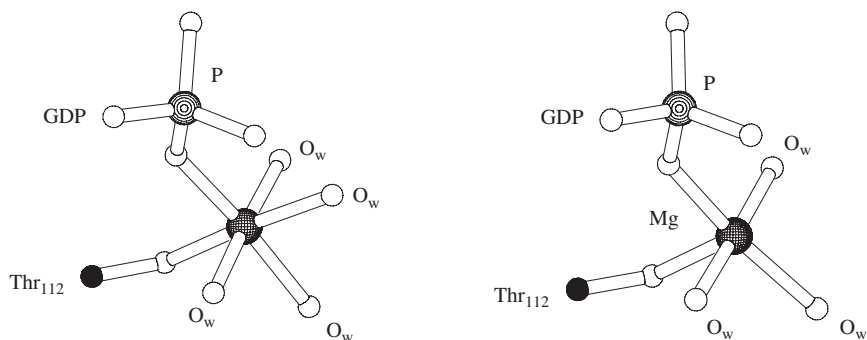


FIGURE 1. The two different coordination geometries of the  $\text{Mg}^{2+}$  cation in the solid-state structure of a  $\text{Mg}^{2+}$ -GDP complex

Quite a few enzymes with specific  $\text{Mg}^{2+}$  binding sites catalyze either the hydrolysis of a phosphate ester or the hydrolytic transfer of a phosphate group<sup>24</sup>. It is often postulated that hydrolysis proceeds over the initial deprotonation of a water ligand to generate a nucleophilic metal-bound hydroxide that is then capable of attacking the substrate. However, very few investigations on species containing a  $\text{Mg}$ -OH functionality have been performed with most of these being theoretical studies in the gas phase on small  $[\text{Mg}(\text{OH})_n]^{2-n}$  ( $n = 1-3$ ) complexes<sup>25</sup>. Only one recent DFT study explicitly considered the deprotonation of  $[\text{Mg}(\text{OH}_2)_6]^{2+}$  and discovered that the expected hexacoordinated  $[\text{Mg}(\text{OH})(\text{OH}_2)_5]^+$  species is intrinsically unstable<sup>14</sup>. Upon deprotonation of a water ligand,  $[\text{Mg}(\text{OH}_2)_6]^{2+}$  spontaneously lowers its coordination number to five with accompanying migration of one water ligand to the second coordination sphere (Figure 2). It is quite interesting that this study (performed at a relatively high level of theory where thermodynamic accuracy can be expected) predicts that deprotonation is a slightly *exothermic* ( $\Delta G = -4.1 \text{ kcal mol}^{-1}$ ) process and thus probably highly relevant in biological processes<sup>14</sup>. Fluoride ligands (isoelectronic with hydroxide) behave quite similarly; DFT calculations predict a pentacoordinate geometry for  $[\text{MgF}(\text{H}_2\text{O})_5]^+$ <sup>14</sup>, a finding which is

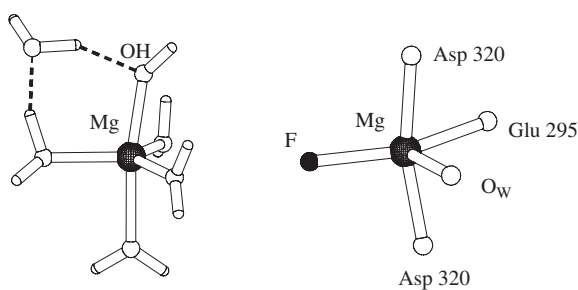


FIGURE 2. Left: deprotonation of  $[\text{Mg}(\text{OH}_2)_6]^{2+}$  lowers the coordination number of magnesium. Reprinted with permission from Reference 14. Copyright 2005 American Chemical Society. Right: pentacoordinate geometry of  $\text{Mg}^{2+}$  in the solid-state structure of the  $\text{Mg}^{2+}$ - $\text{F}^-$ - $\text{P}_i$  complex of yeast enolase

supported by a solid-state structure of the fluoride-inhibited  $\text{Mg}^{2+}-\text{F}^{-}-\text{P}_i$  complex of yeast enolase (Figure 2)<sup>26</sup>.

#### IV. FUNDAMENTAL BINDING MODES

Magnesium differs from all other alkaline earth and transition metal ions in that two fundamentally different binding mechanisms ('outer sphere' and 'inner sphere') occur that are capable of competing with each other (Figure 3)<sup>7,27</sup>. The small ionic radius of  $\text{Mg}^{2+}$  together with its oxophilicity (high affinity for oxygen ligands) results in unusually strong water-metal interactions. As a result, ligand exchange reactions are quite slow, which makes it relatively difficult to replace a water ligand with a bulky organic ligand. As a consequence,  $[\text{Mg}(\text{H}_2\text{O})_6]^{2+}$  has a certain tendency to act as an independent entity when it interacts with biomolecules. Binding interactions in this 'outer sphere' case occur indirectly via strong hydrogen bond interactions between a substrate S and one or more of the water ligands. Alternatively, an organic functionality in a biomolecule may displace one or more of the water ligands in  $[\text{Mg}(\text{H}_2\text{O})_6]^{2+}$ , thus effectively binding the (now partially dehydrated)  $\text{Mg}^{2+}$  cation in an 'inner sphere' coordination mode. Theoretical investigations have indicated that the degree of local solvation is probably one of the major factors in determining the binding mode of a magnesium ion. The tendency for an inner-sphere binding mode increases as the dielectric constant of the local medium decreases (increasing hydrophobicity of an active site binding pocket that is only partially solvent accessible, for example)<sup>28</sup>.

For reasons not yet entirely understood, the oligonucleotides in DNA and RNA often preferably interact with  $[\text{Mg}(\text{H}_2\text{O})_6]^{2+}$  via an outer-sphere binding mode<sup>8</sup>. Extensive hydrogen bonding of magnesium-bound water molecules to heteroatoms in the bases and to the phosphate backbone are the predominant interactions<sup>7</sup>. Guanine, for example, appears to actively promote outer sphere binding of magnesium in RNA; an analysis of a solid-state structure of an RNA strand containing a total of 27 hydrated  $\text{Mg}^{2+}$  ions revealed that 21 of them undergo outer-sphere contacts with guanine; only three inner-sphere contacts were observed<sup>29</sup>. A typical outer-sphere interaction of  $[\text{Mg}(\text{H}_2\text{O})_6]^{2+}$  with two GC base pairs in the major groove of DNA is illustrated in Figure 4<sup>30,31</sup>. A theoretical study (RHF) of this bonding interaction attributed this preference to a cooperative enhancement of charge transfer from guanine to magnesium mediated by the hydration sphere of the ion<sup>32</sup>.

If a magnesium cation is incorporated into the active site of a protein-based enzyme, it usually binds via an inner-sphere mechanism in which one or more water ligands in  $[\text{Mg}(\text{OH}_2)_6]^{2+}$  are exchanged for organic ligands  $\text{L}_x$  originating from side chains. The

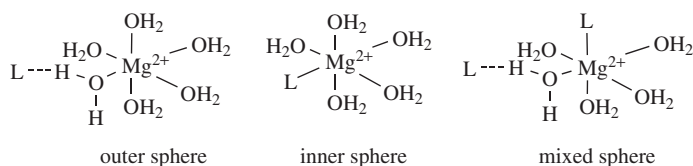


FIGURE 3. Difference between 'outer' and 'inner' sphere coordination modes of magnesium (Reproduced by permission of Elsevier from Reference 7) as well as the possibility of mixed sphere coordination. L is an organic ligand

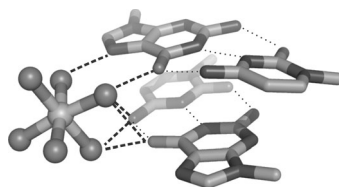


FIGURE 4. Typical outer-sphere interaction of  $[\text{Mg}(\text{H}_2\text{O})_6]^{2+}$  with two GC base pairs in the major groove of a DNA double helix

number of inner-sphere binding contacts is quite variable and values of  $x$  from 1–5 have been observed. Sometimes, a mixed coordination occurs in which ligands ( $\text{L}_x$ ) from protein side chains fix  $\text{Mg}^{2+}$  in the active site. At the same time, a substrate  $\text{S}$  interacts with the magnesium via an outer-sphere binding mechanism (Figure 3). Again, the number of inner-sphere binding contacts is quite variable.

Statistical studies of the inner-sphere binding mode of  $\text{Mg}^{2+}$  in the solid-state structures of metalloproteins have revealed that oxygen, as expected, is the preferred bonding partner<sup>33,34</sup>. Approximately 77% of all  $\text{Mg}-\text{X}$  bonds are  $\text{Mg}-\text{O}$  bonding situations in which either water or negatively charged oxygen functionalities such as carboxylates (Asp, Glu) are the preferred ligands<sup>35</sup>. The second most commonly occurring situation is a  $\text{Mg}-\text{N}$  interaction which can occur either in the form of a porphyrin ring (chlorophyll) or a nitrogen ligand originating from the side chain of lysine or the imidazole ring in histidine. Magnesium–sulfur bonds are extremely seldom in natural systems, having only been observed in a single chlorophyll chromophore<sup>36</sup>.

### A. Carboxylate Ligands

After water, the second most common biological ligand for magnesium is a carboxylate which usually originates from a Glu or Asp side chain. Quite a few theoretical studies of the first coordination sphere of  $\text{Mg}^{2+}$  have therefore included carboxylates<sup>14</sup>. With their negative charge, they are significantly better ligands than water for a hexacoordinated  $\text{Mg}^{2+}$  cation. The equilibrium position is quite favorable for successive exchanges of up to three carboxylates bound in a monodentate manner<sup>14</sup>. However, it is clear that  $\text{Mg}^{2+}$  will not exchange all of its first-shell water molecules<sup>37</sup>. Current calculations indicate that the maximum number of monodentately bound carboxylates will likely not exceed four<sup>38</sup>. In accord with this, a PDB data bank analysis revealed that of 82 solid-state structures available in 2006 for magnesium-containing protein binding sites, 52 contain one, 25 have two, 3 have three and only two structures contain four carboxylate ligands<sup>38</sup>. In the case of two (or more) carboxylate ligands, the resulting  $[\text{Mg}(\text{RCO}_2)_x(\text{OH}_2)_{6-x}]^{2-x}$  complexes are asymmetric and several isomers are possible due to differentiation between axial and equatorial positions. The energy difference between these different possibilities is usually rather small<sup>14,37,38</sup> and examples of both orientations can be found in the PDB data bank. Monodentately bound carboxylates can and do stabilize themselves further via two basic interactions—hydrogen bonding in the first coordination sphere to  $\text{Mg}^{2+}$ -bound water molecules and, as observed in almost all solid-state structures available, additional hydrogen bonding to second-sphere functionalities such as backbone peptide groups, Asn, Gln, Lys or Arg side chains<sup>39</sup>. The situation is further complicated

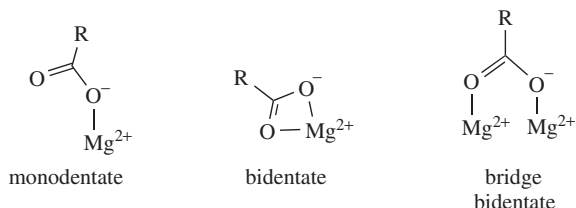


FIGURE 5. Coordination modes available to a carboxylate ligand when interacting with  $\text{Mg}^{2+}$

due to the fact that carboxylates possess three fundamentally different binding modes: mono-, bidentate and bridge bidentate (Figure 5). Until now, only the monodentate mode has been discussed. However, all three have been observed in the solid-state structures of magnesium-containing biomolecules.

It has been suggested that a carboxylate ligand ‘is quite indifferent to its coordination mode’ which is postulated to be mainly determined by the presence/absence of second-sphere hydrogen bonding<sup>40</sup>. It is believed that an equilibrium between both modes (the ‘carboxylate shift’<sup>41</sup>) could be important in enzymatic modes of action<sup>42</sup>. This seems to be especially true for biomolecules that must discriminate between  $\text{Ca}^{2+}$  and  $\text{Mg}^{2+}$ . A survey (2004) of the PDB data bank revealed that  $\text{Mg}^{2+}$  clearly favors the monodentate mode with only 4% of the carboxylate ligands binding in a bidentate manner whereas 29% of the  $\text{Ca}^{2+}$  structures were bidentate<sup>43</sup>. A change in the binding mode (monodentate for  $\text{Mg}^{2+}$ , bidentate for  $\text{Ca}^{2+}$ ) has been postulated to be the deciding factor in discriminating between these ions in *E. coli* ribonuclease H1<sup>44</sup>. Systematic theoretical studies of this equilibrium<sup>43,45</sup> suggest that the binding mode is determined by a fine balance of several factors—only one of them being the identity of the metal ion. The total charge in the region of the metal ion, electrostatic properties of the interacting substrate, the presence/absence of stabilizing H-bond donors in the first and second coordination sphere and the general dielectric medium all play a critical role. The effect of ionic charge density has recently been investigated spectroscopically on droplets of aqueous  $\text{Mg}(\text{OAc})_2$  solutions<sup>46,47</sup>. Significant changes in the coordination mode were observed upon increasing salt concentration—isolated contact ion pairs (outer sphere solvation) are in equilibrium with monodentate coordination at lower salt concentrations. As the solution becomes increasingly saturated, bidentate contacts and then bridge bidentate modes begin to be detected. The bridging bidentate mode is usually only observed in protein-based enzymes where it is a very common motif employed in binuclear active sites in order to position two metal ions in near proximity (3–5 Å) to each other<sup>48,49</sup>.

## B. Phosphate Functionalities

After a carboxylate, the next most significant biological ligand for  $\text{Mg}^{2+}$  is a phosphate. Phosphates, in addition to being present as inorganic phosphate ( $\text{P}_i$ ), also happily polymerize to form not only diphosphates (for example,  $\text{PP}_i$  and ADP) but also triphosphates (nucleoside triphosphates such as ATP). Many of these polyphosphates have fundamental biochemical importance as evidenced by the  $\text{ATP} \rightleftharpoons \text{ADP} + \text{P}_i$  reaction.

Each of the species mentioned above can be expected to exhibit different interactions with  $\text{Mg}^{2+}$  and the binding situation is even more complex than with carboxylates. In addition to outer-sphere interactions, phosphates, like carboxylates, are capable of

monodentate, bidentate and bridge bidentate inner-sphere binding modes. Due to the complexity of naturally occurring phosphorus chemistry, our understanding of the specific interactions of phosphate functionalities with metal ions is still rather limited. Comprehensive statistical analyses of available solid-state structures supported by detailed computational investigations are still missing in the literature. There is a definitive need for such studies since the molecular mechanisms of many biochemical reactions depend upon specific phosphate–metal ion interactions.

A common bonding situation for phosphates is a monodentate inner-sphere mode. An older (1998) study of available solid-state structures, which did not consider outer-sphere binding, concluded that a negatively charged (–1) phosphate group (phosphate diester) clearly favors the monodentate over a bidentate binding situation which had, at that time, not yet been observed for  $\text{Mg}^{2+}$  in a biological molecule<sup>50</sup>. One of the few systems which has been studied in detail is the interaction of a dimethylphosphate monoanion  $[(\text{MeO})_2\text{PO}_2]^-$  with  $[\text{Mg}(\text{OH}_2)_6]^{2+}$ . Recent DFT calculations which explicitly considered solvent effects concluded that an outer-sphere binding situation is preferred over a monodentate inner-sphere mode<sup>51,52</sup>. Most likely, the choice between an outer-sphere and inner-sphere situation is a fine balance between many effects, among the most likely candidates being solvent exposure, identity and number of the organic fragments bound to the phosphate, the charge on the phosphate and the electrostatic potential in the immediate vicinity. A recent QM/MM study on a DNA fragment containing a GC base pair investigated the question of outer- vs. inner-sphere interactions of  $[\text{Mg}(\text{OH}_2)_6]^{2+}$  with a diphosphate linker<sup>53</sup>. Three binding modes (two inner and one outer sphere) are fundamentally possible (Figure 6). Solvent effects were not considered in this study.

Upon dimerization of two phosphates to form pyrophosphate,  $\text{PP}_i$  (with the distinct possibility of various anionic forms depending on the pH), the situation becomes even more complex. Magnesium can now interact with just one of the phosphate groups—or with both simultaneously. In addition, a considerable conformational mobility (rotation about the P–O–P anhydride and R–O–P ester linkages) is present and the number of stable conformers grows exponentially. The dimethyl diphosphate dianion  $[(\text{MeO})_2\text{P}_2\text{O}_7]^{2-}$ , for example, has been reported to exist in at least nine different stable conformations—before interacting with magnesium<sup>54</sup>. Unfortunately, most computational studies have investigated the interaction of a naked  $\text{Mg}^{2+}$  ion with various forms of  $\text{PP}_i$  in the gas phase—results which can scarcely be applied to physiological conditions where  $[\text{Mg}(\text{OH}_2)_6]^{2+}$  is present<sup>54–56</sup>. One theoretical study did, however, partially investigate the interaction of  $[\text{Mg}(\text{OH}_2)_6]^{2+}$  with a simple glycosidic linkage (glucose- $\text{PP}_i$ ) in the gas phase (investigation of the complete manifold of conformational possibilities was not possible)<sup>57</sup>. Even so, eight representative conformations—all with comparable stabilities—were reported.

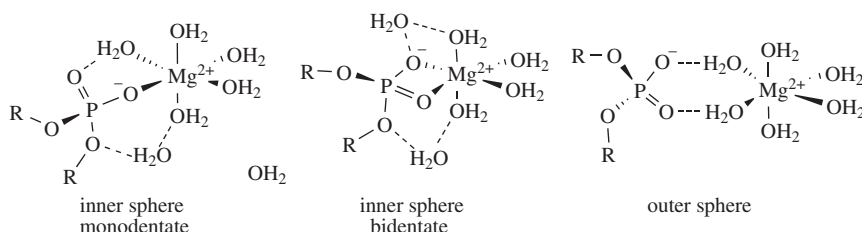


FIGURE 6. Possible binding interactions of a phosphate linker in DNA with  $[\text{Mg}(\text{H}_2\text{O})_6]^{2+}$ . Adapted with permission from Reference 53. Copyright 2006 American Chemical Society

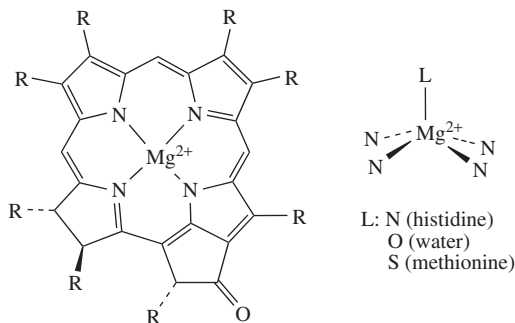


FIGURE 7. Porphyrin ring structure and unusual binding situation of  $\text{Mg}^{2+}$  in chlorophylls and bacteriochlorophylls

In over half of these conformations,  $\text{Mg}^{2+}$  interacted in an inner-sphere binding mode with both phosphate groups (on average with three oxygen ligands). Due to the biological significance of ATP, the interaction of a triphosphate linkage with  $\text{Mg}^{2+}$  has been extensively studied and will be discussed later.

### C. Nitrogen Ligands

Due to the oxophilicity of  $\text{Mg}^{2+}$ , the majority (*ca* 77%) of all bonding interactions are with oxygen ligands<sup>35</sup>. However, magnesium can and does occasionally interact with nitrogen. Usually, the amine group in the side chain of Lys or a nitrogen atom in the imidazole side chain of His replaces a water ligand to form a monodentate  $\text{Mg}-\text{N}$  bond. It is quite characteristic of magnesium that more than a single  $\text{Mg}-\text{N}$  interaction in a biomolecule is seldom observed; the other ligands involved are oxygen based ( $\text{H}_2\text{O}$ , carboxylate etc.)<sup>35</sup>.

However, a discussion of the binding modes of magnesium is not complete without mentioning the extremely unusual situation found in chlorophylls and bacteriochlorophylls (Figure 7) which is the only case where magnesium interacts with *four* (and sometimes five) nitrogen atoms in a biomolecule. The central porphyrin ring in chlorophyll binds  $\text{Mg}^{2+}$  irreversibly to the four ring nitrogens in complete disregard for its preferred hexacoordinate geometry and high oxophilicity. The magnesium is pentacoordinated in a distorted square-pyramidal geometry with the fifth ligand being located above the ring in an apical position. This fifth ligand is usually either an imidazole nitrogen of a histidine side chain or a water molecule<sup>58</sup>. In one remarkable case (a primary electron acceptor in photosystem I), this fifth ligand is a sulfur atom from a methionine residue. This is the only authenticated  $\text{Mg}-\text{S}$  bond found to date in nature<sup>59</sup>.

## V. MAGNESIUM TRANSPORT SYSTEMS

Cation transporters generally function by either partially or completely dehydrating the cation before it is delivered across the membrane<sup>60</sup>. The immense volume change between hydrated and dehydrated  $\text{Mg}^{2+}$  together with the unusually strong  $\text{Mg}^{2+}$ -water ligation energy has the consequence that the demands on a magnesium transporter are much larger than for other cations. It had therefore been postulated, long before specific information was available, that magnesium transporters would lack homology to all other

known transport systems<sup>61</sup>—a hypothesis which has subsequently been supported by all experimental evidence available to date<sup>60</sup>.

It has been recognized for a very long time that cellular  $\text{Mg}^{2+}$  levels depend on a regulated magnesium transmembrane transport. Since the concentration of  $\text{Mg}^{2+}$  is generally an order of magnitude higher inside cells than outside them, magnesium transporters must be capable of working uphill against a considerable thermodynamic gradient<sup>62</sup>. In the case of higher vertebrates, this goes as far as to recover  $\text{Mg}^{2+}$  from bodily secretions such as urine<sup>63</sup>. Although the physiology of  $\text{Mg}^{2+}$  transport in higher organisms (specifically mammals) has been extensively studied, detailed information at a molecular level is still lacking<sup>64,65</sup>. However, three different  $\text{Mg}^{2+}$  transport proteins (CorA, MgtA/B and MgtE) have been identified in bacteria and archaea<sup>3</sup>. Although their precise classification as 'ion channels' or 'transporters' is still being debated<sup>66,67</sup>, these systems do not depend upon ATP for energy but instead utilize membrane potentials to unidirectionally drive  $\text{Mg}^{2+}$  uptake into the cell<sup>66,68</sup>. Only under conditions where the intracellular concentration is dangerously high, is the fluxional direction reversed and  $\text{Mg}^{2+}$  is effluxed<sup>60</sup>.

Of these three transport systems, only CorA has been studied in depth at a molecular level. It does not share a sequence homology with any other known ion transport system and is considered to be the primary  $\text{Mg}^{2+}$  transporter in both bacteria and archaea<sup>3</sup>. In addition to  $\text{Mg}^{2+}$ , CorA is also capable of transporting  $\text{Co}^{2+}$  and  $\text{Ni}^{2+}$ <sup>69</sup>. This 'leakage' is postulated to provide some or even all of the cell's requirements for these trace elements<sup>60</sup>. Most recently, several very similar solid-state structures of a CorA transporter (*Thermatoga maritima*) have become available<sup>67,70–72</sup>. At first considered to be a homotetramer<sup>73,74</sup>, CorA is now known to possess a homopentameric quaternary structure with each subunit containing an extremely long  $\alpha$ -helix. With a total length of *ca* 100 Å, this is the longest  $\alpha$ -helix observed in a protein to date<sup>72</sup>. Five of these helices come together to provide a central ion-conduction channel or pore that transects the membrane and then extends a considerable distance into the cytoplasm (Color Plate 1). This central core of five helices, termed the 'stalk', provides most of the inner surface of the transport channel and has a narrow mouth (*ca* 6 Å) at the membrane surface and a much wider, funnel-like opening into the cell. An unusual feature of CorA is that the inside of the ion channel formed by the five stalk helices is negatively polarized along its entire length but does not contain a single charged residue. CorA obviously mediates the influx of a highly charged cation without the help of specific electrostatic interactions<sup>60</sup>. It should be mentioned that all available structures of CorA represent a 'closed' transporter configuration.

At the entrance of the closed transporter, a ring of highly conserved Asn residues provides a gate. When this gate opens, the initial interaction is believed to be with a fully hydrated  $[\text{Mg}(\text{H}_2\text{O})_6]^{2+}$  cation since CorA transports all hexacoordinated metal ions whose radii are comparable to  $\text{Mg}^{2+}$  ( $\text{Ni}^{2+}$  and  $\text{Co}^{2+}$ )<sup>69</sup>. Discrimination between cations probably occurs at a later stage since  $[\text{Co}(\text{NH}_3)_6]^{3+}$ , very nearly the same size as  $[\text{Mg}(\text{H}_2\text{O})_6]^{2+}$ , is a very potent inhibitor<sup>75</sup>. The incoming  $\text{Mg}^{2+}$  is suspected to be at least partially or even fully dehydrated during passage since ions with larger radii ( $\text{Mn}^{2+}$ , for example) are not transported<sup>75</sup>. In one solid-state structure crystallized in the presence of  $\text{Co}^{2+}$ , a single  $\text{Co}^{2+}$  is trapped just behind the closed Asn gate<sup>71</sup>. Once past the gate, the channel narrows and a passage with a diameter of *ca* 3.3 Å composed of a circular arrangement of conserved residues (a Thr and a Met per stalk), termed the hydrophobic girdle (HG), is encountered. At this point, dehydration is suspected to begin<sup>71</sup>. The real obstacle, however, is encountered somewhat further along at the membrane–cytosol interface. Here, pairs of conserved Leu and Met residues (one pair per subunit) form a hydrophobic belt (HB) that further narrows the passage down to 2.5 Å in the closed conformation. This region is believed to be the primary bottleneck for ion movement<sup>72</sup>.

For the duration of its passage through the membrane, a shorter ring of five additional transmembrane  $\alpha$ -helices provides an outside collar for the stalk. The ends of these helices are arranged so that an unusual ring of 20 positively charged lysine residues—called the sphincter—encircles the stalk at the level of the membrane–cytoplasm interface. At exactly this level, two additional lysine side chains in each helix point outside and away from the central channel which increases the total number of lysine residues in the sphincter region to 30. This sphincter tightly surrounds the hydrophobic girdle. In the closed conformation, the concentrated electrostatic potential generated by the sphincter will strongly repel positively charged  $\text{Mg}^{2+}$  cations, especially if they have already been partially dehydrated. After the hydrophobic girdle, the pore gradually widens into the funnel region. At this point, another metal binding position has been identified<sup>71</sup>. The region from the hydrophobic girdle until the funnel has opened considerably is characterized by successive rings of negative polarity due to side chains bearing negatively polarized hydroxyl and carbonyl ligands<sup>71</sup>.

At the wide cell interface opening, a second array of  $\alpha$ -helices (2 per subunit) also surround the stalk and hang ‘down’ similar to the branches of a weeping willow tree. Surrounding these is an additional arrangement of  $\beta$ -sheets. The tips of these willow helices and  $\beta$ -sheets contain an extraordinary number (a total of 50) of aspartic and glutamic acids which build a ring of negative charge, which undoubtedly helps to counterbalance the positively charged sphincter region. Taken together, the willow helices and  $\beta$ -sheets form an  $\alpha\beta\alpha$  sandwich domain with a novel type of ‘funnel’ fold containing two  $\text{Mg}^{2+}$  binding sites (occupied by either  $\text{Ca}^{2+}$  or  $\text{Co}^{2+}$  ions in some solid-state structures<sup>71</sup>) on the outside of the funnel.

The current model for  $\text{Mg}^{2+}$  transport is illustrated in Figure 8 and is believed to be controlled by a ‘magnesium sensor’ consisting of two specific  $\text{Mg}^{2+}$  binding sites located on the outside of the funnel in the  $\alpha\beta\alpha$  sandwich domain that spans the willow helices and  $\beta$ -sheets<sup>60,71</sup>. Studies of similar binding sites in other proteins<sup>6</sup> indicates that these sites will probably have an affinity for  $\text{Mg}^{2+}$  that is slightly less than the average free concentration of  $\text{Mg}^{2+}$  in cells<sup>60</sup>. When the concentration of  $\text{Mg}^{2+}$  in the cell drops below

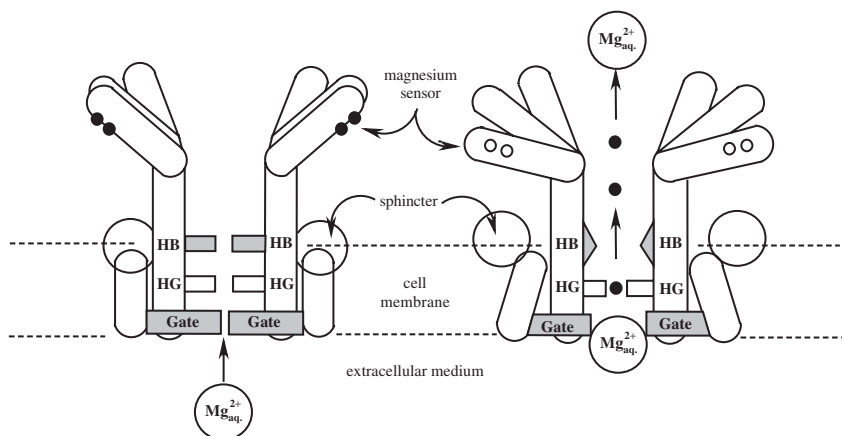


FIGURE 8. Current model for the gating mechanism in the CorA transporter. Left: closed conformation with the magnesium binding sites in the sensor occupied. Right: postulated open conformation allowing ion transport into the cell. Adapted by permission of Macmillan Publishers Ltd. from Reference 71



this critical level, these binding sites will lose their metal cations. It has been suggested that this is the pivot point of a lever system which allows binding/debinding events to drive gate closing/opening<sup>67</sup>. Loss of  $\text{Mg}^{2+}$  in one or more of these binding sites is postulated to trigger rotation or other movement which would move the willow helices away from the stalk, pulling the positively charged sphincter with them and thus opening the Asn gate and the Leu/Met HB bottleneck<sup>71</sup>. Due to the length of the stalk, even a small movement at the binding site could create a large leverage movement<sup>72</sup>. Once  $\text{Mg}^{2+}$  (partially or even fully dehydrated) has passed the bottleneck, it will be drawn along the pore by the successive negatively polarized rings, probably much like a bead on a chain<sup>71</sup>. As the pore widens into the funnel, the  $\text{Mg}^{2+}$  will be spontaneously rehydrated.

## VI. UNIVERSAL ENERGY CURRENCY OF LIFE

Living organisms depend on the continual availability of free energy in an immediately useable bioequivalent form. This fuel of life is used to sustain countless biological functions. For example, mechanical processes (cellular motions, muscle contractions etc.), the active transport of small molecules and ions as well as many enzymatic activities and the synthesis of large biomolecules all require an energy source. The requirements for this biofuel are quite strict. It must be a small organic molecule that contains a large amount of energy stored in its molecular structure that, in addition, is stable under general physiological conditions. However, it must also be able to instantaneously undergo a simple chemical reaction which releases the stored energy upon demand. One of the few organic functionalities that meets these stringent requirements is a phosphorus anhydride bond in a polyphosphate. A P-O-P linkage stores a good deal of chemical energy, is generally immune towards general base or acid catalyzed hydrolysis in aqueous solutions at pH *ca* 7 and can be specifically hydrolyzed upon demand.

It is believed that the energy carrier at the beginning of life was triphosphate ( $\text{P}_3\text{O}_{10}^{4-}$ ), which is often called polyphosphate<sup>76</sup>. A vestige of this activity can still be found in some bacterial enzymes [poly(P)ATP-NAD kinases] which are capable of utilizing triphosphate as an energy source<sup>77,78</sup>. In the meantime, evolutionary adaptation has resulted in the development of nucleoside triphosphates (NTP and dNTP), one of which (adenosine triphosphate, ATP) now represents the general biofuel of life (Figure 9)<sup>79</sup>. Hydrolytic removal of the  $\gamma$ -phosphate to form adenosine diphosphate (ADP) releases a considerable amount of free energy ( $\Delta G \approx -30.5 \text{ kJ mol}^{-1}$ <sup>80</sup>) which can be employed in further chemical reactions. Most biological processes which require energy are now driven by an  $\text{ATP} \rightleftharpoons \text{ADP}$  cycle. As a consequence, the bioturnover of ATP in organisms is extremely high. For example, the daily turnover of ATP in a human approximates half of his/her body weight<sup>81</sup>. In addition to the ATP-ADP cycle, some biosyntheses (synthesis of DNA

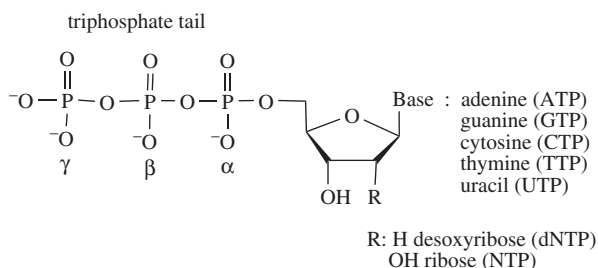


FIGURE 9. The chemical structure of nucleoside triphosphates (NTP and dNTP)

and RNA sequences, for example) are driven by ATP analogues in which adenosine has been substituted for another nucleobase.

### A. $\text{MgATP}^{2-}$

Almost all processes involving ATP depend on magnesium as an essential cofactor. Although this has been recognized since the 1940s, only in the past few years has a detailed understanding of the interaction of magnesium with ATP begun to become available. ATP binds quite strongly to  $\text{Mg}^{2+}$  in aqueous solutions. It has been estimated that 75% or more of all free ATP in cells is actually present in a  $\text{MgATP}^{2-}$  complex which, in addition, is generally accepted as being the biologically active form of ATP<sup>1,5</sup>. ATP has numerous oxygen atoms in the phosphate tail, all of which are capable of binding to  $\text{Mg}^{2+}$ . The sugar and nucleobase components also contain several heteroatoms (oxygen and nitrogen) which could also conceivably interact with  $\text{Mg}^{2+}$ . Solid-state structures of  $\text{MgATP}^{2-}$  are unfortunately not available due to spontaneous nonenzymatic hydrolysis of the triphosphate tail during crystallization<sup>82</sup>. However, one structure of  $\text{MgATP}^{2-}$  was obtained upon cocrystallization with bis(2-pyridyl)amine<sup>83,84</sup>. In this structure, two distinct coordination modes for magnesium are present (Figure 10). An  $[(\text{ATP})_2\text{Mg}]^{6-}$  complex resulted in which all of the water ligands were replaced by monodentate oxygen ligands originating from each of the phosphates in ATP. The second magnesium in the form of  $[\text{Mg}(\text{OH}_2)_6]^{2+}$  stabilizes the complex via outer-sphere coordination. The biological relevance of such a structure is probably minimal.

Although ATP predominantly exists in the 'anti' configuration (the nucleobase points away from the sugar ring) in aqueous solutions, it is an extremely flexible molecule<sup>85</sup>. As has already been discussed for the much simpler pyrophosphate ( $\text{PP}_i$ ), a complex mixture of conformational isomers can be expected. NMR studies on  $\text{ATP}/\text{Mg}^{2+}$  solutions have shown that the triphosphate tail is completely deprotonated at pH 7 and a  $\text{MgATP}^{2-}$  complex is the dominant form<sup>86</sup>. At or around pH 7, magnesium only interacts with ATP via the phosphate chain and the nucleotide part of ATP does not participate in chelation<sup>87</sup>. NMR experiments have furthermore sought to determine exactly how the phosphate tail coordinates with magnesium in solution, with varying results. Some experiments suggest that magnesium coordinates with one oxygen from each of the three phosphates (Figure 10)<sup>88</sup>. Other studies indicate that only one oxygen from the  $\gamma$ - and the  $\beta$ -phosphate coordinate

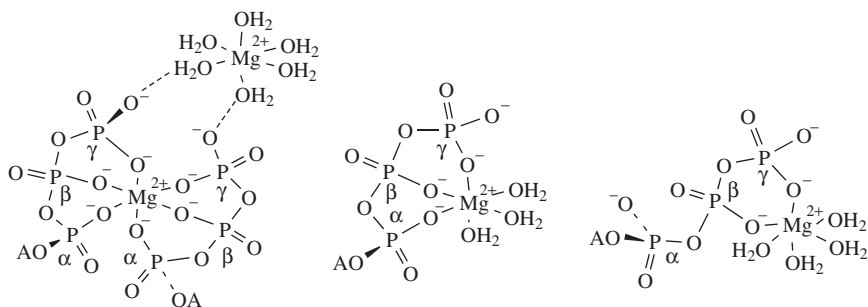


FIGURE 10. Left: solid-state structure of  $\text{MgATP}^{2-}$  (cocrystallized with *bis*(2-pyridyl)amine). Adapted by permission of the Royal Society of Chemistry from Reference 83, and with permission from Reference 84. Copyright 2000 American Chemical Society. Right: the two predominant conformations of  $\text{MgATP}^{2-}$  in aqueous solutions. Adapted by permission of Springer Science and Business Media from Reference 90

and that the  $\alpha$ -phosphate is not involved<sup>87,89</sup>. A more recent molecular dynamics study of  $\text{MgATP}^{2-}$  in water has found a possible explanation for these disparate findings. According to this study, magnesium is equally likely to coordinate an oxygen atom of either the two end phosphates or of all three phosphates<sup>90</sup>. In addition, a relatively high barrier exists between the two conformations; conformational switching is thus rather unlikely to occur<sup>90</sup>.

## B. Biosynthesis of ATP

The biosynthesis of ATP is quite challenging due to the fact that a considerable thermodynamic gradient must be overcome in order to drive this extremely endothermic reaction. This synthesis is achieved in the cell membranes of bacteria and mitochondria through a very effective combination of a complex biomechanical motor with chemical processes<sup>91</sup>. ATP synthases consist of two basic components—a catalytic  $F_1$  unit which is responsible for the chemical reaction (binding of ADP and  $P_i$  with subsequent oxidative phosphorylation) and the  $F_0$  transmembranal unit which delivers the necessary energy in the form of an electrochemical proton gradient (Figure 11)<sup>92</sup>. Solid-state structures of the  $F_1$  unit have revealed that it consists of a hexagonal array of  $\alpha$  and  $\beta$  subunits bound on a shaft comprised of three further subunits ( $\gamma$ ,  $\delta$  and  $\epsilon$ )<sup>93,94</sup> which is driven by  $F_0$  and rotates in discrete  $120^\circ$  steps during catalysis<sup>95,96</sup>. The synthesis of ATP is tightly coupled to and driven by the rotating shaft<sup>97</sup>—quite analogous to a drive shaft in a mechanical motor<sup>98</sup>. The ATPase motor has a further remarkable property. Reversing the rotary motion switches the enzymatic mode from ATP synthesis to ATP hydrolysis<sup>99</sup>.

Energy transmitted over the drive shaft induces the release of newly synthesized ATP on one of the  $\beta$ -subunits, simultaneously promotes ATP synthesis on the next  $\beta$ -subunit and concomitantly binds ADP,  $\text{Mg}^{2+}$  and  $P_i$  to the third<sup>100</sup>. It is suspected that ADP is bound before  $P_i$ <sup>101</sup>. A binding-change mechanism is often used to illustrate this rotational behavior. One of the three  $\beta$ -subunits is believed to be in an ‘open’ O conformation. Upon rotation, this changes to a ‘loose’ L conformation with a high binding affinity for ADP and  $P_i$ . After these substrates are bound, rotation results in a tightly closed conformation T in which ATP is synthesized. Further rotation opens the conformation (now O) and ATP is released<sup>102</sup>. Upon a rotation of  $360^\circ$ , each  $\beta$ -subunit has successively bound ADP and  $P_i$ , synthesized ATP and released it.

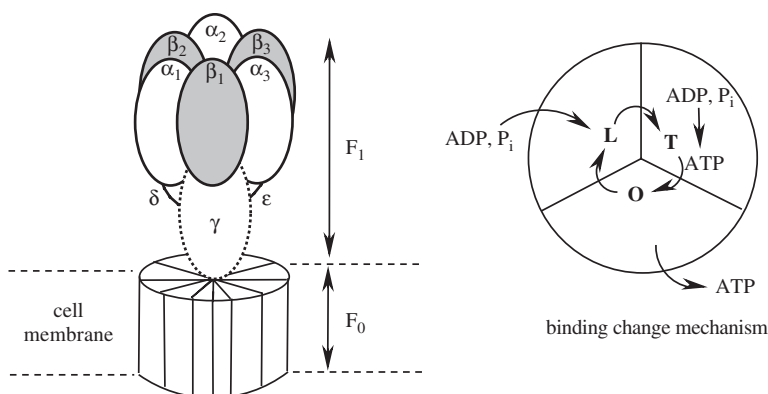


FIGURE 11. Left: simplified schematic diagram of a mitochondrial ATP-synthase. Adapted from Reference 97 with permission from AAAS. Right: binding change mechanism for the synthesis of ATP

Although our knowledge of the general motoric details of ATPase is considerable, critical chemical events taking place in the active sites in the  $\beta$ -subunits, especially the role of the essential  $\text{Mg}^{2+}$  ion, are just now beginning to be unraveled. For quite some time, traditional organic mechanisms (linear pentacoordinated transition structures/intermediates, for example) were postulated as being the critical chemical step in the formation of the  $\beta, \gamma$ -phosphorus anhydride bond in ATP<sup>103</sup>. In these mechanisms, the role of  $\text{Mg}^{2+}$  was believed to be limited to binding, orientating and activating ADP and  $\text{P}_i$ <sup>104</sup>. However, such traditional mechanisms are not capable of explaining exactly how mechanical motion is effectively translated into a single phosphorus anhydride bond<sup>104</sup> and the chemical mechanism of phosphorylation has remained an enigma<sup>105</sup>.

Valuable insights have been gained by a remarkable phenomenon recently discovered: ATPase shows a large magnetic magnesium isotope effect<sup>104</sup>. The rate of ATP synthesis in which  $^{25}\text{Mg}^{2+}$  (nuclear spin 5/2; magnetic moment  $-0.855$  Bohr magneton) is present is twice to three times higher than in the presence of the spinless, nonmagnetic nuclei  $^{24}\text{Mg}^{2+}$  and/or  $^{26}\text{Mg}^{2+}$ <sup>106, 107</sup>. The magnesium isotope effect is a nonclassical phenomenon discovered in 1976<sup>108</sup> and it has since then been shown that *any* reaction involving this isotopic effect is spin-selective; paramagnetic intermediates, e.g. radicals, radical ions and/or radical ion pairs, *must* be involved<sup>109, 110</sup>.

One of the interesting properties of ATPase is that, during or directly after ADP,  $\text{P}_i$  and  $\text{Mg}^{2+}$  are bound, a structural change (mechanical motion) compresses the active site and 'squeezes' water out of the active pocket (change from the 'loose' to the 'closed' conformation). As a result, the primary hydration shell of  $\text{Mg}^{2+}$  is partially removed<sup>104</sup>. This concentrates the positive charge on the ion itself and drastically increases its ability to accept a single electron. The mechanics of ATPase thus directly transforms  $\text{Mg}^{2+}$  into a very reactive electron acceptor (at this point, mechanical energy becomes chemical energy). It is now postulated that the first step in ATP synthesis is a one-electron transfer from the terminal phosphate in ADP to  $\text{Mg}^{2+}$ <sup>104</sup>. A radical-ion pair [ $\text{Mg}^+ - \text{ADP}^\bullet$ ] is generated which, according to the large isotope effect observed, is also the rate-limiting step in the phosphorylation (Figure 12). This primary radical-ion pair is in the singlet spin state, as are all thermally generated radical-ion pairs, and the radical electron is localized on one of the  $\beta$ -oxygen atoms in the phosphate tail of ADP. This extremely reactive oxyradical now attacks the  $\text{P}=\text{O}$  bond in  $\text{P}_i$ . On the way to ATP, a species results in which the  $\gamma$ -phosphate is in a pentacoordinated geometry. This undergoes a fast  $\beta$ -decomposition which releases  $\text{P}_i$  and ATP. A hydroxyl radical in the immediate vicinity of  $\text{Mg}^+$  remains behind. Fast electron spin relaxation in  $\text{OH}^\bullet$  ( $10^{-11}$  s or even shorter)

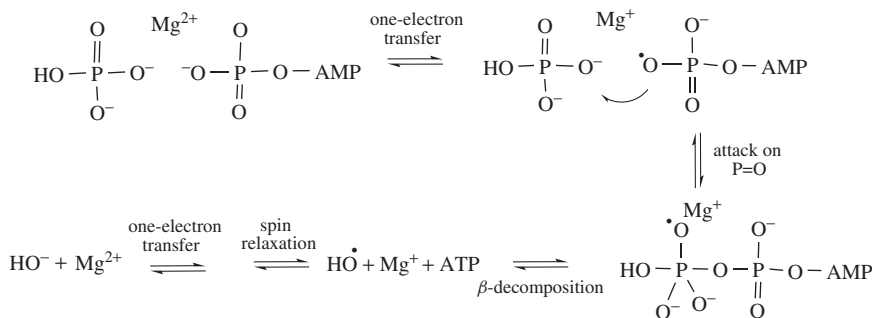


FIGURE 12. Radical-ion pair mechanism for the biosynthesis of ATP. Reproduced by permission of Springer Science and Business Media from Reference 104

makes the reverse electron transfer possible and  $\text{Mg}^{2+}$  is regenerated<sup>104</sup>. The calculated isotope effect for this mechanism is in good agreement with experimental results<sup>111</sup>. Such a radical-ion pair mechanism allows for the possibility of isotopic label ( $^{18}\text{O}$ ) transfer from  $\text{P}_i$  to water. It has been recognized since as early as 1953 that such cross-transfer reactions accompany oxidative phosphorylation<sup>112</sup>; a mechanistic explanation has not, until now, been offered for this finding.

### C. Hydrolysis of ATP

All of the countless biochemical functions of ATP involve specific hydrolysis of either the  $\text{P}_\gamma\text{--O--P}_\beta$  or  $\text{P}_\beta\text{--O--P}_\alpha$  phosphorus anhydride bond. The underlying organic mechanism of phosphorus ester bond hydrolysis has, of course, been the subject of numerous experimental<sup>113</sup> and theoretical<sup>114–116</sup> studies. In the absence of a metal cofactor ( $\text{Mg}^{2+}$ ), two general mechanistic pathways are fundamentally possible: an associative and a dissociative reaction (Figure 13). The associative pathway resembles a general  $\text{S}_\text{N}2$ -type reaction; in-line attack of water initiates hydrolysis which proceeds over a pentacoordinated transition structure or hypervalent intermediate. In the dissociative pathway,  $\text{P--OR}$  bond breakage precedes the water attack. A more or less 'free' metaphosphate ( $\text{PO}_3^-$ ) species is generated which then accepts the water<sup>117,118</sup>. In the dissociative pathway, a linear approach of the water is not absolutely necessary.

The influence of a single hydrated  $\text{Mg}^{2+}$  ion on the general mechanism of hydrolysis has only been considered in two independent studies using  $\text{MeP}_2\text{O}_7^{3-}$  as a model for ATP<sup>119,120</sup>. The presence of  $\text{Mg}^{2+}$  does not change the two possible basic mechanisms (associative vs. dissociative). Both studies concluded that a hydrated  $\text{Mg}^{2+}$  cation helps to promote hydrolysis (as compared to the nonmetallated, gas-phase case) primarily by stabilizing the transition structures/hypervalent intermediates and end products. However, this stabilization is definitely not enough to overcome the considerable kinetic barrier that hinders spontaneous hydrolysis in aqueous solutions. This is in accord with the fact that free  $\text{MgATP}^{2-}$  is quite stable in water at pH 7. Extensive kinetic studies on ATP (and other NTPs) have conclusively demonstrated that *two* metal ions have to be coordinated to the triphosphate chain before hydrolysis can take place<sup>121,122</sup>. These studies clearly indicate that binding of two  $\text{Mg}^{2+}$  ions to the triphosphate tail in a  $\text{M}_{\alpha,\beta}\text{M}_\gamma$  mode (Figure 14) clearly promotes the hydrolysis of the  $\text{O}_\beta\text{--P--O}_\gamma$  bond<sup>123,124</sup>.

Although comprehensive structural analyses of ATP binding sites are not yet available, it is clear that the primary binding interactions usually originate from hydrophobic

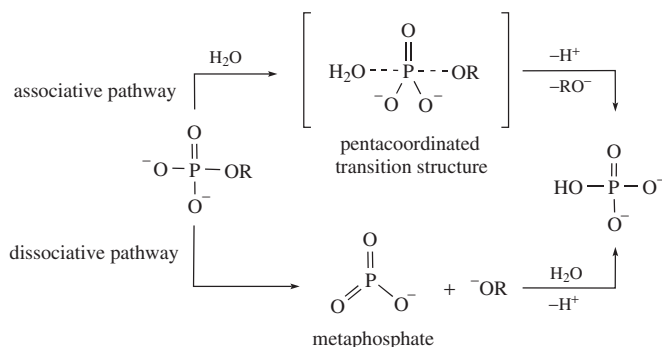


FIGURE 13. Fundamental pathways for the hydrolysis of a phosphorus ester bond

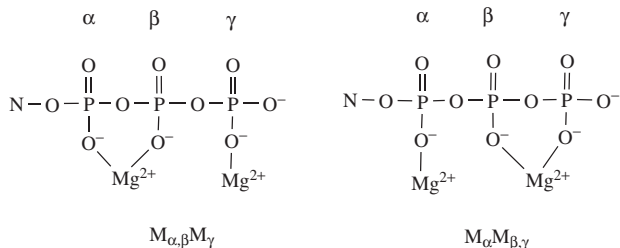


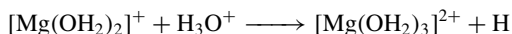
FIGURE 14. General binding modes of two  $\text{Mg}^{2+}$  ions with nucleoside (N) triphosphates. Reproduced by permission of The Royal Society of Chemistry from Reference 123

interactions of adenosine (or other nucleotides) with the enzyme pocket. Interactions between  $\text{Mg}^{2+}$  and protein residues are usually minimal, although a magnesium ion sometimes coordinates in a monodentate fashion with one or maximum two oxygen ligands from protein side chains. This leaves the phosphate tail relatively free and a  $M_{\alpha,\beta}M_{\gamma}$  binding situation is often observed<sup>123</sup>. In the meantime, it is clear that this motif is extremely relevant in the mode of action of enzymes that promote transphosphorylations, i.e. enzymes that transfer the  $\gamma$ -phosphate of an NTP molecule to a substrate<sup>122, 125</sup>. If the active site is unusually hydrophobic, sometimes one of the two metal ions can be replaced by an ionic interaction (e.g. Arg)<sup>126</sup>.

Several other major classes of enzymes, among them the nucleic acid polymerases, activate ATP (and other NTPs) in a completely different manner<sup>127</sup>. Similar to transphosphorylation enzymes, they utilize two metal ions for catalysis<sup>128</sup>. However, steric interactions are purposely employed in order to reverse the preferred binding situation. A  $M_{\alpha}M_{\beta,\gamma}$  motif is generated which weakens the  $P_{\alpha}-O-P_{\beta}$  linkage<sup>123, 124</sup>. This allows a nucleoside monophosphate group to be transferred (under liberation of  $\text{PP}_i$ ), a process which is essential in the biosynthesis of DNA and RNA sequences.

A current molecular dynamics study using a DFT-based method looked at the magnesium-catalyzed hydrolysis of the  $P_{\alpha}-O-P_{\beta}$  linkage in guanosine triphosphate (GTP) and discovered that weakening this linkage may result in a fundamental change in the hydrolytic mechanism<sup>129, 130</sup>. This study explicitly considered solvation effects by performing all computations in a boundary box containing 180 water molecules. As  $[\text{Mg}(\text{OH}_2)_6]^{2+}$  approaches the negatively charged oxygen atoms in the  $P_{\gamma}$  and  $P_{\beta}$  phosphate tail, it begins to bind to them in a bridge bidentate manner (Figure 15). This causes a spontaneous lowering of the coordination number on magnesium from six to four, as four water ligands spontaneously leave. A similar reduction in the coordination number has been previously discussed for hydroxide ligands<sup>14</sup>. This initial tetrahedral complex is unstable; as the simulation time proceeds, it spontaneously embarks on a remarkable reaction path in which  $\text{MgGTP}^{2-}$  is completely decomposed. Four extremely unusual, very unstable species result: two equivalents of metaphosphate ( $\text{PO}_3^-$ ), the radical cation  $[\text{Mg}(\text{OH}_2)_2]^+$ , molecular oxygen O and a  $\text{GMP}^{\bullet-}$  radical anion<sup>129</sup>.

Water immediately transforms the  $\text{PO}_3^-$  into  $\text{HPO}_4^{3-}$  which presents no further problems.  $[\text{Mg}(\text{OH}_2)_2]^+$  also spontaneously reacts with water in the presence of a proton in a series of complex steps to finally yield  $[\text{Mg}(\text{OH}_2)_6]^{2+}$ <sup>129</sup>. High-level quantum-chemical calculations revealed that the first and most important step in this procedure is a single electron transfer from  $\text{Mg}^+$  to  $\text{H}^+$  which occurs in the conical intersection between the singlet and triplet hypersurface of the following reaction<sup>131</sup>:



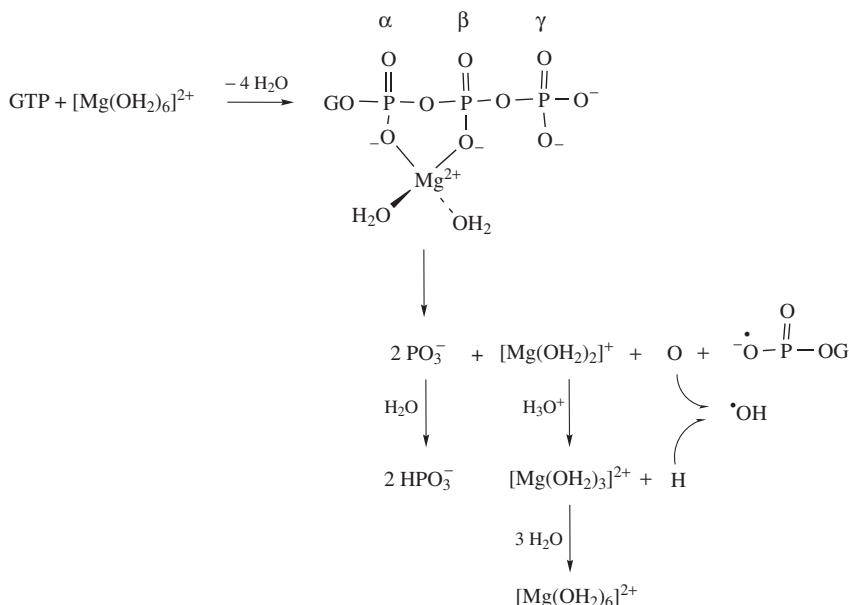


FIGURE 15. Spontaneous decomposition of  $\text{MgGTP}^{2-}$  upon coordination of  $\text{Mg}^{2+}$  in a  $\text{M}_{\gamma,\beta}$  motif. Reproduced by permission of the PCCP Owner Societies from Reference 129

As the proton is converted into molecular hydrogen, it is immediately expelled from the complex at a high velocity<sup>129</sup>. The  $[\text{Mg}(\text{OH}_2)_3]^{2+}$  species left behind is in its ground state and can now simply accept further water ligands until  $\text{Mg}^{2+}$  has restored its optimal octahedral coordination geometry<sup>132</sup>. The proton ejected is assumed to collide with the oxygen atom in the immediate vicinity and a hydroxyl radical ( $\cdot\text{OH}$ ) is produced. If the  $\text{GMP}^{\cdot-}$  radical anion is generated in the heart of an active site with the hydroxyl group of a substrate R already lined up and positioned, it will attack it and form a new  $\text{P}-\text{O}-\text{R}$  bond under ejection of molecular hydrogen from the hydroxyl group. This is immediately trapped by the hydroxyl radical ( $\cdot\text{OH}$ ) and both nasty species end up as water.

This mechanism is still quite controversial<sup>133, 134</sup>. However, CIDNP (chemically induced dynamic nuclear polarization) experiments on a magnesium-dependent DNA-I polymerase (which hydrolyzes the  $\text{P}_\alpha-\text{O}-\text{P}_\beta$  linkage in a NTP in order to insert a new nucleoside in a growing DNA chain) being fed  $\text{MgGTP}^{2-}$  revealed that  $\text{GMP}^{\cdot-}$  radical anions may indeed be involved<sup>129</sup>.

## VII. INTERACTIONS WITH DNA AND RNA

Only four nucleobases encode sequence-specific information in both DNA and RNA. In comparison to proteins, DNA/RNA obviously provides for much less chemical diversity (Figure 16). Nevertheless, nature manages to encode genetic information in its entirety using this simple strategy. Although a fact often forgotten or neglected in textbooks, both DNA and RNA are polyelectrolytes and contain a negatively charged phosphate group per nucleotide. As such, they have an absolute requirement for charge equalization. Usually, hydrated metal cations ( $\text{Na}^+$ ,  $\text{K}^+$ ,  $\text{Mg}^{2+}$  and  $\text{Ca}^{2+}$ ) in the neighborhood of DNA and

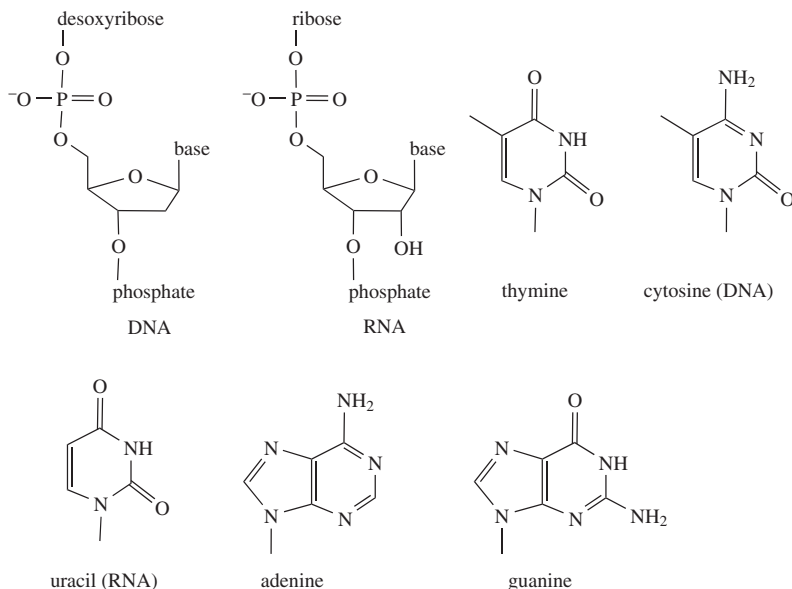


FIGURE 16. Fundamental subunit of the basic polymeric structure of DNA and RNA as well as the individual nucleobases involved

RNA strands take care of this job. However, on occasion, positively charged polyamines or even side chains of proteins can neutralize the backbone charge<sup>135</sup>.

Metal ions interact with DNA or RNA in at least four different ways<sup>136</sup>. The most general mode is that of position unspecific, diffuse binding in which the presence of the (hydrated) metal cation simply provides charge screening to overcome electrostatic repulsions between RNA backbone fragments<sup>10</sup>. These diffuse interactions can be modeled by mathematical approximations such as the Poisson–Boltzman distribution<sup>137, 138</sup>. When DNA or RNA folds, it sometimes creates well-defined sites, ‘holes’, with a high concentration of negative charge. These sites often contain electrostatically localized metal ions that do not further interact with the substructure. Binding is controlled by simple electrostatics and the size of the ‘hole’<sup>139</sup>. Many different ion types, including protonated polyamines, can occupy these sites. Specific binding interactions start with metal ions (often  $Mg^{2+}$ ) bound through outer-sphere coordination modes<sup>140</sup>. In many cases, an extensive network of specific hydrogen-bonding interactions is built up between the DNA or RNA and the water ligands of the metal ion<sup>136</sup>. Finally, the metal ions can interact directly via an inner-sphere coordination. As in the case of protein interactions, this can occur with a variable number (1–3) of ligands, the most common being the phosphoryl oxygens in the backbone, purine N7, base carbonyl groups and the 2′–OH in ribose (RNA)<sup>141</sup>. Finally, a mixed-sphere mode which combines both inner- and outer-sphere binding is sometimes observed<sup>142</sup>.

### A. Magnesium and Structural Stability

The high negative charge in the phosphate backbone of both DNA and RNA is detrimental towards folding into compact structures such as the well-known double-helix motif.



Due to its high charge, small size and propensity for promoting the formation of extensive stabilizing networks of hydrogen bonds,  $\text{Mg}^{2+}$  is often the most effective ion for reducing electrostatic repulsions and promoting folding. As an example, it was recognized very early on (1972) that millimolar concentrations of  $\text{Mg}^{2+}$  stabilize RNA tertiary structures that are only marginally stable in the presence of monovalent ions<sup>143</sup>. In the meantime, a massive amount of data has unequivocally demonstrated the essential role of metal ions in determining the folding kinetics and maintaining the thermal stability of DNA and RNA helices and other secondary structures<sup>10,11</sup>. It is clear that metal ion interactions play a significant role in determining local conformation and topology. However, our understanding of just how important they really are is still rather limited<sup>9</sup>.

Perhaps the most common site-specific magnesium binding sites in both DNA and RNA are localized in the major and minor grooves of double-helix strands. Backbone folding in these regions forms cavities that are lined with lone electron pairs from the nucleobases (typically the N7 purine nitrogen and the O6 carbonyl group) that provide excellently positioned electrostatic contacts for a hydrated  $\text{Mg}^{2+}$  ion<sup>9,144</sup>. An example of this has already been illustrated for a DNA double helix in Figure 4, where crystallization of the Dickerson–Drew dodecamer (sequence CGCCAATTCGCG) revealed one bound  $\text{Mg}^{2+}$  located in the major groove per duplex (helix dimer)<sup>30,31</sup>. Raised  $\text{Mg}^{2+}$  concentrations lead to an improved crystal quality and the use of synchrotron radiation allowed a much better resolution (1.1 Å). Shortly after the first structure was published, five different specific magnesium binding sites were located in this dodecamer (see Color Plate 2)<sup>145</sup>. Four of them bind in an outer-sphere mode. In the major groove,  $\text{Mg}_1$  provides a bridge linking two guanines from opposite strands via an outer-sphere coordination.  $\text{Mg}_1$  is the only ion present in crystals grown with lower  $\text{Mg}^{2+}$  concentrations, which indicates that this binding site has the highest affinity and is the first one to be occupied<sup>145</sup>. This magnesium affects the conformation of the duplex in that it introduces a slight ‘kink’ ( $11^\circ$ ) in the helix axis. In the minor groove,  $\text{Mg}_2$  bridges phosphates from opposite strands. This clearly affects the width of the groove by effectively ‘zipping’ it up, thus allowing the negatively charged backbones to closely approach each other. For example, the width of this groove is 2 Å less than the same dodecamer when crystallized with larger  $\text{Ca}^{2+}$  ions<sup>146</sup>.  $\text{Mg}_3$  is the only ion that interacts via an inner-sphere binding mode and binds in a monodentate manner to the phosphate backbone.  $\text{Mg}_4$  and  $\text{Mg}_5$  are located on the outside of the phosphate backbone and provide charge equalization via outer-sphere interactions.

Many RNA structural motifs also specifically bind  $\text{Mg}^{2+}$  with a striking example being the Loop E motif illustrated in Color Plate 2<sup>147</sup>. In this motif, four magnesium ions provide a zipper for the minor groove which results in a stable, compact secondary structure.  $\text{Mg}_1$  binds monodentately to the backbone and  $\text{Mg}_2$  shows a typical outer-sphere binding pattern. The most interesting feature, however, is a very unusual  $\text{Mg}_2$  cluster in which three water ligands bridge two magnesium ions. This cluster is bound directly to the backbone via a monodentate bridging motif. Such  $\text{Mg}_2$  clusters are occasionally found to stabilize specific RNA folding patterns, a further example being a fragment of a 5S rRNA domain (Color Plate 2)<sup>147</sup>. This fragment adopts its characteristic structure only in the presence of  $\text{Mg}^{2+}$ . Twelve magnesium ions bind in a specific manner<sup>148</sup>. Two binuclear clusters are present: one is buried deep in a major groove and the other is located on the outside of a major groove that has been twisted and compacted by the presence of a twisted Loop E motif in which four further magnesium ions participate. A partial Loop E motif with two more  $\text{Mg}^{2+}$  ions glues the fragment ends together.

## B. Ribozymes

Traditionally seen as a passive carrier of genetic information, it came as a shock when the catalytic properties of RNA were discovered in early 1980s<sup>149,150</sup>. In the meantime,

it is clear that RNA catalysis is quite ancient; it may have played an important role in the early stages of evolution and it is quite possible that RNA was used to support a primitive metabolism<sup>151</sup>. Although some RNA activities may be a 'fossil' remnant of an earlier world, the modern chemical function of RNA is extremely complex and highly varied. RNA is deeply involved in almost every aspect of cellular metabolism. In spite of its basic chemical simplicity, RNA sequences serve in a surprising number of multifunctional roles that vary from structural scaffolds<sup>152</sup>, conformational riboswitches<sup>153</sup>, regulatory signaling<sup>151</sup> and catalytic systems (ribozymes<sup>12</sup>). RNA catalysis is considerably more widespread than was originally believed<sup>154</sup>.

Three different families of naturally occurring ribozymes are known today—the large and small phosphoryl transfer ribozymes and the aminoacyl esterase ribozymes. The large phosphoryl transfer enzymes are a widely varied collection of huge molecular machines which include the group I<sup>155</sup> and group II<sup>156</sup> introns, ribonuclease P<sup>157</sup> and, perhaps, the eukaryotic spliceosome<sup>12</sup>. They all cleave or synthesize phosphodiester linkers in the backbones of RNA (and often DNA), usually via a classical  $S_N2$  mechanism involving the in-line attack of a nucleophile (typically alcohol or water) at phosphorus. The small phosphoryl transfer enzymes are typically found in the genome of primitive viruses. These are small self-cleaving RNA motifs which are responsible for cutting long RNA strands into individual genes<sup>158</sup>. Among others, they include the hammerhead family<sup>159</sup> and the hepatitis delta<sup>160</sup> ribozymes. At the interface between the RNA and protein worlds, the ribosomal aminoacyl esterases catalyze the making and breaking of amide bonds. Since 2000, it has become increasingly clear that ribosomal RNA actually catalyzes the synthesis of proteins<sup>161</sup>.

In contrast to this, catalytic DNA has not yet been observed in nature, although synthetic 'DNAzymes' have been successfully designed<sup>162</sup>. This gives rise to the question of exactly why there are no natural DNAzymes. Is this due to a natural 'fluke' in evolution or does the exchange of one single nucleobase (cytosine for uracil) and the presence of the additional hydroxyl group (ribose instead of deoxyribose) in the sugar have something to do with promoting the catalytic properties of RNA? No satisfactory explanation has yet been offered.

Most ribozymes are folded into compact, stable tertiary structures that possess a unique conformation that is responsible for the chemical activity observed. In addition, most of these systems exhibit a clear requirement for  $Mg^{2+}$  ions<sup>12</sup>. It is currently accepted that the dynamics of RNA folding follows a typical two-step procedure (Figure 17)<sup>12, 163</sup>. In the first step, the secondary structure with regions of single and double strands is formed. It has been recognized for quite some time that this secondary structure formation can be stimulated from almost anything which screens charges and brings polyanionic backbones in close proximity to each other (mono- and divalent metal cations, protonated polyamines and even proteins)<sup>164</sup>. In contrast to this, adoption of the tertiary structure under collapse into a specific 3D conformation (second step) is usually controlled by stringent metal ion requirements (often  $Mg^{2+}$ )<sup>165, 166</sup>. The hypersurface of RNA folding is quite complex and stable misfolded intermediates easily occur. The overall rate of folding is therefore often determined by the time it takes for a misfolded structure to unfold again (kinetic trap)<sup>167</sup>. Metal cations may be solely responsible for directing folding processes and stabilizing the active tertiary structure (structural function). However, they also provide a means of overcoming the deficit of chemical diversity in RNA in a striking manner<sup>12</sup>. One of the greatest challenges in current RNA research is that of separating structural functions from chemical (catalytic) processes<sup>168</sup>.

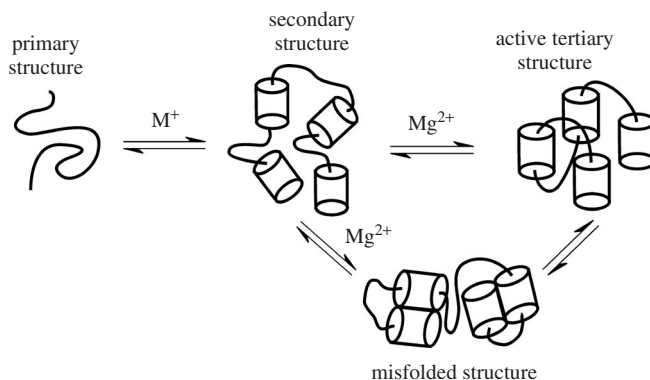


FIGURE 17. Simplified view of two-step folding processes in RNA. Adapted by permission of Springer Science and Business Media from Reference 12

### 1. Self-splicing in group I introns

Group I introns are the most abundant category of ribozymes known to date and more than 2000 sequences have been identified so far<sup>169</sup>. All of these ribozymes self-splice using a common strategy of two consecutive transesterifications using an external guanosine nucleotide as a cofactor<sup>170</sup>. They are distinguished from the group II introns which employ an internal adenosine to initiate self-splicing<sup>154</sup>. It is quite interesting that, apart from a few critical nucleotides, the sequence conservation in the active site is quite poor. However, the 3D core structure of the active site is very well conserved<sup>171</sup>, a fact indicating that the topology of the active site is extremely important. Group I introns have a specific requirement for  $Mg^{2+}$  ions both to ensure proper folding<sup>172</sup> and to promote catalysis<sup>12</sup>.

Although extensively studied for well over two decades (the group I intron from *Tetrahymena thermophila* was the very first ribozyme to be discovered), structural information has been quite elusive. Nevertheless, with the help of 'metal ion rescue experiments'<sup>173</sup>, the general mechanism of self-splicing illustrated in Figure 18 could be elucidated<sup>12, 159</sup>. In the presence of  $Mg^{2+}$  ions, the active site binds an external guanosine nucleotide (G) which then functions as a cofactor. Splicing is initiated by nucleophilic attack of the O3' hydroxyl group of G on the phosphate linker (P) at the 5'-splice site. The attack occurs via an 'in line'  $S_N2$  mechanism over a pentacoordinated intermediate/transition structure<sup>152</sup>. A conformational change then removes the G cofactor from the active site and brings the terminal nucleotide of the hydrolyzed 5'-exon into the proximity of the 3'-splice site and positions it for the second phosphoryl transfer. This time, the nucleophile is believed to be the 5'-hydroxyl group (5'-exon) which attacks the phosphate linker at the 3'-splice site, again via an 'in line'  $S_N2$  mechanism.

Mechanistic studies based mainly on metal ion rescue experiments have identified six oxygen atoms involved in metal ion coordination in the active site (the oxygens in bold font in Figure 19)<sup>174</sup>. Metal ion rescue experiments substitute a potential oxygen ligand with a 'soft' atom, usually sulfur, that is much less inclined to coordinate a 'hard'  $Mg^{2+}$  ion. If the addition of a 'soft' cation such as  $Cd^{2+}$  restores activity, the oxygen

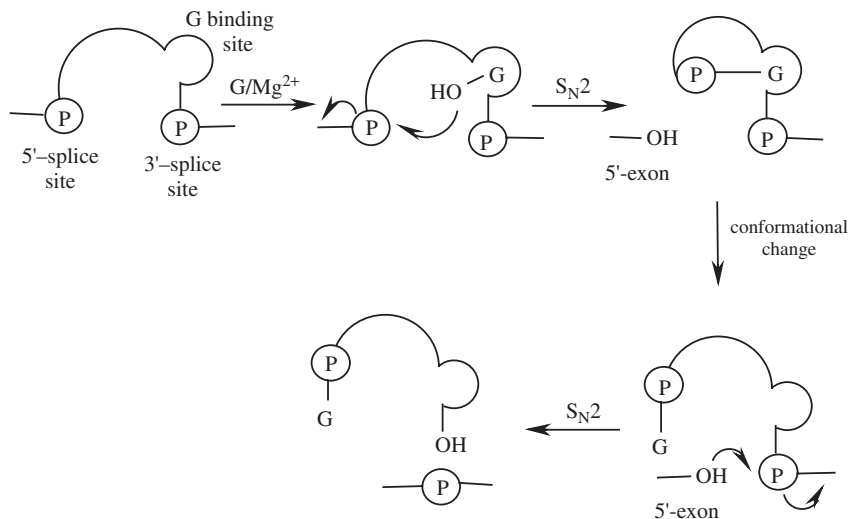


FIGURE 18. Schematic representation of the self-splicing reaction catalyzed by group I introns. G is the guanosine nucleotide cofactor, P a phosphate linker

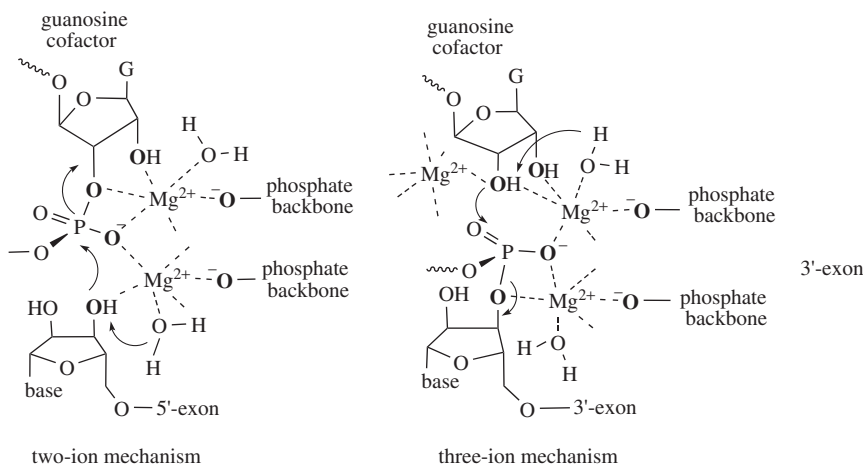


FIGURE 19. The two- and three-metal-ion mechanisms for phosphoryl transfer in the group I introns. Oxygens in bold have been identified as metal ligands by ion rescue experiments. From Reference 177. Reprinted with permission from AAAS

is considered to be a metal ligand<sup>174</sup>. These results have led to possible mechanisms for the phosphoryl transfer steps which involve either two<sup>175</sup> or three<sup>176</sup> metal ions. In the three-ion mechanism, illustrated for the first phosphoryl transfer step, the guanosine cofactor interacts with two  $Mg^{2+}$  ions via both hydroxyl groups. One of the ions activates the nucleophilic hydroxyl group while the other two ions stabilize the developing

pentacoordinated transition structure. As negative charge builds up in the leaving group, it is stabilized by the third metal ion, most probably by providing a proton originating from a water ligand. The two-metal-ion mechanism, illustrated for the second phosphoryl transfer step, is quite similar: one of the magnesium ions activates the nucleophile, both stabilize the pentacoordinated transition structure and the second  $\text{Mg}^{2+}$  stabilizes the developing charge on the leaving group. Only recently have the first solid-state structures for group I introns become available. A total of four are available to date and, in each case, chemical modifications or deletions were made in order to capture one of the reaction intermediates indicated in Figure 19<sup>174</sup>. All four solid-state structures support the two-metal-ion mechanism but do not rule out the possibility of a three-ion mechanism<sup>177</sup>.

## 2. Hammerhead ribozymes

First identified in 1986 as the catalytic active element in the replication cycle of certain viruses, the hammerhead ribozymes (HHRz) are the smallest known, naturally occurring RNA endonucleases<sup>178, 179</sup>. They consist of a single RNA motif which catalyzes a reversible, site-specific cleavage of one of its own phosphodiester bonds<sup>180</sup>. Truncation of this motif allowed a minimal HHRz to be constructed which was the very first ribozyme to be crystallized<sup>181</sup>. HHRz minimal motifs are characterized by a core of eleven conserved nucleotides (bold font in Figure 20) from which three helices of variable length radiate. Selective mutation of any of these conserved residues results in a substantial loss of activity<sup>182</sup>. In the absence of metal ions the structure is relaxed ('extended'), but upon addition of  $\text{Mg}^{2+}$ , hammerhead ribozymes spontaneously fold into a Y-shaped conformation (Figure 20; Color Plate 3)<sup>183</sup>.

It has been postulated that, in this Y-conformation, the 2'-OH functionality of the ribose at C17 initiates a nucleophilic attack on the phosphodiester linkage over a pentacoordinated transition structure (classical  $\text{S}_{\text{N}}2$ -type reaction; Figure 21)<sup>183</sup>. The leaving group is believed to be protonated by a general acid in the vicinity. Quite a bit of experimental support for such an  $\text{S}_{\text{N}}2$  mechanism is available, with perhaps the most important fact being that inversion at phosphorus invariably occurs<sup>184, 185</sup>. However, solid-state structures of minimal HHRz constructs indicate that achievement of the in-line orientation required for an  $\text{S}_{\text{N}}2$  reaction is practically impossible, the angle between the three atoms being

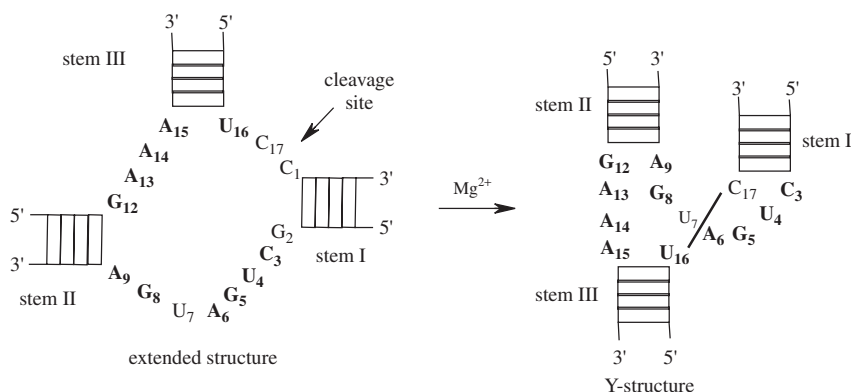


FIGURE 20. The catalytically active RNA sequence of a typical 'minimal' model of hammerhead ribozymes. Reproduced by permission of Wiley-VCH Verlag GmbH & Co. KGaA from Reference 190

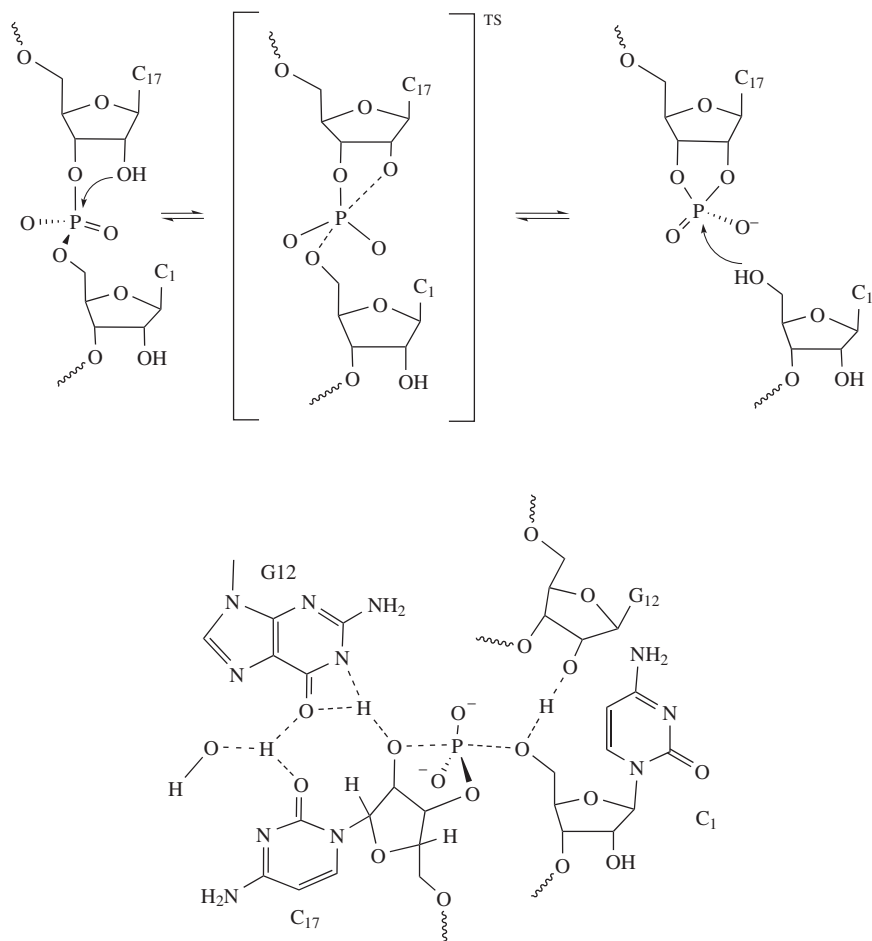


FIGURE 21. Above: initially postulated mechanism of phosphodiester bond cleavage. Below: a modified model of the transition structure in natural hammerhead ribozymes. Reproduced by permission of Wiley-VCH Verlag GmbH & Co. KGaA from Reference 190

nearly  $90^\circ$  instead of the required linear orientation<sup>186,181</sup>. This problem was further compounded by the fact that cleavage could be achieved by soaking the crystals with  $\text{Mg}^{2+}$  ions, which indicated that major structural rearrangements are not necessary to reach the transition structure<sup>187</sup>. Structures of minimal HHRz constructs in the solid state were also consistent with solution data<sup>183</sup>. These findings are incompatible with results obtained from metal ion rescue experiments which clearly indicate that, in the active conformation, a single  $\text{Mg}^{2+}$  ion bridges the phosphate groups of residue A9 and the phosphate being cleaved<sup>188,189</sup>. In the solid-state structures of minimal constructs, these phosphates are over 20 Å apart. Taken together, these disparate findings gave rise to a long-standing debate—the ‘structure-function dilemma’<sup>180</sup>—for the hammerhead ribozymes which is just now beginning to be resolved<sup>190</sup>.

Perhaps the first step in this direction consisted of the realization that the 'minimal' models usually employed for mechanistic investigations (which fold into the Y-structure) are suboptimal<sup>191,192</sup>. These truncated motifs require high (millimolar) concentrations of  $\text{Mg}^{2+}$  ions for proper folding and subsequent catalytic activity (typical rates of *ca*  $1 \text{ min}^{-1}$ )<sup>180</sup>. In contrast to this, natural hammerhead ribozymes are active at submillimolar (physiological) concentrations and exhibit much higher cleavage rates (*ca*  $870 \text{ min}^{-1}$  in the case of HHRzs isolated from schistosomes)<sup>193</sup>.

In a complete hammerhead ribozyme, additional loops and bulges in stems I and II permit tertiary interactions which considerably alter the folding dynamics and allow for activity under physiological conditions<sup>194</sup>. Recent photocross-linking experiments have identified some of these tertiary interactions<sup>195</sup> and a solid-state structure of a new conformation has been determined<sup>196</sup>. This structure is characterized by a much more compact arrangement of the active site with additional tertiary base interactions which are illustrated in Color Plate 3. More important is the fact that a perfect in-line geometry of the 2'-oxygen in C17 with the phosphate and the 5'-oxygen in C1 is now present. Nucleobase A9 is now in the immediate vicinity of the phosphate (not illustrated) and most of the discrepancies which lead to the 'structure-function dilemma' have now been explained. Nucleobase substitution experiments<sup>197</sup> together with kinetic studies<sup>193</sup> have given rise to a modified cleavage mechanism in which N1 of G12 probably functions as the general base to deprotonate the 2'-OH group (Figure 21)<sup>190</sup>. The general acid is postulated to be the hydroxyl group in the sugar functionality of G8. The exact role of  $\text{Mg}^{2+}$  in the mode of action of natural hammerhead ribozymes is still unclear. The bridging  $\text{Mg}^{2+}$  ion indicated by mechanistic experiments<sup>188,189</sup> was not observed in this solid-state structure—probably due to a high concentration of monovalent cations during crystallization<sup>196</sup>. However, the presence of this specific  $\text{Mg}^{2+}$  binding site was recently confirmed spectroscopically<sup>198</sup>. According to this study,  $\text{Mg}^{2+}$  retains 4 water ligands and binds in a monodentate fashion to the N7 atom of guanosine in G10 and to the pro-R phosphate atom in the A9 linkage—which places it in the immediate vicinity of the catalytic activity in the active conformation. However, another study indicated that the A9/G10 site can interact with divalent metal ions via both an inner- and an outer-sphere manner<sup>199</sup>.

Is  $\text{Mg}^{2+}$  solely responsible for achieving proper folding into the transient active conformation (structural role) or does it also actively participate in the catalytic reaction? Again, conflicting information is available in the chemical literature. Originally thought to be absolutely dependent upon  $\text{Mg}^{2+}$ , many studies have now demonstrated that the mode of action is much more complex than previously assumed. Under certain conditions, hammerheads function sluggishly in the presence of (very) high concentrations of monovalent cations such as  $\text{NH}_4^+$  or  $\text{Li}^+$ . In the meantime, there is evidence for the possibility of at least three reaction pathways—a monovalent, a divalent and a cooperative pathway that involves both mono- and divalent metal ions<sup>200,201</sup>.

Although quite some time and effort have been expended to develop computationally based models for direct  $\text{Mg}^{2+}$ -ion participation in the catalysis (both one-<sup>202</sup> and two-ion<sup>203,204</sup> mechanisms have been suggested), it is clear that more information is needed before the relevance of these studies can be judged. It is also quite possible that the mode of action of minimal HHRz constructs could fundamentally differ from the natural ribozymes—and this may be responsible for the differential catalytic rates observed. It is generally accepted that inversion of configuration is conclusive proof for a  $\text{S}_{\text{N}}2$ -type in-line attack. However, a recent computational study argued that, due to the possibility of a facile pseudorotation at phosphorus, an adjacent ( $90^\circ$ ) attack with simultaneous inversion of configuration cannot principally be ruled out<sup>205</sup>. An adjacent attack mechanism requires that a normally unstable apical oxyanion must be stabilized in the transition structure in

order for inversion of configuration to occur. This theoretical study demonstrated that a  $\text{Mg}^{2+}$  ion is capable of such a stabilization<sup>205</sup>.

## VIII. PROTEIN-BASED ENZYMES

In 2000, more than 350 protein-based enzymes (not including the metabolic cycles) with a specific requirement for  $\text{Mg}^{2+}$  had been described in the chemical literature<sup>62</sup> and many more have been discovered since then. In the past three or four years, our knowledge of structural and mechanistic details for many of these enzymes has increased exponentially and currently more than 3000 solid-state structures of protein-based biomolecules containing magnesium are available in the data banks<sup>206</sup>. There is a real need for comprehensive studies, as a systematic description of the common structural characteristics and mode of action of magnesium-based enzymes is not yet available. In an attempt to provide an initial approach to this wide field of current research, this review first provides an overview of general enzymatic modes of action followed by a more detailed discussion of several common types of magnesium-based systems. Selected examples of basic metabolic processes are presented. Magnesium involvement in DNA/RNA replication and repair is illustrated and, finally, the role of magnesium in the important process of photosynthesis is discussed.

### A. General Enzymatic Modes of Action

Quite some progress has been made in understanding general enzymatic catalysis since the first simple 'key and lock' model first proposed by Emil Fischer, still to be found in many biochemistry textbooks. In the meantime, it is clear that such a simple model usually does not represent biochemical reality in the slightest. Enzymes are fascinatingly complex systems—and their individual modes of action can vary quite widely. Perhaps the most convenient categorization for enzymatic reactions to date is to sort them into three different mechanistic classes—the template, sequential and allosteric systems. Of course, some enzymes will show borderline behavior with characteristics belonging to more than one of these categories.

#### 1. Template enzymes

As applied to metalloenzymes in general, the most simple mechanistic behavior—and that corresponding most closely to the earlier key and lock model of enzymatic catalysis—is that of a template system. In these enzymes, the metal cation is irreversibly bound in a well-defined active site on or near the surface of the enzyme with a channel or opening that allows substrate approach and product departure. Template enzymes function primarily via the 'coordination template effect'<sup>207</sup>, also known as the 'scaffold effect'<sup>208</sup>, in which the role of the metal cation is to specifically recognize the substrate(s), bring it/them together and activate it/them (usually through direct metal–substrate interactions) and finally to catalyze the desired chemical reaction, sometimes over one or more metal-bound intermediates, after which the product departs from the active site. Perhaps the best definition of a template metalloenzyme is that the metal ion functions as a 'true catalyst' and, although absolutely necessary in order to catalyze the chemical reaction, it remains bound to the active site and does not directly participate in the catalytic turnover [does not enter or leave the active site with the substrate(s)/product(s)]. The active site of template enzymes is rather small and the chemical reaction is strictly *localized* in the immediate vicinity of the metal ion. Due to this characteristic feature, small organometallo complexes that model the immediate structural and electronic features of the active site sometimes make good biomimetics for template enzymes. As



a consequence, most (probably more than 95%) of the biomimetical work—of both experimental and computational nature—reported in the literature to date is based on template models. Although the majority of template enzymes contain a single metal ion in their active site, quite a few, especially hydrolases, contain two<sup>48,209,210</sup>. Some even contain three metal ions, although the fundamental mode of action should probably be considered borderline, as the third metal ion (often magnesium) usually exhibits sequential or even allosteric behavior. Interestingly enough, very few magnesium-based enzymes exhibit ‘template’ behavior.

## 2. Sequential systems

The next stage of mechanistic complexity occurs in the sequential enzymes. In this case, the metal ion is an intrinsic part of the catalytic turnover. It enters the catalytic circle, interacts with the active site, substrate(s) and/or product and leaves again at some point in the turnover. Due to the ability of water to effectively compete with general organic ligands for magnesium, this metal ion is predestined to display sequential behavior. The resting state of these enzymes does not necessarily contain magnesium in the active site and the enzymatic activity obviously depends on the immediate bioavailability of free  $[\text{Mg}(\text{OH}_2)_6]^{2+}$ . The intracellular  $\text{Mg}^{2+}$  concentration is, however, usually high enough to guarantee enzymatic activity. Many magnesium-based enzymes, especially those involved in metabolic pathways, are suspected to be regulated by controlling the amount of free magnesium present in the immediate vicinity.

The role of magnesium in a sequential enzyme can fall into one of three general categories—two of which involve direct binding interactions with the active site. In the course of a single catalytic turnover,  $\text{Mg}^{2+}$  may enter the active site, bind to it and fulfill a critical catalytic role—one that may even be attributed to ‘template’ behavior, at least for one or more critical steps in the turnover—and then leave again. Alternatively, magnesium binding can trigger a structural change in and around the active site, thus regulating some important aspect of the catalytic turnover. Such binding sites are often termed ‘allosteric’ regulatory sites. Once this function has been fulfilled, it departs again and the structure of the active site returns to its previous state. The third category are enzymes in which  $\text{Mg}^{2+}$  has little or no direct interaction with the active site itself but interacts principally with the substrate(s) and/or product(s). In this case, the magnesium cofactor usually functions as a Lewis acid and helps to activate a bound nucleophile (deprotonation of water, for example), stabilize a critical intermediate and/or transition structure—often via outer-sphere interactions or helps to stabilize a leaving group such as pyrophosphate ( $\text{PP}_i$ ) or inorganic phosphate ( $\text{P}_i$ ).

The active site in a sequential enzyme, which must now accommodate at least one (partially or fully solvated) metal ion as well as substrate/product, is generally a bit larger than those observed for template systems—especially when a regulatory binding site is present. When a metal ion binds to such a site, it usually induces structural changes. In many magnesium-based enzymes, these regulatory conformational changes occur in a relatively limited region (10–50 Å in diameter) in and around the active site, which can still be considered to be localized. Examples of such localized motion include switching between active and inactive conformations, inducing a loop movement that clamps a ‘lid’ on the active site during a critical chemical reaction etc. Sometimes the borderline to true allosteric behavior is quite fluxional.

## 3. Allosteric systems

The most complex mechanistic behavior is displayed by an allosteric system in which metal binding/debinding events trigger structural changes not just in and around the active

site (or sites) but in the *entire* enzyme. Indeed, it is often difficult to speak of an active site as such. The metal ion may bind to a regulatory site far away from where the reaction of interest is taking place. Although the region where the substrate is being transformed into product can often be identified, it is impossible to consider this region as being independent of the rest of the enzyme. As a consequence, it is very difficult to perform mechanistic studies on allosteric systems—and even more difficult to develop models for studying their behavior<sup>211</sup>. Even employing the most simple of molecular modeling techniques, it is still beyond the capacity of modern computers to perform calculations on these enzymes which usually tend to be quite large, often possessing several interacting subunits<sup>212</sup>. Their complexity, together with the fact that  $\text{Mg}^{2+}$  is spectroscopically silent, very small and difficult to detect experimentally, currently limits available knowledge of the mechanistic details occurring in allosteric systems involving magnesium.

One of the few magnesium-based enzymes which exhibits allosteric behavior that has been studied in more detail is alkaline phosphatase (AP), which hydrolyzes phosphate monoesters nonspecifically under both acidic and alkaline conditions<sup>213</sup>. AP is a relatively small enzyme consisting of two subunits. In each subunit is a trinuclear active site which contains two  $\text{Zn}^{2+}$  and one  $\text{Mg}^{2+}$  ion (Figure 22). The two  $\text{Zn}^{2+}$  ions exhibit ‘template’ behavior and are responsible for the catalytic behavior. They are essential for the activity whereas magnesium alone is not active. Reference 214 contains a detailed discussion of the actual hydrolysis; this chapter concentrates on illustrating the ancillary role of  $\text{Mg}^{2+}$  in modifying the behavior of AP. In the solid state, AP consists of two symmetric subunits (homodimer)<sup>215</sup>. In the absence of  $\text{Mg}^{2+}$ , solutions of AP are also homodimeric<sup>216</sup>. However,  $\text{Mg}^{2+}$  binding/debinding triggers reversible dynamic refolding and AP undergoes continual structural rearrangements in solution<sup>217</sup>. Each subunit can assume one of two distinct, inherently nonequivalent conformations which are illustrated by squares and circles in Figure 22<sup>218, 219</sup>. In addition,  $\text{Mg}^{2+}$  binds to AP with negative

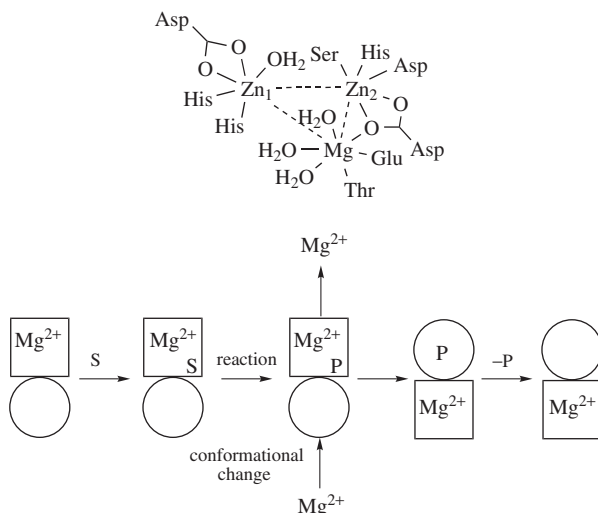


FIGURE 22. The active site of alkaline phosphatase (above) and an allosteric kinetic switch mechanism (below) for the regulatory function of the  $\text{Mg}^{2+}$  ions in controlling the conformation of the nonequivalent subunits (square and circle). Reprinted with permission from Reference 214. Copyright 2005 American Chemical Society

cooperativity and the dimer prefers to have only one  $\text{Mg}^{2+}$  present (square)<sup>220</sup>. The subunit with bound magnesium exhibits a higher binding affinity for both the substrate S (which preferentially docks on this subunit) and the product P. After hydrolysis, the product is not easily displaced from this subunit. However, binding of  $\text{Mg}^{2+}$  to the second subunit (circle) triggers an allosteric conformational change in both subunits. The first subunit now becomes a circle with a drastically reduced affinity for both  $\text{Mg}^{2+}$  and product, both of which are now easily ejected from the active site. Allosteric regulation of AP through reversible binding/debinding of  $\text{Mg}^{2+}$  results in a 'kinetic switch' which accelerates the overall rate via conformationally controlled accelerated dissociation of the product  $\text{P}^{218}$ .

## B. Metabolic Enzymes

Many of the metabolic pathways in higher organisms are mediated by magnesium-dependent enzymes. The well-known glycolytic cycle (found in all biochemistry textbooks and illustrated in Figure 23) is a typical example; of the 10 enzymes involved, half of them have a specific requirement for magnesium. In glycolysis, glucose is oxidized and split in half to create two equivalents of pyruvate. The overall reaction [ $\text{glucose} + 2 \text{ ADP} + 2 \text{ P}_i + 2 \text{ NAD}^+ \rightarrow 2 \text{ pyruvate} + 2 \text{ ATP} + 2 \text{ NADH} + 2 \text{ H}^+ + 2 \text{ H}_2\text{O}$ ] is exothermic and, along the way, the energy released is converted into ATP. In addition, the NADH generated during glycolysis is used to fuel ATP synthases which produce further equivalents of ATP. The net yield of ATP per glucose molecule is either 6 or 8, depending on which shuttle mechanism (glycerol phosphate or malate-aspartate) is employed to transport the electrons from NADH into the mitochondria. The key in regulating the glycolytic pathway is the rate-limiting step catalyzed by the magnesium-dependent enzyme phosphofructokinase. Among other regulatory mechanisms, phosphofructokinase is inhibited by ATP. When ATP is abundant, the turnover of phosphofructokinase slows down, which prevents wasting glucose on making energy when it is not needed.

In spite of the wide chemical variance and high structural and kinetic diversity encountered in magnesium-based metabolic enzymes, they generally follow a common mechanistic theme<sup>6</sup>. They usually possess at least two (and sometimes three) magnesium binding sites and exhibit a typical sequential (and sometimes allosteric) behavior which is illustrated in Figure 24. The catalytic turnover is initiated when  $\text{Mg}^{2+}$  binds to the apoenzyme which triggers local (or even allosteric) conformational changes, thus activating the enzyme towards substrate binding. The second  $\text{Mg}^{2+}$  ion either enters the active site with the substrate ( $\text{MgATP}^{2-}$ , for example) or binds either before or after the substrate (often in a kinetically ordered fashion) and helps to activate the substrate. Reaction then takes place and the product and the second  $\text{Mg}^{2+}$  ion leave (sometimes together as a magnesium complex). The initially generated  $\text{E-Mg}^{2+}$  intermediate remains behind and can then either accept another substrate or lose the first  $\text{Mg}^{2+}$  (this step often underlies external regulatory control mechanisms).

### 1. Protein kinases

Protein kinases catalyze the reversible transfer of the  $\gamma$ -phosphate group in ATP to a hydroxyl group in a substrate. All kinases are dependent upon at least one divalent metal ion, usually  $\text{Mg}^{2+}$ , which they need to assist in the binding of ATP and to facilitate phosphoryl transfer<sup>221</sup>. Such phosphorylations are perhaps one of the most important regulatory reactions occurring in the cell and kinases, as a group, represent one of the fundamental building blocks of complex signal transduction processes. They are 'traffic cops' that help to regulate and/or are intrinsically involved in countless, extremely varied processes that include entire metabolic cycles (glycolysis, for example), DNA transcription/replication,

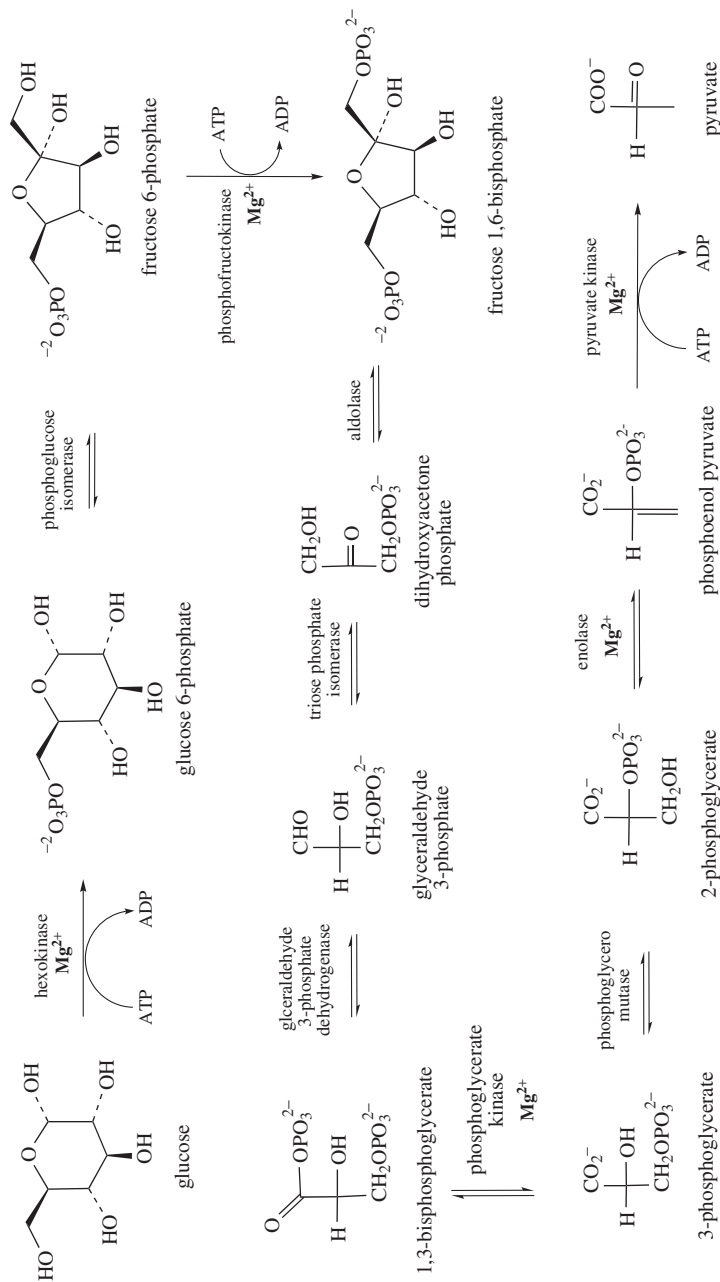


FIGURE 23. Involvement of magnesium in the glycolytic pathway

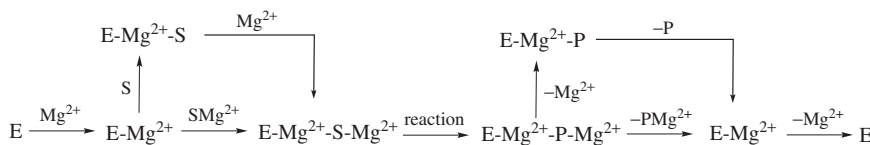


FIGURE 24. General mode of action of magnesium-dependent metabolic enzymes. Reproduced [© 2002 Kluwer Academic Publishers] by permission of Springer Science and Business Media from Reference 6

the biosynthesis of neurotransmitters in the brain—right up to and including events that can be directly observed at the microscopic (cellular differentiation) or macroscopic level (muscle contractions). It is therefore not surprising that higher vertebrates are estimated to have more than 2000 different protein kinases<sup>222</sup>. For example, it has been estimated that *ca* 2% of the human genome (as understood in 2001) contains protein kinase domains<sup>223</sup>. A relatively simple core structure (*ca* 250–300 amino acids) containing the active site is conserved over the entire family<sup>224,225</sup>; however, a kinase frequently has additional auxiliary components<sup>226</sup>, and/or is bound to or otherwise directly interacts with other regulatory proteins<sup>227</sup> or complex domains that either enhance or repress the kinase activity of the core subunit via complex allosteric interactions<sup>228,229</sup>. This gives rise to an incredible degree of familial variance—from both a structural and mechanistic viewpoint.

One kinase, the cAMP-dependent protein kinase (known as PKA), has been the focus of mechanistic research for several decades and is perhaps the best understood member of the kinases to date<sup>221</sup>. PKA catalyzes the phosphorylation of a serine or threonine hydroxyl contained in an Arg–Arg–X–Ser/Thr–Y sequence where X is a small amino acid (Ala, for example) and Y is a hydrophobic residue<sup>230</sup>. In order to maintain cellular homeostasis, hormones are released from organs. These are detected by the G-proteins which then activate adenylate cyclase, which produces a cyclic form of adenosine monophosphate, cAMP. This is a hormonal second messenger and is the regulatory signal controlling the activity of PKA. In the absence of an activating signal (cAMP), PKA is a heterotetramer containing two core catalytic subunits (C) and, as an auxiliary component, a regulatory dimer (R<sub>2</sub>). When the concentration of cAMP in the immediate vicinity rises, the regulatory unit binds four cAMP molecules, an event which instantly causes the heterotetramer to fall apart. A R<sub>2</sub>(cAMP)<sub>4</sub> complex remains behind and two relatively small, active C subunits are released<sup>231</sup>.

The catalytic subunit C of PKA consists of two domains, one composed mostly of  $\alpha$ -helices and one of  $\beta$ -strands, which are connected by a small linker region<sup>232</sup>. The ATP binding site is located deep in the active site between the two domains; the binding site of the larger substrate is at the mouth of the pocket (Color Plate 4). A flexible ‘activation’ loop is postulated to function as a door for the active site and is believed to be directly involved in regulating PKA<sup>221</sup>. PKA has a ‘disordered’ or random binding mechanism. When the ‘door’ is open, both the substrate and ATP have unhindered access to the active site and the binding of one does not influence the other<sup>233</sup>.

Asp184 provides the primary binding site for the catalytic Mg<sup>2+</sup> which probably enters as MgATP<sup>2-</sup> (Figure 25)<sup>234</sup>. This residue is absolutely essential, since mutation to Ala completely destroys the catalytic activity<sup>235</sup>. This catalytic Mg<sup>2+</sup> chelates oxygen atoms from the  $\beta$ - and  $\gamma$ -phosphates and clearly properly positions the phosphate tail and helps to activate the  $\gamma$ -phosphate towards phosphorylation. A second Mg<sup>2+</sup> ion also helps to fix the conformation. This ion is not absolutely required; however, its presence clearly accelerates catalysis<sup>236</sup>. Lys72 is essential for activating ATP, since mutation of this residue destroys the catalytic activity but does not change the ATP binding affinity<sup>237</sup>. Lys168

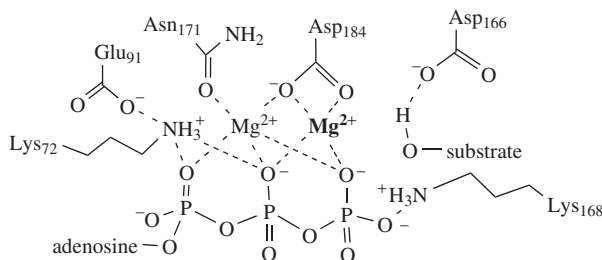


FIGURE 25. Key interactions in the active site of the cAMP-dependent protein kinase (PKA); the additional  $H_2O$  ligands on both hexacoordinated  $Mg^{2+}$  ions have been omitted for clarity and the essential  $Mg^{2+}$  is bold. Modified with permission from reference 234 with permission from cold spring harbor laboratory press

is also involved in positioning the  $\gamma$ -phosphate and, in addition, may be involved in substrate binding<sup>221</sup>. The exact role of Asp166 in the phosphorylation has been a topic of considerable discussion<sup>221, 238</sup>. This residue is not absolutely necessary; however, it considerably enhances the catalytic rate<sup>221</sup>. In the meantime, it is clear that its primary role is that of a general base with only a minor contribution, if any, to substrate binding<sup>239</sup>. It undergoes a direct hydrogen-bonding interaction with the hydroxyl group of the substrate.

The experimental evidence is somewhat contradictory as to whether the phosphate transfer occurs over an associative ( $S_N2$ -type) or dissociative (metaphosphate) pathway (Figure 13). Kinetic experiments demonstrate that the activity is not pH dependent and that a solvent deuterium isotope effect is clearly missing; both facts indicating that the transferred proton is still bound to the hydroxyl in the rate-determining step, as would be expected in the metaphosphate pathway<sup>240</sup>. On the other hand, a solid-state structure of a transition state analogue (PKA was crystallized with a substrate peptide, ADP and  $AlF_3$ ) indicated a strong  $O_{Asp166}-H-O_{hydroxyl}$  interaction in a possible  $S_N2$ -type transition structure<sup>241</sup>. DFT calculations on large models of the active site which included Asp166 (as well as the functional groups of all other conserved residues in the immediate vicinity of both ATP and the substrate) have shown that the two-step dissociative mechanism is probably favored<sup>242, 243</sup>. In the first step, the phosphorus anhydride bond is broken to form a trigonal planar metaphosphate that is stabilized by a hydrogen-bonding interaction with the hydroxyl group in the substrate. In the second step, the hydroxyl group attacks the metaphosphate. It was concluded that Asp166 first helps in substrate binding and then functions as a general base mediator to transfer the hydroxyl proton from serine to the phosphate during the second phosphorylation step. A third computational study using DFT QM/MM methods confirmed that Asp166 primarily functions as a proton trap<sup>244</sup>.

## 2. Enolases

Enolases, also known as 2-phospho-D-glycerate hydrolases, catalyze the reversible dehydration of 2-phosphoglycerate (2-PGA) to phosphoenol pyruvate (PEP) in complex metabolic systems such as the glycolytic pathway illustrated in Figure 23<sup>245</sup>. Eukaryotic enolases generally have a high degree of family resemblance and those isolated from widely varied sources such as yeast, lobster and human usually possess a sequence homology greater than 60%<sup>246</sup>. One member of this very interesting family, yeast enolase, has been studied in quite some detail due to its ease in isolation and propensity towards crystallization. It was one of the very first enzymes to be successfully crystallized (1941)<sup>247</sup>.

Since then, a considerable amount of structural and mechanistic information has been collected and yeast enolase is probably the best understood sequential enzyme to date. It is a homodimer<sup>248</sup> and requires two  $\text{Mg}^{2+}$  ions per active site for catalytic activity under physiological conditions, although magnesium can be replaced with a variety of divalent metal ions *in vitro*<sup>249</sup>. During a catalytic turnover, the metal ions bind to the active site in a kinetically ordered, sequential manner with differential binding affinities<sup>250</sup>. The mode of action of yeast enolase is illustrated in Figure 26 and is unusually well understood since several solid-state structures for each intermediate identified with kinetic methods have been determined.

It is quite interesting that the enolase subunit can exist in four major conformational states—an inactive *apo*-form, as well as open, semiclosed and closed conformations<sup>251, 252</sup>. The resting state of yeast enolase is the *apo*-form. Binding of the first  $\text{Mg}^{2+}$  ion (highest affinity) to the apoenzyme<sup>253</sup> induces a conformational change in the active site which activates it towards substrate binding<sup>249</sup>. This  $\text{Mg}^{2+}$  ion is thus often called the conformational ion. The  $[\text{E}-\text{Mg}^{2+}]$  intermediate is now in the open conformation which is observed in the absence of substrates or inhibitory analogues<sup>254</sup>. The activated  $[\text{E}-\text{Mg}^{2+}]$  complex now binds the substrate (2-PGA) to generate an  $[\text{E}-\text{Mg}^{2+}-\text{S}]$  intermediate<sup>255</sup>. The third step in the catalytic turnover is the binding of the second ‘catalytic’  $\text{Mg}^{2+}$  ion<sup>250, 256</sup>. This causes a concerted movement of three short, flexible loops in the region of the substrate canal which partially closes the active site—similar to placing a lid on a pot (illustrated in Color Plate 5)<sup>253, 257</sup>. Solid-state structures of the  $[\text{E}-\text{Mg}^{2+}-\text{S}-\text{Mg}^{2+}]$  complex<sup>255, 258</sup> exhibit this closed conformation in which the chemical reaction (dehydration) takes place after which a  $[\text{E}-\text{Mg}^{2+}-\text{P}-\text{Mg}^{2+}]$  intermediate results<sup>259</sup>. After the reaction, the ‘lid’ has relaxed somewhat and the product complex exhibits the semiclosed conformation.

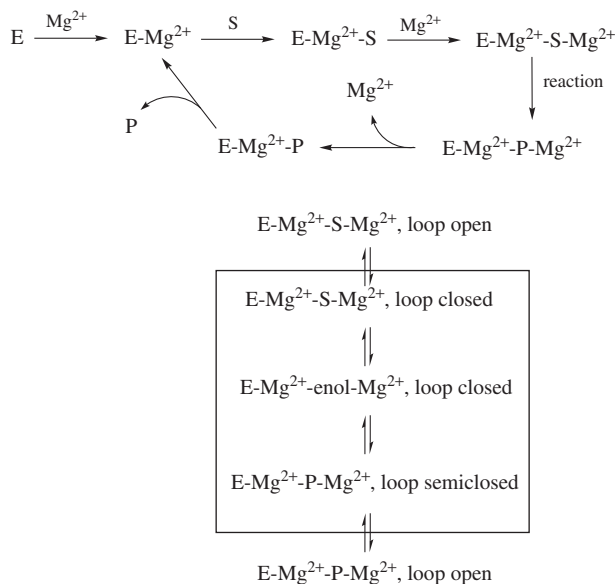


FIGURE 26. Above: the kinetically ordered sequential mode of action of yeast enolase. Reprinted with permission from Reference 250. Copyright 2001 with permission of the American Chemical Society. Below: conformational changes in the chemical step

After a conformational change has opened up the active site, dissociation is kinetically ordered with the catalytic  $\text{Mg}^{2+}$  ion leaving first, followed by the product and then the conformational  $\text{Mg}^{2+}$  ion. It has long been suspected that dehydration occurs via a two-step mechanism over a metastable enol intermediate<sup>260, 261</sup>. This is the only intermediate in the mode of action of yeast enolase that has not yet been either crystallized or observed spectroscopically. However, QM/MM calculations indicate that such an enol intermediate is indeed a viable metastable intermediate along the reaction pathway between the ternary substrate and product complexes<sup>262, 263</sup>.

To date, most quantum-chemical studies on sequential enzymes have been performed using small 'cut outs' of the active site which strongly resemble organometallic template complexes. The electrostatic interactions between the metal ion(s) and organic ligands hold the quantum-chemical model together. While this template strategy may suffice for the proper description of selected intermediates or individual reaction steps, it is fundamentally incapable of being employed for calculating the entire mode of action. Due to the fact that metal ion movement is an intrinsic part of catalysis, the model used needs to be stable towards metal ion exchange as well as ionic movement relative to the amino acid residues that make up the bulk of the active site. Metal-ion-centered template models are incapable of this; they simply fall apart *in silicio* when the metal ions are removed or even slightly displaced from their optimal positions. The only remedy to date is to employ a QM/MM method<sup>264, 265</sup> with a large enough 'cut out' to permit limited ionic movement. QM/MM approaches are based on a method gradient with a small region in the center of the model being calculated with a higher-level, more accurate method and the larger periphery region with a lower-level (and thus faster) method. Due to technical difficulties in implementing the overlap region which is always accompanied by method overlap errors, the results of such calculations are unsystematic and can be quite inaccurate.

Very recently, a new strategy has been developed for systematic quantum-chemical investigations on sequential enzymes. Instead of a method gradient, a structure gradient is employed which generates a 'soccer ball' model<sup>266</sup>. In this approach, all known solid-state structures of the enzyme are overlaid. As long as the mode of action is quasi-localized, the backbone residues will begin to overlap at some point in space moving out and away from the active site. At this point, a sphere containing the active site is cut out. All open valencies of residues on the surface of this sphere are completed with hydrogen atoms and their positions are frozen in space. This creates a hard (fixed) outer shell. Using a structure gradient approach (first dihedral then bond angles and finally bond lengths are freed), the fixed outer shell is connected to a freely optimizable inside<sup>267</sup>. In this manner, not only the limitations of metal-ion-centered models can be completely overcome, but it is possible to employ a single computational method (DFT, for example) with approximately the same size/time advantages as QM/MM methods but without the additional overlap error<sup>268</sup>. The coordinated movement and/or chemical reactions of metal ions, substrate, product as well as flexible side-chain residues (general acids and bases involved in catalysis) and specific solvation waters can now be explicitly studied. This strategy has recently been used to develop an initial model for the active site of yeast enolase (illustrated in Color Plate 5)<sup>269</sup> which is now being enlarged with the goal of studying the localized loop movements in the mode of action.

### C. DNA Replication and Repair

Genetic information necessary for the propagation of all life forms is stored in compressed form in genomes, the data storage compartments of nature, which are basically composed of two long DNA strands wound together in a double helix. Several large, quite diverse classes of enzymes are responsible for manipulating this genetic code. Helicases, for example, unwind double-stranded DNA helices and thus prepare them for further



manipulations<sup>270, 271</sup>. These single (primed) strands are then worked on by the DNA polymerases which are responsible for replicating and maintaining the DNA<sup>272</sup>. During DNA replication, the new DNA is synthesized in a template-dependent process that faithfully copies the original DNA molecule. Replicative DNA polymerases synthesize very long DNA molecules with an incredible accuracy<sup>273, 274</sup>. Usually, these replicases consist of a macromolecular assembly of several proteins that function together as a single unit<sup>275</sup>. As early as 1976, it was realized that the accuracy of this process depends on the presence of  $Mg^{2+}$  ions<sup>276</sup>. Replacing  $Mg^{2+}$  in a DNA polymerase by  $Co^{2+}$  or  $Mn^{2+}$ , for example, usually results in a considerable loss of replication fidelity<sup>277</sup>. Ever since then, almost all newly discovered enzymatic systems for DNA processing also involve  $Mg^{2+}$  as an essential cofactor<sup>278</sup>.

DNA polymerases are now broadly classified into two groups—the DNA replicases that are responsible for copying DNA and the repair polymerases that fix damaged DNA. Far from being the incredibly stable molecule originally believed, it is now known that DNA is a dynamic system that is constantly being damaged by a horde of potential mutagens<sup>279</sup>. These include, among many others, reactive oxygen species formed during metabolic processes, chemical mutagens absorbed over the skin, eaten or breathed, as well as sun light (UV radiation). Damage can also occur as a result of replication or recombination mistakes. Without an ability to repair genomic information, life encoded by DNA would be altered so fast that an organism could not thrive<sup>280</sup>. Cells have therefore developed several different repair mechanisms designed to repair localized damage<sup>272</sup>. Base excision, for example, replaces a damaged nucleobase<sup>280</sup> and nucleotide excision replaces the entire nucleotide<sup>281</sup>. There are also mechanisms for correcting mismatches (replication errors)<sup>282</sup> as well as for repairing breaks in DNA single<sup>283</sup> and double<sup>284</sup> strands. In light of the incredible specificity of enzymes that work on DNA, it is quite remarkable that all of these repair pathways are characterized by the ability to perform broad-band repair with most of the enzymes involved recognizing multiple types of DNA damage<sup>285</sup>.

### 1. DNA replicases

DNA replicases are quite unusual enzymes in that they employ a DNA substrate as a template in order to guide the synthesis of the product (DNA replicant). This is an extremely complex task. The enzyme must first recognize and bind the primed DNA strand. Here the first challenge is encountered. The strand must be bound with a high affinity, but it must be capable of being released—without complete dissociation—to be repositioned at the end of each catalytic turnover so that the next nucleotide can be incorporated. After primer binding, the enzyme must then recognize and bind the proper nucleoside (deoxynucleoside 5'-triphosphate; dNTP). All four dNTPs must be specifically recognized, but how does the enzyme decide that it has the proper one? The next step consists in matching the nucleoside to the template in order to form the proper base pair before it is incorporated, via a chemical reaction into the growing DNA replicant<sup>272</sup>.

The first DNA replicase to be crystallized was the Klenow fragment of the *E. coli* polymerase I<sup>286</sup>. Full length polymerase I is a single polypeptide that contains three functional domains—a polymerization domain, a 3'-exonuclease and a 5'-nuclease. Removal of the 5'-nuclease (a proofreading fragment which reduces the error rate of 1 in  $10^4$  base pairs to 1 in  $10^8$ <sup>272</sup>) yields the Klenow fragment which, in itself, is a fully functional replicase<sup>287</sup>. Subsequent solid-state structures of various other polymerases have revealed that, in spite of considerable sequence inhomogeneity, all DNA replicases share several features that are critical for activity<sup>272</sup>. Perhaps the most important feature common to almost all polymerases is the shape of the catalytic domain. This resembles a half-open

hand with the 'palm' forming a deep cavity with the 'thumb' to the right and the 'fingers' to the left (Color Plate 6). The 'fingers' hold the DNA primer template and interact with the incoming dNTP. The 'thumb' positions and fixes the newly synthesized DNA replicant and the chemistry takes place in the 'palm'. The growing replicant leaves the active site at a  $90^\circ$  angle to the template<sup>288</sup>.

Extensive kinetic experiments on the Klenow fragment (and other replicases) have resulted in the general mechanism illustrated in Figure 27<sup>289, 290</sup>. Except for variations in the individual rate constants, this mechanism seems to be valid for a series of DNA polymerases<sup>127, 291</sup>. The first step is to fetch a nucleoside N ( $\text{MgdNTP}^{2-}$ ). At this point, differentiation between nucleosides occurs; the binding constant of the 'correct' one to form an E-D<sub>n</sub>-N complex is an order of magnitude higher than for an 'incorrect' one<sup>292</sup>. It is believed that nucleoside selection is achieved through geometrical constraints that allow the formation of correct Watson-Crick base pairing to the template and rejects nucleosides that do not have the proper shape<sup>293</sup>. A slow,  $\text{Mg}^{2+}$ -dependent, rate-limiting conformational change which only occurs when the 'correct' nucleoside is present ('induced fit mechanism') now closes the active site<sup>292</sup>. This rearrangement is thought to deliver and bind the nucleoside to the active site. After the chemical reaction (phosphorus anhydride bond formation) which incorporates the nucleoside into the replicant, the conformationally active  $\text{Mg}^{2+}$  ion dissociates. A takes place second conformational change which returns the active site to an open state with concomitant pyrophosphate release (most likely in the form of  $\text{MgPP}_i$ ). Dissociation of either the template or the replicant from the active site is rather slow; replicases tend to function in a repetitive manner<sup>275</sup> and it is not unusual when thousands of nucleosides are processed per binding/debinding event<sup>272</sup>.

A considerable amount of evidence gathered on several replicases strongly indicates that all of them possess the same general phosphorylation mechanism (Figure 28)<sup>272, 288</sup>. The active site contains two absolutely conserved Asp residues that play an essential role in the phosphoryl transfer step<sup>294, 295</sup>. Two  $\text{Mg}^{2+}$  ions are essential<sup>296</sup> and they are fixed in the active site via bridge bidentate coordination with the two Asp residues<sup>297, 298</sup>. This bimetallic arrangement binds and positions the dNTP in a manner in which the usual  $\text{M}_\gamma\text{M}_{\beta\gamma}$  binding motif has been reversed in favor of a  $\text{M}_\alpha\text{M}_{\gamma,\beta}$  motif. One of the metal ions ( $\text{M}_\alpha$ ) is ideally positioned to lower the  $\text{p}K_a$  of the hydroxyl group of the last nucleotide in the growing replicant and is believed to facilitate its deprotonation by a general base in the vicinity<sup>299</sup>. The resulting hydroxide attacks the  $\alpha$ -phosphate of the dNTP<sup>300</sup>. The other  $\text{Mg}^{2+}$  binds to the phosphate tail, holds it in a position favorable for a  $\text{S}_\text{N}2$ -type reaction and stabilizes charge separation in the pentacoordinated transition structure (associative mechanism)<sup>301</sup>. Most likely this second  $\text{Mg}^{2+}$  also stabilizes the pyrophosphate (which is

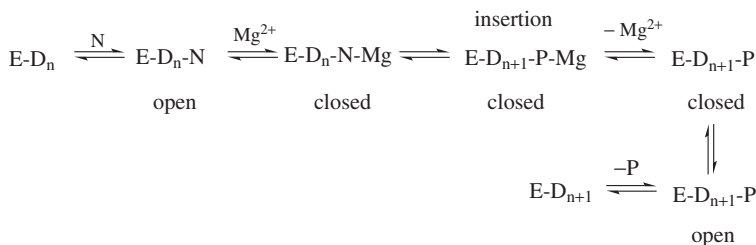


FIGURE 27. General kinetic mechanism of DNA replication. E is the replicase (polymerase), D the growing DNA replicant, N is  $\text{MgdNTP}^{2-}$  and P represents  $\text{MgPP}_i$ . Adapted with permission from Reference 290. Copyright 2006 American Chemical Society

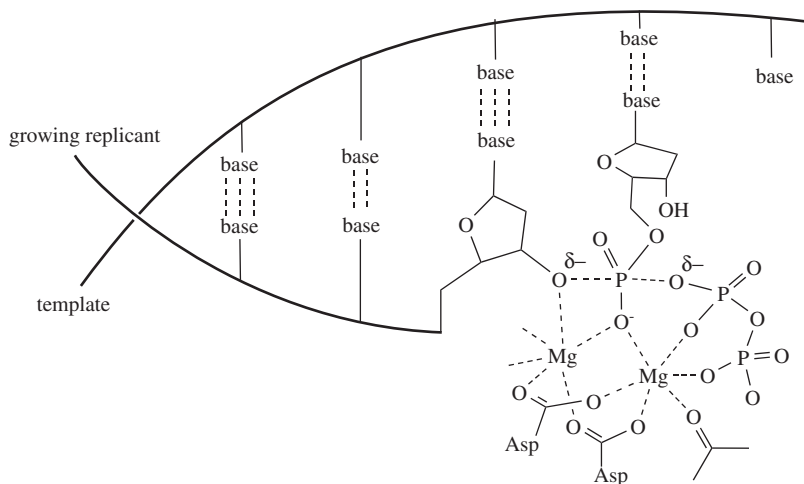


FIGURE 28. Proposed transition structure for the transphosphorylation in DNA replication. Reproduced by permission of Bentham Science Publishers from Reference 272

believed to be protonated by a general acid) as it dissociates from the active site after the nucleoside transfer is complete.

## 2. Base excision repair

Damage to an individual nucleobase is the most common type of DNA damage that occurs<sup>285</sup>. A multitude of environmental factors leads to spontaneous depurinations, depyrimidations, deaminations, oxidations and alkylations of the heterocyclic nucleobase<sup>302</sup>. For example, thousands of damaged nucleobases must be repaired in a single human cell every day of its life in order to maintain genomic integrity<sup>302</sup>. Higher organisms have therefore evolved a common base excision repair (BER) strategy<sup>303</sup>, which is perhaps the major cellular pathway for dealing with most DNA damage<sup>304</sup>. If this damage control system is not working properly, consequences such as early aging, cancer and neurodegenerative diseases result<sup>305</sup>.

Base excision repair is carried out with a 'cut and paste' strategy<sup>306,307</sup>. First, the damaged nucleobase is identified and then excised. This is usually carried out by glycolylases that target distinct nucleobase lesions. They work by flipping the damaged nucleotide out of the helical structure and then cleaving the *N*-glycosidic bond to remove the nucleobase<sup>308</sup>. Monofunctional glycolylases use water as the nucleophile; bifunctional glycolylases employ an amine residue in their active site to first generate a Schiff base (covalently bound intermediate) which then, depending on the glycolase, undergoes either a  $\beta$ - or a  $\beta,\delta$ -elimination (Figure 29). Further processing is pathway-dependent and requires, depending on the intermediate generated by the glycolase, an AP endonuclease, a phosphodiesterase or a phosphatase. After this, a polymerase (usually polymerase  $\beta$ ) pastes in a new nucleotide after which a ligase tucks it back into its proper place in the DNA strand<sup>285</sup>.

The different enzymes involved in base excision repair (and other DNA repair pathways) are quite diverse. Even among the same family, sequence homology is usually

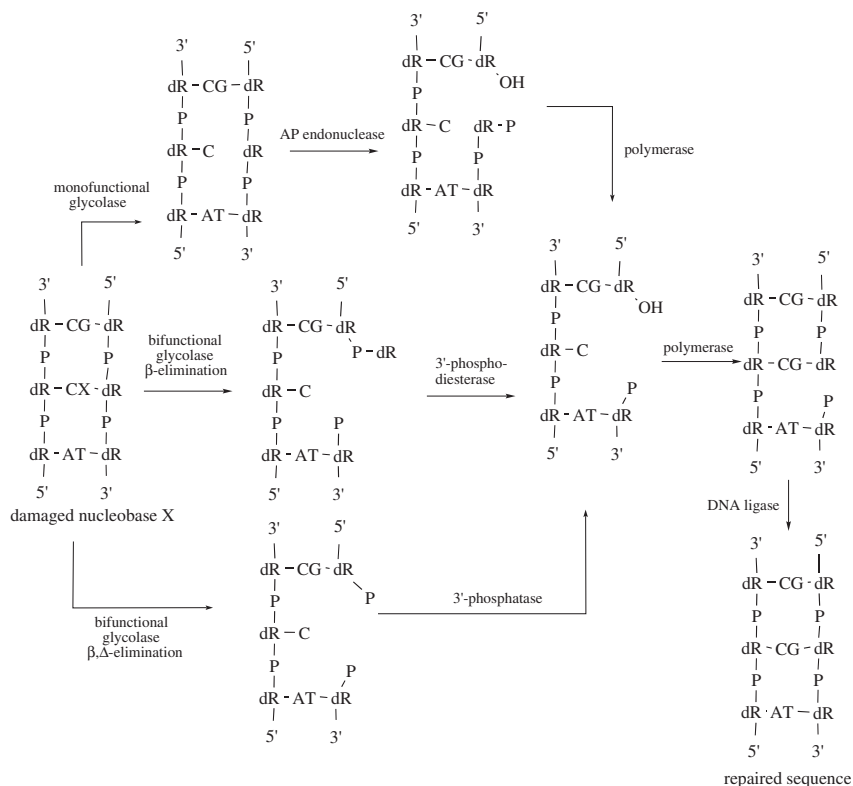


FIGURE 29. Minimal biochemical pathway for base excision repair. Adapted with permission from Reference 285. Copyright 2006 American Chemical Society

severely limited from organism to organism and from task to task. Although more is being learned about these systems on a daily basis, a detailed structure-functional understanding of their individual modes of action is still in the very early stages of being developed. However, recent research efforts have discovered one single feature that all of these enzymes have in common. They normally require divalent metal ions, usually  $\text{Mg}^{2+}$ , for activation<sup>27</sup>.

### 3. Generic two-ion mechanism

DNA and many RNA molecules have helical duplex structures with identical, unvarying phosphate backbones that surround uniformly stacked base pairs that have a very high degree of chemical and topological similarity. This poses the question of exactly how do the countless protein-based enzymes that act upon DNA and RNA (and, in addition, how do ribozymes) manage to pick out their substrate, one particular phosphate linker or nucleotide among literally thousands of others, with such a high degree of selectivity?

A detailed analysis of solid-state structures of several unrelated systems that catalyze the hydrolysis of diphosphate esters (alkaline phosphatase<sup>309</sup> and the Klenow fragment<sup>310</sup>, among others) revealed that their active sites invariably contain conserved carboxylate

residues that are capable of binding two divalent metal ions in a bridge bidentate manner<sup>175</sup>. The metal ions are *ca* 4 Å apart and enzyme–substrate complexes indicate that they are ideally positioned with respect to both the phosphate backbone and the substrate so as to enable a phosphoryl transfer reaction over a linear  $S_N2$ -type transition structure (Figure 19)<sup>175</sup>. This gave rise in 1993 to the postulate of a general ‘two-ion mechanism’ for phosphate ester hydrolysis or transphosphorylation in which one metal ion reduces the  $pK_a$  of the hydroxyl nucleophile (or of  $H_2O$  when a simple hydrolysis is being performed); both support a  $S_N2$ -type associative transition structure and the second ion stabilizes the oxyanion in the leaving group—which is then protonated by a general acid (or water) in the immediate vicinity<sup>175</sup>. Since then, mechanistic investigations on many protein-based enzymes involving various phosphoryl transfer reactions in DNA and RNA have provided concrete evidence for a  $S_N2$ -type reaction involving a pentacoordinated intermediate/transition structure with accompanying inversion of configuration at phosphorus<sup>311,312</sup>. In addition, two metal ions have consistently been found in every DNA and RNA replicase identified to date<sup>313,314</sup>.

A unique characteristic of nucleic acid phosphoryl transfer is an extremely high substrate specificity. For example, the error rate of a replicase inserting a wrong nucleotide is *ca*  $10^{-3}$  to  $10^{-4}$ , even without a proofreading element present<sup>315</sup>. However, the free energy difference between a perfect Watson–Crick base-pair match and a mismatch is *ca* 2 kcal mol<sup>-1</sup>, a value which would lead to an error rate of only  $10^{-1}$  to  $10^{-2}$ <sup>316</sup>. This discrepancy is generally believed to be resolved by the induced-fit mechanism discussed above; however, newer findings indicate that this may not be the sole answer<sup>274</sup>. It is now postulated that the metal ions play an important role in helping to determine substrate specificity<sup>312</sup>.

The situation is not as clear for many other classes of enzymes that act upon DNA and RNA with typical examples being the exo- and endonucleases (exonucleases remove nucleotides from the end of a strand; endonucleases incise internal sites<sup>317</sup>). In order to crystallize nuclease–substrate complexes, this cleavage must be artificially inhibited. Successful strategies include using inert substrate analogues, chemical modification of specific residues or employment of a divalent cation that does not promote catalysis ( $Mn^{2+}$ , for example). This inevitably perturbs the active site and can lead to changes in the positions (and number) of the metal ions and catalytic residues involved<sup>312</sup>. Controversial findings are present in the literature for many systems, thus making it difficult to decide exactly how many metal ions are involved<sup>318</sup>. For example, three different mechanisms involving one, two and even three metal ions have been proposed for the phosphate diester bond cleavage catalyzed by type II restriction endonucleases<sup>319,320</sup>. It is clear that more information is needed before mechanistic similarities for these widely varied enzymes can be recognized.

## D. Magnesium and Photosynthesis

Magnesium is directly involved in one of the most thermodynamically demanding reactions to be found in biology—the synthesis of carbohydrates from  $CO_2$  in plants and cyanobacteria using light energy from the sun. This extremely complex process is considered to be the ‘engine of life’ and is fundamental for sustaining essentially all life on our planet<sup>13</sup>. The first step in this process is initiated by two very large, incredibly complex, coupled biomolecules—the photosystems I (PS-I) and II (PS-II)<sup>321,322</sup>. Oversimply stated, both photosystems work together to convert light energy into electrons, which are then transported across the cell membrane in photosynthesizing organisms where they are used to drive the synthesis of ATP. In addition, photosystem I provides the electrons necessary to reduce  $NADP^+$  to NADPH and photosystem II oxidizes water to  $O_2$  (a major source of

the air we breath) and  $H^+$ . In subsequent reactions, ATP and NADPH are used to convert  $CO_2$  into carbohydrates.

### 1. Chlorophyll

Sunlight is captured in both photosystems by large antenna systems, also known as light harvesting complexes, which basically consist of a complex 3D array of magnesium-based chlorophyll pigments (Figure 7) and carotenoids. The number of chlorophyll cofactors in such antenna systems varies quite widely. For example, six chlorophylls are located in the antenna of both photosystems in purple bacteria<sup>323,324</sup>, 27 in the light harvesting complex (LHC-II) of *Rhodospseudomonas acidophila*<sup>325</sup>, 48 in the LHC-II of spinach<sup>326</sup>, 96 in the PS-I of *Synechococcus elongates*<sup>36</sup>, 200–300 in the PS-I and PS-II of plants and algae and, finally, a huge number (ca 200,000) in the chlorosomes of green bacteria<sup>327</sup>. A subunit of one of the more simple systems is illustrated in Color Plate 7<sup>328</sup>. In this complex process of light harvesting, specific pigment–protein and pigment–pigment interactions are used by nature to finetune the absorption properties of the individual light gathering processes according to environmental demands.

Light energy initially absorbed by the antenna pigments is transferred via complex photochemical processes which are not yet well understood to a primary reaction center located at the base of the antenna, where it is then transformed into electrical energy. An example for such a reaction center is the chlorophyll dimer known as P700 (illustrated for the PS-I of *Synechococcus elongates*; Color Plate 7)<sup>36</sup>. The incoming photoenergy excites the P700 core. A singlet excited P700\* state results which promptly ejects an electron to generate a P700<sup>+</sup> radical cation. The electron is immediately transferred across the thylakoid membrane by a complex chain of electron carriers<sup>329</sup>. The P700<sup>+</sup> species remaining behind is then reduced by either plastocyanine (plants) or cytochrome c6 (cyanobacteria), which returns it to its resting state<sup>322</sup>.

The unusual binding situation of the central  $Mg^{2+}$  ion (illustrated in Figure 7) together with the photophysical properties of the chlorophyll ring system is obviously the key element underlying the transformation of photochemical into electrical energy. However, photoabsorption processes in chlorophylls are extremely complex processes which are still not fully understood—and chemical modifications in the ring periphery as well as very small perturbations in protein–chlorophyll interactions can have large consequences for the photophysical properties<sup>330</sup>. Magnesium coordination to the porphyrin ring results in a quasi-planar system which has two additional axial positions (above and below) available for additional coordination to the central  $Mg^{2+}$ . Most of the chlorophylls in the naturally occurring antenna systems are pentacoordinated to the  $N^T$ -nitrogen of the imidazole ring in a histidine side chain of the protein backbone<sup>331</sup>. The presence of a fifth ligand pulls the central  $Mg^{2+}$  ion slightly out of the porphyrin plane. Biomimetic studies have shown that hexacoordinated species are only formed when the ligand concentration is extremely high<sup>332</sup>. The identity of the fifth ligand on magnesium (usually N, but it can be O or even S) modifies the absorption spectra and it is believed that this ligand is involved in stabilization of the charge separation process in photosynthesis. Not only this, the very presence of a fifth ligand introduces a diastereotopic environment (both *syn* and *anti* diastereomers are possible) which causes small but nontrivial changes in the energetic levels of both ground and excited states<sup>330</sup>.

Unraveling the individual molecular interactions in these very complex photosystems is a challenging focus of current research, particularly since the demand for alternative energy sources has become critical in the past few years. Progress in this area is hampered, however, due to the extreme complexity of the natural systems coupled with the fact that the synthesis of biomimetic porphyrin models is quite challenging. Experimental

methods to directly study the interaction of magnesium with porphyrin systems are still being developed; a new technique is, for example, solid-state  $^{25}\text{Mg}$  NMR spectroscopy<sup>333</sup>. In addition, quantum-chemical studies are just now becoming feasible; calculations of the spectroscopic properties of these extensively conjugated systems have to be performed using higher multireference methodology (which, for these large molecules, is often beyond the limit of available computational capacities) if they are to be at all accurate<sup>334</sup>. Current calculations are often limited to semiempirical methods<sup>335</sup>. However, recent progress in calculating excited-state electron dynamics<sup>336</sup> combined with progress in time-resolved femtosecond spectroscopy<sup>337</sup> is quite promising for future studies on the ultrafast photodynamics in these fascinating systems.

## 2. Rubisco — a photosynthetic $\text{CO}_2$ fixing enzyme

Most of the carbon in us, the food we eat and, in general, the biosphere which surrounds us has been extracted from  $\text{CO}_2$  at some time or another by the world's most abundant enzyme—D-ribulose 1,5-bisphosphate carboxylase/oxygenase (rubisco)<sup>338</sup>. This enzyme catalyzes the initial step of carbon metabolism, the fixation of  $\text{CO}_2$ , in all organisms that rely upon photosynthesis. It has been estimated that the yearly turnover of  $\text{CO}_2$  processed by rubisco is well over  $10^{11}$  metric tons<sup>339</sup>. The overall reaction is the addition of  $\text{H}_2\text{O}$  and  $\text{CO}_2$  to D-ribulose 1,5-bisphosphate, a multistep process which ends up splitting the C2–C3 bond to yield two molecules of 3-phosphoglycerate (Figure 30). One of the interesting things about rubisco is, although it performs an essential biochemical role in sustaining life, it is actually quite a 'bad' enzyme with a very poor performance. It has an extremely low catalytic rate and, among a multitude of other side reactions<sup>340</sup>, a high tendency to confuse  $\text{CO}_2$  with  $\text{O}_2$ , a phenomenon which leads to photorespiration in plants<sup>341</sup>.

The minimal functional unit (quite well conserved among all rubiscos) is a homodimer in which the active sites are located at the subunit interface. Residues from both subunits contribute to each active site, which is illustrated in Color Plate 8. All known forms (at present, four different types) consist of these basic dimeric units which are arranged into various larger multimer arrays—dimers, tetramers and even pentamers<sup>342</sup>. The different forms of rubisco all have a common evolutionary origin and existing solid-state structures of the active sites are nearly superimposable<sup>343</sup>.

Before substrate binding can take place, rubisco must first be activated. This occurs via carbamylation (reaction with  $\text{CO}_2$ ) of an essential Lys residue<sup>344</sup>. This promotes the binding of an essential  $\text{Mg}^{2+}$  ion after which the active site is complete. Rubisco can now recognize and bind the first substrate which is ribulose- $\text{P}_2$  (D-ribulose 1,5-bisphosphate)<sup>345</sup>. The substrate is bound to the  $\text{Mg}^{2+}$  ion via an inner-sphere coordination of the C2-carbonyl and C3-hydroxyl groups which appropriately positions and activates the ribulose- $\text{P}_2$  for subsequent reaction. Substrate binding causes a flexible loop to close over the active site which buries the active site deep within the protein and restricts access to a small channel just large enough for  $\text{CO}_2$  (and  $\text{O}_2$ )<sup>346</sup>.

The catalytic circle begins when the substrate is converted into a reactive enediol or enediolate<sup>345</sup>. The presence of  $\text{CO}_2$  is not required for enolization. This is a reversible process, facilitated by the prepositioning of the  $\text{Mg}^{2+}$ -bound substrate<sup>347</sup>. Isotope exchange experiments indicate that a general base, most likely the carbamate bound to Lys201, could abstract the C3-proton<sup>339</sup>. This carbamate appears to be part of a possible proton relay for transporting  $\text{H}^+$  out and away from the reaction center<sup>339</sup>. Alternatively, a theoretical study indicates that a direct transfer of the hydrogen from the C3 center to the C2 carbonyl group with subsequent proton exchange of the resulting hydroxyl group with the medium is possible<sup>347</sup>.

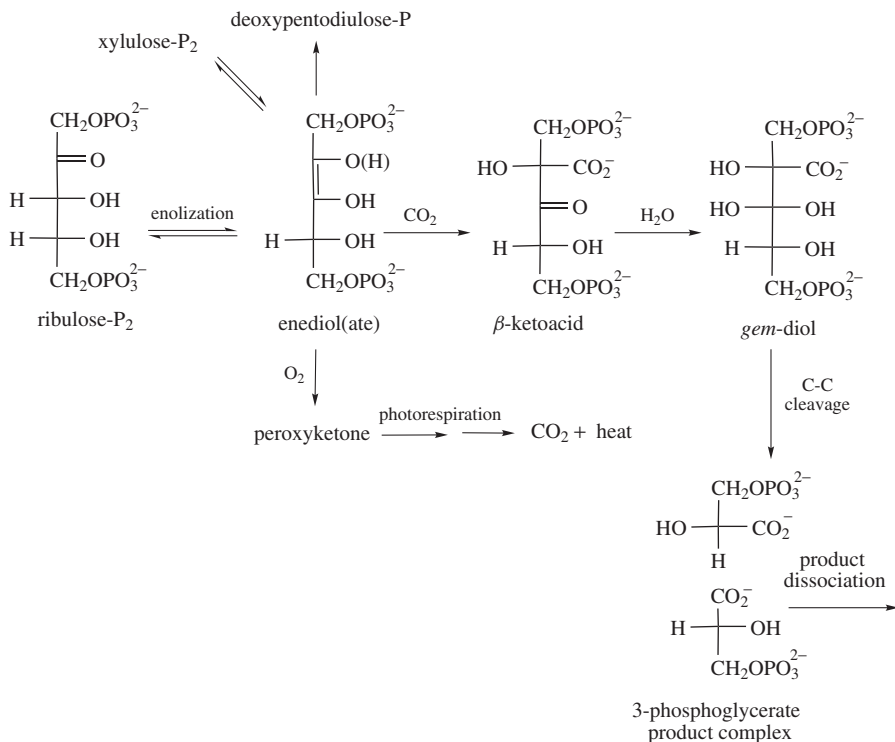


FIGURE 30. The chemical reaction carried out by rubisco

The enediol(ate) has a number of possible fates—it can tautomerize via H-transfer over the ‘wrong’ face of the double bond and xylulose-P<sub>2</sub> results, which is a tightly bound inhibitor<sup>348</sup>. This side reaction is held partially responsible for the low catalytic rate of rubisco<sup>349</sup>. Another nonproductive pathway is elimination of the C1-phosphate which generates deoxypentodiulose-P<sup>350</sup>. If the enediol(ate) survives these processes, a carboxylase/oxygenase bifunctionality becomes possible. The enediol(ate) bound in the active site is not capable of efficiently discriminating between CO<sub>2</sub> and O<sub>2</sub>. If O<sub>2</sub> reacts with the enediol, the secondary pathway of photorespiration is opened up. The products of this reaction are metabolized in the photorespiration pathway which eventually produces CO<sub>2</sub> and dissipates energy as heat—thus wasting important resources. It is estimated that a typical rubisco loses, depending on the relative atmospheric concentrations of CO<sub>2</sub> and O<sub>2</sub>, *ca* 25%–50% of its turnover to photorespiration<sup>341</sup>. This single concurrence reaction dictates the overall efficiency in which plants use their light, water and nitrogen resources—and as such, is currently a target of intense biotechnological efforts aimed at improving the catalytic properties of rubisco and engineering such improvements into crop plants<sup>341</sup>.

DFT calculations indicate that an incoming CO<sub>2</sub> displaces a water ligand at magnesium<sup>351</sup>. Coordination of one of the oxygen atoms in CO<sub>2</sub> to Mg<sup>2+</sup> bends, and thus polarizes, the central carbon atom which becomes sufficiently electrophilic to attack the *Si* face (observed experimentally<sup>352</sup>) of the enediolate C2 atom, which leads to the formation



of the  $\beta$ -ketoacid intermediate over a product-like transition structure. It has recently been suggested that, due to the chemical inertness of  $\text{CO}_2$ , the specificity of rubisco is determined in a late transition structure in which  $\text{CO}_2$  closely resembles a carboxylate group. This would maximize the structural difference between the competing transition structures for carboxylation and oxygenation. However, if the transition structure is too 'close' to the  $\beta$ -ketoacid, this would cause it to bind so tightly that subsequent reactions would be slowed down or even stopped. Rubisco is thus forced to make a compromise between  $\text{CO}_2/\text{O}_2$  selection and the maximum rate of catalytic turnover<sup>353</sup>.

In the subsequent hydration step, a water molecule, which has been positioned by the carbamylated Lys residue (which acts as a general base to accept  $\text{H}^+$ <sup>354</sup>), now adds to the now positive polarized C3 atom to form a *gem*-diol (experimentally verified<sup>355,351</sup>). The C—C bond cleavage step is the rate-determining step and is known to proceed with inversion of configuration at C2 of the first and the addition of a proton to the *Si* face of the *aci*-carboxylate form of the second 3-phosphoglycerate being formed<sup>339</sup>. Computational studies (HF, DFT, MP2) indicate that two completely different mechanisms for C—C bond rupture are theoretically possible—an intramolecular, pericyclic reaction over a five-membered-ring transition structure with a great deal of radical character (homolytic case)<sup>356,357</sup> and a heterolytic bond rupture which is initiated when a general base in the immediate vicinity (possibly Lys201) deprotonates the C3—OH group<sup>351</sup>. However, a much higher level of theory is needed before a differentiation between these two alternatives can be made.

## IX. REFERENCES

1. M. E. Maguire and J. A. Cowan, *Biometals*, **15**, 203 (2002).
2. F. I. Wolf and A. Cittadini, *Mol. Asp. Med.*, **24**, 3 (2003).
3. D. G. Kehres and M. E. Maguire, *Biometals*, **15**, 261 (2002).
4. J. A. Cowan, *Inorg. Chim. Acta*, **275–276**, 24 (1998).
5. R. D. Grubbs, *Biometals*, **15**, 251 (2002).
6. J. A. Cowan, *Biometals*, **15**, 225 (2002).
7. C. B. Black, H. W. Huang and J. A. Cowan, *Coord. Chem. Rev.*, **135–136**, 165 (1994).
8. A. Sreedhara and J. A. Cowan, *Biometals*, **15**, 211 (2002).
9. M. Egli, *Chem. & Biol.*, **9**, 277 (2002).
10. D. E. Draper, *RNA*, **10**, 335 (2004).
11. Z. J. Tan and S. J. Chen, *Biophys. J.*, **90**, 1175 (2006).
12. A. M. Pyle, *J. Biol. Inorg. Chem.*, **7**, 679 (2002).
13. J. F. Kasting and J. L. Siefert, *Science*, **296**, 1066 (2002).
14. S. Kluge and J. Weston, *Biochemistry*, **44**, 4877 (2005).
15. See, for example, the Cambridge Structural Database (CSD): [www.ccdc.cam.ac.uk](http://www.ccdc.cam.ac.uk).
16. H. Einspahr and C. E. Bugg, *Met. Ions Biol. Syst.*, **17**, 51 (1984).
17. R. Caminiti, G. Licheri, G. Piccaluga and G. Pinna, *Chem. Phys. Lett.*, **61**, 45 (1979).
18. H. M. Diebler, G. Eigen, G. Ilgenfritz, G. Maass and R. Winkler, *Pure Appl. Chem.*, **20**, 93 (1969).
19. S. E. Rodriguez-Cruz, R. A. Jockusch and E. R. Williams, *J. Am. Chem. Soc.*, **121**, 1986 (1999).
20. S. E. Rodriguez-Cruz, R. A. Jockusch and E. R. Williams, *J. Am. Chem. Soc.*, **121**, 8898 (1999).
21. P. J. Focia, H. Alam, T. Lu, U. D. Ramirez and D. M. Freymann, *Proteins: Struct. Funct. Bioinf.*, **54**, 222 (2004).
22. P. R. Markies, O. S. Akkerman, F. Bickelhaupt, W. J. J. Smeets and A. L. Spek, *Adv. Organomet. Chem.*, **32**, 147 (1991).
23. N. Walker, M. P. Dobson, R. R. Wright, P. E. Barran, J. N. Murrell and A. J. Stace, *J. Am. Chem. Soc.*, **122**, 11138 (2000).
24. W. W. Cleland and A. C. Hengge, *Chem. Rev.*, **106**, 3252 (2006).

25. M. Trachtman, G. D. Markham, J. P. Glusker, P. George and C. W. Bock, *Inorg. Chem.*, **40**, 4230 (2001).
26. L. Leiboda, E. Zhang, K. Lewinski and J. M. Brewer, *Proteins: Struct. Funct. Gen.*, **16**, 219 (1993).
27. J. A. Cowan, *Chem. Rev.*, **98**, 1067 (1998).
28. T. Dudev and C. Lim, *Chem. Rev.*, **103**, 773 (2003).
29. K. Juneau, E. Podell, D. J. Harrington and T. R. Cech, *Structure*, **9**, 221 (2001).
30. X. Shui, L. McFail-Isom, G. G. Hu and L. D. Williams, *Biochemistry*, **37**, 8341 (1998).
31. I. Berger, V. Tereshko, H. Ikeda, V. E. Marquez and M. Egli, *Nucleic Acids Res.*, **26**, 2473 (1998).
32. A. S. Petrov, G. Lamm and G. R. Pack, *J. Phys. Chem. B*, **106**, 3294 (2002).
33. M. M. Harding, *Acta Crystallogr.*, **D62**, 678 (2006).
34. M. M. Harding, *Acta Crystallogr.*, **D57**, 401 (2001) and literature contained therein.
35. C. W. Bock, A. K. Katz, G. D. Markham and J. P. Glusker, *J. Am. Chem. Soc.*, **121**, 7360 (1999).
36. P. Jordan, P. Fromme, H. T. Witt, O. Klukas, W. Saenger and N. Krauß, *Nature*, **411**, 909 (2001).
37. T. Dudev, J. A. Cowan and C. Lim, *J. Am. Chem. Soc.*, **121**, 7665 (1999).
38. T. Dudev and C. Lim, *J. Am. Chem. Soc.*, **128**, 1553 (2006).
39. T. Dudev, Y. L. Lin, M. Dudev and C. Lim, *J. Am. Chem. Soc.*, **125**, 3168 (2003).
40. U. Ryde, *Biophys. J.*, **77**, 2777 (1999).
41. R. L. Rardin, W. B. Tolmann and S. J. Lippard, *New J. Chem.*, **15**, 417 (1991).
42. G. C. Dismukes, *Chem. Rev.*, **96**, 2909 (1996).
43. T. Dudev and C. Lim, *J. Phys. Chem. B*, **108**, 4546 (2004).
44. C. S. Babu, T. Dudev, R. Casareno, J. A. Cowan and C. Lim, *J. Am. Chem. Soc.*, **125**, 9318 (2003).
45. E. Rezabal, J. M. Mercero, X. Lopez and J. M. Ugalde, *J. Inorg. Biochem.*, **100**, 374 (2006).
46. L. Y. Wang, Y. H. Zhang and L. J. Zhao, *J. Phys. Chem. A*, **109**, 609 (2005).
47. A. Wahab, S. Mahiuddin, G. Hefter, W. Kunz, B. Minofar and P. Jungwirth, *J. Phys. Chem. B*, **109**, 24108 (2005).
48. D. E. Wilcox, *Chem. Rev.*, **96**, 2435 (1996).
49. N. Sträter, W. N. Lipscomb, T. Klabunde and B. Krebs *Angew. Chem., Int. Ed. Engl.*, **35**, 2024 (1996).
50. B. Schneider and M. Kabeláč, *J. Am. Chem. Soc.*, **120**, 161 (1998).
51. A. S. Petrov, J. Funseth-Smotzer and G. R. Pack, *Int. J. Quantum Chem.*, **102**, 645 (2005).
52. A. S. Petrov, G. R. Pack and G. Lamm, *J. Phys. Chem. B*, **108**, 6072 (2004).
53. N. Sundaresan, C. K. S. Pillai and C. H. Suresh, *J. Phys. Chem. A*, **110**, 8826 (2006).
54. I. Tvaroska, I. André and J. P. Carver, *J. Mol. Struct. (Theochem.)*, **469**, 103 (1999).
55. W. J. McCarthy, D. M. A. Smith, L. Adamowicz, H. Saint-Martin and I. Ortega-Blake, *J. Am. Chem. Soc.*, **120**, 6113 (1998).
56. H. Saint-Martin, L. E. Ruiz-Vicent, A. Ramírez-Solís and I. Ortega-Blake, *J. Am. Chem. Soc.*, **118**, 12167 (1996).
57. I. André, I. Tvaroska and J. P. Carter, *J. Phys. Chem. A*, **104**, 4609 (2000).
58. S. M. Prince, M. Z. Papiz, A. A. Freer, G. McDermott, A. M. Hawthornthwaite-Lawless, R. J. Cogdell and N. W. Isaacs, *J. Mol. Biol.*, **268**, 412 (1997).
59. A. S. Pedrares, W. Teng and K. Ruhlandt-Senge, *Chem. Eur. J.*, **9**, 2019 (2003).
60. M. E. Maguire, *Front. Biosci.*, **11**, 3149 (2006).
61. R. D. Grubbs and M. E. Maguire, *Magnesium*, **6**, 113 (1987).
62. A. M. P. Romani and A. Scarpa, *Front. Biosci.*, **5**, 720 (2000).
63. J. Sahni, B. Nelson and A. M. Scharenberg, *Biochem. J.*, **401**, 505 (2007).
64. A. M. P. Romani and M. E. Maguire, *Biometals*, **15**, 271 (2002).
65. A. M. P. Romani, *Front. Biosci.*, **12**, 308 (2007).
66. M. Kolisek, G. Zsurka, J. Samaj, J. Weghuber, R. J. Schweyen and M. Schweigel, *EMBO J*, **22**, 1235 (2003).
67. V. V. Lunin, E. Dobrovetsky, G. Khutoreskaya, R. Zhang, A. Joachimiak, D. A. Doyle, A. Bochkarev, M. E. Maguire, A. M. Edwards and C. M. Koth, *Nature*, **440**, 833 (2006).
68. E. M. Froschauer, M. Kolisek, F. Dieterich, M. Schweigel and R. J. Schweyen, *FEMS Microbiol. Lett.*, **237**, 49 (2004).

69. M. D. Snively, J. B. Florer, C. G. Miller and M. E. Maguire, *J. Bacteriol.*, **171**, 4761 (1989).
70. S. Eshaghi, D. Niegowski, A. Kohl, D. M. Molina, S. A. Lesley and P. Nordlund, *Science*, **313**, 354 (2006).
71. J. Payandeh and E. F. Pai, *EMBO J.*, **25**, 3762 (2006).
72. M. E. Maguire, *Cur. Opin. Struct. Biol.*, **16**, 432 (2006).
73. S. Z. Wang, Y. Chen, Z. H. Sun, Q. Zhou and S. F. Sui, *J. Biol. Chem.*, **281**, 26813 (2006).
74. M. A. Warren, L. M. Kucharski, A. Veenstra, L. Shi, P. F. Grulich and M. E. Maguire, *J. Bacteriol.*, **186**, 4605 (2004).
75. L. M. Kucharski, W. J. Lubbe and M. E. Maguire, *J. Biol. Chem.*, **275**, 16767 (2000).
76. A. Kornberg, *J. Bacteriol.*, **177**, 491 (1995).
77. S. Garavaglia, A. Galizzi and M. Rizzi, *J. Bacteriol.*, **185**, 4844 (2003).
78. S. Kawai, S. Mori, T. Mukai, S. Suzuki, T. Yamada, W. Hashimoto and K. Murata, *Biochem. Biophys. Res. Commun.*, **276**, 57 (2000).
79. H. Sigel, *Inorg. Chim. Acta*, **198–200**, 1 (1992).
80. L. Stryer, *Biochemie*, 4<sup>th</sup> Edition, Spectrum Akademischer Verlag, Heidelberg, 1996.
81. G. Oster, *Nature*, **417**, 25 (2002).
82. M. Souhassou, C. Lecomte and R. H. Blessing, *Acta Crystallogr.*, **B48**, 370 (1992).
83. R. Cini, M. C. Burla, A. Nunzi, G. P. Polidori and P. F. Zanazzi, *J. Chem. Soc., Dalton Trans.*, 2467 (1984).
84. C. V. Grant, V. Frydman and L. Frydman, *J. Am. Chem. Soc.*, **122**, 11743 (2000).
85. P. Wang, R. M. Izatt, J. L. Oscarson and S. E. Gillespie, *J. Phys. Chem.*, **100**, 9556 (1996).
86. P. Wang, J. L. Oscarson, R. M. Izatt, G. D. Watt and C. D. Larsen, *J. Solution Chem.*, **24**, 989 (1995).
87. L. Jiang and X. A. Mao, *Spectrochim. Acta*, **A57**, 1711 (2001).
88. A. S. Mildvan, *Magnesium*, **6**, 28 (1987).
89. M. Cohn and T. R. Hughes Jr., *J. Biol. Chem.*, **237**, 176 (1962).
90. J. C. Liao, S. Sun, D. Chandler and G. Oster, *Eur. Biophys. J.*, **33**, 29 (2004).
91. P. D. Boyer, *Annu. Rev. Biochem.*, **66**, 717 (1997).
92. T. M. Duncan, V. V. Bulgin, Y. Zhou, M. L. Hutcheon and R. L. Cross, *Proc. Natl. Acad. Sci. U.S.A.*, **92**, 10964 (1995).
93. M. A. Bianchet, J. Hullihen, P. L. Pedersen and L. M. Amzel, *Proc. Natl. Acad. Sci. U.S.A.*, **95**, 11065 (1998).
94. J. P. Abrahams, A. G. W. Leslie, R. Lutter and J. E. Walker, *Nature*, **370**, 621 (1994).
95. D. Sabbert, S. Engelbrecht and W. Junge, *Nature*, **381**, 623 (1996).
96. H. Noji, R. Yasuda, M. Yoshida and K. Kinosita Jr., *Nature*, **386**, 299 (1997).
97. Y. Sambongi, Y. Iko, M. Tanabe, H. Omote, A. Iwamoto-Kihara, I. Ueda, T. Yanagida, Y. Wada and M. Futai, *Science*, **286**, 1722 (1999).
98. H. Noji and M. Yoshida, *J. Biol. Chem.*, **276**, 1665 (2001).
99. Y. Rondelez, G. Tresset, T. Nakashima, Y. Kato-Yamada, H. Fujita, S. Takeuchi and H. Noji, *Nature*, **433**, 773 (2005).
100. R. Yasuda, H. Noji, M. Yoshida, K. Kinosita Jr. and H. Itoh, *Nature*, **410**, 898 (2001).
101. V. N. Kasho, M. Stengelin, I. N. Smirnova and L. D. Faller, *Biochemistry*, **36**, 8045 (1997).
102. J. P. Abrahams, A. G. W. Leslie, R. Lutter and J. E. Walker, *Nature*, **370**, 621 (1994).
103. Y. H. Ko, S. Hong and P. L. Pedersen, *J. Biol. Chem.*, **274**, 28853 (1999).
104. A. L. Buchachenko and D. A. Kuznetsov, *Mol. Biol.*, **40**, 9 (2006).
105. J. Weber and A. E. Senior, *FEBS Lett.*, **545**, 61 (2003).
106. A. L. Buchachenko, D. A. Kouznetsov, S. E. Arkhangelsky, M. A. Orlova and A. A. Markarian, *Mitochondrion*, **5**, 67 (2005).
107. A. L. Buchachenko, D. A. Kouznetsov, S. E. Arkhangelsky, M. A. Orlov and A. A. Markarian, *Cell. Biochem. Biophys.*, **43**, 243 (2005).
108. A. L. Buchachenko, E. M. Galimov, V. V. Ershov, G. A. Nikiforov and A. P. Pershin, *Proc. USSR Acad. Sci.*, **228**, 379 (1976).
109. A. L. Buchachenko and V. L. Berdinsky, *Chem. Rev.*, **102**, 603 (2002).
110. A. L. Buchachenko, *J. Phys. Chem. A*, **105**, 9995 (2001).
111. A. L. Buchachenko, N. N. Lukzen and J. B. Pedersen, *Chem. Phys. Lett.*, **434**, 139 (2007).
112. M. Cohn, *J. Biol. Chem.*, **201**, 735 (1953).
113. G. R. J. Thatcher and R. Kluger, *Adv. Phys. Org. Chem.*, **25**, 99 (1989).
114. M. Bianciotto, J. C. Barthelat and A. Vigroux, *J. Am. Chem. Soc.*, **124**, 7573 (2002).

115. N. Iché-Tarrat, J. C. Barthelat, R. Rinaldi and A. Vigroux *J. Phys. Chem. B.*, **109**, 22570 (2005).
116. N. Iché-Tarrat, M. Ruiz-Lopez, J. C. Barthelat and A. Vigroux, *Chem. Eur. J.*, **13**, 3617 (2007).
117. B. L. Grigorenko, A. V. Nemukhin, M. S. Shadrina, I. A. Topol and S. K. Burt, *Proteins; Struct. Funct. Bioinf.*, **66**, 456 (2007).
118. B. L. Grigorenko, A. V. Nemukhin, I. A. Topol, R. E. Cachau and S. K. Burt, *Proteins; Struct. Funct. Bioinf.*, **60**, 495 (2005).
119. E. Franzini, P. Fantucci and L. De Gioia, *J. Mol. Catal. A*, **204–205**, 409 (2003).
120. J. Akola and R. O. Jones, *J. Phys. Chem. B*, **107**, 11774 (2003).
121. H. Sigel, *Pure Appl. Chem.*, **70**, 969 (1998).
122. H. Sigel, *Coord. Chem. Rev.*, **100**, 453 (1990).
123. H. Sigel and R. Griesser, *Chem. Soc. Rev.*, **34**, 875 (2005).
124. H. Sigel, *Chem. Soc. Rev.*, **33**, 191 (2004).
125. L. W. Tari, A. Matte, H. Goldie and L. T. J. Delbaere, *Nat. Struct. Biol.*, **4**, 990 (1997).
126. H. Sigel and R. Tribolet, *J. Inorg. Biochem.*, **40**, 163 (1990).
127. T. A. Steitz, *J. Biol. Chem.*, **274**, 17395 (1999).
128. P. H. Patel and L. A. Loeb, *Nat. Struct. Biol.*, **8**, 656 (2001).
129. A. A. Tulub, *Phys. Chem. Chem. Phys.*, **8**, 2187 (2006).
130. A. A. Tulub, *Russ. J. Inorg. Chem.*, **50**, 1884 (2005).
131. W. Domcke, D. Yarkony and H. Koppel, *Conical Intersections: Electronic Structure, Dynamics and Spectroscopy*, World Scientific Press, New York, 2004.
132. S. A. Pavlenko and A. A. Voitjuk, *J. Struct. Chem.*, **32**, 590 (1991).
133. J. N. Harvey, J. Zureck, U. Pentikäinen and A. J. Mulholland, *Phys. Chem. Chem. Phys.*, **8**, 5366 (2006).
134. A. A. Tulub, *Phys. Chem. Chem. Phys.*, **8**, 5368 (2006).
135. J. A. Subirana and M. Soler-López, *Annu. Rev. Biophys. Biomol. Struct.*, **32**, 27 (2003).
136. R. K. O. Sigel and A. M. Pyle, *Chem. Rev.*, **107**, 97 (2007).
137. G. S. Manning, *Biopolymers*, **69**, 137 (2003).
138. I. A. Shkel, O. V. Tsidikov and M. R. Record Jr., *Proc. Natl. Acad. Sci. U.S.A.*, **99**, 2597 (2002).
139. V. K. Misra and D. E. Draper, *Proc. Natl. Acad. Sci. U.S.A.*, **98**, 12456 (2001).
140. R. T. Batey, R. P. Rambo, L. Lucast, R. Rha and J. A. Doudna, *Science*, **287**, 1232 (2000).
141. D. J. Klein, P. B. Moore and T. A. Steitz, *RNA*, **10**, 1366 (2004).
142. J. Anastassopoulou, *J. Mol. Struct.*, **651–653**, 19 (2003).
143. P. E. Cole, S. K. Yang and D. M. Crothers, *Biochemistry*, **11**, 4358 (1972).
144. T. K. Chiu and R. E. Dickerson, *J. Mol. Biol.*, **301**, 915 (2000).
145. V. Tereshko, G. Minasov and M. Egli, *J. Am. Chem. Soc.*, **121**, 470 (1999).
146. G. Minasov, V. Tereshko and M. Egli, *J. Mol. Biol.*, **291**, 83 (1999).
147. C. C. Correll, B. Freeborn, P. B. Moore and T. A. Steitz, *Cell*, **91**, 705 (1997).
148. N. B. Leontis, P. Gosh and P. B. Moore, *Biochemistry*, **25**, 7386 (1986).
149. K. Kruger, P. J. Grabowski, A. J. Zaug, J. Sands, D. E. Gottschling and T. R. Cech, *Cell*, **31**, 147 (1982).
150. C. Guerrier-Takada, K. Gardiner, T. Marsh, N. Pace and S. Altman, *Cell*, **35**, 849 (1983).
151. G. F. Joyce, *Nature*, **418**, 214 (2002).
152. D. M. Zhou and K. Taira, *Chem. Rev.*, **98**, 991 (1998).
153. B. J. Tucker and R. R. Breaker, *Cur. Opin. Struct. Biol.*, **15**, 342 (2005).
154. J. A. Doudna and T. R. Cech, *Nature*, **418**, 222 (2002).
155. S. A. Woodson, *Cur. Opin. Struct. Biol.*, **15**, 324 (2005).
156. R. K. O. Sigel, *Eur. J. Inorg. Chem.*, 2281 (2005).
157. A. V. Kazantsev and N. R. Pace, *Nat. Rev. Microbiol.*, **4**, 729 (2006).
158. R. H. Symons, *Nucl. Acid Res.*, **25**, 2683 (1997).
159. R. G. Kuimelis and L. W. McLaughlin, *Chem. Rev.*, **98**, 1027 (1998).
160. H. Liu, J. J. Robinet, S. Ananvoranich and J. W. Gauld, *J. Phys. Chem. B*, **111**, 439 (2007).
161. N. Ban, P. Nissen, J. Hansen, P. B. Moore and T. A. Steitz, *Science*, **289**, 905 (2000).
162. R. Fiammengio and A. Jäschke, *Cur. Opin. Biotech.*, **16**, 614 (2005).
163. I. Tinoco Jr. and C. Bustamante, *J. Mol. Biol.*, **293**, 271 (1999).
164. D. E. Draper, D. Grilley and A. M. Soto, *Annu. Rev. Biophys. Biomol. Struct.*, **34**, 221 (2005).

165. S. A. Woodson, *Cur. Opin. Chem. Biol.*, **9**, 104 (2005).
166. V. K. Misra and D. E. Draper, *J. Mol. Biol.*, **317**, 507 (2002).
167. T. R. Sosnick and T. Pan, *Cur. Opin. Struct. Biol.*, **13**, 309 (2003).
168. V. J. DeRose, *Cur. Opin. Struct. Biol.*, **13**, 317 (2003).
169. J. J. Cannone, S. Subramanian, M. N. Schnare, J. R. Collett, L. M. D'Souza, Y. Du, B. Feng, N. Lin, L. V. Madabusi, K. M. Müller, N. Pande, Z. Shang, N. Yu and R. R. Gutell, *BMC Bioinformatics*, **3**, 2 (2002).
170. T. R. Cech, *Annu. Rev. Biochem.*, **59**, 543 (1990).
171. Q. Vicens and T. R. Cech, *Trends Biochem. Sci.*, **31**, 41 (2006).
172. J. Pan, D. Thirumalai and S. A. Woodson, *Proc. Natl. Acad. Sci. U.S.A.*, **96**, 6149 (1999).
173. E. L. Christian and M. Yarus, *Biochemistry*, **32**, 4475 (1993).
174. M. R. Stahley and S. A. Strobel, *Cur. Opin. Struct. Biol.*, **16**, 319 (2006).
175. T. A. Steitz and J. A. Steitz, *Proc. Natl. Acad. Sci. U.S.A.*, **90**, 6498 (1993).
176. S. Shan, A. V. Kravchuk, J. A. Piccirilli and D. Herschlag, *Biochemistry*, **40**, 5161 (2001).
177. M. R. Stahley and S. A. Strobel, *Science*, **309**, 1587 (2005).
178. G. A. Prody, J. T. Bakos, J. M. Buzayan, I. R. Schneider and G. Bruening, *Science*, **231**, 1577 (1986).
179. C. J. Hutchins, P. D. Rathjen, A. C. Forster and R. H. Symons, *Nucl. Acids Res.*, **14**, 3627 (1986).
180. K. F. Blount and O. C. Uhlenbeck, *Annu. Rev. Biophys. Biomol. Struct.*, **34**, 415 (2005).
181. H. W. Pley, K. M. Flaherty and D. B. McKay, *Nature*, **372**, 68 (1994).
182. D. E. Ruffner, G. D. Stormo and O. C. Uhlenbeck, *Biochemistry*, **29**, 10695 (1990).
183. C. Hamman and D. M. Lilley, *ChemBioChem*, **3**, 690 (2002).
184. G. Slim and M. J. Gait, *Nucl. Acids Res.*, **19**, 1183 (1991).
185. M. Koizumi and E. Ohtsuka, *Biochemistry*, **30**, 5145 (1991).
186. W. G. Scott, J. T. Finch and A. Klug, *Cell*, **81**, 991 (1995).
187. J. B. Murray, D. P. Terwey, L. Maloney, A. Karpeisky, N. Usman, L. Beigelman and W. G. Scott, *Cell*, **92**, 665 (1998).
188. S. Wang, K. Karbstein, A. Peracchi, L. Beigelman and D. Herschlag, *Biochemistry*, **38**, 14363 (1999).
189. K. Suzmura, M. Warashina, K. Yoshinari, Y. Tanaka, T. Kuwabara, M. Orita and K. Taira, *FEBS Lett.*, **473**, 106 (2000).
190. R. Przybilski and C. Hammann, *ChemBioChem*, **7**, 1641 (2006).
191. M. de la Peña, S. Gago and R. Flores, *EMBO J.*, **22**, 5561 (2003).
192. A. Khvorova, A. Lescoute, E. Westhof and S. D. Jayasena, *Nat. Struct. Biol.*, **10**, 708 (2003).
193. M. Roychowdhury-Saha and D. H. Burke, *RNA*, **12**, 1846 (2006).
194. J. C. Penedo, T. J. Wilson, S. D. Jayasena, A. Khvorova and D. M. J. Lilley, *RNA*, **10**, 880 (2004).
195. D. Lambert, J. E. Heckman and J. M. Burke, *Biochemistry*, **45**, 7140 (2006).
196. M. Martick and W. G. Scott, *Cell*, **126**, 309 (2006).
197. J. Han and J. M. Burke, *Biochemistry*, **44**, 7864 (2005).
198. M. Vogt, S. Lahiri, C. G. Hoogstraten, R. D. Britt and V. J. DeRose, *J. Am. Chem. Soc.*, **128**, 16764 (2006).
199. Y. Tanaka, Y. Kasai, S. Mochizuki, A. Wakisaka, E. H. Morita, C. Kojima, A. Toyozawa, Y. Kondo, M. Taki, Y. Takagi, A. Inoue, K. Yamasaki and K. Taira, *J. Am. Chem. Soc.*, **126**, 744 (2004).
200. Y. Takagi, A. Inoue and K. Taira, *J. Am. Chem. Soc.*, **126**, 12856 (2004).
201. J. M. Zhou, D. M. Zhou, Y. Takagi, Y. Kasai, A. Inoue, T. Baba and K. Taira, *Nucl. Acids Res.*, **30**, 2374 (2002).
202. R. A. Torres, F. Himo, T. C. Bruice, L. Noodleman and T. Lovell, *J. Am. Chem. Soc.*, **125**, 9861 (2003).
203. F. Leclerc and M. Karplus, *J. Phys. Chem. B*, **110**, 3395 (2006).
204. M. Boero, M. Tateno, K. Terakura and A. Oshiyama, *J. Chem. Theory Comput.*, **1**, 925 (2005).
205. R. Stowasser and D. A. Usher, *Bioorg. Chem.*, **30**, 420 (2002).
206. See, for example, the Jena library of biological macromolecules at [www.fli-leibniz.de/IMAGE.html](http://www.fli-leibniz.de/IMAGE.html).
207. D. H. Busch and N. A. Stephenson, *Coord. Chem. Rev.*, **100**, 119 (1990).
208. S. W. Ragsdale, *Chem. Rev.*, **106**, 3317 (2006).

209. W. T. Lowther and B. W. Matthews, *Chem. Rev.*, **102**, 4581 (2002).
210. N. Miti, S. J. Smith, A. Neves, L. W. Guddat, L. R. Gahan and G. Schenk, *Chem. Rev.*, **106**, 3338 (2006).
211. J. A. Hardy and J. A. Wells, *Cur. Opin. Struct. Biol.*, **14**, 706 (2004).
212. D. Kern and E. R. P. Zuiderweg, *Cur. Opin. Struct. Biol.*, **13**, 748 (2003).
213. G. Parkin, *Chem. Rev.*, **104**, 699 (2004).
214. J. Weston, *Chem. Rev.*, **105**, 2151 (2005).
215. M. H. Le Du, C. Lamoure, B. H. Muller, O. V. Bulgakov, E. Lajeunesse, A. Ménez and J. C. Boulain, *J. Mol. Biol.*, **316**, 941 (2002).
216. E. Dirnbach, D. G. Steel and A. Gafni, *Biochemistry*, **40**, 11219 (2001).
217. V. Subramaniam, N. C. H. Bergenhem, A. Gafni and D. G. Steel, *Biochemistry*, **34**, 1133 (1995).
218. V. Bučević-Popović, M. Pavela-Vrančić and R. Dieckmann, *Biochimie*, **86**, 403 (2004).
219. S. Orhanović and M. Pavela-Vrani, *Eur. J. Biochem.*, **270**, 4356 (2003).
220. M. F. Hoylaerts, T. Manes and J. L. Millán, *J. Biol. Chem.*, **272**, 22781 (1997).
221. J. A. Adams, *Chem. Rev.*, **101**, 2271 (2001).
222. T. Hunter, *Semin. Cell Biol.*, **5**, 367 (1994).
223. E. S. Lander *et al.*, *Nature*, **409**, 860 (2001).
224. S. K. Hanks and T. Hunter, *FASB J.*, **9**, 576 (1995).
225. S. S. Taylor and E. Radzio-Andezelm, *Structure*, **2**, 345 (1994).
226. M. G. Gold, D. Barford and D. Komander, *Curr. Opin. Struct. Biol.*, **16**, 693 (2006).
227. P. Pellicena and J. A. Kuriyan, *Curr. Opin. Struct. Biol.*, **16**, 702 (2006).
228. Z. Shi, K. A. Resing and N. G. Ahn, *Curr. Opin. Struct. Biol.*, **16**, 686 (2006).
229. A. Reményi, M. C. Good and W. A. Lim, *Curr. Opin. Struct. Biol.*, **16**, 676 (2006).
230. B. E. Kemp, D. J. Graves, E. Benjamini and E. G. Krebs, *J. Biol. Chem.*, **252**, 4888 (1977).
231. S. S. Taylor, J. A. Buechler and W. Yonemoto, *Annu. Rev. Biochem.*, **59**, 971 (1990).
232. J. Zheng, D. R. Knighton, L. F. Ten Eyck, R. Karlsson, N. H. Xuong, S. S. Taylor and J. M. Sowadski, *Biochemistry*, **32**, 2154 (1993).
233. B. Grant and J. A. Adams, *Biochemistry*, **35**, 2022 (1996).
234. Madhusudan, E. A. Trafny, N. H. Xuong, J. A. Adams, L. F. Ten Eyck, S. S. Taylor and J. M. Sowadski, *Prot. Sci.*, **3**, 176 (1994).
235. C. S. Gibbs and M. J. Zoller, *J. Biol. Chem.*, **266**, 8923 (1991).
236. P. F. Cook, M. E. Neville Jr., K. E. Vrana, F. T. Hartl and J. R. Roskoski Jr., *Biochemistry*, **21**, 5794 (1982).
237. M. J. Robinson, P. C. Harkins, J. Zhang, R. Baer, J. W. Haycock, M. H. Cobb and E. J. Goldsmith, *Biochemistry*, **35**, 5641 (1996).
238. V. E. Anderson, M. W. Ruszczycki and M. E. Harris, *Chem. Rev.*, **106**, 3236 (2006).
239. V. T. Skamaki, D. J. Owen, M. E. M. Noble, E. D. Lowe, G. Lowe, N. G. Oikonomakos and L. N. Johnson *Biochemistry*, **38**, 14718 (1999).
240. J. Zhou and J. A. Adams, *Biochemistry*, **36**, 2977 (1997).
241. Madhusudan, P. Akamine, N. H. Xuong and S. S. Taylor, *Nat. Struct. Biol.*, **9**, 273 (2002).
242. N. Diaz and M. J. Field, *J. Am. Chem. Soc.*, **126**, 529 (2004).
243. M. Valiev, R. Kawai, J. A. Adams and J. H. Weare, *J. Am. Chem. Soc.*, **125**, 9926 (2003).
244. Y. Cheng, Y. Zhang and J. A. McCammon, *J. Am. Chem. Soc.*, **127**, 1553 (2005).
245. J. Stubbe and R. H. Abeles, *Biochemistry*, **19**, 5505 (1980).
246. S. Duquerooy, C. Camus and J. Janin, *Biochemistry*, **34**, 12513 (1995).
247. O. Warburg and W. Christian, *Biochem. Z.*, **310**, 384 (1941).
248. B. Stec and L. Leiboda, *J. Mol. Biol.*, **211**, 235 (1990).
249. J. M. Brewer and G. Weber, *J. Biol. Chem.*, **241**, 2550 (1966).
250. R. R. Poyner, W. W. Cleland and G. H. Reed, *Biochemistry*, **40**, 8009 (2001).
251. J. Qin, G. Chai, J. M. Brewer, L. L. Loveland and L. Leiboda, *Biochemistry*, **45**, 793 (2006).
252. P. A. Sims, A. L. Menefee, T. M. Larsen, S. O. Mansoorabadi and G. H. Reed, *J. Mol. Biol.*, **355**, 422 (2006).
253. J. E. Wedekind, R. R. Poyner, G. H. Reed and I. Rayment, *Biochemistry*, **33**, 9333 (1994).
254. L. Leiboda, B. Stec and J. M. Brewer, *J. Biol. Chem.*, **264**, 3685 (1989).
255. T. M. Larsen, J. E. Wedekind, I. Rayment and G. H. Reed, *Biochemistry*, **35**, 4349 (1996).
256. E. Zhang, M. Hatada, J. M. Brewer and L. Leiboda, *Biochemistry*, **33**, 6295 (1994).
257. J. M. Brewer, C. V. C. Glover, M. J. Holland and L. Leiboda, *J. Prot. Chem.*, **22**, 353 (2003).

258. E. Zhang, J. M. Brewer, W. Minor, L. A. Carreira and L. Lebioda, *Biochemistry*, **36**, 12526 (1997).
259. G. H. Reed, R. R. Poyner, T. M. Larsen, J. E. Wedekind and I. Rayment, *Cur. Opin. Struct. Biol.*, **6**, 736 (1996).
260. D. A. Vinarov and T. Nowak, *Biochemistry*, **38**, 12138 (1999).
261. S. Duquerroy, C. Camus and J. Janin, *Biochemistry*, **34**, 12513 (1995).
262. H. Liu, Y. Zhang and W. Yang, *J. Am. Chem. Soc.*, **122**, 6560 (2000).
263. C. Alhambra, J. Gao, J. C. Corchado, J. Villà and D. G. Truhlar, *J. Am. Chem. Soc.*, **121**, 2253 (1999).
264. H. M. Senn and W. Thiel, *Curr. Opin. Chem. Biol.*, **11**, 182 (2007).
265. R. A. Friesner and V. Guallar, *Annu. Rev. Phys. Chem.*, **56**, 389 (2005).
266. J. Weston, unpublished results (2007).
267. I. Wagner, Diplomarbeit (Master's thesis), Friedrich-Schiller-Universität, Jena, Germany (2006).
268. S. Kluge, PhD Dissertation, Friedrich-Schiller-Universität, Jena, Germany (2007).
269. D. Mollenhauer, Diplomarbeit (Master's thesis), Friedrich-Schiller-Universität, Jena, Germany (2007).
270. E. Delagoutte and P. H. von Hippel, *Q. Rev. Biophys.*, **36**, 1 (2003).
271. E. Delagoutte and P. H. von Hippel, *Q. Rev. Biophys.*, **35**, 431 (2002).
272. M. M. Hingorani and M. O'Donnel, *Cur. Org. Chem.*, **4**, 887 (2001).
273. T. A. Kunkel, *J. Biol. Chem.*, **279**, 16895 (2004).
274. C. M. Joyce and S. J. Benkovic, *Biochemistry*, **43**, 14317 (2004).
275. T. A. Baker and S. P. Bell, *Cell*, **92**, 295 (1998).
276. M. A. Sirover and L. A. Loeb, *Biochem. Biophys. Res. Commun.*, **70**, 812 (1976).
277. M. A. Sirover and L. A. Loeb, *J. Biol. Chem.*, **252**, 3605 (1977).
278. A. Hartwig, *Mutat. Res.*, **475**, 113 (2001).
279. J. H. J. Hoeijmakers, *Nature*, **411**, 366 (2001).
280. J. J. Truglio, D. L. Croteau, B. Van Houten and C. Kisker, *Chem. Rev.*, **106**, 233 (2006).
281. A. Sancar, *Annu. Rev. Biochem.*, **65**, 43 (1996).
282. R. D. Kolodner and G. T. Marsischky, *Cur. Opin. Gen. Devel.*, **9**, 89 (1999).
283. K. W. Caldecott, *DNA Repair*, **6**, 443 (2007).
284. X. Xing and C. E. Bell, *Biochemistry*, **43**, 16142 (2004).
285. P. J. O'Brian, *Chem. Rev.*, **106**, 720 (2006).
286. D. L. Ollis, P. Brick, R. Hamlin, N. G. Xuong and T. A. Steitz, *Nature*, **313**, 762 (1985).
287. H. Klenow and I. Henningsen, *Proc. Natl. Acad. Sci. U.S.A.*, **65**, 168 (1970).
288. W. A. Beard and S. H. Wilson, *Chem. Rev.*, **106**, 361 (2006).
289. S. S. Patel, I. Wong and K. A. Johnson, *Biochemistry*, **30**, 511 (1991).
290. A. K. Showalter, B. J. Lamarche, M. Bakhtina, M. I. Su, K. H. Tang and M. D. Tsai, *Chem. Rev.*, **106**, 340 (2006).
291. K. A. Johnson, *Annu. Rev. Biochem.*, **62**, 685 (1993).
292. I. Wong, S. S. Patel and K. A. Johnson, *Biochemistry*, **30**, 526 (1991).
293. S. Lone and L. J. Romano, *Biochemistry*, **46**, 2599 (2007).
294. J. Wang, A. K. M. A. Satar, C. C. Wang, J. D. Karam, W. H. Konigsberg and T. J. Steitz, *Cell*, **89**, 1087 (1997).
295. C. A. Brautigam and T. J. Steitz, *Cur. Opin. Struct. Biol.*, **8**, 54 (1998).
296. X. Zhong, S. S. Patel and M. D. Tsai, *J. Am. Chem. Soc.*, **120**, 235 (1998).
297. C. M. Joyce and T. A. Steitz, *Annu. Rev. Biochem.*, **63**, 777 (1994).
298. S. Doublié, S. Tabor, A. M. Long, C. C. Richardson and T. Ellenberger, *Nature*, **391**, 251 (1998).
299. P. Lin, L. C. Pedersen, V. K. Batra, W. A. Beard, S. H. Wilson and L. G. Pedersen, *Proc. Natl. Acad. Sci. U.S.A.*, **103**, 13294 (2006).
300. J. Florián, M. F. Goodman and A. Warshel, *J. Am. Chem. Soc.*, **125**, 8163 (2003).
301. C. Castro, E. Smidansky, K. R. Maksimchuk, J. J. Arnold, V. S. Korneeva, M. Götte, W. Konigsberg and C. E. Cameron, *Proc. Natl. Acad. Sci. U.S.A.*, **104**, 4267 (2007).
302. T. Lindahl, *Nature*, **362**, 709 (1993).
303. J. L. Huffman, O. Sundheim and J. A. Tainer, *Mutat. Res. Fund. Mol. Mech. Mut.*, **577**, 55 (2005).
304. R. D. Wood, *Annu. Rev. Biochem.*, **65**, 135 (1996).

305. D. M. Wilson III and V. A. Bohr, *DNA Repair*, **6**, 544 (2007).
306. K. Hitomi, S. Iwai and J. A. Tainer, *DNA Repair*, **6**, 410 (2007).
307. T. Izumi, L. R. Wiederhold, G. Roy, R. Roy, A. Jaiswal, K. K. Bhakat, S. Mitra and T. K. Hazra, *Toxicology*, **193**, 43 (2003).
308. J. T. Stivers and Y. L. Yang, *Chem. Rev.*, **103**, 2729 (2003).
309. E. E. Kim and H. W. Wyckoff, *J. Mol. Biol.*, **218**, 449 (1991).
310. L. S. Beese and T. A. Steitz, *EMBO J.*, **10**, 25 (1991).
311. K. Mizuuchi, T. J. Nobbs, S. E. Halford, K. Adzuma and J. Qin, *Biochemistry*, **38**, 4640 (1999).
312. W. Yang, J. Y. Lee and M. Nowotny, *Mol. Cell*, **22**, 5 (2006).
313. K. D. Westover, D. A. Bushnell and R. D. Kornberg, *Cell*, **119**, 481 (2004).
314. Y. W. Yin and T. A. Steitz, *Cell*, **116**, 393 (2004).
315. T. A. Kunkel and K. Bebenek, *Annu. Rev. Biochem.*, **69**, 497 (2000).
316. E. C. Friedberg, G. C. Walker, W. Siede, R. D. Wood, R. A. Schultz and T. Ellenberger, *DNA Repair and Mutagenesis*, 2<sup>nd</sup> edition, ASM Press, Washington DC, 2005.
317. T. M. Marti and O. Fleck, *Cell Mol. Life Sci.*, **61**, 336 (2004).
318. A. Pingoud and A. Jeltsch, *Nucl. Acids Res.*, **29**, 3705 (2001).
319. A. Pingoud, M. Fuxreiter and W. Wende, *Cell. Mol. Life Sci.*, **62**, 685 (2005).
320. A. Jeltsch, J. Alves, H. Wolfes, G. Maass and A. Pingoud, *Proc. Natl. Acad. Sci. U.S.A.*, **90**, 8499 (1993).
321. J. Barber, *Q. Rev. Biophys.*, **36**, 71 (2003).
322. P. Fromme, P. Jordan and N. Krauß, *Biochim. Biophys. Acta*, **1507**, 5 (2001).
323. N. Kamiya and J. R. Shen, *Proc. Natl. Acad. Sci. U.S.A.*, **100**, 98 (2003).
324. A. Zouni, H. T. Witt, J. Kern, P. Fromme, N. Krauß, W. Saenger and P. Orth, *Nature*, **409**, 739 (2001).
325. G. McDermott, S. M. Price, A. A. Freer, A. M. Hawthornthwaite-Lawless, M. Z. Papiz, R. J. Cogdell and N. W. Isaacs, *Nature*, **374**, 517 (1995).
326. Z. Liu, H. Yan, K. Wang, T. Kuang, J. Zhang, L. Gui, X. An and W. Chang, *Nature*, **428**, 287 (2004).
327. G. A. Montaña, B. P. Bowen, J. T. LaBelle, N. W. Woodbury, V. B. Pizziconi and R. E. Blankenship, *Biophys. J.*, **85**, 2560 (2003).
328. W. Kühlbrandt, D. N. Wang and Y. Fujiyoshi, *Nature*, **367**, 614 (1994).
329. S. Santabarbara, P. Heathcote and M. C. W. Evans, *Biochim. Biophys. Acta*, **1708**, 283 (2005).
330. T. S. Balaban, P. Fromme, A. R. Holzwarth, N. Krauß and V. I. Prokhorenko, *Biochim. Biophys. Acta*, **1556**, 197 (2002).
331. S. M. Prince, M. Z. Papiz, A. A. Freer, G. McDermott, A. M. Hawthornthwaite-Lawless, R. J. Cogdell and N. W. Isaacs, *J. Mol. Biol.*, **268**, 412 (1997).
332. A. J. van Gammeren, F. B. Hulsbergen, C. Erkelens and H. J. M. de Groot, *J. Biol. Inorg. Chem.*, **9**, 109 (2004).
333. A. Wong, R. Ida, X. Mo, Z. Gan, J. Poh and G. Wu, *J. Phys. Chem. A*, **110**, 10084 (2006).
334. J. Linnanto and J. Korppi-Tommola, *Phys. Chem. Chem. Phys.*, **8**, 663 (2006).
335. M. Nsango, A. B. Fredj, N. Jaidane, M. G. K. Njock and Z. B. Lakhdar, *J. Mol. Struct. (Theochem.)*, **681**, 213 (2004).
336. I. Barth, J. Manz, Y. Shigeta and K. Yagi, *J. Am. Chem. Soc.*, **128**, 7043 (2006).
337. B. Dietzek, R. Maksimenka, W. Kiefer, G. Hermann, J. Popp and M. Schmidt, *Chem. Phys. Lett.*, **415**, 94 (2005).
338. S. Gutteridge and J. Pierce, *Proc. Natl. Acad. Sci. U.S.A.*, **103**, 7203 (2006).
339. W. W. Cleland, T. J. Andrews, S. Gutteridge, F. C. Hartman and G. H. Lorimer, *Chem. Rev.*, **98**, 549 (1998).
340. F. G. Pearce, *Biochem. J.*, **399**, 525 (2006).
341. R. J. Spreitzer and M. E. Salvucci, *Annu. Rev. Plant Biol.*, **53**, 449 (2002).
342. H. J. Imker, A. A. Fedorov, E. V. Fedorov, S. C. Almo and J. A. Gerlt, *Biochemistry*, **46**, 4077 (2007).
343. I. Andersson and T. C. Taylor, *Arch. Biochem. Biophys.*, **414**, 130 (2003).
344. G. H. Lorimer, *Biochemistry*, **20**, 1236 (1981).
345. J. Pierce, G. H. Lorimer and G. S. Reddy, *Biochemistry*, **25**, 1636 (1986).
346. J. Newman and S. Gutteridge, *J. Biol. Chem.*, **268**, 25876 (1993).
347. O. Tapia, M. Oliva, V. S. Safont and J. Andrés, *Chem. Phys. Lett.*, **323**, 29 (2000).



- 348. D. L. Edmondson, H. J. Kane and T. J. Andrews, *FEBS Lett.*, **260**, 62 (1990).
- 349. F. G. Pearce and T. J. Andrews, *Plant Physiol.*, **117**, 1059 (1998).
- 350. F. G. Pearce and T. J. Andrews, *J. Biol. Chem.*, **278**, 32526 (2003).
- 351. H. Mauser, W. A. King, J. E. Gready and T. J. Andrews, *J. Am. Chem. Soc.*, **123**, 10821 (2001).
- 352. J. V. Schloss and G. H. Lorimer, *J. Biol. Chem.*, **257**, 4691 (1982).
- 353. G. G. B. Tcherkez, G. D. Farquhar and T. J. Andrews, *Proc. Natl. Acad. Sci. U.S.A.*, **103**, 7246 (2006).
- 354. T. C. Taylor and I. Andersson, *J. Mol. Biol.*, **265**, 432 (1997).
- 355. G. Schneider, Y. Lindqvist and C. I. Brändén, *Annu. Rev. Biophys. Biomol. Struct.*, **21**, 119 (1992).
- 356. M. Oliva, V. S. Safont, J. Andrés and O. Tapia, *Chem. Phys. Lett.*, **340**, 391 (2001).
- 357. M. Oliva, V. S. Safont, J. Andrés and O. Tapia, *J. Phys. Chem. A*, **105**, 9243 (2001).

## CHAPTER 9

# Theoretical studies of the addition of RMgX to carbonyl compounds

SHINICHI YAMABE and SHOKO YAMAZAKI

Department of Chemistry, Nara University of Education, Takabatake-cho, Nara  
630-8528, Japan

Fax: +81-742-27-9208; e-mail: yamabes@nara-edu.ac.jp

---

I. INTRODUCTION .....	369
II. EXPERIMENTAL BACKGROUND .....	370
III. CALCULATIONS OF GRIGNARD REAGENTS .....	374
IV. CALCULATIONS OF MODEL GRIGNARD REACTIONS .....	380
V. A COMPREHENSIVE COMPUTATIONAL STUDY OF GRIGNARD REACTIONS .....	384
A. Computational Methods .....	384
B. Structures of Grignard Reagents .....	384
C. Additions of Grignard Reagents to Carbonyl Compounds without Solvent Molecules .....	387
D. Additions with Solvent Molecules .....	389
E. Chelation-controlled Addition Models .....	391
F. A Model for SET .....	396
G. Concluding Remarks .....	399
VI. REFERENCES .....	401

---

### I. INTRODUCTION

In this chapter, theoretical studies of geometries of Grignard reagents and paths of Grignard reactions are presented. Since numerous theoretical studies have been reported, we confine ourselves here to *ab initio* studies which are thought to give reliable results. Molecular orbital calculations began to be practical when examining reactions of small model systems with the software GAUSSIAN of computational organic chemistry. It had the function of geometry optimizations (GAUSSIAN 80<sup>1</sup>). However, around the year 1980, only small model systems were used to simulate reactions. With the version GAUSSIAN 92/DFT<sup>2</sup>, the density functional theory calculations became available. DFT calculations

---

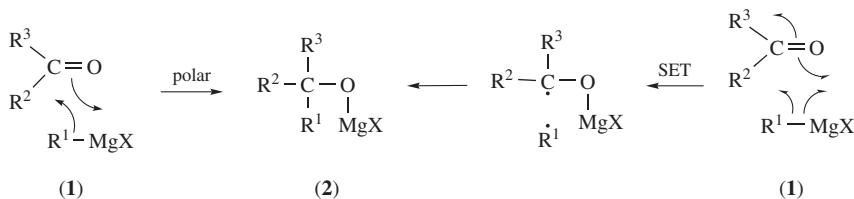
*The chemistry of organomagnesium compounds*

Edited by Z. Rappoport and I. Marek © 2008 John Wiley & Sons, Ltd. ISBN: 978-0-470-05719-3

display a good compromise between the accuracy of calculated results and performance. Then, from 1993, reliable reacting systems began to be studied to trace the paths. At present, the computational study is thought to be an indispensable tool to precisely understand the reaction mechanism. As for the Grignard reactions, however, the mechanism has been veiled for a long time. One difficulty in dealing with the reaction is a well known problem: there are both polar and single-electron-transfer (SET) mechanisms. One question is why the closed-shell system, ketone plus Grignard reagent, is converted to singlet biradical species. In other words, what is the driving force for forming the biradical species? Those questions have been recently solved and will be discussed in Section V of this chapter. However, we will first present the experimental background and earlier theoretical studies.

## II. EXPERIMENTAL BACKGROUND

The Grignard reaction has a 100-year history and is one of the most important organic reactions for C–C bond formation<sup>3</sup>, and is still extensively utilized in organic syntheses nowadays. The structure of Grignard reagents has been gradually revealed by X-ray analyses and other spectroscopic methods<sup>3b,c</sup>. However, the detailed mechanism (in particular, C–C bond formation) of carbonyl addition of Grignard reagents is still unclear. The mechanism is considered to be complex and varies depending on alkyl groups, halogens, solvent, concentration and temperature. The two mechanistic possibilities, polar vs SET (single-electron transfer) shown in the process, **1** → **2**, of Scheme 1 have been discussed for many years<sup>3b,c,f–k</sup>.

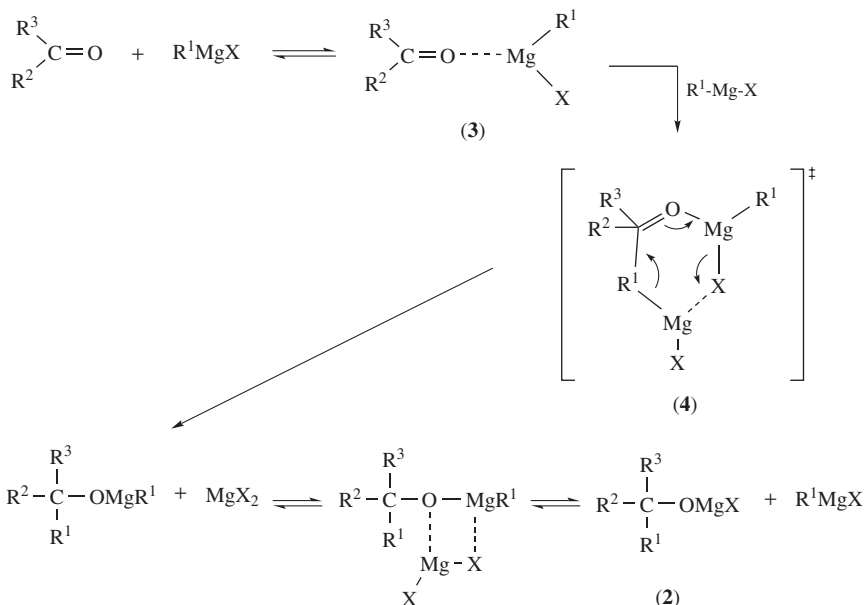


SCHEME 1. Two traditional mechanisms for C–R<sup>1</sup> bond formation

Numerous stereoselective carbonyl additions of Grignard reagents, including enantioselective examples, have been developed recently. Such stereoselective additions have been considered through the polar mechanism, and Cram's selectivity involving chelation control is used in order to explain the high diastereoselectivity<sup>4,5</sup>. Since the detailed C–C bond formation steps including transition states has not been clear, further development of higher efficiency (improving yields), chemoselectivity (minimizing side-reactions) and stereoselectivity in the addition steps is difficult.

The actual composition/structure of Grignard reagents—commonly written as RMgX—has been a matter of some dispute<sup>6</sup>. It appears to depend on the nature of R and also on the solvent. Thus, the <sup>1</sup>H NMR spectrum of MeMgBr in Et<sub>2</sub>O indicates that it is present largely as MgMe<sub>2</sub> + MgBr<sub>2</sub><sup>3k</sup>. On the other hand, X-ray measurements on crystals of PhMgBr, isolated from Et<sub>2</sub>O solution, indicate that it has the composition PhMgBr·2Et<sub>2</sub>O, with the four ligands arranged tetrahedrally around the Mg atom<sup>3b,c</sup>. In any event, Grignard reagents may be regarded as acting as sources of negatively polarized carbon, i.e. as δ<sup>−</sup>-R(MgX)<sup>δ<sup>+</sup></sup>.

There is evidence of complexing the Mg atom of the Grignard reagent with the carbonyl oxygen atom (**3** in Scheme 2), and it is found that two molecules of R<sup>1</sup>MgX are involved

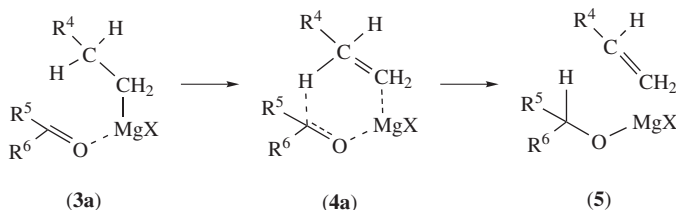


SCHEME 2. A termolecular mechanism for Grignard reagent addition to carbonyl compounds via the cyclic transition state **4**

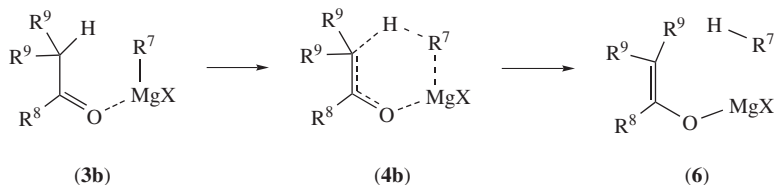
in the termolecular addition reaction, in some cases at least, possibly via a cyclic transition state such as **4** (Scheme 2)<sup>7,8</sup>.

In this termolecular mechanism, the second molecule of R<sup>1</sup>MgX could be regarded as a Lewis acid catalyst, increasing the positive polarization of the carbonyl carbon atom through complexing with oxygen. In practice, it is found that the addition of Lewis acids such as MgBr<sub>2</sub><sup>3f</sup> enhances the rate of Grignard additions. The details of the mechanism of Grignard reagent addition to C=O have been scarcely studied for such a well-known reaction; however, pathways closely analogous to that shown above (i.e. via **4** in Scheme 2) can be invoked to explain the following two further important observations.

The first is that Grignard reagents bearing hydrogen atoms on the β-carbon atom of the alkyl group (R<sup>4</sup>CH<sub>2</sub>CH<sub>2</sub>MgX in **3a**) tend to reduce the extent of the transformation, carbonyl group → an alcohol, while being converted to alkenes (R<sup>4</sup>CH=CH<sub>2</sub> in **5**). In this process, transfer of H rather than R<sup>4</sup>CH<sub>2</sub>CH<sub>2</sub> takes place via **4a** (Scheme 3).



SCHEME 3. A mechanism for alkene formation via a Grignard reaction



SCHEME 4. The mechanism for alkane formation in a Grignard reaction

The second is that sterically hindered ketones bearing hydrogen atoms on their  $\alpha$ -carbons,  $\text{R}_2^9\text{CH}(\text{CO})\text{R}^8$  (cf. **3b**), tend to be converted to their enolates (**6**), where the Grignard reagent,  $\text{R}^7\text{MgX}$ , is lost as  $\text{R}^7\text{---H}$  in the process via **4b** (Scheme 4).

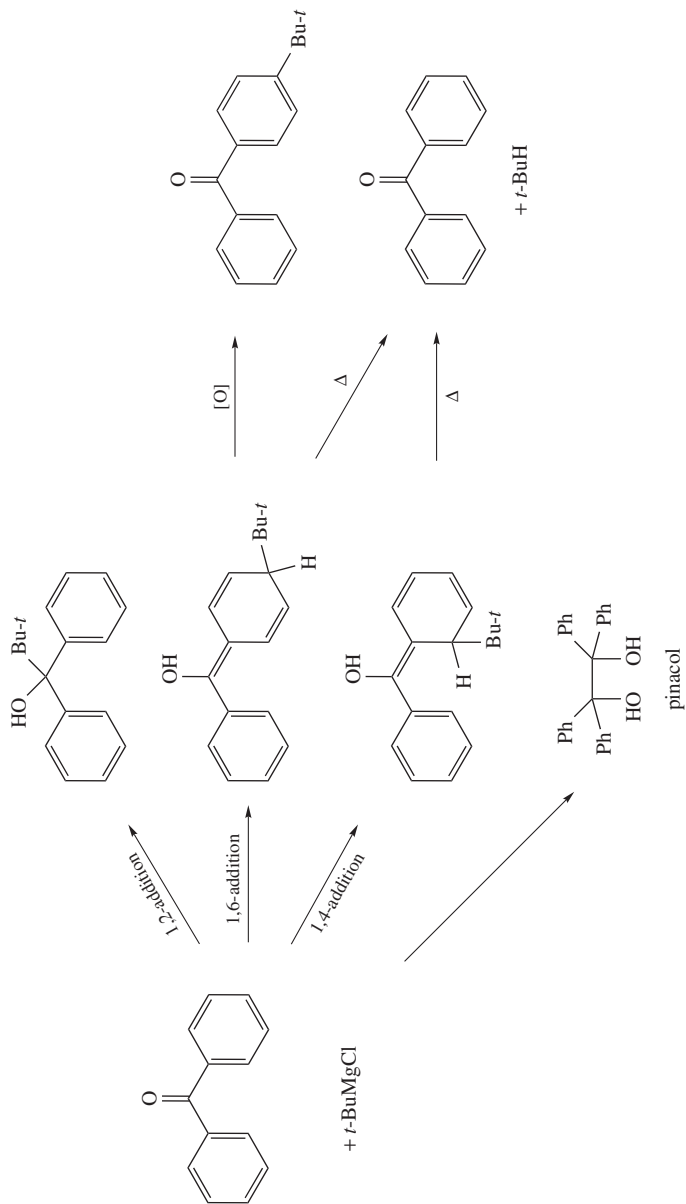
Grignard reagents act as strong nucleophiles and the addition reaction is almost always substantially irreversible (cf. conjugate addition to  $\text{C}=\text{C}=\text{O}$ ). The initial products are alcohols, but it is important to emphasize that the utility of Grignard and similar additions to  $\text{C}=\text{O}$  is a general method of connecting different carbon atoms together, i.e. the original products can then be further modified in a wide variety of reactions. In the past organozinc compounds were used in a similar way, but they are largely displaced by Grignard reagents. In turn, Grignard reagents tend to be displaced gradually by lithium alkyls  $\text{RLi}$  and aryls  $\text{ArLi}$ , respectively. These latter reagents ( $\text{RLi}$  and  $\text{ArLi}$ ) tend to give more of the normal addition product with sterically hindered ketones than Grignard reagents, as well as more of the 1,2-product and less 1,4-additions with  $\text{C}=\text{C}=\text{O}$  than Grignard reagents.

Holm and Crossland reported the product distribution (Scheme 5 and Table 1)<sup>9</sup> in a reaction between *t*-BuMgCl and benzophenone. While the 1,2-addition affords the normal product, 1,6- and 1,4-additions should involve the *tert*-butyl radical for *ortho*- and *para*-additions, and the mechanism involves a single-electron transfer (SET). The product distribution indicates that the more sterically crowded benzophenones give more of the SET products. Ashby and Smith<sup>10a</sup> obtained relative rates for reactions of acetone and benzophenone (Table 2)<sup>10b</sup>. Noteworthy is that those ketones have opposite reactivity orders toward  $\text{R}^1\text{MgCl}$  for the  $\text{R}^1$  variation.

There are now two types of Grignard reagents<sup>11</sup>; one gives a large kinetic isotope effect (KIE), a large Hammett  $\rho$  value for the substituted benzophenones and large steric rate retardation. Examples are  $\text{MeMgX}$ ,  $\text{ArMgBr}$  and  $\text{PhCH}_2\text{MgBr}$ , and  $\text{R}$  transfer is regarded as rate-determining. The other (e.g. allylic  $\text{MgBr}$ ) gives a near-unity KIE, a small  $\rho$  value and negligible steric rate retardation, and SET is regarded as rate-determining. However, as shown in Scheme 6, *t*-BuMgCl shows a different pattern, i.e. a small KIE, a large  $\rho$  value and no steric rate retardation. The two last reactivity features reported by Holm were interpreted in terms of the rate-determining SET mechanism<sup>9</sup>. Yamataka and coworkers

TABLE 1. Product distributions in the reaction of substituted benzophenones and *t*-BuMgCl

Benzophenone	Pinacol (%)	1,2-Adduct (%)	1,4-Adduct (%)	1,6-Adduct (%)
Parent	6	44	0	50
4,4'-Dimethyl	12	55	0	33
4,4'-Di- <i>t</i> -butyl	21	40	39	0
4,4'-Dichloro	0	50	21	29
2,4,6-Trimethyl	0	0	0	100
2,4,6,4'-Tetramethyl	0	0	0	100
2,3,5,6-Tetramethyl	0	0	0	100

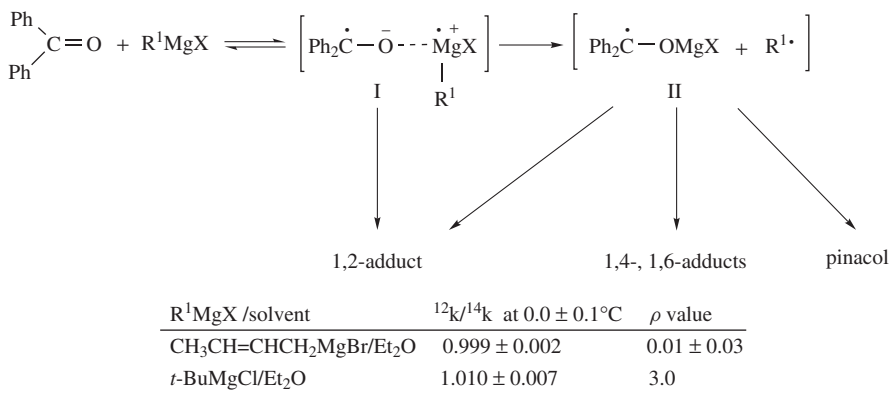


SCHEME 5. The product distribution in the 1,2-, 1,4- and 1,6-additions of *t*-BuMgCl to benzophenone

TABLE 2. Relative reaction rates of typical ketones and Grignard reagents  $R^1MgCl$ 

$R^1$	Acetone	Benzophenone
$CH_3$	1114	30
$CH_3CH_2$	2324	408
$(CH_3)_2CH$	272	4027
$(CH_3)_3C$	9	5363

suggested<sup>11</sup>, however, that the Hammett  $\rho$  value for the SET step is small as observed in the reactions of allylic Grignard reagents. The large  $\rho$  value of 3.0 reported for the reaction of *t*-BuMgCl with benzophenones is rather indicative of the presence of electron-transfer equilibrium prior to the rate-determining step. It is assumed that in the *t*-BuMgCl reaction the product formation from the first intermediate, I, is retarded compared to the rate with MeMgCl due to the steric bulk of *t*-Bu, and another route via the second intermediate, II, becomes important. The rate-determining step of the reaction is then the isomerization of I to II. This interpretation is consistent with the large  $\rho$  value as well as a small KIE observed for this reaction.

SCHEME 6. Kinetic isotope effect (KIE) and Hammett  $\rho$  value in the SET mechanism

### III. CALCULATIONS OF GRIGNARD REAGENTS

First, the geometry, stability and harmonic frequency of the  $CH_3MgCl$  monomer are reported. The calculations confirm the  $C_{3v}$ -symmetric,  $CH_3MgCl$  structure for the Grignard reagent and indicate that the  $Mg + CH_3Cl \rightarrow CH_3MgCl$  reaction is quite exothermic, with the heat of reaction being 58.8 and 47.5 kcal mol<sup>-1</sup> in the 3-21G and 6-31G\* basis sets, respectively<sup>12</sup>. The calculated energies, dipole moments, and geometrical parameters for  $CH_3Cl$ , and  $CH_3MgCl$  are listed in Table 3, together with the experimental values<sup>13</sup> of  $CH_3Cl$ . For  $CH_3Cl$ , the geometry calculated from the 6-31G\* basis set is found to be in good agreement with the experimental data. The 3-21G geometry is similar except that, due to the neglect of d functions on the heavy atoms, the C—Cl bond turns out to be much too long. It is of interest to note that the 6-31G\* C—Mg bond length (2.09 Å) is in fair agreement with the value of 2.16 Å found experimentally for the C—Mg bond of

TABLE 3. Energies, dipole moments and geometries of CH<sub>3</sub>Cl and CH<sub>3</sub>MgCl

Parameter	CH <sub>3</sub> Cl			CH <sub>3</sub> MgCl	
	3-21G	6-31G*	exptl	3-21G	6-31G*
<i>r</i> (C-Cl), Å	1.892	1.785	1.778		
<i>r</i> (C-H), Å	1.074	1.078	1.084	1.088	1.088
<i>r</i> (C-Mg), Å				2.090	2.090
<i>r</i> (Mg-Cl), Å				2.278	2.211
∠(HCCl or HCMg), deg	106.3	108.6	108.4	111.3	111.7
μ, Debye	2.87	2.44	1.94	3.52	2.42

Reprinted with permission from Reference 12. Copyright 1982 American Chemical Society

TABLE 4. Normal-mode vibrational frequencies (cm<sup>-1</sup>) of CH<sub>3</sub>Cl and CH<sub>3</sub>MgCl

		CH <sub>3</sub> Cl		CH <sub>3</sub> MgCl			
		theory		experimental <sup>a</sup>		theory	
	Mode	3-21G	6-31G*	normal modes	measured	3-21G	6-31G* exptl <sup>b</sup>
a <sub>1</sub>	sym C-H st <sup>c</sup>	3282	3280	3074.4	2967.8	3156	3179 2805
	sym C-H d <sup>d</sup>	1501	1538	1382.6	1354.9	1371	1327 1306
	C-Cl st	663	782	740.2	732.8		
	C-Mg st					656	647
	Mg-Cl st					370	376
e	asym C-H st	3401	3376	3165.9	3039.2	3224	3235
	asym C-H d	1639	1641	1481.8	1452.1	1642	1607
	rocking	1096	1138	1038.0	1017.3	703	637 530
	Me-Mg-Cl					119	123
	bend						

<sup>a</sup> From Reference 16. For CH<sub>3</sub>Cl 'normal modes' are frequencies corrected by the anharmonicity effects for measured frequencies.<sup>b</sup> From Reference 17.<sup>c</sup> Stretch.<sup>d</sup> Deformation.

Reprinted with permission from Reference 12. Copyright 1982 American Chemical Society.

MgC<sub>2</sub>H<sub>5</sub>BrEt<sub>2</sub>O<sup>14</sup>, and the 6-31G\* Mg-Cl bond length is only 0.04 Å larger than that determined for MgCl<sub>2</sub><sup>15</sup>.

The calculated normal-mode vibrational frequencies are compared with the available experimental values<sup>16</sup> in Table 4. For CH<sub>3</sub>Cl, the 3-21G and 6-31G\* basis sets yield similar results except that the former basis underestimates the C-Cl stretching frequency. With the 6-31G\* basis utilized in assignments of the CH<sub>3</sub>MgCl modes, the harmonic frequencies of CH<sub>3</sub>Cl are overestimated on an average by 7%, and the assignment of the modes of CH<sub>3</sub>Cl is straightforward.

Second, formation of CH<sub>3</sub>MgX is reported. Theoretical calculations using self-consistent field (SCF) and Møller-Plesset perturbation theory, up to the fourth order (MP4), have been carried out on the gas-phase Mg + CH<sub>3</sub>X → CH<sub>3</sub>MgX reaction surface for X = F and Cl<sup>18</sup>. The transition-state energies, geometries and vibrational frequencies for both reactions are presented and compared to those of the Mg + HX → HMgX reaction. The transition states for both X = F and X = Cl are found to possess *C<sub>s</sub>* symmetry and to be almost identical in structure. The activation energy for the Mg + fluoromethane reaction is found to be 31.2 kcal mol<sup>-1</sup>, while that for the chloromethane reaction is



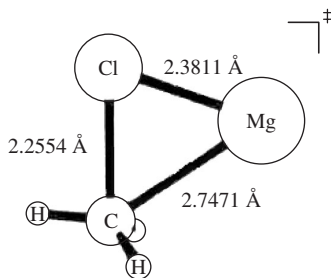


FIGURE 1. Transition-state structure for  $\text{Mg} + \text{CH}_3\text{Cl} \rightarrow \text{CH}_3\text{MgCl}$  optimized at the MP2/6-311G(d,p) level. Reprinted with permission from Reference 18. Copyright 1991 American Chemical Society

substantially higher, at  $39.4 \text{ kcal mol}^{-1}$ , calculated at the MP4SDTQ level by using the 6-311G(d,p) basis set. The intrinsic reaction coordinate has been followed down from the transition state toward both reactants and product for the  $\text{Mg} + \text{CH}_3\text{F} \rightarrow \text{CH}_3\text{MgF}$  reaction, confirming the connection of these points on the potential energy surface. The structure for the transition state of  $\text{Mg} + \text{CH}_3\text{Cl} \rightarrow \text{CH}_3\text{MgCl}$  is shown in Figure 1. The  $\text{H}-\text{C}-\text{Cl}-\text{Mg}$  dihedral angle of  $180.0^\circ$  in the transition state is found to be the same at both the SCF and MP2 levels, in contrast to that found for the  $\text{CH}_3\text{FMg}^\ddagger$ . Therefore, both the  $\text{CH}_3\text{FMg}^\ddagger$  and  $\text{CH}_3\text{ClMg}^\ddagger$  transition states have analogous structures at the MP2 level, belonging to the  $C_s$  point group. The following comparisons between the two TS structures will be for those calculated at the MP2 level. The  $\text{C}-\text{Mg}$  bond length is slightly longer by  $0.11 \text{ \AA}$  in the  $\text{CH}_3\text{ClMg}^\ddagger$  transition state than that for  $\text{CH}_3\text{FMg}^\ddagger$ , while the  $\text{C}-\text{H}$  bond lengths are the same to within a few thousandths of an angstrom. The  $\text{C}-\text{Cl}$  and  $\text{Mg}-\text{Cl}$  bonds are necessarily longer due to the larger size of the Cl atom. The  $\text{H}-\text{C}-\text{Cl}$  angle is within only  $0.4^\circ$  of that in  $\text{CH}_3\text{FMg}^\ddagger$ , and the  $\text{H}'-\text{C}-\text{Cl}$  angles differ by only  $0.56^\circ$ . Here,  $\text{H}'$  refers to the hydrogen atom in the  $C_s$  symmetry plane. The  $\text{H}'-\text{C}-\text{X}-\text{H}$  dihedral angles are also about the same (only a  $1.5^\circ$  difference). The  $\text{Mg}-\text{Cl}$  bond distance in the transition state is fairly close to its value in the  $\text{CH}_3\text{MgCl}$  Grignard structure, indicative of a strong interaction between these two atoms.

Theoretical calculations using self-consistent field and Møller–Plesset perturbation theory through second order (MP2) have been carried out on the gas-phase  $\text{Mg} + \text{C}_2\text{H}_3\text{X} \rightarrow \text{C}_2\text{H}_3\text{MgX}$  reaction for  $\text{X} = \text{F}, \text{Cl}$ <sup>19</sup>. Optimized geometries for the reactants, transition states (TSs) and products have been determined along with relative energies and vibrational frequencies. The intrinsic reaction coordinate has been followed from the TS to reactants and products, confirming that the located structures all lie on the reaction potential energy surface (Figure 2). The transition state is found to possess  $C_1$  symmetry, while the product belongs to point group  $C_s$  (Figure 3). The activation energies are calculated to be  $22.8 \text{ kcal mol}^{-1}$  for the  $\text{Mg} + \text{C}_2\text{H}_3\text{F}$  reaction and  $29.7 \text{ kcal mol}^{-1}$  for the  $\text{Mg} + \text{C}_2\text{H}_3\text{Cl}$  reaction. The overall exothermicity for both reactions is  $54.3 \text{ kcal mol}^{-1}$  at the MP2/6-31G\*\* level. The geometry of  $\text{Cl}-\text{Mg}-\text{C}_2\text{H}_3$  is shown in Figure 4.

The mechanism of the Grignard reagent formation was studied.<sup>20</sup> The results of density functional calculations are reported for  $\text{CH}_3\text{Mg}_2$ ,  $\text{CH}_3\text{Mg}_{4(\text{T})}$  and for  $\text{CH}_3\text{Mg}_{5(\text{TB})}\text{Cl}$  model clusters, with T = tetrahedral and TB = trigonal bipyramid. These calculations aim at a simulation of the migration of a methyl group in the proposed intermediates  $\text{RMg}_n^{(1)}$  ( $n = 2$  and 4) and of the succession of steps from the substrate to  $\text{RMgX}$ . The mono-coordination of the methyl group in the clusters  $\text{CH}_3\text{Mg}_n$  ( $n = 2$  or 4) represents the most stable structure. The  $\text{CH}_3\text{Mg}_5\text{Cl}$  geometries and energies are shown in Figure 5. The energy

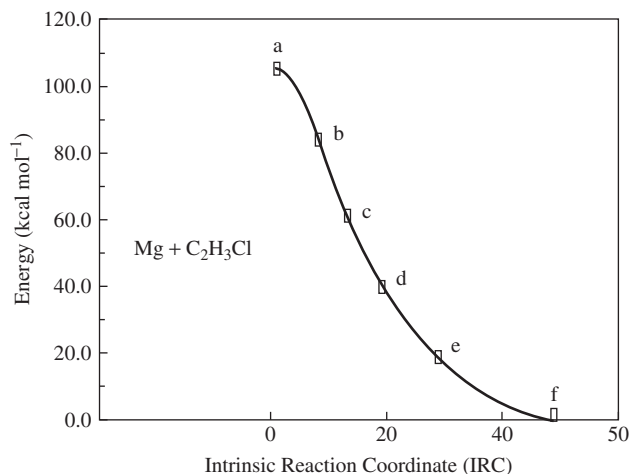


FIGURE 2. Potential energy profile along the reaction surface for  $\text{Mg} + \text{C}_2\text{H}_3\text{Cl} \rightarrow \text{C}_2\text{H}_3\text{MgCl}$  at the RHF/3-21G\* level. The zero point on the abscissa along the IRC is the TS and the product is toward the positive direction. Reprinted with permission from Reference 19. Copyright 1991 American Chemical Society

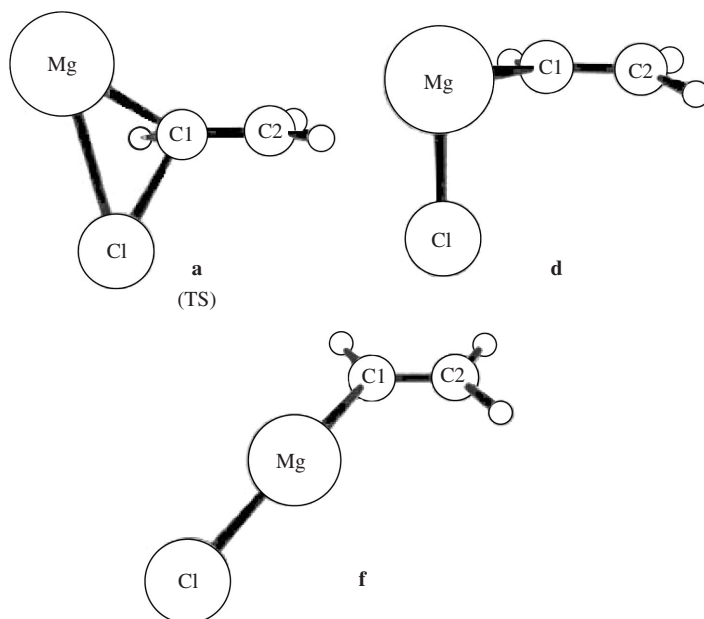


FIGURE 3. Optimized geometries for selected points along the IRC for the  $\text{Mg} + \text{C}_2\text{H}_3\text{Cl} \rightarrow \text{C}_2\text{H}_3\text{MgCl}$  reaction calculated at the RHF/3-21G\* level. See Figure 2 for the points selected. Reprinted with permission from Reference 19. Copyright 1991 American Chemical Society.

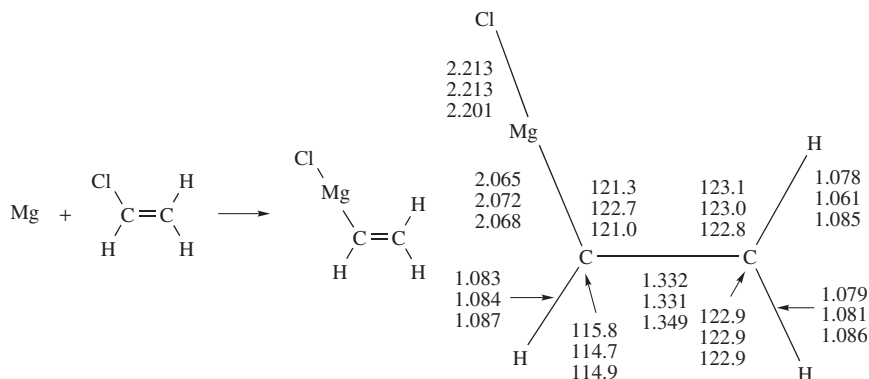


FIGURE 4. Optimized geometries for the  $\text{C}_2\text{H}_3\text{MgCl}$  Grignard molecule. Units are in angstroms and degrees. Values from top to bottom are at the RHF/3-21G\*, RHF/6-31G\*\* and MP2/6-31G\*\* levels, respectively

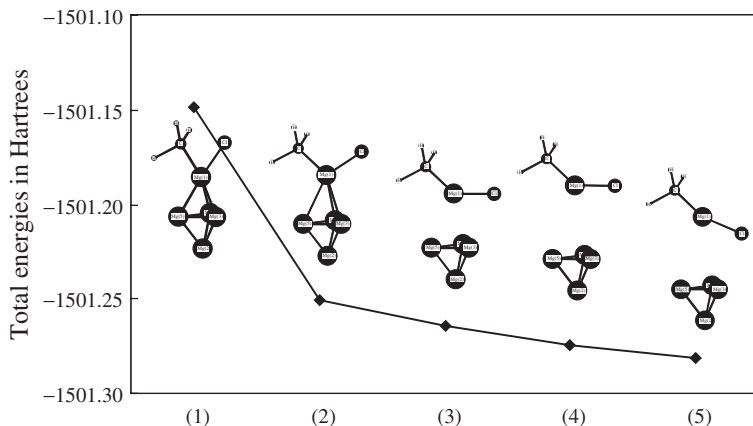
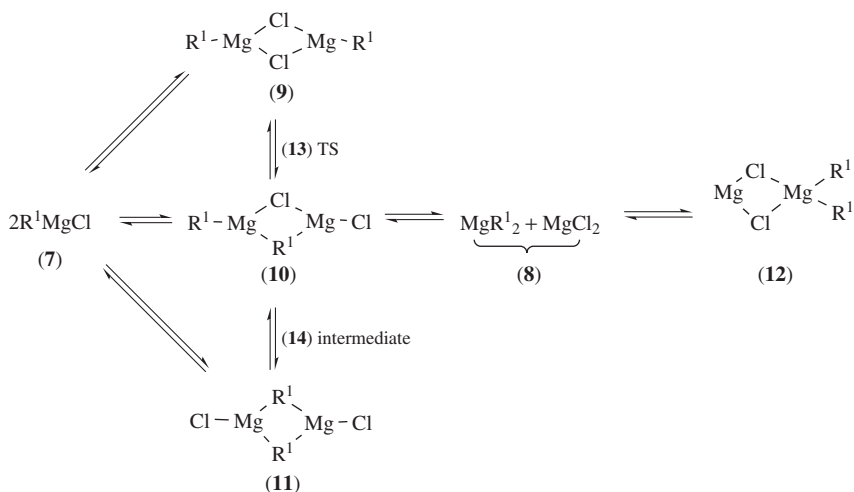


FIGURE 5. Formation of the Grignard reagent  $\text{CH}_3\text{MgCl}$ <sup>20</sup>. 1 Hartree = 627.51 kcal mol<sup>-1</sup>. Along the abscissa, sequential changes of geometries, (1) → (2) → (3) → (4) → (5), are shown

barrier to pass from poly-coordination structure to mono-coordination structure is low (1.213 eV = 27.9 kcal mol<sup>-1</sup>). It is sufficient, however, to prevent the methyl migration from a magnesium atom to another one and the migration motion is probably frozen at lower temperatures. The reaction would evolve then in an irreversible pathway toward the Grignard reagent  $\text{RMgX}$  and a magnesium cluster with  $n - 1$  magnesium atoms.

*Ab initio* molecular orbital calculations were used to study the modified Schlenk equilibrium<sup>21</sup>:  $2\text{R}^1\text{MgCl}$  (**7**)  $\rightleftharpoons (\text{R}^1\text{MgCl})_2 \rightleftharpoons \text{MgR}_2^1 + \text{MgCl}_2 \rightleftharpoons \text{Mg}(\text{Cl}_2)\text{MgR}_2^1$  with  $\text{R}^1 = \text{H}$  and  $\text{CH}_3$  (Scheme 7) by Axten and coworkers.<sup>22</sup> In the absence of a solvent, calculations indicate that the formation of the various possible bridged dimers  $(\text{R}^1\text{MgCl})_2$  (**9**, **10** and **11**) is substantially exothermic (Figure 6). When the dimer **10** is decomposed nonequivalently, **8** is obtained. It is very unstable (Figure 6) and formation of its dimeric form (**12**) is further unlikely. With dimethyl ether as a model solvent, only the formation



SCHEME 7. Schlenk equilibrium which describes the composition of a wide range of Grignard solutions,  $\text{R}^1 = \text{Me}$

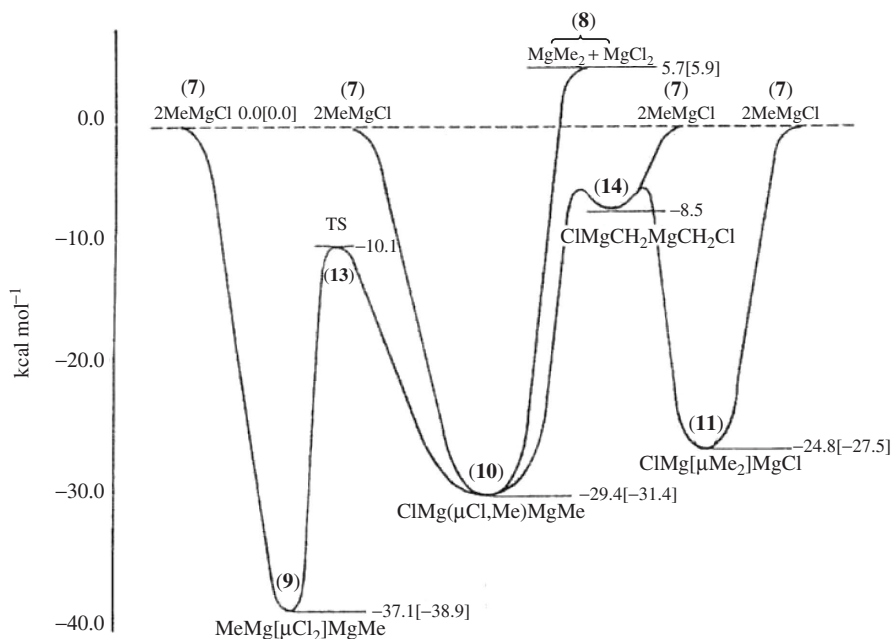


FIGURE 6. Energies (kcal mol<sup>-1</sup>) of the various reaction channels for  $\text{CH}_3\text{MgCl}$ . Unbracketed values are at the MP4SDTQ/6-31G\*//HF/6-31G\* level and bracketed values are at the MP2/6-31G\*//MP2/6-31G\* level. Reproduced by permission of Springer Science + Business Media from Reference 22

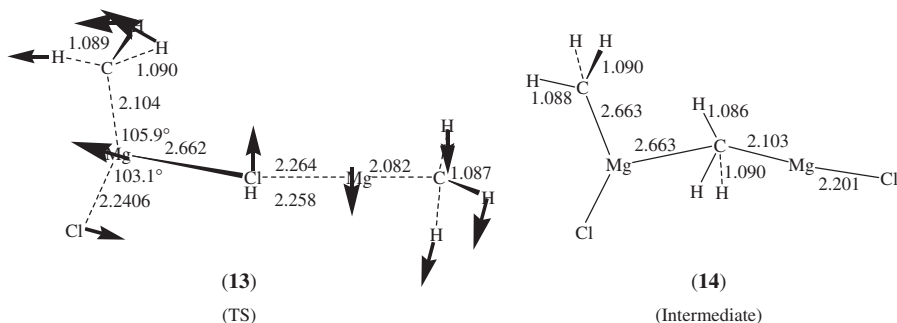


FIGURE 7. Optimized geometries of structures **13** and **14**. Distances are in angstrom. For **13**, reaction-coordinate vectors are also shown. Reproduced by permission of Springer Science + Business Media from Reference 22

of the dimer  $(\text{Me}_2\text{O})(\text{CH}_3)\text{Mg}(\mu\text{Cl}_2)\text{Mg}(\text{CH}_3)(\text{OMe}_2)$  is exothermic when entropic effects are included (i.e. in Gibbs free energies). Geometries of the isomerization TS (**13**) and the transient intermediate (**14**) are shown in Figure 7.

#### IV. CALCULATIONS OF MODEL GRIGNARD REACTIONS

The mechanism of the Grignard reaction was investigated for the first time by *ab initio* SCF MO theory by Nagase and Uchibori<sup>23</sup> for a model reaction composed of formaldehyde and  $\text{MgH}_2$  molecules. A reactant complex **3c** is formed, which is stabilized by  $23.4 \text{ kcal mol}^{-1}$  (Figure 8) relative to the isolated molecules. Complex **3c** is isomerized to a four-centered transition state (TS) with a small activation energy of  $12.7 \text{ kcal mol}^{-1}$ . The product,  $\text{H}_3\text{COMgH}$ , is afforded with a large exothermic energy,  $63.4 \text{ kcal mol}^{-1}$ . The geometries of the complex **3c** and TS are shown in Figure 9. Although the model,  $\text{H}_2\text{C=O} + \text{MgH}_2$ , is far from real reacting systems, this pioneering work prompted further computational studies of reaction paths.

Electronic and conformational effects on  $\pi$ -facial stereoselectivity in nucleophilic additions to carbonyl compounds have been studied by the use of RHF/3-21G and RHF/6-31G\* methods<sup>24</sup>. Figure 10 shows a comparison of predicted and experimental selectivities for methyl Grignard additions. Satisfactory agreement of the ratios of *anti* and equatorial attacks of  $\text{MeMgX}$  on the carbonyl carbon atoms was reported.

A theoretical study on the addition of organomagnesium reagents ( $\text{CH}_3\text{Mg}^+$ ,  $\text{CH}_3\text{MgCl}$ ,  $2\text{CH}_3\text{MgCl}$ ) to the carbonyl group of chiral  $\alpha$ -alkoxy carbonyl compounds (2-hydroxypropanal, 3-hydroxybutanone, and 3,4-di-*O*-methyl-1-*O*-(trimethylsilyl)-*L*-erythrose) was carried out<sup>25,26</sup>. Analytical gradients SCF MO and second derivatives at the *ab initio* method at the HF/3-21G basis set level were applied to identify the stationary points on potential energy surfaces. The geometry, harmonic vibrational frequencies, transition vectors and electronic structures of the transition structures were obtained. The dependence of the results obtained upon the computation method and the model system is analyzed, discussed and compared with available experimental data (Scheme 8). The first step corresponds to the exothermic formation of a chelate complex **17** without energy barrier. This stationary point corresponds to a puckered five-membered ring, determining the stereochemistry of the global process, which is retained throughout the reaction pathway. The second and rate-limiting step is associated with the C–C bond formation via 1,3-migration of the nucleophilic methyl group (R in M–R) from the organomagnesium compound to the carbonyl carbon. For an intramolecular mechanism, the transition

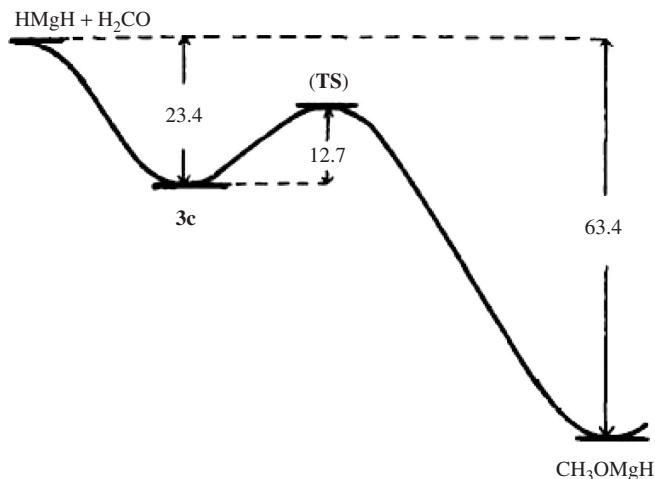


FIGURE 8. The energy profile ( $\text{kcal mol}^{-1}$ ) for the  $\text{HMgH} + \text{H}_2\text{CO}$  reaction along a polar pathway. Reprinted from Reference 23, copyright 1982, with permission from Elsevier

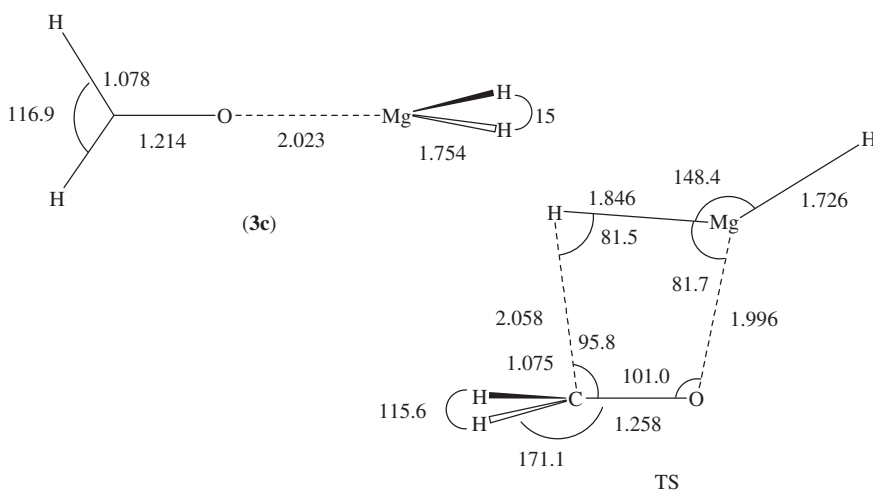
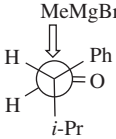


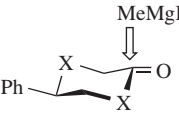
FIGURE 9. Optimized geometries in Å and deg. for an intermediate (**3c**) and a transition state (TS). Reprinted from Reference 23, copyright 1982, with permission from Elsevier

structure can be described as a four-membered ring (TS in Scheme 8). The inclusion of a second equivalent of  $\text{CH}_3\text{MgCl}$ , corresponding to an intermolecular mechanism, decreases the barrier height, and the process can be considered as an assisted intermolecular mechanism: the first equivalent forms the chelate structure and the second  $\text{CH}_3\text{MgCl}$  carries out the nucleophilic addition to the carbonyl group. The most favorable pathway corresponds to an intermolecular mechanism via an *anti* attack. Analysis of the results reveals that

(*anti* attack)

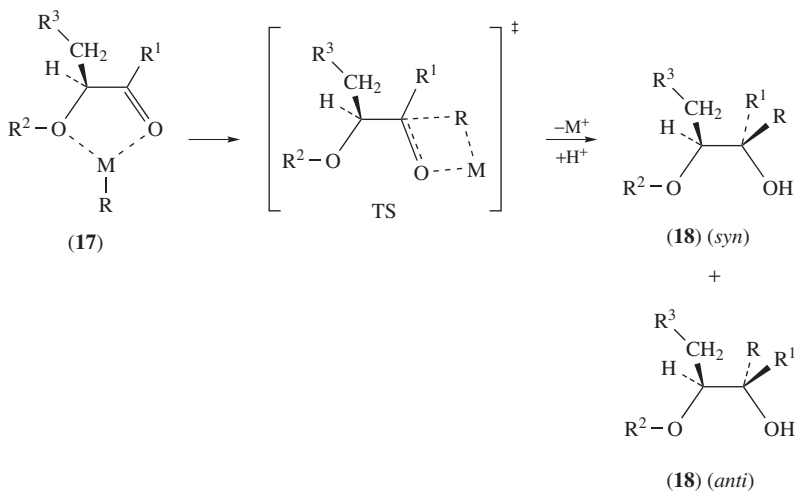


(15)



(16)

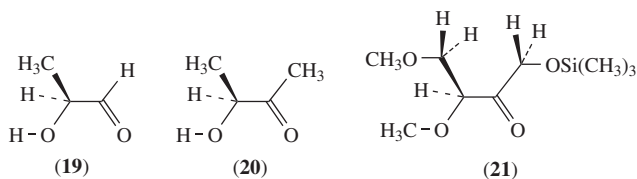
Substrate	Stereochemistry	
	Exptl.	Calc.
<b>15</b>	45:55	36:64
<b>16a</b> X=CH <sub>2</sub>	45:55	68:32
<b>16b</b> X=O	98:2	94:6
<b>16c</b> X=S	7:93	3:97

FIGURE 10. Comparisons of experimental and calculated *anti* to equatorial isomer ratios

SCHEME 8. Schematic representation for the chelate-controlled addition of an organometallic reagent ( $M-R$ ) to the carbonyl group of a chiral  $\alpha$ -alkoxy carbonyl compound (**17**). Two diastereomers **18** with different orientation of  $R$  with respect to  $CH_2R^3$  can be obtained. The *syn* diastereomer is obtained when the nucleophilic attack of  $R$  takes place on the same face of the plane, defined by the carbonyl group and the  $R$ -substituted carbon atom, where  $CH_2R^3$  is located in the chelate complex

the nature of transition structures for the intramolecular and intermolecular mechanisms is a rather robust entity. There is a minimal molecular model with a transition structure which describes the essentials of the chemical addition process, and the corresponding transition vector is an invariant feature.

The following results were derived from those calculations for the paths shown in Figure 11 (see also Scheme 9).



SCHEME 9. 2-Hydroxypropanal (19), 3-hydroxy-2-butanone 20 and 3,4-di-O-methyl-1-O-(tri-methylsilyl)-L-erythrose (21), used as the carbonyl substrate in 17

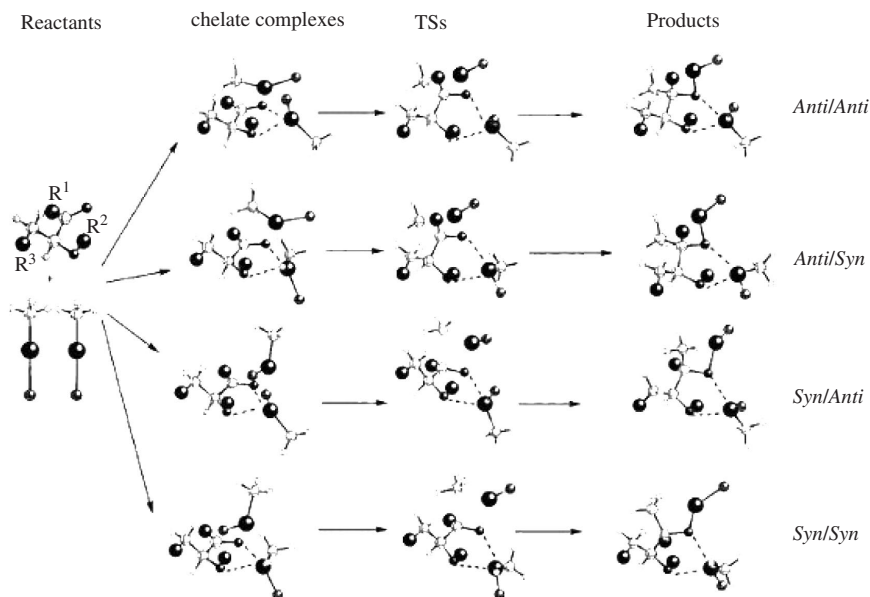


FIGURE 11. Reactants, chelate complexes, TSs and products for the *anti* (two upper paths) and *syn* (two lower paths) addition of  $\text{CH}_3\text{MgCl}$  to 19, 20 and 21 with the participation of 2 equivalents of  $\text{CH}_3\text{MgCl}$ . The relative orientation of the methyl group of the chelating  $\text{CH}_3\text{MgCl}$  can be *anti* (first and third paths) or *syn* (second and fourth paths) with respect to the  $\text{CH}_2\text{R}^3$  group of the model. Reprinted with permission from Reference 25. Copyright 1996 American Chemical Society

(i) The formation of *syn* and *anti* chelate complexes is the first step in the addition process and takes place without an energy barrier.

(ii) The magnesium is coordinated to the lone pair of the carbonyl oxygen and to the methoxy oxygen. The chelate complexes can be described as puckered five-membered rings.

(iii) The chelate conformation is maintained throughout the reaction path, being the thermodynamic controls for the *syn* and *anti* pathways dominated by the relative stability between the corresponding chelate complexes and products. Cram's model based on chelation-controlled carbonyl addition can explain the energetic results.

(iv) The C-C bond-forming stage is the second and rate-limiting step for the addition process. The TSs are four-membered rings, corresponding to the 1,3-intramolecular migration from the chelate complex to products. The calculations<sup>25</sup> adopted models of



$\alpha$ -hydroxy aldehyde **19** and ketones (**20** and **21**) along with the  $\text{CH}_3\text{MgCl}$  dimer. The dimer-participating reactions were computed to be favorable energetically. However, one  $\text{CH}_3\text{MgCl}$  molecule is retained as a chelate complexed catalyst. The dimer formed in the Schlenk equilibrium seems to be more active in general Grignard reactions.

## V. A COMPREHENSIVE COMPUTATIONAL STUDY OF GRIGNARD REACTIONS

In spite of various theoretical studies of Grignard reactions shown in the previous section, their mechanisms seem to be as yet unsettled. In particular, the connection between the  $\text{R}^1\text{MgX}$  dimer in the Schlenk equilibrium and its reactivity toward carbonyl groups is still unclear. In this section, a systematic computational study of several Grignard reactions is presented<sup>27</sup> in order to reveal their unclear points. The polar vs. SET problem will be explained in a forthcoming new mechanism.

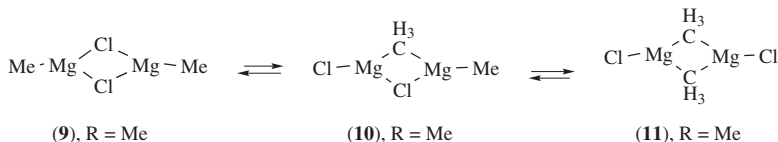
### A. Computational Methods

Geometries were fully optimized by the B3LYP density functional theory (DFT) method<sup>28</sup> together with the SCRF<sup>29</sup> solvent effect (dimethyl ether  $\text{Me}_2\text{O}$ , dielectric constant = 5.02). The basis set used is 6-31G\*. Vibrational frequency calculations gave a sole imaginary frequency for all transition structures, which verifies that the geometries obtained are correctly of the saddle point. From the reactant precursor, partial geometry optimizations were repeatedly carried out with fixed Mg–O and C–C distances. Through the partial optimizations, an approximate transition state (TS) structure could be obtained. Next, by use of the approximate structure and the force constants (second derivatives of total energies), TS geometries were determined. In this case, the negative values (*ca*  $-0.05$  hartree  $\text{au}^{-2}$ ) of the Hessian diagonal force constants of the bond-forming Mg–O and C–C distances should be included in the input line. All calculations were performed using GAUSSIAN 98<sup>30</sup>.

### B. Structures of Grignard Reagents

Grignard reagents ( $\text{R}^1\text{MgX}$ ) in ether solution form aggregates<sup>3b, c, 21</sup>. The degree of aggregation depends on the halogen (X), the concentration, the alkyl group  $\text{R}^1$  and the solvent. For simple alkyl or aryl magnesium chlorides in diethyl ether, the predominant species is considered to be a solvated halogen-bridged dimer<sup>3f, g</sup>. As described in Section III, Axten and coworkers revealed by *ab initio* calculations that the dimer of  $\text{MeMgCl}$  is much more stable than the monomer in calculations which do not take the solvent into account<sup>22</sup>.

The dimers of the Schlenk equilibrium (Scheme 10) have been investigated by B3LYP/6-31G\* calculations. The coordination of the dimethyl ether solvent was included along with the SCRF solvent effect. In Figure 12, three constitutional isomers of  $(\text{Me-Mg-Cl})_2(\text{Me}_2\text{O})_n$  ( $n = 2$  and 4) are compared. For both  $n = 2$  and 4, **9a** and **9b** are most stable and have two bridged Cl atoms. This result is in accord with Axten's results<sup>22</sup>, although our present model with ether molecules is more realistic. The structure shows good resemblance to the crystal structures of halogen-bridged dimers  $(\text{MgX})_2$ <sup>31</sup>.



SCHEME 10. Schlenk equilibrium for methylmagnesium chloride

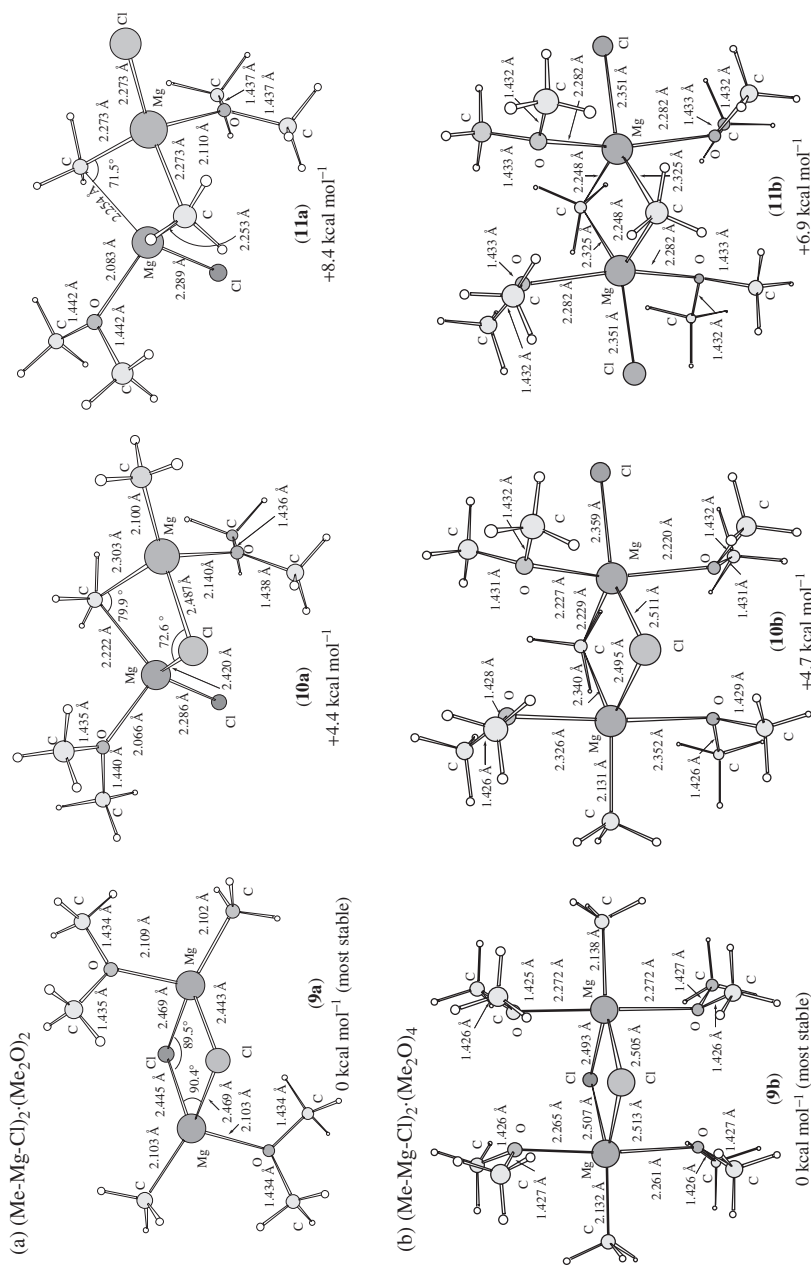


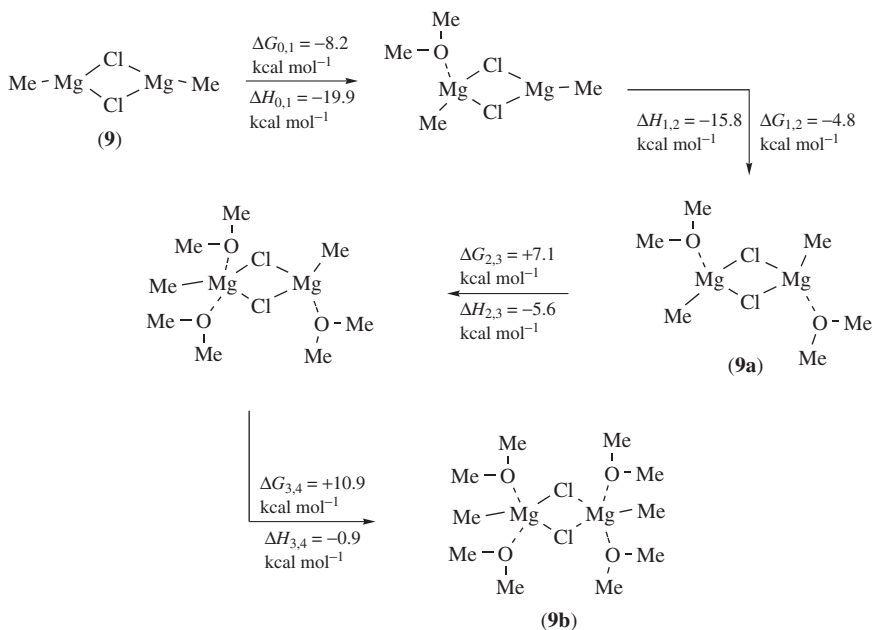
FIGURE 12. Three geometric isomers of Schlenk equilibrium (Grignard reagents) with two solvent molecules (a) are shown in the upper row. Those with four solvent molecules (b) are shown in the lower row. Relative energies to **9a** and **9b** are also shown, where the positive values correspond to less stable systems. The stability of the dimer **9a** relative to that of two monomers,  $\text{MeMgCl} \cdot \text{Me}_2\text{O} \rightarrow (\text{MeMgCl} \cdot \text{Me}_2\text{O})_2 \cdot (\text{Me}_2\text{O})_2$  (**9a**), is also calculated. The energy change  $\Delta E_{\text{cl}}$  for dimerization is  $-23.1 \text{ kcal mol}^{-1}$ .

In order to determine how many ether molecules are favored by the Schlenk dimer,  $\text{MeMgCl}_2\text{MgMe}$  in Scheme 10, the geometry of **9b** (four ethers) is compared to that of **9a** (two ethers). In **9a**, two  $\text{Mg}-\text{O}$  distances (2.103 Å and 2.109 Å) are close to that (2.104 Å) of the  $\text{MgO}$  ionic crystal. In **9b**, they are 2.265 Å, 2.261 Å, 2.272 Å and 2.272 Å and are larger than those in **9a**. In spite of the large  $\text{Mg}$  to  $\text{O}$  affinity, two  $\text{Mg}$  atoms do not favor the coordination of four ether molecules. Thus, **9a** is a saturated complex, although there seems to be room on the two  $\text{Mg}$  atoms for further nucleophilic coordination.  $\text{Mg}$  atoms seem to persist in tetra-coordination. Ether solvation of the Schlenk equilibrium species does not block reaction channels completely.

In order to confirm the saturation in **9a**, free-energy changes for the following stepwise clustering reactions were calculated:



When the addition of the  $n$ -th ether molecule gives a negative  $\Delta G_{n-1,n}$  value, the addition is favored. In contrast, a positive  $\Delta G_{n-1,n}$  value means that the  $n$ -th molecule is not bound to the  $(n-1)$  cluster. The calculated values are  $\Delta G_{0,1} = -8.2$ ,  $\Delta G_{1,2} = -4.8$ ,  $\Delta G_{2,3} = +7.1$  and  $\Delta G_{3,4} = +10.9$  kcal mol<sup>-1</sup> as shown in Scheme 11;  $\Delta H_{n-1,n}$  values are also given in Scheme 11. The addition of the third and fourth ether molecules are less exothermic ( $\Delta H_{2,3} = -5.6$  and  $\Delta H_{3,4} = -0.9$  kcal mol<sup>-1</sup>), which are overcome by entropy changes leading to the positive  $\Delta G_{2,3}$  and  $\Delta G_{3,4}$  values.



SCHEME 11. Free-energy differences  $\Delta G_{n-1,n}$  and enthalpy differences  $\Delta H_{n-1,n}$  for the successive addition (see above) of  $\text{Me}_2\text{O}$  molecules to  $(\text{Me-Mg-Cl})_2$

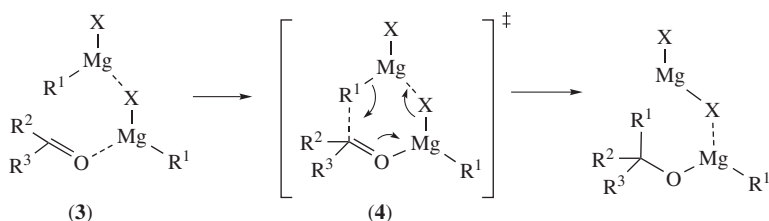
Clearly, the third and fourth molecules cannot be bound to the  $(\text{Me-Mg-Cl})_2(\text{Me}_2\text{O})_2$  cluster, **9a**. Therefore, **9a** is a saturated shell. Since the double trigonal-bipyramidal geometry of **9b** ( $n = 4$ ) in Figure 12 does not involve significant steric congestion, expulsion

of  $n = 3$  and 4 ether molecules arises from the poor ability of Mg atoms for the fifth coordination. Among Schlenk equilibrium dimers in Figure 12, **9a** is a most likely reactant for Grignard reactions.

### C. Additions of Grignard Reagents to Carbonyl Compounds without Solvent Molecules

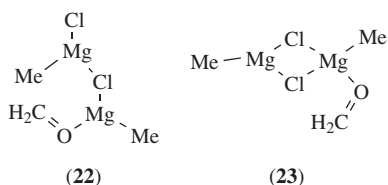
The SET mechanism is known to be operative for reactions of Grignard reagents and aromatic ketones such as benzophenone<sup>3f,h,k,11</sup>. In reactions of Grignard reagents and aliphatic ketones and aldehydes, the polar mechanism seems to be major<sup>3b,c</sup>. The reactions of aliphatic ketones and aldehydes are more widely utilized in organic syntheses. Thus, at first, the polar addition mechanism was examined.

First, a mechanism without solvent molecules was examined for simplification and initial formation of a carbonyl–Mg atom complex was expected. The previously proposed polar addition mechanism is shown in Scheme 12<sup>7,8</sup>, which has been quoted widely<sup>32</sup>.

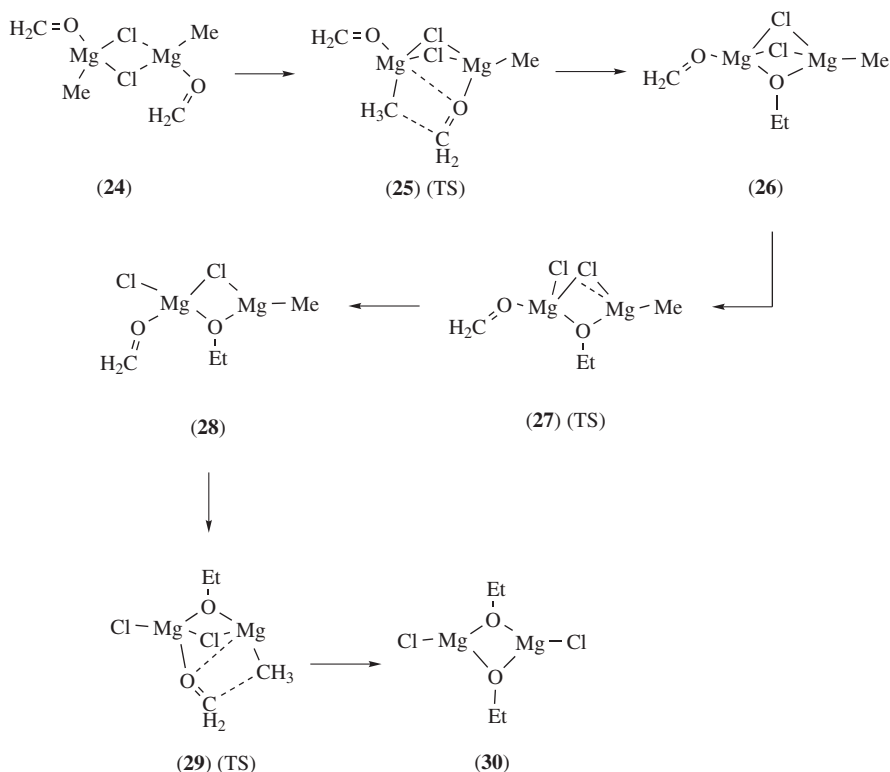


SCHEME 12. Termolecular polar mechanism proposed by Swain and Boyles<sup>7</sup> and Ashby and coworkers<sup>8</sup>. The first reaction in Scheme 2

The potential intermediacy of precursor **22** (a model of **3**) was investigated. However, the initial geometry of the model **22** converged by geometry optimizations to that of  $\text{MeMgCl}_2\text{MgMe}-\text{O}=\text{CH}_2$  (**23**).



The convergence arises from the stability of the two chlorine-bridged structures in the Schlenk equilibrium (i.e. **9** in Scheme 10). Thus, the proposed concerted mechanism containing a cyclic transition state in Scheme 12 is unlikely for Grignard reactions. This result is in contrast to the carbonyl additions with organolithium reagents<sup>33</sup>. The formation of a 1:1 complex was reported for the reactions of Grignard reagents and ketones<sup>3i,j</sup>. Also, stoichiometric amounts of Grignard reagent to carbonyl compounds are generally enough. Therefore, an intermediate model **24** consisting of  $\text{MeMgCl}_2\text{MgMe}$  and two formaldehyde molecules was calculated. Reactions between the Schlenk dimer,  $(\text{MeMgCl})_2$ , and two formaldehyde molecules are shown in Scheme 13. The (**24**  $\rightarrow$  **25**  $\rightarrow$  **26**) process is shown in Figure 13 and the (**26**  $\rightarrow$  **27**  $\rightarrow$  **28**  $\rightarrow$  **29**  $\rightarrow$  **30**) process in Figure 14. Geometries of

SCHEME 13. Reactions between the Schlenk dimer,  $(\text{MeMgCl})_2$ , and two formaldehyde molecules

the bromide analogue of Figure 13 will be shown in Figure 15. Solvent ether molecules will be taken into account in Figure 16.

In the reactant-like complex **24**,  $\text{H}_2\text{C}=\text{O}$  molecules are bound to Mg atoms. One  $\text{H}_2\text{C}=\text{O}$  is shifted leftward to be linked with the left methyl group. At the same time, the carbonyl oxygen of  $\text{H}_2\text{C}=\text{O}$  is directed to the left Mg atom. Thus, a concerted C-C and O-Mg bond formation is shown in TS **25**. Reaction-coordinate vectors in Figure 17 indicate the formation clearly. A C-C covalent bond (1.525 Å in **26**) is established, and the original dichlorine bridge **24** in the square is replaced by the dichlorine and oxygen bridges. The two strong Mg-O bonds (1.943 Å and 2.008 Å) in the bridge of **26** are reflected by a large exothermic energy ( $-49.3 \text{ kcal mol}^{-1}$ ). The triply-bridged structure of **26** is presumably caused by preference of tetra-coordination of magnesium atoms. The reaction pathway **24**  $\rightarrow$  **25**(TS)  $\rightarrow$  **26** would be very important among the polar Grignard reactions; the minimum essential is a four-center reaction (Scheme 14).

For the addition transition state structure **25**, a remarkable feature has been found: the bond-forming carbonyl carbon and the Me group do not reside on the same magnesium atom but on the vicinal magnesium atom of the bridged dimer. The di-Cl- and O-bridged product **26** has newly formed Mg-O and C-C bonds. The energy barrier for this process (**24**  $\rightarrow$  **25**(TS)) is very small ( $+2.4 \text{ kcal mol}^{-1}$ ).

The first addition product **26** can proceed to the second addition stage (Scheme 13 and Figure 14). The intermediate **26** transforms to **28** through bridged-Cl opening TS **27**. **28**

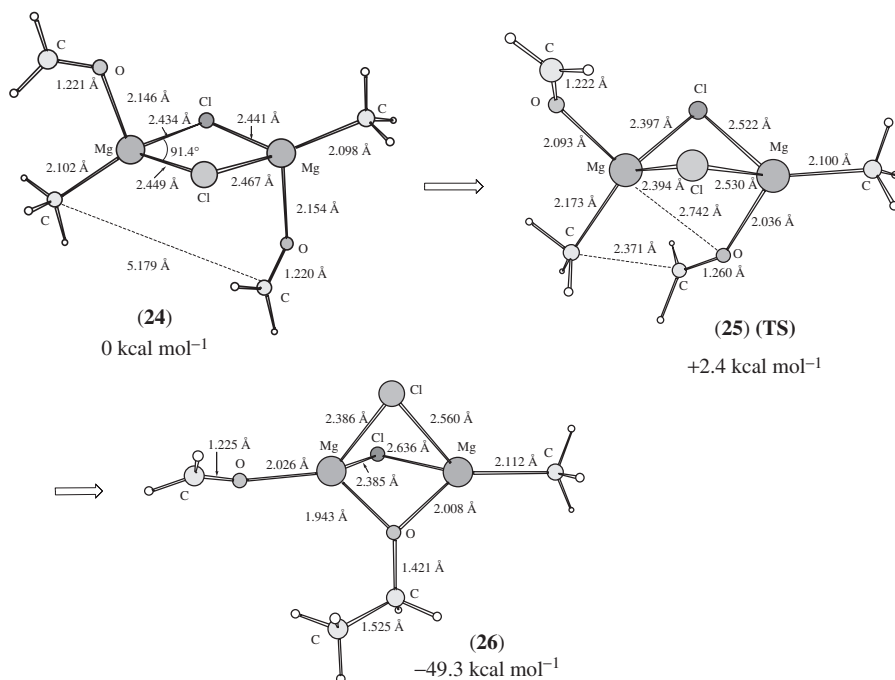


FIGURE 13. Carbonyl addition 1:1 complex (no solvent molecule) (the first stage) corresponding to that of Scheme 13. The geometry of **24** was determined in the intrinsic reaction coordinate to **25** (TS). A symmetric reactant geometry ( $C_{2h}$ ) is 1.8 kcal mol<sup>-1</sup> less stable than **24**

undergoes the second addition step (**28** → **29**(TS) → **30**), similar to the first addition step (**24** → **25**(TS) → **26**). The final product **30** is highly stable due to the four Mg–O bonds. Although the energy barrier for the second addition step (+12.9 kcal mol<sup>-1</sup>) is larger than the first addition step (+2.4 kcal mol<sup>-1</sup>), transformation of **28** to **30** is a highly exothermic process (−97.5 − (−52.6) = −44.9 kcal mol<sup>-1</sup>).

The calculation of the bromide analog for the first critical addition step **24-Br** → **25-Br** (TS) → **26-Br** was also carried out for comparison with that in (Me-Mg-Cl)<sub>2</sub>(H<sub>2</sub>C=O)<sub>2</sub> of Figure 13 (Figure 15). The structure of the intermediates, and transition state and energy barriers, are similar to those of the chloride models. This similarity suggests that the addition of bromo-Grignard reagent requires dimeric species. Although Grignard reagents are known to be in a different aggregate state depending on halogen atoms<sup>3f,g</sup>, this result shows that the reactivity toward carbonyl compounds does not depend on whether the halogen is Br or Cl. The high reactivity of Grignard reagents toward carbonyl compounds can be understood by the model of Scheme 14 starting from the coordination of the magnesium to the carbonyl oxygen and transforming the C–Mg to strong C–C and O–Mg bonds.

#### D. Additions with Solvent Molecules

The polar addition process was investigated also by calculation with dimethyl ether molecules as a more realistic system. Two H<sub>2</sub>C=O molecules were added to the sole

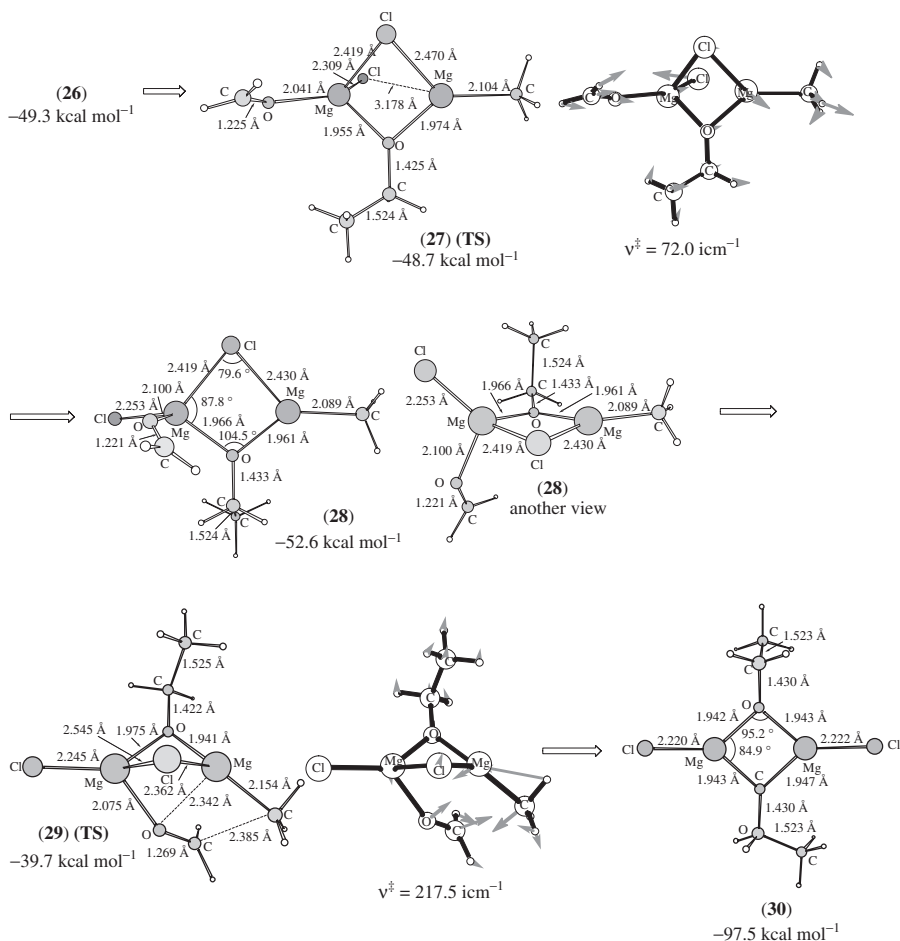
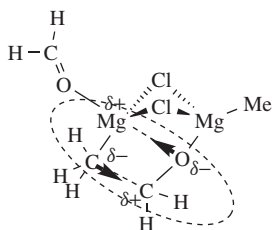


FIGURE 14. Carbonyl addition 1:1 complex (no solvent molecules) (the second stage) corresponding to that of Scheme 13



SCHEME 14. A four-center reaction in 25(TS)

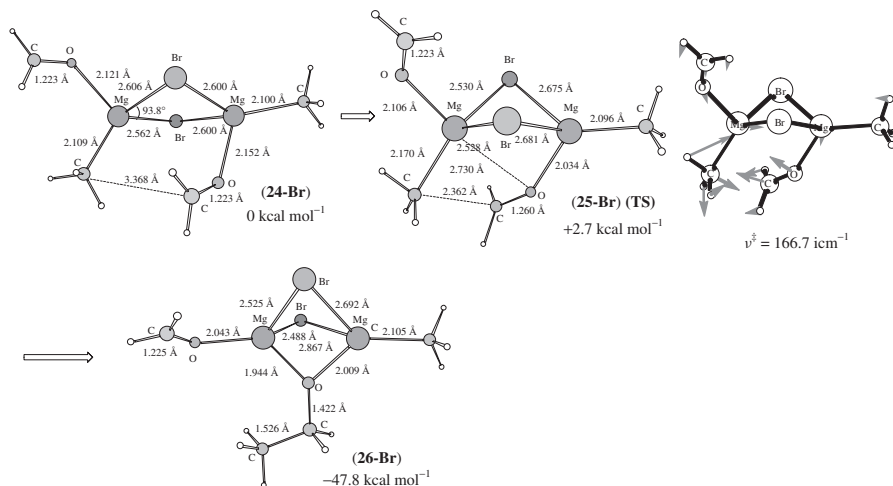


FIGURE 15. The first reaction channel in  $(\text{Me-Mg-Br})_2(\text{H}_2\text{C=O})_2$ , **24-Br**  $\rightarrow$  **25-Br** (TS)  $\rightarrow$  **26-Br**

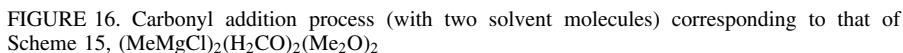
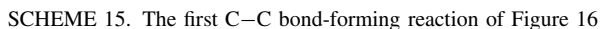
reactant **9a** in Scheme 11 and Figure 12. The dimer **31**, the transition state **32** and a product **33** were calculated (Scheme 15). Their geometries are shown in Figure 16. The structure obtained for the precursor **31** has dimeric five-coordinated magnesiums. The structure is similar to the reported X-ray structure having dimeric five-coordinated magnesium atoms<sup>34</sup>. As in the non-solvated model system (**25**(TS) in Figure 13), the bond-forming carbonyl carbon and Me group reside on vicinal magnesium atoms of the bridged dimer in the addition transition state structure **32**(TS) (see the reaction-coordinate vectors in Figure 17). The energy barrier for this process is very small (+0.3 kcal mol<sup>-1</sup>) and shows that the process is very facile. Conversion from **31** to the product **33** takes place exothermally (-69.3 kcal mol<sup>-1</sup>). Thus, the dichlorine-bridged four-membered structure is retained in the transition state.

In Figure 16, the  $\text{Me}_2\text{O}$  molecules do not affect the polar reaction path significantly in comparison with the path in Figure 13. However, some bond distances are appreciably different between the two precursors **24** (Figure 13) and **31** (Figure 16). A Mg-Cl distance is 2.449 Å in **24**, while it is 2.739 Å in **31**. When the Mg-OMe distances of **9a** (Figure 12) and **31** are compared, the distance of 2.368 Å in **31** is larger than that (2.109 Å) in **9a**. These results indicate that the tetravalent Mg atoms form tight covalent and coordination bonds and the pentavalent Mg atoms form somewhat loose chemical bonds.

## E. Chelation-controlled Addition Models

The high diastereoselectivity for the addition of Grignard reagents to carbonyl compounds is explained by the proposed four-centered process (Scheme 14). Reactions of chiral carbonyl compounds (Scheme 16a) and chiral Grignard reagents (Scheme 16b) are examined. The examples in Scheme 16a are stereoselective addition reactions of Grignard reagents to chiral  $\alpha$ -alkoxy ketones<sup>4a</sup>. Some other examples of stereoselective Grignard reagent addition to various  $\alpha$ -alkoxy carbonyl derivatives<sup>4b-d, 26</sup> and a related chiral sulfinyl imine<sup>35</sup> were reported. The reaction examples of Scheme 16b are additions of chiral  $\gamma$ -alkoxy magnesium halides to ketones<sup>36</sup>. Some other examples of chelated





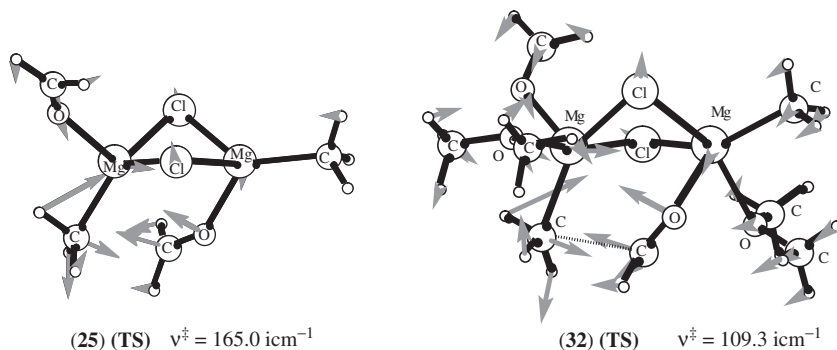
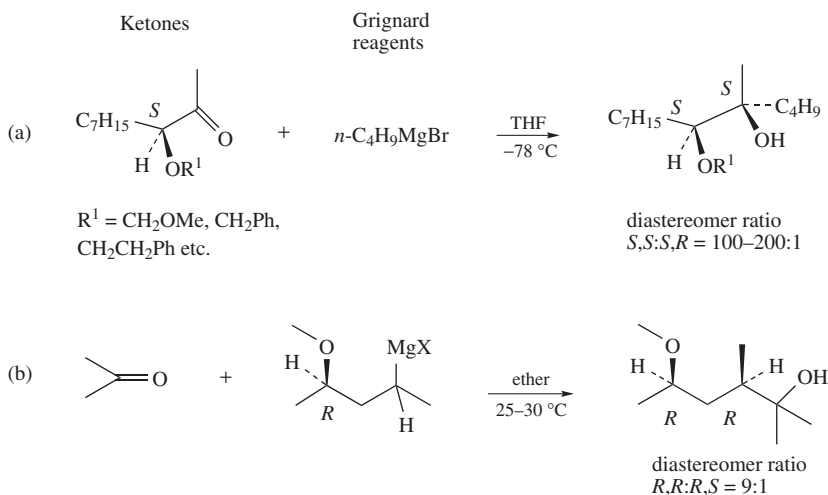


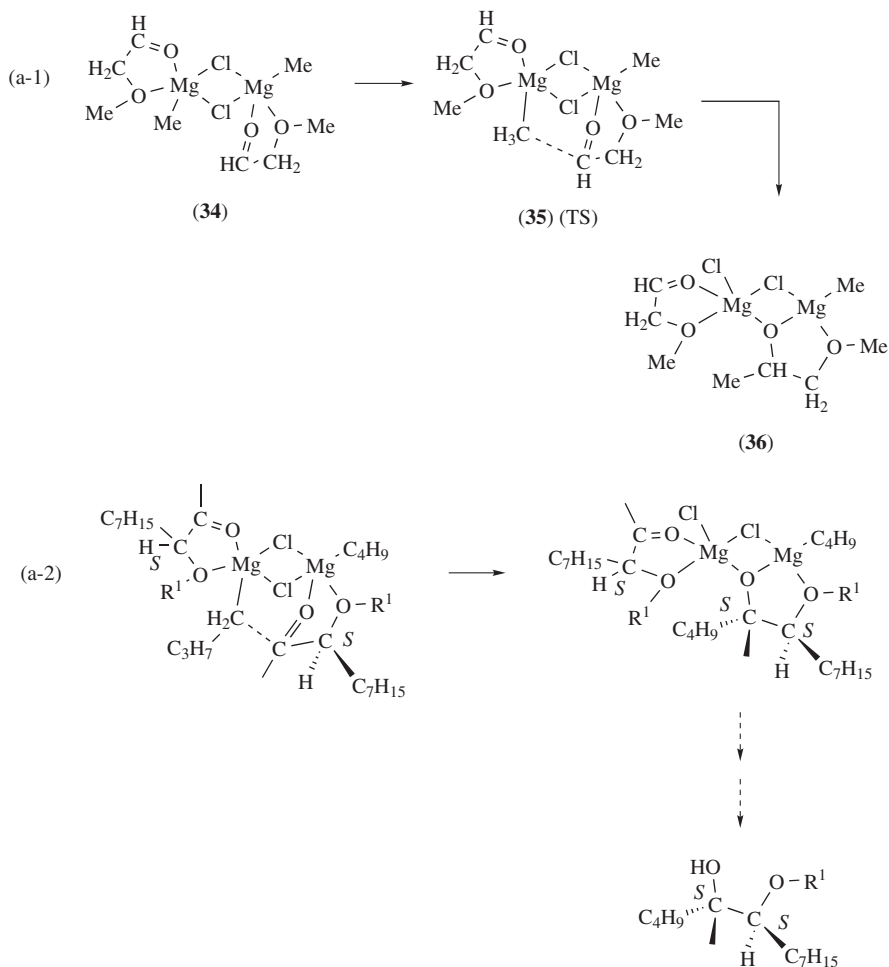
FIGURE 17. Reaction-coordinate vectors corresponding to the sole imaginary frequencies  $\nu^\ddagger$  for **25**(TS) in Figure 13 and **32**(TS) in Figure 16

Grignard reagents, such as tetrahydroisoquinoline Grignard species discovered by Seebach and coworkers<sup>37</sup> and  $\alpha$ -alkoxy Grignard reagents<sup>38</sup>, were also reported. Because a stable coordination of an ether solvent to magnesium is shown in the model system of Figure 16, the coordination of the ether oxygen in substrates to magnesium may work effectively to form chelation. The proposed mechanism of chelation-controlled addition could be determined by a theoretical study.



SCHEME 16. The observed stereochemistry of the reported reactions by the use of (a) chiral ketones<sup>4a</sup> and (b) Grignard reagents<sup>36</sup> in Grignard reactions. Asymmetric carbon atoms are denoted by *R* or *S*

The addition paths of two separated  $\text{MeMgCl}$  molecules to the carbonyl group of chiral  $\alpha$ -alkoxy carbonyl compounds<sup>25</sup>, which are shown in Schemes 8 and 9 and in Figure 11 in Section IV, were traced. However, in these models, one  $\text{MeMgCl}$  molecule bridges two oxygen atoms and acts merely as a catalyst. Instead, the Schlenck dimer  $(\text{MeMgCl})_2$  should be considered for the carbonyl reactant coordination.



SCHEME 17a. Reaction of methylmagnesium chloride and 2-methoxyacetaldehyde (a-1) and its extension to the chiral reaction (a-2)

As an example of a reaction in Scheme 16a, the reaction between  $\text{MeMgCl}$  and 2-methoxyacetaldehyde as a model for chelated carbonyl compounds was investigated. By taking the dimeric forms in Scheme 11 and Figure 12, the dimeric addition process of  $(\text{MeMgCl}/\text{OHCCCH}_2\text{OMe})$  was examined. In Scheme 17a-1 and Figure 18a, a reaction pathway with effective chelation at Mg was obtained. Geometries of **34**, **35** and **36** are shown in Figure 18a. The polar addition precursor as a dimer **34**, transition state **35** and product **36** have features similar to that of the solvent-attached  $\text{MeMgCl}/\text{O}=\text{CH}_2$  system in Figure 16. In the first addition transition-state structure **35**, the bond-forming carbonyl carbon and Me group reside on vicinal magnesium atoms of the bridged dimer. The dichlorine-bridged four-membered structure is retained in the transition state as well.

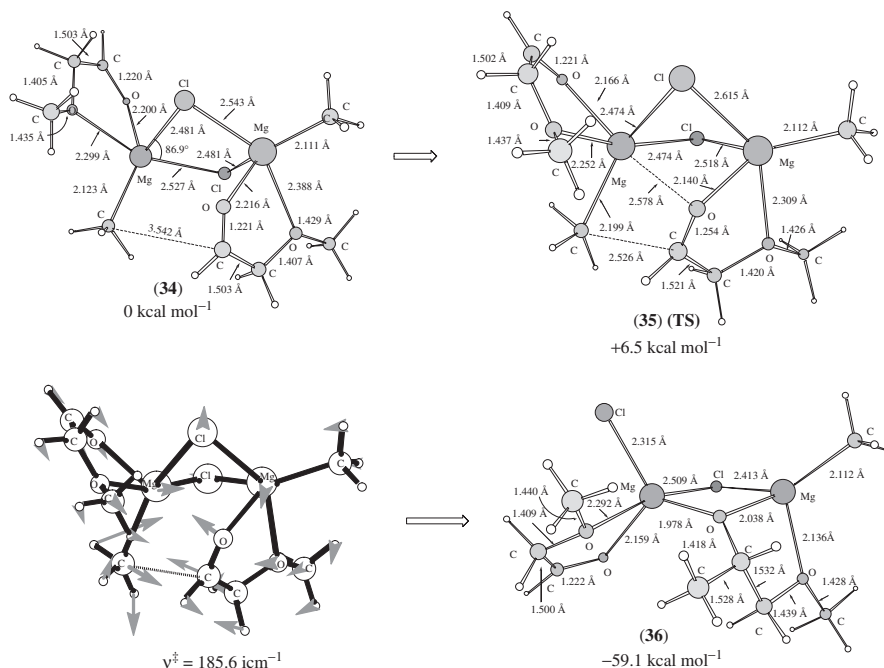
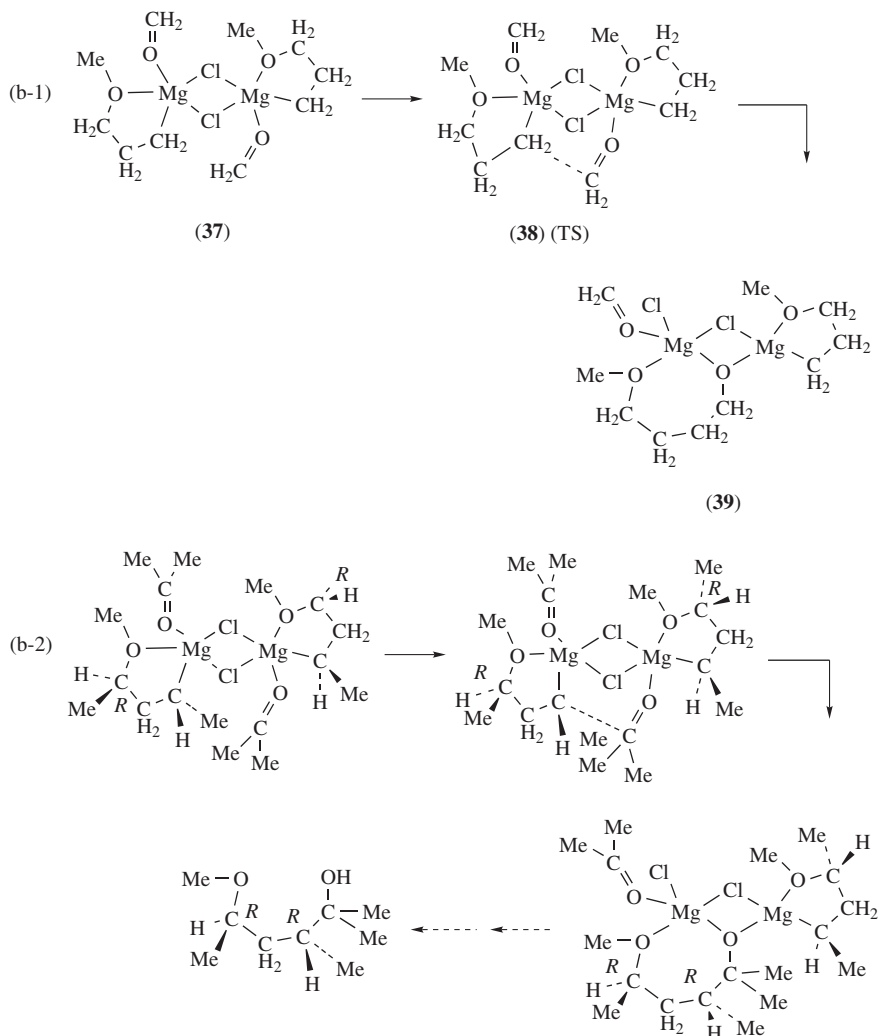


FIGURE 18a. Carbonyl addition process for the alkoxy carbonyl compound model corresponding to that of Scheme 17a-1

Owing to chelation of the OMe group, the aldehyde was fixed configurationally. Thus, the present model calculation has revealed that the chelation control results in the highly stereoselective addition processes observed. The reaction occurs via a dimeric form which has not been considered so far. This model uses achiral substrates and does not create asymmetric carbons. However, through replacement of the  $\alpha$ -H of an aldehyde by a heptyl group, in addition to some other substitutions (Scheme 17a-2), the stereoselective pathway can be explained as follows. The  $\text{C}_7\text{H}_{15}$  group would be located on the outside of the dimer. The configuration is fixed by chelation. The nucleophile ( $n\text{-C}_4\text{H}_9$  group) would attack from the less hindered H side. The stereochemical result is the same as in Cram's original concept<sup>5</sup>. The result from the extension of the model study is in accord with the major product stereochemistry in Scheme 16a.

As an example of Scheme 16b, the reaction between 3-methoxypropylmagnesium chloride which is a model for chelated Grignard reagents and formaldehyde was adopted. The first addition process of  $(\text{MeOCH}_2\text{CH}_2\text{CH}_2\text{MgCl/O}=\text{CH}_2)_2$  was examined (Scheme 17b-1). A pathway with an effective chelation was also obtained in this model reaction and geometries of **37**, **38** (TS) and **39** are shown in Figure 18b. Thus, the example of Scheme 16b also shows that the effective chelation control works in a dimeric form as well as that of Scheme 16a. When the magnesium-substituted carbon configuration is fixed by chelation, stereoselection by steric effects could occur. In the example of Scheme 17b-2, the stereoselectivity is determined by the step of the formation of the conformationally stable Grignard reagent. Various remote steric effects based on the chelation control to create diastereomeric carbons have been suggested so far<sup>4a,34-38</sup>. The present



SCHEME 17b. An example of Scheme 16b

dimeric intermediate model rather than the monomeric one may reasonably describe the stereochemistry of Grignard reactions in the framework of the polar mechanism.

## F. A Model for SET

In order to facilitate the four-center reaction in Scheme 14, steric congestion between the alkyl group  $R^1$  and the carbonyl carbon needs to be avoided. In Scheme 18, a reaction using the bulky  $(t\text{-BuMgCl})_2(\text{acrolein})_2$  system was examined.

Here a model conjugate ketone, i.e. *cis*-acrolein, was adopted. From the dimeric precursor **40**, the four-center reaction path was traced but could not be accomplished. The

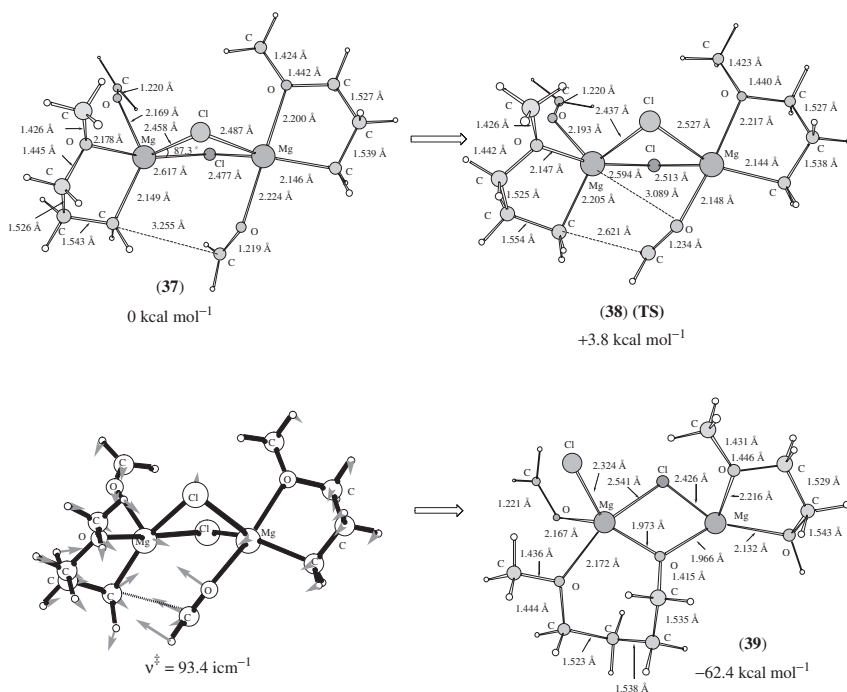
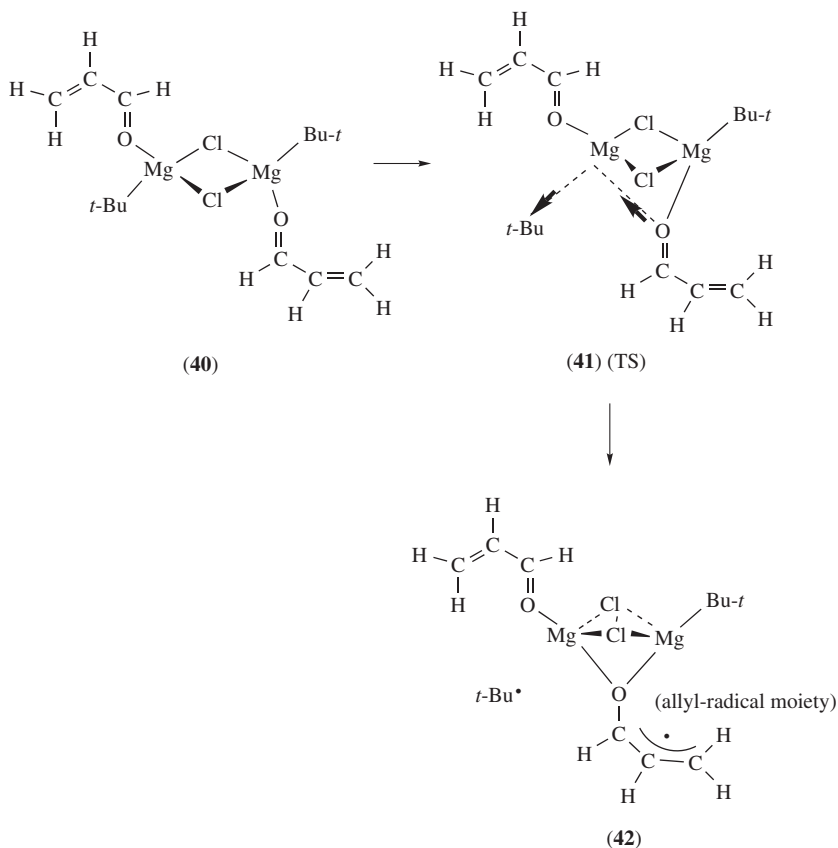


FIGURE 18b. Carbonyl addition process for the alkoxy Grignard model corresponding to that of Scheme 17b-1

nucleophilic center is blocked by the bulky *t*-Bu group. Other paths were sought starting from **40**. As a result, a singlet biradical forming path was found uniquely and is shown in Scheme 18 and Figure 19. The carbonyl oxygen approaches the left-side Mg, in a process similar to the four-center reaction in Scheme 14. However, instead of the simultaneous C–C bond formation, the *t*-Bu group is pushed away from Mg. The motion is described in TS **41** (see the reaction-coordinate vectors in Figure 19). With the decrease in the Mg–O distance, the Mg–C distance is gradually enlarged. Partial optimizations with a fixed Mg–O distance were repeated, and a complex potential surface with various extremely shallow energy minima was found. A local minimum with smaller relative energy than that (=8.5 kcal mol<sup>-1</sup>) of TS **41** was sought. However, the attempted geometry converged to that of **42**, probably due to the complex potential curve and spin contamination, and **42** was calculated to be slightly less stable than TS **41**. A singlet biradical **42** is obtained, where the spin densities are localized on the tertiary carbon of *t*-Bu and on three carbon atoms of the reaction-center acrolein. Noteworthy is a very small spin density on the left-side Mg atom despite the Mg–C homolytic dissociated product. The left-side Mg persists in its tetravalency, and the *t*-Bu group has been pushed away. In **42**, two singlet radical centers (*t*-Bu<sup>•</sup> and O–CH=CH–CH<sub>2</sub><sup>•</sup>) are distant; the corresponding triplet state has similar geometry and spin density (except signs) distributions. In **42**, an allyl radical moiety is formed. Radical–radical recombinations leading to the normal Grignard addition and the conjugate addition are possible. In fact, the reactions of  $\alpha,\beta$ -unsaturated carbonyl compounds (e.g. 3-hexen-2-one, 4-methyl-3-penten-2-one, 2-cyclohexenone, *t*-butyl crotonate and crotonaldehyde) give 1,2-adducts and 1,4-adducts<sup>39</sup>. As explained for Scheme 5 and



SCHEME 18. A singlet-biradical forming process. When the Mg–O bond formation proceeds, the left-side *t*-Bu group is pushed away as a *t*-Bu<sup>•</sup> via homolytic C–Mg cleavage

Table 1, a kinetic study suggested both polar and homolytic mechanisms for conjugate addition, depending on the substrate and the substrate conformation<sup>39a</sup>.

The singlet biradical intermediate **42** is less stable ( $\Delta E_{\text{el}} = +8.7 \text{ kcal mol}^{-1}$ , the difference of total electronic energies) than precursor **40**. When the *tert*-butyl group was separated infinitely, the instability,  $\Delta E_{\text{el}} = +13.7 \text{ kcal mol}^{-1}$ , was calculated. However, the instability is cancelled out in Gibbs free energies. This Gibbs free energy ( $T = 300 \text{ K}$ ) of *t*-Bu<sup>•</sup> and the residual radical (= (**42**–*t*-Bu)<sup>•</sup>) is  $1.0 \text{ kcal mol}^{-1}$  smaller (i.e. the species is more stable) than that of **40**. As the temperature is raised to  $> 300 \text{ K}$ , the biradical separated state is even more stable than precursor **40**. This stability ( $\Delta G = -1.0 \text{ kcal mol}^{-1}$ ,  $T = 300 \text{ K}$ ) of the homolytically dissociated products (two doublet radicals, *t*-Bu<sup>•</sup> and (**42**–*t*-Bu)<sup>•</sup>) compared to **40** is in sharp contrast to the significant instability ( $\Delta G = +24.9 \text{ kcal mol}^{-1}$ ) of homolytically dissociated products from **24** (Figure 13), Me<sup>•</sup> and the residual radical, (**24**–Me)<sup>•</sup>. The precursor **24** cannot cause such a reaction as in Figure 19. SET is *entropy-driven* in the reaction between *t*-BuMgCl and acrolein.

In Scheme 5 and Table 1, the product distributions in reactions between the substituted benzophenones and *t*-BuMgCl have been shown. While the parent benzophenone

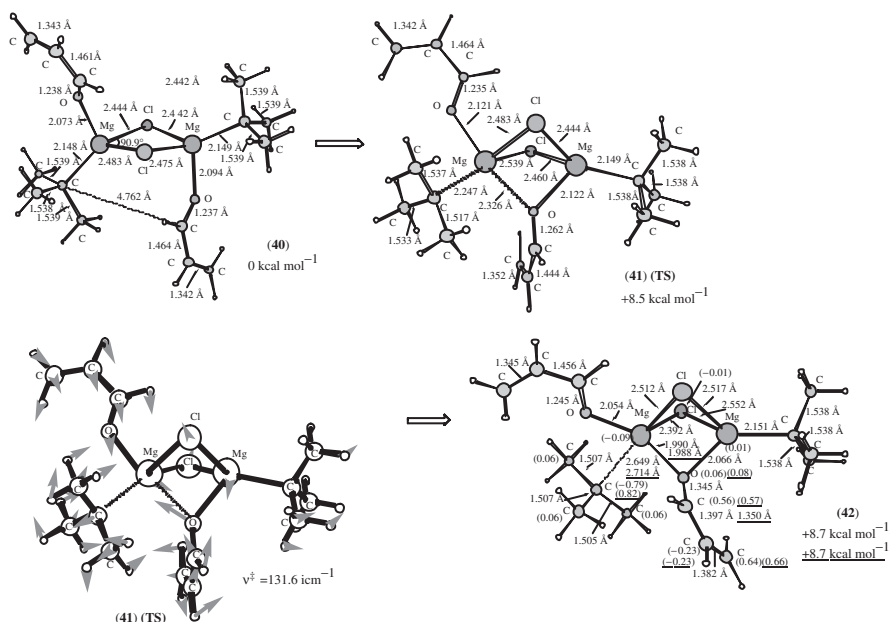


FIGURE 19. Geometries of  $(t\text{-BuMgCl})_2(\text{acrolein})_2$  optimized by (U)B3LYP/6-31G\*SCRF and reaction-coordinate vectors corresponding to the sole imaginary frequencies  $\nu^\ddagger$  for **41**(TS). Those models are explained in Scheme 18. For **41** and **42**, the singlet biradical state was calculated with the symmetry-broken (iop(4/13 = 1)) initial orbitals. In **42**, the triplet-spin geometry optimized data are shown by the underlined numbers. In **42**, spin densities are exhibited in parentheses

affords 1,2-(normal) and 1,6-adducts almost equally, 2,4,6-trimethylbenzophenone form the 1,6-(abnormal) adduct exclusively. The geometries of two singlet biradicals **43** and **44** (Scheme 19) were determined and are shown in Figure 20. In the biradical intermediate **43**, the evolved  $t\text{-Bu}$  radical may recombine with the bridged coordinated benzophenone which lacks steric crowding. That is, the carbonyl carbon C may undergo addition of  $t\text{-Bu}$  leading to the normal 1,2-adduct.

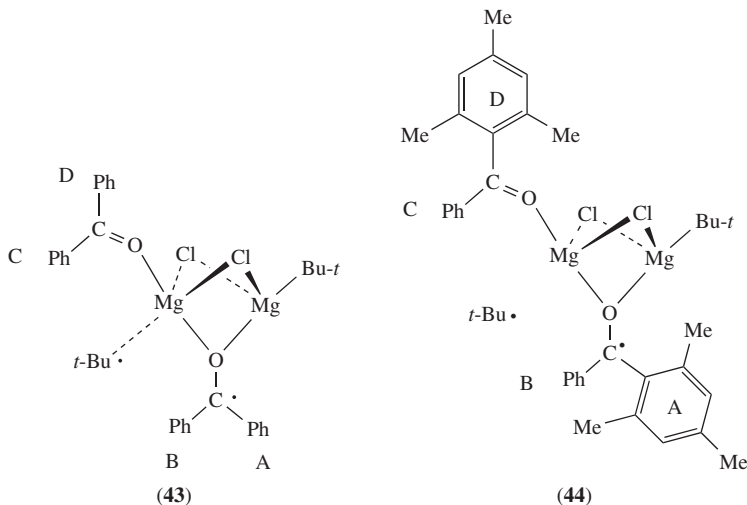
In contrast, in the radical **44** there is steric congestion (particularly by the *ortho* methyl groups) around the carbonyl carbon,  $\text{C}^\bullet$ . The  $t\text{-Bu}$  radical cannot be bound to the carbonyl carbon  $\text{C}^\bullet$  anymore, and normal Grignard adduct formation is prohibited. The steric hindrance in **44** is consistent with the experimental evidence (no normal adduct).

In view of the present calculated results, the SET mechanism would be described as follows. Basically, the polar four-center reaction in Scheme 14 leads to C–C bond formation. However, when the alkyl group is bulky, only the two-center (Mg–O) reaction takes place. The alkyl–Mg bond is cleaved homolytically owing to the persistent Mg tetravalency and the stability of the resultant radical species. Hence, biradical intermediates are formed not by a single electron transfer but by the C–Mg homolytic scission.

## G. Concluding Remarks

Section V has revealed a new mechanism of addition of Grignard reagents to carbonyl compounds. The mechanism was thought to be very complex due to aggregation and a competing SET mechanism. No attempts to elucidate the correlation between the





SCHEME 19. The singlet biradical **43** is formed in the reaction between the two parent benzophenones and  $(t\text{-BuMgCl})_2$ . The radical **44** is formed from the two 2,4,6-trimethylbenzophenones and  $(t\text{-BuMgCl})_2$ . A, B, C and D denote for the respective phenyl and mesityl rings

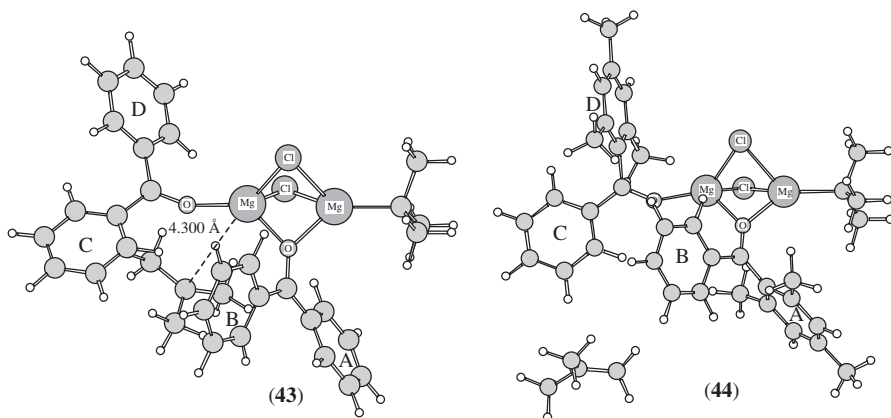
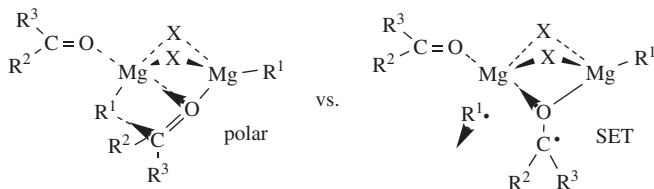


FIGURE 20. Geometries of the two singlet-biradical intermediates, **43** and **44**, corresponding to those in Scheme 19. In **43**, the  $t\text{-Bu}$  group is adjacent to the carbonyl carbon of the bridged benzophenone molecule. In **44**, the group is far away from it and cannot be bound with the carbon atom owing to the steric crowding

Schlenk intermediates and the addition path have been made so far. However, our results seem to provide simple and realistic pathways. The Grignard addition occurs in a dimeric dichlorine-bridged form. A vicinal-magnesium bonding alkyl and  $\text{C}=\text{O}$  interaction causes  $\text{C}-\text{C}$  bond formation via a four-center interaction as shown in Scheme 20 (polar mechanism). When the interaction is improbable owing to the steric effect, the  $\text{Mg}-\text{O}=\text{C}$  bond formation precedes the  $\text{C}-\text{C}$  bond formation and the  $\text{Mg}-\text{C}$  bond is ruptured (SET).



SCHEME 20. Slightly different geometric changes lead to two mechanisms

The rupture is caused by the preference of the tetravalency of the Mg atom, whereas the preference is ambiguous (e.g., elongation and weakening of the bridged Mg—Cl bonds) in the polar mechanism.

Solvent ether molecules may be bound effectively and flexibly to Mg atoms in retaining their tetravalency. When only the reactants  $(R^1MgX)_2$  and  $(R^2R^3C=O)_2$  are taken into account (e.g. in Scheme 13), trivalent Mg states such as **28** and **30** are inevitably formed. The solvent molecules compensate for the lack of chemical bonds to the Mg atoms, through formation of appropriate Mg—O coordination bonds. Even in this case they do not interfere with intrinsic reaction channels.

## VI. REFERENCES

1. J. S. Binkley, R. A. Whiteside, R. Krishnan, R. Seeger, D. J. Defrees, H. B. Schlegel, S. Topiol, L. R. Kahn and J. A. Pople, *Gaussian 80*, Carnegie-Mellon Quantum Chemistry Publishing Unit, Pittsburgh, PA, 1980.
2. M. J. Frisch, G. W. Trucks, H. B. Schlegel, P. M. W. Gill, B. G. Johnson, M. W. Wong, J. B. Foresman, M. A. Robb, M. Head-Gordon, E. S. Replogle, R. Gomperts, J. L. Andres, K. Raghavachari, J. S. Binkley, C. Gonzalez, R. L. Martin, D. J. Fox, D. J. Defrees, J. Baker, J. J. P. Stewart and J. A. Pople, *Gaussian 92/DFT*, Gaussian, Inc., Pittsburgh, PA, 1993.
3. (a) V. Grignard, *Compt. Rend.*, **130**, 1322 (1900).  
(b) G. S. Silvermann and P. E. Rakita (Eds.), *Handbook of Grignard Reagents*, Marcel Dekker, New York, 1996.  
(c) H. G. Richey Jr. (Ed.), *Grignard Reagents: New Developments*, Wiley, New York, 2000.  
(d) B. J. Wakefield, *Organomagnesium Methods in Organic Synthesis*, Academic Press, London, 1995.  
(e) M. S. Kharasch and O. Reinmuth, *Grignard Reactions of Nonmetallic Substances*, Prentice-Hall, NJ, 1954.  
(f) E. C. Ashby, *Pure Appl. Chem.*, **52**, 545 (1980).  
(g) E. C. Ashby and W. E. Becker, *J. Am. Chem. Soc.*, **85**, 118 (1963).  
(h) K. Maruyama and T. Katagiri, *J. Am. Chem. Soc.*, **108**, 6263 (1986).  
(i) T. Holm, *Acta Chem. Scand.*, **20**, 2821 (1966).  
(j) S. G. Smith and G. Su, *J. Am. Chem. Soc.*, **86**, 2750 (1964).  
(k) E. C. Ashby, J. Laemmle and H. M. Newmann, *Acc. Chem. Res.*, **7**, 272 (1974).
4. (a) W. C. Still and J. H. McDonald, *Tetrahedron Lett.*, **21**, 1031 (1980).  
(b) K-Y. Ko and E. L. Eliel, *J. Org. Chem.*, **51**, 5353 (1986).  
(c) S. V. Frye and E. L. Eliel, *J. Am. Chem. Soc.*, **110**, 484 (1988).  
(d) W. F. Bailey, D. P. Reed, D. R. Clark and G. N. Kapur, *Org. Lett.*, **3**, 1865 (2001).
5. D. J. Cram and K. R. Kopecky, *J. Am. Chem. Soc.*, **81**, 2748 (1959).
6. P. Sykes, *A Guidebook to Mechanism in Organic Chemistry*, 5th edn., Chap. 8, Longman Group Ltd, London & New York, 1981.
7. C. G. Swain and H. B. Boyles, *J. Am. Chem. Soc.*, **73**, 870 (1951).
8. E. C. Ashby, R. B. Duke and H. M. Neumann, *J. Am. Chem. Soc.*, **89**, 1964 (1967).
9. T. Holm and I. Crossland, *Acta Chem. Scand.*, **25**, 59 (1971).
10. (a) E. C. Ashby and R. S. Smith, unpublished results.  
(b) M. Okubo and K. Maruyama, *Kagaku*, **35**, 338 (1980); *Chem. Abstr.* **94**, 14633 (1981).

11. H. Yamataka, T. Matsuyama and T. Hanafusa, *J. Am. Chem. Soc.*, **111**, 4912 (1989).
12. S. Sakai and K. D. Jordan, *J. Am. Chem. Soc.*, **104**, 4019 (1982).
13. *Tables of Interatomic Distances*; *Chem. Soc. Spec. Publ.*, No. 18, Suppl., 1965.
14. L. J. Guggenberger and R. E. Rundle, *J. Am. Chem. Soc.*, **86**, 5344 (1964).
15. P. A. Akishin and V. P. Spiridonov, *Sov. Phys. Crystallogr. (Engl. Transl.)*, **2**, 472 (1957).
16. J. L. Duncan, A. Allan and D. C. McKean, *Mol. Phys.*, **18**, 289 (1970).
17. B. S. Ault, *J. Am. Chem. Soc.*, **102**, 3480 (1980).
18. S. R. Davis, *J. Am. Chem. Soc.*, **113**, 4145 (1991).
19. L. Liu and S. R. Davis, *J. Phys. Chem.*, **95**, 8619 (1991).
20. E. Pérez, J.-C. Négrel, A. Goursot and M. Chanon, *Main Group Metal Chem.*, **22**, 201 (1999).
21. W. Schlenk and W. Schlenk, Jr. *Ber. Dtsch. Chem. Ges.*, **62**, 920 (1929).
22. J. Axten, J. Troy, P. Jiang, M. Trachtman and C. W. Bock, *Struct. Chem.*, **5**, 99 (1994).
23. S. Nagase and Y. Uchibori, *Tetrahedron Lett.*, **23**, 2585 (1982).
24. Y.-D. Wu and K. N. Houk, *J. Am. Chem. Soc.*, **109**, 908 (1987).
25. V. S. Safont, V. Moliner, M. Oliva, R. Castillo, J. Andrés, F. González and M. Carda, *J. Org. Chem.*, **61**, 3467 (1996).
26. (a) M. Carda, F. González, S. Rodríguez and J. A. Marco, *Tetrahedron: Asymmetry*, **3**, 1511 (1992).  
(b) M. Carda, F. González, S. Rodríguez and J. A. Marco, *Tetrahedron: Asymmetry*, **4**, 1799 (1993).
27. S. Yamazaki and S. Yamabe, *J. Org. Chem.*, **67**, 9346 (2002).
28. (a) A. D. Becke, *J. Chem. Phys.*, **98**, 5648 (1993).  
(b) C. Lee, W. Yang and R. G. Parr, *Phys. Rev. B*, **37**, 785 (1988).
29. L. Onsager, *J. Am. Chem. Soc.*, **58**, 1486 (1936).
30. M. J. Frisch, G. W. Trucks, H. B. Schlegel, G. E. Scuseria, M. A. Robb, J. R. Cheeseman, V. G. Zakrzewski, J. A. Montgomery, R. E. Stratmann, J. C. Burant, S. Dapprich, J. M. Millam, A. D. Daniels, K. N. Kudin, M. C. Strain, O. Farkas, J. Tomasi, V. Barone, M. Cossi, R. Cammi, B. Mennucci, C. Pomelli, C. Adamo, S. Clifford, J. Ochterski, G. A. Petersson, P. Y. Ayala, Q. Cui, K. Morokuma, D. K. Malick, A. D. Rabuck, K. Raghavachari, J. B. Foresman, J. Cioslowski, J. V. Ortiz, B. B. Stefanov, G. Liu, A. Liashenko, P. Piskorz, I. Komaromi, R. Gomperts, R. L. Martin, D. J. Fox, T. Keith, M. A. Al-Laham, C. Y. Peng, A. Nanayakkara, C. Gonzalez, M. Challacombe, P. M. W. Gill, B. G. Johnson, W. Chen, M. W. Wong, J. L. Andres, M. Head-Gordon, E. S. Replogle, and J. A. Pople, *Gaussian 98, Revision A.7*, Gaussian, Inc., Pittsburgh, PA, 1998.
31. (a) A. L. Spek, P. Voorbergen, G. Schat, C. Blomberg and F. Bickelhaupt, *J. Organomet. Chem.*, **77**, 147 (1974).  
(b) J. Toney and G. D. Stucky, *J. Chem. Soc., Chem. Commun.*, 1168 (1967).
32. For example, see: F. A. Carey and R. J. Sundberg, *Advanced Organic Chemistry Part B: Reactions and Synthesis*, Plenum Press, New York, 1990, p. 376.
33. M. Nakamura, E. Nakamura, N. Koga and K. Morokuma, *J. Am. Chem. Soc.*, **115**, 11016 (1993).
34. M. Marsch, K. Harms, W. Massa and G. Boche, *Angew. Chem., Int. Ed. Engl.*, **26**, 696 (1987).
35. B. Z. Lu, C. Senanayake, N. Li, Z. Han, R. P. Bakale and S. A. Wald, *Org. Lett.*, **7**, 2599 (2005).
36. W. H. Miles, S. L. Rivera and J. D. del Rosario, *Tetrahedron Lett.*, **33**, 305 (1992).
37. (a) D. Seebach and M. A. Syfrig, *Angew. Chem., Int. Ed. Engl.*, **23**, 248 (1984).  
(b) D. Seebach, J. Hansen, P. Seiler and J. M. Gromek, *J. Organomet. Chem.*, **285**, 1 (1985).  
(c) P. Zhang and R. E. Gawley, *Tetrahedron Lett.*, **33**, 2945 (1992).
38. G. J. McGarvey and M. Kimura, *J. Org. Chem.*, **47**, 5422 (1982).
39. (a) T. Holm, *Acta Chem. Scand.*, **45**, 925 (1991).  
(b) E. R. Coburn, *Organic Synthesis*, Wiley, New York, 1955; Collect. Vol. No. III, p. 696.  
(c) J. Munch-Petersen, *Organic Synthesis*, Wiley, New York, 1973; Collect. Vol. No. V, p. 762.  
(d) F. S. Prout, R. J. Hartman, P.-Y. Huang, C. J. Korpics and G. R. Tichelaar, *Organic Synthesis*, Wiley, New York, 1963; Collect. Vol. No. IV, p. 93.

## CHAPTER 10

# Organomagnesium-group 15- and Organomagnesium-group 16-bonded complexes

KATHERINE L. HULL and KENNETH W. HENDERSON

*Department of Chemistry and Biochemistry, 251 Nieuwland Science Hall, University of Notre Dame, Notre Dame, IN 46556, USA*

*Fax: +57 46 31 66 52; e-mail: khenders@nd.edu*

---

I. INTRODUCTION .....	403
II. ORGANOMAGNESIUM-GROUP 15-BONDED COMPLEXES .....	404
A. Organomagnesium Amides .....	404
1. Synthesis .....	404
2. Structural characterization .....	412
3. Reactivity studies .....	419
a. Metalation reactions .....	419
b. Disproportionation reactions .....	422
c. Reactions with oxygen .....	422
d. Reactions with aldehydes and ketones .....	423
B. Organomagnesium Heavy Pnictogenides .....	427
III. ORGANOMAGNESIUM-GROUP 16-BONDED COMPLEXES .....	427
A. Organomagnesium Alkoxides and Aryloxides .....	428
1. Synthesis .....	428
2. Structural characterization .....	428
3. Reactivity studies .....	432
B. Organomagnesium Heavy Chalcogenides .....	433
IV. REFERENCES .....	434

---

### I. INTRODUCTION

This chapter is devoted to the chemistry of organomagnesium-group 15- and group 16-bonded complexes, with emphasis on their synthesis, structural characterization and utility. In particular, organomagnesium amides will be the central focus of the first section, as

---

*The chemistry of organomagnesium compounds*

Edited by Z. Rappoport and I. Marek © 2008 John Wiley & Sons, Ltd. ISBN: 978-0-470-05719-3

these complexes have received by far the most attention. For the purposes of this particular review the compounds of discussion are limited to those that contain both magnesium to carbon and magnesium to pnictogen or chalcogen bonds. Metal species containing dative interactions to the group 15 or group 16 elements will not be considered and charge-separated species containing these elements are also excluded. Also, only homometallic complexes will be considered. It should, however, be noted that a set of heterodimetallic reagents containing magnesium has recently received a good deal of interest due to their ability to act as highly selective Brönsted bases. Selections of these reagents contain alkyl units, amide units, an alkali metal and a divalent or a trivalent metal (Mg, Zn, Mn or Al). These are highly interesting compounds from both a structural and a synthetic perspective and have been recently reviewed extensively elsewhere<sup>1,2</sup>. A good deal of work has been carried out on organomagnesium  $\beta$ -diketiminates and tris(pyrazolyl)-hydroborates, and these complexes are included as they illustrate general reactivity patterns for this class of complexes.

## II. ORGANOMAGNESIUM-GROUP 15-BONDED COMPLEXES

### A. Organomagnesium Amides

#### 1. Synthesis

A summary of the general routes for the synthesis of organomagnesium amides is given in Scheme 1. The most commonly used synthesis of organomagnesium amides is by the reaction of a diorganomagnesium,  $R_2Mg$ , with one molar equivalent of a protic amine. This simple procedure is over a century old and is still the most convenient method for preparing a wide variety of compounds within this class<sup>3</sup>. In general, dialkylmagnesium bases have been most commonly employed in these reactions, although a few examples of diaryl or mixed alkyl/aryl magnesium reagents have also been utilized. Also, the commercial availability of the reagent dibutylmagnesium has made this route attractive for many researchers.

Alkane elimination:



Ligand Redistribution:



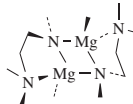
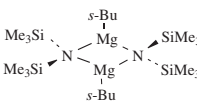
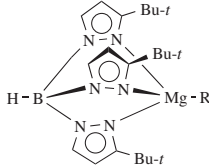
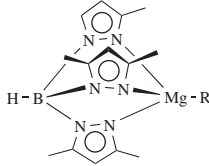
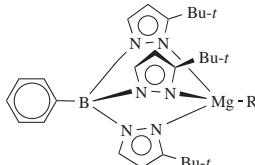
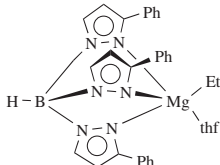
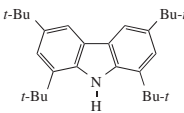
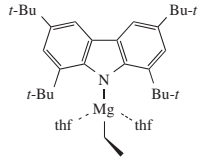
Metathesis:



SCHEME 1

Table 1 gives a complete list of the crystallographically characterized compounds synthesized from the reaction of diorganomagnesium compounds with protic amines or metal amides. A variety of dialkylmagnesium precursors have been used in these reactions. In general, one alkyl group acts as the base and extracts the amine's proton, while the second alkyl group remains attached to the magnesium center. It should be noted that the identity of the alkyl and amide groups present is important for the successful completion

TABLE 1. Structurally characterized organomagnesium amides synthesized from the reaction of amines or metal amides with diorganomagnesium precursors

Amine/Amide	R <sub>2</sub> Mg	Solvent	Product number	Product	Reference
Me <sub>2</sub> NCH <sub>2</sub> CH <sub>2</sub> NHMe	Me <sub>2</sub> Mg	Et <sub>2</sub> O	1		4
(Me <sub>3</sub> Si) <sub>2</sub> NH	<i>n</i> -Bu( <i>s</i> -Bu)Mg	Hexane	2		5
Tl{HB(3-C <sub>3</sub> N <sub>2</sub> - <i>t</i> -BuH <sub>2</sub> ) <sub>3</sub> }	R <sub>2</sub> Mg R=Me, <i>i</i> -Pr	THF	3a,b		6-8
K{HB(3,5-C <sub>3</sub> N <sub>2</sub> (CH <sub>3</sub> ) <sub>2</sub> H) <sub>3</sub> }	R <sub>2</sub> Mg R=CH <sub>2</sub> SiMe <sub>3</sub>	THF	4		8, 9
Tl{PhB(3-C <sub>3</sub> N <sub>2</sub> - <i>t</i> -BuH <sub>2</sub> ) <sub>3</sub> }	R <sub>2</sub> Mg R=Me, Et	Benzene	5a,b		10
Tl{HB(3-C <sub>3</sub> N <sub>2</sub> PhH <sub>2</sub> ) <sub>3</sub> }	Et <sub>2</sub> Mg	THF	6		11
	Et <sub>2</sub> Mg	THF	7		12

(continued overleaf)

TABLE 1. (continued)

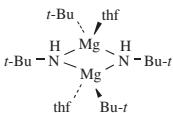
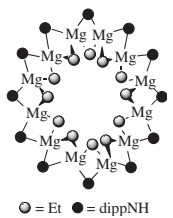
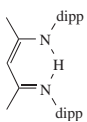
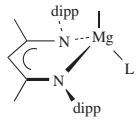
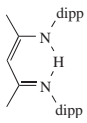
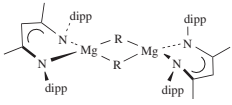
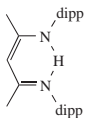
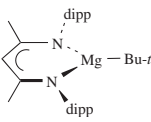
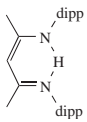
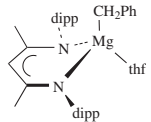
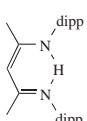
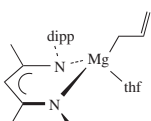
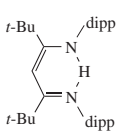
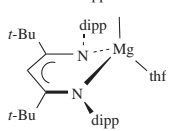
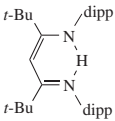
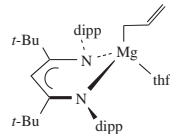
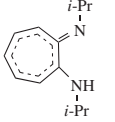
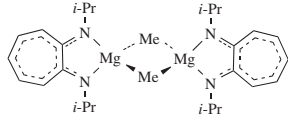
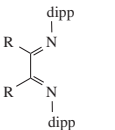
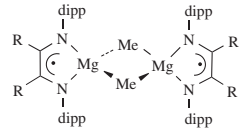
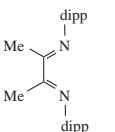
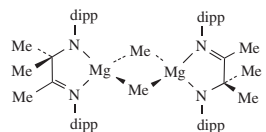
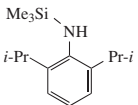
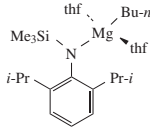
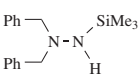
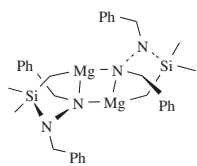
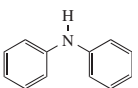
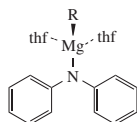
Amine/Amide	R <sub>2</sub> Mg	Solvent	Product number	Product	Reference
<i>t</i> -BuNH <sub>2</sub>	<i>t</i> -Bu <sub>2</sub> Mg	Toluene	<b>8</b>		13
RNH <sub>2</sub> R=dipp dipp = 2,6- <i>i</i> -Pr <sub>2</sub> -C <sub>6</sub> H <sub>3</sub>	Et <sub>2</sub> Mg	Toluene	<b>9</b>	 ○ = Et    ● = dippNH	13
	Me <sub>2</sub> Mg	Et <sub>2</sub> O or THF	<b>10a,b</b>	 L = Et <sub>2</sub> O, THF	14, 15
	R <sub>2</sub> Mg R=Me, <i>n</i> -Bu	Toluene	<b>11a,b</b>		14–16
	<i>t</i> -Bu <sub>2</sub> Mg	Toluene	<b>12</b>		14
	[(PhCH <sub>2</sub> ) <sub>2</sub> Mg(thf) <sub>2</sub> ]	THF	<b>13</b>		17
	[La(η <sup>3</sup> -C <sub>3</sub> H <sub>5</sub> ) <sub>3</sub> (μ-C <sub>4</sub> H <sub>8</sub> O <sub>2</sub> )•Mg(η <sup>1</sup> -C <sub>3</sub> H <sub>5</sub> ) <sub>2</sub> (μ-C <sub>4</sub> H <sub>8</sub> O <sub>2</sub> ) <sub>1.5</sub> ] <sub>n</sub>	THF	<b>14</b>		18
	Me <sub>2</sub> Mg	THF	<b>15</b>		19

TABLE 1. (continued)

Amine/Amide	R <sub>2</sub> Mg	Solvent	Product number	Product	Reference
	[(C <sub>3</sub> H <sub>5</sub> ) <sub>2</sub> Mg(thf) <sub>n</sub> ]	Toluene	16		20
	Me <sub>2</sub> Mg	Toluene	17		15
	Me <sub>2</sub> Mg	Et <sub>2</sub> O	18a,b	 <p>R = 1, 8-naphthdiyl R = Me</p>	21, 22
	Me <sub>2</sub> Mg	Toluene/THF	19		21, 22
	Bu <sub>2</sub> Mg	Hexane/THF	20		23
	Bu <sub>2</sub> Mg	Hexane	21		24
	R <sub>2</sub> Mg R=Et, <i>i</i> -Pr	THF	22a,b		25

(continued overleaf)



TABLE 1. (continued)

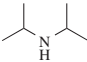
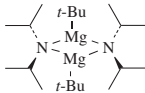
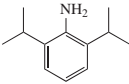
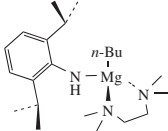
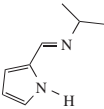
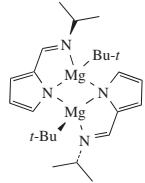
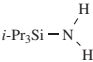
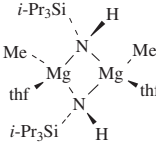
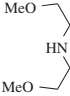
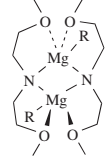
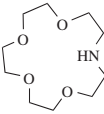
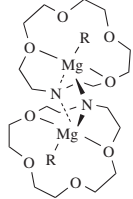
Amine/Amide	R <sub>2</sub> Mg	Solvent	Product number	Product	Reference
PhCN	Cp <sub>2</sub> Mg	Et <sub>2</sub> O	<b>23</b>		26
NHRR <sup>1</sup> R=R <sup>1</sup> =Ph R=H, R <sup>1</sup> =CH( <i>i</i> -Pr) <sub>2</sub> R=H, R <sup>1</sup> =2,6- <i>i</i> -Pr <sub>2</sub> -C <sub>6</sub> H <sub>3</sub> R= <i>i</i> -Pr, R <sup>1</sup> =CH <sub>2</sub> Ph	[CpMgMe(OEt <sub>2</sub> )] <sub>2</sub>	Et <sub>2</sub> O	<b>24a–d</b>		27
	[CpMgMe(OEt <sub>2</sub> )] <sub>2</sub>	Et <sub>2</sub> O	<b>25</b>		27
	[CpMgMe(OEt <sub>2</sub> )] <sub>2</sub>	Et <sub>2</sub> O	<b>26</b>		27
	[CpMgMe(OEt <sub>2</sub> )] <sub>2</sub>	Et <sub>2</sub> O	<b>27</b>		28
	[CpMgMe(OEt <sub>2</sub> )] <sub>2</sub>	THF	<b>28</b>		28
	[CpMgMe(OEt <sub>2</sub> )] <sub>2</sub>	Et <sub>2</sub> O	<b>29</b>		29
	[CpMgMe(OEt <sub>2</sub> )] <sub>2</sub>	(4- <i>t</i> -Bu-Py) Et <sub>2</sub> O	<b>30</b>		29

TABLE 1. (continued)

Amine/Amide	R <sub>2</sub> Mg	Solvent	Product number	Product	Reference
	Me <sub>2</sub> Mg	Toluene/THF	31		30
	<i>n</i> -Bu <sub>2</sub> Mg	Et <sub>2</sub> O	32		31
	<i>i</i> -Pr <sub>2</sub> Mg	Toluene	33		32
	R <sub>2</sub> <sup>3</sup> Mg	Toluene/Et <sub>2</sub> O	34a-d		33
				$R^1 = R^2 = \text{Me}, R^3 = \text{Et}$ $R^1 = R^2 = \text{Me}, R^3 = i\text{-Pr}$ $R^1 = \text{Et}, R^2 = \text{Me}, R^3 = i\text{-Pr}$ $R^1 = i\text{-Pr}, R^2 = \text{Me}$	
	Bu <sub>2</sub> Mg	Hexane/Et <sub>2</sub> O	35		34
	Bu <sub>2</sub> Mg, <i>t</i> -BuLi	Heptane	36		35

(continued overleaf)

TABLE 1. (continued)

Amine/Amide	R <sub>2</sub> Mg	Solvent	Product number	Product	Reference
	Bu <sub>2</sub> Mg, <i>t</i> -BuLi	Heptane	37		35
	Bu <sub>2</sub> Mg	Heptane (TMEDA)	38		35
	<i>t</i> -Bu <sub>2</sub> Mg	Toluene	39		36
	Me <sub>2</sub> Mg	THF	40		37
	R <sub>2</sub> Mg R=Me, Et, Np	Et <sub>2</sub> O	41		38
	R <sub>2</sub> Mg R=Me, Et, Np	THF/Et <sub>2</sub> O	42		38

of this route. For example, if the dialkylamide is small, the reaction may not cease at the alkyl(amido) stage but proceed to the dialkyl and bis(amido) species (Scheme 2)<sup>39</sup>. In such instances it is likely that the formation of insoluble polymeric products drives the reaction. In some cases mixed alkyl/aryl (methyl/cyclopentadienyl) R<sub>2</sub>Mg bases have been employed. For example, compounds **24–30** were synthesized using [CpMgMe(OEt<sub>2</sub>)<sub>2</sub>]<sub>2</sub> as a convenient reagent (Table 1)<sup>27–29</sup>. In each case the alkyl group acts as the base, producing methane gas, whereas the cyclopentadienyl ring remains  $\pi$ -coordinated to the

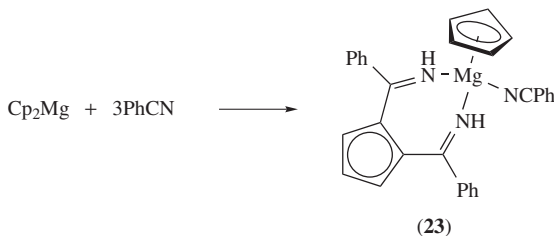


SCHEME 2

magnesium center. Several extensions and exceptions to these alkane elimination reactions have also been utilized, and are outlined below.

Ligand redistribution between magnesium bis(amides) and diorganomagnesium may take place. For instance, simply mixing the two metal reagents together results in the preparation of the heteroleptic organomagnesium amide complex **33**. Mixed-metal reagents have also been employed, including a mixed magnesium/lanthanum complex for the synthesis of  $\beta$ -diketiminate **14**<sup>18</sup>. A mixed-metal route was also used to prepare compounds **36** and **37**<sup>35</sup>. Specifically, heptane solutions of *n*-Bu(*s*-Bu)Mg were reacted with dibenzylamine and diisopropylamine to produce mixtures of the respective *n*- or *s*-BuMgNR<sub>2</sub> complexes. These mixtures proved difficult to separate but subsequent treatment with *t*-BuLi gave the *t*-BuMgNR<sub>2</sub> complexes, which were crystallized as pure solids from solution<sup>35</sup>. Another series of reactions using a second metal center are those involving the preparation of the  $\{\eta^3\text{-tris(pyrazolyl)borato}\}$  derivatives **3–6**. These compounds are conveniently synthesized by reaction of diorganomagnesium reagents with either the thallium or potassium precursors rather than protonated ligand<sup>6–11</sup>. Thus, these reactions proceed by metathesis rather than by deprotonation.

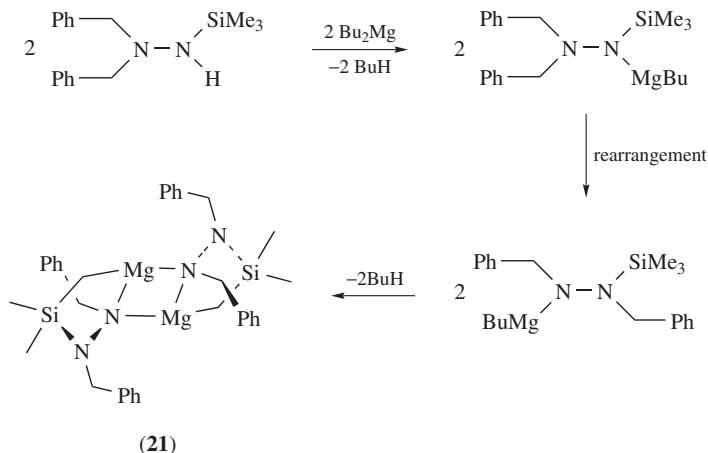
Addition reactions between diorganomagnesium compounds and organic nitriles may be used to produce organomagnesium imides<sup>40</sup>. The 1,2-cyclopentadienyl diimine complex **23** was synthesized from the reaction between Cp<sub>2</sub>Mg and benzonitrile<sup>26</sup>. This is an unusual reaction in the organomagnesium amide series as one of the cyclopentadienyl rings remains  $\pi$ -bound to the magnesium center while two benzonitriles add sequentially to the second ring (Scheme 3)<sup>26</sup>. Protons from the cyclopentadienyl ring are transferred to the benzonitriles, reducing the nitrile group to a carbon–nitrogen double bond. Another example of an addition reaction comes from the preparation of compound **34**, where *N*-alkylation occurs on reaction of the base with the bis(imino)pyridine ligand<sup>33</sup>.



SCHEME 3

Compound **21** is formed upon reaction of Bu<sub>2</sub>Mg with a silyl hydrazine (Scheme 4)<sup>24</sup>. In this instance the base removes a proton from the hydrazine followed by an unexpected migration of the benzyl group, and subsequent deprotonation of the trimethylsilyl group<sup>24</sup>.

The reactions involving diorganomagnesium reagents may be carried out in solvents ranging from saturated hydrocarbons to polar etheral solvents. The ability of these reactions to be conducted in hydrocarbon solvents gives them a distinct advantage over the alternative Grignard route. The Grignard route involves the reaction of a metal amide (typically an alkali metal amide) with a classic Grignard reagent of the form RMgX (X = halide). An alkali metal halide is eliminated upon formation of the organomagnesium



SCHEME 4

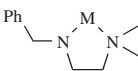
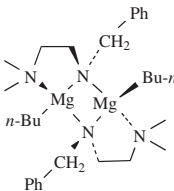
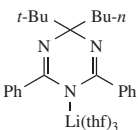
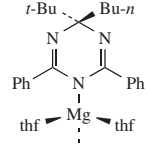
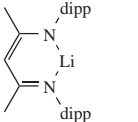
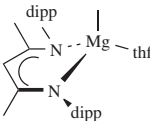
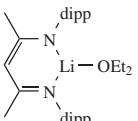
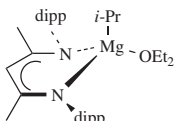
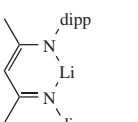
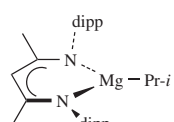
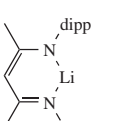
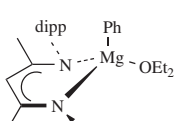
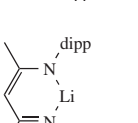
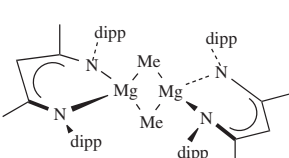
amide complex. Table 2 contains a complete list of organomagnesium amides produced from Grignard reagents which have been characterized in the solid state. These reactions are typically carried out in mixed solvent systems. The Grignard reagent, which is generally insoluble in hydrocarbons, is prepared as a solution in polar solvents such as THF or Et<sub>2</sub>O, then combined with a hydrocarbon/arene solution of the metal amide. Although this method provides a simple and straightforward means to organomagnesium amides, it is limited in its application for subsequent organic syntheses because of these solvent restrictions. Furthermore, the presence of Lewis base donor solvent is a drawback in some instances as it may cause disproportionation of organomagnesium complexes, resulting in the formation of bis(amide) and dialkylmagnesium species<sup>41,47</sup>. This possibility will be discussed in more detail in Section II.A.3.

A final set of miscellaneous organomagnesium amides that have been structurally characterized is outlined in Table 3. These were synthesized by neither R<sub>2</sub>Mg bases nor by Grignard reagents. Compounds **11a**, **55** and **56** were generated by heating existing compounds **10b**, **16** and **47**, respectively, under vacuum<sup>15,20,44</sup>. The coordinated solvent in each of the precursor compounds was eliminated, yielding desolvated dimeric, hexameric and monomeric species, respectively<sup>15,20,44</sup>. Compounds **57–59** were synthesized by reacting a magnesium bis(amide) base with an acetylene<sup>25,48</sup>. The terminal carbon was deprotonated, yielding the corresponding alkynylmagnesium amide species. Finally, reaction of MgBr<sub>2</sub> with a potassium amide was used to prepare compound **60**<sup>49</sup>.

## 2. Structural characterization

By the end of 2006 over seventy organomagnesium amides were present in the Cambridge Structural Database. Rather surprisingly, although Magnuson and Stucky reported the first crystal structure of this class of compound in 1969, it has only been in the last few years that the majority of work has appeared<sup>4</sup>. The complex [Me<sub>2</sub>NCH<sub>2</sub>CH<sub>2</sub>N(Me)MgMe]<sub>2</sub>, **1**, is shown in Figure 1, and consists of two metal centers bridged by two amido nitrogen centers<sup>4</sup>. The tetracoordinate coordination sphere of the metals is completed by binding to a methyl unit and a chelating dimethylamido function. This early structural analysis possesses several features that have proved to be typical for these compounds. In general the metals tend to be tetracoordinate, either through chelation or

TABLE 2. Structurally characterized organomagnesium amides synthesized from the reaction of metal amides with Grignard reagents

Amide	Grignard	Solvent	Product number	Product	Ref- erence
 M = Li or Na	<i>n</i> -BuMgCl	Hexane/THF	<b>43</b>		41
	MeMgCl	Toluene/THF	<b>44</b>		42
	MeMgCl	THF	<b>10b</b>		15
	<i>i</i> -PrMgCl	Et <sub>2</sub> O	<b>45</b>		43
	<i>i</i> -PrMgCl	Toluene/Et <sub>2</sub> O	<b>46</b>		44
	PhMgBr	Toluene/Et <sub>2</sub> O	<b>47</b>		44
	MeMgBr	Toluene/Et <sub>2</sub> O	<b>11a</b>		44

(continued overleaf)

TABLE 2. (continued)

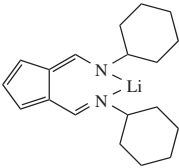
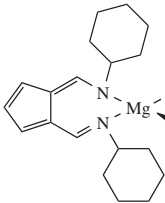
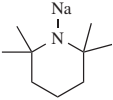
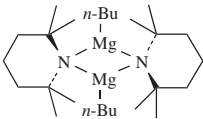
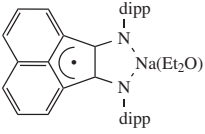
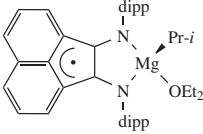
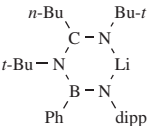
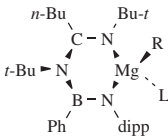
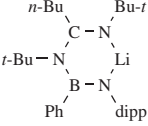
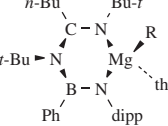
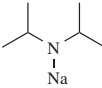
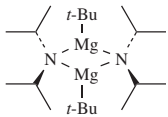
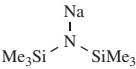
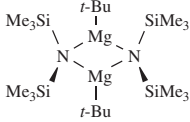
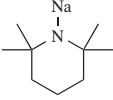
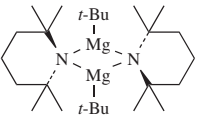
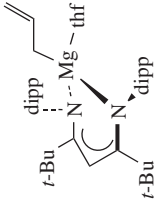
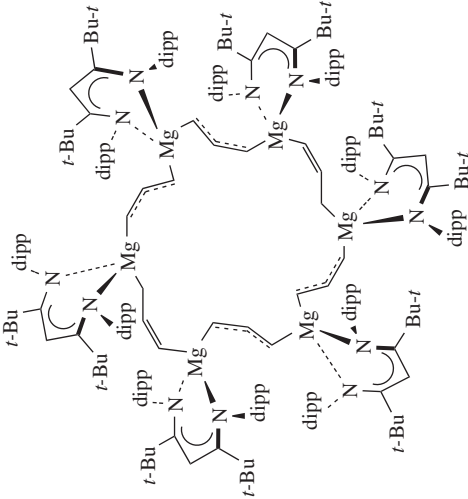
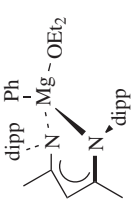
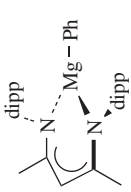
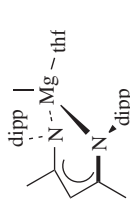
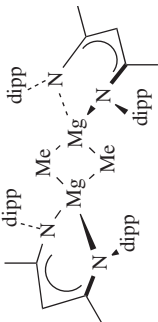
Amide	Grignard	Solvent	Product number	Product	Reference
	MeMgBr	Toluene/THF	48		45
	BuMgCl	Hexane/Et <sub>2</sub> O	49		46
	<i>i</i> -PrMgCl	Hexane/Et <sub>2</sub> O	50		32
	RMgX	Toluene/Et <sub>2</sub> O	51	 R = Me, X = Br, L = OEt <sub>2</sub> R = <i>t</i> -Bu, X = Cl, L = none R = Mes, X = Br, L = none	34
	RMgCl R = Ph, <i>i</i> -Pr	Toluene/THF	52		34
	<i>t</i> -BuMgCl	Hexane/Et <sub>2</sub> O	37		35
	<i>t</i> -BuMgCl	Hexane/Et <sub>2</sub> O	53		35
	<i>t</i> -BuMgCl	Hexane/Et <sub>2</sub> O	54		35

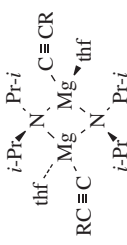
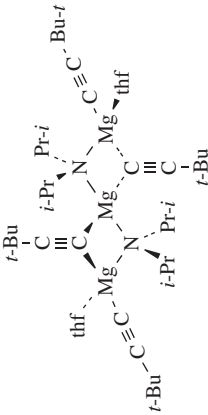
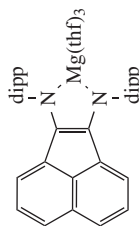
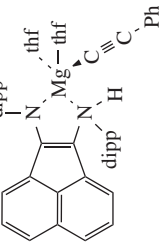
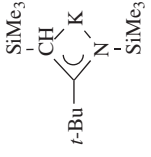
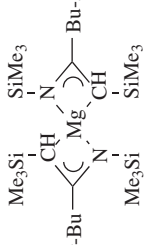
TABLE 3. Structurally characterized organomagnesium amides synthesized by miscellaneous methods

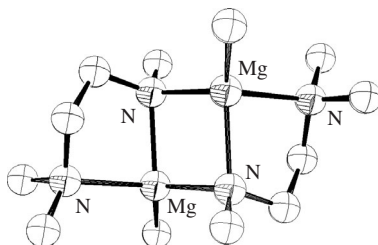
Mg precursor	Precursor 2	Solvent	Product Number	Product	Reference
	—	150 °C vacuum	<b>55</b>		20
	—	150 °C vacuum	<b>56</b>		44
	—	150 °C vacuum	<b>11a</b>		15

(continued overleaf)



TABLE 3. (continued)

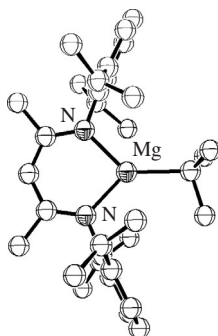
Mg precursor	Precursor 2	Solvent	Product Number	Product	Reference
$(i\text{-Pr}_2\text{N})_2\text{Mg}$	$\text{R}-\text{C}\equiv\text{C}-\text{H}$ $\text{R}=\text{Ph}, \text{SiMe}_3$	THF	57		25
$(i\text{-Pr}_2\text{N})_2\text{Mg}$	$t\text{-Bu}-\text{C}\equiv\text{C}-\text{H}$	THF	58		25
	$\text{Ph}-\text{C}\equiv\text{C}-\text{H}$	Toluene/THF	59		48
$\text{MgBr}_2$		pentane	60		49

FIGURE 1. Dimeric molecular structure of **1** with hydrogens omitted

through interactions with donor solvents. A small number of three-coordinate compounds are known, where sterically bulky groups are bound to the metal center. The dimeric arrangement of **1**, with bridging nitrogen groups, is also commonplace<sup>4</sup>. Preferential bridging by the alkyl units is limited to instances where the nitrogen centers are part of a large ligand set such as some  $\beta$ -diketimines.

Monomeric complexes typically only arise when the materials are crystallized in the presence of donor solvents, producing solvated solid-state compounds. A few exceptions to the solvation of monomers can be seen. One notable example is compound **12**, which was prepared by the reaction of  $t\text{-Bu}_2\text{Mg}$  with the corresponding protic amine (Figure 2)<sup>14</sup>. The related  $\beta$ -diketiminato **46** (Table 2) was also obtained as an unsolvated monomeric compound and was prepared from a reaction conducted in toluene with only small amounts of diethyl ether present<sup>44</sup>. The  $\eta^3$ -tris(pyrazolyl)borate complexes **3–5** (Table 1) also typically crystallize solvent-free, as the metal achieves tetracoordination through binding to the tridentate ligand and the terminal organic fragment<sup>6–10</sup>.

There are only two examples of structurally characterized  $\text{R}_2\text{NMgR}$  compounds which have aggregation states larger than dimers. The remarkable dodecameric complex  $[\text{DippN(H)MgEt}]_{12}$ , **9** (Table 1), forms a ring structure composed of twelve interconnected  $\text{MgNMgC}$  rings (Figure 3)<sup>13</sup>. (Dipp = 2,6-diisopropylphenyl). It is noteworthy that both the amine and the ethyl groups bridge between the magnesium atoms. The large ring is slightly bowed, deviating at most *ca* 0.24 Å from the average plane of the magnesium atoms. In turn, the 2,6-diisopropylphenylamido groups point out from the magnesium atoms and away from the ring, while all of the smaller ethyl groups project towards the center of the ring. The second highly aggregated structure is allylmagnesium  $\beta$ -diketiminato **55** (Table 3), which is obtained upon sublimation of the monomeric THF

FIGURE 2. Monomeric three-coordinate structure of **12** with hydrogens omitted

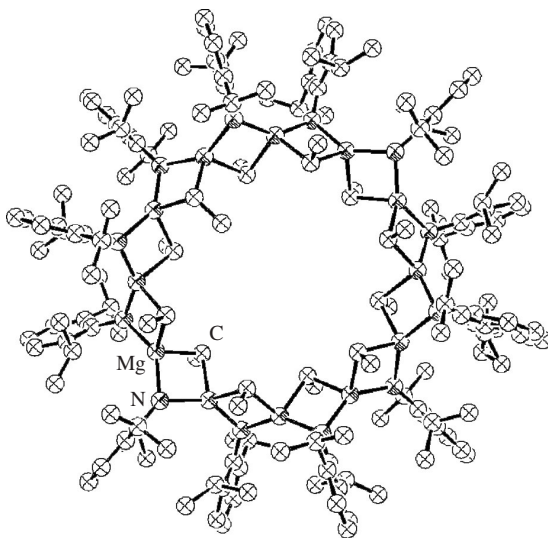


FIGURE 3. Ring hexameric structure of **9** with hydrogens omitted

derivative<sup>20</sup>. This hexameric ring is similar to **9**, although the deviations from the mean plane of the ring are slightly more significant. Each of the magnesium atoms is bridged by allyl groups while the bulky amides project outward from the ring.

The  $\eta^3$ -tris(pyrazolyl)borato-based compounds **3–6** (Table 1) are a unique subset of the organomagnesium amides<sup>6–11</sup>. The sterically-demanding environment of the  $\eta^3$ -tris(pyrazolyl)borato ligand strongly controls the overall structure of these compounds. Three nitrogens from each of three five-membered pyrazolyl rings coordinate to the magnesium center and provide an overall  $-1$  charge to the complex. Two of the pyrazolyl rings are coplanar with each other and the magnesium, while the third ring sits perpendicular to this plane above the magnesium center. This magnesium atom, which is highly protected within this amido pocket, is then available to bond to a variety of organic fragments to complete its coordination sphere. The compounds within this series are exclusively monomeric and, though sometimes synthesized in ethereal solvent, compound **6** is the only solvated complex<sup>11</sup>. The nature of the organic group within this set of complexes appears to have little influence upon the metrical parameters of the overall structures.

Many organomagnesium complexes containing  $\beta$ -diketiminate ligands have been structurally characterized. Typically, the metal center lies in the NCCCN plane and is equivalently coordinated to both nitrogen atoms and is further bonded to an alkyl fragment. The nature of the alkyl group on the magnesium and the presence of polar solvent both influence the aggregation state of the resulting solid-state structure. For example, methyl- and butyl-substituted compounds **11a** and **11b** (Table 1) form dimeric aggregates in the solid state when generated in non-polar solvent<sup>14–16</sup>. However, the analogous compound **12** (Table 1), which is *t*-butyl-substituted, is monomeric when crystallized from non-polar solvent<sup>14</sup>. The steric bulk of the *t*-butyl ligand blocks the magnesium's coordination sphere and prevents dimerization. Furthermore, when solvated monomeric **10a** and **10b** are compared with unsolvated dimeric **11a**, it becomes evident that the presence of donor solvent reduces the aggregation state of the complex through solvation of the magnesium center<sup>14–16</sup>.

The cyclopentadienyl-containing compounds **23–30** (Table 1) adopt another structure type for organomagnesium amides<sup>26–29</sup>. In all cases, the structures consist of one  $\eta^5$ -cyclopentadienyl ligand that is bound to the magnesium centers with the metal–cyclopentadienyl centroid distances lying in a narrow range between 2.0 and 2.1 Å. Both monomeric and dimeric aggregates are observed, which again is primarily related to the steric bulk present on the amide group.

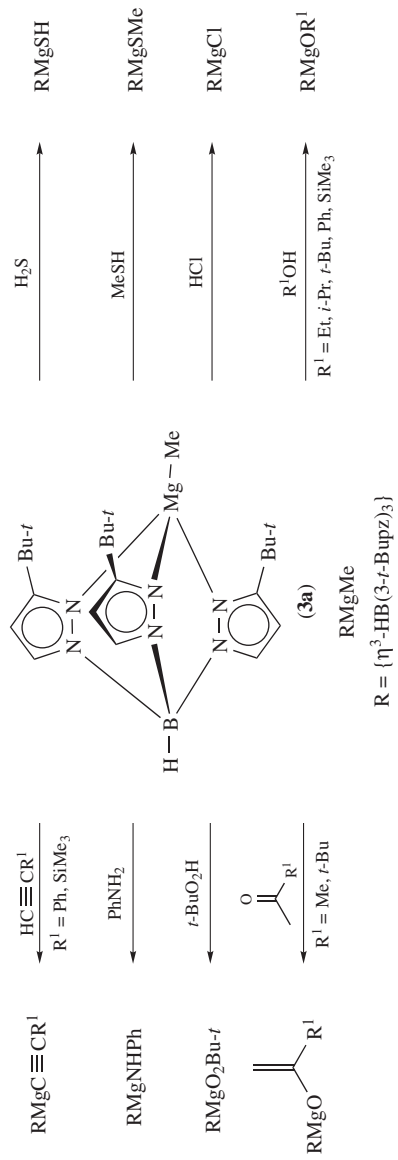
### 3. Reactivity studies

*a. Metalation reactions.* The most commonly studied reaction of organomagnesium amides is their use in metalation reactions. It is generally assumed that the organic group is the most reactive unit of the reagent, and is consequently involved in these reactions. It should, however, be noted that the involvement of the alkyl or the amide unit has been a subject of some debate in the reactions of the mixed-metal reagents<sup>50,51</sup>. A number of general reactivity patterns for organomagnesium amides has been demonstrated using the  $\eta^3$ -tris(pyrazolyl)-hydroborate framework. As shown in Scheme 5, the complex  $\{\eta^3\text{-HB}(3\text{-}t\text{-Bupz})_3\}\text{MgMe}$ , **3a**, has been employed in a wide range of reactions<sup>6,52</sup>. In all of these cases the methyl unit is used as a base to perform a series of deprotonation reactions. The use of the bulky  $\eta^3$ -tris(pyrazolyl)-hydroborate ligand prevents complications due to oligomerization of the products or ligand rearrangement.

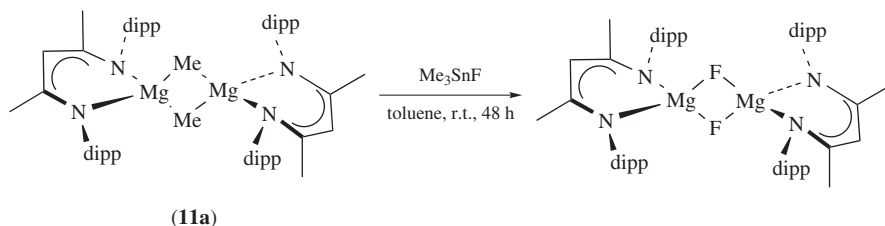
Similarly, the unsolvated  $\beta$ -diketiminato complex  $\{\text{HC}(\text{C}(\text{Me})\text{N-2,6-}(i\text{-Pr})_2\text{C}_6\text{H}_3)_2\}\text{MgBu}$ , which is generated *in situ* by reacting  $\text{Bu}_2\text{Mg}$  with  $\text{HC}(\text{C}(\text{Me})\text{N-2,6-}(i\text{-Pr})_2\text{C}_6\text{H}_3)_2$ , has been shown to be reactive towards alcohols, amines and carboxylic acids to form the corresponding amidomagnesium alkoxides, amides and carboxylates<sup>44</sup>. Another noteworthy example of a reaction involving a  $\beta$ -diketiminato complex is shown in Scheme 6. Reaction of **11a** with  $\text{Me}_3\text{SnF}$  under mild conditions yields a fluorine-bridged dimer<sup>16</sup>. This is a rare example of a molecular magnesium fluoride complex and it is presumably stabilized towards disproportionation to  $\text{MgF}_2$  by the bulk of the amide ligand<sup>16</sup>.

Organomagnesium amides have been utilized as alternatives to standard Grignard reagents<sup>53–55</sup>. These reagents are believed to be less nucleophilic than classic Grignard reagents. The slight reduction in their reactivity allows their use in reactions where a mild base is desired. A significant potential advantage of using alkylmagnesium amides over either lithium amides or magnesium bis(amides) in the deprotonation of relatively weak acids is that the reactions are driven to completion due to the irreversible loss of alkane. This is particularly useful in instances when the pKa of the carbon acid and the amine are similar. The reactions of commercially available butylmagnesium diisopropylamide,  $\text{BuMgDA}$ , with cyclopropane carboxamides are good examples of this reactivity<sup>56</sup>. As shown in Scheme 7,  $\text{BuMgDA}$  reacts with cyclopropane carboxamides to give the  $\beta$ -magnesiato species, which readily undergoes a variety of substitution reactions. Another useful variation in this reactivity pattern was found by altering the stoichiometry of amide and alkyl present in the magnesium base reagent. Specifically, whereas  $\text{BuMgDA}$  reacts with the cyclopropanes to give the  $\beta$ -magnesiato species, mixing  $\text{Bu}_2\text{Mg}$  and diisopropylamine in a 1:0.5 molar ratio produces a system that gives predominantly the  $\alpha$ -metallated product. It was assumed that this is due to the kinetic selectivity of this reagent mixture. In any event, the intermediate may be trapped to produce  $\alpha$ -carboxy,  $\alpha$ -iodo or  $\alpha$ -alkyl products that are difficult to prepare by other means. Another demonstration of the utility of this reagent has been the  $\beta$ -metalation of amide-activated cyclobutanes<sup>57</sup>. This reaction is notable since equivalent lithium amide systems are unreactive with such weakly acidic substrates.

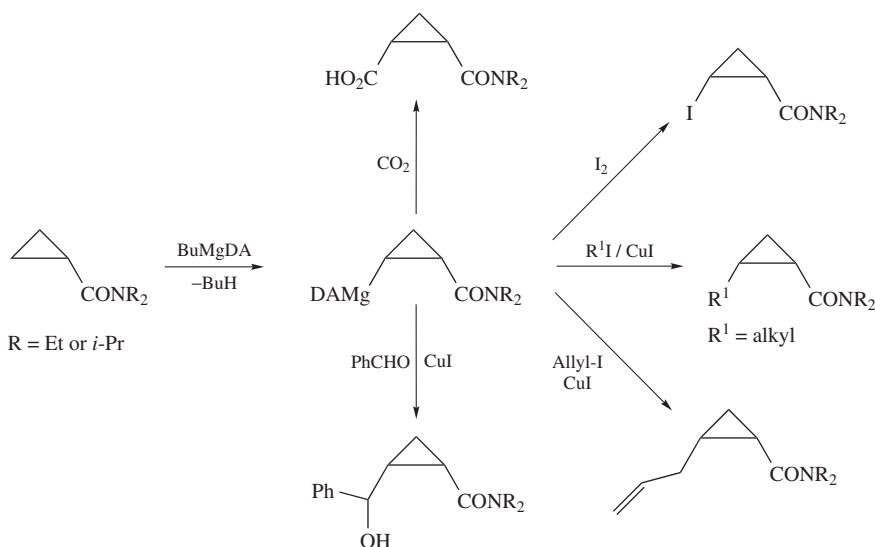
The magnesium bis(amide)  $\text{Mg}(\text{TMP})_2$  ( $\text{TMP} = 2,2,6,6\text{-tetramethylpiperidide}$ ) has been shown to be a useful base in the selective deprotonation of arenes to produce arylmagnesium amide intermediates<sup>54</sup>. For example, reaction of  $\text{Mg}(\text{TMP})_2$  with methyl benzoate



SCHEME 5



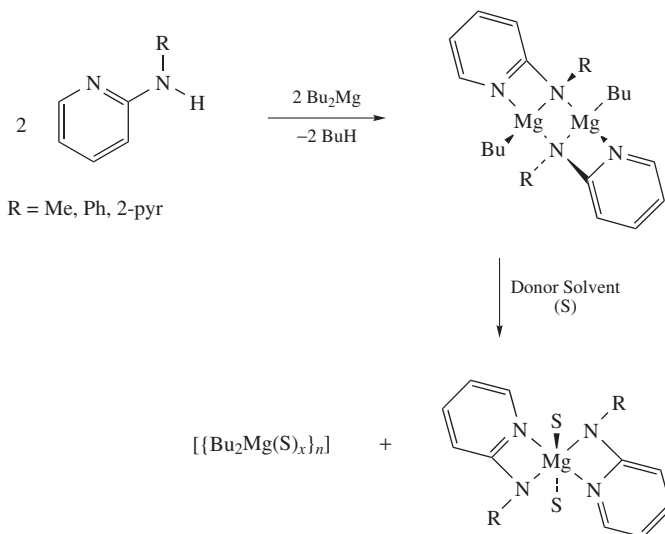
SCHEME 6



followed by quenching with carbon dioxide gives dimethyl *ortho*-phthalate in over 80% yield. In comparison, reaction with amido Grignard reagents,  $R_2NMgX$ , results in condensation with the ester group. Similarly, arylmagnesium amides are proposed to be key intermediates in the directed metalation of benzamides, cyclopropanes and carbocubanes.

Organomagnesium amide complexes have also been studied for use as reagents in the halogen–magnesium exchange reactions of halogenated arenes and indoles<sup>58</sup>. The reagent  $i\text{-PrMgN}(i\text{-Pr})_2$  proved to be useful for magnesiation of iodophenoxyalcohols. However, poor yields were obtained using iodophenols and iodoindoles. Also, related bromine–magnesium exchange reactions using  $i\text{-PrMgN}(i\text{-Pr})_2$  with bromophenoxyalcohols, phenols and indoles were unsuccessful, requiring application of the mixed-metal reagents of the type  $i\text{-PrMgBu}_2\text{Li}$ . Organomagnesium amides have been applied to the carbomagnesation of olefins, although the yields of each of the addition products are substantially lower than when using the dialkylmagnesium analogues<sup>53</sup>. Also, a small number of these complexes have been used as catalysts for the polymerization of *rac*-lactide and  $\epsilon$ -caprolactone<sup>18,34</sup>.

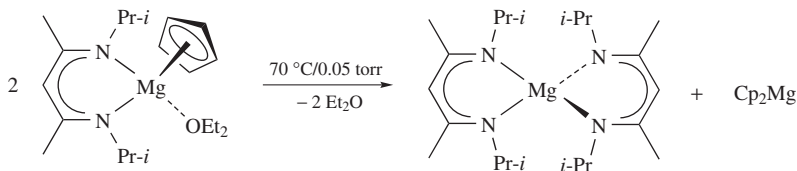
*b. Disproportionation reactions.* Many organomagnesium amide complexes are sensitive to the presence of coordinating solvents. Addition of polar solvents to arene or hydrocarbon solutions of alkyl(amido)magnesium species may result in disproportionation, yielding the bis(amido) and dialkylmagnesium complexes<sup>25, 41, 47</sup>. At least in some instances the driving force for the disproportionation is the increase in coordination number at the metal center. As shown in Scheme 8, chelation of two (2-pyridyl)amido units on the metal center allows coordination by additional donor solvent, increasing the coordination number at the metal from four to six<sup>47</sup>. Studies have shown that modest variations of the organic unit on the (2-pyridyl)amido substituent does not effect this reaction. Another important factor in such disproportionation reactions appears to be the relative strength of the donor solvent. The alkyl magnesium amides  $[\text{Ph}_2\text{NMgR}(\text{THF})_2]$  ( $\text{R}=\text{Et}$  or  $i\text{-Pr}$ ) are readily crystallized from THF solutions upon reaction of  $\text{MgR}_2$  with  $\text{HNPh}_2$ <sup>25</sup>. However, addition of the strong donor solvent HMPA,  $(\text{Me}_2\text{N})_3\text{PO}$ , results in exclusive isolation of the bis(amide)  $[(\text{Ph}_2\text{N})_2\text{Mg}(\text{HMPA})_2]$ . Therefore, the nature of the equilibrium between the hetero- and homoleptic magnesium species is similar to the Schlenk equilibrium in Grignard reagents and related complexes<sup>59</sup>.



SCHEME 8

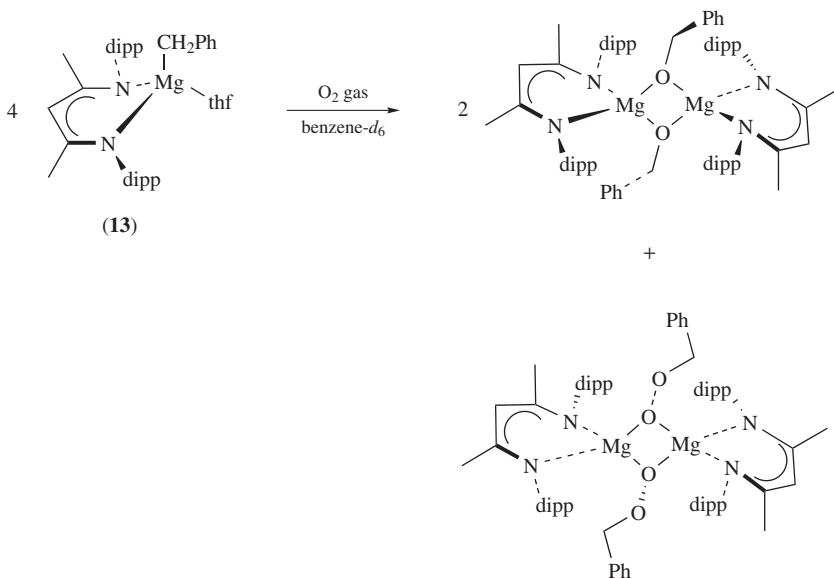
Many monomeric organomagnesium amide solvates may be transformed on heating under vacuum. In some instances this leads to simple desolvation of the complexes and in turn gives rise to dimerization or even further aggregation<sup>15, 20, 28, 29, 44, 60</sup>. Another outcome is disproportionation<sup>15, 28, 29, 60</sup>. For example, the disproportionation of an ether-solvated  $\beta$ -diketiminate complex upon sublimation is shown in Scheme 9<sup>29</sup>.

*c. Reactions with oxygen.* Organomagnesium amides are air- and moisture-sensitive, and several studies have been carried out demonstrating their reactivity towards  $\text{O}_2$ <sup>8, 9, 15, 17</sup>. The most common outcome of this reaction is insertion of oxygen into the metal–carbon bond to form either alkoxide or alkylperoxide species. Reaction of the solvated magnesium  $\beta$ -diketiminate complex,  $[\text{MeMg}\{\eta^2\text{-(}i\text{-Pr)}_2\text{ATI}\}(\text{THF})]$ , where ATI = aminotroponimin-ate, with  $\text{O}_2$  produced the methoxy-bridged dimer  $[\text{MeOMg}\{\eta^2\text{-(}i\text{-Pr)}_2\text{ATI}\}(\text{THF})_2]$ <sup>15</sup>.



SCHEME 9

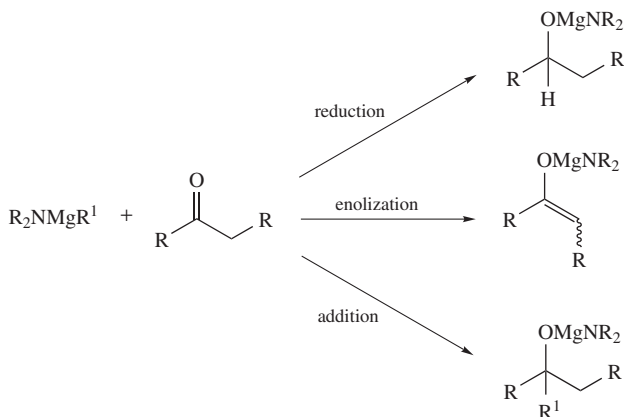
*In situ* <sup>1</sup>H NMR monitoring of this reaction in THF-*d*<sub>8</sub> showed the loss of the methyl signal and the concomitant appearance of the methoxy signal, confirming the insertion of O<sub>2</sub> into the magnesium–carbon bond. The solvated β-diketiminato complex, **13**, has also been observed to undergo O<sub>2</sub> insertion<sup>17</sup>. The <sup>13</sup>C{<sup>1</sup>H} NMR spectrum obtained upon addition of dry O<sub>2</sub> gas to a benzene-*d*<sub>6</sub> solution of **13** revealed the presence of two species in a 2:1 ratio. Crystallization yielded both the benzyloxo and benzylperoxo products, which are shown in Scheme 10. An unusual reaction was observed on addition of O<sub>2</sub> to {η<sup>3</sup>-HB(3-*t*-Bupz)<sub>3</sub>}MgCH<sub>2</sub>SiMe<sub>3</sub>, **4**. In this case the siloxide {η<sup>3</sup>-HB(3-*t*-Bupz)<sub>3</sub>}MgOSiMe<sub>3</sub> was produced due to cleavage of the Si–C bond<sup>8,9</sup>. It was proposed that this reaction involves a radical process whereby the initially prepared organoperoxide rearranges to form the thermodynamically stable Si–O bond and formaldehyde.



SCHEME 10

*d. Reactions with aldehydes and ketones.* The most common outcomes of the reaction of organomagnesium amides with aldehydes or ketones are reduction, enolization and addition, as shown generically in Scheme 11. The specific reaction occurring (or competitive reactions) is determined by the interplay of the sterics and electronic effects of the reagent and substrate carbonyl compound.



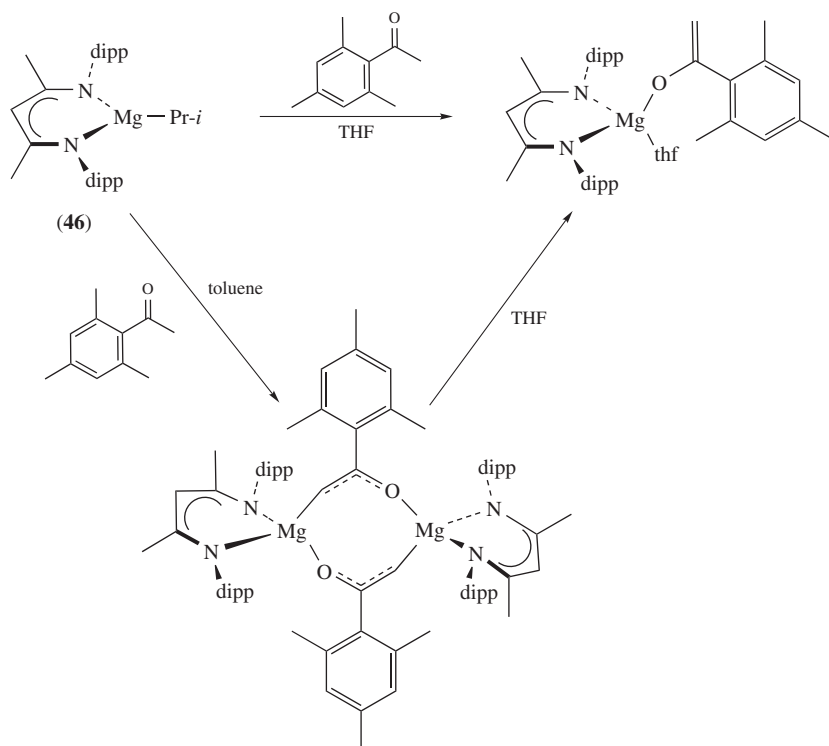


SCHEME 11

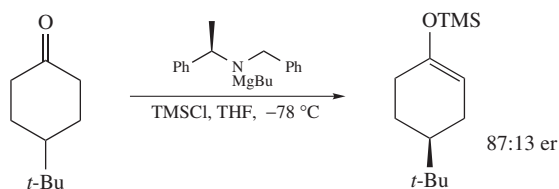
Generally, enolization reactions will occur when the organo group on the reagent is relatively large and the ketone contains an acidic  $\alpha$ -proton. This is the preferred pathway for the reaction of  $\beta$ -diketiminate complex **46** with 2',4',6'-trimethylacetophenone (Scheme 12)<sup>44</sup>. Enolization is also favored in this case as the ketone is sterically protected toward attack by nucleophilic addition<sup>61, 62</sup>. Another feature of this reaction is that the structure of the products is dependent upon the solvent media present. In THF, the amido(enolate) is a solvated monomer whereas in toluene, an unusual dimer is produced which utilizes both the carbon and the oxygen centers of the enolate group to bridge the metal centers. However, addition of THF to the toluene solution containing the dimer produces the same monomeric solvate generated directly in THF solution.

An interesting case is the reaction of  $\{\eta^3\text{-HB}(3\text{-}t\text{-Bupz})_3\}\text{MgMe}$ , **3a**, with acetone and *t*-butyl methyl ketone<sup>10, 16</sup>. As outlined in Scheme 5, despite carrying a small methyl unit the reagent acts as a base rather than a nucleophile on reaction with unhindered ketones to produce enolates. In this instance it appears that the steric bulk of the  $\eta^3$ -tris(pyrazolyl)-hydroborate ligand dominates the reaction pathway. Enantioselective deprotonation reactions of conformationally-locked ketones have also been mediated by organomagnesium amides, which carry chiral amide groups (Scheme 13)<sup>63</sup>. These reagents show similar selectivities to their bis(amido) counterparts but have the advantage of requiring only half the amount of chiral starting material<sup>64–67</sup>. It is also worth noting that the heteroleptic reagents react chemoselectively with the ketones under study to produce only the enolate products. In comparison, reaction of the dialkylmagnesium starting material with the substituted cyclohexanones results in substantial quantities of both secondary and tertiary alcohol after workup due to participation of competitive reduction and alkylation reactions.

Addition reactions dominate when the organic group is relatively small and can act as a good nucleophile for attack of unhindered ketones or aldehydes. For example, reaction of the methylmagnesium amides,  $R_2NMgMe$  ( $NR_2 = N(\text{Pr-}i)_2$ ,  $NPh_2$  and  $c\text{-NC}_5\text{H}_8\text{Me}_2$ ) with either 4-*t*-butylcyclohexanone or the more sterically encumbered 2,2,6,6-tetramethyl-4-*t*-butylcyclohexanone have been reported to display good stereoselectivity for alkylating ketones<sup>68</sup>. A combination of the steric bulk of the amide and the ketone, as well as the nature of the solvent media present was found to effect the selectivity obtained. Asymmetric alkylation reactions have also been completed using these reagents. Optically active aldehydes have been shown to react with alkylmagnesium amides to produce chiral



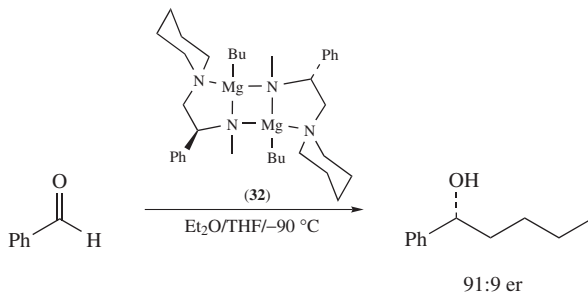
SCHEME 12



SCHEME 13

secondary alcohols with essentially complete Cram selectivity<sup>69</sup>. Furthermore, incorporation of a chiral amide unit into the reagent allows the possibility of heteromolecular asymmetric induction reactions with unsaturated groups. This approach has been demonstrated to be highly successful using potentially chelating chiral amides, including the structurally characterized complex **32**<sup>31</sup>. These very simply-prepared reagents display selectivities up to 91:9 er using a variety of alkyl and aryl nucleophiles, and also for a wide range of aldehydes (Scheme 14).

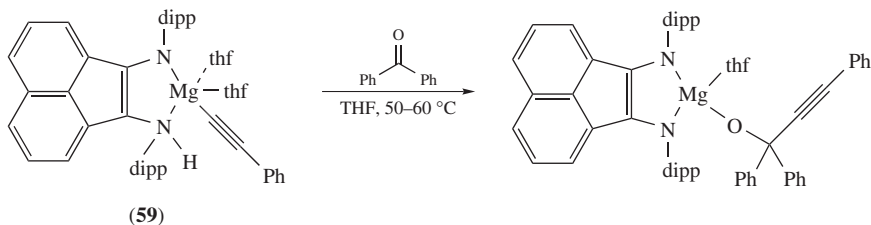
Reduction of ketones may occur if the alkyl group contains a  $\beta$ -hydrogen that is available for abstraction. For example, addition of benzophenone to the *in situ* prepared complex BuMgN(SiMe<sub>3</sub>)<sub>2</sub> results in  $\beta$ -hydride transfer from the butyl group leading to the formation of the reduction product<sup>70</sup>. This type of reaction has also been conducted in an



SCHEME 14

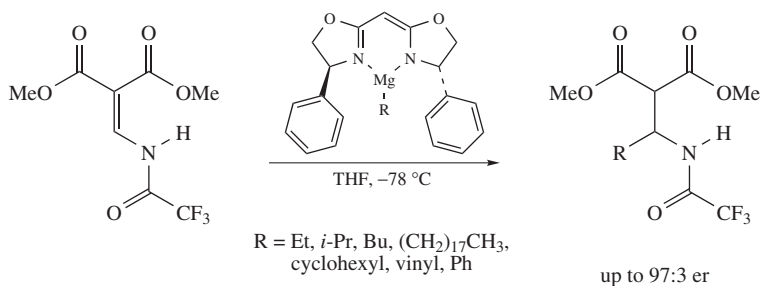
asymmetric manner through application of chiral amides as described previously for the alkylation reactions<sup>31</sup>. Specifically, reaction of *in situ* prepared chiral organomagnesium amides with a number of aldehydes yield secondary alcohols in excellent yields and selectivities (typically >95% and >85% respectively).

Another interesting example of an insertion reaction is found through the addition of benzophenone to complex **59** (Scheme 15)<sup>48</sup>. In this case hydrogen is abstracted from an amine group with addition of an alkyne unit across the carbonyl to produce a radical anion.



SCHEME 15

A useful application of organomagnesium amides is in the enantioselective conjugate addition to enamidomalonate to prepare  $\beta$ -amino acid derivatives (Scheme 16)<sup>71</sup>. The alkylmagnesium amide complexes provided both high yields and high selectivity in the organic transformation.

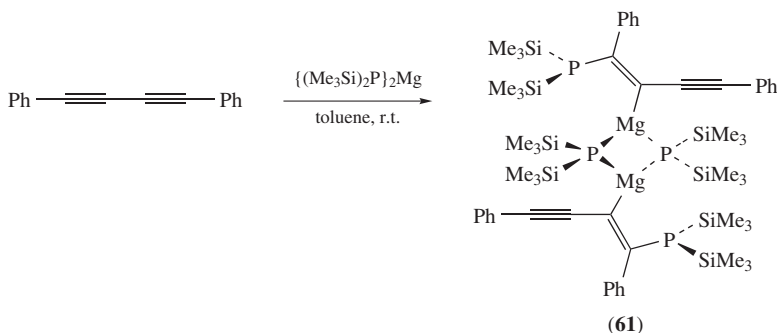


SCHEME 16

## B. Organomagnesium Heavy Pnictogenides

Organomagnesium complexes of heavy group 15 elements are much more rare than their amido analogues. In fact, only three examples of structurally authenticated complexes have been reported in the literature, all containing magnesium–phosphorus bonds<sup>72,73</sup>. The limited number of these compounds is at least in part a consequence of the lability of the bonds between magnesium and the heavy group 15 elements. However, this is an area that has received generally little attention and certainly merits further study.

The first example of a structurally characterized organomagnesium phosphanide only appeared in 1998 with the synthesis of complex **61**<sup>72</sup>. As shown in Scheme 17, this complex is produced upon the addition reaction between magnesium bis[(bis(trimethylsilyl) phosphanide)] and 1,4-diphenylbutadiyne<sup>72</sup>. Compound **61** is dimeric in the solid state, forming a central  $\text{Mg}_2\text{P}_2$  ring with magnesium–phosphorus bond lengths of 2.559(2)/2.569(2) Å. The second phosphorus atom of the ligand then forms a dative interaction to each magnesium center, with a Mg–P distance of 2.708(3) Å. Replacing magnesium for barium in this reaction results in a more reactive intermediate that immediately undergoes further reaction with butadiene present in solution to produce a phosphacyclopentadienide<sup>72</sup>.

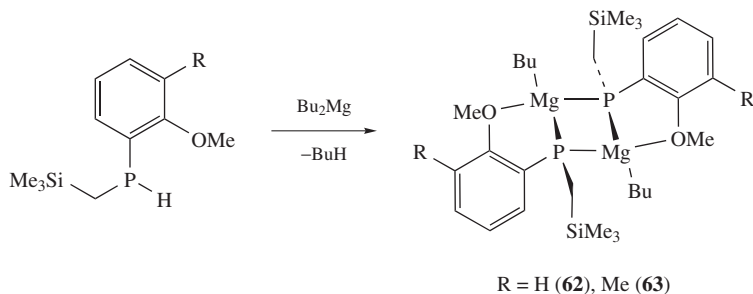


SCHEME 17

The organomagnesium phosphanide complexes **62** and **63** shown in Scheme 18 were directly prepared by metalation of the appropriate secondary phosphanes<sup>73</sup>. Reaction of two equivalents of the phosphanes with  $\text{Bu}_2\text{Mg}$  again only produced **62** and **63** rather than the expected bis(phosphanide) derivatives. It was speculated that this may be a consequence of steric hindrance caused by chelation in the heteroleptic complexes. Both complexes again form dimers with tetracoordinated metals and central  $\text{Mg}_2\text{P}_2$  rings, with magnesium–phosphorus distances of 2.5760(8)/2.5978(8) Å for **62** and 2.5765(17)/2.5730(16) and 2.6138(16)/2.6105(17) Å for **63**. These distances are comparable to the magnesium–phosphorus bonds of the four-membered ring in **61**. They are also similar to the magnesium–phosphorus distances in bisphosphanides<sup>74,75</sup>. These compounds are found to rapidly decompose in  $\text{THF-d}_8$  solution and are believed to undergo ligand degradation.

## III. ORGANOMAGNESIUM-GROUP 16-BONDED COMPLEXES

Organomagnesium complexes of the group 16 elements have been even less studied than their group 15 analogues. A summary of the known and relevant chemistry of these species is given below.



SCHEME 18

## A. Organomagnesium Alkoxides and Aryloxides

### 1. Synthesis

Organomagnesium alkoxides and aryloxides are typically synthesized by methods which are comparable to the synthesis of organomagnesium amides. The two most common routes again are the deprotonation of alcohols by  $\text{R}_2\text{Mg}$  bases or the reaction of a Grignard reagent with a metal alkoxide. Table 4 gives a summary of the structurally characterized organomagnesium alkoxides and aryloxides, and details of their methods of preparation. Complexes **64–67** were generated by the alkane elimination method<sup>76–78</sup>. Similarly, a series of methyl- and cyclopentadienylmagnesium alkoxides has also been prepared in this manner, although they have not been structurally characterized<sup>83,84</sup>. The Grignard transmetalation procedure was used in the synthesis of **68–70**<sup>77,79,80</sup>, and also to prepare a series of phenyl- and butylmagnesium alkoxides<sup>85</sup>. Phenylmagnesium carboxylates have also been synthesized by reacting sodium salts of carboxylic acids with phenylmagnesium bromide<sup>86</sup>. Alternative methods, however, were used in the synthesis of compounds **71** and **72**<sup>81,82</sup>. Complex **71** was unexpectedly formed via cleavage of 2,1,1-cryptand upon addition of dineopentylmagnesium<sup>81</sup>. The mixed alkyl, amide, alkoxide complex **72** was first formed as a low yield product by reacting  $n\text{-BuMgCl}$  with  $\text{NaN(H)Dipp}$  in ether. It was then rationally prepared by combining stoichiometric quantities of  $\text{Bu}_2\text{Mg}$ ,  $\text{Mg[N(H)Dipp]}_2$  and  $n\text{-BuOH}$  in heptane<sup>82</sup>.

### 2. Structural characterization

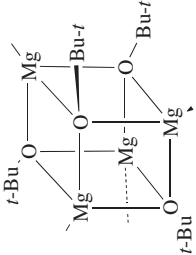
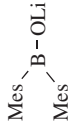

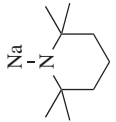
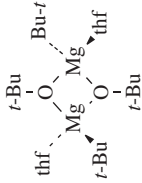
Monomeric, dimeric and tetrameric aggregation states of organomagnesium alkoxides and aryloxides have all been observed. Monomeric structures **66** and **67** consist of magnesium centers that are coordinated by the sterically encumbering donor ligands 18-crown-6-ether and TMEDA, preventing further aggregation<sup>78</sup>. Complex **68** is the sole tetrameric cubane structure for this class of compounds that has been characterized in the solid state thus far (Figure 4)<sup>79</sup>. This complex was prepared by transmetalation in a mixture of toluene and THF (5:1) followed by sublimation. Nevertheless, the solution chemistry of a variety of alkylmagnesium alkoxides has been studied in detail and found to form numerous oligomers<sup>83,87</sup>. As expected, the type of aggregate formed is determined by the extent of the branching of the alkyl and alkoxy groups and the strength of the donor solvent present. In contrast with organomagnesium amides, none of the structures consists of organo-bridged magnesium centers.

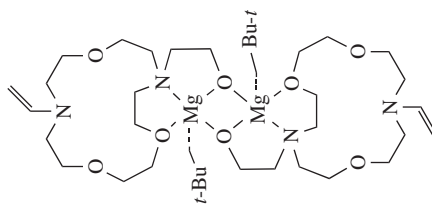
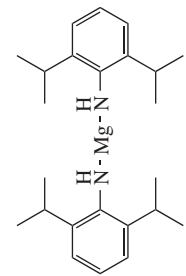
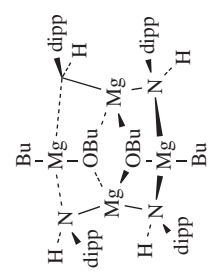
TABLE 4. Structurally characterized organomagnesium alkoxides and aryloxides, showing their methods of preparation

Mg precursor	Precursor 2	Solvent	Product number	Product	Reference
$\text{Bu}_2\text{Mg}$		Hexane/Toluene	<b>64</b>		76
$\text{Bu}_2\text{Mg}$		THF	<b>65</b>		77
$i\text{-Bu}_2\text{Mg}$		$\text{Et}_2\text{O}$ (crystallization from benzene after addition of 18-crown-6- ether)	<b>66</b>		78
$\text{Et}_2\text{Mg}$		$\text{Et}_2\text{O}$ (crystallization from benzene after addition of TMEDA)	<b>67</b>		78

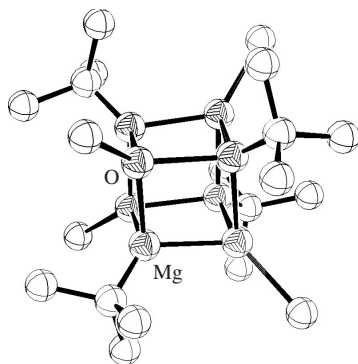
(continued overleaf)

TABLE 4. (continued)

Mg precursor	Precursor 2	Solvent	Product number	Product	Reference
MeMgBr	<i>t</i> -BuOK	Toluene	68		79
MeMgCl		Et <sub>2</sub> O	69		77
<i>t</i> -BuMgCl		Hexane/THF/O <sub>2</sub>	70		80

$(\text{Me}_3\text{CH}_2)_2\text{Mg}$	2,1,1,1-cryptand	Benzene/ $\text{Et}_2\text{O}$	71		81
	$\text{Bu}_2\text{Mg}$	Heptane ( $\text{BuOH}$ )	72		82

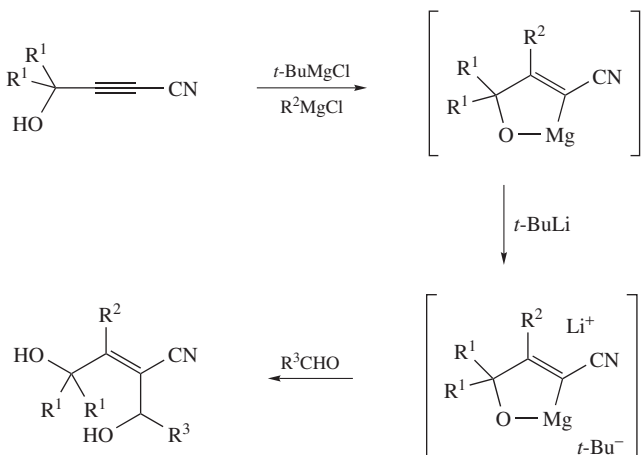


FIGURE 4. Tetrameric cubane structure of **68** with hydrogens omitted

### 3. Reactivity studies

Organomagnesium alkoxides and aryloxides have been utilized in only a few applications. Methylmagnesium *t*-butoxide **68** has been used in the chemical vapor deposition of MgO films onto silicon substrates<sup>79</sup>. MgO films with good crystallinity were grown at 800 °C on Si(111) surfaces, whereas polycrystalline films were formed at 400 °C. Intermediate temperatures produced multiple crystallite orientations. Similar results were obtained for deposition onto Si(100) surfaces over this range of temperatures.

Tri- and tetra-substituted alkenenitriles can be generated by the addition of Grignard reagents to  $\gamma$ -hydroxyalkynenitriles<sup>88</sup>. It was proposed that deprotonation of the hydroxyl group by *t*-butylmagnesium chloride followed by addition of a second Grignard reagent,  $R^2MgX$ , results in the formation of a chelated organomagnesium alkoxide intermediate (Scheme 19). Subsequent addition of *t*-butyllithium to this intermediate followed by alkylation with an electrophile yields tetra-substituted nitriles. Alternatively, the cyclic magnesium chelate can be protonated to yield tri-substituted nitriles.



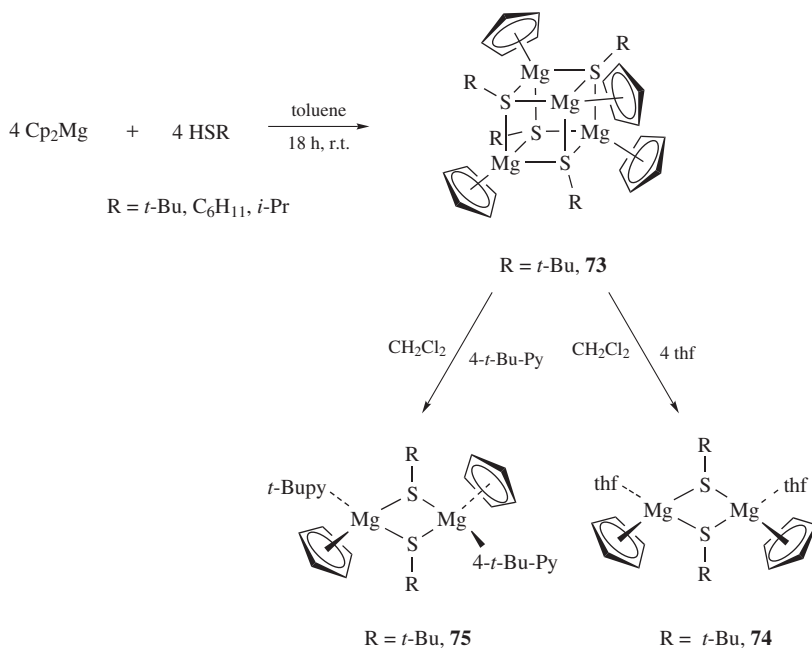
SCHEME 19

## B. Organomagnesium Heavy Chalcogenides

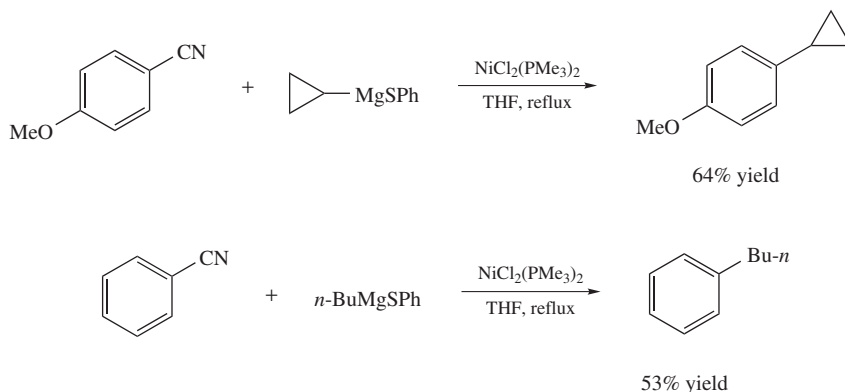
Analogous to heavy group 15 organomagnesium complexes, there are very few organomagnesium heavy group 16 complexes which have been synthesized or structurally characterized. Indeed, only three examples of structurally characterized organomagnesium sulfides have appeared, and no heavier chalcogenides are known. A series of cyclopentadienyl-based thiol complexes has been prepared by treating  $\text{Cp}_2\text{Mg}$  with three different alkanethiols (Scheme 20)<sup>89</sup>.

Each of the three complexes was obtained as a crystalline solid, but only the *t*-butyl derivative **73** has been structurally characterized. X-ray crystallography reveals a tetrameric cubane structure composed of four magnesium centers each coordinated to three sulfur atoms. Each magnesium center is additionally bonded to the  $\pi$ -face of a cyclopentadienyl ring. When THF or 4-*t*-butylpyridine is added to a solution of dichloromethane, two new complexes **74** and **75** are formed. Both compounds were found to be dimeric with central  $\text{Mg}_2\text{S}_2$  rings, as expected upon solvation of the cubane complex. The two dimeric aggregates have slightly different geometries. The cyclopentadienyl rings of the thf-coordinated dimer **74** are oriented in *cis* fashion whereas they are *trans* in the 4-*t*-butylpyridine-coordinated dimer **75**.

Limited reactivity studies of organomagnesium sulfides have also been conducted. These complexes have recently been employed as modified Grignard reagents in the cross-coupling of benzonitriles<sup>90</sup>. The advantage of these complexes over Grignard reagents is that nucleophilic addition across the nitrile is inhibited. The alkylmagnesium sulfide complexes shown in Scheme 21 were prepared *in situ* by transmetalation, then reacted with the appropriate benzonitrile species. The aryl alkanes were produced in good yields upon heating the THF solutions at reflux overnight.



SCHEME 20



SCHEME 21

## IV. REFERENCES

1. R. E. Mulvey, *Organometallics*, **25**, 1060 (2006).
2. R. E. Mulvey, F. Mongin, M. Uchiyama and Y. Kondo, *Angew. Chem., Int. Ed.*, **46**, 3802 (2007).
3. L. Menunier, *Compt. Rend.*, **136C**, 758 (1903).
4. V. R. Magnuson and G. D. Stucky, *Inorg. Chem.*, **8**, 1427 (1969).
5. L. M. Engelhardt, B. S. Jolly, P. C. Junk, C. L. Raston, B. W. Skelton and A. H. White, *Aust. J. Chem.*, **39**, 1337 (1986).
6. R. Han, A. Looney and G. Parkin, *J. Am. Chem. Soc.*, **111**, 7276 (1989).
7. R. Han and G. Parkin, *J. Am. Chem. Soc.*, **112**, 3662 (1990).
8. R. Han and G. Parkin, *Organometallics*, **10**, 1010 (1991).
9. R. Han and G. Parkin, *Polyhedron*, **9**, 2655 (1990).
10. J. L. Kisko, T. Fillebeen, T. Hascall and G. Parkin, *J. Organomet. Chem.*, **596**, 22 (2000).
11. M. H. Chisholm, N. W. Eilerts, J. C. Huffman, S. S. Iyer, M. Pacold and K. Phomphrai, *J. Am. Chem. Soc.*, **122**, 11845 (2000).
12. N. Kuhn, M. Schulten, R. Boese and D. Bläser, *J. Organomet. Chem.*, **421**, 1 (1991).
13. M. M. Olmstead, W. J. Grigsby, D. R. Chacon, T. Hascall and P. P. Power, *Inorg. Chim. Acta*, **251**, 273 (1996).
14. V. C. Gibson, J. A. Segal, A. J. P. White and D. J. Williams, *J. Am. Chem. Soc.*, **122**, 7120 (2000).
15. P. J. Bailey, C. M. Dick, S. Fabre and S. Parsons, *J. Chem. Soc., Dalton Trans.*, 1655 (2000).
16. H. Hao, H. W. Roesky, Y. Ding, C. Cui, M. Schormann, H.-G. Schmidt, M. Noltemeyer and B. Žemva, *J. Fluorine Chem.*, **115**, 143 (2002).
17. P. J. Bailey, R. A. Coxall, C. M. Dick, S. Fabre, L. C. Henderson, C. Herber, S. T. Liddle, D. Loroño-González, A. Parkin and S. Parsons, *Chem. Eur. J.*, **9**, 4820 (2003).
18. L. F. Sánchez-Barba, D. L. Hughes, S. M. Humphrey and M. Bochmann, *Organometallics*, **25**, 1012 (2006).
19. P. J. Bailey, R. A. Coxall, C. M. Dick, S. Fabre and S. Parsons, *Organometallics*, **20**, 798 (2001).
20. P. J. Bailey, S. T. Liddle, C. A. Morrison and S. Parsons, *Angew. Chem., Int. Ed.*, **40**, 4463 (2001).
21. P. J. Bailey, R. A. Coxall, C. M. Dick, S. Fabre, S. Parsons and L. J. Yellowlees, *Chem. Commun.*, 4563 (2005).
22. P. J. Bailey, C. M. Dick, S. Fabre, S. Parsons and L. J. Yellowlees, *Dalton Trans.*, 1602 (2006).
23. W. Vargas, U. Englich and K. Ruhlandt-Senge, *Inorg. Chem.*, **41**, 5602 (2002).
24. H. Sachdev and C. Preis, *Eur. J. Inorg. Chem.*, 1495 (2002).

25. K.-C. Yang, C.-C. Chang, J.-Y. Huang, C.-C. Lin, G.-H. Lee, Y. Wang and M. Y. Chiang, *J. Organomet. Chem.*, **648**, 176 (2002).
26. N. Etkin, C. M. Ong and D. W. Stephan, *Organometallics*, **17**, 3656 (1998).
27. A. Xia, M. J. Heeg and C. H. Winter, *Organometallics*, **21**, 4718 (2002).
28. A. Xia, H. M. El-Kaderi, M. J. Heeg and C. H. Winter, *J. Organomet. Chem.*, **682**, 224 (2003).
29. H. M. El-Kaderi, A. Xia, M. J. Heeg and C. H. Winter, *Organometallics*, **23**, 3488 (2004).
30. M. Westerhausen, T. Bollwein, N. Makropoulos, S. Schneiderbauer, M. Suter, H. Nöth, P. Mayer, H. Piotrowski, K. Polborn and A. Pfitzner, *Eur. J. Inorg. Chem.*, 389 (2002).
31. K. H. Yong and J. M. Chong, *Org. Lett.*, **4**, 4139 (2002).
32. I. L. Fedushkin, A. A. Skatova, M. Hummert and H. Schumann, *Eur. J. Inorg. Chem.*, 1601 (2005).
33. I. J. Blackmore, V. C. Gibson, P. B. Hitchcock, C. W. Rees, D. J. Williams and A. J. P. White, *J. Am. Chem. Soc.*, **127**, 6012 (2005).
34. T. Chivers, C. Fedorchuk and M. Parvez, *Organometallics*, **24**, 580 (2005).
35. B. Conway, E. Hevia, A. R. Kennedy, R. E. Mulvey and S. Weatherstone, *Dalton Trans.*, 1532 (2005).
36. J. Lewiński, M. Dranka, I. Kraszewska, W. Sliwiński and I. Justyniak, *Chem. Commun.*, 4935 (2005).
37. M. Westerhausen, T. Bollwein, N. Makropoulos and H. Piotrowski, *Inorg. Chem.*, **44**, 6439 (2005).
38. E. P. Squiller, A. D. Pajerski, R. R. Whittle, and H. G. Richey, Jr., *Organometallics*, **25**, 2465 (2006).
39. G. E. Coates and D. Ridley, *J. Chem. Soc. A*, 56 (1967).
40. E. C. Ashby, L. C. Chao and H. M. Neumann, *J. Am. Chem. Soc.*, **95**, 5186 (1973).
41. K. W. Henderson, R. E. Mulvey, W. Clegg and P. A. O'Neil, *J. Organomet. Chem.*, **439**, 237 (1992).
42. D. R. Armstrong, K. W. Henderson, M. MacGregor, R. E. Mulvey, M. J. Ross, W. Clegg and P. A. O'Neil, *J. Organomet. Chem.*, **486**, 79 (1995).
43. J. Prust, K. Most, I. Müller, E. Alexopoulos, A. Stasch, I. Usón and H. W. Roesky, *Z. Anorg. Allg. Chem.*, **627**, 2032 (2001).
44. A. P. Dove, V. C. Gibson, P. Hormnirum, E. L. Marshall, J. A. Segal, A. J. P. White and D. J. Williams, *Dalton Trans.*, 3088 (2003).
45. P. J. Bailey, D. Loroño-González and S. Parsons, *Chem. Commun.*, 1426 (2003).
46. E. Hevia, A. R. Kennedy, R. E. Mulvey and S. Weatherstone, *Angew. Chem., Int. Ed.*, **43**, 1709 (2004).
47. K. W. Henderson, R. E. Mulvey and A. E. Dorigo, *J. Organomet. Chem.*, **518**, 139 (1996).
48. I. L. Fedushkin, N. M. Khvoynova, A. A. Skatova, and G. K. Fukin, *Angew. Chem., Int. Ed.*, **42**, 5223 (2003).
49. C. F. Caro, P. B. Hitchcock, and M. F. Lappert, *Chem. Commun.*, 1433 (1999).
50. P. C. Andrikopoulos, D. R. Armstrong, H. R. L. Barley, W. Clegg, S. H. Dale, E. Hevia, G. W. Honeyman, A. R. Kennedy and R. E. Mulvey, *J. Am. Chem. Soc.*, **127**, 6184 (2005).
51. M. Uchiyama, Y. Matsumoto, D. Nobuto, T. Furuyama, K. Yamaguchi and K. Morokuma, *J. Am. Chem. Soc.*, **128**, 8748 (2006).
52. R. Han and G. Parkin, *J. Am. Chem. Soc.*, **114**, 748 (1992).
53. U. M. Dzhemilev and O. S. Vostrikova, *J. Organomet. Chem.*, **285**, 43 (1985).
54. P. E. Eaton, C.-H. Lee and Y. Xiong, *J. Am. Chem. Soc.*, **111**, 8016 (1989).
55. H. Böhlend, F. R. Hofmann, W. Hanay and H. J. Berner, *Z. Anorg. Allg. Chem.*, **577**, 53 (1989).
56. M.-X. Zhang and P. E. Eaton, *Angew. Chem., Int. Ed.*, **41**, 2169 (2002).
57. P. E. Eaton, M. X. Zhang, N. Komiya, C. G. Yang, I. Steele and R. Gilardi, *Synlett*, 1275, (2003).
58. J. Xu, N. Jain and Z. Sui, *Tetrahedron Lett.*, **45**, 6399 (2004).
59. J. F. Allan, W. Clegg, K. W. Henderson, L. Horsburgh and A. R. Kennedy, *J. Organomet. Chem.*, **559**, 173 (1998).
60. R. Han and G. Parkin, *J. Organomet. Chem.*, **393**, C43 (1990).
61. J. F. Allan, K. W. Henderson, A. R. Kennedy and S. J. Teat, *Chem. Commun.*, 1059 (2000).
62. Z. S. Sales, R. Nassar, J. J. Morris and K. W. Henderson, *J. Organomet. Chem.*, **690**, 3474 (2005).
63. E. L. Carswell, D. Hayes, K. W. Henderson, W. J. Kerr and C. J. Russell, *Synlett*, 1017 (2003).

64. M. J. Bassindale, J. J. Crawford, K. W. Henderson and W. J. Kerr, *Tetrahedron Lett.*, **45**, 4175 (2004).
65. K. W. Henderson, W. J. Kerr and J. H. Moir, *Tetrahedron*, **58**, 4573 (2002).
66. J. D. Anderson, P. García García, D. Hayes, K. W. Henderson, W. J. Kerr, J. H. Moir and K. Pai Fondekar, *Tetrahedron Lett.*, **42**, 7111 (2001).
67. K. W. Henderson, W. J. Kerr and J. H. Moir, *Chem. Commun.*, 479 (2000).
68. E. C. Ashby and G. F. Willard, *J. Org. Chem.*, **43**, 4094 (1978).
69. M. F. Reetz, N. Harmat and R. Mahrwald *Angew. Chem., Int. Ed. Engl.*, **31**, 342 (1992).
70. K. W. Henderson, J. R. Allan and A. R. Kennedy, *J. Chem. Soc., Chem. Commun.*, 1149 (1997).
71. M. P. Sibi and Y. Asano, *J. Am. Chem. Soc.*, **123**, 9708 (2001).
72. M. Westerhausen, M. H. Digeser, H. Nöth, T. Seifert and A. Pfitzner, *J. Am. Chem. Soc.*, **120**, 6722 (1998).
73. S. Blair, K. Izod, W. Clegg and R. W. Harrington, *Eur. J. Inorg. Chem.*, 3319 (2003).
74. E. Hey, L. M. Engelhardt, C. L. Raston and A. H. White, *Angew. Chem., Int. Ed. Engl.*, **26**, 81 (1987).
75. M. Westerhausen and A. Pfitzner, *J. Organomet. Chem.*, **479**, 141 (1994).
76. K. W. Henderson, G. W. Honeymoon, A. R. Kennedy, R. E. Mulvey, J. A. Parkinson and D. C. Sherrington, *Dalton Trans.*, 1365 (2003).
77. S. C. Cole, M. P. Coles and P. B. Hitchcock, *Organometallics*, **23**, 5159 (2004).
78. A. D. Pajerski, E. P. Squiller, M. Parvez, R. R. Whittle and H. G. Richey, Jr., *Organometallics*, **24**, 809 (2005).
79. M. M. Sung, C. G. Kim, J. Kim and Y. Kim, *Chem. Mater.*, **14**, 826 (2002).
80. B. Conway, E. Hevia, A. R. Kennedy, R. E. Mulvey and S. Weatherstone, *Dalton Trans.*, 1532 (2005).
81. E. P. Squiller, R. R. Whittle and H. G. Richey, Jr. *Organometallics*, **4**, 1154 (1985).
82. E. Hevia, A. R. Kennedy, R. E. Mulvey and S. Weatherstone, *Angew. Chem., Int. Ed.*, **43**, 1709 (2004).
83. E. C. Ashby, J. Nackashi and G. E. Paris, *J. Am. Chem. Soc.*, **97**, 3162 (1975).
84. O. N. D. Mackey and C. P. Morley, *J. Organomet. Chem.*, **426**, 279 (1992).
85. S. Gupta, S. Sharma and A. K. Narula, *J. Organomet. Chem.*, **452**, 1 (1993).
86. P. N. Kapoor, A. K. Bhagi, H. K. Sharma and R. N. Kapoor, *J. Organomet. Chem.*, **369**, 281 (1989).
87. G. E. Coates, J. A. Heslop, M. E. Redwood and D. Ridley, *J. Chem. Soc. A*, 1118 (1968).
88. F. F. Fleming, V. Gudipati and O. W. Steward, *Tetrahedron*, **59**, 5585 (2003).
89. A. Xia, M. J. Heeg and C. H. Winter, *J. Organomet. Chem.*, **669**, 37 (2003).
90. J. A. Miller and J. W. Dankwardt, *Tetrahedron Lett.*, **44**, 1907 (2003).

## CHAPTER 11

# Preparation and reactivity of magnesium enolates

CLAUDE GRISON

UMR CNRS-Université de Montpellier 2 5032, ENSCM, 8 rue de l'Ecole Normale,  
F-34296 Montpellier, France  
Fax: +33-4-67-14-43-42; e-mail: cgrison@univ-montp2.fr

---

I. INTRODUCTION . . . . .	438
II. PREPARATION OF MAGNESIUM ENOLATES . . . . .	438
A. Reductive Metal Insertion into Carbon–Halogen Bonds . . . . .	438
B. Permutation Heteroatom/Metal . . . . .	441
C. Permutational Metal/Metal Salts Interconversions (Transmetallations) . . . . .	445
D. Conjugate Addition . . . . .	450
E. Permutational Hydrogen/Metal Interconversions (Metallations) . . . . .	457
F. Miscellaneous Methods . . . . .	471
III. REACTIVITY OF ENOLATES . . . . .	472
A. Introduction . . . . .	472
B. Reactions of Magnesium Ketone Enolates with Electrophiles . . . . .	472
C. Reactions of Magnesium Ester Enolates and Magnesium Lactone Enolates with Electrophiles . . . . .	484
D. Reactions of Magnesium Dicarboxyl Enolates with Electrophiles . . . . .	489
1. Reactions of magnesium $\alpha$ -ketoester enolates . . . . .	489
2. Reactions of magnesium chelates of $\beta$ -ketoesters or $\beta$ -diketones . . . . .	493
3. Reactions of magnesium dialkyl malonate or magnesium hydrogen alkyl malonate . . . . .	494
E. Reactions of Magnesium Amide and Lactam Enolates with Electrophiles . . . . .	499
F. Reactions of Magnesium Thioesters and Thioamide Enolates with Electrophiles . . . . .	500
G. Reactions of Carboxylic Acid Dianions with Electrophiles . . . . .	503
H. Reactions with Anions of Chiral Oxazolidinones and Derivatives with Electrophiles . . . . .	503
I. Reactions of Miscellaneous Magnesium Chiral Enolates . . . . .	505
IV. REFERENCES . . . . .	506

---

*The chemistry of organomagnesium compounds*

Edited by Z. Rapoport and I. Marek © 2008 John Wiley & Sons, Ltd. ISBN: 978-0-470-05719-3

## I. INTRODUCTION

Enolate anions are among the most important synthetic intermediates, largely because of their great utility to form carbon–carbon bonds. In this field, lithium enolates have been used extensively in modern synthetic organic chemistry and asymmetric synthesis. Recently, increasing interest has been directed toward new developments of magnesium enolates that may be advantageous in chemio-, regio- and stereoselective transformations. Magnesium enolates are highly suitable metal synthons. Using a divalent metal reagent allows one to formally bond two chiral ligands to the Mg center. Moreover, this higher degree of covalency leads to simpler and more stable systems than lithium analogues. Because they are good candidates in stereoselective carbon–carbon bond formation, there is a need for a comprehensive survey covering new developments of magnesium enolates.

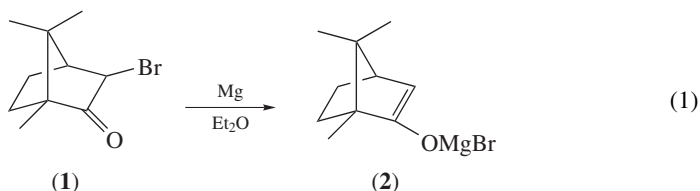
The chapter is organized under the headings *Preparation* and *Reactivity* of magnesium enolates.

## II. PREPARATION OF MAGNESIUM ENOLATES

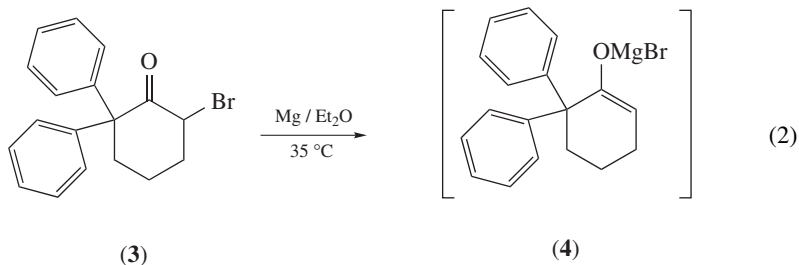
### A. Reductive Metal Insertion into Carbon–Halogen Bonds

Grignard reagents are usually prepared from the corresponding halides by reaction with metallic magnesium. This method has been used to prepare magnesium enolates of ketones. The problem with the reductive metal insertion in an  $\alpha$ -halo carbonyl compound is the presence of the electrophilic carbonyl function. Preparation of magnesium enolate by this route can lead to the formation of an intractable mixture of products, including addition, reduction or coupling of the substrate. Thus, the preparation of magnesium enolates with elemental magnesium is often described with highly sterically hindered bromo ketones, therefore minimizing the possibility of side reactions with the carbonyl group.

The action of magnesium on  $\alpha$ -halo ketone has been used by Malmgren, for the synthesis of bromomagnesium enolate **2** derived from 3-bromocamphor **1** (equation 1)<sup>1</sup>.

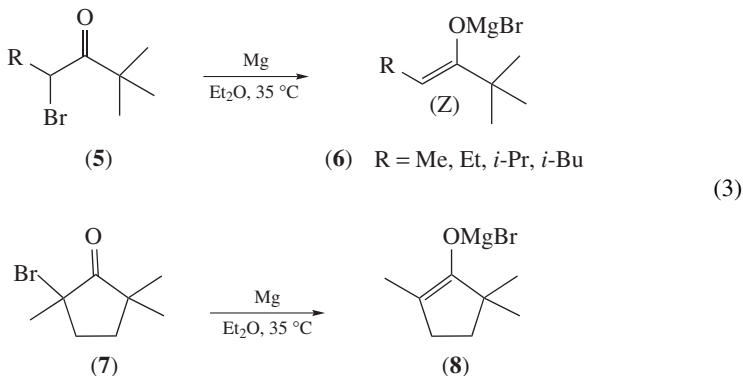


Similarly, the bromo magnesium enolate **4** of 2,2-diphenylcyclohexanone has been prepared by the action of magnesium on 6-bromo-2,2-diphenylcyclohexanone **3** (equation 2). A small amount of iodine is added to initiate the reaction. The enolate **4** is obtained in 79% yield after 15 min at reflux<sup>2</sup>.

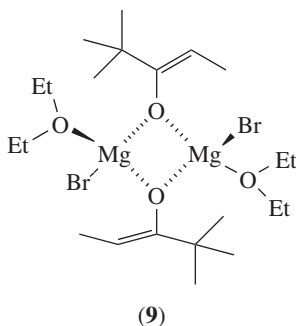


Colonge and Grenet have reported that this type of reaction may be utilized in the preparation of magnesium enolates from simple aliphatic  $\alpha$ -bromo ketones<sup>3</sup>.

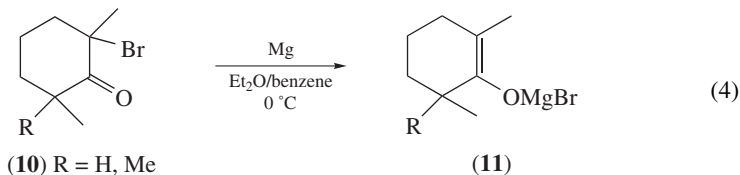
The treatment of  $\alpha$ -bromo *t*-butyl alkyl ketone **5** with magnesium gives almost exclusively the (*Z*)-enolate **6**. The process can be extended to cyclic systems, such as 2-bromo-2,5-trimethyl cyclopentanone **7** that leads to the enolate **8** (equation 3)<sup>4</sup>.



In diethyl ether, the bromo magnesium enolate derived from *t*-butyl ethyl ketone has been characterized as the dimer **9** with bridging enolate residues<sup>5</sup>.



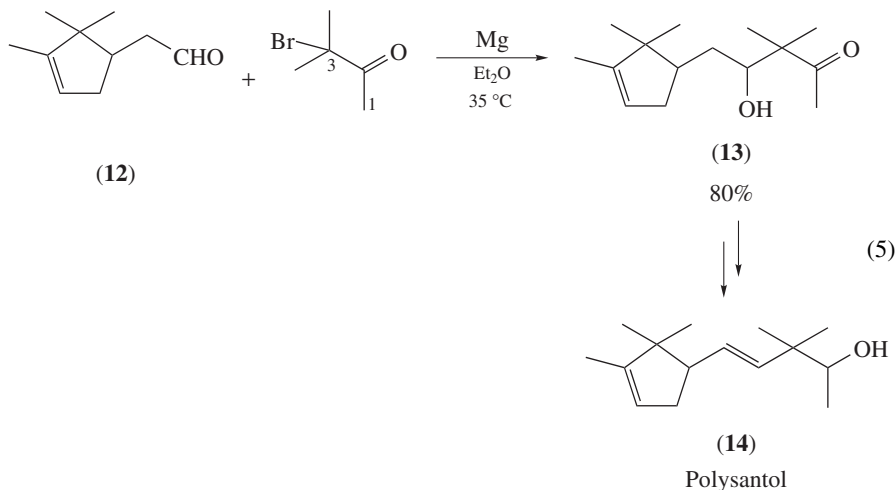
The procedure for the preparation of magnesium enolates from  $\alpha$ -bromo ketones does not need a particular purity or nature of the metal. Magnesium turnings are often convenient to use and sufficiently reactive in many cases. Thus, magnesium enolates **11** of 2,6-dimethyl- and 2,2,6-trimethylcyclohexanones are obtained by treatment of the corresponding 2-bromo ketones **10** with magnesium turnings in a benzene/ether mixture (equation 4). These magnesium reagents are prepared and used at  $0^\circ\text{C}$ , whereas the lithium and titanium analogues are obtained at  $-78^\circ\text{C}$ . These experimental conditions illustrate the higher thermal stability of the magnesium species<sup>6</sup>.





Side-reactions can sometimes be avoided by preparing the magnesium enolate in the presence of the electrophile.

Recently, Altarejos and coworkers have described the direct coupling of  $\alpha$ -campholenic aldehyde **12** with  $\alpha$ -bromoketone by a magnesium-mediated aldol-type reaction<sup>7</sup>. Thus, under conditions similar to a classical Grignard reaction, the reaction of 3-bromo-3-methyl-2-butanone with magnesium in refluxing diethyl ether generates the corresponding bromomagnesium enolate and subsequent coupling with  $\alpha$ -campholenic aldehyde **12** gives the  $\beta$ -hydroxyketone **13** (equation 5). In contrast to the direct aldolisation reaction between the  $\alpha$ -campholenic aldehyde and aliphatic ketones, the process allows the regioselective preparation of disubstituted keto-enolate and the aldol condensation through the sole carbon C-3. It limits the other aldol condensation product through the terminal carbon C-1, and opens an interesting route to the synthesis of the sandalwood-type odorant Polysantol **14**.

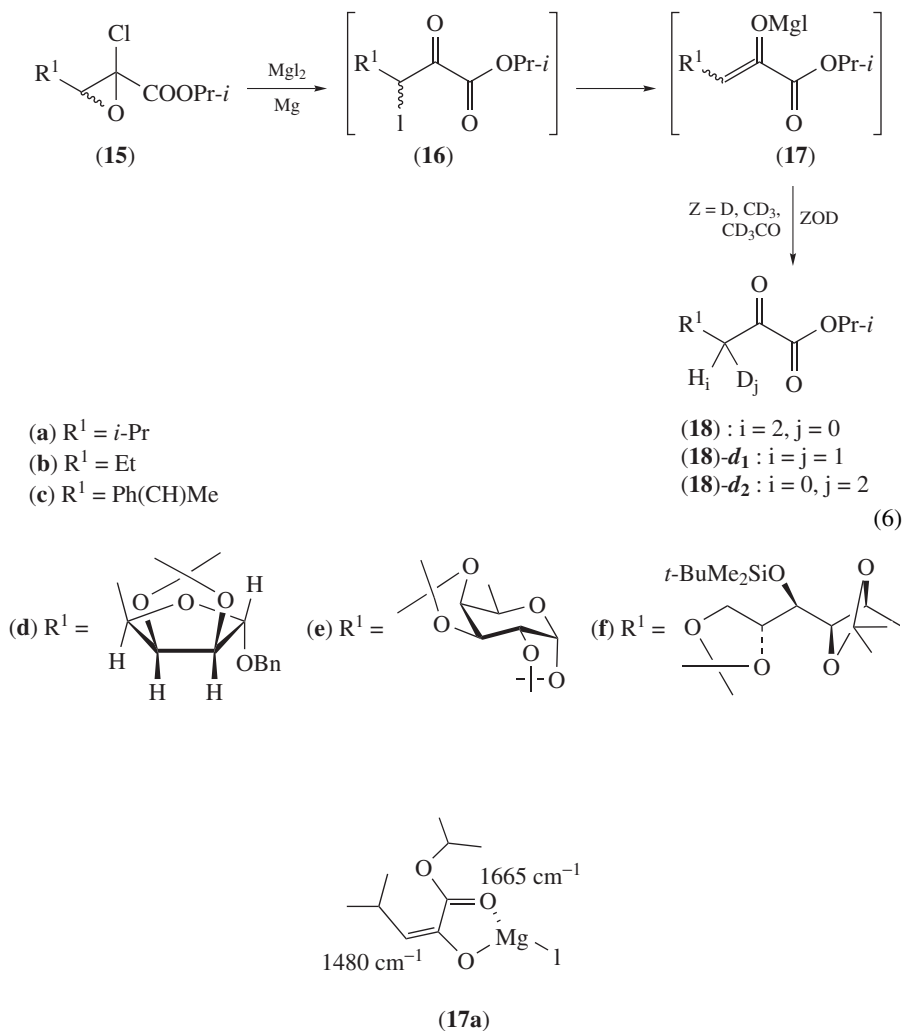


The authors have extended this methodology to other  $\alpha$ -bromoketones in order to determine the scope of the reaction and prepared several Polysantol structurally related compounds. Noteworthy is the excellent chemoselectivity without any side reactions on the aldehyde moiety.

Recently, a reductive magnesium insertion into a carbon–iodine bond of a  $\beta$ -iodo- $\alpha$ -ketoester has been described<sup>8</sup>. The preparation of the iodomagnesium enolate **17** derived from an  $\alpha$ -ketoester is the first preparation of such metallic species in this series. It was obtained from the reaction between the  $\beta$ -iodo- $\alpha$ -ketoester precursor **16** and magnesium. In this case, the form of the metal is critical and magnesium powder with a large surface area is necessary (equation 6).

The  $\beta$ -iodo- $\alpha$ -ketoester precursor **16** is previously obtained from the reaction between the  $\alpha$ -chloroglycidic ester **15** and  $\text{MgI}_2$  in ether. The  $\beta$ -iodo- $\alpha$ -ketoester **16** is not isolated and is *in situ* transformed into the iodomagnesium enolate **17** by the presence of the active magnesium produced during the preparation of  $\text{MgI}_2$  (the 2/1 magnesium–iodine ratio was used intentionally for the preparation of  $\text{MgI}_2$ )<sup>9</sup>.

The enolate structure of **17** is deduced from the IR data of the reaction medium as a result of the presence of absorption bands at  $1490\text{ cm}^{-1}$  for the  $\text{C}=\text{C}$  bond and  $1665\text{ cm}^{-1}$  for the  $\text{C}=\text{O}$  bond of the ester group, characteristic for an internal coordination of the enolate magnesium atom with the ester  $\text{C}=\text{O}$ <sup>9</sup>.



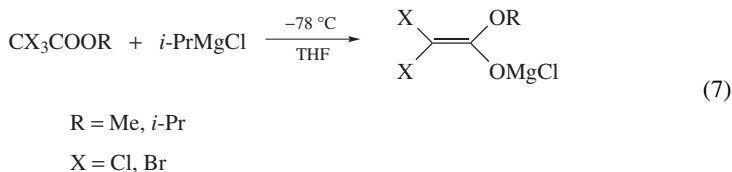
All prepared magnesium enolates **17** are stable in refluxing diethyl ether. Deuteration, and reactions with various electrophiles confirm their structure (see section III). It is noteworthy that the lithiated carbanion-enolate analogue, directly obtained by deprotonation of an  $\alpha$ -ketoester **18** with lithiated bases (LDA, for example), is not stable and immediately degrades in the medium, whatever the temperature. Comparatively, the magnesium chelate **17** shows a higher stability, which allows its preparation and synthetic applications.

## B. Permutation Heteroatom/Metal

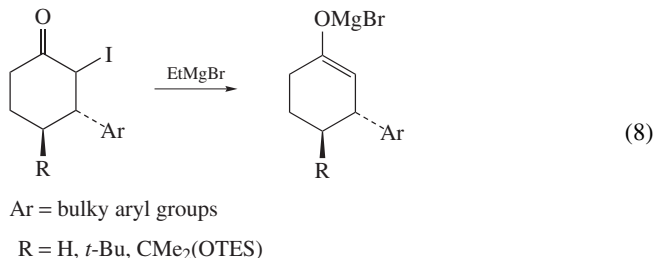
Metal-halogen interconversions are primarily used to prepare organolithium compounds from alkyl and aryl halides. Particular Grignard reagents can be prepared from this methodology. They often give better yields than reactions between halides and magnesium

metal due to less side reactions. This method has found applications in the preparation of magnesium enolates, even in the presence of functional groups.

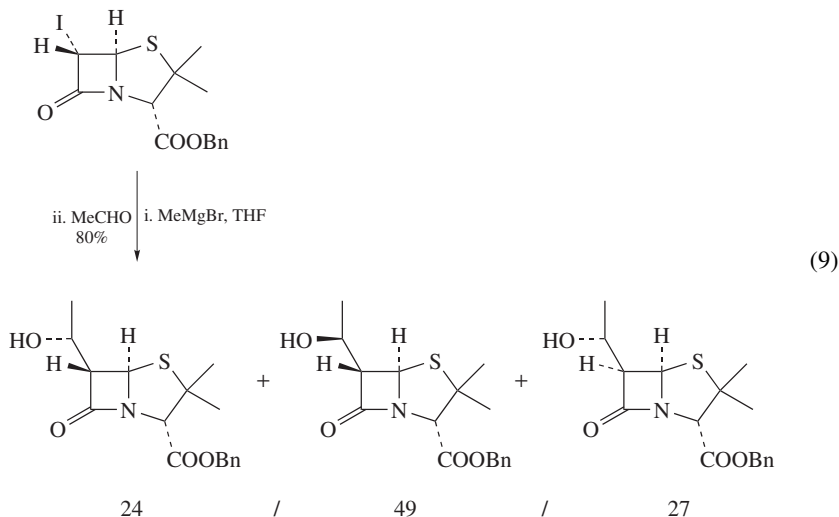
Several years ago, Castro, Villieras and coworkers described the preparation of the magnesium enolate derived from an alkyl  $\alpha,\alpha$ -dihaloacetate by halogen-metal exchange between isopropylmagnesium chloride and alkyl trihaloacetate. THF is required as solvent (equation 7)<sup>10</sup>.



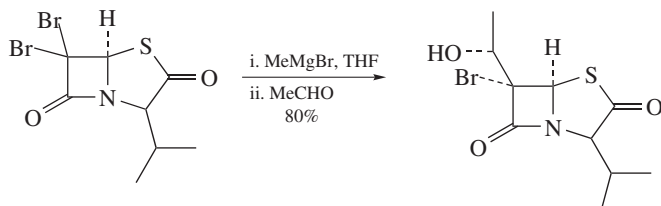
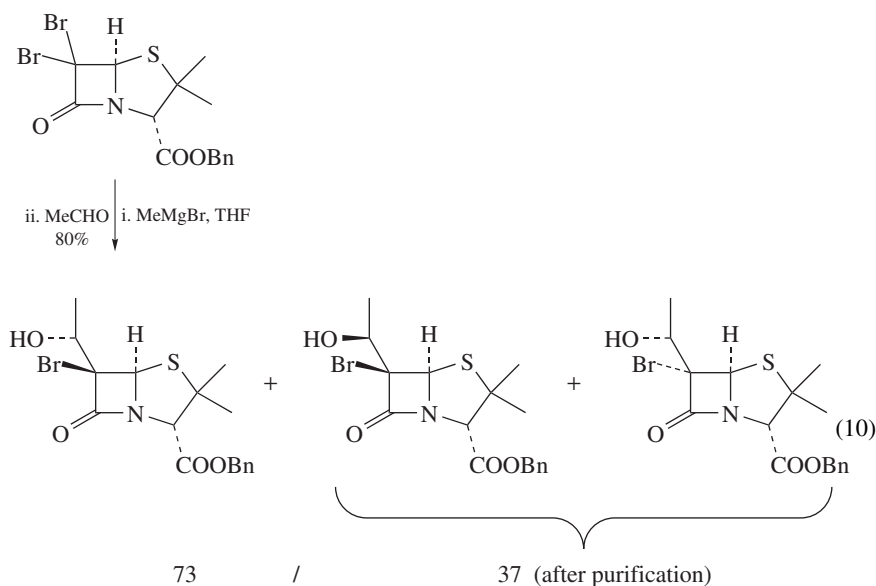
Different protocols have been tested to prepare enolates from  $\beta$ -aryl- $\alpha$ -iodoketones. Reactions using  $\text{Et}_3\text{B}/\text{Ph}_3\text{SnH}$  in benzene,  $\text{Et}_3\text{B}$  in benzene or ether and  $n\text{-BuLi}$  in ether failed to provide the corresponding enolates. Alternatively, the use of  $\text{EtMgBr}$  succeeds in generating reactive magnesium enolates from  $\alpha$ -iodo ketones. In most cases, the formation of the enolate in THF is cleaner than that in  $\text{Et}_2\text{O}$ <sup>11,12</sup> (equation 8).



This method has been used to prepare the antibiotic thienamycin. The magnesium enolate of the  $\beta$ -lactam was prepared from the 6-iodo derivative in THF (equation 9)<sup>4b</sup>.

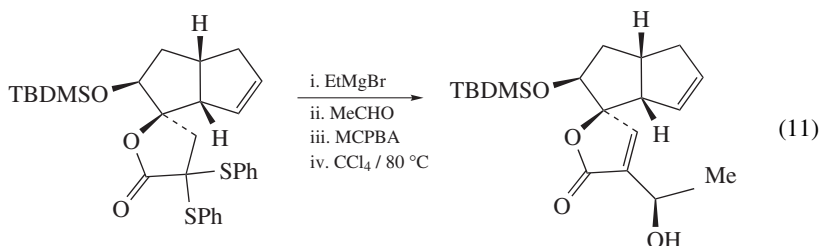


To increase the stereoselectivity of the aldol reaction, successful reaction of dibromo- $\beta$ -lactams with methylmagnesium bromide followed by addition of acetaldehyde has been studied (equation 10)<sup>4b</sup>.



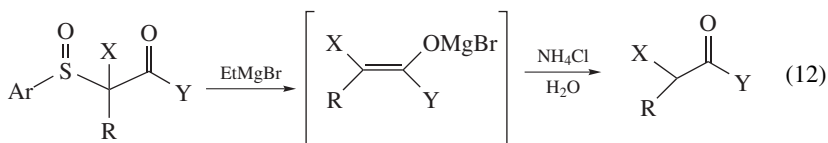
If the metal-halogen interconversions were originally used to prepare magnesium enolates, other heteroatoms than halogen can undergo the exchange. Sulfur atom is often employed.

For instance, Trost, Mao and coworkers use  $\alpha,\alpha$ -disulphenylated lactones as enolate precursors<sup>13</sup>. Reaction of ethylmagnesium bromide and  $\alpha,\alpha$ -di-(phenylthio)- $\gamma$ -butyrolactone provides such an enolate that is quenched by ethanal (equation 11).




The process has been employed with  $\alpha,\alpha$ -disulfonylated ketones, but it needs a catalytic amount of copper(I) bromide in the reaction mixture.

Ligand exchange reaction of sulfoxides has been reported as a novel method for the generation of magnesium enolates. Reaction of a sulfinyl group of  $\beta$ -keto-sulfoxides, sulfinylamides, sulfinylesters and sulfinylcarboxylic acids with ethylmagnesium bromide gives the corresponding magnesium enolates at low temperature<sup>14-17</sup> (equation 12). The results for EtMgBr-promoted desulfinylation of  $\alpha$ -halo- $\alpha$ -sulfinyl derivatives are summarized in Table 1 after quenching the magnesium enolates with aqueous  $\text{NH}_4\text{Cl}$ .



It should be noted that this desulfinylation is totally regioselective and gives the trisubstituted enolate. In the cases of  $\alpha$ -halo  $\alpha$ -sulfinyl ketones, reactions are carried out at  $-78^\circ\text{C}$  in  $\text{Et}_2\text{O}$  with 1.1 equivalent of ethylmagnesium bromide. Interesting results have been obtained with  $\alpha$ -fluoro-,  $\alpha$ -bromo- and  $\alpha$ -chloro  $\alpha$ -sulfinyl ketones. Because of the

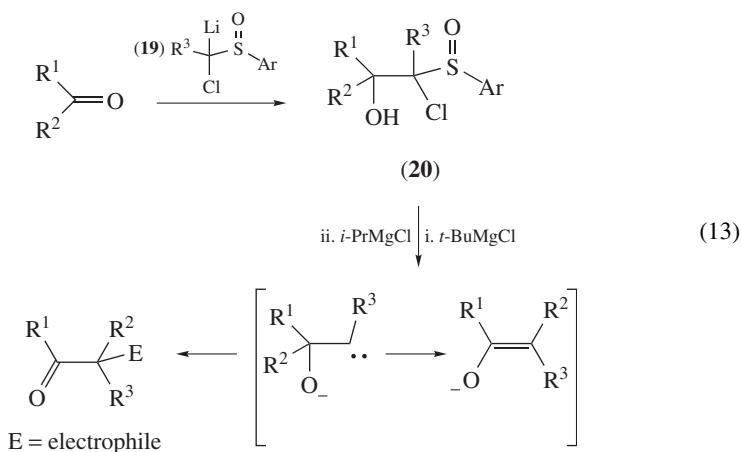
TABLE 1. Synthesis of  $\alpha$ -haloketones from  $\alpha$ -halosulfoxides

X	Ar	R	Y	Yield (%)
F	Ph	$(\text{CH}_2)_3\text{CH}_3$	$(\text{CH}_2)_2\text{Ph}$	79
F	Ph	$(\text{CH}_2)_3\text{CH}_3$	$(\text{CH}_2)_8\text{CH}_3$	90
F	Ph	$(\text{CH}_2)_3\text{CH}_3$	Ph	82
F	Ph	$(\text{CH}_2)_3\text{CH}_3$	<i>c</i> -Hex	85
Cl	<i>p</i> -Tol	$(\text{CH}_2)_3\text{CH}_3$	$(\text{CH}_2)_2\text{Ph}$	91
Cl	<i>p</i> -Tol	$(\text{CH}_2)_3\text{CH}_3$	$(\text{CH}_2)_8\text{CH}_3$	93
Cl	<i>p</i> -Tol	$(\text{CH}_2)_3\text{CH}_3$	Ph	78
Cl	Ph	$(\text{CH}_2)_3\text{CH}_3$	<i>c</i> -Hex	95
Br	<i>p</i> -Tol	$(\text{CH}_2)_3\text{CH}_3$	$(\text{CH}_2)_2\text{Ph}$	68
Br	Ph	$(\text{CH}_2)_3\text{CH}_3$	$(\text{CH}_2)_8\text{CH}_3$	70
Br	Ph	$(\text{CH}_2)_3\text{CH}_3$	Ph	56
Br	Ph	$(\text{CH}_2)_3\text{CH}_3$	<i>c</i> -Hex	59
F	<i>p</i> -Tol	$(\text{CH}_2)_2\text{Ph}$	H	82
F	<i>p</i> -Tol	$(\text{CH}_2)_9\text{CH}_3$	H	95
Cl	Ph	$(\text{CH}_2)_2\text{Ph}$	H	73
Cl	Ph	$(\text{CH}_2)_9\text{CH}_3$	H	91
Cl	<i>p</i> -Tol	$(\text{CH}_2)_2\text{CH}_3$	CON 	78
Cl	<i>p</i> -Tol	$(\text{CH}_2)_2\text{CH}_3$	CONH $(\text{CH}_2)_5\text{CH}_3$	73
Cl	<i>p</i> -Tol	$(\text{CH}_2)_2\text{CH}_3$	CONHCH <sub>2</sub> Ph	80
Cl	<i>p</i> -Tol	$(\text{CH}_2)_2\text{CH}_3$	CONH <sub>2</sub>	78
F	<i>p</i> -Tol	CH <sub>2</sub> -Ph	COOEt	60
F	<i>p</i> -Tol	$(\text{CH}_2)_9\text{CH}_3$	COOEt	58
Cl	<i>p</i> -Tol	CH <sub>2</sub> -Ph	COOEt	72
Cl	<i>p</i> -Tol	$(\text{CH}_2)_9\text{CH}_3$	COOEt	91
Cl	<i>p</i> -Tol	CH <sub>2</sub> -Ph	COOBu- <i>i</i>	93
Cl	<i>p</i> -Tol	$(\text{CH}_2)_9\text{CH}_3$	COOBu- <i>i</i>	67
Cl	<i>p</i> -Tol	CH <sub>3</sub>	COOH	67

unstable nature of the products containing bromine, the yields for the synthesis of  $\alpha$ -bromoketones are lower than for other  $\alpha$ -haloketones.

With  $\alpha$ -chloro  $\alpha$ -sulfinylcarboxylic acids and their derivatives, the optimal conditions are different. Treatment of primary or secondary  $\alpha$ -chloro  $\alpha$ -sulfinylamides with 3 equivalents of EtMgBr in THF at  $-78^\circ\text{C}$  for 10 min gives cleanly the desulfinylated  $\alpha$ -chloroamides in good yields. An excess of Grignard reagent is necessary for completion of the reaction. Similar conditions (EtMgBr, 2 equiv/ $-78^\circ\text{C}$ /THF) for the  $\alpha$ -chloro  $\alpha$ -sulfinylesters give  $\alpha$ -chloroesters with better yields. It is worth noting that even  $\alpha$ -chloro  $\alpha$ -sulfinylcarboxylic acid gives  $\alpha$ -chloropropionic acid.

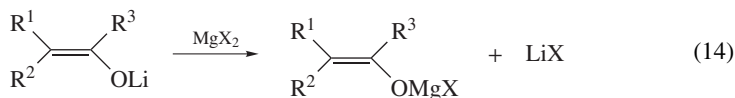
The reductive removal of a sulfinyl group to prepare magnesium enolates is also mentioned from  $\alpha$ -chloro- $\beta$ -hydroxy sulfoxides **20**. These latter are obtained by reaction between lithium carbanions derived from 1-chloroalkyl *p*-tolyl sulfoxides **19** and carbonyl compounds. These substrates are treated with *t*-BuMgCl to give magnesium alkoxides, which reacted with *i*-PrMgCl to afford the magnesium enolates via the rearrangement of  $\beta$ -oxido carbenoids<sup>18</sup> (equation 13).



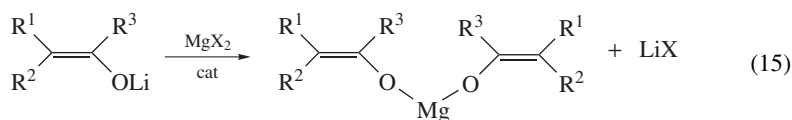
### C. Permutational Metal/Metal Salts Interconversions (Transmetalations)

The preparation of magnesium enolate by addition of one equivalent of magnesium dihalide to a solution of lithium enolate is a commonly used procedure.

The reactions covered in this section may be represented for convenience by equation 14.



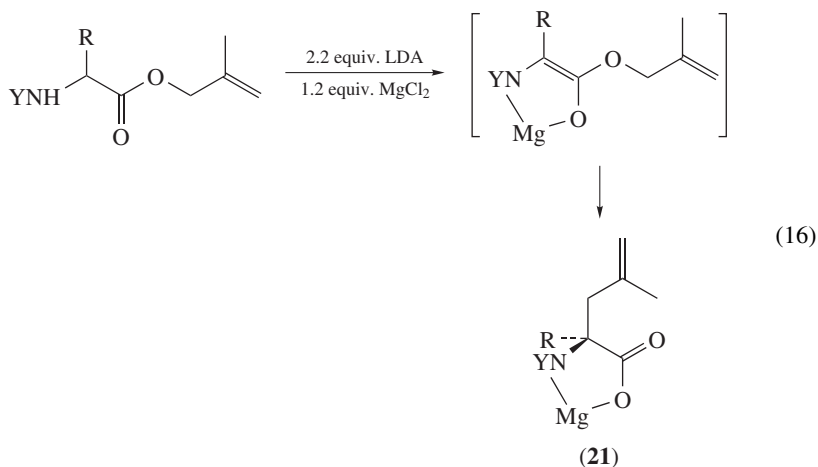
MgX<sub>2</sub> can be used in catalytic amount and leads to magnesium dienolate (equation 15).



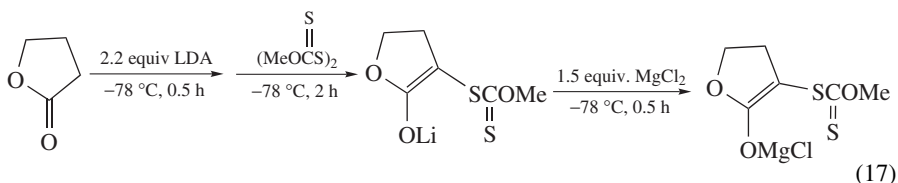
It should be emphasized that, in many cases, these equations are oversimplified. In many of the reported examples, the produced enolate is used *in situ*, and its real structure and nature of the counterion (Mg or Li) are obscured.

However, the formation of a conformationally rigid chelate with a fixed geometry is generally admitted in the transmetalation of organolithiums with magnesium halides. That explains the stability of the enolate and the stereoselectivity of its reactions.

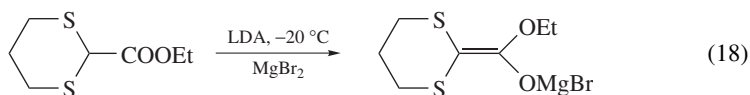
Some synthetic applications of this methodology are the synthesis of sterically high demanding  $\alpha$ -alkylated unsaturated amino acids **21**. Deprotonation of allylic *N*-protected aminoesters with LDA at  $-78^\circ\text{C}$  and subsequent addition of  $\text{MgCl}_2$  result in the formation of a chelated magnesium enolate (equation 16). In contrast to the corresponding lithium enolates, which decompose by warming, the chelate magnesium enolates are more stable and can be used for stereoselective ester enolate Claisen rearrangements<sup>19</sup>.

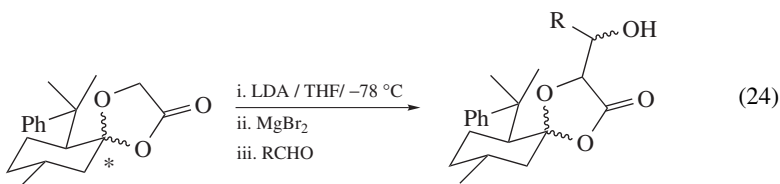
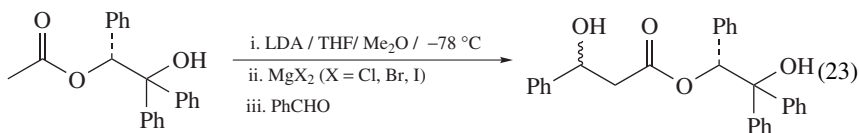
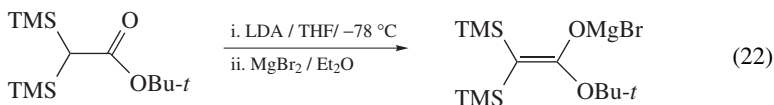
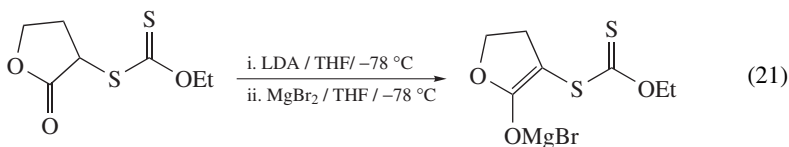
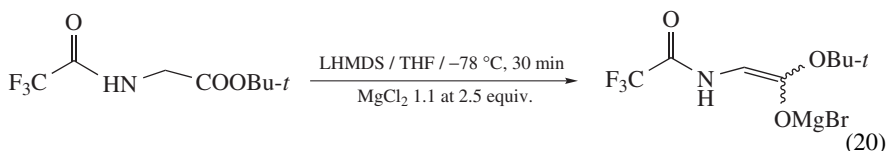
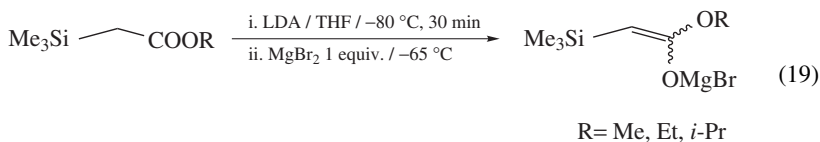


The method has been extended to other polyfunctional systems, such as *O*-ethyl *S*-(tetrahydro-2-oxo-3-furanyl)dithiocarbonate. Treatment of  $\gamma$ -butyrolactone with bis [methoxy(thiocarbonyl)]disulfide in the presence of 2.2 equivalents of lithium diisopropylamide at  $-78^\circ\text{C}$  in THF provides the lithium enolate which reacts with  $\text{MgCl}_2$  to furnish the magnesium enolate<sup>20</sup> (equation 17).



Reactions presented below show that this method is used frequently to prepare magnesium enolates derived from functionalized carboxylic esters or lactones<sup>21–23,4</sup> (equations 18–24, Tables 2 and 3).





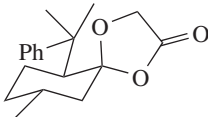
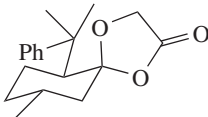
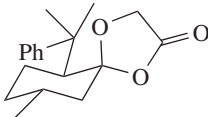
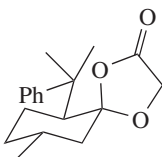
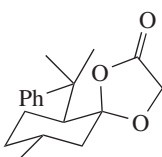
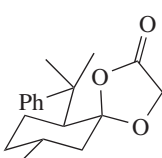
The chelation between a Boc group and Mg(II) is often used to control the stereochemistry in aldol reactions. For instance, Donohoe and House have reported the diastereoselective reductive aldol reactions of Boc-protected electron-deficient pyrroles. The key step of the synthesis is the preparation of an exocyclic magnesium enolate of Boc-protected 2-substituted pyrroles<sup>24</sup>.

TABLE 2. Aldol stereochemistry of chiral acetates

X	dr
Cl	96/4
Br	97/3
I	98/2



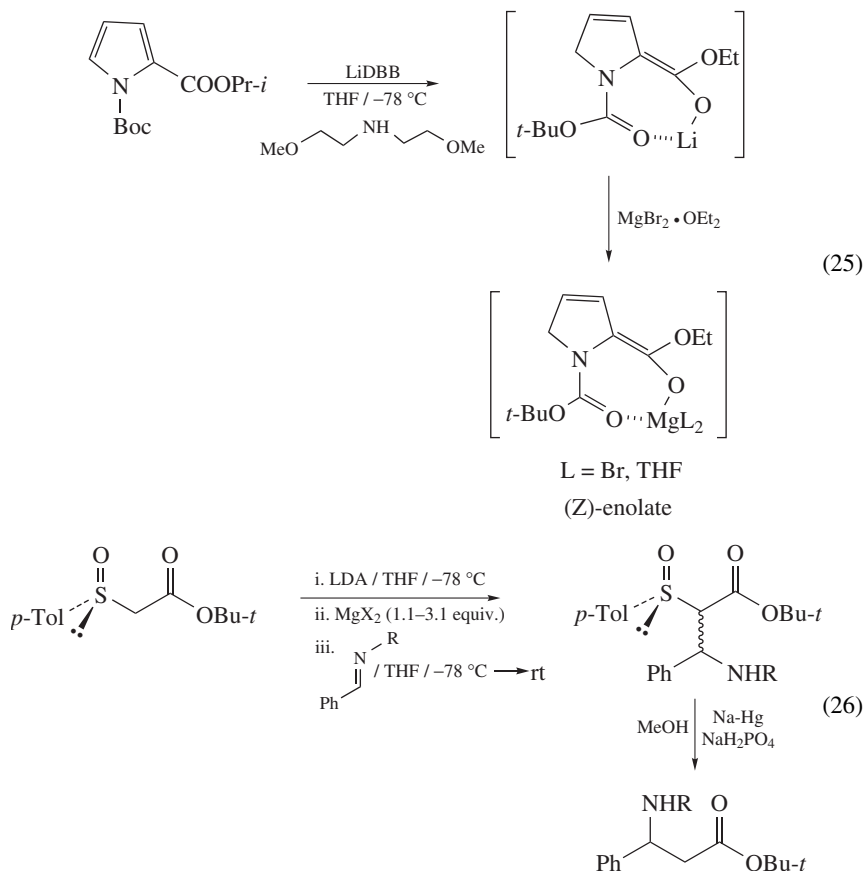
TABLE 3. Yields and aldol stereochemistry of chiral dioxolones

Dioxolone	R	Yield (%)	dr
	Ph	92	83/17
	<i>n</i> -Pr	86	90/10
	<i>i</i> -Pr	86	73/27
	Ph	89	75/25
	<i>n</i> -Pr	92	74/26
	<i>i</i> -Pr	89	89/11

Once the substrate is reduced by a LiDBB (4,4'-di-*tert*-butyl-biphenyllithium) solution, the transmetallation of the produced lithium enolate is performed with 1 equiv. of the complex magnesium bromide-diethyl ether ( $\text{MgBr}_2$ ,  $\text{Et}_2\text{O}$ ) leading to the chelated (*Z*)-magnesium enolate (equation 25).

Enantiomerically pure sulfoxides have been investigated as precursors of  $\alpha$ -sulfinyl carbanions for asymmetric synthesis. The results are rationalized in terms of chelated intermediates. In the case of the addition of  $\beta$ -sulfinyl ester enolates on benzaldimines, interesting and surprising results were obtained with magnesium enolates<sup>25</sup>. The preparation of these magnesium enolates is based on the transmetallation of the corresponding lithium species (equation 26). The reaction is carried out by a successive deprotonation of the  $\beta$ -sulfinyl ester with LDA, and a subsequent addition of  $\text{MgX}_2$  ( $\text{MgBr}_2 \cdot \text{OEt}_2$  or  $\text{MgI}_2$ ) to the lithium enolate. The imine is added to the resulting magnesium species at  $-78^\circ\text{C}$ .

Bromo- and iodomagnesium enolates lead to different diastereoselections (Table 4). The discrepancy results from the difference of the Lewis acidity between magnesium bromide and magnesium iodide, and the bulkiness of the halogen atoms. The possible transition states of this asymmetric addition are presented in Section III. Most probably the reaction proceeds through a chelated model with bromomagnesium enolates, and through a nonchelated model with two equivalents of magnesium iodide<sup>25</sup>.

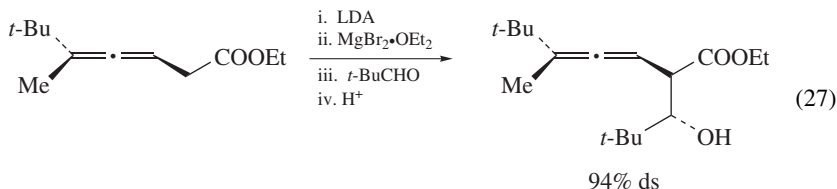


Transfer of chirality in aldol reactions has been attempted using  $\beta$ -allenyl ester enolates. These ambident nucleophiles have an axis of chirality, and such compounds have been less utilized in stereoselective reactions. They are prepared by transmetalation of the

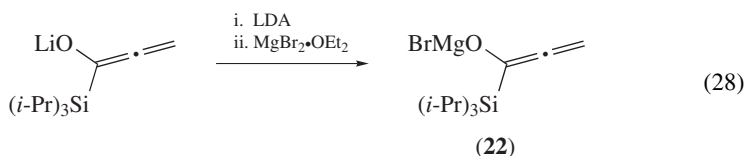
TABLE 4. Yields and selectivities of asymmetric addition of  $\alpha$ -sulfinyl ester enolate with benzaldimines

X	R	Yield (%)	dr
Br	Ts, COOMe	99	91/9
I	Ts, COOMe	81	30/70

lithium enolate with magnesium bromide etherate and are used in stereoselective aldol reaction (equation 27)<sup>26</sup>.

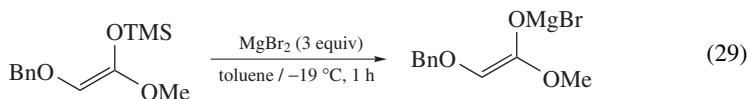


Other magnesium allenyl enolates, such as **22**, obtained by transmetalation of the lithium species have been used successfully in the preparation of  $\alpha,\beta$ -unsaturated acyl silanes (equation 28)<sup>27</sup>.

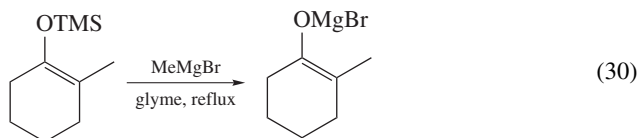


It should be noted that the sequence deprotonation/reverse Brook rearrangement between the triisopropylsilyloxy allene and isopropylmagnesium chloride in THF does not provide the magnesium enolate.

Permutational silicon/magnesium salts interconversion can occur with silylenol ethers. Indeed, several metal salts such as  $\text{TiCl}_4$  and  $\text{Bu}_2\text{BOTf}$  are known to promote the corresponding trialkylsilyl/metal salt exchange with silylenol ether, and consequently this reaction is called a transmetalation reaction. This type of reaction with magnesium salts has been reported recently by Mukaiyama (equation 29)<sup>28</sup>. The reaction is carried out with  $\text{MgBr}_2\cdot\text{OEt}_2$  in toluene at  $-19^\circ\text{C}$ . It has to be noted that the magnesium enolate is not formed if the silylenol ether is treated with  $\text{MgI}_2$ ,  $\text{MgCl}_2$ ,  $\text{Mg}(\text{OTf})_2$  or  $\text{Mg}(\text{ClO}_4)_2$ .



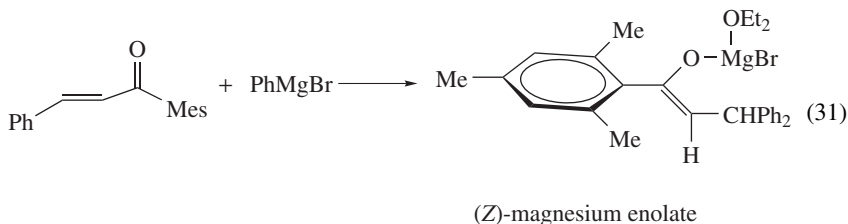
An additional silicon/magnesium exchange reaction of silylenol ether with alkyl Grignard reagents was reported. Such reaction is generally employed for the regiospecific generation of magnesium enolates from the corresponding silyl enolate (equation 30)<sup>4a</sup>.



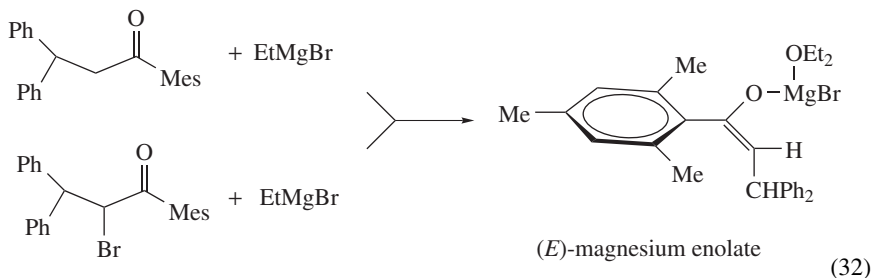
## D. Conjugate Addition

The conjugate addition of organometallic reagents to an electron-deficient carbon-carbon double bond is one of the most widely used synthetic methods to generate enolate. It is well known that Grignard reagents usually give a mixture of 1,2- and 1,4-addition

products in which the proportions vary depending upon the steric constraints imposed and the reaction conditions. Thus, by careful choice of the reagent (tertiary organomagnesium reagent or magnesium-ate complexes) and the Michael acceptor (bulky substituents on the carbonyl group, electron-withdrawing group), it is possible to achieve either 1,2- or 1,4-addition<sup>29</sup>. As a result, the Michael addition of magnesium anions has been developed as a new source of magnesium enolates, and several different types are now available<sup>30,31</sup>.



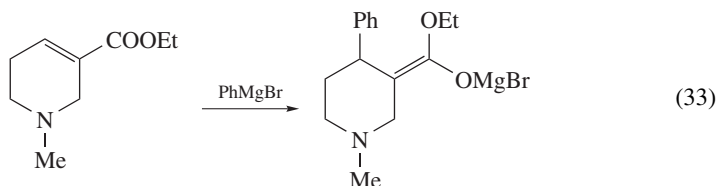
One of the simplest methods is the addition of Grignard reagent onto a sterically hindered enone<sup>32</sup>. For example, the (Z)-magnesium enolate is formed from the reaction of benzalacetomesitylene and phenylmagnesium bromide (equation 31).



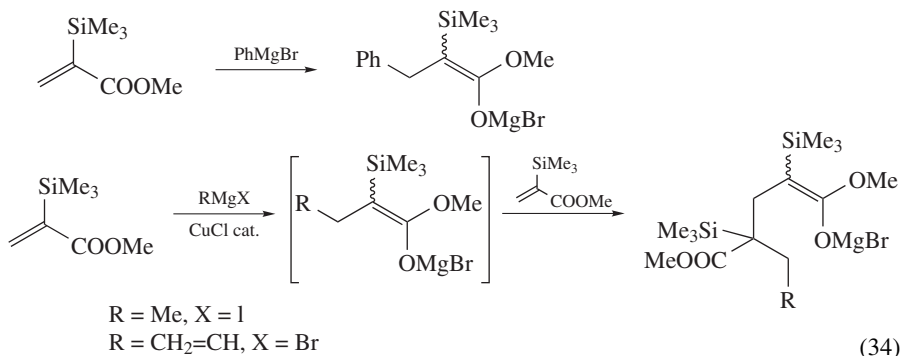
It should be noted that the reaction of EtMgBr either on the 2,2-diphenyl 2,4,6-trimethylphenyl ketone or on 2,2-diphenyl-1-bromoethyl 2,4,6-trimethylphenylketone gave the (E)-magnesium enolate (equation 32). Cryoscopic studies in naphthalene show that (Z)- and (E)-magnesium enolates are both monomeric; they contain tricoordinate magnesium analogous to the Grignard compound derived from isopropyl mesityl ketone. IR spectra confirm the enolic nature of the magnesium adducts<sup>32</sup>.

The mechanism of these reactions has been extensively studied. A recent book summarizes this literature<sup>30</sup>. A review refers to many other examples involving conjugate addition of organomagnesium reagents to  $\alpha,\beta$ -unsaturated ketones. It includes the stereochemistry of the reaction and copper-induced conjugate additions<sup>33</sup>.

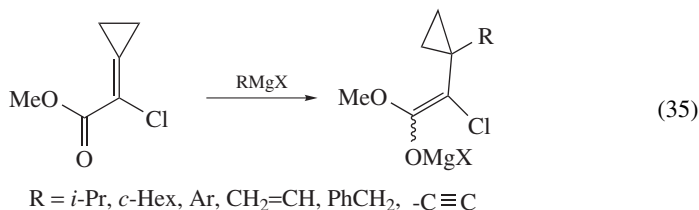
The Michael acceptor can be an  $\alpha,\beta$ -unsaturated carboxylic ester. This possibility is illustrated with the conjugate addition of phenylmagnesium bromide to ethyl arecadinatate, which leads to 4-phenylnipecotic acid<sup>34</sup> (equation 33).



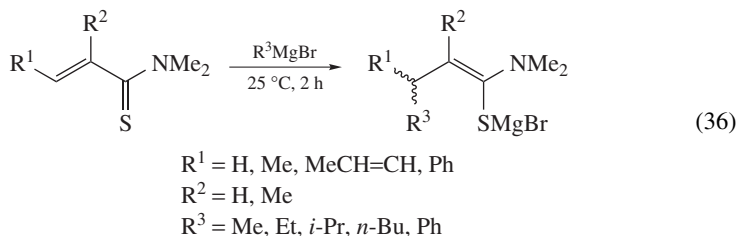
Methyl 2-(trimethylsilyl)propenoate serves as an excellent Michael acceptor in the reactions with Grignard reagents (equation 34). The resulting adduct anions can be applied to the subsequent condensation with a variety of carbonyl compounds. Such Michael addition is sensitive to the reaction conditions and to the nature of the organomagnesium species. With a stoichiometric amount of PhMgBr, the Michael adduct is the major product, whereas the copper-catalyzed addition of MeMgI and CH<sub>2</sub>=CHMgBr leads to a double reaction resulting from the reaction of magnesium enolate with the Michael acceptor<sup>35</sup>.



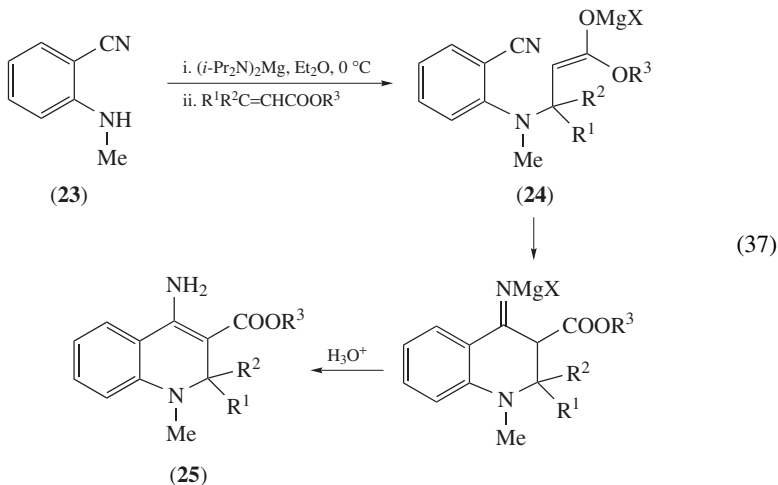
Interestingly, even methyl 2-bromo- or 2-chloro-2-cyclopropylideneacetate reacts cleanly with various Grignard reagents in a 1,4-addition without any chlorine–metal exchange side reactions (equation 35). These *in situ* generated magnesium enolates are particularly reactive with aromatic aldehydes<sup>36</sup>.



*N,N*-Dialkyl- $\alpha$ -methacrylthioamides are other examples of Michael acceptors that generate magnesium enolates and as such they undergo conjugate addition reactions with Grignard reagents<sup>37</sup>. It is believed that the conjugate addition provides (*Z*)-enolates, via a cyclic, six-centered transition state (equation 36)<sup>4b</sup>.

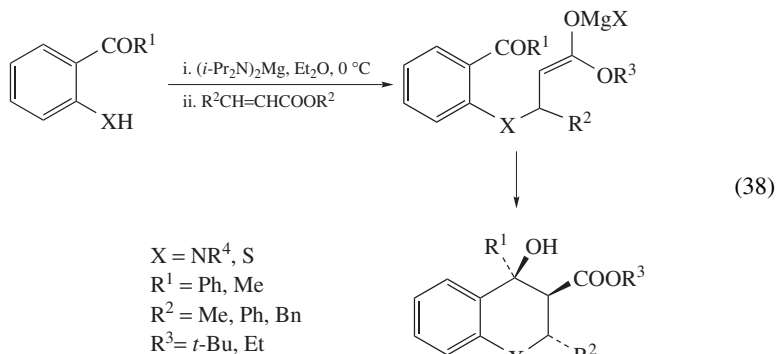


Surprisingly, hard magnesium nucleophiles can serve as Michael donors. For example, magnesium amide, derived from deprotonation of **23** with magnesium diisopropylamide, adds to an  $\alpha,\beta$ -unsaturated ester to give the corresponding magnesium enolate **24** via a conjugate addition (equation 37)<sup>38</sup>. Subsequent internal cyclic addition of the magnesium enolate onto the next nitrile yields 4-amino-1,2-dihydro-3-quinolinecarboxylic acid derivatives **25**.

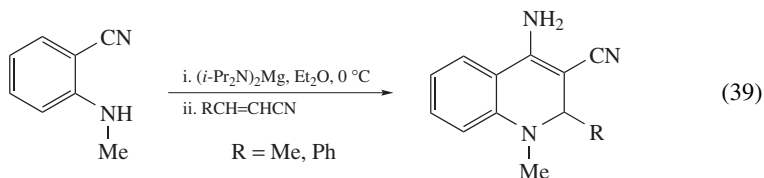


It can be assumed that the bivalent magnesium ion, which probably stabilizes the cyclic anionic intermediate, promotes further coupling reactions.

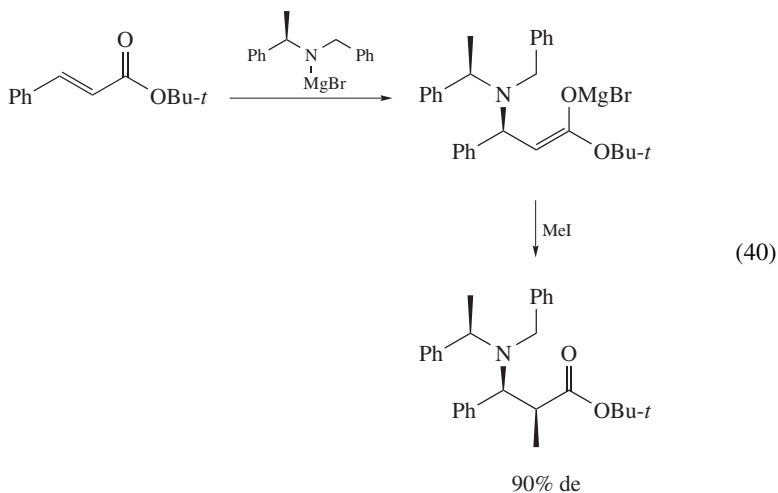
The same type of reaction has been applied to the preparation of 1,2-dihydroquinoline-3- and 2*H*-1-benzothiopyran-3-carboxylic acid derivatives (equation 38) via a magnesium amide-induced sequential conjugate addition–aldol condensation reaction between 2-(alkylamino)phenylketones or 2-mercaptobenzophenones<sup>39</sup>.



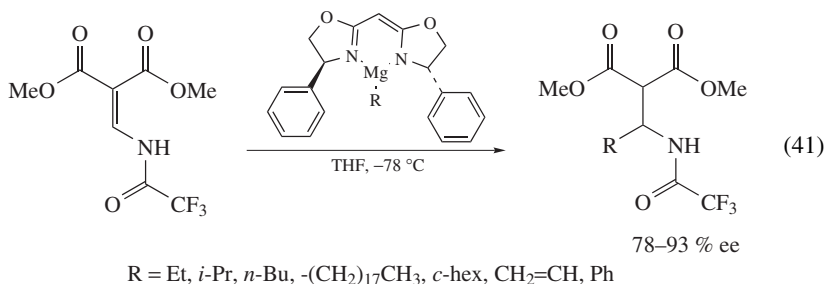
2,3-Dihydroquinoline-3-carbonitriles can also be prepared by the tandem reaction between 2-(methylamino)-benzophenone and  $\alpha,\beta$ -unsaturated carbonitriles in the presence of magnesium amide under the same conditions as for the reaction with  $\alpha,\beta$ -unsaturated carboxylates (equation 39).



The propensity of magnesium amide to undergo Michael additions with  $\alpha,\beta$ -unsaturated esters has been developed into a general protocol using homochiral amide to give magnesium  $\beta$ -aminoenolate intermediates<sup>40</sup> (equation 40).



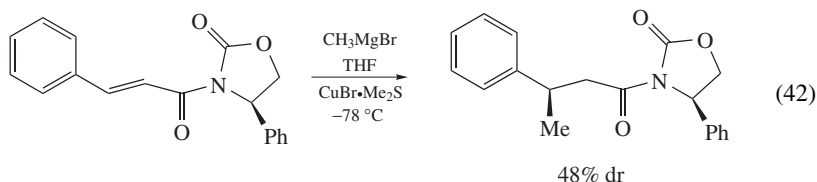
Chiral organomagnesium amides form an efficient method to realize enantioselective conjugate addition. Sibi and Asano have reported the Michael addition of  $\sigma$ -bound magnesium reagents derived from bisoxazolines to enamidomalonates (equation 41). The enantioselectivity of the addition is discussed in Section III. This method allows the preparation of chiral  $\beta$ -amino acid derivatives<sup>41</sup>.



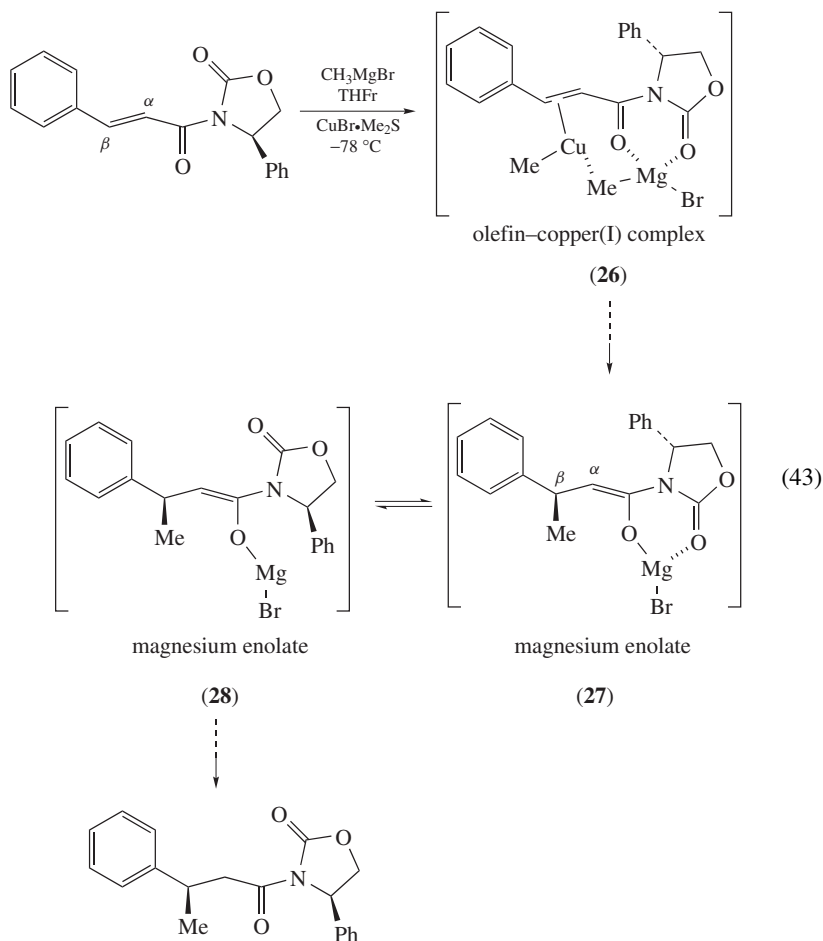
The introduction of asymmetry in conjugate additions can be promoted by chiral acceptors. The preparation of regio-defined magnesium enolates from copper(I)-mediated conjugate addition of Grignard reagents has been extensively used in many important

syntheses. The understanding of these reactions is important to improve the reaction conditions<sup>42</sup>.

A convenient and interesting way to control the absolute stereochemistry is to use the Evans-type 4-phenyloxazolidinone auxiliary. Studies of the mechanism for such conjugate addition have been made by Hruby and coworkers (equation 42)<sup>43</sup>.

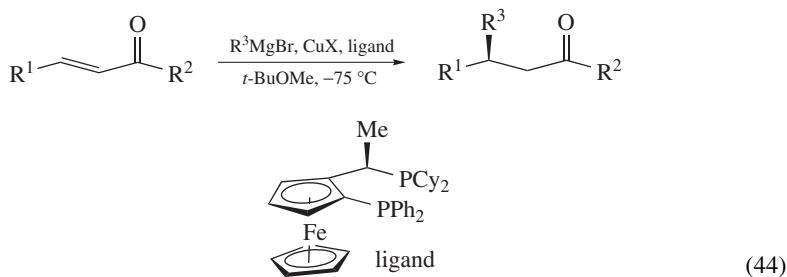


Three chiral intermediates are observed directly by <sup>1</sup>H and <sup>13</sup>C NMR spectroscopy: one olefin–copper(I) complex **26** and two magnesium enolates **27** and **28** (equation 43).





The two methyl groups in the olefin–copper(I) complex **26** are crucial for asymmetric induction. The  $150^\circ$  dihedral angle between the  $\alpha$ - and  $\beta$ -protons of the magnesium enolate **27** provides valuable information to determine the stereochemical effects on the  $\alpha$  center. The two magnesium enolates **27** and **28** are reversibly temperature-dependent. Enolate **27** is the major component at 253 K, while enolate **28** becomes the major component at 293 K. Therefore, temperature lower than *ca* 256 K is required to obtain high stereoselectivity.



$R^1 = \text{Me, Et, } n\text{-Pr, } n\text{-Bu, } n\text{-Pent,}$   
 $\text{BnO}(\text{CH}_2)_3, \text{Ph}$

$R^2 = \text{SMe, SEt}$

$R^3 = \text{Me, Et, } n\text{-Pr, } i\text{-Pr, } n\text{-Bu, } i\text{-Bu}$

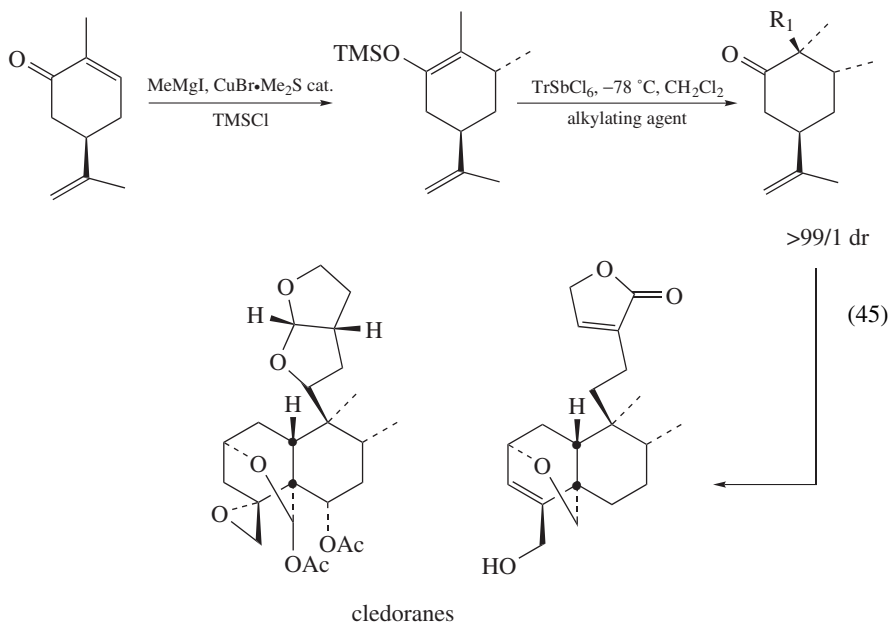
$X = \text{Br.Me}_2\text{S}$

$R^1 = \text{Me, Et, } n\text{-Pr, } n\text{-Bu, } n\text{-Pent}$

$R^2 = \text{Me, } n\text{-Bu, } t\text{-Bu}$

$R^3 = \text{Me, Et, } n\text{-Pr, } i\text{-Pr, } n\text{-Bu, } i\text{-Bu,}$   
 $\text{Cl-Bu, } i\text{-Pr}(\text{CH}_2)_2, \text{Ph}$

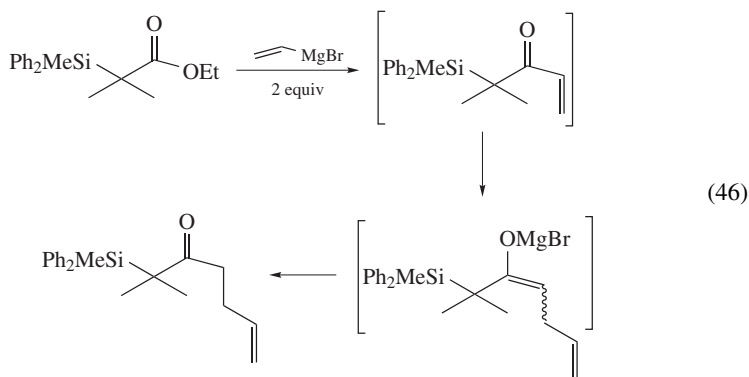
$X = \text{Cl, Br.Me}_2\text{S, I}$



Numerous other protocols have been developed to prepare magnesium enolates by asymmetric 1,4-addition of Grignard reagents to electron-deficient alkenes. Recently, an enantioselective metal-catalyzed version of this key reaction has been studied with enones and  $\alpha,\beta$ -unsaturated thioesters<sup>44–46</sup>. Using chiral ferrocenyl-based diphosphines leads to interesting results (equation 44).

The copper-catalyzed conjugate addition of methylmagnesium iodide to cyclohexenone and trapping of the resulting enolate as its trimethylsilyl enolate, followed by  $\text{TrSbCl}_6$ -catalyzed Mukaiyama reaction, are the first steps of an elegant synthesis of enantiomerically pure clerodanes<sup>47</sup> (equation 45).

Tandem reactions attract significant research interest as they can lead to new methodologies to generate metal enolates. For example, the reaction of ethyl 2-methyl-2-(diphenylmethylsilyl)propionate with vinylmagnesium bromide (or 2-methyl-1-propenylmagnesium bromide) results in the addition of two equivalents of the Grignard reagent. The first addition gives the enone intermediate while the second undergoes a Michael reaction. This sequence allows the synthesis of  $\beta$ -ketosilanes and tetrasubstituted ketones<sup>48</sup> (equation 46).



### E. Permutational Hydrogen/Metal Interconversions (Metallations)

As in the preceding section, it should be emphasized that the exact constitution of magnesium enolates is still undetermined, since they are generally produced and used *in situ*. Consequently, the general equations may be oversimplified, since they do not take into account solvation, association or interactions between different species.

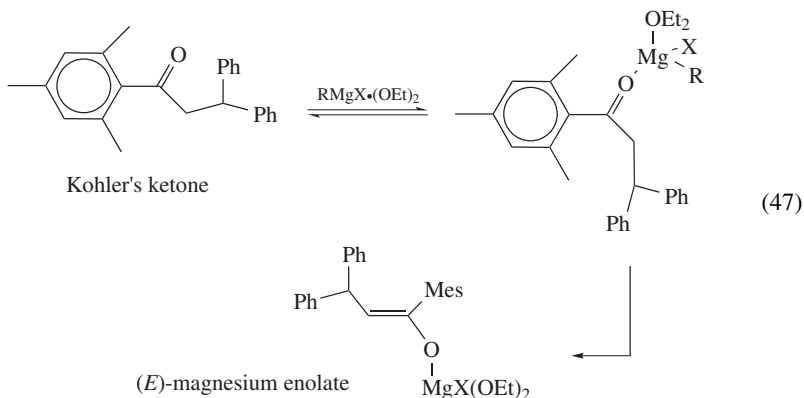
The preparation of magnesium enolates by metallation competes with nucleophilic addition. Thus, until recently, this strategy was only valuable for sterically hindered or relatively acidic substrates, which were metallated by Grignard reagents or magnesium dialkoxides.

However, it has now been reported that sterically hindered magnesium amides analogous to LDA or LTMP are effective and selective metallating reagents. By comparison with the lithium reagents, they have distinctive stability (even in boiling THF), reactivity (they are compatible with a number of functional groups) and selectivity (they are useful in regio- and stereoselective formation of magnesium enolates) properties. Finally, they are also good candidates for enantioselective deprotonation.

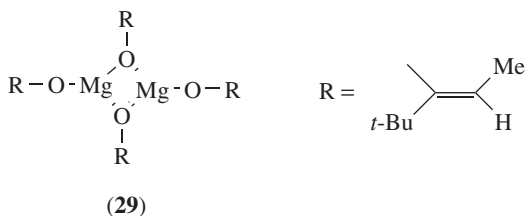
In view of the importance currently attached to the usefulness and synthesis of magnesium enolates, these different aspects are discussed in this section.

Alkylmagnesium halides and dialkylmagnesium compounds are efficient metallating agents toward alkyl mesityl ketones such as Kohler's ketone (2,2-diphenylethyl 2,4,6-trimethylphenyl ketone) and hindered carboxylic esters such as *t*-butyl acetate.

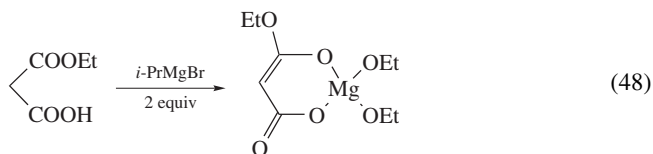
A study of the enolisation mechanism with Kohler's ketone has shown the formation of an (*E*)-magnesium enolate<sup>49</sup>(equation 47).



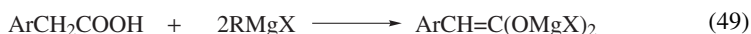
Bertrand and coworkers have studied the complexity of magnesium enolates in solution. The NMR and IR of the products generated from alkyl- and dialkylmagnesium reagents with enolizable ketones indicate that enolates as well as solvent-separated carbonyl conjugated carbanion ion pairs are formed. The analysis of the reaction mixture is complicated by the occurrence of ketone reduction<sup>50</sup>.



Fellmann and Dubois<sup>51</sup> have described the structure of the enolate **29** derived from the reaction of *t*-butyl acetate with (MeO)<sub>2</sub>Mg. The <sup>13</sup>C NMR spectrum reveals two *O*-metallated species, which should be symmetric enolates as proposed by Pinkus and Wu for the bromomagnesium enolate of methylmesityl ketone (metal is tricoordinated)<sup>32</sup>.



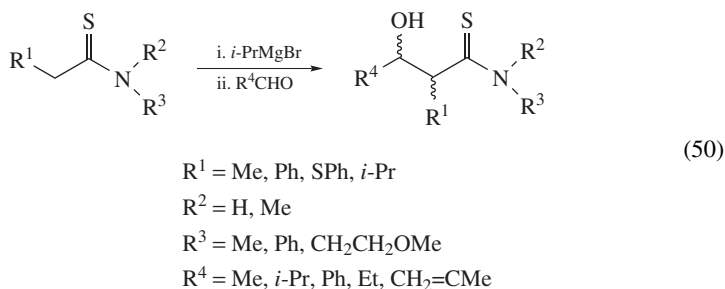
Magnesium enolates derived from  $\beta$ -dicarbonyl compounds can be easily obtained by metallation with *i*-PrMgBr. A stable cyclic chelate is obtained<sup>52</sup>. As example, the magnesium enolate of mixed malonate is shown in equation 48.



The bis-deprotonation of arylacetic acids by Grignard reagents is known<sup>53</sup> and the resulting bis(bromomagnesium) salts (equation 49) have been used for preparing  $\beta$ -hydroxy acids (Ivanov reaction).

Extensive studies have been performed on the metallation of thioamides, sulfones and sulfoxides.

Thioamides of secondary amines are deprotonated with isopropylmagnesium to give (*Z*)-enolates. Thioamides of primary amines react with two equivalents of *i*-PrMgBr to afford dianions that have been shown to have the (*Z*)-configuration. These magnesium species are versatile intermediates in stereoselective aldol reaction (equation 50, Table 5; see Section III).



$\alpha$ -Sulfinyl magnesium carbanion enolates have been also investigated as reagents for asymmetric aldol reactions. The first example was introduced by Solladié<sup>54</sup>. The magnesium enolate is prepared by reaction of the sulfinyl ester with *t*-butylmagnesium bromide. It reacts with aldehydes and ketones with high levels of asymmetric induction. The results are rationalized in terms of rigid chelated intermediates (see Section III). This method has been extended to acetamides. It is illustrated by the preparation of the magnesium enolate derived from *N,N*-diethyl 2-acetyl-1,3-dithiolane-*S*-oxide (equation 51). This metal anion is an interesting chiral synthon, which has found applications in asymmetric aldol-type addition<sup>55</sup>.

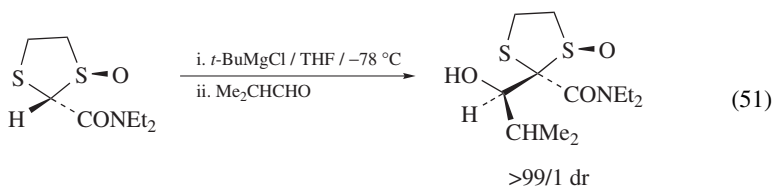


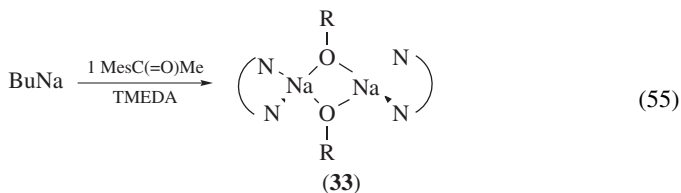
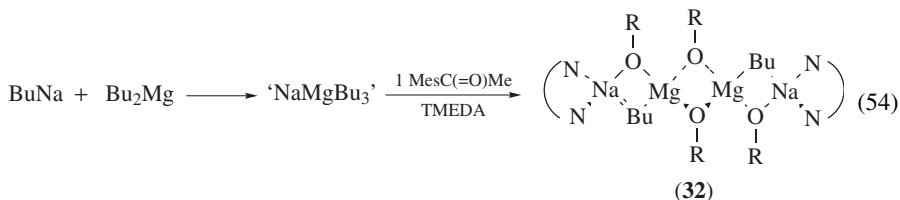
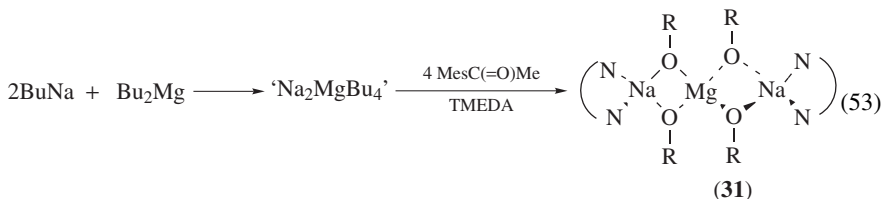
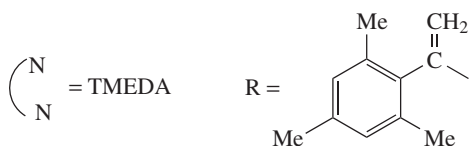
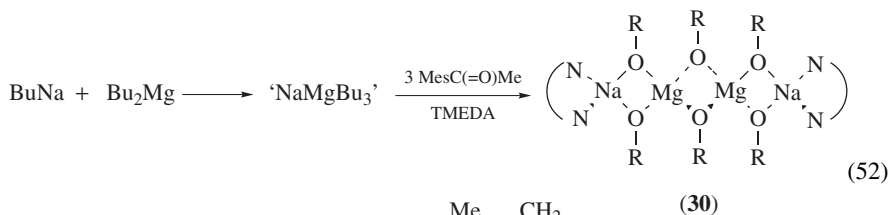
TABLE 5. Stereochemistry of aldol reaction of magnesium enolates derived from thioamides with aldehydes

R <sup>1</sup>	R <sup>2</sup>	R <sup>3</sup>	R <sup>4</sup>	dr
Me	Me	Me	<i>i</i> -Pr	95/5
Me	Me	Me	Ph	93/7
Me	Me	Me	CH <sub>2</sub> =CH	89/11
Ph	Me	Me	<i>i</i> -Pr	72/28
Ph	Me	Me	CH <sub>2</sub> =CH	73/27
PhS	Me	Me	<i>i</i> -Pr	66/34
<i>i</i> -Pr	Me	Me	Ph	34/66
Ph	Me	H	<i>i</i> -Pr	98/2
Ph	Me	H	Ph	94/6
Ph	CH <sub>2</sub> CH <sub>2</sub> OMe	H	Ph	97/3

To find a synergic mixed-metal reagent, Hevia and coworkers have investigated the reactivity of variant monosodium–monomagnesium trialkyl  $\text{NaMgBu}_3$  and disodium–monomagnesium  $\text{Na}_2\text{MgBu}_4$  complexes toward the sterically demanding 2,4,6-trimethylacetophenone<sup>56</sup>.

Reactions occur smoothly at room temperature, affording the enolate products **30–32** as isolated crystalline solids (in 35–78% yields). In these reactions, 2,4,6-trimethylacetophenone is selectively deprotonated at the methyl position and no nucleophilic side-reactions take place.

The solid-state structures of the homoanionic magnesium enolates **30** and **31** and heteroanionic enolate **33** have been determined by X-ray crystallography, establishing as a common motif a polymetallic chain of four members for **30** and **32** or three members for **31**, with the anionic ligands in each case bridging the different metals together (equations 52–55).

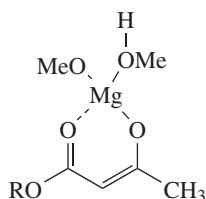


A problem inherent in metallation reactions with Grignard reagents is the poor chemoselectivity of the reactions. The most common side-reactions are the competing nucleophile addition and the reduction of the carbonyl compounds. An interesting alternative would be to use the high electrophilicity of the  $\text{Mg}^{2+}$  cation and its tendency to form a multi-coordinate complex. The preformation of a  $\text{Mg}(\text{II})$  complex with a carbonyl compound or a carboxylic acid derivative enhances the acidity of the substrate to the point where a relatively mild base can be used.

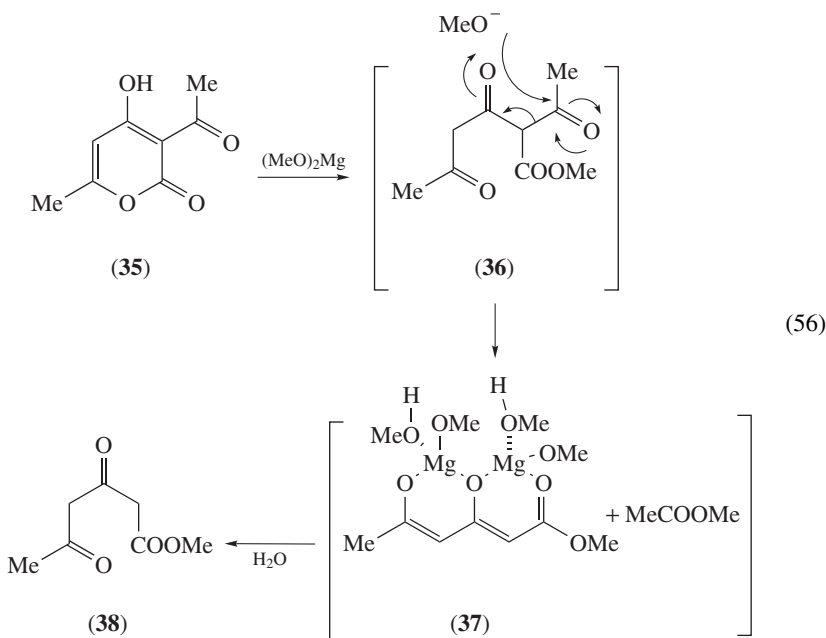
Two simple basic systems are described:  $\text{Mg}(\text{OR})_2$  and  $\text{MgX}_2/\text{Et}_3\text{N}$ .

Magnesium alkoxide, simply prepared by dissolving magnesium in alcohol in the presence of a crystal of iodine, can be used to prepare magnesium enolates of bifunctional compounds.

For example, the chelated magnesium enolate of a  $\beta$ -diketone or a  $\beta$ -ketoester **34** (formed via **33**) can be easily prepared using  $(\text{MeO})_2\text{Mg}/\text{MeOH}$  as a base. It is stable in a refluxing solution of the reagent, in contrast with the sodium enolate analogue, which is unstable in these conditions.

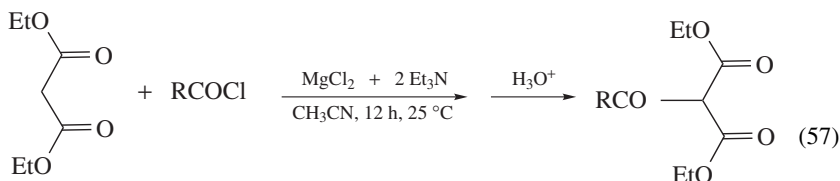


(34)



Thus, the methanolysis of the lactone **35** by MeONa or (MeO)<sub>2</sub>Mg produces initially the triketoester **36**, which is subsequently deacylated *in situ* to give after hydrolysis the diketone ester **38**. The yield of **38** is considerably better with (MeO)<sub>2</sub>Mg, as the result of the formation in the reaction medium of a chelated bis-enolate **37** which protects **38** from degradation. Extensive degradation is observed with the sodium enolate analogue of **37** which is unstable in these conditions (equation 56)<sup>57</sup>.

Rathke and Cowan have used the combination MgCl<sub>2</sub>/R<sub>3</sub>N for the metallation of  $\beta$ -dicarbonyl compounds<sup>58</sup>. In the presence of magnesium chloride and 2 equivalents of Et<sub>3</sub>N, diethyl malonate is easily metallated. The C-acylation of the resulting anion with acid chloride gives excellent yields (equation 57). Other metal chlorides (ZnCl<sub>2</sub>, CuCl<sub>2</sub>, FeCl<sub>3</sub>, LiCl, TiCl<sub>4</sub>, AlCl<sub>3</sub>) are ineffective. Similarly, ethyl acetoacetate is C-acylated by acid chlorides in the presence of magnesium chloride and 2 equivalents of pyridine. The reaction of diethyl malonate or ethyl acetoacetate with tertiary amine and MgCl<sub>2</sub> provides a remarkably simple entry into the enolate chemistry derived from dialkyl malonate, which will be described in Section III.

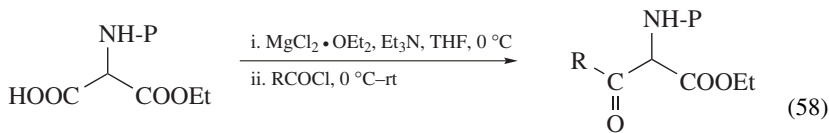


R = Me, *n*-Pr, *i*-Pr, *t*-Bu, Ph

85–92% isolated yields

The same process has been extended to trialkylphosphonoacetates. Acylation with acid chlorides of the magnesium enolates derived from trimethyl and triethyl phosphonoacetates using a MgCl<sub>2</sub>/Et<sub>3</sub>N system provides 2-acyl dialkylphosphonoacetates. Further decarboxylation of these latter compounds affords  $\beta$ -ketophosphonates<sup>59</sup>.

A similar procedure for the synthesis of  $\alpha$ -acyl aminoesters has been proposed using a MgCl<sub>2</sub>/R<sub>3</sub>N base system to generate the magnesium enolates of a series of  $\alpha$ -carboxy aminoesters. These reagents react smoothly at 0 °C with a variety of acid chlorides to give  $\alpha$ -acyl aminoesters in good to excellent yields<sup>60</sup> (equation 58).

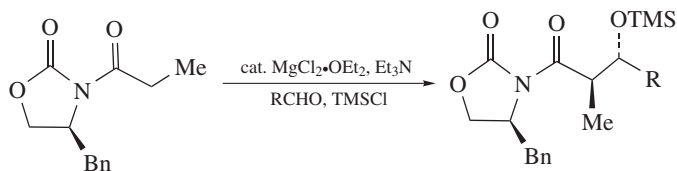


P = Boc, Cbz, Bz

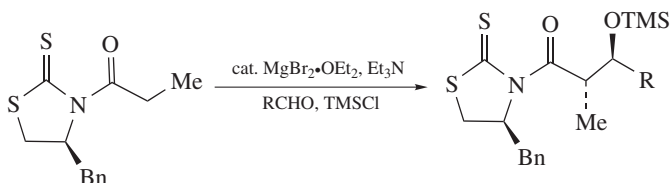
77–92%

R = Ar, Me, *n*-Pr, *i*-Pr

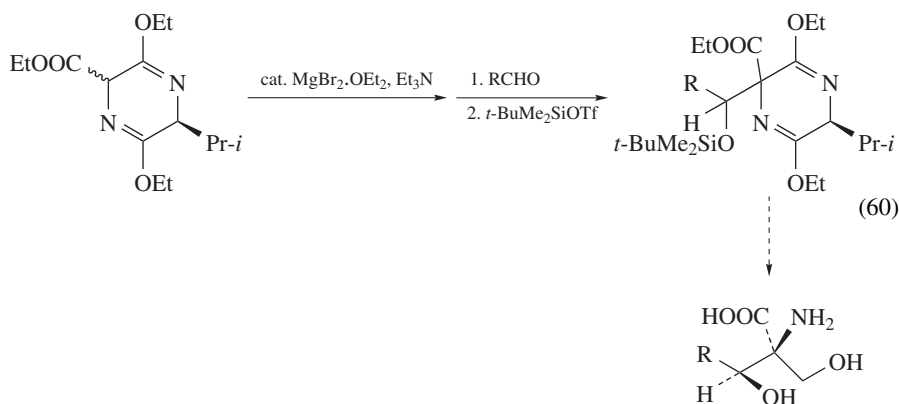
The MgX<sub>2</sub>/R<sub>3</sub>N systems offer another useful synthetic interest. Recently, Evans and coworkers have demonstrated that substoichiometric amounts of magnesium halides in the presence of an amine and chlorotrimethylsilane catalyze the direct aldol reaction of *N*-acyloxazolidinones and *N*-acylthiazolidinethiones with high diastereoselectivity<sup>61, 62</sup> (equation 59).



(59)



Interestingly, another Mg(II)-mediated aldol-type reaction has been investigated by using  $\text{MgBr}_2\text{--Et}_3\text{N}$  with bislactim ethers and aliphatic aldehydes. The aldol products are converted in  $\alpha$ -substituted serines<sup>63</sup> (equation 60, Table 6).



(60)

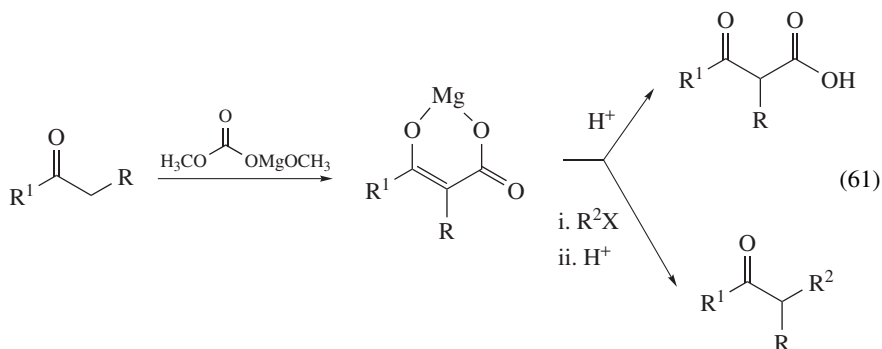
Stile has developed an alternative way to generate magnesium enolate under mild basic conditions<sup>64</sup>. Ketones react with magnesium methyl carbonate (MMC or Stile's reagent)

TABLE 6. Diastereoselective aldol-type reaction of bislactim ether with aldehydes

R	Yield (%)	dr
<i>i</i> -Pr	86	7/83/1/9
<i>n</i> -Bu	75	7/75/2/16
Ph	70	18/72/0/10
$\text{Me}_2\text{C}=\text{CH}$	74	16/64/3/17



to give stable chelated adducts, which are converted to  $\beta$ -keto carboxylic acids or  $\alpha$ -substituted ketones after alkylation and subsequent decarboxylation (equation 61). The process is compatible with carboxylic acid derivatives (nitrile, ester and amide)<sup>65</sup>.



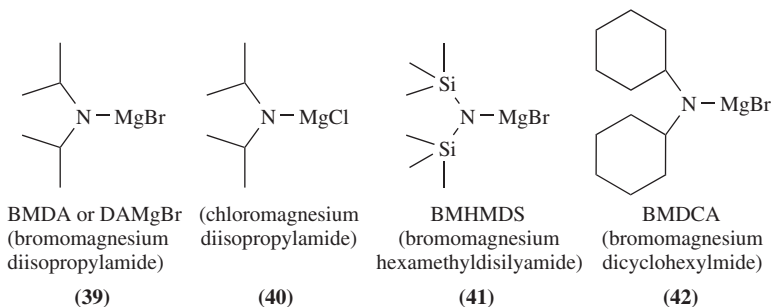
In recent years, a variety of hindered magnesium amides have been used to produce magnesium enolates. The versatility of these bases is now well recognized. Some typical examples are presented below.

The magnesium amides may be prepared either by reaction of lithium amide and magnesium bromide, by reaction of DIBAL-H with  $R_2Mg$ , or by reaction of the corresponding amine with a Grignard reagent<sup>66-68</sup>.

For instance, BMDA **39**, the LDA-analogue, is generated by treatment of diisopropylamine with ethylmagnesium bromide at  $0^\circ C$  in diethyl ether and the mixture is stirred for 1 h at the same temperature.

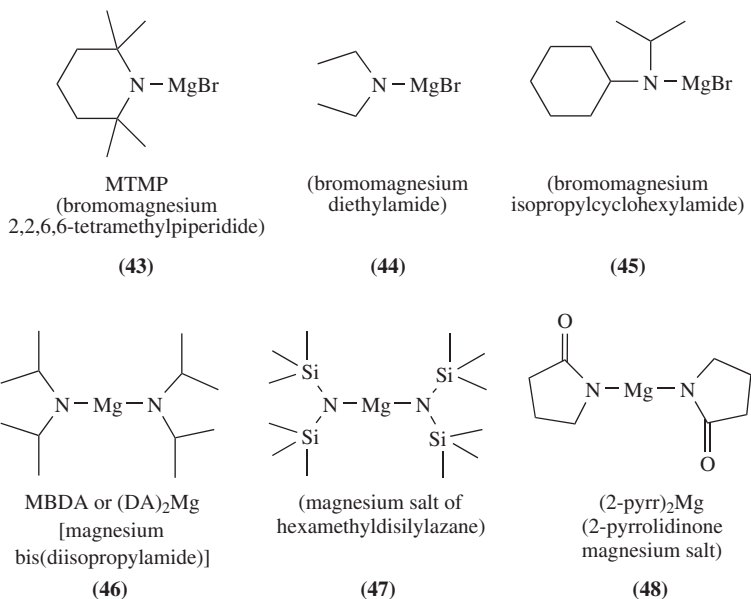
The magnesium amides and diamides are more thermally stable and less reactive than their lithium analogues, leading to different selectivities.

Examples for the preparation of magnesium enolates (or further subsequent reactions of the enolates) by magnesium amides are listed in Table 7.

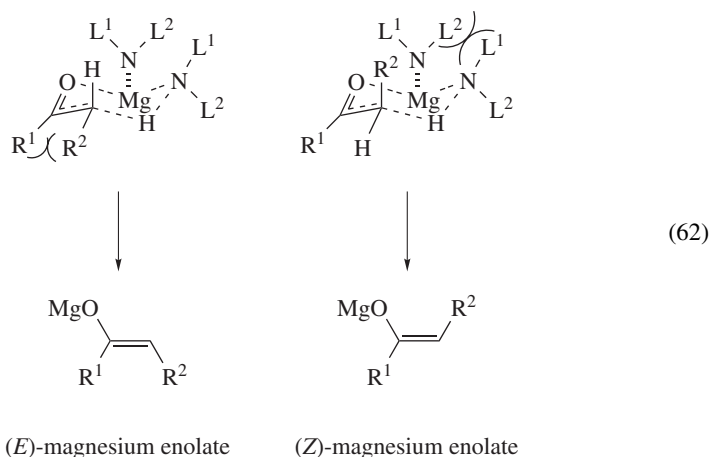


The magnesium amides of choice for the preparation of magnesium enolates via metallation are the Hauser bases, such as **39** and **40**, or (bis)amidomagnesium reagents, such as **46** and **47**. The reaction has been successfully applied to the preparation of enolates derived from cyclic, acyclic and  $\alpha$ -siloxyketones, benzylic ketones, aldehydes, carboxylic esters and amides, even with the less hindered Hauser bases.

However, these reagents show significant differences in their reactivity and in their selectivity as compared to their lithium analogues. It is possible to control the regioselective formation of enolate. By a careful choice of base, (bis)amidomagnesium reagent such



as **46** [(DA)<sub>2</sub>Mg] in THF/heptane or the electrogenerated base **47** in DME/HMPA leads to kinetic enolates of cyclic and acyclic ketones via an *in situ* reaction with TMSCl. Yields are high and the regioselectivity is similar to the one obtained with LDA/DME at  $-78^\circ\text{C}$ , although the reaction with **46** is performed at room temperature. It should be noted that the high *E*-enol stereoselectivity for benzylic ketones is opposite to the one obtained with LDA. This result can be rationalized considering steric interactions in Ireland's transition state model<sup>74</sup> (equation 62).



The use of DAMgBr **39** in Et<sub>2</sub>O/HMPA/TMSCl/Et<sub>3</sub>N leads to the thermodynamic enolates or silyl enol ethers. This methodology is one of the best direct regioselective preparations of thermodynamic silylenol ethers from unsymmetric cyclic ketones.

TABLE 7. Examples for the preparation of magnesium enolates (or reaction products after trapping) by magnesium amides

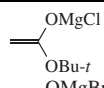
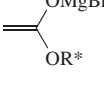
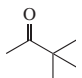
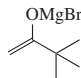
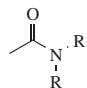
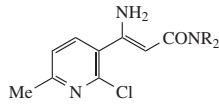
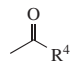
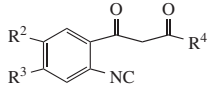
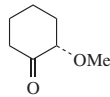
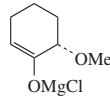
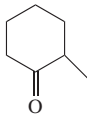
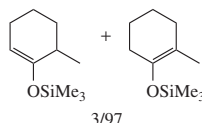
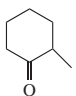
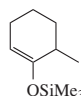
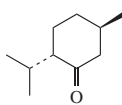
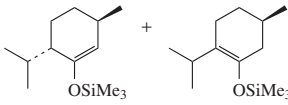
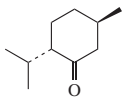
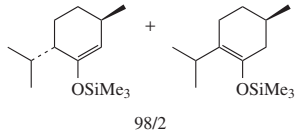
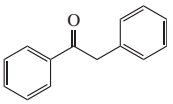
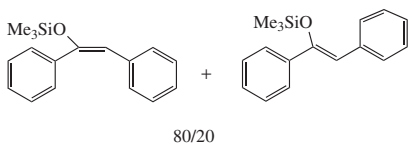
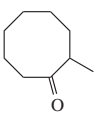
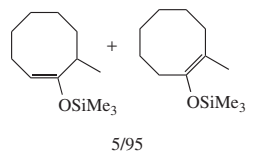
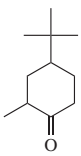
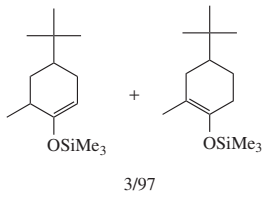
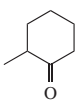
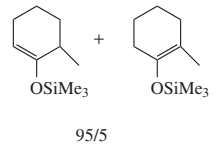
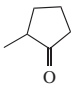
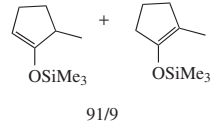
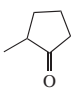
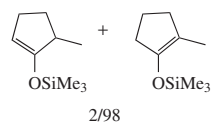
Substrate	Magnesium amide	Magnesium enolate or reaction product after trapping procedure of enolates	Reference
$\text{CH}_3\text{COOBu-}t$	<b>46</b>		66, 68
$\text{CH}_3\text{COOR}^*$ ( $\text{R}^* = (-)\text{-menthyl, (+)-bornyl}$ )	<b>44</b>		69
	<b>39</b>		70
 $\text{R} = \text{Me, piperidin-1-yl, morpholin-4-yl, 4-methylpiperazin-1-yl}$	<b>46</b>		71
 $\text{R}^4 = \text{OMe, OEt, OPr-}n, \text{OBu-}n, \text{OBu-}t, \text{NMe}_2$	<b>46</b>		68, 72
	<b>40</b>		73
	<b>39/</b> TMSCl/ $\text{Et}_3\text{N}/\text{Et}_2\text{O}/\text{HMPA}$	 3/97	74
	<b>46/</b> TMSCl/THF/heptane		74
	<b>33/</b> TMSCl/ $\text{Et}_3\text{N}/\text{Et}_2\text{O}/\text{HMPA}$	 3/97	75

TABLE 7. (continued)

Substrate	Magnesium amide	Magnesium enolate or reaction product after trapping procedure of enolates	Reference
	<b>46</b> / TMSCl/THF/ heptane	 98/2	74
	<b>46</b> / TMSCl/THF/ heptane	 80/20	74
	<b>39</b> / TMSCl/Et <sub>3</sub> N/Et <sub>2</sub> O/ HMPA	 5/95	75
	<b>39</b> / TMSCl/Et <sub>3</sub> N/Et <sub>2</sub> O/ HMPA	 3/97	75
	<b>47</b> electrogenerated base DME/ HMPA	 95/5	76
	<b>47</b> electrogenerated base DME/ HMPA	 91/9	76
	<b>48</b> electrogenerated base DME/ HMPA	 2/98	77

(continued overleaf)

TABLE 7. (continued)

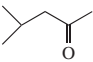
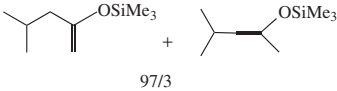
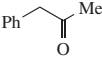
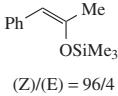
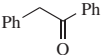
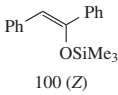
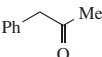
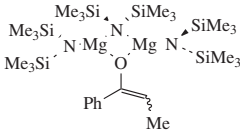
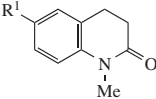
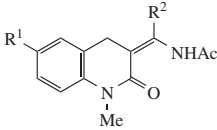
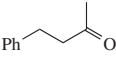
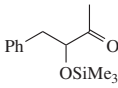
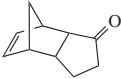
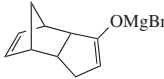
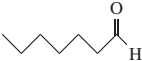
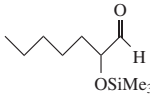
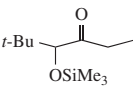
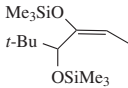
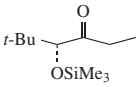
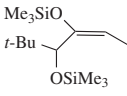
Substrate	Magnesium amide	Magnesium enolate or reaction product after trapping procedure of enolates	Reference
	<b>47</b> electrogenerated base DME/ HMPA	 97/3	76
	<b>47</b> electrogenerated base DME/ HMPA	 (Z)/(E) = 96/4	76
	<b>47</b> electrogenerated base DME/ HMPA	 100 (Z)	76
	<b>47</b> (2 equiv.) toluene	 (E)/(Z) = 74/26	78, 79
	<b>39</b>		80
	<b>46</b>		81
	<b>39</b>		82
	<b>46</b>		81
	<b>43</b>		83

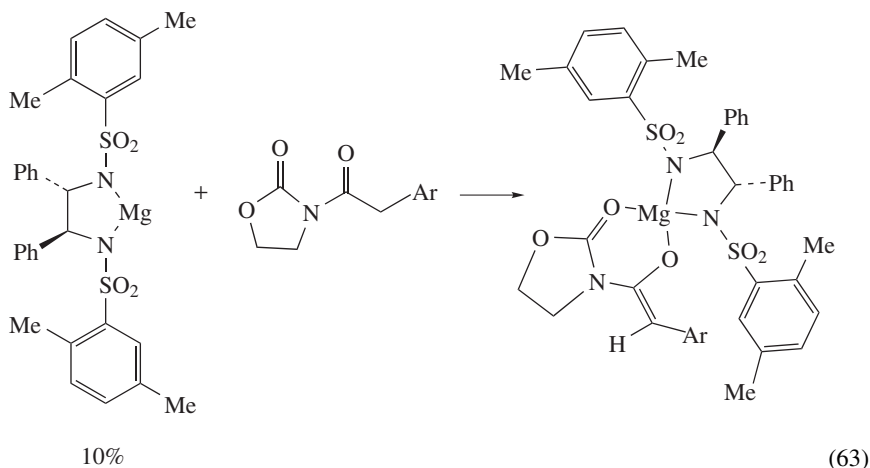
TABLE 7. (continued)

Substrate	Magnesium amide	Magnesium enolate or reaction product after trapping procedure of enolates	Ref.
	45	 (E)/(Z) = 91/9	84

The increasing interest in enolization reactions mediated by magnesium amides led to new investigations for structural features of these reagents<sup>78,79</sup>.

Magnesium amides have also found good utility in enantioselective deprotonation processes. A range of chiral amines has been prepared by Henderson and coworkers and it was found after conversion to their Mg-bisamide derivatives that it react with 4- and 2,6-substituted cyclohexanones with good to excellent selectivities<sup>85-89</sup> (see Section III). Structures of some chiral magnesium amides are given in Chart 1.

The concept of chiral magnesium amides for the preparation of magnesium enolates has been extended to chiral magnesium bis(sulfonamide) complexes as catalysts for the enolization of *N*-acyloxazolidines<sup>90</sup> (equation 63).



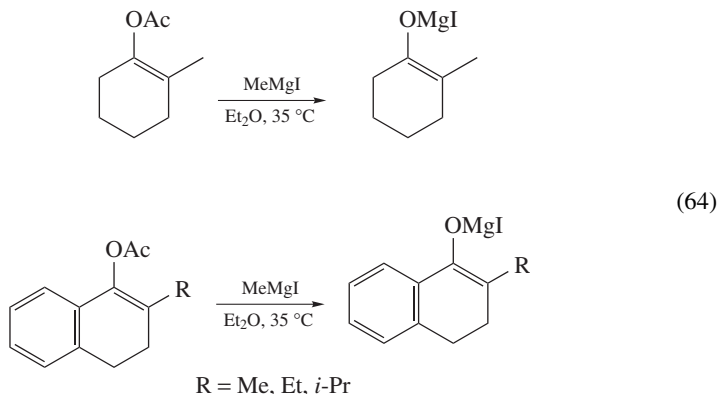
The metallation should proceed via the formation of a chelated tetrahedral magnesium enolate complex, with a (*Z*)-geometry. The conformational rigidity would be enforced by chelation of both the imide enolate and bis(sulfonamide) ligand to the tetrahedral magnesium ion.



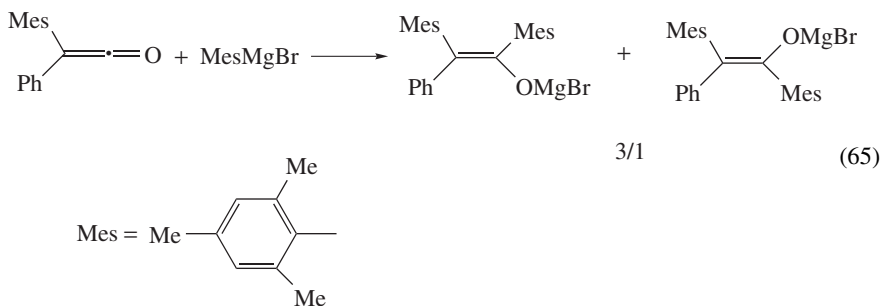
### F. Miscellaneous Methods

Other methods to prepare magnesium enolates were also reported. They involve the addition to carbon–carbon multiple bonds. Two different mechanisms are possible: (a) the addition–elimination sequence to a carbon–carbon double bond, (b) the addition to a carbon–carbon of a ketene.

Uncatalyzed addition reactions of Grignard reagents with nonconjugated alkenes and alkynes are of limited use in synthesis. However, carbon–carbon double bonds substituted by a leaving group, such as an acetate, are susceptible to be displaced by organomagnesium compounds presumably by an addition–elimination pathway. A few examples have been reported<sup>91,92</sup> (equation 64).



Early investigations of reactions of organomagnesium compounds with ketenes are described, as illustrated by the example of mesitylketene described by Rappoport and coworkers<sup>93</sup> (equation 65).

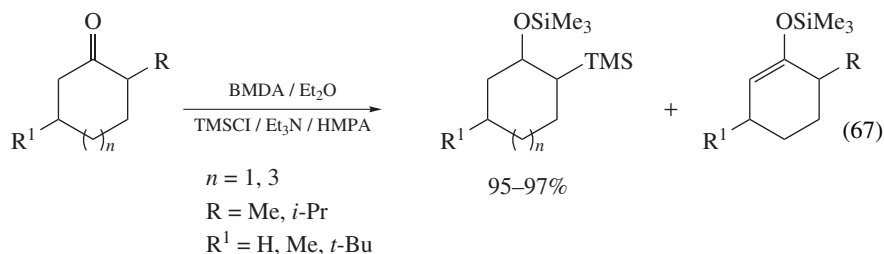


The preference for the formation of the major (*E*)-enolate indicates that the attack occurs preferentially from the side of the formally bulkier mesityl ring. *Ab initio* calculations allow one to rationalize this result. The ketene adopts a conformation with a planar Ph–C=C moiety while the mesityl is nearly perpendicular to this plane. Since the attack onto the C=O group occurs in the plane of the C=C double bond, the coplanar Ph is effectively bulkier and the preferred attack is from the mesityl side.

Recently, Verkade and coworkers have reported the successful synthesis of  $\beta$ -hydroxy-nitriles from carbonyl compounds in a reaction promoted by strong nonionic bases, such as proazaphosphatrane types. The reaction occurs in the presence of magnesium sulfate,

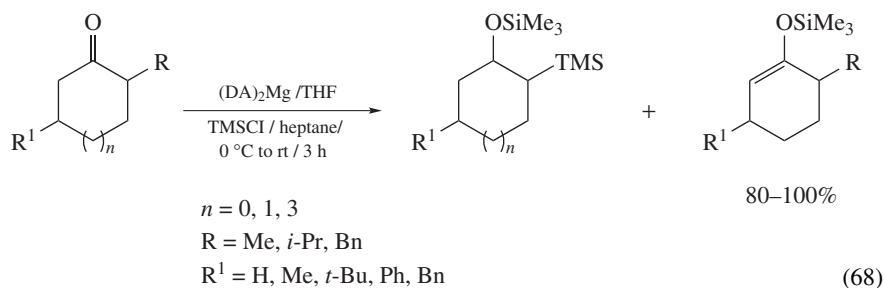




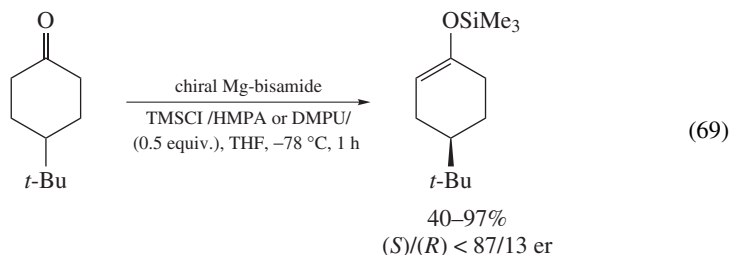


The effectiveness of magnesium enolates as nucleophilic agents limits the interest of the reaction. With less substituted substrates ( $R = \text{H}$ ), the aldol reaction is faster than the silylation. Moreover, due to solubility limitations, the authors are unable to determine whether the high thermodynamic:kinetic ratio of silylenol ethers obtained accurately represents the magnesium enolate composition. Nonetheless, this method is an excellent procedure to selectively prepare the thermodynamic silylenol ether from an unsymmetrical ketone<sup>75</sup>.

Bordeau and coworkers have described an efficient and stereoselective synthesis of kinetic silylenol ethers<sup>74</sup>. Less highly substituted silylenolates are regiospecifically prepared in high yield, around room temperature under kinetic conditions, from unsymmetric cyclic ketones and  $[(\text{DA})_2\text{Mg}]$  in THF/heptane (equation 68).

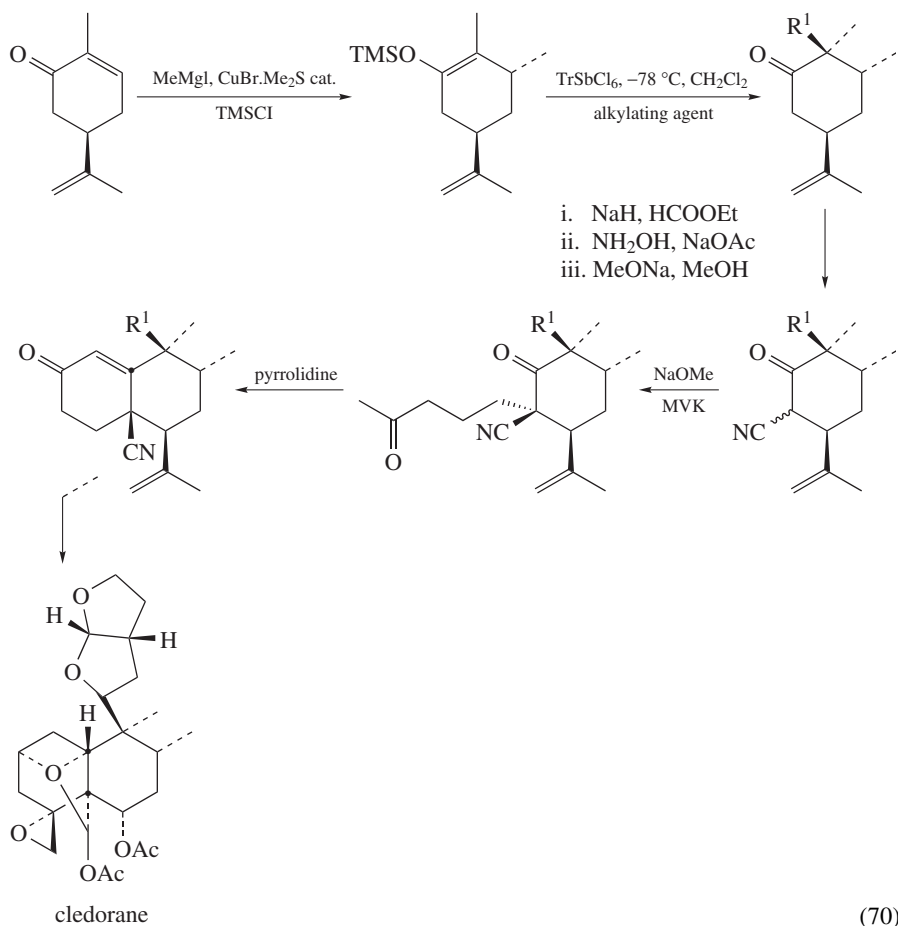


Recently, Henderson has investigated the effect of Lewis base additives such as HMPA in enantioselective deprotonation of ketones mediated by chiral magnesium amide bases. In almost all reactions investigated, the additive HMPA could be replaced by DMPU without any undue effect on either selectivity or conversion (equation 69)<sup>85-89</sup>.

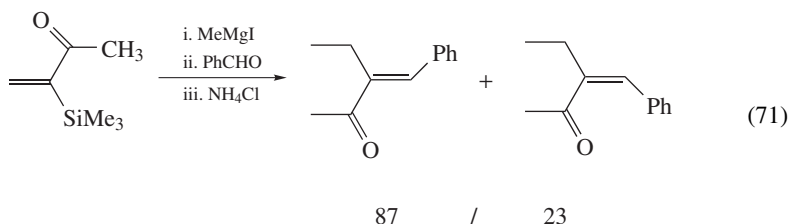


An important reaction of silylenol ethers is their use as enolate equivalent in Mukaiyama aldol additions. An example of the synthetic utility of this reaction with a magnesium enolate as starting reagent is shown below.

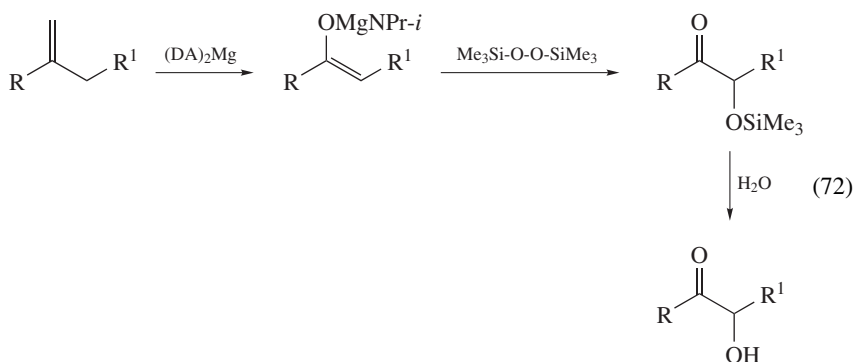
The copper-catalyzed conjugate addition of methyl magnesium iodide to cyclohexenone and trapping the enolate as its trimethylsilyl enol ether, followed by a trityl hexachloroantimonate-catalyzed Mukaiyama reaction, is applied to *R*-(-)-carvone. C-2, C-3 functionalized chiral cyclohexanones are converted into their  $\alpha$ -cyano ketones, which are submitted to Robinson annulation with methyl vinyl ketone. Highly functionalized chiral decalones are obtained that can be used as starting compounds in the total synthesis of enantiomerically pure clerodanes<sup>47</sup> (equation 70).



The conjugate addition of a Grignard reagent (often copper-induced) to an enone, followed by reaction of the resulting enolate with an electrophile, provides numerous examples of tandem vicinal functionalizations<sup>95</sup>. For example, equation 71 depicts the generation of an  $\alpha$ -magnesium enolate by the addition of methylmagnesium iodide to 3-trimethylsilylbut-3-en-2-one; the subsequent addition of benzaldehyde generates an alkene via a Peterson olefination<sup>96</sup>.



To develop new electrophilic reagents, Ricci and coworkers have described the synthesis of trimethylsilyloxy and hydroxy compounds from magnesium enolates and bis(trimethylsilyl)peroxide. Magnesium enolates, generated using magnesium diisopropylamide,  $(\text{DA})_2\text{Mg}$ , give the hydroxycarbonyl compounds in excellent yields<sup>81</sup> (equation 72, Table 8).

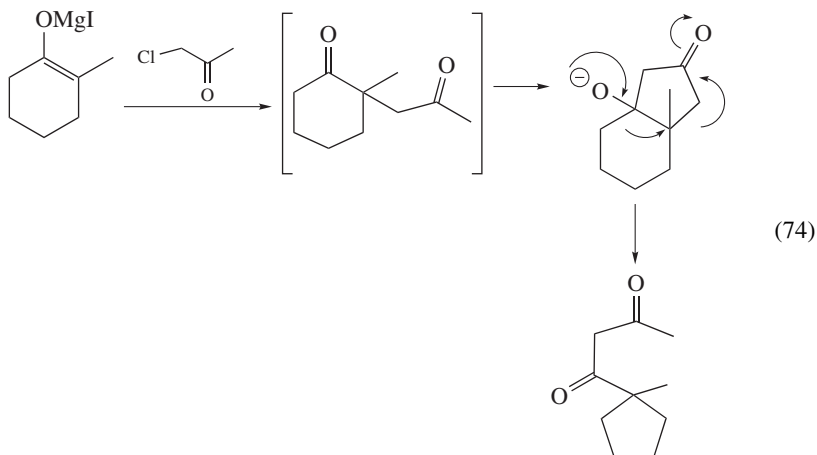
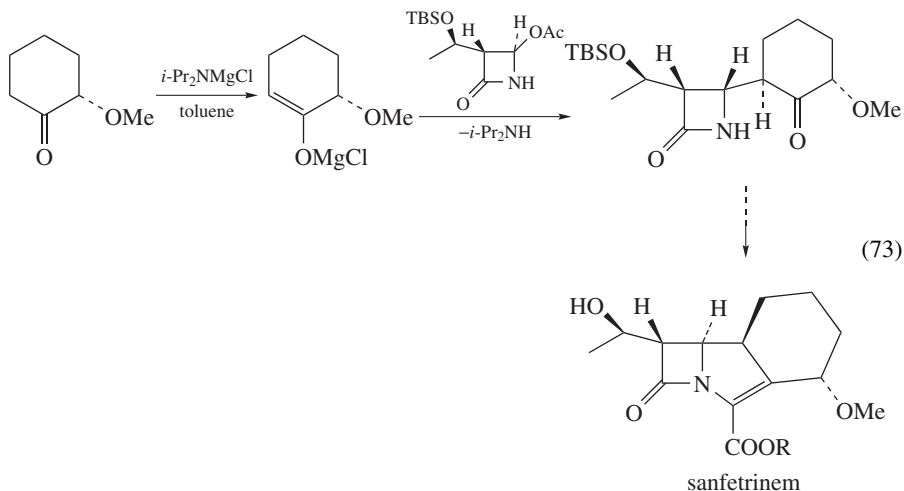


Magnesium ketone enolates are capable of C-alkylation. In general O-alkylated compounds are not observed. Matsumoto and coworkers have reported a diastereoselective synthesis for the preparation of tricyclic  $\beta$ -lactam antibiotics<sup>73</sup>. The key step is the reaction between magnesium enolate of (2*S*)-2-methoxycyclohexanone and 4-acetoxiazetidinone (equation 73). The direct coupling reaction between the magnesium enolate and the acetoxiazetidinone proceeds with high yield, regio- and diastereoselectively. Several similar methods are reported with tin and lithium enolates but, among the various enolates screened, the magnesium enolate is found to be the most simple and efficient.

TABLE 8. Synthesis of trimethylsilyloxy and hydroxy compounds from magnesium enolates and bis(trimethylsilyl)peroxide

R	R <sup>1</sup>	Yield of trimethylsilyloxy derivatives (%)	Yield of hydroxyl derivatives (%)
<i>n</i> -Hex	H	100	46
PhCH <sub>2</sub> CH <sub>2</sub>	H	100	42
(CH <sub>2</sub> ) <sub>6</sub>		100	61
(CH-CH <sub>3</sub> )(CH <sub>2</sub> ) <sub>6</sub>		100	40

Surprisingly, the magnesium enolate of 2-methylcyclohexen-1-one reacts with chloroacetone to give an unexpected product via a cyclohexane ring contraction<sup>91</sup> (equation 74).



Stile, then Baker and coworkers<sup>64, 65a</sup>, have shown that certain magnesium ketone enolates react with magnesium methyl carbonate (MMC: Stiles reagent) to give stable chelated adducts, which are either converted to  $\beta$ -keto carboxylic acids by treatment with aqueous HCl, or to the methyl esters by reaction with methanolic HCl. MMC adducts can be alkylated *in situ* with various alkyl halides. For example, the MMC adduct of 8-[1-(*t*-butyldimethylsiloxy)2-phenylethyl]-2-(1-oxoethyl)dibenzofuran reacts with  $\omega$ -halo compounds bearing nitrile, ester or amide groups (equation 75, Table 9). The obtained dibenzofuranic derivatives are important intermediates in the synthesis of a series of leukotriene B<sub>4</sub> antagonists. Good to moderate yields (40–86%) of monoalkylated products are formed. In contrast to the unsubstituted  $\beta$ -ketoacids, all  $\alpha$ -alkyl  $\beta$ -ketoacids intermediates decarboxylate during the reaction or workup.

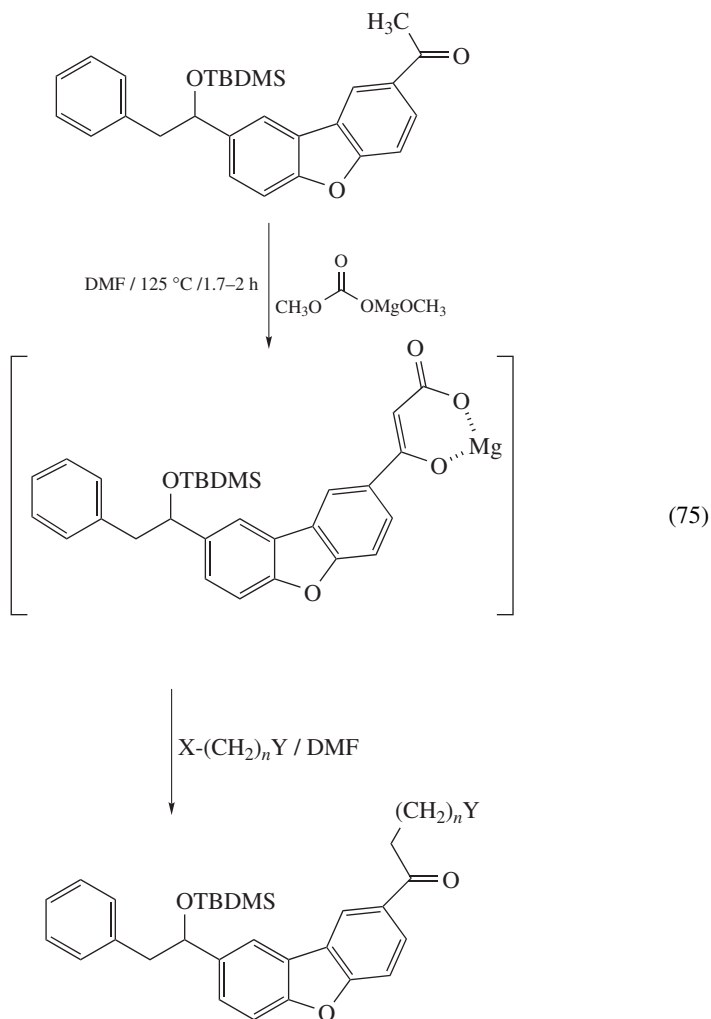
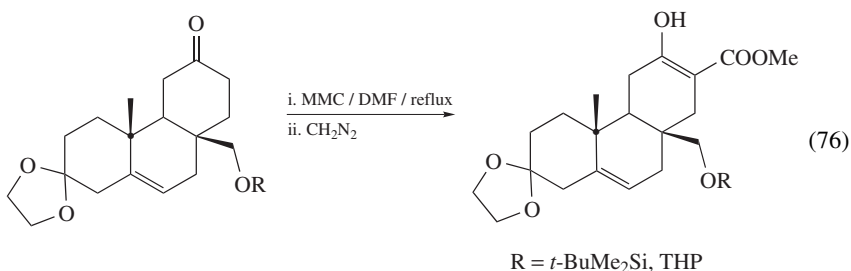


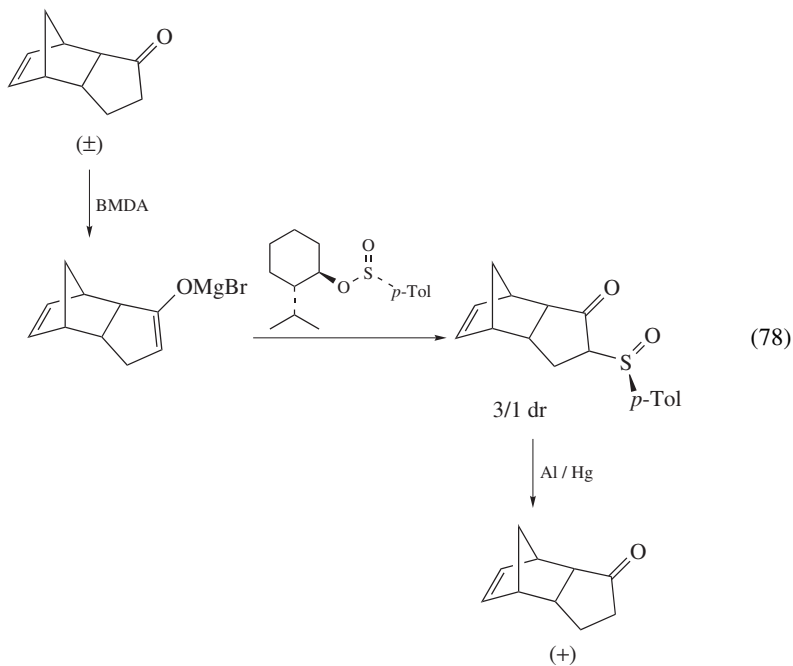
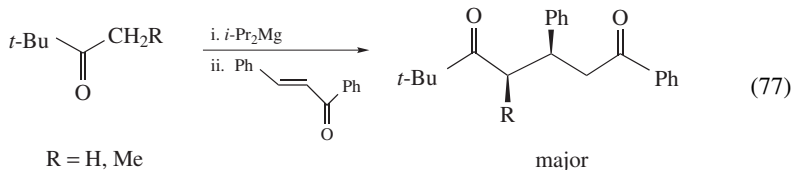
TABLE 9. Reactants and products of MMC-activated substitution reactions

X	Y	n
Br	COOMe	1
Br	CN	1
Br	CONMe <sub>2</sub>	1
Br	CON(Pr- <i>i</i> ) <sub>2</sub>	1
Br	CON(CH <sub>2</sub> ) <sub>4</sub>	1
Br	CON(CH <sub>2</sub> ) <sub>5</sub>	2
I	COOMe	2
Br	COOMe	3

A similar procedure has been applied to the preparation of tetracyclic intermediates having the Bruceantin tetrahydrofuran ring<sup>65b</sup>. The enolic  $\beta$ -ketoesters are isolated with excellent yields (85–95%) (equation 76).

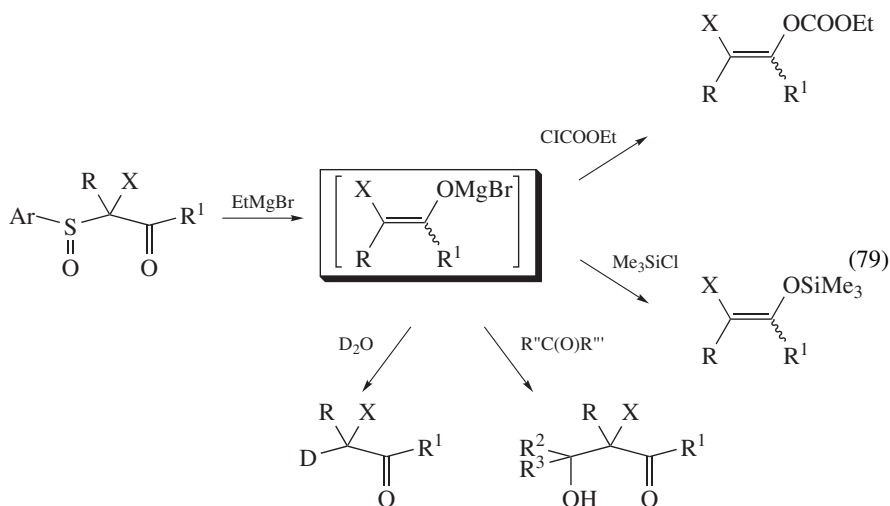


Magnesium enolates derived from hindered ketones are also possible Michael donors. For example, enolization of *t*-butyl alkylketones with (*i*-Pr)<sub>2</sub>Mg allows the 1,4-addition on the chalcone. A long reaction time (>3 h) limits the competing 1,2-addition and increases the proportion of the threo isomer<sup>97</sup> (equation 77).



The main access to pure enantiomer of chiral sulfoxides is the reaction of Grignard reagents with sulfinate esters. The reaction has been extended to magnesium enolates. It proceeds with clean inversion of configuration at the sulfur atom to yield the  $\beta$ -ketosulfoxide as a single diastereomer. An interesting example of kinetic resolution has been observed by Childs and Edwards<sup>82</sup> for the preparation of  $\beta$ -ketosulfoxide from a racemic ketone and the  $S_S$ -menthyl-*p*-toluensulfinate (equation 78). The rate of reaction of the (+)- and (–)-magnesium enolates with chiral sulfinate differs markedly and leads to the formation of two diastereomers in a 3/1 ratio. The two diastereomers cannot be separated by column chromatography, but the parent ketone is regenerated in optically active form by reductive desulfination.

Due to their inherent polarizability,  $\alpha$ -halo- $\beta$ -ketosulfoxides may be used as electrophilic partners in desulfination reaction to generate metal enolate. Therefore, treatment of  $\alpha$ -halo- $\beta$ -ketosulfoxides with EtMgBr gives magnesium enolates. Trapping these reagents with various electrophiles allows the preparation of  $\alpha$ -haloketones<sup>14,16</sup> (equation 79, Table 10).



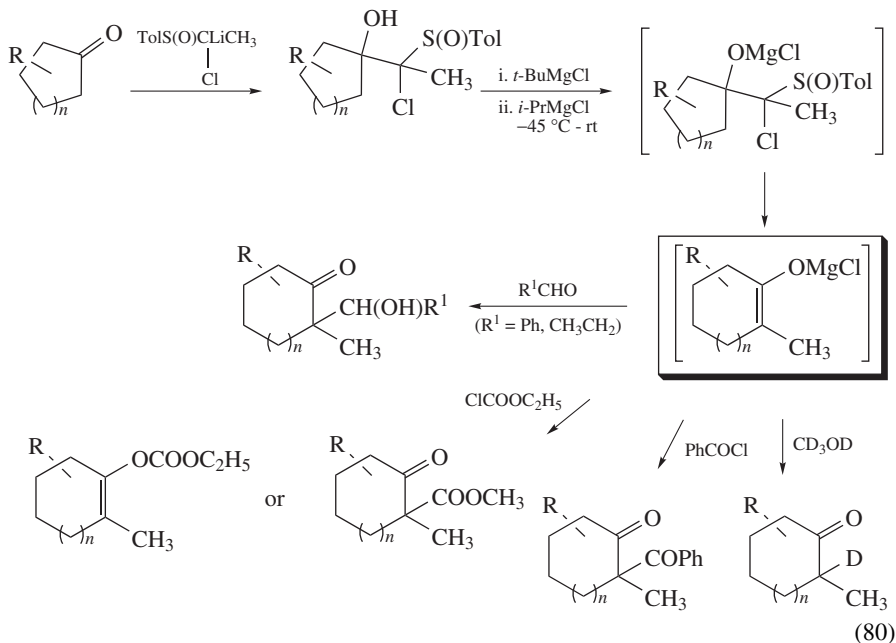
In contrast to  $\alpha$ -halo- $\beta$ -ketosulfoxides, 1-chloroalkyl aryl sulfoxides react with Grignard reagents to give  $\beta$ -oxido carbenoids. The rearrangement of these intermediates leads

TABLE 10. Substrates and reagents for synthesis of  $\alpha$ -halocarbonyl compounds

Ar	X	R	R <sup>1</sup>	R <sup>2</sup>	R <sup>3</sup>
Ph	F	CH <sub>3</sub>	Ph	CH <sub>3</sub>	CH <sub>3</sub>
Tol	Cl	CH <sub>3</sub> (CH <sub>2</sub> ) <sub>2</sub>	PhCH <sub>2</sub> CH <sub>2</sub>	Ph	H
	Br	CH <sub>3</sub> (CH <sub>2</sub> ) <sub>7</sub>	CH <sub>3</sub> (CH <sub>2</sub> ) <sub>8</sub>	PhCH <sub>2</sub> CH <sub>2</sub>	
			<i>c</i> -Hex	CH <sub>3</sub>	
				CH <sub>3</sub> (CH <sub>2</sub> ) <sub>8</sub>	
				<i>c</i> -Hex	
				(CH <sub>2</sub> ) <sub>5</sub>	



to magnesium enolates, which can be trapped with various electrophiles to give  $\alpha,\alpha$ -disubstituted carbonyl compounds in moderate to good yields<sup>18</sup> (equation 80).



Magnesium enolates generated by interconversion metal/halogen show a high reactivity toward diethylphosphorochloridate to furnish enol phosphates. This reaction has been used in the synthesis of tetrahydrocannabinols<sup>11,12</sup> as illustrated in equation 81. Reaction of the  $\alpha$ -iodo- $\beta$ -aryl-cyclohexanone **49** with EtMgBr gives the magnesium enolate **50** by metal-halogen exchange, which upon reaction with ClP(O)(OEt)<sub>2</sub> provides the enol diethyl phosphate **51**. The enol phosphate thus formed is converted in silyl derivative **52** by treatment with ClMgCH<sub>2</sub>SiMe<sub>2</sub>(OPr-*i*) in the presence of Ni(acac)<sub>2</sub> as a catalyst in THF. The product **52** is the direct precursor of  $\Delta_9$ -THC metabolites.

It should be noted that the reaction of boron and lithium enolates analogues of **50** with ClP(O)(OEt)<sub>2</sub> are unsuccessful.

Enantioselective protonation of ketone metal enolates constitutes an important method for the preparation of optically active ketones. Fuji and coworkers<sup>92</sup> have shown interest in the magnesium counteraction in the enantioselective protonation of such enolates. Pertinent results are obtained with protonation of Mg(II) enolates of 2-alkyltetralones and carbamates derived from 1,1'-binaphthalene-2,2'-diol as chiral proton sources, as indicated in equation 82 and Table 11.

Magnesium enolates react with aldehydes and ketones to give aldol products after hydrolysis. The reaction proceeds both regio- and stereoselectively and has found many applications in the synthesis of natural products.

By a careful choice of the base and of the experimental conditions, either the kinetic or the thermodynamic magnesium enolate could be prepared (see Section II).

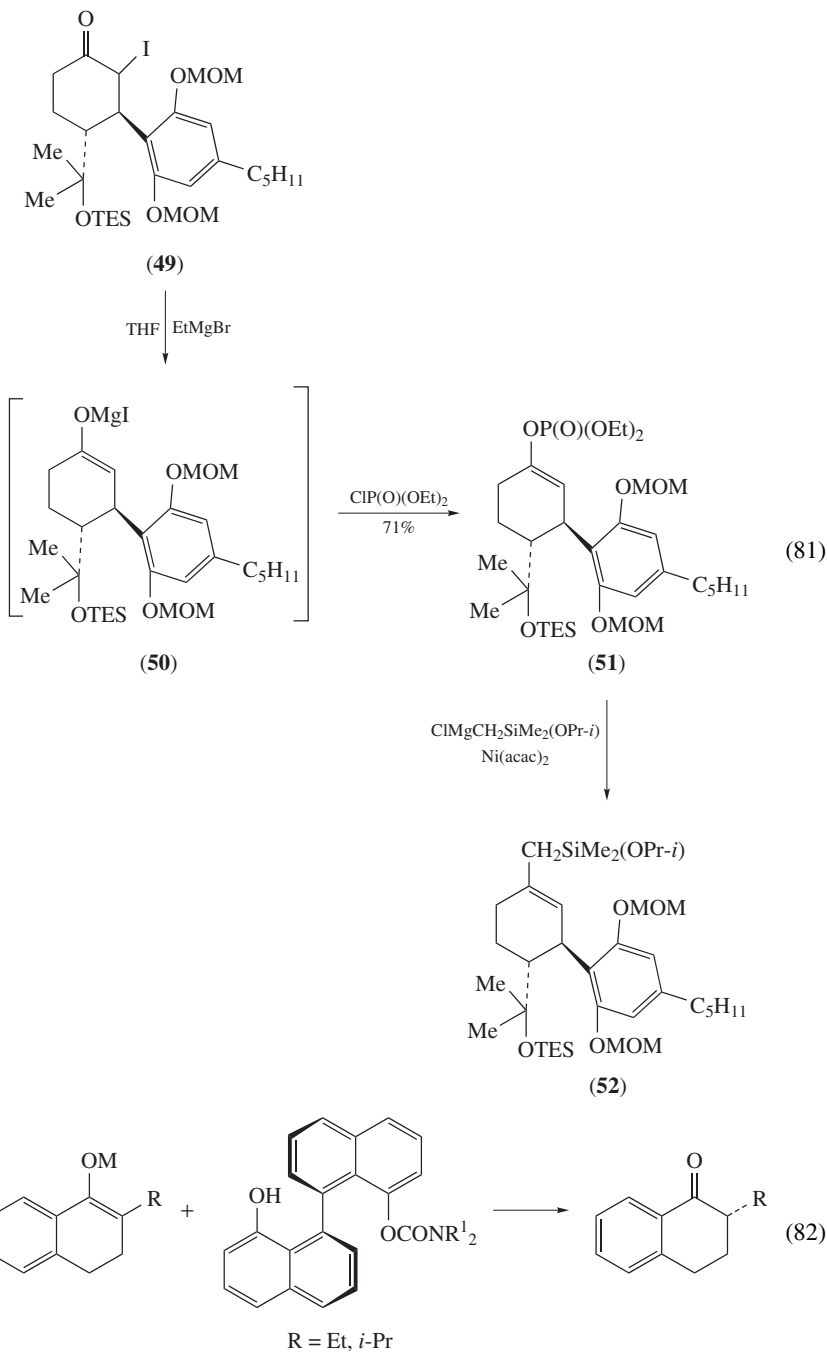
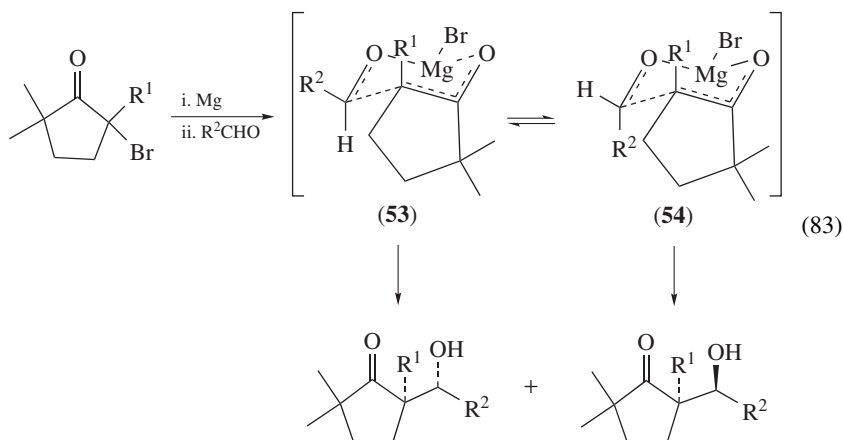


TABLE 11. Enantioselective protonation of magnesiumenolates

M	R	R <sup>1</sup>	ee (%)
MgI	<i>i</i> -Pr	<i>i</i> -Pr	9
Li	<i>i</i> -Pr	<i>i</i> -Pr	92
MgI	<i>i</i> -Pr	Et	15
Li	<i>i</i> -Pr	Et	93

Aldol reactions of magnesium enolates are frequently more diastereoselective than the corresponding reactions of lithium enolates. The aldol condensation proceeds via a cyclic transition state in agreement with the Zimmerman–Traxler chelated model<sup>53b</sup>.

A few years ago, Fellmann and Dubois<sup>98</sup> studied the aldol reaction of magnesium enolates of trialkyl-substituted  $\alpha$ -bromocyclopentanones with different aldehydes, as exemplified in equation 83 and Table 12. Upon addition of aldehydes, 2-unsubstituted cyclopentanone magnesium enolates (obtained by magnesium insertion in the C–Br bond) are converted to the *threo* aldol products via a *lk* approach. A chair-like transition state, in which the R<sup>2</sup> substituent of the aldehyde is placed in an equatorial position to prevent unfavorable 1,3-diaxial interactions with the cyclopentane ring, explains the stereochemical result. The *threo* isomer is also observed with a small alkyl group R<sup>1</sup> for the same reasons. When R<sup>1</sup> is larger, the *gauche* R<sup>1</sup>/R<sup>2</sup> interactions become important and disfavor **53** favoring **54**. This decreases the energy difference between both transition states and smaller selectivity is therefore observed.



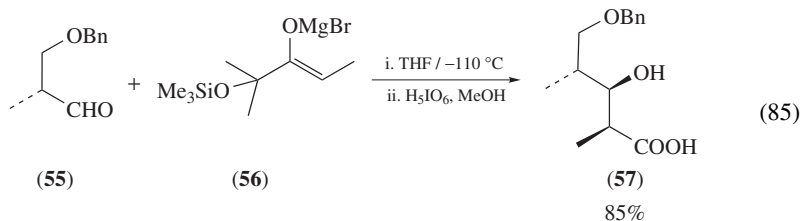
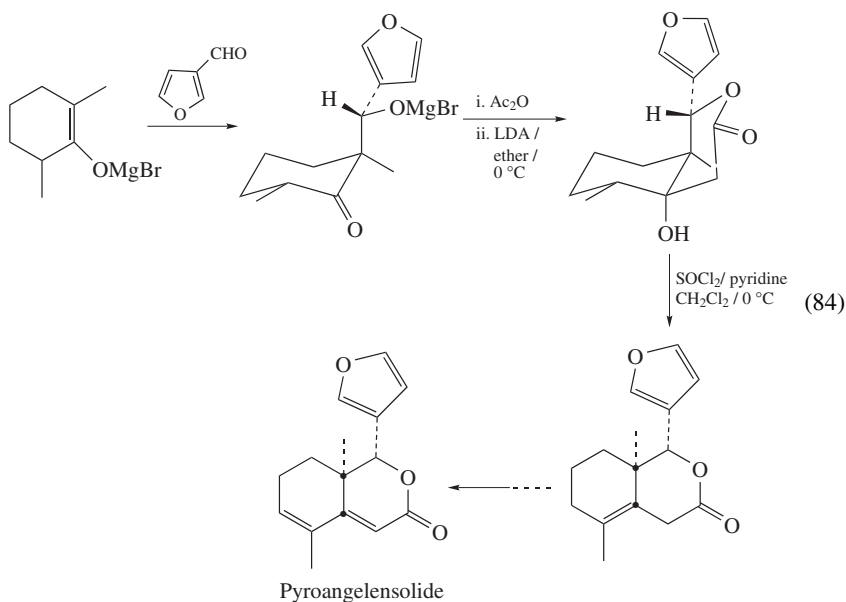
The study of Mateos and Fuente Blanco<sup>6</sup> on the aldol condensation between magnesium enolate of 2,2,6-trimethylcyclohexanone and 3-furaldehyde is in accord with the preceding stereochemical results. Application to the preparation of model compounds of limonoid, such as pyroangelensolide, is described (equation 84).

In addition to the structural effects due to the geometry of a substituted magnesium enolate, the stereochemistry of the reaction with a chiral aldehyde can be controlled, as described in equation 85. The aldol reaction based on the addition of magnesium enolate **56** to aldehyde **55** has been applied to the synthesis of monensin. The chiral center in the aldehyde induces the preferential approach of one diastereotopic face of the aldehyde by

TABLE 12. Stereochemistry of cyclopentanones

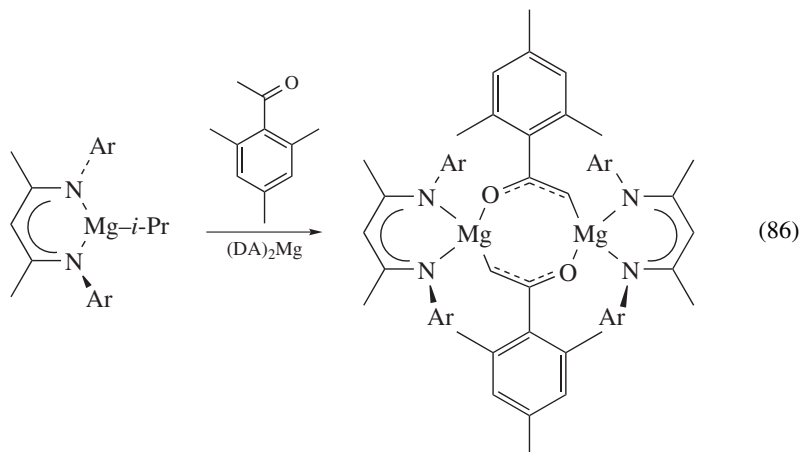
R <sup>1</sup>	R <sup>2</sup>		
H	Me	93.5	6.5
H	Et	94	6
H	<i>i</i> -Bu	93.5	6.5
H	<i>neo</i> -Pe	94	6
H	<i>i</i> -Pr	97	3
H	<i>t</i> -Bu	>99	<1
Me	Me	93.5	6.5
Et	Me	87.5	12.5
<i>i</i> -Bu	Me	80	20
<i>i</i> -Pr	Me	46	54
<i>i</i> -Bu	Me	29	71

the magnesium enolate; the aldol product formed is converted into a carboxylic acid (cf. **57**) by H<sub>5</sub>IO<sub>6</sub> with a facial preference of 5/1.



Magnesium enolates derived from hindered ketones are able to initiate polymerization.

For example, addition of 2',4',6'4-trimethylacetophenone in toluene to a suspension of  $(\text{DA})_2\text{Mg}$  results in the isolation of  $(\text{DA})\text{Mg}(\text{OC}(=\text{CH}_2)\text{-2,4,6-Me}_3\text{C}_6\text{H}_2)$ , which is found to be an excellent initiator for the living syndiospecific ( $\sigma_r > 0.95$ ) polymerization of methyl methacrylate<sup>99</sup> (equation 86).



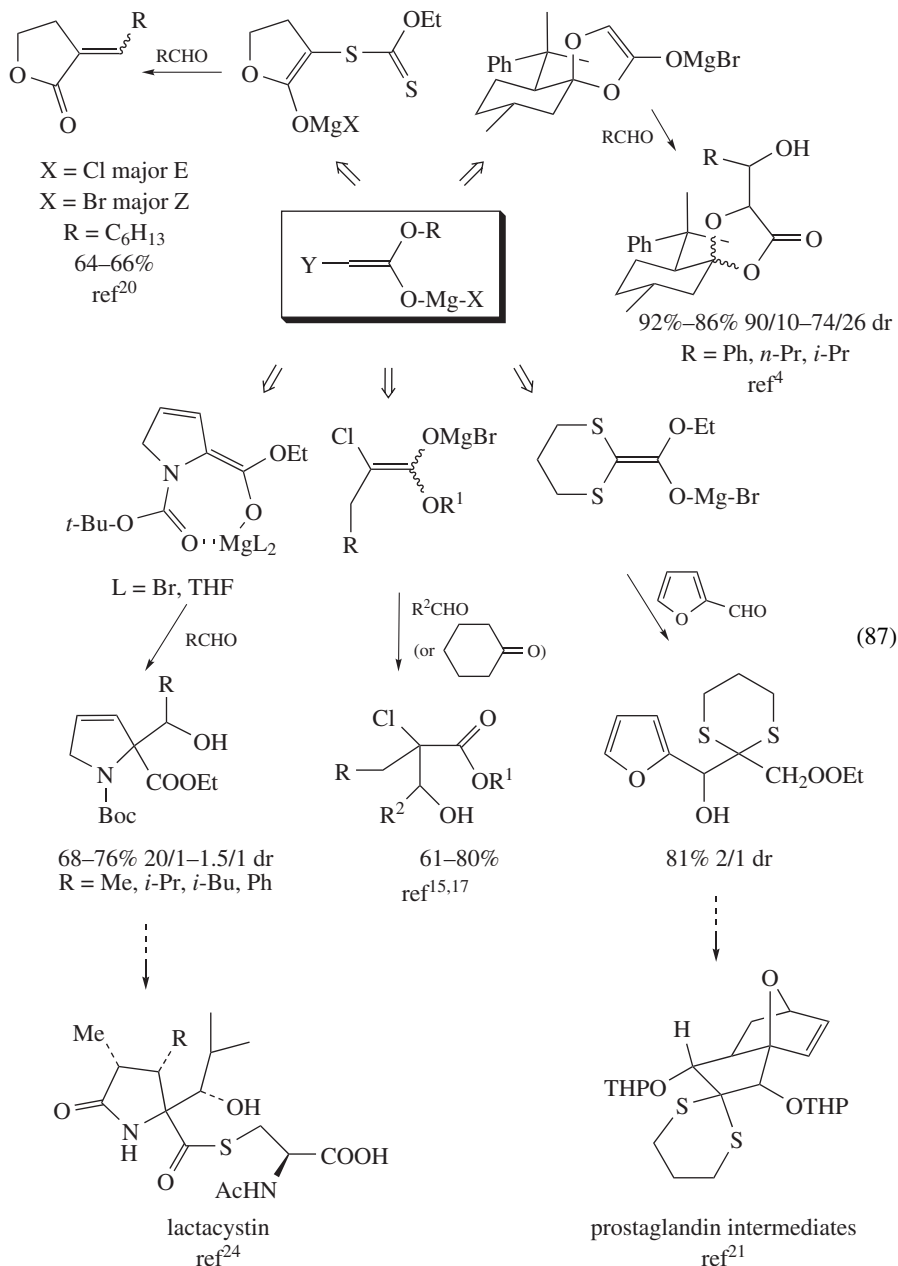
### C. Reactions of Magnesium Ester Enolates and Magnesium Lactone Enolates with Electrophiles

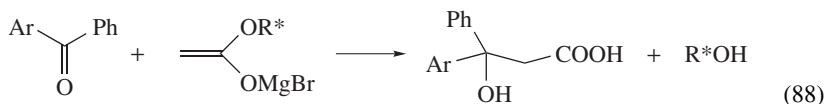
Different approaches for the stereoselective transformations and applications of magnesium ester and lactone enolates to organic synthesis have been reported. In most cases, a second functional group is present in the  $\beta$  position. This can be explained by an easy preparation and by a greater stability of the enolate. They are useful reagents in aldol reactions and are attractive for the construction of biologically active products. Equation 87 describes a few types of bifunctional compounds involving magnesium ester and lactone enolates and typical examples of synthetic utility.

Asymmetric synthesis in aldol-type reaction involving magnesium ester or lactone enolates has also been reported. Enolate of (–)-menthyl or (+)-bornyl acetate reacts with substituted benzophenones or  $\alpha$ -naphthophenones to yield, upon hydrolysis of the resulting esters, optically active  $\beta$ -hydroxyacids. Although these results are interpreted in terms of a steric factor, Prelog's rules are not applicable to these reactions<sup>69</sup> (equation 88).

The reaction of alkyl dihalogenoacetate magnesium enolates with 2,3-isopropylidene-D-glyceraldehyde affords the expected  $\beta$ -hydroxy- $\alpha$ -dihalogenoesters<sup>100</sup>. The *erythro* isomer is obtained with isopropyl dichloroacetate magnesium enolate. This result is in agreement with theoretical models. 2-Deoxy-pentono-1,4-lactones are obtained after removal of the halogen atom by either Raney nickel or tributyltin hydride reduction (equation 89).

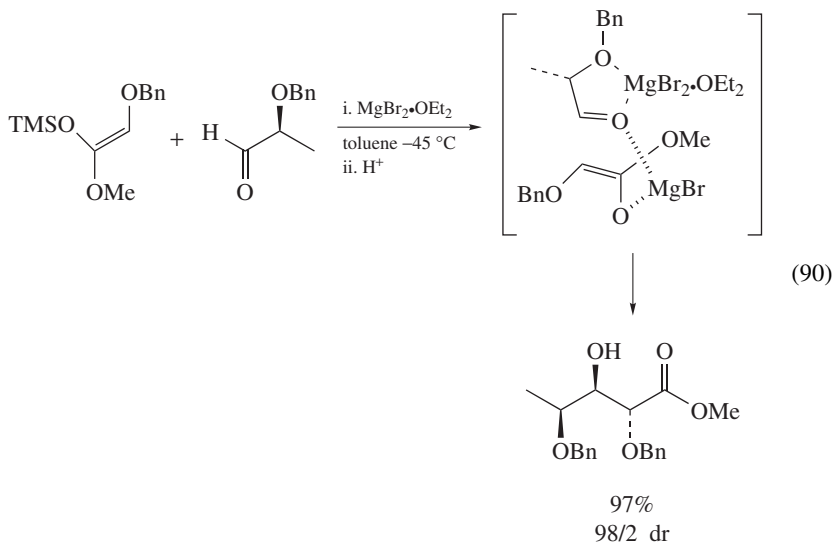
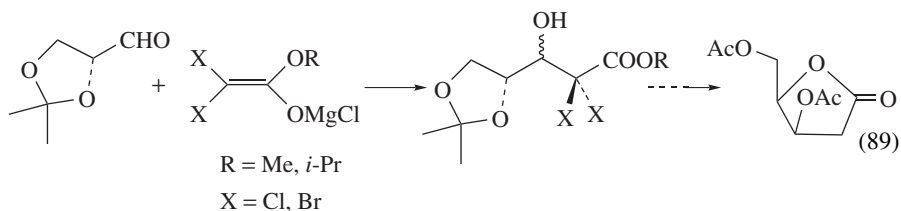
Magnesium-halide-mediated aldol reactions are often reported using magnesium salts simply as Lewis acids<sup>101–103</sup>. More recently, Mukaiyama and coworkers<sup>28</sup> have described a highly diastereoselective aldol reaction between chiral alkoxy aldehydes and magnesium enolate, formed by transmetalation from a silylenol ether and  $\text{MgBr}_2 \cdot \text{OEt}_2$  via a six-membered chelated cyclic transition state. High yield and excellent diastereoselectivity are observed (equation 90).





$\text{R}^* = (-)\text{-menthyl}, (+)\text{-bornyl}$

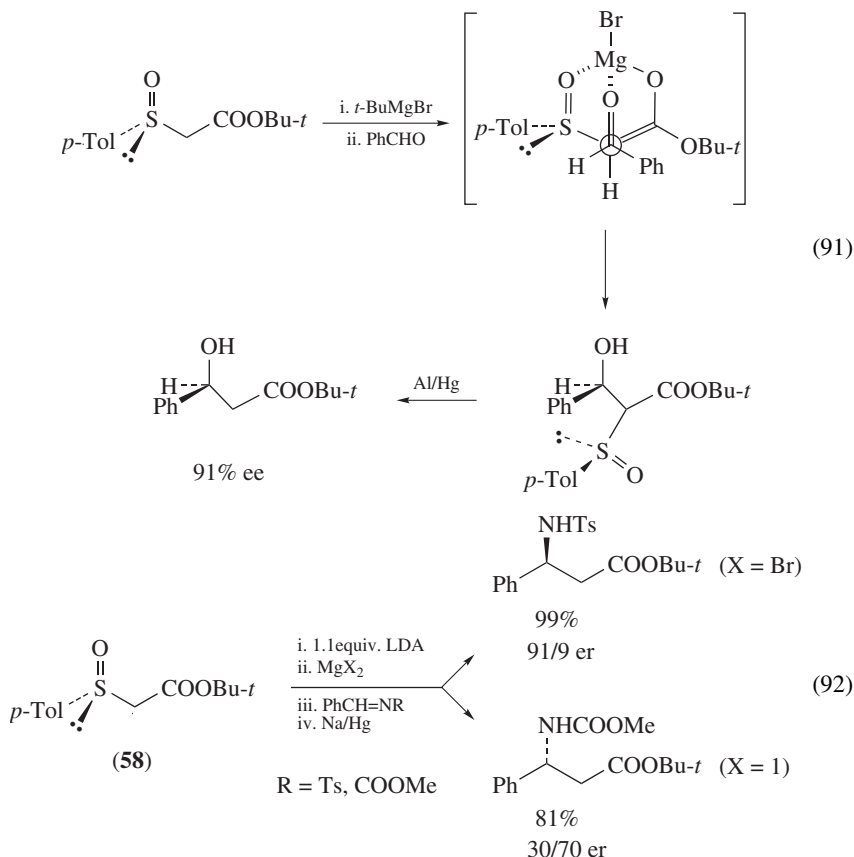
69–82% yield  
4–48% optical yield



Carbanions of enantiomerically pure sulfoxides have been investigated as precursors for asymmetric synthesis. However, they react with carbonyl compounds with modest selectivity. This selectivity is increased by the incorporation of an ester group adjacent to the carbanionic center. The observed stereochemistry in this reaction is consistent with chelated intermediates, where magnesium chelate is particularly efficient, as illustrated in equation 91<sup>54,55</sup>.

Fujisawa and coworkers<sup>25</sup> have studied the reaction of pure  $\alpha$ -sulfinyl ester enolate **58** with benzaldimines possessing an electron-withdrawing group at the nitrogen atom. The reaction gives  $\beta$ -aminoester in both enantiomeric forms in satisfactory yields (67–99%), in which the changeover of the diastereofacial selectivity was induced by the choice of the protecting group at the nitrogen and the use of additives. Two transition states are proposed. With the magnesium bromide, the reaction probably proceeds through a

chelated model, whereas by using the less reactive magnesium iodide, it proceeds through a nonchelated model (equation 92).

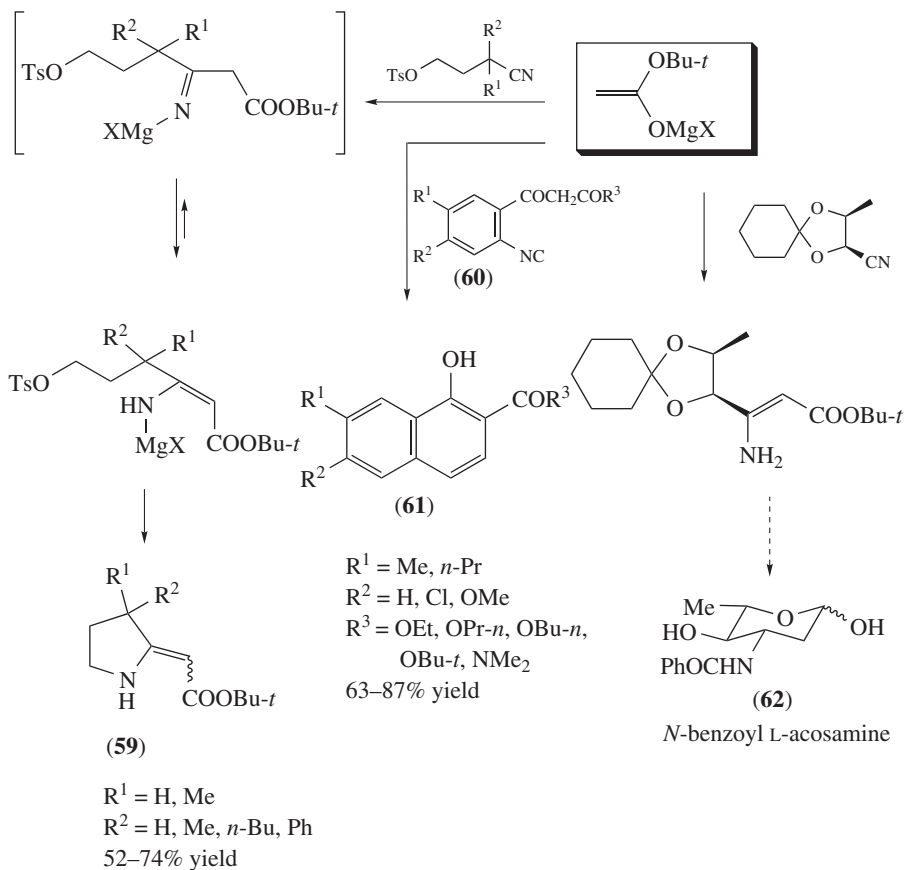


Hiyama and Kobayashi have studied the reaction between magnesium enolates of *t*-butyl (or ethyl) acetate or *t*-butyl propionate and nitriles. The reaction furnishes 3-amino-2-alkenoates **59** having *Z* configuration<sup>68</sup>. It has been successfully extended to isonitriles. The addition of magnesium enolate of alkyl acetate to isonitriles **60** affords 4-hydroxy-3-quinolinecarboxylic esters or amides **61** by a tandem Claisen-type condensation/cyclization sequence<sup>72</sup>. This approach has also been used for the synthesis of heterocycles<sup>67</sup> and aminosugar such as L-acosamine **62**<sup>104</sup> (equation 93).

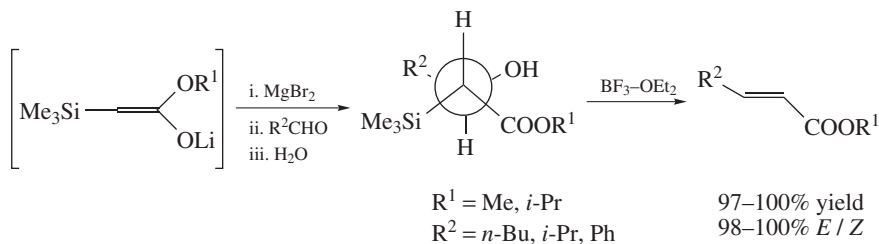
The transmetalation of  $\alpha$ -silylated ester lithium enolates by magnesium bromide and subsequent Peterson olefination provides a stereoselective synthesis of  $\alpha,\beta$ -unsaturated esters<sup>22</sup> (equation 94).

Magnesium aminoester enolates are of much interest for the synthesis of complex aminoacids and peptides. These chelate enolates have been used as nucleophiles for a wide range of stereoselective transformations, as diastereoselective Michael additions<sup>23</sup> and Claisen rearrangement<sup>19</sup>. Two typical examples are presented in equation 95.



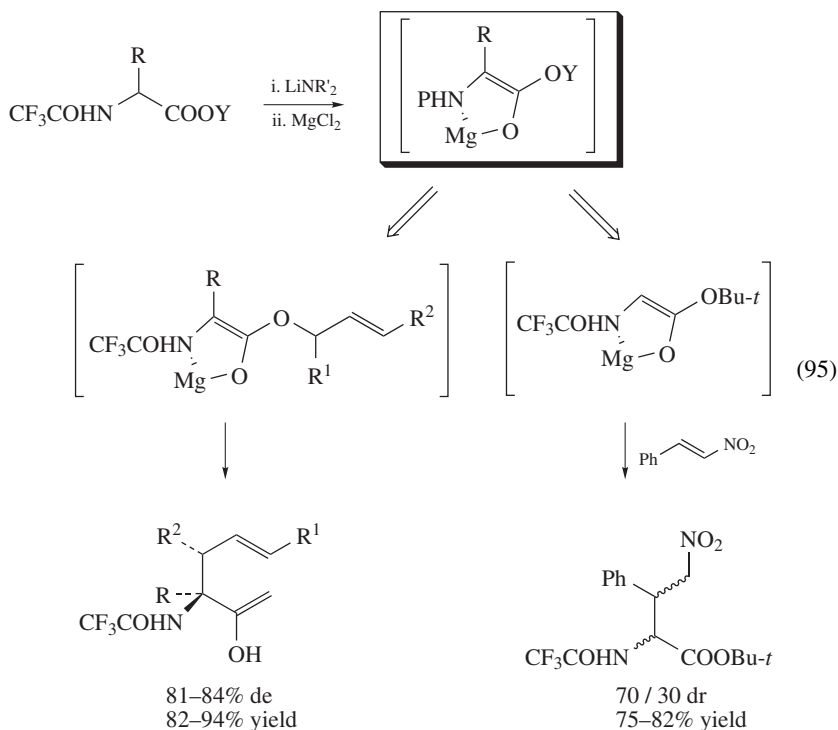


(93)



(94)

The formation of chelated magnesium enolate presents three advantages: the enolate is stable and doesn't decompose during the rearrangement; the chelation accelerates the Claisen rearrangement; the fixed enolate geometry that results from the chelation leads to interesting degrees of diastereoselectivity.



## D. Reactions of Magnesium Dicarboxyl Enolates with Electrophiles

### 1. Reactions of magnesium $\alpha$ -ketoester enolates

Iodomagnesium enolates **17** derived from  $\alpha$ -ketoesters are obtained as indicated in Section II from  $\alpha$ -chloro glycidic esters **15**. They can react with different electrophiles. Hydrolysis of the magnesium enolates **17** yielded the  $\alpha$ -ketoesters **18**. A detailed study on deuteriolysis reports the regioselective C-mono **18-d<sub>1</sub>** and C-dideuteriation **18-d<sub>2</sub>** products using [D<sub>4</sub>] acetic acid as deuterium donor (94–99% yield) (see equation 6, Section II). This constitutes an efficient method to introduce the pyruvic moiety, deuteriated or not deuteriated, into aliphatic or glucidic substrates<sup>8</sup>. Knowing the biological interest of  $\alpha$ -ketoacid group, this first example of deuterium incorporation in such moiety appears especially important as it opens the route to radioactive tracers in this series.

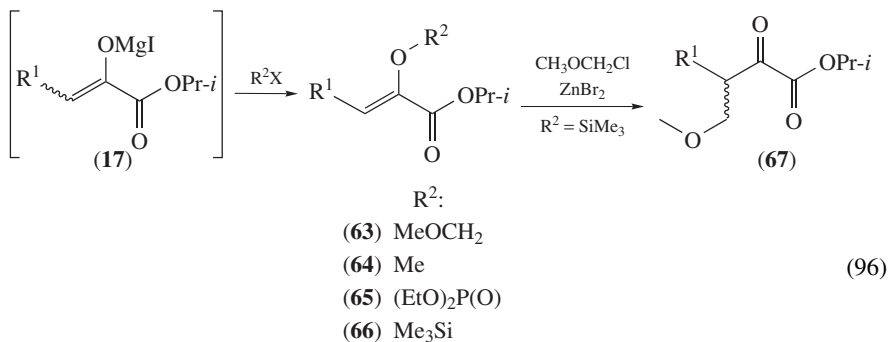
However, due to the high stability of these magnesium enolates, it is necessary to add an excess of HMPA to increase their nucleophilicity toward other electrophiles. Under these conditions, the aliphatic and glucidic magnesium enolates **17** react with hard alkylating reagents such as chloromethylmethyl ether, dimethyl sulfate, diethyl phosphorochloridate and chlorotrimethylsilane to provide O-alkylation products **63–66** in fair to good yields<sup>9</sup> (equation 96, Table 13). Enol ether moieties of different resistance to acid-catalyzed hydrolysis are therefore obtained. It is noteworthy that the steric hindrance of a glucidic residue is not the limiting factor and the phosphorylation of enolates is even more efficient with derivatives of D-galactose and D-lyxose. This procedure constitutes an interesting

TABLE 13. Reactions of magnesium enolates **17**

R <sup>2</sup>	X	Yield (%)	E/Z	Yield (%)	E/Z	Yield (%)	E/Z	Yield (%)	E/Z	Yield (%)	E/Z		
H <sup>a</sup>	OH <sup>a</sup>	98	—	18b	95	—	18c	100	—	18d	99	18e	98
MeOCH <sub>2</sub>	Cl	75	13/87	63b	58	10/90	63c	53	19/81	63d	47	63e	62
Me	SO <sub>4</sub> Me	76	0/100	64b	34	0/100	64c	54	0/100	64d	20	64e	44
(EtO) <sub>2</sub> P(O)	Cl	28	93/7	65b	34	95/5	65c	28	92/8	65d	45	65e	43
Me <sub>3</sub> Si	Cl	78	15/85	66b	86	7/93	66c	62	19/81	66d	90	66e	50

<sup>a</sup> See equation 6, Section II.

alternative to the Perkow reaction for the preparation of glucidic phosphoenolpyruvic acid derivatives **65d–e**.



The reaction is stereoselective giving the *Z*-isomer as the major product with alkyl halides and silyl halides. Interestingly, *E* selectivity is observed with enolphosphates.

In the aliphatic series, the C-alkylation of enolates **17** is achieved through their O-silylated derivatives **66**. In the presence of a catalytic amount of  $\text{ZnBr}_2$ , the silyl enol ether **66** reacted with  $\text{ClCH}_2\text{OCH}_3$  to give only the C-alkylated  $\alpha$ -ketoester **67**. The alkylation is regiospecific but the ketoesters (**67a**, **c**) are obtained with modest yields (about 50% yield).

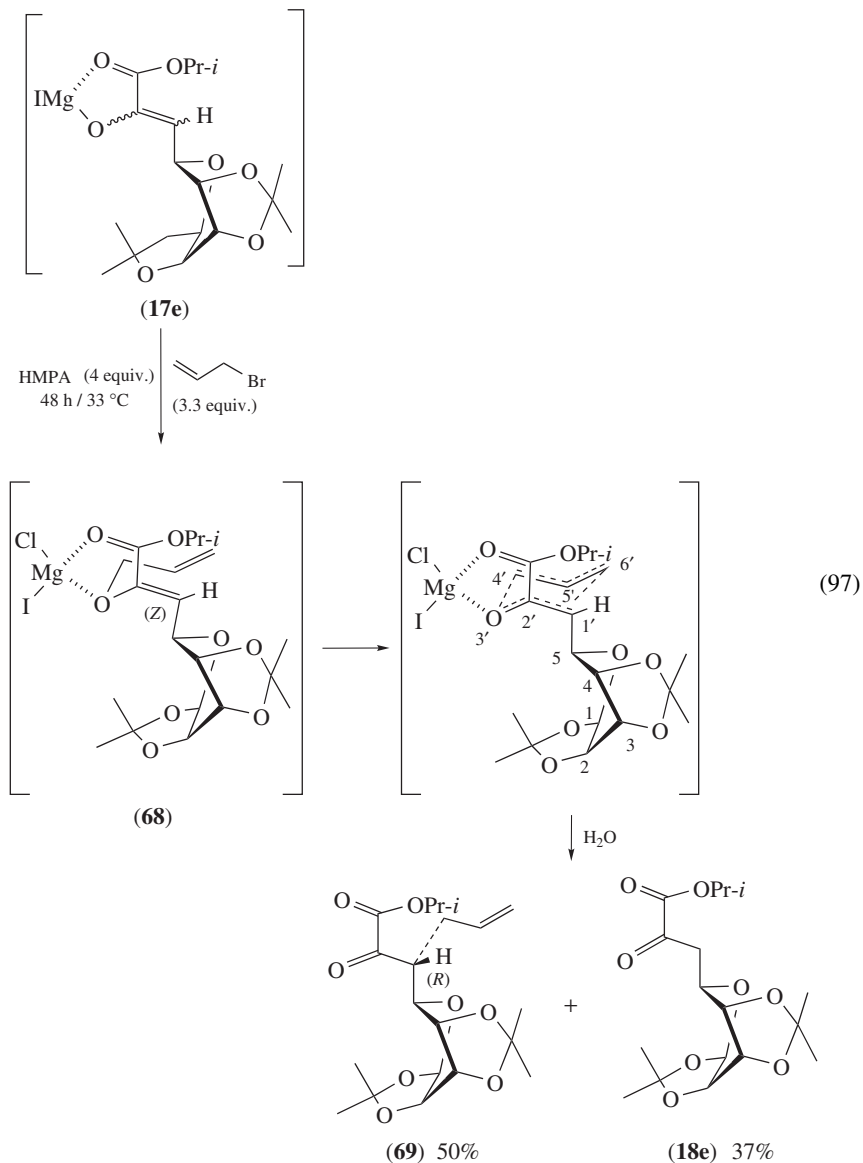
An interesting application in the glucidic series concerns the one-pot magnesium dihalide-catalyzed Claisen rearrangement of 2-alkoxycarbonyl allyl vinyl ethers obtained from the iodomagnesium enolate **17e**. This represents the first synthetic application for the stereoselective construction of a disaccharide analogue **70** including a galactosyl and an ulosonic isopropyl ester moiety<sup>105</sup>. Thus, the reaction of the magnesium enolate **17e** with allyl bromide led to the  $\alpha$ -ketoester enol precursor **68** (equation 97). The reaction is rather slow, due to the poor reactivity of enolate **17e**, so that, as the slow O-allylation proceeds, a mild Claisen rearrangement occurs, catalyzed by the magnesium salts present in the reaction medium. Finally, after 48 h at  $33^\circ\text{C}$ , the C-allylation product **69** is obtained in 50% yield accompanied by  $\alpha$ -ketoester **18e**. The latter compound **18e** results from the hydrolysis of the unreacted starting magnesium enolate **17e** and is easily separated from **69** (37% yield after a chromatographic purification).

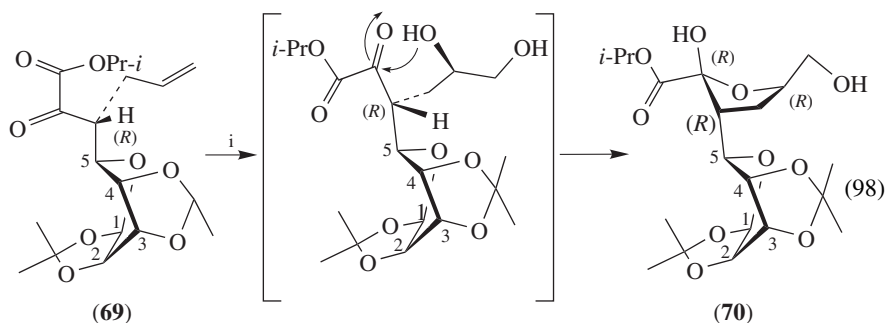
The reaction is 100% stereoselective and affords **69** as a unique stereomer with the (*R*)-configuration at C-6, assigned by X-ray analysis. Consequently, the configuration at C-6 results from the well-known chair transition state model for the (*Z*)-O-allyl enol **68** in which the allyl unit is on the opposite side to the isopropylidene ketal at C3–C4 and reacts on the *Si* face of the trisubstituted carbon–carbon double bond. Such a transition state leads to the sole (*R*)-configuration in **69**.

The asymmetric inducing effect of the chiral pyranic ring placed outside of the six centers of the chair transition state has to be noted. In the present case, magnesium dihalide seems to play a crucial role in terms of stereocontrol as an efficient tool to fix a defined

and single transition state conformation and to maximize asymmetric induction. It allows one also to carry out the rearrangement under mild reaction conditions at low temperature.

The C-allyl ketoester **69** represents a key precursor for the stereoselective synthesis of the disaccharide analogue **70** in which an ulosonic residue could be installed via the dihydroxylation of the double bond of **69** (equation 98). These glucidic  $\alpha$ -ketoacids are involved in biosynthetic pathways of bacteria and constitute important targets for the design of new antibacterial agents.



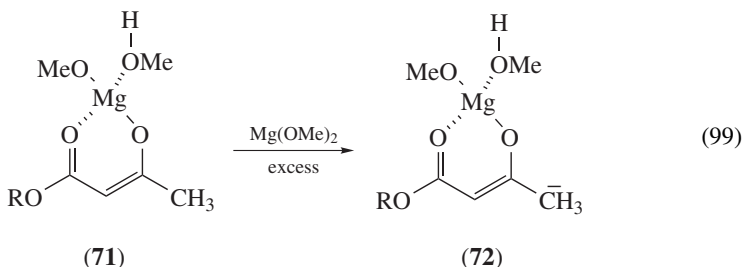


$i = \text{OsO}_4 / \text{NMO}$ , 24 h (95% yield, de: 3/2) or AD-mix- $\beta$ , 48 h (90% yield, 9/1 dr)

## 2. Reactions of magnesium chelates of $\beta$ -ketoesters or $\beta$ -diketones

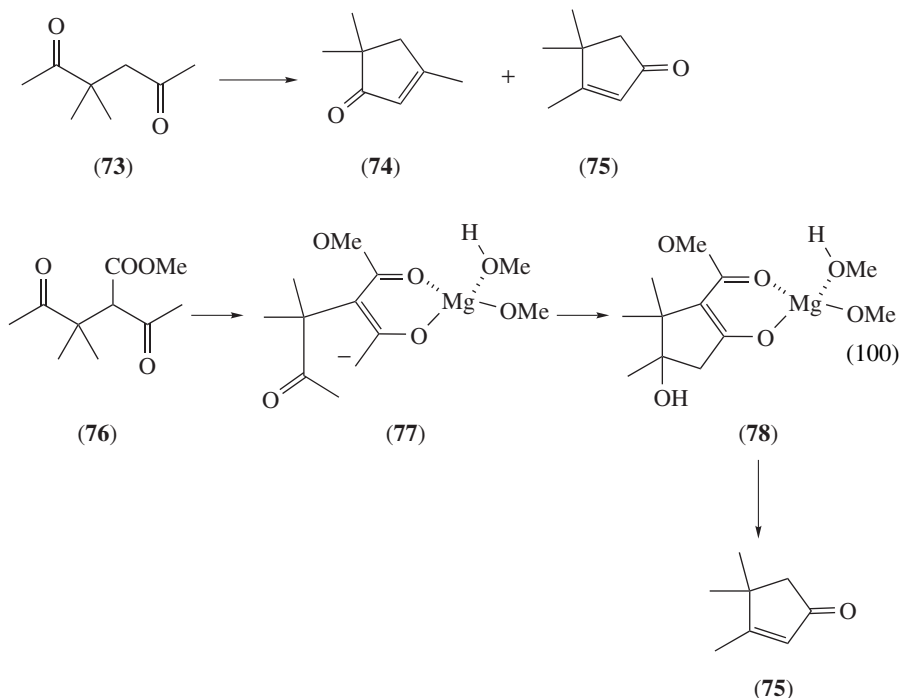
Prepared from  $(\text{MeO})_2\text{Mg}/\text{MeOH}$ , the magnesium chelates of  $\beta$ -ketoesters or  $\beta$ -diketones show high stability and sometimes a particular reactivity<sup>106, 107</sup> (see Section II).

Base-catalyzed transformations can be carried out elsewhere on a complex molecule in the presence of such protected  $\beta$ -dicarbonyl magnesium chelate. For example, the chelated magnesium enolate of a  $\beta$ -ketoester such as **71** prevents the carbonyl keto group becoming an acceptor in aldol condensations. However, in the presence of excess of magnesium methanolate, exchange of the acetyl methyl protons can occur via a carbanion **72** stabilized by delocalization into the adjacent chelate system (equation 99).



Consequently, the magnesium chelate **71** can also react as a nucleophilic donor in aldol reactions. In the chemistry involving magnesium chelates, these two aspects model their mode of action as nucleophilic partners in aldol condensations. This is exemplified in aldol condensations of  $\gamma$ -diketones<sup>106</sup>. Thus, sodium hydroxyde catalyzed cyclization of diketone **73** to give a mixture of 3,5,5-trimethyl-cyclopent-2-enone **74** and 3,4,4-trimethyl-cyclopent-2-enone **75** in a 2.2/1 isomeric ratio (equation 100). When treated with magnesium methanolate, the insertion of a  $\alpha$ -methoxy carbonyl group as control element, as in **76**, allows the formation of a chelated magnesium enolate **77**, and the major product is now mainly the aldol **78**. This latter treated with aqueous NaOH provides the trimethylcyclopent-2-enones **74** and **75** in a 1/49 ratio.

Alternatively, the displacement of alkoxide by attack of a nucleophile at the carbonyl unit of complexed magnesium  $\beta$ -ketoester can proceed smoothly according to a Claisen-type reaction, as described in the transformation of xantophanic enol **79** into resorcinol **80** (equation 101)<sup>107</sup>.



Other examples including the compared reactivity of sodium and magnesium enolates of  $\beta$ -ketoester, especially in xanthrynone and glaucyrynone chemistry, are detailed in the review of L. Crombie<sup>108</sup>.

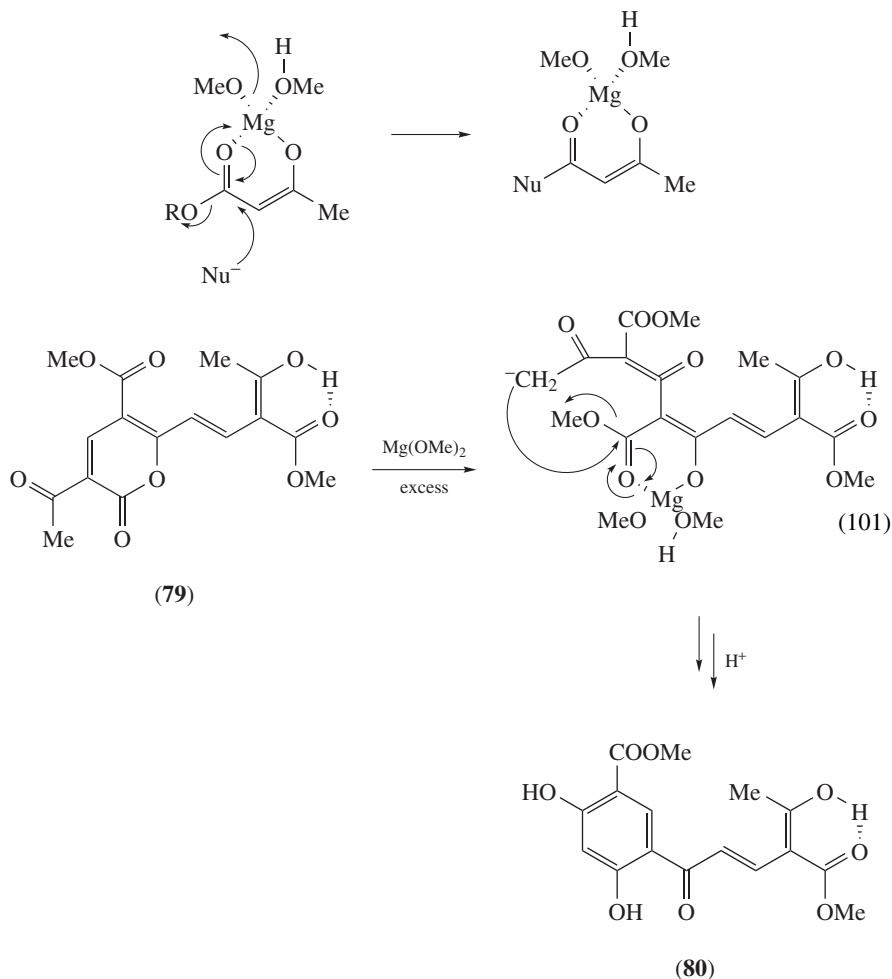
### 3. Reactions of magnesium dialkyl malonate or magnesium hydrogen alkyl malonate

Anions derived from malonates are ambident nucleophiles, which can react at the carbon or oxygen atom. Therefore, carbon-carbon bond-forming reactions by alkylation or acylation of enolates have been encountered with difficulties. Side reactions which may cause problems are the above-mentioned competing O-reaction and dialkylation<sup>109</sup>.

Ireland and Marshall<sup>110</sup> have shown that the use of magnesium malonate enolates offered several advantages: (a) magnesium stabilizes the malonate anion and allows some selective C-alkylation and acylation; (b) magnesium malonate is more soluble and more stable than the corresponding lithium malonate.

Thus, magnesium malonate enolates are useful tools for C-acylation reactions in the synthesis of  $\beta$ -ketoesters. Two reagents could be used for such purposes: magnesium malonate derived from hydrogen methylmalonate, and magnesium malonate derived from dialkylmalonate.

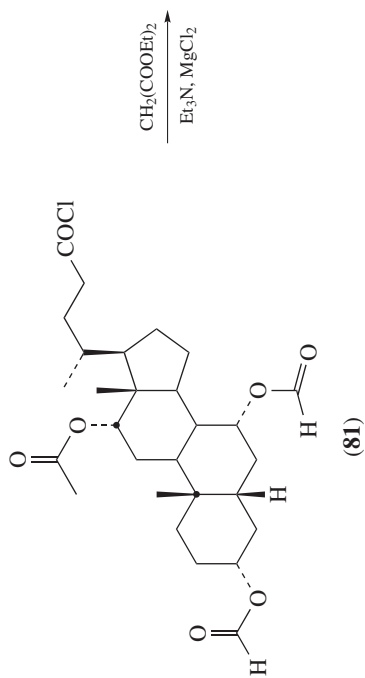
They are easily prepared from Grignard reagents, magnesium ethoxide or with the complex magnesium chloride-trialkylamine (see Section II where the generation of these reagents is discussed). The acylation of anions derived from malonates can be achieved with acyl chlorides, acyl imidazoles, alkoxycarbonylimidazoles or mixed anhydrides.



This acylation procedure is very useful in the synthesis of biologically active products, such as steroids and aminoacids.

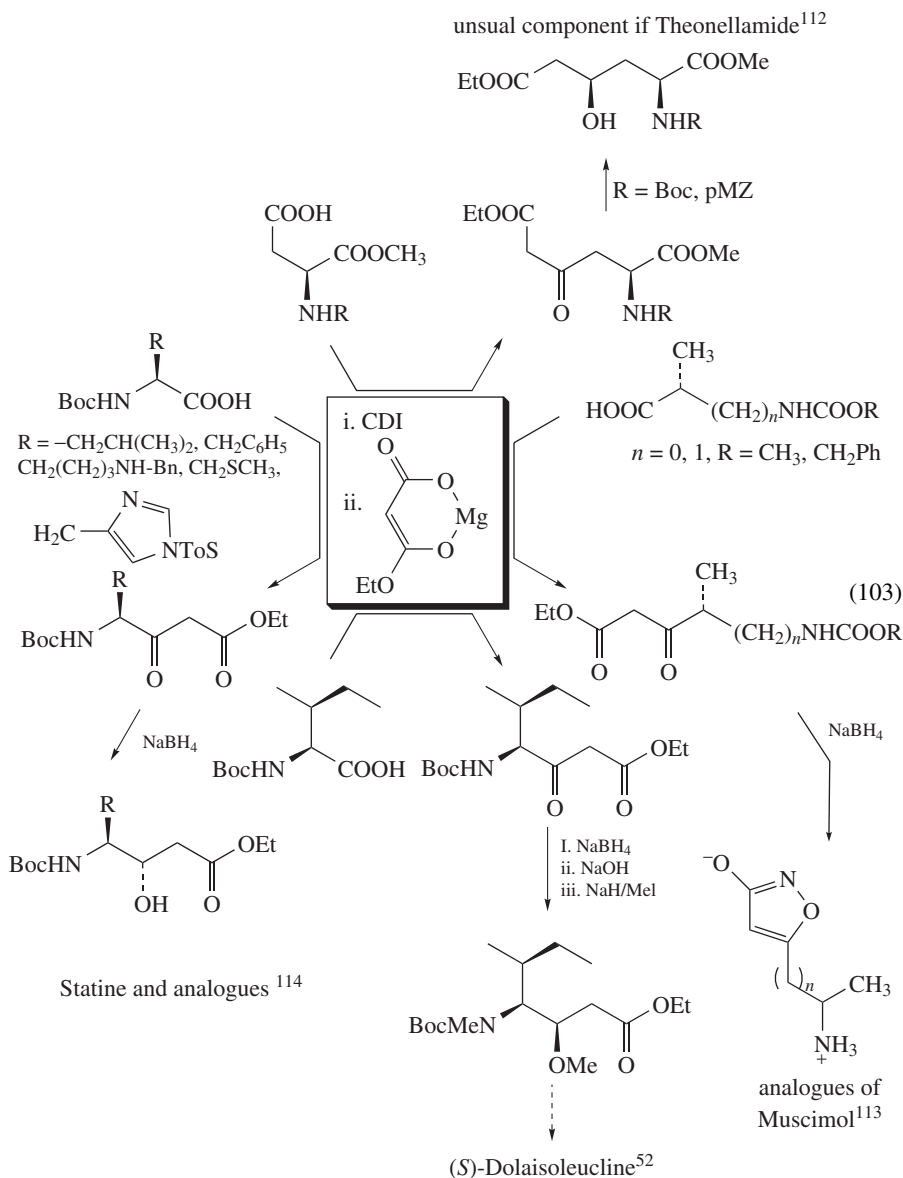
Recently, Francis and coworkers<sup>111</sup> have reported a scalable stereoselective synthesis of Scymnol. Scymnol is a derivative of cholic acid, which finds applications in the treatment of various skin problems and liver dysfunction. Triformyloxycholeic acid chloride **81** is treated with the magnesium enolate of diethylmalonate to afford the  $\beta$ -ketodiester diethyl 3 $\alpha$ ,7 $\alpha$ ,12 $\alpha$ -triformyloxy-24-oxo-5 $\beta$ -cholestane-26,27-dioate (**82**). The stereoselective hydrogenation of **82** gives the corresponding  $\beta$ -hydroxy diester **83** using a BINAP ruthenium(II) catalyst. Subsequent reduction of the diester moiety and deprotection of the hydroxyl groups afforded Scymnol, **84** (equation 102).





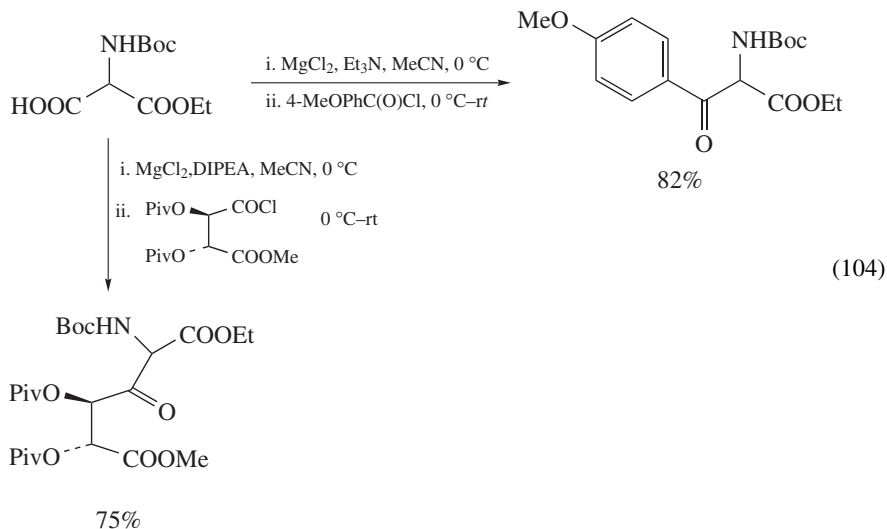
(84) Scymnol

Different syntheses of  $\gamma$ -amino- $\beta$ -ketoester derivatives from *N*-protected L-aminoacids by *N,N'*-carbonyldiimidazole activation and treatment with the magnesium enolate of hydrogen ethyl malonate are described. These compounds are useful intermediates in the preparation of active amino acid analogues, as illustrated and summarized in equation 103.

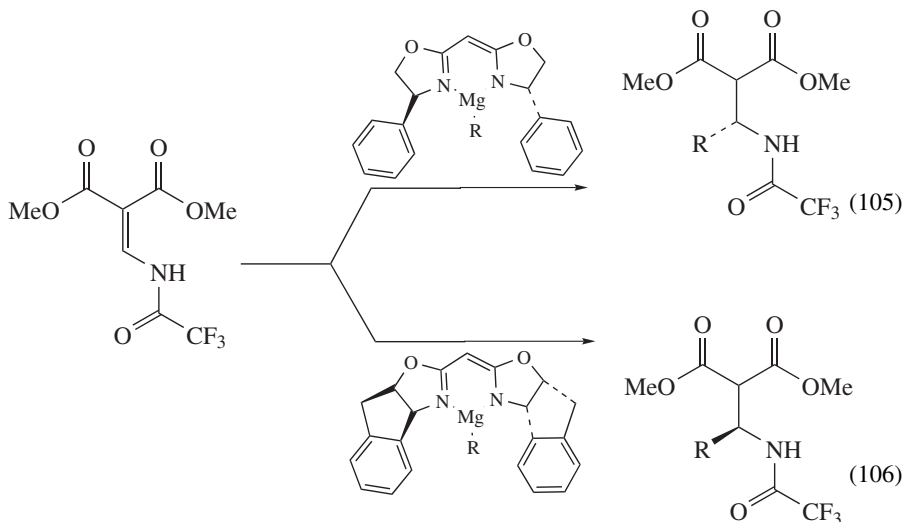


With a similar procedure, Krysan<sup>60</sup> has described a practical synthesis of  $\alpha$ -acylamino- $\beta$ -ketoesters. The combination of  $\text{MgCl}_2$  and  $\text{R}_3\text{N}$  is used to metallate a series of alkyl

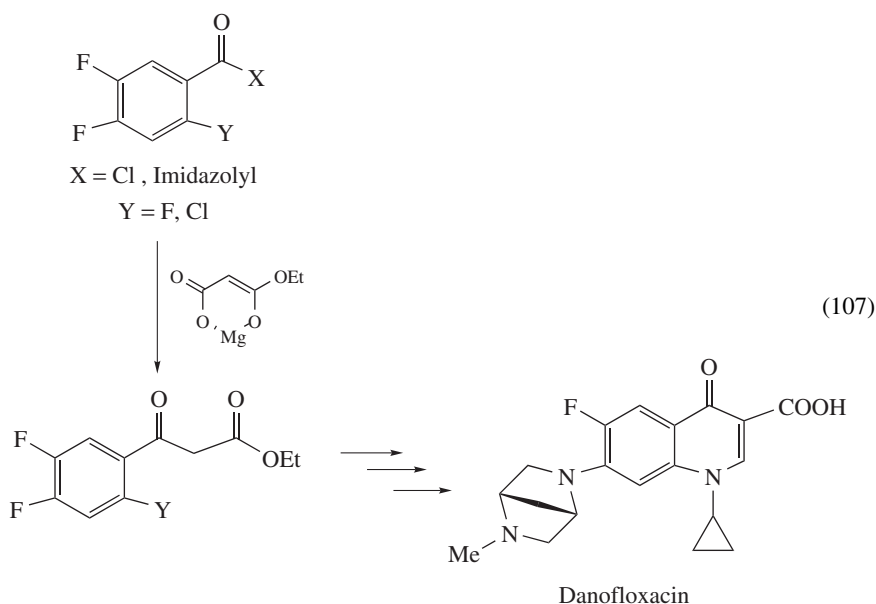
hydrogen (acylamino)malonates at 0 °C. The resulting magnesium enolates react with a wide range of acid chlorides to give the corresponding  $\alpha$ -acylamino- $\beta$ -keto esters in good to excellent yields (equation 104).



A general methodology for the preparation of  $\beta$ -amino- $\alpha,\beta$ -diesters has been developed by Sibi and Asano<sup>41</sup>. It is based on an enantioselective conjugate addition of chiral organomagnesium amides to enamidomalonates. Addition of a large variety of nucleophiles gives adducts in good yields and enantioselectivities. Alkyl, vinyl and aryl nucleophiles are compatible in this method. It should be noted that a simple change of the chiral ligand allows one to prepare products with an opposite configuration (equations 105 and 106, Table 14).



The simplicity and convenience of this chemistry led to an industrial application on a large scale, as illustrated by the synthesis of Danofloxacin, an animal health quinolone antibiotic<sup>115</sup> (equation 107).



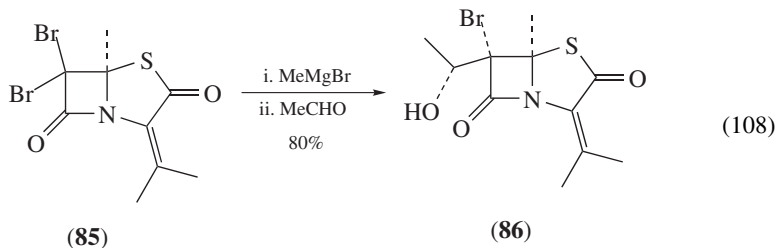
### E. Reactions of Magnesium Amide and Lactam Enolates with Electrophiles

Aldol reactions of simple amide enolates give poor stereoselection. Stimulated by the interest in  $\beta$ -lactams, the stereochemistry of aldol reactions of chiral magnesium enolates of  $\beta$ -lactams has been studied<sup>116,117</sup>. The best results have been obtained with 6,6-dibromopenams **85** (equation 108). After bromine–magnesium exchange with MeMgBr,

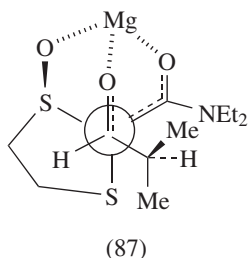
TABLE 14. Conjugate addition of different nucleophiles to enamidomalonates

R	Yield % (ee%)	Yield % (ee%)
Et	79 (78)	65 (–78)
<i>i</i> -Pr	72 (83)	62 (–80)
<i>n</i> -Bu	72 (81)	65 (–70)
(CH <sub>2</sub> ) <sub>17</sub> CH <sub>3</sub>	71 (83)	68 (–70)
Cyclohexyl	69 (93)	64 (–74)
CH <sub>2</sub> =CH	65 (86)	58 (–59)
phenyl	70 (81)	65 (–56)

then addition of ethanal, a single isomer **86** is obtained in excellent yield. It results from the attack of the concave face of the bicyclic system<sup>118</sup>.



Other chiral magnesium enolates derived from amides are known to react with aldehydes. For example, the aldol-type reaction of magnesium enolate of (–)-*trans*-2-*N,N*-diethylacetamide-1,3-dithiolanes-*S*-oxide with isobutyraldehyde affords a single diastereomer in 82%. The relative stereochemistry of the adduct originates from a rigid transition state **87** where the oxygen atoms of the enolate and the aldehyde are coordinated to the magnesium atom<sup>55</sup>.



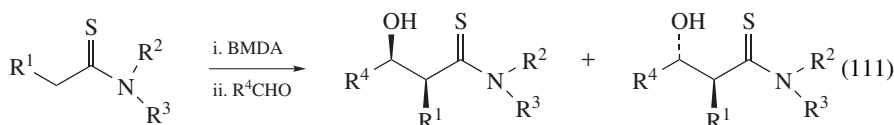
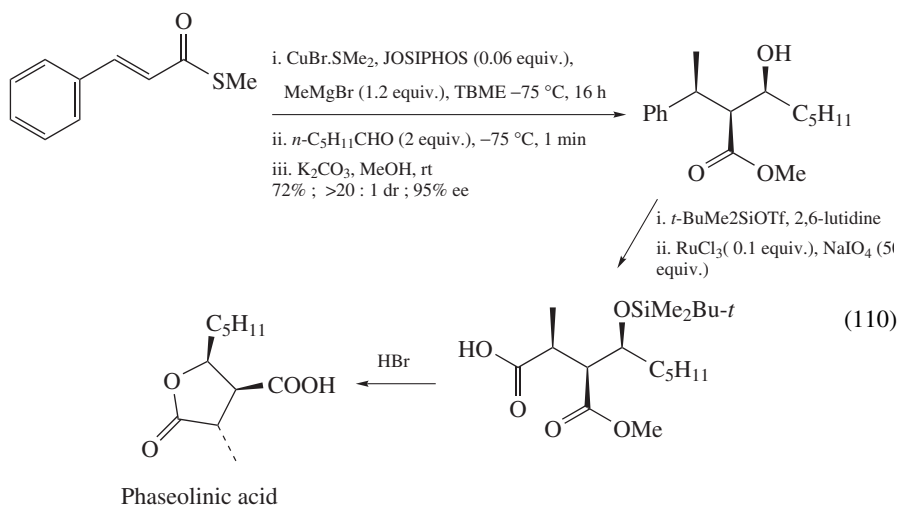
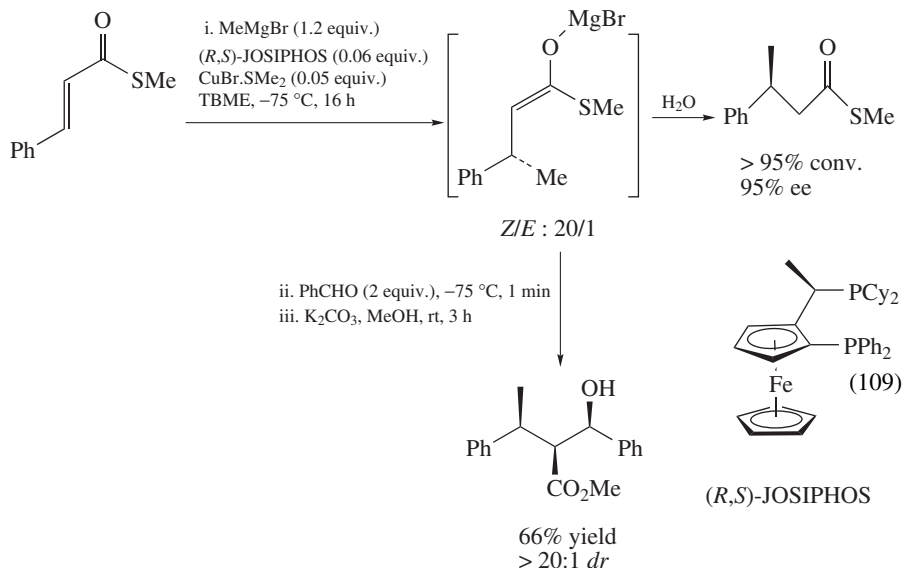
## F. Reactions of Magnesium Thioesters and Thioamide Enolates with Electrophiles

Recently, Feringa and coworkers<sup>46</sup> have described a very interesting protocol for the catalytic asymmetric 1,4-addition of Grignard nucleophiles to  $\alpha,\beta$ -unsaturated thioesters. These conjugate thioesters may be also used to perform some tandem 1,4-addition-aldol reactions via the copper-catalyzed 1,4-addition of organomagnesium derivatives, in the presence of a catalytic amount of JOSIPHOS, in high yields and level of stereocontrol. It was found that the magnesium enolate intermediate readily undergoes aldol reaction with benzaldehyde after 1 min at  $-75^\circ\text{C}$  (equation 109).

The utility and efficiency of this methodology is demonstrated by the first catalytic asymmetric synthesis of (–)-phaseolinic acid<sup>46</sup>, a natural product displaying useful antifungal, antitumor and antibacterial properties, as illustrated in equation 110.

This elegant tandem protocol allows the synthesis of this natural product in a good 54% overall yield.

Thioamide enolates are also interesting substrates for the stereoselective aldol-type reactions. The aldol stereochemistry is very sensitive to the conditions of preparation of magnesium thioamide enolates and it generally gives different results depending on the procedure used. Illustrations of some aspects of the reactivity are provided in the examples presented below.



The products obtained after treatment of thioamides with magnesium bromide diisopropylamide (BMDA) and subsequent aldol condensation are presented in equation 111. The difference in the stereochemistry between thioamides of secondary amines and primary amines should be noted (Table 15). Although, in each case, the metallation leads to

TABLE 15. Aldol stereochemistry of thioamides

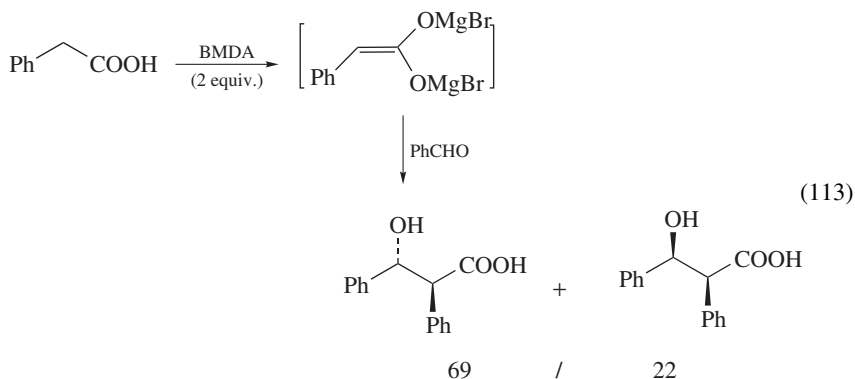
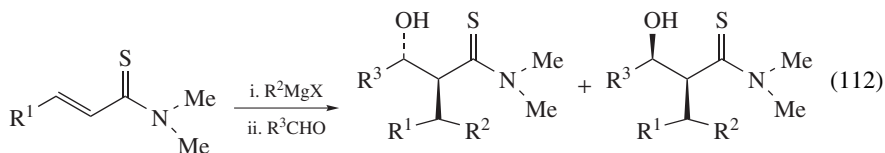
R <sup>1</sup>	R <sup>2</sup>	R <sup>3</sup>	R <sup>4</sup>	<i>syn/anti</i>
Me	Me	Me	<i>i</i> -Pr	95/5
Me	Me	Me	Ph	93/7
Me	Me	Me	CH <sub>2</sub> =CH	89/11
Ph	Me	Me	<i>i</i> -Pr	72/28
Ph	Me	H	<i>i</i> -Pr	2/98
Ph	Me	H	Ph	6/94

TABLE 16. Aldol stereochemistry of  $\alpha,\beta$ -unsaturated thioamides

R <sup>1</sup>	R <sup>2</sup>	R <sup>3</sup>	X	<i>syn/anti</i>
Me	Me	Me	I	4/96
Me	Me	<i>i</i> -Pr	I	<1/99
Me	Et	Ph	Br	15/85
Ph	<i>i</i> -Pr	Me	Br	<1/99
Ph	<i>i</i> -Pr	<i>i</i> -Pr	Br	<1/99
Ph	<i>i</i> -Pr	H	Br	18/82

the (*Z*)-enolates, dianions of thioamides derived from primary amines react with aldehydes to afford predominantly the *anti* aldols whereas enolates of thioamides derived from secondary amines give the *syn* aldols.

If thioamide enolates are prepared by conjugate addition of Grignard reagents to  $\alpha,\beta$ -unsaturated thioamides of secondary amines, the reaction of these enolates with aldehydes affords *anti* aldols. These results are rationalized by the formation of a boat-like, chelate transition state<sup>119,120</sup>. Representative examples are provided in equation 112 and Table 16.

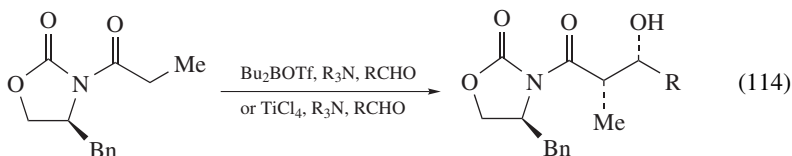


### G. Reactions of Carboxylic Acid Dianions with Electrophiles

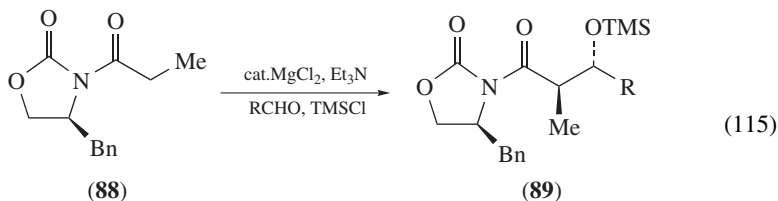
A few years ago, Blagouev and Ivanov described the bis-deprotonation of aryl acetic acids by Grignard reagents<sup>121</sup>. These magnesium dianions, known as Ivanov reagents, react with aldehydes and ketones. Reaction between dianions of phenylacetic acid and benzaldehyde yields the *anti*  $\beta$ -hydroxy acid as the major diastereomer (*anti/syn* 69/22) (equation 113). This result is in agreement with the formation of a cyclic chair-like transition state according to the model of Zimmerman–Traxler<sup>53b</sup>.

### H. Reactions with Anions of Chiral Oxazolidinones and Derivatives with Electrophiles

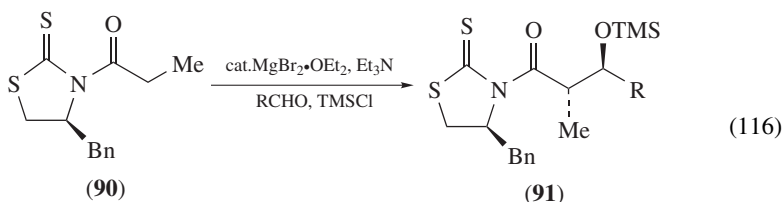
The oxazolidinones have been used as chiral auxiliaries for enolate alkylation and aldol reactions in enantioselective and total syntheses<sup>122–124</sup>. The interest in these substrates is largely known for *syn*-diastereoselective aldol reactions with chlorotitanium or dialkylboron oxazolidinone enolates<sup>123, 124</sup> (equation 114).



Recently, Evans has reported diastereoselective magnesium halide-catalyzed *anti*-aldol reactions of chiral *N*-acyloxazolidinones **88** (equation 115)<sup>61</sup> and *N*-acylthiazolidine-thiones **90** (equation 116)<sup>62</sup>.



32/1–14/1 dr

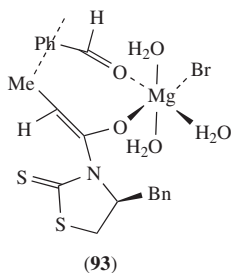
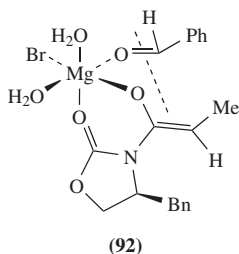


19/1–7/1 dr

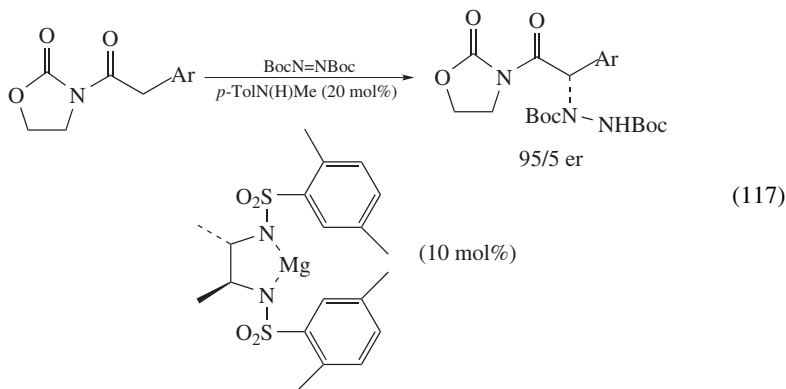
Although *N*-acyloxazolidinones **88** and *N*-acylthiazolidine-thiones **90** lead to an *anti* aldol, the respective products **89** and **91** present a different *anti* configuration. Consequently, the corresponding derived magnesium enolates exhibit the opposite face selection in these reactions. On the basis of previous results involving enolates of various metal complexes such as boron, titanium, lithium or sodium enolates, the (Z)-metal enolate



is always formed. Evans suggests that these reactions proceed via either a five- or six-coordinate magnesium chair-like transition state **92** for *N*-acyloxazolidinones **88** and a boat-like transition state **93** for *N*-acylthiazolidinethiones **90**. The observed stereochemical results negate the possibility that the thione C=S moiety is coordinated to the magnesium center in the aldol transition state **93**, whereas a chair Zimmerman–Traxler transition state is assumed in the case of magnesium enolate **92**. Semiempirical calculations support such hypotheses.



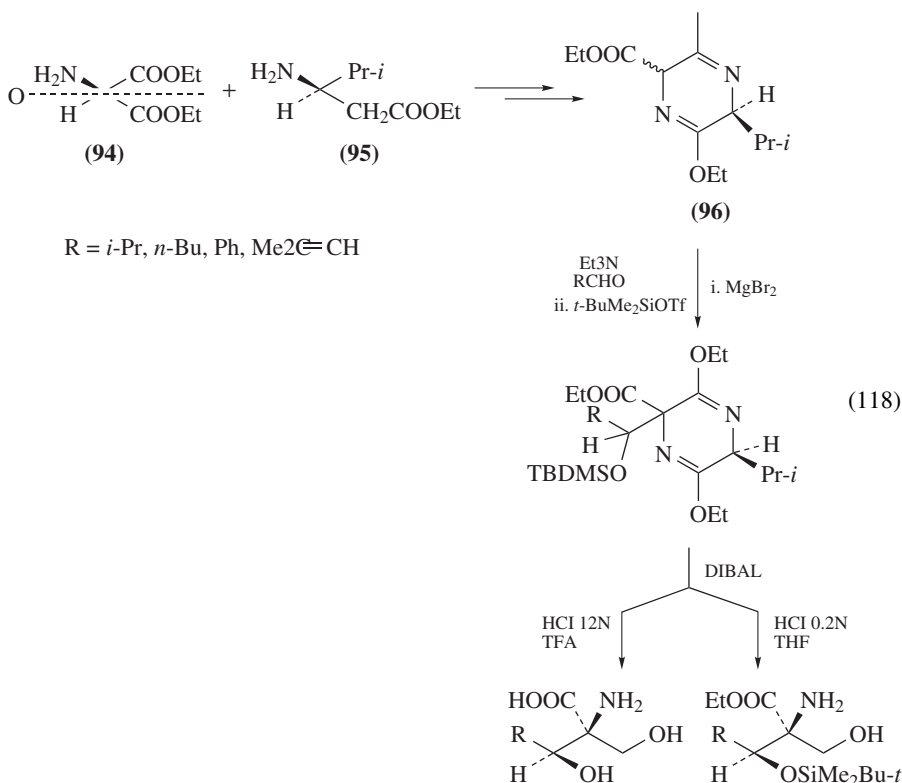
The enantioselective amination of *N*-acyl oxazolidinones has been studied as part of a general approach to the synthesis of arylglycines. In this case, the enolization is initiated by a chiral magnesium bis(sulfonamide) complex. The oxazolidinone imide enolates are generated using catalytic conditions (10 mol% of magnesium complex) and treated *in situ* with BocN=NBoc to provide the corresponding hydrazide. 20 mol% of *N*-methyl-*p*-toluensulfonamide are added to accelerate the reaction<sup>90</sup> (equation 117).



The procedure is applicable to a variety of aryl-substituted imides incorporating either electron-withdrawing or electron-donating substituents. The reaction leads to high enantiomeric ratio (95/5 er) and the products are easily purified by recrystallization (84–97% yields).

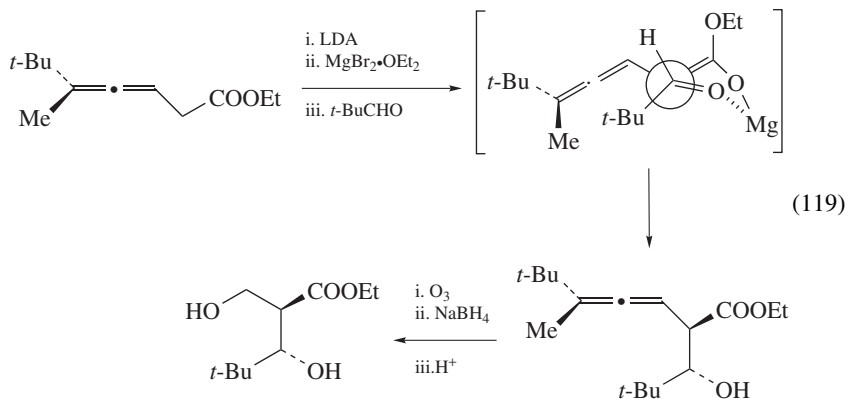
### I. Reactions of Miscellaneous Magnesium Chiral Enolates

A straightforward example of asymmetric synthesis is the enantioselective synthesis of  $\alpha$ -amino acid which uses (S)-valine ethyl ester **95** as a chiral auxiliary<sup>61</sup> (equation 118). In the process, the chiral auxiliary **95** is condensed with  $\sigma$ -asymmetric  $\alpha$ -amino diethylmalonate **94**. Treatment of the product with trimethyloxonium tetrafluoroborate provides the bis-imino ether **96**, which is enolized with  $\text{MgBr}_2$ /triethylamine. The geometry of this enolate is fixed by a six-membered ring, and the isopropyl group of the valine residue imposes a strong facial bias by hindering the 'lower' face of the enolate. The aldehyde is directed to the 'upper' face. Silylation, reduction and hydrolysis provide the acids **97** or esters **98** of alkylated serine derivatives. Four diastereomers are obtained and separated by chromatography (70–86% yields).



An interesting class of chiral enolates are allenyl enolates. These ambident nucleophiles bear an axis of chirality. Krause and coworkers have found that an axis to center chirality transfer takes place in the aldol reaction of chiral magnesium allenyl enolate with pivalic aldehyde<sup>26</sup>. The aldol reaction proceeds with good diastereofacial selectivity if

the lithium enolate is transmetalated with magnesium bromide etherate. The traditional Zimmerman–Traxler chair-like transition state doesn't explain the *u*-configuration of the aldol adduct. However, the stereochemical course of this axis to center chirality transfer can be rationalized by assuming a boat transition state, as illustrated in equation 119.



This reaction was used to prepare enantiomerically pure ethyl (2*S*,3*S*)-4,4-dimethyl-3-hydroxy-2-hydroxymethylpentanoate.

#### IV. REFERENCES

1. S. M. Malmgren, *Chem. Ber.*, **35**, 3910 (1902).
2. J. P. Collman, *J. Org. Chem.*, **26**, 3162 (1961).
3. J. Colonge and S. Grenet, *Bull. Soc. Chim. Fr.*, **10**, C41 (1953).
4. (a) H. B. Meikelburger and C. S. Wilcox, in *Comprehensive Organic Synthesis* (Eds. B. M. Trost and I. Fleming), Vol. 2, Pergamon Press, Oxford, 1991, pp. 99–128.  
(b) C. H. Heathcock, in *Comprehensive Organic Synthesis* (Eds. B. M. Trost and I. Fleming), Vol. 2, Pergamon Press, Oxford, 1991, pp. 181–235.
5. P. G. Williard, *Comprehensive Organic Synthesis* (Eds. B. M. Trost and I. Fleming), Vol. 1, Pergamon Press, Oxford, 1991, pp. 1–42.
6. A. F. Mateos and J. A. de la Fuente Blanco, *J. Org. Chem.*, **56**, 7084 (1991).
7. J. M. Castro, P. J. Linares-Palomino, S. Salido, J. Altarejos, M. Nogueras and A. Sánchez, *Tetrahedron Lett.*, **45**, 2619 (2004).
8. C. Grison, S. Petek and P. Coutrot, *Tetrahedron*, **61**, 7193 (2005).
9. C. Grison, S. Petek and P. Coutrot, *Synlett*, 331 (2005).
10. J. Villieras, B. Castro and N. Ferracutti, *C. R. Acad. Sci., Ser. C*, **267**, 915 (1968).
11. A. D. William and Y. Kobayashi, *Org. Lett.*, **3**, 2017 (2001).
12. A. D. William and Y. Kobayashi, *J. Org. Chem.*, **67**, 8771 (2002).
13. B. M. Trost, M. K. T. Mao, J. M. Balkovec and P. Buhlmayer, *J. Am. Chem. Soc.*, **108**, 4965 (1986).
14. T. Satoh, K.-I. Onda, N. Itoh and K. Yamakawa, *Tetrahedron Lett.*, **32**, 5599 (1991).
15. T. Satoh, Y. Kitoh, K.-I. Onda and K. Yamakawa, *Tetrahedron Lett.*, **34**, 2331 (1993).
16. T. Satoh, N. Itoh, K.-I. Onda, Y. Kitoh and K. Yamakawa, *Bull. Chem. Soc. Jpn.*, **65**, 2800 (1992).
17. T. Satoh, Y. Kitoh, K.-I. Onda, K. Takano and K. Yamakawa, *Tetrahedron*, **50**, 4957 (1994).
18. T. Satoh and K. Miyashita, *Tetrahedron Lett.*, **45**, 4859 (2004).
19. U. Kazmaier and S. Maier, *Chem. Commun.*, 1991 (1995).
20. S. Matsui, *Bull. Chem. Soc. Jpn.*, **60**, 1853 (1987).
21. D. D. Sternbach, D. M. Rossana and K. D. Onan, *J. Org. Chem.*, **49**, 3427 (1984).
22. M. Larchevêque and A. Debal, *J. Chem. Soc., Chem. Commun.*, 877, (1981).

23. B. Mendler and U. Kazmaier, *Synthesis*, 2239 (2005).
24. T. J. Donohoe and D. House, *Tetrahedron Lett.*, **44**, 1095 (2003).
25. M. Shimizu, Y. Kooriyama and T. Fujisawa, *Chem. Lett.*, 2419 (1994).
26. M. Laux, N. Krause and U. Koop, *Synlett*, 87 (1996).
27. I. A. Stergiades and M. A. Tius, *J. Org. Chem.*, **64**, 7547 (1999).
28. H. Fujisawa, Y. Sasaki and T. Mukaiyama, *Chem. Lett.*, 190 (2001).
29. T. Eicher, in *The Chemistry of the Carbonyl Group* (Ed. S. Patai), Interscience, New York, 1966, p. 638.
30. T. Holm and L. Crossland, *Grignard Reagents New Developments* (Ed. H. G. Richey, Jr.), Wiley, Chichester, 2000, p. 19.
31. B. J. Wakefield, *Organomagnesium Methods in Organic Synthesis*, Academic Press, London, 1995, p. 124.
32. A. G. Pinkus and A-B. Wu, *J. Org. Chem.*, **40**, 2816 (1975).
33. M. J. Chapdelaine and M. Hulce, *Org. React.*, **38**, 225 (1990).
34. D. D. Weller, R. D. Gless and H. Rapoport, *J. Org. Chem.*, **42**, 1485 (1977).
35. J. Tanaka, S. Kanemasa, Y. Ninomiya and O. Tsuge, *Bull. Chem. Soc. Jpn.*, **63**, 466 (1990).
36. S. Dalai, M. Limbach, L. Zhao, M. Tamm, M. Sevvana, V. V. Sokolov and A. de Meijere, *Synthesis*, 471 (2006).
37. Y. Tamaru, T. Hioki, S.-I. Kawamura, H. Satomi and Z.-I. Yoshida, *J. Am. Chem. Soc.*, **106**, 3876 (1984).
38. K. Kobayashi, H. Takabatake, T. Kitamura, O. Morikawa and H. Konishi, *Bull. Chem. Soc. Jpn.*, **70**, 1697 (1997).
39. K. Kobayashi, R. Nakahashi, A. Shimizu, T. Kitamura, O. Morikawa and H. Konishi, *J. Chem. Soc., Perkin Trans. 1*, 1547 (1999).
40. M. E. Bunnage, S. G. Davies, C. J. Goodwin and I. A. S. Walters, *Tetrahedron: Asymmetry*, **5**, 35 (1994).
41. M. P. Sibi and Y. Asano, *J. Am. Chem. Soc.*, **123**, 9708 (2001).
42. B. Breit and P. Demel, *Modern Organic Chemistry* (Ed. N. Krause), Wiley-VCH, Weinheim, 2002, p. 188.
43. B.-S. Lou, G. Li, F.-D. Lung and V. J. Hruby, *J. Org. Chem.*, **60**, 5509 (1995).
44. F. Lopez, S. R. Harutyunyan, A. J. Minnaard and B. L. Feringa, *J. Am. Chem. Soc.*, **126**, 12784 (2004).
45. R. Des Mazery, M. Pullez, F. Lopez, S. R. Harutyunyan, A. J. Minnaard and B. L. Feringa, *J. Am. Chem. Soc.*, **127**, 9966 (2005).
46. G. P. Howell, S. P. Fletcher, K. Geurts, B. ter Horst and B. L. Feringa, *J. Am. Chem. Soc.*, **128**, 14977 (2006).
47. B. J. M. Jansen, C. J. Hendrikx, N. Masalov, G. A. Stork, T. M. Meulemans, F. Z. Macaeve and A. de Groot, *Tetrahedron*, **56**, 2075 (2000).
48. G. L. Larson, D. Hernandez, I. Montes de Lopez-Cepero and L. E. Torres, *J. Org. Chem.*, **50**, 5260 (1985).
49. A. G. Pinkus, D. F. Mullica, W. O. Milligan, D. A. Grossie and P. W. Hurd, *Tetrahedron*, **40**, 4829 (1984).
50. Y. Maroni-Barnaud, J. Bertrand, F. Ghosland, L. Gorrichon-Guigon, Y. Koudsi, P. Maroni and R. Meyer, *C. R. Acad. Sci. Paris*, **280**, C-221 (1975).
51. P. Fellmann and J.-E. Dubois, *Tetrahedron Lett.*, **3**, 247 (1977).
52. (a) T. Shioiri, K. Hayashi and Y. Hamada, *Tetrahedron*, **49**, 1913 (1993).  
(b) Y. Hamada, K. Hayashi and T. Shioiri, *Tetrahedron Lett.*, **32**, 931 (1991).
53. (a) D. Ivanov and N. Nicoloff, *Bull. Soc. Chim. Fr.*, **51**, 1325 (1932).  
(b) H. E. Zimmerman and M. D. Traxler, *J. Am. Chem. Soc.*, **79**, 1920 (1957).
54. G. Solladié, in *Asymmetric Synthesis* (Ed. J. D. Morrison), Vol. 2, Academic Press, New York, 1983, p. 157.
55. M. Corich, F. Di Furia, G. Licini and G. Modena, *Tetrahedron Lett.*, **33**, 3043 (1992).
56. E. Hevia, K. W. Henderson, A. R. Kennedy and R. E. Mulvey, *Organometallics*, **25**, 1778 (2006).
57. L. Crombie, D. F. Games and A. W. G. James, *J. Chem. Soc., Perkin Trans. 1*, 2715 (1996).
58. M. W. Rathke and P. J. Cowan, *J. Org. Chem.*, **50**, 2622 (1985).
59. B. Corbel, I. L'Hostis-Kervella and J. P. Haelters, *Synth. Commun.*, **26**, 2561 (1996).
60. D. J. Krysan, *Tetrahedron Lett.*, **37**, 3303 (1996).

61. D. A. Evans, J. S. Tedrow, J. T. Shaw and C. Wade Downey, *J. Am. Chem. Soc.*, **124**, 392 (2002).
62. D. A. Evans, C. Wade Downey, J. T. Shaw and J. S. Tedrow, *Org. Lett.*, **4**, 1127 (2002).
63. S. Sano, T. Miwa, X-K. Liu, T. Ishii, T. Takehisa, M. Shiro and Y. Nagao, *Tetrahedron: Asymmetry*, **9**, 3615 (1998).
64. M. Stile, *J. Am. Chem. Soc.*, **81**, 2598 (1959).
65. (a) E. S. Hand, S. C. Johnson and D. C. Baker, *J. Org. Chem.*, **62**, 1348 (1997).  
(b) S. M. Kerwin, A. G. Paul and C. H. Heathcock, *J. Org. Chem.*, **52**, 1686 (1987).
66. P. E. Eaton, C. H. Lee and Y. Xiong, *J. Am. Chem. Soc.*, **111**, 6016 (1989).
67. K. Kobayashi and H. Suginome, *Bull. Chem. Soc. Jpn.*, **59**, 2635 (1986).
68. T. Hiyama and K. Kobayashi, *Tetrahedron Lett.*, **23**, 1597 (1982).
69. K. Sisido, K. Kumazawa and H. Nozaki, *J. Am. Chem. Soc.*, **82**, 125 (1960).
70. H. Yamataka, M. Shimizu and M. Mishima, *Bull. Chem. Soc. Jpn.*, **75**, 127 (2002).
71. K. Kobayashi, D. Iitsuka, O. Morikawa and H. Konishi, *Synthesis*, 51 (2007).
72. K. Kobayashi, T. Nakashima, M. Mano, O. Morikawa and H. Konishi, *Chem. Lett.*, 602 (2001).
73. T. Matsumoto, T. Murayama, S. Mitsunashi and T. Miura, *Tetrahedron Lett.*, **40**, 5043 (1999).
74. G. Lessène, R. Tripoli, P. Cazeau, C. Biran and M. Bordeau, *Tetrahedron Lett.*, **40**, 4037 (1999).
75. M. E. Krafft and R. A. Holton, *Tetrahedron Lett.*, **24**, 1345 (1983).
76. D. Bonafoux, M. Bordeau, C. Biran, P. Cazeau and J. Dunogues, *J. Org. Chem.*, **61**, 5532 (1996).
77. D. Bonafoux, M. Bordeau, C. Biran and J. Dunogues, *Synth. Commun.*, **28**, 93 (1998).
78. X. He, J. Jacob Morris, B. C. Noll, S. N. Brown and K. W. Henderson, *J. Am. Chem. Soc.*, **128**, 13599 (2006).
79. X. He, J. F. Allan, B. C. Noll, A. R. Kennedy and K. W. Henderson, *J. Am. Chem. Soc.*, **127**, 6920 (2005).
80. K. Kobayashi, Y. Fuchimoto, K. Hayashi, M. Mano, M. Tanmatsu, O. Morikawa and H. Konishi, *Synthesis*, 2673 (2005).
81. L. Camici, P. Dembech, A. Ricci, G. Seconi and M. Taddei, *Tetrahedron*, **44**, 4197 (1988).
82. B. J. Childs and G. L. Edwards, *Tetrahedron Lett.*, **34**, 5341 (1993).
83. N. A. Van Draanen, S. Arseniyadis, M. T. Crimmins and C. H. Heathcock, *J. Org. Chem.*, **56**, 2499 (1991).
84. C. H. Heathcock and S. Arseniyadis, *Tetrahedron Lett.*, **49**, 6009 (1985).
85. J. D. Anderson, P. Garcia Garcia, D. Hayes, K. W. Henderson, W. J. Kerr, J. H. Moir and K. P. Fondecar, *Tetrahedron Lett.*, **42**, 7111 (2001).
86. M. J. Bassindale, J. J. Crawford, K. W. Henderson and W. J. Kerr, *Tetrahedron Lett.*, **45**, 4175 (2004).
87. K. W. Henderson, W. J. Kerr and J. H. Moir, *Chem. Commun.*, 479 (2000).
88. K. W. Henderson, W. J. Kerr and J. H. Moir, *Synlett*, 1253 (2001).
89. E. L. Carswell, D. Hayes, K. W. Henderson, W. J. Kerr and C. J. Russell, *Synlett*, 1017 (2003).
90. D. A. Evans and S. G. Nelson, *J. Am. Chem. Soc.*, **119**, 6452 (1997).
91. C. J. R. Adderley, G. V. Baddeley and F. R. Hewgill, *Tetrahedron*, **23**, 4143 (1967).
92. K. Fuji, T. Kawabata and A. Kuroda, *J. Org. Chem.*, **60**, 1914 (1995).
93. H. Yamataka, O. Aleksyuk, S. E. Biali and Z. Rappoport, *J. Am. Chem. Soc.*, **118**, 12580 (1996).
94. P. Kisanga, D. McLeod, B. D' Sa and J. Verkade, *J. Org. Chem.*, **64**, 3090 (1999).
95. R. K. Dieter, in *Modern Organic Chemistry* (Ed. N. Krause), Wiley-VCH, Weinheim, 2002, p. 79.
96. J. Tanaka, H. Kobayashi, S. Kanemasa and O. Tsuge, *Bull. Chem. Soc. Jpn.*, **62**, 1193 (1989).
97. J. Bertrand, N. Cabrol, L. Gorrichon-Guigon and Y. Maroni-Barnaud, *Tetrahedron Lett.*, **47**, 4683 (1973).
98. P. Fellmann and J. E. Dubois, *Tetrahedron*, **34**, 1349 (1978).
99. A. P. Dove, V. C. Gibson, E. L. Marshall, A. J. P. White and D. J. Williams, *J. Chem. Soc., Chem. Commun.*, 1208 (2002).
100. B. Rague, Y. Chapleur and B. Castro, *J. Chem. Soc., Perkin Trans. 1*, 2063 (1982).

101. A. Bernardi, S. Cardani, L. Colombo, G. Poli, G. Schimperna and C. Scolastico, *J. Org. Chem.*, **52**, 888 (1987).
102. E. J. Corey, W. Li and G. A. Reichard, *J. Am. Chem. Soc.*, **120**, 2330 (1998).
103. K. Takai and C. H. Heathcock, *J. Org. Chem.*, **50**, 3247 (1985).
104. T. Hiyama, K. Nishide and K. Kobayashi, *Tetrahedron Lett.*, **25**, 569 (1984).
105. C. Grison, T. K. Olszewski, C. Crauste, A. Fruchier, C. Didierjean and P. Coutrot, *Tetrahedron Lett.*, **47**, 6583 (2006).
106. M. L. F. Cadman, L. Crombie, S. Freeman and J. Mistry, *J. Chem. Soc., Perkin Trans. 1*, 1397 (1995).
107. L. Crombie, M. Eskins, D. E. Games and C. Loader, *J. Chem. Soc., Perkin Trans. 1*, 472 (1979).
108. L. Crombie, *Tetrahedron*, **54**, 8243 (1998).
109. M. W. Rathke and P. J. Cowan, *J. Org. Chem.*, **50**, 2622 (1985).
110. R. E. Ireland and J. A. Marshall, *J. Am. Chem. Soc.*, **81**, 2907 (1959).
111. R. Adhikari, D. J. Cundy, C. L. Francis, M. Gebara-Coghlan, B. Krywult, C. Lubin, G. W. Simpson and Qi Yang, *Aust. J. Chem.*, **58**, 34 (2005).
112. K. Tohdo, Y. Hamada and T. Shioiri, *Synlett*, 105 (1994).
113. P. Krogsgaard-Larsen, A. L. Nordahl Larsen and K. Thyssen, *Acta Chem. Scand., Ser. B*, **32**, 469 (1978).
114. J. Maibaum and D. H. Rich, *J. Org. Chem.*, **53**, 869 (1988).
115. F. R. Busch, R. S. Lehner and B. T. O'Neil, *U.S. Patent* **5**, 380,860 (1995).
116. F. Di Ninno, T. Beattie and B. G. Christensen, *J. Org. Chem.*, **42**, 2960 (1977).
117. J. A. Aimetti and M. S. Kellog, *Tetrahedron Lett.*, 3805 (1979).
118. A. Martel, J. P. Daris, C. Bachand and M. Menard, *Can. J. Chem.*, **65**, 2179 (1987).
119. Y. Tamura, T. Hioki, S. Nishi and Z. I. Yoshida, *Tetrahedron Lett.*, **23**, 2383 (1982).
120. Y. Tamura, T. Hioki and Z. I. Yoshida, *Tetrahedron Lett.*, **25**, 5793 (1984).
121. B. Blagouev and D. Ivanov, *Synthesis*, 615 (1970).
122. G. Procter, *Asymmetric Synthesis*, Chap 5, Oxford University Press, New York, 1999.
123. D. A. Evans, D. L. Rieger, M. T. Bilodeau and F. J. Urpi, *J. Am. Chem. Soc.*, **113**, 111 (1991).
124. J. R. Gaje and D. A. Evans, *Org. Synth.*, **68**, 83 (1990).

## CHAPTER 12

# Functionalized organomagnesium compounds: Synthesis and reactivity

PAUL KNOCHEL, ANDREY GAVRYUSHIN and KATJA BRADE

*Department Chemie und Biochemie, Ludwig-Maximilians-Universität München, Butenandtstr. 5-13, D-81377 München, Germany*

*Fax: +49-89-2180-77680; e-mail: paul.knochel@cup.uni-muenchen.de*

---

I. INTRODUCTION . . . . .	512
II. PREPARATION OF FUNCTIONALIZED GRIGNARD REAGENTS . . . . .	512
A. Direct Oxidative Addition of Magnesium to Organic Halides . . . . .	512
B. The Halogen–Magnesium Exchange Reaction . . . . .	515
1. Early studies . . . . .	515
2. Application of the halogen–magnesium exchange reaction for the synthesis of functionalized Grignard reagents . . . . .	517
a. Scope and limitations . . . . .	517
b. Functional group tolerance . . . . .	530
C. Metalation Reactions with Magnesium Amide Bases . . . . .	537
D. Miscellaneous Methods . . . . .	540
III. REACTIVITY OF GRIGNARD REAGENTS . . . . .	543
A. Substitutions at an $sp^3$ -center . . . . .	543
1. Transition-metal-catalyzed cross-coupling reactions . . . . .	543
2. Ring-opening of small cycles . . . . .	547
3. Diverse reactions . . . . .	547
B. Substitutions at an $sp^2$ -center . . . . .	550
1. Transition-metal-catalyzed cross-coupling reactions . . . . .	550
2. Transition-metal-free cross-coupling reactions . . . . .	556
3. Allylic substitution reactions . . . . .	557
4. Synthesis of carbonyl compounds . . . . .	559
C. Substitutions at an $sp$ -center . . . . .	559
D. Addition of Organomagnesium Reagents to Multiple Bonds . . . . .	559
1. Addition to carbon–carbon bonds . . . . .	559

---

*The chemistry of organomagnesium compounds*

Edited by Z. Rapoport and I. Marek © 2008 John Wiley & Sons, Ltd. ISBN: 978-0-470-05719-3

a. Catalyzed addition to non-activated C=C bonds . . . . .	559
b. 1,4-Addition to Michael acceptors . . . . .	563
c. Addition to other activated alkenes . . . . .	565
d. Addition to carbon–carbon triple bonds . . . . .	567
2. Addition to carbon–oxygen bonds . . . . .	569
3. Addition to carbon–nitrogen bonds . . . . .	571
E. Diverse Reactions . . . . .	575
1. Amination reactions . . . . .	575
a. Electrophilic amination reactions . . . . .	575
b. Oxidative coupling of polyfunctional aryl and heteroaryl amidocuprates . . . . .	580
2. Synthesis of cyclopropanes . . . . .	582
3. Synthesis of chiral sulfoxides . . . . .	582
IV. REFERENCES . . . . .	583

## I. INTRODUCTION

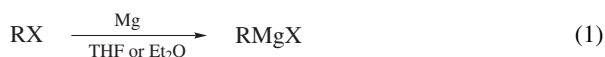
Organomagnesium reagents now play one of the key roles in organic synthesis. Since their discovery at the beginning of the last century by Victor Grignard<sup>1</sup>, the development of new methods for their preparation opened a way toward highly functionalized organomagnesium reagents. Their practical synthesis, good stability and excellent reactivity make organomagnesium compounds indispensable organometallic intermediates for industry and academic laboratory. Transmetalation to less reactive but more chemoselective organometallic species (zinc, copper<sup>2</sup>, titanium etc.) allows additional fine-tuning of their reactivity pattern.

Several comprehensive reviews and books have been published, encompassing the preparation and use of Grignard reagents<sup>3</sup>, their chemical and physical properties<sup>4</sup>, mechanistic investigations of their formation<sup>3b,5</sup> and studies of their structures in solution and in solid state<sup>5d,6</sup>. In the present chapter, emphasis will be placed on synthetic methods for the preparation of *functionalized* organomagnesium compounds as well as their applications in organic synthesis.

## II. PREPARATION OF FUNCTIONALIZED GRIGNARD REAGENTS

### A. Direct Oxidative Addition of Magnesium to Organic Halides

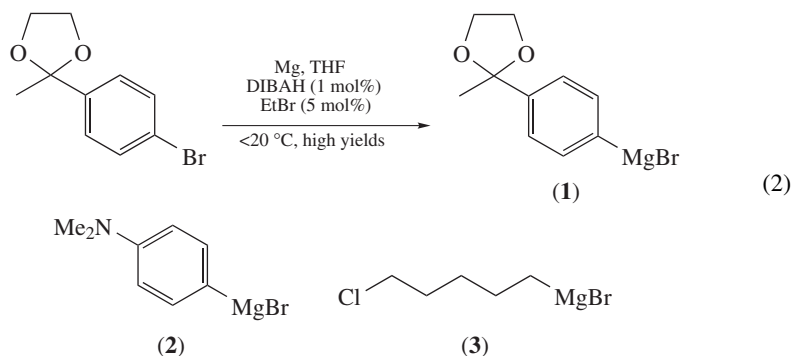
A widely used route for the synthesis of Grignard reagents is the oxidative addition of magnesium metal to organic halides in a polar, aprotic solvent like THF or diethyl ether (equation 1).



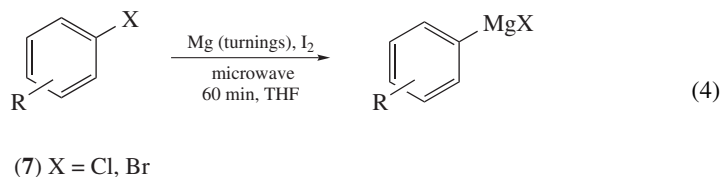
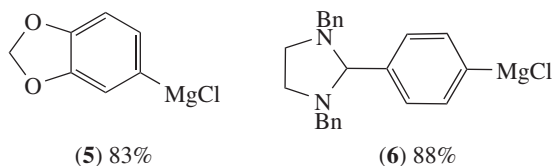
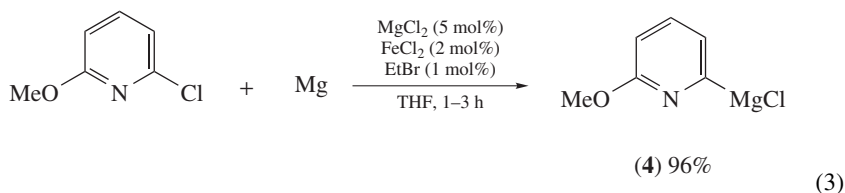
Nevertheless, these solvents represent a safety hazard for large-scale industrial processes<sup>7</sup>. They can be substituted by less flammable high boiling glycol ethers like ‘butyl diglyme’ (C<sub>4</sub>H<sub>9</sub>O(CH<sub>2</sub>)<sub>2</sub>OC<sub>4</sub>H<sub>9</sub>). Additional possibilities might arise from the use of non-ethereal solvents like toluene<sup>8</sup>, though the presence of one or two equivalents of diethyl ether or THF was found to be beneficial<sup>9</sup>. Controlling the reactant feed rate by on-line concentration monitoring using near-IR spectroscopy can help to further improve the safety of especially large scale processes<sup>10</sup>. Using this method, excessive reactant accumulations leading to unsafe situations like overpressure in the reactor system can be avoided.



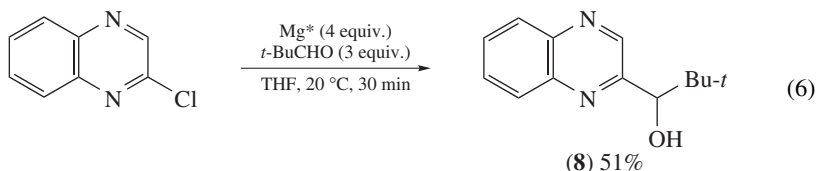
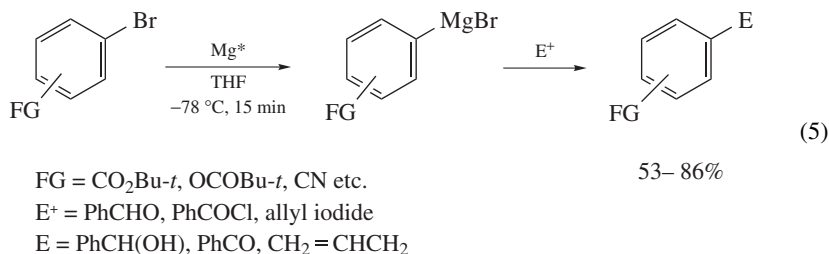
Usually, magnesium metal is covered with an 'oxide layer' which mainly consists of  $\text{Mg}(\text{OH})_2$ <sup>11</sup>. The nature of this metal surface plays a pivotal role in the oxidative addition reaction<sup>12</sup>. Thus, to shorten the induction period and obtain a better reproducibility of the reaction time, activation of the magnesium surface with agents as 1,2-dibromoethane prior to reaction is normally desired<sup>13</sup>. A radical mechanism for this reaction is widely accepted<sup>14</sup>, though details are still being discussed<sup>15</sup>. Another method of activation of Mg metal using diisobutylaluminium hydride (DIBAH) allows lowering of the reaction temperature ( $0-10^\circ\text{C}$ ), which can be crucial for the preparation of less stable compounds like **1–3** (equation 2)<sup>16</sup>.



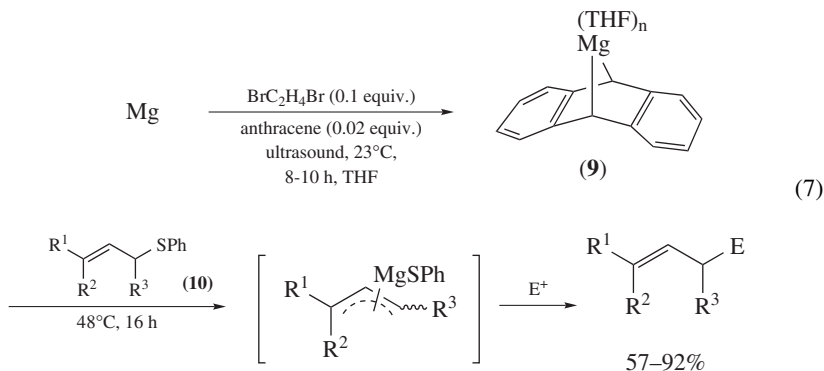
Low reactive aryl chlorides are converted to the respective organomagnesium species in excellent yields through transition metal catalysis using 2 mol%  $\text{FeCl}_2$  (**4–6**, equation 3)<sup>17</sup>. Alternatively, a safe and reproducible method for activation of aryl chlorides or bromides **7** uses microwave irradiation (equation 4). In a synthesis of a novel HIV-1 protease inhibitor, microwave irradiation was essential to generate the starting arylmagnesium halide as well as to promote the subsequent Kumada coupling reaction<sup>18</sup>.



For the synthesis of functionalized Grignard reagents bearing sensitive functional groups, highly reactive Rieke magnesium ( $\text{Mg}^*$ ) can be used<sup>19</sup>. The low reaction temperatures ( $-78^\circ\text{C}$ ) allow the presence of a number of functional groups, which are not compatible with the usual methodology (equation 5)<sup>20</sup>. Direct trapping of the resulting Grignard reagents with an electrophile (Barbier conditions), e.g. in the formation of **8**, sometimes improves these results even further (equation 6)<sup>21</sup>.

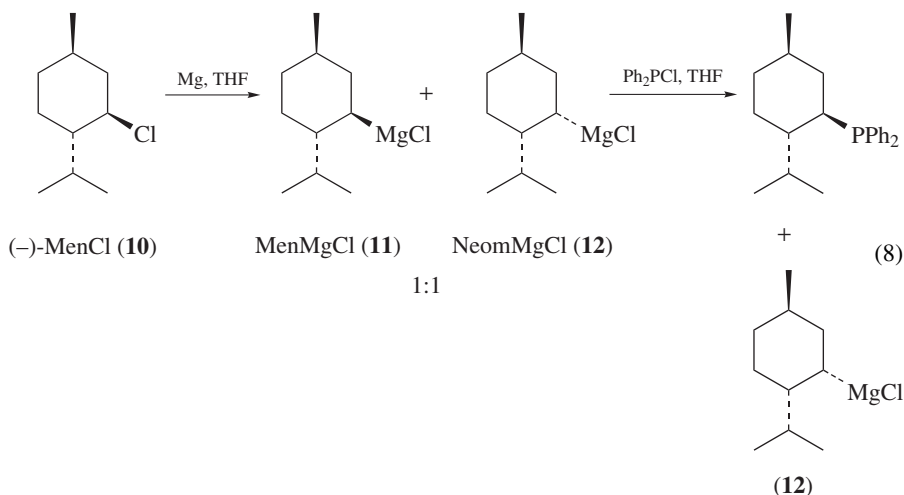


Another source for highly reactive magnesium is soluble Mg-anthracene **9**<sup>22</sup>. It can be used for the reductive metalation of allylic phenyl sulfides **10** (equation 7)<sup>23</sup>.

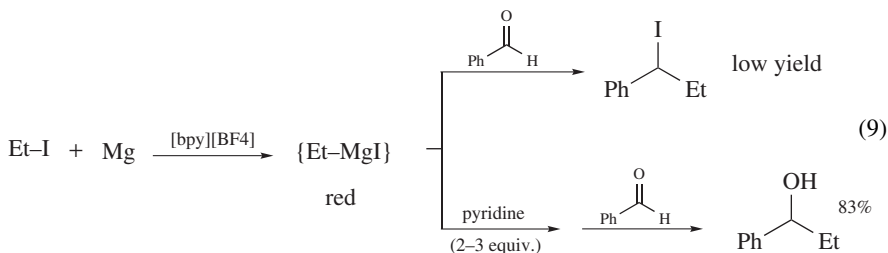


Interesting information on their configurational stability was obtained in the direct synthesis of Grignard reagents from enantiomerically pure alkyl halides like (–)-menthyl chloride ( $\text{MenCl}$ , **10**)<sup>24</sup>. The corresponding Grignard reagents  $\text{MenMgCl}$  (**11**) and  $\text{Neom-MgCl}$  (**12**) are formed in a 1:1 ratio, with no equilibrium between them. If the reactivity of the two epimers differs significantly, as in the present case, it is possible to selectively use each component in reactions with electrophiles by using kinetic or thermodynamic reaction control. Thus, reaction with diphenylphosphine chloride leads to full consumption of the more reactive epimer  $\text{MenMgCl}$  (**11**), while the pure chiral Grignard reagent

**12** (NeomMgCl) remains in the reaction mixture (equation 8).



Grignard reagents can be generated from organic iodides and magnesium in ionic liquids<sup>25</sup> like *n*-butylpyridinium tetrafluoroborate ([bpy][BF<sub>4</sub>])<sup>26</sup>. The resulting Grignard reagents show a different reactivity in this solvent (equation 9).

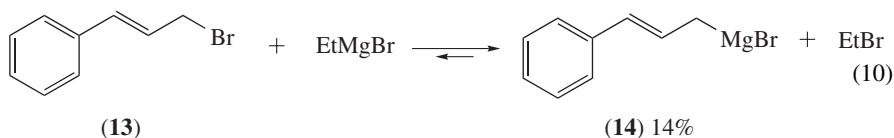


Unfortunately, the preparation of functionalized Grignard reagents via direct oxidative addition of magnesium metal to organic halides still suffers from severe limitations. This is mainly due to the intrinsic high reducing potential of magnesium metal.

## B. The Halogen–Magnesium Exchange Reaction

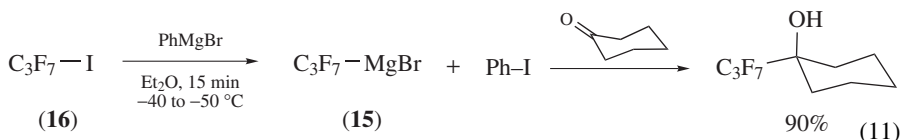
### 1. Early studies

In 1931 Prévost reported the reaction of cinnamyl bromide (**13**) to cinnamylmagnesium bromide (**14**), which was the first example of a bromine–magnesium exchange reaction (equation 10)<sup>27</sup>.

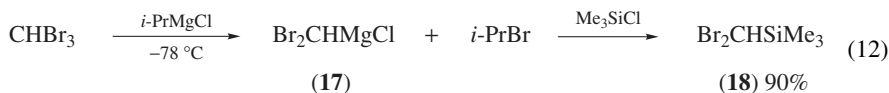


The halogen–magnesium exchange is an equilibrium process, where the formation of the most stable organomagnesium compound is favored ( $sp > sp^2(\text{vinyl}) > sp^2(\text{aryl}) > sp^3(\text{prim.}) > sp^3(\text{sec.})$ ). The mechanism of the exchange reaction is not yet fully clarified, but calculations show that it proceeds via a concerted 4-centered mechanism, in contrast to the halogen–lithium exchange that goes via the formation of a halogenated complex<sup>28</sup>.

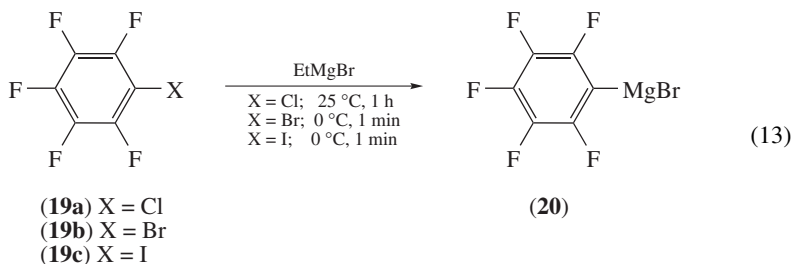
One of the first synthetically useful procedures, employing a halogen–magnesium exchange reaction, is the synthesis of perfluoroalkylmagnesium halides of type **15** starting from the perfluorinated iodide **16** (equation 11)<sup>29</sup>. This procedure showed significant advantages compared to the oxidative addition reaction, such as higher yields and less side reactions. It is one of the best methods for the synthesis of perfluorinated Grignard reagents<sup>30</sup>.



The halogen–magnesium exchange reaction was later used as a general approach to magnesium carbenoids<sup>31</sup>. Reaction of *i*-PrMgCl with CHBr<sub>3</sub> at  $-78^\circ\text{C}$  furnishes the corresponding magnesium carbenoid **17** which is trapped with chlorotrimethylsilane, leading to (dibromomethyl)trimethylsilane **18** in 90% yield (equation 12).



This pioneering work paved the way to the systematic study of magnesium carbenoids<sup>32</sup>. Furthermore, it demonstrated that the halogen–magnesium exchange rate is enhanced by the presence of electronegative substituents. A few years later, it could be shown that the formation rate of the new Grignard reagent does not only depend on the electronic properties of the organic molecule, but on the halogen atom as well<sup>33</sup>. The reactivity order ( $\text{I} > \text{Br} > \text{Cl} \gg \text{F}$ ) is influenced by the bond strength of the carbon–halogen bond, the halide electronegativity and polarizability. Only for very electron-poor systems, such as the tetra- or pentafluorobenzenes, is the exchange of a chlorine possible, requiring elevated temperatures and longer reaction times. For instance, the exchange reaction of 1-chloro-2,3,4,5,6-pentafluorobenzene (**19a**) with EtMgBr requires 1 h at room temperature to reach complete conversion to the Grignard reagent. The corresponding bromo- and iodo-perfluorobenzenes **19b** and **19c** react already at  $0^\circ\text{C}$ , leading to perfluorophenylmagnesium bromide **20** within 1 min (equation 13).

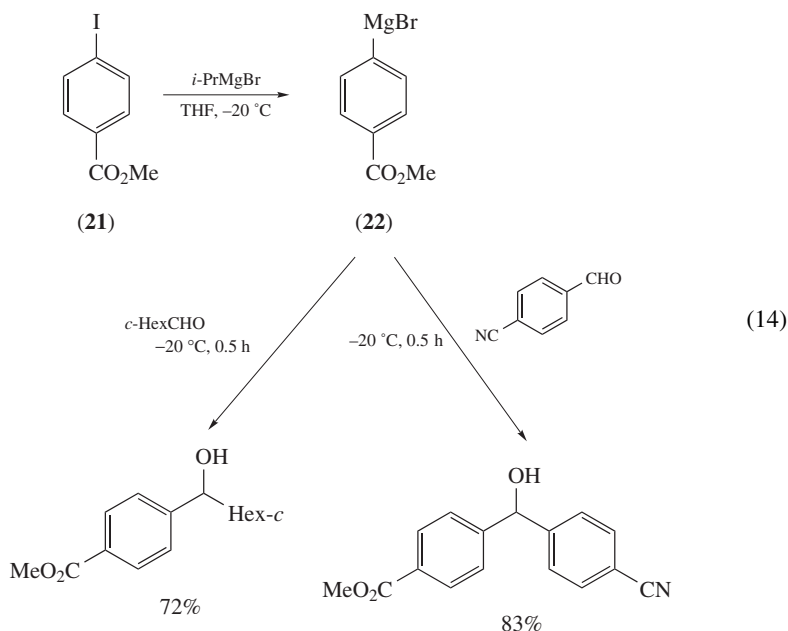


The strong dependency of the reactivity of carbon–magnesium bonds on the reaction temperature, as well as the fact that only reactive electrophiles like aldehydes and most ketones react rapidly at temperatures below 0 °C, turned the halogen–magnesium exchange reaction into a first choice method for the preparation of magnesium organometallics bearing reactive functional groups<sup>34</sup>.

## 2. Application of the halogen–magnesium exchange reaction for the synthesis of functionalized Grignard reagents

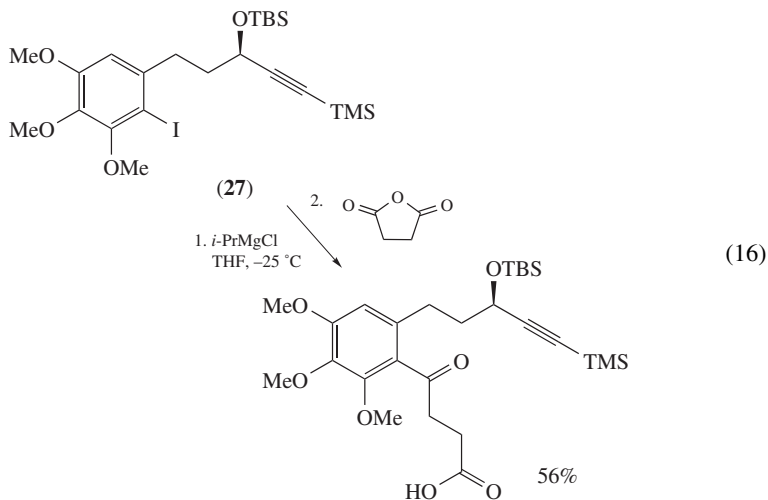
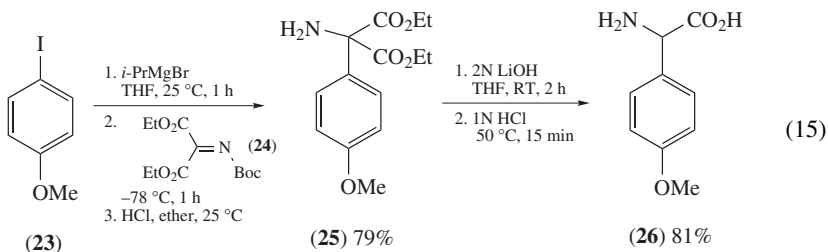
*a. Scope and limitations.* Functionalized iodoarenes react readily with *i*-PrMgCl or *i*-PrMgBr in THF at temperatures below 0 °C, sometimes even at –78 °C, affording a range of functionalized arylmagnesium compounds. Sensitive carbonyl group derivatives like nitriles, esters or amides are well tolerated under such conditions<sup>35</sup>.

Thus, treatment of methyl 4-iodobenzoate (**21**) with *i*-PrMgBr in THF at –20 °C provides the corresponding Grignard reagent **22** after 30 min. The magnesium reagent **22** reacts smoothly with aldehydes at this temperature (equation 14)<sup>36</sup>.



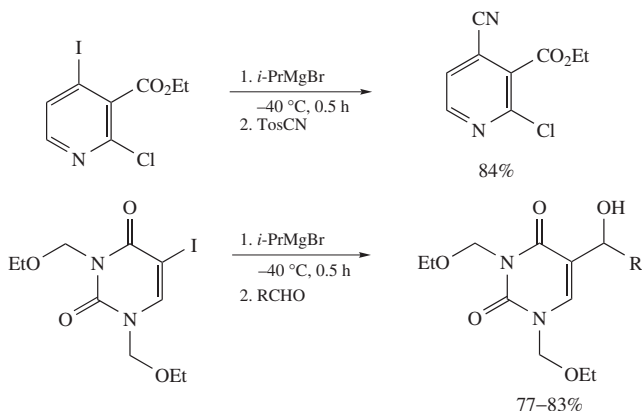
Process safety evaluations of the exchange reaction on aryl iodides using *i*-PrMgCl revealed the danger of a highly exothermic decomposition reaction at elevated temperatures (>80 °C)<sup>37</sup>.

Aromatic iodides bearing electron-donating groups, such as compound **23**, can be subjected to an iodine–magnesium exchange as well. They usually require higher temperatures (25 °C) and longer reaction times<sup>35,38</sup>. Addition of the resulting arylmagnesium species to diethyl *N*-Boc-iminomalonate (**24**)<sup>39</sup> furnishes adduct **25** in 79% yield. Saponification followed by decarboxylation provides the  $\alpha$ -amino acid **26** in 81% yield (equation 15)<sup>38</sup>. Even a highly electron-rich system like **27** possessing three methoxy groups undergoes the iodine–magnesium reaction as shown in a total synthesis of colchicines (equation 16)<sup>40</sup>.

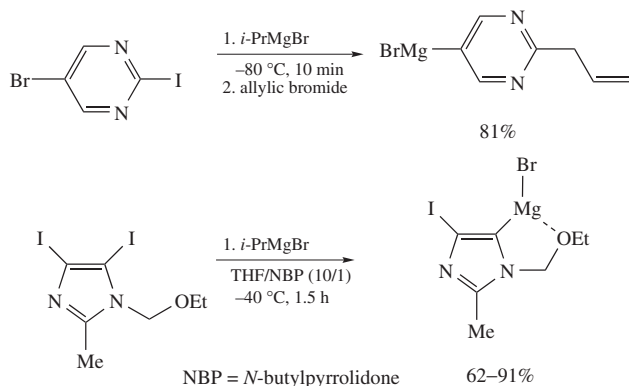


Likewise, heteroaryl iodides react with *i*-PrMgCl in THF giving the corresponding magnesium compounds in excellent yields (Scheme 1)<sup>36,41</sup>.

The I/Mg-exchange reaction can be extended to the use of iodo-substituted pyridines<sup>42,43</sup>, uracils<sup>42,44</sup>, purines<sup>45</sup>, imidazoles<sup>42,46</sup>, quinolines<sup>47</sup>, imidazo[1,2-*a*]-pyridines<sup>48</sup>, pyrroles<sup>49</sup>



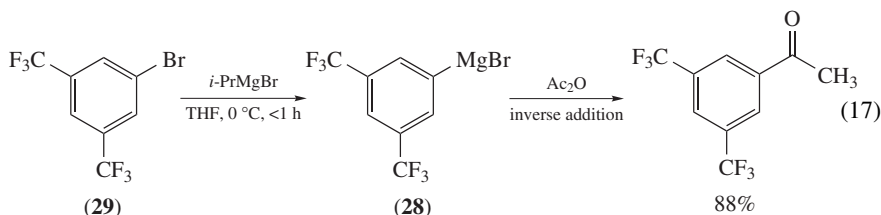
SCHEME 1



SCHEME 1. (continued)

and isoxazoles<sup>50</sup>. Functional groups like an ester or a nitrile are well tolerated at the temperatures which are required for the exchange.

The Br/Mg-exchange reaction is significantly slower than the I/Mg exchange. Using *i*-PrMgCl or *i*-PrMgBr, a fast exchange at temperatures below 0 °C can only be achieved for systems bearing strong electron-withdrawing groups<sup>41a,51</sup>. For example, Grignard reagent **28**, a valuable building block for the synthesis of a neurokinin 1 receptor agonist, is obtained from the readily available aryl bromide **29** using *i*-PrMgBr (equation 17)<sup>52</sup>.

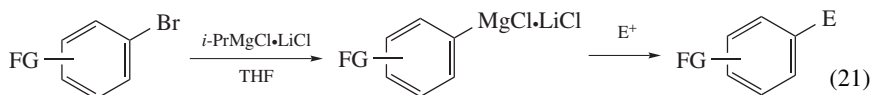
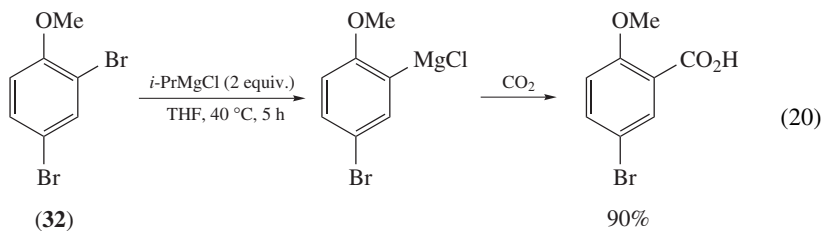
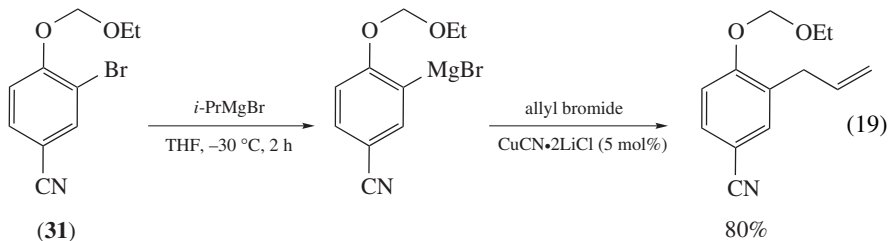
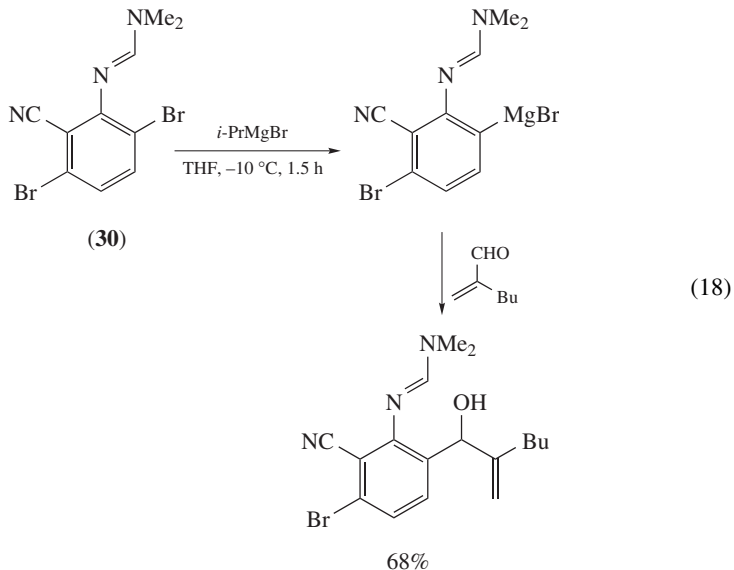


A low reaction temperature (0 °C) allows a safe synthesis of the highly useful, but explosive class of trifluoromethylphenyl Grignard reagents<sup>53</sup>. Polyfunctional aryl bromides **30** and **31**, bearing a chelating function at the *ortho*-position to the bromine, undergo a bromine–magnesium exchange much easier (equations 18 and 19)<sup>41a,51</sup>. Even the less effective methoxy group directs and facilitates the exchange as in the case of 2,4-dibromoanisole (**32**) (equation 20)<sup>54</sup>, although its electron-releasing nature requires a higher reaction temperature.

Inactivated aryl bromides do not react with *i*-PrMgCl in a sufficient rate even at temperatures as high as room temperature. However, the presence of 1 equivalent of LiCl in the reaction mixture enhances the rate of the exchange reaction tremendously, thus even allowing the use of electron-rich aryl bromides (equation 21)<sup>55</sup>.

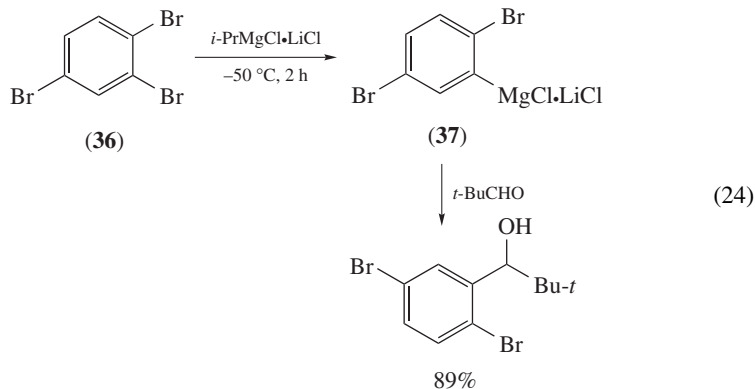
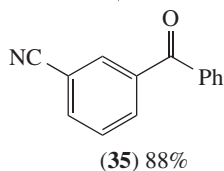
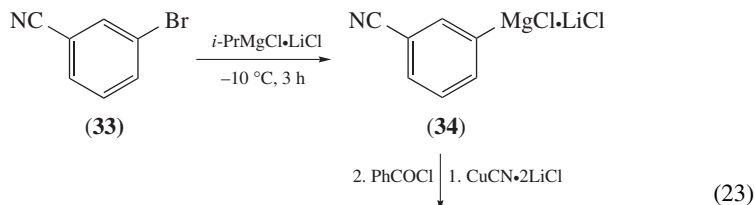
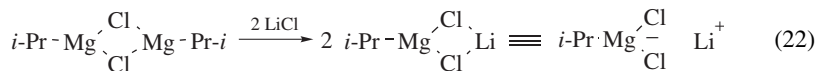
The addition of a stoichiometric amount of LiCl breaks the aggregates of the otherwise dimeric *i*-PrMgCl producing a highly reactive Grignard reagent *i*-PrMgCl•LiCl (equation 22). Commercially available *i*-PrMgCl•LiCl can be used for the preparation of a variety of substrates bearing functional groups. Thus, 3-bromobenzonitrile (**33**) undergoes a fast Br/Mg exchange at –10 °C, leading to the 3-magnesiated species **34** which reacts upon transmetalation with CuCN•2LiCl using benzoyl chloride furnishing ketone

**35** (equation 23). The exchange in the presence of LiCl can further be successfully used for the functionalization of *ortho*-dibromo- and tribromobenzenes like **36**, since low reaction temperatures permit the generation of unstable *o*-bromoarylmagnesium species **37** (equation 24)<sup>55</sup>. The addition of LiCl also proved to be beneficial for industrial-scale Grignard reactions, since it avoids the formation of gaseous side products<sup>56</sup>.



FG = F, Cl, Br, CN, CO<sub>2</sub>R, OMe

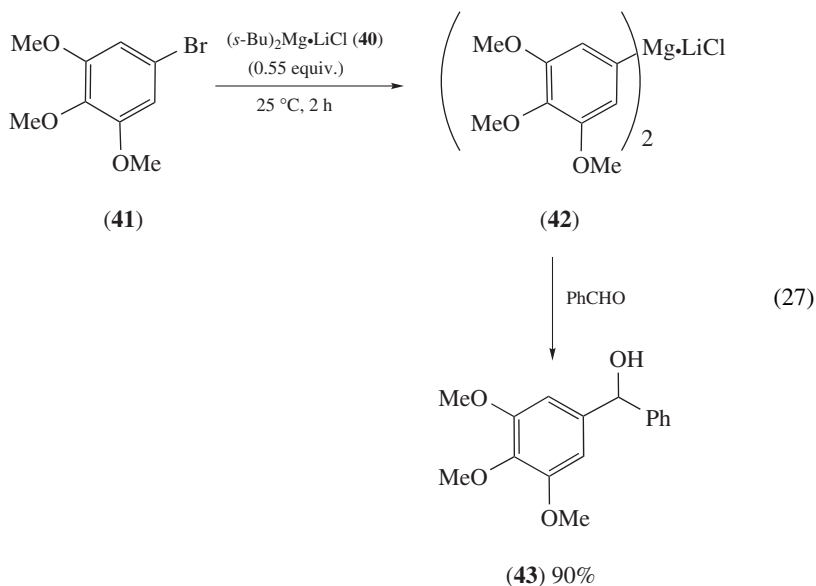
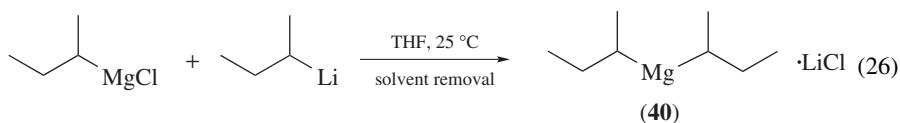
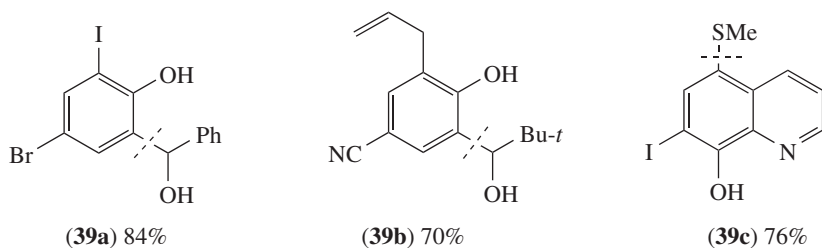
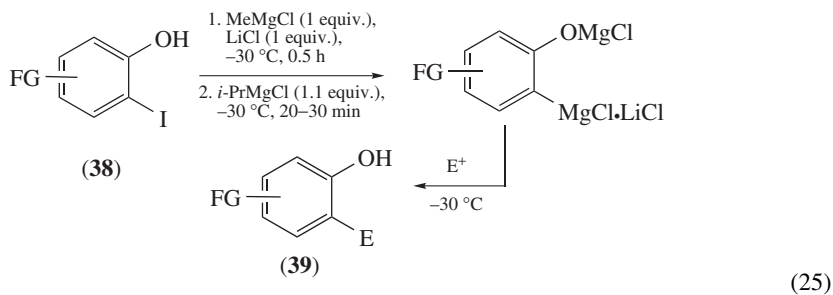


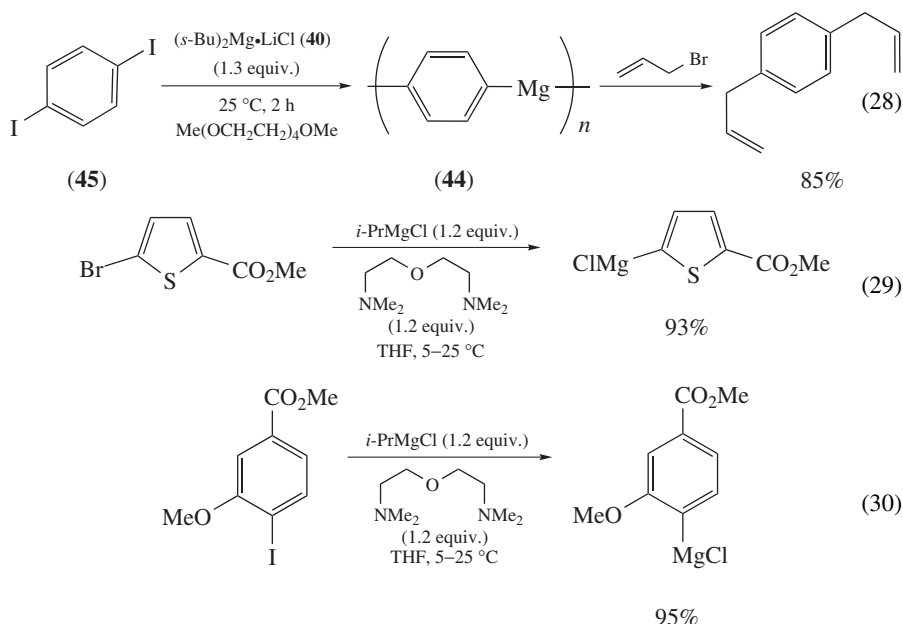


Additionally, the yields of the reactions of arylmagnesium reagents with electrophiles are higher in the presence of LiCl. The ionic salt LiCl ensures a good solubility of the reaction products, such as magnesium alcoholates, in the reaction mixture, making the whole process much easier to handle. For example, the addition of MeMgCl in the presence of LiCl followed by the addition of *i*-PrMgCl to aromatic and heteroaromatic substrates **38** bearing a hydroxy function leads to the corresponding THF-soluble dimagnesiates species, which can be reacted with electrophiles to give *ortho*-functionalized phenols **39a–c** (equation 25)<sup>57</sup>.

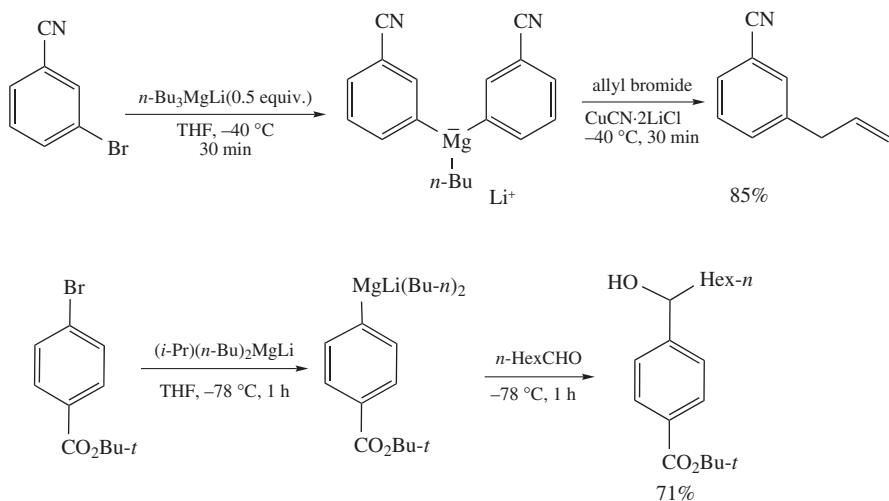
In an extension to this method, lithium magnesiate **40** was prepared (equation 26). This new class of highly reactive exchange reagents allows fast conversion of the electron rich aryl bromide **41** to the corresponding diarylmagnesium reagent **42**, which is trapped with benzaldehyde to give alcohol **43** in 40% yield (equation 27)<sup>28d</sup>. The exchange reagent **40** further allows a facile preparation of the polymeric aryl-bis-magnesium reagent **44** (*n* not determined) starting from diiodobenzene (**45**) (equation 28).

The presence of bis[2-(*N,N*-dimethylamino)ethyl]ether allows a selective halogen–magnesium exchange of iodo- and bromoaromatics at ambient temperature using isopropylmagnesium chloride. Sensitive carboxylic ester and cyano groups are well tolerated (equations 29 and 30)<sup>58</sup>.



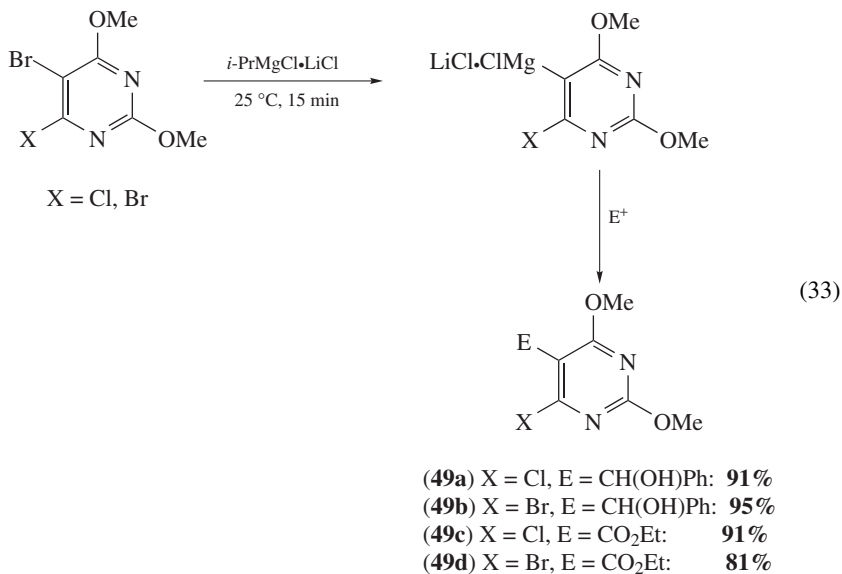
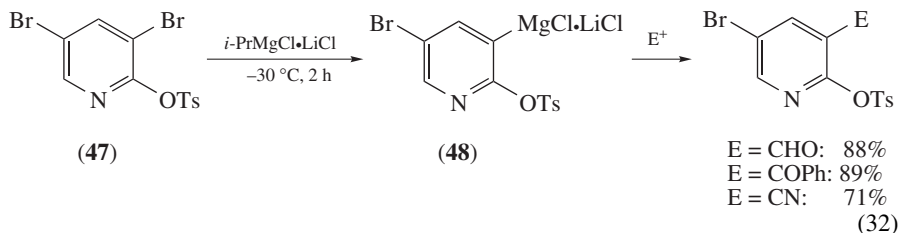
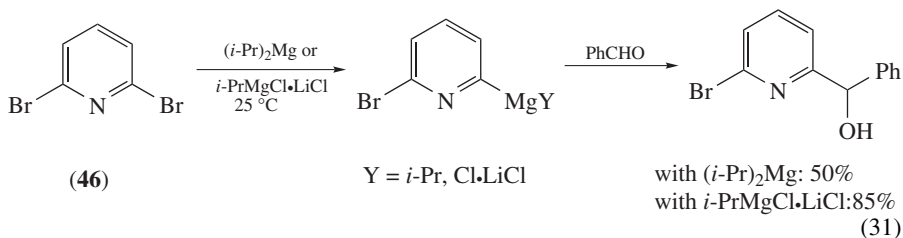


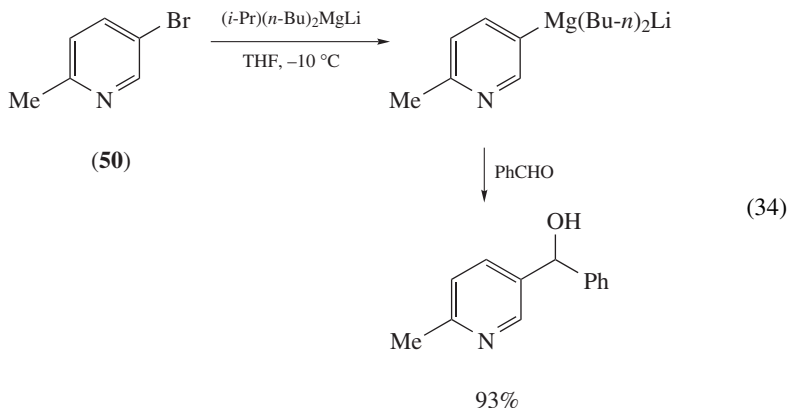
Lithium magnesiates are another class of highly reactive exchange reagents. They are prepared by reacting an organolithium reagent (2 equiv.) with an alkylmagnesium halide (1 equiv.). These lithium magnesiates are substantially more reactive than usual Grignard reagents and undergo a Br/Mg exchange on various aryl bromides<sup>59</sup>. Even 0.5 equiv. of the lithium dibutylmagnesiolate relative to the aromatic halide can be sufficient to achieve complete conversion (Scheme 2).



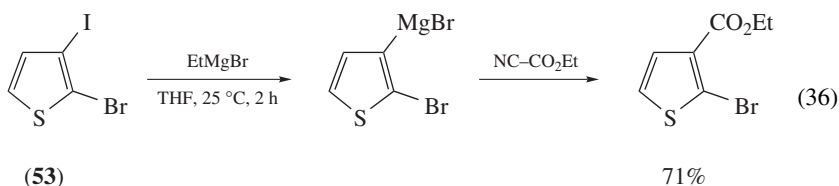
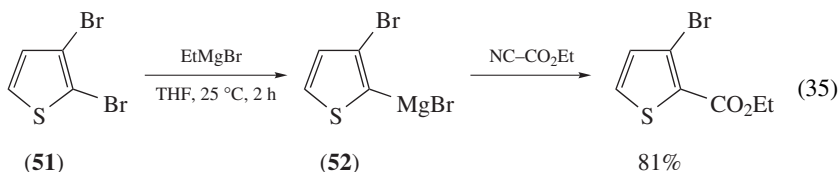
SCHEME 2

Although bromopyridines like **46** are reactive enough to undergo the exchange with *i*-PrMgCl at room temperature, higher yields are obtained using *i*-PrMgCl•LiCl (equation 31)<sup>60</sup>. A tosyloxy substituent in position 2 allows regioselective Br/Mg exchange on position 3 of 3,5-dibromopyridine derivatives **47** (equation 32). The resulting pyridylmagnesium species **48** reacts readily with various electrophiles<sup>61</sup>. Even functionalized uracil derivatives **49a–c** can be obtained via Br/Mg exchange using *i*-PrMgCl•LiCl allowing an efficient synthesis of the HIV replication inhibitor Emivirine (MKC-442, equation 33)<sup>62</sup>. Also, lithium magnesiates can be successfully applied for the bromine–magnesium exchange of heteroaryl bromides like **50** (equation 34)<sup>63</sup>.



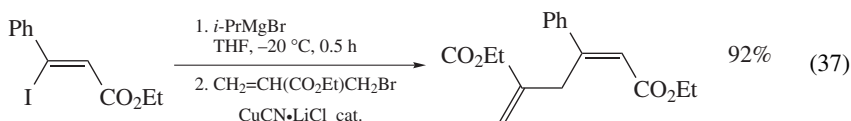


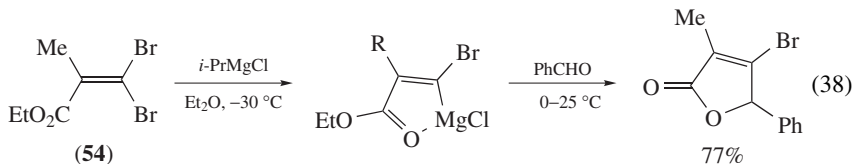
Selective formation of 2- or 3-substituted bromothiophenes can be achieved via halogen–magnesium exchange using  $\text{EtMgBr}$ . Thus, treatment of 2,3-dibromothiophene (**51**) gives solely the 2-magnesiated product **52** (equation 35), whereas 2-bromo-3-iodothiophene (**53**) selectively exchanges the iodine atom (equation 36)<sup>41a,64</sup>.



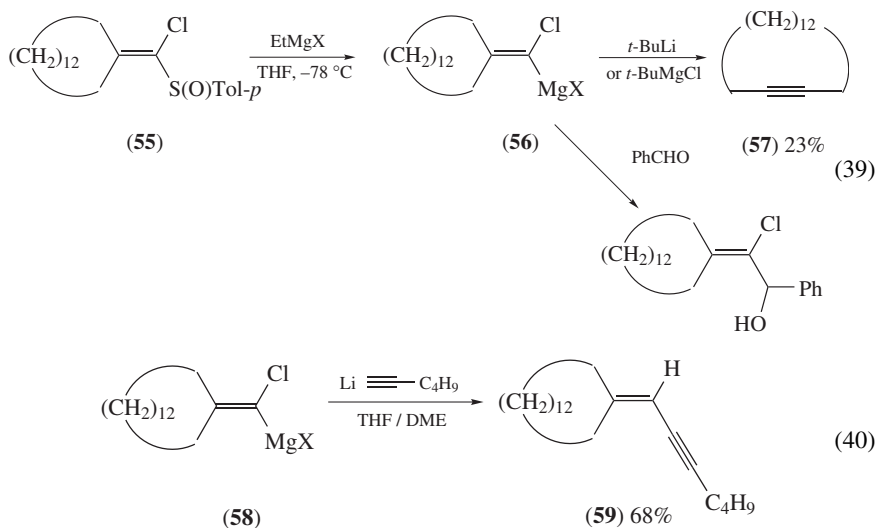
A selective exchange reaction was observed on 2,4-dibromothiazoles allowing the synthesis of substituted 4-bromothiazoles<sup>65</sup>. The use of functionalized organomagnesium compounds as intermediates for the synthesis of polyfunctionalized heterocycles has been reviewed recently<sup>66</sup>.

For a long time, the exchange reaction on functionalized alkenyl halides was limited to reactions on systems either bearing an electron-withdrawing group in  $\alpha$ -position<sup>67</sup> or a coordinating substituent in  $\beta$ -position (equation 37)<sup>68</sup>. In the case of  $\beta$ -dibromoacrylic esters like **54**, only the halogen placed *cis*- to the ester function is exchanged due to the strong intramolecular coordination (equation 38)<sup>69</sup>.

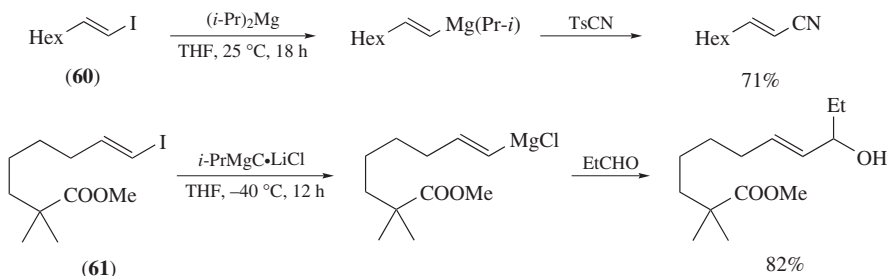




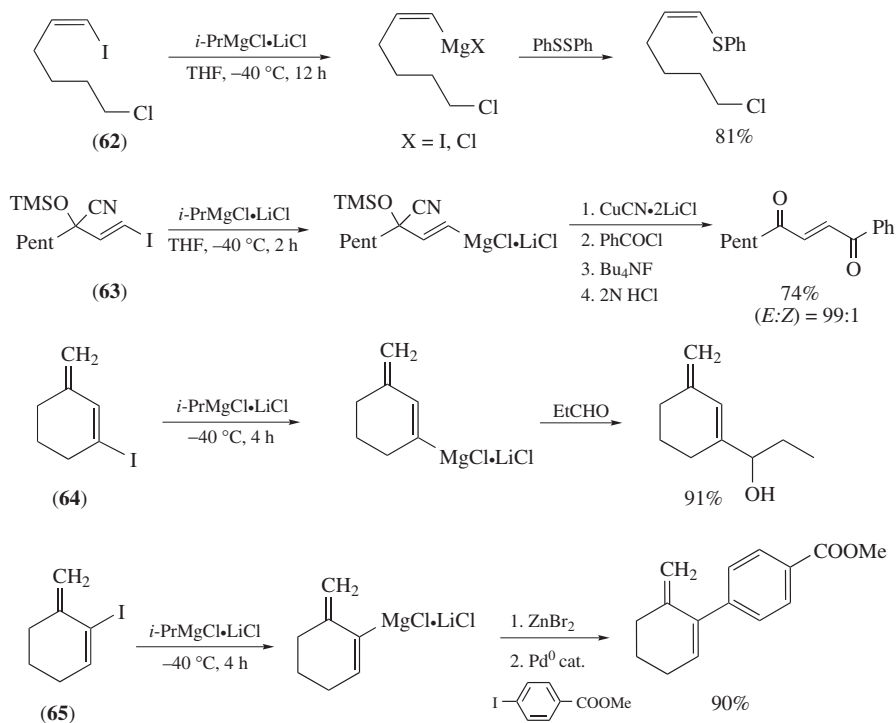
The aryl sulfoxide moiety may serve as a good leaving group in the exchange reaction. Thus, 1-haloalkenyl sulfoxide **55** undergo the exchange at  $-78\text{ }^\circ\text{C}$  to give carbenoid compounds **56** which can be trapped by electrophiles or converted to acetylenes **57** (equation 39)<sup>70</sup>. Reaction of carbenoid **58** with lithium acetylides leads to the formation of enynes **59** (equation 40)<sup>71</sup>.



Unfunctionalized alkenyl iodides like **60** react with  $i\text{-PrMgCl}$  or  $i\text{-Pr}_2\text{Mg}$  (Scheme 3). Unfortunately, the exchange reaction requires high temperatures like room temperature or higher to take place, thus precluding the presence of sensitive groups. By using  $i\text{-PrMgCl}\cdot\text{LiCl}$  as exchange reagent, the reaction of unactivated, but functionalized alkenyl iodides **61–63** and iodiienes **64** and **65** as substrates can be realized. Complete retention of the double bond configuration is observed (Scheme 3)<sup>72</sup>.

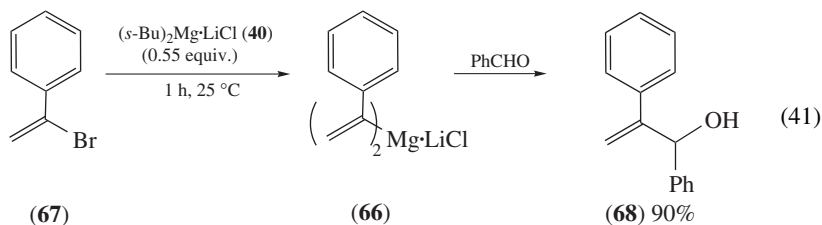


SCHEME 3



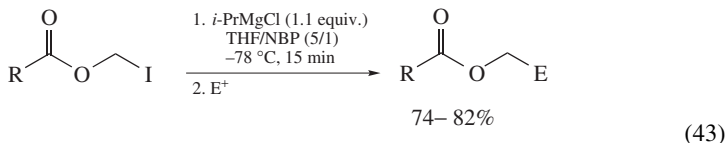
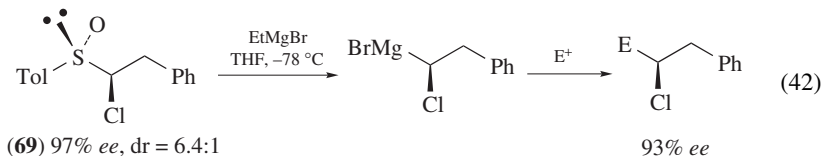
SCHEME 3. (continued)

The Br/Mg-exchange reactions on alkenyl bromides are very sluggish. This problem was overcome by the use of  $s\text{-Bu}_2\text{Mg}\cdot\text{LiCl}$ <sup>28d</sup>. For example, Grignard reagent **66** is obtained by reaction of  $\alpha$ -bromostyrene (**67**) with the complex **40** for 1 h at 25 °C. Quenching with benzaldehyde gives the allylic alcohol **68** in 93% yield (equation 41).

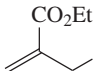


Iodine–magnesium exchange of allenyl iodides takes place on reaction with  $i\text{-PrMgBr}$  in ether. Subsequent reaction with aldehydes or ketones provides homopropargylic alcohols with high regioselectivity<sup>73</sup>. Exchange on chloroalkyl phenyl sulfoxides **69** can also be performed successfully<sup>74–76</sup>. It can be applied for the synthesis of olefins<sup>77</sup> as well as for the preparation of chiral Grignard reagents starting from a chiral sulfoxide as described in equation 42<sup>78,79</sup>.

The aspects of the preparation and reactions of chiral Grignard reagents were reviewed<sup>80</sup>. Exchange of alkyl halides is synthetically useful mostly if  $\alpha$ -halogen or  $\alpha$ -acyloxy substituents are present. The resulting Grignard reagents react smoothly with various electrophiles (equation 43)<sup>77,81</sup>.

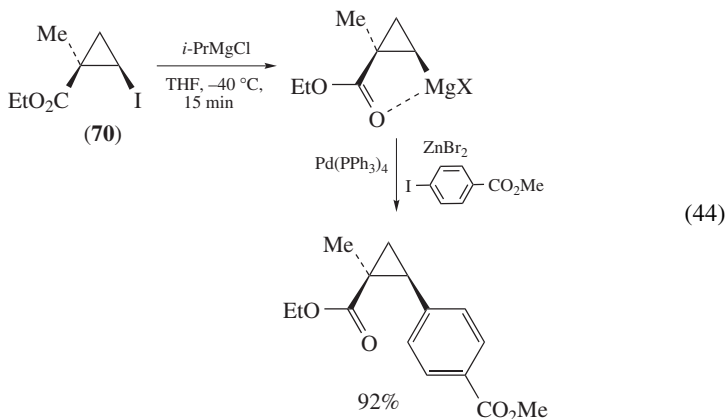


R = *c*-Hex, *t*-Bu

E<sup>+</sup> = ArCHO, (PhS)<sub>2</sub>, Ph<sub>2</sub>PCl, , etc.

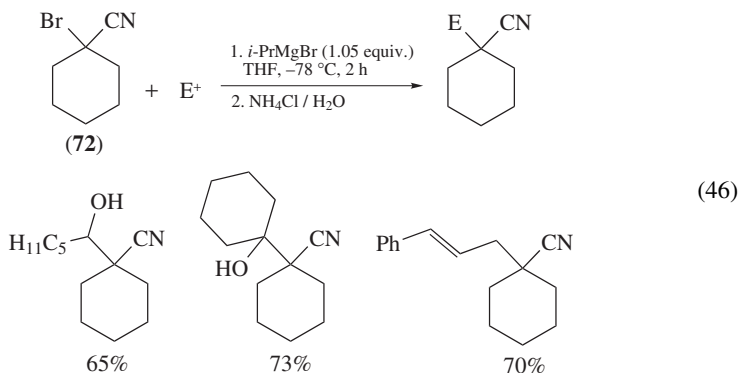
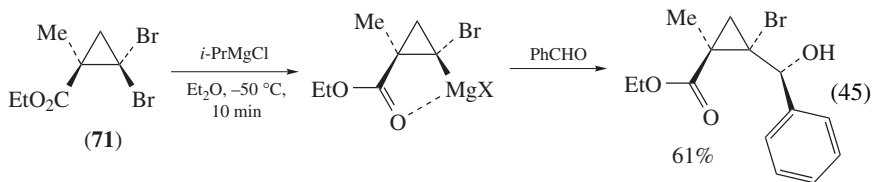
NBP: *N*-butyl-2-pyrrolidinone

Cyclopropyl iodides like **70** and bromides are good substrates for the exchange reaction (equation 44)<sup>77,82,83</sup>. The reaction is stereoselective and sufficiently fast at low temperatures, thus allowing the preparation of functionalized compounds. If a coordinating group like an ester is present in a *gem*-dihalocyclopropane like **71**, the *cis*-halogen substituent is exchanged selectively in ether (equation 45)<sup>84</sup>.

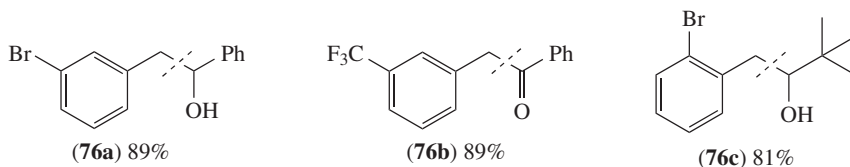
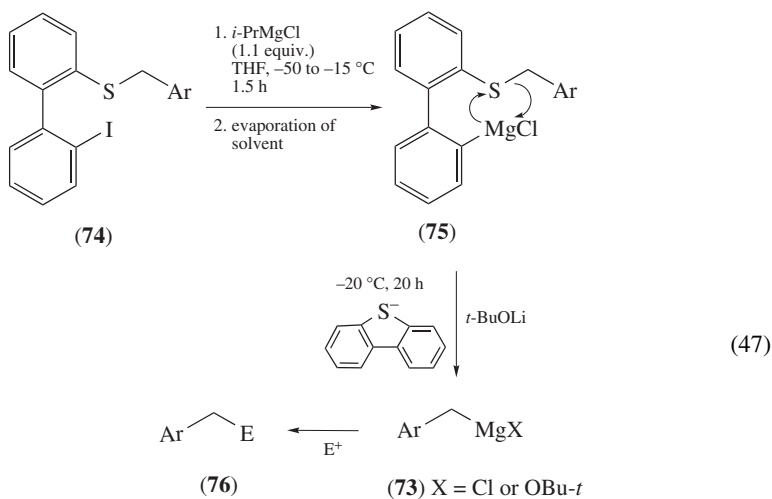


$\alpha$ -Metalated nitriles are versatile nucleophiles<sup>85</sup>. They combine a high nucleophilicity with a small steric hindrance of the CN unit, thus allowing sterically demanding alkylation reactions. Afterwards, the nitriles are converted into a large variety of other functional groups<sup>86</sup>.  $\alpha$ -Magnesiated nitriles can be obtained via Br/Mg exchange starting from  $\alpha$ -bromo nitriles like **72**<sup>87</sup>. The rapid exchange at low temperature ( $-78^\circ\text{C}$ ) allows an *in situ* reaction protocol, where the exchange reaction selectively takes place in the presence of reactive electrophiles including aldehydes (equation 46).



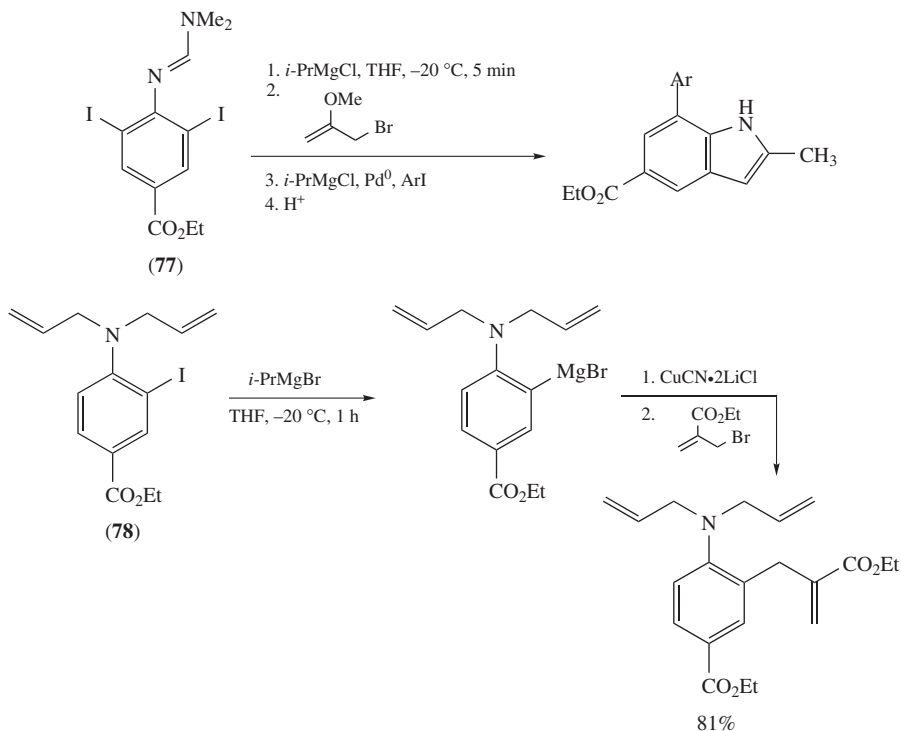


Recently, the preparation of functionalized benzylic magnesium reagents **73** could be realized by using a new sulfur–magnesium exchange reaction (equation 47)<sup>88</sup>. I/Mg



exchange on *o*-(*o*-iodophenyl)phenylthio derivative **74** affords the expected exchange product **75** which undergoes an intramolecular sulfur–magnesium exchange reaction after treatment with *t*-BuOLi leading to the desired Grignard reagent **73**. It can be trapped with electrophiles leading to functionalized benzylic compounds **76a–c**.

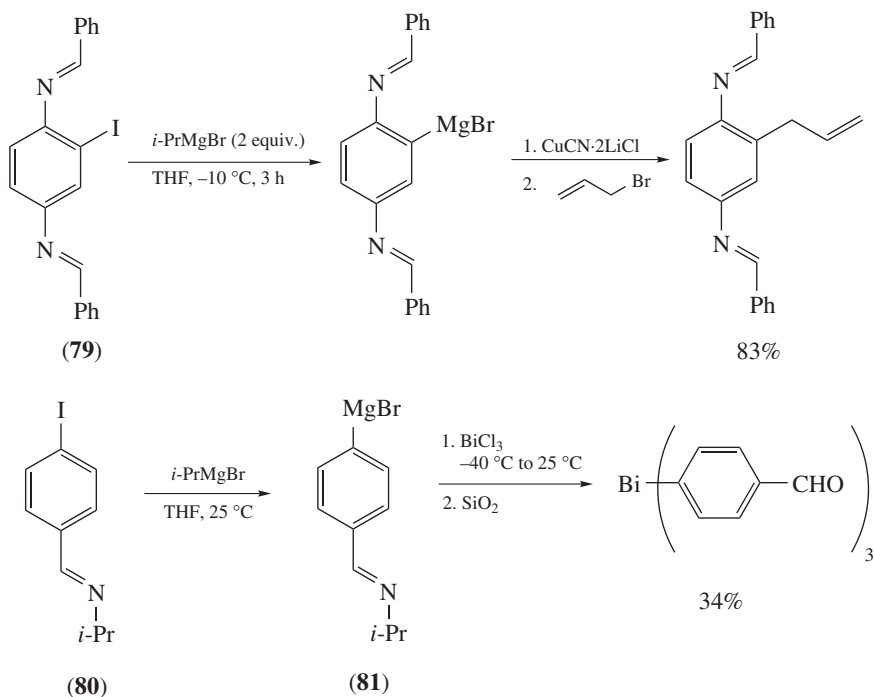
*b. Functional group tolerance.* The magnesium exchange reaction tolerates an impressive number of functional groups. For example, the amino function is tolerated after protection as amidine **77** or as diallyl derivative **78** (Scheme 4). Imines like **79** and **80** are suitable protecting groups of anilines and aromatic aldehydes during exchange reactions (Scheme 5)<sup>89</sup>.



SCHEME 4

While aryl iodides bearing an aldehyde group preferentially react with the aldehyde function during attempted iodine–magnesium exchange, the corresponding imine **80** undergoes a smooth exchange reaction leading to the Grignard reagent **81** (Scheme 5).

The tedious protection and deprotection sequence of anilines can be avoided through the formation of magnesium amides. Halogen–lithium exchange reactions on aryl halides bearing acidic protons have been successfully conducted with alkyllithium reagents. But the necessity of low reaction temperatures ( $-78^{\circ}\text{C}$ ) and the considerable amounts of side products make this methodology less attractive, while the formation of unprotected functionalized Grignard reagents can be easily accomplished (Scheme 6). The acidic amine proton of the functionalized aniline **82** is first abstracted with methyl- or phenylmagnesium chloride. These two Grignard reagents only reluctantly undergo exchange reactions



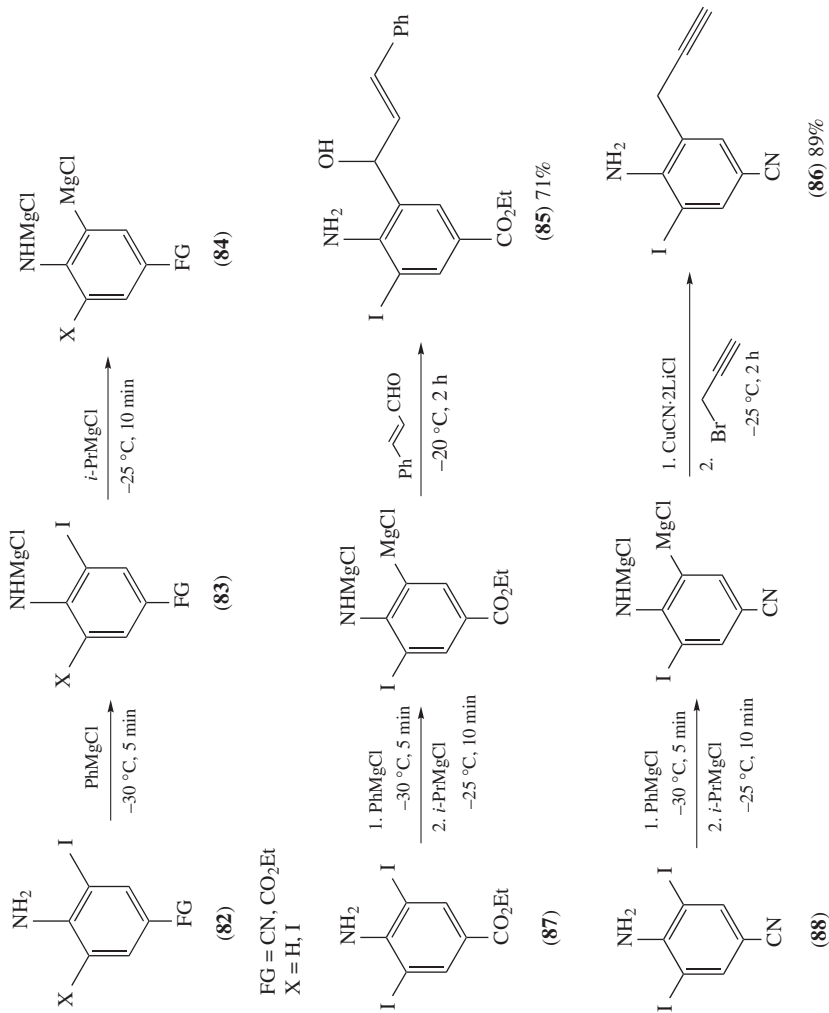
SCHEME 5

and lead to an intermediate of type **83**. In a second step, the actual I/Mg-exchange reaction is carried out with *i*-PrMgCl, leading to the desired Grignard reagent **84** (Scheme 6).<sup>89</sup>

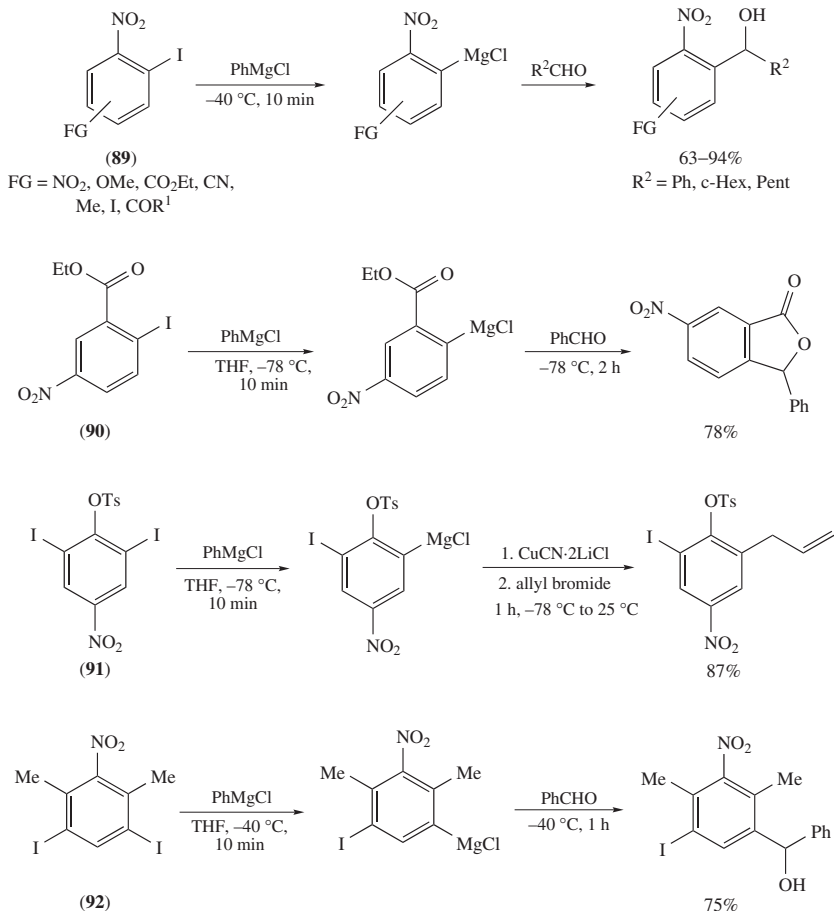
Thus, the functionalized anilines **85** and **86** are obtained in 71–89% yield starting from diiodoanilines **87** and **88** (Scheme 6). Other proton-donating groups like hydroxy groups (equation 25)<sup>57</sup>, acids, amides or benzylic alcohols<sup>90</sup> are also compatible with this approach.

Nitro compounds are key intermediates in organic synthesis<sup>91</sup> and are rather reactive toward organomagnesium reagents. They are in general believed not to be compatible with organometallic functionalities. The I/Mg-exchange reaction proceeds readily in the case of *ortho*-nitroaryl iodides such as **89** by using the less reactive PhMgCl instead of *i*-PrMgCl<sup>92</sup>. For nitro-containing substrates, bearing an additional coordinating group such as **90** and **91**, or *ortho*-disubstituted substrates like **92**, the exchange on *meta*- and *para*-aryl iodides is also possible (Scheme 7).

The triazene group is a convenient synthetic equivalent of a diazonium salt and is readily converted to an iodine functionality<sup>93</sup>. It reacts with *i*-PrMgCl when an I/Mg exchange with an iodoarene bearing a triazene functionality is attempted. By using the more reactive *i*-PrMgCl·LiCl, the exchange reaction can be realized at lower temperatures (−40 °C) allowing an excellent compatibility with a triazene group. Thus, the reaction of the iodotriazene **93** with *i*-PrMgCl·LiCl provides the desired Grignard reagent which undergoes a smooth addition–elimination with 3-iodo-2-cyclohexenone in the presence of CuCN·2LiCl. The resulting enone **94** is readily converted to aryl iodide **95** by treatment with CH<sub>3</sub>I (equation 48)<sup>94</sup>. This iodine can be subjected to further functionalizations<sup>95</sup>.

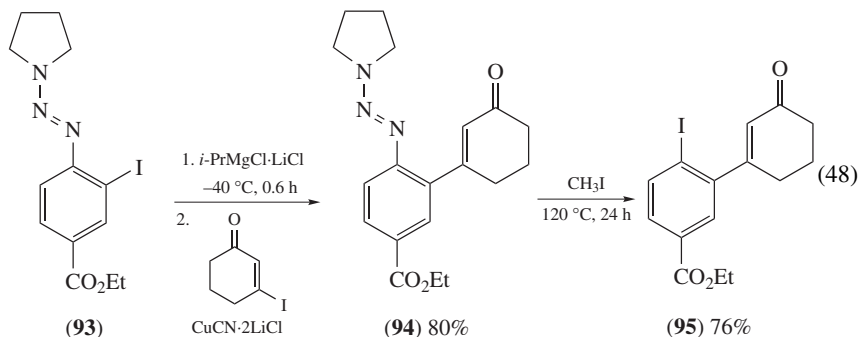


SCHEME 6

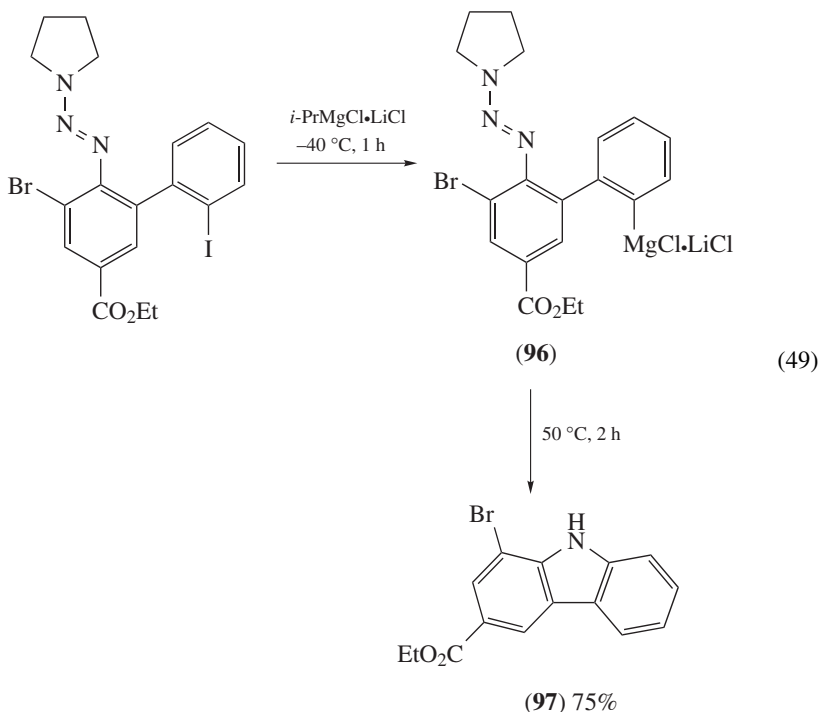


SCHEME 7

Magnesiated triazene derivatives like **96** can further be used for the preparation of functionalized carbazoles **97** (equation 49)<sup>95</sup>.

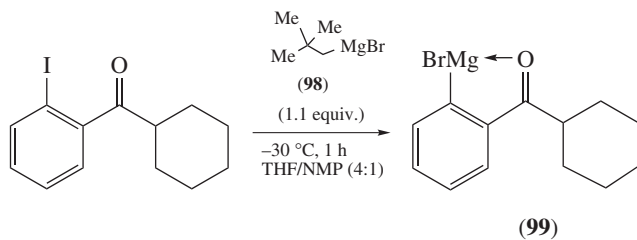


By carefully tuning the reaction conditions, the preparation of ketone group-containing arylmagnesium species can be achieved. To avoid side reactions, neopentylmagnesium bromide (NpMgBr) **98**, a sterically hindered but reactive Grignard reagent, is used. In conjunction with *N*-methylpyrrolidinone (NMP) as a polar cosolvent, complete conversion to the organomagnesium species **99** is observed at  $-30^{\circ}\text{C}$  within 1 h (equation 50)<sup>96</sup>. The *ortho*-keto function actually facilitates the formation of the Grignard reagent by pre-coordination of NpMgBr **98** and stabilizes the resulting arylmagnesium species **99** by chelation. Iodo-substituted aryl or heteroaryl ketones or cycloalkenyl ketones can alternatively be protected as cyanohydrins **100** and **101** allowing I/Mg-exchange reactions with *i*-PrMgCl•LiCl<sup>97</sup>. After deprotection the functionalized products **102** and **103** are obtained in 76–87% yield (equations 51 and 52). This protocol can also be applied to aromatic iodoaldehydes<sup>97</sup>.

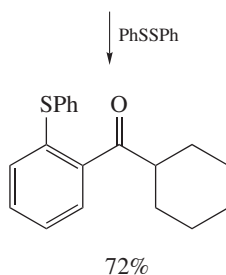


Electrophilic functional groups in *ortho*-position to the carbon–magnesium bond allow two sequential alkylations. Starting from *ortho*-iodobenzyl chloride **104**, the benzannulated heterocycles **105** and **106** are obtained after the reaction with appropriate electrophiles (Scheme 8)<sup>98</sup>.

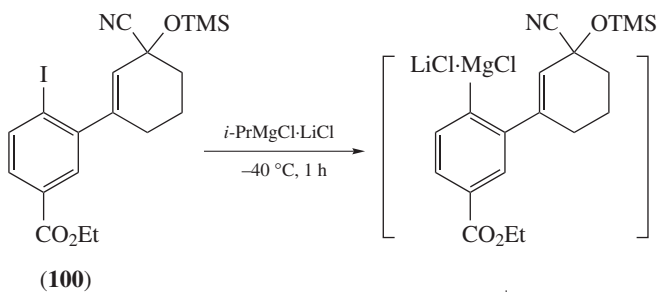
The high activity of *i*-PrMgCl•LiCl in exchange reactions allows the preparation of highly functionalized aryl and hetaryl pinacolborates **107**, e.g. **107a**, **b** (bimetallic reagents, equation 53)<sup>99</sup>. The halogen–magnesium exchange reaction can be easily applied to solid-phase synthesis<sup>81b, 100, 101</sup>, affording polymer-bound Grignard reagent **108** (equation 54).



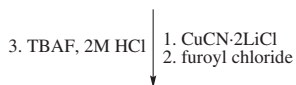
(50)



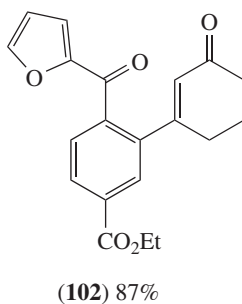
72%



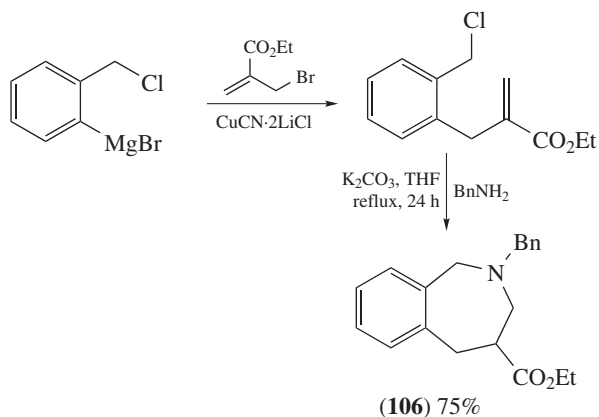
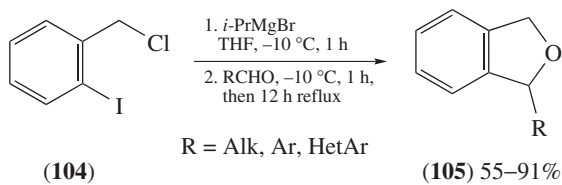
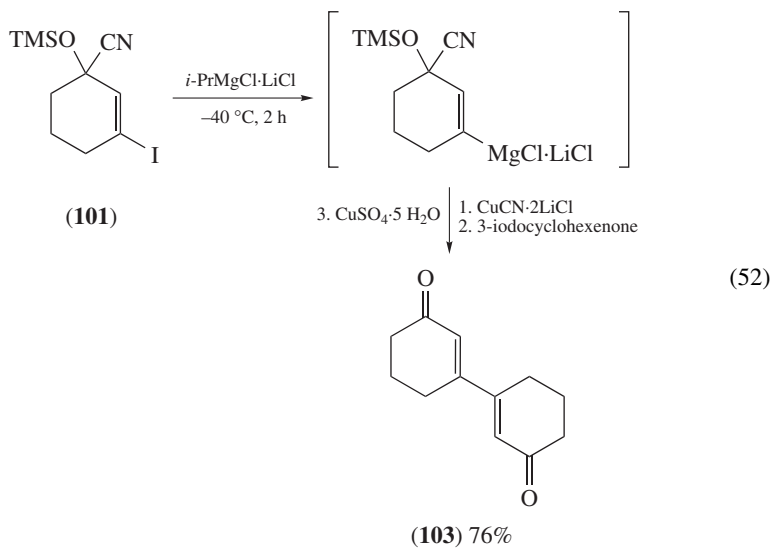
(100)



(51)

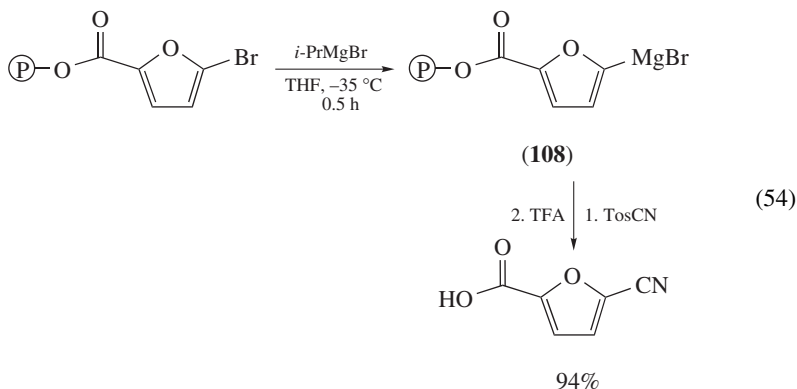
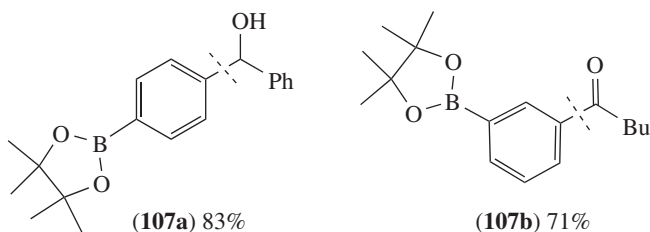
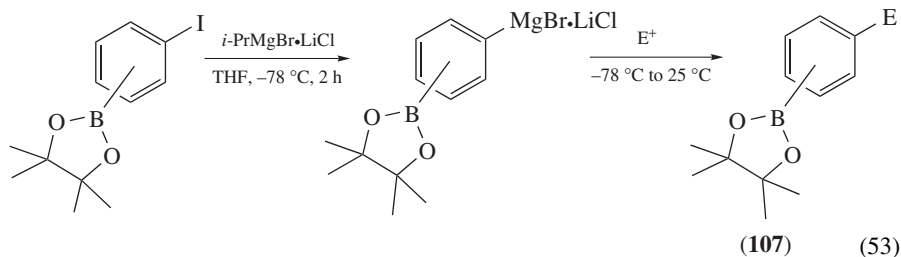


(102) 87%



SCHEME 8



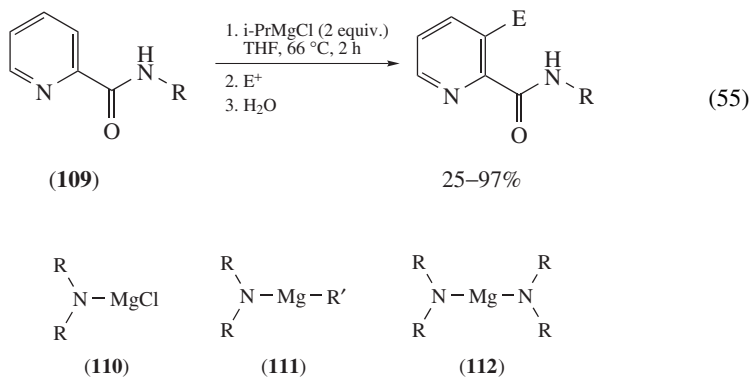


### C. Metalation Reactions with Magnesium Amide Bases

Alkyl lithium reagents (RLi) or lithium dialkylamides ( $R_2NLi$ ) have been widely used for the *ortho*-metalation reactions of aromatic and heteroaromatic compounds<sup>102</sup>, although their use is usually complicated by the presence of undesired side reactions as a result of their reactivity and strong nucleophilicity and by a low compatibility of functional groups. To overcome low reaction temperatures ( $-78$  to  $-90$  °C) and ensure the presence of various functional groups, magnesium amides and to a smaller extent Grignard reagents have been developed as metalating agents. Alkylmagnesium reagents are strongly basic. Nevertheless, their low kinetic basicity allows only successful magnesiations in a few cases such as the pyridyl amide **109**. The activating group both directs the Grignard reagent and breaks magnesium aggregates. Unfortunately, the attempted metalation often competes with addition reactions (equation 55)<sup>103</sup>.

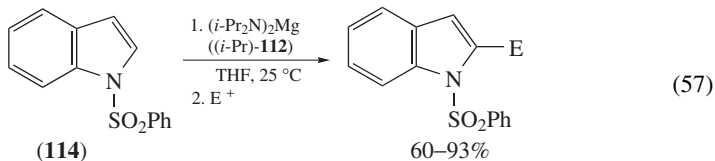
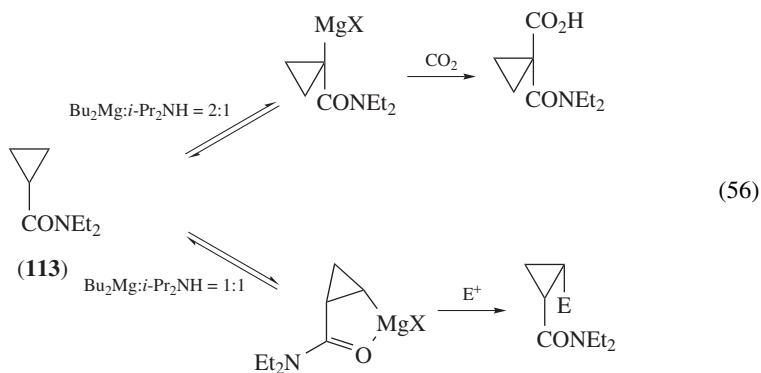
3-Substituted pyridines undergo exclusively 1,4-addition, while 4-substituted pyridines give a mixture of products<sup>103</sup>. The metalation of alkynes by *n*-BuMgCl is often used<sup>104</sup>.

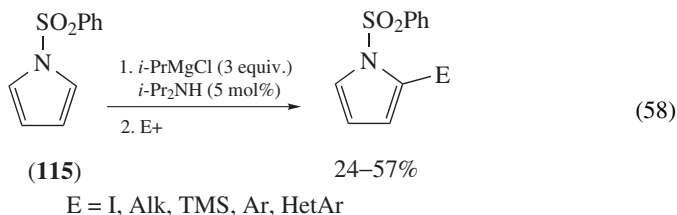
Reaction of alkylmagnesium reagents with sterically hindered amines leads to the formation of magnesium amides **110**–**112**<sup>105</sup>, reacting much faster than the parent alkylmagnesium derivatives with C–H acidic substrates (Scheme 9).



SCHEME 9

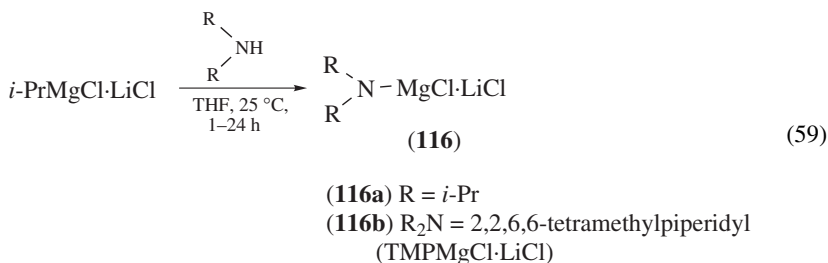
The low solubility of the amides  $\text{R}_2\text{NMgCl}$  (**110**),  $\text{R}_2\text{NMgR}'$  (**111**) or  $(\text{R}_2\text{N})_2\text{Mg}$  (**112**) has hampered a general application of these bases. Usually, a large excess (up to 5 equiv.) is necessary to ensure a complete magnesiation. This is disadvantageous, since the range of electrophiles added to quench the newly generated magnesium reagent may be limited due to side reactions of some electrophiles with the excess of magnesium base. Nevertheless, cyclopropyl amides such as **113** can be functionalized (equation 56)<sup>106</sup>. Also, the magnesiation of indoles like **114** can be realized (equation 57)<sup>107,108</sup>. Finally, the catalytic generation of the magnesium base may be advantageous in the case of the magnesiation of pyrrole **115** (equation 58)<sup>109</sup>.





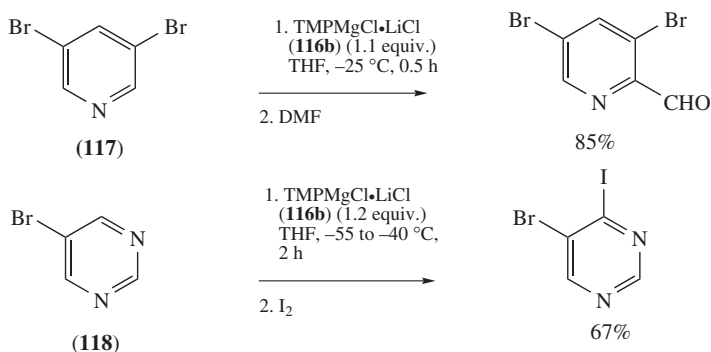
The chemistry of magnesium bisamides has been reviewed<sup>110</sup>. They can be used for the regio- and stereoselective formation of enolates<sup>111</sup>, while chiral magnesium amides are applied in asymmetric synthesis for enantioselective enolisations<sup>112</sup>.

A large excess of the magnesium amides can be avoided by using highly soluble mixed Mg/Li amides  $\text{R}_2\text{NMgCl}\cdot\text{LiCl}$  **116**<sup>113</sup>. Reaction of  $i\text{-PrMgCl}\cdot\text{LiCl}$  with sterically hindered secondary amines affords Mg/Li reagents **116** (e.g. **116a,b**) which display high kinetic activity, excellent solubility combined with a better stability upon storage as THF solutions (equation 59).

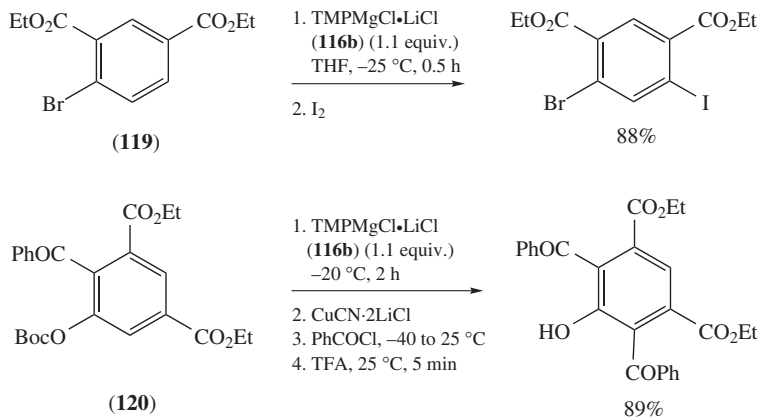


TMPMgCl $\cdot$ LiCl (**116b**) is an especially efficient base for the regioselective magnesiation of various heteroaromatics (**117** and **118**) and aromatics (**119** and **120**) species (Scheme 10)<sup>113,114</sup>.

Even a multiple functionalization of a bisubstituted aromatic compound such as **121** can be achieved by successive magnesiation with TMPMgCl $\cdot$ LiCl (**116b**) and quench-



SCHEME 10



SCHEME 10

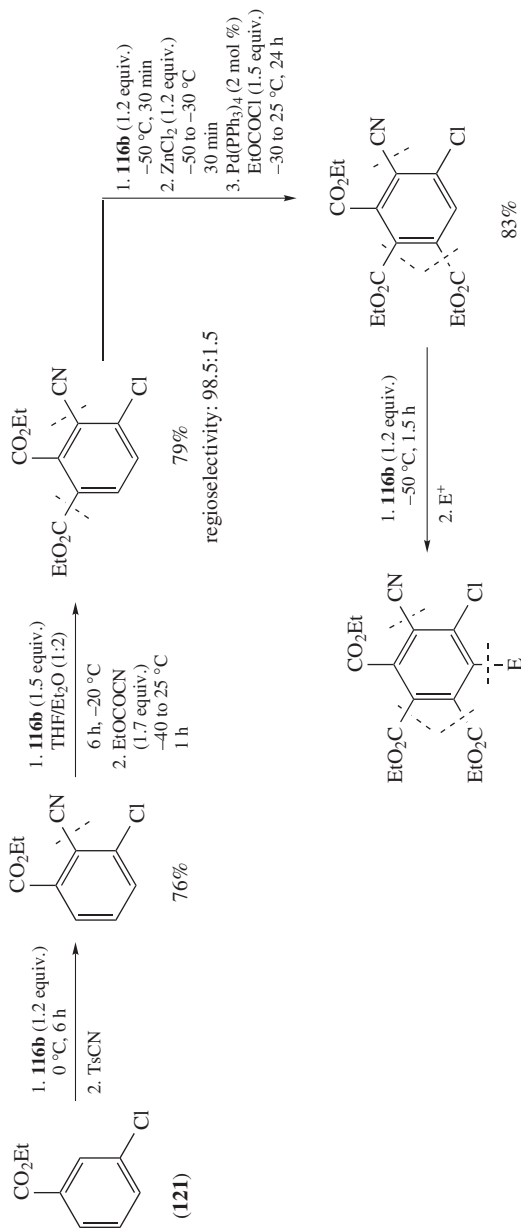
ing with various electrophiles leading to hexasubstituted benzene derivatives **122a–d** (Scheme 11)<sup>114</sup>.

#### D. Miscellaneous Methods

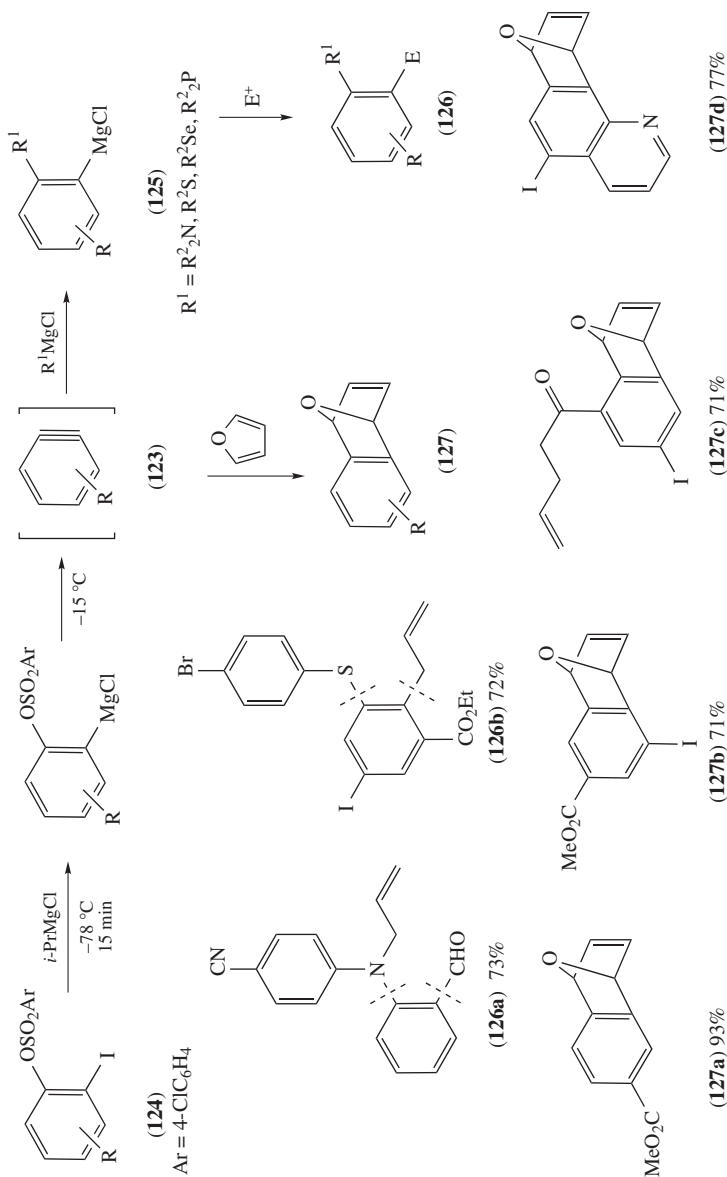
Arynes are valuable intermediates in synthetic organic chemistry<sup>115</sup>. The triple bond of an aryne is highly reactive toward reactions with nucleophiles. For example, functionalized arynes **123**, prepared from *ortho*-iodoaryl sulfonates **124** by an iodine–magnesium exchange followed by the elimination reaction of *ortho*-magnesio-arylsulfonates, react with a number of heteroatomic nucleophiles, like  $\text{R}_2\text{NMgX}$ ,  $\text{RSMgX}$ ,  $\text{RSeMgX}$  and partially with  $\text{R}_2\text{PMgX}$ , generating novel Grignard species of type **125**. These reagents can be trapped by electrophiles leading to functionalized aromatics **126**. Alternatively, arynes **123** undergo cyclization reactions with furan leading to cycloadducts of type **127** (Scheme 12)<sup>116</sup>. Following this protocol, various functionalized arynes **126a, b** and **127a, c** and heteroaryne **127d** have been prepared.

The nature of the sulfonate leaving group proved to be crucial for an efficient elimination reaction leading to arynes of type **123** (Scheme 12). Best results are obtained with 4-chlorobenzenesulfonate as leaving group. Similarly, the reaction of arylmagnesium reagents with arynes, prepared *in situ* from 2-fluorophenyllithium, gave sterically encumbered substituted 2-iodobiphenyls after iodolysis<sup>117</sup>. The addition of  $\text{MgH}_2$  to olefins is leading to Grignard reagents<sup>118</sup>. Also, the reaction of Mg metal with 1,4-diarylbutadienes gives magnesium derivatives behaving as Grignard reagents (equation 60)<sup>119</sup>.

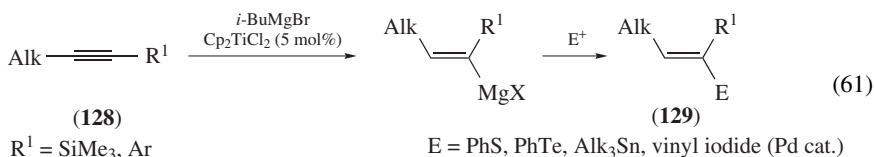
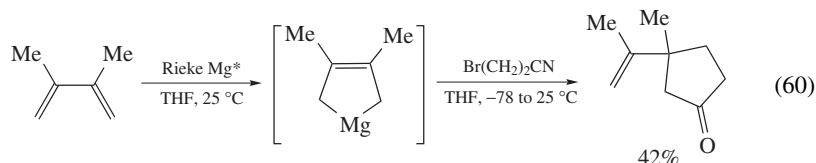
Hydromagnesiation of acetylenes, catalyzed by titano- and zirconocenes, can be readily achieved. A regioselective reaction occurs only if one of the substituents on the triple bond is silicon or an aryl group **128** (equation 61). Mechanistic studies on this hydromagnesiation have been reported<sup>120,121</sup>. This reaction has been applied to the synthesis of polysubstituted alkenes of type **129**<sup>122</sup>. The non-catalyzed hydromagnesiation of 1,3-alkadienes with *i*-PrMgCl gives only mixtures of magnesiated alkenes<sup>123</sup>. Reaction of 2-alkyl-1,3-butadienes with *n*-PrMgX in the presence of  $\text{Cp}_2\text{TiCl}_2$  affords allylmagnesium



SCHEME 11



reagents as single regioisomers<sup>124</sup>.



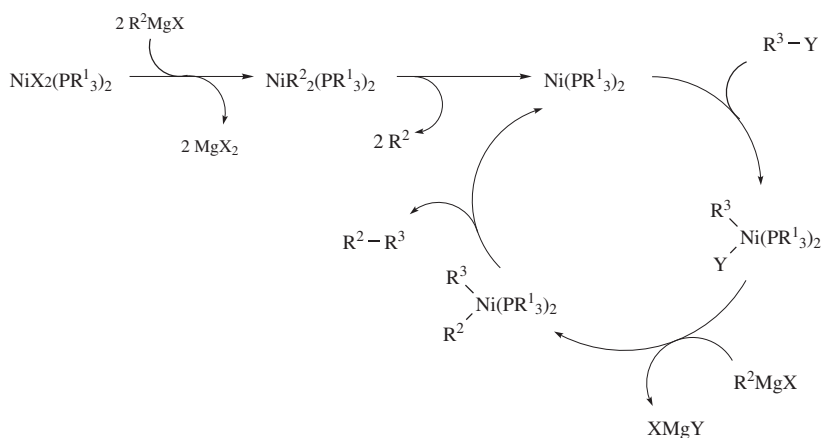
### III. REACTIVITY OF GRIGNARD REAGENTS

Organomagnesium compounds are versatile reagents for organic synthesis<sup>125</sup>. They undergo a multitude of reactions, which will be divided in this section into two major groups: substitution and addition reactions. Cross-coupling reactions<sup>126</sup>, allylic substitutions and ring-opening of small cyclic molecules will be considered as substitution reactions. Carbomagnesiation and 1,4-addition reactions will be discussed in the addition part. Cases of mechanistically complex reactions will be classified according to the structure of the final product, i.e. addition–elimination reactions will be included in the substitution part. The substitution reactions are further subdivided into three groups according to the degree of unsaturation at the electrophilic center of the substrate.

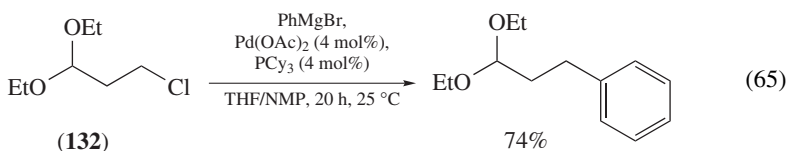
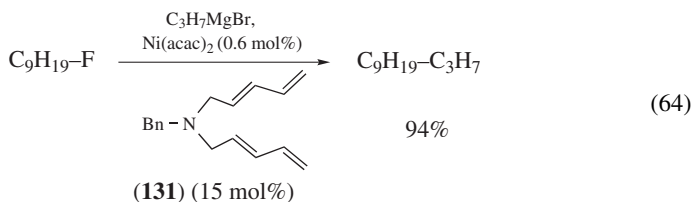
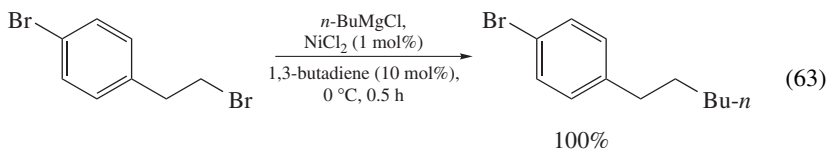
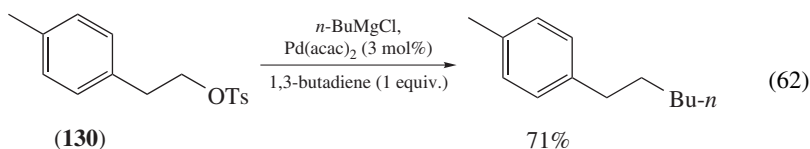
#### A. Substitutions at an $\text{sp}^3$ -center

##### 1. Transition-metal-catalyzed cross-coupling reactions

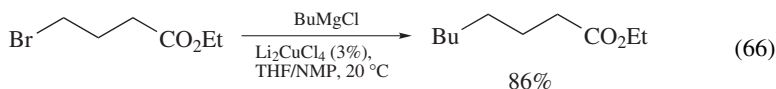
Pd- and Ni-catalyzed coupling reactions follow a mechanism which is described in Scheme 13.



Compared to the formation of  $\text{Csp}^2\text{--Csp}^2$  bonds,  $\text{Csp}^3\text{--Csp}^2$  couplings are difficult to perform. Unactivated alkyl electrophiles only reluctantly undergo the oxidative addition to a metal center, while  $\beta$ -hydride elimination is generally fast. *n*-Alkyl bromides and tosylates like **130** can be coupled successively with aryl- and alkylmagnesium reagents in the presence of 1,3-butadiene, using 3%  $\text{Pd}(\text{acac})_2$  as a catalyst (equation 62)<sup>127</sup>. Using 1 mol%  $\text{NiCl}_2$  and 10 mol% butadiene, the reactions can even be performed at 0 °C (equation 63)<sup>128</sup>. With 1,3,8,10-tetraenes like **131** as additives, the nickel-catalyzed cross-coupling of alkyl halides with organozinc or Grignard reagents proceeds readily (equation 64). In the presence of strong electron-donating ligands ( $\text{PCy}_3$ , IMes), arylmagnesium bromides can be coupled with primary alkyl chlorides like **132** using Pd catalysis (equation 65)<sup>129, 130</sup>.



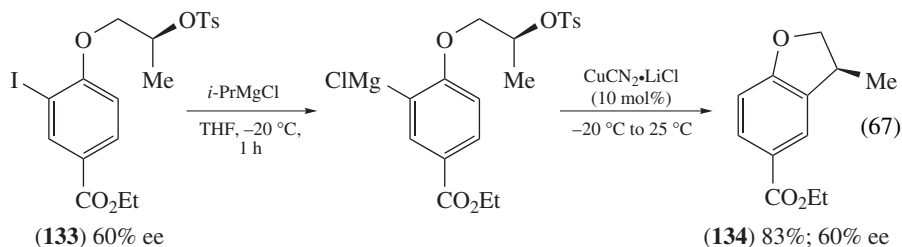
Enol phosphates can be coupled with alkyl or aryl magnesium reagents using  $\text{NiCl}_2(\text{dppe})$ <sup>131</sup> or  $\text{PdCl}_2(\text{PPh}_3)_2$ <sup>132</sup>. Copper-catalyzed cross-coupling of alkyl halides or sulfonates with Grignard reagents has become a popular method for constructing alkyl chains. For example,  $\text{Li}_2\text{CuCl}_4$  in THF-NMP efficiently catalyses the reaction of alkyl- and vinylmagnesium reagents with primary alkyl halides. Functional groups (ketone, ester, nitrile, sulfonate) are tolerated in this reaction (equation 66)<sup>133</sup>.



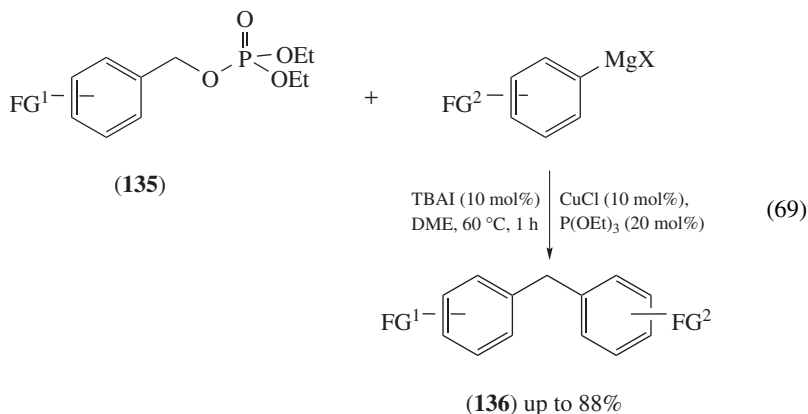
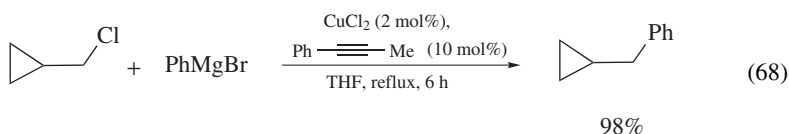
If an organomagnesium reagent bears a remote leaving group, cyclizations can be achieved. Starting from the tosylate **133**, a stereoselective substitution using  $\text{CuCN}\cdot 2\text{LiCl}$



afforded the benzotetrahydrofuran **134** without loss of optical purity (equation 67).

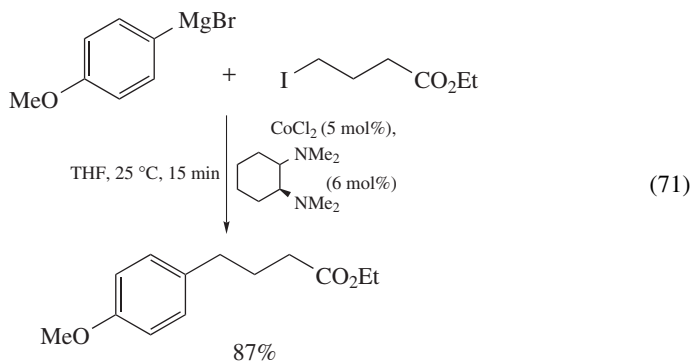
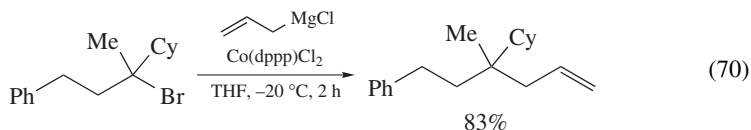


Copper thiophenolate-LiBr has proven to be a superior catalyst for special cases like the reaction of arylmagnesium compounds with primary alkyl tosylates and *n*-alkylmagnesium bromides with secondary tosylates<sup>134</sup>. Primary alkyl fluorides react smoothly with tertiary alkylmagnesium halides in the presence of  $\text{CuCl}_2$ , while primary and secondary alkyl magnesium reagents require the addition of butadiene. Arylmagnesium derivatives only react at elevated temperatures, while alkyl chlorides give poor results<sup>135</sup>. The latter can be efficiently coupled in the presence of 1-phenylpropyne as an additive (equation 68)<sup>136</sup>. Various alkylmagnesium chlorides can be reacted with alkyl bromides in the presence of an amino-organomanganese complex and  $\text{CuCl}$ <sup>137</sup>. A combination of  $\text{CuCl}$ , triethyl phosphate and tetrabutylammonium iodide (TBAI) efficiently couples aryl- or heteroarylmagnesium halides with benzylic phosphates **135** forming polyfunctionalized diarylmethanes **136** (equation 69)<sup>138</sup>.

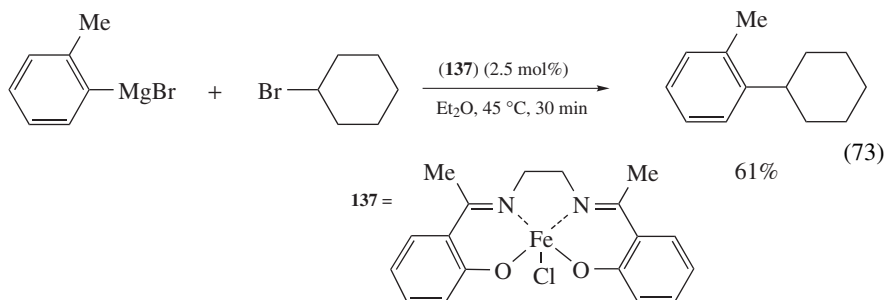
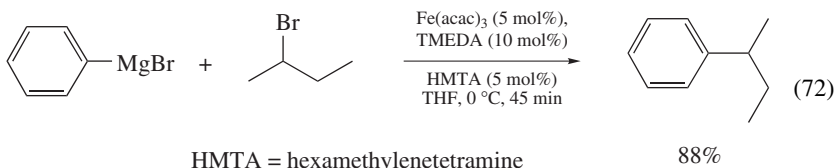


Other possible catalysts for the reaction of various alkyl bromides with allylmagnesium halides in THF are cobaltbis(1,3-diphenylphosphino)propane complex (equation 70)<sup>139</sup> or cobalt chloride in combination with a diamine (equation 71)<sup>140</sup>. Cyclization products can

be obtained in good yields in the presence of a suitably placed double bond<sup>141</sup>.



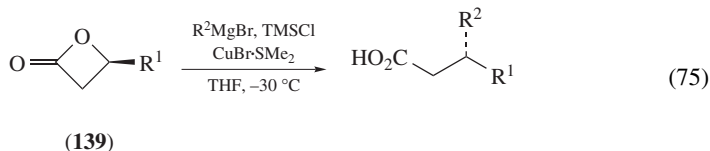
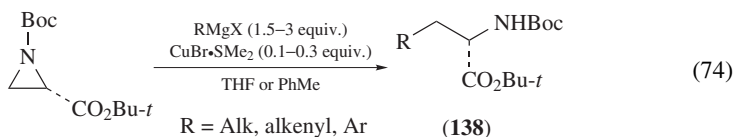
Fe<sup>III</sup> salts have been successfully used for coupling reactions of various organomagnesium reagents with alkyl electrophiles. Thus, FeCl<sub>3</sub> and TMEDA<sup>142</sup>, Fe(acac)<sub>3</sub> (equation 72)<sup>143</sup> or Fe<sup>III</sup> salen-type complexes (**137**, equation 73)<sup>144</sup> catalyze the coupling of arylmagnesium reagents with primary and secondary alkyl bromides. Fe(MgX)<sub>2</sub> is believed to be the active catalyst. It is formed in the reaction mixture by the *in situ* reduction of Fe<sup>III</sup> salts by the Grignard reagent<sup>145</sup>. The Fe<sup>II</sup> complex [Li(TMEDA)]<sub>2</sub>[Fe(C<sub>2</sub>H<sub>4</sub>)<sub>4</sub>] is another efficient catalyst for the cross-coupling reaction between alkyl electrophiles and arylmagnesium compounds<sup>145</sup> affording complete conversion within minutes even at -20 °C.



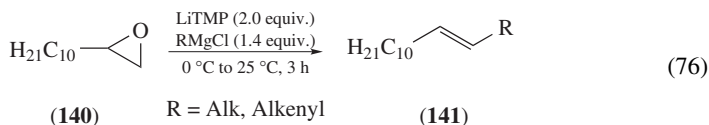
Oxidative homo-coupling of alkyl magnesium reagents possessing  $\beta$ -hydrogens is achieved in the presence of silver tosylate (AgOTs, 1 mol%) as a catalyst and 1,2-dibromoethane as a reoxidant<sup>146</sup>.

## 2. Ring-opening of small cycles

Organomagnesium reagents can effect ring-opening of aziridines in the presence of a catalytic amount of  $\text{Cu}^{\text{I}}$  salt<sup>147</sup>. The aziridines must bear a phosphinoyl, sulfonyl or carbamate group on the nitrogen. This method can be used for the synthesis of chiral  $\beta$ -(het)arylalkylamines<sup>148</sup> or  $\alpha$ -amino acids like **138** (equation 74)<sup>149</sup>. The easily available chiral  $\beta$ -propiolactones of type **139** undergo similar ring-opening reactions, thus offering an alternative to enantioselective 1,4-addition reactions (equation 75)<sup>150</sup>.



Terminal epoxides **140** are deprotonated at  $0^\circ\text{C}$  using lithium tetramethylpiperidide (LiTMP). The resulting anion reacts with alkyl- and alkenylmagnesium reagents under ring-opening.  $\text{Li}_2\text{O}$  is eliminated and alkenes **141** are formed (equation 76)<sup>151</sup>.



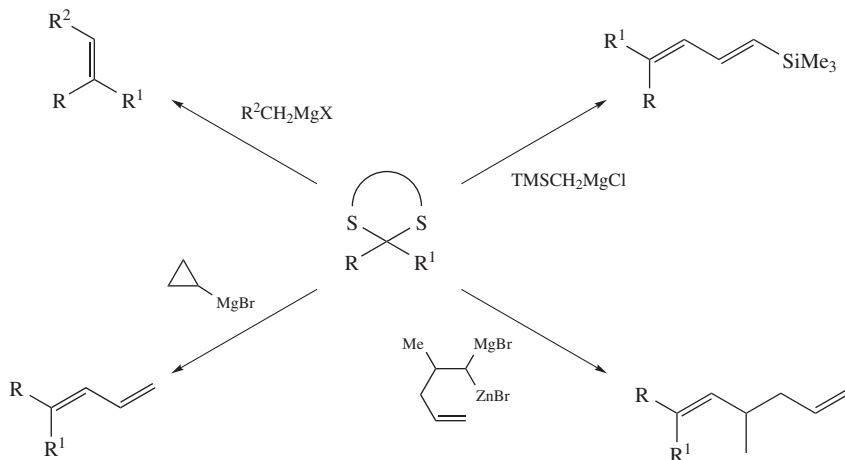
Reaction of ketone dithioacetals with Grignard reagents opens synthetic routes to a variety of substituted alkenes (Scheme 14)<sup>152</sup>. For the reactions of simple aliphatic dithioacetals the presence of a Ni-trialkylphosphine catalyst is needed<sup>153</sup>.

Chiral acetals undergo diastereoselective ring-opening with Grignard reagents in toluene<sup>154</sup>. Ketals, derived from  $\omega$ -bromoketones, react with  $\text{Mg}/\text{MgBr}_2$ , giving cycloalkanol ethers after Lewis-acid-assisted ring-opening and intramolecular quench of the alkylmagnesium species. Substituted cyclopropanes and cyclobutanes are obtained by this method<sup>155</sup>.

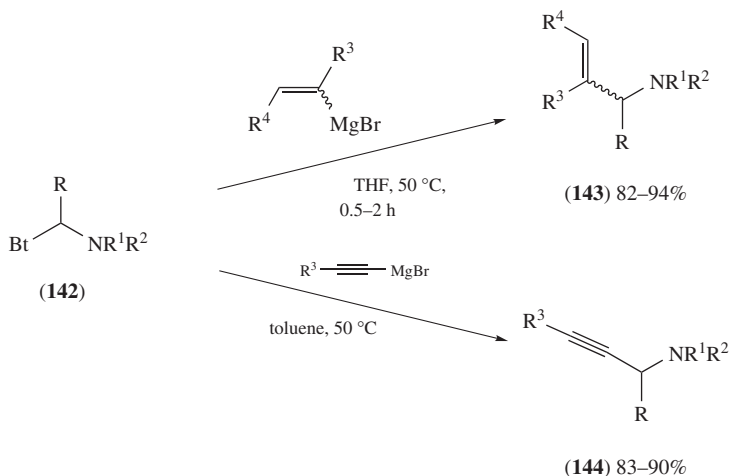
## 3. Diverse reactions

Benzotriazole (Bt) may serve as a leaving group in reactions with organometallic species<sup>156</sup>. Thus, polysubstituted  $\alpha$ -aminobenzotriazoles **142** react with Grignard reagents as imine equivalents and the use of alkenyl- or propargylmagnesium reagents allows the synthesis of allyl- or propargylamines **143** and **144** in good yields (Scheme 15)<sup>157</sup>.

This reaction can furthermore be applied on chiral amins, affording a straightforward route to optically pure *trans*-2,5-pyrrolidines<sup>158</sup> or chiral alkyl-substituted 1,3-oxazolidines. This method was used for the enantioselective synthesis of substituted piperidines<sup>159</sup>.



SCHEME 14

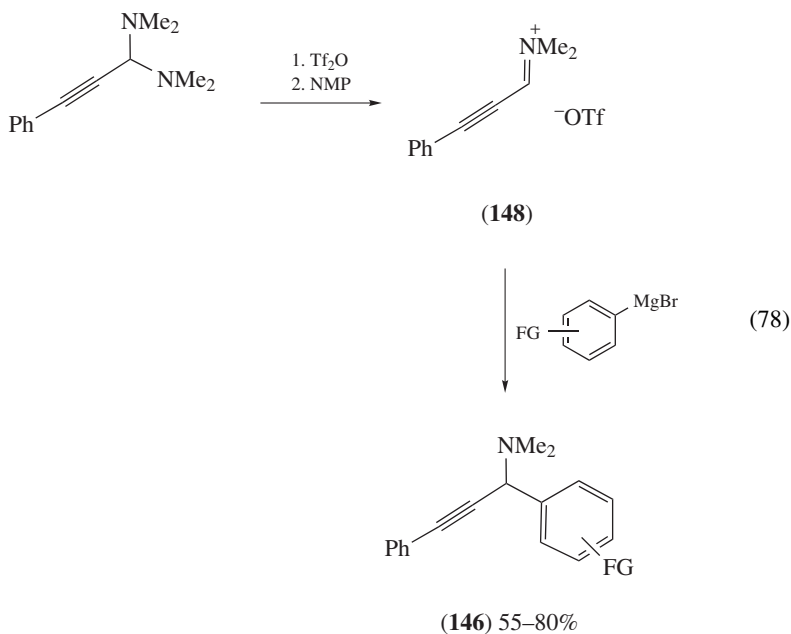
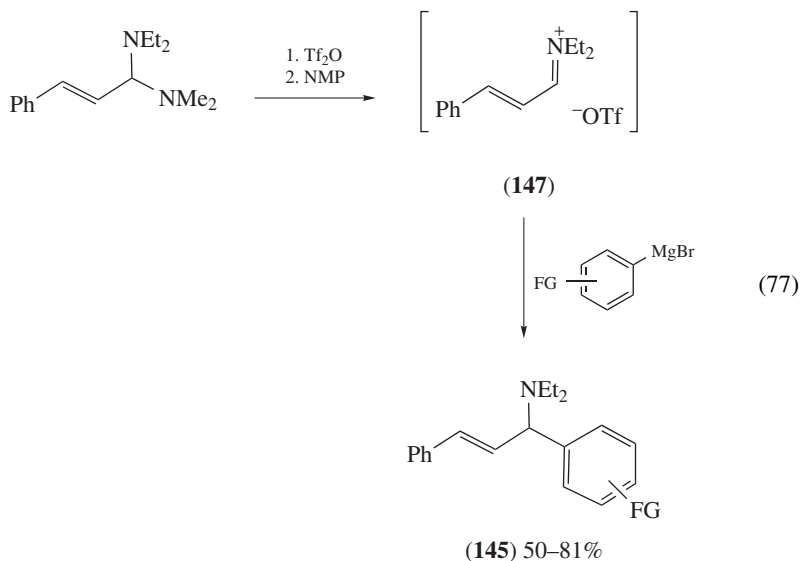


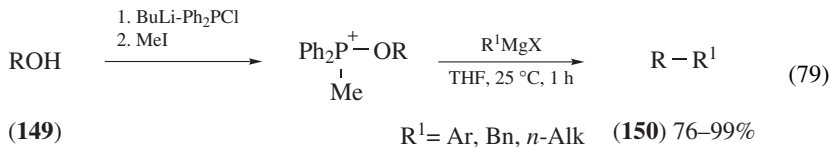
SCHEME 15

An alternative route to tertiary allyl- and propargylamines **145** and **146** is the reaction of Grignard compounds with iminium triflates **147** and **148** (equations 77 and 78). The intermediate iminium triflates **147** and **148** are obtained from the corresponding aminals by reaction with  $Tf_2O$ . Primary propargylamines can be prepared from tetraallylated aminals<sup>160</sup>.

Other functionalities than halides, sulfonates or benzotriazoles (Scheme 15) might serve as leaving groups in substitution reactions with organomagnesium reagents. For example, benzylic  $\alpha$ -azidoethers react with a substitution of the azide group<sup>161</sup>. Primary and benzylic alcohols **149** can be converted into good leaving groups by their transformation into

diphenylphosphinites followed by quaternization with MeI. Reaction with alkyl-, benzyl- and arylmagnesium compounds gives the corresponding coupling products of type **150** (equation 79)<sup>162</sup>.





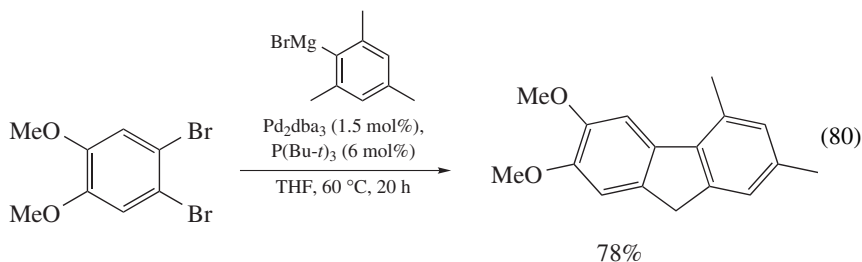
The transmetalation of alkylmagnesium reagents to Cu, Mn and Zn was performed by using an optically enriched Grignard reagent. Transmetalation to zinc proceeds with complete retention of configuration (concerted mechanism), while the transformations to copper and manganese organometallics<sup>163</sup> as well as trialkyltin halides<sup>164</sup> are rather complicated.

## B. Substitutions at an sp<sup>2</sup>-center

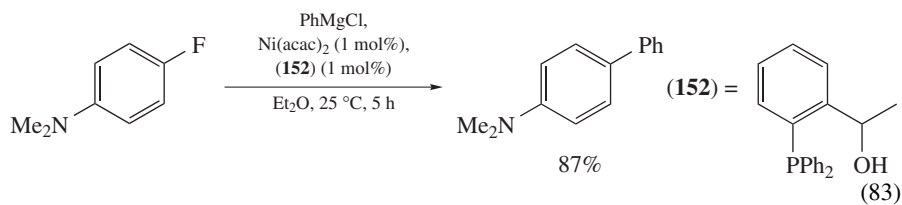
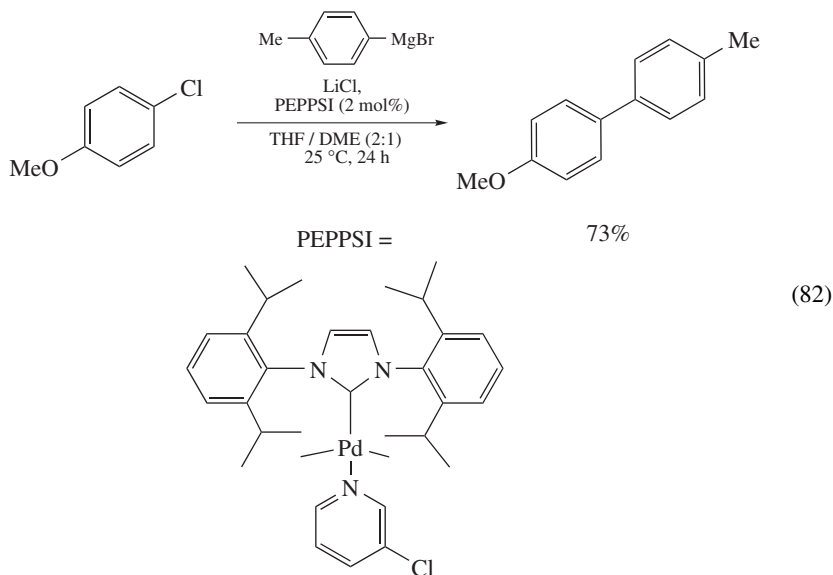
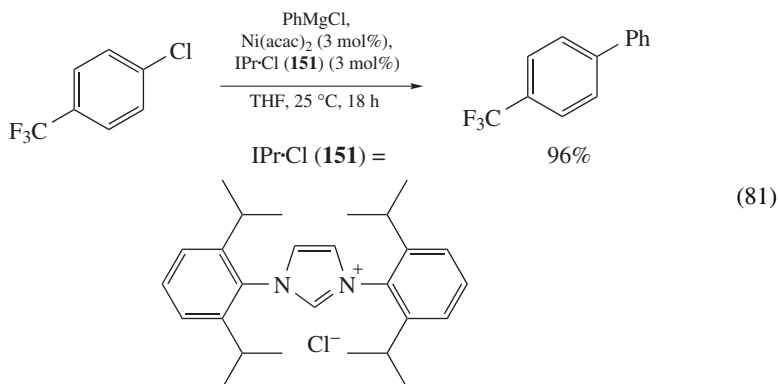
### 1. Transition-metal-catalyzed cross-coupling reactions

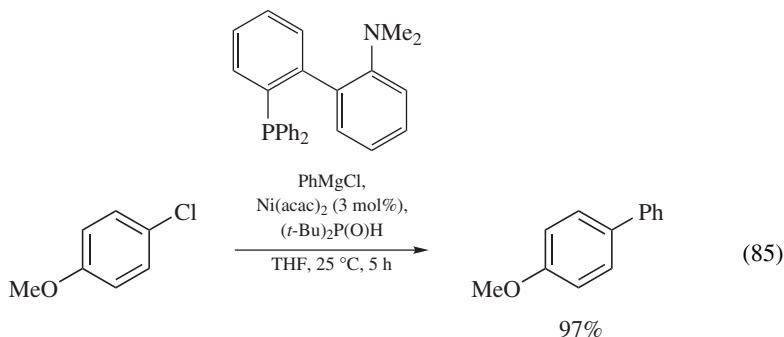
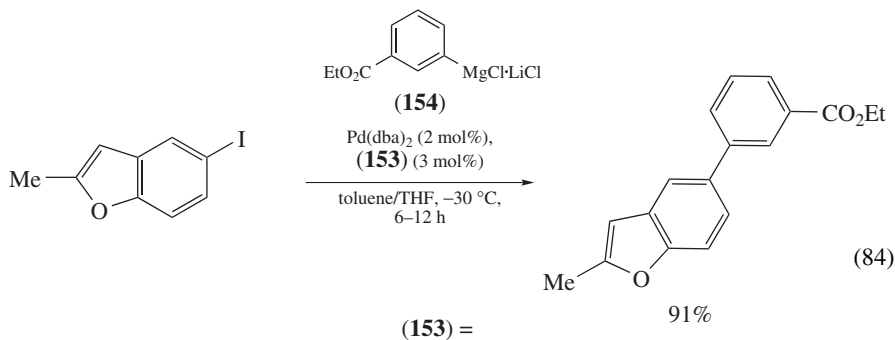
The reaction of aryl electrophiles with organomagnesium compounds is known as Kumada or Kumada–Tamao–Corriu reaction. The most common leaving groups in the electrophile are halogen atoms and, among them, chlorine is the most wanted due to the good availability and the low price of aryl or heteroaryl chlorides. Unfortunately, the oxidative addition of a metal center to an aryl chloride is a difficult reaction and many efforts have been made to overcome existing limitations.

More efficient ligands were recently developed. In the case of Pd and Ni, electron-rich ligands like bulky trialkylphosphines (equation 80)<sup>165</sup> or stable carbenes like *N*-heterocyclic carbenes (NHC, **151**, equation 81)<sup>166</sup> and PEPPSI (equation 82)<sup>167</sup> can be used with good success. The combination of Ni with a NHC ligand allows coupling at room temperature and permits the coupling with aryl fluorides<sup>168</sup>. These fluorides can be coupled as well using triarylphosphine ligand **152** bearing a hydroxyl group in close vicinity (equation 83)<sup>169</sup>. Using biaryl ligand **153**, the coupling reactions can be carried out at temperatures below 0 °C, thus allowing the use of functionalized Grignard reagents like **154** (equation 84)<sup>170</sup>.

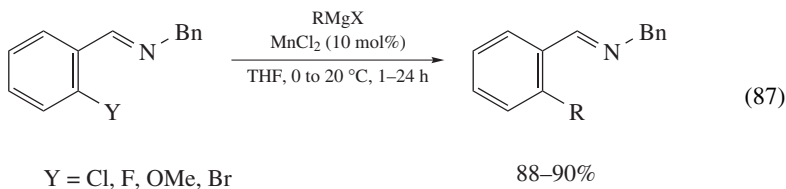
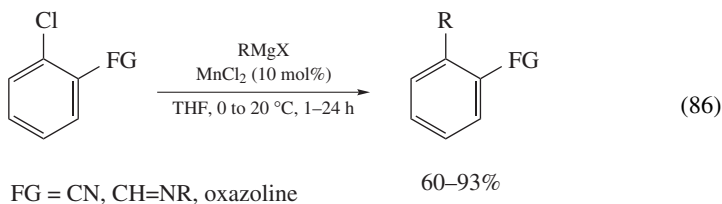


Dialkylphosphine oxides are another class of highly efficient ligands for coupling reactions using Pd<sup>171</sup> or Ni<sup>172</sup> (equation 85). Electron-poor fluoroazines and -diazines react already in the presence of NiCl<sub>2</sub>(dppp)<sup>173</sup>, while hindered and electron-rich P(*Bu-t*)<sub>3</sub><sup>126</sup> and (*t*-Bu)<sub>2</sub>P(S)H<sup>174</sup> can be used for the coupling of unactivated aryl chlorides in the presence of Ni.



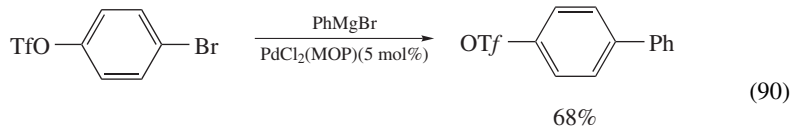
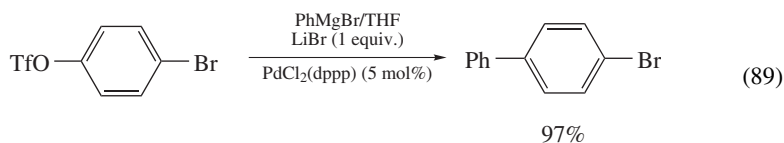
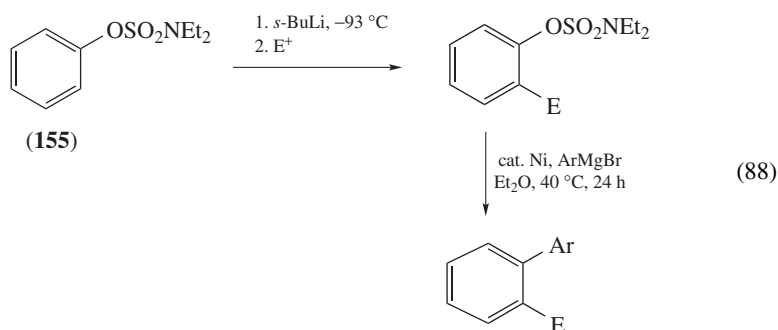


Transmetalation of organomagnesium compounds to zinc reagents opens new pathways for their coupling. It allows the use of conventional ligands like  $\text{PPh}_3$  for nickel-catalyzed coupling reactions<sup>175</sup>. Manganese salts in NMP are effective catalysts for the coupling of aryl chlorides bearing an *ortho*-coordinating group with alkyl, alkenyl or aryl Grignard reagents (equation 86)<sup>176</sup>. Using this method, other halogens or even a methoxy group can serve as a leaving group (equation 87). Heteroaromatic chlorides can be also coupled with aryl- and alkylmagnesium halides using manganese chloride as catalyst<sup>177</sup>.



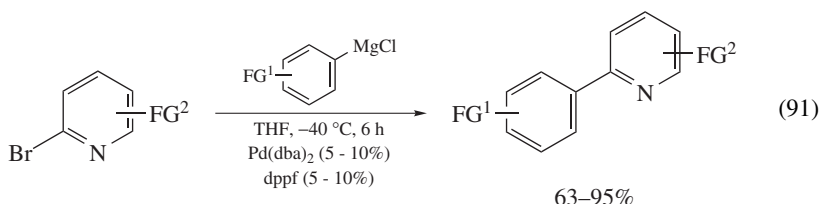


Besides developing new ligand systems, much effort has been made toward other leaving groups than halogens. Sulfonates<sup>178</sup>, sulfones<sup>179</sup>, tosylates<sup>180</sup>, nitriles<sup>181</sup>, alkyl ethers<sup>182</sup> or sulfonamides<sup>183</sup> can serve as leaving groups. The *N,N*-dialkyl sulfamate group can further function as *ortho*-directing group, thus allowing sequential functionalization of aromatic compounds like **155** (equation 88)<sup>184</sup>. Of special interest is the selectivity of coupling reactions of an electrophile bearing various leaving groups. Although iodine is almost always the most active leaving group, the choice between bromine or triflate can be made by selecting the appropriate catalyst (equations 89 and 90)<sup>185</sup>.

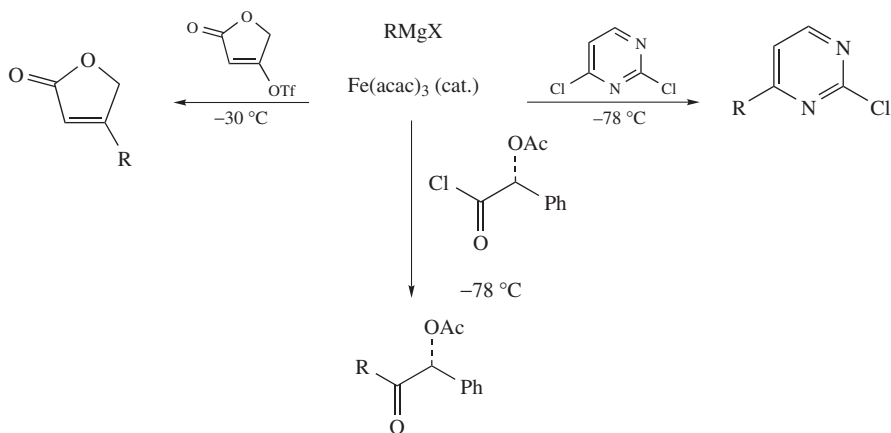


MOP = 2-diphenylphosphino-2'-methoxy-1,1'-binaphthyl

Substituted pyridines, quinolines and diazines react with polyfunctionalized arylmagnesium reagents under very mild conditions in the presence of  $\text{PdCl}_2(\text{dppf})$  as a catalyst (equation 91)<sup>186</sup>.



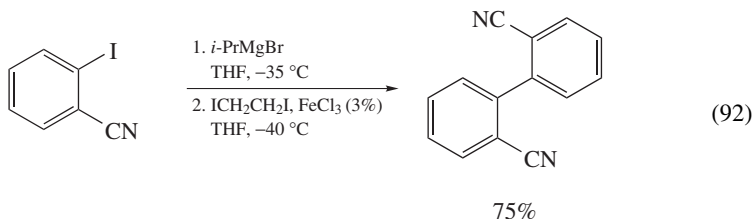
Bromo- and iodoanilines, -phenols and -benzoic acids are first deprotonated *in situ* by an excess of the organomagnesium reagent and then coupled ( $\text{PdCl}_2(\text{dppf})$ , 1 mol%, THF, 25 °C, 3 h) with organomagnesium halides, thus avoiding tedious protection-deprotection steps<sup>187</sup>. Iron(III) salts can also serve as appropriate catalysts for various cross-coupling



SCHEME 16

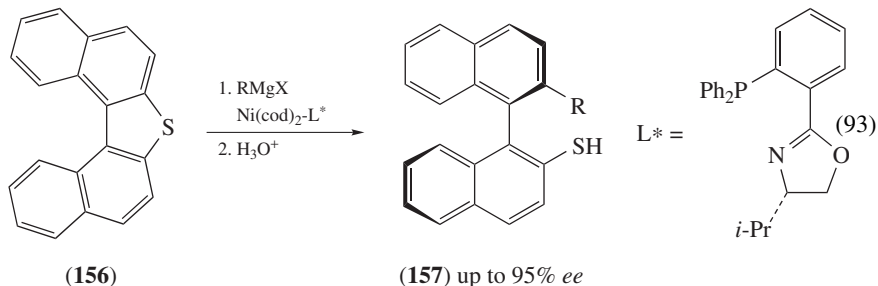
reactions<sup>188</sup>. They are cheap, non-toxic, environmentally friendly and effective for  $\text{Csp}^3$ – $\text{Csp}^2$  couplings, allowing the reactions of alkylmagnesium reagents with aryl chlorides, triflates and tosylates as well as heteroaryl chlorides (Scheme 16)<sup>189</sup>.

However, arylmagnesium organometallics can only be used in a few cases<sup>190</sup> like an iron-catalyzed homocoupling (equation 92)<sup>191</sup>. Iron catalysis is further used for the dechlorination of electron-rich aryl chlorides by Grignard reagents<sup>192</sup>.

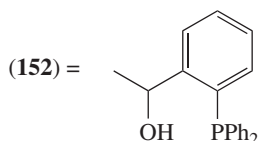
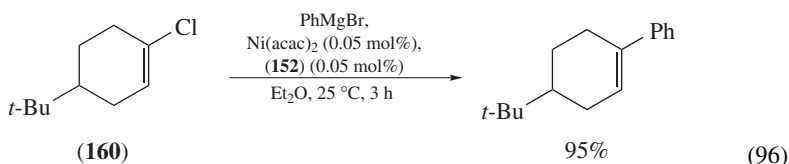
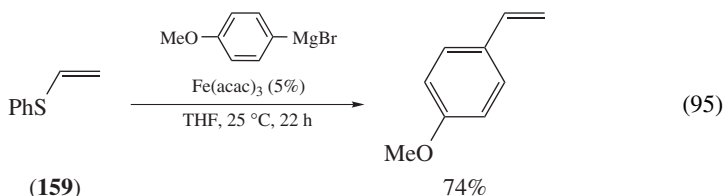
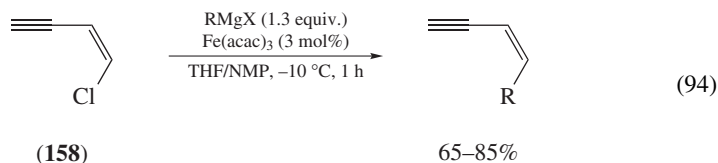


Another way toward more cost-efficient and environmentally friendly catalysts is their immobilization on a solid phase as could be realized with nickel on charcoal<sup>193</sup>.

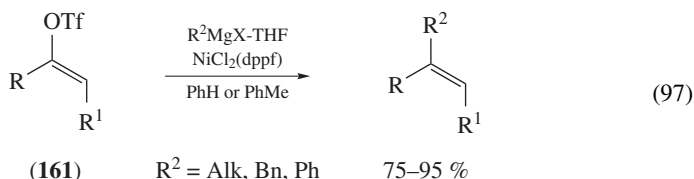
Substituted dibenzothiophenes **156** react with Grignard reagents to give products of the thiophene ring cleavage. With a chiral Ni catalyst, axially chiral biaryl compounds **157** can be obtained in high enantioselectivities (equation 93)<sup>194</sup>.



Substituted alkenes can serve as electrophiles in cross-coupling reactions. For example, chloroenynes **158** and chlorodienes react with Grignard reagents with retention of the stereochemistry using Pd<sup>195</sup>, Mn<sup>196</sup> or Fe<sup>197</sup> (equation 94). Iron catalysis usually proceeds under mild reaction conditions<sup>198</sup> as shown in the coupling of alkenyl sulfides **159** (equation 95)<sup>199</sup>. Alkenyl chlorides like **160** undergo smooth cross-couplings with arylmagnesiums using nickel catalysis in the presence of hydroxyphosphine ligand **152** (equation 96)<sup>200</sup>.

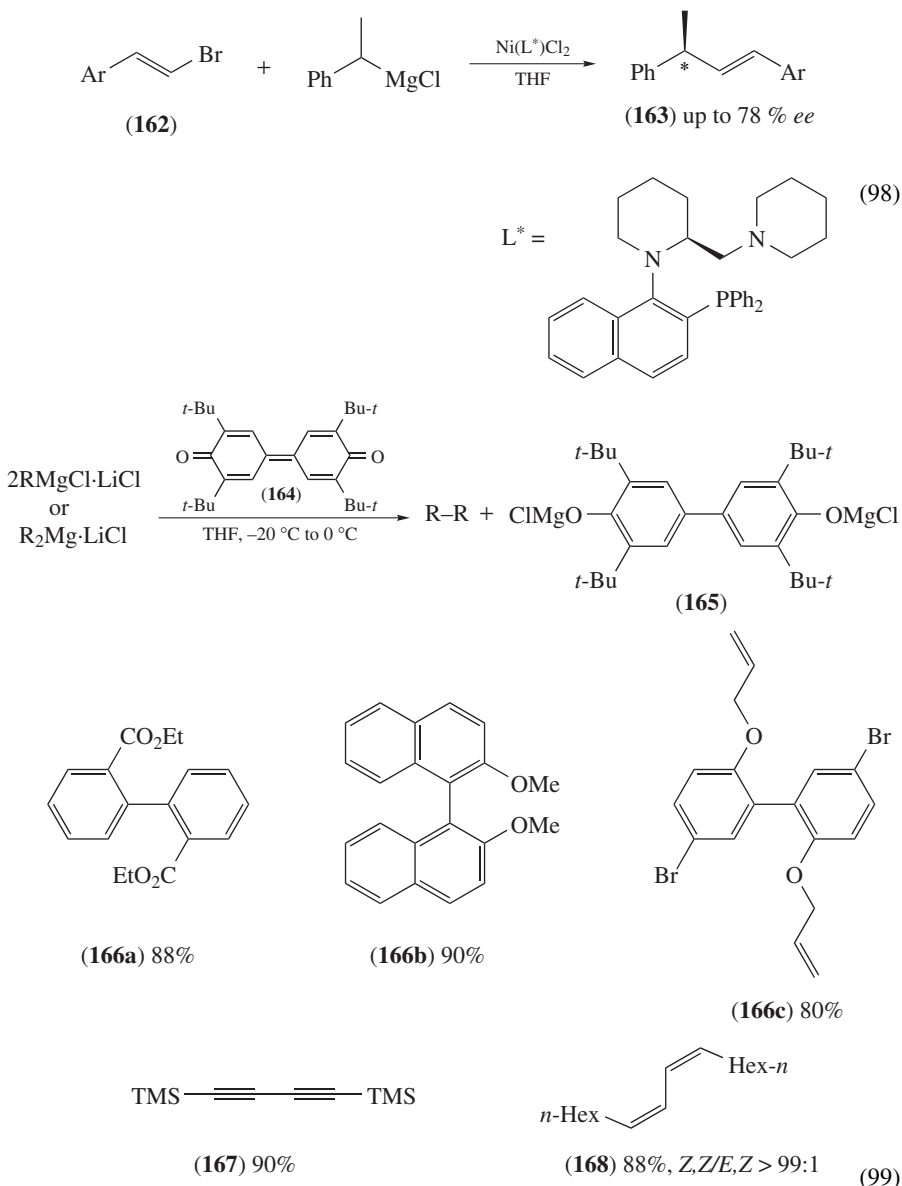


1,3-Dienyl triflates<sup>201</sup> and enol triflates derived from  $\beta$ -ketoesters<sup>202</sup> can be coupled with Grignard reagents in the presence of Cu<sup>I</sup> species. Enol triflates **161** have been successfully coupled with NiCl<sub>2</sub>(dppp) as a catalyst (equation 97)<sup>203</sup>. High yields in the coupling of dienyl phosphates can only be achieved in the presence of nickel salts<sup>204</sup>, whereas enol phosphates, which can be derived *in situ* from ketones, can be coupled with an arylmagnesium species using a palladium catalyst<sup>205</sup>.



2-Bromostyrenes **162** react with 1-ethylphenylmagnesium chloride under Ni catalysis providing 1,3-diaryl-1-butenes **163**. When chiral nickel complexes are used, the products

**163** are obtained with up to 78% *ee* (equation 98)<sup>206,207</sup>.



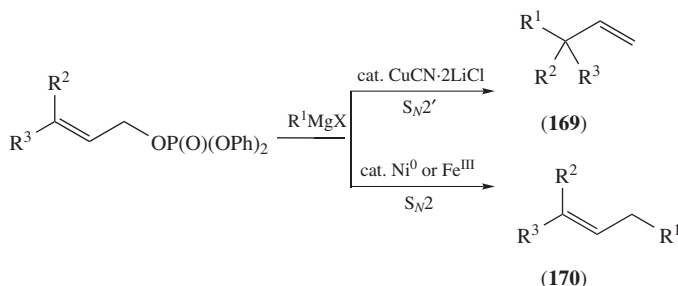
## 2. Transition-metal-free cross-coupling reactions

Besides all achievements in the area of transition-metal catalysis, there is a need for finding new catalytic systems which meet the requirements of high efficiency, low

price and environmental friendliness. Such conditions are realized in transition-metal-free homocoupling of organomagnesium compounds, where mono- or diorganomagnesium compounds, that are complexed with lithium chloride, are oxidatively coupled using the readily available 3,3',5,5'-tetra-*tert*-butyldiphenylquinone (**164**) (equation 99)<sup>208</sup>. The resulting biphenyldiolate **165** can be easily separated from the reaction mixture and reoxidized to **164** with air. The method allows the synthesis of various biaryls **166a–c**, diynes **167** and dienes **168** with retention of the double bond configuration.

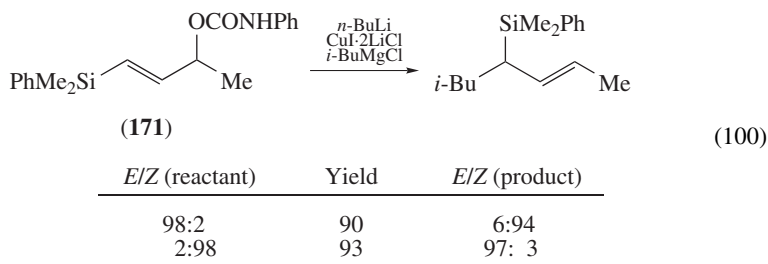
### 3. Allylic substitution reactions

Reactions of organomagnesium compounds with allylic electrophiles usually require transition metal catalysis in order to achieve good regio- and stereoselectivities<sup>209</sup>. If Cu<sup>I</sup> salts are used as catalysts, increased reaction temperatures and amounts of catalyst as well as slow addition of Grignard reagent favor the formation of the  $\gamma$ -adduct **169**<sup>210</sup>. The transmetalation of Grignard reagents to zinc organometallics prior to the addition of the Cu<sup>I</sup> catalyst strongly favor  $S_N2'$ -substitutions. In contrast, Fe<sup>III</sup> catalysis for the reaction of Grignard reagents with allyl diphenylphosphates leads almost exclusively to the  $\alpha$ -substitution products **170** (Scheme 17)<sup>211</sup>.



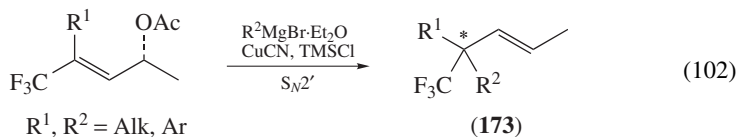
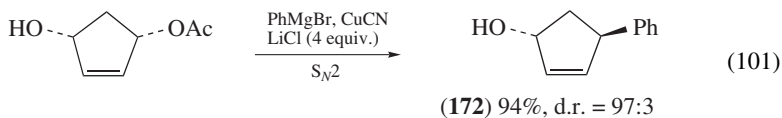
SCHEME 17

The presence of electron-donor sites in the substrates like a diphenylphosphinyl moiety<sup>212</sup> or *o*-diphenylphosphinobenzoate as leaving group<sup>213</sup> allows high levels of stereoselectivity (*syn*  $S_N2'$ ). High regio- and stereoselectivities can also be obtained using allylic carbamates **171**<sup>214</sup> or allylic cyclic carbonates<sup>215</sup> (equation 100). Allylic ethers are coupled using cobalt or rhodium catalysis<sup>216</sup>.

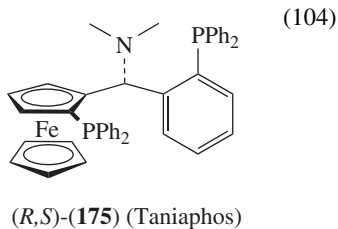
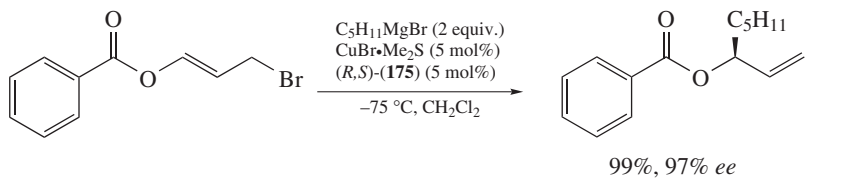
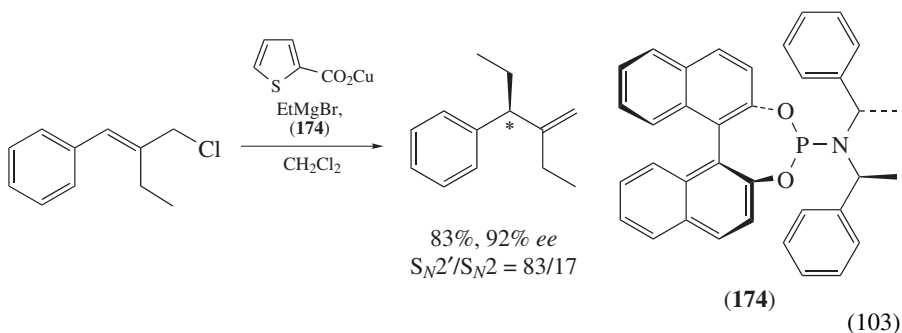


Allylic substitution reactions are valuable for the asymmetric synthesis of complex organic molecules, since they allow enantioselective C–C bond formations. One approach

is to use readily available chiral allylic alcohols or derivatives. The resulting substitution products **172** and **173**, which contain tertiary or quaternary chiral centers, are obtained in high diastereomeric purities (equations 101 and 102)<sup>217,218</sup>.

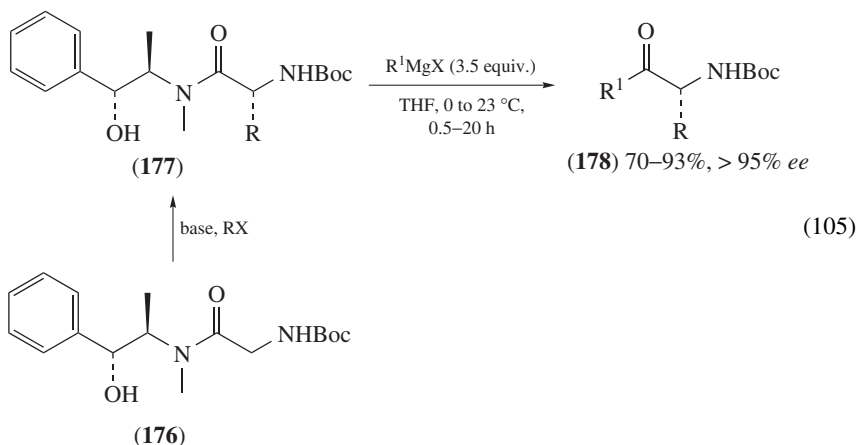


The second approach starts from achiral allylic substrates and uses a chiral metal catalyst. Among all ligands which have been tested<sup>218,219</sup>, binaphthol-derived phosphoramidites like **174** have led to excellent regio- and enantioselectivities (equation 103)<sup>220</sup>. Highly stereoselective substitutions are also obtained using ligand **175** (*Taniaphos*, equation 104)<sup>221</sup>.



#### 4. Synthesis of carbonyl compounds

The acylation of organometallic reagents with acyl chlorides has been reviewed<sup>222</sup>. The presence of catalytic amounts of  $\text{Fe}(\text{acac})_3$  allows these reactions to proceed at  $-78^\circ\text{C}$  and thus undesired side reactions, like a subsequent attack on the resulting ketone, are completely suppressed<sup>223</sup>. Even aryl cyanides can be coupled using this method to form benzophenones. Besides *N*-*tert*-butoxy-*N*-methyl amides, Weinreb amides are efficient acylation reagents which suppress the formation of side products<sup>224</sup>. Alternatively, acyl halides first react with tri-*n*-butylphosphine to form acylphosphonium salts. These salts react smoothly with Grignard reagents giving ketones in good yields<sup>225</sup>. Various carboxylic acids are converted quantitatively with 2-chloro-4,6-dimethoxy-1,3,5-triazine to activated amides, which react *in situ* with Grignard reagents in the presence of copper iodide. Quantitative yields of ketones have been achieved<sup>226</sup>. The conversion of  $\alpha$ -amino acids into  $\alpha$ -aminoketones without epimerisation of the chiral center has been achieved<sup>227, 228</sup>. Thus, protected pseudoephedrine glycineamide **176** is first diastereoselectively alkylated in the presence of a base. Treatment of the resulting alkylated amino acid derivative **177** with organomagnesium compounds gives the protected  $\alpha$ -aminoketones **178** in good yields with complete retention of configuration at the  $\alpha$ -carbon (equation 105)<sup>229</sup>.



#### C. Substitutions at an $\text{sp}$ -center

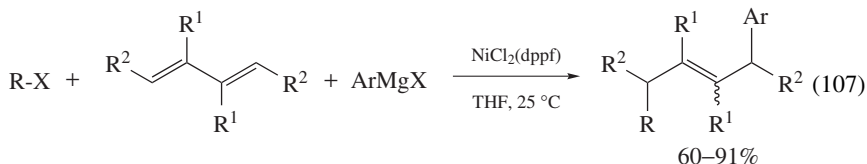
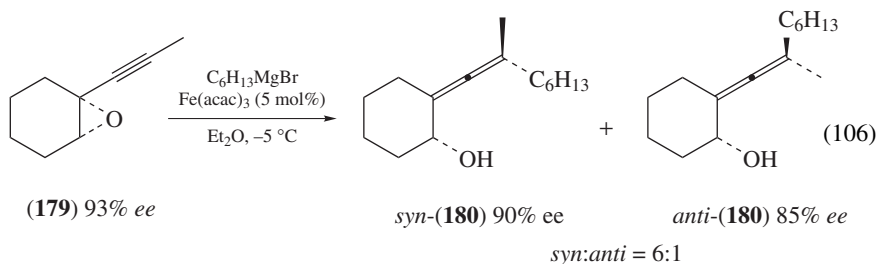
There are only few reactions known where a  $\text{sp}$ -carbon is subjected to the attack of a Grignard reagent leading to allenes. For example, propargylic dithioacetals react with organomagnesium compounds to yield substituted allenes<sup>230</sup>. Alkynyl oxiranes **179** furnish 2,3-allenols such as **180** with good chirality transfer in the presence of an iron catalyst (equation 106)<sup>231</sup>. Arylbenzotriazolylacetylenes, which are derived from  $\text{BtCH}_2\text{SiMe}_3$  and aryl chlorides, react with organomagnesium compounds to provide disubstituted acetylenes<sup>232</sup>.

#### D. Addition of Organomagnesium Reagents to Multiple Bonds

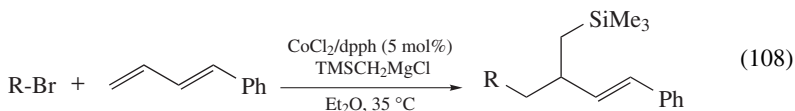
##### 1. Addition to carbon-carbon bonds

*a. Catalyzed addition to non-activated  $\text{C}=\text{C}$  bonds.* The uncatalyzed reaction of Grignard reagents with a non-activated double bond is generally difficult, with the exception of

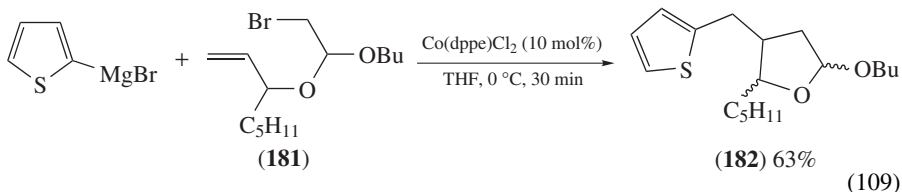
allylmagnesium and/or conjugated dienes as substrates. Another exception is the addition to cyclopropenes, occurring in a highly stereoselective fashion<sup>233</sup>. Recently, a number of synthetically useful addition methods involving transition metal catalysis were developed. Stereoselective addition of Grignard reagents to alkenes, mostly catalyzed by nickel and zirconium, has been reviewed<sup>234</sup>. The nickel complex  $\text{NiCl}_2(\text{dppf})$  efficiently promotes the three-component coupling of alkyl halides, butadienes and arylmagnesium halides (equation 107)<sup>235</sup>.



A combination of  $\text{CoCl}_2$  and 1,6-bis(diphenylphosphino)hexane catalyzes a similar reaction of an alkyl bromide with a 1,3-diene and trimethylsilylmethylmagnesium chloride, giving homoallylic silanes (equation 108)<sup>236</sup>.

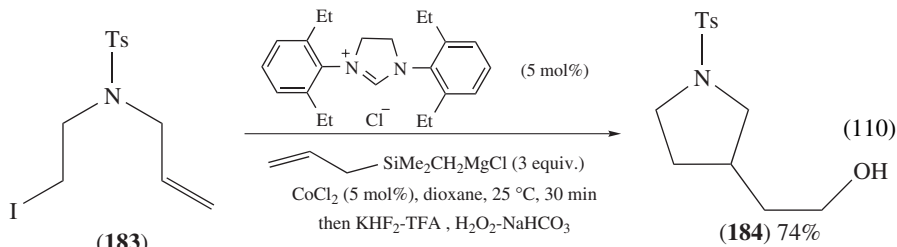


A similar Co-catalyzed reaction with arylmagnesium halides and alkenes **181**, bearing a halogen in a suitable position, occurs via a radical intermediate, leading to cyclic acetals **182** (equation 109)<sup>237</sup>.

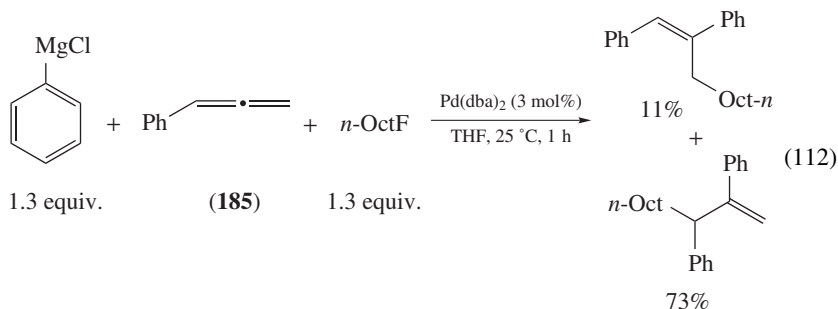
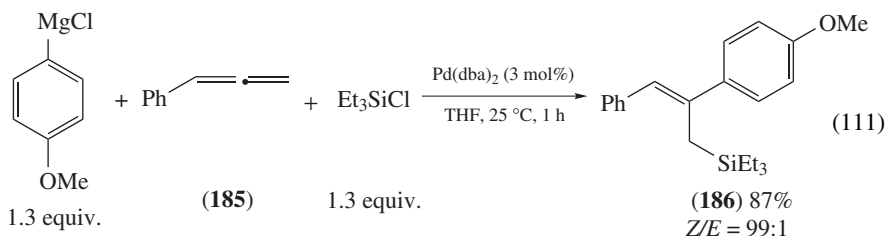


6-Halo-1-hexene and heteroatom-substituted analogues **183** react with allyldimethylsilylmethylmagnesium chloride, giving 5-membered cyclic products **184** (equation 110)<sup>238</sup>. This method has been used for the synthesis of substituted pyrrolidines, otherwise difficult to prepare.





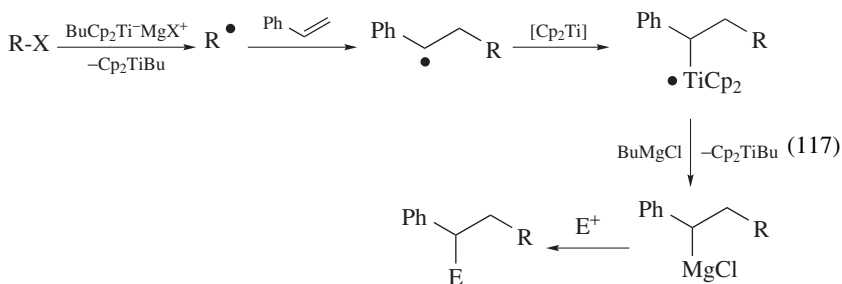
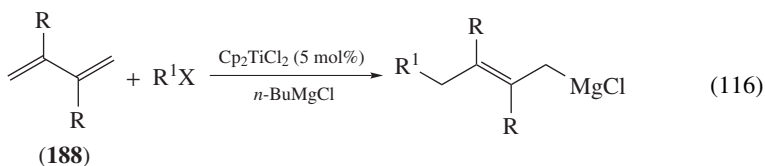
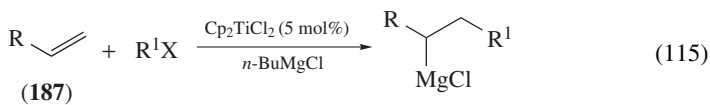
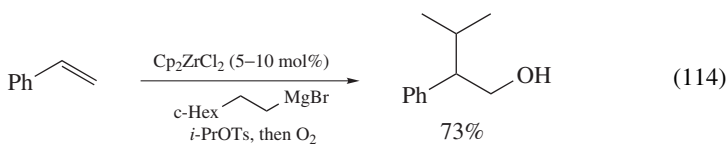
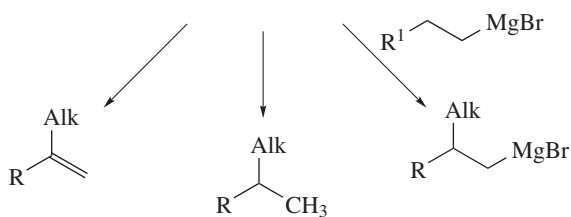
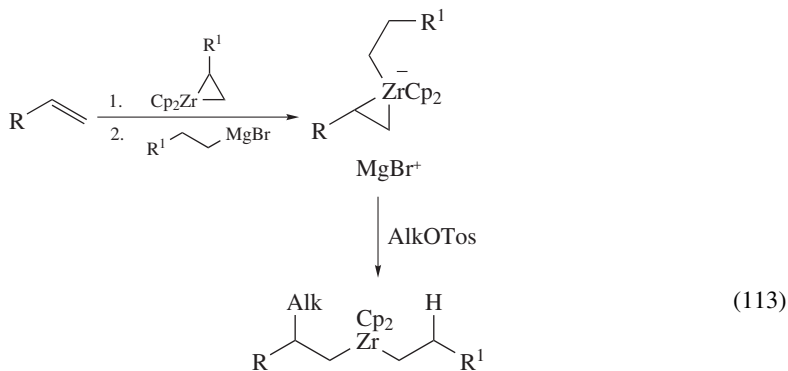
Allenes **185** react with arylmagnesium chlorides in the presence of trialkylsilyl chlorides and a Pd<sup>0</sup> catalyst, furnishing substituted allylsilanes **186** with high (*Z*)-stereoselectivity (equation 111). Alkyl halides afford in this reaction mixtures of regioisomeric trisubstituted alkenes (equation 112)<sup>239</sup>.



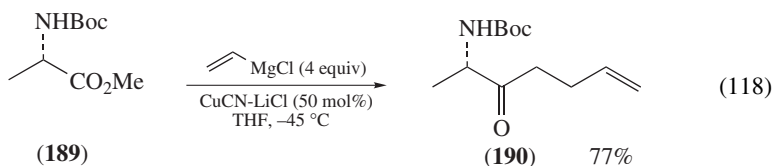
Titanocene and zirconocene dichlorides efficiently catalyze the addition of Grignard reagents to unactivated alkenes. In the presence of Cp<sub>2</sub>ZrCl<sub>2</sub>, alkylmagnesium bromides react with monosubstituted alkenes and alkyl tosylates leading potentially to three different types of products (equation 113). In many cases the reaction is highly selective, providing the formal carbomagnesiation product which reacts with oxygen or electrophiles like NBS yielding the corresponding alcohols or bromides (equation 114)<sup>240</sup>.

Titanocene dichloride also catalyzes a regioselective carbomagnesiation of alkenes **187** (equation 115) and dienes **188** (equation 116). The reaction proceeds at 0 °C in THF in the presence of Cp<sub>2</sub>TiCl<sub>2</sub>, an organic halide and *n*-BuMgCl which leads to the catalytic species, affording benzyl, allyl or  $\alpha$ -silyl alkylmagnesium halides, which are trapped with electrophiles (equation 117)<sup>241</sup>.

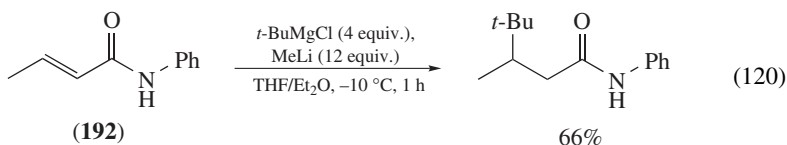
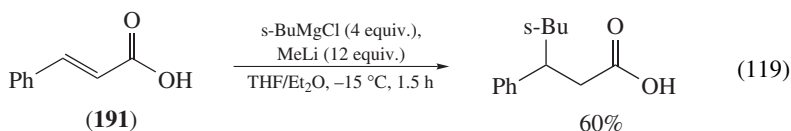
A dimerization reaction of alkenylmagnesium reagents in the presence of chlorosilanes, catalyzed by Cp<sub>2</sub>TiCl<sub>2</sub>, furnishing 1,4-disilyl-2-butenes has been reported<sup>242</sup>. Transition-metal-catalyzed carbon-carbon bond formation, promoted by Mn, Cr, Fe and Co, has been reviewed<sup>243</sup>.



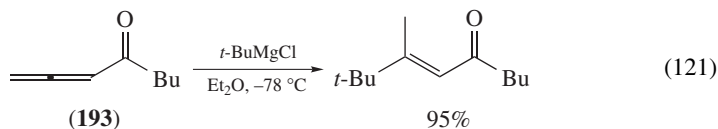
*b. 1,4-Addition to Michael acceptors.* The Michael addition of Grignard reagents to various unsaturated carbonyl compounds has been extensively studied. New developments in this field were recently reviewed<sup>244</sup>. Functionalized organomagnesium reagents, obtained by a low-temperature iodine–magnesium exchange reaction, add in 1,4-fashion to  $\alpha,\beta$ -enones in the presence of  $\text{CuCN}\cdot 2\text{LiCl}$  (5–10 mol%)<sup>245</sup>. Treatment of aromatic, aliphatic or  $\alpha$ -aminomethyl carboxylates **189** with an excess of an alkenylmagnesium bromide in the presence of a catalytic amount of copper salts provides homoallylic ketones **190** in 26–77% yield. The reaction proceeds as a sequence of a Grignard acylation followed by a 1,4-addition (equation 118)<sup>246</sup>. 3-Substituted glutarate diesters are easily obtained in good yields by the reaction of various Grignard reagents with dimethyl 1,3-propenedicarboxylate<sup>247</sup>.



Substituted acrylic acids **191** and amides **192** usually do not react with organomagnesium reagents, but  $\text{MeLi}$  allows a smooth addition even at  $-15\text{ }^{\circ}\text{C}$ , if an excess of Grignard reagent is used (equations 119 and 120)<sup>248</sup>.

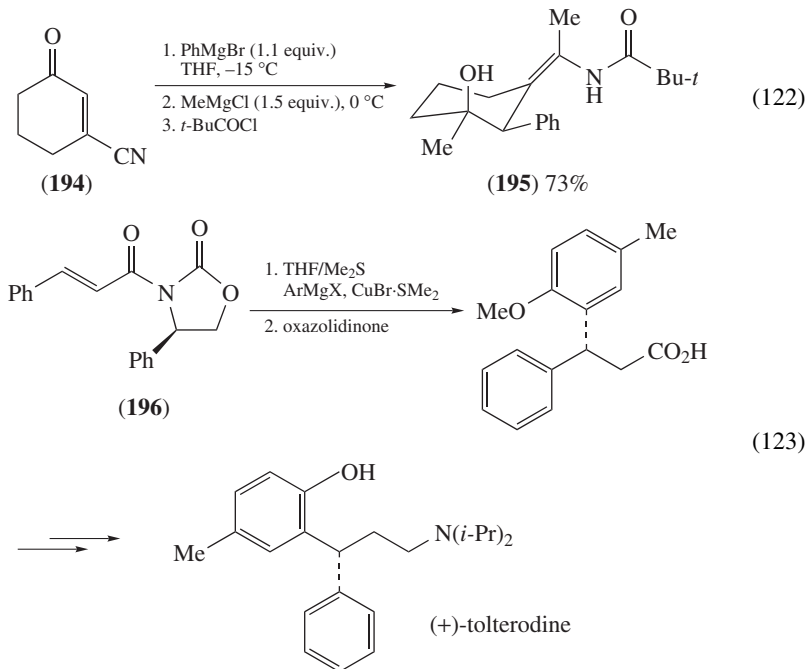


Conjugated allenyl ketones **193** react smoothly with Grignard reagents in ether at  $-78\text{ }^{\circ}\text{C}$  without a catalyst, yielding  $\alpha,\beta$ -enones in excellent yields and with complete (*E*)-selectivity (equation 121)<sup>249</sup>.



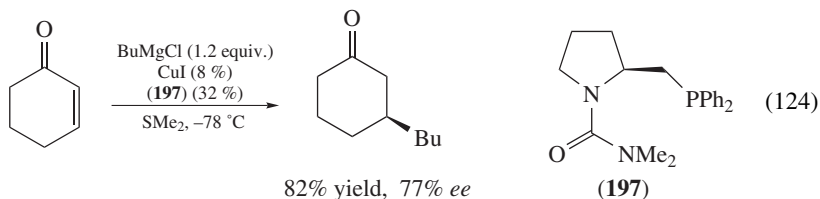
Cyclic  $\gamma$ -oxonitriles **194** react sequentially with two different Grignard reagents, affording enamides **195** with high diastereoselectivity (equation 122)<sup>250</sup>. A number of chiral auxiliaries have been developed for performing enantioselective 1,4-addition to  $\alpha,\beta$ -unsaturated carbonyl compounds. Chiral oxazolidinones are often highly effective, affording the Michael adducts with up to 99% *ee*. Optically active amidoacrylates, prepared from acryloyl oxazolidinone in four steps, react with Grignard reagents in the presence of a catalytic amount of  $\text{Cu}^{\text{I}}$ . This reaction was applied for the synthesis of  $\alpha$ -amino acids with up to 97% *ee*<sup>251</sup>. Asymmetric conjugate addition of an arylmagnesium reagent

to cinnamoyloxazolidinone **196** is the key step in the synthesis of (+)-tolterodine<sup>252</sup>, a pharmacologically important muscarinic receptor agonist (equation 123).



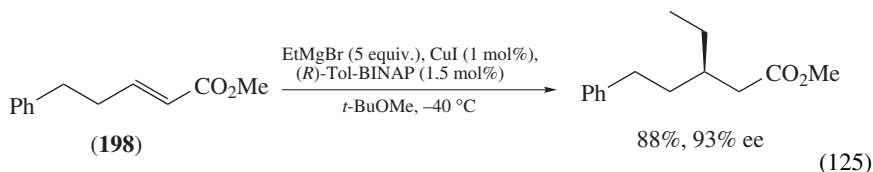
Similar acryloyl imidazolidinones have been used for the asymmetric 1,4-addition of organomagnesium compounds in the presence of a Lewis acid. The diastereoselectivity is variable and was found to be highly depending on the nature of all substrates<sup>253</sup>.

The proline-derived carbamoylphosphine **197** catalyzes the asymmetric 1,4-addition of Grignard reagents to 2-cyclohexenone although a high catalyst loading is required in this case (equation 124). Changing the solvent to diethyl ether and lowering the catalyst loading to 3 mol% leads to the 1,4-adduct with 67% *ee*<sup>254</sup>.

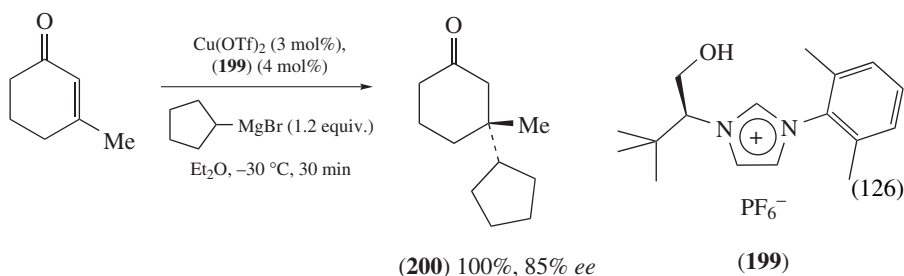


Ferrocene-derived ligand (*R,S*)-Josiphos, which is widely used for catalytic asymmetric hydrogenation reactions, is also a good catalyst for the asymmetric copper-catalyzed 1,4-addition. Reaction in *t*-BuOMe in the presence of 6 mol% of this ligand gives products with up to 98% *ee*<sup>255</sup>.

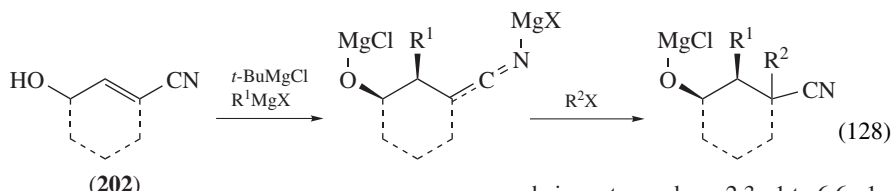
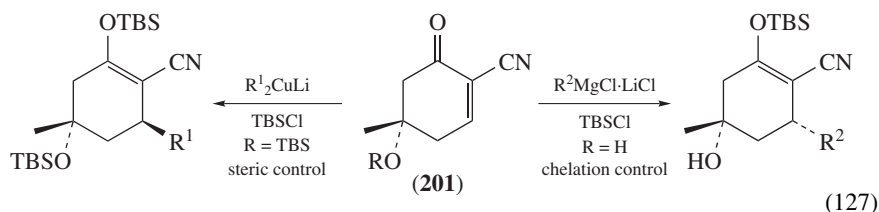
Unsaturated esters like **198** react with Grignard reagents under similar conditions, giving excellent yields and enantioselectivities. The catalyst is a Cu<sup>I</sup>–Tol-BINAP complex

(equation 125)<sup>256</sup>.

The creation of all-carbon quaternary chiral centers by asymmetric conjugate addition is a challenging task. A chiral heterocyclic carbene **199** has been used as a ligand for this reaction. Chiral 3,3-disubstituted cyclohexanones **200** were obtained by this method with up to 85% *ee* (equation 126)<sup>257</sup>.

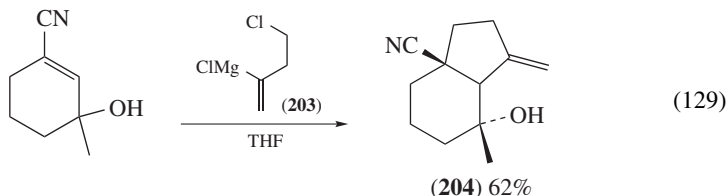


*c. Addition to other activated alkenes.* Addition to  $\alpha,\beta$ -unsaturated nitriles has been reviewed<sup>258</sup>. Addition to cyclic oxo-nitriles **201** can be directed either by using steric effects or by chelation (equation 127).  $\gamma$ -Hydroxy- $\alpha,\beta$ -unsaturated nitriles like **202** are subjected to a one-pot addition–alkylation sequence, leading to polysubstituted nitriles. In the case of open-chain systems, diastereoselectivities up to 6.6:1 are achieved, while cyclic systems may lead to highly diastereoselective reactions (equation 128)<sup>259</sup>.  $\omega$ -Chloroalkyl-alkenylmagnesium halides **203** give bicyclic hydroxynitriles **204** (equation 129)<sup>260,261</sup>.

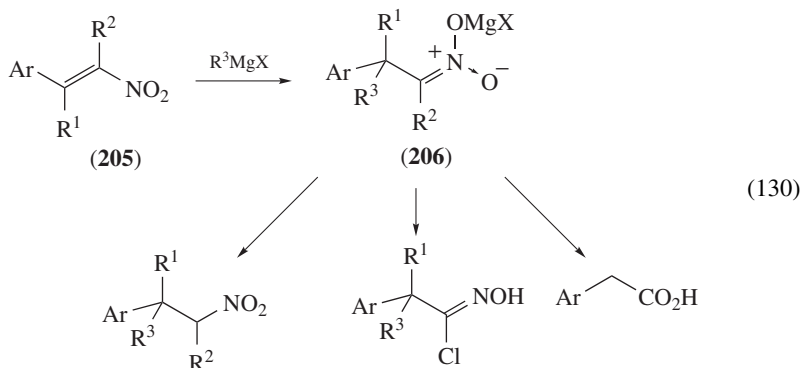


$R^1 = \text{Me, Ar}$   
 $R^2X = \text{PhCHO, BnBr}$

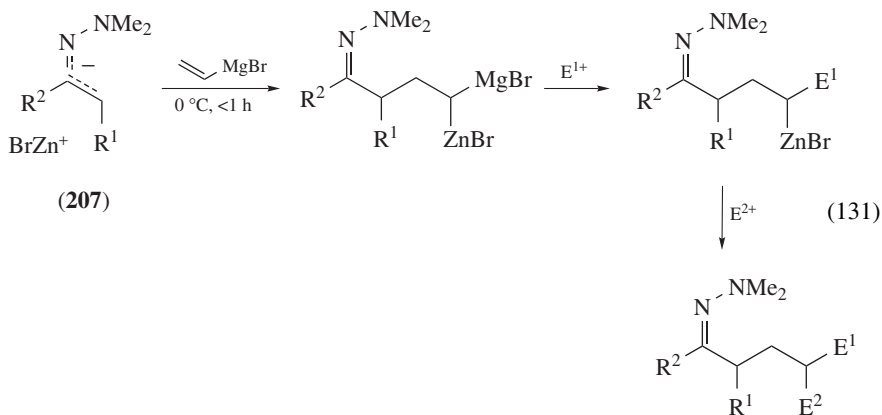
open-chain systems: d.r. = 2.3 : 1 to 6.6 : 1  
 cyclic systems: completely stereoselective

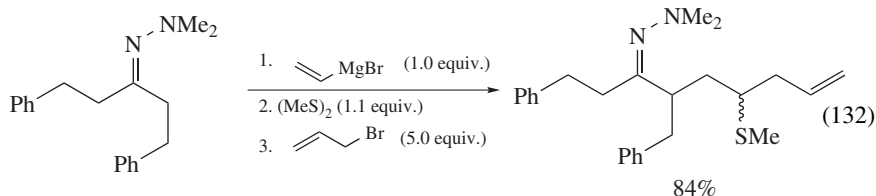


The addition of Grignard reagents to nitroalkenes like **205** gives *aci*-salts **206**, which can be further transformed into nitroalkanes, hydroxymoyl halides or carboxylic acids (equation 130)<sup>262</sup>. Reaction of  $\text{RMgX}$  with nitroalkenes in the presence of  $\text{CeCl}_3$ , followed by treatment with 100% acetic acid, was developed as efficient synthesis of complex nitroalkanes<sup>263</sup>.

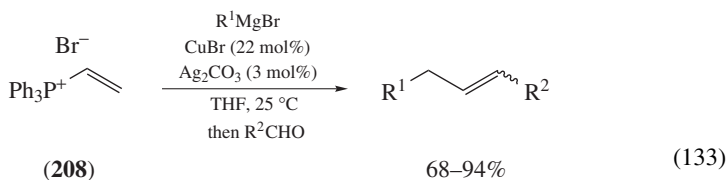


Organomagnesium compounds react with imines, prepared from 3-methoxy-2-naphthaldehydes by a 1,4-addition mechanism. This reaction can be performed with high diastereoselectivity. The method was applied for the synthesis of optically pure  $\beta$ -tetralones<sup>264</sup>. Vinylmagnesium bromide reacts as an acceptor with a ketone dimethyl hydrazone zincate **207**, yielding a 1,1-bimetallic species, which can be reacted sequentially with two different electrophiles (equations 131 and 132)<sup>265</sup>. The reaction proceeds via a metalla-aza-Claisen rearrangement, where the dimethylhydrazone anion behaves as an ‘aza-allylic’ system<sup>266</sup>.

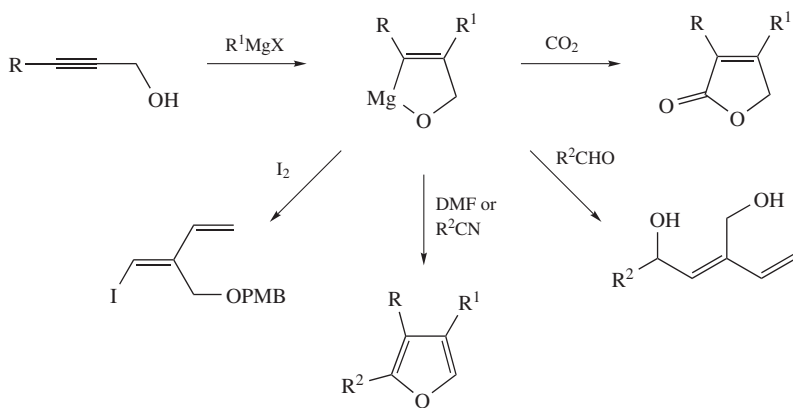




Vinylphosphonium bromide **208** reacts with Grignard reagents, forming alkylphosphonium ylides. These ylides react with aldehydes, giving alkenes in a one-pot sequence. In this reaction, catalytic amounts of both copper and silver salts are necessary (equation 133)<sup>267</sup>.



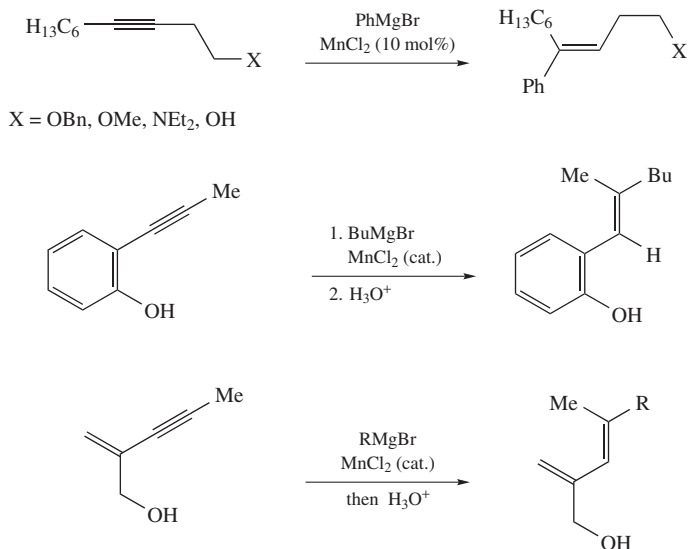
*d. Addition to carbon–carbon triple bonds.* Addition of Grignard reagents to an unactivated alkyne usually requires a coordinating group and/or a transition metal catalyst. Propargyl alcohols react with  $\text{RMgX}$  regioselectively without catalysis. This reaction allows a number of synthetically useful transformations (Scheme 18)<sup>268</sup>.



SCHEME 18

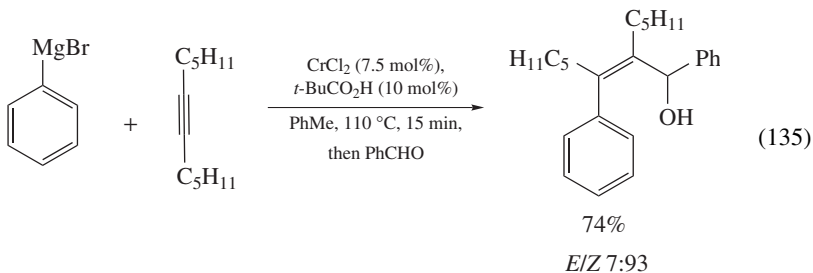
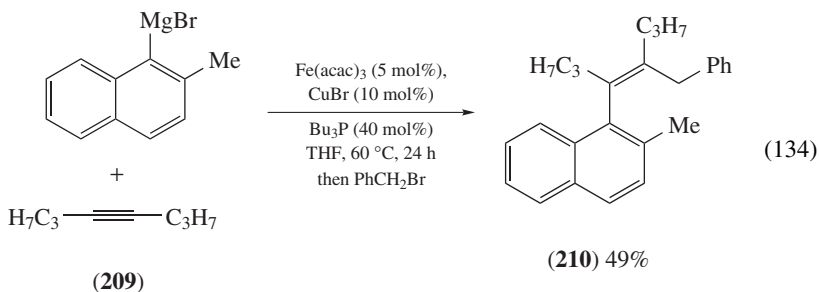
Homopropargylic alcohols or *ortho*-ethynylphenols and -benzylic alcohols react with Grignard compounds by using a manganese salt catalysis. The corresponding propargylic alcohols give under these conditions substituted allenes (Scheme 19)<sup>269, 270</sup>. Secondary and tertiary propargylic alcohols react with primary alkylmagnesium reagents with a high selectivity under  $\text{Cu}^{\text{I}}$  catalysis<sup>271</sup>.

Unactivated alkynes **209** undergo the addition of arylmagnesium reagents under cooperative iron and copper catalysis, yielding trisubstituted alkenylmagnesium species. They can be trapped with electrophiles, giving tetrasubstituted alkenes such as **210**. In some



SCHEME 19

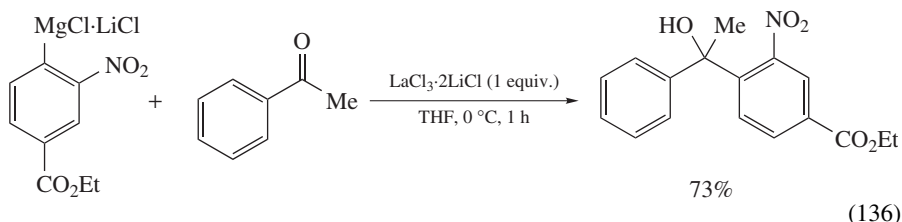
cases, unsymmetrical alkynes react completely regioselectively (equation 134)<sup>272</sup>. A similar process has been developed using chromium catalysis and toluene as the solvent<sup>273</sup>. In this case, the reactions with aldehydes provide highly substituted allylic alcohols (equation 135).



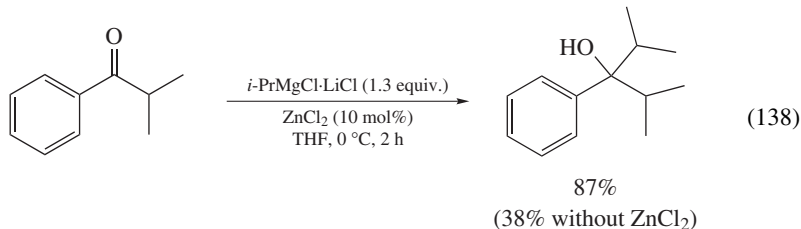
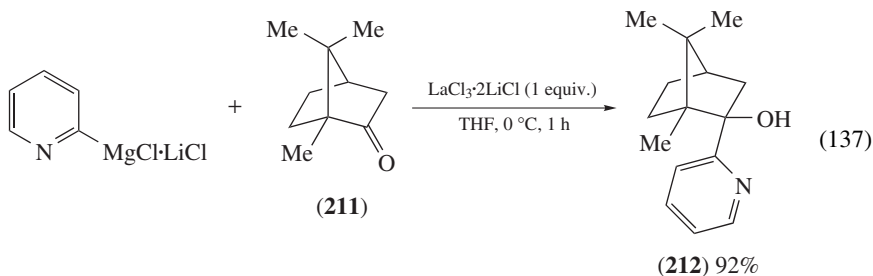


## 2. Addition to carbon–oxygen bonds

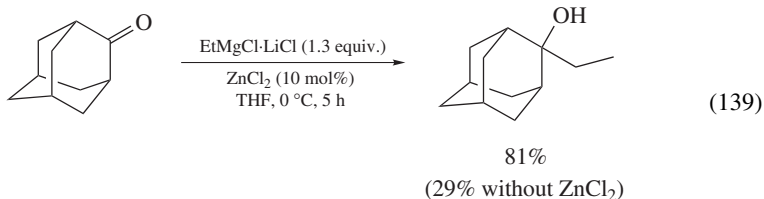
Recent advances in the selective addition of organometallic reagents to carbonyl compounds have been reviewed<sup>274</sup>. A computational study of the mechanism of 1,2-addition reactions of Grignard compounds to carbonyl compounds was also reported<sup>275</sup>. The addition of organomagnesium species to carbonyl compounds is usually complicated by side processes like reduction or enolization. Often, these processes are even dominating. Many efforts were dedicated to the development of more selective and practical processes. The use of rare-earth metal salts like cerium(III) chloride, giving after transmetalation reaction highly nucleophilic, but less basic species, is one of the most widespread methods<sup>276</sup>. However, the heterogeneity of the reaction mixture due to the low solubility of  $\text{CeCl}_3$  in THF causes significant problems; besides, this method is usually not suitable for reactions with highly functionalized Grignard reagents. The addition of LiCl increases the solubility of metal salts. This allowed the development of an excellent and very general method for the addition of various Grignard reagents to carbonyl compounds, making use of soluble complexes of lanthanide salts with LiCl in THF (equation 136)<sup>277</sup>. This protocol is particularly useful in the case of polyfunctionalized arylmagnesium reagents.



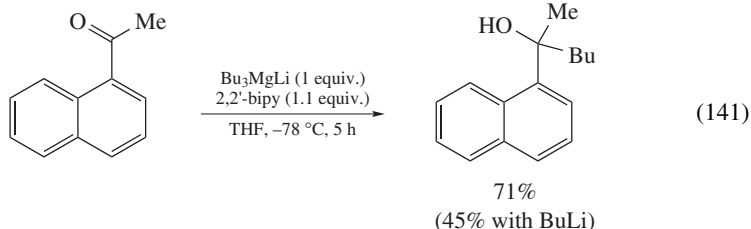
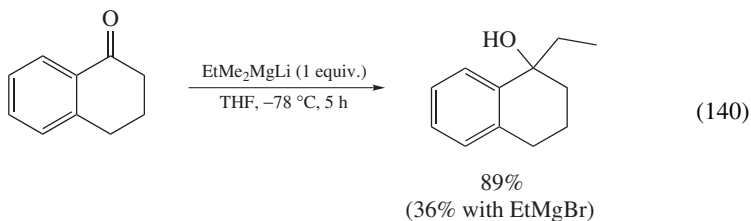
No product was formed in this reaction in the absence of the soluble lanthanide salt or even in the presence of  $\text{CeCl}_3$ . Heteroaryl Grignard reagents react smoothly in the presence of  $\text{LaCl}_3 \cdot 2\text{LiCl}$  even with highly sterically hindered ketones like **211** (equation 137).



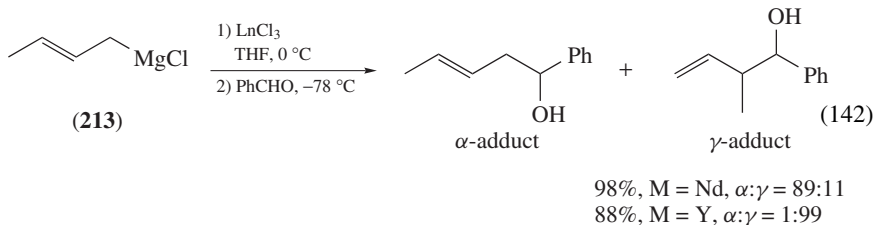
In the absence of additives the yield of the alcohol **212** is only 17%, and 53% in the presence of  $\text{CeCl}_3$ . Catalytic amounts of zinc chloride in the presence of LiCl were found to have a similar positive effect on the outcome of the 1,2-addition reaction of alkylmagnesium halides to enolizable ketones (equations 138 and 139)<sup>278</sup>. Due to the low price of  $\text{ZnCl}_2$ , this method seems promising for large-scale applications.



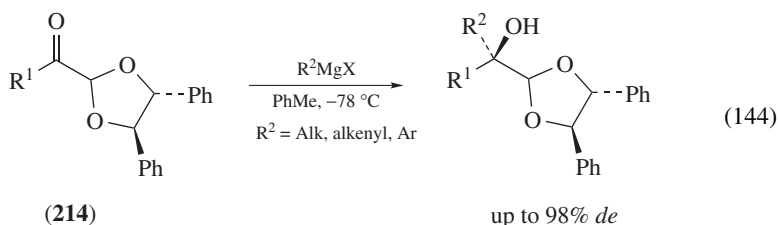
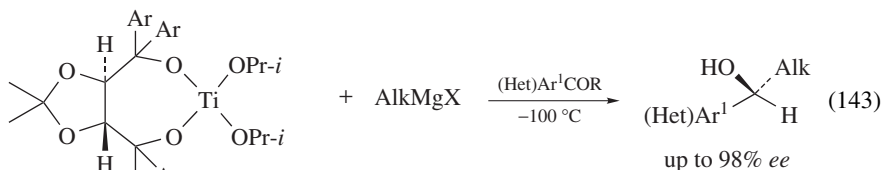
Addition of a primary alkyl group to enolizable ketones can be performed using magnesium–ate complexes<sup>279</sup>. The additional presence of 2,2'-bipyridyl (1 equiv.) in the reaction mixture improves the yields. The ate complexes are prepared *in situ* from the corresponding Grignard reagents and alkyllithium compounds (equations 140 and 141).



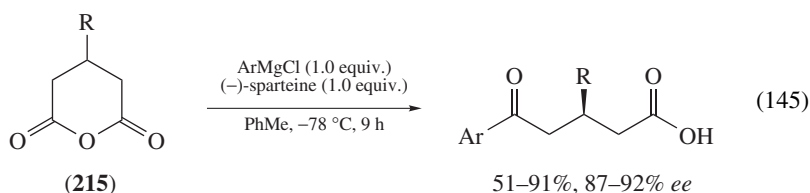
An interesting selectivity in the transfer of alkyl groups ( $n\text{-Alk} > \text{Me}$ ) is observed in these addition reactions. The regioselectivity of the reaction of crotylmagnesium chloride (**213**) with benzaldehyde strongly depends on the presence of various rare-earth metal chlorides. The  $\alpha$ - to  $\gamma$ -ratio of products can be switched to the opposite by using only another metal salt. Yttrium trichloride gives exclusively  $\gamma$ -product, while neodymium trichloride leads to 89% of the  $\alpha$ -attack (with 92% of (*E*)-isomer) (equation 142)<sup>280</sup>.



The enantioselective addition of organomagnesium compounds to ketones can be most conveniently performed by using a chiral auxiliary in the substrate molecule. Primary alkylmagnesium reagents react with aryl and heteroaryl ketones in the presence of magnesium TADDOLate at  $-100^{\circ}\text{C}$ , yielding products with up to 98% *ee* (equation 143)<sup>281</sup>. Chiral  $\alpha$ -ketoacetals **214**, prepared in two steps from  $\alpha$ -substituted cinnamic aldehydes, add organomagnesium species with up to 98% diastereoselectivity (equation 144).



*N*-Boc-leucinal may react with allyl- and alkenylmagnesium halides giving *syn*- and *anti*-products in *ca* 9:1 ratio. This method was used for the asymmetric synthesis of important amino acids like statine and norstatine<sup>282</sup>. An enantioselective desymmetrization of anhydrides was reported. Arylmagnesium chlorides react in toluene in the presence of (–)-sparteine (1 equiv.) with 3-substituted glutaric anhydrides **215**, giving aryl ketones with 87–92% *ee* (equation 145)<sup>283</sup>.

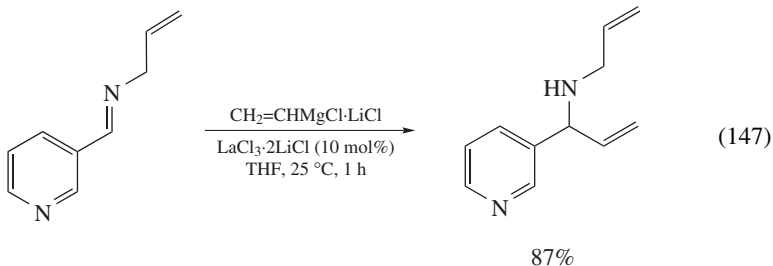
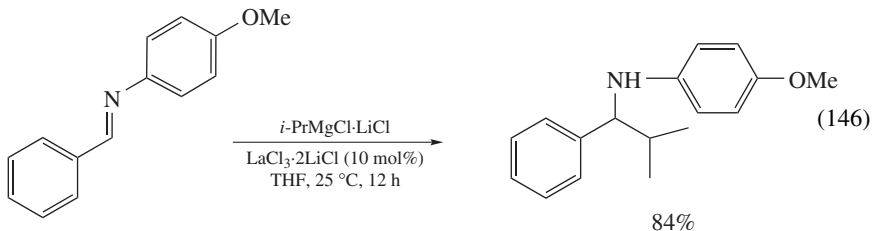


### 3. Addition to carbon–nitrogen bonds

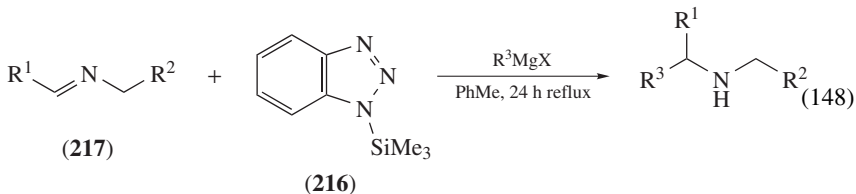
The reaction of Grignard reagents with imines and nitriles is an important method for the preparation of primary amines. In comparison with organolithium reagents, the addition of  $\text{RMgX}$  to imines shows a complex behavior which depends on the nature of the reagents. A directing group on the aldimine facilitates the reaction. A stoichiometric amount of a Lewis acid can be added to enhance the rate and 1,2-selectivity<sup>284</sup>. The addition reaction of organometallic reagents to imines has been reviewed<sup>285, 286</sup>.

Grignard reagents add with difficulty to imines derived from enolizable carbonyl compounds. The activation of the  $\text{C}=\text{N}$  bond can be achieved either by attachment of an electron-withdrawing group or *N*-coordination with a Lewis acid<sup>285</sup>. The use of a catalytic amount of the soluble rare-earth metal complex  $\text{LnCl}_3 \cdot 2\text{LiCl}$  allows the addition of

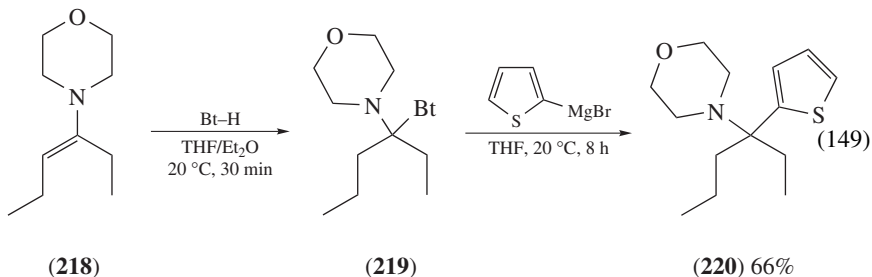
various Grignard reagents to imines (equations 146 and 147)<sup>276</sup>.



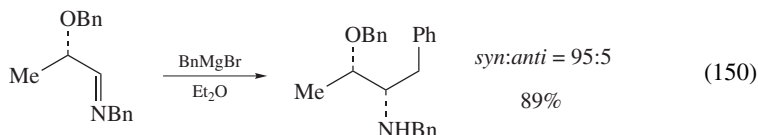
The addition of allylmagnesium halides (2 equiv.) to 1,3-azadienes affords after *in situ* alkylation dihomoaallylamines, which are useful intermediates in the synthesis of azepines or related heterocycles<sup>287</sup>. Activation of the C=N moiety of aldimines by 1-benzotriazolyltrimethylsilane minimizes side reactions. The mechanism involves reversible addition of **BTMS (216)** to the imine **217** followed by displacement of the benzotriazolyl group by a Grignard reagent (equation 148)<sup>288</sup>.



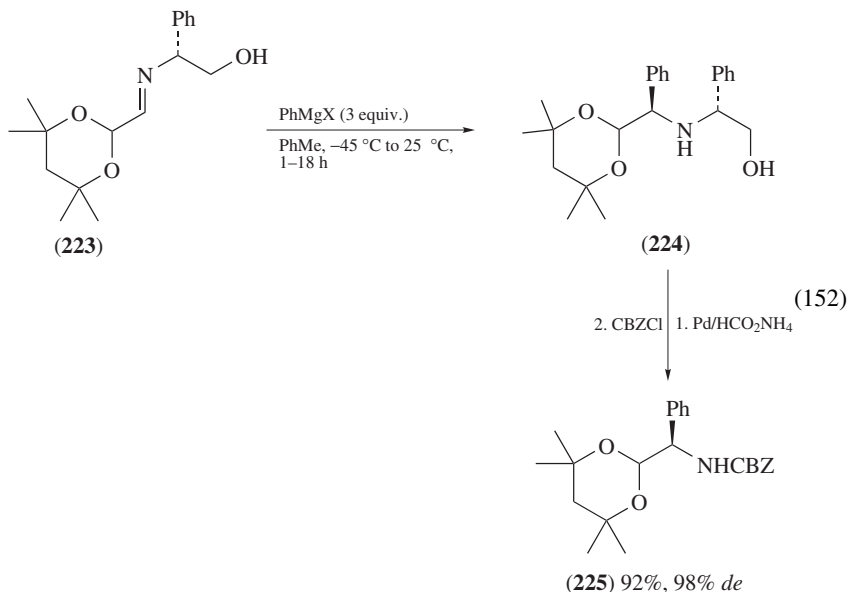
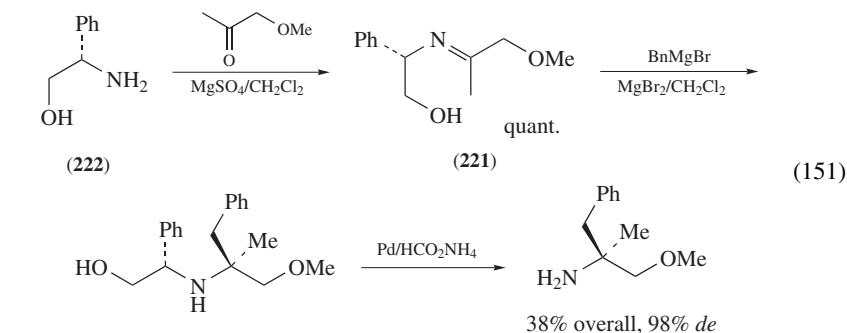
Similarly, reaction of enamines such as **218** with benzotriazole affords  $\alpha$ -aminoalkyl-benzotriazoles **219**, which react smoothly with organomagnesium compounds, giving tertiary alkyl carbylamines **220** (equation 149)<sup>289</sup>. The whole sequence can therefore be considered as the addition of Grignard reagents to imines.



Imines, derived from *O*-benzylaldehyde and benzylamine, react with non-stabilized Grignard reagents in ether yielding products with excellent diastereoselectivities (equation 150)<sup>290</sup>.

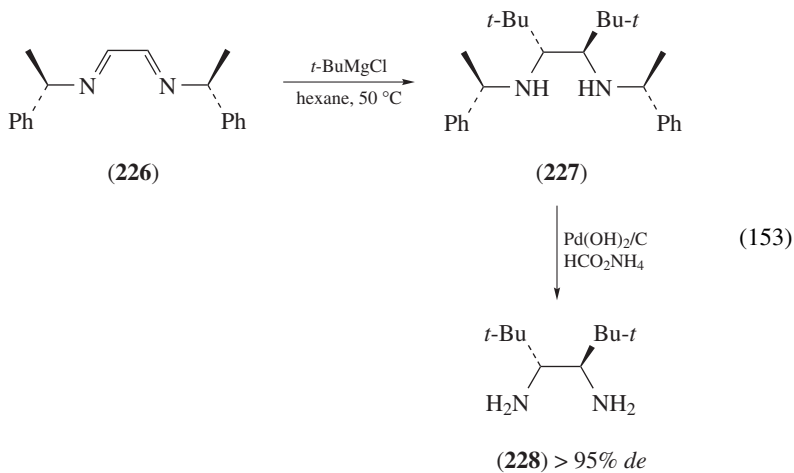


High yields and diastereoselectivities have also been observed for the addition of Grignard reagents to imines like **221** derived from phenylglycinol (**222**), which are existing in equilibria with 1,3-oxazolidines. Also, the imine derived from methoxyacetone affords amino-ethers with excellent diastereoselectivities. The addition of a Lewis acid ( $\text{MgBr}_2$ ) has a strong effect on both the yield and the selectivity (equation 151)<sup>291</sup>.

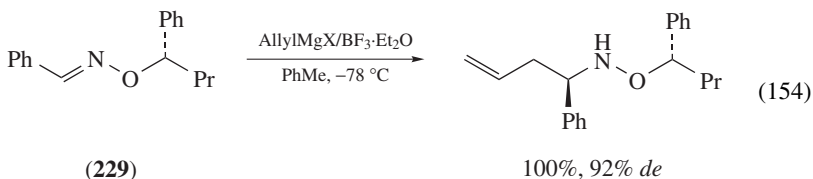


Imines **223** derived from glyoxal acetals react with various organomagnesium compounds with high diastereoselectivity (equation 152)<sup>292</sup>. The 1,2-aminoalcohols **224** can be converted into the protected enantiopure aminoaldehydes **225**. For these reactions toluene was found to be a superior solvent.

The addition reaction of 1,2-bisimine **226**, prepared from glyoxal and chiral  $\alpha$ -phenylethylamine, gives diastereomerically pure product **227**, which was converted to the chiral 1,2-diamine **228** (equation 153)<sup>293</sup>. Decreasing the temperature below 50 °C leads to a sharp drop of the stereoselectivity.

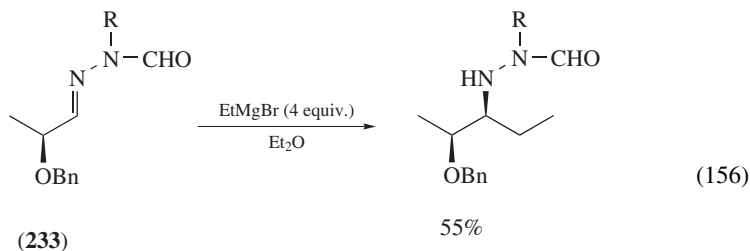
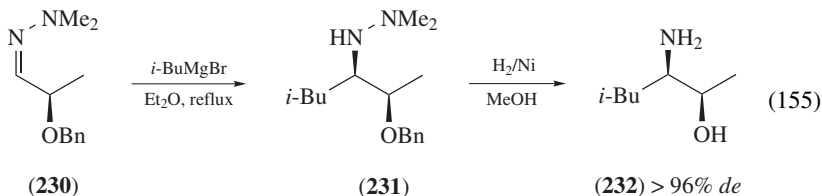
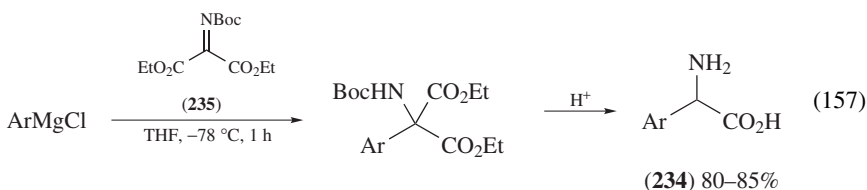


Chiral oxime ethers **229** of (*R*)- and (*S*)-*O*-(1-phenylbutyl)-hydroxylamine (ROPhy/SOPHy) react with Grignard reagents in the presence of  $\text{BF}_3 \cdot \text{OEt}_2$  in toluene at  $-78^\circ\text{C}$  yielding addition products with high diastereoselectivities (equation 154)<sup>294</sup>. The resulting chiral hydroxylamine derivatives have been converted enantioselectively to primary amines, or (when R = allyl) to  $\beta$ -amino acids.

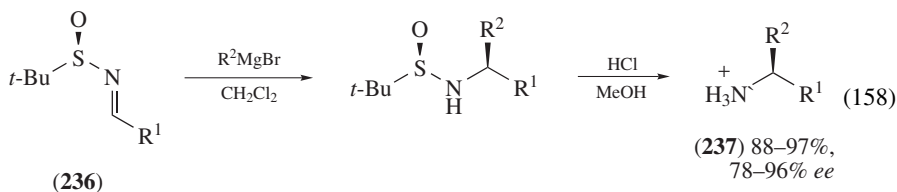


*O*-Benzylactaldehyde dimethylhydrazone **230** allows a substrate control in the addition reaction of organomagnesium halides, leading almost exclusively to the *syn*-isomer **231** (equation 155)<sup>295</sup>. The resulting hydrazide can be reduced on Raney Ni to the corresponding *syn*-aminoalcohol **232**. The stereoselective Grignard addition to a similar *N*-formyl hydrazone **233** proceeds with 92% diastereoselectivity (equation 156). The silylation of the amide nitrogen by TMSCl provides the pure *syn*-adduct<sup>296</sup>.

A convenient synthesis of aryl glycines **234** is performed by the addition of arylmagnesium chlorides to *N*-Boc-iminomalonate (**235**) (prepared from diethyl mesoxalate and  $\text{BocN=PPh}_3$ ). This reaction proceeds smoothly at low temperatures and is tolerating many functional groups in the Grignard reagent leading to amino acids of type **234** (equation 157)<sup>297</sup>.

R = H: 92% *de*R = SiMe<sub>3</sub>: 99.6% *de*

Chiral sulfinimines **236** are very useful intermediates for the preparation of enantiomerically pure primary amines **237** (equation 158)<sup>298</sup>. This reaction has been applied to the synthesis of  $\alpha$ -amino acids<sup>299</sup>. For sulfinimines obtained from simple ketones, lithium reagents are preferable for the addition<sup>298b</sup>, while for cyclic ketones organomagnesium compounds gave the best results. Addition of alkyl and aryl Grignard compounds to sulfinimines, derived from 3- and 4-substituted cyclohexanones, proceeds with excellent diastereoselectivity, depending on the stereochemistry of the ring substituents rather than the sulfinyl group<sup>300</sup>.

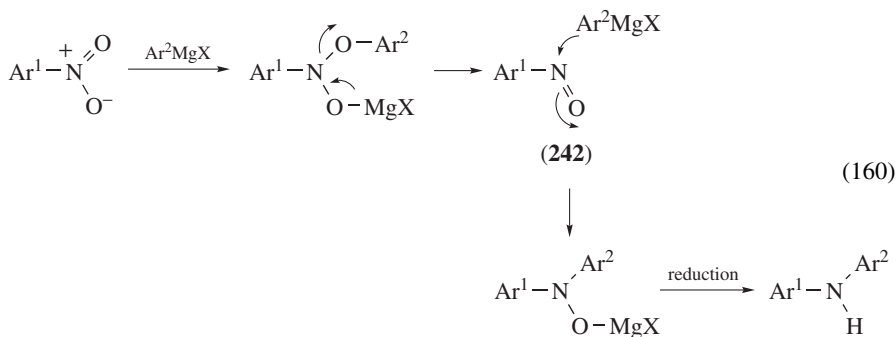
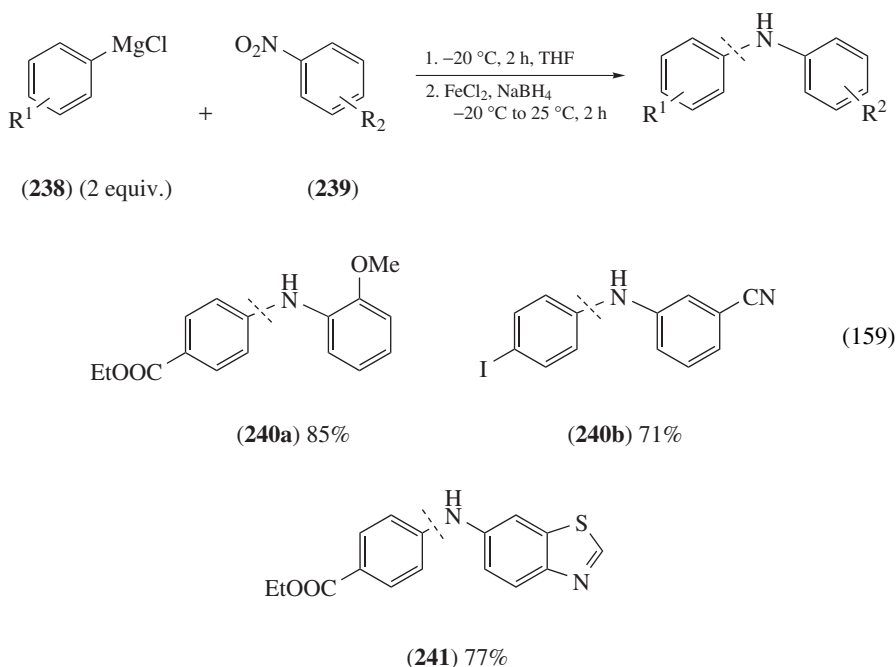


## E. Diverse Reactions

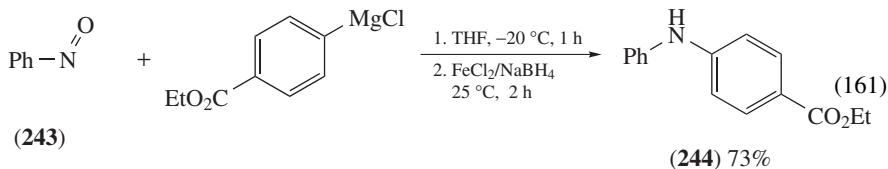
### 1. Amination reactions

*a. Electrophilic amination reactions.* The reaction of nucleophilic Grignard reagents with electrophilic aromatic nitrogen compounds in a higher oxidation state is a versatile

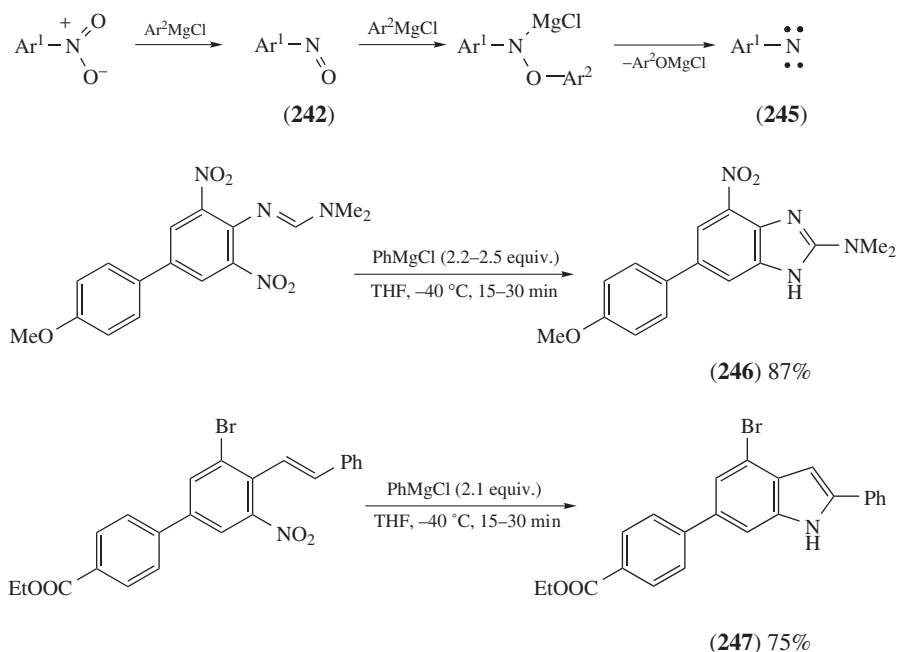
method for the synthesis of amines<sup>301</sup>. The reaction of functionalized arylmagnesium halides such as **238** with nitroarenes **239** followed by a reductive workup<sup>302</sup> provides polyfunctionalized diarylamines **240a, b** and heterocyclic amines like **241** in high yields (equation 159). The use of two equivalents of the Grignard reagent is crucial to obtain complete conversion as explained by considering the reaction mechanism (equation 160)<sup>303</sup>. The intermediate arylnitroso derivative **242** is a proposed reactive species. Thus, nitrosoarenes like **243** can be directly used as starting materials, allowing the synthesis of various functionalized diarylamines like **244** (equation 161)<sup>304</sup>.







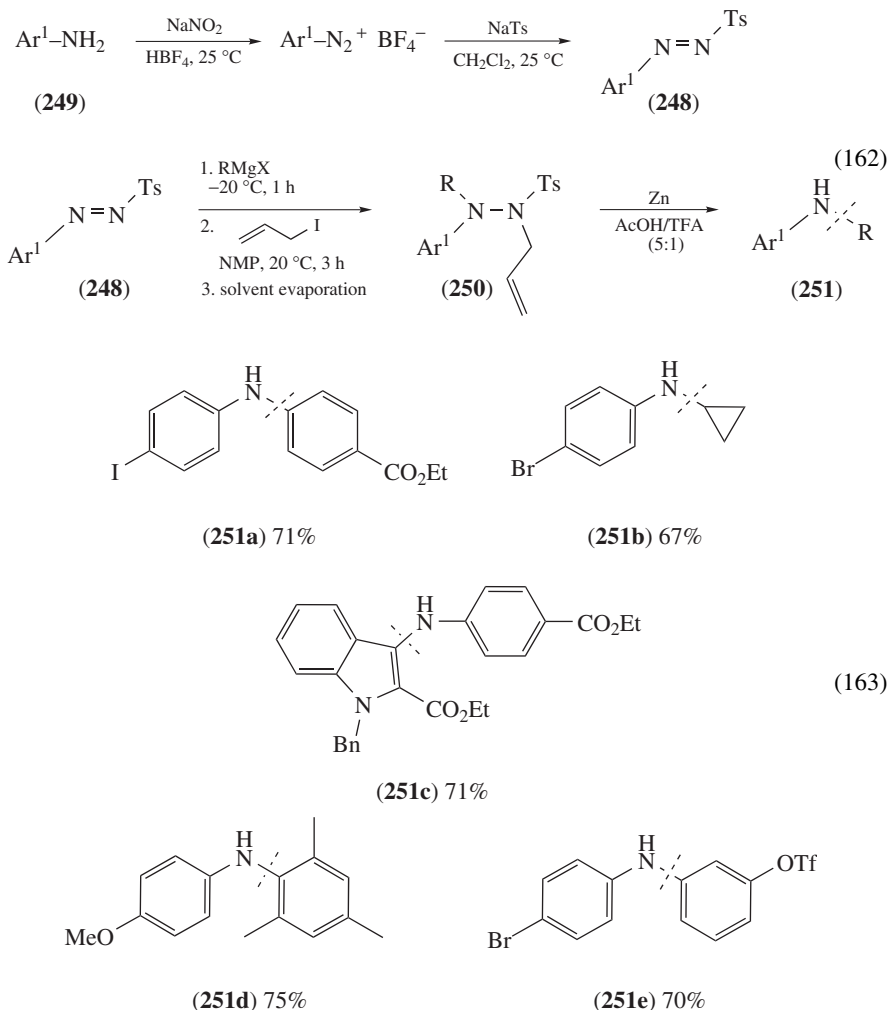
Nitroarenes, bearing bulky substituents next to the nitro function, are not reduced to the corresponding diarylamines<sup>305</sup>. Although the formation of the intermediate nitrosoarene **242** is still observed, due to steric hindrance the second equivalent of the Grignard reagent adds to the oxygen atom resulting in the formation of the nitrene **245**. This reactive intermediate **245** can be used for the mild synthesis of benzimidazoles like **246** or indoles like **247** bearing a broad range of functional groups (Scheme 20).



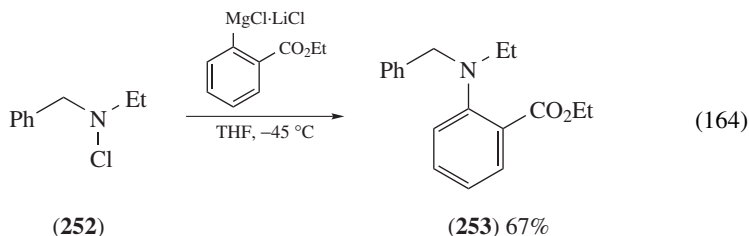
SCHEME 20

Arylazo tosylates of type **248**, which are readily obtained from aniline derivatives **249** in a two-step procedure (equation 162), can be alternatively used as starting materials<sup>306</sup>. This electrophilic nitrogen equivalent **248** reacts with a broad range of functionalized Grignard reagents under mild conditions. Subsequent allylation of the addition products with allyl iodide, followed by reductive cleavage of the resulting hydrazine derivatives

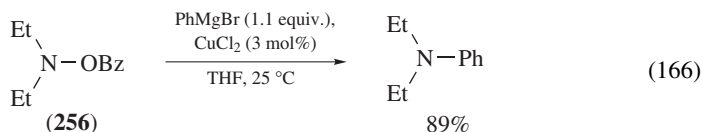
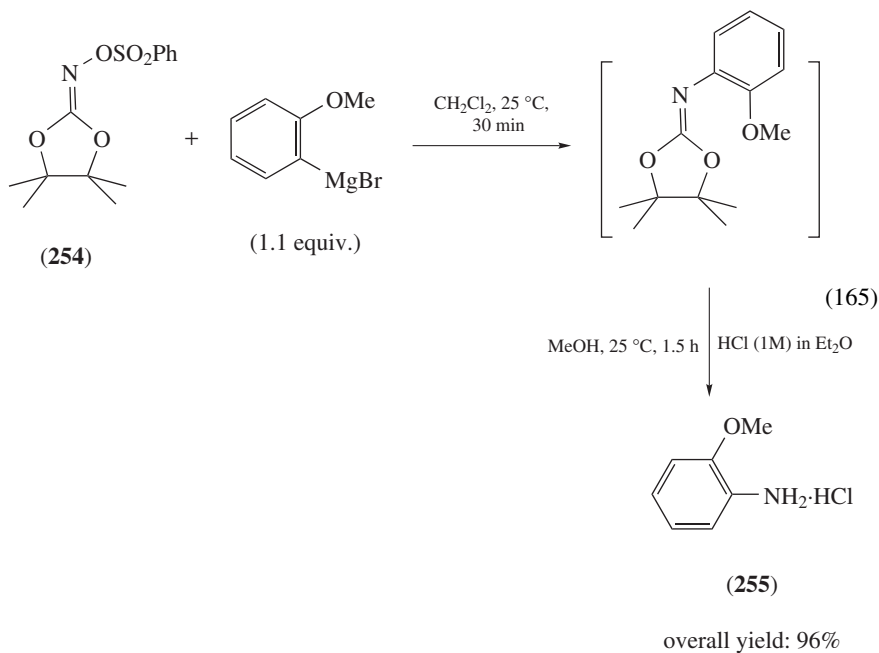
**250**, furnishes polyfunctionalized amines **251a–e** (equation 163).

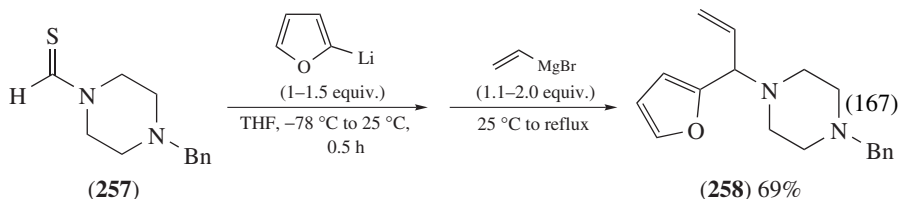


The electrophilic amination reaction of organometallic species using mono-, di- and trihaloamines has attracted a lot of attention for the synthesis of amines. Only a few cases have been reported using alkylchloroamines as precursors for the synthesis of tertiary amines<sup>307</sup>. One example is the reaction of functionalized arylmagnesium compounds with benzyl-*N*-chloroamines **252** providing polyfunctional tertiary amines **253** (equation 164)<sup>308</sup>. The procedure was also applied for the preparation of chiral *N*-chloroamines with retention of chirality at the  $\alpha$ -carbon. However, the amination process is limited to benzyl-*N*-chloroamines.



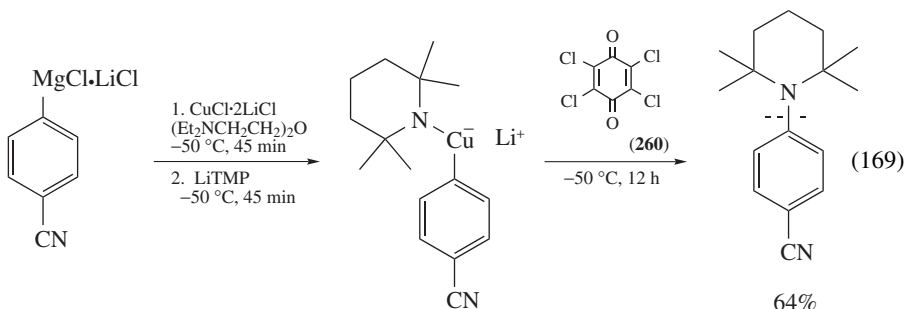
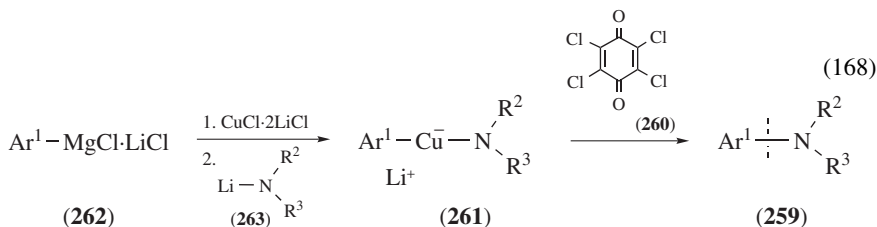
Another electrophilic amination method uses 4,4,5,5-tetramethyl-1,3-dioxolan-2-one *O*-phenylsulfoxime **254** as an electrophilic nitrogen equivalent<sup>309</sup>. It proved suitable for the amination of alkyl- and arylmagnesium reagents affording the respective primary alkyl or aryl amines **255** (equation 165). Electrophilic amination of Grignard reagents can further be achieved using *O*-benzoyl-*N,N*-dialkylhydroxylamines **256** and a catalytic amount of  $\text{CuCl}_2$  (equation 166)<sup>310</sup>. A three-component coupling reaction of thioformamides **257** with organolithium and Grignard reagents allows the formation of tertiary amines like **258** (equation 167)<sup>311</sup>.





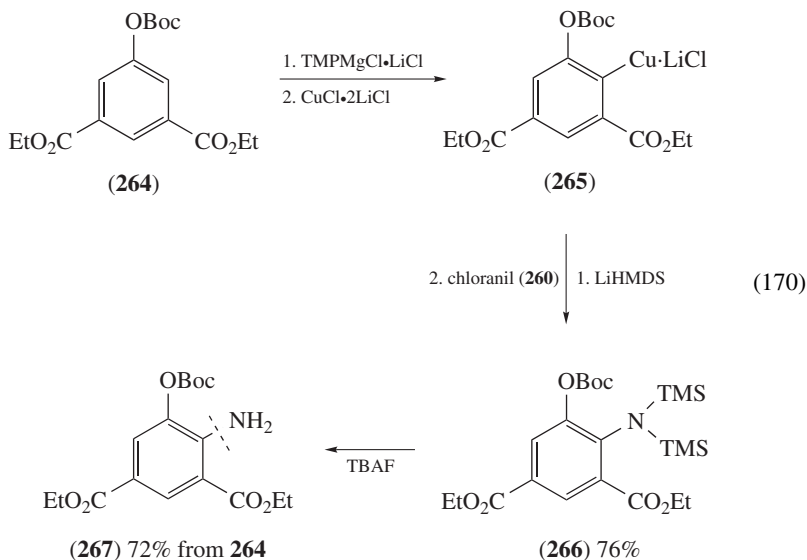
*b. Oxidative coupling of polyfunctional aryl and heteroaryl amidocuprates.* The oxidative amination of amidocuprates is a complement to the electrophilic amination reaction. Previous work<sup>312,313</sup> focused on the use of oxygen as oxidant for converting amidocuprates to various amines.

In a new synthetic protocol for the preparation of polyfunctional primary, secondary and tertiary aryl and heteroaryl amines **259**, chloranil (**260**) proves to be an efficient oxidant<sup>314</sup>. The required functionalized amidocuprates **261** are prepared starting from organomagnesium reagents **262** by transmetalation with  $\text{CuCl}\cdot 2\text{LiCl}$  followed by treatment with a lithium amide **263**. Oxidation of **261** with chloranil (**260**) affords the amines **259** in 70–80% yield (equation 168). This sequence can be performed with arylmagnesium reagents **262** bearing various functional groups such as a methoxy, an iodide and an amide group, as well as with various lithium amides **263** bearing functional groups like a bromide, a nitrile and an ester group, allowing the synthesis of the polyfunctionalized amines **259**. Steric hindrance of either the copper reagent or the lithium amide **263** is well tolerated (equation 169).

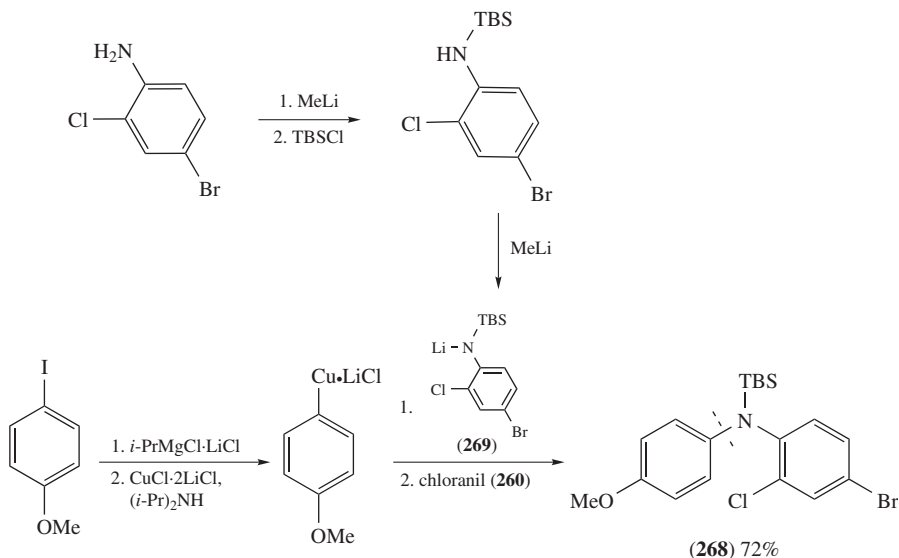


For the synthesis of primary amines, the diester **264** is magnesiated with  $\text{TMPMgCl}\cdot \text{LiCl}$  and transmetalated with  $\text{CuCl}\cdot 2\text{LiCl}$ , affording the corresponding arylcopper derivative **265**. Addition of LiHMDS furnishes the corresponding amidocuprate, which is reacted

with chloranil (**260**) leading to the *N,N*-bis(trimethylsilyl)amine derivative **266**. Desilylation with TBAF results in the formation of the arylamine **267** in 72% yield (equation 170).



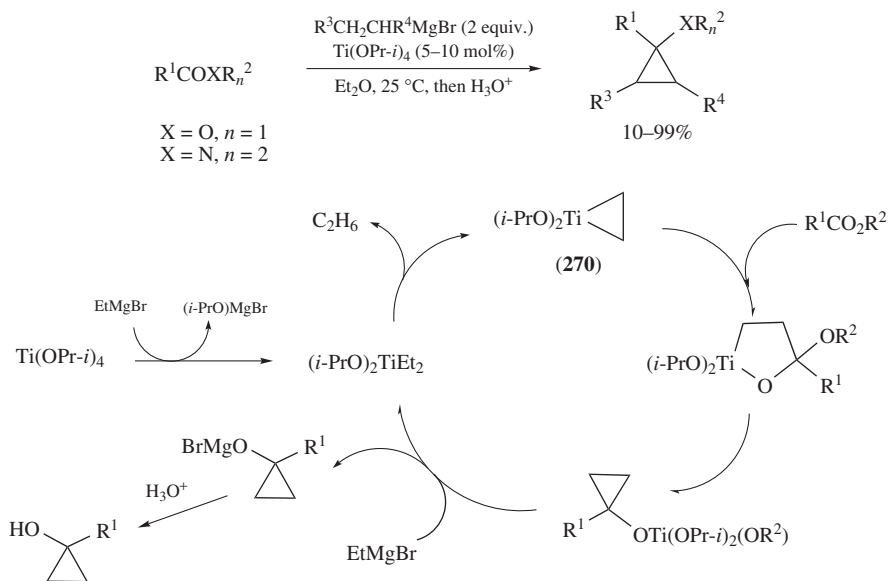
Secondary amines **268** are prepared using TBS-protected lithium amides **269** (Scheme 21), while the preparation of polyfunctional triarylamines applies lithium amides which are derived from secondary amines.



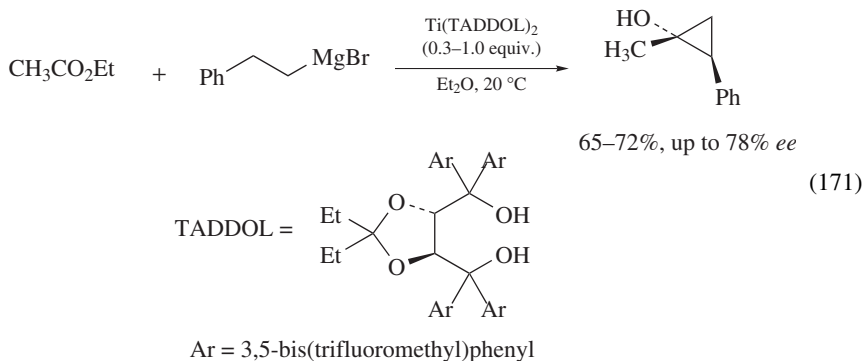
SCHEME 21

## 2. Synthesis of cyclopropanes

Cyclopropylamines and cyclopropanols can be prepared from alkylmagnesium halides<sup>315</sup>. The reaction is catalyzed by titanium alcoholates and its mechanism includes the formation of a dialkoxytitanacyclopropane **270**, which reacts with a carbonyl compound or nitrile (Scheme 22). The use of chiral titanium alcoholates allows the reaction to be performed with up to 78% *ee* (equation 171)<sup>316</sup>.



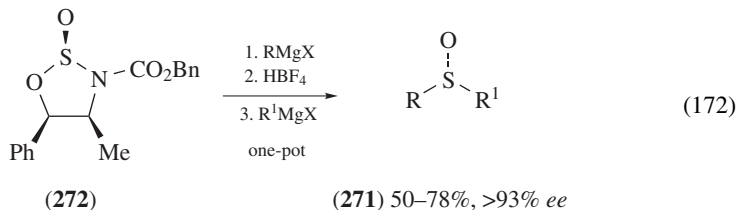
SCHEME 22



## 3. Synthesis of chiral sulfoxides

Chiral sulfoxides are useful intermediates in asymmetric synthesis. A number of methods can be used for their preparation. For example, enantiomerically pure *p*-tolylsulfoxides can be obtained by displacing a dimethylphosphonylmethyl moiety, a carbon leaving

group, from sulfur by Grignard reagents<sup>317</sup>. Optically pure menthyl 4-bromophenyl sulfinate can be sequentially displaced, yielding unsymmetrical dialkyl sulfoxides in 60–97% yield and >98% ee<sup>318</sup>. A simple one-pot synthesis of chiral sulfoxides **271** in high optical purity was developed recently. It starts from norephedrine-derived sulfamidites **272**<sup>319</sup> (equation 172).



#### IV. REFERENCES

1. V. Grignard, *Compt. Rend. Acad. Sci. Paris*, **130**, 1322 (1900).
2. B. H. Lipshutz and S. Sengupta, *Org. React.*, **41**, 135 (1992).
3. (a) H. G. Richey, Jr., *Grignard Reagents*, Wiley, New York, 2000.  
(b) M. S. Kharasch and O. Reinmuth, *Grignard Reactions of Nonmetallic Substances*, Prentice-Hall, New York, 1954.  
(c) G. S. Silverman and P. E. Rakita, *Handbook of Grignard Reagents*, Marcel Dekker, New York, 1996.  
(d) B. J. Wakefield, *Organomagnesium Methods in Organic Synthesis*, Academic Press, London, 1995.
4. W. E. Lindsell, in *Comprehensive Organometallic Chemistry II* (Eds. E. W. Abel, F. G. A. Stone and G. Wilkinson), Vol. 1 (Vol. Ed. C. E. Housecroft), Chap. 3, Pergamon Press, Oxford, 1995, pp. 72–78 and references therein.
5. (a) C. Hamdouchi and H. M. Walborsky, in *Handbook of Grignard Reagents* (Eds. G. S. Silverman and P. E. Rakita), Marcel Dekker, New York, 1996, p. 145.  
(b) J. F. Garst and F. Ungváry, in *Grignard Reagents: New Developments* (Ed. H. G. Richey, Jr.), Wiley, Chichester, 2000, p. 185.  
(c) J. F. Garst, F. Ungváry and J. T. Baxter, *J. Am. Chem. Soc.*, **119**, 253 (1997).  
(d) J. F. Garst and M. P. Soriaga, *Coord. Chem. Rev.*, **248**, 623 (2004).
6. (a) F. Bickelhaupt, in *Grignard Reagents: New Developments* (Ed. H. G. Richey, Jr.), Wiley, Chichester, 2000, p. 299.  
(b) H. L. Uhm, in *Handbook of Grignard Reagents* (Eds. G. S. Silverman and P. E. Rakita), Marcel Dekker, New York, 1996, p. 117.
7. P. E. Rakita, J. F. Aultman and L. Stapleton, *Chem. Eng.*, **97**, 110 (1990).
8. (a) A. Tuulmets, M. Marvi and D. Panov, *J. Organomet. Chem.*, **523**, 133 (1996).  
(b) M. Sassian, D. Panov and A. Tuulmets, *Appl. Organomet. Chem.*, **16**, 525 (2002).
9. H. Simuste, D. Panov, A. Tuulmets and B. T. Nguyen, *J. Organomet. Chem.*, **690**, 3061 (2005).
10. J. Wiss and G. Ermini, *Org. Process Res. Dev.*, **10**, 1282 (2006).
11. J. F. Garst and M. P. Soriaga, *Coord. Chem. Rev.*, **248**, 623 (2004).
12. (a) H. M. Walborsky and M. Topolski, *J. Am. Chem. Soc.*, **114**, 3455 (1992).  
(b) C. E. Teerlinck and W. J. Bowyer, *J. Org. Chem.*, **61**, 1059 (1996).
13. For factors controlling Grignard reagent formation, see: W. E. Lindsell, in *Comprehensive Organometallic Chemistry I* (Eds. G. Wilkinson, F. G. S. Stone and G. E. Ebel), Vol. 1, Chap. 3, Pergamon Press, Oxford, 1982, pp. 155–252 and references therein.
14. (a) H. M. Walborsky, *Acc. Chem. Res.*, **23**, 286 (1990).  
(b) J. F. Garst, *Acc. Chem. Res.*, **24**, 95 (1991).  
(c) C. Walling, *Acc. Chem. Res.*, **24**, 255 (1991).  
(d) H. R. Rogers, C. L. Hill, Y. Fujiwara, R. J. Rogers, H. L. Mitchell and G. M. Whitesides, *J. Am. Chem. Soc.*, **102**, 217 (1980).

- (e) K. S. Root, C. L. Hill, L. M. Lawrence and G. M. Whitesides, *J. Am. Chem. Soc.*, **111**, 5404 (1989).
- (f) E. C. Ashby and J. Oswald, *J. Org. Chem.*, **53**, 6068 (1988).
15. F. Kanoufi, C. Combellas, H. Hazimeh, J.-M. Mattalia, C. Marchi-Delapierre and M. Chanon, *J. Phys. Org. Chem.*, **19**, 847 (2006).
16. U. Tilstam and H. Weinmann, *Org. Process Res. Dev.*, **6**, 906 (2002).
17. B. Bogdanović and M. Schwickardi, *Angew. Chem., Int. Ed.*, **39**, 4610 (2000).
18. H. Gold, M. Larhed and P. Nilsson, *Synlett*, 1596 (2005).
19. (a) R. D. Rieke and M. V. Hanson, *Tetrahedron*, **53**, 1925 (1997).
- (b) R. D. Rieke, M. S. Sell, W. R. Klein, T.-A. Chen, J. D. Brown and M. U. Hansen, in *Active Metals. Preparation, Characterization, Application* (Ed. A. Fürstner), Wiley-VCH, Weinheim, 1996, p. 1.
20. J. Lee, R. Velarde-Ortiz, A. Guijarro, J. R. Wurst and R. D. Rieke, *J. Org. Chem.*, **65**, 5428 (2000).
21. (a) O. Sugimoto, S. Yamada and K. Tanji, *Tetrahedron Lett.*, **43**, 3355 (2002).
- (b) O. Sugimoto, S. Yamada and K. Shigeru, *J. Org. Chem.*, **68**, 2054 (2003).
22. B. Bogdanović, *Acc. Chem. Res.*, **21**, 261 (1988).
23. D. Cheng, S. Zhu, Z. Yu and T. Cohen, *J. Am. Chem. Soc.*, **123**, 30 (2001).
24. J. Beckmann, D. Dakternieks, M. Draeger and A. Duthie, *Angew. Chem., Int. Ed.*, **45**, 6509 (2006).
25. S. T. Handy, *J. Org. Chem.*, **71**, 4659 (2006).
26. M. C. Law, K.-Y. Wong and T. H. Chan, *Chem. Commun.*, 2457 (2006).
27. C. Prévost, *Bull. Soc. Chim. Fr.*, 1372 (1931).
28. (a) W. F. Bailey and J. J. Patricia, *J. Organomet. Chem.*, **352**, 1 (1988).
- (b) H. J. Reich, N. H. Phillips and I. L. Reich, *J. Am. Chem. Soc.*, **107**, 4101 (1985).
- (c) W. B. Farnham and J. C. Calabrese, *J. Am. Chem. Soc.*, **108**, 2449 (1986).
- (d) A. Krasovskiy, B. F. Straub and P. Knochel, *Angew. Chem., Int. Ed.*, **45**, 159 (2006).
29. (a) O. R. Pierce, A. F. Meiners and E. T. McBee, *J. Am. Chem. Soc.*, **75**, 2516 (1953).
- (b) E. T. McBee, C. W. Roberts and A. F. Meiners, *J. Am. Chem. Soc.*, **79**, 335 (1957).
- (c) P. Moreau, R. Albachi and A. Commeyras, *Nouv. J. Chim.*, **1**, 497 (1977).
30. (a) R. D. Chambers, W. K. R. Musgrave and J. Savory, *J. Chem. Soc.*, 1993 (1962).
- (b) For a review on fluorinated organometallics, see: D. J. Burton and Z. Y. Yang, *Tetrahedron*, **48**, 189 (1992).
31. (a) J. Villiéras, *Bull. Soc. Chim. Fr.*, 1520 (1967).
- (b) J. Villiéras, B. Kirschleger, R. Tarhouni and M. Rambaud, *Bull. Soc. Chim. Fr.*, 470 (1986).
32. For recent examples, see:
- (a) A. Müller, M. Marsch, K. Harms, J. C. W. Lohrenz and G. Boche, *Angew. Chem., Int. Ed.*, **35**, 1518 (1996).
- (b) R. W. Hoffmann, M. Julius, F. Chemla, T. Ruhland and G. Frenzen, *Tetrahedron*, **50**, 6049 (1994).
33. C. Tamborski and G. J. Moore, *J. Organomet. Chem.*, **26**, 153 (1971).
34. (a) N. Furukawa, T. Shibutani and H. Fujihara, *Tetrahedron Lett.*, **28**, 5845 (1987).
- (b) D. J. Burton and Z. Y. Yang, *Tetrahedron*, **48**, 189 (1992).
- (c) R. D. Chambers, W. K. R. Musgrave and J. Savory, *J. Chem. Soc.*, 1993 (1962).
- (d) H. H. Paradies and M. Görbing, *Angew. Chem., Int. Ed. Engl.*, **8**, 279 (1969).
- (e) G. Cahiez, D. Bernard and J. F. Normant, *J. Organomet. Chem.*, **113**, 107 (1976).
- (f) D. Seyferth and R. L. Lambert, *J. Organomet. Chem.*, **54**, 123 (1973).
- (g) H. Nishiyama, K. Isaka, K. Itoh, K. Ohno, H. Nagase, K. Matsumoto and H. Yoshiwara, *J. Org. Chem.*, **57**, 407 (1992).
- (h) C. Bolm and D. Pupowicz, *Tetrahedron Lett.*, **38**, 7349 (1997).
35. L. Boymond, M. Rottländer, G. Cahiez and P. Knochel, *Angew. Chem., Int. Ed.*, **37**, 1701 (1998).
36. A. E. Jensen, W. Dohle, I. Sapountzis, D. M. Lindsay, V. A. Vu and P. Knochel, *Synthesis*, 565 (2002).
37. J. T. Reeves, M. Sarvestani, J. J. Song, Z. Tan, L. Nummy, H. Lee, N. K. Yee and C. H. Senanayake, *Org. Process Res. Dev.*, **10**, 1258 (2006).
38. P. Cali and M. Begtrup, *Synthesis*, 6 (2002).



39. (a) R. Kober, W. Hammes and W. Steglich, *Angew. Chem., Int. Ed.*, **21**, 203 (1982).  
(b) D. von der Brück, R. Bühler and H. Plieninger, *Tetrahedron*, **28**, 791 (1972).
40. T. Graening, W. Friedrichsen, J. Lex and H.-G. Schmalz, *Angew. Chem., Int. Ed.*, **41**, 1524 (2002).
41. (a) M. Abarbri, J. Thibonnet, L. Bérillon, F. Dehmel, M. Rottländer and P. Knochel, *J. Org. Chem.*, **65**, 4618 (2000).  
(b) P. Knochel, E. Hupe, W. Dohle, D. M. Lindsay, V. Bonnet, G. Quéguiner, A. Boudier, F. Kopp, S. Demay, N. Seidel, M. I. Calaza, V. A. Vu, I. Sapountzis and T. Bunlaksananusorn, *Pure Appl. Chem.*, **74**, 11 (2002).
42. P. Knochel, W. Dohle, N. Gommermann, F. F. Kneisel, T. Korn, I. Sapountzis and V. A. Vu, *Angew. Chem., Int. Ed.*, **42**, 4302 (2003).
43. L. Bérillon, A. Leprêtre, A. Turck, N. Ple, G. Quéguiner, G. Cahiez and P. Knochel, *Synlett*, 1359 (1998).
44. M. Abarbri and P. Knochel, *Synlett*, 1577 (1999).
45. T. Tobrman and D. Dvorak, *Org. Lett.*, **5**, 4289 (2003).
46. F. Dehmel, M. Abarbri and P. Knochel, *Synlett*, 345 (2000).
47. A. Staubitz, W. Dohle and P. Knochel, *Synthesis*, 233 (2003).
48. C. Jaramillo, J. C. Carretero, J. E. de Diego, M. del Prado, C. Hamdouchi, J. L. Roldán and C. Sánchez-Martínez, *Tetrahedron Lett.*, **43**, 9051 (2002).
49. (a) M. Bergauer and P. Gmeiner, *Synthesis*, 2281 (2001).  
(b) J. Felding, J. Kristensen, T. Bjerregaard, L. Sander, P. Vedsø and M. Begtrup, *J. Org. Chem.*, **64**, 4196 (1999).
50. H. Kromann, F. A. Slok, T. N. Johansen and P. Krogsgaard-Larsen, *Tetrahedron*, **57**, 2195 (2001).
51. (a) M. Abarbri, F. Dehmel and P. Knochel, *Tetrahedron Lett.*, **40**, 7449 (1999).  
(b) G. Varchi, A. E. Jensen, W. Dohle, A. Ricci, G. Cahiez and P. Knochel, *Synlett*, 477 (2001).
52. J. L. Leazer Jr., R. Cvetovich, F.-R. Tsay, U. Dolling, T. Vickery and D. Bachert, *J. Org. Chem.*, **68**, 3695 (2003).
53. (a) E. C. Ashby and D. M. Al-Ferki, *J. Organomet. Chem.*, **390**, 275 (1990).  
(b) M. C. Jones, *Plant Oper. Prog.*, **8**, 200 (1989).  
(c) J. Broeke, B.-J. Deelman and G. van Koten, *Tetrahedron Lett.*, **42**, 8085 (2001).  
(d) P. Pinho, D. Guijarro and P. Andersson, *Tetrahedron*, **54**, 7897 (1998).  
(e) F. A. R. Kaul, G. T. Puchta, H. Schneider, M. Grosche, D. Mihalios and W. A. Herrmann, *J. Organomet. Chem.*, **621**, 184 (2001).
54. H. Nishiyama, K. Isaka, K. Itoh, K. Ohno, H. Nagase, K. Matsumoto and H. Yoshiwara, *J. Org. Chem.*, **57**, 407 (1992).
55. A. Krasovskiy and P. Knochel, *Angew. Chem., Int. Ed.*, **43**, 3333 (2004).
56. D. Hauk, S. Lang and A. Murso, *Org. Process Res. Dev.*, **10**, 733 (2006).
57. F. Kopp, A. Krasovskiy and P. Knochel, *Chem. Commun.*, 2288 (2004).
58. X.-J. Wang, X. Sun, L. Zhang, Y. Xu, D. Krishnamurthy and C. H. Senanayake, *Org. Lett.*, **8**, 305 (2006).
59. K. Kitagawa, A. Inoue, H. Shinokubo and K. Oshima, *Angew. Chem., Int. Ed.*, **39**, 2481 (2000).
60. F. Trécourt, G. Breton, V. Bonnet, F. Mongin, F. Marsais and G. Quéguiner, *Tetrahedron Lett.*, **40**, 4339 (1999).
61. H. Ren and P. Knochel, *Chem. Commun.*, 726 (2006).
62. N. Boudet and P. Knochel, *Org. Lett.*, **8**, 3737 (2006).
63. S. Kii, A. Akao, T. Iida, T. Mase and N. Yasuda, *Tetrahedron Lett.*, **47**, 1877 (2006).
64. C. Christophersen, M. Begtrup, S. Ebdrup, H. Petersen and P. Vedsø, *J. Org. Chem.*, **68**, 9513 (2003).
65. A. Spiess, G. Heckmann and T. Bach, *Synlett*, 131 (2004).
66. (a) H. Ila, O. Baron, A. J. Wagner and P. Knochel, *Chem. Commun.*, 583 (2006).  
(b) H. Ila, O. Baron, A. J. Wagner and P. Knochel, *Chem. Lett.*, **35**, 2 (2006).
67. J. Thibonnet, V. A. Vu, L. Bérillon and P. Knochel, *Tetrahedron*, **58**, 4787 (2000).
68. I. Sapountzis, W. Dohle and P. Knochel, *Chem. Commun.*, 2068 (2001).
69. V. A. Vu, I. Marek and P. Knochel, *Synthesis*, 1797 (2003).

70. T. Satoh, K. Takano, H. Ota, H. Someya, K. Matsuda and M. Koyama, *Tetrahedron*, **54**, 5557 (1998).
71. M. Watanabe, M. Nakamura and T. Satoh, *Tetrahedron*, **61**, 4409 (2005).
72. (a) H. Ren, A. Krasovskiy and P. Knochel, *Org. Lett.*, **6**, 4215 (2004).  
(b) H. Ren, A. Krasovskiy and P. Knochel, *Chem. Commun.*, 543 (2005).
73. H. Shinokubo, H. Miki, T. Yokoo, K. Oshima and K. Utimoto, *Tetrahedron*, **51**, 11681 (1995).
74. T. Satoh, A. Kondo and J. Musashi, *Tetrahedron*, **60**, 5453 (2004).
75. R. W. Hoffmann, B. Holzer, O. Knopff and K. Harms, *Angew. Chem., Int. Ed.*, **39**, 3072 (2000).
76. R. W. Hoffmann and P. G. Nell, *Angew. Chem., Int. Ed.*, **38**, 338 (1999).
77. A. Inoue, J. Kondo, H. Shinokubo and K. Oshima, *Chem. Eur. J.*, **8**, 1730 (2002).
78. R. W. Hoffmann, O. Knopff and A. Kusche, *Angew. Chem., Int. Ed.*, **39**, 1462 (2000).
79. O. Knopff, H. C. Stiasny and R. W. Hoffmann, *Organometallics*, **23**, 705 (2004).
80. R. W. Hoffmann, *Chem. Soc. Rev.*, **32**, 225 (2003).
81. (a) R. W. Hoffmann and A. Kusche, *Chem. Ber.*, **127**, 1311 (1994).  
(b) M. Rottländer, L. Boymond, L. Bérillon, A. Leprière, G. Varchi, S. Avolio, H. Laaziri, G. Quéguiner, A. Ricci, G. Cahiez and P. Knochel, *Chem. Eur. J.*, **6**, 767 (2000).  
(c) S. Avolio, C. Malan, I. Marek and P. Knochel, *Synlett*, 1820 (1999).
82. M. S. Baird, A. V. Nizovtsev and I. G. Bolesov, *Tetrahedron*, **58**, 1581 (2002).
83. (a) V. A. Vu, I. Marek and P. Knochel, *Angew. Chem., Int. Ed.*, **41**, 351 (2002).  
(b) J. Kondo, A. Inoue, H. Shinokubo and K. Oshima, *Angew. Chem., Int. Ed.*, **40**, 2085 (2001).
84. F. Kopp, G. Sklute, K. Polborn, I. Marek and P. Knochel, *Org. Lett.*, **7**, 3789 (2005).
85. (a) F. F. Fleming and B. C. Shook, *Tetrahedron*, **58**, 1 (2002).  
(b) S. Arseniyadis, K. S. Kyler and D. S. Watt, *Org. React.*, **31**, 1 (1984).
86. A. J. Fatiadi, in *The Chemistry of Triple-Bonded Functional Groups. Supplement C* (Eds. S. Patai and Z. Rappoport), Wiley, New York, 1983, p. 1157.
87. F. F. Fleming, Z. Zhang, W. Liu and P. Knochel, *J. Org. Chem.*, **70**, 2200 (2005).
88. A. H. Stoll, A. Krasovskiy and P. Knochel, *Angew. Chem., Int. Ed.*, **45**, 606 (2006).
89. G. Varchi, C. Kofink, D. M. Lindsay, A. Ricci and P. Knochel, *Chem. Commun.*, 396 (2003).
90. S. Kato, N. Nonoyama, K. Tomimoto and T. Mase, *Tetrahedron Lett.*, **43**, 7315 (2002).
91. N. Ono, *The Nitro Group in Organic Synthesis*, Wiley-VCH, New York, 2001.
92. (a) I. Sapountzis and P. Knochel, *Angew. Chem., Int. Ed.*, **41**, 1610 (2002).  
(b) I. Sapountzis, H. Dube, R. Lewis and P. Knochel, *J. Org. Chem.*, **70**, 2445 (2005).
93. (a) S. Bräse, *Acc. Chem. Res.*, **37**, 804 (2004).  
(b) D. B. Kimball and M. M. Haley, *Angew. Chem., Int. Ed.*, **41**, 3338 (2002).  
(c) A. de Meijere, P. von Zezschwitz, H. Nuske and B. Stulgies, *J. Organomet. Chem.*, **653**, 129 (2002).
94. W. B. Wan, R. C. Chiechi, T. J. R. Weakley and M. M. Haley, *Eur. J. Org. Chem.*, **18**, 3485 (2001).
95. C.-Y. Liu and P. Knochel, *Org. Lett.*, **7**, 2543 (2005).
96. For the utility of neopentyl organometallics in zinc and copper chemistry, see:  
(a) P. Jones, C. K. Reddy and P. Knochel, *Tetrahedron*, **54**, 1471 (1998).  
(b) P. Jones and P. Knochel, *J. Chem. Soc., Perkin Trans. 1*, 3117 (1997).  
(c) F. F. Kneisel and P. Knochel, *Synlett*, 1799 (2002).
97. C.-Y. Liu, H. Ren and P. Knochel, *Org. Lett.*, **8**, 617 (2006).
98. T. Delacroix, L. Bérillon, G. Cahiez and P. Knochel, *J. Org. Chem.*, **65**, 8108 (2000).
99. O. Baron and P. Knochel, *Angew. Chem., Int. Ed.*, **44**, 3133 (2005).
100. L. Boymond, M. Rottländer, G. Cahiez and P. Knochel, *Angew. Chem., Int. Ed.*, **37**, 1701 (1998).
101. R. G. Franzen, *Tetrahedron*, **56**, 685 (2000).
102. (a) V. Snieckus, *Chem. Rev.*, **90**, 879 (1990).  
(b) E. J.-G. Anctil and V. Snieckus, *J. Organomet. Chem.*, **653**, 150 (2002).
103. V. Bonnet, F. Mongin, F. Trécourt and G. Quéguinér, *J. Chem. Soc., Perkin Trans. 1*, 4245 (2000).
104. A. B. Holmes and C. N. Sporikou, *Org. Synth.*, **65**, 61 (1987).  
(b) H. J. Bestman, T. Brosche, K. H. Koschatzky, K. Michaelis, H. Platz, K. Roth, J. Suess, O. Vostrowsky and W. Knauf, *Tetrahedron Lett.*, **23**, 4007 (1982).

- (c) L. Poncini, *Bull. Soc. Chim. Belg.*, **92**, 215 (1983).
105. (a) M.-X. Zhang and P. E. Eaton, *Angew. Chem., Int. Ed.*, **41**, 2169 (2002).  
 (b) Y. Kondo, Y. Akihiro and T. Sakamoto, *J. Chem. Soc., Perkin Trans. 1*, 2331 (1996).  
 (c) P. E. Eaton, C. H. Lee and Y. Xiong, *J. Am. Chem. Soc.*, **111**, 8016 (1989).  
 (d) P. E. Eaton, M.-X. Zhang, N. Komiya, C.-G., Yang, I. Steele, and R. Gilardi, *Synlett*, 1275 (2003).  
 (e) P. E. Eaton and R. M. Martin, *J. Org. Chem.*, **53**, 2728 (1988).  
 (f) M. Shilai, Y. Kondo and T. Sakamoto, *J. Chem. Soc., Perkin Trans. 1*, 442 (2001).
106. P. E. Eaton and M.-X. Zhang, *Angew. Chem., Int. Ed.*, **41**, 2169 (2002).
107. W. Schlecker, A. Huth, E. Ottow and J. Mulzer, *J. Org. Chem.*, **60**, 8414 (1995).
108. Y. Kondo, A. Yoshida and T. Sakamoto, *J. Chem. Soc., Perkin Trans. 1*, 2331 (1996).
109. A. Dinsmore, D. G. Billing, K. Mandy, J. P. Michael, D. Mogano and S. Patil, *Org. Lett.*, **6**, 293 (2004).
110. K. W. Henderson and W. J. Kerr, *Chem. Eur. J.*, **7**, 3431 (2001).
111. (a) D. Benafoux, M. Bordeaux, C. Biran and J. Dunogues, *J. Organomet. Chem.*, **993**, 27 (1995).  
 (b) G. Lesseue, R. Tripoli, P. Cazeau, C. Brian and M. Bordeaux, *Tetrahedron Lett.*, **40**, 4037 (1999).
112. (a) D. A. Evans and S. G. Nelson, *J. Am. Chem. Soc.*, **119**, 6452 (1997).  
 (b) K. W. Hendersson, W. J. Kerr and J. H. Mair, *Tetrahedron*, **58**, 4573 (2002).
113. A. Krasovskiy, V. Krasovskaya and P. Knochel, *Angew. Chem., Int. Ed.*, **45**, 2958 (2006).
114. W. Lin, O. Baron and P. Knochel, *Org. Lett.*, **8**, 5673 (2006).
115. For reviews, see:  
 (a) A. Sauer and R. Huisgen, *Angew. Chem.*, **72**, 294 (1960).  
 (b) R. W. Hoffmann, *Dehydrobenzene and Cycloalkynes*, Academic Press, New York, 1967.  
 (c) L. Castedo and E. Guitian, in *Studies in Natural Products Chemistry*, Vol. 3, Part B (Ed. A. U. Rahman), Elsevier, Amsterdam, 1989, p. 417.  
 (d) S. V. Kessar, in *Comprehensive Organic Synthesis*, Vol. 4 (Eds. B. M. Trost, I. Fleming and H. F. Semmelhack), Pergamon, Oxford, 1991, p. 483.  
 (e) R. F. C. Brown, *Synlett*, 9 (1993).  
 (f) W. Sander, *Acc. Chem. Res.*, **32**, 669 (1999).  
 (g) H. Pellissier and M. Santelli, *Tetrahedron*, **59**, 701 (2003).
116. (a) I. Sapountzis, W. Lin, M. Fischer and P. Knochel, *Angew. Chem., Int. Ed.*, **43**, 4364 (2004).  
 (b) W. Lin, I. Sapountzis and P. Knochel, *Angew. Chem., Int. Ed.*, **44**, 4258 (2005).  
 (c) W. Lin, F. Ilgen and P. Knochel, *Tetrahedron Lett.*, **47**, 1941 (2006).
117. N. Hartmann and M. Niemeyer, *Synth. Commun.*, **31**, 3839 (2001).
118. B. Bogdanović, P. Bons, S. Konstantinović, M. Schwickardi and U. Westeppe, *Chem. Ber.*, **126**, 1371 (1993).
119. (a) Y. Kai, N. Kanegisa, K. Miki, N. Kasai, K. Mashima, H. Yasuda and A. Nakamura, *Chem. Lett.*, 3976 (1982).  
 (b) R. D. Rieke and H. Xiong, *J. Org. Chem.*, **56**, 3109 (1991).
120. Y. Gao and F. Sato, *J. Chem. Soc., Chem. Commun.*, 659 (1995).
121. M. Cai, J. Xia and G. Chen, *J. Organomet. Chem.*, **689**, 2531 (2004).
122. (a) M. Cai, J. Xia, and W. Hao, *Heteroat. Chem.*, **16**, 65 (2005).  
 (b) M. Cai, W. Hao, H. Zhao and J. Xia, *J. Organomet. Chem.*, **689**, 3593 (2004).  
 (c) M. Cai, J. Xia and G. Chen, *J. Organomet. Chem.*, **689**, 1714 (2004).  
 (d) H. Shinokubo, H. Miki, T. Yokoo, K. Oshima and K. Utimoto, *Tetrahedron*, **51**, 11681 (1995).
123. N. B. Victorov and L. M. Zubritskii, *Russ. J. Org. Chem.*, **33**, 1706 (1997).
124. F. Sato and H. Vrade, 'Hydromagnesiation of alkenes and alkynes', in *Grignard Reagents—New Developments* (Ed. H. G. Richey, Jr.), Wiley, New York, 2000, pp. 65–105.
125. P. Knochel, A. Krasovskiy and I. Sapountzis, 'Polyfunctional magnesium organometallics for organic synthesis', Chapter 4, in *Handbook of Functionalized Organometallics* (Ed. P. Knochel), Wiley-VCH, 2005.
126. P. Knochel, I. Sapountzis and N. Gommermann, 'Carbon–carbon bond-forming reactions mediated by organomagnesium reagents', in *Metal-Catalyzed Cross-Coupling Reactions* (Eds. A. de Meijere and F. Diederich), 2nd edn., Wiley-VCH, 2004, pp. 619–670.

127. J. Terao, Y. Naitoh, H. Kuniyasu and N. Kambe, *Chem. Lett.*, **32**, 890 (2003).
128. J. Terao, H. Hideyuki, A. Ikumi, H. Kuniyasu and N. Kambe, *J. Am. Chem. Soc.*, **124**, 4222 (2002).
129. A. C. Frisch, N. Shaikh, A. Zapf and M. Beller, *Angew. Chem., Int. Ed.*, **41**, 4056 (2002).
130. A. C. Frisch, F. Rataboul, A. Zapf and M. Beller, *J. Organomet. Chem.*, **687**, 403 (2003).
131. A. Sofia, E. Karlström, K. Itami and J.-E. Bäckvall, *J. Org. Chem.*, **64**, 1745 (1999).
132. J. A. Miller, *Tetrahedron Lett.*, **43**, 7111 (2002).
133. G. Cahiez, C. Chaboche and M. Jezequel, *Tetrahedron*, **56**, 2733 (2000).
134. D. H. Burns, J. D. Miller, H.-K. Chan and M. O. Delaney, *J. Am. Chem. Soc.*, **119**, 2125 (1997).
135. J. Terao, A. Ikumi, H. Kuniyasu and N. Kambe, *J. Am. Chem. Soc.*, **125**, 5646 (2003).
136. J. Terao, H. Todo, S. A. Begum, H. Kuniyasu and N. Kambe, *Angew. Chem., Int. Ed.*, **46**, 2086 (2007).
137. J. G. Donkervoort, J. L. Vicario, J. T. B. H. Jastrzebski, R. A. Gossage, G. Cahiez and G. van Koten, *J. Organomet. Chem.*, **558**, 61 (1998).
138. C. C. Kofink and P. Knochel, *Org. Lett.*, **8**, 4121 (2006).
139. (a) T. Tsuji, H. Yorimitsu and K. Oshima, *Angew. Chem., Int. Ed.*, **41**, 4137 (2002).  
(b) H. Ohmiya, T. Tsuji, Y. Hideki and K. Oshima, *Chem. Eur. J.*, **10**, 5640 (2004).
140. H. Ohmiya, H. Yorimitsu and K. Oshima, *J. Am. Chem. Soc.*, **128**, 1886 (2006).
141. H. Ohmiya, T. Tsuji, H. Yorimitsu and K. Oshima, *Chem. Eur. J.*, **10**, 5640 (2004).
142. M. Nakamura, K. Matsuo, S. Ito and E. Nakamura, *J. Am. Chem. Soc.*, **126**, 3686 (2004).
143. (a) T. Nagano and T. Hayashi, *Org. Lett.*, **6**, 1297, (2004).  
(b) G. Cahiez, V. Habiak, C. Duplais and A. Moyeux, *Angew. Chem., Int. Ed.*, **46**, 4364 (2007).
144. R. B. Bedford, D. W. Bruce, R. M. Frost, J. W. Goodby and M. Hird, *Chem. Commun.*, 2822 (2004).
145. M. Ruben and A. Fürstner, *Angew. Chem., Int. Ed.*, **43**, 3955 (2004).
146. T. Nagano and T. Hayashi, *Chem. Lett.*, **34**, 1152 (2005).
147. (a) H. M. I. Osborn, J. B. Sweeney and W. Howson, *Tetrahedron Lett.*, **35**, 2739 (1994).  
(b) T. Gajda, A. Napieraj, K. Osowska-Pacewiczka, S. Zawadzki and A. Zwierzak, *Tetrahedron*, **53**, 4935 (1997).  
(c) K. Osowska-Pacewiczka and A. Zwierzak, *Synthesis*, 333 (1996).
148. V. G. Nenajdenko, A. S. Karpov and E. S. Balenkova, *Tetrahedron: Asymmetry*, **12**, 2517 (2001).
149. J. E. Baldwin, C. N. Farthing, A. T. Russell, C. J. Schofield and A. C. Spivey, *Tetrahedron Lett.*, **37**, 3761 (1996).
150. S. G. Nelson, Z. Wan and M. A. Stan, *J. Org. Chem.*, **67**, 4680 (2002).
151. D. M. Hodgson, M. J. Fleming and S. J. Stanway, *J. Am. Chem. Soc.*, **126**, 12250 (2004).
152. T.-Y. Luh, *J. Organomet. Chem.*, **653**, 209 (2002) and references therein.
153. L.-F. Huang, C.-H. Huang, B. Stulgies, A. de Meijere and T.-Y. Luh, *Org. Lett.*, **5**, 4489 (2003).
154. (a) T.-M. Yuan, S.-M. Yeh, Y.-T. Hsieh and T.-Y. Luh, *J. Org. Chem.*, **59**, 8192 (1994).  
(b) W.-L. Cheng, Y.-J. Shaw, S.-M. Yeh, P. P. Kanakamma, Y.-H. Chen, C. Chen, J.-C. Shieue, S.-J. Yiin, G.-H. Lee, Y. Wang and T.-Y. Luh, *J. Org. Chem.*, **64**, 532 (1999).
155. J.-W. Huang, C.-D. Chen and M.-K. Leung, *Tetrahedron Lett.*, **40**, 8647 (1999).
156. A. R. Katritzky, X. Lan, J. Z. Yang and O. V. Denisko, *Chem. Rev.*, **98**, 409 (1998).
157. (a) A. R. Katritzky, S. K. Nair and G. Qiu, *Synthesis*, 199 (2002).
158. A. R. Katritzky, X.-L. Cui, B. Yang and P. J. Steel, *Tetrahedron Lett.*, **39**, 1698 (1998).
159. H. Poerwono, K. Higashiyama and H. Takahashi, *J. Org. Chem.*, **63**, 2711 (1998).
160. N. Gommermann, C. Koradin and P. Knochel, *Synthesis*, 2143 (2002).
161. M. Baruah and M. Bols, *J. Chem. Soc., Perkin Trans. 1*, 509 (2002).
162. T. Shintou, W. Kikuchi and T. Mukaiyama, *Chem. Lett.*, **32**, 676 (2003).
163. R. W. Hoffmann and B. Hoelzer, *J. Am. Chem. Soc.*, **124**, 4204 (2002).
164. D. Dakternieks, K. Dunn, D. J. Henry, C. H. Schiesser and E. R. Tieckinck, *Organometallics*, **18**, 3342 (1999).
165. C.-G. Dong and Q.-S. Hu, *Angew. Chem., Int. Ed.*, **45**, 2289 (2006).
166. (a) J. Huang and S. P. Nolan, *J. Am. Chem. Soc.*, **121**, 9889 (1999).

- (b) V. P. W. Böhm, T. Weskamp, C. W. K. Gstöttmayr and W. A. Herrmann, *Angew. Chem., Int. Ed.*, **39**, 1602 (2000).
167. M. G. Organ, M. Mashima and E. Nakamura, *J. Am. Chem. Soc.*, **127**, 17978 (2005).
  168. W. A. Herrmann, V. P. W. Böhm, C. W. K. Gstöttmayr, M. Grosche, C.-P. Reisinger and T. Weskamp, *J. Organomet. Chem.*, **617–618**, 616 (2001).
  169. N. Yoshikai, H. Mashima and E. Nakamura, *J. Am. Chem. Soc.*, **127**, 17978 (2005).
  170. R. Martin and S. L. Buchwald, *J. Am. Chem. Soc.*, **129**, 3844 (2007).
  171. (a) G. Y. Li, *J. Organomet. Chem.*, **653**, 63 (2002).  
(b) L. Ackermann and A. Althammer, *Org. Lett.*, **8**, 3457 (2006).
  172. L. Ackermann, R. Born, J. H. Spatz and D. Meyer, *Angew. Chem., Int. Ed.*, **44**, 7216 (2005).
  173. F. Mongin, L. Mojovic, B. Guillet, F. Trécout, and G. Quéguiner, *J. Org. Chem.*, **67**, 8991 (2002).
  174. G. Y. Li and W. J. Marshall, *Organometallics*, **21**, 590 (2002).
  175. J. Miller and R. P. Farrell, *Tetrahedron Lett.*, **39**, 7275 (1998).
  176. G. Cahiez, F. Lepifre and P. Ramiandrasoa, *Synthesis*, 2138 (1999).
  177. M. Rueping and W. Ieawsuwan, *Synlett*, 247 (2007).
  178. (a) A. H. Roy and J. F. Hartwig, *J. Am. Chem. Soc.*, **125**, 8704 (2003).  
(b) C.-H. Cho, H.-S. Yun and K. Park, *J. Org. Chem.*, **68**, 3017 (2003).  
(c) C.-H. Cho, M. Sun, Y.-S. Seo, C.-B. Kim and K. Park, *J. Org. Chem.*, **70**, 1482 (2005).
  179. J. Clayden, J. J. A. Cooney and M. Julia, *J. Chem. Soc., Perkin Trans. 1*, 7 (1995).
  180. A. M. Roy and J. F. Hartwig, *J. Am. Chem. Soc.*, **125**, 8704 (2003).
  181. J. A. Miller, *Tetrahedron Lett.*, **42**, 6991 (2001).
  182. J. W. Dankwardt, *Angew. Chem., Int. Ed.*, **43**, 2428 (2004).
  183. R. R. Milburn and V. Snieckus, *Angew. Chem., Int. Ed.*, **43**, 888 (2004).
  184. T. K. Macklin and V. Snieckus, *Org. Lett.*, **7**, 2519 (2005).
  185. T. Kamikawa and T. Hayashi, *Tetrahedron Lett.*, **38**, 7087 (1997).
  186. (a) V. Bonnet, F. Mongin, F. Trécout, G. Quéguiner and P. Knochel, *Tetrahedron Lett.*, **42**, 5717 (2001).  
(b) V. Bonnet, F. Mongin, F. Trécout, G. Quéguiner and P. Knochel, *Tetrahedron*, **58**, 4429 (2002).
  187. N. A. Bumagin and E. V. Luzikova, *J. Organomet. Chem.*, **532**, 271 (1997).
  188. Review on advances in iron-catalyzed cross-coupling reactions: A. Fürstner and R. Martin, *Chem. Lett.*, **34**, 624 (2005).
  189. (a) A. Fürstner, A. Leitner, M. Mendez and H. Krause, *J. Am. Chem. Soc.*, **124**, 13856 (2002).  
(b) B. Scheiper, M. Bonnekessel, H. Krause and A. Fürstner, *J. Org. Chem.*, **69**, 3943 (2004).  
(c) A. Fürstner and A. Leitner, *Angew. Chem., Int. Ed.*, **41**, 609 (2002).  
(d) G. Seidel, D. Laurich and A. Fürstner, *J. Org. Chem.*, **69**, 3950 (2004).
  190. J. Quintin, X. Franck, R. Hocquemiller and B. Figadère, *Tetrahedron Lett.*, **43**, 3547 (2002).
  191. (a) T. Nagano and T. Hayashi, *Org. Lett.*, **7**, 491 (2005).  
(b) G. Cahiez, C. Chaboche, F. Mahuteau-Betzer and M. Ahr, *Org. Lett.*, **7**, 1943 (2005).
  192. H. Guo, K.-I. Kanno and T. Takahashi, *Chem. Lett.*, **33**, 1356 (2004).
  193. (a) S. Tasler and B. H. Lipshutz, *J. Org. Chem.*, **68**, 1190 (2003).  
(b) B. H. Lipshutz, S. Tasler, W. Chrisman, B. Spliethoff and B. Tesche, *J. Org. Chem.*, **68**, 1177 (2003).
  194. Y.-H. Cho, A. Kina, T. Shimada and T. Hayashi, *J. Org. Chem.*, **69**, 3811 (2004).
  195. P. Ramiandrasoa, B. Brehon, A. Thivet, M. Alami and G. Cahiez, *Tetrahedron Lett.*, **38**, 2447 (1997).
  196. M. Alami, P. Ramiandrasoa and G. Cahiez, *Synlett*, 325 (1998).
  197. M. Seck, X. Franck, R. Hocquemiller, B. Figadère, J.-F. Peyrat, O. Provot, J.-D. Brion and M. Alami, *Tetrahedron Lett.*, **45**, 1881 (2004).
  198. (a) W. Dohle, F. Kopp, G. Cahiez and P. Knochel, *Synlett*, 1901 (2001).  
(b) G. Cahiez and H. Avedissian, *Synthesis*, 1199 (1998).  
(c) M. Dos Santos, X. Franck, R. Hocquemiller, B. Figadère, J.-F. Peyrat, O. Provot, J.-D. Brion and M. Alami, *Synlett*, 2697 (2004).
  199. K. Itami, S. Higashi, M. Mineno and J.-I. Yoshida, *Org. Lett.*, **7**, 1219 (2005).
  200. N. Yoshikai, H. Mashima and E. Nakamura, *J. Am. Chem. Soc.*, **127**, 17978 (2005).

201. A. S. E. Karlstroem, M. Roenn, A. Thorarensen and J.-E. Bäckvall, *J. Org. Chem.*, **63**, 2517 (1998).
202. M. Die and M. Nakata, *Synlett*, 1511 (2001).
203. C. A. Busacca, M. C. Eriksson and R. Fiaschisi, *Tetrahedron Lett.*, **40**, 3101 (1999).
204. A. S. E. Karlstroem, K. Itami and J.-E. Bäckvall, *J. Org. Chem.*, **64**, 1745 (1999).
205. J. A. Miller, *Tetrahedron Lett.*, **43**, 7111 (2002).
206. G. C. Lloyd-Jones and C. P. Butts, *Tetrahedron*, **54**, 901 (1998).
207. H. Horibe, K. Kazuta, M. Kotoku, K. Kondo, H. Okuno, Y. Murakami and T. Aoyama, *Synlett*, 2047 (2003).
208. A. Krasovskiy, A. Tishkov, V. del Amo, H. Mayr and P. Knochel, *Angew. Chem., Int. Ed.*, **45**, 5010 (2006).
209. A. Kar and N. P. Argade, *Synthesis*, 2995 (2005).
210. J.-E. Bäckvall, E. S. M. Persson and A. Brombrun, *J. Org. Chem.*, **59**, 4126 (1994).
211. A. Yanagisawa, N. Nomura and H. Yamamoto, *Tetrahedron*, **50**, 6017 (1994).
212. M. T. Didiuk, J. P. Morken and A. H. Hoveyda, *J. Am. Chem. Soc.*, **117**, 7273 (1995).
213. B. Breit, P. Demel and C. Studte, *Angew. Chem., Int. Ed.*, **43**, 3786 (2004).
214. (a) J. H. Smitrovich and K. A. Woerpel, *J. Am. Chem. Soc.*, **120**, 12998 (1998).  
(b) J. H. Smitrovich and K. A. Woerpel, *J. Org. Chem.*, **65**, 1601 (2000).
215. S.-K. Kang, D.-G. Cho, C.-H. Park, E.-Y. Namkoong and J.-S. Shin, *Synth. Commun.*, **25**, 1659 (1995).
216. H. Yasui, K. Mizutani, H. Yorimitsu and K. Oshima, *Tetrahedron*, **62**, 1410 (2006).
217. (a) Y. Kobayashi, K. Nakata and T. Ainai, *Org. Lett.*, **7**, 183 (2005).  
(b) M. Ito, M. Matsumi, M. G. Muruges and Y. Kobayashi, *J. Org. Chem.*, **66**, 5881 (2001).
218. (a) M. Kimura, T. Yamazaki, T. Kitazume and T. Kubota, *Org. Lett.*, **6**, 4651 (2004).  
(b) G. J. Meuzelaar, A. S. E. Karlstrom, M. Van Klaveren, E. Persson, A. Del Villar, G. Van Koten and J.-E. Bäckvall, *Tetrahedron*, **56**, 2895 (2000).  
(c) B. Heckmann, C. Mioskowski, R. K. Bhatt and J. R. Falck, *Tetrahedron Lett.*, **37**, 1421 (1996).
219. (a) A. Alexakis, C. Malan, L. Lea, C. Benhaim and X. Fournieux, *Synlett*, 927 (2001).  
(b) K.-G. Chung, Y. Miyake and S. Uemura, *J. Chem. Soc., Perkin Trans. 1*, 2725 (2000).
220. (a) C. A. Falcicola, K. Tissot-Croset and A. Alexakis, *Angew. Chem., Int. Ed.*, **45**, 5995 (2006).  
(b) K. Tissot-Croset, D. Polet and A. Alexakis, *Angew. Chem., Int. Ed.*, **43**, 2426 (2004).  
(c) K. Tissot-Croset and A. Alexakis, *Tetrahedron Lett.*, **45**, 7375 (2004).  
(d) B. L. Feringa, *Acc. Chem. Res.*, **33**, 346 (2000).
221. K. Geurts, S. P. Fletcher and B. L. Feringa, *J. Am. Chem. Soc.*, **128**, 15572 (2006).
222. R. K. Dieter, *Tetrahedron*, **55**, 4177 (1999).
223. C. Duplais, F. Bures, I. Sapountzis, T. J. Korn, G. Cahiez and P. Knochel, *Angew. Chem., Int. Ed.*, **43**, 2968 (2004).
224. O. Labeeuw, P. Phansavath and J.-P. Genet, *Tetrahedron Lett.*, **45**, 7107 (2004).
225. (a) H. Maeda, K. Takahashi and H. Ohmori, *Tetrahedron*, **54**, 12233 (1998).  
(b) H. Maeda, N. Hino, Y. Yamauchi and H. Ohmori, *Chem. Pharm. Bull.*, **48**, 1196 (2000).
226. L. De Luca, G. Giacomelli and A. Porcheddu, *Org. Lett.*, **3**, 1519 (2001).
227. R. C. Klix, S. A. Chamberlin, A. V. Bhatia, D. A. Davis, T. K. Hayes, F. G. Rojas and R. W. Koops, *Tetrahedron Lett.*, **36**, 1791 (1995).
228. B. F. Bonini, M. Comes-Franchini, M. Fochi, G. Mozzanti, A. Ricci and G. Varchi, *Synlett*, 1013 (1998).
229. A. G. Myers and T. Yoon, *Tetrahedron Lett.*, **36**, 9429 (1995).
230. (a) H.-R. Tseng and T.-Y. Luh, *J. Org. Chem.*, **61**, 8685 (1996).  
(b) H.-R. Tseng, C.-F. Lee, L.-M. Yang and T.-Y. Luh, *J. Org. Chem.*, **64**, 8582 (1999).
231. A. Fürstner and M. Mendez, *Angew. Chem., Int. Ed.*, **42**, 5355 (2003).
232. A. R. Katritzky, A. A. A. Abdel-Fattah and M. Wang, *J. Org. Chem.*, **67**, 7526 (2002).
233. (a) X. Liu and J. M. Fox, *J. Am. Chem. Soc.*, **128**, 5600 (2006).  
(b) S. Simaan and I. Marek, *Org. Lett.*, **9**, 2569 (2007).
234. A. H. Hoveyda, N. M. Heron and J. A. Adams, *Grignard Reagents*, Wiley, Chichester, 2000, pp. 107–137.
235. J. Terao, S. Nii, F. A. Chowdhury, A. Nakamura and N. Kambe, *Adv. Synth. Catal.*, **346**, 905 (2004).
236. K. Mizutani, H. Shinokubo and K. Oshima, *Org. Lett.*, **5**, 3959 (2003).

237. H. Ohmiya, K. Wakabayashi, H. Yorimitsu and K. Oshima, *Tetrahedron*, **62**, 2207 (2006).  
238. H. Someya, H. Ohmiya, H. Yorimitsu and K. Oshima, *Org. Lett.*, **9**, 1565 (2007).  
239. Y. Fujii, J. Terao, H. Kuniyasu and N. Kambe, *J. Organomet. Chem.*, **692**, 375 (2007).  
240. J. de Armas and A. H. Hoveyda, *Org. Lett.*, **3**, 2097 (2001).  
241. S. Nii, J. Terao and N. Kambe, *J. Org. Chem.*, **69**, 573 (2004).  
242. H. Watabe, J. Terao and N. Kambe, *Org. Lett.*, **3**, 1733 (2001).  
243. H. Shinokubo and K. Oshima, *Eur. J. Org. Chem.*, **10**, 2081 (2004).  
244. F. Lopez, A. J. Minnaard and B. L. Feringa, *Acc. Chem. Res.*, **40**, 179 (2007).  
245. G. Varchi, A. Ricci, G. Cahiez and P. Knochel, *Tetrahedron*, **56**, 2727 (2000).  
246. K. A. Hansford, J. E. Dettwiler and W. D. Lubell, *Org. Lett.*, **5**, 4887 (2003).  
247. G. J. Leotta, L. E. Overman and G. S. Welmaker, *J. Org. Chem.*, **59**, 1946 (1994).  
248. M. Kikuchi, S. Niikura, N. Chiba, N. Terauchi and M. Asaoko, *Chem. Lett.*, **36**, 736 (2007).  
249. N. Chinkov, N. Morlender-Vais and I. Marek, *Tetrahedron Lett.*, **43**, 6009 (2002).  
250. F. F. Fleming, G. Wei, Z. Zhang and O. W. Steward, *Org. Lett.*, **8**, 4903 (2006).  
251. P. A. Lander and L. S. Hegedus, *J. Am. Chem. Soc.*, **116**, 8126 (1994).  
252. P. G. Andersson, H. E. Schink and K. Oesterlund, *J. Org. Chem.*, **63**, 8067 (1998).  
253. A. Bongini, G. Cardillo, A. Mingardi and C. Tomasini, *Tetrahedron: Asymmetry*, **7**, 1457 (1996).  
254. M. Kanai and K. Tomioka, *Tetrahedron Lett.*, **36**, 4275 (1995).  
255. (a) F. Lopez, S. R. Harutyunyan, A. J. Minnaard and B. L. Feringa, *J. Am. Chem. Soc.*, **126**, 12784 (2004).  
(b) A. Alexakis and C. Benhaim, *Eur. J. Org. Chem.*, **19**, 3221 (2002).  
256. S. Wang, S. Ji and T. Loh, *J. Am. Chem. Soc.*, **129**, 276 (2007).  
257. D. Martin, S. Kehrli, M. D'Augustin, H. Clavier, M. Mauduit and A. Alexakis, *J. Am. Chem. Soc.*, **128**, 8416 (2006).  
258. F. F. Fleming and Q. Wang, *Chem. Rev.*, **103**, 2035 (2003).  
259. (a) F. F. Fleming, V. Gudipati and O. W. Steward, *Org. Lett.*, **4**, 659 (2002).  
(b) F. F. Fleming, V. Gudipati and O. W. Steward, *Tetrahedron*, **59**, 5585 (2003).  
(c) F. F. Fleming, Q. Wang and O. W. Steward, *J. Org. Chem.*, **68**, 4235 (2003).  
(d) F. F. Fleming, Q. Wang and O. W. Steward, *Org. Lett.*, **2**, 1477 (2000).  
260. F. F. Fleming, Z. Zhang, Q. Wang and O. W. Steward, *Angew. Chem., Int. Ed.*, **43**, 1126 (2004).  
261. F. F. Fleming, Z. Zhang, Q. Wang and O. W. Steward, *J. Org. Chem.*, **68**, 7646 (2003).  
262. C.-F. Yao, K.-H. Kao, T.-J. Liu, C.-M. Chu, Y. Wang, W.-C. Chen, Y.-M. Lin, W.-W. Lin, M.-C. Yan, J.-Y. Liu, M.-C. Chuang and J.-L. Shiue, *Tetrahedron*, **54**, 791 (1998).  
263. G. Bartoli, M. Bosco, L. Sembri and E. Marcantoni, *Tetrahedron Lett.*, **35**, 8651 (1994).  
264. S. V. Kolotuchin and A. I. Meyers, *J. Org. Chem.*, **65**, 3018 (2000).  
265. E. Nakamura, K. Kubota and G. Sakata, *J. Am. Chem. Soc.*, **119**, 5457 (1997); mechanism: I. Marek and J.-F. Normant, *Chem. Rev.*, **96**, 3241 (1996).  
266. I. Sapountzis, W. Lin, M. Fischer and P. Knochel, *Angew. Chem., Int. Ed.*, **43**, 4364 (2004).  
267. Y. Shen and J. Yao, *J. Org. Chem.*, **61**, 8659 (1996).  
268. (a) P. Forgione and A. G. Fallis, *Tetrahedron Lett.*, **41**, 11 (2000).  
(b) P. E. Tessier, A. J. Penwell, F. E. S. Souza and A. G. Fallis, *Org. Lett.*, **5**, 2989 (2003).  
(c) A. G. Fallis, *Acc. Chem. Res.*, **32**, 464 (1999).  
269. H. Yorimitsu, J. Tang, K. Okada, H. Shinokubo and K. Oshima, *Chem. Lett.*, **11** (1998).  
270. S. Nishimae, R. Inoue, H. Shimokubo and K. Oshima, *Chem. Lett.*, 785 (1998).  
271. S. Ma and Z. Lu, *Adv. Synth. Catal.*, **348**, 1894 (2006).  
272. E. Shirakawa, T. Yamagami, K. Takafumi, S. Yamaguchi and T. Hayashi, *J. Am. Chem. Soc.*, **127**, 17164 (2005).  
273. K. Murakami, H. Ohmiya, H. Yorimitsu and K. Oshima, *Org. Lett.*, **9**, 1569 (2007).  
274. M. Hatano, T. Miyamoto and K. Ishihara, *Curr. Org. Chem.*, **11**, 127 (2007).  
275. S. Yamazaki and S. Yamabe, *J. Org. Chem.*, **67**, 9346 (2002).  
276. H.-J. Liu, K.-S. Shia, X. Shang and B.-Y. Zhu, *Tetrahedron*, **55**, 3803 (1999).  
277. A. Krasovskiy, F. Kopp and P. Knochel, *Angew. Chem., Int. Ed.*, **45**, 497 (2006).  
278. M. Hatano, S. Suzuki and K. Ishihara, *J. Am. Chem. Soc.*, **128**, 9998 (2006).  
279. M. Hatano, T. Matsumura and K. Ishihara, *Org. Lett.*, **7**, 573 (2005).  
280. S. Matsukawa, Y. Funabashi and T. Imamoto, *Tetrahedron Lett.*, **44**, 1007 (2003).  
281. B. Weber and D. Seebach, *Tetrahedron*, **50**, 6117 (1994).

282. G. Verresha and A. Datta, *Tetrahedron Lett.*, **38**, 5223 (1997).  
283. R. Shintani and G. C. Fu, *Angew. Chem., Int. Ed.*, **41**, 1057 (2002).  
284. S. E. Denmark, Q. Nakajama and O. J.-C. Nicaise, *J. Am. Chem. Soc.*, **116**, 8797 (1994).  
285. R. Bloch, *Chem. Rev.*, **98**, 1407 (1998).  
286. S. E. Denmark and O. J.-C. Nicaise, *Chem. Commun.*, 999 (1996).  
287. H. Urabe, D. Shikanai, K. Arayama, T. Sato and R. Tanaka, *Chem. Lett.*, **36**, 556 (2007).  
288. A. R. Katritzky, Q. Hong and Z. Yang, *J. Org. Chem.*, **60**, 3405 (1995).  
289. A. R. Katritzky, H. Yang and S. K. Singh, *J. Org. Chem.*, **70**, 286 (2005).  
290. T. Franz, M. Hein, U. Veith, V. Jäger, E.-M. Peters, K. Peters and H. G. von Schnering, *Angew. Chem., Int. Ed.*, **33**, 1298 (1994).  
291. A. G. Steinig and D. M. Spero, *J. Org. Chem.*, **64**, 2406 (1999).  
292. K. R. Muralidharan, M. K. Mokhallalati and L. N. Pridgen, *Tetrahedron Lett.*, **35**, 7489 (1994).  
293. S. Roland and P. Mangeney, *Eur. J. Org. Chem.*, 611 (2000).  
294. J. C. A. Hunt, C. Lloyd, C. J. Moody, A. M. Z. Slawin and A. K. Takle, *J. Chem. Soc., Perkin Trans. 1*, 3443 (1999).  
295. A. Solladié-Cavallo and F. Bonne, *Tetrahedron: Asymmetry*, **7**, 171 (1996).  
296. A. K. Saksena, V. M. Girijavallabhan, H. Wang, R. G. Lovey, F. Guenter, I. Mergelsberg and M. S. Puar, *Tetrahedron Lett.*, **45**, 8249 (2004).  
297. P. Cali and M. Begtrup, *Synthesis*, 63 (2002).  
298. (a) J. A. Ellman, T. D. Owens and T. P. Tang, *Acc. Chem. Res.*, **35**, 984 (2002).  
(b) J. A. Ellman, *Pure Appl. Chem.*, **75**, 39 (2003).  
(c) G. Liu, D. A. Cogan and J. A. Ellman, *J. Am. Chem. Soc.*, **119**, 9913 (1997).  
299. (a) F. A. Davis and W. McCoull, *J. Org. Chem.*, **64**, 3396 (1999).  
(b) D. A. Cogan and J. A. Ellman, *J. Am. Chem. Soc.*, **121**, 268 (1999).  
(c) D. A. Cogan, G. Liu and J. A. Ellman, *Tetrahedron*, **55**, 8883 (1999).  
300. J. P. McMahon and J. A. Ellman, *Org. Lett.*, **6**, 1645 (2004).  
301. (a) I. Sapountzis and P. Knochel, *J. Am. Chem. Soc.*, **124**, 9390 (2002).  
(b) Review on the reaction between nitroarenes and Grignard reagents: A. Ricci and M. Fochi, *Angew. Chem., Int. Ed.*, **42**, 1444 (2003).  
(c) Review on modern amination methods: M. Kienle, S. R. Dubbaka, K. Brade and P. Knochel, *Eur. J. Org. Chem.*, **20**, 4166 (2007).  
302. A. Ono, H. Sasaki and F. Yaginuma, *Chem. Ind. (London)*, 480 (1983).  
303. (a) K. Feldman, B. Colasson and V. V. Fokin, *Org. Lett.*, **6**, 3897 (2004).  
(b) C. W. Tornøe, C. Christensen and M. Meldal, *J. Org. Chem.*, **67**, 3057 (2002).  
(c) V. V. Rostovtsev, L. G. Green, V. V. Fokin and K. B. Sharpless, *Angew. Chem., Int. Ed.*, **41**, 2596 (2002).  
(d) J. S. Yadav, B. V. Subba Reddy and V. Geetha, *Synlett*, 513 (2002).  
(e) G. Koebrich and P. Buck, *Chem. Ber.*, **103**, 1412 (1970).  
304. F. Kopp, I. Sapountzis and P. Knochel, *Synlett*, 885 (2003).  
305. W. Dohle, A. Staubitz and P. Knochel, *Chem. Eur. J.*, **9**, 5323 (2003) and references cited therein.  
306. (a) I. Sapountzis and P. Knochel, *Angew. Chem., Int. Ed.*, **43**, 897 (2004).  
(b) P. Sinha and P. Knochel, *Synlett*, 3304 (2006).  
307. (a) G. H. Coleman, *J. Am. Chem. Soc.*, **55**, 3001 (1933).  
(b) F. Klages, G. Neber and F. Kirchner, *Liebigs Ann. Chem.*, **547**, 25 (1941).  
308. P. Sinha and P. Knochel, *Synlett*, 3304 (2006).  
309. (a) M. Kitamura, T. Suga, S. Chiba and K. Narasaka, *Org. Lett.*, **6**, 4619 (2004).  
(b) M. Kitamura, S. Chiba and K. Narasaka, *Bull. Chem. Soc. Jpn.*, **76**, 1063 (2003).  
(c) H. Tsutsui, T. Ichikawa and K. Narasaka, *Bull. Chem. Soc. Jpn.*, **72**, 1869 (1999).  
(d) E. Erdik and T. Daskapan, *J. Chem. Soc., Perkin Trans. 1*, 3139 (1999).  
(e) E.-U. Würthwein and R. Weigmann, *Angew. Chem., Int. Ed.*, **26**, 923 (1987).  
(f) R. A. Hagopian, M. J. Therien and J. R. Murdoch, *J. Am. Chem. Soc.*, **106**, 5753 (1984).  
310. M. J. Campbell and J. S. Johnson, *Org. Lett.*, **9**, 1521 (2007).  
311. T. Murai and F. Asai, *J. Am. Chem. Soc.*, **129**, 780 (2007).  
312. H. Yamamoto and K. Maruoka, *J. Org. Chem.*, **45**, 2739 (1980).  
313. (a) A. Casarini, P. Dembech, D. Lazzari, E. Marini, G. Reginato, A. Ricci and G. Seconi, *J. Org. Chem.*, **58**, 5620 (1993).



- (b) A. Alberti, F. Canè, P. Dembech, D. Lazzari, A. Ricci and G. Seconi, *J. Org. Chem.*, **61**, 1677 (1996).
- (c) F. Canè, D. Brancaleoni, P. Dembech, A. Ricci and G. Seconi, *Synthesis*, 545 (1997).
- (d) P. Bernardi, P. Dembech, G. Fabbri, A. Ricci and G. Seconi, *J. Org. Chem.*, **64**, 641 (1999).
314. (a) V. del Amo, S. R. Dubbaka, A. Krasovskiy and P. Knochel, *Angew. Chem., Int. Ed.*, **45**, 7838 (2006).
- (b) M. Kienle, S. R. Dubbaka, V. del Amo and P. Knochel, *Synthesis*, 1272 (2007).
315. (a) O. Kulinkovich, S. V. Sviridov and D. A. Vasilevski, *Synthesis*, 234 (1991).
- (b) Review on the Kulinkovich reaction: O. G. Kulinkovich and A. de Meijere, *Chem. Rev.*, **100**, 2789 (2000).
- (c) Review on the titanium-mediated synthesis of cyclopropylamines from Grignard reagents and nitriles: A. de Meijere, S. I. Kozhushkov and A. I. Savchenko, *J. Organomet. Chem.*, **689**, 2033 (2004).
316. E. J. Corey, S. A. Rao and M. C. Noe, *J. Am. Chem. Soc.*, **116**, 9345 (1994).
317. C. Cardellicchio, A. Iacuone, F. Naso and P. Tortorella, *Tetrahedron Lett.*, **37**, 6017 (1996).
318. (a) M. A. M. Capozzi, C. Cardellicchio, F. Naso, G. Spina and P. Tortorella, *J. Org. Chem.*, **66**, 5933 (2001).
- (b) M. A. M. Capozzi, C. Cardellicchio, F. Naso and P. Tortorella, *J. Org. Chem.*, **65**, 2843 (2000).
- (c) M. A. M. Capozzi, C. Cardellicchio, F. Naso and V. Rosito, *J. Org. Chem.*, **67**, 7289 (2002).
319. (a) J. L. Garcia Ruano, C. Alemparte, M. Teresa Aranda and M. M. Zarzuelo, *Org. Lett.*, **5**, 75 (2003).
- (b) Z. Han, D. Krishnamurthy, P. Grover, H. S. Wilkinson, Q. K. Fang, X. Su, Z.-H. Lu, D. Magiera and C. H. Senanayake, *Angew. Chem., Int. Ed.*, **42**, 2032 (2003).

## CHAPTER 13

# Iron-Catalyzed Reactions of Grignard Reagents

GÉRARD CAHIEZ and CHRISTOPHE DUPLAIS

*Laboratoire de Synthèse Organique Sélective et de Chimie Organométallique (SOSCO), UMR 8123 CNRS-ESCOM-UCP, 5 Mail Gay Lussac, Neuville <sup>s</sup>/Oise, F-95092 Cergy-Pontoise, France*

*Fax: +33 1 34 25 73 83; e-mail: g.cahiez@escom.fr*

---

I. INTRODUCTION . . . . .	595
II. DEPROTONATION OF KETONES . . . . .	596
III. IRON-CATALYZED ACYLATION OF GRIGNARD REAGENTS . . . . .	599
IV. IRON-CATALYZED CROSS-COUPPLING REACTIONS . . . . .	604
A. Iron-catalyzed Alkenylation of Grignard Reagents . . . . .	604
1. From alkenyl halides . . . . .	604
2. From other alkenyl derivatives . . . . .	608
B. Iron-catalyzed Arylation and Heteroarylation of Alkyl Grignard Reagents . . . . .	610
C. Iron-catalyzed Heteroarylation of Aryl Grignard Reagents . . . . .	614
D. Iron-catalyzed Alkylation of Aryl Grignard Reagents . . . . .	615
V. IRON-CATALYZED HOMOCOUPPLING OF AROMATIC GRIGNARD REAGENTS . . . . .	619
VI. OTHER REACTIONS . . . . .	621
A. Iron-catalyzed Substitution . . . . .	621
B. Carbometallation . . . . .	622
C. Radical Cyclization . . . . .	623
D. Addition to Conjugated Unsaturated Carbonyl Compounds . . . . .	624
VII. APPLICATIONS OF IRON-CATALYZED REACTIONS OF GRIGNARD REAGENTS IN ORGANIC SYNTHESIS . . . . .	625
VIII. REFERENCES . . . . .	628

---

## I. INTRODUCTION

The first attempts to modify the course of the reaction of Grignard reagents with various substrates by using iron salts as a catalyst were reported by Kharasch and coworkers<sup>1–8</sup>

---

*The chemistry of organomagnesium compounds*

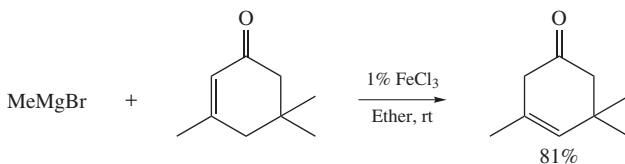
Edited by Z. Rappoport and I. Marek © 2008 John Wiley & Sons, Ltd. ISBN: 978-0-470-05719-3

from 1941 on. The reports mainly treat of the reactions with organic halides and unsaturated ketones. Undoubtedly, Kharasch is the pioneer of the iron-catalyzed reactions of Grignard reagents. Some time afterwards, in 1971, Kochi and coworkers<sup>9–17</sup> published interesting results about the mechanism of the reaction between alkenyl halides and Grignard reagents in the presence of iron salts. Surprisingly, the chemistry of iron-catalyzed Grignard reagents had never been significantly developed until recent years. Indeed, for about 25 years (1975–2000), most of the studies concerning transition-metal-catalyzed Grignard reactions involved copper<sup>18–21</sup> or palladium<sup>22,23</sup> and nickel complexes<sup>24</sup>, and the impressive number of results obtained with these metals<sup>25–28</sup> put the development of the iron chemistry on the back burner.

As a major tool resulting from this period, palladium- and nickel-catalyzed cross-coupling reactions are now increasingly used for industrial applications. However, sustainable development is currently an essential part in the strategy of chemical industries and the search for more economic and more eco-friendly synthetic methods is of vital concern. As a consequence, palladium and nickel complexes, which are toxic and/or expensive, have to be replaced by other more convenient catalysts. Iron salts are good candidates since iron is a very cheap metal having no significant toxicological properties. Because of this, in the last decade, the iron-catalyzed cross-coupling reactions of Grignard reagents have been extensively studied. Since the first preparative procedure reported by Cahiez and Avedissian<sup>29</sup> in 1998, the number of publications<sup>30–32</sup> has clearly increased.

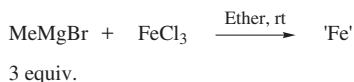
## II. DEPROTONATION OF KETONES

During their investigations, Kharasch and Tawney<sup>2,6</sup> studied the reaction of methylmagnesium bromide with isophorone in the presence of various transition metal salts in diethyl ether. In a first report<sup>2</sup>, they showed that with iron(III) chloride a major product is formed, but they failed to characterize it. A few years later<sup>6</sup>, they established that this product is the deconjugated ketone (Scheme 1).



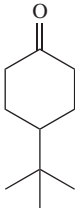
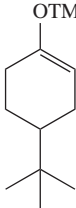
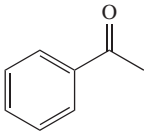
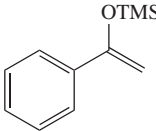
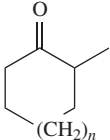
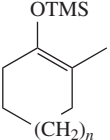
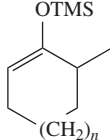
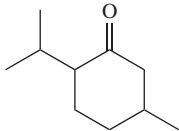
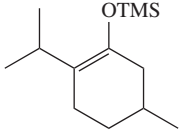
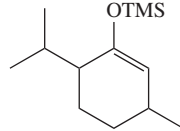
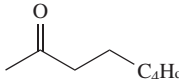
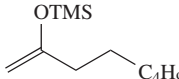
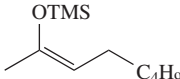
SCHEME 1

This result received no attention until 1984 when Krafft and Holton<sup>33,34</sup> decided to reinvestigate this reaction. The expected enolate was trapped with trimethylchlorosilane to form the corresponding silyl enol ether. Their first attempts showed that unsaturated and saturated ketones react with Grignard reagents in the presence of iron salts to produce substantial amount of a tertiary alcohol resulting from a 1,2-addition. They discovered that this side reaction can be suppressed by using a reagent ('Fe') (see Section IV.B) prepared by addition of three equivalents of methylmagnesium bromide to one equivalent of iron(III) chloride (Scheme 2).



SCHEME 2

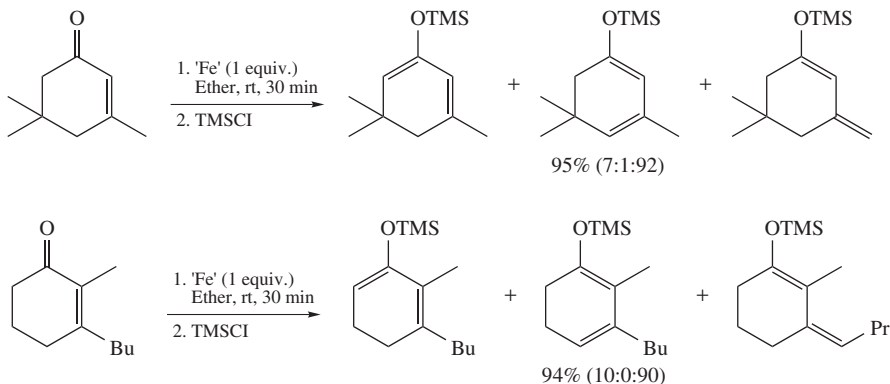
TABLE 1. Regioselective preparation of trimethylsilyl enol ether

$\text{R}^1\text{---CH}_2\text{---C(=O)---R}^2 \xrightarrow[\text{2. TMSCl}]{\text{1. 'Fe' (1. equiv.)}, \text{Ether, rt, 30 min}} \text{R}^1\text{---CH=C(OTMS)---R}^2$		
Ketone	Trimethylsilyl enol ethers (ratio)	Yield (%)
		98
		92
	 (97:3)  (93:7)	99 90
$n = 1$ $n = 2$		
	 (98:2) 	97
	 (80:20) 	95

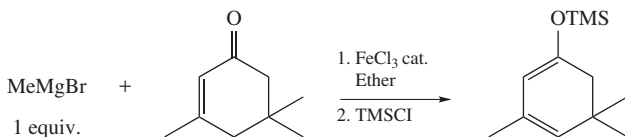
Under these conditions<sup>33</sup>, various cyclic and acyclic ketones were successfully deprotonated. After addition of trimethylchlorosilane, the thermodynamically more stable trimethylsilyl enol ether was obtained as a major product in excellent yield (Table 1).

It is important to note that, under the same conditions, isophorone or other  $\beta$ -alkyl cyclic enones predominantly afford the exocyclic conjugated silyl dienol ether<sup>34</sup> (Scheme 3).

On the contrary, the endocyclic conjugated silyl dienol ether is almost exclusively formed under the Kharasch conditions<sup>33</sup> (Scheme 4).



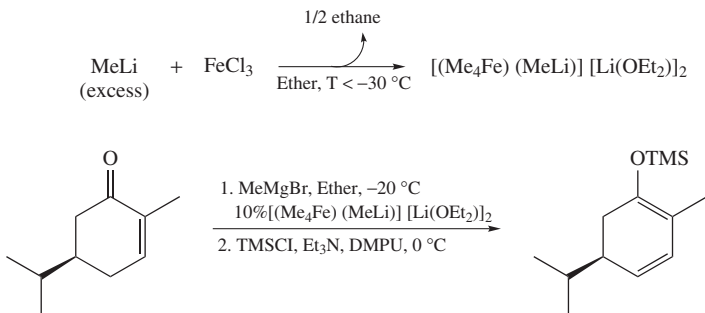
SCHEME 3



SCHEME 4

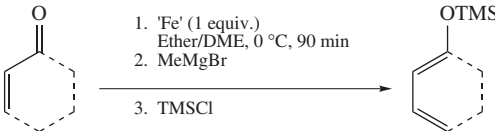
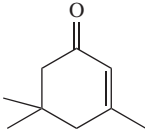
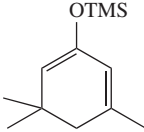
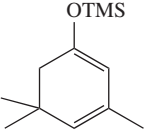
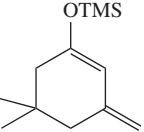
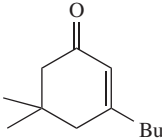
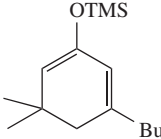
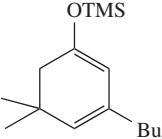
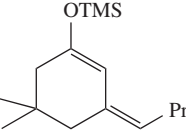
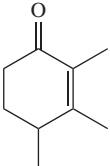
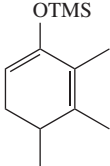
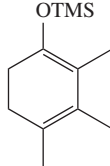
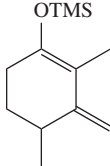
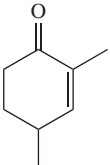
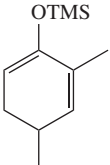
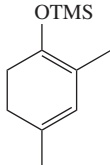
The endocyclic silyl dienol ether<sup>34</sup> is also obtained as the major product when the conjugated cyclic enone is successively treated with the 'Fe' complex prepared according to Scheme 2, then with one equivalent of methylmagnesium bromide (Table 2). This is interesting since these products are difficult to obtain otherwise. The mechanism of this unusual reaction remains obscure.

Recently, F rstner and coworkers<sup>35</sup> have prepared a 'super-ate' complex of iron(II) as shown in Scheme 5. The structure was fully characterized by X-ray crystallography. They have shown that methylmagnesium bromide reacts with pulegone in the presence of this complex to give the corresponding endocyclic silyl dienol ether. Consequently, they have proposed that a similar 'ate-complex' is probably involved when the reaction is performed under the Kharasch conditions.



SCHEME 5

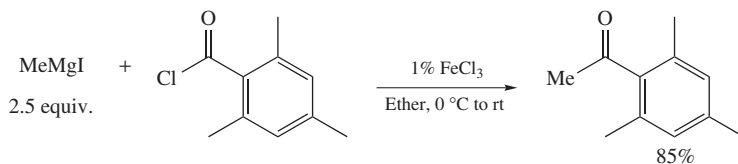
TABLE 2. Regioselective preparation of trimethylsilyl dienol ethers

				
Enone	Dienol ethers (ratio)			Yield (%)
				99
	(2:96:2)			
				98
	(1:99:0)			
				90
	(4:92:4)			
				93
	(5:95)			

### III. IRON-CATALYZED ACYLATION OF GRIGNARD REAGENTS

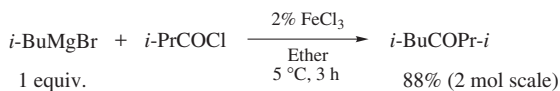
The first iron-catalyzed acylation of Grignard reagents was described by Kharasch and coworkers<sup>5</sup> in 1944 (Scheme 6). They reported only one example of reaction between methylmagnesium iodide and mesitoyl chloride in the presence of iron(III) chloride in diethyl ether.

In 1953, Percival and coworkers<sup>36</sup> showed that aliphatic ketones can be prepared under these conditions. Unfortunately, in the case of linear aliphatic ketones the reaction only gives moderate yields, since the Grignard reagent adds to the ketone or behaves as a base



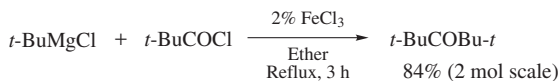
SCHEME 6

to deprotonate the starting carboxylic acid chloride (dehydrochlorination). However, in the case of hindered ketones both side reactions are considerably limited. As an example, 2,5-dimethylhexan-3-one was obtained in 88% yield by reacting isobutyryl chloride with *i*-butylmagnesium bromide, in diethyl ether at 5 °C, in the presence of 2% iron(III) chloride (Scheme 7).



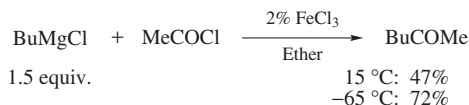
SCHEME 7

It is necessary to operate under reflux to obtain good yields when more hindered Grignard reagents are used (Scheme 8).



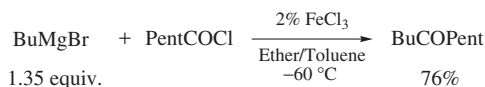
SCHEME 8

With linear aliphatic carboxylic acid chlorides, such as acetyl chloride, Percival and coworkers pointed out that it is possible to prevent the side reactions previously described by performing the reaction at low temperature (Scheme 9).

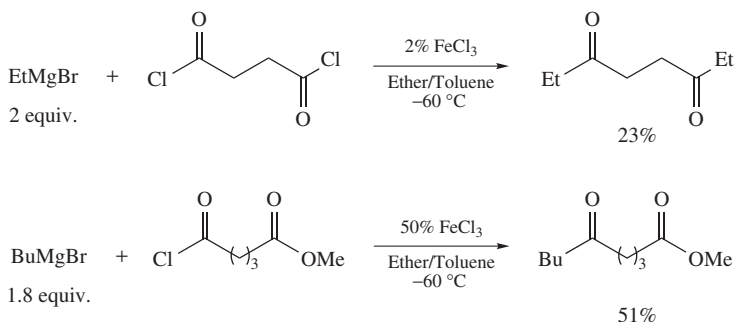


SCHEME 9

In 1961, to improve these results, Cason and Kraus<sup>37</sup> used a diethyl ether/toluene mixture as a solvent. Unfortunately, yields of ketone are never better than 80% (Scheme 10).



SCHEME 10

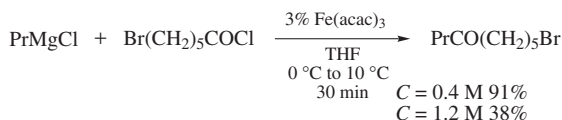


SCHEME 11

In addition, the reaction is not chemoselective, thus carboxylic diacid chlorides and carboxylic acid chlorides bearing an ester group give unsatisfactory yields of ketone (Scheme 11)<sup>38,39</sup>.

Twenty-five years later, a dramatic improvement was reported by Fiandanese, Marchese and coworkers<sup>40–42</sup>. They discovered that excellent yields of ketone were obtained when diethyl ether is replaced by THF. Moreover, iron acetylacetonate is used as a catalyst instead of iron(III) chloride because it is not hygroscopic and easier to handle. The scope of the procedure is very large and the reaction occurs highly chemoselectively under mild conditions (0 °C). It should be noted that excellent yields are obtained from stoichiometric amounts of Grignard reagents (Table 3).

Unfortunately, the yield depends highly on the concentration of the reaction mixture (Scheme 12). As shown below<sup>43</sup>, in the case of the reaction of 6-bromohexanoyl chloride with propylmagnesium chloride, the yield jumps from 38% to 91% when the concentration decreases from 1.2 M to 0.4 M. It is a drawback for large-scale applications since the concentration cannot be higher than 0.5 M.



SCHEME 12

The main limitation of this procedure is the preparation of aromatic ketones from aryl Grignard reagents and aromatic carboxylic acid chlorides that are clearly less reactive than their aliphatic analogues. In this case, the ketones are only obtained in moderate yields because of the formation of a large amount of homocoupling product (diaryl). It is possible to improve the yield of diaryl ketone by using an excess of aryl Grignard reagent, but the purification of the product is then very delicate due to the presence of a huge amount of homocoupling product. Cahiez, Knochel and coworkers<sup>44</sup> showed that the side reaction is completely avoided when the starting aromatic carboxylic acid chloride is replaced by the corresponding cyanide (Scheme 13).

Functionalized aryl Grignard compounds, prepared by iodine–magnesium exchange according to the procedure reported by Cahiez, Knochel and coworkers<sup>45</sup> in 1998, can be efficiently acylated. It is thus possible to prepare various polyfunctionalized diaryl ketones (Scheme 14)<sup>44</sup>.

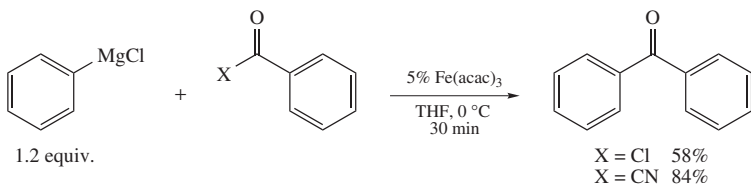


TABLE 3. Iron-catalyzed acylation of Grignard reagents in THF

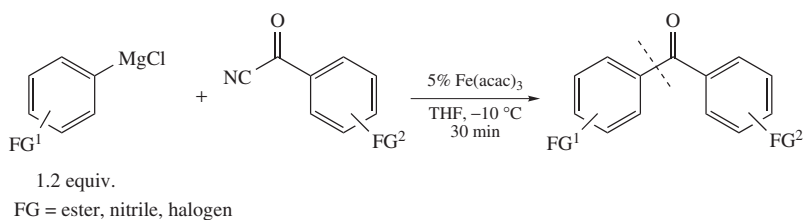
$  \begin{array}{c}  \text{R}^1\text{MgCl} + \text{Cl}-\text{C}(=\text{O})-\text{R}^2 \\  \text{1 equiv.} \quad \text{1 equiv.}  \end{array}  \xrightarrow[\text{0 } ^\circ\text{C to rt, 30 min}]{\text{3\% Fe(acac)}_3, \text{THF}}  \text{R}^1-\text{C}(=\text{O})-\text{R}^2  $			
R <sup>1</sup>	R <sup>2</sup> COCl	Product	Yield (%)
Me	DecCOCl		84
Pent	PentCOCl		82
Dec	MeCOCl		80
<i>i</i> -Pr	BuCOCl		80
<i>t</i> -Bu	BuCOCl		70
Ph	BuCOCl		83
Ph	<i>i</i> -PrCOCl		92
Bu	PhCOCl		90
Et <sup>a</sup>			90
Me	NCC <sub>6</sub> H <sub>4</sub> COCl		75

TABLE 3. (continued)

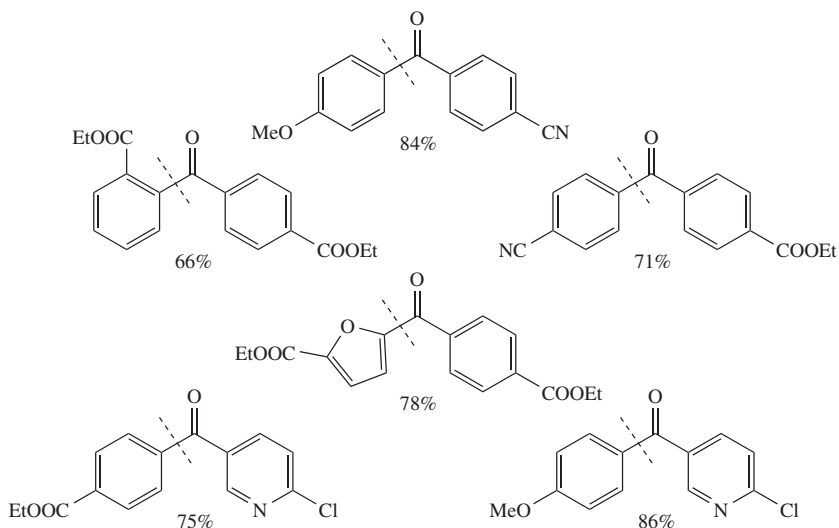
R <sup>1</sup>	R <sup>2</sup> COCl	Product	Yield (%)
Bu	MeOOCCH <sub>2</sub> H <sub>4</sub> COCl		78

<sup>a</sup> 2 equivalents of EtMgBr were used.

SCHEME 13



The following diaryl ketones were prepared according to this procedure.



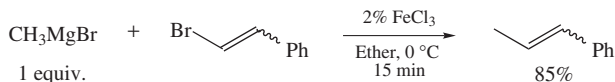
SCHEME 14

#### IV. IRON-CATALYZED CROSS-COUPLING REACTIONS

##### A. Iron-catalyzed Alkenylation of Grignard Reagents

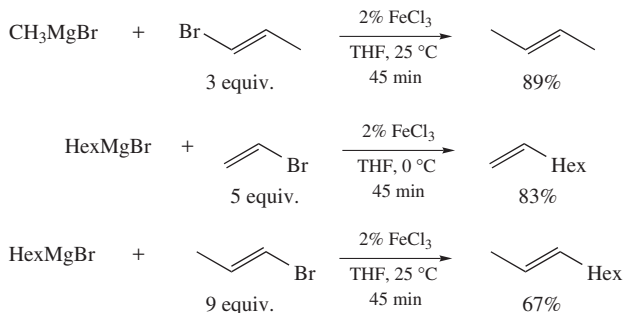
###### 1. From alkenyl halides

The first example of iron-catalyzed cross-coupling reaction between Grignard reagents and alkenyl bromides was reported by Kharasch and Fuchs<sup>7</sup> in 1945 (Scheme 15).



SCHEME 15

In 1971, Tamura and Kochi<sup>9,10</sup> described the reaction of alkyl Grignard reagents with alkenyl bromides in the presence of iron(III) chloride in THF. Only very reactive substrates such as vinyl and propenyl bromide were used (Scheme 16). Yields of coupling product are moderate to good but, unfortunately, a large excess of alkenyl bromide is required (3 to 9 equivalents). (*E*)-Bromopropene reacts 15 times faster than the (*Z*)-isomer. It should be noted that the reaction is stereoselective.



SCHEME 16

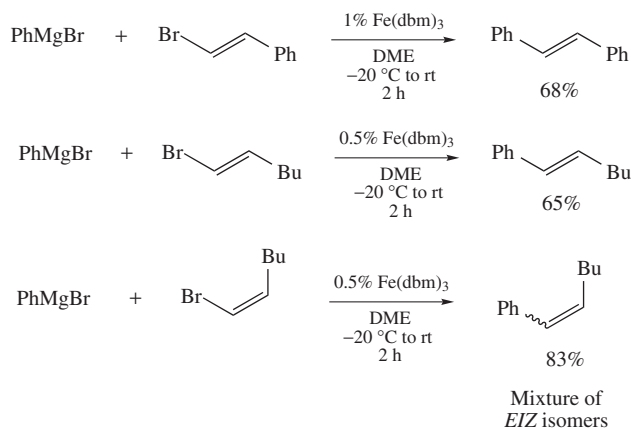
The results published thereafter by Kochi's group are especially interesting from a mechanistic point of view<sup>13-15</sup>. Indeed, for preparative chemistry the yields are not satisfactory and the reaction is limited to reactive alkenyl bromides such as propenyl and styryl bromides (Table 4). Neumann and Kochi<sup>13</sup> were the first to replace iron(III) chloride by iron(III) acetylacetonate or related complexes such as Fe(dbm)<sub>3</sub> (iron tris-dibenzoylmethanato) that are less hygroscopic and easier to handle.

In 1983, Molander and coworkers<sup>46</sup> studied the coupling of aromatic Grignard reagents with 2-bromostyrene. They showed that the use of dimethoxyethane (DME) instead of tetrahydrofuran as a solvent significantly increases the yields (from *ca* 30% to 60–70%). However, the reaction is always limited to reactive alkenyl bromides. Moreover, while (*E*)-alkenyl bromides always lead to satisfactory yields, the corresponding (*Z*)-stereomers give either low yields of coupling product or mixtures of stereomers (Scheme 17). Similar results were observed by Smith and Kochi<sup>14</sup> in other cases when a hindered Grignard reagent was used.

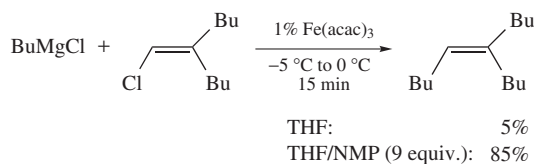
In 1998, Cahiez and Avedissian<sup>29</sup> discovered that the addition of *N*-methylpyrrolidinone (NMP, 4 to 9 equivalents) to the reaction mixture allows one to obtain excellent yields (Scheme 18). In addition, only a stoichiometric amount of alkenyl halide is then required. Under these conditions, the reaction takes place almost instantaneously even from low

TABLE 4. Iron-catalyzed coupling of Grignard reagents with alkenyl bromides

$\text{R}^1\text{MgBr} + \text{Br}-\text{CH}=\text{CH}-\text{R}^2 \xrightarrow[\text{THF, 25 } ^\circ\text{C, 45 min}]{3\% \text{ Fe(dbm)}_3} \text{R}^1-\text{CH}=\text{CH}-\text{R}^2$ $3 \text{ equiv.}$		
R <sup>1</sup>	R <sup>2</sup>	Yield (%)
Et	Me	58
Ph	Ph	32
Et	Ph	59
<i>i</i> -Pr	Me	60
<i>c</i> -Hex	Me	54
<i>t</i> -Bu	Me	27



SCHEME 17



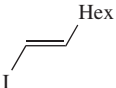

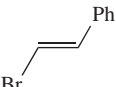
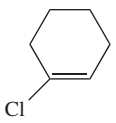
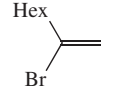
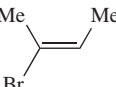
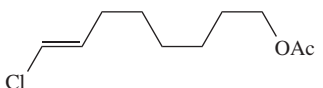
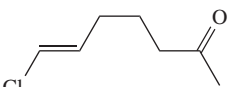
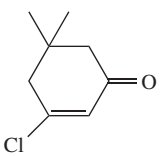
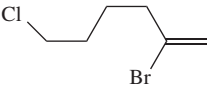
SCHEME 18

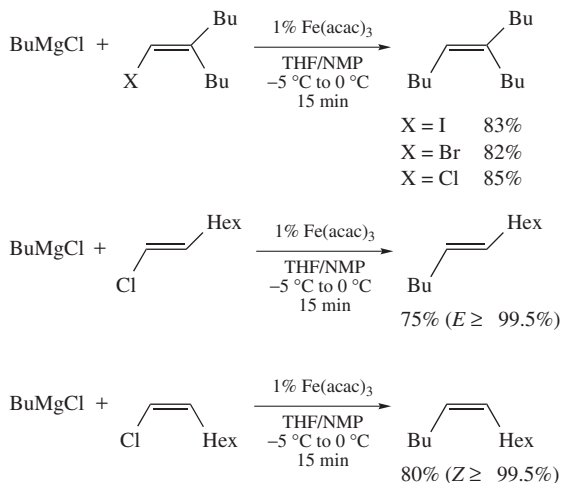
reactive substrates such as  $\beta,\beta$ -disubstituted alkenyl chlorides. It should be noted that NMP is a very cheap additive that was not frequently used before with Grignard reagents.

Only 1 to 3% iron(III) acetylacetonate are required and the scope of the reaction is very large. A vast array of alkenyl iodides, bromides and even chlorides can be successfully used and the stereoselectivity is excellent even in the case of the *Z*-alkenyl halides (Scheme 19).

In addition, the reaction is very chemoselective and even a keto group is tolerated (Table 5). It should be underlined that this procedure compares advantageously to the corresponding palladium- or nickel-catalyzed coupling reactions.

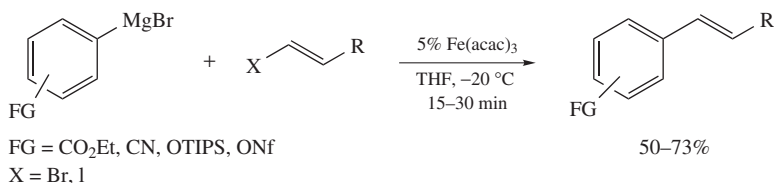
TABLE 5. Iron-catalyzed coupling of Grignard reagents with alkenyl halides

$R^1MgCl$ 1.1 equiv.	$  \begin{array}{c}  R^2 \quad R^3 \\  \diagdown \quad \diagup \\  C=C \\  \diagup \quad \diagdown \\  X \quad R^4  \end{array}  $	$  \xrightarrow[\substack{\text{THF/NMP} \\ -5^\circ\text{C to } 0^\circ\text{C} \\ 15 \text{ min}}]{1\% \text{ Fe}(\text{acac})_3}  $	$  \begin{array}{c}  R^2 \quad R^3 \\  \diagdown \quad \diagup \\  C=C \\  \diagup \quad \diagdown \\  R^1 \quad R^4  \end{array}  $
$R^1$	Alkenyl Halides		Yield (%)
<i>s</i> -Bu			80
<i>c</i> -Hex			89
<i>t</i> -Bu			64
Bu			75
<i>i</i> -Pr			72
Oct			84
Bu			80
Bu			80
Bu			79
Bu			79



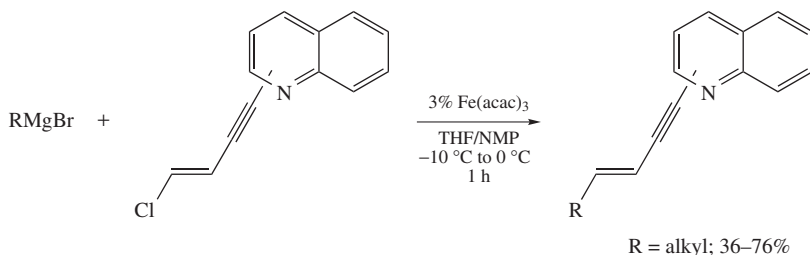
SCHEME 19

In 2001, Cahiez, Knochel and coworkers<sup>47</sup> reported an extension of this work to the coupling of functionalized arylmagnesium compounds with alkenyl bromides or iodides (Scheme 20). It should be noted that with aryl Grignard reagents the use of NMP is not necessary.

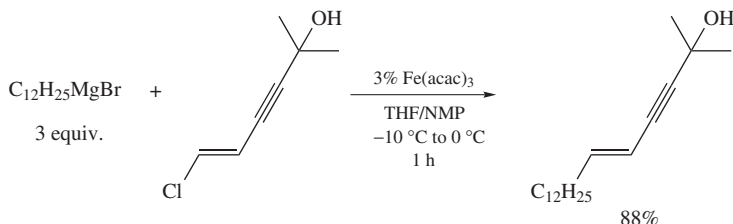


SCHEME 20

The conditions described above were used by Figadère, Alami and coworkers<sup>48</sup> to prepare analogues of meglumine antimonate (Glucantime<sup>®</sup>), a product used in chemotherapy, from chloroenynes or chlorodienes (Scheme 21). The reaction was further extended to various chloroenynes (Scheme 22).

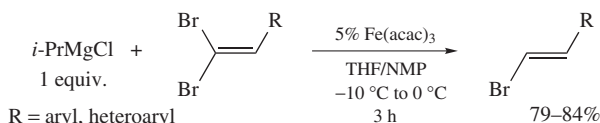


SCHEME 21



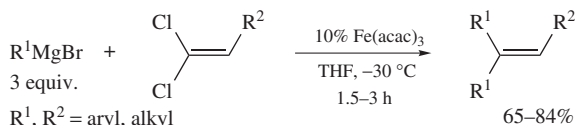
SCHEME 22

In 2002, Figad re and coworkers<sup>49,50</sup> reported the mono-reduction of 2-aryl (or heteroaryl)-1,1-dibromo-1-alkenes (Scheme 23). The reaction is achieved with one equivalent of isopropylmagnesium chloride in the presence of iron(III) acetylacetonate. Pure (*E*)-alkenyl bromides are obtained. With two equivalents of alkyl Grignard reagent, the mono-substituted product is obtained in moderate yield.



SCHEME 23

It is noteworthy that 1,1-dichloro-1-alkenes behave differently; the reduction is not observed and both chlorine atoms are substituted<sup>51</sup>. Satisfactory yields are obtained by using an excess of Grignard reagent (Scheme 24).



SCHEME 24

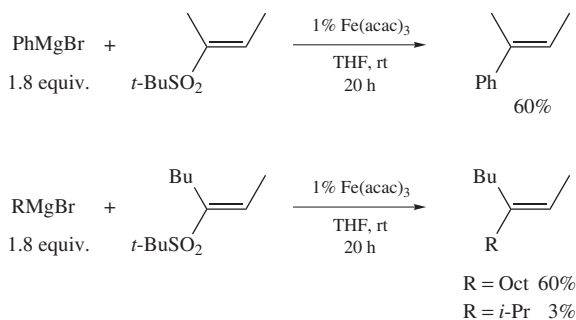
## 2. From other alkenyl derivatives

In 1982, Julia's group<sup>52–55</sup> showed that vinyl sulfones react with Grignard reagents in the presence of iron salts to afford moderate yields of coupling product (Scheme 25). The reaction is stereoselective but its scope is limited. Thus, with secondary alkylmagnesium halides, only the reduction product is formed.

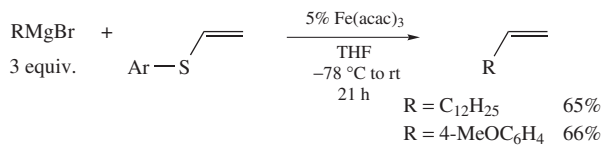
The iron-catalyzed cross-coupling between Grignard reagents and alkenyl sulfides was also studied (Scheme 26)<sup>56</sup>. Unfortunately, this reaction is very sensitive to steric and electronic effects and only two products were synthesized in modest yields. In fact, the scope of the reaction is very limited since only vinyl sulfides can be used.

In 1998, Cahiez and Avedissian<sup>29</sup> reported that enol phosphates can be used instead of alkenyl halides (Scheme 27).

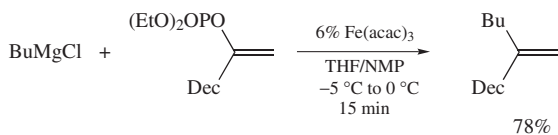
As expected, enol triflates also couple under these conditions (Scheme 28). Thus, F rstner and coworkers<sup>57</sup> have recently shown that various cyclic and acyclic enol triflates can be used successfully.



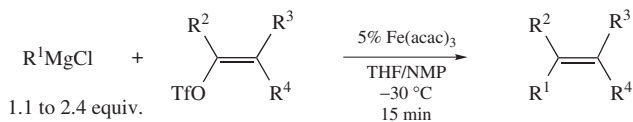
SCHEME 25



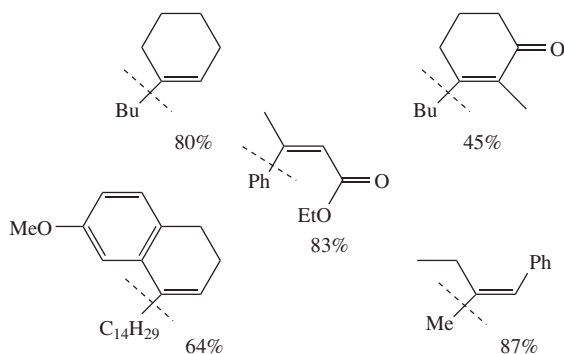
SCHEME 26



SCHEME 27

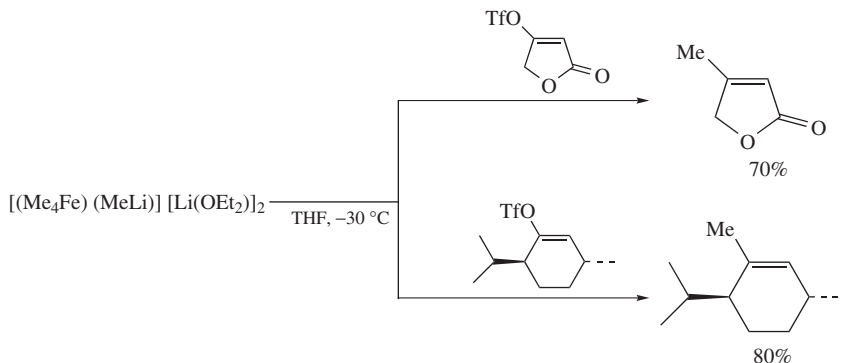


The following coupling products were prepared according to this procedure



SCHEME 28



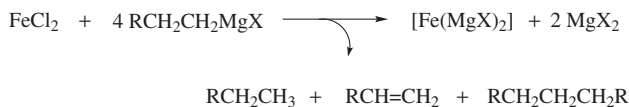


SCHEME 29

It is interesting to note that the ‘super’ iron(II) ate complex prepared by F rstner and coworkers<sup>35</sup> leads to good yields of methylated product (Scheme 29).

## B. Iron-catalyzed Arylation and Heteroarylation of Alkyl Grignard Reagents

In 2002, F rstner and coworkers<sup>58,59</sup> reported that aryl halides react with Grignard reagents under the conditions previously used for the coupling of alkenyl halides. They proposed that the active iron species is  $\text{Fe}(\text{MgX})_2$ , a complex described by Bogdanovic and coworkers<sup>60</sup> a few years earlier (Scheme 30). This iron(-II) species is formed by addition of four equivalents of the Grignard compounds to  $\text{FeCl}_2$ .



SCHEME 30

The tentative catalytic cycle is presented in Figure 1. The scope of this reaction is unusual since excellent yields are obtained from aryl chlorides, tosylates and triflates

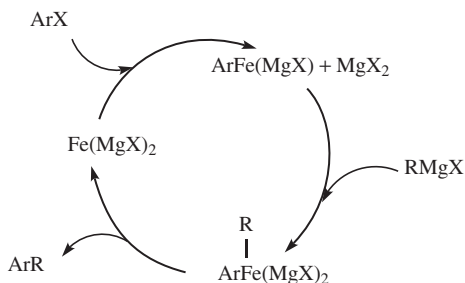
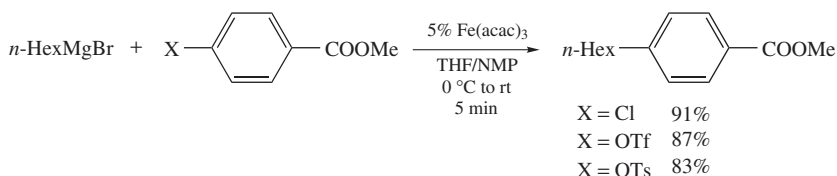
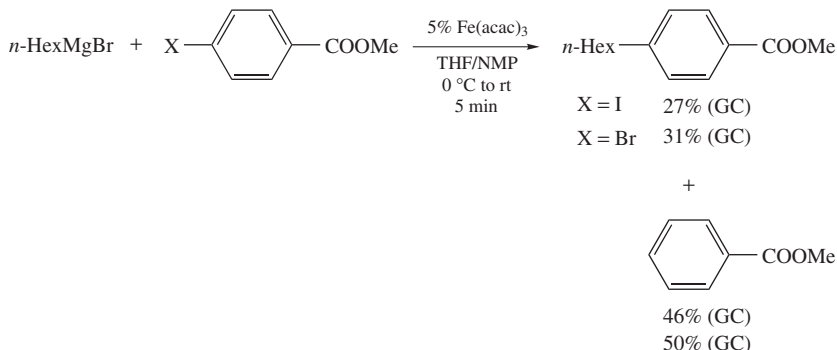


FIGURE 1



SCHEME 31



SCHEME 32

(Scheme 31), whereas the corresponding bromides and iodides lead to a mixture of coupling and reduction products (Scheme 32).

All electron-poor aryl chlorides, tosylates, triflates and heteroaryl chlorides react to give good to excellent yields. However, in the case of electron-rich aryl groups, only aryl triflates are reactive enough to give satisfactory yields of coupling product. It should be noted that a vast array of heteroaryl chlorides were used successfully (Table 6). The scope of the reaction is more limited regarding the nature of the Grignard reagents. Thus, only primary alkyl Grignard reagents afford good yields. With secondary alkylmagnesium halides, the yield of coupling product never rises above 50%.

Hocek and coworkers<sup>61–63</sup> studied the regioselectivity of the cross-coupling reaction between methylmagnesium bromide and various dichloropurines. With 2,6- and 2,8-dichloropurines, it is possible to obtain the monomethylated product with an excellent regioselectivity (Scheme 33). It is important to notice that such a regioselectivity is not observed under palladium or nickel catalysis.

However, the selectivity depends closely on the difference in reactivity between the two chlorine atoms. As an example, 6,8-dichloropurine gives a mixture of monosubstituted products (Scheme 34).

Sometimes, by using an excess of Grignard reagents, both chlorine atoms can be substituted (Scheme 35).

Recently, Olsson and coworkers<sup>64</sup> have reported a cross-coupling reaction between seven-membered cyclic imidoyl chlorides and alkyl Grignard reagents (Scheme 36). The corresponding substituted imines, which are very difficult to prepare otherwise, are synthesized in good to excellent yields.

Later, Olsson and coworkers<sup>64</sup> proposed a general method to prepare simple acyclic imines from amides according to a two-step procedure (Scheme 37).

TABLE 6. Cross-coupling between alkyl Grignard reagents and aryl or heteroaryl chlorides, triflates, and tosylates

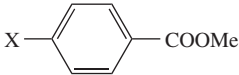
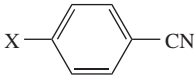
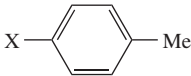
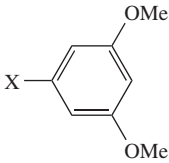
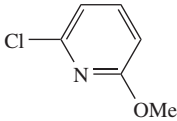
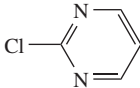
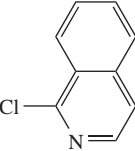
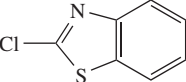
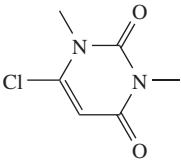
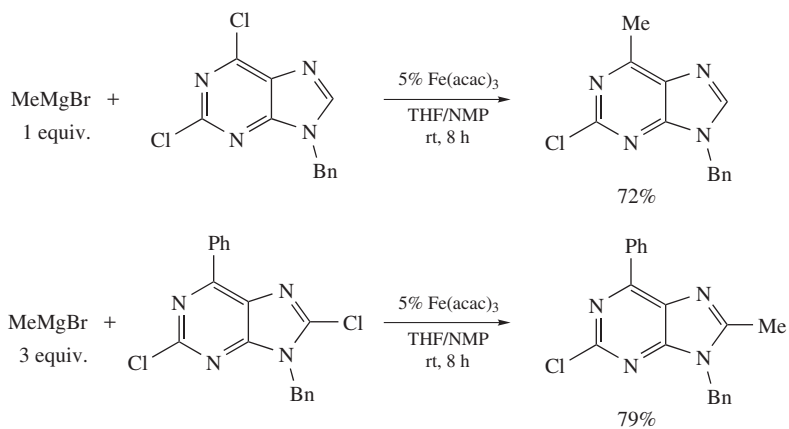
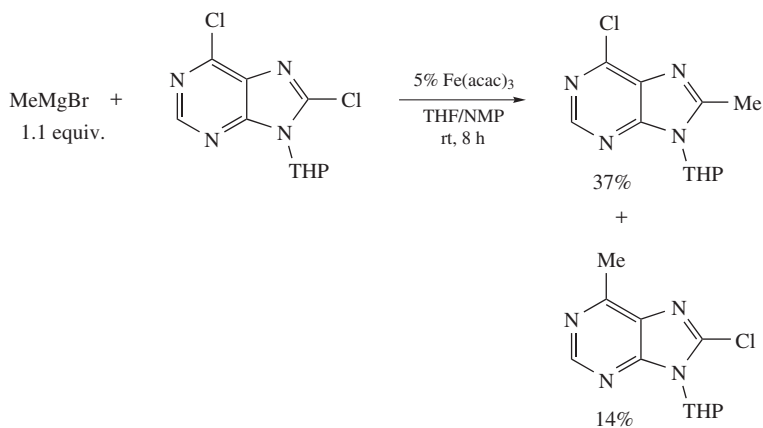
$n\text{-HexMgBr} + \text{ArX} \xrightarrow[\text{THF/NMP, 0 } ^\circ\text{C to rt, 20 min}]{5\% \text{ Fe(acac)}_3}$ $1.2 \text{ equiv.}$ $\text{X} = \text{Cl, OTs, OTf}$		$n\text{-Hex}-\text{Ar}$	
ArX		Yield (%)	
		91 (X = Cl)	
		87 (X = OTf)	
		83 (X = OTs)	
		91 (X = Cl)	
		87 (X = OTf)	
		83 (X = OTs)	
		0 (X = Cl)	
		81 (X = OTf)	
		0 (X = Cl)	
		90 (X = OTf)	
		95	
		93	
		95	
		68	

TABLE 6. (continued)

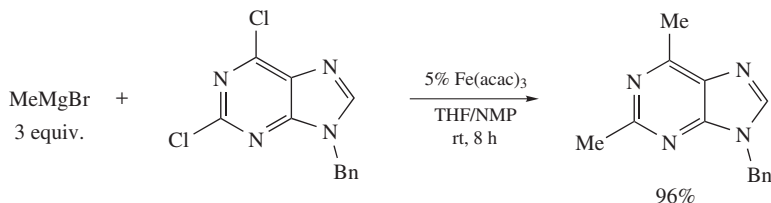
ArX	Yield (%)
	60



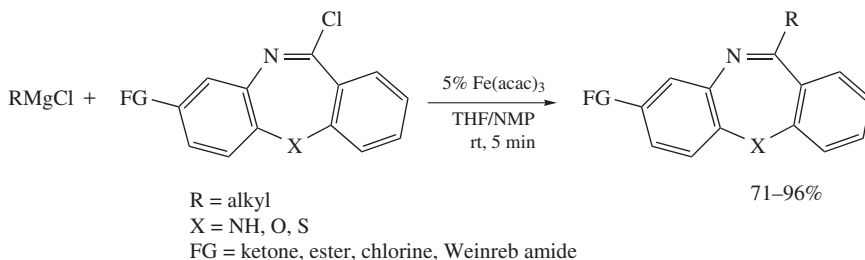
SCHEME 33



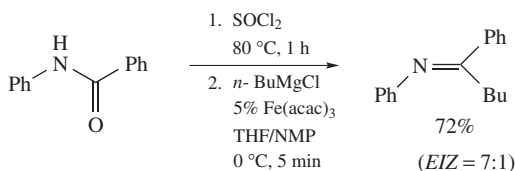
SCHEME 34



SCHEME 35



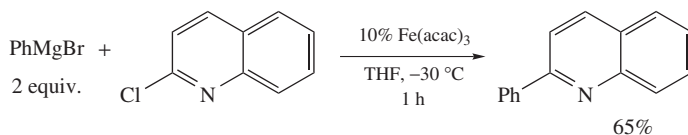
SCHEME 36



SCHEME 37

### C. Iron-catalyzed Heteroarylation of Aryl Grignard Reagents

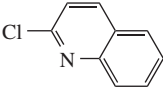
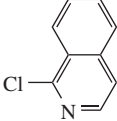
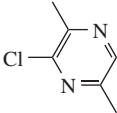
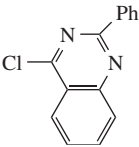
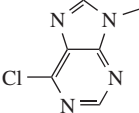
Iron-catalyzed aryl–aryl coupling reactions generally lead to poor yields of cross-coupling product since the homocoupling of the starting Grignard reagent mainly occurs (see above). However, in the case of heteroaryl halides, moderate yields of cross-coupling product can be obtained by using an excess of aryl Grignard reagent. Thus, Figad re and coworkers<sup>65</sup> synthesized 2-phenylquinoline in 65% yield (Scheme 38).



SCHEME 38

F rstner and coworkers<sup>58,59</sup> also reported various examples of coupling with nitrogen heteroaryl chlorides (Table 7). In all cases, at least two equivalents of phenylmagnesium bromide are required and the yield never rises above 71%.

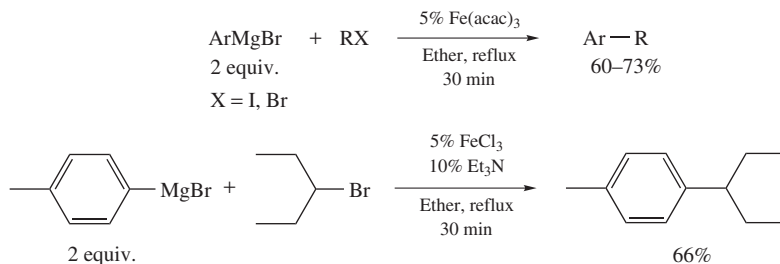
TABLE 7. Cross-coupling between phenylmagnesium bromide and heteroaryl chlorides

PhMgBr + RCl	$\xrightarrow[\text{THF, } -30\text{ }^{\circ}\text{C}]{5\% \text{ Fe(acac)}_3, 20 \text{ min}}$	Ar—R
2.3 equiv.		
R = heteroaryl		
RCl	Yield (%)	
	71	
	57	
	64	
	66	
	60	

#### D. Iron-catalyzed Alkylation of Aryl Grignard Reagents

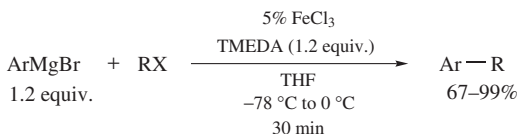
Recently, this reaction has been extensively studied since it is currently the only method to couple aryl Grignard reagents with secondary alkyl halides<sup>12,16</sup>. Indeed, secondary alkyl halides do not react under palladium or nickel catalysis<sup>66</sup>. On the other hand, let us recall that the coupling of secondary alkyl Grignard reagents with aryl halides leads to poor results (see above).

The reaction can be performed in diethyl ether in the presence of iron(III) acetylacetonate, as reported by Nagano and Hayashi<sup>67</sup> in 2004, or in the presence of FeCl(salen) or iron(III) chloride/triethylamine, as described by Bedford and coworkers<sup>68</sup> (Scheme 39). The latter compared several ligands (amines<sup>69</sup>, phosphines<sup>70</sup>) and the best results were obtained with triethylamine, TMEDA or DABCO. In all cases, the reactions have to be performed in refluxing diethyl ether and the Grignard reagent has to be added at once! Unfortunately, these reaction conditions are only useable on a very small scale (1 mmol) but they cannot be used for large-scale applications.



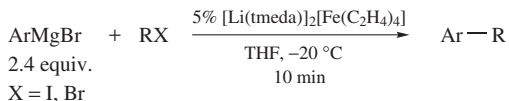
SCHEME 39

As shown by Nakamura and coworkers<sup>71</sup> in 2004, the reaction also takes place in THF in the presence of iron(III) chloride (Scheme 40). However, it is necessary to add a huge amount of TMEDA (120% for 5% FeCl<sub>3</sub>). Primary and secondary alkyl halides were coupled successfully. It is important to note that the results clearly depend on the origin of the iron(III) chloride<sup>72</sup>.

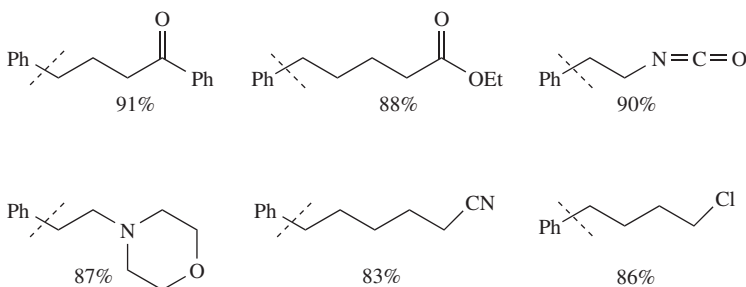


SCHEME 40

Martin and F rstner<sup>73</sup> showed that an iron(-II) complex can be used as a precatalyst. This result is very interesting for mechanistic considerations. Unfortunately, this sophisticated complex is not very attractive for large-scale applications. The reaction is remarkably chemoselective, thus the presence of ketone, ester, isocyanide, chloride and nitrile is tolerated (Scheme 41).

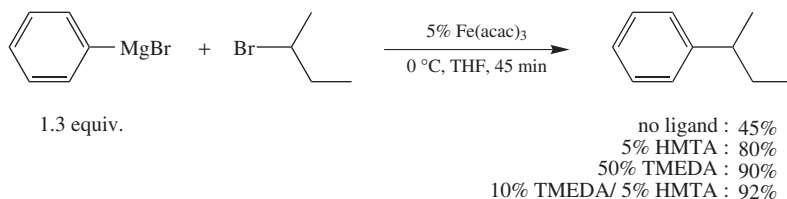


The following coupling products were prepared according to this procedure.



SCHEME 41

In 2007, Cahiez and coworkers<sup>72</sup> disclosed two new catalytic systems to improve the reaction, especially for large-scale syntheses. In the first catalytic system, iron(III) acetylacetonate is used instead of iron(III) chloride. In addition, the use of hexamethylenetetramine (HMTA, 5%), a very cheap new ligand, allows one to significantly lower the amount of TMEDA (10% instead of 120%) (Scheme 42). This catalytic system is based on a synergy between TMEDA and HMTA.



SCHEME 42

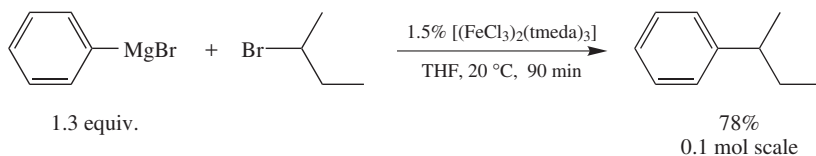
The reaction can be applied to various secondary and primary alkyl bromides (Table 8).

The second procedure uses 1.5% [(FeCl<sub>3</sub>)<sub>2</sub>(tmeda)<sub>3</sub>] as a catalyst (Scheme 43). The complex, which is not hygroscopic, is very easily obtained by adding 1.5 equivalents of TMEDA to a solution of iron(III) chloride in THF (Scheme 44). It is quantitatively isolated by filtration.

TABLE 8. Cross-coupling between aryl Grignard reagents and alkyl bromides

$\text{ArMgX} + \text{RBr} \xrightarrow[\text{THF, 0 } ^\circ\text{C, 45 min}]{\substack{5\% \text{ Fe(acac)}_3 \\ 10\% \text{ TMEDA} \\ 5\% \text{ HMTA}}} \text{Ar-R}$		
1.3 equiv.		
ArMgBr	RBr	Yield (%)
PhMgBr		75
		72
PhMgBr		94
		93
		88
		85





SCHEME 43



SCHEME 44

Recently, Fu and coworkers<sup>66</sup> have shown that secondary alkyl halides do not react under palladium catalysis since the oxidative addition is too slow. They have demonstrated that this lack of reactivity is mainly due to steric effects. Under iron catalysis, the coupling reaction is clearly less sensitive to such steric influences since cyclic and acyclic secondary alkyl bromides were used successfully. Such a difference could be explained by the mechanism proposed by Cahiez and coworkers<sup>72</sup> (Figure 2). Contrary to Pd<sup>0</sup>, which reacts with alkyl halides according to a concerted oxidative addition mechanism, the iron-catalyzed reaction could involve a two-step monoelectronic transfer.

Finally, Bica and Gaertner<sup>74</sup> have recently shown that an ionic liquid can be used as a solvent to perform the reaction.

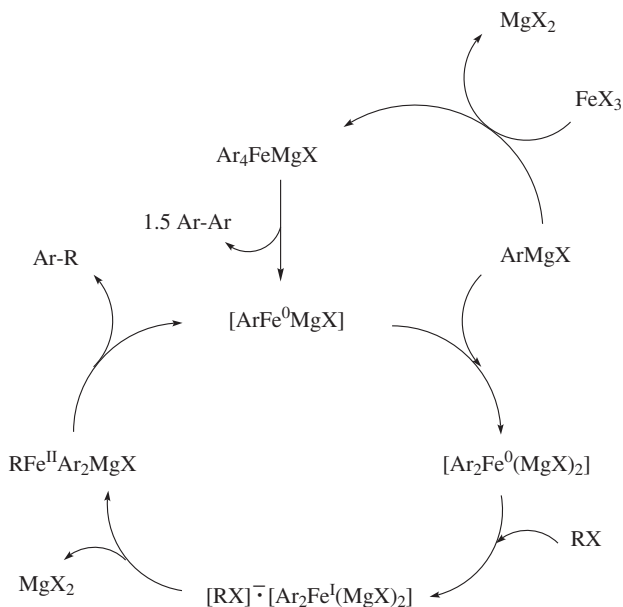
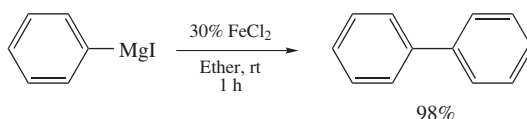


FIGURE 2

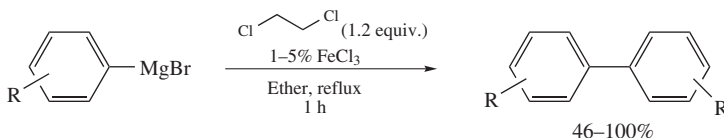
## V. IRON-CATALYZED HOMOCOUPLING OF AROMATIC GRIGNARD REAGENTS

The first iron-mediated homocoupling reaction was described in 1939 by Gilman and Lichtenwalter<sup>75</sup>. They showed that phenylmagnesium iodide reacts with a sub-stoichiometric amount of iron(II) chloride, in diethyl ether, to give biphenyl in 98% yield (Scheme 45).



SCHEME 45

In 2005, Cahiez and coworkers<sup>76</sup> and Nagano and Hayashi<sup>77</sup> showed that a catalytic amount of iron(III) chloride is efficient when a suitable oxidant is added to the reaction mixture (Figure 3). Nagano and Hayashi used an excess of 1,2-dichloroethane (the stoichiometric amount is 0.5 equivalent) in refluxing diethyl ether to couple various aryl Grignard reagents in high yield (Scheme 46).



SCHEME 46

Cahiez decided to develop the reaction in THF. Indeed, diethyl ether is not convenient for large-scale applications (especially at reflux). Moreover, many aromatic Grignard reagents can only be obtained in THF e.g. by preparation of arylmagnesium chlorides from aryl chlorides or preparation of functionalized arylmagnesium halides from the corresponding aryl iodides by iodide–magnesium exchange<sup>45</sup>.

The coupling procedure requires only 0.6 equivalent of 1,2-dihalogenoethane as an oxidant and can be applied to various simple aryl and heteroaryl Grignard reagents. It should be noted that in the case of hindered and functionalized aryl Grignard reagents, a dramatic improvement was observed by using 1,2-dibromo- or 1,2-diiodoethane instead of 1,2-dichloroethane (Table 9).

Pei and coworkers<sup>78</sup> reported that the homocoupling product can be obtained by adding an aryl bromide to a mixture of magnesium and 2% iron salts in THF (Scheme 47). All reactions were performed on a 1 mmol scale.

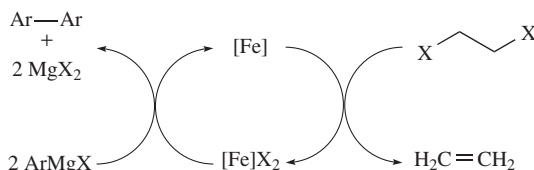
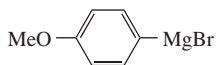
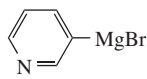
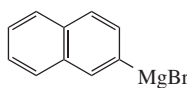
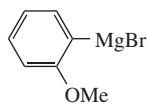
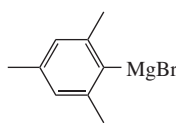
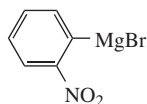
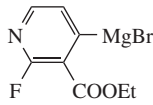
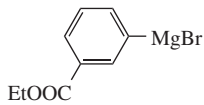
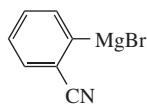
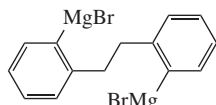
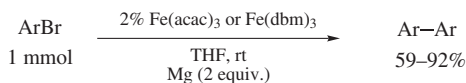


FIGURE 3

TABLE 9. Homocoupling of aryl and heteroaryl Grignard reagents

$  \begin{array}{c}  \text{X} \text{---} \text{CH}_2 \text{---} \text{X} \text{ (0.6 equiv.)} \\  \text{3\% FeCl}_3 \\  \text{THF, } -40^\circ\text{C or rt} \\  \text{1 h}  \end{array}  $		
ArMgBr	X	Yield (%)
	Cl	90
	Cl	82
	Cl	81
	Cl	21
	Br	73
	Cl	5
	Br	60
	Br	41
	Br	41
	I	33
	I	67
	I	75
	Br	76



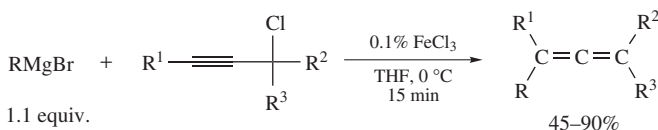
SCHEME 47

According to our experience, these results are not reproducible on a larger scale since, in all cases, the main product is the Grignard reagent and not the homocoupling product. In fact, it is not surprising since iron salts have been successfully used by Bogdanovic and Schwickardi<sup>79</sup> to catalyze the formation of aryl Grignard reagents from aryl halides and magnesium.

## VI. OTHER REACTIONS

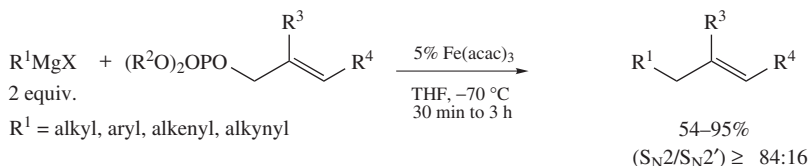
### A. Iron-catalyzed Substitution

In 1976, Pasto and coworkers<sup>80</sup> described the  $S_N2'$  reaction of primary and secondary alkyl Grignard reagents with terminal and non-terminal propargylic chlorides (Scheme 48). Only 0.1% iron(III) chloride is necessary to obtain various allenes in good yields.



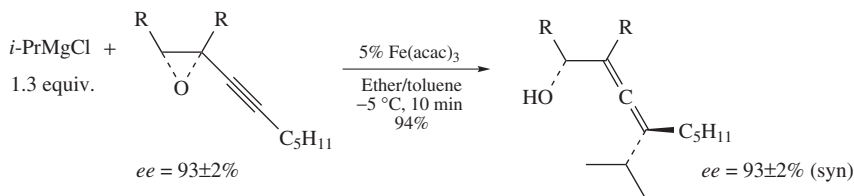
SCHEME 48

Yamamoto and coworkers<sup>81,82</sup> studied the substitution of allylic phosphates by Grignard reagents in the presence of copper or iron salts. Only the  $S_N2'$  product is formed under copper catalysis whereas, in the presence of iron(III) acetylacetonate, the  $S_N2$  product is generally obtained with an excellent selectivity (Scheme 49). It should be noted that aryl-, alkenyl-, alkynyl- and alkylmagnesium halides can be used successfully.



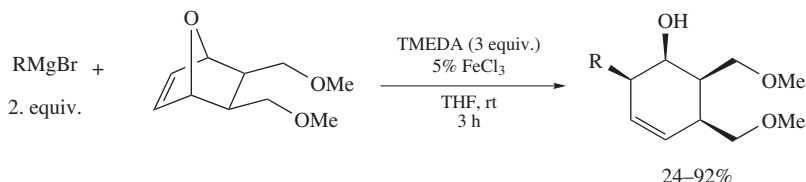
SCHEME 49

In 2003, Fürstner and Méndez<sup>83</sup> reported an elegant reaction between optically active propargylic epoxides and organomagnesium compounds in the presence of iron(III) acetylacetonate (Scheme 50). Interestingly, the chirality of the starting product is transferred to the final 2,3-allenols which are obtained with a good enantiomeric purity.



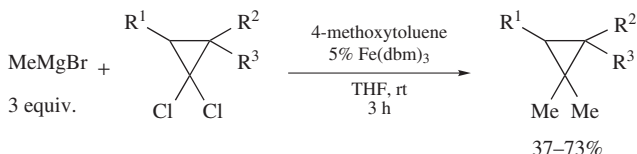
SCHEME 50

In the same year, Nakamura and coworkers<sup>84</sup> published an iron-catalyzed ring opening reaction of oxabicyclic alkenes by Grignard reagents (Scheme 51). This reaction is highly regio- and stereoselective.



SCHEME 51

Finally, Tanabe and coworkers<sup>85</sup> reported that treatment of *gem*-dichlorocyclopropanes with methylmagnesium bromide in the presence of 5%  $\text{Fe(dbm)}_3$  and 4-methoxytoluene (1 equiv.) affords the dimethylated product (Scheme 52).



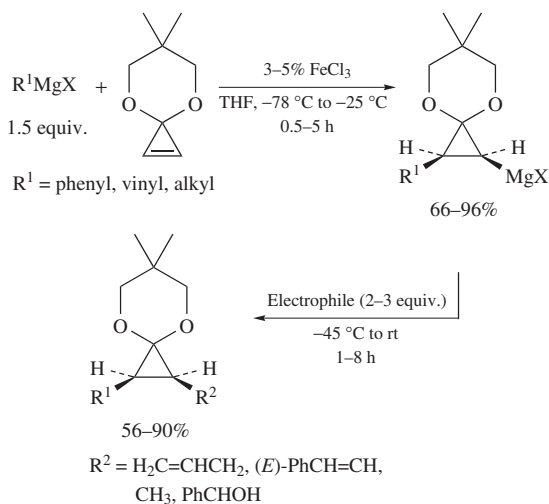
SCHEME 52

## B. Carbometallation

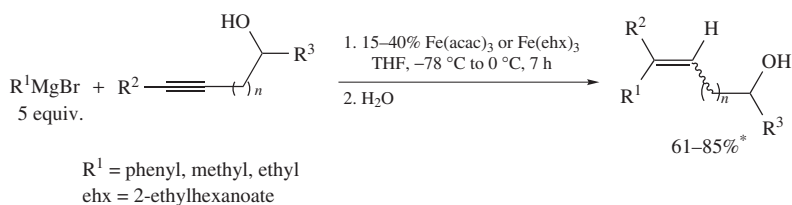
In 2000, Nakamura and coworkers<sup>86</sup> described the iron-catalyzed addition of Grignard reagents to the cyclopropenone derivatives depicted in Scheme 53. Phenyl, vinyl and alkyl Grignard reagents lead to good to excellent yields. The carbometallation is highly stereoselective and the resulting cyclopropylmagnesium halide reacts with various electrophiles with retention of configuration.

Recently, Zhang and Ready<sup>87</sup> published an iron-catalyzed carbometallation of propargylic and homopropargylic alcohols. This reaction generates regioselectively tri- and tetrasubstituted olefins in satisfactory yields (Scheme 54). Unfortunately, a large excess of the Grignard reagents is required and sub-stoichiometric amounts of iron salts are necessary.

In 2005, Hayashi and coworkers<sup>88</sup> reported the iron/copper co-catalyzed arylmagnesylation of alkynes. This method gives only moderate yields but the stereoselectivity is generally excellent (Scheme 55).

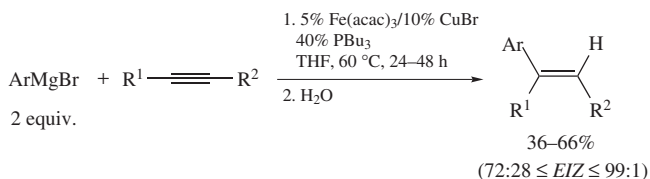


SCHEME 53



\*When  $\text{R}^1 = \text{Me}$  only the (Z)-stereomer was obtained

SCHEME 54



SCHEME 55

Two years later, Hayashi and coworkers<sup>89</sup> showed that the use of an *N*-heterocyclic carbene ligand (IPr) allows one to perform the iron-catalyzed addition of arylmagnesium bromides to conjugated arylalkynes in high yields and with a good stereoselectivity (Scheme 56).

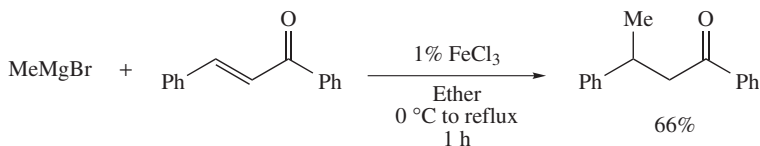
### C. Radical Cyclization

In 1998, Oshima and coworkers<sup>90</sup> reported few examples of radical cyclization mediated by Grignard reagents in the presence of iron(II) chloride (Scheme 57). However, this reaction often gives moderate yields.



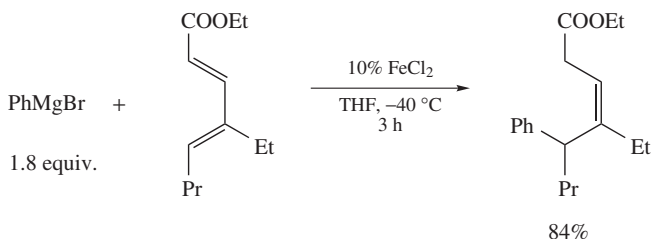
#### D. Addition to Conjugated Unsaturated Carbonyl Compounds

In 1941, Kharasch and Sayles<sup>4</sup> reported the 1,4-addition of methylmagnesium bromide to chalcone in the presence of iron salts (Scheme 59).



SCHEME 59

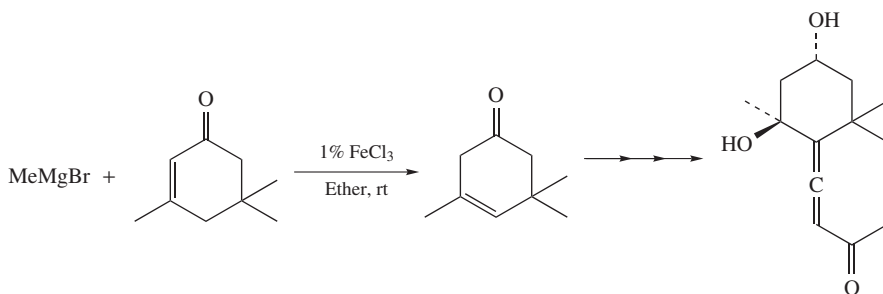
Many years later, Fukuhara and Urabe<sup>91</sup> showed that aryl Grignard reagents react with ethyl 2,4-dienoates or 2,4-dienamides, in the presence of iron salts, to give the 1,6-addition products (Scheme 60). This reaction is stereoselective and leads to the (*Z*)-trisubstituted olefins.



SCHEME 60

## VII. APPLICATIONS OF IRON-CATALYZED REACTIONS OF GRIGNARD REAGENTS IN ORGANIC SYNTHESIS

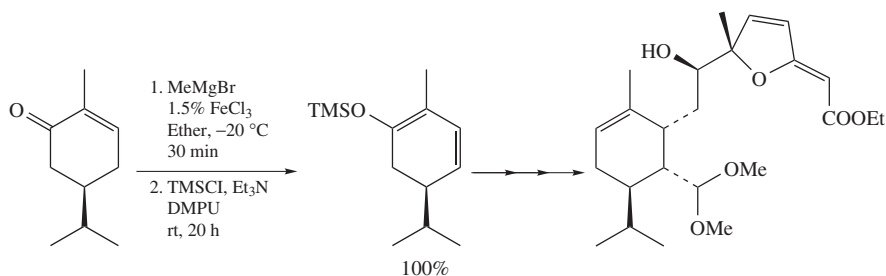
These last years, several syntheses of natural products using an iron-catalyzed reaction of Grignard reagents have been published. In 1969, Meinwald and Hendry<sup>92</sup> used the reaction discovered by Kharasch and Tawney<sup>2,6</sup> to prepare an allenic sesquiterpenoid isolated from the grasshopper *Romalea Microptera* (Scheme 61).



SCHEME 61

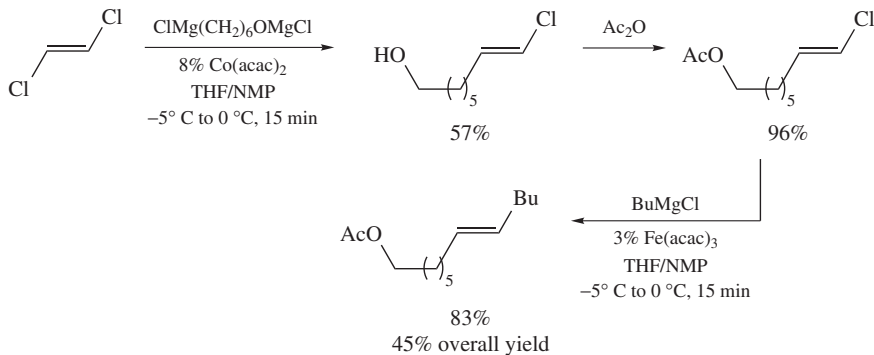
The Kharasch reaction has also been employed by Gennari and coworkers<sup>93</sup> to synthesize, from (*L*)-carvone, a potential functionalized precursor of sarcodictyins and eleutherobin (Scheme 62).





SCHEME 62

Iron-catalyzed alkenylation of Grignard reagents was used by Cahiez and Avedissian<sup>29</sup> to prepare the pheromone of *Argyroplaca Leucotetra* in three steps from 1,2-(*E*)-dichloroethene (Scheme 63). Two successive alkenylation reactions, the first involving a cobalt catalysis, the second an iron catalysis, allow one to obtain the desired product in 45% overall yield.



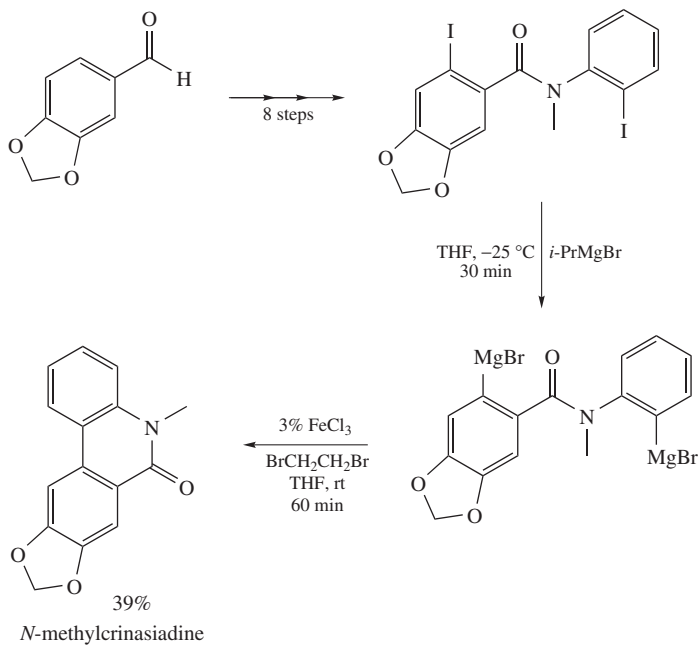
SCHEME 63

The iron-catalyzed homocoupling of Grignard reagents was successfully applied to the synthesis of *N*-methylcrinasiadine by Cahiez and coworkers<sup>76</sup> (Scheme 64).

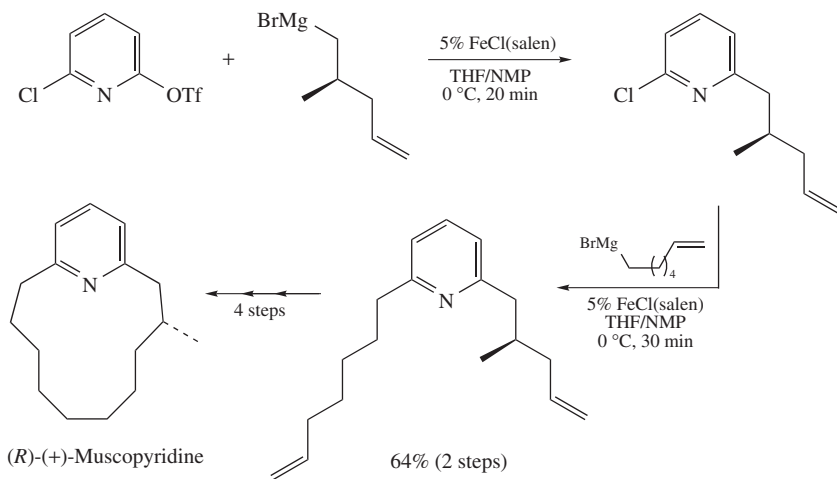
F rstner and Leitner<sup>94</sup> have recently described the synthesis of (*R*)-(+)-muscopyridine. This elegant strategy is based on two regioselective iron-catalyzed heteroaryl-alkyl coupling reactions (Scheme 65).

A similar cross-coupling reaction was used for the synthesis of the immunosuppressive agent FTY720 (Scheme 66)<sup>95</sup>.

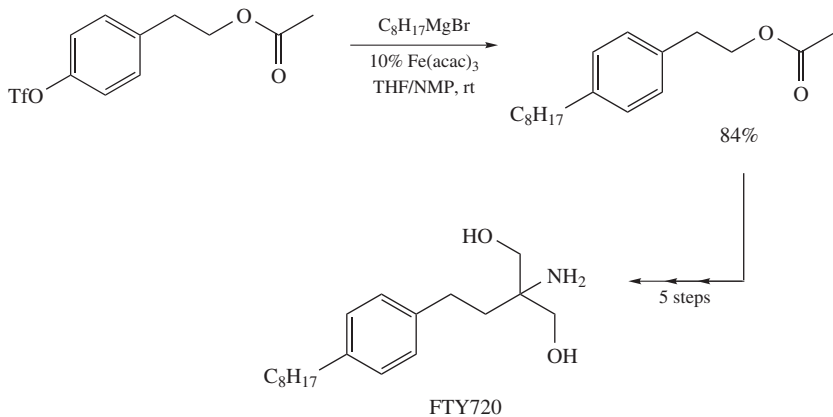
The iron-catalyzed addition of Grignard reagents to propargylic epoxides developed by F rstner and M ndez<sup>83</sup> allows one to prepare a *syn*-allenol, which is an important intermediate for the synthesis of a precursor of the amphidinolide X<sup>96</sup> (Scheme 67).



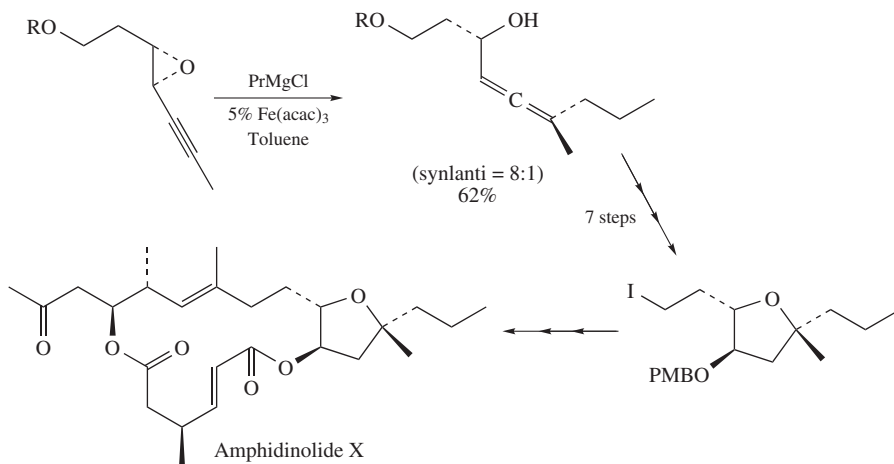
SCHEME 64



SCHEME 65



SCHEME 66



SCHEME 67

### VIII. REFERENCES

1. M. S. Kharasch, S. C. Kleiger, J. A. Martin and F. R. Mayo, *J. Am. Chem. Soc.*, **63**, 2305 (1941).
2. M. S. Kharasch and P. O. Tawney, *J. Am. Chem. Soc.*, **63**, 2308 (1941).
3. M. S. Kharasch and E. K. Fields, *J. Am. Chem. Soc.*, **63**, 2316 (1941).
4. M. S. Kharasch and D. C. Sayles, *J. Am. Chem. Soc.*, **64**, 2972 (1942).
5. M. S. Kharasch, R. T. Morrison and W. H. Hurry, *J. Am. Chem. Soc.*, **66**, 368 (1944).
6. M. S. Kharasch and P. O. Tawney, *J. Am. Chem. Soc.*, **67**, 128 (1945).
7. M. S. Kharasch and C. F. Fuchs, *J. Org. Chem.*, **10**, 292 (1945).
8. M. S. Kharasch, M. Weiner, W. Nudenberg, A. Bhattacharya, T. Wang and N. C. Yang, *J. Am. Chem. Soc.*, **83**, 3232 (1961).
9. M. Tamura and J. K. Kochi, *J. Am. Chem. Soc.*, **93**, 1487 (1971).
10. M. Tamura and J. K. Kochi, *Synthesis*, 303 (1971).
11. S. M. Neumann and J. K. Kochi, *J. Organomet. Chem.*, **31**, 289 (1971).

12. J. K. Kochi, *Acc. Chem. Res.*, **7**, 351 (1974).
13. S. M. Neumann and J. K. Kochi, *J. Org. Chem.*, **40**, 599 (1975).
14. R. S. Smith and J. K. Kochi, *J. Org. Chem.*, **41**, 502 (1976).
15. C. L. Kwan and J. K. Kochi, *J. Am. Chem. Soc.*, **98**, 4903 (1976).
16. K. L. Rollick, W. A. Nugent and J. K. Kochi, *J. Organomet. Chem.*, **225**, 279 (1982).
17. J. K. Kochi, *J. Organomet. Chem.*, **653**, 11 (2002).
18. G. H. Posner, *Org. React.*, **19**, 1 (1972).
19. G. H. Posner, *Org. React.*, **22**, 253 (1975).
20. B. H. Lipshutz and S. Sengupta, *Org. React.*, **41**, 135 (1992).
21. N. Krause (Ed.), *Modern Organocopper Chemistry*, Wiley-VCH, Weinheim, 2002.
22. N. Miyaura and A. Suzuki, *Chem. Rev.*, **95**, 2457 (1995).
23. J. P. Corbet and G. Mignani, *Chem. Rev.*, **106**, 2651 (2006).
24. Y. Tamaru (Ed.), *Modern Organonickel Chemistry*, Wiley-VCH, Weinheim, 2005.
25. S. Stanford, *Tetrahedron*, **54**, 263 (1998).
26. J. Hassan, M. Sévignon, C. Gozzi, E. Schultz and M. Lemaire, *Chem. Rev.*, **102**, 1359 (2002).
27. A. C. Frisch and M. Beller, *Angew. Chem., Int. Ed.*, **44**, 674 (2005).
28. A. de Meijere and P. J. Stang (Eds.), *Metal-Catalyzed Cross-Coupling Reactions*, 2nd edn., Wiley-VCH, Weinheim, 2004.
29. G. Cahiez and H. Avedissian, *Synthesis*, 1199 (1998).
30. C. Bolm, J. Legros, J. Le Paith and L. Zani, *Chem. Rev.*, **104**, 6217 (2004).
31. H. Shinokubo and K. Oshima, *Eur. J. Org. Chem.*, 2081 (2004).
32. A. Fürstner and R. Martin, *Chem. Lett.*, **34**, 624 (2005).
33. M. E. Krafft and R. A. Holton, *J. Org. Chem.*, **49**, 3669 (1984).
34. M. E. Krafft and R. A. Holton, *J. Am. Chem. Soc.*, **106**, 7619 (1984).
35. A. Fürstner, H. Krause and C. W. Lehmann, *Angew. Chem., Int. Ed.*, **45**, 440 (2006).
36. W. C. Percival, R. C. Wagner and N. C. Cook, *J. Am. Chem. Soc.*, **75**, 3731 (1953).
37. J. Cason and K. W. Kraus, *J. Org. Chem.*, **26**, 1768 (1961).
38. J. Cason and E. J. Reist, *J. Org. Chem.*, **23**, 1668 (1958).
39. J. Cason and K. W. Kraus, *J. Org. Chem.*, **26**, 1772 (1961).
40. V. Fiandanese, G. Marchese, V. Martina and L. Ronzini, *Tetrahedron Lett.*, **25**, 4805 (1984).
41. C. Cardellicchio, V. Fiandanese, G. Marchese and L. Ronzini, *Tetrahedron Lett.*, **26**, 3595 (1985).
42. C. Cardellicchio, V. Fiandanese, G. Marchese and L. Ronzini, *Tetrahedron Lett.*, **28**, 2053 (1987).
43. G. Cahiez, Unpublished results.
44. C. Duplais, F. Bures, I. Sapountzis, T. J. Korn, G. Cahiez and P. Knochel, *Angew. Chem., Int. Ed.*, **43**, 2968 (2004).
45. L. Boymond, M. Röttländer, G. Cahiez and P. Knochel, *Angew. Chem., Int. Ed.*, **37**, 1701 (1998).
46. G. A. Molander, B. J. Rahn, D. C. Shubert and S. E. Bonde, *Tetrahedron Lett.*, **24**, 5449 (1983).
47. W. Dohle, F. Kopp, G. Cahiez and P. Knochel, *Synlett*, **12**, 1901 (2001).
48. M. Seck, X. Franck, R. Hocquemiller, B. Figadère, J. F. Peyrat, O. Provot, J. D. Brion and M. Alami, *Tetrahedron Lett.*, **45**, 1881 (2004).
49. M. A. Fakhfakh, X. Franck, R. Hocquemiller and B. Figadère, *J. Organomet. Chem.*, **624**, 131 (2001).
50. M. A. Fakhfakh, X. Franck, A. Fournier, R. Hocquemiller and B. Figadère, *Synth. Commun.*, **32**, 2863 (2002).
51. M. Dos Santos, X. Franck, R. Hocquemiller, B. Figadère, J. F. Peyrat, O. Provot, J. D. Brion and M. Alami, *Synlett*, 2697 (2004).
52. J. L. Fabre, M. Julia and J. N. Verpeaux, *Tetrahedron Lett.*, **23**, 2469 (1982).
53. J. L. Fabre, M. Julia and J. N. Verpeaux, *Bull. Soc. Chim. Fr.*, **5**, 772 (1985).
54. E. Alvarez, T. Cuvigny, C. Hervé du Penhoat and M. Julia, *Tetrahedron*, **44**, 111 (1988).
55. E. Alvarez, T. Cuvigny, C. Hervé du Penhoat and M. Julia, *Tetrahedron*, **44**, 119 (1988).
56. K. Itami, S. Higashi, M. Mineno and J. Yoshida, *Org. Lett.*, **7**, 1219 (2005).
57. B. Scheiper, M. Bonnekessel, H. Krause and A. Fürstner, *J. Org. Chem.*, **69**, 3943 (2004).
58. A. Fürstner and A. Leitner, *Angew. Chem., Int. Ed.*, **41**, 609 (2002).
59. A. Fürstner, A. Leitner, M. Méndez and H. Krause, *J. Am. Chem. Soc.*, **124**, 13856 (2002).

60. L. E. Aleandri, B. Bogdanovic, P. Bons, C. D rr, A. Gaidies, T. Hartwig, S. C. Hockett, M. Lagarden, U. Wilczok and R. A. Brand, *Chem. Mater.*, **7**, 1153 (1995).
61. M. Hocek and H. Dvor kov , *J. Org. Chem.*, **68**, 5773 (2003).
62. M. Hocek, D. Hockov  and H. Dvor kov , *Synthesis*, 889 (2004).
63. M. Hocek and R. Pohl, *Synthesis*, 2869 (2004).
64. L. K. Ottesen, F. Ek and R. Olsson, *Org. Lett.*, **8**, 1771 (2006).
65. J. Quintin, X. Franck, R. Hocquemiller and B. Figad re, *Tetrahedron Lett.*, **43**, 3547 (2002).
66. I. D. Hills, N. R. Netherton and G. C. Fu, *Angew. Chem., Int. Ed.*, **42**, 5749 (2003).
67. T. Nagano and T. Hayashi, *Org. Lett.*, **6**, 1297 (2004).
68. R. B. Bedford, D. W. Bruce, R. M. Frost, J. W. Goodby and M. Hird, *Chem. Commun.*, 2822 (2004).
69. R. B. Bedford, D. W. Bruce, R. M. Frost and M. Hird, *Chem. Commun.*, 4161 (2005).
70. R. B. Bedford, M. Betham, D. W. Bruce, A. A. Danopoulos, R. M. Frost and M. Hird, *J. Org. Chem.*, **71**, 1104 (2006).
71. M. Nakamura, K. Matsuo, S. Ito and E. Nakamura, *J. Am. Chem. Soc.*, **126**, 3686 (2004).
72. G. Cahiez, V. Habiak, C. Duplais and A. Moyeux, *Angew. Chem., Int. Ed.*, **46**, 4364 (2007).
73. R. Martin and A. F rstner, *Angew. Chem., Int. Ed.*, **43**, 3955 (2004).
74. K. Bica and P. Gaertner, *Org. Lett.*, **8**, 733 (2006).
75. H. Gilman and M. Lichtenwalter, *J. Am. Chem. Soc.*, **61**, 957 (1939).
76. G. Cahiez, C. Chaboche, F. Mahuteau-Betzer and M. Ahr, *Org. Lett.*, **7**, 1943 (2005).
77. T. Nagano and T. Hayashi, *Org. Lett.*, **7**, 491 (2005).
78. X. Xu, D. Cheng and W. Pei, *J. Org. Chem.*, **71**, 6637 (2006).
79. B. Bogdanovic and M. Schwickardi, *Angew. Chem., Int. Ed.*, **39**, 4610 (2000).
80. D. J. Pasto, G. F. Hennion, R. H. Shults, A. Waterhouse and S. K. Chou, *J. Org. Chem.*, **41**, 3496 (1976).
81. A. Yanagisawa, N. Nomura and H. Yamamoto, *Synlett*, 513 (1991).
82. A. Yanagisawa, N. Nomura and H. Yamamoto, *Tetrahedron*, **50**, 6017 (1994).
83. A. F rstner and M. M ndez, *Angew. Chem., Int. Ed.*, **42**, 5355 (2003).
84. M. Nakamura, K. Matsuo, T. Inoue and E. Nakamura, *Org. Lett.*, **5**, 1373 (2003).
85. Y. Nishii, K. Wakasugi and Y. Tanabe, *Synlett*, 67 (1998).
86. M. Nakamura, A. Hirai and E. Nakamura, *J. Am. Chem. Soc.*, **122**, 978 (2000).
87. D. Zhang and J. M. Ready, *J. Am. Chem. Soc.*, **128**, 15050 (2006).
88. E. Shirakawa, T. Yamagami, T. Kimura, S. Yamaguchi and T. Hayashi, *J. Am. Chem. Soc.*, **127**, 17164 (2005).
89. T. Yamagami, R. Shintani, E. Shirakawa and T. Hayashi, *Org. Lett.*, **9**, 1045 (2007).
90. Y. Hayashi, H. Shinokubo and K. Oshima, *Tetrahedron Lett.*, **39**, 63 (1998).
91. K. Fukuhara and H. Urabe, *Tetrahedron Lett.*, **46**, 603 (2005).
92. J. Meinwald and L. Hendry, *Tetrahedron Lett.*, 1657 (1969).
93. S. M. Ceccarelli, U. Piarulli and C. Gennari, *Tetrahedron*, **57**, 8531 (2001).
94. A. F rstner and A. Leitner, *Angew. Chem., Int. Ed.*, **42**, 308 (2003).
95. G. Seidel, D. Laurich and A. F rstner, *J. Org. Chem.*, **69**, 3950 (2004).
96. O. Lepage, E. Kattnig and A. F rstner, *J. Am. Chem. Soc.*, **126**, 15970 (2004).

## CHAPTER 14

# Carbomagnesiation reactions

KENICHIRO ITAMI

*Department of Chemistry and Research Center for Materials Science, Nagoya University, Chikusa-ku, Nagoya 464-8602, Japan*  
Fax: +81-52-788-6098; e-mail: itami@chem.nagoya-u.ac.jp

and

JUN-ICHI YOSHIDA

*Department of Synthetic Chemistry and Biological Chemistry, Graduate School of Engineering, Kyoto University, Nishikyo-ku, Kyoto 615-8510, Japan*  
Fax: +81-75-383-2727; e-mail: yoshida@sbchem.kyoto-u.ac.jp

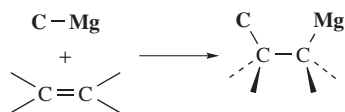
---

I. INTRODUCTION .....	632
II. CARBOMAGNESIATION REACTIONS OF ALKYNES .....	633
A. Intramolecular Addition to Simple Alkynes .....	633
B. Intermolecular Addition to Simple Alkynes .....	635
C. Addition to Alkynylsilanes .....	639
D. Addition to Nitrogen-, Oxygen- and Sulfur-Attached Alkynes .....	641
E. Addition to Propargyl Alcohols .....	645
F. Addition to Propargyl Amines .....	652
III. CARBOMAGNESIATION REACTIONS OF ALKENES .....	653
A. Addition to Simple Alkenes .....	653
B. Allylmagnesiation of Alkenes .....	655
C. Addition to Strained Alkenes .....	657
D. Addition to Vinylsilanes .....	661
E. Addition to Allyl and Homoallyl Alcohols .....	664
F. Zirconium-catalyzed Ethylmagnesiation of Alkenes .....	671
IV. CARBOMAGNESIATION REACTIONS OF AROMATICS .....	674
V. SUMMARY .....	675
VI. REFERENCES .....	676

---

## I. INTRODUCTION

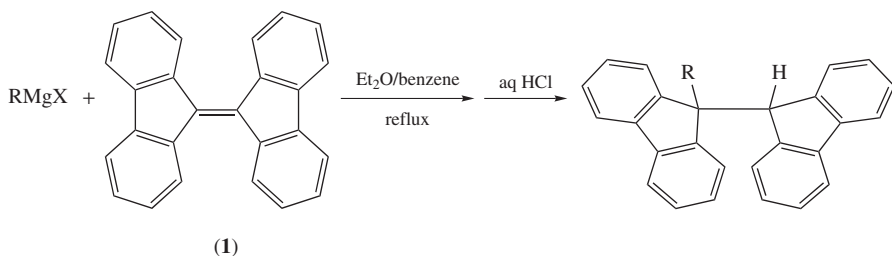
Among various reactions of organomagnesium compounds (Grignard reagents), the addition reaction of a carbon–magnesium bond of an organomagnesium compound across a carbon–carbon multiple bond (a so-called carbomagnesiation reaction) has found many uses in organic synthesis (Scheme 1)<sup>1</sup>. It not only forms a carbon–carbon bond but also produces a new organomagnesium compound, which can react with other reactants.



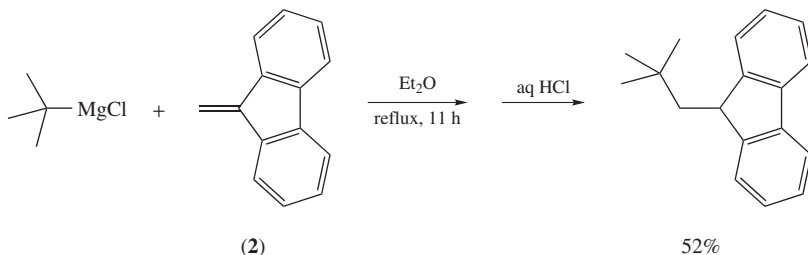
Carbomagnesiation



SCHEME 1



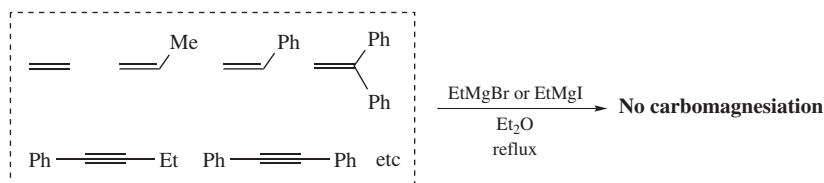
RMgX	Yield (%)
<i>t</i> -BuMgCl	68
PhCH <sub>2</sub> MgCl	58
MeMgI	0
PhMgBr	0



SCHEME 2

One of the earliest examples of the addition of Grignard reagents to a carbon–carbon multiple bond may be the following results reported by Fuson and Porter in 1948<sup>2</sup>. They demonstrated that reactive Grignard reagents such as *t*-BuMgCl and PhCH<sub>2</sub>MgCl could add across the C=C bond of fulvene derivatives **1** and **2** (Scheme 2)<sup>2–5</sup>. The addition does not take place with MeMgI or PhMgBr. Although it is obvious that the carbomagnesiation is made possible by a judicious combination of highly reactive Grignard reagents and C=C bonds, this represents the first example of carbomagnesiation of alkenes.

However, it has been known that the addition of a simple organomagnesium compound across an isolated (non-activated) carbon–carbon multiple bond is a sluggish process (Scheme 3)<sup>6–8</sup>. Over the last half-century of extensive worldwide research, synthetic chemists have devised a number of solutions to overcome the low reactivity of organomagnesium compounds and carbon–carbon multiple bonds<sup>1</sup>. Those include (i) the use of transition metal catalysts, (ii) the use of electronically activated alkenes and alkynes, (iii) the use of alkenes and alkynes bearing metal-directing functionalities and (iv) the use of functionalized organomagnesium compounds. This chapter summarizes the state of the art as well as synthetic utilities of carbomagnesiation reactions in organic synthesis. The Michael addition (1,4-addition) of Grignard reagents to simple  $\alpha,\beta$ -unsaturated carbonyl compounds, which perhaps is one of the most studied organic reactions, will not be treated as a major topic in this chapter<sup>9</sup>, but only some selected examples for this type of carbomagnesiation will be discussed.



SCHEME 3

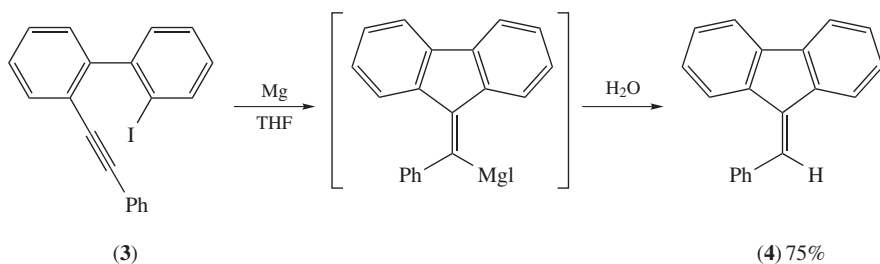
## II. CARBOMAGNESIATION REACTIONS OF ALKYNES

### A. Intramolecular Addition to Simple Alkynes

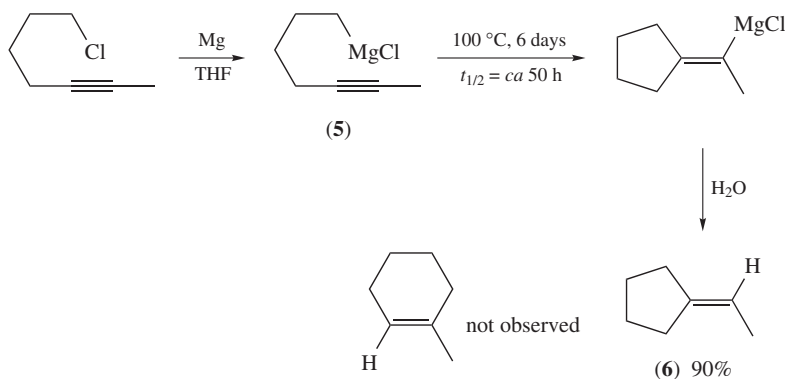
As stated in the introduction, the addition of a simple organomagnesium compound (Grignard reagent) across an isolated carbon–carbon triple bond is very hard to achieve<sup>7</sup>. However, intramolecular carbomagnesiation across a carbon–carbon triple bond proceeds more easily. For example, treatment of iodobenzene **3** bearing a tolane unit in *ortho* position undergoes cyclization to produce the ring-closed alkenylmagnesium compound, which yields benzyldenefluorene **4** upon hydrolysis (Scheme 4)<sup>10</sup>. Although this might be one of the oldest examples of intramolecular carbomagnesiation reactions of alkynes, there is no evidence for the presence of uncyclized organomagnesium compound.

Intramolecular carbomagnesiation across an unconjugated (unactivated) carbon–carbon triple bonds in aliphatic systems is mechanistically interesting. Heating a THF solution of 5-heptynylmagnesium chloride (**5**) for 6 days at 100 °C followed by hydrolysis furnishes ethyldenecyclopentane (**6**) in 90% yield (Scheme 5)<sup>11</sup>. The carbomagnesiation proceeds exclusively with 5-*exo-dig* fashion and the corresponding 6-*endo-dig* cyclization product (1-methylcyclohexene) is not observed. Kinetic experiments indicates that  $t_{1/2}$  of carbomagnesiation is *ca* 50 hours at 100 °C. In contrast, hydrolysis immediately after preparation of organomagnesium compound **5** in refluxing THF furnishes only a few percent of ethyldenecyclopentane (**6**), which indicates that the cyclization occurs after the formation of the Grignard reagent.



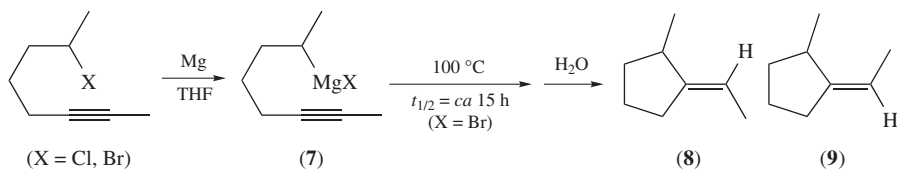


SCHEME 4



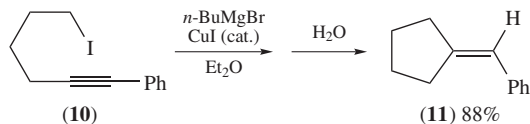
SCHEME 5

Similar experiments using substrates having a methyl group  $\alpha$  to magnesium **7** furnishes a mixture of stereoisomers **8** and **9** (Scheme 6)<sup>11</sup>. Whether the mixture of *cis* and *trans* isomers is formed in the carbomagnesiation step, or by isomerization of a single isomer after addition, has not been discussed. Kinetic experiments indicate that  $t_{1/2}$  of cyclization using bromide is *ca* 15 hours at 100 °C.



SCHEME 6

Copper salts serve as good catalysts for intramolecular carbomagnesiation. For instance, Crandall and coworkers reported that the treatment of acetylenic iodide **10** with an excess of *n*-BuMgBr in the presence of a catalytic amount of CuI affords the cyclic product **11** after hydrolytic workup (Scheme 7)<sup>12</sup>. Quenching with D<sub>2</sub>O leads to 85% incorporation of deuterium at vinylic position in the cyclized product. The reaction probably proceeds by metal-halogen exchange leading to an organomagnesium species which is subsequently

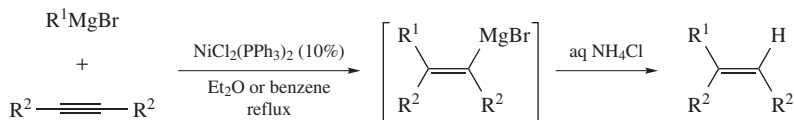


SCHEME 7

transmetalated into an organocopper and cyclizes into the corresponding alkenylmagnesium compound. Overall, this reaction represents a catalytic carbomagnesiation reaction.

## B. Intermolecular Addition to Simple Alkynes

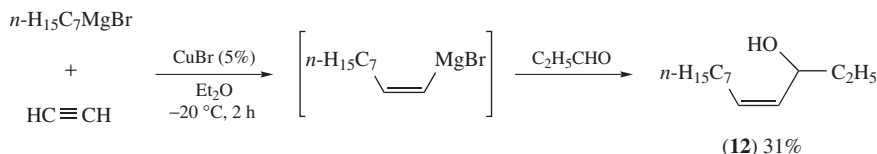
The development of a catalytic system leading to an intermolecular carbomagnesiation of simple alkynes has been a challenge. In 1972, Duboudin and Jousseume reported the Ni-catalyzed carbomagnesiation of alkynes (Scheme 8)<sup>13–15</sup>. Although this may be one of the early successes in the intermolecular carbomagnesiation of alkynes, the scope is somewhat limited: low yielding with dialkylacetylenes, and inapplicable to alkyl Grignard reagents other than MeMgBr.



R <sup>1</sup>	R <sup>2</sup>	Yield (%)
Me	Ph	65
Ph	Ph	50
Ph	Et	30
Ph	<i>n</i> -Pr	31

SCHEME 8

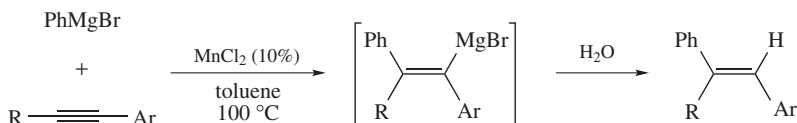
Normant and coworkers demonstrated that the intermolecular carbomagnesiation across acetylene ( $\text{HC}\equiv\text{CH}$ ) could be catalyzed by a copper salt<sup>16</sup>. The treatment of *n*-heptylmagnesium bromide with acetylene in the presence of a catalytic amount of CuBr (5 mol%) in Et<sub>2</sub>O at  $-20^\circ\text{C}$  followed by the reaction with  $\text{C}_2\text{H}_5\text{CHO}$  and quenching with  $\text{H}_2\text{O}$  results in the formation of allylic alcohol **12** in 31% yield (Scheme 9)<sup>16</sup>. The carbomagnesiation takes place in a *syn*-addition manner.



SCHEME 9

Since this report on the copper catalysis in carbomagnesiation across acetylene, a variety of Cu-catalyzed carbomagnesiation reactions of alkynes have been reported. However, the applicable alkynes are somewhat limited to electronically biased (activated) or heteroatom-containing alkynes, which will be discussed later.

Oshima and coworkers reported that  $\text{MnCl}_2$  could catalyze the phenylmagnesiation of arylalkynes (Scheme 10)<sup>17</sup>. Although phenylacetylene itself cannot be used, the phenylmagnesiation takes place with a range of arylalkynes at 100 °C in toluene. The methoxy and dimethylamino groups in the *ortho* position of benzene ring of arylalkynes dramatically facilitate the reaction most likely through chelation assistance. They further extended such a chelation-assisted carbomagnesiation to 2-alkynylphenols<sup>18</sup>.



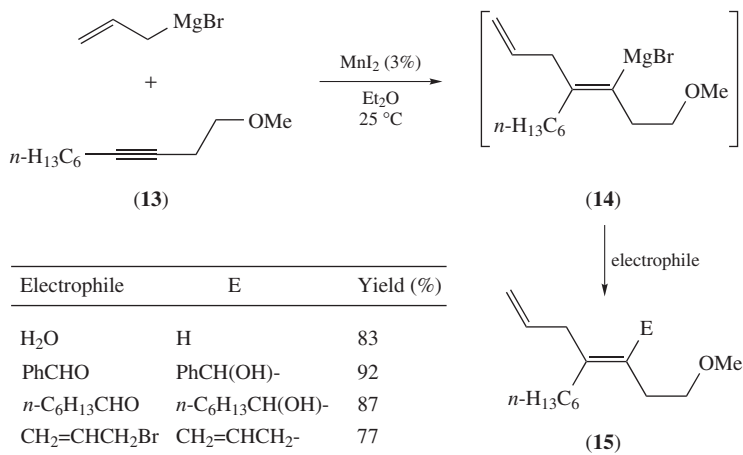
R	Ar	Yield (%)
<i>n</i> -C <sub>6</sub> H <sub>13</sub>	Ph	66
Ph	Ph	60
<i>n</i> -C <sub>6</sub> H <sub>13</sub>	2-MeOC <sub>6</sub> H <sub>4</sub>	80
<i>n</i> -C <sub>6</sub> H <sub>13</sub>	3-MeOC <sub>6</sub> H <sub>4</sub>	63
<i>n</i> -C <sub>6</sub> H <sub>13</sub>	4-MeOC <sub>6</sub> H <sub>4</sub>	38
<i>n</i> -C <sub>6</sub> H <sub>13</sub>	2-Me <sub>2</sub> NC <sub>6</sub> H <sub>4</sub>	94

SCHEME 10

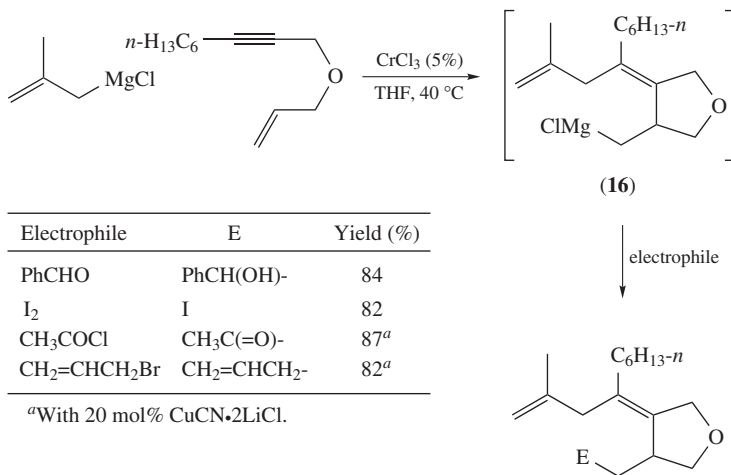
As in the previous examples, the presence of polar functionality near the alkyne affects the rate, regioselectivity and stereoselectivity of carbometalation reaction. Oshima, Utimoto and coworkers reported such a substituent effect in the Mn-catalyzed allylmagnesiation of alkynes<sup>19</sup>. The treatment of homopropargylic alcohol methyl ether **13** with allylmagnesium bromide in the presence of  $\text{MnI}_2$  catalyst (3 mol%) provides the allylated alkenylmagnesium species **14** in a regio- and stereoselective fashion (Scheme 11). The Mn-catalyzed allylmagnesiation proceeds well with the corresponding benzyl and tetrahydropyranyl ethers also. The thus-generated alkenylmagnesium species **14** is allowed to react with electrophiles such as aldehydes and allyl bromides to give tetrasubstituted olefins **15** in good yields (Scheme 11)<sup>19</sup>. The *syn* addition of an allylmagnesium component has been also confirmed. The reaction is clearly oxygen-assisted since 6-dodecyne is completely recovered unchanged even at elevated temperature.

Chromium salts can catalyze the carbomagnesiation reactions of 1,6-enynes with cyclization (Scheme 12)<sup>20,21</sup>. This reaction is probably initiated by carbometalation of the alkyne unit. The resultant organomagnesium species **16** undergoes further functionalization upon treatment with various electrophiles (Scheme 12)<sup>21</sup>.

Yorimitsu, Oshima and coworkers reported the Cr-catalyzed arylmagnesiation of simple alkynes<sup>22</sup>. In early experiments, they found that the phenylmagnesiation of 6-dodecyne could be catalyzed by  $\text{CrCl}_2$  in toluene at 100 °C (Scheme 13). They further found that some alcohols as additives have an accelerating effect on the reaction. The investigation



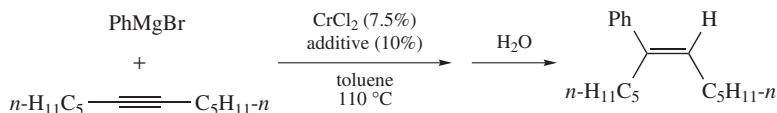
SCHEME 11



SCHEME 12

into the additive effect in this transformation finally led to the discovery of pivalic acid (*t*-BuCOOH) as an optimal promoter, providing the addition product in high yield with virtually complete stereoselectivity (>99% *E*). Although the reason for the dramatic effect of additives is not clear, the regio- and stereoselective arylmagnesiation takes place with a range of dialkylacetylenes and aryl(alkyl)acetylenes. The use of silyl-substituted alkynes results in low stereoselectivity.

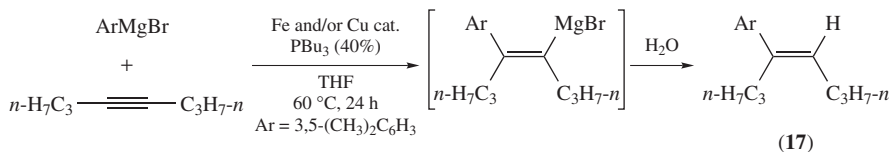
Shirakawa, Hayashi and coworkers disclosed that the arylmagnesiation of simple alkynes could be effectively catalyzed by a catalytic system consisting of iron and copper (Scheme 14)<sup>23</sup>. For example, the treatment of 3,5-dimethylphenylmagnesium bromide (2 equiv) with 4-octyne (1 equiv) under the catalytic influence of Fe(acac)<sub>3</sub> (5 mol%), CuBr



Additive	Time (h)	Yield (%)	E/Z
none	18	81	91:9
MeOH	2	77	95:5
PhOH	2	77	95:5
PhCOOH	0.25	81	>99:1
<b><i>t</i>-BuCOOH</b>	<b>0.25</b>	<b>87</b>	<b>&gt;99:1</b>

SCHEME 13

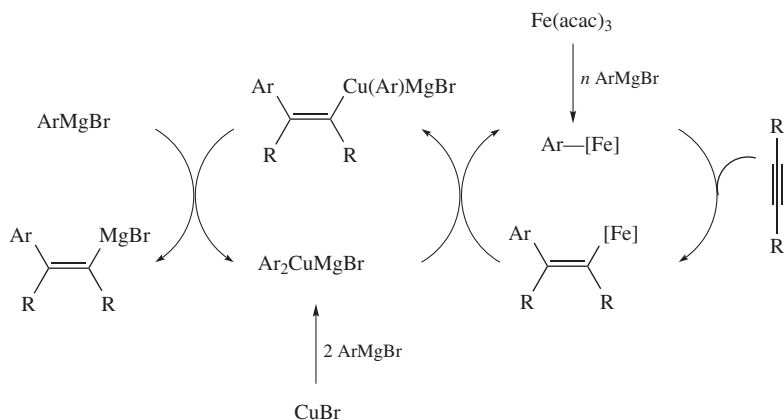
(10 mol%) and  $\text{PBU}_3$  (40 mol%) in THF at  $60^\circ\text{C}$  for 24 h followed by hydrolysis furnishes 74% of hydroarylation product **17** with 95% *E* selectivity. Quenching the reaction with  $\text{D}_2\text{O}$  results in the formation of arylalkene with exclusive incorporation of deuterium at its olefinic methyne, indicating the carbomagnesiation process. Omission of either  $\text{Fe}(\text{acac})_3$  or  $\text{CuBr}$  results in dramatic decrease in carbomagnesiation efficiency (26% and 0% yield, respectively). These control experiments clearly indicate a unique iron/copper cooperative catalysis in this reaction. This catalytic system can be applied to various aryl Grignard reagents. On the basis of several control experiments, a possible mechanism, given in Scheme 15, has been proposed.



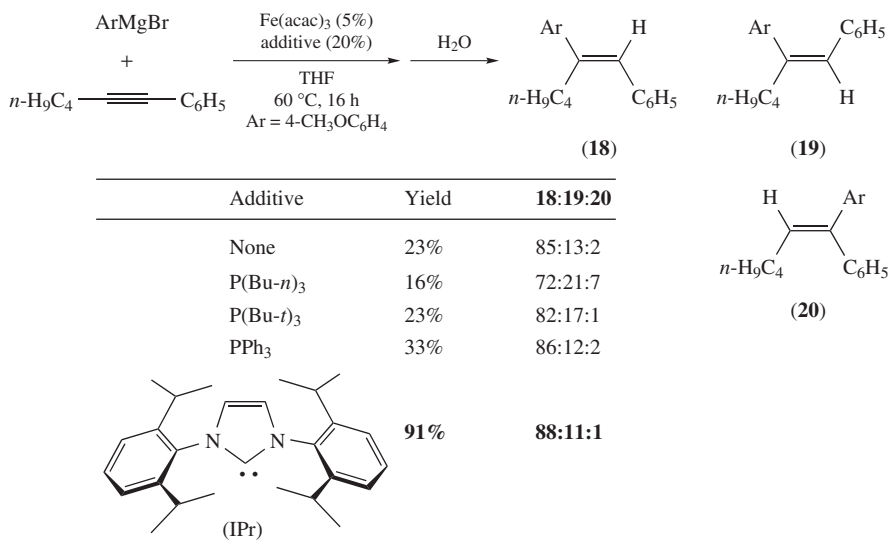
Catalyst system	Yield (%)
<b>Fe(acac)<sub>3</sub> (5%), CuBr (10%)</b>	<b>74</b>
Fe(acac) <sub>3</sub> (5%)	26
CuBr (10%)	0

SCHEME 14

In connection with the aforementioned Fe/Cu co-catalyzed arylmagnesiation, Shirakawa, Hayashi and coworkers further investigated the iron catalysis focusing on aryl(alkyl)acetylenes as substrates<sup>24</sup>. As already stated in their previous work, a combination of iron salt with a phosphine does not have high activity (Scheme 16). However, the Fe-catalyzed arylmagnesiation of aryl(alkyl)acetylenes is greatly improved by addition of a catalytic amount of 1,3-bis-(2,6-diisopropylphenyl)imidazol-2-ylidene (IPr) (Scheme 16)<sup>24</sup>. With this improved catalyst system, a range of arylmagnesium bromides can be added across various aryl(alkyl)acetylenes.



SCHEME 15

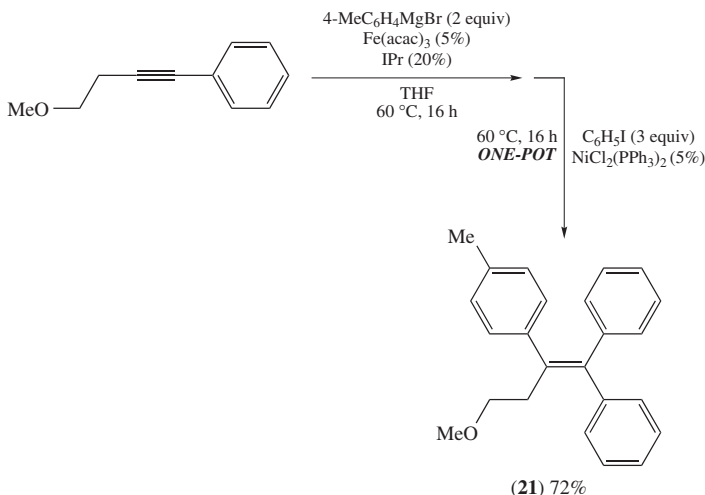


SCHEME 16

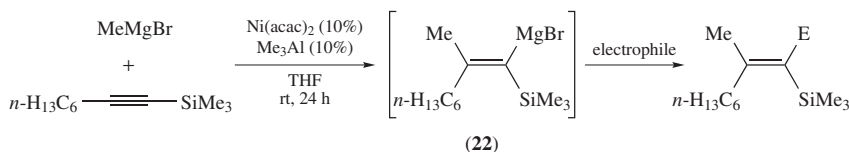
The alkenylmagnesium species generated by the Fe-catalyzed arylmagnesiation can be trapped by electrophiles. For example, the cross-coupling reaction of the alkenylmagnesium species with an aryl halide is achieved with a nickel catalyst, giving a tetrasubstituted olefin **21** in good overall yield (Scheme 17)<sup>24</sup>.

### C. Addition to Alkynylsilanes

A carbomagnesiation of alkynylsilanes is an attractive method generating synthetically versatile silyl-substituted alkenylmagnesium species. Snider and coworkers reported the



SCHEME 17

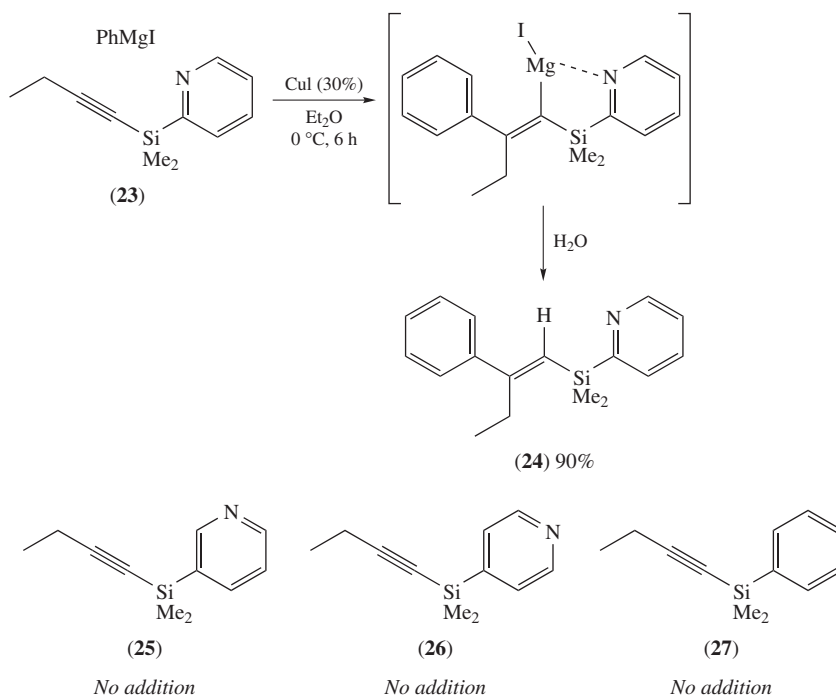


Electrophile	E	Yield (%)	Z/E
H <sub>2</sub> O	H	80	90:10
D <sub>2</sub> O	D	75	90:10
CH <sub>3</sub> CHO	CH <sub>3</sub> CH(OH)-	75	85:15
CH <sub>2</sub> =CHBr	CH <sub>2</sub> =CH-	48	85:15

SCHEME 18

Ni-catalyzed addition of MeMgBr to alkynylsilanes (Scheme 18)<sup>25,26</sup>. A combination of Ni(acac)<sub>2</sub> and Me<sub>3</sub>Al seems to be crucial; NiBr<sub>2</sub> and Ni(acac)<sub>2</sub> show lower activity, and NiCl<sub>2</sub>(phosphine) complexes are totally inactive. Some of the methyl groups transferred may arise from Me<sub>3</sub>Al since the use of Ni(acac)<sub>2</sub>/(*i*-Bu)<sub>2</sub>AlH as catalyst leads to small amounts of hydrometalation. Although this catalytic system is somewhat limited to methylmagnesiation, the resultant alkenylmagnesium species **22** can be trapped by various electrophiles (Scheme 18)<sup>25</sup>. Quenching the reaction with H<sub>2</sub>O and D<sub>2</sub>O leads to the incorporation of H and D, respectively. The reaction with acetaldehyde gives an allylic alcohol. The reaction with vinyl bromide affords a 1,3-diene that is most likely nickel-catalyzed (Tamao–Kumada–Corriu-type cross-coupling). The presence of a coordinating heteroatom on the side chain of the alkyne influences the stereoselectivity of methylmagnesiation reaction of alkynylsilanes<sup>26</sup>.

Itami, Yoshida and coworkers reported an efficient protocol for the carbomagnesiation of alkynylsilanes bearing a metal-coordinating 2-pyridyl group on silicon



SCHEME 19

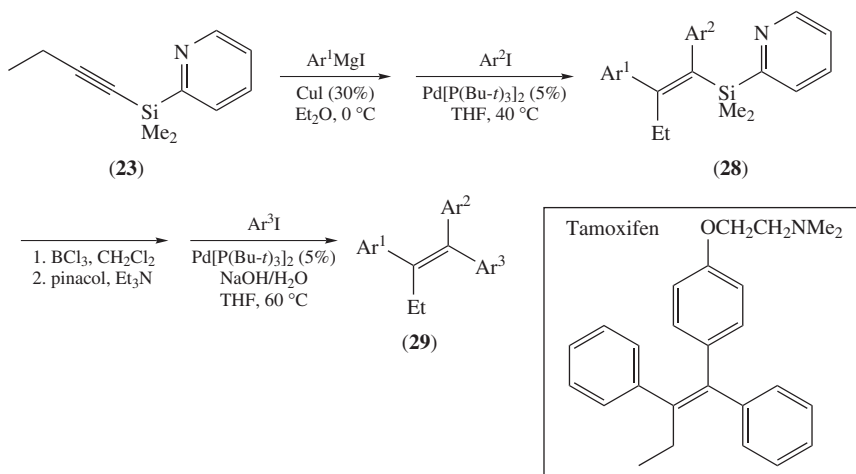
(Scheme 19)<sup>27,28</sup>. The regio- and stereoselective addition of arylmagnesium iodides (ArMgI) to 2-pyridylsilylalkyne **23** proceeds in the presence of CuI catalyst, furnishing alkenylsilanes **24** in high yields after quenching the reaction with water (Scheme 19). The use of ArMgBr, ArMgCl or Ar<sub>2</sub>Mg in place of ArMgI results in lower addition efficiency. The Cu-catalyzed addition does not occur at all with the corresponding 3-pyridyl, 4-pyridyl and phenylsilanes (**25–27**), which clearly implicates the strong directing effect of the 2-pyridyl group on silicon.

By using this reaction as a key step, a programmed and diversity-oriented synthesis of tamoxifen-type tetrasubstituted olefins can be accomplished (Scheme 20)<sup>27,28</sup>. Thus, by adding a Pd catalyst and aryl iodides (Ar<sup>2</sup>I) to the solution of alkenylmagnesium species generated by the Cu-catalyzed carbomagnesiation of 1-butyndimethyl(2-pyridyl)silane **23**, a regio- and stereoselective introduction of two aryl groups onto the alkenylsilane is achieved in one-pot. Although direct C–Si bond arylation of the resultant alkenylsilanes **28** is not feasible, a borodesilylation/cross-coupling sequence of the alkenylsilanes allows the installation of the third aryl group at C–Si bonds yielding the tamoxifen-type tetrasubstituted olefins **29**.

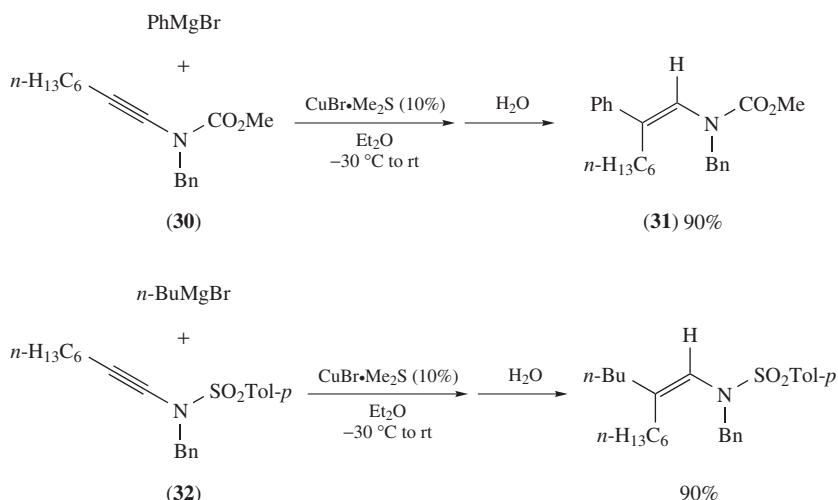
#### D. Addition to Nitrogen-, Oxygen- and Sulfur-Attached Alkynes

Marek and coworkers have developed the regio- and stereocontrolled carbomagnesiation of alkynyl amine derivatives. For example, PhMgBr adds across the triple bond ofynamide **30** in the presence of a catalytic amount of CuBr·Me<sub>2</sub>S (10 mol%). The following





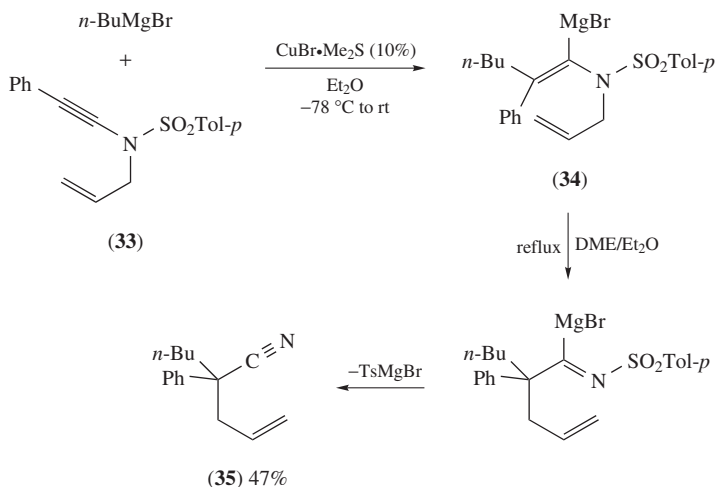
SCHEME 20



SCHEME 21

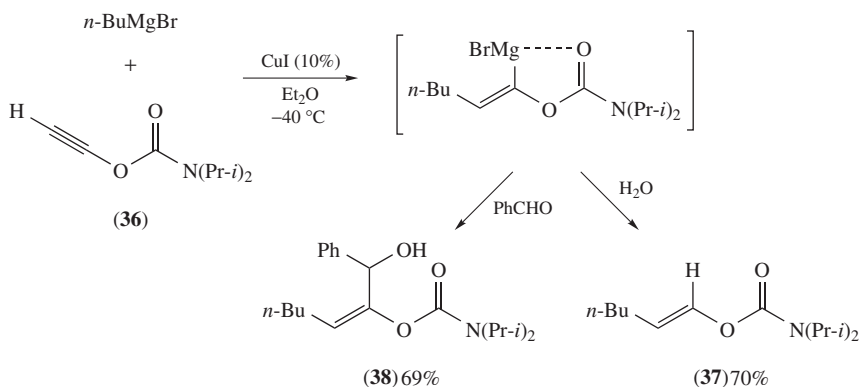
hydrolysis affords the enamide **31** in 90% yield (Scheme 21)<sup>29</sup>. The stereochemical assignment of the product by NOE experiments indicates that the carbometalation proceeds in a *syn*-addition fashion. As for catalyst precursor,  $\text{CuBr}\cdot\text{Me}_2\text{S}$  is optimal. The Cu-catalyzed carbomagnesiation also takes place with sulfonyl-substituted ynamide **32** with high regio- and stereoselectivity (Scheme 21)<sup>29</sup>. The chelation of the carbamoyl and sulfonyl moieties to the organometallic species has been proposed to be of primary importance for controlling the regiochemistry of reaction. In line with such an assumption, the use of coordinating solvent such as THF erodes the regioselectivity of the carbomagnesiation.

The Cu-catalyzed carbomagnesiation of alkynylsulfonamide **33** having an allyl group on the nitrogen atom also takes place. Interestingly, the organomagnesium species **34** thus generated undergoes aza-Claisen rearrangement to yield pentenenitrile **35** (Scheme 22)<sup>30</sup>.



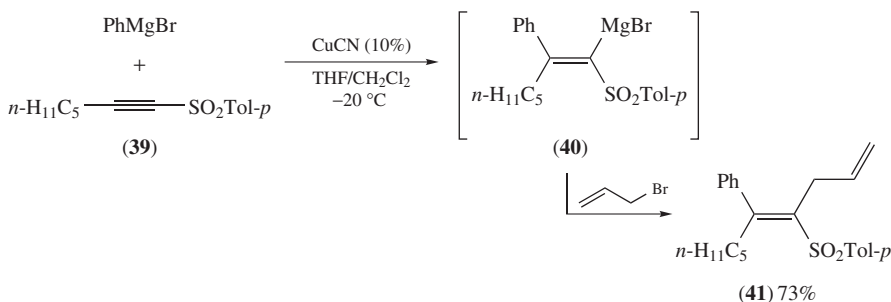
SCHEME 22

Marek and Chechik-Lankin have demonstrated that the stereoselective Cu-catalyzed carbomagnesiation reactions of alkynyl carbamates is a straightforward means for the preparation of synthetically versatile alkenyl enol carbamates. When ethynylcarbamate **36** is added to a stoichiometric amount of *n*-BuMgBr in Et<sub>2</sub>O in the presence of CuI (10 mol%), the addition takes place smoothly at -40 °C giving (*E*)-alkenyl carbamate **37** in 70% yield (Scheme 23)<sup>31</sup>. The addition of benzaldehyde as an electrophile gives **38** in 69% yield. An intramolecular coordination of the sp<sup>2</sup> organometallic species (Cu or Mg) by the carbamate moiety has been proposed.



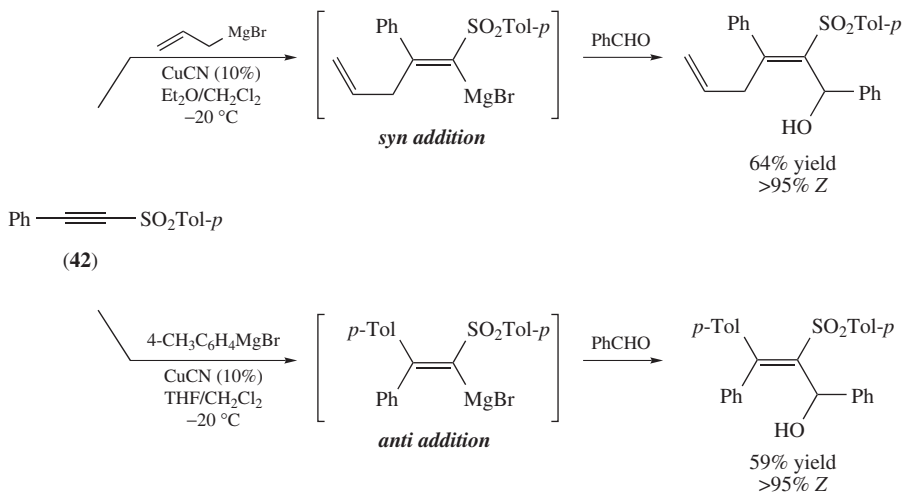
SCHEME 23

The carbomagnesiation of alkynyl sulfones takes place in the presence of copper catalyst. For example, the addition of PhMgBr to *p*-tolylsulfonylheptyne **39** in the presence of CuCN (10 mol%) occurs at  $-20^{\circ}\text{C}$  in THF/CH<sub>2</sub>Cl<sub>2</sub> yielding the corresponding alkenylmagnesium species **40**, which then is allowed to react with allyl bromide to afford trisubstituted vinyl sulfone **41** in 73% yield (Scheme 24)<sup>32</sup>. The stereochemistry of the product has been verified by NMR experiment (NOESY) and X-ray crystal structure analysis. These results demonstrate that the addition of Grignard reagent occurs in a *syn* fashion. The advantage of this catalytic protocol is obvious since it has been known that (i) the reaction of Grignard reagent with alkynyl sulfones typically yields the products of overall substitution of sulfone moiety, and (ii) organocopper reagents add to alkynyl sulfones with low stereoselectivity.



SCHEME 24

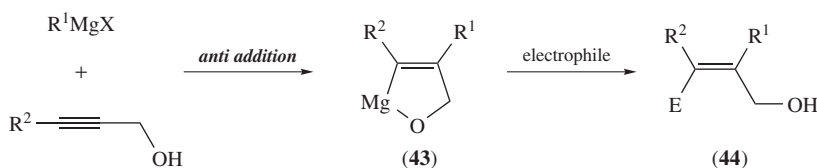
When the phenyl-substituted alkynyl sulfone **42** is used as a substrate for the Cu-catalyzed carbomagnesiation, interesting nucleophile-dependent stereoselectivity is observed. While the use of allyl Grignard reagent results in a *syn* addition, the use of aryl Grignard reagent results in an *anti*-carbomagnesiation (Scheme 25)<sup>33</sup>.



SCHEME 25

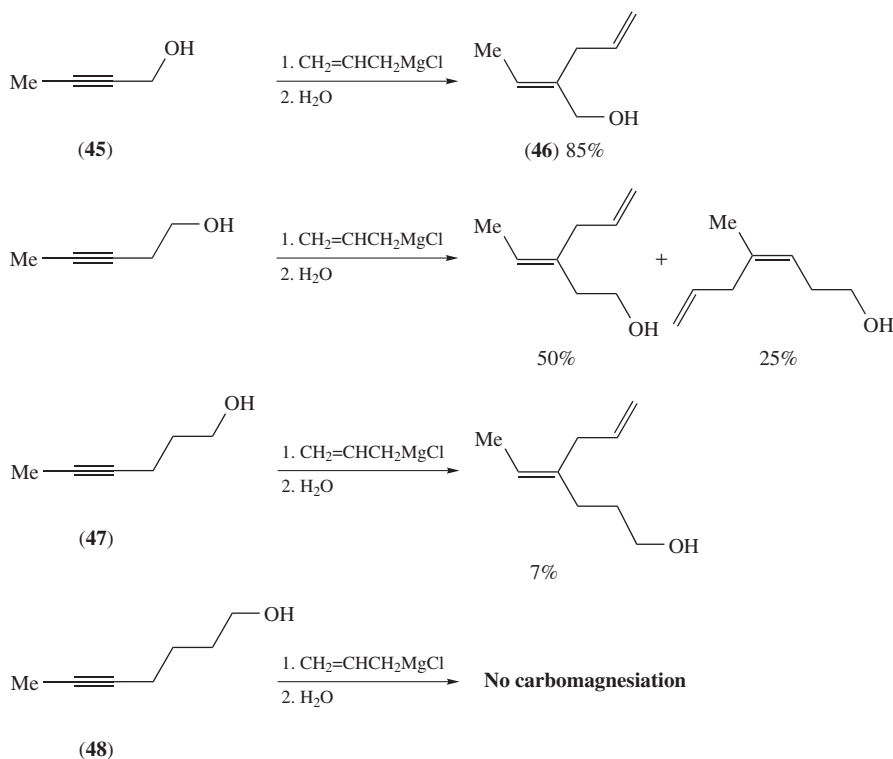
### E. Addition to Propargyl Alcohols

Although the typical carbomagnesiation to alkynes proceeds in a *syn*-addition fashion, propargyl alcohols react with organomagnesium compounds in an *anti*-addition manner (Scheme 26). The reactions are believed to proceed through the formation of a magnesium–oxygen bond, making a five-membered cyclic organomagnesium compound **43**, which then reacts with electrophiles to give substituted allylic alcohols **44** stereoselectively (Scheme 26). The unique *anti*-carbomagnesiation process may be closely related to the *anti*-hydroalumination of propargyl alcohols with  $\text{LiAlH}_4$  or Red-Al<sup>34</sup>.



SCHEME 26

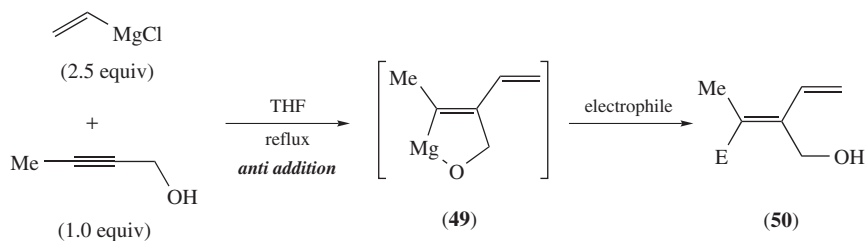
For example, the treatment of 2-butyne-1-ol (**45**) with allylmagnesium chloride in refluxing ether followed by hydrolysis affords **46** in 85% yield (Scheme 27)<sup>35,36</sup>. Although the use of vinylmagnesium chloride also provides the corresponding *anti*-addition product in



SCHEME 27

60% yield, no addition takes place with PhMgBr, MeMgCl and *t*-BuMgCl. The reaction is clearly oxygen-assisted since the yields of addition product substantially decrease in the case of **47** (7%) and **48** (0%), where the oxygen atom is too far remote for efficient assistance. In the homopropargyl series, both regioisomers are obtained.

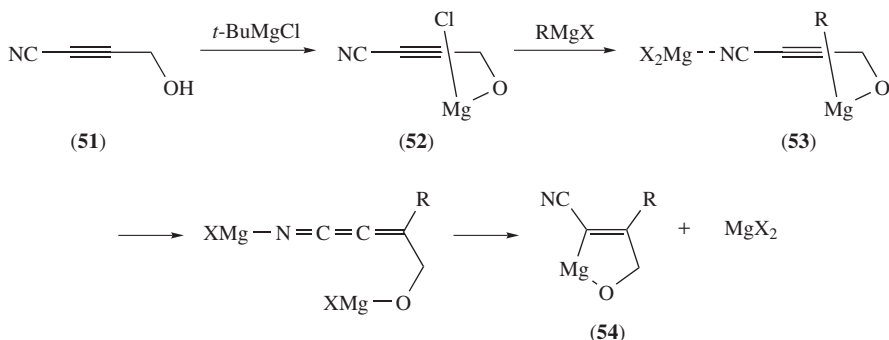
Useful 1,3-dienylmagnesium species can be generated through an *anti*-vinylmagnesiation of 2-butyne-1-ol (Scheme 28)<sup>37</sup>. The resultant organomagnesium species **49** is allowed to react with electrophiles, such as iodine, aldehydes and ketones, to furnish a range of substituted 1,3-dienes **50** in reasonable overall yields (Scheme 28)<sup>37,38</sup>.



Electrophile	E	Yield (%)
aq NH <sub>4</sub> Cl	H	75
I <sub>2</sub>	I	60
PhCHO	PhCH(OH)-	80
PhCOMe	PhCMe(OH)-	44

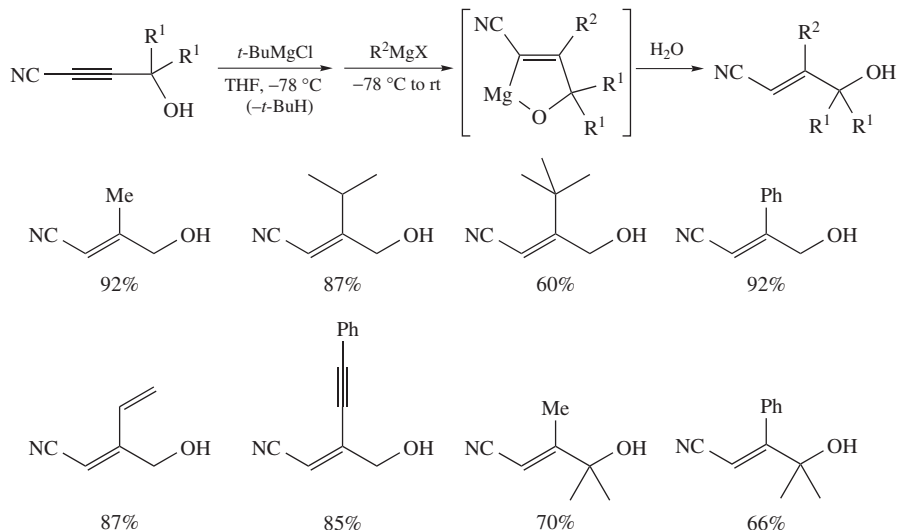
SCHEME 28

Propargylic alcohols having a cyano group **51** also undergo *anti*-carbomagnesiation (Scheme 29)<sup>39</sup>. Mechanistically, the reaction most likely proceeds through initial formation of halomagnesium alkoxide **52** followed by halogen-alkyl exchange. Alkyl transfer from the resulting alkoxide **53** leads to an intermediate chelate **54**. Fleming and coworkers found that *t*-BuMgCl serves as an excellent sacrificial base for initial deprotonation<sup>39</sup>.



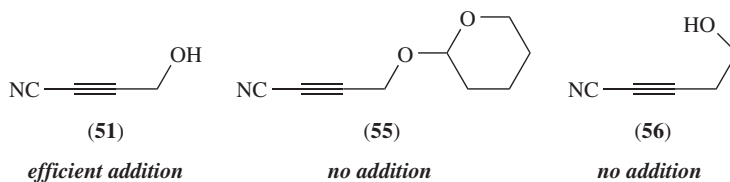
SCHEME 29

The carbomagnesiation reaction proceeds with a range of organomagnesium compounds (Scheme 30)<sup>39,40</sup>. Not only aryl, alkenyl and alkynyl groups, but also alkyl groups were found to add across a triple bond. The enhanced reactivity of cyano-substituted alkynes is worthwhile, and this may be due to accelerated alkyl transfer from **53** with activation of the cyano group by  $\text{MgX}_2$  (Scheme 29).



SCHEME 30

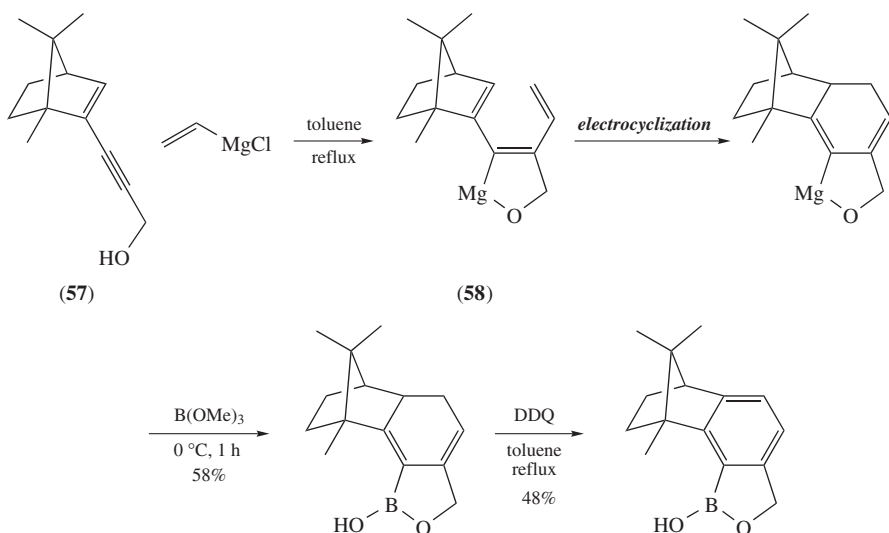
Chelation is essential for this carbomagnesiation. A control experiment, in which the THP-protected cyanoalkyne **55** is exposed to  $n\text{-BuMgCl}$ , leads to 90% recovery of unchanged alkyne (Scheme 31). In addition, homopropargylic alcohol **56** does not undergo carbomagnesiation<sup>40</sup>.



SCHEME 31

When enyne alcohol **57** is subjected to *anti*-carbomagnesiation using vinylmagnesium chloride, the resultant triene **58** undergoes further electrocyclicization (Scheme 32)<sup>41</sup>.

Fallis and coworkers reported the synthesis of a tricyclic ABC ring-system of paclitaxel using the three-component assembly of Grignard reagent, propargylic alcohol and aldehyde as a key step (Scheme 33)<sup>42,43</sup>.



SCHEME 32

By using dimethylformamide or benzonitrile as an electrophile after the *anti*-carbomagnesiation of propargylic alcohols, substituted furans **59** are obtained by treatment with *p*-TsOH (Scheme 34)<sup>44</sup>.

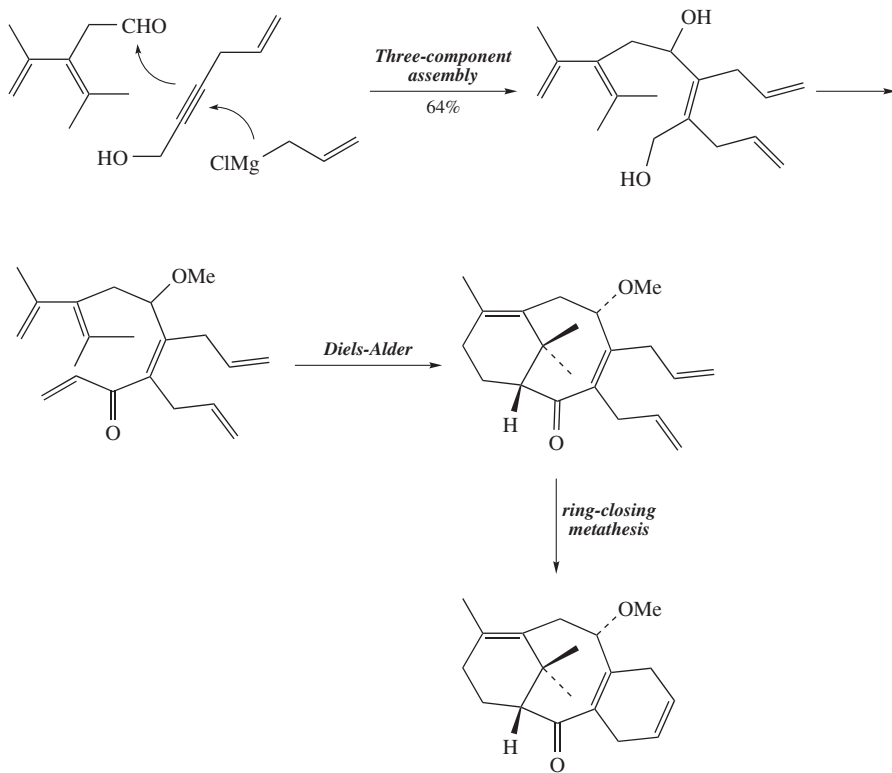
The use of CO<sub>2</sub> and SOCl<sub>2</sub> as electrophiles furnishes furanones and sultines, respectively (Scheme 35)<sup>45–47</sup>. By using this method, Fallis and coworkers demonstrated a facile synthesis of Vioxx, Merck's anti-inflammatory drug, as well as 'thio-Vioxx' which has been revealed to be a selective COX-2 (cyclooxygenase-2) inhibitor<sup>45</sup>.

As electrophiles for post-functionalization of *anti*-carbomagnesiation, aryl and alkenyl halides can also be used when Pd catalyst is employed. By merging such Pd-catalyzed arylation, tamoxifen can be synthesized in a stereoselective manner (Scheme 36)<sup>48</sup>.

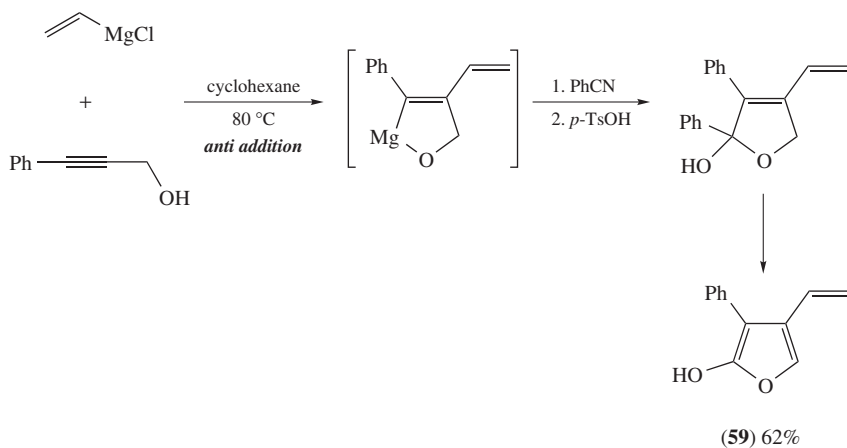
Several catalytic procedures have been also developed for the carbomagnesiation of propargylic alcohols. For example, Duboudin and Jousseume reported that the Cu-catalyzed carbomagnesiation of propargylic alcohols **60** leads to the selective formation of 2,3-disubstituted propyn-2-ols **61** via the hydroxyl-controlled *anti*-carbomagnesiation (Scheme 37)<sup>49,50</sup>. The copper catalyst not only allows the addition under much milder conditions (0 °C), but also allows the use of a wide range of organomagnesium compounds (Me, Et, *i*-Pr, *t*-Bu, Ph, PhCH<sub>2</sub>, CH<sub>2</sub>=CHCH<sub>2</sub>).

Quite interestingly, propargyl alcohol itself can be applied in the copper-catalyzed protocol. In the absence of copper catalyst, only the metalation (deprotonation) of terminal hydrogen occurs (Scheme 38)<sup>49,50</sup>.

The use of secondary propargylic alcohols affords a mixture of two regioisomeric products, while the reaction of tertiary propargylic alcohols gives the linear products selectively. Ma and Lu reported a highly regioselective Cu-catalyzed *anti*-carbomagnesiation of secondary terminal propargylic alcohols affording 2-substituted allylic alcohols<sup>51,52</sup>. For example, when 3-butyne-2-ol (**62**) is treated with a THF solution of *n*-pentylmagnesium bromide in the presence of CuI (0.5 equiv), *anti*-carbomagnesiation occurs (Scheme 39). When iodine is added as a quenching agent, alkenyl iodide **63** is obtained in high

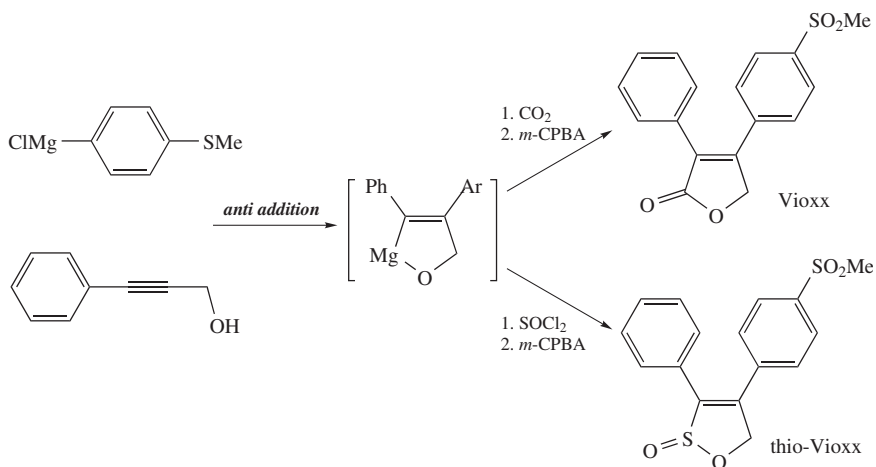


SCHEME 33

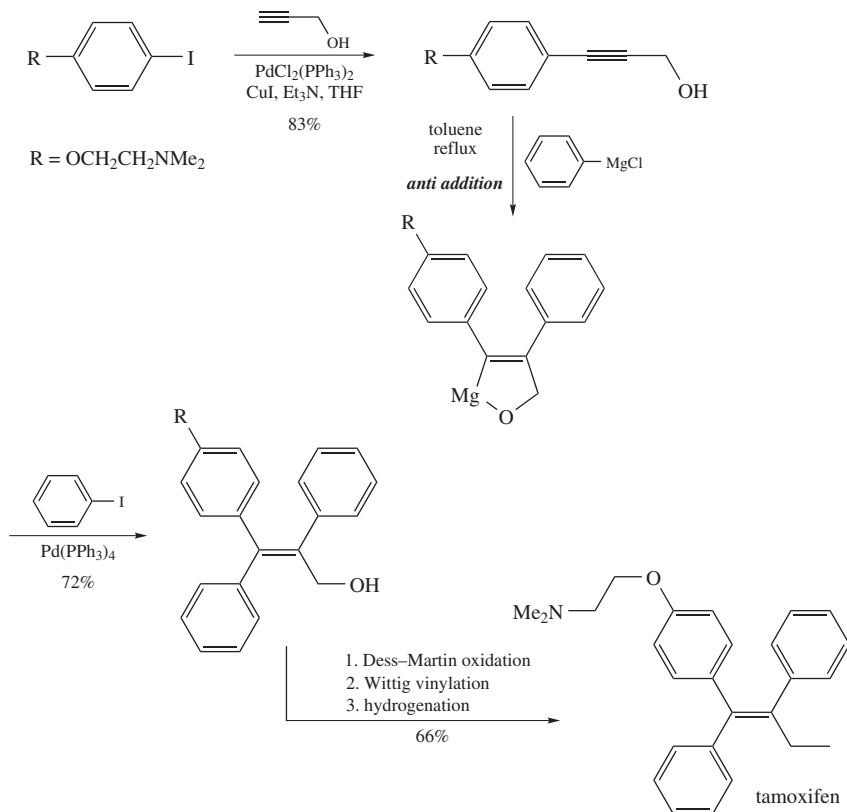


SCHEME 34

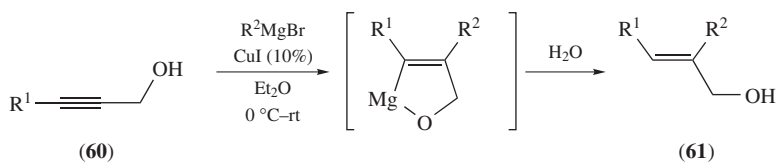




SCHEME 35

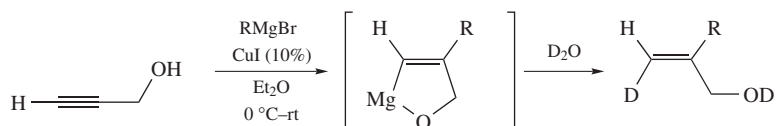


SCHEME 36



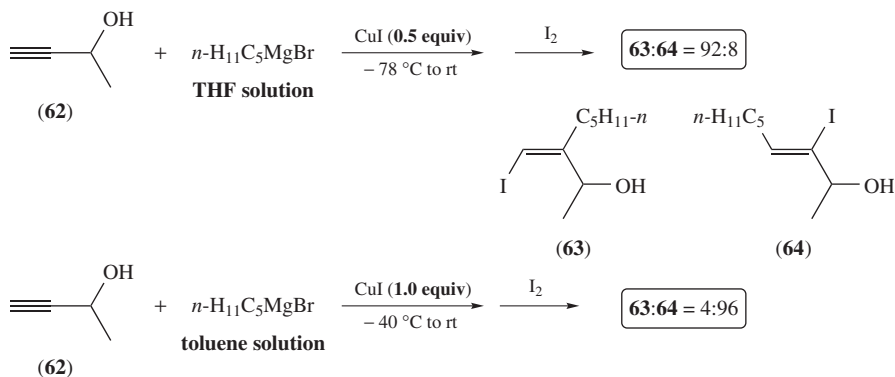
R <sup>1</sup>	R <sup>2</sup>	Yield (%)	R <sup>1</sup>	R <sup>2</sup>	Yield (%)
Me	allyl	80	Ph	Ph	55
Me	Ph	40	Ph	Me	58
Me	Et	55	Ph	Et	70
Me	<i>i</i> -Pr	45	Ph	<i>i</i> -Pr	60
Me	<i>t</i> -Bu	20	Ph	<i>t</i> -Bu	55

SCHEME 37



R	Yield (%)	R	Yield (%)
Allyl	60	Me	53
PhCH <sub>2</sub>	80	Et	60
Ph	73	<i>t</i> -Bu	45

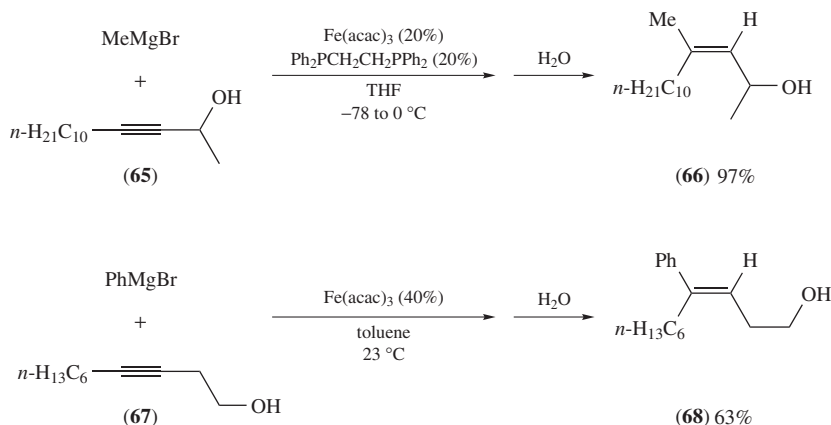
SCHEME 38



SCHEME 39

selectivity. The reaction also takes place with other copper salts such as CuCl, albeit with lower efficiency. Quite interestingly, however, the use of a stoichiometric amount of CuI results in reverse selectivity in product distribution (**63** vs **64**). Changing the solvent of Grignard reagent from THF to toluene results in exclusive formation of **64** (Scheme 39). This highly stereoselective *syn*-carbometalation can also be applied to tertiary propargylic alcohols.

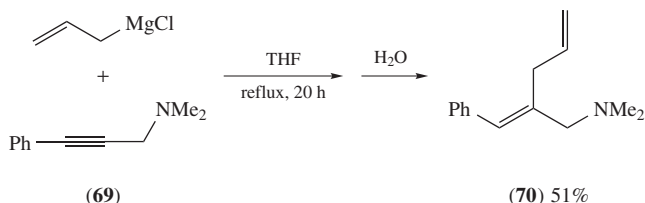
When an iron salt is used as a catalyst in the addition of Grignard reagents to propargylic alcohols, *syn*-carbomagnesiation takes place (Scheme 40)<sup>53</sup>. For example, when a catalytic amount of Fe(acac)<sub>3</sub> and Ph<sub>2</sub>PCH<sub>2</sub>CH<sub>2</sub>PPh<sub>2</sub> (dppe) are subjected to the reaction of MeMgBr and propargylic alcohol **65**, the carbomagnesiation takes place to give allylic alcohol **66** selectively. Important findings are not only that MeMgBr does not add to **65** in the absence of iron catalyst, but also that the present catalysis provides access to a different isomer of the addition product. Other metal salts such as Co(OAc)<sub>2</sub> and Ni(acac)<sub>2</sub> also show catalytic activity, but the efficiency is not as high as iron salts. Homopropargylic alcohol **67** also provides the corresponding homoallylic alcohol **68**. The directing effect of oxygen atom has been proposed as a possible scenario for highly regio- and stereoselective carbometalation<sup>53</sup>.



SCHEME 40

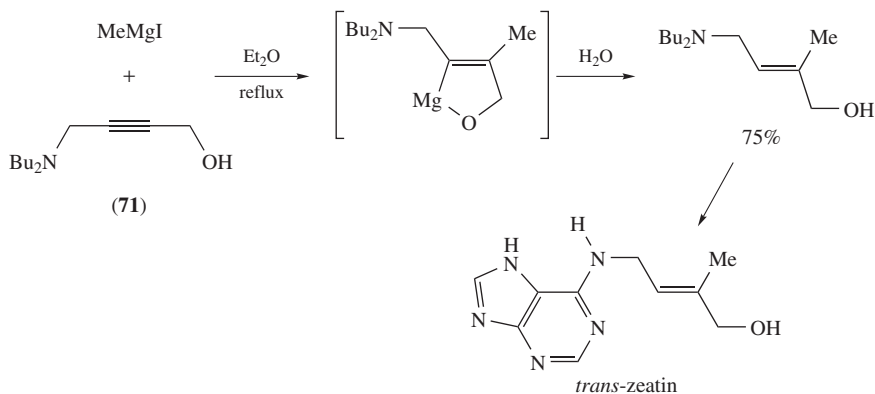
## F. Addition to Propargyl Amines

Similarly to propargylic alcohols, propargylic amines also undergo regio- and stereoselective carbomagnesiation (Scheme 41)<sup>54,55</sup>. For example, when propargylic amine **69** is treated with allylmagnesium chloride in refluxing THF, allylated product **70** is obtained in 51% yield<sup>54</sup>.



SCHEME 41

When an alkyne bears both a hydroxyl and an amino group at different propargylic positions, there is a regioselectivity issue with regard to the addition of organomagnesium compounds. When **71** is subjected to the reaction with organomagnesium compounds, organic groups are introduced at the carbon proximal to hydroxyl group (Scheme 42)<sup>56</sup>. These results clearly indicate the superior directing power of the hydroxyl group. By using such hydroxyl-assisted carbomagnesiation, a short synthesis of *trans*-zeatin has been accomplished<sup>56</sup>.

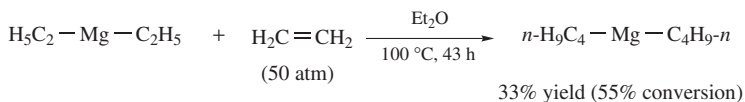


SCHEME 42

### III. CARBOMAGNESIATION REACTIONS OF ALKENES

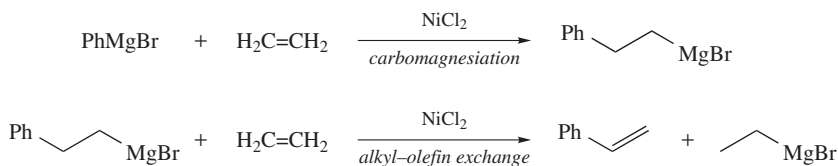
#### A. Addition to Simple Alkenes

As already stated in the introductory part of this chapter, the careful investigations of Gilman and coworkers revealed that ethylmagnesium halides do not add across simple alkenes in refluxing ether<sup>6,8</sup>. However, the carbomagnesiation of simple alkenes does take place under forcing conditions. In 1958, Podall and Foster reported that diethylmagnesium in ether reacts with ethylene at 50 atm and 100 °C to yield dibutylmagnesium (Scheme 43)<sup>57</sup>. Later, Shepherd<sup>58</sup> and Lehmkuhl and coworkers<sup>59–66</sup> obtained a 1:1 ratio of ethylene and other 1-alkenes by the addition of *sec*-alkyl, *tert*-alkyl and allylic Grignard reagents under high pressure and temperature (30–70 atm and 50–175 °C).



SCHEME 43

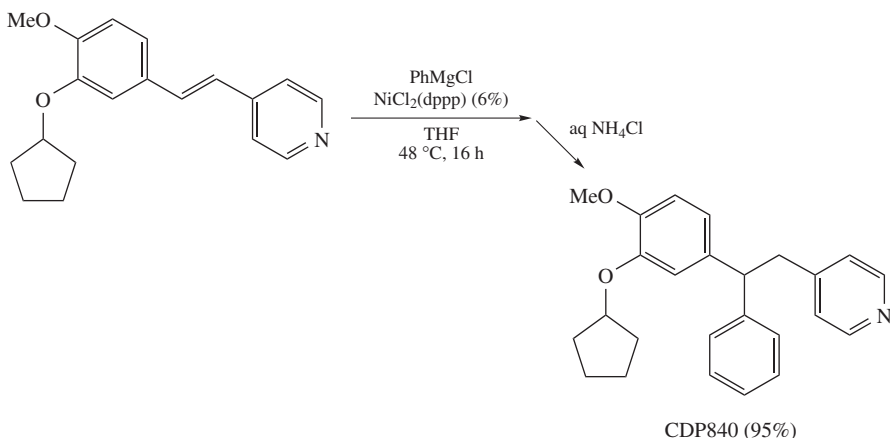
The presence of transition metal assists the insertion of C=C bond into the carbon-magnesium bond of Grignard reagents<sup>67</sup>. For example, Job and Reich as early as 1924 noticed that a mixture of PhMgBr and NiCl<sub>2</sub> in a Et<sub>2</sub>O solution absorbs ethylene<sup>68</sup>. Later, it was found that NiCl<sub>2</sub> does catalyze an insertion of ethylene into the Ph–Mg bond giving PhCH<sub>2</sub>CH<sub>2</sub>MgBr (Scheme 44)<sup>69–71</sup>. However, it was also found that this catalytic carbomagnesiation is accompanied by subsequent alkyl–olefin exchange reaction, which is also catalyzed by NiCl<sub>2</sub> (Scheme 44)<sup>69–71</sup>. Because of the occurrence of the alkyl–olefin



SCHEME 44

exchange, this catalytic carbomagnesiation has not received much attention in organic synthesis.

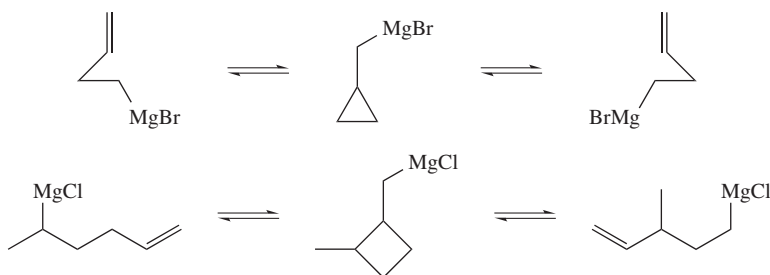
Although it may be regarded as an example of catalytic conjugate addition, Ni-catalyzed carbomagnesiation is possible for 4-vinylpyridines (Scheme 45)<sup>72</sup>. Under the influence of nickel catalyst, the addition of phenyl, vinyl and benzyl Grignard reagents takes place to give the addition products in good yields. As nickel catalysts,  $\text{NiCl}_2(\text{dppp})$ ,  $\text{NiCl}_2(\text{PPh}_3)_2$  and  $\text{Ni}(\text{acac})_2$  have sufficient activity. Unfortunately, Grignard reagents bearing  $\beta$ -hydrogen atom(s) cannot be applied. By using this method, a rapid synthesis of CDP840, a phosphodiesterase IV inhibitor, has been accomplished (Scheme 45)<sup>72</sup>.



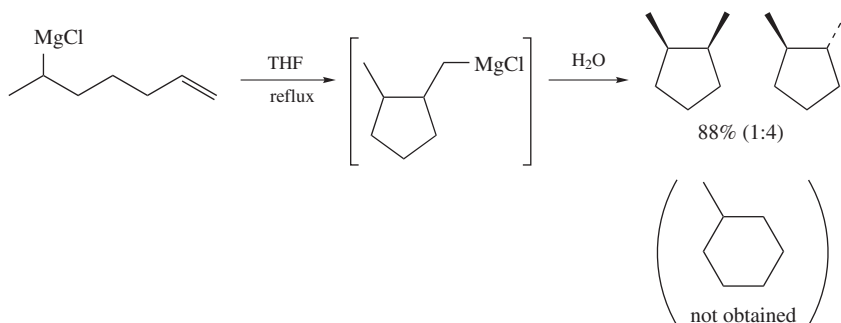
SCHEME 45

Similar to the carbomagnesiation of alkynes, the low reactivity of simple alkenes can be alleviated by performing intramolecular carbomagnesiation<sup>73</sup>. For example, it has been reported that intramolecular carbomagnesiation is involved in the rearrangements of butenyl- and pentenylmagnesium compounds (Scheme 46)<sup>74–78</sup>. However, cyclic products are often not observed because they are usually much less stable than the ring-opening products.

A facile intramolecular carbomagnesiation becomes possible by inserting one more carbon between the reactive magnesium center and the double bond. For example, when a 6-chloro-1-heptene was refluxed with magnesium, 1,2-dimethylcyclopentane (*cis/trans* = *ca* 1/4) was obtained in 88% yield after hydrolysis (Scheme 47)<sup>79,80</sup>. The cyclization shows a 5-*exo-trig* selectivity and the product derived from 6-*endo-trig* cyclization (methylcyclohexane) is not observed.



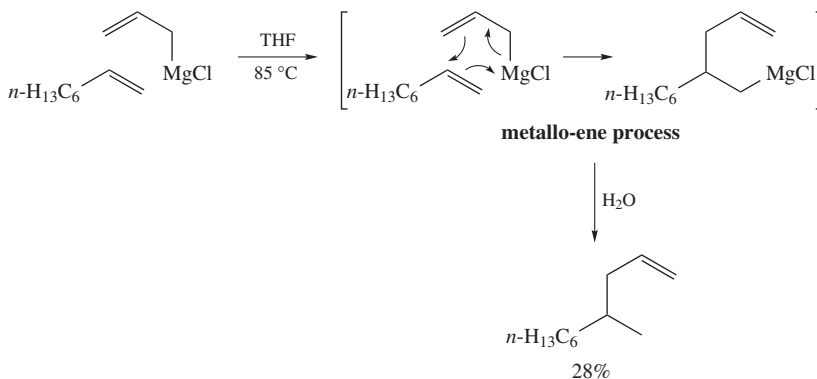
SCHEME 46



SCHEME 47

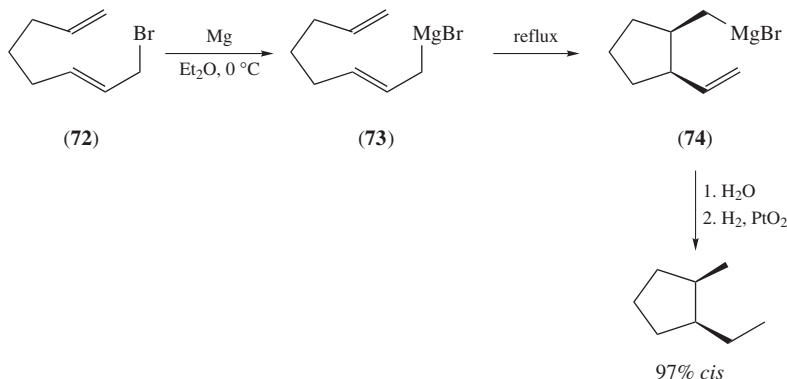
## B. Allylmagnesiation of Alkenes

Allylic Grignard reagents are known to possess exceptionally high reactivity toward alkenes in comparison with other Grignard reagents (Scheme 48)<sup>59–61, 63–65, 81</sup>. The process has been now recognized as a metallo-ene reaction. Even with enhanced reactivity, however, intermolecular carbomagnesiation to simple alkenes is still low-yielding, and thus has received virtually no attention as a strategic tool in organic synthesis.



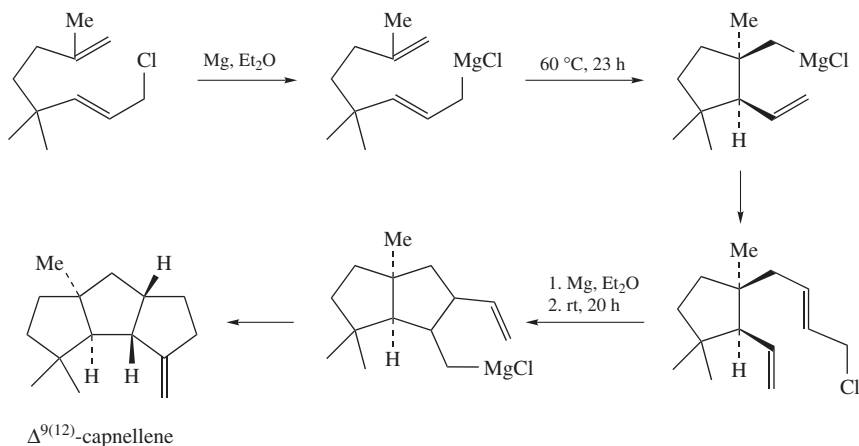
SCHEME 48

In contrast to intermolecular versions, intramolecular allylmagnesiation of alkenes (metallo-ene reaction) is entropically favored, and thus more efficient and selective<sup>82</sup>. Felkin and coworkers have demonstrated that 2,7-octadienylmagnesium bromide **73** prepared from **72** undergoes intramolecular allylmagnesiation in refluxing ether to give **74** stereoselectively (Scheme 49)<sup>83</sup>.



SCHEME 49

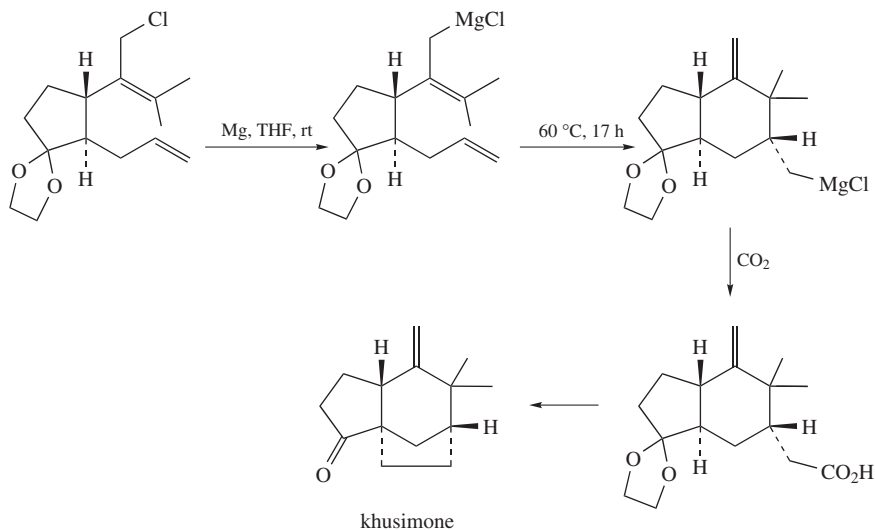
Oppolzer and coworkers extensively utilized such intramolecular ‘magnesium-ene’ reaction in the synthesis of complex natural products<sup>82</sup>. For example,  $\Delta^{9(12)}$ -capnellene has been synthesized by using this intramolecular allylmagnesiations iteratively (Scheme 50)<sup>84</sup>.



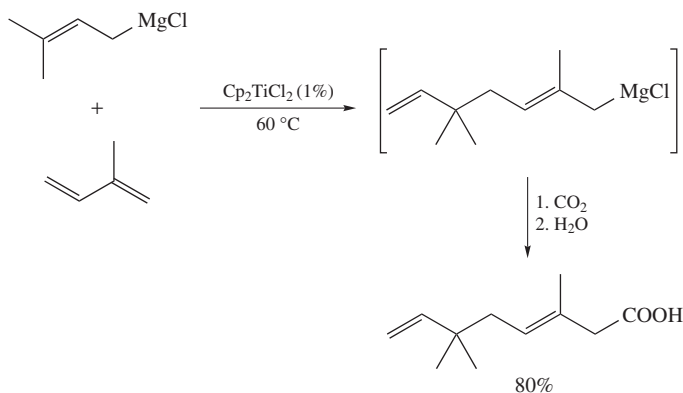
SCHEME 50

Oppolzer and coworkers further demonstrated that an alternative mode of cyclization<sup>85</sup> led to the total synthesis of khusimone (Scheme 51)<sup>86</sup>.

Allylic Grignard reagents also react with dienes such as butadiene or isoprene<sup>87</sup>. However, the reaction tends to produce oligomeric products. Otsuka and Akutagawa have



SCHEME 51



SCHEME 52

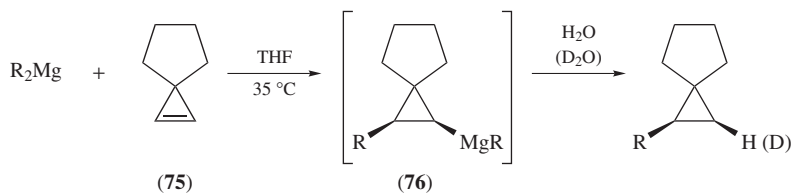
demonstrated that the use of  $\text{Cp}_2\text{TiCl}_2$  or  $\text{TiCl}_2(\text{OEt})_2$  as a catalyst promotes the selective formation of 1:1 adduct (Scheme 52)<sup>88,89</sup>. By using this method, a range of natural terpenes, such as lanceol and lavandurol, have been synthesized<sup>88</sup>.

### C. Addition to Strained Alkenes

Cyclopropenes possess appreciable high reactivity toward carbomagnesiation<sup>90</sup>. For example, dialkylmagnesium compounds react with spiro[2.4]hept-1-ene (**75**) to give the carbometalated products **76** (Scheme 53)<sup>91</sup>. The *syn*-addition has been confirmed by  $\text{D}_2\text{O}$  quenching of the reaction.

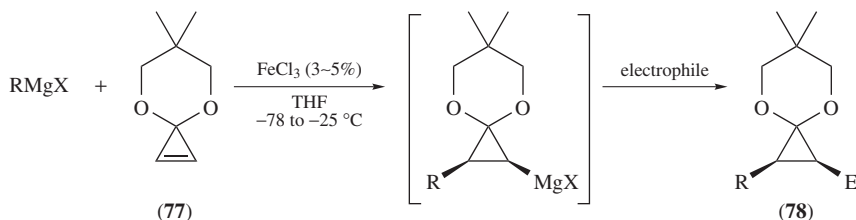
Nakamura and coworkers reported that the carbomagnesiation of cyclopropenone acetal **77** is significantly promoted by the addition of a catalytic amount of  $\text{FeCl}_3$  (Scheme 54)<sup>92</sup>.





R = Me, Et, *i*-Pr, *t*-Bu

SCHEME 53

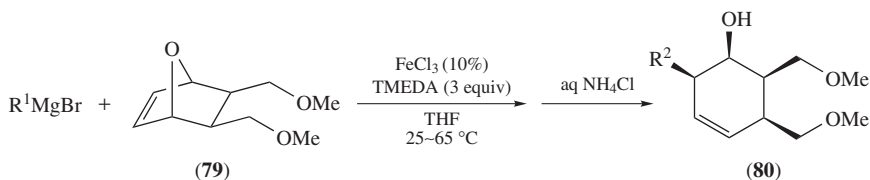


RMgX	Electrophile	E	Yield (%)
C <sub>6</sub> H <sub>5</sub> MgBr	H <sub>2</sub> O	H	96
C <sub>6</sub> H <sub>5</sub> MgBr	CH <sub>2</sub> =CHCH <sub>2</sub> Br	CH <sub>2</sub> =CHCH <sub>2</sub> -	85
C <sub>6</sub> H <sub>5</sub> MgBr	CH <sub>3</sub> I	CH <sub>3</sub>	90
C <sub>6</sub> H <sub>5</sub> MgBr	C <sub>6</sub> H <sub>5</sub> CHO	C <sub>6</sub> H <sub>5</sub> CH(OH)-	56
CH <sub>2</sub> =CHMgBr	H <sub>2</sub> O	H	75
CH <sub>3</sub> MgBr	H <sub>2</sub> O	H	66
C <sub>6</sub> H <sub>5</sub> CH <sub>2</sub> CH <sub>2</sub> MgCl	H <sub>2</sub> O	H	85

SCHEME 54

The reactions using phenyl, vinyl and alkyl Grignard reagents afford the substituted cyclopropanone acetals **78** in good to excellent yields after hydrolysis. Notably, the reaction of the Grignard reagent possessing  $\beta$ -hydrogen atoms takes place in good yield. The *syn*-carbometalation has been confirmed by employing carbon electrophiles.

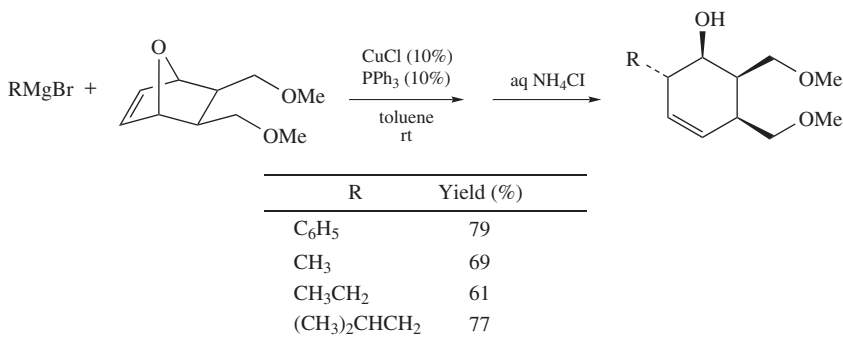
This Fe-catalyzed carbomagnesiation reaction can be extended to other strained alkenes as well. For example, the treatment of aryl Grignard reagents with 7-oxabicyclo[2.2.1]heptane derivative **79** induces the stereoselective arylative ring-opening reaction in the presence of FeCl<sub>3</sub> catalyst to give the densely substituted cyclohexene derivative **80** in good yields (Scheme 55)<sup>92,93</sup>. Addition of *N,N,N',N'*-tetramethylethylenediamine (TMEDA) to the reaction mixture facilitates the ring-opening reaction<sup>93</sup>. The reaction takes place in such a manner that the aryl group attacks the carbon–carbon double bond from the *exo*-face of the substrate to give all-*cis*-substituted cyclohexenol product **80** after subsequent  $\beta$ -eliminative ring opening of the oxygen bridge. The reaction can be extended to alkenyl Grignard reagents but the use of EtMgBr and *i*-PrMgBr results in the production of vinyl- and hydrogen-transferred products, respectively ( $\text{R}^1 \neq \text{R}^2$ )<sup>93</sup>. Lautens and coworkers reported that the nickel-based catalytic system is also effective in the ring-opening reactions of oxabicyclic alkenes<sup>94</sup>.



R <sup>1</sup>	R <sup>2</sup>	Yield (%)
C <sub>6</sub> H <sub>5</sub>	C <sub>6</sub> H <sub>5</sub>	74
4-MeC <sub>6</sub> H <sub>4</sub>	4-MeC <sub>6</sub> H <sub>4</sub>	72
2-MeC <sub>6</sub> H <sub>4</sub>	2-MeC <sub>6</sub> H <sub>4</sub>	75
CH <sub>2</sub> =CH	CH <sub>2</sub> =CH	41
CH <sub>3</sub> CH <sub>2</sub>	CH <sub>2</sub> =CH	24
(CH <sub>3</sub> ) <sub>2</sub> CH	H	92

SCHEME 55

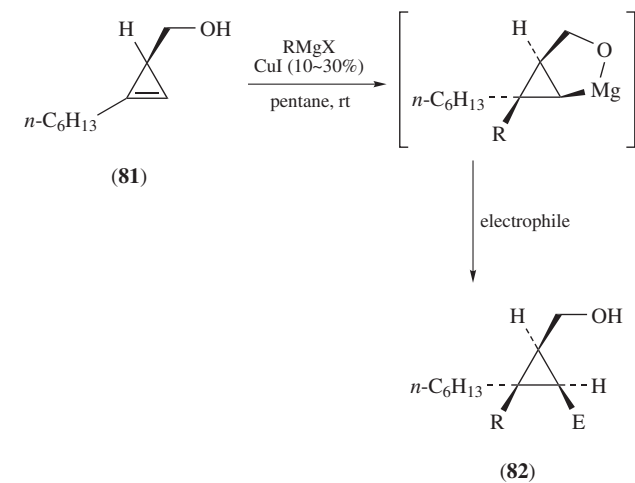
Arrayás, Carretero and coworkers have demonstrated that the CuCl/PPh<sub>3</sub> system also induces the ring opening of oxacyclic alkenes but with completely opposite (*anti*) stereoselectivity (Scheme 56)<sup>95</sup>. The introduction of methyl and alkyl groups, which was not possible with the iron-based system (Scheme 55), is also feasible with high fidelity. Miller and coworkers reported the Cu-catalyzed regio- and stereoselective ring openings of 3-aza-2-oxabicyclo[2.2.1]hept-5-ene systems with Grignard reagents<sup>96</sup>.



SCHEME 56

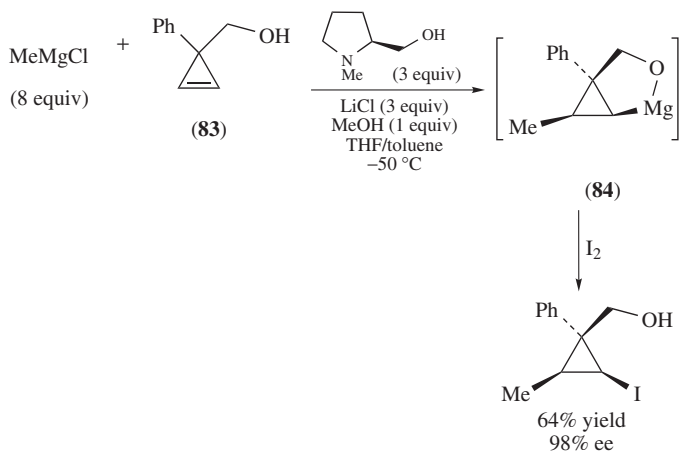
Hydroxymethylated cyclopropanes, which can be readily prepared by Rh-catalyzed reaction of diazoesters and alkynes, are good substrates for uncatalyzed<sup>97</sup> and Cu-catalyzed<sup>98</sup> carbomagnesiation. For example, a range of substituted cyclopropanes **82** can be synthesized in a regio- and stereoselective fashion by the Cu-catalyzed addition of Grignard reagents to (3-hydroxymethyl)cyclopropanes **81** (Scheme 57)<sup>98, 99</sup>.

Fox and Lui have demonstrated that the addition of *N*-methylprolinol can induce high enantioselectivity in the methylmagnesiation of (3-hydroxymethyl)cyclopropane **83** (Scheme 58)<sup>100</sup>. The fact that the reaction produces only one diastereomer, where the methyl and hydroxymethyl groups on cyclopropane ring are *syn*, may be rationalized by



R	Electrophile	E	Yield (%)
Methyl	H <sub>2</sub> O	H	83
Methyl	I <sub>2</sub>	I	81
Benzyl	H <sub>2</sub> O	H	78
Vinyl	H <sub>2</sub> O	H	81
Vinyl	I <sub>2</sub>	I	83
Vinyl	Bu <sub>3</sub> SnCl	Bu <sub>3</sub> Sn	71
Phenylethynyl	H <sub>2</sub> O	H	75

SCHEME 57

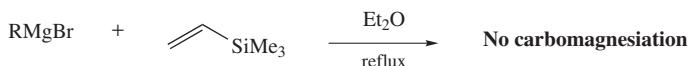


SCHEME 58

the intermediacy of magnesium chelate **84**. The application to other organomagnesium compounds results in much lower enantioselectivity.

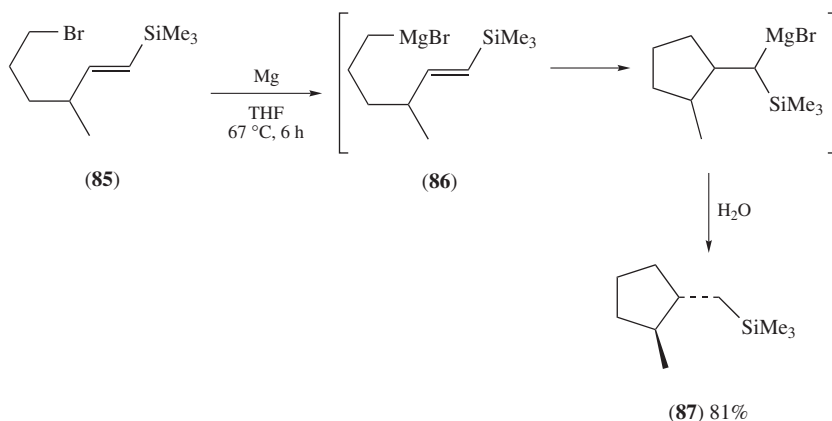
### D. Addition to Vinylsilanes

The carbomagnesiation of vinylsilanes is a powerful method for the generation of synthetically useful  $\alpha$ -silyl carbanions. However, simple vinylsilanes such as trimethyl(vinyl) silane do not undergo carbometalation with Grignard reagents (Scheme 59)<sup>101</sup>. In early days, only limited success had been achieved by using perfluorovinylsilanes<sup>102</sup>.



SCHEME 59

One of the classical solutions to overcome the low reactivity is to render the carbomagnesiation intramolecular. For example, Utimoto and coworkers reported that the reaction of (*E*)-6-bromo-3-methyl-1-trimethylsilyl-1-hexene (**85**) with magnesium produces the corresponding Grignard reagent **86**, which intramolecularly adds to the vinylsilane moiety from the less hindered side affording a single stereoisomer of cyclized product **87** (Scheme 60)<sup>103</sup>.

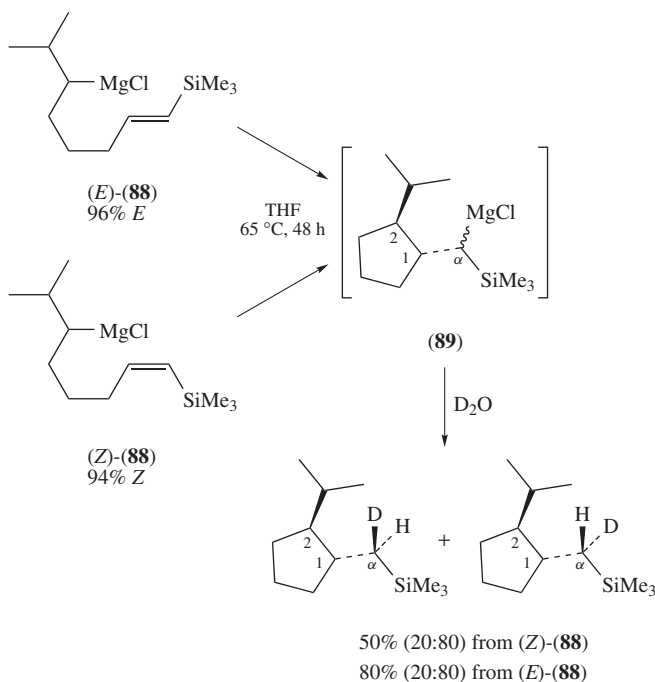


SCHEME 60

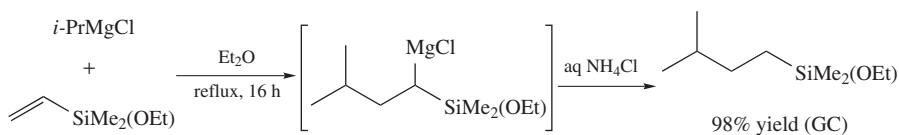
Hoffmann and coworkers have further carefully examined the intramolecular carbomagnesiation of a vinylsilane (Scheme 61)<sup>104</sup>. Both (*E*)- and (*Z*)-isomers of **88** undergo an intramolecular carbomagnesiation and a stereospecific (>95%) *syn*-addition of the carbon–magnesium bond to the double bond takes place. The resulting  $\alpha$ -silylalkylmagnesium compounds **89** are not configurationally stable under the reaction conditions. They epimerize with a half-life of 2.7 days at room temperature.

Electron-withdrawing groups such as alkoxy and chloro groups on silicon activate vinylsilanes toward the addition of secondary and tertiary alkylmagnesium halides (Scheme 62)<sup>101, 105</sup>.

Subsequent reactions of thus-generated organomagnesium species are also possible<sup>106, 107</sup>. For example,  $\alpha$ -silylorganomagnesium compound **91** is allowed to react with



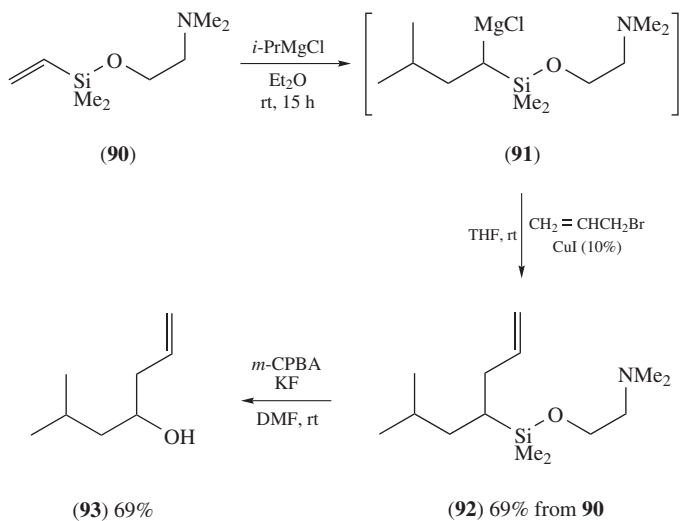
SCHEME 61



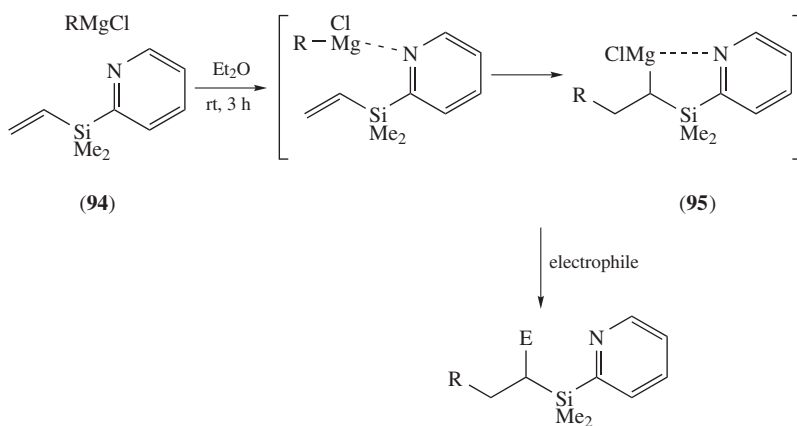
SCHEME 62

allyl bromide in the presence of CuI catalyst to give **92** in 69% yield (Scheme 63)<sup>106</sup>. The subsequent oxidative cleavage of the carbon–silicon bond then affords the secondary alcohol **93** in 69% yield (Scheme 63).

Although Grignard reagents become viable for the addition reaction to vinylsilanes, serious limitations still exist. For example, substitution reactions at the silicon atom are often observed as unavoidable side reactions when activating groups (e.g. chloro, alkoxy and amino groups) are used. In addition, primary alkyl Grignard reagents are not applicable. Itami, Yoshida and coworkers have developed a novel strategy for intermolecular carbomagnesiation of vinylsilanes by exploiting the 2-pyridylsilyl group as a removable directing group (Scheme 64)<sup>108,109</sup>. The reaction presumably involves a pre-equilibrium complex of **94** and a Grignard reagent, making the subsequent carbomagnesiation intramolecular in nature. The importance of this pre-equilibrium complex was further supported by the observation of a dramatic solvent effect: weakly coordinating solvents such as Et<sub>2</sub>O favor this reaction, whereas strongly coordinating solvents such as THF disfavor it. In addition to this kinetic preference, stabilization of the resultant organomagnesium species **95** by intramolecular coordination of the pyridyl group might



SCHEME 63

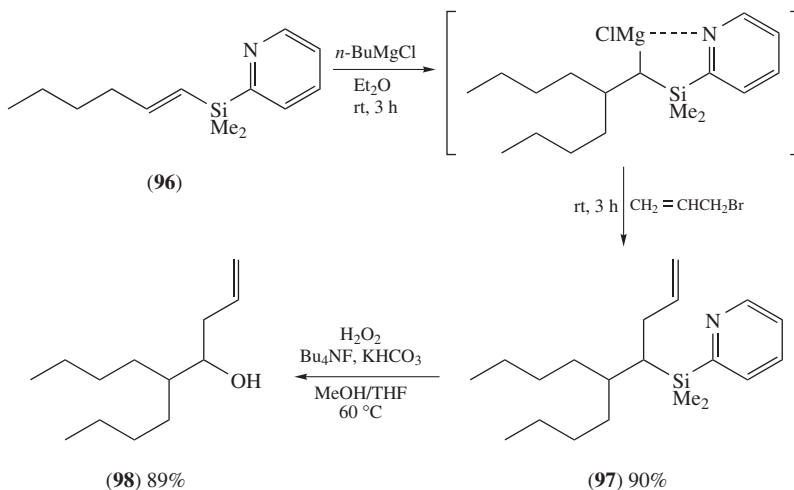


R	Electrophile	E	Yield (%)
<i>n</i> -Butyl	D <sub>2</sub> O	D	83
<i>n</i> -Butyl	CH <sub>2</sub> =CHCH <sub>2</sub> Br	CH <sub>2</sub> =CHCH <sub>2</sub> -	91
<i>n</i> -Butyl	CH <sub>2</sub> =N <sup>+</sup> Me <sub>2</sub> I <sup>-</sup>	Me <sub>2</sub> NCH <sub>2</sub> -	93
<i>n</i> -Butyl	C <sub>6</sub> H <sub>5</sub> I [5% Pd(PPh <sub>3</sub> ) <sub>4</sub> ]	C <sub>6</sub> H <sub>5</sub>	77
<i>i</i> -Propyl	CH <sub>2</sub> =CHCH <sub>2</sub> Br	CH <sub>2</sub> =CHCH <sub>2</sub> -	91
Allyl	4-ClC <sub>6</sub> H <sub>4</sub> Br [2.5% Pd(PPh <sub>3</sub> ) <sub>4</sub> ]	4-ClC <sub>6</sub> H <sub>4</sub>	93
Phenyl	H <sub>2</sub> O	H	73

SCHEME 64

also be responsible for the efficiency of this carbomagnesiation process. Nevertheless, by using this protocol, facile addition of primary alkyl Grignard reagents to vinylsilanes has been realized for the first time. Secondary alkyl, allyl and phenyl Grignard reagents also add across **94**. The addition of various electrophiles in the subsequent reactions is also possible (Scheme 64).

The carbomagnesiation also takes place with  $\beta$ -substituted vinylsilane **96**, which represents a more difficult class of substrate (Scheme 65)<sup>108</sup>. The three-component assembled product **97** is converted to the corresponding secondary alcohol **98** by fluoride-mediated oxidative cleavage of the carbon–silicon bond (Scheme 65).



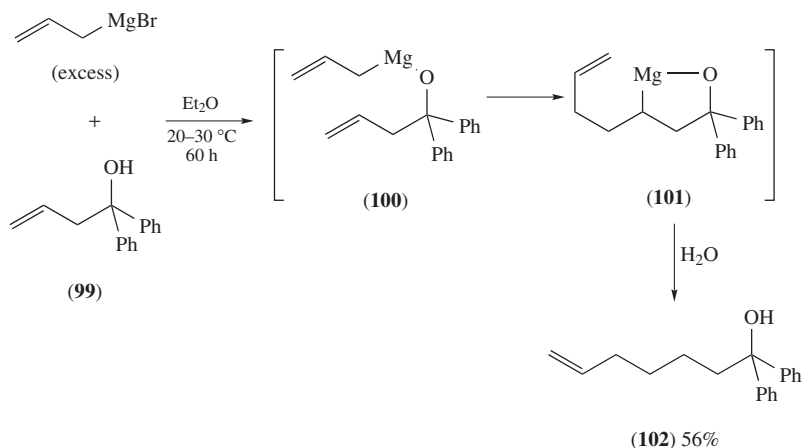
SCHEME 65

### E. Addition to Allyl and Homoallyl Alcohols

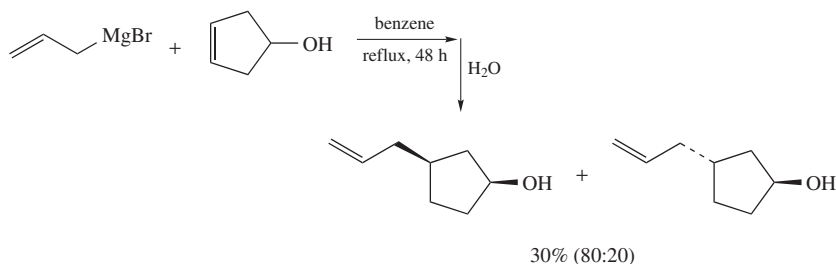
The presence of a neighboring hydroxyl group facilitates the carbomagnesiation of alkenes. For example, Eisch and Husk unexpectedly found that homoallylic alcohol **99** reacts with an excess amount of allylmagnesium bromide at room temperature to give the carbomagnesiation product **102** in 56% yield (Scheme 66)<sup>110</sup>. At this time, it was one of the few examples of carbomagnesiation to unconjugated ethylenic linkage taking place under mild conditions. However, the reaction is somewhat limited to allyl Grignard reagent: *t*-BuMgBr and PhCH<sub>2</sub>MgBr exhibit extremely low reactivity, and no reaction occurs with PhMgBr<sup>111</sup>. An analysis of this facile carbomagnesiation in terms of substrate, magnesium reagent and medium has led to the suggestion that the reaction occurs via the intramolecular rearrangement of **100** to **101**<sup>111,112</sup>. In line with such a hydroxyl-assisted proximity effect, an insertion of methylene spacer(s) between the hydroxyl group and the double bond leads to substantial decrease in reaction efficiency<sup>112</sup>. In some instances when the carbomagnesiation is slow, the dehydration of the initial product often occurs<sup>112</sup>.

When allylmagnesium bromide is allowed to react with 3-cyclopentanol, the allylated product (3-allylcyclopentanol) is obtained as an 80:20 mixture of *cis*- and *trans*-isomers (Scheme 67)<sup>113</sup>. The reaction of 3-cyclopentanol with diallylmagnesium in refluxing benzene proceeds slowly but cleanly to yield only the *cis*-isomer.

Ni(acac)<sub>2</sub> acts as a catalyst for this carbomagnesiation<sup>112</sup>. The remarkable effect of nickel salts on this allylation reaction has three interconnected advantages: more rapid



SCHEME 66



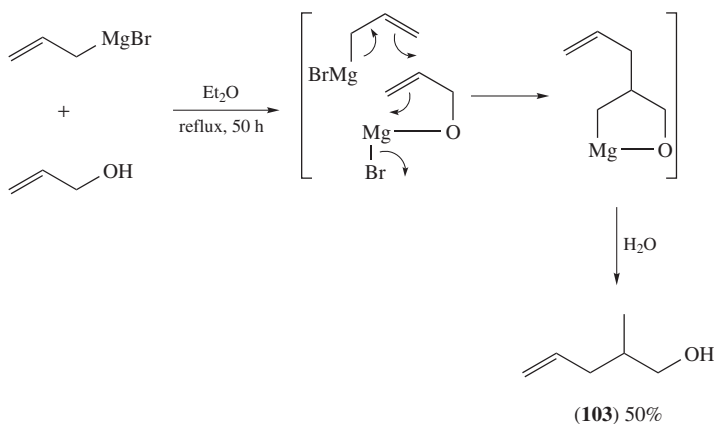
SCHEME 67

reaction, higher conversion to product and less dehydration of the initial alcohol. Although (allyl)nickel species seems to be involved, the mechanism of nickel catalysis is still unknown.

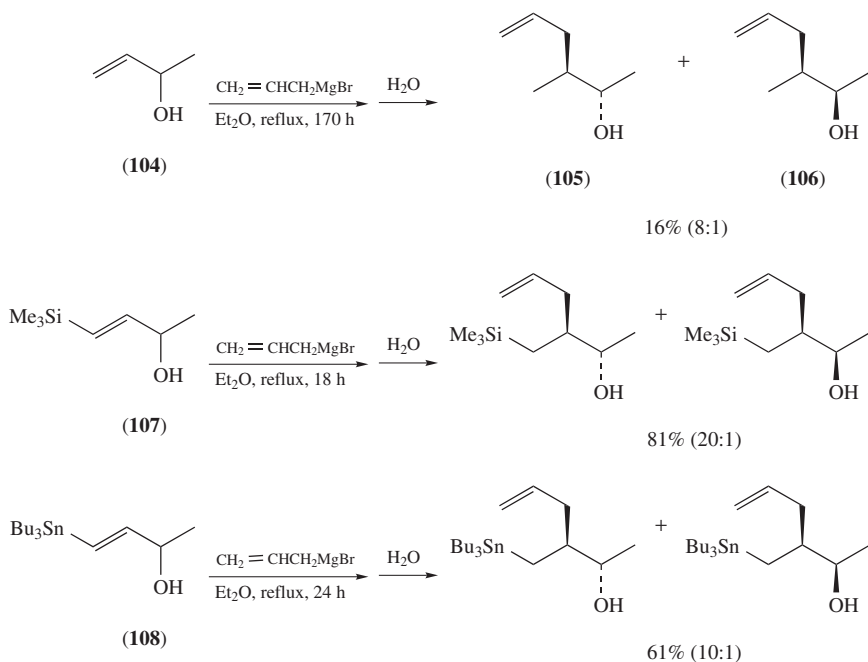
At about the same time that Eisch and coworkers discovered the hydroxyl-assisted carbomagnesiation of homoallylic alcohol, Felkin and coworkers reported a different carbomagnesiation that was also assisted by hydroxyl group. Allylmagnesium bromide adds regioselectively to allyl alcohol, and the alcohol **103** was obtained in 50% yield after hydrolysis (Scheme 68)<sup>114</sup>. The use of  $\text{PhCH}_2\text{MgCl}$  affords a 10% yield of 2-benzylpropanol (benzene, reflux, 170 h), but the reaction does not take place with *t*-BuMgCl, *i*-BuMgCl, *i*-PrMgCl and EtMgBr. Although cinnamyl alcohol is an excellent substrate for the reaction with allylmagnesium bromide (99% yield,  $\text{Et}_2\text{O}$ , room temperature)<sup>115</sup>, crotyl alcohol and  $\beta$ -methallyl alcohol are poor substrates (<5%,  $\text{Et}_2\text{O}$ , reflux, 170 h)<sup>114</sup>. The protection of the hydroxyl group completely suppresses the reaction, which clearly indicates that the reaction is assisted by the hydroxyl group. It has been proposed that it follows the magnesium-ene mechanism, which is promoted by coordination of alkene  $\pi$ -bond to a covalently bound magnesium atom (Scheme 68). This is in sharp contrast to the mechanism proposed for the allylmagnesiation of homoallylic alcohol, where the allyl group is transferred intramolecularly (Scheme 66).

A concerted addition of this kind, involving simultaneous intramolecular electrophilic assistance by the magnesium bound to oxygen, and intermolecular nucleophilic attack by





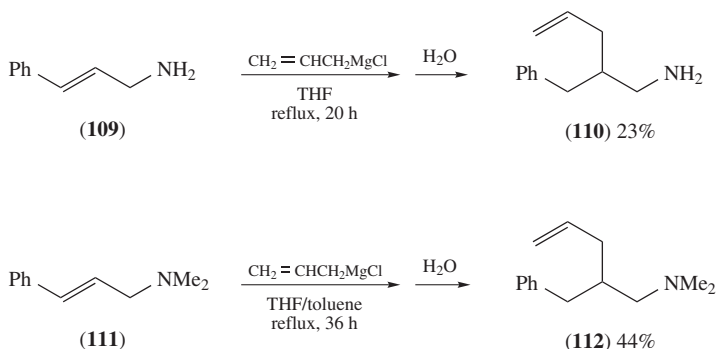
SCHEME 68



SCHEME 69

allylmagnesium bromide, is consistent not only with the kinetic data, but also with the stereochemical course of the reaction. For example, the reaction of  $\alpha$ -methallyl alcohol (**104**) with allylmagnesium bromide gives the product alcohol **105** and **106** (16% yield) in a ratio of 8:1 (Scheme 69)<sup>114</sup>. The reactions of silylated and stannylated  $\alpha$ -methallyl alcohols (**107** and **108**) give carbometalated products in much higher yields with preference for the *erythro* isomers<sup>116</sup>.

Similarly to the case of the hydroxyl group, the amino group also exhibits an acceleration effect in carbomagnesiation reaction. For example, allylic amines such as **109** and **111** undergo regioselective carbomagnesiation with allylmagnesium chloride giving the adducts **110** and **112** in 23% and 44% yield, respectively (Scheme 70)<sup>54</sup>. The failure to observe addition to the related unsaturated hydrocarbon (1-phenyl-1-propene), even when amine function are present in other molecules in the solution, suggests that the amine functions promotes the additions to **109** and **111**. Hence, an amine-assisted carbomagnesiation mechanism similar to that proposed for allylic alcohol (Scheme 68) has been suggested.



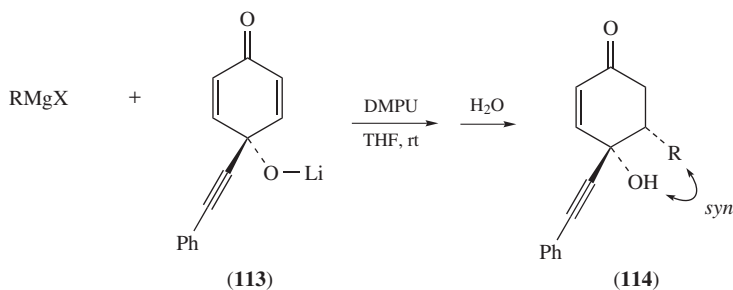
SCHEME 70

As in the cases of many types of carbomagnesiation reactions mentioned before, a chelating auxiliary on olefinic substrates has a strong impact on the reactivity and selectivity in conjugate addition. Chelation-controlled conjugate additions have been investigated with quinol alkoxide **113** that reacts with Grignard reagents to afford conjugate addition products **114** (Scheme 71)<sup>117–119</sup>. Chelation between the alkoxide and the Grignard reagent results in a transient complex that delivers the nucleophile from the same face and establishes the *syn* stereochemistry between the installed organic group and the hydroxyl group.

Such an alkoxide-assisted (hydroxyl-assisted) conjugate addition methodology has been exploited in the key step toward (±)-euonyminol (Scheme 72)<sup>120</sup>.

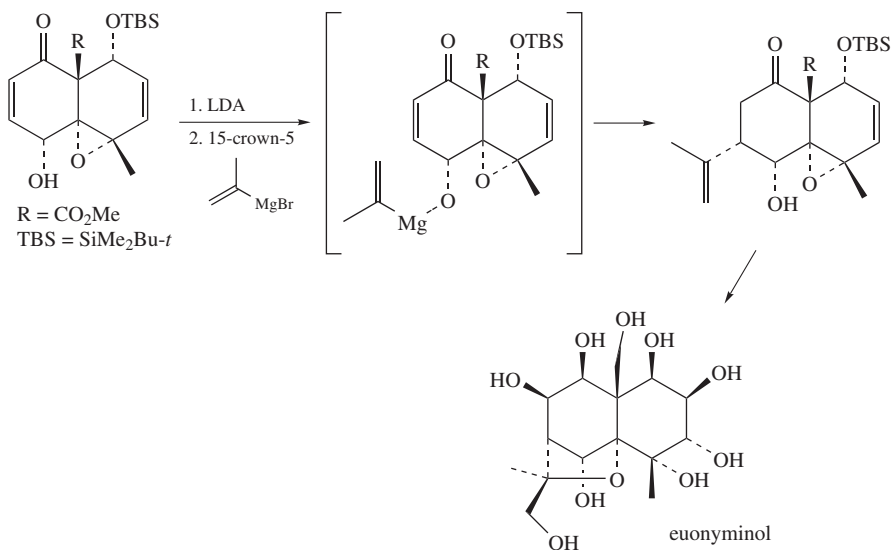
Addition of Grignard reagents to hydroxyl-containing unsaturated nitrile **115** provides conjugate addition products with virtually complete stereocontrol (Scheme 73)<sup>121</sup>. Mechanistic evidence supports a chelation-controlled conjugate addition via alkylmagnesium alkoxide intermediates. Diverse Grignard reagents having  $sp^3$ -,  $sp^2$ - and  $sp$ -hybridized carbons react with high efficiency ( $-78^\circ\text{C}$ , 5 min).

Fleming and coworkers further extended the chelation-controlled conjugate addition strategy to  $\gamma$ -hydroxy unsaturated nitriles (Scheme 74)<sup>122, 123</sup>. A treatment of a Grignard reagent with  $\gamma$ -hydroxy unsaturated nitrile **116** results in clean and regioselective carbomagnesiation. Mechanistically, deprotonation of the hydroxyl group generates the alkoxymagnesium halide **117** that rapidly engages in halogen–alkyl exchange with the Grignard reagent. The resulting alkylmagnesium alkoxide initiates a smooth conjugate addition, ultimately generating the conjugate adduct **118** after treatment with acetic acid. The substantial rate difference between deprotonation and conjugate addition allows *t*-BuMgCl to be employed as a sacrificial base. The hydroxyl-assisted mechanism resembles that suggested for the carbomagnesiation of allylic alcohol. In line with such a chelation-controlled mechanism, control experiments involving addition of *n*-BuMgCl to



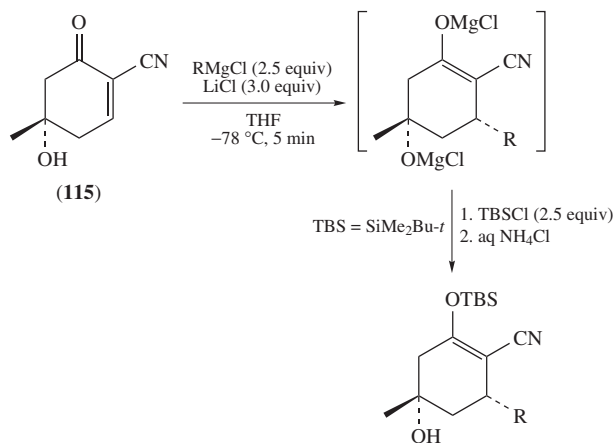
RMgX	Yield (%)
MeMgCl	85
EtMgBr	86
<i>n</i> -BuMgCl	83
CH <sub>2</sub> =CHMgCl	68
PhMgBr	81

SCHEME 71



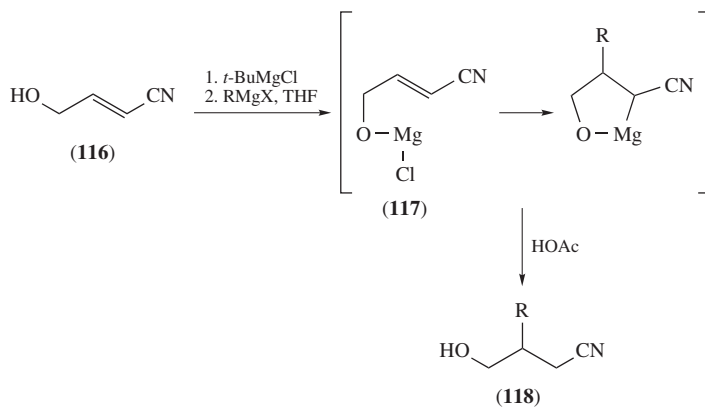
SCHEME 72

the substrates lacking the hydroxyl group (**119**) afford only recovered starting materials. Chelation apparently requires the hydroxyl group adjacent to the double bond since relocating the hydroxyl group three or four carbons away, as in **120** and **121**, precludes conjugate addition.

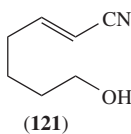
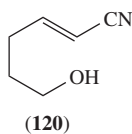
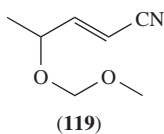


R	Yield (%)
Methyl	58
<i>t</i> -Butyl	43
Phenyl	58
Vinyl	49
Ethynyl	47

SCHEME 73

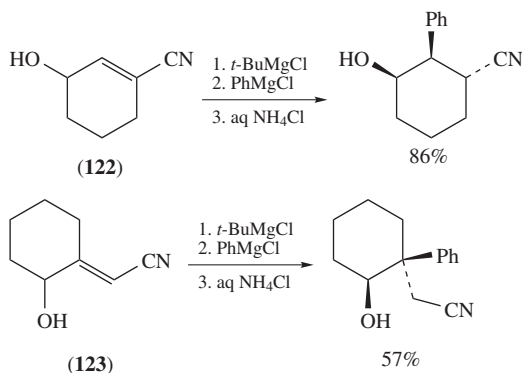


No carbomagnesiation with



R	Yield (%)
Methyl	74
<i>n</i> -Butyl	80
Phenyl	76
Vinyl	63
Phenylethynyl	62

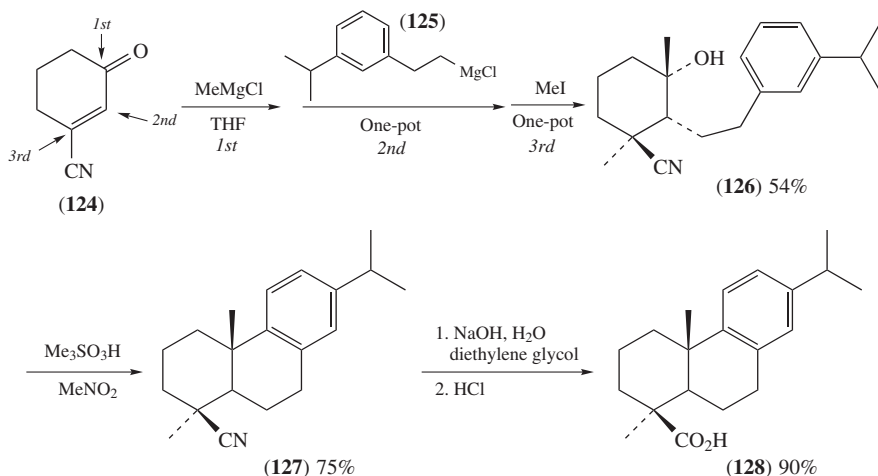
SCHEME 74



SCHEME 75

Conjugate additions to cyclic unsaturated nitriles such as **122** and **123** also proceed smoothly with virtually complete stereocontrol (Scheme 75)<sup>123</sup>. Given the long-standing difficulty of performing conjugate additions to  $\alpha,\beta$ -unsaturated nitrile compounds<sup>124</sup>, the present chelation-assisted methodology is extremely powerful and might provide a practical solution.

The clean and facile chelation-controlled carbomagnesiation of hydroxylated unsaturated nitriles offers an opportunity for further multicomponent assembly through the reactions of the resultant organomagnesium species with electrophiles. The following example accessing terpenoid structures may illustrate the power of a multicomponent assembling reaction (Scheme 76)<sup>125</sup>. The sequential addition of MeMgCl, second Grignard reagent **125** and MeI to cyanocyclohexenone **124** gave **126** in 54% yield. Obviously MeMgCl adds to carbonyl group forming the alkoxide, which triggers the chelation-controlled conjugate addition of **125** to the C=C bond. The follow-up methylation of the resultant organomagnesium species with MeI then furnishes the entire abietane carbon



SCHEME 76

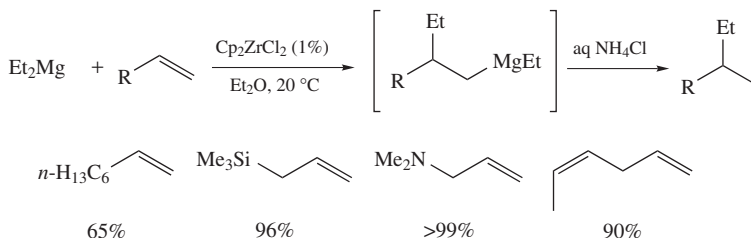
skeleton in one-pot. Intramolecular Friedel–Crafts alkylation of **126** affords predominantly the *cis*-abietane **127**. Finally, the nitrile hydrolysis completes the synthesis of *epi*-dehydroabietic acid **128**.

Fleming and coworkers have developed a number of such multicomponent assembling reactions using alkyl halides, aldehydes, ketones and acid chlorides as electrophiles for post-functionalization of carbomagnesiation<sup>126–130</sup>. The stereoselectivity of the reaction with electrophiles is not only generally high but also highly dependent on the nature of electrophiles.

## F. Zirconium-catalyzed Ethylmagnesiation of Alkenes

Despite impressive development in the addition reaction of Grignard reagents to carbon–carbon multiple bonds, a facile intermolecular carbomagnesiation reaction of simple alkenes has been a long-standing goal. Although somewhat limited to ethylmagnesium compounds, the zirconium-catalyzed ethylmagnesiation of terminal alkenes, originally discovered by Dzhemilev and extensively investigated by Hoveyda and others, has attracted great attention in the synthetic community.

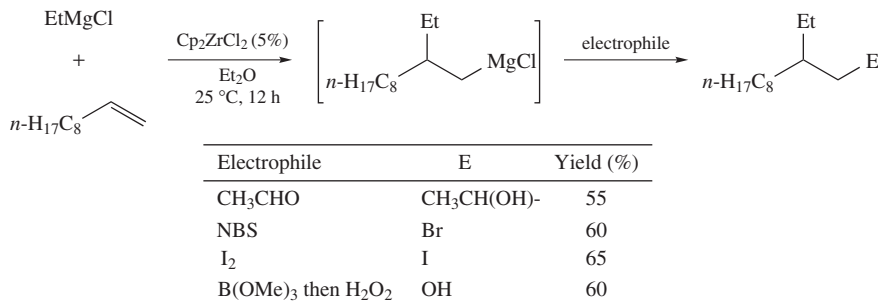
In 1983, Dzhemilev and coworkers reported that  $\text{Cp}_2\text{ZrCl}_2$  catalyzes the addition of ethylmagnesium compounds, such as ethylmagnesium halides and diethylmagnesium, to simple alkenes. For example, under the catalytic influence of  $\text{Cp}_2\text{ZrCl}_2$  (1 mol%),  $\text{Et}_2\text{Mg}$  reacts with a range of terminal alkenes at room temperature in  $\text{Et}_2\text{O}$  furnishing the ethylmagnesiation product in good to excellent yields (Scheme 77)<sup>131–133</sup>. Although the addition to internal alkenes such as 2-hexene and cyclohexene does not take place, strained cyclic alkenes such as norbornene and norbornadiene undergo ethylmagnesiation. The use of other alkylmagnesium compounds results in the formation of many unwanted side products<sup>133–135</sup>.



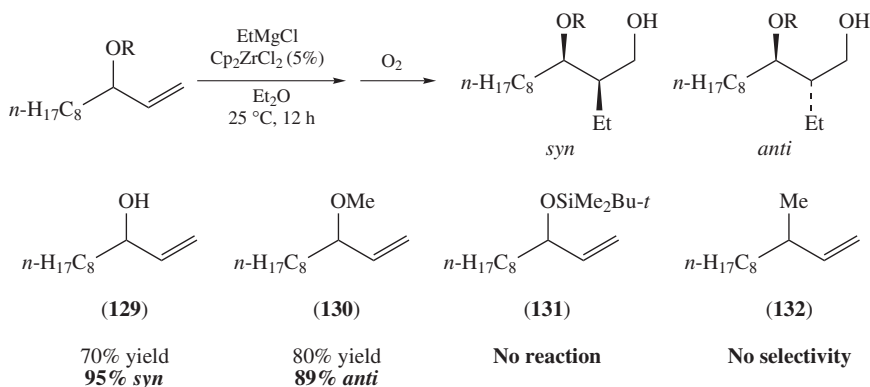
SCHEME 77

Hoveyda and coworkers have demonstrated that ethylmagnesiation of simple 1-alkenes by  $\text{EtMgCl}$  can proceed more efficiently than was originally reported by Dzhemilev, and that the resulting organomagnesium species can undergo further bond-forming processes such as reaction with aldehyde, borylation followed by oxidation, and halogenation using NBS or  $\text{I}_2$  (Scheme 78)<sup>136</sup>. In all cases examined, the ethylmagnesiation proceeds with an excellent level of regiocontrol (>99:1).

Hoveyda and coworkers have further demonstrated that allylic alcohols and ethers are good substrates exhibiting notable diastereocontrol (Scheme 79)<sup>136</sup>. The ethylmagnesiation of allylic alcohol **129** affords the *syn* diol with 95:5 diastereoselectivity (70% yield). On the other hand, the reaction of the corresponding methyl ether **130** affords the monoprotected alcohol with opposite sense of diastereoselectivity (*syn:anti* = 11:89). The corresponding *t*-butyldimethylsilyl ether **131** is recovered unchanged, and oxygen-free substrate **132** provides an equal mixture of diastereomers. The chelation between the



SCHEME 78

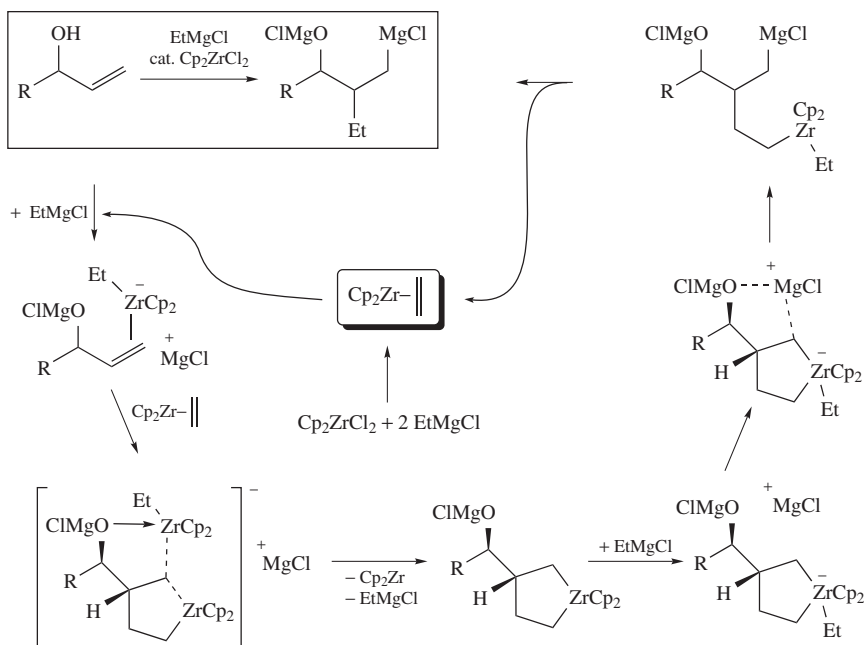


SCHEME 79

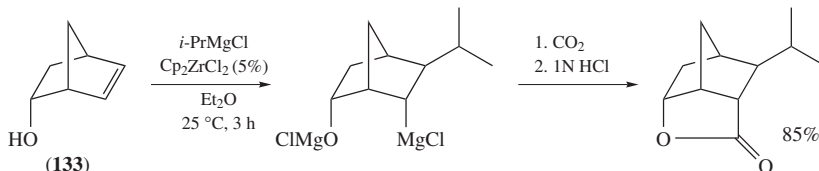
Lewis basic heteroatom and a metal center (Zr or Mg) in a transition state organization seems to be responsible for high diastereocontrol<sup>137</sup>.

In analogy to other zirconium-catalyzed reactions, a possible pathway has been thought to involve oxidative cyclization of Cp<sub>2</sub>Zr(CH<sub>2</sub>=CH<sub>2</sub>) and 1-alkene giving zirconacyclopentane species, which further reacts with EtMgCl leading to the formal ethylmagnesium product. On the basis of extensive mechanistic studies, the mechanistic picture that includes a biszirconocene complex as its centerpiece has been proposed by Hoveyda and coworkers (Scheme 80)<sup>137</sup>. The proposed mechanistic hypothesis rationalizes (i) the requirement for excess EtMgCl, (ii) the necessity for the presence of a Lewis basic heteroatom for diastereocontrol and (iii) the reaction for the highly regioselective rupture of the intermediate zirconacyclopentane.

The dramatic influence of internal Lewis bases on reactivity/selectivity can be seen in other systems such as homoallylic alcohols<sup>138</sup> and substituted norbornenes<sup>139</sup>. For example, when *endo*-5-norbornen-2-ol (**133**) is used as a substrate, the Zr-catalyzed carbomagnesiation occurs with a range of alkyl Grignard reagents in an *anti*-addition manner (Scheme 81)<sup>139</sup>. It is reasonable to suggest that with the Mg salt of **133**, the heteroatom binds and delivers the magnesium ion to initiate a complete reversal in the regioselective zirconacyclopentane cleavage.



SCHEME 80

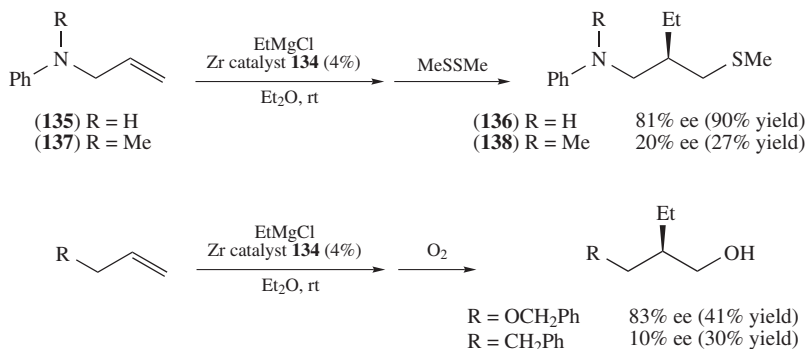


SCHEME 81

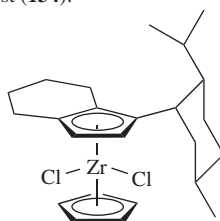
Enantioselective ethylmagnesiation can be achieved by using a chiral Zr catalyst<sup>140–149</sup>. Whitby and coworkers reported that the  $C_1$ -symmetric zirconocene dichloride **134** serves as a cheap, active and selective catalyst precursor for the enantioselective ethylmagnesiation of unactivated terminal alkenes (Scheme 82)<sup>140,141</sup>. For example, the reaction of *N*-allylaniline (**135**) and  $\text{EtMgCl}$  in  $\text{Et}_2\text{O}$  followed by quenching with  $\text{MeSSMe}$  gives **136** in 81% ee (90% yield). Dramatic decrease in enantioselectivity is observed when the  $\text{NH}$  functionality of **135** is protected as  $\text{NMe}$  moiety (**137**). The reaction using allyl benzyl ether gives high enantioselectivity (83% ee) whereas the use of simple 4-phenyl-1-butene as a substrate results in very poor yield and enantioselectivity (Scheme 82)<sup>141</sup>. Attractive heteroatom-coordination to the metal (Zr or Mg) may be involved in the stereo-determining transition structure of this reaction.

Hoveyda and coworkers have also developed a number of useful asymmetric transformations by judicious modification of Zr-catalyzed ethylmagnesiation of alkenes into other reactions<sup>142–149</sup>.





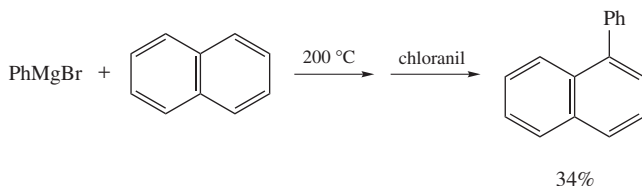
Chiral Zr catalyst (**134**):



SCHEME 82

#### IV. CARBOMAGNESIATION REACTIONS OF AROMATICS

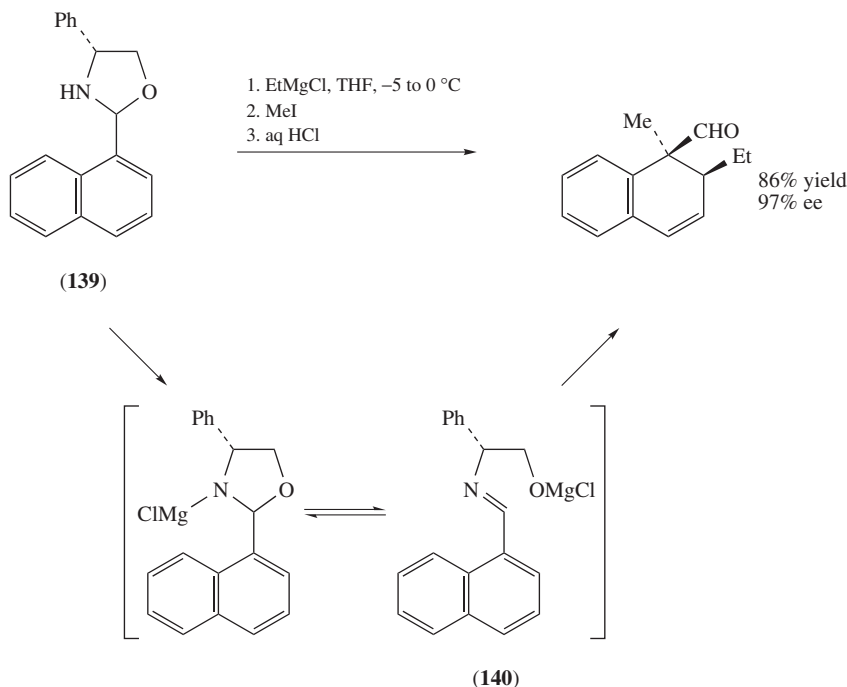
Under forcing conditions, Grignard reagents add to certain aromatic compounds. For example, the addition of PhMgBr to naphthalene takes place at 200 °C (Scheme 83)<sup>150</sup>. After treatment of the crude product with chloranil (for dehydrogenation), 1-phenylnaphthalene is obtained in 34% yield.



SCHEME 83

On the other hand, aromatic compounds substituted by electron-withdrawing groups such as nitro group are surprisingly susceptible to attack by Grignard reagents<sup>151</sup>. Such a reaction may be regarded as a variant of conjugate addition. It was also reported that the addition of Grignard reagent to naphthyloxazolidine **139** takes place in much milder conditions (Scheme 84)<sup>152, 153</sup>. It has been proposed that the Grignard reagents add to the naphthylimine **140**, which is formed by the ring opening of oxazolidine ring with the action of Grignard reagent, in a 1,4-addition manner.

It is well-known that [60]fullerene is a fairly electronegative system having a low-lying LUMO. Therefore, [60]fullerene behaves like an electron-poor conjugated polyolefin

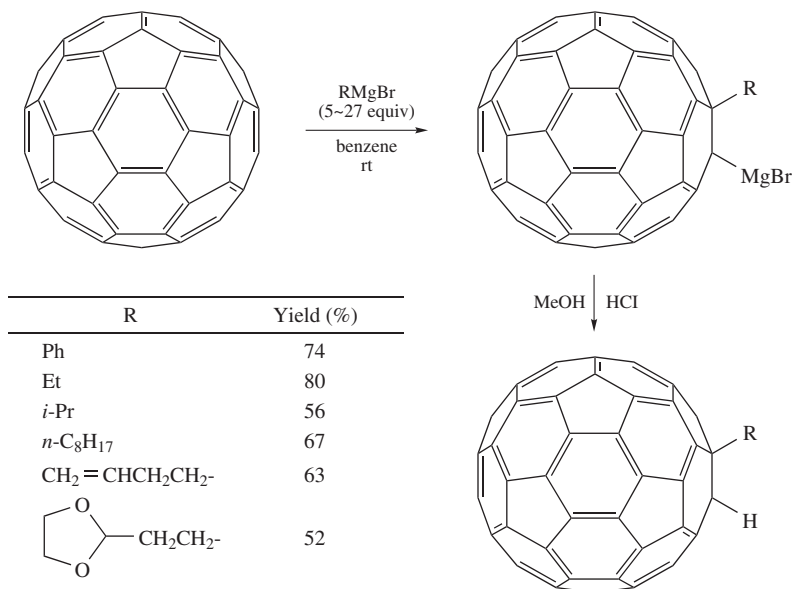


SCHEME 84

rather than a 'superarene'. Consequently, [60]fullerene undergoes nucleophilic additions with various nucleophiles<sup>154</sup>. In 1992, Hirsch and coworkers demonstrated that Grignard reagents can be used as nucleophiles for [60]fullerene (Scheme 85)<sup>155, 156</sup>. Phenyl and alkyl Grignard reagents add across [60]fullerene, but it is typically necessary to monitor the reaction by titration in order to maximize the yield of mono-adducts  $\text{RC}_{60}\text{H}$ <sup>156</sup>. The addition takes place across the  $\text{C}=\text{C}$  bond between two six-membered rings of [60]fullerene. An interesting solvent effect in the addition of silylmethyl Grignard reagents to [60]fullerene has been demonstrated by Nagashima and coworkers. Although the use of THF results in the production of mono-adduct  $\text{RC}_{60}\text{H}$  as usual, the use of toluene provides bis-adduct  $\text{RC}_{60}\text{R}$ <sup>157, 158</sup>. Hirsch and coworkers have also demonstrated that [70]fullerene also reacts with  $\text{PhMgBr}$  in a regioselective fashion giving  $\text{PhC}_{70}\text{H}$  as an isometrically pure compound<sup>156</sup>.

## V. SUMMARY

Carbomagnesiation reactions became an important and powerful tool in organic synthesis. Although a truly universal reaction system that allows the regio- and stereoselective carbomagnesiation of unactivated alkenes and alkynes has not yet been described, the last half-century of extensive worldwide research has resulted in impressive progress for making useful organic frameworks. We believe that the development of new catalysts, reagents and strategies in carbomagnesiation will be a topic of unparalleled importance in all aspects of pure and applied chemistry.



SCHEME 85

## VI. REFERENCES

1. I. Marek, N. Chinkov and D. Banon-Tenne, in *Metal-Catalyzed Cross-Coupling Reactions*, 2nd edn. (Eds. A. de Meijere and F. Diederich), Chap. 7, Wiley-VCH, Weinheim, 2004; I. Marek and J. Normant, in *Metal-Catalyzed Cross-Coupling Reactions* (Eds. F. Deiderich and P. J. Stang), Chap. 7, Wiley-VCH, New York, 1998; B. J. Wakefield, *Organomagnesium Methods in Organic Synthesis*, Academic Press, London, 1995; A. Inoue and K. Oshima, in *Main Group Metals in Organic Synthesis* (Eds. H. Yamamoto and K. Oshima), Vol. 1, Chap. 3, Wiley-VCH, Weinheim, 2004; P. Knochel, A. Gavryushin, A. Krasovskiy and H. Leuser, in *Comprehensive Organometallic Chemistry III* (Eds. D. M. P. Mingos, R. H. Crabtree and P. Knochel), Vol. 9, Chap. 9.03, Elsevier, Oxford, 2007; J. F. Normant and A. Alexakis, *Synthesis*, 841 (1981); A. G. Fallis and P. Forgione, *Tetrahedron*, **57**, 5899 (2001).
2. R. C. Fuson and H. D. Porter, *J. Am. Chem. Soc.*, **70**, 895 (1948).
3. R. C. Fuson, H. A. DeWald and R. Gaertner, *J. Org. Chem.*, **16**, 21 (1951).
4. R. C. Fuson and F. E. Mumford, *J. Org. Chem.*, **17**, 255 (1952).
5. R. C. Fuson and O. York, Jr., *J. Org. Chem.*, **18**, 570 (1953).
6. H. Gilman and H. M. Crawford, *J. Am. Chem. Soc.*, **45**, 554 (1923).
7. H. Gilman and J. B. Shumaker, *J. Am. Chem. Soc.*, **47**, 514 (1925).
8. H. Gilman and J. M. Peterson, *J. Am. Chem. Soc.*, **48**, 423 (1926).
9. G. H. Posner, *Org. React.*, **19**, 1 (1972); N. Krause (Ed.), *Modern Organocopper Chemistry*, Wiley-VCH, Weinheim, 2002.
10. S. A. Kandil and R. E. Dessy, *J. Am. Chem. Soc.*, **88**, 3027 (1966).
11. H. G. Richey, Jr. and A. M. Rothman, *Tetrahedron Lett.*, 1457 (1968).
12. J. K. Crandall, P. Battioni, J. T. Wehlacz and R. Bindra, *J. Am. Chem. Soc.*, **97**, 7171 (1975).
13. J.-G. Duboudin and B. Jousseau, *J. Organomet. Chem.*, **44**, C1 (1972).
14. J.-G. Duboudin and B. Jousseau, *J. Organomet. Chem.*, **96**, C47 (1975).
15. J.-G. Duboudin and B. Jousseau, *J. Organomet. Chem.*, **162**, 209 (1978).
16. A. Alexakis, G. Cahiez and J. F. Normant, *J. Organomet. Chem.*, **177**, 293 (1979).
17. H. Yorimitsu, J. Tang, K. Okada, H. Shinokubo and K. Oshima, *Chem. Lett.*, 11 (1998).
18. S. Nishimae, R. Inoue, H. Shinokubo and K. Oshima, *Chem. Lett.*, 785 (1998).
19. K. Okada, K. Oshima and K. Utimoto, *J. Am. Chem. Soc.*, **118**, 6076 (1996).

20. T. Nishikawa, H. Shinokubo and K. Oshima, *J. Am. Chem. Soc.*, **123**, 4629 (2001).
21. T. Nishikawa, H. Shinokubo and K. Oshima, *Org. Lett.*, **4**, 2795 (2002).
22. K. Murakami, H. Ohmiya, H. Yorimitsu and K. Oshima, *Org. Lett.*, **9**, 1569 (2007).
23. E. Shirakawa, T. Yamagami, T. Kimura, S. Yamaguchi and T. Hayashi, *J. Am. Chem. Soc.*, **127**, 17164 (2005).
24. T. Yamagami, R. Shintani, E. Shirakawa and T. Hayashi, *Org. Lett.*, **9**, 1045 (2007).
25. B. B. Snider, M. Karras and R. S. E. Conn, *J. Am. Chem. Soc.*, **100**, 4624 (1978).
26. B. B. Snider, R. S. E. Conn and M. Karras, *Tetrahedron Lett.*, 1679 (1979).
27. K. Itami, T. Kamei and J. Yoshida, *J. Am. Chem. Soc.*, **125**, 14670 (2003).
28. T. Kamei, K. Itami and J. Yoshida, *Adv. Synth. Catal.*, **346**, 1824 (2004).
29. H. Chechik-Lankin, S. Livshin and I. Marek, *Synlett*, 2098 (2005).
30. H. Yasui, H. Yorimitsu and K. Oshima, *Chem. Lett.*, **36**, 32 (2007).
31. H. Chechik-Lankin and I. Marek, *Org. Lett.*, **5**, 5087 (2003).
32. M. Xie and X. Huang, *Synlett*, 477 (2004).
33. M. Xie, L. Liu, J. Wang and S. Wang, *J. Organomet. Chem.*, **690**, 4058 (2005).
34. J. A. Marshal and B. S. DeHoff, *J. Org. Chem.*, **51**, 863 (1986).
35. H. G. Richey, Jr. and F. W. Von Rein, *J. Organomet. Chem.*, **20**, P32 (1969).
36. F. W. Von Rein and H. G. Richey, Jr., *Tetrahedron Lett.*, 3777 (1971).
37. T. Wong, M. W. Tjepkema, H. Audrain, P. D. Wilson and A. G. Fallis, *Tetrahedron Lett.*, **37**, 755 (1996).
38. P. Forgione and A. G. Fallis, *Tetrahedron Lett.*, **41**, 11 (2000).
39. F. F. Fleming, V. Gudipati and O. W. Steward, *Org. Lett.*, **4**, 659 (2002).
40. F. F. Fleming, V. Gudipati and O. W. Steward, *Tetrahedron*, **59**, 5585 (2003).
41. P. E. Tessier, N. Nguyen, M. D. Clay and A. G. Fallis, *Org. Lett.*, **7**, 767 (2005).
42. N. P. Villalva-Servin, A. Laurent, G. P. A. Yap and A. G. Fallis, *Synlett*, 1263 (2003).
43. P. Forgione, P. D. Wilson, G. P. A. Yap and A. G. Fallis, *Synlett*, 921 (2000).
44. P. Forgione, P. D. Wilson and A. G. Fallis, *Tetrahedron Lett.*, **41**, 17 (2000).
45. D. V. Smil, F. E. S. Souza and A. G. Fallis, *Bioorg. Med. Chem. Lett.*, **15**, 2057 (2005).
46. M. A. Franks, E. A. Schrader, E. C. Pietsch, D. R. Pennella, S. V. Torti and M. E. Welker, *Bioorg. Med. Chem.*, **13**, 2221 (2005).
47. F. C. Engelhardt, Y.-J. Shi, C. J. Cowden, D. A. Conlon, B. Pipik, G. Zhou, J. M. McNamara and U.-H. Dolling, *J. Org. Chem.*, **71**, 480 (2006).
48. P. E. Tessier, A. J. Penwell, F. E. S. Souza and A. G. Fallis, *Org. Lett.*, **5**, 2989 (2003).
49. B. Jousseau and J.-G. Duboudin, *J. Organomet. Chem.*, **91**, C1 (1975).
50. J.-G. Duboudin and B. Jousseau, *J. Organomet. Chem.*, **168**, 1 (1979).
51. Z. Lu and S. Ma, *J. Org. Chem.*, **71**, 2655 (2006).
52. S. Ma and Z. Lu, *Adv. Synth. Catal.*, **348**, 1894 (2006).
53. D. Zhang and J. M. Ready, *J. Am. Chem. Soc.*, **128**, 15050 (2006).
54. H. G. Richey, W. E. Erickson and A. S. Heyn, *Tetrahedron Lett.*, 2183 (1971).
55. R. Mornet and L. Gouin, *Bull. Soc. Chim. Fr.*, 737 (1977).
56. R. Mornet and L. Gouin, *Tetrahedron Lett.*, 167 (1977).
57. H. E. Podall and W. E. Foster, *J. Org. Chem.*, **23**, 1848 (1958).
58. L. H. Shepherd, Jr., U.S. Patent 3 597 488; *Chem. Abstr.*, **75**, 88751 (1971).
59. H. Lehmkuhl and D. Reinehr, *J. Organomet. Chem.*, **25**, C47 (1970).
60. H. Lehmkuhl and D. Reinehr, *J. Organomet. Chem.*, **34**, 1 (1972).
61. H. Lehmkuhl and D. Reinehr, *J. Organomet. Chem.*, **57**, 29 (1973).
62. H. Lehmkuhl, D. Reinehr, J. Frandt and G. Schroth, *J. Organomet. Chem.*, **57**, 39 (1973).
63. H. Lehmkuhl, D. Reinehr, D. Henneberg and G. Schroth, *J. Organomet. Chem.*, **57**, 49 (1973).
64. H. Lehmkuhl, D. Reinehr, G. Schomburg, D. Henneberg, H. Damen and G. Schroth, *Justus Liebigs Ann. Chem.*, 103 (1975).
65. H. Lehmkuhl, D. Reinehr, D. Henneberg, G. Schomburg and G. Schroth, *Justus Liebigs Ann. Chem.*, 119 (1975).
66. H. Lehmkuhl, O. Olbrysch, D. Reinehr, G. Schomburg and D. Henneberg, *Justus Liebigs Ann. Chem.*, 145 (1975).
67. M. S. Kharasch, *J. Org. Chem.*, **19**, 1600 (1954).
68. A. Job and R. Reich, *Compt. Rend.*, **179**, 330 (1924).
69. L. Farády, L. Bencze and L. Markó, *J. Organomet. Chem.*, **10**, 505 (1967).
70. L. Farády, L. Bencze and L. Markó, *J. Organomet. Chem.*, **17**, 107 (1969).

71. L. Farády and L. Markó, *J. Organomet. Chem.*, **28**, 159 (1971).
72. I. N. Houpin, J. Lee, I. Dorziotis, A. Molina, B. Reamer, R. P. Volante and P. J. Reider, *Tetrahedron*, **54**, 1185 (1998).
73. E. A. Hill, *J. Organomet. Chem.*, **91**, 123 (1975).
74. M. S. Silver, P. R. Shafer, J. E. Nordlander, C. Rüchardt and J. D. Roberts, *J. Am. Chem. Soc.*, **82**, 2646 (1960).
75. E. A. Hill, H. G. Richey, Jr. and T. C. Rees, *J. Org. Chem.*, **28**, 2161 (1963).
76. D. J. Patel, C. L. Hamilton and J. D. Roberts, *J. Am. Chem. Soc.*, **87**, 5144 (1965).
77. M. E. H. Howden, A. Maercker, J. Burdon and J. D. Roberts, *J. Am. Chem. Soc.*, **88**, 1732 (1966).
78. A. Maercker and J. D. Roberts, *J. Am. Chem. Soc.*, **88**, 1742 (1966).
79. H. G. Richey, Jr. and T. C. Rees, *Tetrahedron Lett.*, 4297 (1966).
80. W. C. Kossa, Jr., T. C. Rees and H. G. Richey, Jr., *Tetrahedron Lett.*, 3455 (1971).
81. H. Lehmkuhl, *Bull. Soc. Chim. Fr. Part II*, 87 (1981).
82. W. Oppolzer, *Angew. Chem., Int. Ed. Engl.*, **28**, 38 (1989).
83. H. Felkin, J. D. Umpleby, E. Hagaman and E. Wenkert, *Tetrahedron Lett.*, 2285 (1972).
84. W. Oppolzer and K. Bätting, *Tetrahedron Lett.*, **23**, 4669 (1982).
85. W. Oppolzer, R. Pitteloud and H. F. Strauss, *J. Am. Chem. Soc.*, **104**, 6476 (1982).
86. W. Oppolzer and R. Pitteloud, *J. Am. Chem. Soc.*, **104**, 6478 (1982).
87. H. Lehmkuhl and D. Reinehr, *J. Organomet. Chem.*, **34**, 1 (1972).
88. S. Akutagawa and S. Otsuka, *J. Am. Chem. Soc.*, **97**, 6870 (1975).
89. F. Barbot and P. Miginiac, *J. Organomet. Chem.*, **145**, 269 (1978).
90. B. J. Wakefield, in *Comprehensive Organometallic Chemistry* (Eds. G. Wilkinson, F. G. A. Stone and E. W. Abel), Chap. 44, Pergamon, Oxford, 1982.
91. E. K. Watkins and H. G. Richey, Jr., *Organometallics*, **11**, 3785 (1992).
92. M. Nakamura, A. Hirai and E. Nakamura, *J. Am. Chem. Soc.*, **122**, 978 (2000).
93. M. Nakamura, K. Matsuo, T. Inoue and E. Nakamura, *Org. Lett.*, **5**, 1373 (2003).
94. M. Lautens and S. Ma, *J. Org. Chem.*, **61**, 7246 (1996).
95. R. G. Arrayás, S. Carrera and J. C. Carretero, *Org. Lett.*, **5**, 1333 (2003).
96. M. D. Surman, M. J. Mulvihill and M. J. Miller, *J. Org. Chem.*, **67**, 4115 (2002).
97. H. G. Richey, Jr. and R. M. Bension, *J. Org. Chem.*, **45**, 5036 (1980).
98. L.-a. Liao and J. M. Fox, *J. Am. Chem. Soc.*, **124**, 14322 (2002).
99. L.-a. Liao, F. Zhang, N. Yan, J. A. Golen and J. M. Fox, *Tetrahedron*, **60**, 1803 (2004).
100. X. Lui and J. M. Fox, *J. Am. Chem. Soc.*, **128**, 5600 (2006).
101. K. Tamao, R. Kanatani and M. Kumada, *Tetrahedron Lett.*, **25**, 1905 (1984).
102. D. Seyferth and T. Wada, *Inorg. Chem.*, **1**, 78 (1962).
103. K. Utimoto, K. Imi, H. Shiragami, S. Fujikura and H. Nozaki, *Tetrahedron Lett.*, **26**, 2101 (1985).
104. R. W. Hoffmann, O. Knopff and T. Faber, *J. Chem. Soc., Perkin Trans. 2*, 1785 (2001).
105. G. R. Buell, R. Corriu, C. Guerin and L. Spialter, *J. Am. Chem. Soc.*, **92**, 7424 (1970).
106. K. Tamao, T. Iwahara, R. Kanatani and M. Kumada, *Tetrahedron Lett.*, **25**, 1909 (1984).
107. K. Tamao, R. Kanatani and M. Kumada, *Tetrahedron Lett.*, **25**, 1913 (1984).
108. K. Itami, K. Mitsudo and J. Yoshida, *Angew. Chem., Int. Ed.*, **40**, 2337 (2001).
109. K. Itami and J. Yoshida, *Synlett*, 157 (2006).
110. J. J. Eisch and G. R. Husk, *J. Am. Chem. Soc.*, **87**, 4194 (1965).
111. J. J. Eisch and J. H. Merkley, *J. Organomet. Chem.*, **20**, P27 (1969).
112. J. J. Eisch and J. H. Merkley, *J. Am. Chem. Soc.*, **101**, 1148 (1979).
113. J. J. Eisch, J. H. Merkley and J. E. Galle, *J. Org. Chem.*, **44**, 587 (1979).
114. M. Chérest, H. Felkin, C. Frajerma, C. Lion, G. Roussi and G. Swierczewski, *Tetrahedron Lett.*, 875 (1966).
115. H. Felkin and C. Kaeseberg, *Tetrahedron Lett.*, 4587 (1970).
116. P. Kocienski, C. Love and D. A. Roberts, *Tetrahedron Lett.*, **30**, 6753 (1989).
117. K. A. Swiss, W. Hinkley, C. A. Maryanoff and D. C. Liotta, *Synthesis*, 127 (1992).
118. M. Solomon, W. C. L. Jamison, M. McCormick, D. C. Liotta, D. A. Cherry, J. E. Mills, R. D. Shah, J. D. Rodgers and C. A. Maryanoff, *J. Am. Chem. Soc.*, **110**, 3702 (1988).
119. K. A. Swiss, D. C. Liotta and C. A. Maryanoff, *J. Am. Chem. Soc.*, **112**, 9393 (1990).
120. J. D. White, H. Shin, T.-S. Kim and N. S. Cutshall, *J. Am. Chem. Soc.*, **119**, 2404 (1997).
121. F. F. Fleming, J. Guo, Q. Wang and D. Weaver, *J. Org. Chem.*, **64**, 8568 (1999).

122. F. F. Fleming, Q. Wang and O. W. Steward, *Org. Lett.*, **2**, 1477 (2000).
123. F. F. Fleming, Q. Wang, Z. Zhang and O. W. Steward, *J. Org. Chem.*, **67**, 5953 (2002).
124. F. F. Fleming and Q. Wang, *Chem. Rev.*, **103**, 2035 (2003).
125. F. F. Fleming, Z. Zhang, Q. Wang and O. W. Steward, *Angew. Chem., Int. Ed.*, **43**, 1126 (2004).
126. F. F. Fleming, Q. Wang and O. W. Steward, *J. Org. Chem.*, **68**, 4235 (2003).
127. F. F. Fleming, Z. Zhang, Q. Wang and O. W. Steward, *J. Org. Chem.*, **68**, 7646 (2003).
128. F. F. Fleming, Z. Zhang, G. Wei and O. W. Steward, *Org. Lett.*, **7**, 447 (2005).
129. F. F. Fleming, Z. Zhang, G. Wei and O. W. Steward, *J. Org. Chem.*, **71**, 1430 (2006).
130. F. F. Fleming, G. Wei, Z. Zhang and O. W. Steward, *Org. Lett.*, **8**, 4903 (2006).
131. U. M. Dzhemilev, O. S. Vostrikova and R. M. Sultanov, *Izv. Akad. Nauk SSSR, Ser. Khim.*, 218 (1983); *Chem. Abstr.*, **98**, 160304 (1983).
132. U. M. Dzhemilev, O. S. Vostrikova, R. M. Sultanov, A. G. Kukovinets and A. M. Khalilov, *Izv. Akad. Nauk SSSR, Ser. Khim.*, 2053 (1984); *Chem. Abstr.*, **102**, 165971 (1985).
133. U. M. Dzhemilev and O. S. Vostrikova, *J. Organomet. Chem.*, **285**, 43 (1985).
134. C. J. Rousset, E. Negishi, N. Suzuki and T. Takahashi, *Tetrahedron Lett.*, **33**, 1965 (1992).
135. U. M. Dzhemilev, *Tetrahedron*, **51**, 4333 (1995).
136. A. H. Hoveyda and Z. Xu, *J. Am. Chem. Soc.*, **113**, 5079 (1991).
137. A. F. Hour, M. T. Didiluk, Z. Xu, N. R. Horan and A. H. Hoveyda, *J. Am. Chem. Soc.*, **115**, 6614 (1993).
138. A. H. Hoveyda, Z. Xu, J. P. Morken and A. F. Hour, *J. Am. Chem. Soc.*, **113**, 8950 (1991).
139. A. H. Hoveyda, J. P. Morken, A. F. Hour and Z. Xu, *J. Am. Chem. Soc.*, **114**, 6692 (1992).
140. L. Bell, R. J. Whitby, R. V. H. Jones and M. C. H. Standen, *Tetrahedron Lett.*, **37**, 7139 (1996).
141. L. Bell, D. C. Brookings, G. J. Dawson, R. J. Whitby, R. V. H. Jones and M. C. H. Standen, *Tetrahedron*, **54**, 14617 (1998).
142. A. H. Hoveyda and J. P. Morken, *J. Org. Chem.*, **58**, 4237 (1993).
143. J. P. Morken, M. T. Didiuk and A. H. Hoveyda, *J. Am. Chem. Soc.*, **115**, 6997 (1993).
144. J. P. Morken, M. T. Didiuk, M. S. Visser and A. H. Hoveyda, *J. Am. Chem. Soc.*, **116**, 3123 (1994).
145. A. F. Hour, Z. Xu, D. A. Cogan and A. H. Hoveyda, *J. Am. Chem. Soc.*, **117**, 2943 (1995).
146. M. S. Visser and A. H. Hoveyda, *Tetrahedron*, **51**, 4383 (1995).
147. M. S. Visser, J. P. A. Harritty and A. H. Hoveyda, *J. Am. Chem. Soc.*, **118**, 3779 (1996).
148. N. M. Heron, J. A. Adams and A. H. Hoveyda, *J. Am. Chem. Soc.*, **119**, 6205 (1997).
149. J. A. Adams, N. M. Heron, A.-M. Koss and A. H. Hoveyda, *J. Org. Chem.*, **64**, 854 (1999).
150. D. Bryce-Smith and B. J. Wakefield, *Tetrahedron Lett.*, 3295 (1964).
151. G. Bartoli, M. Bosco and G. Baccolini, *J. Org. Chem.*, **45**, 522 (1980).
152. L. N. Pridgen, M. K. Mokhallalati and M.-J. Wu, *J. Org. Chem.*, **57**, 1237 (1992).
153. M. K. Mokhallalati, K. R. Muralidharan and L. N. Pridgen, *Tetrahedron Lett.*, **35**, 4267 (1994).
154. A. Hirsch and M. Brettreich, *Fullerenes: Chemistry and Reactions*, Wiley-VCH, Weinheim, 2005.
155. A. Hirsch, A. Soi and H. R. Karfunkel, *Angew. Chem., Int. Ed. Engl.*, **31**, 766 (1992).
156. A. Hirsch, T. Gröser, A. Skiebe and A. Soi, *Chem. Ber.*, **126**, 1061 (1993).
157. H. Nagashima, H. Terasaki, E. Kimura, K. Nakajima and K. Itoh, *J. Org. Chem.*, **59**, 1246 (1994).
158. H. Nakajima, M. Saito, Y. Kato, H. Goto, E. Osawa, M. Haga and K. Itoh, *Tetrahedron*, **52**, 5053 (1996).

# The chemistry of organomagnesium ate complexes

HIDEKI YORIMITSU and KOICHIRO OSHIMA

*Department of Material Chemistry, Graduate School of Engineering, Kyoto University, Kyoto-daigaku Katsura, Nishikyo, Kyoto 615-8510, Japan*  
 Fax: +81-75-383-2438; e-mail: yori@orgrxn.mbox.media.kyoto-u.ac.jp;  
 oshima@orgrxn.mbox.media.kyoto-u.ac.jp

I. INTRODUCTION	681
II. PREPARATION OF TRIORGANOMAGNESATES	682
III. REACTIONS OF TRIORGANOMAGNESATES	683
A. Nucleophilic Addition Reactions	683
B. Deprotonation Reactions	686
C. Halogen–Magnesium Exchange	690
IV. ADDITIONAL IMPORTANT CHEMISTRY OF ORGANOMAGNESATES	711
A. Alkoxydialkylmagnesate $R_2MgOR$	711
B. Lithium Tris(2,2,6,6-tetramethylpiperidino)magnesate $(TMP)_3MgLi$	713
C. Combination of Isopropylmagnesium Chloride and Lithium Chloride $i\text{-PrMgCl}\cdot LiCl$	714
V. SUMMARY	714
VI. REFERENCES	714

## I. INTRODUCTION

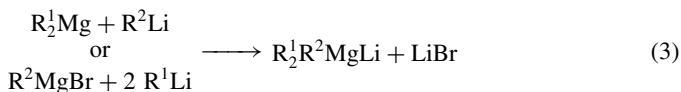
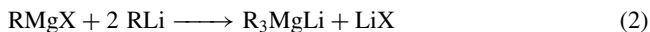
Ate complexes have formed a structurally intriguing entity for chemists working on organometallics. Organomagnesium ate complexes, organomagnesates, emerged in 1951, when Wittig and coworkers proposed the formation of lithium triphenylmagnesate  $Ph_3MgLi$  by mixing phenyllithium and diphenylmagnesium<sup>1</sup>. NMR studies of the reaction of methyllithium and dimethylmagnesium in 1967 strongly supported the formation of lithium trimethylmagnesate<sup>2</sup>. Finally, in 1978, X-ray crystallographic analysis by Thoennes and Weiss unambiguously provided evidence of the existence of

organomagnesates<sup>3</sup>. Since the latter report, a number of chemists have devoted themselves to crystallographic studies on organomagnesium ate complexes. Some reports help to overview structural studies on organomagnesates<sup>4-6</sup>.

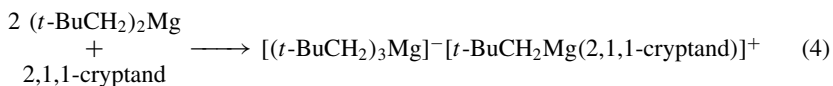
Ate complexation is a promising method to enhance the reactivity of organometallic reagents. Ate complexes such as organocuprates, -zincates, -aluminates, -borates and -silicates are hence useful in organic synthesis. In contrast, the application of organomagnesates in organic synthesis had been largely unexplored. During the last decade, organomagnesates have been attracting the increasing attention of synthetic organic chemists. The recent progress is largely due to lithium triorganomagnesates  $R_3MgLi$  and alkylmagnesium chloride–lithium chloride complex  $RMgCl \cdot LiCl$ . This chapter mainly summarizes the preparation and reactions of triorganomagnesate reagents, as the chemistry of  $RMgCl \cdot LiCl$  is summarized in Chapter 12 by Knochel<sup>7,8</sup>. The  $RMgCl \cdot LiCl$  reagents are now used on industrial scales<sup>9</sup>.

## II. PREPARATION OF TRIORGANOMAGNESATES

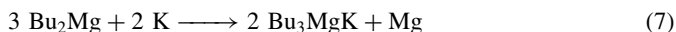
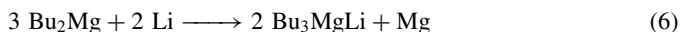
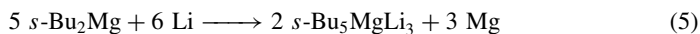
The easiest and reliable way to prepare triorganomagnesates is the reaction of diorganomagnesium with one molar equivalent of organolithium (equation 1). Organometallic chemists synthesized triorganomagnesates by this method<sup>1-3</sup>, and sodium triorganomagnesates were also synthesized in a similar fashion<sup>10</sup>. Synthetic organic chemists prefer the more convenient route, the reaction of alkylmagnesium halide with two molar equivalents of organolithium (equation 2)<sup>11</sup>. They use the triorganomagnesates in the same pot without isolation. The triorganomagnesates prepared by the latter method can exist as mixtures of  $R_2Mg$ ,  $R_3MgLi$ ,  $R_4MgLi_2$  etc. in solution. One can prepare mixed organomagnesates  $R^1_2R^2MgLi$  by using a combination of  $R^1_2Mg + R^2Li$  or  $R^2MgBr + 2 R^1Li$  (equation 3), although the exact structure in solutions is not clear<sup>11,12</sup>.



Trialkylmagnesate species could be isolated by treatment of diorganomagnesium compounds with cryptands,<sup>13</sup> 15-crown-5<sup>14</sup> or a tetraazamacrocyclic<sup>5</sup>. An equilibrium as shown in equation 4 rationalizes the formation of trialkylmagnesate.



The reduction of dialkylmagnesiums by alkali metals in hydrocarbon solvent yielded the corresponding ate complexes of definite stoichiometries<sup>15</sup>. Lithium reacted with dialkylmagnesium to form both  $R_5MgLi_3$  and  $R_3MgLi$  according to the stoichiometry used (equations 5 and 6). Reduction with sodium afforded  $R_5Mg_2Na$  as well as  $R_3MgNa$ . Potassium, rubidium and cesium reduced dialkylmagnesium to yield trialkylmagnesates (equation 7).

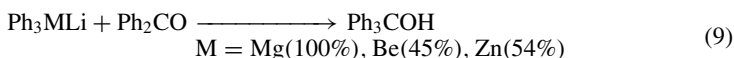
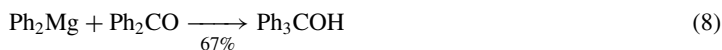




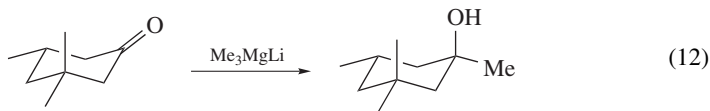
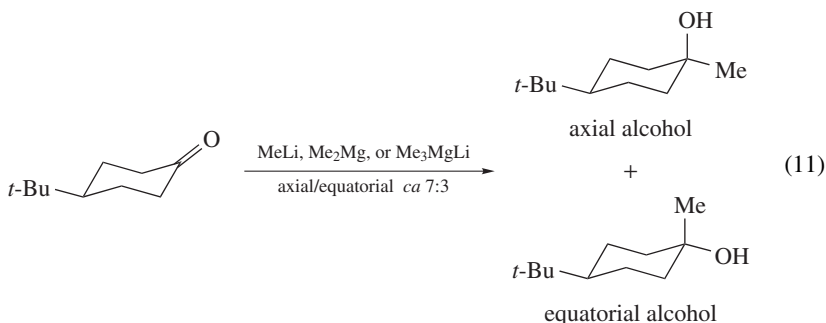
### III. REACTIONS OF TRIORGANOMAGNESATES

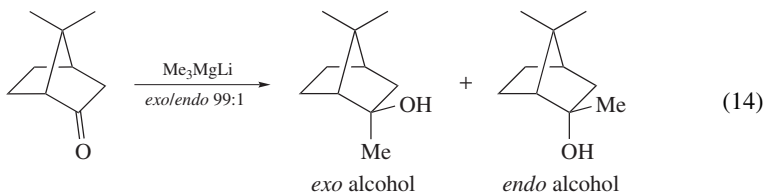
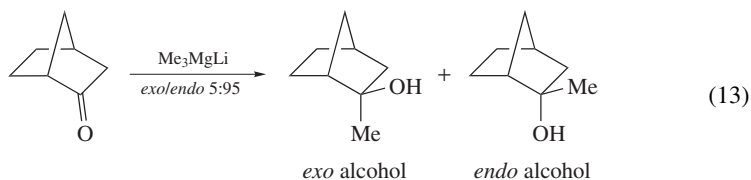
#### A. Nucleophilic Addition Reactions

Wittig's pioneering work includes the reactions of benzophenone and chalcone with lithium triphenylmagnesate<sup>1</sup>. The reaction of benzophenone with diphenylmagnesium afforded triphenylmethanol in 67% yield (equation 8). Lithium triphenylmagnesate was more reactive than diphenylmagnesium, and as reactive as phenyllithium, resulting in a quantitative formation of triphenylmethanol (equation 9). The magnesate was more reactive than the corresponding beryllium and zinc ate complexes, which provided triphenylmethanol in 45% and 54% yields, respectively. With chalcone, diphenylmagnesium and lithium triphenylmagnesate both yielded mainly the corresponding 1,4-adduct (equation 10), whereas phenyllithium alone yielded the 1,2-adduct.



Ashby and coworkers reported in 1974 stereochemical studies on addition of lithium trimethylmagnesate to several ketones<sup>16</sup>. The reactions of 4-*tert*-butylcyclohexanone with methyl lithium, with dimethylmagnesium and with lithium trimethylmagnesate in ether afforded mixtures of the corresponding axial and equatorial alcohols in ratios of 65:35, 70:30 and 69:31, respectively (equation 11). Reaction of 3,3,5-trimethylcyclohexanone with lithium trimethylmagnesate yielded exclusively the axial alcohol (equation 12). Reaction of norcamphor provided 95% of the *endo* alcohol and 5% of the *exo* alcohol (equation 13). In contrast, reaction of camphor yielded the *exo* alcohol with high stereoselectivity (equation 14). Among the methylmetals examined, no difference in the stereoselectivity was virtually observed.





Richey and King found in 1982 that addition of 15-crown-5 to a THF solution of diethylmagnesium and pyridine significantly accelerated the nucleophilic addition of the organomagnesium compound to pyridine (Table 1)<sup>17</sup>. Interestingly, the reaction led to the formation of a significant amount of 4-ethylpyridine. It is noteworthy that diethylmagnesium and pyridine react very slowly in the absence of the crown ether to produce 2-ethylpyridine as a sole product. A similar phenomenon was observed by using cryptand as an additive<sup>13</sup>. Richey conjectured, and finally confirmed, that organomagnesium complexes are formed *in situ* (equation 4), and that the complex is responsible for the unusual reactivity. Richey and Farkas showed that reactions of pyridine with solutions prepared by mixing diethylmagnesium and ethyllithium solutions yielded a mixture of 4-ethylpyridine and 2-ethylpyridine<sup>18</sup>. Reaction of 2-cyclohexen-1-one with diethylmagnesium in the presence of 2,1,1-cryptand gave much more of 1,4-addition product, 3-ethylcyclohexanone, than that with either organometallic compound alone (Table 2)<sup>18</sup>.

Very recently, Ishihara and coworkers developed a highly efficient nucleophilic addition of magnesiate reagents to ketones, which is very useful in organic synthesis<sup>19</sup>. The nucleophilicity of the alkyl group in lithium trialkylmagnesiate is markedly enhanced compared to that of the parent alkyl lithium or alkylmagnesium halide. Butylation of acetophenone was examined with several organolithium and organomagnesium reagents (Table 3). Reaction with butyllithium gave the corresponding tertiary alcohol in modest yield, along with a small amount of an undesired aldol product (entry 1). The basic nature of butyllithium

TABLE 1. Reactions of pyridine with ethylmetals

Ethylmetal	Time	2-Ethylpyridine (%)	4-Ethylpyridine (%)
Et <sub>2</sub> Mg	22 h	0.3	0
Et <sub>2</sub> Mg + 15-crown-5	20 h <sup>a</sup>	13	37
Et <sub>2</sub> Mg + 2,1,1-cryptand	24 h	14	31
Et <sub>2</sub> Mg + EtLi	22 h	37	6
EtLi	0.5 h	39	0

<sup>a</sup> Performed at 40 °C.

TABLE 2. Reactions of 2-cyclohexen-1-one with ethylmetals

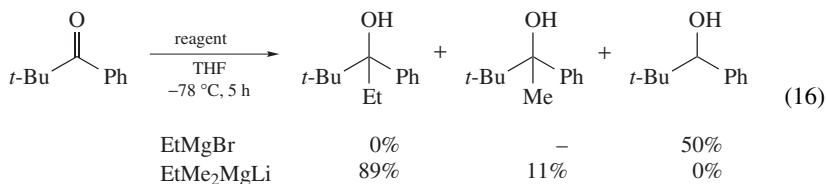
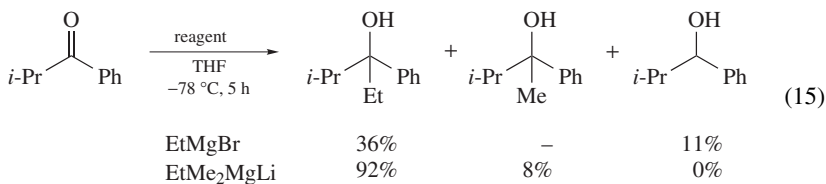
Ethylmetal	1,4-Adduct (%)	1,2-Adduct (%)
Et <sub>2</sub> Mg	2	67
Et <sub>2</sub> Mg + 15-crown-5	34	57
Et <sub>2</sub> Mg + 2,1,1-cryptand	30	40
EtLi	0	73

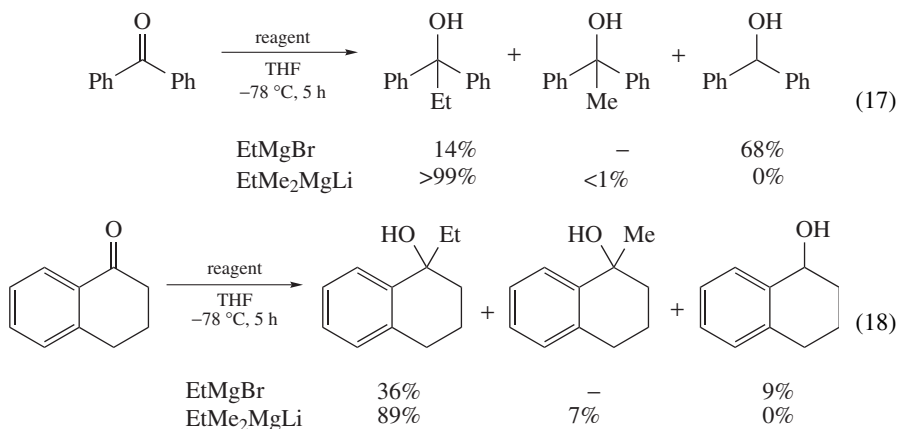
TABLE 3. Reactions of acetophenone with butylmetals

Entry	Butylmetal	1,2-Adduct (%)	Aldol product (%)	Reduced product (%)
1	BuLi	62	7	0
2	BuMgCl	50	9	8
3	Bu <sub>2</sub> Mg	48	27	20
4	Bu <sub>3</sub> MgLi	99	0	0

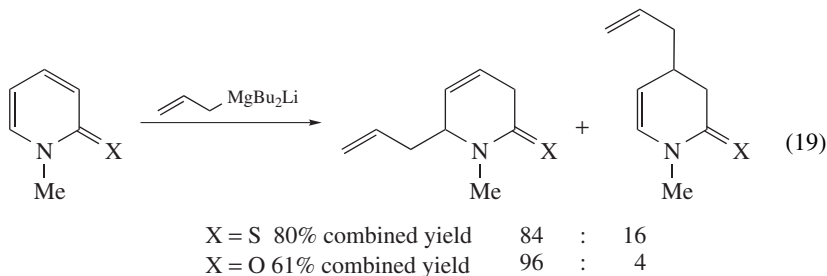
would produce the enolate of acetophenone. Use of butylmagnesium chloride also led to a similar result, except for the additional production of a small amount of 1-phenylethanol (entry 2). Although dibutylmagnesium effected butylation, the selectivity of the desired product was considerably diminished (entry 3). When lithium tributylmagnesate, prepared from butylmagnesium chloride and butyllithium in a 1:2 molar ratio, was examined, a highly selective and efficient butylation took place (entry 4).

Interestingly, mixed magnesate reagents, RMe<sub>2</sub>MgLi (R ≠ Me), could transfer the R group selectively to ketones (equations 15–18). Surprisingly, readily enolizable ketones such as β-tetralone were ethylated in excellent yields (equation 18).





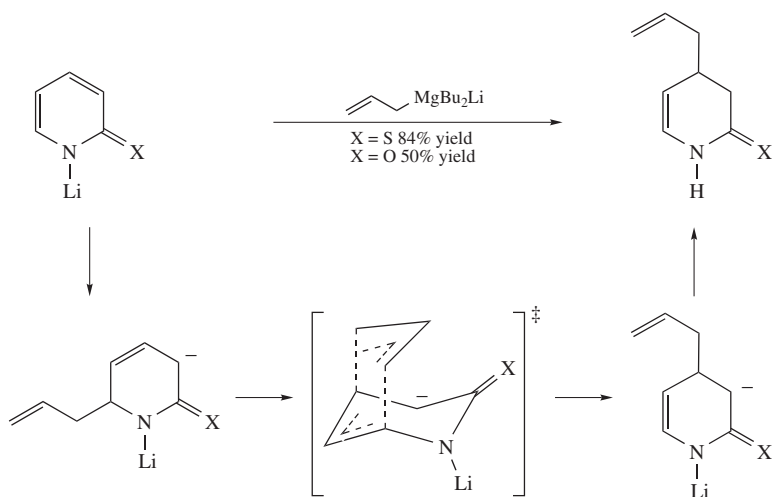
Lithium allyldibutylmagnesate can be formed easily by mixing allylmagnesium chloride and two molar equivalents of butyllithium. The allyldibutylmagnesate was nucleophilic enough to allylate pyridine-2-thiones and pyridin-2-ones<sup>20</sup>. Treatment of 1-methylpyridine-2-thione and 1-methylpyridin-2-one with lithium allyldibutylmagnesate gave rise to the allylation at the 6 positions (equation 19). On the other hand, 1-lithiopyridine-2-thione and 1-lithiopyridin-2-one underwent the allylation at the 4 positions (Scheme 1). By careful monitoring of the reaction mixture, it was concluded that the 4-allylpyridine derivatives were obtained via the [3,3] sigmatropic rearrangement of the initially formed 6-allylpyridine intermediates.



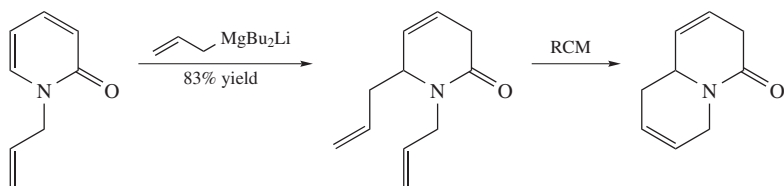
The reaction of a 1-allylpyridin-2-one derivative with lithium allyldibutylmagnesate followed by ring-closing metathesis (RCM) yielded tetrahydroquinolizin-4-one (Scheme 2)<sup>21</sup>.

## B. Deprotonation Reactions

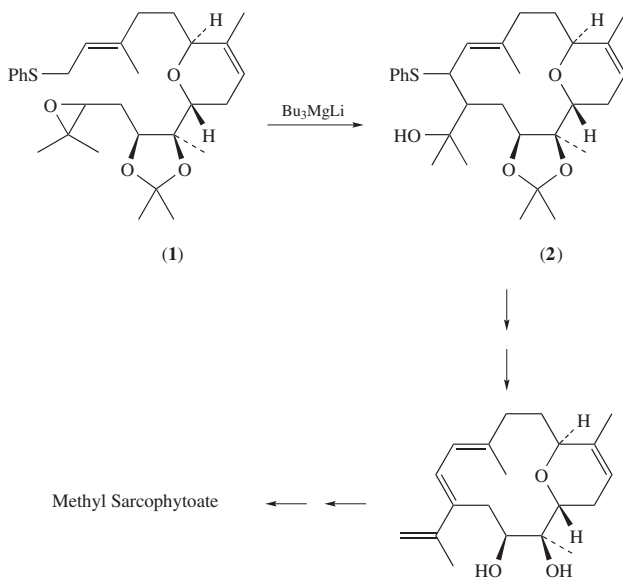
The efficiency of deprotonation reaction of fluorene was a benchmark of the enhanced reactivity of triorganomagnesates<sup>1,17</sup>. The deprotonation with triorganomagnesates has emerged as a useful tool in modern synthetic organic chemistry since the work by Nakata and coworkers in 1997<sup>22</sup>. As a key step in the asymmetric synthesis of the fourteen-membered unit of methyl sarcophytoate, lithium tributylmagnesate was highly effective to metalate **1** at the allylic sulfide moiety (Scheme 3). The anion generated underwent cyclization to yield **2**, whereas the original protocol using butyllithium/DABCO system or other surrogates suffered from substantial decomposition of **1** as well as poor reproducibility.



SCHEME 1



SCHEME 2



SCHEME 3

TABLE 4. Generation of sulfur-stabilized anion with organometallic reagents

Base	%D
BuLi	86
0.25 BuLi + Bu <sub>2</sub> Mg	85
1.0 BuLi + Bu <sub>2</sub> Mg	62
Bu <sub>2</sub> Mg	0

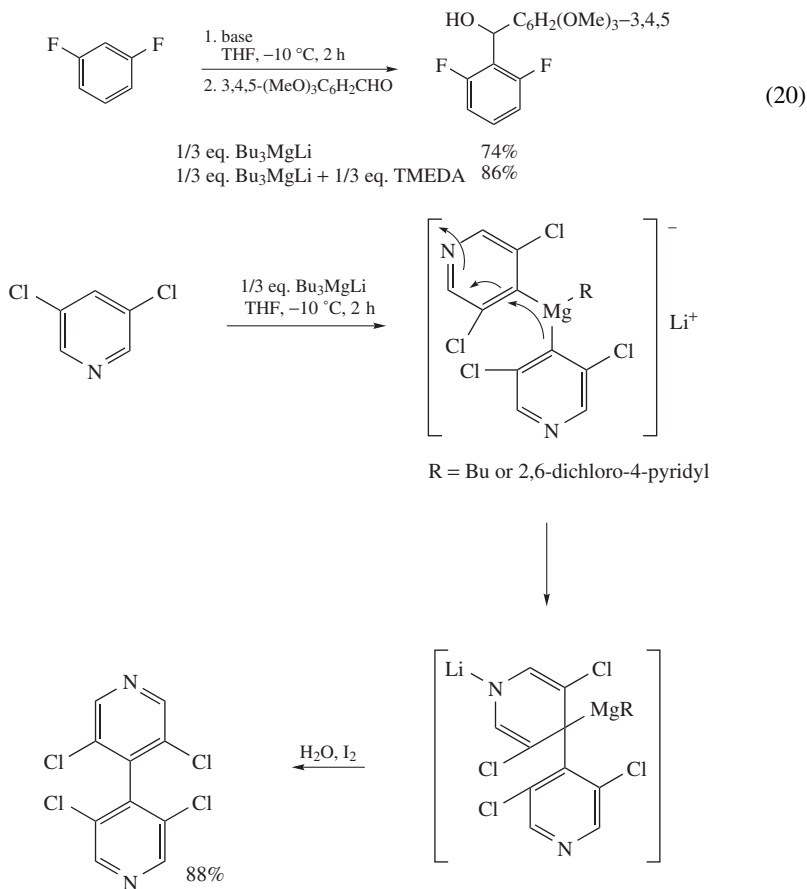
TABLE 5. Metalation of 3-fluoropyridine

E <sup>+</sup>	E	Yield (%)
I <sub>2</sub>	I	64
4-MeOC <sub>6</sub> H <sub>4</sub> CHO	4-MeOC <sub>6</sub> H <sub>4</sub> CHOH	50
3,4,5-(MeO) <sub>3</sub> C <sub>6</sub> H <sub>2</sub> CHO	3,4,5-(MeO) <sub>3</sub> C <sub>6</sub> H <sub>2</sub> CHOH	55 <sup>a</sup>
CH <sub>2</sub> =CHCH <sub>2</sub> Br	CH <sub>2</sub> =CHCH <sub>2</sub>	40
2-Bromopyridine	2-Pyridyl	51 <sup>b</sup>

<sup>a</sup> 74% in the presence of 0.33 molar equivalents of TMEDA.<sup>b</sup> With PdCl<sub>2</sub>(dppf).

Nakata and coworkers also found that a mixture of butyllithium and dibutylmagnesium generated the anion of a 1,3-dithiane derivative (Table 4)<sup>23</sup>. It is worth noting that their reagent consisted of dibutylmagnesium and 0.25 molar equivalents of butyllithium. The reagent was more effective for the deprotonation than lithium tributylmagnesium. The sulfur-stabilized anion which was generated by the action of their reagent had a longer lifetime than that generated by using butyllithium alone or lithium tributylmagnesium.

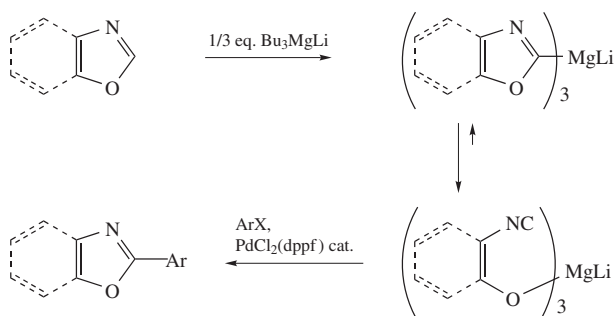
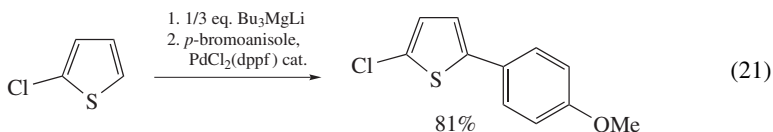
Mongin and coworkers have been focusing on deprotonation reactions of aromatic hydrogens with magnesate reagents. Treatment of 3-fluoropyridine with 0.33 molar equivalents of lithium tributylmagnesium in THF at  $-10^{\circ}\text{C}$  resulted in deprotonation at the 4 position (Table 5)<sup>24</sup>. The intermediate lithium tripyridylmagnesium reacted with electrophiles as well as underwent a palladium-catalyzed cross-coupling reaction. Use of TMEDA as an additive proved to enhance the reactivity of the magnesate complexes. Deprotonation also took place at the 2 position of 1,3-difluorobenzene (equation 20). 3,5-Dichloropyridine was involved in a deprotonation reaction in which it was transformed into the tetrachloro-4,4'-bipyridyl via 1,2-migration of the lithium pyridylmagnesium formed by deprotonation (Scheme 4)<sup>25</sup>.



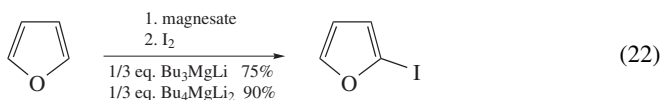
SCHEME 4

Deprotonation reactions of other heteroaromatics were also reported. Thiophene was regioselectively deprotonated at the 2 position by the action of 0.33 molar equivalents of lithium tributylmagnesate in THF at room temperature<sup>26</sup>. Deprotonation took place at the 5 position upon treatment of 2-chloro- and 2-methoxythiophenes (equation 21). The lithium trithienylmagnesate underwent reactions with electrophiles and cross-coupling reactions. Deprotonation reactions of oxazole and benzoxazole proceeded smoothly with lithium tributylmagnesate in THF at room temperature (Scheme 5)<sup>27</sup>. Interestingly, tri(2-oxazolyl)- and tri(2-benzoxazolyl)magnesates isomerized very rapidly and completely to the isocyano-substituted enolate of acetaldehyde and 2-isocyano-phenolate, respectively. The reactions of the metalated intermediates with various electrophiles occurred easily with concomitant recovery of the original aromaticity. Furan and benzofuran were deprotonated upon treatment with 0.33 molar equivalents of lithium tributylmagnesate (equation 22)<sup>28</sup>. Dilithium tetrabutylmagnesate, prepared from magnesium dibromide and

four molar equivalents of butyllithium, was more reactive than lithium tributylmagnesate.



SCHEME 5



### C. Halogen–Magnesium Exchange

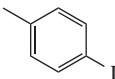
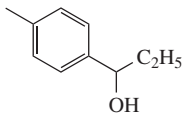
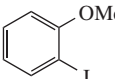
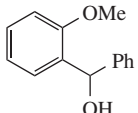
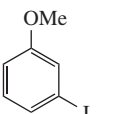
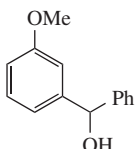
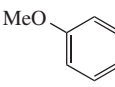
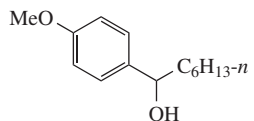
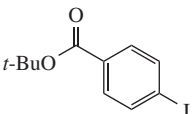
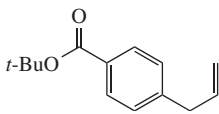
Although halogen–lithium exchange reactions are among the most important methods for the preparation of organolithium compounds, the functional group compatibility of the exchange is not satisfactory. Despite their promising functional group compatibility, halogen–magnesium exchange reactions are thought to be slower, to require higher temperature, and thus to be less useful. For the last decade, halogen–magnesium exchange has been recognized as a powerful tool for preparation of organomagnesium reagents<sup>29</sup>. The significant development has been observed since 1998, when Knochel and coworkers reported isopropylmagnesium-induced exchange reactions that are applicable to polyfunctional organomagnesium reagents<sup>30</sup>. Knochel's group also disclosed very recently that an isopropylmagnesium chloride/lithium chloride system is highly efficient for the exchange reactions (Chapter X by Knochel)<sup>7,8</sup>.

Halogen–magnesium exchange reactions with triorganomagnesates were reported independently from academia<sup>11</sup> and industry<sup>31</sup> in 2001.

Treatment of various aryl iodides with 1.2 (or 0.5) molar equivalents of lithium tributylmagnesate, prepared from butylmagnesium bromide and butyllithium in a 1:2 ratio in THF, led to iodine–magnesium exchange<sup>11</sup>. The arylmagnesium reagents thus formed were trapped by electrophiles (Table 6). Electron-rich as well as electron-deficient arylmagnesium reagents were prepared. Functional groups such as ester were tolerated during the exchange procedure, as the exchange reactions proceeded even at  $-78^\circ\text{C}$ . For instance, treatment of *tert*-butyl *p*-iodobenzoate with 0.5 molar equivalents of lithium tributylmagnesate at  $-78^\circ\text{C}$  furnished the corresponding arylmagnesium reagent, which then reacted with allyl bromide under the catalysis of  $\text{CuCN}\cdot 2\text{LiCl}$  (Table 6, last entry). Intriguingly,

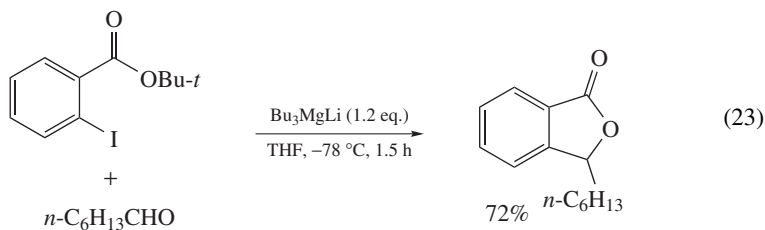


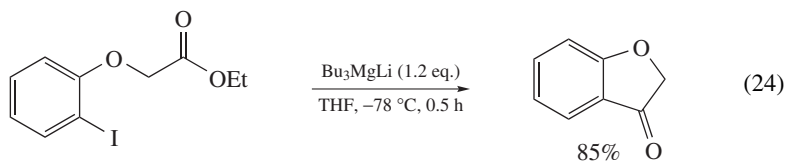
TABLE 6. Iodine–magnesium exchange of aryl iodides

$\text{Ar-I} \xrightarrow[\text{THF, } -78^\circ\text{C, 30 min}]{\text{Bu}_3\text{MgLi (1.2 eq.)}} \text{Ar-Bu}_2\text{MgLi} \xrightarrow{\text{Electrophile}} \text{Ar-E}$			
Ar-I	Electrophile	Ar-E	Yield (%)
	$\text{C}_2\text{H}_5\text{CHO}$		75 <sup>a</sup>
	$\text{PhCHO}$		92
	$\text{PhCHO}$		93
	$n\text{-C}_6\text{H}_{13}\text{CHO}$		94
	$\text{CH}_2=\text{CHCH}_2\text{Br}^b$		88

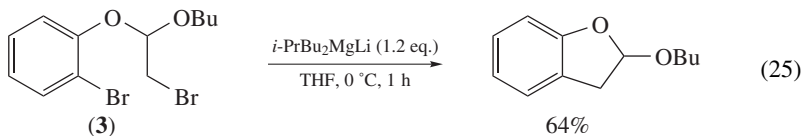
<sup>a</sup> 0.5 molar equivalents of  $\text{Bu}_3\text{MgLi}$  was used.<sup>b</sup> A catalytic amount of  $\text{CuCN}\cdot 2\text{LiCl}$  was added.

the magnesiation reaction of *t*-butyl *o*-iodobenzoate was faster than the nucleophilic butylation of an aldehyde (equation 23). Addition of lithium tributylmagnesate to a mixture of the iodobenzoate and heptanal afforded the corresponding phthalide in a good yield. Ethyl (2-iodophenoxy)acetate underwent iodine–magnesium exchange to give 3-coumaranone in excellent yield (equation 24).



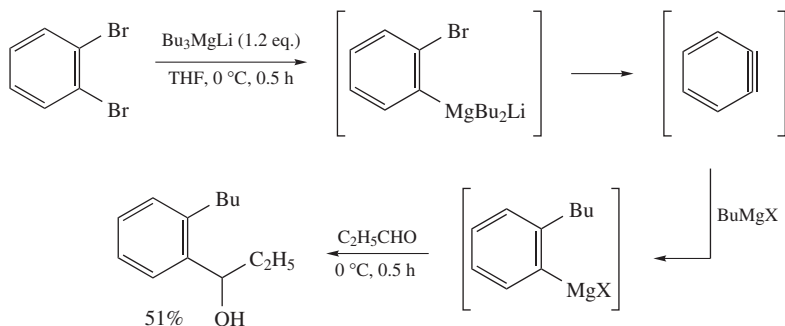


Since the exchange reaction of aryl bromides did not proceed to completion at  $-78^{\circ}\text{C}$  in some cases, bromine–magnesium exchange with lithium tributylmagnesate should be performed at  $0^{\circ}\text{C}$  (Table 7)<sup>11</sup>. Cyano groups survived even at  $-40^{\circ}\text{C}$  (last two entries). Unfortunately, one needs to avoid using aryl bromides with carbonyl groups due to the higher temperature. To attain more efficient bromine–magnesium exchange reactions at  $-78^{\circ}\text{C}$ , lithium dibutylisopropylmagnesate proved to be suitable (Table 8). Functional groups such as carbonyl groups tolerated the magnesate reagent. The exchange reaction of aryl bromide **3** led to the formation of 2-alkoxycoumaran in good yield via intramolecular nucleophilic substitution (equation 25).



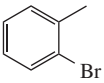
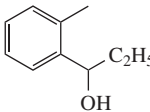
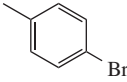
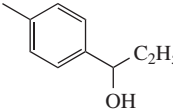
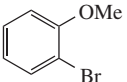
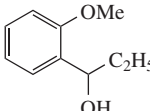
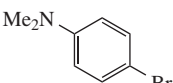
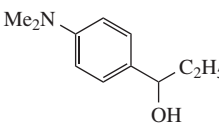
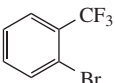
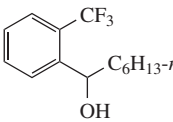
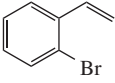
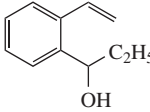
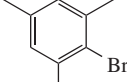
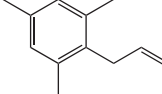
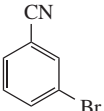
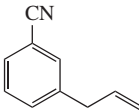
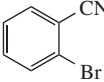
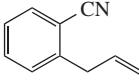
Controlled metalation of dihaloarenes provides an efficient method to synthesize disubstituted aromatic compounds (Table 9)<sup>11</sup>. In the case of *p*-bromiodobenzene, no bromine–magnesium exchange took place with a stoichiometric amount of a magnesate reagent (entry 1). Only one of two bromides in *m*- or *p*-dibromobenzene underwent the exchange (entries 2 and 3). On the other hand, *p*-diiodobenzene was converted to dimagnesiated benzene upon treatment with 1.0 molar equivalent of lithium tributylmagnesate (entry 4). Dimetalation of *m*-diiodobenzene needed 2.0 molar equivalents of the reagent (entry 5). Lithium butyldimethylmagnesium allowed for selective monomagnesiation of *p*-diiodobenzene (entry 6). The lower reactivity of the methyl group would decelerate the second exchange reaction. Thus, properly mixed triorganomagnesates can control the reactivity in halogen–magnesium exchange.

Treatment of *o*-dibromobenzene with lithium tributylmagnesate yielded 2-butylphenylmagnesium reagent, which was formed via benzyne (Scheme 6)<sup>11</sup>.



SCHEME 6

TABLE 7. Bromine–magnesium exchange of aryl bromides with Bu<sub>3</sub>MgLi

$\text{Ar-Br} \xrightarrow[\text{THF, 0 } ^\circ\text{C, 30 min}]{\text{Bu}_3\text{MgLi (1.2 eq.)}} \text{Ar-Bu}_2\text{MgLi} \xrightarrow{\text{Electrophile}} \text{Ar-E}$			
Ar-Br	Electrophile	Ar-E	Yield (%)
	C <sub>2</sub> H <sub>5</sub> CHO		88
	C <sub>2</sub> H <sub>5</sub> CHO		85
	C <sub>2</sub> H <sub>5</sub> CHO		90 <sup>a</sup>
	C <sub>2</sub> H <sub>5</sub> CHO		94
	<i>n</i> -C <sub>6</sub> H <sub>13</sub> CHO		76
	C <sub>2</sub> H <sub>5</sub> CHO		52
	CH <sub>2</sub> =CHCH <sub>2</sub> Br <sup>b</sup>		93
	CH <sub>2</sub> =CHCH <sub>2</sub> Br <sup>b</sup>		85 <sup>a,c</sup>
	CH <sub>2</sub> =CHCH <sub>2</sub> Br <sup>b</sup>		80 <sup>a,c</sup>

<sup>a</sup> 0.5 molar equivalents of Bu<sub>3</sub>MgLi was used.<sup>b</sup> A catalytic amount of CuCN•2LiCl was added.<sup>c</sup> The reaction was performed at -40 °C.

TABLE 8. Bromine–magnesium exchange of aryl bromides with *i*-PrBu<sub>2</sub>MgLi

$\text{Ar-Br} \xrightarrow[\text{THF, } -78^\circ\text{C, 1 h}]{i\text{-PrBu}_2\text{MgLi (1.2 eq.)}} \text{Ar-Bu}_2\text{MgLi} \xrightarrow[\text{-78}^\circ\text{C, 1 h}]{\text{Electrophile}} \text{Ar-E}$			
Ar-Br	Electrophile	Ar-E	Yield (%)
	CH <sub>2</sub> =CHCH <sub>2</sub> Br <sup>a</sup>		99
	<i>n</i> -C <sub>6</sub> H <sub>13</sub> CHO		71
	CH <sub>2</sub> =CHCH <sub>2</sub> Br <sup>a</sup>		80
	CH <sub>2</sub> =CHCH <sub>2</sub> Br <sup>a</sup>		87

<sup>a</sup> A catalytic amount of CuCN•2LiCl was added.

Lithium butyldimethylmagnesate was preferable to tributylmagnesate in the bromine–magnesium exchange of 3-bromopyridine since the latter afforded a rather complex mixture (Table 10)<sup>11</sup>. 2-Bromopyridine and 2-bromothiophene were also converted to the corresponding magnesium reagents which then reacted with aldehydes.

Stereospecific magnesianation was observed in the exchange reactions of alkenyl iodides with lithium dibutylisopropylmagnesate (Table 11)<sup>11</sup>. The magnesianation could be completed within 1 h at  $-78^\circ\text{C}$ , where the ester functionality was compatible with the reaction (last entry). Unfortunately, the bromine–magnesium exchange of alkenyl bromide was disappointing since, due to the slow exchange, sequential dehydrobromination and deprotonation took place to yield the relevant magnesium acetylide as a by-product (equation 26). The exchange reaction of 1-silyl-1-haloalkenes proceeded smoothly, along with considerable isomerization to give mainly the *E* isomer (Scheme 7). Obviously, these results reflect the strong preference of the bulky silyl group to be in the *trans* position to the alkyl group.

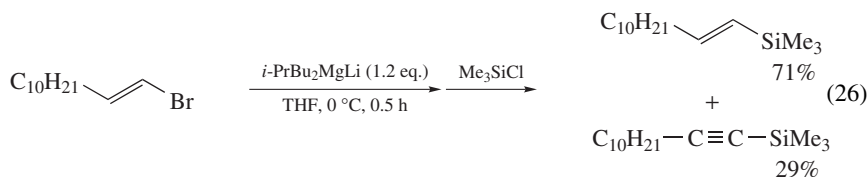


TABLE 9. Halogen–magnesium exchange of dihaloarenes followed by reaction with propanal

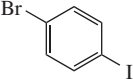
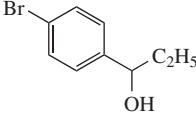
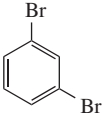
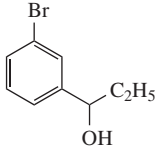
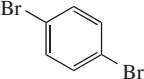
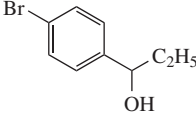
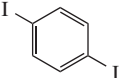
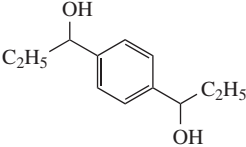
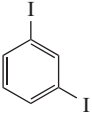
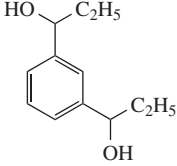
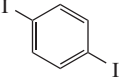
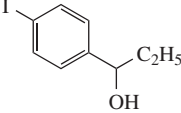
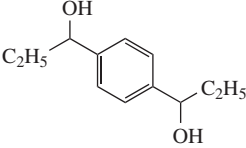
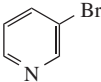
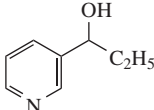
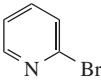
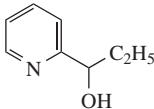
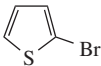
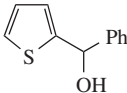
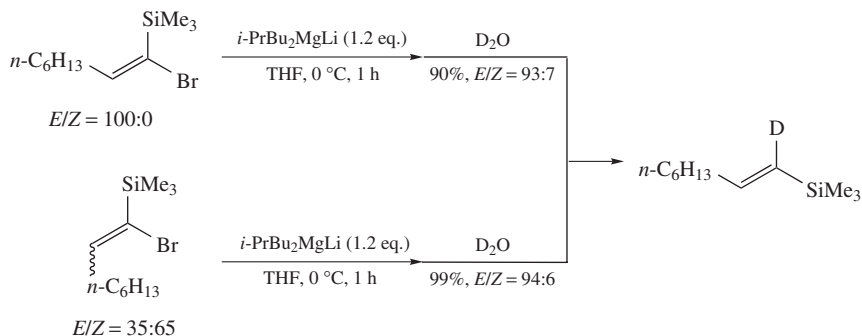
Entry	Ar–I	Conditions	Product	Yield (%)
1		<i>i</i> -PrBu <sub>2</sub> MgLi (1.0 eq.) –78 °C, 0.5 h		65
2		<i>i</i> -PrBu <sub>2</sub> MgLi (1.0 eq.) 0 °C, 0.5 h		78
3		Bu <sub>3</sub> MgLi (1.0 eq.) –78 °C, 0.5 h		85
4		Bu <sub>3</sub> MgLi (1.0 eq.) –78 °C, 0.5 h		80
5		Bu <sub>3</sub> MgLi (2.0 eq.) –78 °C, 0.5 h		48
6		BuMe <sub>2</sub> MgLi (1.0 eq.) –78 °C, 0.5 h	  	64  9

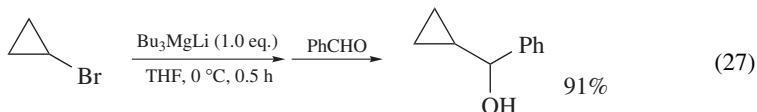
TABLE 10. Bromine–magnesium exchange of heteroaryl bromides with  $\text{BuMe}_2\text{MgLi}$ 

HeteroAr–Br $\xrightarrow[\text{THF, 0 } ^\circ\text{C, 0.5 h}]{\text{BuMe}_2\text{MgLi (1.0 eq.)}}$ $\xrightarrow[\text{0 } ^\circ\text{C, 0.5 h}]{\text{RCHO}}$ HeteroAr–CH(OH)R			
HeteroAr–Br	RCHO	HeteroAr–CH(OH)R	Yield (%)
	$\text{C}_2\text{H}_5\text{CHO}$		73
	$\text{C}_2\text{H}_5\text{CHO}$		67
	$\text{PhCHO}$		78 <sup>a</sup>

<sup>a</sup> Lithium tributylmagnesate was used.

SCHEME 7

Since the carbon–carbon bonds in strained cyclopropane rings have large s-character, cyclopropyl bromides underwent smooth bromine–magnesium exchange by the action of lithium tributylmagnesate (equation 27)<sup>11</sup>.



Chemists in Banyu Pharmaceutical discovered that lithium tributylmagnesate, prepared from butylmagnesium chloride and two molar equivalents of butyllithium, is quite

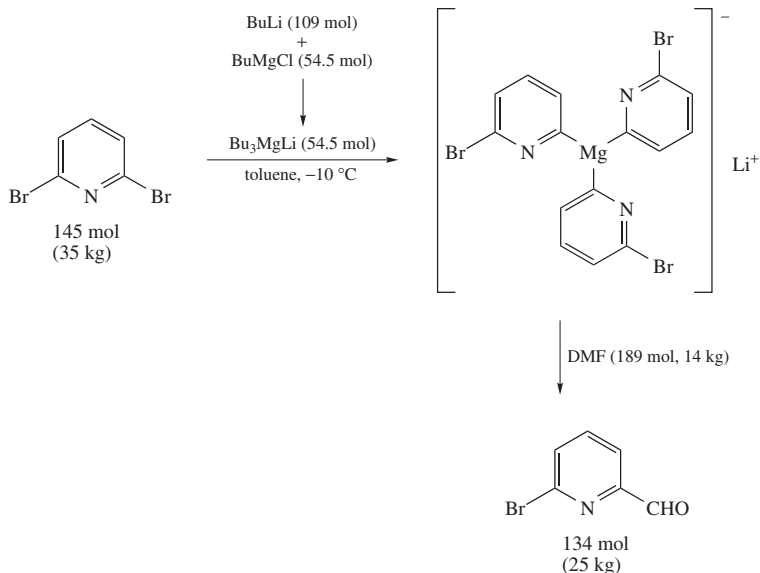
TABLE 11. Iodine–magnesium exchange of alkenyl iodides

$$\text{R}^1\text{C}(\text{R}^2)=\text{C}(\text{R}^3)\text{I} \xrightarrow[\text{THF, 0 } ^\circ\text{C, 1 h}]{i\text{-PrBu}_2\text{MgLi (1.2 eq.)}} \xrightarrow{\text{Electrophile}} \text{Product}$$

Entry	Alkenyl iodide	Electrophile	Product	Yield (%)
1		Me <sub>3</sub> SiCl		93
2		CH <sub>2</sub> =CHCH <sub>2</sub> Br <sup>a</sup>		70
3		Me <sub>2</sub> CO		75
4		Me <sub>3</sub> SiCl		87
5		CH <sub>2</sub> =CHCH <sub>2</sub> Br <sup>a</sup>		70
6		Me <sub>2</sub> CO		75
7		PhCHO		87
8		PhCHO		70
9		C <sub>2</sub> H <sub>5</sub> CHO		80 <sup>b</sup>

<sup>a</sup> A catalytic amount of CuCN•2LiCl was added.<sup>b</sup> Performed at −78 °C.

efficient for the selective monomagnesiation of 2,6-dibromopyridine (Scheme 8)<sup>31</sup>. The bromine–magnesium exchange reaction of 2,6-dibromopyridine with the magnesate reagent (0.35 molar equivalents) proceeded efficiently under noncryogenic conditions (−10 °C) in toluene, affording a virtually pure mono-magnesiated intermediate. Subsequent treatment with DMF provided the desired aldehyde in 95% yield. In the Banyu protocol, all the three butyl groups in the ate complex participated in the exchange.



SCHEME 8

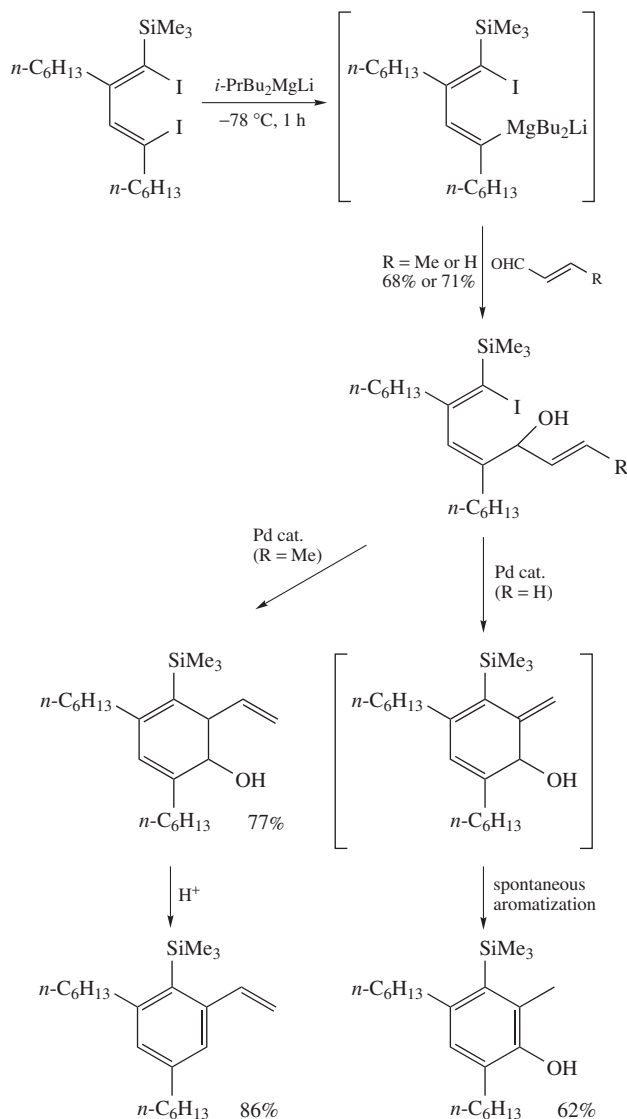
TABLE 12. Monoformylation of dibromoarenes by the Banyu protocol [(1) 0.35–0.40 molar equivalents of Bu<sub>3</sub>MgLi, (2) 1.3 molar equivalents of DMF, (3) aq. citric acid or aq. acetic acid]

Dibromoarene	Conditions	Magnesiation (mono-/di-)	Product	Yield (%)
	toluene 0 °C, 5 h	88.5:< 0.1		84
	toluene 0 °C, 1.5 h	92.0:< 0.1		99
	toluene/THF (5:1) 0 °C, 1 h	91.9:< 2		92
	toluene/THF (1:1) -10 °C, 1.5 h	97.7:< 0.1		78
	toluene -10 °C, 3 h	90.7:1.6		73

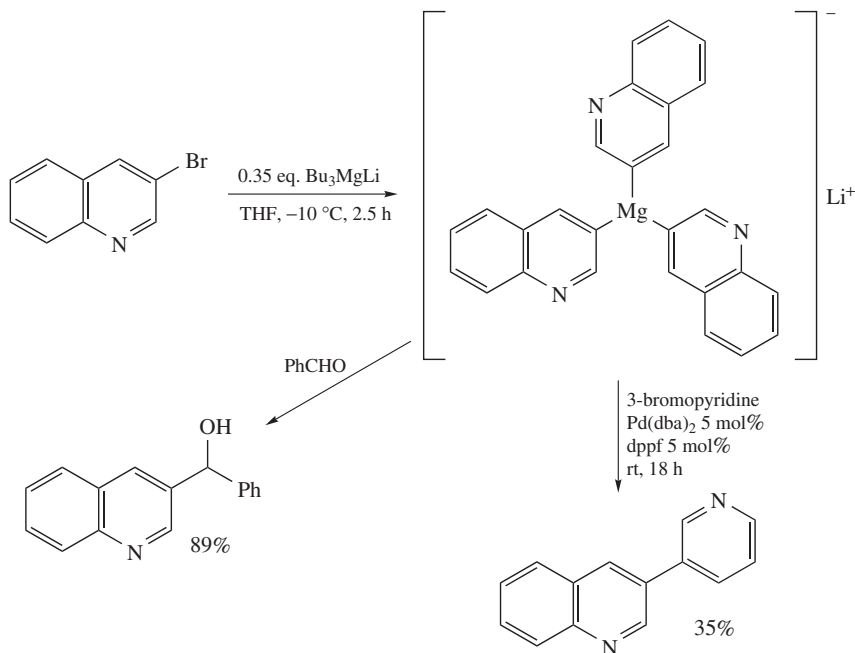


The protocol is used for the preparation of 25 kg of the aldehyde in Banyu, and applied to the synthesis of a muscarinic receptor agonist. It is noteworthy that halogen-metal exchange reactions with other metal reagents such as butyllithium or isopropylmagnesium bromide led to more complex mixtures. The Banyu protocol was applicable to similar monoformylation reactions of dibromoheteroarenes (Table 12).

Since the two pioneering reports from academia<sup>11</sup> and industry<sup>31</sup>, organomagnesium ate reagents have been recognized as reliable reagents in organic synthesis. Most of the



SCHEME 9



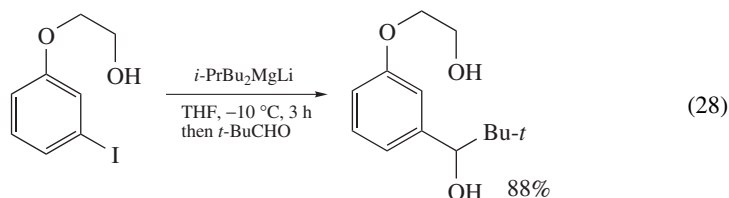
SCHEME 10

examples of the nucleophilic addition reactions and the deprotonation reactions in the previous sections were reported after these two reports. This is also the case for halogen–magnesium exchange reactions.

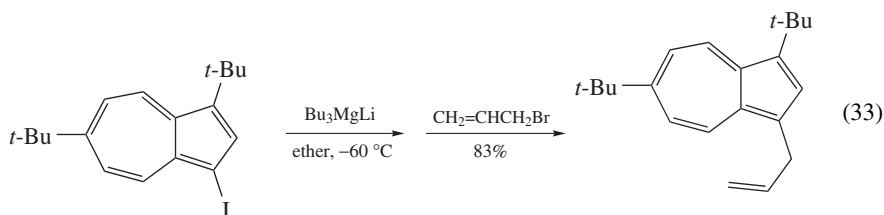
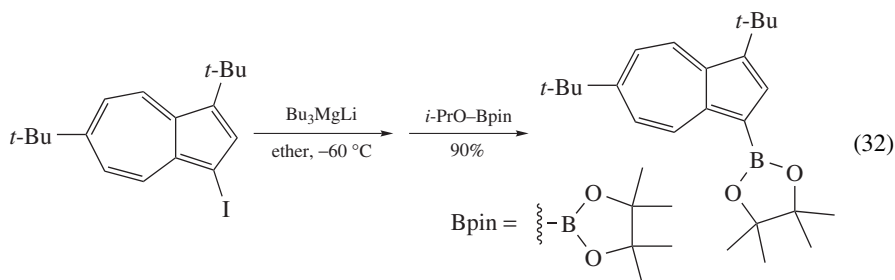
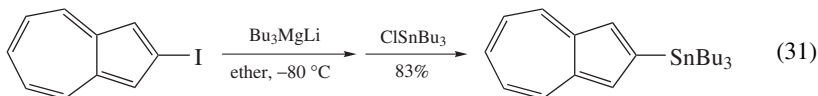
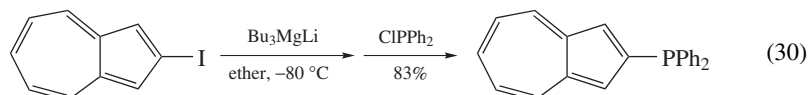
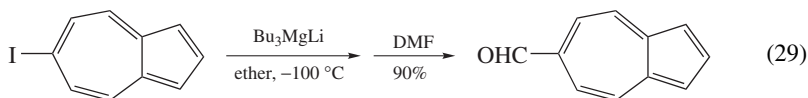
Sato and coworkers found that site-selective iodine–magnesium exchange reactions of 1,4-diiodo-1,3-alkadienes were attained only by using the organomagnesium ate complex, lithium dibutylisopropylmagnesate (Scheme 9)<sup>32</sup>. The magnesiated iodoalkadienes were transformed into polysubstituted styrenes and phenols.

Although isopropylmagnesium chloride, *tert*-butylmagnesium chloride and diisopropylmagnesium failed to effect the bromine–magnesium exchange reaction of 3-bromoquinoline, 0.35 molar equivalents of lithium tributylmagnesate smoothly promoted the metalation at  $-10^\circ\text{C}$  in THF (Scheme 10)<sup>33</sup>. Lithium tris(3-quinolyl)magnesate reacted with benzaldehyde to yield the corresponding alcohol. Intriguingly, the yields largely depended on the amount of the magnesate reagent used, i.e. 0% yield with 1 molar equivalent of the reagent, and 5–10% with 0.66 molar equivalents. Butylated products were obtained in these cases through addition of the remaining butylmagnesium species to the quinoline ring. Similar bromine–magnesium exchange occurred in the reactions of 2- or 4-bromoquinolines. The tris(quinolyl)magnesates and related tris(heteroaryl)magnesates are involved in palladium- and nickel-catalyzed cross-coupling reactions, albeit the yields were moderate<sup>34</sup>.

Selective halogen–magnesium exchange of *m*- and *p*-halobenzene derivatives having *ortho*-directing groups took place with magnesate reagents (equation 28)<sup>35</sup>. Lithium dibutylisopropylmagnesate proved to be superior in preventing *ortho*-metalation to other metalation agents such as isopropylmagnesium bromide.



Preparation of some azulenyilmagnesium species was achieved by the halogen–magnesium exchange reactions of iodoazulenes with lithium tributylmagnesate at low temperatures (equations 29–33)<sup>36</sup>. The reactions offer access to a variety of functionalized azulenes including azulenylphosphine, -stannane and -boronic ester.

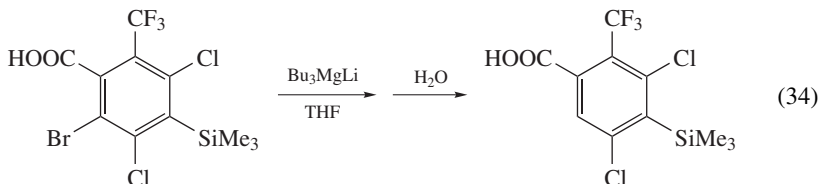


A halogen–magnesium exchange reaction of 4-iodo-6-phenylthieno[2,3-*d*]pyrimidine with various magnesate reagents had taken place (Table 13)<sup>37</sup>. Among the magnesate reagents, lithium butyldimethylmagnesium was the most efficient. The magnesate reagent was superior to butyllithium since the reaction with the magnesate under Barbier-type conditions was performed at 0 °C. The reaction with butyllithium at 0 °C afforded none of the desired product.

TABLE 13. Barbier-type reaction of iodopyrimidine derivative with aldehyde

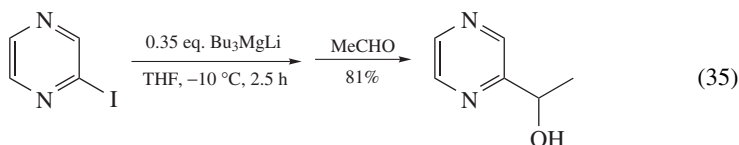
Conditions	Yield (%)
BuMe <sub>2</sub> MgLi, −76 °C	60
BuMe <sub>2</sub> MgLi, 0 °C	62
Bu <sub>3</sub> MgLi, −76 °C	19
PhBu <sub>2</sub> MgLi, −76 °C	56
BuPh <sub>2</sub> MgLi, −76 °C	trace
BnPh <sub>2</sub> MgLi, −76 °C	41
BuLi, −76 °C	57
BuLi, 0 °C	0

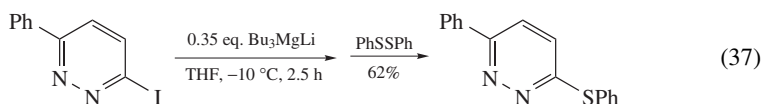
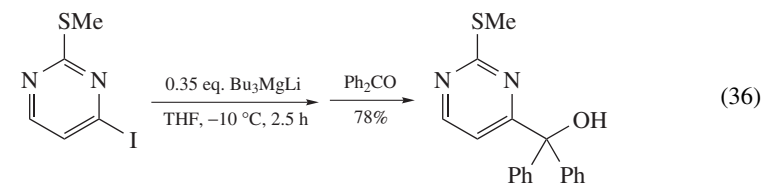
Metalation of only the bromine of 2-bromo-3,5-dichloro-6-(trifluoromethyl)-4-trimethylsilylbenzoic acid proceeded smoothly with lithium tributylmagnesate (equation 34)<sup>38</sup>.



Lithium dibutylisopropylmagnesate proved to be quite efficient for the bromine–magnesium exchange of 5-bromo-2-picoline at −10 °C (Table 14)<sup>39</sup>. The resulting picolylmagnesium reagent reacted with electrophiles including thiuram disulfide (last entry).

The reactions of 2-iodopyrazine, 2-methylsulfanyl-4-iodopyrimidine and 3-iodo-6-phenylpyridazine with lithium tributylmagnesate resulted in very efficient iodine–magnesium exchange to yield the corresponding heteroarylmagnesium species (equations 35–37)<sup>40</sup>. The reactions with carbonyl compounds and diphenyl disulfide proceeded with good yields. The reactions proceeded smoothly, and neither the starting iodide nor any butylated compounds derived from nucleophilic addition to the heteroaromatic nuclei were observed.



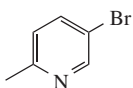
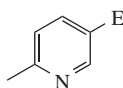


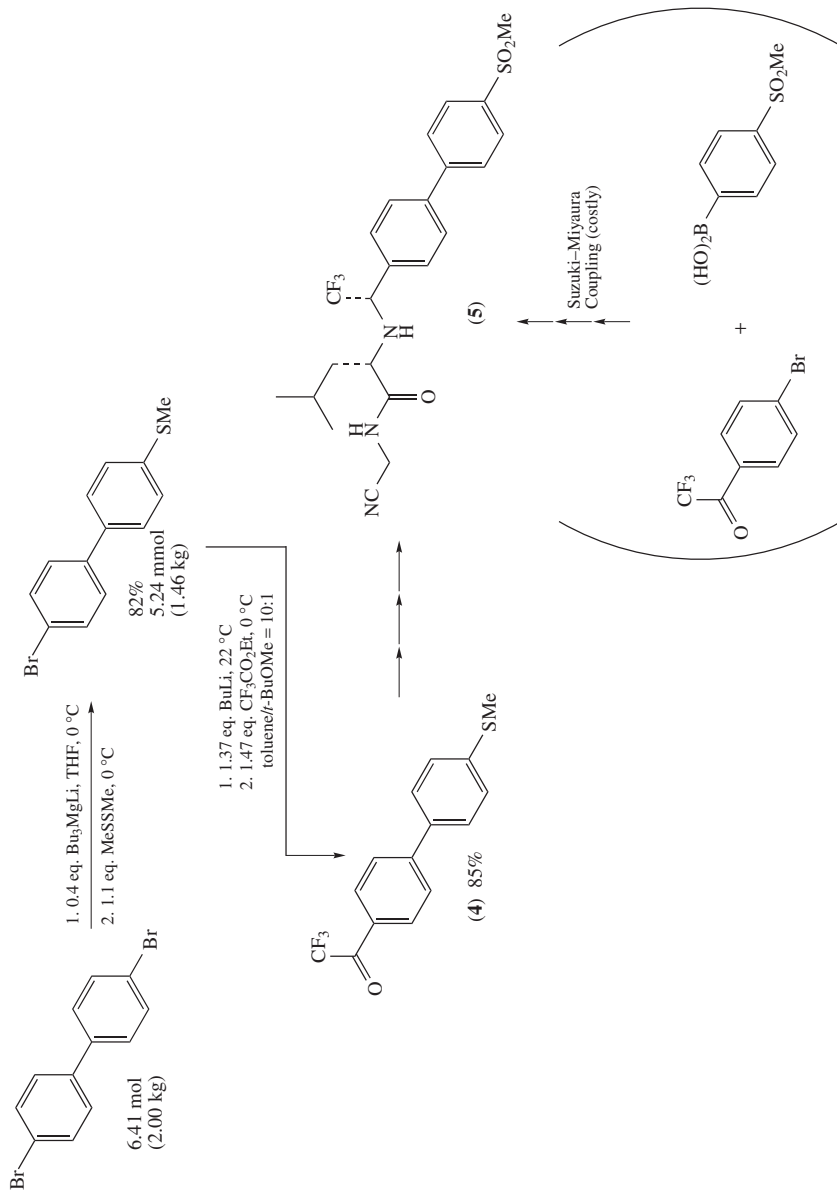
Chemists in Merck sought to develop a cost-efficient and practical synthesis of biphenyl ketone **4**, a precursor to potent cathepsin K Inhibitor **5** (Scheme 11). Instead of an obvious retrosynthetic analysis via a Suzuki–Miyaura cross-coupling between the corresponding arylboronic acid and aryl bromide, they have found the following new route to the ketone **4**<sup>41</sup>. A selective halogen–magnesium exchange/dimethyl disulfide quench protocol on 4,4'-dibromobiphenyl with lithium tributylmagnesate proceeded smoothly under non-cryogenic conditions on a large scale. The magnesate showed superb reactivity, whereas other metalation agents such as butyllithium, isopropylmagnesium chloride and Knochel's isopropylmagnesium chloride–lithium chloride system were less selective or completely unreactive.

The reactions of *gem*-dibromocyclopropanes with dialkylcuprates, trialkylzincates and trialkylmanganates were well known, and afforded alkylated cyclopropylmetals. Lithium trialkylmagnesates also participated in similar alkylative metalation (Scheme 12)<sup>42</sup>. Treatment of dibromocyclopropane **6** with lithium tributylmagnesate at low temperatures followed by addition of electrophiles provided the corresponding butylated products as mixtures of diastereomers **7** and **8**. The reactions should be performed at  $-78^\circ\text{C}$  to  $-30^\circ\text{C}$ . At higher temperatures, formation of 1,2-nonadiene was inevitable. 1,2-Migration of the butyl group was incomplete at  $-78^\circ\text{C}$ .

Treatment of dibromomethyl methylphenylsilane with lithium tributylmagnesate at  $-78^\circ\text{C}$  induced very efficient bromine–magnesium exchange to yield the bromomethylsilane upon protonolysis at  $-78^\circ\text{C}$  (Scheme 13)<sup>42,43</sup>. Warming the reaction mixture in the presence of a copper salt before protonolysis led to smooth migration of one of the butyl groups to afford 1-silylpentylmetal.

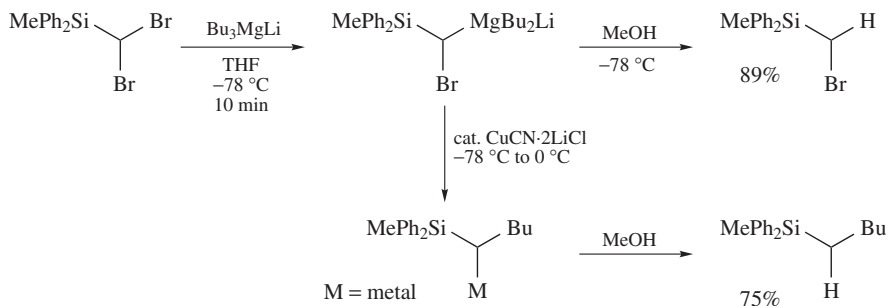
TABLE 14. Preparation of picolylmagnesium and its reactions with electrophiles

	$\xrightarrow[\text{THF, } -10^\circ\text{C, 0.5 h}]{i\text{-PrBu}_2\text{MgLi (0.50 eq.)}}$	$\xrightarrow{\text{electrophile}}$	
Electrophile	E	Yield (%)	
PhCHO	CH(OH)Ph	93	
PhCOCl	PhCO	52	
<i>t</i> -BuCOCl	<i>t</i> -BuCO	57	
DMF	CHO	85	
CH <sub>2</sub> =CHCH <sub>2</sub> Br	CH <sub>2</sub> =CHCH <sub>2</sub>	92	
<i>i</i> -Pr <sub>2</sub> NC(S)SSC(S)N(Pr- <i>i</i> ) <sub>2</sub>	SC(S)N(Pr- <i>i</i> ) <sub>2</sub>	89	

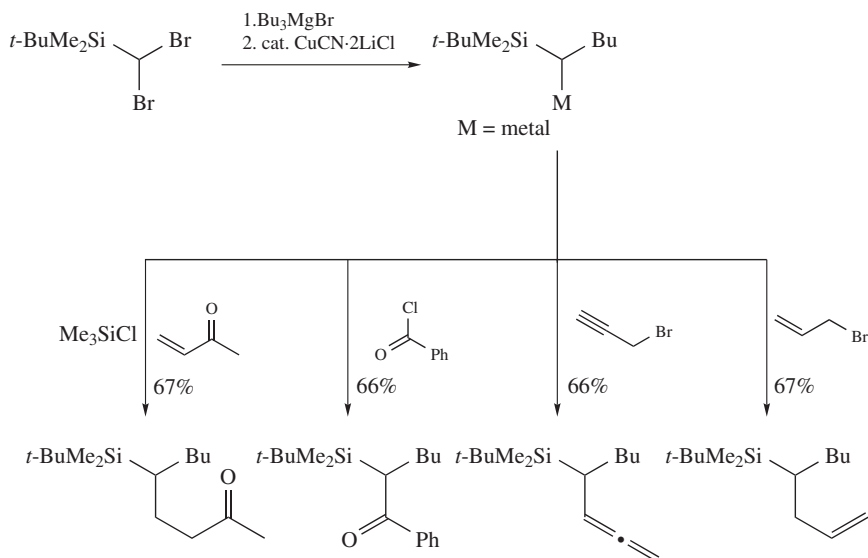


SCHEME 11





SCHEME 13



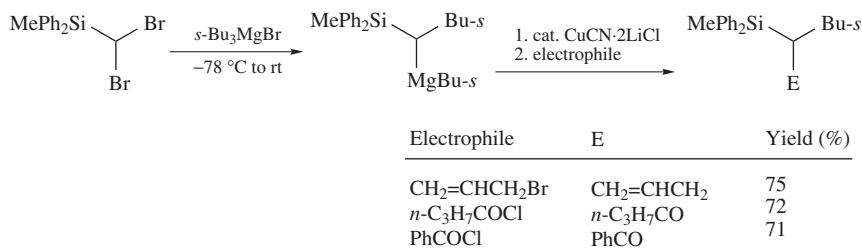
SCHEME 14

The 1-silylpentylmetal species thus formed could react with allyl bromide, propargyl bromide, acid chlorides and  $\alpha,\beta$ -unsaturated ketones (Scheme 14).

Lithium tris(*sec*-butyl)magnesate underwent bromine–magnesium exchange, which was followed by 1,2-migration in the absence of  $\text{CuCN}\cdot 2\text{LiCl}$  at room temperature (Scheme 15). However,  $\text{CuCN}\cdot 2\text{LiCl}$  was essential for the acylation and allylation.

The reactions of dibromomethylsilanes with lithium trimethylmagnesate proceeded via a reaction course different from that with lithium tributylmagnesate<sup>42,44</sup>. One of the two bromine atoms was substituted by the methyl group, and the other bromine atom remained intact (Table 15). Dibromo compounds such as dibromomethylsilane (entry 1), 1,1-dibromoethylsilane (entry 2) and dibromodisilylmethanes (entries 3–8) were transformed into the corresponding monomethylated products in high yields, regardless of the bulkiness of the silyl groups.





SCHEME 15

TABLE 15. Monomethylation with lithium trimethylmagnesate

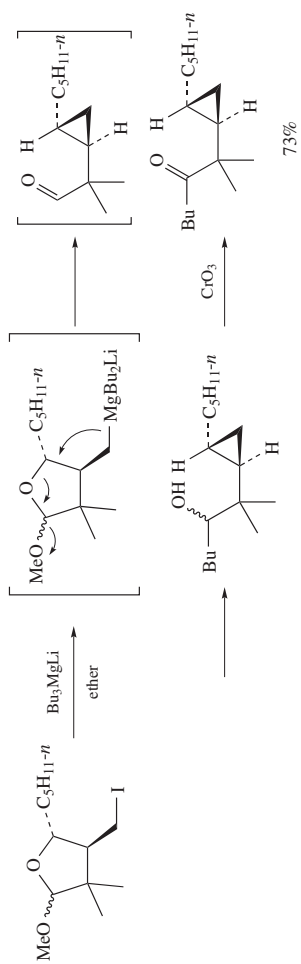
$\text{R}^1-\text{C}(\text{Br})_2-\text{R}^2 \xrightarrow[\text{THF, } -78^\circ\text{C, 0.5 h}]{\text{Me}_3\text{MgLi (1.0 eq.)}} \text{R}^1-\text{C}(\text{Me})(\text{Br})-\text{R}^2$			
Entry	R <sup>1</sup>	R <sup>2</sup>	Yield (%)
1	Ph <sub>2</sub> MeSi	H	98
2	Ph <sub>2</sub> MeSi	Me	89
3	Ph <sub>2</sub> MeSi	Me <sub>3</sub> Si	93
4	Et <sub>3</sub> Si	Et <sub>3</sub> Si	90
5	<i>t</i> -BuMe <sub>2</sub> Si	Me <sub>3</sub> Si	82
6	Me <sub>3</sub> Si	Me <sub>3</sub> Si	89
7	PhMe <sub>2</sub> Si	PhMe <sub>2</sub> Si	80
8	Ph <sub>2</sub> MeSi	Ph <sub>2</sub> MeSi	90

Lithium tributylmagnesate induced iodine–magnesium exchange reaction of 5-alkoxy-3-iodomethyl-1-oxacyclopentanes (Scheme 16)<sup>45</sup>. A following intramolecular nucleophilic substitution led to construction of a cyclopropane with concomitant opening of the oxacyclopentane ring.

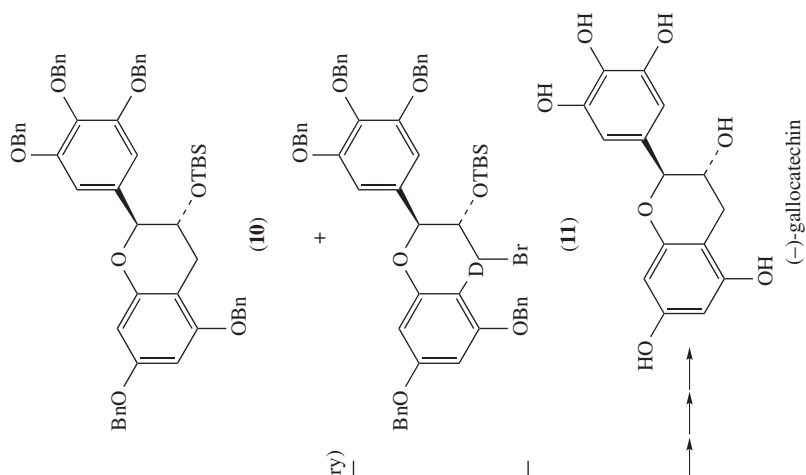
Suzuki and coworkers found an application of magnesate reagents in the stereoselective synthesis of (–)-gallo catechin (Scheme 17)<sup>46</sup>. They examined chemoselective iodine–metal exchange of **9** followed by intramolecular cyclization by using various metalation agents. The use of organolithium reagents resulted in limited success. The metalation with isopropylmagnesium chloride resulted in slow halogen–metal exchange at  $-40^\circ\text{C}$ , yet afforded no cyclic product **10**. With isopropylmagnesium chloride, uncyclized product **11** was completely deuteriated, which suggests that the corresponding arylmagnesium reagent has a long lifetime. The use of a magnesate reagent,  $\text{Ph}_3\text{MgLi}$ , improved the yield of **10**, compared to isopropylmagnesium chloride. Almost quantitative transformation of **9** to **10** was attained by a combined use of  $\text{Ph}_3\text{MgLi}$  and HMPA.

Trost and coworkers employed a magnesate reagent in the formal synthesis of fostricin (Scheme 18)<sup>47</sup>. Stereoselective addition of the corresponding alkenylmagnesium to  $\alpha$ -alkoxyketone proceeded smoothly in 75% yield with more than 20:1 diastereoselectivity.

Magnesate reagents are reactive enough to enable magnesiations on polymer beads. Schreiber and coworkers reported diversity-oriented synthesis of biaryl-containing medium rings using a one bead/one stock solution platform<sup>48</sup>. For the diversity-oriented synthesis of biaryl-containing medium rings in an atropdiastereoselective fashion, they investigated the development of the oxidation of organocuprates. The reactions were performed on

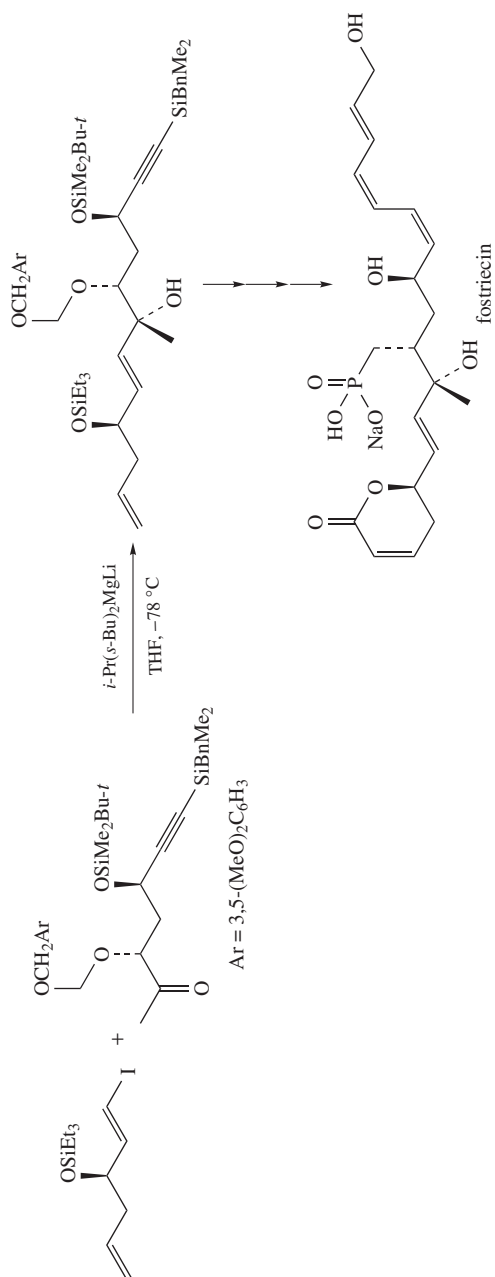


SCHEME 16



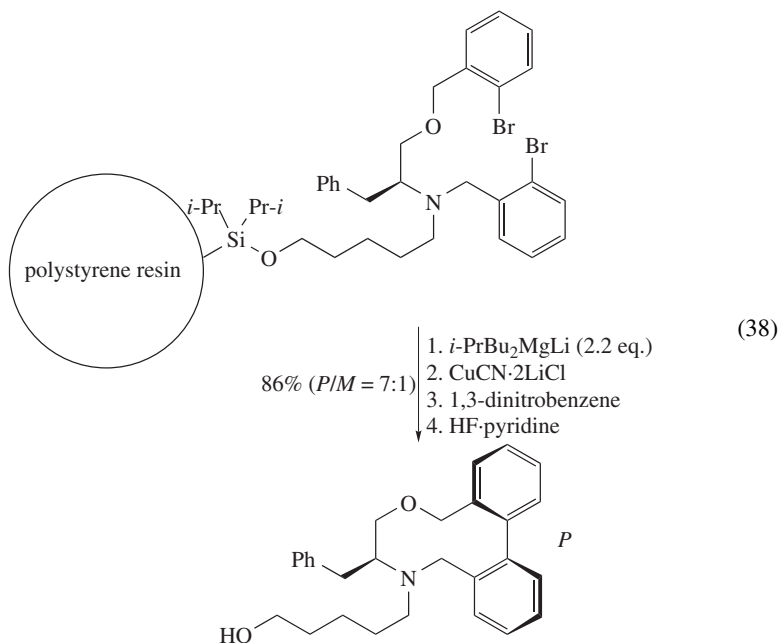
Reagent	10	11 (%D)	9 (recovery)
BuLi (1.0 eq.)	77%	5% (0)	6%
<i>t</i> -BuLi (2.0 eq.)	53%	—	—
<i>i</i> -PrMgCl (1.2 eq.)	—	28% (100)	72%
Bu <sub>3</sub> MgLi (1.2 eq.)	84%	12% (0)	—
Ph <sub>3</sub> MgLi (1.2 eq.)	76%	14% (86)	—
Ph <sub>3</sub> MgLi (2.5 eq.), HMPA (10 eq.)	96%	—	—

SCHEME 17



SCHEME 18

polystyrene beads by metalating polymer-supported aryl bromides with lithium dibutylisopropylmagnesate, followed by transmetalation with copper and then oxidation with 1,3-dinitrobenzene (equation 38).



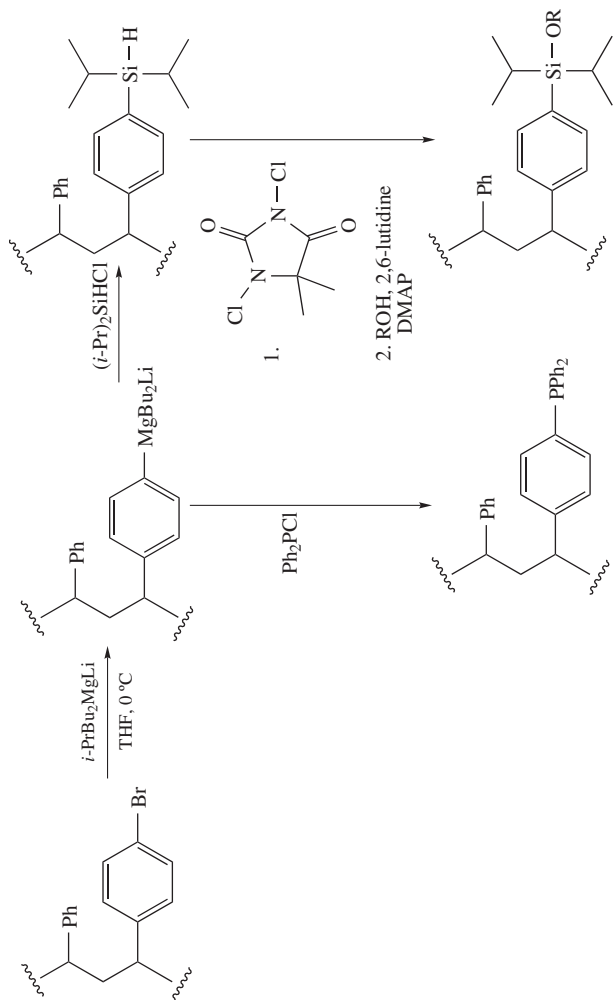
Polystyrene beads which are composed of 74% styrene, 25% 4-bromostyrene and 1% divinylbenzene were completely metalated with lithium dibutylisopropylmagnesate (Scheme 19)<sup>49</sup>. The polymagnesiated polystyrene then reacted with a variety of electrophiles to yield high quality solid-supported reagents. For instance, the use of chlorodiphenylphosphine as an electrophile generated polystyrene beads (150–600  $\mu\text{m}$ ) having diphenylphosphinophenyl groups. It is noteworthy that treatment with isopropylmagnesium chloride or butyllithium alone resulted in incomplete functionalization of the beads. An additional example is the synthesis of diisopropylsilane-functionalized polystyrene and its use for covalently attaching alcohols onto the polystyrene solid-support. The chemical stability was comparable to that of a triisopropylsilyl protecting group.

Synthesis of copolysiloxanes **14**, a candidate for dental and medical devices and sensors, required the preparation of the substituted allylbenzene **13** (Scheme 20)<sup>50</sup>. However, attempted cross-coupling reaction of **12** with allylzinc bromide resulted in failure. Alternatively, the magnesiation of **12** with lithium tributylmagnesate followed by the addition of allyl bromide provided **13** in excellent yield.

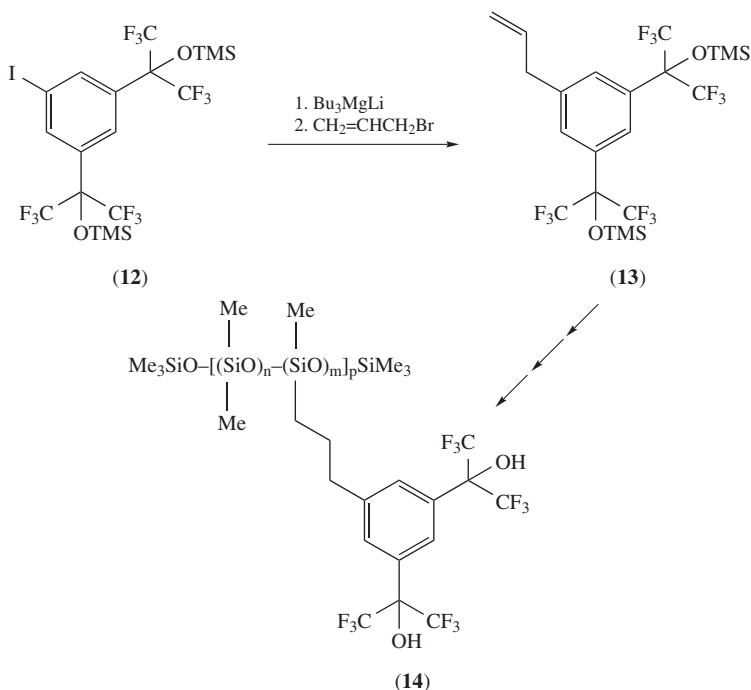
#### IV. ADDITIONAL IMPORTANT CHEMISTRY OF ORGANOMAGNESATES

##### A. Alkoxydialkylmagnesate $\text{R}_2\text{MgOR}$

Hanawalt and Richey observed that additions of alkali-metal alkoxides to dialkylmagnesium led in some reactions to behavior resembling that of trialkylmagnesates<sup>51</sup>. This includes enhanced reactivities in addition to pyridine leading to 4- or 2-alkyl-substituted

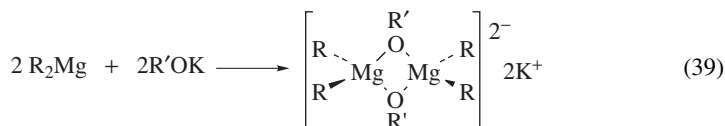


SCHEME 19



SCHEME 20

pyridines, additions to ketones in which the accompanying reduction of the ketones are suppressed<sup>52</sup> and halogen-metal exchange with aryl halides<sup>53</sup>. NMR studies revealed the formation of the dinuclear magnesate complexes from the dialkylmagnesium and the alkoxides (equation 39).



### B. Lithium Tris(2,2,6,6-tetramethylpiperidino)magnesate (TMP)<sub>3</sub>MgLi

The title reagent has no carbon-magnesium bonds. However, the 'inorganic' magnesate reagent is to be noted since it showed excellent reactivity in deprotonation reactions. The reagent is readily available by mixing lithium tributylmagnesate and three molar equivalents of 2,2,6,6-tetramethylpiperidine, and has much less nucleophilicity than triorganomagnesate<sup>24,25</sup>. Triamidomagnesates are structurally intriguing since they are recognized as 'inverse crown ethers.'<sup>54</sup>. Zinc analogs of the reagent are also useful for deprotonation reactions<sup>55</sup>.

### C. Combination of Isopropylmagnesium Chloride and Lithium Chloride *i*-PrMgCl•LiCl

Knochel and coworkers showed that *i*-PrMgCl•LiCl is a useful reagent for the simple and high-yielding preparation of a broad range of functionalized arylmagnesium reagents starting from readily available aryl bromides (Chapter X by Knochel)<sup>7,8</sup>. The exchange reactions proceed under noncryogenic conditions and are scalable. The reactivity is comparable to or a little lower than that of triorganomagnesates, and hence a wider variety of functional groups are tolerant. In order to perform unknown halogen–magnesium exchange reactions, *i*-PrMgCl•LiCl and lithium trialkylmagnesates are the first choices.

## V. SUMMARY

Triorganomagnesates are establishing their positions in modern organic synthesis. Grignard reagents RMgX have a long history and outstanding utility and their ate complexation significantly enhanced their reactivity. We believe that magnesates will find as many applications as Grignard reagents in organic synthesis.

## VI. REFERENCES

1. G. Wittig, F. J. Meyer and G. Lange, *Justus Liebigs Ann. Chem.*, **571**, 167 (1951).
2. L. M. Seitz and T. L. Brown, *J. Am. Chem. Soc.*, **88**, 4140 (1966); **89**, 1602 (1967).
3. D. Thoenes and E. Weiss, *Chem. Ber.*, **111**, 3726 (1978).
4. K. M. Waggoner and P. P. Power, *Organometallics*, **11**, 3209 (1992).
5. A. D. Pajerski, D. M. Kushlan, M. Parvez and H. G. Richey, Jr., *Organometallics*, **25**, 1206 (2006).
6. R. E. Mulvey, *Chem. Commun.*, 1049 (2001).
7. A. Krasovskiy and P. Knochel, *Angew. Chem. Int. Ed.*, **43**, 3333 (2004); A. Krasovskiy, B. F. Straub and P. Knochel, *Angew. Chem. Int. Ed.*, **45**, 159 (2006).
8. P. Knochel, A. Krasovskiy and I. Sapountzis, *Polyfunctional Magnesium Organometallics for Organic Synthesis*, in *Handbook of Functionalized Organometallics* (Ed. P. Knochel), Wiley-VCH, Weinheim, 2005.
9. D. Hauk, S. Lang and A. Murso, *Org. Proc. Res. Devel.*, **10**, 733 (2006).
10. M. Geissler, J. Kopf and E. Weiss, *Chem. Ber.*, **122**, 1395 (1989).
11. K. Kitagawa, A. Inoue, H. Shinokubo and K. Oshima, *Angew. Chem. Int. Ed.*, **39**, 2481 (2000); A. Inoue, K. Kitagawa, H. Shinokubo and K. Oshima, *J. Org. Chem.*, **66**, 4333 (2001).
12. G. E. Coates and J. A. Heslop, *J. Chem. Soc., A*, 514 (1968).
13. E. P. Squiller, R. R. Whittle and H. G. Richey, Jr., *J. Am. Chem. Soc.*, **107**, 432 (1985).
14. A. D. Pajerski, M. Parvez and H. G. Richey, Jr., *J. Am. Chem. Soc.*, **110**, 2660 (1988).
15. D. B. Malpass and J. F. Eastham, *J. Org. Chem.*, **38**, 3718 (1973).
16. E. C. Ashby, L.-C. Chao and J. Laemmle, *J. Org. Chem.*, **39**, 3258 (1974).
17. H. G. Richey, Jr. and B. A. King, *J. Am. Chem. Soc.*, **104**, 4672 (1982).
18. H. G. Richey, Jr. and J. Farkas, Jr., *Tetrahedron Lett.*, **26**, 275 (1985); H. G. Richey, Jr. and J. Farkas, Jr., *Organometallics*, **9**, 1778 (1990).
19. M. Hatano, T. Matsumura and K. Ishihara, *Org. Lett.*, **7**, 573 (2005).
20. J. G. Sosnicki, *Tetrahedron Lett.*, **46**, 4295 (2005).
21. J. G. Sosnicki, *Tetrahedron Lett.*, **47**, 6809 (2006).
22. M. Yasuda, M. Ide, Y. Matsumoto and M. Nakata, *Synlett*, 899 (1997); *Bull. Chem. Soc. Jpn.*, **71**, 1417 (1998).
23. M. Ide, M. Yasuda and M. Nakata, *Synlett*, 936 (1998); M. Ide and M. Nakata, *Bull. Chem. Soc. Jpn.*, **72**, 2491 (1999).
24. H. Awad, F. Mongin, F. Trécourt, G. Quéguiner, F. Marsais, F. Blanco, B. Abarca and R. Ballesteros, *Tetrahedron Lett.*, **45**, 6697 (2004).
25. H. Awad, F. Mongin, F. Trécourt, G. Quéguiner and F. Marsais, *Tetrahedron Lett.*, **45**, 7873 (2004).



26. O. Bayh, H. Awad, F. Mongin, C. Hoarau, F. Trécourt, G. Quéguiner, F. Marsais, F. Blanco, B. Abarca and R. Ballesteros, *Tetrahedron*, **61**, 4779 (2005).
27. O. Bayh, H. Awad, F. Mongin, C. Hoarau, L. Bischoff, F. Trécourt, G. Quéguiner, F. Marsais, F. Blanco, B. Abarca and R. Ballesteros, *J. Org. Chem.*, **70**, 5190 (2005).
28. F. Mongin, A. Bucher, J. P. Bazureau, O. Bayh, H. Awad and F. Trécourt, *Tetrahedron Lett.*, **46**, 7989 (2005).
29. A. Inoue and K. Oshima, 'Magnesium in Organic Synthesis', in *Main Group Metals in Organic Synthesis* (Eds. H. Yamamoto and K. Oshima), Volume 1, Chapter 3.4, Wiley-VCH, Weinheim, 2004; P. Knochel, A. Krasovskiy and I. Sapountzis, 'Functional Magnesium Organometallics for Organic Synthesis', in *Handbook of Functionalized Organometallics* (Ed. P. Knochel), Volume 1, Chapter 4.2.3, Wiley-VCH, Weinheim, 2005; B. J. Wakefield, *Organomagnesium Methods in Organic Synthesis*, Chapter 3.2.2, Academic Press, London, 1995.
30. L. Boymond, M. Rottländer, G. Cahiez and P. Knochel, *Angew. Chem. Int. Ed.*, **37**, 1701 (1998).
31. T. Iida, T. Wada, K. Tomimoto and T. Mase, *Tetrahedron Lett.*, **42**, 4841 (2001); T. Mase, I. N. Houpis, A. Akao, I. Dorziotis, K. Emerson, T. Hoang, T. Iida, T. Itoh, K. Kamei, S. Kato, Y. Kato, M. Kawasaki, F. Lang, J. Lee, J. Lynch, P. Maligres, A. Molina, T. Nemoto, S. Okada, R. Reamer, J. Z. Song, D. Tschaen, T. Wada, D. Zewge, R. P. Volante, P. J. Reider and K. Tomimoto, *J. Org. Chem.*, **66**, 6775 (2001).
32. K. Fukuhara, Y. Takayama and F. Sato, *J. Am. Chem. Soc.*, **125**, 6884 (2003).
33. S. Dumouchel, F. Mongin, F. Trécourt and G. Quéguiner, *Tetrahedron Lett.*, **44**, 2033 (2003).
34. S. Dumouchel, F. Mongin, F. Trécourt and G. Quéguiner, *Tetrahedron Lett.*, **44**, 3877 (2003).
35. J. Xu, N. Jain and Z. Sui, *Tetrahedron Lett.*, **45**, 6399 (2004).
36. S. Ito, T. Kubo, N. Morita, Y. Matsui, T. Watanabe, A. Ohta, K. Fujimori, T. Murafuji, Y. Sugihara and A. Tajiri, *Tetrahedron Lett.*, **45**, 2891 (2004).
37. F. D. Therkelsen, M. Rottländer, N. Thorup and E. B. Pedersen, *Org. Lett.*, **6**, 1991 (2004).
38. E. Masson, E. Marzi, F. Cottet, C. Bobbio and M. Schlosser, *Eur. J. Org. Chem.*, 4393 (2005).
39. S. Kii, A. Akao, T. Iida, T. Mase and N. Yasuda, *Tetrahedron Lett.*, **47**, 1877 (2006).
40. F. Buron, N. Plé, A. Turck and F. Marsais, *Synlett*, 1586 (2006).
41. S. J. Dolman, F. Gosselin, P. D. O'Shea and I. W. Davis, *Tetrahedron*, **62**, 5092 (2006).
42. A. Inoue, J. Kondo, H. Shinokubo and K. Oshima, *Chem. Eur. J.*, **8**, 1730 (2002).
43. J. Kondo, A. Inoue, H. Shinokubo and K. Oshima, *Angew. Chem. Int. Ed.*, **40**, 2085 (2001).
44. A. Inoue, J. Kondo, H. Shinokubo and K. Oshima, *Chem. Lett.*, **30**, 956 (2001).
45. T. Tsuji, T. Nakamura, H. Yorimitsu, H. Shinokubo and K. Oshima, *Tetrahedron*, **60**, 973 (2004).
46. T. Higuchi, K. Ohmori and K. Suzuki, *Chem. Lett.*, **35**, 1006 (2006).
47. B. M. Trost, M. U. Frederiksen, J. P. N. Papillon, P. E. Harrington, S. Shin and B. T. Shireman, *J. Am. Chem. Soc.*, **127**, 3666 (2005).
48. D. R. Spring, S. Krishnan, H. E. Blackwell and S. L. Schreiber, *J. Am. Chem. Soc.*, **124**, 1354 (2002); S. Krishnan and S. L. Schreiber, *Org. Lett.*, **6**, 4021 (2004).
49. G. L. Thomas, M. Ladlow and D. R. Spring, *Org. Biomol. Chem.*, **2**, 1679 (2004); G. L. Thomas, C. Böhner, M. Ladlow and D. R. Spring, *Tetrahedron*, **61**, 12153 (2005).
50. B. Boutevin, M. Gaboyard, F. Guida-Pietrasanta, L. Hairault, B. Lebreton and E. Pasquinet, *J. Polym. Sci., A, Polym. Chem.*, **41**, 1400 (2003).
51. E. M. Hanawalt and H. G. Richey Jr., *J. Am. Chem. Soc.*, **112**, 4983 (1990).
52. J. E. Chubb and H. G. Richey, Jr., *Organometallics*, **21**, 3661 (2002).
53. J. Farkas, Jr., S. J. Stoudt, E. M. Hanawalt, A. D. Pajerski and H. G. Richey, Jr., *Organometallics*, **23**, 423 (2004).
54. R. E. Mulvey, *Organometallics*, **25**, 1060 (2006).
55. Y. Kondo, M. Shirai, M. Uchiyama and T. Sakamoto, *J. Am. Chem. Soc.*, **121**, 3539 (1999); M. Uchiyama and Y. Kondo, *J. Synth. Org. Chem. Jpn.*, **64**, 1180 (2006).

## CHAPTER 16

# The chemistry of magnesium carbenoids

TSUYOSHI SATOH

*Department of Chemistry, Faculty of Science, Tokyo University of Science; Ichigaya-funagawara-machi 12, Shinjuku-ku, Tokyo 162-0826, Japan*  
*Fax: 81-3-5261-4631; e-mail: tsatoh@rs.kagu.tus.ac.jp*

---

I. INTRODUCTION .....	718
II. GENERATION OF MAGNESIUM CARBENOIDS .....	718
A. Generation of Magnesium Carbenoids by Halogen–Magnesium Exchange Reaction .....	718
B. Generation of Magnesium Carbenoids by Sulfoxide–Magnesium Exchange Reaction .....	720
1. Generation of racemic magnesium carbenoids .....	720
2. Generation of optically active magnesium carbenoids .....	721
III. REACTIONS AND SYNTHETIC USES OF MAGNESIUM CARBENOIDS .....	722
A. Cyclopropanation of Allylic Alcohols with Magnesium Carbenoids ...	722
B. Electrophilic Reactions of Magnesium Carbenoids .....	723
1. Reaction of magnesium carbenoids with Grignard reagents .....	723
2. Synthesis of secondary chiral Grignard reagents .....	725
3. Reaction of magnesium carbenoids with $\alpha$ -sulfonyl lithium carbanions .....	727
4. Reaction of magnesium carbenoids with <i>N</i> -lithio arylamines .....	728
5. 1,3-Carbon–hydrogen (C,H) insertion reaction of magnesium carbenoids .....	729
IV. MAGNESIUM CYCLOPROPYLIDENES .....	735
A. Magnesium Cyclopropylidenes as Intermediates in the Doering–LaFlamme Allene Synthesis .....	735
B. Nucleophilic Reactions of Magnesium Cyclopropylidenes .....	738
C. Electrophilic Reactions of Magnesium Cyclopropylidenes .....	739
V. MAGNESIUM ALKYLIDENE CARBENOIDS .....	742
A. Generation and Nucleophilic Property of Magnesium Alkylidene Carbenoids, the Fritsch–Buttenberg–Wiechell Rearrangement .....	742

---

*The chemistry of organomagnesium compounds*

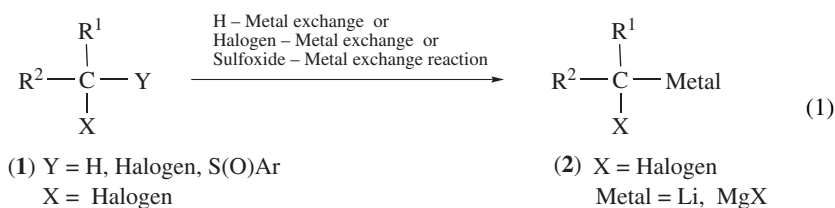
Edited by Z. Rapoport and I. Marek © 2008 John Wiley & Sons, Ltd. ISBN: 978-0-470-05719-3

B. Electrophilic Reactions of Magnesium Alkylidene Carbenoids . . . . .	746
1. One-pot synthesis of tetrasubstituted olefins . . . . .	746
2. Synthesis of allenes by alkenylation of magnesium alkylidene carbenoids with $\alpha$ -sulfonyl lithium carbanions . . . . .	748
3. Reaction of magnesium alkylidene carbenoids with <i>N</i> -lithio arylamines . . . . .	748
4. Reaction of magnesium alkylidene carbenoids with <i>N</i> -lithio nitrogen-containing heterocycles, lithium acetylides and lithium thiolates . . . . .	755
VI. MAGNESIUM $\beta$ -OXIDO CARBENOIDS . . . . .	760
VII. OTHER MAGNESIUM CARBENOIDS . . . . .	767
VIII. CONCLUSIONS AND PERSPECTIVE . . . . .	767
IX. REFERENCES . . . . .	767

## I. INTRODUCTION

Carbenes and carbenoids<sup>1</sup> have long been recognized as a highly reactive species and are frequently used as intermediates in organic synthesis<sup>2</sup>. From a synthetic perspective, however, most of the carbenes are relatively short-lived and are too reactive to be controlled. Recently, metal–carbene complexes (or metallocarbenes) were found to be easier to control and are nowadays widely used in organic synthesis<sup>2b</sup>.

Carbenoids (**2**) have been generated from alkyl halides (**1**; Y = H or halogen) by hydrogen–metal or halogen–metal exchange reactions (equation 1). Especially, lithium carbenoids (**2**; Metal = Li) were generated from alkyl halides with butyllithium; however, they are so reactive that the H–Li or halogen–Li exchange reaction must be usually conducted below  $-90^{\circ}\text{C}$ . On the other hand, from recent cumulative investigations, magnesium carbenoids (**2**; Metal = MgX) could be generated from alkyl iodides (**1**; Y = I) or sulfoxides (**1**; Y = S(O)Ar) by iodine–magnesium or sulfoxide–magnesium exchange reaction and were found to be much more stable as compared to lithium carbenoids. As a result, magnesium carbenoids can be generated around  $-78^{\circ}\text{C}$ , are relatively easy to handle and present interesting reactivities. In this chapter, generation, properties and synthetic uses of magnesium carbenoids will be discussed.

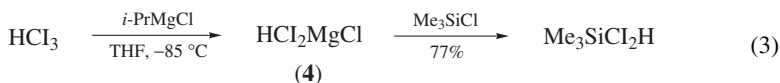


## II. GENERATION OF MAGNESIUM CARBENOIDS

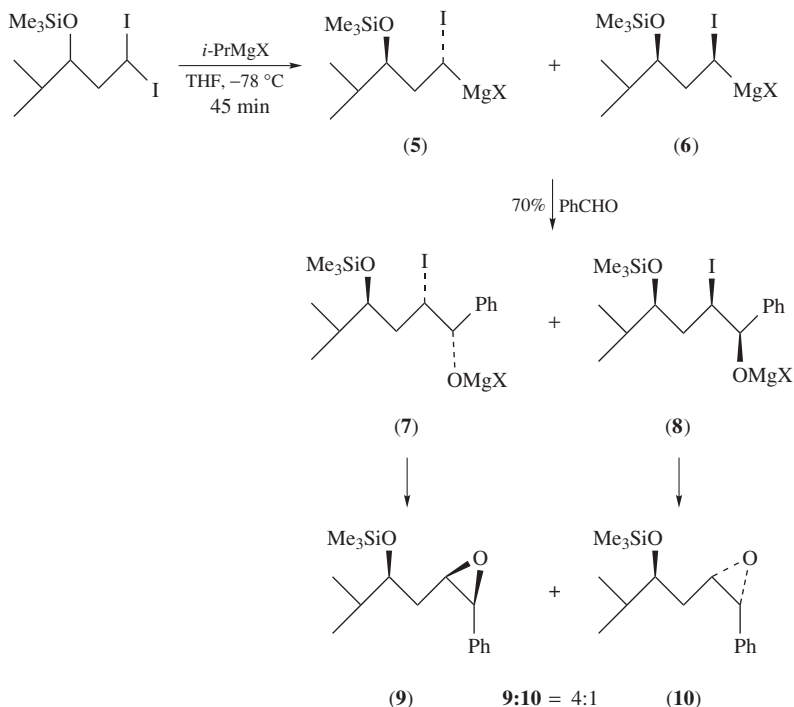
### A. Generation of Magnesium Carbenoids by Halogen–Magnesium Exchange Reaction

The halogen–metal exchange is a well-known reaction for the generation of alkyl-, alkenyl- and arylmetals from the corresponding halides and alkyl metals. Especially the bromine- or iodine–lithium exchange reaction is widely used for the preparation of lithium carbanions. Lithium carbenoids have also been generated from polyhaloalkyl compounds by halogen–lithium exchange reaction.

On the other hand, a rather limited number of examples were reported for the generation of magnesium carbenoids via the halogen–magnesium exchange reaction before 2000. Seyferth and coworkers reported the synthesis of bromochloromethylmagnesium chloride (**3**) from chlorodibromomethane in THF by bromine–magnesium exchange with isopropylmagnesium chloride at  $-95^{\circ}\text{C}$  (equation 2)<sup>3</sup>. Diiodomethylmagnesium chloride (**4**) was also derived from triiodomethane with isopropylmagnesium chloride at  $-85^{\circ}\text{C}$  by iodine–magnesium exchange reaction (equation 3). The magnesium carbenoids (**3** and **4**) were found to be sufficiently stable at low temperature and could react with electrophiles. For example, treatment of **3** and **4** with chlorotrimethylsilane resulted in the formation of trimethylsilylbromochloromethane and trimethylsilyldiiodomethane in 63 and 77% yield, respectively.



Magnesium carbenoids (**5** and **6**) were generated from a geminal diiodoalkane by diastereoselective iodine–magnesium exchange reaction with isopropylmagnesium halide in THF at  $-78^{\circ}\text{C}$  for 45 min (Scheme 1)<sup>4</sup>. Subsequent reaction of the magnesium



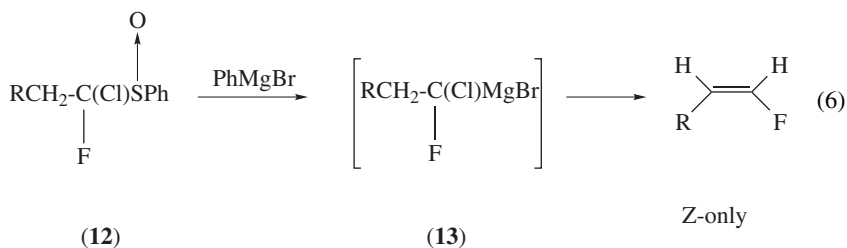
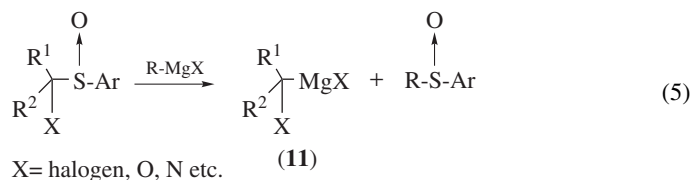
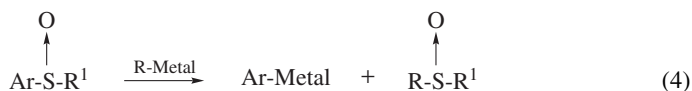
SCHEME 1

carbenoids with benzaldehyde gave *cis*-disubstituted epoxides (**9** and **10**) via the adducts **7** and **8** in 70% yield as a 4:1 mixture of diastereomers. It was concluded that the configuration of the carbenoid was stable at temperatures up to  $-20^{\circ}\text{C}$ . Further studies on the diastereoselective addition reactions of magnesium carbenoids with benzaldehyde were reported<sup>5</sup>. Mechanistic study of the iodine–magnesium exchange<sup>6</sup> and  $^{13}\text{C}$  NMR study of the resulting magnesium carbenoid<sup>7</sup> were reported by Hoffmann and coworkers.

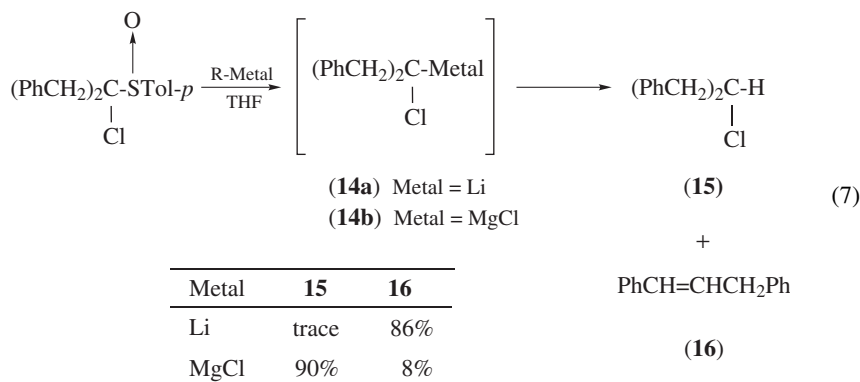
## B. Generation of Magnesium Carbenoids by Sulfoxide–Magnesium Exchange Reaction

### 1. Generation of racemic magnesium carbenoids

Treatment of alkyl aryl sulfoxides with an alkylmetal results in sulfur–aryl (or sulfur–alkyl) bond-cleavage to give a new arylmetal (or alkylmetal) and a new sulfoxide. This reaction is called sulfoxide–metal exchange reaction or ligand exchange reaction of sulfoxides (equation 4)<sup>8</sup>. When the sulfoxide has an alkyl group with a halogen or heteroatom at its  $\alpha$ -position, the sulfoxide–metal exchange reaction exclusively takes place between the sulfur–alkyl bond to give carbenoid **11** (equation 5). For example, treatment of  $\alpha$ -chlorofluoro sulfoxide (**12**) with phenylmagnesium bromide leads initially to the unstable magnesium carbenoid **13** and then to the alkenylfluoride (equation 6)<sup>9</sup>.

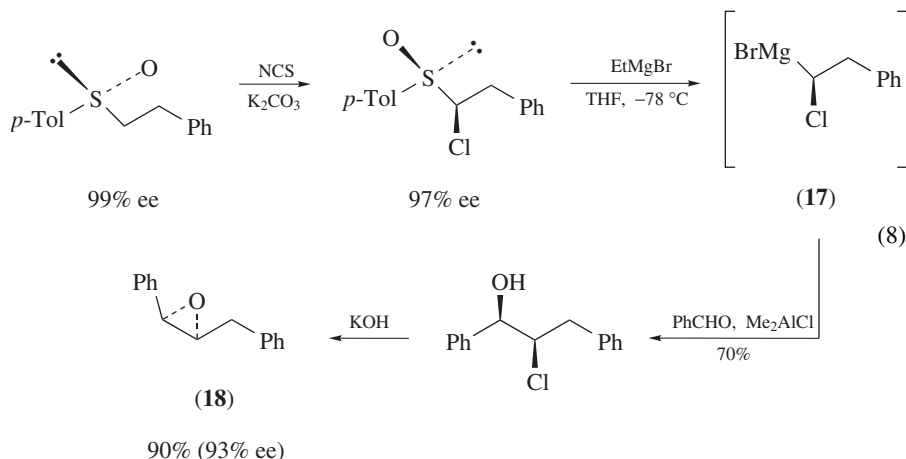


The sulfoxide–metal exchange reaction using *t*-BuLi and EtMgCl was also investigated (equation 7)<sup>10</sup>. Treatment of  $\alpha$ -chloroalkyl *p*-tolyl sulfoxide with *t*-BuLi in THF at  $-100^{\circ}\text{C}$  for 5 min afforded olefin (**16**) in 86% yield with traces of chloride **15**. This result shows that the intermediate lithium carbenoid **14a** is highly reactive and decomposes rapidly. On the other hand, treatment of the same  $\alpha$ -chloroalkyl sulfoxide with EtMgCl at  $-78^{\circ}\text{C}$  for 5 min gave the chloride **15** in 90% yield with 8% of **16**. Even when the reaction was maintained at  $-78^{\circ}\text{C}$  for 2 h the chloride **15** was still obtained in 85% yield with 15% of the olefin **16** after hydrolysis. This suggests that magnesium carbenoid **14b** is stable at  $-78^{\circ}\text{C}$ .

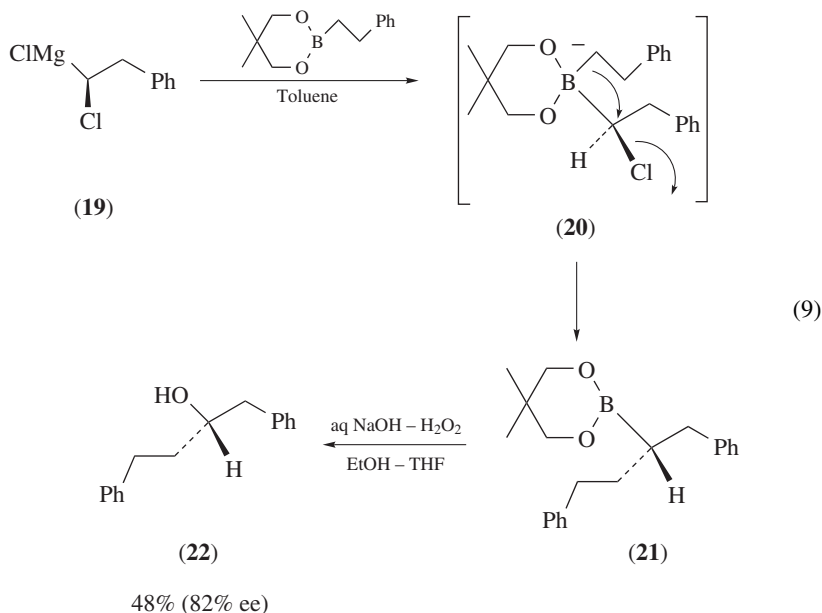


## 2. Generation of optically active magnesium carbenoids

Optically active  $\alpha$ -chloroalkyl aryl sulfoxides can be prepared from optically active alkyl aryl sulfoxides by chlorination with NCS in the presence of K<sub>2</sub>CO<sub>3</sub><sup>11</sup>. Hoffmann and Nell reported the preparation of optically active magnesium carbenoid **17**, with over 90% ee from the optically active  $\alpha$ -chloroalkyl *p*-tolyl sulfoxide via a sulfoxide–magnesium exchange reaction (equation 8)<sup>12</sup>. Indeed, 1-chloro-2-phenylethyl *p*-tolyl sulfoxide of 97% ee was treated with EtMgBr at  $-78^\circ\text{C}$  and the resulting magnesium carbenoid **17** was treated with benzaldehyde activated by dimethylaluminum chloride to give an (*R,R*)-chlorohydrin. The latter was treated with KOH to afford *cis*-epoxide **18** in 90% yield with 93% ee (equation 8). Three important conclusions were obtained from the above-mentioned investigations. First, the sulfoxide–magnesium exchange reaction can be applied to generate optically enriched Grignard reagent **17**. Second, the sulfoxide–magnesium exchange reaction occurs with retention of configuration at the carbon bearing the chlorine atom. Third, only very slow racemization of magnesium carbenoid **17** took place under the reaction conditions.



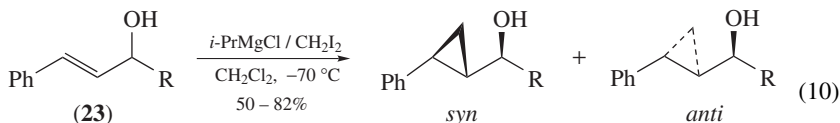
An asymmetric homologation of boronic esters was realized by using chiral magnesium carbenoid **19** (equation 9)<sup>13</sup>. When optically active magnesium carbenoid (**19**), derived from the reaction of  $\alpha$ -chloroalkyl *p*-tolyl sulfoxide with EtMgCl (see equation 8), reacts with boronic ester, the optically active ate-complex **20** was obtained. 1,2-Nucleophilic rearrangement then took place from the complex with inversion of configuration at the migratory terminus to give the boronate intermediate **21**. Then, the optically active secondary alcohol **22** was obtained in 82% ee after oxidation of the boronate **21**.



### III. REACTIONS AND SYNTHETIC USES OF MAGNESIUM CARBENOIDS

#### A. Cyclopropanation of Allylic Alcohols with Magnesium Carbenoids

The Simmons–Smith-type cyclopropanation of olefins<sup>14</sup> is one of the most well-known reactions of carbenes and carbenoids. However, cyclopropanation of simple olefins with magnesium carbenoids is usually very difficult and only cyclopropanation of allylic alcohols was reported<sup>15</sup>. Thus, treatment of allylic alcohols (**23**) in CH<sub>2</sub>Cl<sub>2</sub> at  $-70^\circ\text{C}$  with *i*-PrMgCl and diiodomethane for 48 to 60 h afforded cyclopropanes in up to 82% yield as a mixture of *syn*- and *anti*-isomers. In this reaction, *syn*-isomers were mainly or exclusively obtained (*syn:anti* = 5:1–400:1) (equation 10).



R = Me, Et, *i*-Pr, *t*-Bu

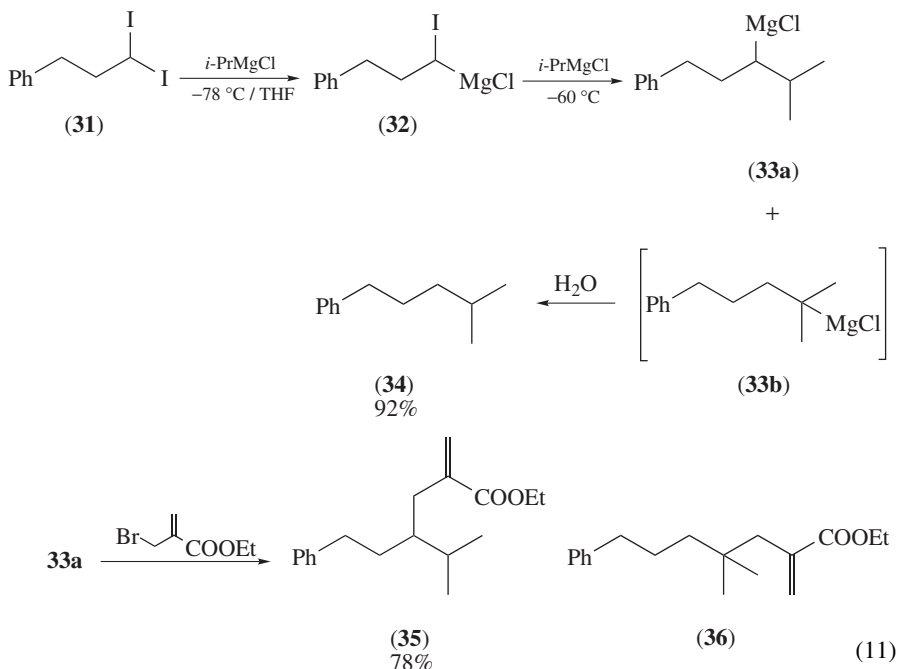
*syn:anti* = 5:1 – over 400:1



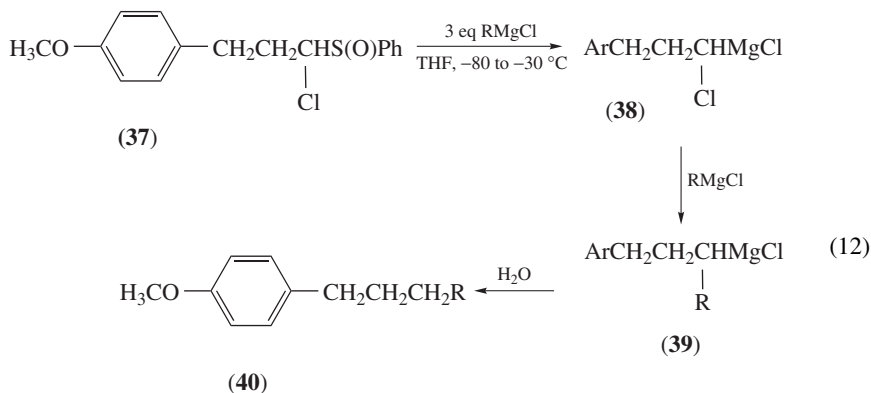


Thus, reaction of a Grignard reagent (**24**) with chloriodomethane in THF at 0 °C resulted in the formation of iodide **25** and a mixture of multi-carbon homologated alkyl iodides (**26**). The mechanism of this interesting reaction was thought to be as follows: First, iodine–magnesium exchange reaction between the Grignard reagent **24** and chloriodomethane occurred to give iodide **25** and magnesium carbenoid **27**. As magnesium carbenoid **27** has an electrophilic nature, the reaction of the Grignard reagent **24** with **27** afforded a one-carbon homologated Grignard reagent **28** and bromochloromagnesium. Reaction of the Grignard reagent **28** with chloriodomethane gave one-carbon homologated alkyl iodide **29** and magnesium carbenoid **27**. On the other hand, reaction of **28** with magnesium carbenoid **27** resulted in the formation of a two-carbon homologated Grignard reagent **30**.

Formation of homologated reagents by the reaction of a Grignard reagent with magnesium carbenoid was reported (equation 11)<sup>17</sup>. Treatment of a diiodide **31** with *i*-PrMgCl at –78 °C in THF for 1 h afforded  $\alpha$ -iodoalkylmagnesium compound **32**. By warming the reaction mixture to –60 °C, magnesium carbenoid **32** reacted with *i*-PrMgCl to afford the Grignard reagent **33a**. Hydrolysis gave the corresponding hydrocarbon **34** in 92% yield. Reaction of the Grignard reagent **33a** with ethyl ( $\alpha$ -bromomethyl)acrylate gave **35** in 79% yield with some amounts of **36**, which indicated that the intermediate **33a** was contaminated with the ‘rearranged’ Grignard reagent **33b**. Interestingly, when this reaction was carried out in diisopropyl ether, instead of THF, the ‘rearranged’ Grignard reagent **33b** was formed as the main product. As Grignard reagents **33a** and **33b** did not interconvert, the Grignard reagents were anticipated to be formed from **32** by reaction with *i*-PrMgCl in two independent pathways. A plausible mechanism of this very interesting reaction was proposed<sup>17</sup>.



The reaction of a Grignard reagent with magnesium carbenoids, derived from 1-chloroalkyl aryl sulfoxides by sulfoxide–magnesium exchange reaction, was also reported (equation 12)<sup>18</sup>. Thus, treatment of 1-chloroalkyl phenyl sulfoxide (**37**) with 3 eq of EtMgCl at  $-80^{\circ}\text{C}$  followed by slowly warming the reaction to  $-30^{\circ}\text{C}$  gave first **39** and then the ethylated product (**40**,  $\text{R} = \text{CH}_2\text{CH}_3$ ) in 80% yield. The sulfoxide–magnesium exchange reaction was found to be completed within 10 min at  $-80^{\circ}\text{C}$  and the resulting magnesium carbenoid **38** was stable below  $-60^{\circ}\text{C}$  for a long period of time. By warming the reaction mixture, the magnesium carbenoid **38** reacts with the Grignard reagents in excess to afford first **39** and then the alkylated products **40** in good yields, as indicated in equation 12. Primary and secondary Grignard reagents react well with carbenoid **38**; however, *tert*-BuMgCl did not react with 1-chloroalkyl phenyl sulfoxide (**37**).



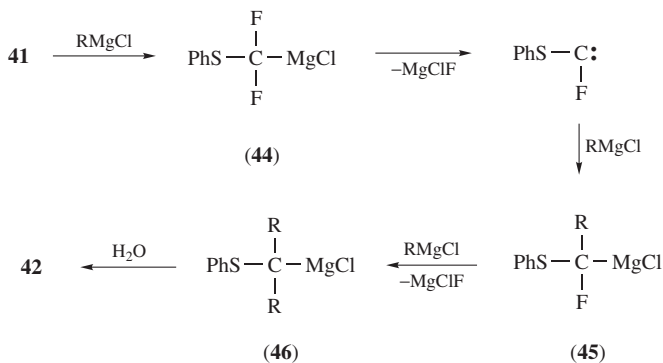
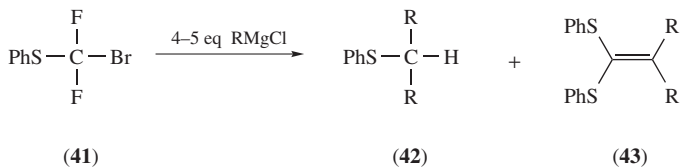
$\text{R} = \text{CH}_2\text{CH}_3$  (80%),  $\text{CH}_2(\text{CH}_2)_4\text{CH}_3$  (87%),  $\text{CH}(\text{CH}_3)_2$  (87%), cyclopentyl (94%), cyclohexyl (75%), *tert*-Bu (0%)

Reaction of phenylthiobromodifluoromethane (**41**) with a Grignard reagent gave the alkyl phenyl sulfide **42** as the main product along with ketenedithioacetal (**43**) (Scheme 3)<sup>19</sup>. The proposed mechanism is as follows: The bromine–magnesium exchange reaction of **41** affords magnesium carbenoid **44**. Then,  $\alpha$ -elimination of the dihalomagnesium results in the formation of a carbene-like intermediate, which reacts with RMgCl to give the second magnesium carbenoid **45**. The same reaction takes place to afford the  $\alpha$ -sulfur-stabilized Grignard reagent **46**. Acidic work-up of the reaction furnished sulfide **42**. Furthermore, trapping the intermediate **46** with electrophiles, such as iodoalkanes, aldehydes and benzoyl cyanide, were also successfully performed.

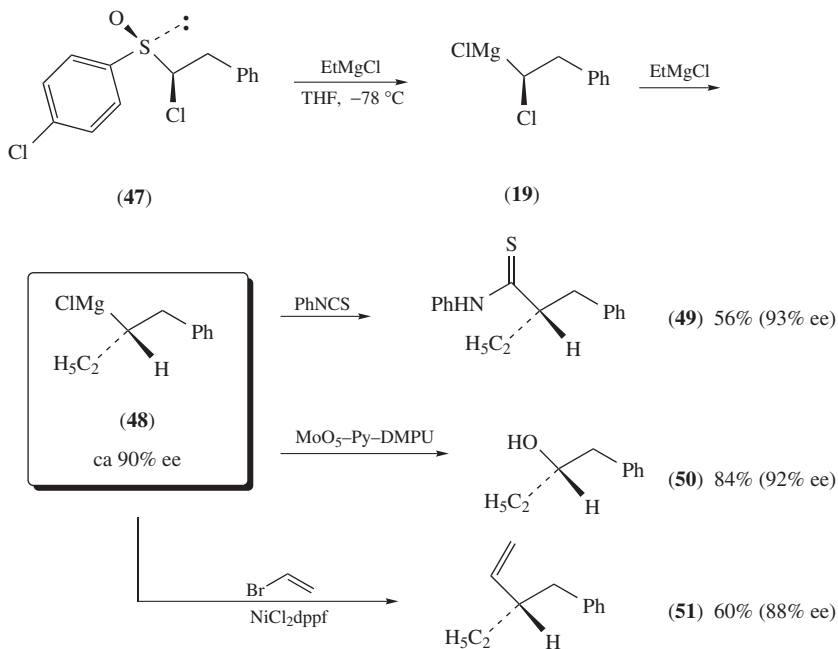
## 2. Synthesis of secondary chiral Grignard reagents

As mentioned above, the configuration of the magnesium carbenoid is rather stable at low temperature; chiral Grignard reagents having over 90% ee could be generated from optically active 1-chloroalkyl aryl sulfoxides (Scheme 4)<sup>20–22</sup>.

Treatment of optically pure 1-chloroalkyl aryl sulfoxide **47** with excess EtMgCl gave initially the optically active magnesium carbenoid **19** via a sulfoxide–magnesium exchange reaction. The electrophilic reaction of carbenoid **19** with EtMgCl gave the optically active secondary Grignard reagent **48** with inversion of configuration at the chiral carbon



SCHEME 3

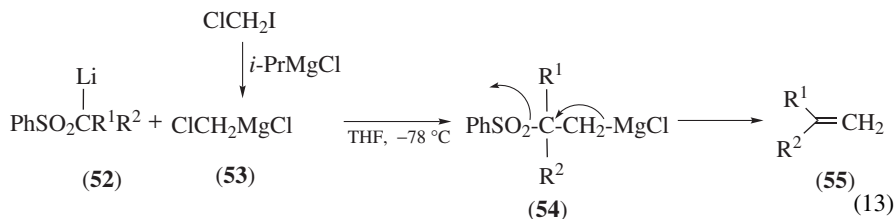


SCHEME 4

center. Quenching this reaction with phenylisothiocyanate gave thioamide **49** in 56% yield with 93% ee. Quite interestingly, from this experiment it appeared that the secondary Grignard reagent **48** is configurationally stable at  $-78^{\circ}\text{C}$ . Oxidation of **48** with molybdenum peroxide gave alcohol **50** with retention of configuration and the enantiomeric purity of **48** was retained. Kumada–Corriu coupling of **48** with vinyl bromide in the presence of Ni-catalyst gave the coupling product **51** with full retention of the configuration<sup>21</sup>.

### 3. Reaction of magnesium carbenoids with $\alpha$ -sulfonyl lithium carbanions

Magnesium carbenoids react not only with Grignard reagents but also with other carbanions such as  $\alpha$ -sulfonyl lithium carbanions to afford olefins (equation 13)<sup>23</sup>. Thus, chloromethylmagnesium chloride (**53**), generated in THF at  $-78^{\circ}\text{C}$  from chloriodomethane and *i*-PrMgCl, reacts with  $\alpha$ -sulfonyl lithium carbanion (**52**) to give the olefin **55**. The mechanism of this reaction was thought to be as described in equation 13. The electrophilic reaction of carbenoid **53** with the carbanion **52** gave a new Grignard reagent having a sulfonyl group at the  $\beta$ -position (**54**).  $\beta$ -Elimination then took place to afford olefin **55**. Moderate to good yields of the olefins **55**, which are summarized in Table 1, were obtained by this reaction.

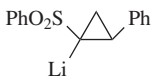
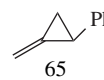


Similarly, the reaction of 1-chloropentylmagnesium chloride (**56**), derived from 1-chloro-1-iodopentane, with  $\alpha$ -sulfonyl lithium carbanions (**52**) affords 1,2-di- or 1,1,2-trisubstituted olefins (**57**) in moderate to good yields (equation 14). This reaction represents an elegant preparation of olefins from sulfones.

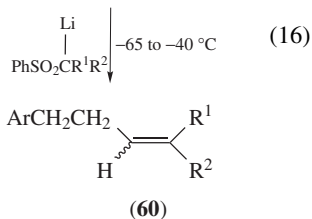
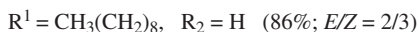
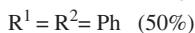
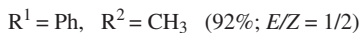
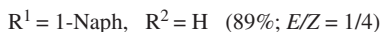
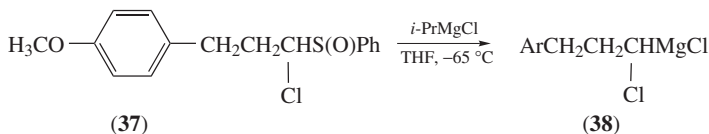
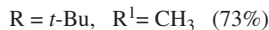
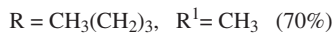
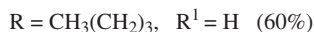
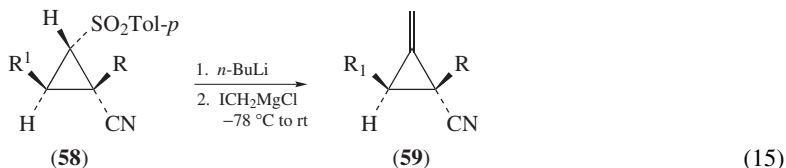
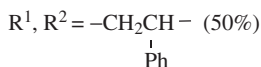
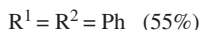
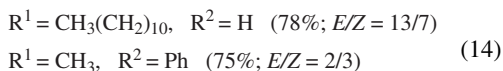
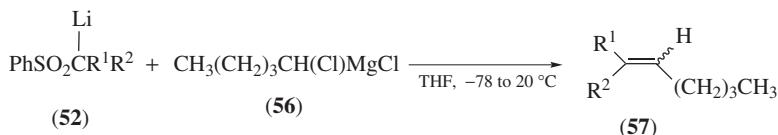
Optically pure methylenecyclopropanes **59** were synthesized from cyclopropyl sulfones **58** and the carbenoid, iodomethylmagnesium chloride, in moderate to good yields (equation 15)<sup>24</sup>.

The olefin formation described above can be conducted with magnesium carbenoids derived from 1-chloroalkyl phenyl sulfoxides<sup>18</sup>. An example is shown in equation 16.

TABLE 1. Reaction of  $\alpha$ -sulfonyl lithium carbanions (**52**) with chloromethylmagnesium chloride (**53**)

$\alpha$ -Sulfonyl lithium carbanion ( <b>52</b> )		Olefin ( <b>55</b> )
R <sup>1</sup>	R <sup>2</sup>	Yield (%)
CH <sub>2</sub> (CH <sub>2</sub> ) <sub>9</sub> CH <sub>3</sub>	H	82
CH <sub>2</sub> (CH <sub>2</sub> ) <sub>8</sub> COOH	H	60
CH <sub>2</sub> (CH <sub>2</sub> ) <sub>4</sub> CH <sub>3</sub>	CH <sub>3</sub>	68
CH <sub>3</sub>	Ph	76
-(CH <sub>2</sub> ) <sub>6</sub> -		76
		65

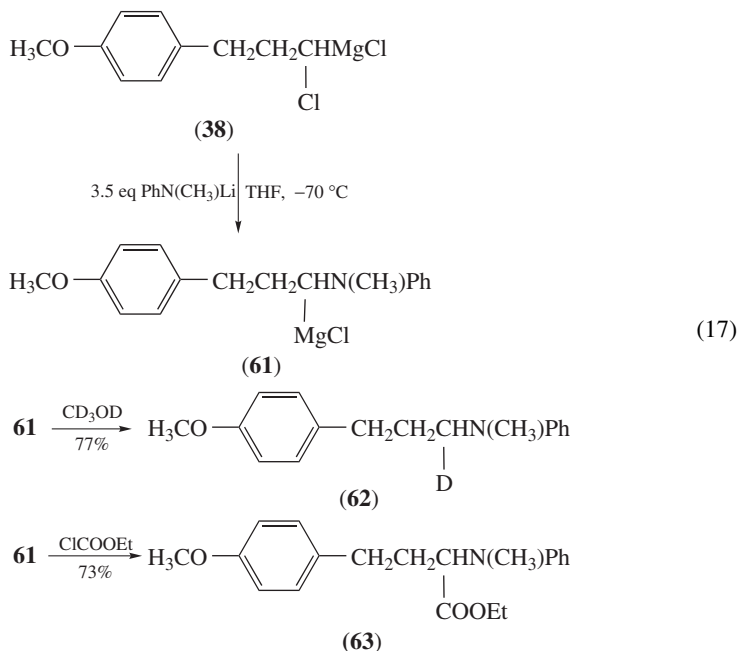
Thus, magnesium carbenoid **38**, generated from 1-chloroalkyl phenyl sulfoxide (**37**) in THF at  $-65^{\circ}\text{C}$  with 2.8 eq of *i*-PrMgCl, reacts with  $\alpha$ -sulfonyl lithium carbanion to lead to 1,2-di- and 1,1,2-trisubstituted olefins (**60**). Yields are better in such conditions as compared to the reaction described in equation 14.



#### 4. Reaction of magnesium carbenoids with *N*-lithio arylamines

The electrophilic reaction of magnesium carbenoids with *N*-lithio arylamines was found to give non-stabilized  $\alpha$ -amino-substituted carbanions (equation 17)<sup>25</sup>. Treatment of magnesium carbenoid **38** with 3.5 eq of *N*-lithio *N*-methylaniline at  $-70^{\circ}\text{C}$  followed

by slowly warming the reaction mixture to  $-40^{\circ}\text{C}$  gave the non-stabilized  $\alpha$ -amino-substituted carbanion ( $\alpha$ -amino-substituted Grignard reagent) **61** in good yield. The presence of the non-stabilized  $\alpha$ -amino-substituted carbanion **61** was confirmed by quenching the reaction with deuterated methanol to give *N*-methylaniline having an  $\alpha$ -deuteriated alkyl group (**62**) in 77% yield with 91% deuterium incorporation. The preparation of  $\alpha$ -amino-substituted carbanions is well recognized to be rather difficult from non-activated amines<sup>26</sup>. Therefore, the results obtained in this study are rewarding and can be considered as an excellent alternative for the preparation of non-stabilized  $\alpha$ -amino carbanions.



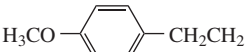
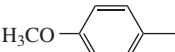
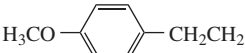
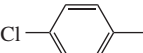
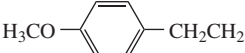
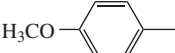
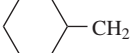
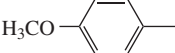
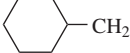
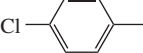
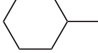
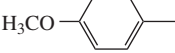
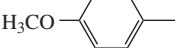
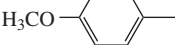
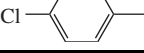
Reactions of  $\alpha$ -amino-substituted carbanion **61** with several electrophiles were investigated and, for instance, ethyl chloroformate was found to give the  $\alpha$ -amino acid derivative **63** in 73% yield. This reaction represents a very interesting and unprecedented one-pot synthesis of  $\alpha$ -amino acid derivative from 1-chloroalkyl aryl sulfoxide (see Table 2).

The reaction of the magnesium carbenoid having a 2-arylethyl group (Table 2, entries 1–3) with *N*-lithio *N*-methyl-*p*-anisidine, *N*-methyl-*p*-chloroaniline and *N*-benzyl-*p*-anisidine gave equally good yields (67–74%) of the  $\alpha$ -amino esters. The reaction of the magnesium carbenoid having a cyclohexylmethyl group (Table 2, entries 4 and 5) gave a similar yield (68%); however, the reaction of the magnesium carbenoid having a cyclohexyl group showed markedly diminished yield (48%, Table 2, entry 6). Glycine derivatives could be synthesized starting from chloromethyl *p*-tolyl sulfoxide via a magnesium carbenoid, chloromethylmagnesium chloride, in 30–61% yields (Table 2, entries 7–9).

### 5. 1,3-Carbon–hydrogen (C,H) insertion reaction of magnesium carbenoids

The carbon–hydrogen insertion (C,H insertion) is one of the most striking reactions of carbenes and carbenoids. The reaction is interesting and very useful for the construction

TABLE 2. Synthesis of  $\alpha$ -amino esters from magnesium carbenoids by the reaction with *N*-lithio *N*-substituted arylamines followed by ethyl chloroformate
$$\text{R}-\underset{\text{Cl}}{\text{CHS}}(\text{O})\text{Ph} \xrightarrow{i\text{-PrMgCl}} \left[ \underset{\text{Cl}}{\text{R}-\text{CHMg}} \right] \xrightarrow[2. \text{ClCOOEt}]{1. \text{ArN}(\text{R}^1)\text{Li}} \underset{\text{COOEt}}{\text{R}-\text{CHN}(\text{R}^1)\text{Ar}}$$

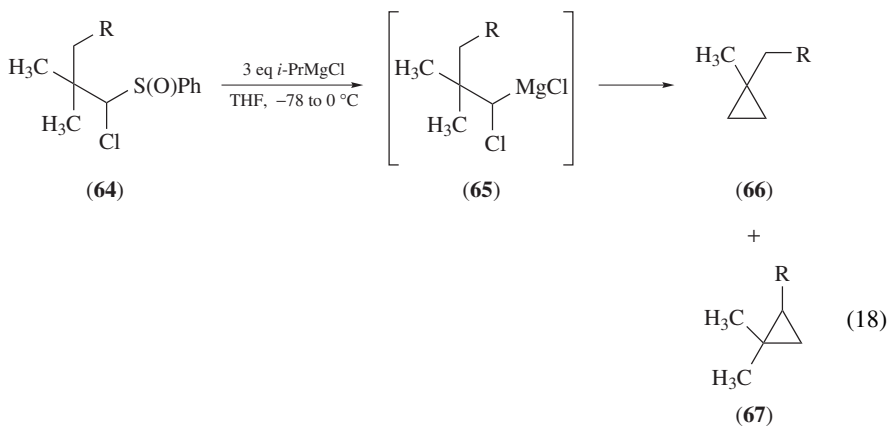
R	Ar	R <sup>1</sup>	Yield (%)
		CH <sub>3</sub>	74
		CH <sub>3</sub>	73
		PhCH <sub>2</sub>	67
		CH <sub>3</sub>	68
		CH <sub>3</sub>	68
		CH <sub>3</sub>	48
H		CH <sub>3</sub>	61
H		PhCH <sub>2</sub>	58
H		CH <sub>3</sub>	30

of complex molecules, due to the formation of a new carbon–carbon bond between a carbene (or carbenoid) and an unactivated carbon center. The author studied the C,H insertion of magnesium carbenoids starting from 1-chloroalkyl phenyl sulfoxides (**64**) and a representative example is described in equation 18<sup>27</sup>.

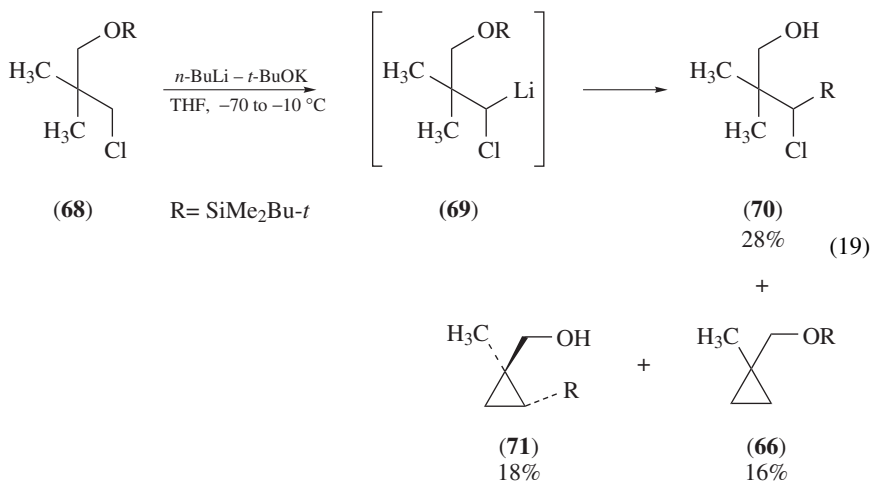
When 1-chloroalkyl phenyl sulfoxide (**64**) was treated with 3 eq of *i*-PrMgCl in THF at  $-78^\circ\text{C}$  and the reaction mixture was slowly allowed to warm to  $0^\circ\text{C}$ , the resulting cyclopropanes **66** and **67** were formed in good to high yields. Magnesium carbenoid **65**, first intermediate in this reaction, undergoes a 1,3-C,H insertion reaction with either the methyl or methylene carbon center. Interestingly, when the substituent R has an oxygen functional group, the C,H insertion exclusively takes place with one of the two methyl groups to afford cyclopropane (**66**) after the 1,3-elimination reaction. As recognized from the results in equation 18, the C,H insertion of magnesium carbenoids gives high yields of cyclopropanes under mild conditions.

Clayden and Julia reported the 1,3-C,H insertion reaction of lithium carbenoid (**69**) derived from a primary alkyl chloride (**68**) by H–Li exchange reaction (equation 19)<sup>28</sup>. Treatment of **68** with a mixture of *n*-BuLi and *tert*-BuOK gave three products. These

were silicon-migrated chloride **70** and cyclopropanes **66** and **71**. Obviously, the 1,3-C,H insertion through magnesium carbenoids **65** proceeds more selectively and in better yields.



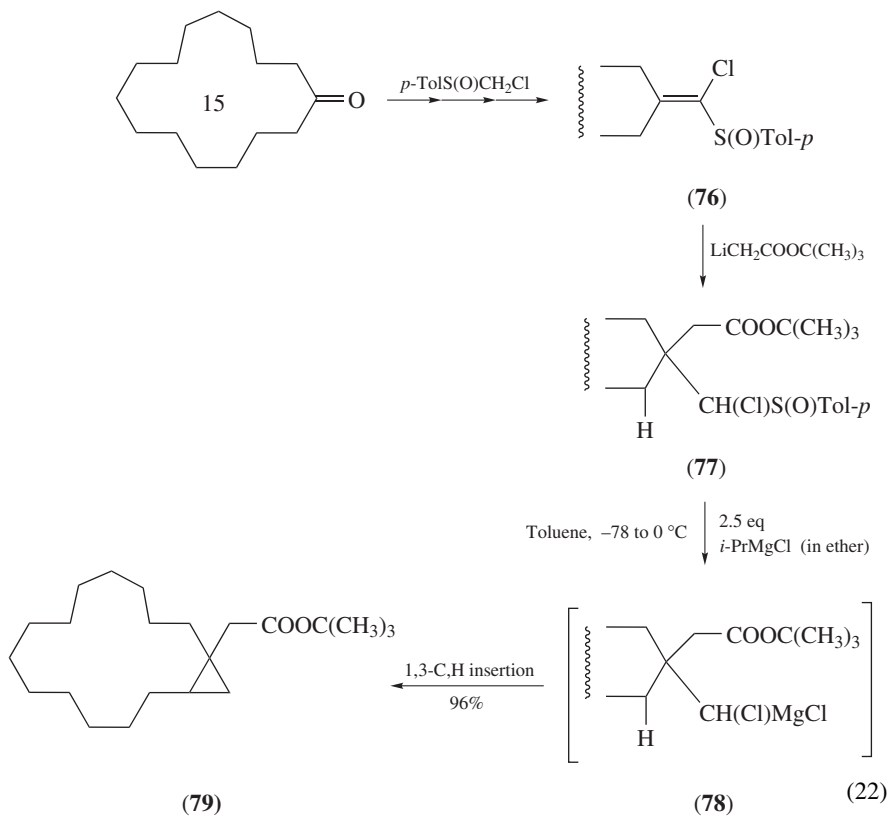
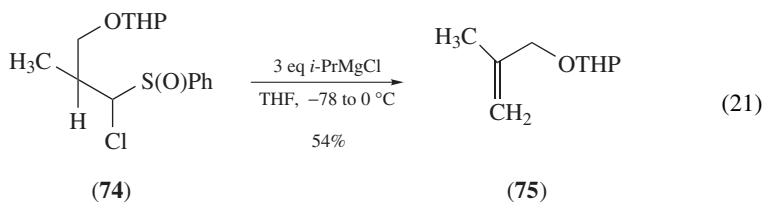
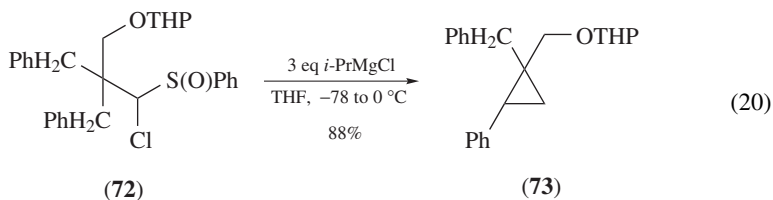
R	<b>66</b> Yield (%)	<b>67</b> Yield (%)
1-Naph	65	32
OTHP	97	0
OSiMe <sub>2</sub> Bu- <i>t</i>	85	0
OCH <sub>2</sub> OCH <sub>2</sub> CH <sub>2</sub> OCH <sub>3</sub>	89	0



The 1,3-C,H insertion of magnesium carbenoid occurs not only between the carbenoid carbon center and methyl groups but also with the methylene group. For instance, when **72** was treated with *i*-PrMgCl, the cyclopropane (**73**) was obtained in 88% yield as a



5:1 mixture of two diastereomers (equation 20). Interestingly, when 1-chloroalkyl phenyl sulfoxide (**74**) was subjected to the sulfoxide–magnesium exchange, the alkene **75** was isolated in 54% yield suggesting that the 1,2-C,H insertion competes favorably with the 1,3-C,H insertion reaction (equation 21).

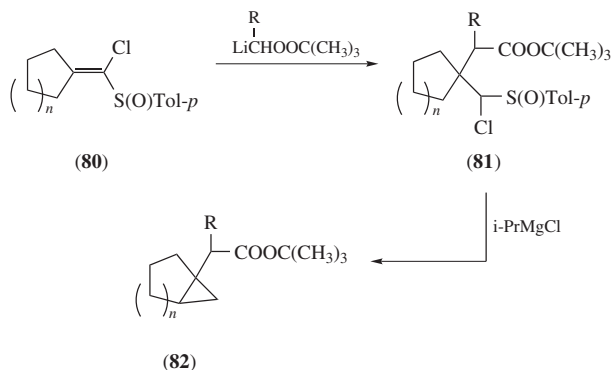


A very interesting synthetic method of bicyclo[*n*.1.0]alkanes from cyclic ketones via this 1,3-C,H insertion of magnesium carbenoid as a key reaction was reported (equation 22)<sup>29</sup>. 1-Chlorovinyl *p*-tolyl sulfoxide (**76**) was synthesized from cyclopentadecanone and chloromethyl *p*-tolyl sulfoxide in three steps in high overall yield. Lithium enolate of *tert*-butyl acetate was added to **76** to give the adduct **77** in quantitative yield.  $\alpha$ -Chlorosulfoxide (**77**) in a toluene solution was treated with *i*-PrMgCl in ether at  $-78^\circ\text{C}$  and the reaction mixture was slowly warmed to  $0^\circ\text{C}$  to afford the bicyclo[13.1.0]hexadecane derivative **79** in 96% yield through the reaction of the intermediate magnesium carbenoid **78**.

It is worth noting that use of *i*-PrMgCl in ether (not in THF) and toluene as solvent for the reaction is essential for the reaction to proceed. Otherwise, the protonated product of magnesium carbenoid **78**, obtained as by-product, was very difficult to separate from the desired compound (**79**). Interestingly, the 1,3-C,H insertion reaction is highly regioselective.

The synthesis of bicyclo[*n*.1.0]alkanes (**82**) from various 1-chlorovinyl *p*-tolyl sulfoxides (**80**) and lithium enolate of *tert*-butyl acetate, propionate and hexanoate through the adducts (**81**) are summarized in Table 3. As shown in Table 3, addition reaction of *tert*-butyl carboxylates to 1-chlorovinyl *p*-tolyl sulfoxides (**80**) proceeds smoothly to afford the adducts (**81**) in high to quantitative yields. Cyclopropanation of **81** with *i*-PrMgCl

TABLE 3. Synthesis of bicyclo [*n*.1.0]alkanes (**82**) from 1-chlorovinyl *p*-tolyl sulfoxides (**80**) with lithium enolate of *tert*-butyl acetate, propionate and hexanoate through the adduct (**81**)

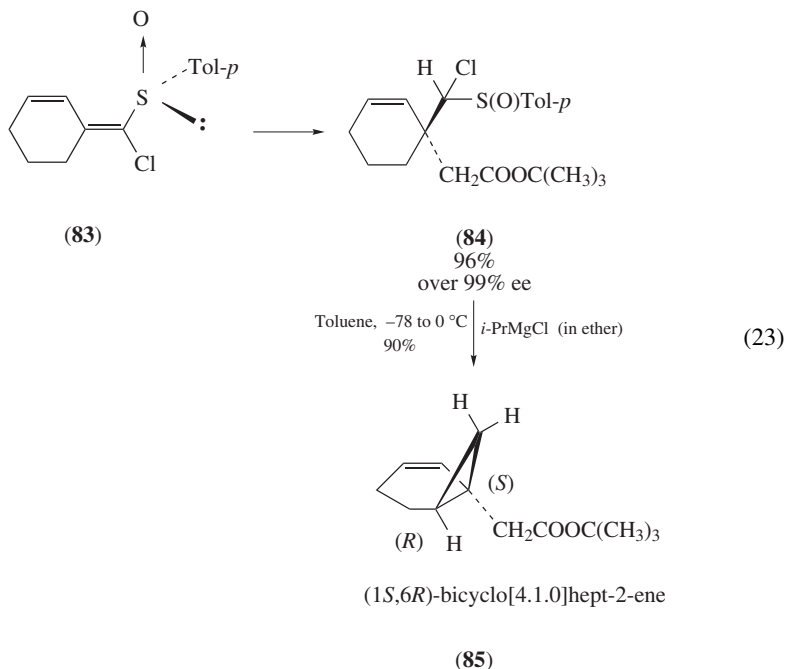


<i>n</i>	R	<b>81</b>	<b>82</b>
		Yield (%)	Yield (%)
1	H	98	74
2	H	97	68
4	H	97	90
2	CH <sub>3</sub>	99	76 <sup>a</sup>
4	CH <sub>3</sub>	88	96 <sup>a</sup>
11	CH <sub>3</sub>	93	95 <sup>a</sup>
2	CH <sub>2</sub> CH <sub>2</sub> CH <sub>2</sub> CH <sub>3</sub>	99	95 <sup>a</sup>
4	CH <sub>2</sub> CH <sub>2</sub> CH <sub>2</sub> CH <sub>3</sub>	78	89 <sup>a</sup>
11	CH <sub>2</sub> CH <sub>2</sub> CH <sub>2</sub> CH <sub>3</sub>	89	99 <sup>a</sup>

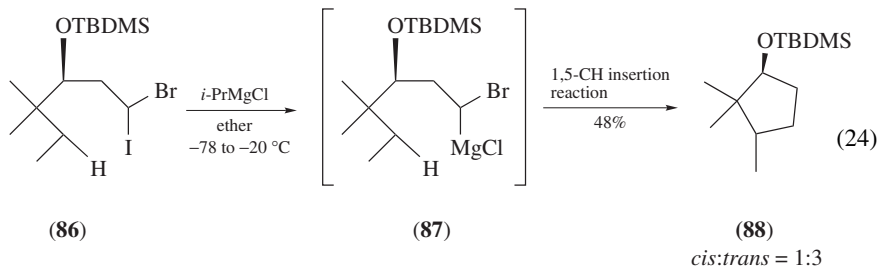
<sup>a</sup> A single isomer was obtained.

afforded bicyclo[*n*.1.0]alkanes having a *tert*-butyl carboxylate moiety (**82**) in 68–99% yields with very high regioselectivity.

Starting from optically active 1-chlorovinyl *p*-tolyl sulfoxide derived from 2-cyclohexenone, the asymmetric synthesis of cyclopropane derivative (**85**) was realized (equation 23)<sup>29</sup>. Addition reaction of lithium enolate of *tert*-butyl acetate to **83** gave the adduct (**84**) in 96% yield with over 99% ee. Treatment of the latter with *i*-PrMgCl in a similar way as described above afforded optically pure (1*S*,6*R*)-bicyclo[4.1.0]hept-2-ene (**85**) in 90% yield.



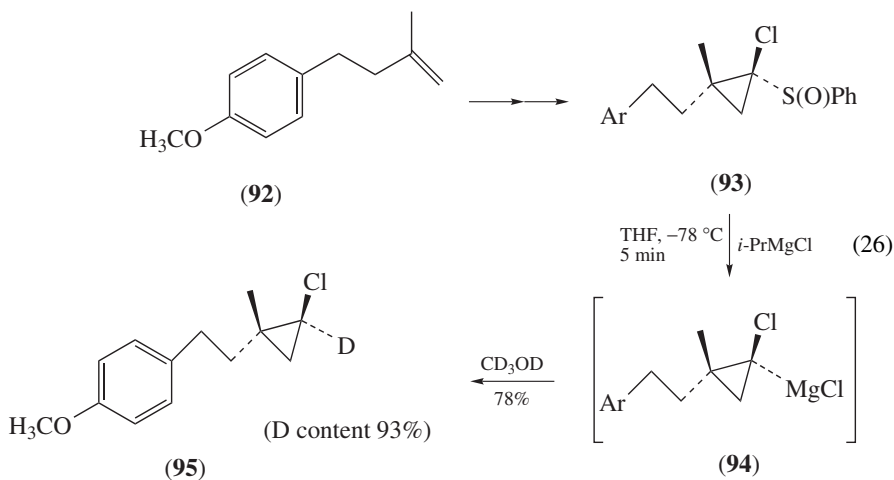
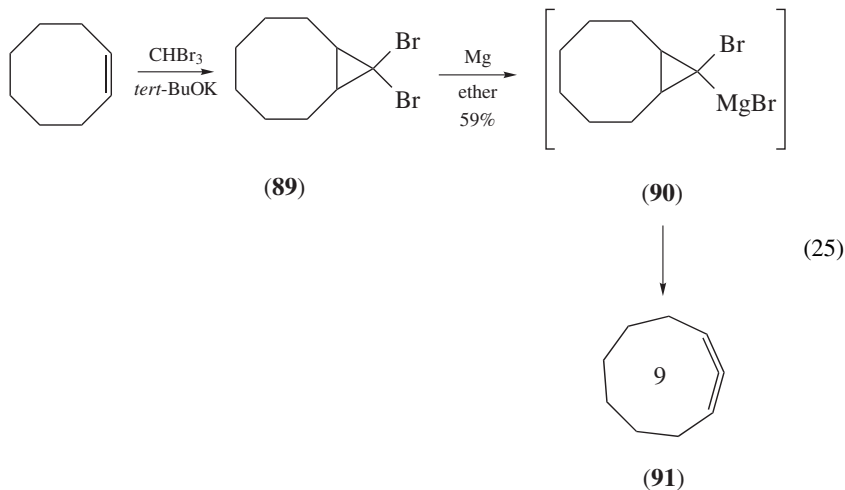
An intramolecular 1,5-C,H insertion reaction was reported from substituted bromoiodoalkane and halogen–magnesium exchange reaction (equation 24)<sup>30</sup>. Indeed, treatment of bromoiodoalkane (**86**) with *i*-PrMgCl in ether at -78 °C to -20 °C resulted in the formation of magnesium carbenoid **87**. The 1,5-C,H insertion of **87** took place to afford a cyclopentane derivative (**88**); however, the yield was not satisfactory.

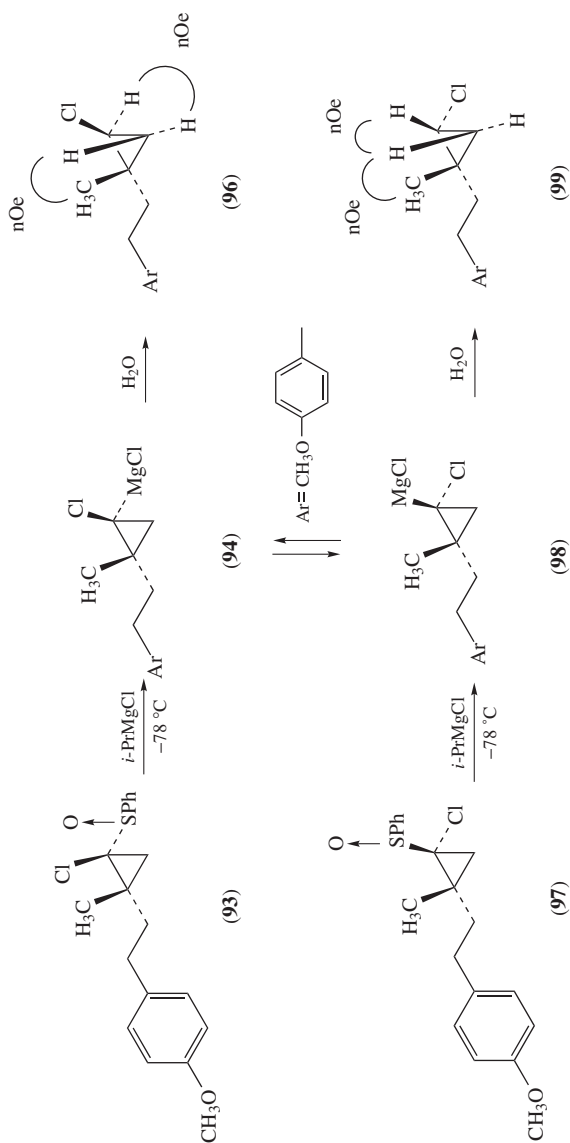


## IV. MAGNESIUM CYCLOPROPYLIDENES

## A. Magnesium Cyclopropylidenes as Intermediates in the Doering–LaFlamme Allene Synthesis

Cyclopropylidenes (carbenacyclopropanes) are carbenes generated from cyclopropanes and are known to be highly reactive intermediates leading to allenes. They are usually prepared from the reaction of 1,1-dihalocyclopropanes with alkylmetal derivatives. This reaction is now called the Doering–LaFlamme allene synthesis<sup>14</sup>. For example, when 9,9-dibromobicyclo[6.1.0]nonane (**89**), derived from cyclooctene, was treated with magnesium in ether under reflux, 1,2-cyclononadiene (**91**) was obtained in 59% yield. Magnesium cyclopropylidene (**90**) is thought to be the intermediate of this reaction (equation 25)<sup>31</sup>.





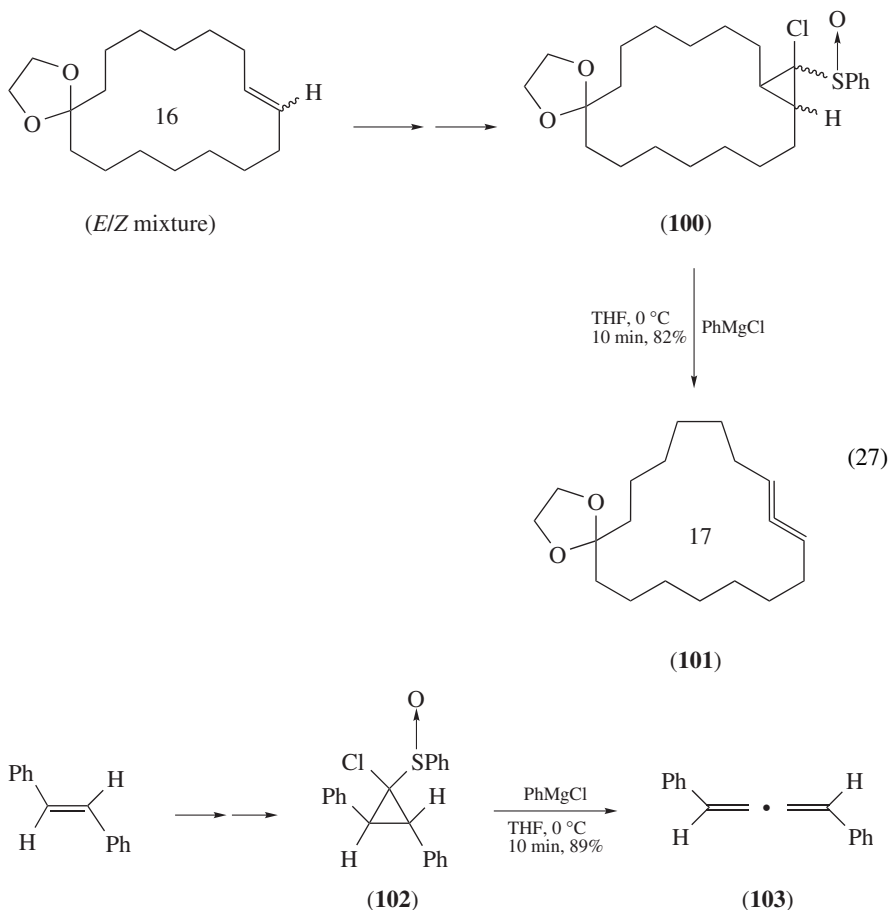
Conditions		-78 to -60 °C, 1 h		-78 to -60 °C, 1 h; then -60 °C, 3 h	
From					
<b>93</b>	<b>96</b> only	<b>96</b> + trace of <b>99</b>		<b>96</b> : <b>99</b> = 5 : 2 <sup>a</sup>	
<b>97</b>	<b>99</b> only	<b>99</b> + trace of <b>96</b>		<b>96</b> : <b>99</b> = 1 : 5 <sup>a</sup>	

<sup>a</sup> The ratio was determined by  $^1\text{H}$  NMR.

SCHEME 5

Since cyclopropylidenes were generated from 1,1-dihalocyclopropanes with either alkyllithiums or Grignard reagent but as well with lithium, or magnesium metal, at room or even higher temperature, the generated carbenoids quickly afforded allenes (or decomposed). As the stability and chemical nature of magnesium cyclopropylidenes was not investigated, Satoh and coworkers studied, in 2001, the preparation of such magnesium cyclopropylidenes from 1-chlorocyclopropyl phenyl sulfoxides at  $-78^{\circ}\text{C}$  by sulfoxide–magnesium exchange reaction<sup>32</sup>.

At first, 1-chlorocyclopropyl phenyl sulfoxide (**93**) was synthesized from the olefin **92** in three steps in good yield. Treatment of sulfoxide **93** with 2.5 eq of *i*-PrMgCl in THF at  $-78^{\circ}\text{C}$  for 5 min followed by quenching with  $\text{CD}_3\text{OD}$  afforded the deuteriated chlorocyclopropane (**95**) in 78% yield with high deuterium incorporation. From this experiment, it was proved that the intermediate of the reaction is a magnesium cyclopropylidene species **94** (equation 26).



Then, the magnesium cyclopropylidene (**94**) generated at  $-78^{\circ}\text{C}$  was slowly warmed to  $-60^{\circ}\text{C}$  and stirred at this temperature for 3 h. Deuterolysis of the reaction mixture with  $\text{CD}_3\text{OD}$  afforded the chlorocyclopropane in 81% yield with 95% D-content. From

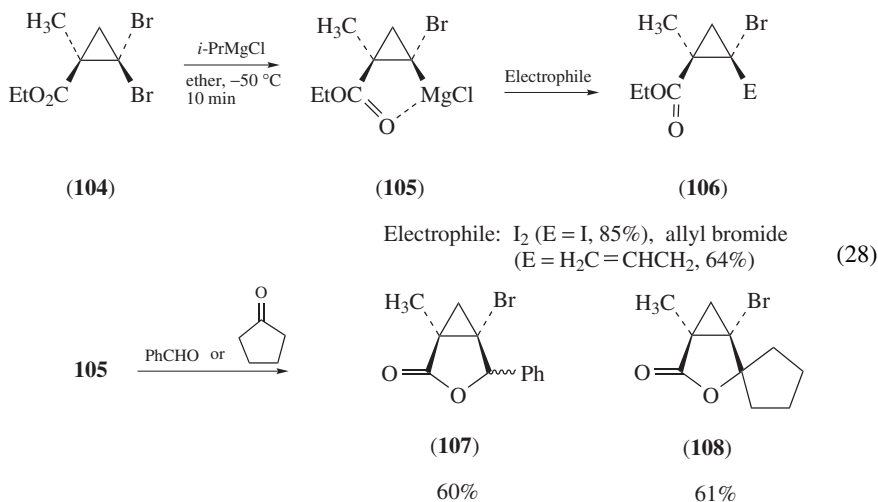
this result, it was concluded that magnesium cyclopropylidene (**94**) is stable at  $-60^{\circ}\text{C}$  for at least 3 h.

Interestingly, inversion of stereochemistry of the magnesium cyclopropylidenes was observed in this study (Scheme 5). Both diastereomers of  $\alpha$ -chlorocyclopropyl phenyl sulfoxides (**93** and **97**) were treated with *i*-PrMgCl and the generated magnesium cyclopropylidenes (**94** and **98**) were allowed to stand at several different temperatures. As shown in Scheme 5, after quenching the carbenoid with water after 5 min at  $-78^{\circ}\text{C}$ , **96** and **99** were obtained without any contamination of their diastereomers. On the other hand, when the reaction mixture was kept at  $-60^{\circ}\text{C}$  for 1 to 3 h, a mixture of both chlorocyclopropanes (**96** and **99**) was obtained. From these results, it was concluded that magnesium cyclopropylidenes **94** and **98** are configurationally stable below  $-60^{\circ}\text{C}$  and pyramidal inversion of the magnesium cyclopropylidenes slowly takes place at temperature around  $-60^{\circ}\text{C}$ .

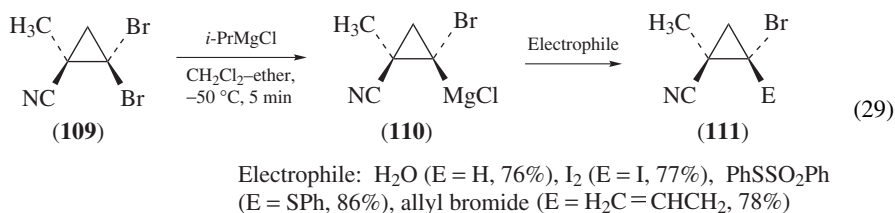
To extend this chemistry as a new method for the synthesis of allenes, temperatures of the reaction and the nature of the Grignard reagent were investigated. PhMgCl at  $0^{\circ}\text{C}$  was found to give the optimal condition for the preparation of allenes in good isolated yields (equation 27). Large-membered ring olefin, cyclohexadecene and *trans*-stilbene were converted to  $\alpha$ -chlorocyclopropyl phenyl sulfoxides **100** and **102**. When treated with 2.5 eq of PhMgCl at  $0^{\circ}\text{C}$  for 10 min, the one-carbon ring-expansion occurs to lead to the allene **101** and diphenylallene **103** in good yields. This reaction provided a general method for the synthesis of allenes from olefins with one-carbon elongation.

## B. Nucleophilic Reactions of Magnesium Cyclopropylidenes

As mentioned above, carbenoids have both a nucleophilic and an electrophilic nature. Generation of a magnesium cyclopropylidene and its nucleophilic behavior were reported (equation 28)<sup>33</sup>. Treatment of ethyl dibromocyclopropanecarboxylate (**104**) with *i*-PrMgCl in ether at  $-50^{\circ}\text{C}$  for 10 min lead, via stereoselective bromine–magnesium exchange, to the formation of magnesium cyclopropylidene (**105**). The generated carbenoid **105** was found to be stable at  $-50^{\circ}\text{C}$  due to the interaction between the ester group and the magnesium. Reaction of carbenoid **105** with iodine and allyl bromide gave the products **106**, both as single isomers, in good yields. The reaction of **105** with benzaldehyde and cyclopentanone gave  $\gamma$ -lactones **107** and **108** in 60% yield.

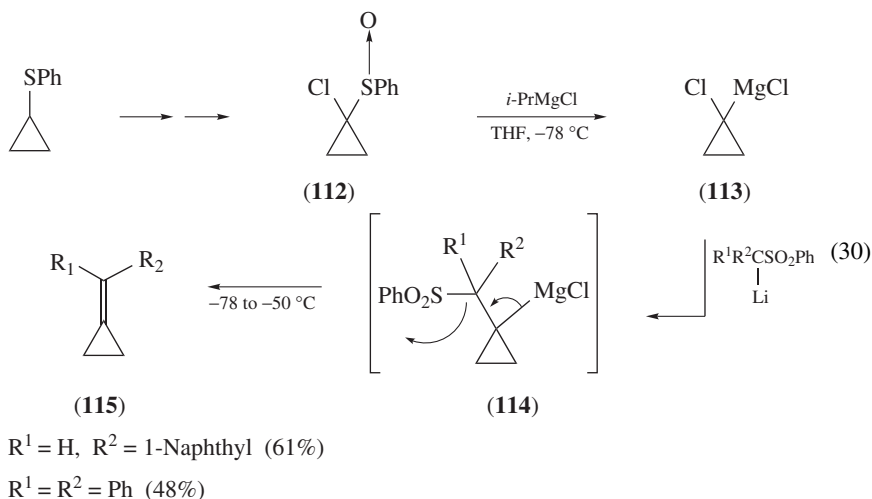


A similar chemistry was carried out from 2,2-dibromocyclopropanecarbonitrile (**109**) (equation 29)<sup>34</sup>. Thus, treatment of dibromide (**109**) with *i*-PrMgCl in a mixture of dichloromethane and ether (4:1) at  $-50^{\circ}\text{C}$  for 5 min resulted in the formation of magnesium cyclopropylidene (**110**) via a stereoselective bromine–magnesium exchange reaction. The nucleophilic reaction of carbenoid **110** with several electrophiles afforded the products **111** in about 80% yield. From the products **111**, highly substituted cyclopropanes could be synthesized using bromine– and sulfoxide–magnesium exchange reactions.



### C. Electrophilic Reactions of Magnesium Cyclopropylidenes

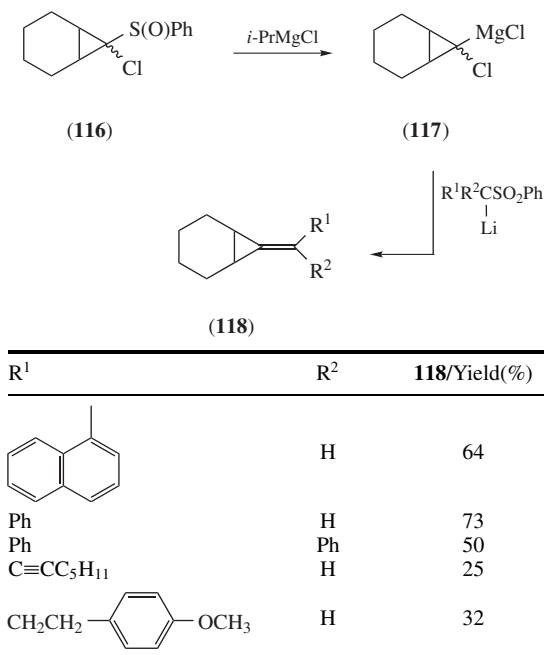
An interesting reaction using the electrophilic nature of magnesium carbenoids with  $\alpha$ -sulfonyl lithium carbanion giving alkylidenecyclopropanes was reported by Satoh and Saito (equation 30)<sup>35</sup>. 1-Chlorocyclopropyl phenyl sulfoxide (**112**), synthesized from commercially available cyclopropyl phenyl sulfide in 93% overall yield, was treated with 2.5 eq of *i*-PrMgCl at  $-78^{\circ}\text{C}$ . The sulfoxide–magnesium exchange reaction was found to take place instantaneously to give magnesium cyclopropylidene (**113**). To this carbenoid, three equivalents of an  $\alpha$ -sulfonyl lithium carbanion was added and the reaction mixture was allowed to warm to  $-50^{\circ}\text{C}$  to give alkylidenecyclopropane (**115**) in moderate yield.



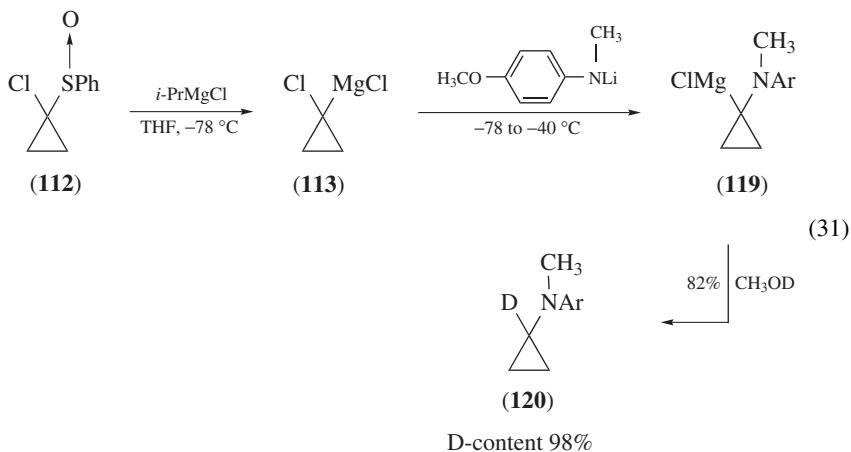
The proposed mechanism of this reaction is composed by an initial  $\text{S}_{\text{N}}2$ -type nucleophilic substitution reaction of **113** with the nucleophilic  $\alpha$ -sulfonyl lithium carbanion to give the alkylmagnesium species (**114**) having a sulfonyl group at the  $\beta$ -position. Then, a  $\beta$ -elimination reaction of magnesium sulfinate from the intermediate (**114**) occurs



TABLE 4. Synthesis of alkyldenecyclopropanes (**118**) from 1-chlorocyclopropyl phenyl sulfoxide (**116**) and  $\alpha$ -sulfonyl lithium carbanions through magnesium cyclopropylidene (**117**)



to give the expected alkyldenecyclopropane (**115**). Examples for the synthesis of alkyldenecyclopropanes (**118**) from 1-chlorocyclopropyl phenyl sulfoxide (**116**) via magnesium cyclopropylidene (**117**) are summarized in Table 4.

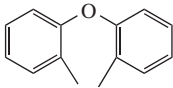
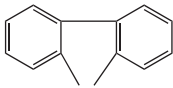
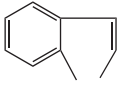
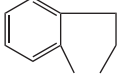


The electrophilic reaction of magnesium cyclopropylidene (**113**) with *N*-lithioarylamines was reported (equation 31)<sup>36</sup>. Thus, electrophilic reaction of magnesium cyclopropylidene (**113**) derived from **112** with *N*-lithio *N*-methyl *p*-anisidine resulted in the formation of  $\alpha$ -amino-substituted cyclopropylmagnesium (**119**) in good yield. Methanolysis of the reaction mixture with CH<sub>3</sub>OD gave  $\alpha$ -deuteriated *N*-cyclopropyl-*N*-methyl-*p*-anisidine (**120**) in 82% yield with 98% D-content.

The reaction of **113** with several *N*-lithioamines was investigated and the results are summarized in Table 5. *N*-Methylaniline, *p*-chloro-*N*-methylaniline and *N*-benzyl-*p*-anisidine gave 60–67% yield of the desired *N*-cyclopropyl arylamines. Diphenylamine gave the desired product; however, the yield was not satisfactory. Interestingly, dibenzylamine did not afford the desired product at all. This result indicated that the magnesium cyclopropylidene (**113**) only reacts with *N*-lithio arylamines. The reaction of **113** with *N*-lithio nitrogen-containing heterocyclic compounds was also studied. From the results shown in Table 5, the yields of the reaction are variable as a function of the heterocyclic compounds used.

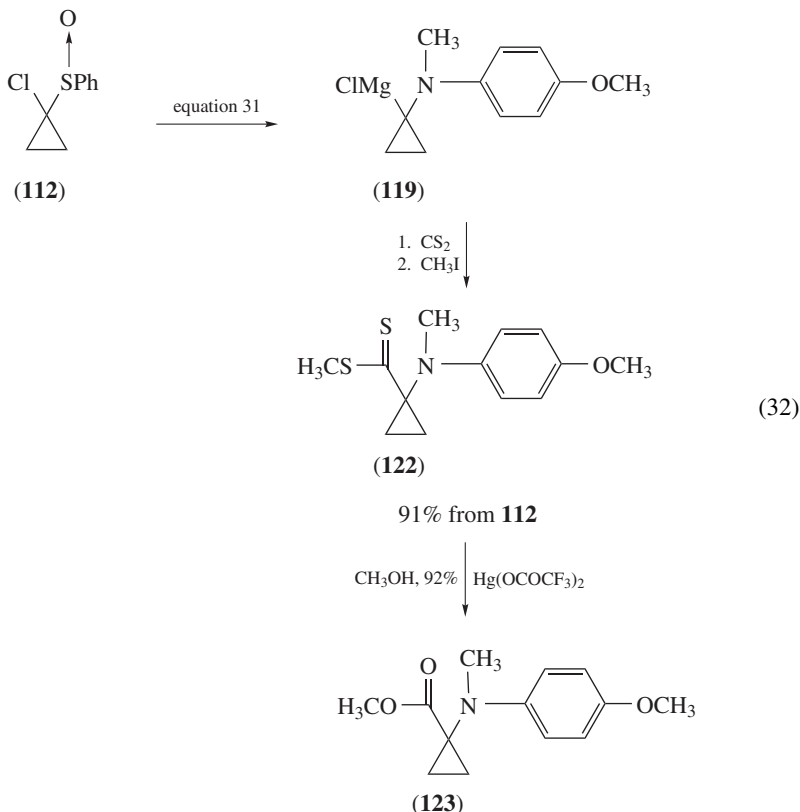
The reactivity of the formed  $\alpha$ -amino-substituted cyclopropylmagnesium (**119**) with some electrophiles was investigated<sup>36</sup>. Cyclopropylmagnesium (**119**) was found to have a low nucleophilicity and, for example, reaction with benzaldehyde gave only 40% yield

TABLE 5. Reaction of magnesium cyclopropylidene (**113**) derived from 1-chlorocyclopropyl phenyl sulfoxide (**112**) with *N*-lithio amines

$  \begin{array}{c} \text{O} \\ \uparrow \\ \text{Cl} \text{---} \text{SPh} \\ \diagup \quad \diagdown \\ \triangle \end{array} \xrightarrow[\text{THF, } -78^\circ\text{C}]{i\text{-PrMgCl}} \begin{array}{c} \text{Cl} \quad \text{MgCl} \\ \diagup \quad \diagdown \\ \triangle \end{array} \xrightarrow[2. \text{CH}_3\text{OH}]{1. \begin{array}{c} \text{R}^1 \\   \\ \text{LiN} \text{---} \text{R}^2 \\ -78 \text{ to } -40^\circ\text{C} \end{array}} \begin{array}{c} \text{R}^1 \\   \\ \text{H} \text{---} \text{N} \text{---} \text{R}^2 \\ \diagup \quad \diagdown \\ \triangle \end{array}  $			
(112)	(113)		(121)
R <sup>1</sup>	R <sup>2</sup>	Equiv of amine	<b>121</b> /Yield(%)
CH <sub>3</sub>	Ph	3.5	67
CH <sub>3</sub>	<i>p</i> -Chlorophenyl	3.5	60
CH <sub>2</sub> Ph	<i>p</i> -Methoxyphenyl	3.5	60
Ph	Ph	3.5	42
CH <sub>2</sub> Ph	CH <sub>2</sub> Ph	3.5	0
		2.0	87
		2.0	43
		2.0	21
		2.0	75

of the adduct. The reaction of **119** with ethyl chloroformate gave maximum 20% yield of the desired ethoxycarbonylated product.

On the other hand, the reaction of **119** with carbon disulfide followed by iodomethane gave dithioester **122** in high yield (equation 32). Methanolysis of the dithioester **122** in methanol with excess  $\text{Hg}(\text{OCOCF}_3)_2$  gave the cyclopropyl  $\alpha$ -amino acid derivative **123** in high yield.



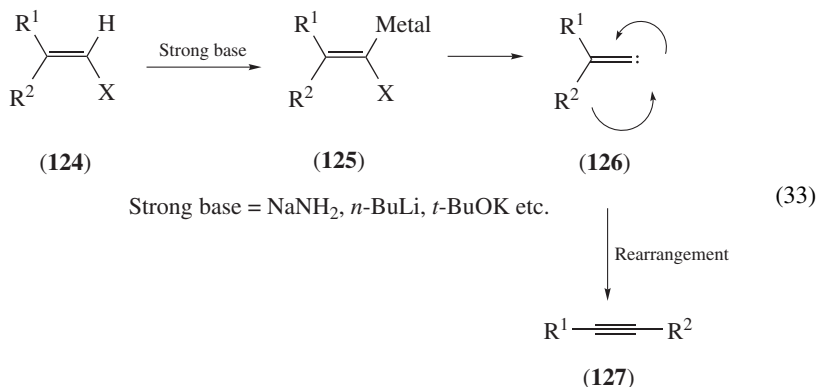
## V. MAGNESIUM ALKYLIDENE CARBENOIDS

### A. Generation and Nucleophilic Property of Magnesium Alkylidene Carbenoids, the Fritsch–Buttenberg–Wiechell Rearrangement

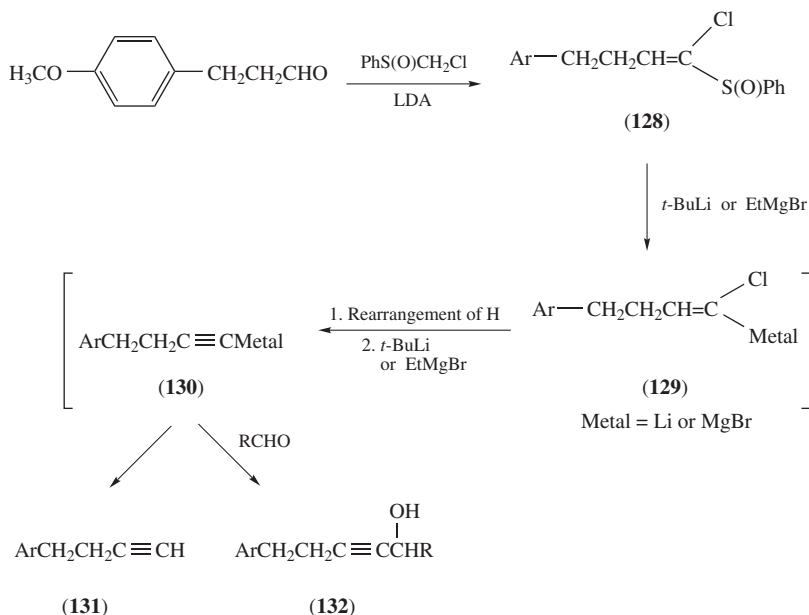
Alkylidene carbenoids are  $\text{sp}^2$  carbenoids and are known to be very interesting reactive intermediates<sup>37</sup>. The most famous reaction of alkylidene carbenoids is the Fritsch–Buttenberg–Wiechell rearrangement (equation 33)<sup>14</sup>.

Treatment of 1-haloalkene (**124**) with a strong base resulted in the formation of carbenoid **125** by the hydrogen–metal exchange reaction. The metal in **125** is usually Na, Li or K and the organometals were found to be highly unstable; elimination of Metal-X resulted in the formation of alkylidene carbene **126**. The Fritsch–Buttenberg–Wiechell rearrangement takes place either from the alkylidene carbenoid or carbene to afford

acetylene (**127**). As the alkylidene carbenoid (**125**) was usually generated at room temperature or higher, the behavior of the alkylidene carbenoid was unclear until recently.



In 1993, Satoh and coworkers reported the preparation of lithium- and magnesium-alkylidene carbenoids from 1-chlorovinyl phenyl sulfoxides by sulfoxide–metal exchange reaction at low temperature (Scheme 6)<sup>38</sup>. 1-Chlorovinyl phenyl sulfoxide (**128**) is easily synthesized from the corresponding aldehyde and chloromethyl phenyl sulfoxide in high yield. Sulfoxide **128** was treated with *t*-BuLi in THF at –78 °C to give the terminal alkyne **131**. Obviously, the intermediate of this reaction was the alkylidene carbenoid **129**.

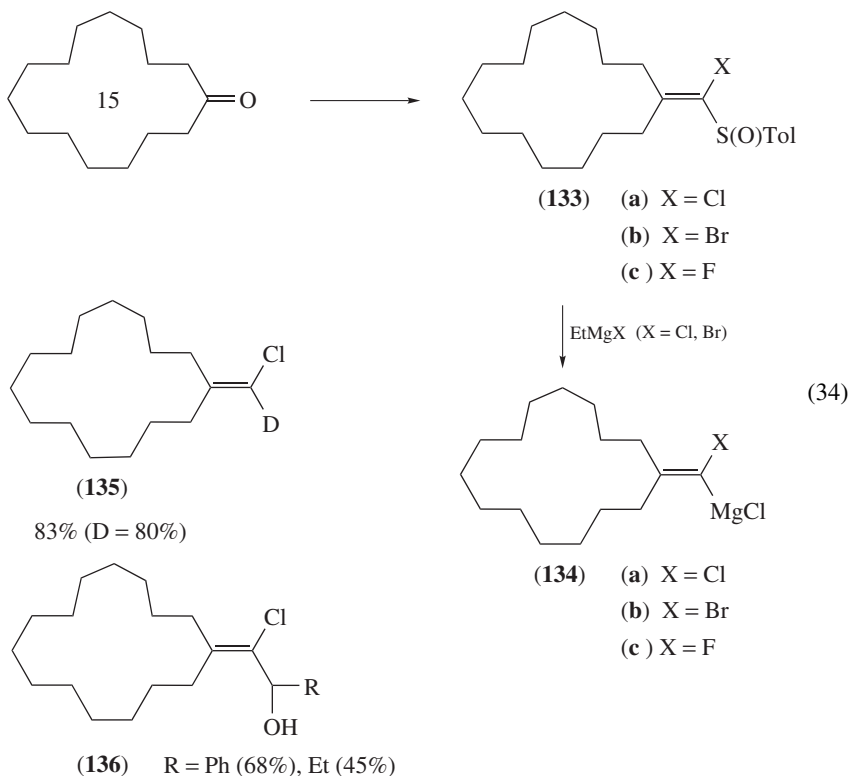


SCHEME 6

The Fritsch–Buttenberg–Wiechell rearrangement of the carbenoid gave the alkyne **131**, which was further metallated in the reaction mixture with the excess of the alkylmetal to

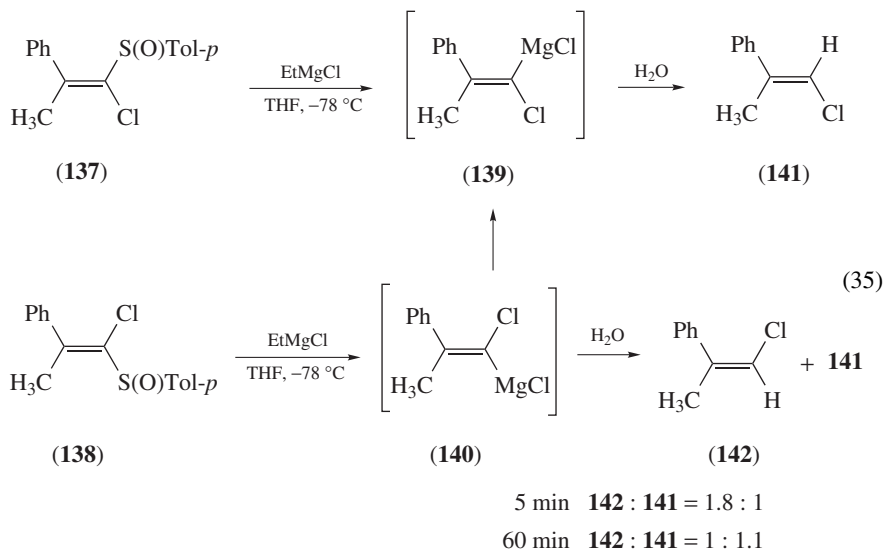
give the acetylide **130**. Addition of an aldehyde gave the propargylic alcohol **132**. When this reaction was carried out with EtMgBr, the corresponding magnesium alkylidene carbenoid (**129**; Metal = MgBr) was generated; however, even at  $-78^{\circ}\text{C}$  the rearrangement took place to give the alkyne **131**.

On the other hand, magnesium alkylidene carbenoid **134** derived from 1-halovinyl *p*-tolyl sulfoxides **133**, easily prepared from ketones (cyclopentadecanone is shown as representative example) and halomethyl aryl sulfoxide in three steps in high overall yields, showed quite interesting properties (equation 34)<sup>39</sup>. For instance, treatment of 1-chlorovinyl *p*-tolyl sulfoxide (**133a**) with EtMgCl in THF at  $-78^{\circ}\text{C}$  resulted instantaneously in the formation of magnesium alkylidene carbenoid **134a**. The formation of carbenoid **134a** was confirmed by quenching the reaction mixture with  $\text{CD}_3\text{OD}$  to afford deuteriated chloroalkene (**135**) in high yield.

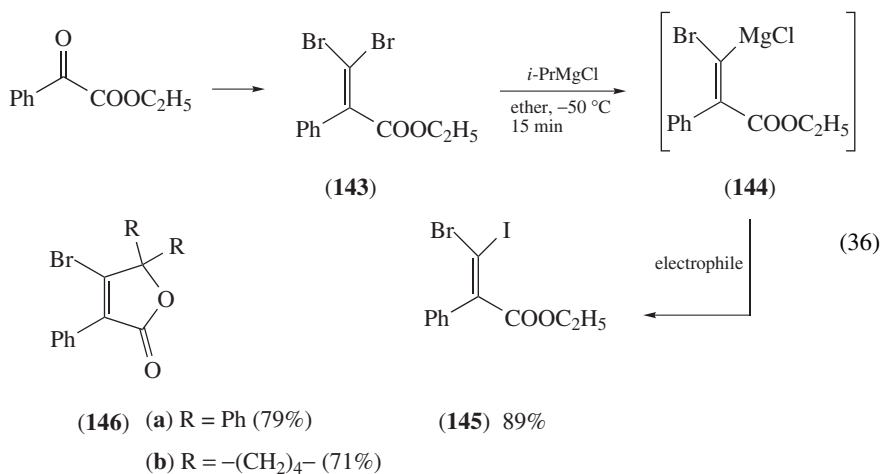


Moreover, magnesium carbenoid **134a** was found to be stable below  $-78^{\circ}\text{C}$  for at least 30 min. The carbenoid (**134b**; X = Br) showed similar properties compared with **134a**; however, **134c** (X = F) was found to be relatively unstable. The nucleophilicity of **134a** was examined by classical reaction with ketones and aldehydes and it was found that carbenoid **134a** has a rather low nucleophilicity; only aldehydes reacted to give the adduct **136** in about 60% yields. Interestingly, the Fritsch–Buttenberg–Wiechell rearrangement was rarely observed from the magnesium alkylidene carbenoids derived from ketones.

The configurational stability of the magnesium alkylidene carbenoids was examined (equation 35)<sup>39b</sup>. Thus, at first, (*E*)-1-chlorovinyl *p*-tolyl sulfoxide (**137**) and its (*Z*)-isomer (**138**) were synthesized from acetophenone. Sulfoxide **137** was treated with EtMgCl in THF at  $-78^{\circ}\text{C}$  for 5 min to give (*E*)-chloroalkene **141** in 95% as a single isomer after hydrolysis. Prolonging the reaction time to 60 min gave a similar result.



On the other hand, treatment of (*Z*)-1-chlorovinyl *p*-tolyl sulfoxide (**138**) with EtMgCl for 5 min gave a mixture of *Z*-chloroalkene **142** accompanied by its *E*-isomer (**141**) in a ratio of 1.8:1. Prolonging the reaction time to 60 min gave an almost equimolar mixture of **142** and **141** in a 1:1.1 ratio. These results indicated that magnesium alkylidene carbenoid **140** isomerizes even at  $-78^{\circ}\text{C}$ . Magnesium alkylidene carbenoid **139** is therefore thermodynamically more stable than **140**.

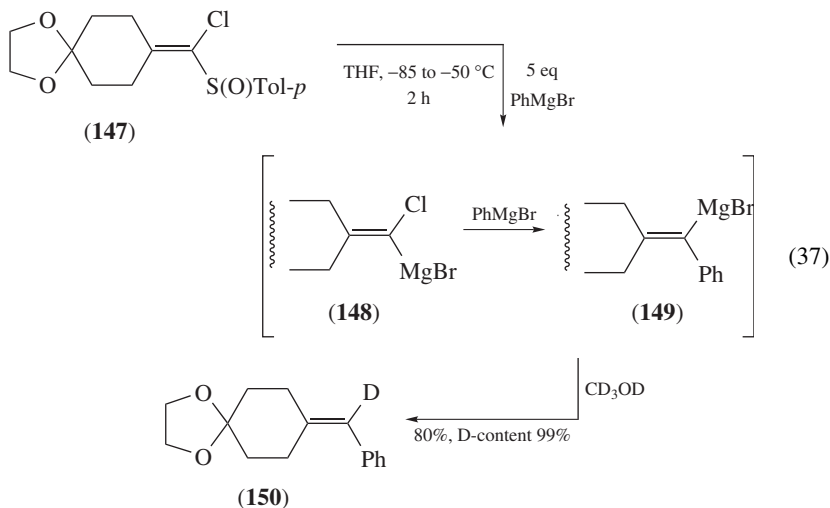


The nucleophilic nature of magnesium alkylidene carbenoids was also reported (equation 36)<sup>40</sup>. Treatment of dibromoalkene **143**, derived from ethyl phenylglyoxylate, with *i*-PrMgCl in ether at  $-50^{\circ}\text{C}$  for 15 min resulted in the formation of the magnesium alkylidene carbenoid having an ethyl ester group in the molecule (**144**). Carbenoid **144** could be trapped with several electrophiles such as iodine, or benzophenone and cyclopentanone to afford the iodide **145** and lactones **146a** and **146b**, respectively, in good yields.

## B. Electrophilic Reactions of Magnesium Alkylidene Carbenoids

### 1. One-pot synthesis of tetrasubstituted olefins

From a synthetic organic chemistry point of view, the electrophilic nature of magnesium alkylidene carbenoids is much more interesting than their nucleophilic nature. Satoh and coworkers found that treatment of 1-chlorovinyl *p*-tolyl sulfoxide (**147**) with an excess of PhMgBr in THF at  $-85$  to  $-50^{\circ}\text{C}$  for 2 h followed by  $\text{CD}_3\text{OD}$  gave the deuterio styrenyl derivative **150** in 80% yield with a complete deuterium incorporation (equation 37)<sup>39b</sup>.

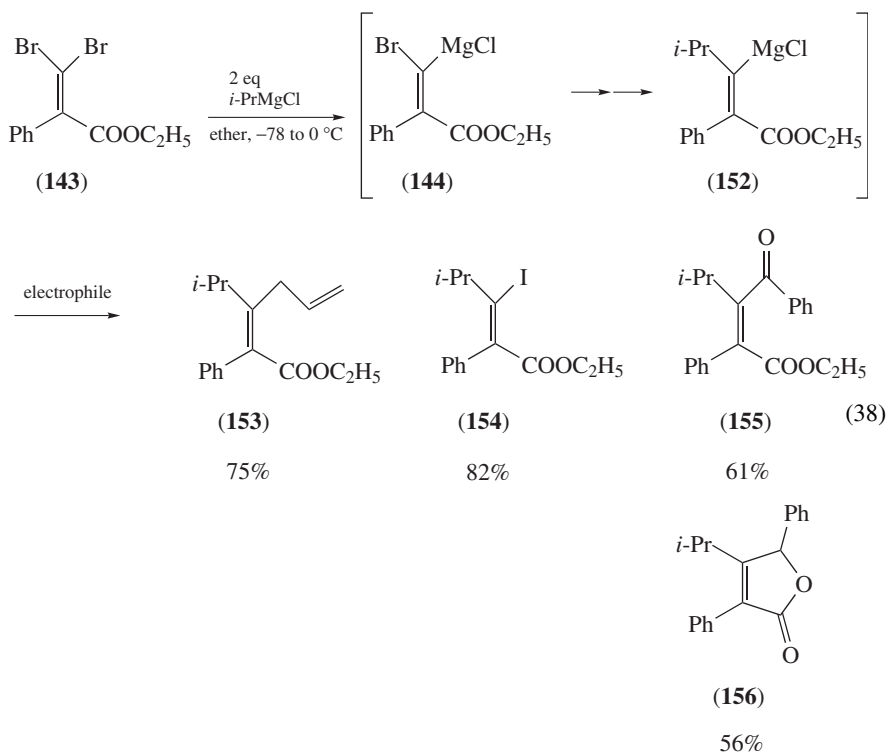


The reaction proceeds as follows. At first, the sulfoxide–magnesium exchange reaction of **147** gave the magnesium alkylidene carbenoid **148**. Based on the electrophilic nature of carbenoid **148**, nucleophilic substitution of **148** on the  $\text{sp}^2$  carbon atom by PhMgBr resulted in the formation of alkenyl Grignard reagent **149**. Finally, the carbanion was quenched with  $\text{CD}_3\text{OD}$  to afford the deuteriated olefin **150**. This reaction resulted in an interesting double substitution of sulfinyl and chloro groups by phenyl and deuterio groups on the olefinic  $\text{sp}^2$  carbon in a one-pot procedure.

Selected examples of this new method are summarized in Table 6. As shown in this Table, PhMgBr and *p*-methoxyphenylmagnesium bromide reacted well with **147** to give first the magnesium alkylidene carbenoid and, after nucleophilic substitution with an additional equivalent of Grignard, the corresponding alkenyl Grignard reagent. A large variety of electrophiles can be added to the reaction mixture and the corresponding tetrasubstituted olefins **151** are obtained in good yields (with the exception of the reaction of acetone).

TABLE 6. Synthesis of tetrasubstituted olefins (**151**) by the reaction of 1-chlorovinyl *p*-tolyl sulfoxide (**147**) with ArMgBr followed by addition of electrophiles

Ar	Electrophile	<b>151</b>	
		E	Yield (%)
Ph	CH <sub>3</sub> CH <sub>2</sub> CHO	CH <sub>3</sub> CH <sub>2</sub> CHOH	81
Ph	CH <sub>3</sub> COCH <sub>3</sub>	CH <sub>3</sub> CH(OH)CH <sub>3</sub>	21
Ph	ClCOOEt	EtOCO	65
Ph	I <sub>2</sub>	I	53
Ph		PhCH <sub>2</sub> CH <sub>2</sub> CH(OH)CH <sub>2</sub>	42
Ph	PhNCO	PhNHCO	87
<i>p</i> -Methoxyphenyl	PhCHO	PhCH(OH)	87
<i>p</i> -Methoxyphenyl	ClCOOEt	EtOCO	67
<i>p</i> -Methoxyphenyl	PhNCO	PhNHCO	87

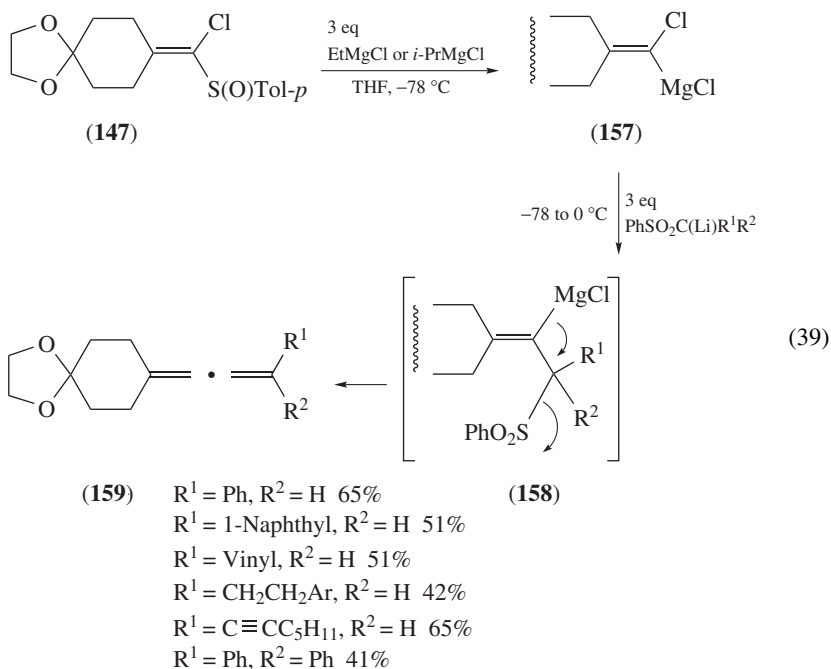




A similar reaction was reported by Knochel, Marek and coworkers (equation 38)<sup>40</sup>. Thus, dibromide **143** was treated with 2 equivalents of *i*-PrMgCl at  $-78^{\circ}\text{C}$  and the reaction mixture was warmed to  $0^{\circ}\text{C}$  to give the functionalized alkenyl Grignard reagent **152** through magnesium alkylidene carbenoid intermediate **144**. Trapping the alkenyl Grignard reagent **152** with different electrophiles such as allyl bromide, iodine, benzoyl chloride and benzaldehyde gave the corresponding olefins **153–156** respectively in moderate to good yields.

## 2. Synthesis of allenes by alkenylation of magnesium alkylidene carbenoids with $\alpha$ -sulfonyl lithium carbanions

The electrophilic reaction of magnesium alkylidene carbenoids with other nucleophiles than the original Grignard reagent can also be carried out. For example, treatment of magnesium alkylidene carbenoid **157**, derived from **147**, with  $\alpha$ -sulfonyl lithium carbanion afforded allenes **159** in moderated yields (equation 39)<sup>41</sup>.

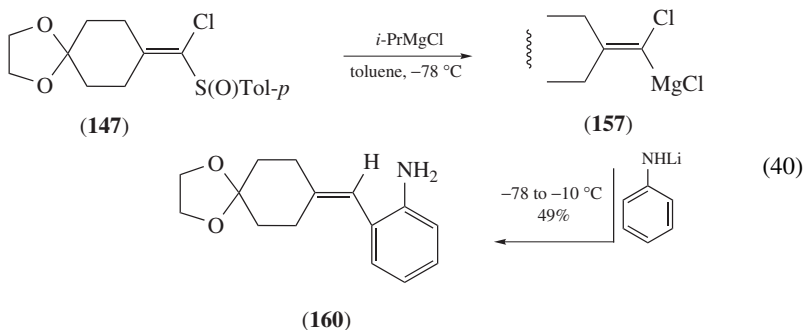


The proposed mechanism is as follows: First, the  $\alpha$ -sulfonyl lithium carbanion attacks the electrophilic carbenoid carbon atom to give the vinylmagnesium intermediate (**158**). As the sulfonyl moiety is a good leaving group, a  $\beta$ -elimination takes place to afford the allenes (**159**).

## 3. Reaction of magnesium alkylidene carbenoids with *N*-lithio arylamines

A very interesting direct alkenylation of arylamines at the *ortho*-position by the reaction of magnesium alkylidene carbenoids with *N*-lithio arylamines to give **162** was reported by Satoh and coworkers (equation 40)<sup>42</sup>. Magnesium alkylidene carbenoid **157**, derived

from **147**, was treated with three equivalents of *N*-lithio aniline at  $-78^{\circ}\text{C}$  and the reaction mixture was gradually allowed to warm to  $-10^{\circ}\text{C}$  to give *ortho*-alkenylated aniline **160** in 49% yield. Toluene was found to be the best solvent for this reaction. The generality of this unprecedented reaction was investigated and selected results are summarized in Table 7.



Magnesium alkylidene carbenoid **157** reacted with *p*-anisidine in 44% yield; however, the yield decreased with *p*-chloroaniline. 2-Methylaniline gave only *ortho*-alkenylated product and 2,6-dimethylaniline gave no alkenylated product. These results indicate that this reaction only gives *ortho*-alkenylated products. Interestingly, the reaction with 1-aminonaphthalene and 1-aminoanthracene gave much better yields. Magnesium alkylidene carbenoid **161**, generated from 1-chlorovinyl *p*-tolyl sulfoxide synthesized from acetone, reacts similarly with *N*-lithio arylamines to give **162**. Especially, the reaction with 1-aminonaphthalene and 1-aminoanthracene gave about 80% yields of *ortho*-alkenylated arylamines.

Very interesting results were obtained from the reaction of magnesium alkylidene carbenoids with *meta*-substituted arylamines (Table 8)<sup>42b</sup>. The reaction of magnesium alkylidene carbenoids **157** and **161** with three *meta*-substituted anilines was carried out and the results are summarized in Table 8. The reaction of **157** with *meta*-anisidine gave two products **163** and **164** (in a 30:13 ratio) in 43% yield. The main product was found to have the alkenyl group at the more hindered position (**163**). As shown in the Table, all the other *meta*-substituted aniline derivatives also gave the more hindered alkenylated compounds as the main product in variable ratio.

To gain a better understanding of the regioselectivity of the reaction, theoretical study using the Gaussian 98 program was performed<sup>42b</sup>. Thus, electrostatic potential-derived charges using the CHelpG scheme of Breneman were calculated with the structures optimized at the MP2/6-31(+)G\* level and the more negative charge was found to be on carbon-2 in the most stable conformer.

Stereochemistry of this reaction is also quite interesting. Thus, both geometrical isomers of 1-chlorovinyl *p*-tolyl sulfoxides (**165**–**167**) were synthesized from 2-cyclohexenone, methyl vinyl ketone and 2-heptanone respectively, and the corresponding magnesium alkylidene carbenoids were generated and treated with *N*-lithio aniline or *N*-lithio 1-aminonaphthalene. The results are summarized in Table 9.

Interestingly, the reaction of the magnesium alkylidene carbenoids derived from *E*-**165** and *Z*-**165** with *N*-lithio aniline gave *Z*-*ortho*-alkenylated aniline *Z*-**168** and *E*-*ortho*-alkenylated aniline *E*-**168**, respectively, with high stereospecificity (entries 1 and 2). The same results were obtained from *E*-**165** and *Z*-**165** with *N*-lithio 1-aminonaphthalene which gives *Z*-**169** and *E*-**169** (entries 3 and 4). Furthermore, the reaction of the magnesium alkylidene carbenoid derived from *E*-**166** and *Z*-**166** with *N*-lithio 1-aminonaphthalene (entries 5 and 6) again showed high stereospecificity in products *Z*-**170** and

TABLE 7. Synthesis of *ortho*-alkenylated arylamines (**162**) by the reaction of the magnesium alkylidene carbenoids with *N*-lithio arylamines

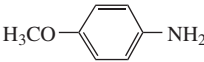
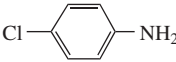
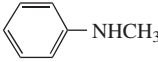
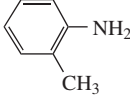
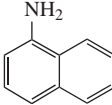
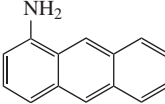
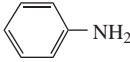
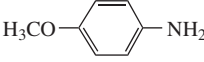
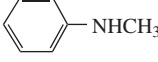
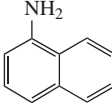
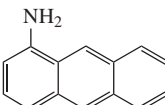
$  \begin{array}{c}  \text{R} \quad \text{Cl} \\  \diagdown \quad / \\  \text{C} \\  / \quad \diagdown \\  \text{R} \quad \text{MgCl}  \end{array}  $ <b>(157)</b> <b>(161)</b> R = CH <sub>3</sub>		$  \begin{array}{c}  \text{N(Li)R}^1 \\    \\  \text{C}_6\text{H}_4\text{-X}  \end{array}  $ toluene, -78 to -10 °C	$  \begin{array}{c}  \text{R} \quad \text{H} \quad \text{NHR}^1 \\  \diagdown \quad / \quad   \\  \text{C} \\  / \quad \diagdown \\  \text{R} \quad \text{C}_6\text{H}_3\text{-X}  \end{array}  $ <b>(162)</b>
R	R	Arylamine	<b>162</b> /Yield (%)
CH <sub>3</sub>	CH <sub>3</sub> <b>(161)</b>		44
			28
			38
			32
			66
			60
			43
			43
			46
			81
			79



TABLE 9. The reaction of magnesium alkylidene carbenoids derived from *E*- and *Z*-1-chlorovinyl *p*-tolyl sulfoxides with *N*-lithio aniline and *N*-lithio 1-aminonaphthalene

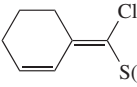
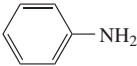
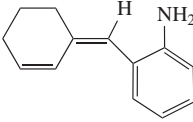
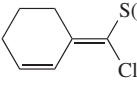
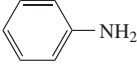
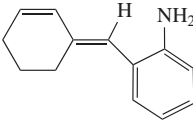
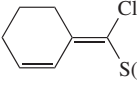
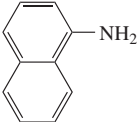
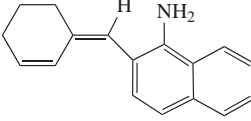
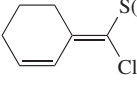
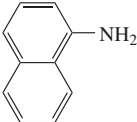
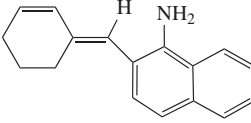
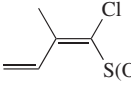
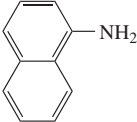
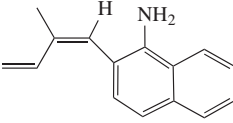
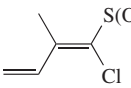
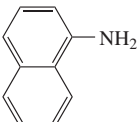
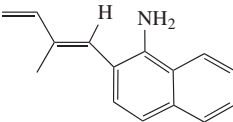
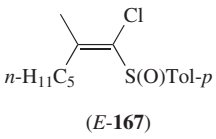
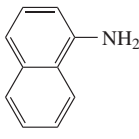
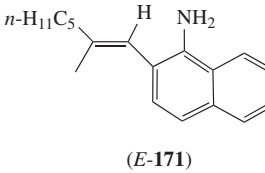
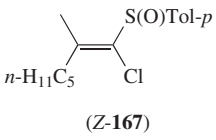
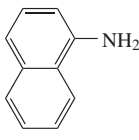
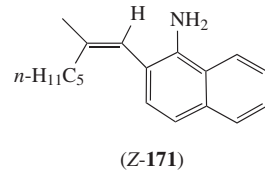
Entry	1-Chlorovinyl <i>p</i> -tolyl sulfoxide	Arylamine	Product	<i>E</i> : <i>Z</i>	Yield (%)
1	 ( <i>E</i> -165)		 ( <i>Z</i> -168)	6:94	53
2	 ( <i>Z</i> -165)		 ( <i>E</i> -168)	94:6	46
3	 ( <i>E</i> -165)		 ( <i>Z</i> -169)	3:97	65
4	 ( <i>Z</i> -165)		 ( <i>E</i> -169)	95:5	71
5	 ( <i>E</i> -166)		 ( <i>Z</i> -170)	4:96	68
6	 ( <i>Z</i> -166)		 ( <i>E</i> -170)	94:6	62

TABLE 9. (continued)

Entry	1-Chlorovinyl <i>p</i> -tolyl sulfoxide	Arylamine	Product	<i>E</i> : <i>Z</i>	Yield (%)
7	 ( <i>E</i> -167)		 ( <i>E</i> -171)	44:56	54
8	 ( <i>Z</i> -167)		 ( <i>Z</i> -171)	34:66	55

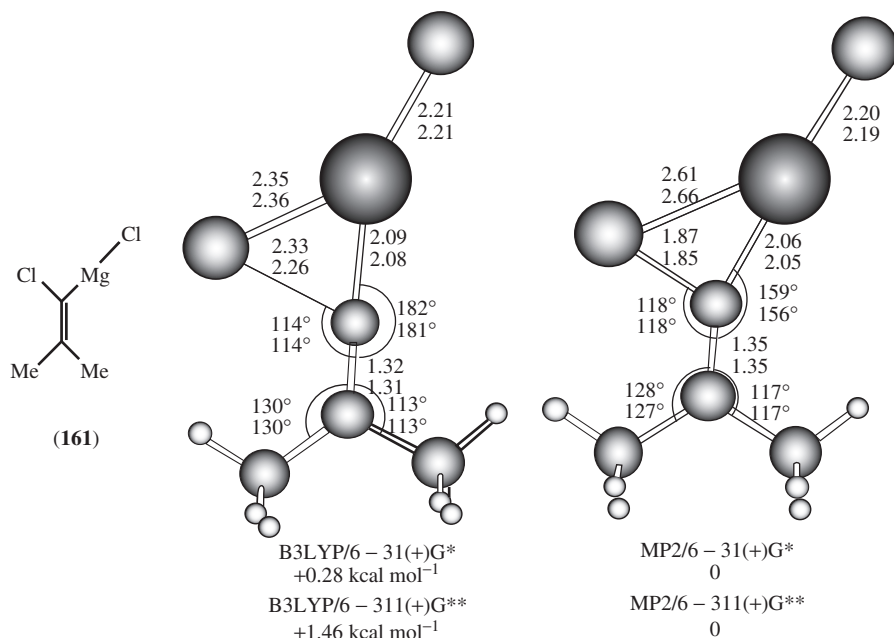


FIGURE 1. Geometries of 1-chloro-2-methylpropenylmagnesium chloride **161** optimized at the RHF, B3LYP and MP2 levels of theory with the 6-31(+)*G*\* and 6-311(+)*G*\*\* basis sets. The energies of these geometries were calculated by the CCSD(T) method with the corresponding basis set

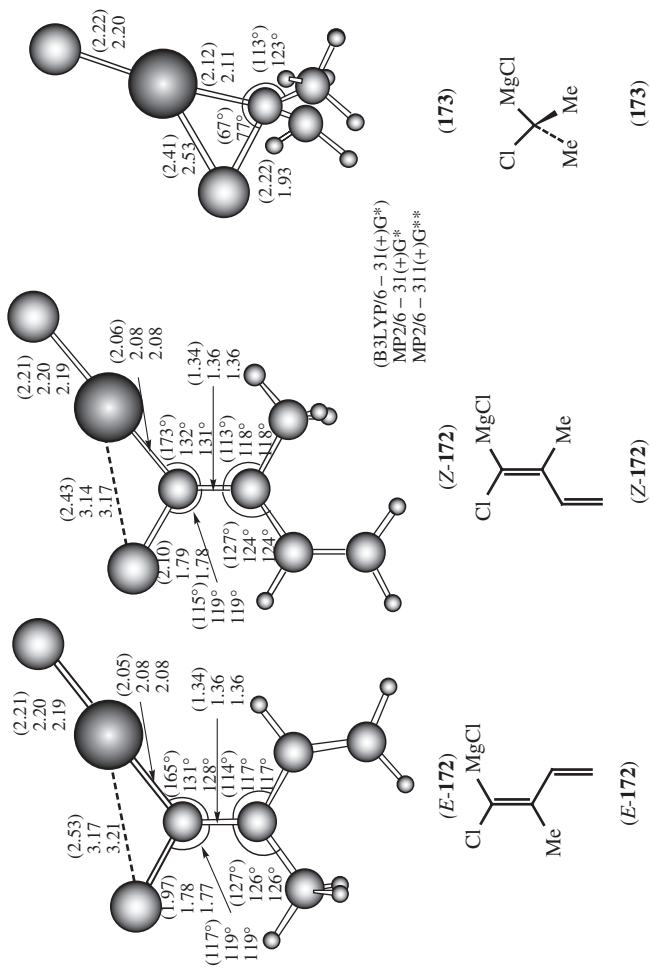


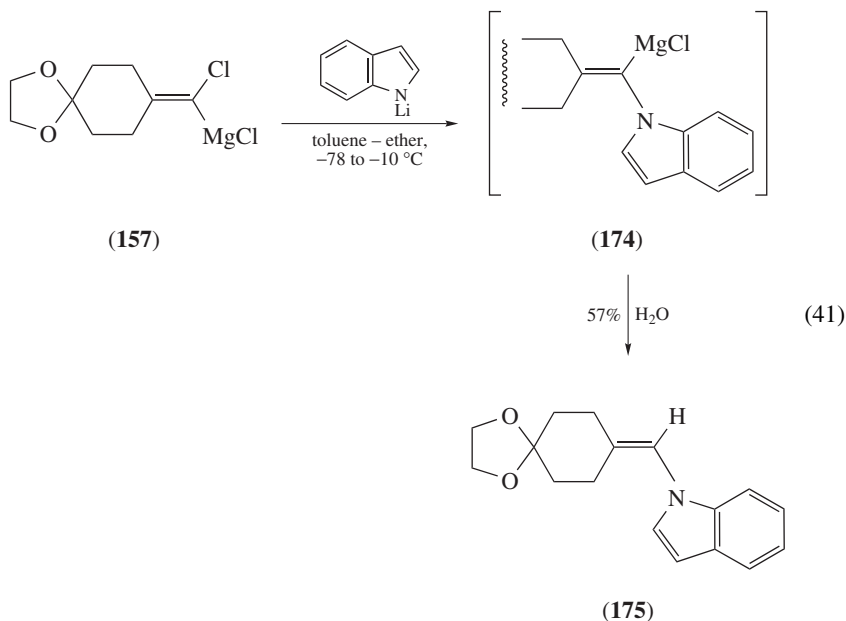
FIGURE 2. Geometries of *E*-172, *Z*-172 and 173 optimized at B3LYP/6-31(+)*G*<sup>\*</sup>, MP2/6-31(+)*G*<sup>\*</sup> and MP2/6-311(+)*G*<sup>\*\*</sup>

distance between the Mg and the vinyl-Cl is much longer, the C-Cl bond is shorter and the C=C-Mg angle is smaller as compared to **161**. Thus, the conjugated system is geometrically stabilized.

#### 4. Reaction of magnesium alkylidene carbenoids with *N*-lithio nitrogen-containing heterocycles, lithium acetylides and lithium thiolates

Magnesium alkylidene carbenoids were found to be reactive with different nucleophiles to give new alkenylmagnesium compounds which could be trapped with electrophiles. As a whole, novel methods for the synthesis of tri- or tetrasubstituted olefins from the 1-chlorovinyl *p*-tolyl sulfoxides in a one-pot reaction are realized.

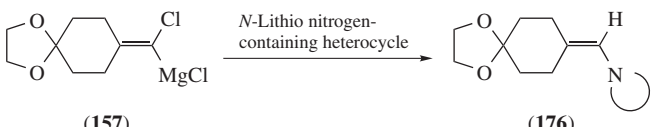
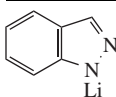
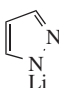
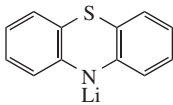
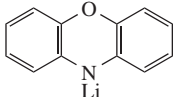
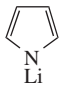
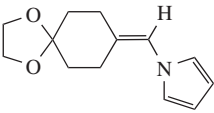
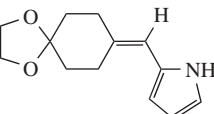
Thus, treatment of magnesium alkylidene carbenoid **157** with *N*-lithio indole in a toluene/ether mixture of solvents resulted in the formation of *N*-alkenylated indole **175** in 57% yield through the alkenylmagnesium intermediate **174** (equation 41)<sup>43</sup>. The generality of this reaction to give **176** was investigated and the results are shown in Table 10. Indazole gave the desired *N*-alkenylated product in 51% yield; however, pyrazole gave only 15% yield. Phenothiazine and phenoxazine gave good yields of the products. Interestingly, the simplest heterocycle pyrrole gave the *N*-alkenylated product in only 14% yield whereas the 2-alkenylated pyrrole (**177**) was obtained as a main product in 56% yield.



The stereochemistry of this reaction was also investigated (equation 42). Thus, geometrical isomers of 1-chlorovinyl *p*-tolyl sulfoxides *Z*-**178** and *E*-**178** were synthesized from 4-phenyl-2-butanone and they were treated with *i*-PrMgCl followed by *N*-lithio indole. As shown in equation 42, this reaction gave a mixture of isomers (*E*-**179** and *Z*-**179**) in relatively good yields but with low stereoselectivity.

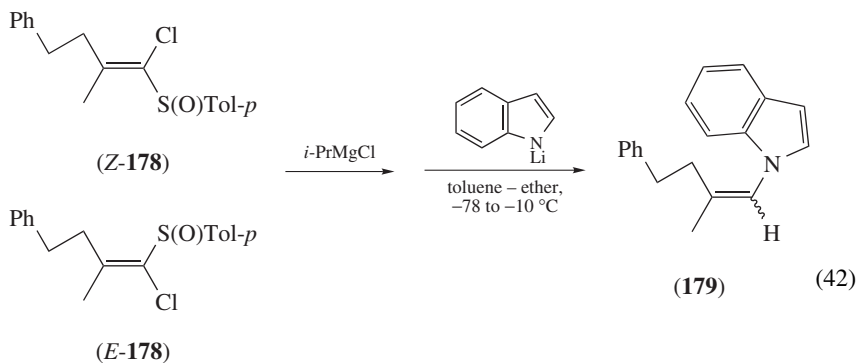


TABLE 10. Reaction of magnesium alkylidene carbenoid **157** with *N*-lithio nitrogen-containing heterocycles

	
<i>N</i> -Lithio nitrogen-containing heterocycle	<b>176</b> Yield (%)
	51
	15
	71
	70
	 14
	 56
	(177)

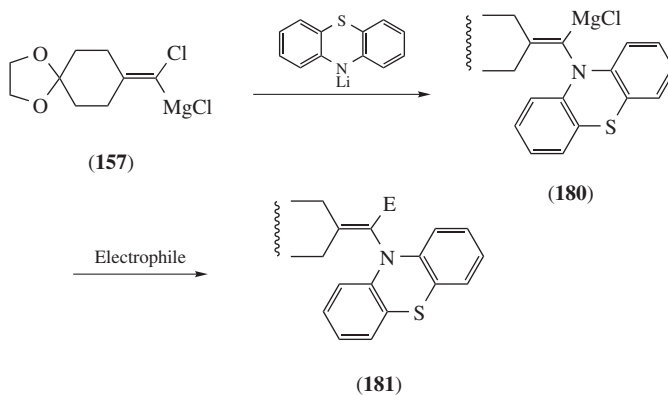
From a more synthetic perspective, reaction of the alkenylmagnesium derivatives with electrophiles is very interesting. Indeed, if the intermediates could be trapped with electrophiles, the reaction would provide a novel route to the preparation of nitrogen-containing heterocycles having a fully substituted enamine structure. This expectation proved to be possible (Table 11)<sup>43</sup>.

The reaction of the magnesium alkylidene carbenoid **157** with *N*-lithio phenothiazine gave the alkenylmagnesium intermediate **180** in good yield. Quenching the reaction with deuteriomethanol gave the deuterio olefin (**181**, Table 11, E = D) in 71% yield with a deuterium incorporation of 98%. The reaction with iodomethane did not take place; however, using 5 mol% of CuI as a catalyst at room temperature resulted in the formation of the methylated olefin in 62% yield. The alkylation and allylation required CuI as a catalyst. Benzoyl chloride and phenyl isocyanate reacted with the alkenylmagnesium intermediate **180** to give the desired products (**181**).



178	179 / Yield (%)	E-179 : Z-179
Z-178	64	44 : 56
E-178	65	29 : 71

TABLE 11. Synthesis of phenothiazine having a fully substituted enamine structure (181)



Electrophile	181	
	E	Yield (%)
CH <sub>3</sub> OD	D	71 <sup>a</sup>
CH <sub>3</sub> I	CH <sub>3</sub>	62 <sup>b</sup>
CH <sub>3</sub> CH <sub>2</sub> I	CH <sub>3</sub> CH <sub>2</sub>	55 <sup>b</sup>
CH <sub>2</sub> =CHCH <sub>2</sub> I	CH <sub>2</sub> =CHCH <sub>2</sub>	63 <sup>b</sup>
PhCH <sub>2</sub> Br	PhCH <sub>2</sub>	30 <sup>b</sup>
PhCOCl	PhCO	59
PhNCO	PhNHCO	39

<sup>a</sup> Deuterium content 98%.

<sup>b</sup> The reaction was carried out with CuI as a catalyst.

TABLE 12. Synthesis of enyne **183** from magnesium alkylidene carbenoids **134a** with lithium acetylides and electrophiles

R	Electrophile	<b>183</b>	
		E	Yield (%)
CH <sub>3</sub> (CH <sub>2</sub> ) <sub>3</sub>	H <sub>2</sub> O	H	63
	H <sub>2</sub> O	H	41
H <sub>3</sub> CO-	H <sub>2</sub> O	H	49
F-	H <sub>2</sub> O	H	38
(CH <sub>3</sub> ) <sub>3</sub> Si	H <sub>2</sub> O	H	16
CH <sub>3</sub> (CH <sub>2</sub> ) <sub>3</sub>	I <sub>2</sub>	I	44

Lithium acetylides were found to react with magnesium alkylidene carbenoids to afford enynes (Table 12)<sup>44</sup>. Thus, magnesium alkylidene carbenoid **134a**, generated from 1-chlorovinyl *p*-tolyl sulfoxide **133a**, reacts with 1-hexynyl lithium (3 equivalents) to give, via **182**, the conjugated enyne **183** in 63% yield after hydrolysis. In this reaction, the presence of cyclopentylmethyl ether (CPME) as an additive was found to be effective. The scope of this reaction was investigated and the results are summarized in Table 12. Unfortunately, yields were moderate.

The reaction of magnesium alkylidene carbenoids with lithium thiolates gave trisubstituted alkenyl sulfides (**185**) in good yields through the alkenylmagnesium intermediates **184** (Table 13)<sup>44</sup>. Thus, to the magnesium alkylidene carbenoid **157**, prepared in toluene at  $-78^{\circ}\text{C}$ , was added lithium *p*-toluenethiolate (3 equivalents) and alkenylsulfide **185** was obtained in 80% yield after hydrolysis. In this reaction, the presence of 1,2-dimethoxyethane (DME) as an additive was found to be effective. As shown in Table 13, the reaction with arenethiolates gave better yields as compared to the reaction with alkyl thiolates.

TABLE 13. Synthesis of vinyl sulfides (**185**) by the reaction of magnesium alkylidene carbenoids with lithium thiolates

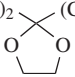
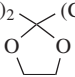
$  \begin{array}{c} \text{R} \\ \diagup \\ \text{C}=\text{C} \\ \diagdown \\ \text{R} \end{array} \begin{array}{c} \text{Cl} \\ \diagup \\ \text{C} \\ \diagdown \\ \text{MgCl} \end{array} \xrightarrow[\text{-78 to 0 } ^\circ\text{C}]{\text{RSLi, toluene-DME,}} \begin{array}{c} \text{R} \\ \diagup \\ \text{C}=\text{C} \\ \diagdown \\ \text{R} \end{array} \begin{array}{c} \text{MgCl} \\ \diagup \\ \text{C} \\ \diagdown \\ \text{SR} \end{array} \xrightarrow{\text{H}_2\text{O}} \begin{array}{c} \text{R} \\ \diagup \\ \text{C}=\text{C} \\ \diagdown \\ \text{R} \end{array} \begin{array}{c} \text{H} \\ \diagup \\ \text{C} \\ \diagdown \\ \text{SR} \end{array}  $			
		( <b>184</b> )	( <b>185</b> )
R	R	Lithium thiolate	<b>185</b> /Yield (%)
$-(\text{H}_2\text{C})_2$  ( <b>157</b> )		$\text{H}_3\text{C}-\text{C}_6\text{H}_4-\text{SLi}$	80
		$\text{H}_3\text{CO}-\text{C}_6\text{H}_4-\text{SLi}$	82
		$\text{Cl}-\text{C}_6\text{H}_4-\text{SLi}$	72
		$n\text{-C}_{12}\text{H}_{25}\text{SLi}$	60
		$(\text{CH}_3)_3\text{CSLi}$	39
$-(\text{CH}_2)_{14}-$	( <b>134a</b> )	$\text{H}_3\text{C}-\text{C}_6\text{H}_4-\text{SLi}$	51
$\text{CH}_3$	$\text{CH}_3$ ( <b>161</b> )	$\text{H}_3\text{C}-\text{C}_6\text{H}_4-\text{SLi}$	77
$\text{Ph}$	$\text{Ph}$	$\text{H}_3\text{C}-\text{C}_6\text{H}_4-\text{SLi}$	68

TABLE 14. Synthesis of vinyl sulfides (**186**) by the reaction of magnesium alkylidene carbenoids with lithium *p*-toluenethiolate followed by some electrophiles

$  \begin{array}{c} \text{R} \\ \diagup \\ \text{C}=\text{C} \\ \diagdown \\ \text{R} \end{array} \begin{array}{c} \text{Cl} \\ \diagup \\ \text{C} \\ \diagdown \\ \text{MgCl} \end{array} \xrightarrow[\text{-78 to 0 } ^\circ\text{C}]{\text{H}_3\text{C}-\text{C}_6\text{H}_4-\text{SLi, toluene-DME,}} \begin{array}{c} \text{R} \\ \diagup \\ \text{C}=\text{C} \\ \diagdown \\ \text{R} \end{array} \begin{array}{c} \text{MgCl} \\ \diagup \\ \text{C} \\ \diagdown \\ \text{STol-}p \end{array} \xrightarrow{\text{Electrophile}} \begin{array}{c} \text{R} \\ \diagup \\ \text{C}=\text{C} \\ \diagdown \\ \text{R} \end{array} \begin{array}{c} \text{E} \\ \diagup \\ \text{C} \\ \diagdown \\ \text{STol-}p \end{array}  $			
		( <b>184</b> )	( <b>186</b> )
R	R	Electrophile	<b>186</b>
			E      Yield (%)
$-(\text{H}_2\text{C})_2$  ( <b>157</b> )		$\text{D}_2\text{O}$	D      80 <sup>a</sup>
		PhCHO	PhCHOH      64
		$\text{CH}_3\text{CH}_2\text{CHO}$	$\text{CH}_3\text{CH}_2\text{CHOH}$ 39
		PhCOCl	PhCO      54
		ClCOOEt	EtOCO      11
		$\text{I}_2$	I      50
$\text{CH}_3$ ( <b>161</b> )	$\text{CH}_3$	PhCHO	PhCHOH      58
		$\text{I}_2$	I      72

<sup>a</sup> Deuterium content 98%.

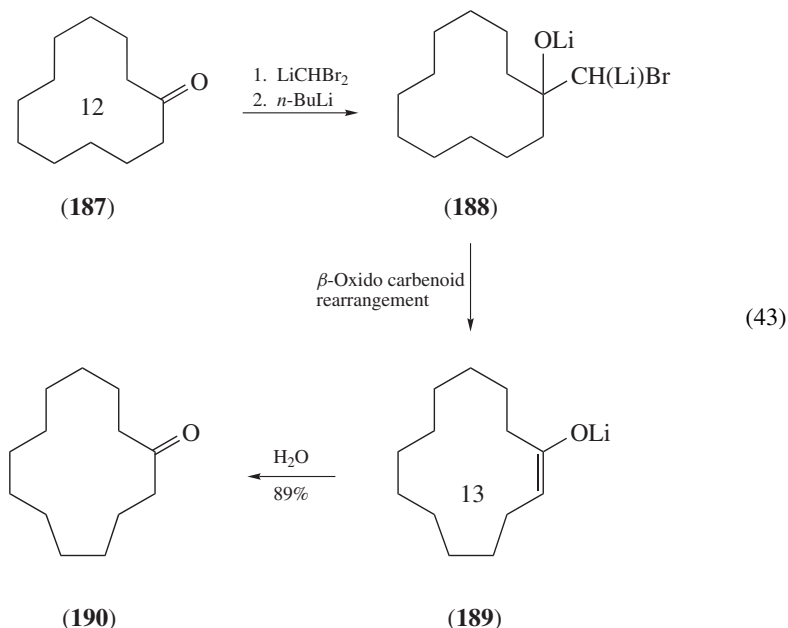
Reaction of the alkenylmagnesium intermediates **184** with several electrophiles led to trisubstituted alkenyl sulfides **186** (Table 14). Thus, when the reaction was quenched with  $D_2O$ , the deuteriated vinyl sulfide (**186**;  $E = D$ ) was obtained in 80% yield with 98% deuterium incorporation. The reaction with aldehydes, benzoyl chloride and iodine gave moderate to good yields of the desired functionalized alkenyl sulfides (**186**); however, ethyl chloroformate did not give good result.

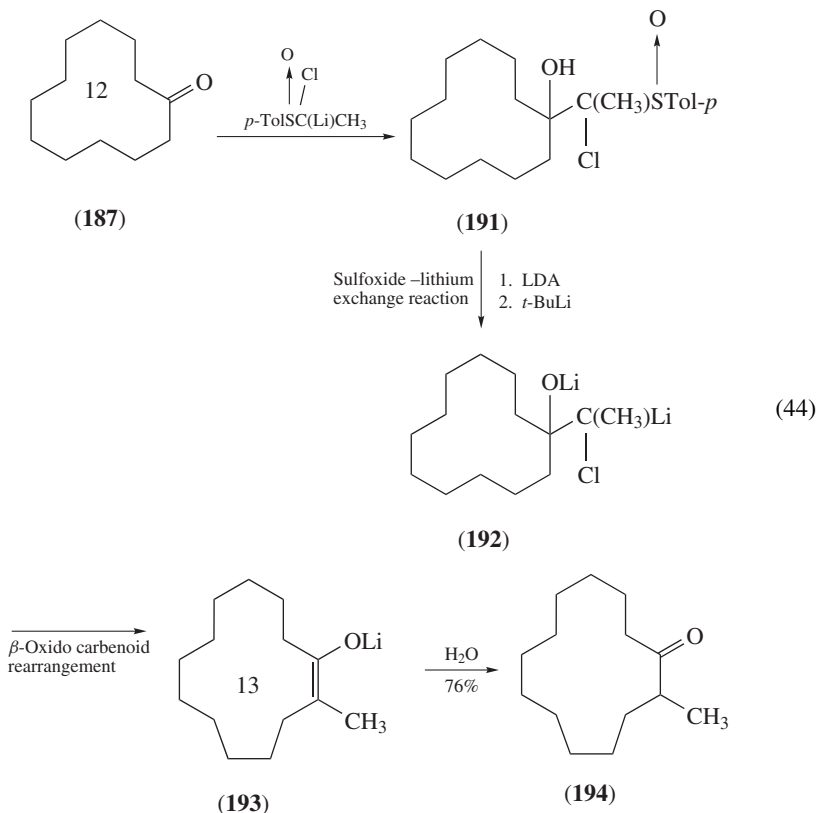
Development of new synthetic methods from aryl 1-chlorovinyl sulfoxides including the chemistry of magnesium alkylidene carbenoids has been reviewed by the author<sup>45</sup>.

## VI. MAGNESIUM $\beta$ -OXIDO CARBENOIDS

A one-carbon homologation of carbonyl compounds is an important and extensively used method for the preparation of desired carbonyl compounds<sup>46</sup>. One-carbon ring-expansion<sup>47</sup> or one-carbon homologation of ketones or aldehydes via a  $\beta$ -oxido carbenoid is a representative example of the homologation, but few methods have been reported<sup>48, 49</sup>.

For example, as shown in equation 43, Taguchi, Nozaki and coworkers reported in 1974 a one-carbon ring enlargement of cyclododecanone (**187**) to cyclotridecanone (**190**) with dibromomethyl lithium through  $\beta$ -oxido carbenoid (**188**)<sup>48a,c</sup>. This reaction was expected to proceed via a one-carbon expanded enolate (**189**). Cohen and coworkers used the bis(phenylthio)methyl lithium<sup>49</sup> whereas Satoh and coworkers used  $\alpha$ -sulfinyl lithium carbanion of 1-chloroalkyl aryl sulfoxides as the source of  $\beta$ -oxido carbenoids (equation 44)<sup>50</sup>.

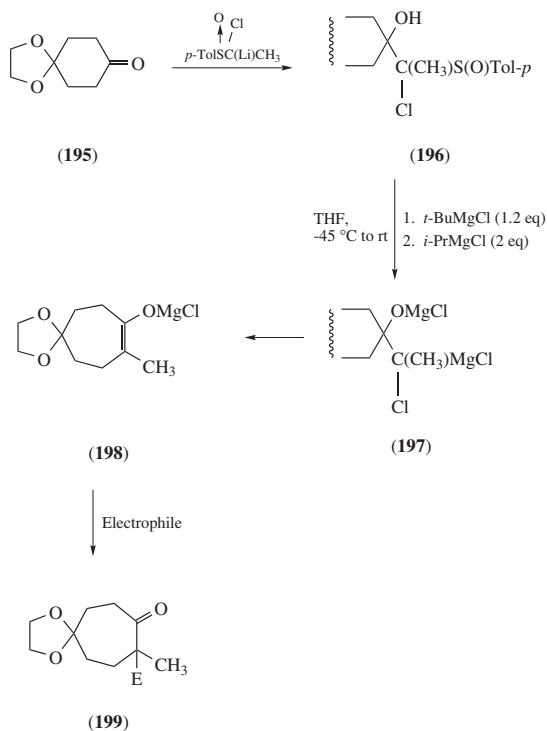


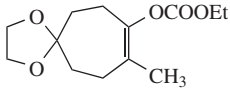
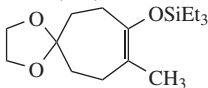


Thus, treatment of  $\alpha$ -sulfinyl lithium carbanion of 1-chloroethyl *p*-tolyl sulfoxide with cyclododecanone gave the adduct **191** in high yield. This adduct was further treated with LDA (to form the lithium alkoxide) followed by *tert*-butyllithium to give the  $\beta$ -oxido carbenoid **192** via the sulfoxide-lithium exchange reaction. The  $\beta$ -oxido carbenoid rearrangement then takes place to afford one-carbon elongated enolate **193**, which was finally treated with water to give a one-carbon homologated cyclotridecanone having a methyl group at the  $\alpha$ -position (**194**) in 76% yield.

Sato and coworkers further investigated this reaction and found that, in some cases, magnesium  $\beta$ -oxido carbenoids gave better results. Trapping of the enolate intermediates with several electrophiles was successfully carried out and a new method for the synthesis of one-carbon expanded cyclic  $\alpha,\alpha$ -disubstituted ketones from lower cyclic ketones was realized. An example using 1,4-cyclohexanedione mono ethylene ketal (**195**) as a representative cyclic ketone is shown in Table 15<sup>51</sup>.

Thus,  $\alpha$ -sulfinyl lithium carbanion of 1-chloroethyl *p*-tolyl sulfoxide was reacted with 1,4-cyclohexanedione mono ethylene ketal (**195**) to afford the adduct (**196**) in quantitative yield. The adduct was treated with *tert*-butylmagnesium chloride (magnesium alkoxide was initially formed) followed by isopropylmagnesium chloride to result in the formation of magnesium  $\beta$ -oxido carbenoid **197**. The  $\beta$ -oxido carbenoid rearrangement then takes place to give one-carbon expanded magnesium enolate **198**. Finally, an electrophile was

TABLE 15. Synthesis of 2-methyl-2-(substituted)cycloheptanones (**199**) from cyclohexanone derivative **195**, 1-chloroethyl *p*-tolyl sulfoxide, and electrophiles

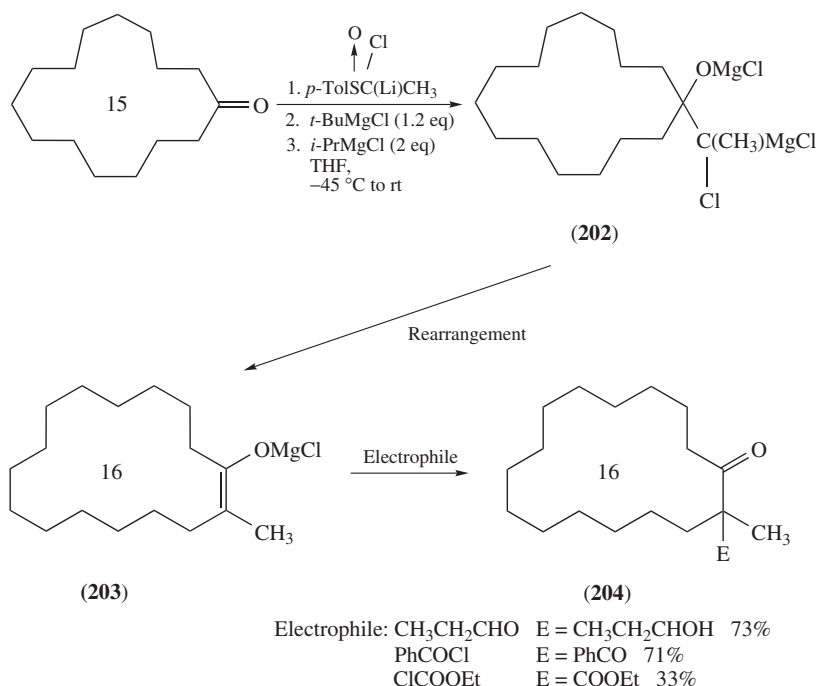
Electrophile	<b>199</b>	
	E	Yield (%)
CD <sub>3</sub> OD	D	75 <sup>a</sup>
CH <sub>3</sub> CH <sub>2</sub> CHO	CH <sub>3</sub> CH <sub>2</sub> CHOH	71
PhCHO	PhCHOH	64
PhCOCl	PhCO	63
CH <sub>3</sub> I	CH <sub>3</sub>	73 <sup>b</sup>
PhCH <sub>2</sub> Br	PhCH <sub>2</sub>	75 <sup>b</sup>
CH <sub>2</sub> =CHCH <sub>2</sub> I	CH <sub>2</sub> =CHCH <sub>2</sub>	59 <sup>b</sup>
ClCOOEt	 <b>(200)</b>	74
Et <sub>3</sub> SiCl	 <b>(201)</b>	75 <sup>b</sup>

<sup>a</sup> Deuterium content 95%.<sup>b</sup> HMPA was added as an additive.

added to the reaction mixture to give one-carbon expanded ketone having a quaternary center at the  $\alpha$ -position (**199**).

Quenching this reaction with deuteriomethanol gave 2-methylcycloheptanone having deuterium at the 2-position (**199**; E = D) in 75% yield with 95% deuterium incorporation. Aldehydes and benzoyl chloride gave the desired products in 60–70% yields. Alkylation of the enolate intermediate (**198**) was successfully carried out with alkyl halides in the presence of HMPA in good yields. The reaction with ethyl chloroformate and chlorotriethylsilane gave enol carbonate (**200**) and silyl enol ether (**201**) in 74 and 75% yield, respectively.

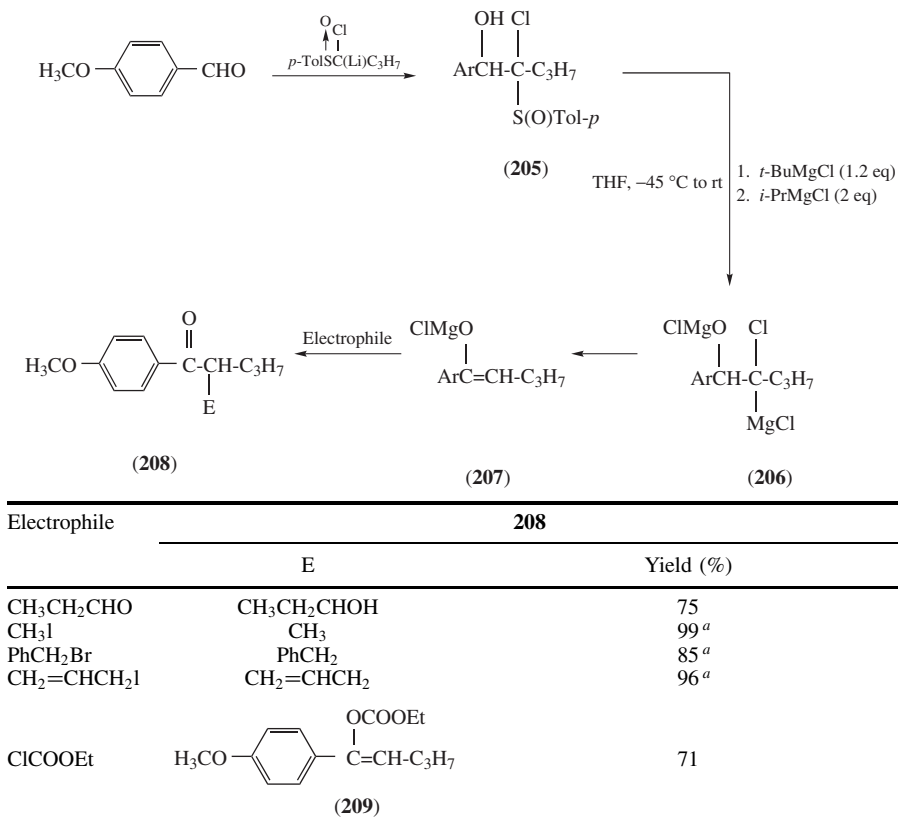
This chemistry was found to be applicable to large-membered cyclic ketones, for example cyclopentadecanone, and selected results are shown in Scheme 7. The reaction of  $\alpha$ -sulfinyl lithium carbanion of 1-chloroethyl *p*-tolyl sulfoxide gave the adduct in almost quantitative yield. The adduct was treated with *tert*-butylmagnesium chloride followed by isopropylmagnesium chloride to result in the formation of magnesium  $\beta$ -oxido carbenoid **202**. The  $\beta$ -oxido carbenoid rearrangement then takes place to give one-carbon expanded magnesium enolate **203**. Quenching of this enolate intermediate with propanal afforded  $\alpha,\alpha$ -disubstituted cyclohexadecanone (**204**) in 73% yield. Benzoyl chloride gave  $\alpha$ -benzoylated ketone (**204**; E = C(=O)Ph) in 71% yield. Interestingly, the reaction with ethyl chloroformate gave not the enol carbonate but an  $\alpha$ -ethoxycarbonylated product (**204**; E = COOEt), though the yield was not satisfactory.



SCHEME 7

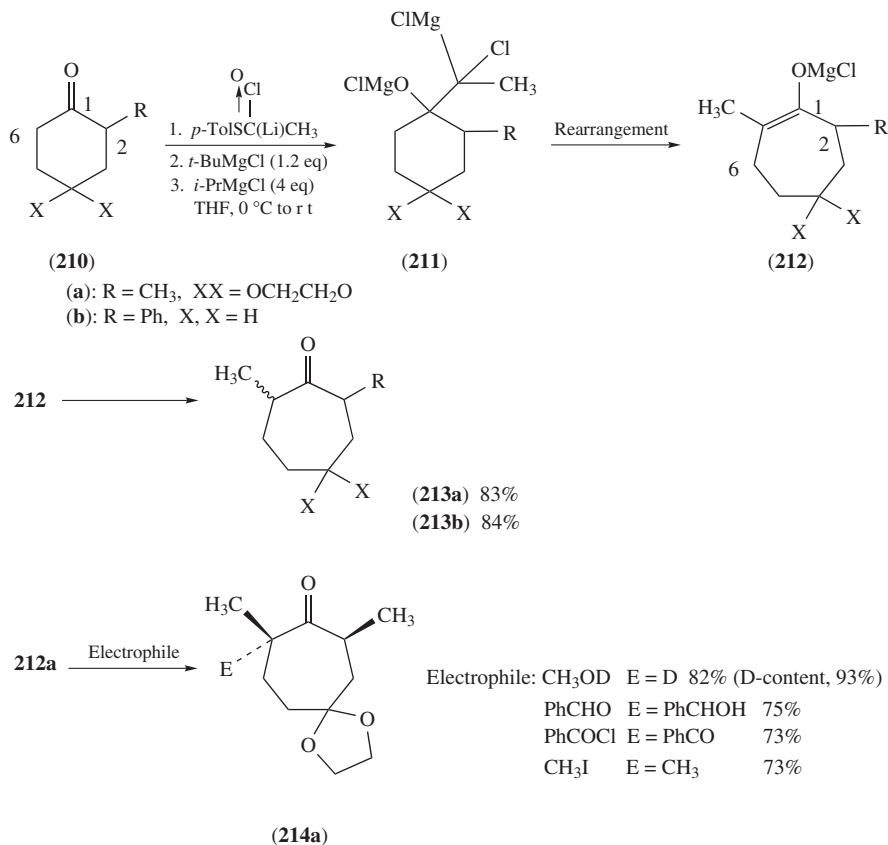
The chemistry mentioned above could also be applied to aldehydes. As an example, *p*-anisaldehyde and 1-chlorobutyl *p*-tolyl sulfoxide were used as shown in Table 16. Thus, treatment of  $\alpha$ -sulfinyl lithium carbanion of 1-chlorobutyl *p*-tolyl sulfoxide with



TABLE 16. Synthesis of  $\alpha$ -substituted ketones (**208**) from *p*-anisaldehyde, 1-chlorobutyl *p*-tolyl sulfoxide and electrophiles<sup>a</sup> HMPA was added as an additive.

*p*-anisaldehyde gave a mixture of two diastereoisomers (**205**) in quantitative yield. Treatment of the main isomer with *tert*-butylmagnesium chloride followed by isopropylmagnesium chloride resulted in the formation of magnesium  $\beta$ -oxido carbenoid **206**. In this case, rearrangement of the hydrogen on the carbon bearing the oxygen took place to give magnesium enolate **207**. Quenching this enolate intermediate with propanal gave the desired  $\alpha$ -substituted ketone (**208**) in 75% yield. Alkylation of the enolate **207** with iodomethane, benzyl bromide and allyl iodide gave  $\alpha$ -alkylated ketones **208** in good to quantitative yields. The reaction of the enolate **207** with ethyl chloroformate gave again the enol carbonate **209** in 71% yield.

Application of the method described above to unsymmetrical cyclic ketones such as 2-substituted cyclohexanones gave 2,7-disubstituted and 2,2,7-trisubstituted cycloheptanones (Scheme 8)<sup>52</sup>. Treatment of  $\alpha$ -sulfinyl lithium carbanion of 1-chloroethyl *p*-tolyl sulfoxide with 2-substituted cyclohexanones (**210a** and **210b**) afforded adducts as a mixture of two diastereomers. The main adducts were first treated with *t*-BuMgCl followed by *i*-PrMgCl (4 equiv) at 0°C to room temperature to give the magnesium  $\beta$ -oxido carbenoid **211**. The



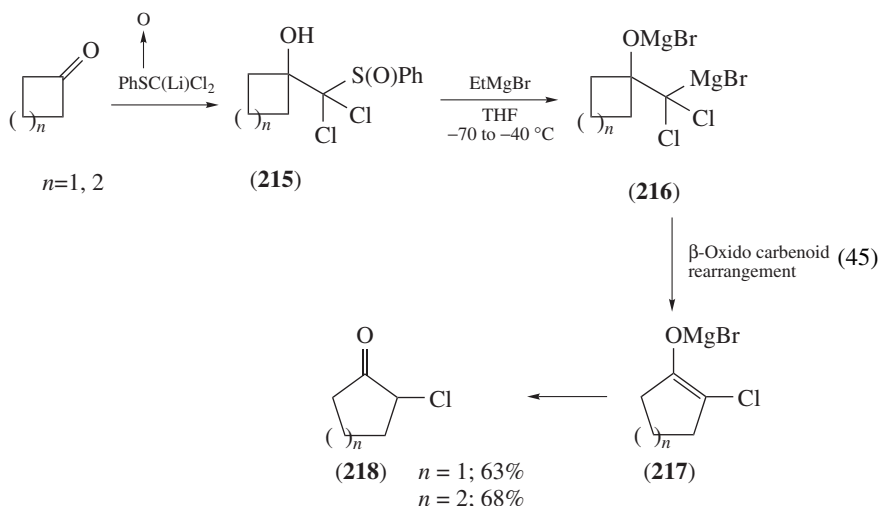
SCHEME 8

$\beta$ -oxido carbenoid rearrangement then took place to afford one-carbon ring-expanded magnesium enolates **212**. Hydrolysis of the magnesium enolate afforded 2,7-disubstituted cycloheptanone derivatives **213a** and **213b** in 83 and 84% yields, respectively.

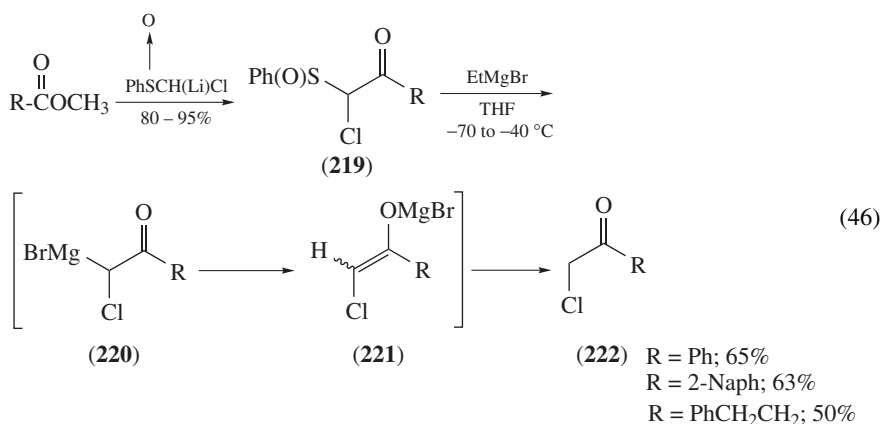
Interestingly, the formation of **213** implies that the carbon–carbon insertion took place between the carbons C<sub>1</sub> and C<sub>6</sub> of the starting cyclohexanone (**210**). The migrating group is not the same as that usually reported in this type of rearrangement<sup>48</sup>. In addition, magnesium enolate intermediate **212** could be trapped with several electrophiles such as benzaldehyde, benzoyl chloride and iodomethane to give 2,2,7-trisubstituted cycloheptanones (**214a**) in good yields. This method is very useful for the synthesis of 2,7-disubstituted and 2,2,7-trisubstituted cycloheptanones from 2-substituted cyclohexanones with one-carbon ring-expansion in only two chemical steps.

Using dichloromethyl phenyl sulfoxide in this procedure as a one-carbon homologating agent gave interesting results (equation 45)<sup>53</sup>. Thus, treatment of the  $\alpha$ -sulfinyl lithium carbanion of dichloromethyl phenyl sulfoxide at  $-60^\circ\text{C}$  with cyclobutanone and cyclopentanone gave the adducts **215** in almost quantitative yields. The sulfoxide–magnesium exchange reaction of the adducts **215** with EtMgBr gave magnesium  $\beta$ -oxido carbenoids

**216.** The  $\beta$ -oxido carbenoid rearrangement then took place to give one-carbon expanded magnesium enolate having a chlorine atom (**217**), which was treated with water to afford  $\alpha$ -chloroketone (**218**) in moderate yield. Unfortunately, this method could not be applied to larger cycloalkanones and acyclic ketones. Application of this method to aldehydes gave chloromethyl aryl ketones and chloromethyl alkyl ketones in moderate yields<sup>53</sup>.



Finally, magnesium carbenoid  $\alpha$  to carbonyl moiety was reported (equation 46)<sup>53</sup>. The  $\alpha$ -sulfinyl lithium carbanion of chloromethyl phenyl sulfoxide was reacted with methyl esters to give  $\alpha$ -chloro- $\alpha$ -sulfinylmethyl ketones (**219**) in 80–95% yields. Treatment of **219** with EtMgBr in THF at low temperature resulted in the formation of magnesium carbenoid **220** and  $\alpha$ -chloroketones **222** in moderate yields after hydrolysis. Obviously, the sulfoxide–magnesium exchange reaction of **219** proceeded to give magnesium carbenoid **220**; however, Wolff-type rearrangement does not take place, but instead, magnesium enolates (**221**) were produced in this reaction.



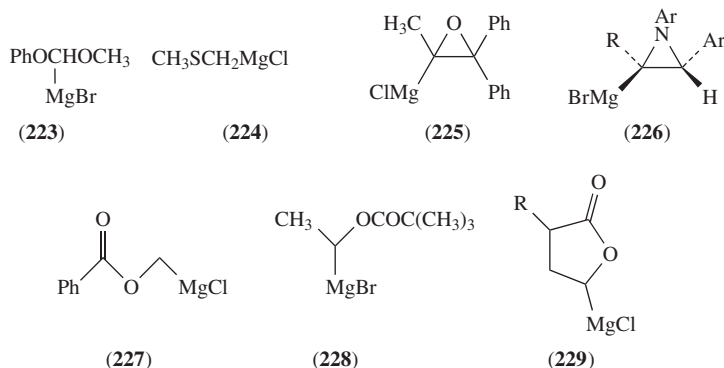


FIGURE 3

### VII. OTHER MAGNESIUM CARBENOIDS

Some other  $\alpha$ -heteroatom-substituted Grignard reagents, such as magnesioacetal (**223**)<sup>54</sup>, methylthiomethyl Grignard reagent **224**<sup>55</sup>, oxiranyl Grignard reagent **225**<sup>56</sup>, aziridinyl-magnesium halide (**226**)<sup>57</sup>, functionalized magnesim carbenoids **227** and **228**<sup>58</sup> and  $\gamma$ -magnesio- $\gamma$ -butyrolactones (**229**)<sup>59</sup>, have been reported (Figure 3).

In some cases, they act as magnesium carbenoids; however, they usually react as  $\alpha$ -heterosubstituted Grignard reagents. Therefore, the author will not address the chemistry of these  $\alpha$ -heteroatom-substituted Grignard reagents in detail.

### VIII. CONCLUSIONS AND PERSPECTIVE

As outlined in this chapter, magnesium carbenoids are relatively stable compounds as compared to the corresponding lithium carbenoids. Therefore, we can prepare the corresponding carbenoids in a similar way to the usual preparation of more classical Grignard reagents. Generation of the magnesium carbenoids can be performed mainly in two ways: the halogen–magnesium exchange and the sulfoxide–magnesium exchange reactions at low temperature, usually at  $-78^\circ\text{C}$ . As mentioned above, the preparation of magnesium carbenoids, from sulfoxides having a halogen on the  $\alpha$ -position using the sulfoxide–magnesium exchange reaction, has a much higher versatility than the halogen–magnesium exchange reaction. The magnesium carbenoids show both nucleophilic and electrophilic properties; however, the electrophilic reaction of the magnesium carbenoids is far more interesting for synthetic purposes as mentioned above.

The chemistry of magnesium carbenoids started practically in the last 20 years; in other words, it is rather a new field in chemistry. Many new and interesting results will be forthcoming from this field.

### IX. REFERENCES

1. In this chapter, the term 'carbenoid' is suggested for the description of intermediates which exhibit reactions qualitatively similar to those of free carbenes.
2. Some monographs and reviews concerning carbenes and carbenoids:
  - (a) W. Kirmse, *Carbene Chemistry*, Academic Press, New York, 1971.
  - (b) F. Z. Dorwald, *Metal Carbenes in Organic Synthesis*, Wiley-VCH, Weinheim, 1999.
  - (c) G. Bertrand (Ed.), *Carbene Chemistry*, Marcel Dekker, New York, 2002.
  - (d) G. Kobrich, *Angew. Chem., Int. Ed. Engl.*, **11**, 473 (1972).

- (e) P. J. Stang, *Chem. Rev.*, **78**, 383 (1978).  
(f) S. D. Burke and P. A. Grieco, *Org. React.*, **26**, 361 (1979).  
(g) H. F. Schaefer III, *Acc. Chem. Res.*, **12**, 288 (1979).  
(h) H. Wynberg and E. W. Meijer, *Org. React.*, **28**, 1 (1982).  
(i) A. Oku and T. Harada, *J. Synth. Org. Chem. Jpn.*, **44**, 736 (1986).  
(j) A. Oku, *J. Synth. Org. Chem. Jpn.*, **48**, 710 (1990).  
(k) A. Padwa and K. E. Krumpe, *Tetrahedron*, **48**, 5385 (1992).  
(l) A. Padwa and M. D. Weingarten, *Chem. Rev.*, **96**, 223 (1996).  
(m) M. Braun, *Angew. Chem. Int. Ed.*, **37**, 430 (1998).
3. D. Seyferth, R. L. Lambert, Jr. and E. M. Hanson, *J. Organomet. Chem.*, **24**, 647 (1970).  
4. R. W. Hoffmann and A. Kusche, *Chem. Ber.*, **127**, 1311 (1994).  
5. V. Schulze, P. G. Nell, A. Burton and R. W. Hoffmann, *J. Org. Chem.*, **68**, 4546 (2003).  
6. V. Schulze, M. Bronstrup, V. P. W. Bohm, P. Schwerdtfeger, M. Schimeczek and R. W. Hoffmann, *Angew. Chem. Int. Ed.*, **37**, 824 (1998).  
7. V. Schulze, R. Lowe, S. Fau and R. W. Hoffmann, *J. Chem. Soc., Perkin Trans. 2*, 463 (1998).  
8. (a) S. Oae, *Reviews on Heteroatom Chemistry*, MYU, Tokyo, **4**, 196 (1991).  
(b) B. J. Wakefield, *Organomagnesium Methods in Organic Synthesis*, Academic Press, London, 1995, p. 58.
9. (a) H. Uno, F. Semba, T. Tasaka and H. Suzuki, *Chem. Lett.*, 309 (1989).  
(b) H. Uno, K. Sakamoto, F. Semba and H. Suzuki, *Bull. Chem. Soc. Jpn.*, **65**, 210 (1992).  
(c) H. Uno, K. Sakamoto, F. Semba and H. Suzuki, *Bull. Chem. Soc. Jpn.*, **65**, 218 (1992).
10. (a) T. Satoh and K. Takano, *Tetrahedron*, **52**, 2349 (1996).  
(b) T. Satoh, *J. Synth. Org. Chem. Jpn.*, **61**, 98 (2003).
11. (a) T. Satoh, T. Oohara, Y. Ueda and K. Yamakawa, *Tetrahedron Lett.*, **29**, 313 (1988).  
(b) T. Satoh, T. Oohara, Y. Ueda and K. Yamakawa, *J. Org. Chem.*, **54**, 3130 (1989).
12. R. W. Hoffmann and P. G. Nell, *Angew. Chem. Int. Ed.*, **38**, 338 (1999).  
13. P. R. Blakemore, S. P. Marsden and H. D. Vater, *Org. Lett.*, **8**, 773 (2006).
14. (a) A. Hassner and C. Stumer, *Organic Synthesis Based on Name Reactions*, Second edition, Pergamon, Amsterdam, 2002.  
(b) B. P. Mundy, M. G. Ellerd and F. G. Favaloro, Jr., *Name Reactions and Reagents in Organic Synthesis*, Second edition, Wiley-Interscience, New York, 2005.  
(c) L. Kurti and B. Czako, *Strategic Applications of Named Reactions in Organic Synthesis*, Elsevier, Amsterdam, 2005.
15. C. Bolm and D. Pupowicz, *Tetrahedron Lett.*, **42**, 7349 (1997).  
16. R. C. Hahn and J. Tompkins, *Tetrahedron Lett.*, **31**, 973 (1990).  
17. R. W. Hoffmann, O. Knopff and A. Kusche, *Angew. Chem. Int. Ed.*, **39**, 1462 (2000).  
18. T. Satoh, A. Kondo and J. Musashi, *Tetrahedron*, **60**, 5453 (2004).  
19. M. Pohmakotr, W. Jeawsuwan, P. Tuchinda, P. Kongsaree, S. Prabpai and V. Reutrakul, *Org. Lett.*, **6**, 4547 (2004).
20. R. W. Hoffmann, B. Holzer, O. Knopff and K. Harms, *Angew. Chem. Int. Ed.*, **39**, 3072 (2000).  
21. B. Holzer and R. W. Hoffmann, *Chem. Commun.*, 732 (2003).  
22. R. W. Hoffmann, *Chem. Soc. Rev.*, **32**, 225 (2003).  
23. C. D. Lima, M. Julia and J.-N. Verpeaux, *Synlett*, 133 (1992).  
24. J. L. G. Ruano, S. A. Alonso de Diego, M. R. Martin, E. Torrente and A. M. M. Castro, *Org. Lett.*, **6**, 4945 (2004).
25. (a) T. Satoh, A. Osawa and A. Kondo, *Tetrahedron Lett.*, **45**, 6703 (2004).  
(b) T. Satoh, A. Osawa, T. Ohbayashi and A. Kondo, *Tetrahedron*, **62**, 7892 (2006).
26. (a) S. V. Kessar and P. Singh, *Chem. Rev.*, **97**, 721 (1997).  
(b) A. R. Katritzky and M. Qi, *Tetrahedron*, **54**, 2647 (1998).  
(c) W. H. Pearson and P. Stoy, *Synlett*, 903 (2003).
27. T. Satoh, J. Musashi and A. Kondo, *Tetrahedron Lett.*, **46**, 599 (2005).  
28. J. Clayden and M. Julia, *Synlett*, 103 (1995).  
29. T. Satoh, S. Ogata and D. Wakasugi, *Tetrahedron Lett.*, **47**, 7249 (2006).  
30. O. Knopff, C. Stiasny and R. W. Hoffmann, *Organometallics*, **23**, 705 (2004).  
31. P. D. Gardner and M. Narayana, *J. Org. Chem.*, **26**, 3518 (1961).  
32. T. Satoh, T. Kurihara and K. Fujita, *Tetrahedron*, **57**, 5369 (2001).  
33. V. A. Vu, I. Marek, K. Polborn and P. Knochel, *Angew. Chem. Int. Ed.*, **41**, 351 (2002).  
34. F. Kopp, G. Sklute, K. Polborn, I. Marek and P. Knochel, *Org. Lett.*, **7**, 3789 (2005).

35. T. Satoh and S. Saito, *Tetrahedron Lett.*, **45**, 347 (2004).
36. T. Satoh, M. Miura, K. Sakai and Y. Yokoyama, *Tetrahedron*, **62**, 4253 (2006).
37. P. J. Stang, *Chem. Rev.*, **78**, 383 (1978).
38. T. Satoh, Y. Hayashi and K. Yamakawa, *Bull. Chem. Soc. Jpn.*, **66**, 1866 (1993).
39. (a) T. Satoh, K. Takano, H. Someya and K. Matsuda, *Tetrahedron Lett.*, **36**, 7097 (1995).  
(b) T. Satoh, K. Takano, H. Ota, H. Someya, K. Matsuda and M. Koyama, *Tetrahedron*, **54**, 5557 (1998).
40. V. A. Vu, I. Marek and P. Knochel, *Synthesis*, 1797 (2003).
41. (a) T. Satoh, T. Sakamoto and M. Watanabe, *Tetrahedron Lett.*, **43**, 2043 (2002).  
(b) T. Satoh, T. Sakamoto, M. Watanabe and K. Takano, *Chem. Pharm. Bull.*, **51**, 966 (2003).
42. (a) T. Satoh, Y. Ogino and M. Nakamura, *Tetrahedron Lett.*, **45**, 5785 (2004).  
(b) T. Satoh, Y. Ogino and K. Ando, *Tetrahedron*, **61**, 10262 (2005).
43. T. Satoh, J. Sakurada and Y. Ogino, *Tetrahedron Lett.*, **46**, 4855 (2005).
44. M. Watanabe, M. Nakamura and T. Satoh, *Tetrahedron*, **61**, 4409 (2005).
45. T. Satoh, *The Chemical Record*, The Japan Chemical Journal Forum and Wiley Periodicals, Inc. **3**, 329 (2004).
46. (a) O. W. Lever, Jr., *Tetrahedron*, **32**, 1943 (1976).  
(b) S. F. Martin, *Synthesis*, 633 (1979).  
(c) J. C. Stowell, *Chem. Rev.*, **84**, 409 (1984).  
(d) N. F. Badham, *Tetrahedron*, **60**, 11 (2004).
47. (a) G. R. Krow, *Tetrahedron*, **43**, 3 (1987).  
(b) M. Hesse, *Ring Enlargement in Organic Chemistry*, Wiley-VCH, Weinheim, 1991.  
(c) P. Dowd and W. Zhang, *Chem. Rev.*, **93**, 2091 (1993).
48. (a) H. Taguchi, H. Yamamoto and H. Nozaki, *J. Am. Chem. Soc.*, **96**, 6510 (1974).  
(b) H. Taguchi, H. Yamamoto and H. Nozaki, *Tetrahedron Lett.*, 2617 (1976).  
(c) H. Taguchi, H. Yamamoto and H. Nozaki, *Bull. Chem. Soc. Jpn.*, **50**, 1592 (1977).  
(d) J. Villieras, P. Perriot and J. F. Normant, *Synthesis*, 968 (1979).  
(e) H. D. Ward, D. S. Teager and R. K. Murray, Jr., *J. Org. Chem.*, **57**, 1926 (1992).
49. W. D. Abraham, M. Bhupathy and T. Cohen, *Tetrahedron Lett.*, **28**, 2203 (1987).
50. (a) T. Satoh, N. Itoh, K. Gengyo and K. Yamakawa, *Tetrahedron Lett.*, **33**, 7543 (1992).  
(b) T. Satoh, N. Itoh, K. Gengyo, S. Takada, N. Asakawa, Y. Yamani and K. Yamakawa, *Tetrahedron*, **50**, 11839 (1994).
51. (a) T. Satoh and K. Miyashita, *Tetrahedron Lett.*, **45**, 4859 (2004).  
(b) K. Miyashita and T. Satoh, *Tetrahedron*, **61**, 5067 (2005).
52. T. Satoh, S. Tanaka and N. Asakawa, *Tetrahedron Lett.*, **47**, 6769 (2006).
53. T. Satoh, Y. Mizu, T. Kawashima and K. Yamakawa, *Tetrahedron*, **51**, 703 (1995).
54. I. Tabushi, K. Takagi and R. Oda, *Nippon Kagaku Zasshi*, **85**, 302 (1964); *Chem. Abstr.*, **61**, 13226g (1964).
55. K. Ogura, M. Fujita, K. Takahashi and H. Iida, *Chem. Lett.*, 1697 (1982).
56. T. Satoh, S. Kobayashi, S. Nakanishi, K. Horiguchi and S. Irida, *Tetrahedron*, **55**, 2515 (1999).
57. (a) T. Satoh, R. Matsue, T. Fujii and S. Morikawa, *Tetrahedron Lett.*, **41**, 6495 (2000).  
(b) T. Satoh, R. Matsue, T. Fujii and S. Morikawa, *Tetrahedron*, **57**, 3891 (2001).
58. S. Avolio, C. Malan, I. Marek and P. Knochel, *Synlett*, 1820 (1999).
59. S. Sugiyama, H. Shimizu and T. Satoh, *Tetrahedron Lett.*, **47**, 8771 (2006).

## CHAPTER 17

# Catalytic enantioselective conjugate addition and allylic alkylation reactions using Grignard reagents

FERNANDO LÓPEZ

*Departamento de Química Orgánica, Facultad de Química, Universidad de Santiago de Compostela, Avda. de las ciencias, s/n, 15782, Santiago de Compostela, Spain  
e-mail: qofer@usc.es*

and

ADRIAAN J. MINNAARD and BEN L. FERINGA

*Stratingh Institute for Chemistry, University of Groningen, Nijenborgh 4, 9747 AG Groningen, The Netherlands*

*Fax: ++31 503634296; e-mails: A.J.Minnaard@rug.nl and B.L.Feringa@rug.nl*

---

I. INTRODUCTION .....	772
II. ENANTIOSELECTIVE CONJUGATE ADDITION TO CYCLIC ENONES .....	774
III. ENANTIOSELECTIVE CONJUGATE ADDITION TO ACYCLIC ENONES .....	779
IV. ENANTIOSELECTIVE CONJUGATE ADDITION TO $\alpha,\beta$ -UNSATURATED ESTERS AND THIOESTERS .....	779
V. APPLICATION OF THE CONJUGATE ADDITION OF GRIGNARD REAGENTS TO $\alpha,\beta$ -UNSATURATED THIOESTERS IN THE SYNTHESIS OF NATURAL PRODUCTS .....	786
VI. MECHANISTIC STUDIES .....	788
VII. ENANTIOSELECTIVE ALLYLIC ALKYLATION WITH GRIGNARD REAGENTS .....	791
VIII. CONCLUSIONS .....	798
IX. REFERENCES AND NOTES .....	800

---

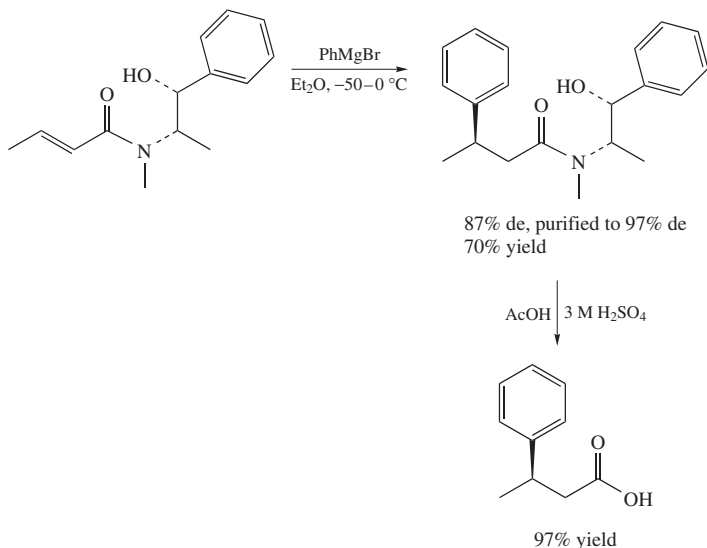
*The chemistry of organomagnesium compounds*

Edited by Z. Rappoport and I. Marek © 2008 John Wiley & Sons, Ltd. ISBN: 978-0-470-05719-3

## I. INTRODUCTION

The conjugate addition of organometallic reagents to  $\alpha,\beta$ -unsaturated compounds is one of the basic methods in our repertoire for the construction of carbon–carbon bonds<sup>1</sup>. These addition reactions have been used as key steps in the synthesis of numerous biologically active compounds, and show a broad scope due to the large variety of donor and acceptor compounds that can be employed. It is evident that a tremendous effort has been devoted over the last three decades to develop asymmetric variants of this reaction<sup>2</sup>.

The first successful approaches were based on the, often Cu-mediated, conjugate addition of organolithium and organomagnesium (Grignard) reagents to  $\alpha,\beta$ -unsaturated systems covalently modified with chiral auxiliaries (Scheme 1)<sup>3</sup><sup>4</sup>.



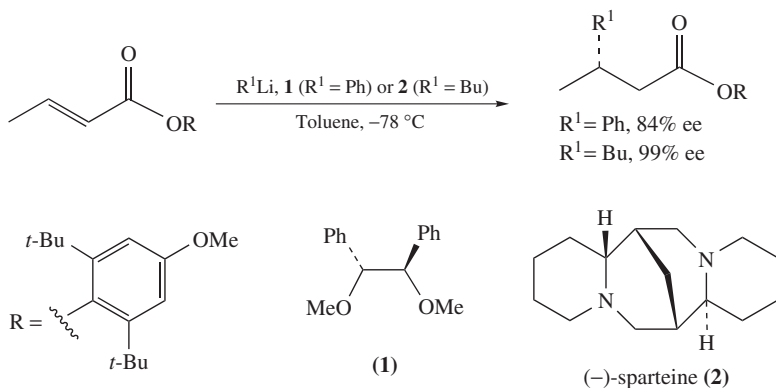
SCHEME 1. Asymmetric conjugate addition of Grignard reagents to substrates containing chiral auxiliaries

Other strategies made use of organocopper compounds with chiral nontransferable groups, such as chiral alkoxycuprates and amidocuprates<sup>2,4</sup>. For instance, Corey and coworkers reported in 1986 enantioselectivities of over 90% by using a chiral ephedrine-derived alkoxycuprate<sup>5</sup>. The use of organolithium reagents in the presence of stoichiometric amounts of chiral ether **1** or amine **2** ligands was also explored, providing high enantioselectivities in the conjugate addition to  $\alpha,\beta$ -unsaturated *N*-cyclohexylimines and sterically crowded esters (Scheme 2)<sup>6</sup>.

Although some of these strategies provide high enantioselectivities with a number of substrates, the development of catalytic rather than stoichiometric processes is the main challenge in order to provide truly efficient synthetic methods.

It was not until the late 1980s that the feasibility of a catalytic ( $\leq 10$  mol% chiral catalyst) and enantioselective conjugate addition was demonstrated. Lippard and coworkers reported the first enantioselective conjugate addition of a Grignard reagent to an enone, using catalytic amounts of Cu–amide complex **3** (Figure 1)<sup>7</sup>. Subsequently, a variety of catalytic systems, based on, e.g., Cu thiolates **4–7**<sup>8</sup>, and phosphine–oxazoline ligand **8**<sup>9</sup>, was introduced for the conjugate addition of Grignard reagents. Although the





SCHEME 2. Asymmetric conjugate addition of organolithium reagents with stoichiometric chiral ligands. Adapted with permission from *Acc. Chem. Res.*, **40**, 179–188 (2007). Copyright 2007 American Chemical Society

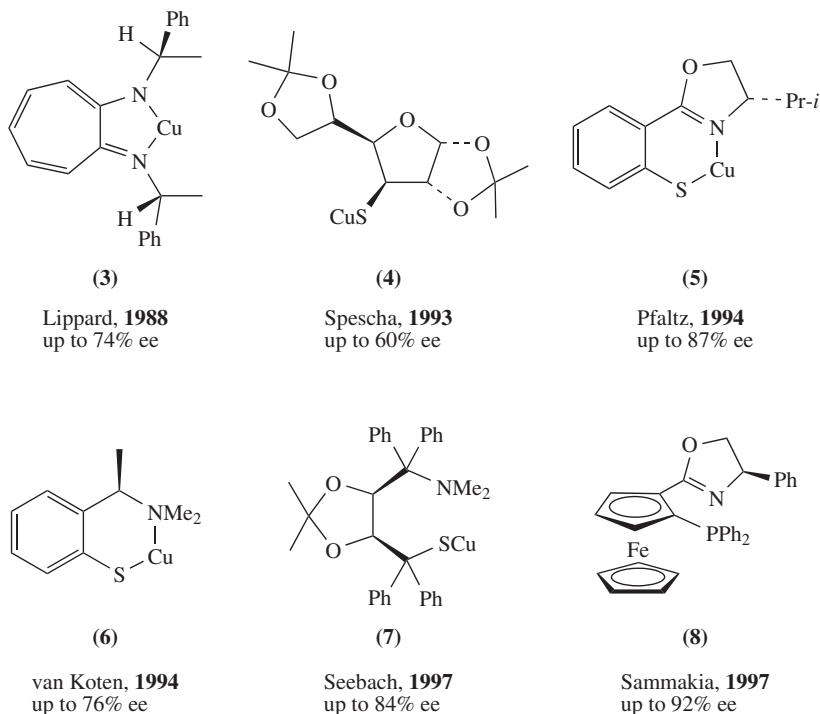


FIGURE 1. Selected catalysts developed for the conjugate addition of Grignard reagents to enones. Adapted with permission from *Acc. Chem. Res.*, **40**, 179–188 (2007). Copyright 2007 American Chemical Society

scope remained limited and ee values infrequently reached the 90% level (Figure 1), high enantioselectivity (92%) was observed in two examples for ligand **8**. Despite the fact that the parameters governing the stereocontrol were not completely clear, these excellent contributions provided an important basis to allow the development of the catalytic methodology.

The development of a catalytic enantioselective method for the conjugate addition of Grignard reagents was for a long time hampered by the reactivity of the Grignard which causes a fast uncatalyzed reaction. In addition, organomagnesium reagents are 'hard' nucleophiles which as such prefer direct addition above conjugate addition<sup>1,2,10</sup>. Therefore, the development of catalytic conjugate addition reactions using less reactive organometallics such as organozinc, organocopper, organoaluminum, or arylboron and arylsilicon reagents dominated. These reagents are used with catalysts based on copper, rhodium, palladium, nickel and cobalt.

Early work by Soai and coworkers showed the viability of performing the conjugate addition of dialkylzinc reagents to enones with modest enantioselectivities using sub-stoichiometric amounts of chiral complexes of Ni and Co<sup>11</sup>. Dialkylzinc reagents have distinct advantages compared to Grignard reagents, because they show low reactivity in the uncatalyzed reaction and a high tolerance of functional groups, both in the substrate and zinc reagent. A Cu-catalyzed conjugate addition of Et<sub>2</sub>Zn to 2-cyclohexenone with 32% ee was subsequently reported<sup>12</sup>. The discovery by Feringa and coworkers in 1996 that chiral monodentate phosphoramidites are excellent ligands for the asymmetric Cu-catalyzed conjugate addition of R<sub>2</sub>Zn reagents<sup>13</sup> led to a method for the highly enantioselective Cu-catalyzed conjugate addition of dialkylzinc reagents to enones<sup>14,15</sup>. This, in turn, stimulated the development of a broad range of efficient phosphorus-based catalysts for the Cu-catalyzed conjugate addition of dialkylzinc reagents. In addition, this methodology found application in natural product synthesis<sup>16–20</sup>.

Complementary to the use of zinc reagents for the introduction of (functionalized) alkyl groups is the rhodium-catalyzed conjugate addition of aryl- and alkenylboron reagents. This method rapidly became popular, also because arylboron reagents are air and moisture stable and a large variety of them is commercially available<sup>21</sup>.

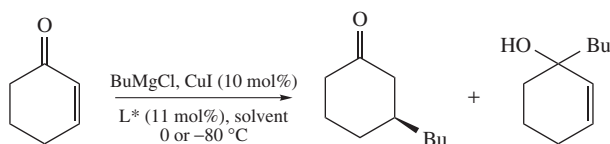
The efficiency of dialkylzinc and boron reagents in the catalytic enantioselective conjugate addition clearly displaced for a number of years the use of Grignard reagents in this transformation<sup>22</sup>. Compared to dialkylzinc reagents, Grignard reagents are known to show lower functional group tolerance, although recently considerable advances have been made in the use of functionalized organomagnesium compounds<sup>23</sup>. Nevertheless, there are significant incentives to use Grignard reagents instead of dialkylzinc or organoboron compounds. Grignard reagents are cheap and readily available from all kinds of alkyl, alkenyl, aryl and alkynyl halides. This is in contrast to diorganozincs. In fact, as most zinc and boron reagents themselves originate from the corresponding Grignard, it serves atom economy to use the latter reagents directly. For large-scale synthesis, Grignard reagents are preferred over organozincs for environmental reasons and are commonly used in fine chemical and pharmaceutical industries. A disadvantage of the conjugate addition of boronic acids is the concomitant protonation of the resulting enolate that precludes its use in tandem reactions<sup>24</sup>.

## II. ENANTIOSELECTIVE CONJUGATE ADDITION TO CYCLIC ENONES

Most ligands used so far in the field of the copper-catalyzed conjugate addition of Grignard reagents combine phosphorus, sulfur or selenium with nitrogen or oxygen donor atoms in their structure, to coordinate selectively with copper and magnesium of the organometallic species, respectively<sup>8,9,25</sup>. The fact that free Cu salts show high activity in the conjugate addition of Grignard reagents, even at low temperature, makes tight binding of Cu ions by

bidentate ligands probably essential to avoid a nonselective background reaction. Interestingly, although chiral diphosphine ligands have dominated the field of asymmetric catalysis in the last 30 years<sup>26</sup>, until very recently none of these ligands was reported to be effective in the conjugate addition of Grignard reagents. *A priori*, diphosphines would not match with the metal-differentiating coordination concept, although in several of these diphosphine ligands the two phosphorus atoms have very different electronic and steric properties<sup>27</sup>.

In 2004, our group reported the highly regio- and enantioselective conjugate addition of Grignard reagents using copper catalysts with ferrocenyl-based diphosphine ligands. Where bidentate phosphines such as BINAP, Trost ligand and DuPHOS led to poor enantioselectivities in the model reaction (5–28% ee) (Scheme 3, Figure 2), promising enantioselectivities (45–70% ee) were obtained with MandypHos, Walphos and Josiphos. Among the ferrocenyl ligands, Taniaphos<sup>28</sup> (Figure 2), provided in the preliminary screening the highest enantioselectivity (95% ee), although with modest regioselectivity (conjugate addition *versus* direct addition = 60:40).



SCHEME 3. Enantioselective copper-catalyzed addition of butylmagnesium chloride to 2-cyclohexenone

Optimization of the reaction parameters led to conditions using 5 mol% of CuCl, 6 mol% of Taniaphos and 1.15 equiv of EtMgBr in Et<sub>2</sub>O at 0 °C, which afforded full conversion in 15 min with a regioselectivity of 95% and an excellent 96% ee<sup>29</sup>. The results with a variety of Grignard reagents using these optimal conditions are shown in Table 1.

The products were obtained with 90–96% ee using RMgBr reagents with linear alkyl chains (R = Me, *n*-Pr, *n*-Bu). Employing Grignard reagents with branched alkyl chains, a strong influence of the substitution pattern on the enantioselectivity was observed. In particular, the incorporation of isopropyl and isobutyl fragments resulted in poor ee values, although isoamylmagnesium bromide afforded the corresponding 1,4-addition product with 95% ee. Noteworthy is that, with the  $\alpha$ - and  $\beta$ -branched Grignard reagents *i*-PrMgBr and *i*-BuMgBr, Josiphos provides excellent regiocontrol (99%) with moderate to high (54%–92%) enantioselectivities. Contrary to Taniaphos, Josiphos is more effective at low temperatures (e.g. –60 °C *vs* 0 °C) and in combination with CuBr•SMe<sub>2</sub> instead of CuCl.

Therefore, the proper selection of Taniaphos or Josiphos in a complementary way allows the use of a broad range of Grignard reagents. Moreover, the reaction turned out to be not limited to cyclohexenone, as other cyclic enones as well as lactones provided high levels of regio- and enantioselectivity (Figure 3)<sup>29</sup>.

Recently, diaminocarbenes, also called NHCs (for *N*-heterocyclic carbenes), have been shown to be a viable alternative to phosphorus ligands. Almost simultaneously, both the copper/NHC-catalyzed enantioselective conjugate addition of dialkylzincs<sup>30</sup> and Grignard reagents to 3-substituted enones was reported. For the Grignard addition reactions, the groups of Mauduit, Alexakis and coworkers<sup>31</sup> studied a series of chiral imidazolium salts as precatalysts, whereupon **9** and **10** turned out to be the most efficient (Figure 4). Good yields and high to excellent enantioselectivities were obtained (Table 2) apparently in the complete absence of direct addition product.

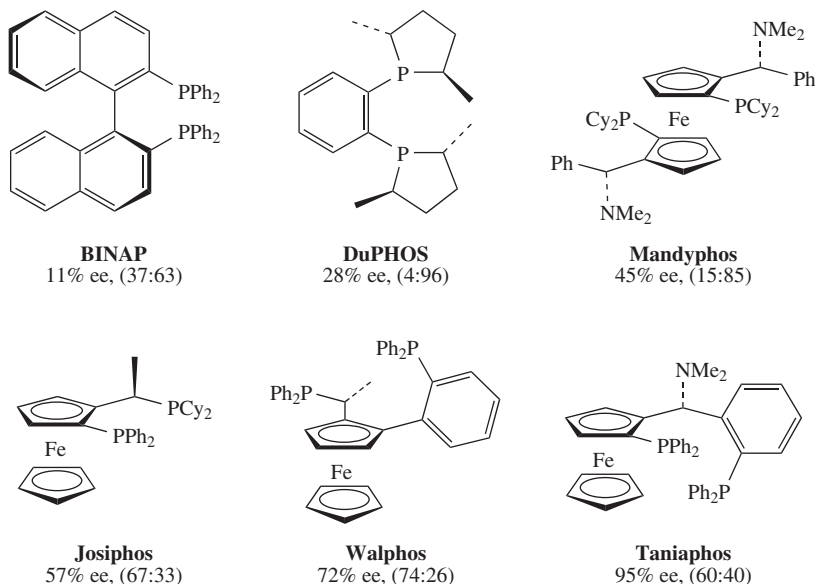


FIGURE 2. Selectivity of several diphosphine ligands in the model reaction. In parentheses, regioselectivity: (conjugate addition versus direct addition). Adapted with permission from *Acc. Chem. Res.*, **40**, 179–188 (2007). Copyright 2007 American Chemical Society

TABLE 1. Enantioselective copper-catalyzed conjugate addition of Grignard reagents to 2-cyclohexenone<sup>a,b</sup>

RMgBr	L*	1,4:1,2	ee (%) (1,4)
EtMgBr	Taniaphos	95:5	96
MeMgBr	Taniaphos	83:17	90
<i>n</i> -PrMgBr	Taniaphos	81:19	94
<i>n</i> -BuMgBr	Taniaphos	88:12	96
<i>i</i> -PrMgBr	Taniaphos	78:22	1
<i>i</i> -BuMgBr	Taniaphos	62:38	33
MgBr	Taniaphos	76:24	95
<i>i</i> -PrMgBr <sup>c</sup>	Josiphos	99:1	54
<i>i</i> -BuMgBr <sup>c</sup>	Josiphos	99:1	92
EtMgBr <sup>c</sup>	Josiphos	99:1	56

<sup>a</sup> >98% conversion after 15 min at 0 °C using CuCl.

<sup>b</sup> >98% conversion after 2 h at –60 °C using CuBr•SMe<sub>2</sub>.

<sup>c</sup> Adapted with permission from *Acc. Chem. Res.*, **40**, 179–188 (2007). Copyright 2007 American Chemical Society.

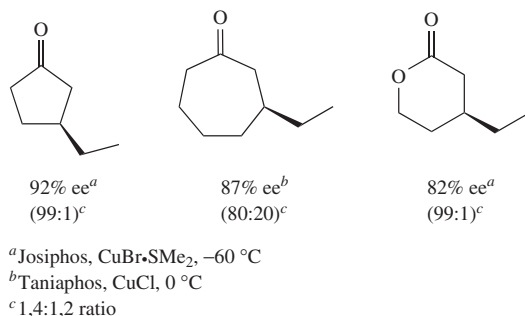


FIGURE 3. Representative examples of conjugate addition products using Cu/ferrocenyl diphosphine catalysts. Adapted with permission from *Acc. Chem. Res.*, **40**, 179–188 (2007). Copyright 2007 American Chemical Society

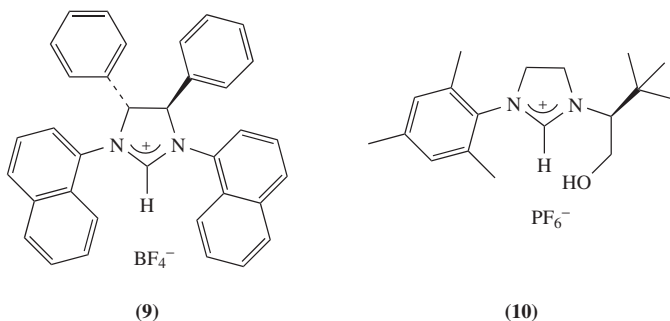
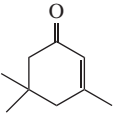
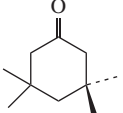
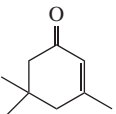
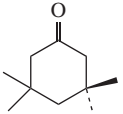
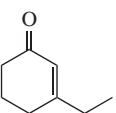
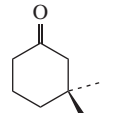
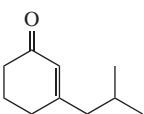
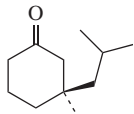
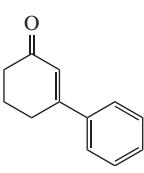
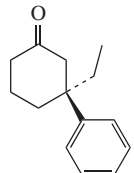
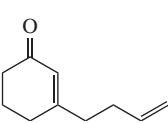
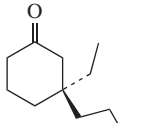
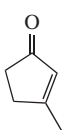
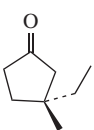
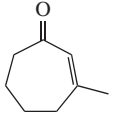
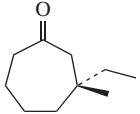


FIGURE 4. Chiral NHC ligands for the enantioselective copper-catalyzed conjugate addition of Grignard reagents

TABLE 2. Cu/NHC-catalyzed addition of Grignard reagents to 3-substituted 2-cyclohexenones

RMgBr	L*	Yield (%)	ee (%)
EtMgBr	<b>9</b>	90	73 ( <i>S</i> )
EtMgBr	<b>10</b>	81	80 ( <i>R</i> )
BuMgBr	<b>10</b>	100 (conv)	77 ( <i>R</i> )
ButenylMgBr	<b>10</b>	80	90 ( <i>S</i> )
<i>i</i> -BuMgBr	<b>10</b>	72	96 ( <i>S</i> )
<i>i</i> -PrMgBr	<b>10</b>	77	77 ( <i>R</i> )
<i>c</i> -pentMgBr	<b>10</b>	80	85 ( <i>S</i> )
<i>c</i> -hexMgBr	<b>10</b>	79	74 ( <i>R</i> )
<i>t</i> -BuMgBr	<b>10</b>	0	
PhMgBr	<b>10</b>	61	66 ( <i>R</i> )

TABLE 3. Cu/NHC-catalyzed addition of Grignard reagents to 3-substituted-2-cycloalkenones

RMgBr	L*	Enone	Yield (%)	ee (%)	Product
EtMgBr	<b>9</b>		57	71 ( <i>S</i> )	
EtMgBr	<b>10</b>		85	82 ( <i>R</i> )	
MeMgBr	<b>10</b>		67	68 ( <i>S</i> )	
EtMgBr	<b>10</b>		69	81 ( <i>S</i> )	
EtMgBr	<b>10</b>		87	72 ( <i>S</i> )	
EtMgBr	<b>10</b>		84	69 ( <i>R</i> )	
EtMgBr	<b>10</b>		90	46 ( <i>R</i> )	
EtMgBr	<b>10</b>		99 (conv)	82 ( <i>R</i> )	

A series of differently substituted cyclic enones was used as substrate. Using a seven-membered ring enone the enantioselectivity remained high, but for a five-membered ring analogue the ee dropped (Table 3).

### III. ENANTIOSELECTIVE CONJUGATE ADDITION TO ACYCLIC ENONES

The method developed for the conjugate addition of Grignard reagents using Cu complexes of ferrocenyl-based diphosphines was subsequently expanded to linear enones<sup>32</sup>. The  $\beta$ -substituted ketones resulting from the conjugate addition to linear enones are common subunits in natural products and important building blocks for the synthesis of physiologically active molecules. A number of procedures for their enantioselective preparation has been reported to date although the enantioselectivities are usually substrate and ligand dependent<sup>19a, 20, 22, 33</sup>.

Initially, the addition of EtMgBr to (*E*)-3-nonen-2-one was investigated, catalyzed by CuCl and Taniaphos (Table 4). The product was obtained with good regioselectivity at 0°C, but surprisingly with complete lack of enantioselectivity. Performing the conjugate addition at low temperature and in particular using Josiphos dramatically enhanced the selectivity up to 86% ee. Further improvement could be obtained by using the less coordinating solvent *t*-BuOMe instead of Et<sub>2</sub>O.

These conditions resulted also in high selectivities when Grignard reagents with different linear alkyl chains were used, whereas the substrate scope included a variety of aliphatic linear enones (Scheme 4). Particularly noteworthy is the addition of MeMgBr (e.g. to octenone), which provides the corresponding ketones with 97–98% ee, even when only 1 mol% of catalyst is employed<sup>34</sup>.

Both  $\beta$ -substituted aliphatic and aromatic enones can be used. For instance, benzyldeneacetone,  $\beta$ -thienyl- and  $\beta$ -furyl-substituted enones reacted smoothly in *t*-BuOMe at –75°C with RMgBr reagents to give the corresponding ketones with high yields, regioselectivities and enantioselectivities of 90–97% (Scheme 4). In contrast, the conjugate addition of  $\alpha$ -branched and aryl Grignard reagents or the use of sterically hindered enones provided only moderate enantioselectivities<sup>32</sup>.

### IV. ENANTIOSELECTIVE CONJUGATE ADDITION TO $\alpha,\beta$ -UNSATURATED ESTERS AND THIOESTERS

The conjugate addition of Grignard reagents to  $\alpha,\beta$ -unsaturated acid derivatives, in particular to esters, is highly attractive. Despite the enormous synthetic potential of the resulting

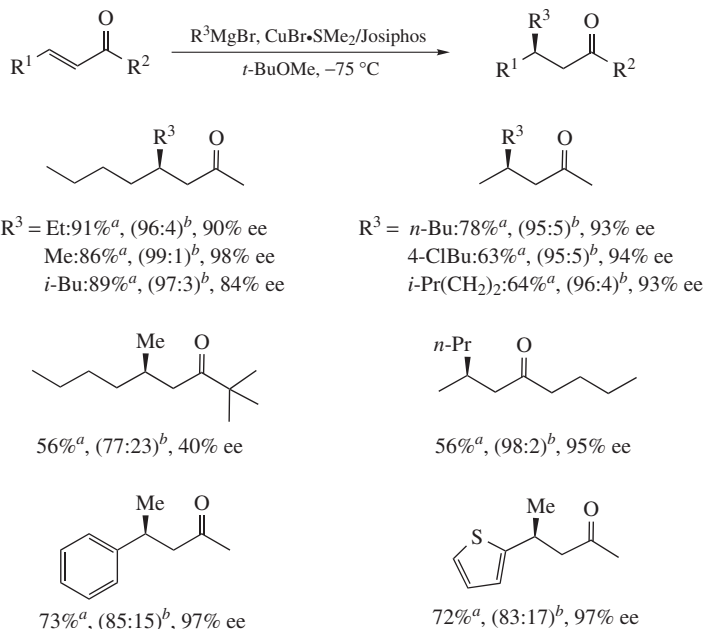
TABLE 4. Enantioselective conjugate addition of EtMgBr to (*E*)-3-nonen-2-one<sup>a,b,c</sup>

L*	CuX	Solvent	<i>T</i> (°C)	1,4:1,2	ee (%) (1,4)
Taniaphos	CuCl	Et <sub>2</sub> O	0	84:16	1
Taniaphos	CuCl	Et <sub>2</sub> O	–75	70:30	48
Josiphos	CuBr•SMe <sub>2</sub>	Et <sub>2</sub> O	–75	91:9	86
Josiphos	CuBr•SMe <sub>2</sub>	<i>t</i> -BuOMe	–75	99:1	90

<sup>a</sup> EtMgBr added to a solution of (*E*)-3-nonen-2-one, 5 mol% CuX and 6 mol% ligand.

<sup>b</sup> All conversions are >98%.

<sup>c</sup> Adapted with permission from *Acc. Chem. Res.*, **40**, 179–188 (2007). Copyright 2007 American Chemical Society.



<sup>a</sup> Isolated yield <sup>b</sup> 1,4:1,2 ratio.

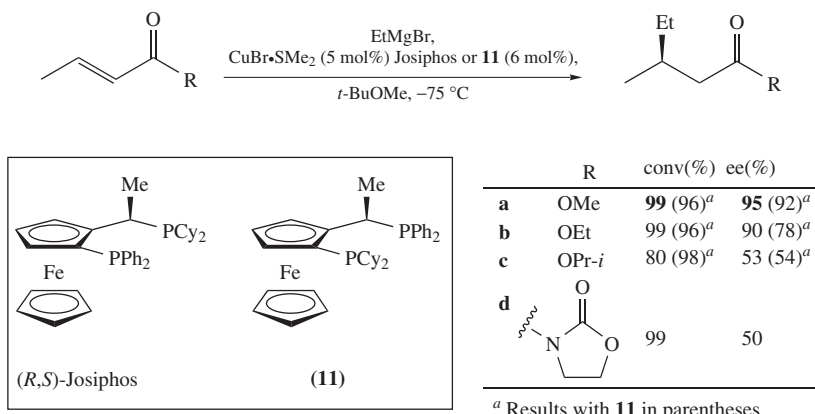
SCHEME 4. Enantioselective conjugate addition of RMgBr reagents to linear enones. Adapted with permission from *Acc. Chem. Res.*, **40**, 179–188 (2007). Copyright 2007 American Chemical Society

$\beta$ -substituted esters as chiral building blocks for natural product synthesis, progress during the last decades in the enantioselective conjugate addition of organometallic reagents to unsaturated esters has been limited<sup>35</sup>. The lower intrinsic reactivity of  $\alpha,\beta$ -unsaturated esters compared to that of enones may account for this paucity of methodologies. Indeed, no combinations of catalysts and alkyl organometallic reagents had previously been shown to be successful for these conjugate additions, although an enantioselective conjugate addition of dialkylzinc reagents to the more reactive  $\alpha,\beta$ -unsaturated *N*-acyloxazolidinones has been reported by Hird and Hoveyda<sup>36,37</sup>.

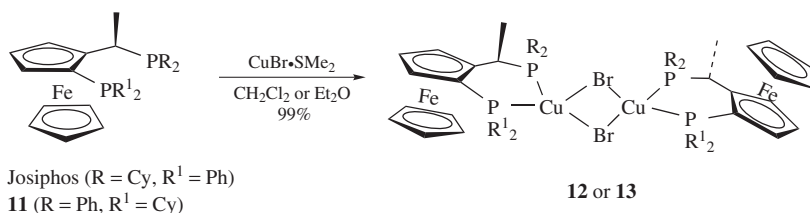
An initial study demonstrated that Josiphos and its 'inverted' analogue **11** were very effective in promoting the Cu-catalyzed conjugate addition of EtMgBr to unsaturated crotonates (Scheme 5). It is noteworthy that the use of sterically hindered esters, which usually helps to avoid undesired 1,2-additions, or alternatives for esters such as an oxazolidinone, are not required. Indeed, the highest conversions and stereoselectivities are obtained with methyl crotonate<sup>38</sup>.

Interestingly, the dinuclear Cu complexes **12** and **13** (Scheme 6) could be recovered from the crude reaction mixtures or, alternatively, prepared independently by mixing equimolar amounts of ligands and CuBr·SMe<sub>2</sub> in an appropriate solvent. It was established that these Cu complexes participate in the catalytic cycle, as the reaction of methyl crotonate and EtMgBr with the independently prepared (or recovered) complexes (0.5 mol%) afforded the product with the same yields and enantioselectivities as previously obtained with the complexes prepared *in situ*.





SCHEME 5. Screening of catalysts and crotonic acid derivatives in the copper-catalyzed Grignard addition. Adapted with permission from *Acc. Chem. Res.*, **40**, 179–188 (2007). Copyright 2007 American Chemical Society




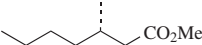
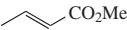
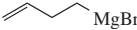


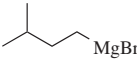
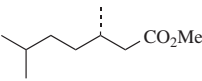
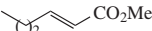
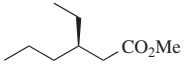
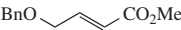
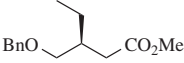
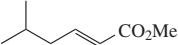
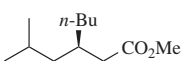
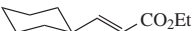
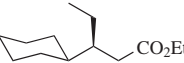
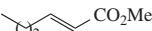
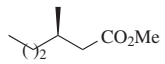
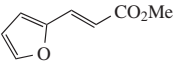
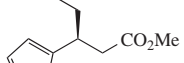
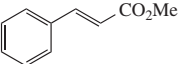
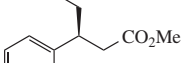
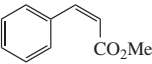
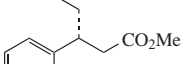
SCHEME 6. Preparation of the Cu complexes **12** and **13**. Adapted with permission from *Acc. Chem. Res.*, **40**, 179–188 (2007). Copyright 2007 American Chemical Society

Table 5 summarizes the scope of the reaction. As a general trend, linear aliphatic Grignard reagents provided excellent results in the conjugate addition to methyl crotonate, affording the products with excellent regio- and enantioselectivities and complete conversions using 0.5 mol% of catalyst. With regard to the substrates, less hindered  $\alpha,\beta$ -unsaturated esters, without branching at the  $\gamma$  position, afford better results with the Cu complex of Josiphos (**12**). However, for substrates with bulky groups or aromatic rings at the double bond, a superior efficiency is observed when catalyst **13** is used instead.

The conjugate addition of Grignard reagents can also be performed with the corresponding *Z*-enoates, leading to the products with opposite absolute configurations. However, lower ee values were consistently obtained in these reactions. In the reaction with *Z*-methyl cinnamate, analysis of the reaction mixture at different times revealed that an isomerization of the *Z*-enoate to the corresponding *E*-enoate occurred during the reaction, causing the decrease in ee.

From the perspective of potential applications to the synthesis of biologically active compounds, the introduction of a methyl group via the conjugate addition of MeMgBr to  $\alpha,\beta$ -unsaturated esters is a particularly relevant goal. Unfortunately, the addition of MeMgBr to methyl-2-hexenoate showed the limitation of the methodology. Although the product was formed with high enantioselectivity (93% ee) the reaction rate was prohibitively low due to the decreased reactivity of MeMgBr.

TABLE 5. Enantioselective Cu/ferrocenyl diphosphine-catalyzed conjugate addition to  $\alpha,\beta$ -unsaturated esters <sup>a,b</sup>

Substrate	RMgBr	Product	Cat (mol%)	Yield (%) <sup>f</sup>	ee (%)
	<i>n</i> -BuMgBr		<b>12</b> (0.5)	92	95
			<b>12</b> (0.5)	67	85
			<b>12</b> (0.5)	90	96
	EtMgBr		<b>12</b> (0.5)	99 <sup>c</sup>	93
	EtMgBr		<b>12</b> (2.5)	85	86
	<i>n</i> -BuMgBr		<b>12</b> (2.5)	99 <sup>c</sup>	92
	EtMgBr		<b>13</b> (2.5)	86 <sup>d</sup>	98
	MeMgBr		<b>12</b> (2.5)	19 <sup>c</sup>	93
	EtMgBr		<b>13</b> (0.5)	90 <sup>d</sup>	95
	EtMgBr		<b>13</b> (1.5)	94 <sup>d,e</sup>	98 (S)
	EtMgBr		<b>13</b> (1.5)	100 <sup>c-e</sup>	53 (R)

<sup>a</sup> Cu complex (see table), 1.15 equiv. of RMgBr, *t*-BuOMe, −75 °C.<sup>b</sup> Adapted with permission from *Acc. Chem. Res.*, **40**, 179–188 (2007). Copyright 2007 American Chemical Society.<sup>c</sup> Conversation(GC)<sup>d</sup> 2.5 equiv. of RMgBr employed.<sup>e</sup> Carried out in CH<sub>2</sub>Cl<sub>2</sub>.<sup>f</sup> Isolated yield.

The above-mentioned study was followed by a report of the groups of Ji, Loh and coworkers, who reported the application of a catalyst based on cuprous iodide and Tol-BINAP for the same purpose<sup>39</sup>. Noteworthy is that the effective use of a C<sub>2</sub>-symmetric ligand in this reaction marks the end of the aforementioned metal-differentiating coordination concept. It was shown that a variety of Grignard reagents could be used for the

TABLE 6. CuI/Tol-BINAP-catalyzed conjugate addition of Grignard reagents

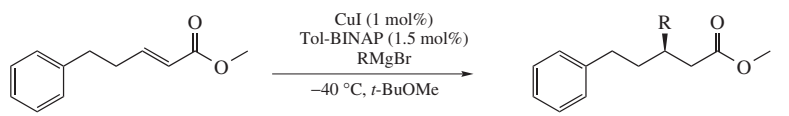
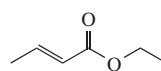
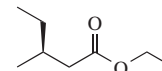
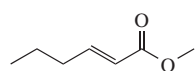
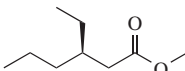
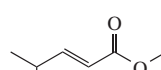
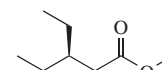
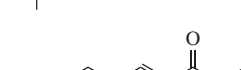


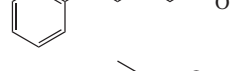

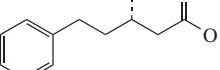
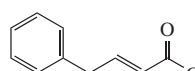
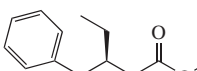
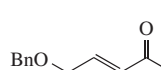
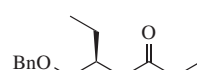
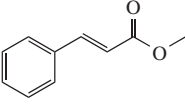
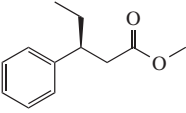
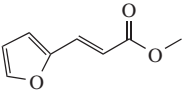
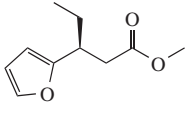
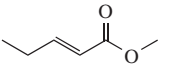
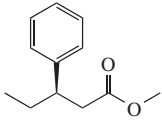
		
RMgBr	Yield (%)	ee (%)
EtMgBr	88	93
PrMgBr	90	92
<i>i</i> -PrMgBr	89	91
BuMgBr	90	92
PentMgBr	86	90
HeptMgBr	89	92
ButenylMgBr	90	94
<i>i</i> -BuMgBr	91	86
MeMgBr	20	98

TABLE 7. CuI/Tol-BINAP-catalyzed conjugate addition of EtMgBr

Unsaturated ester	Yield (%)	ee (%)	Product
	83	74	
	85	87	
	67	68	
	88	93	
	86	94 ( <i>S</i> )	
	85	94	
	83	73	
	86	87	

(continued overleaf)

TABLE 7. (continued)

Unsaturated ester	Yield (%)	ee (%)	Product
	90 <sup>a</sup>	93	
	80 <sup>a</sup>	85	
	80 <sup>b</sup>	74	

<sup>a</sup> 5 mol% CuI and 7.5 mol% Tol-BINAP were used.<sup>b</sup> PhMgBr was used.

highly enantioselective addition to unsaturated methyl esters (Table 6). Table 7 shows the scope of the reaction using EtMgBr as the nucleophile. As in the case of Cu/Josiphos and Cu/Taniaphos, *Z*-enoates give the opposite configuration of the product, in this case apparently without concomitant isomerization of the substrate as the ee is not compromised. As for the Cu/ferrocenyl diphosphine catalysts, enantioselectivities drop considerably when PhMgBr is used as the nucleophile and conversions are significantly lower with MeMgBr.

To address the lack of reactivity in the methyl Grignard additions, we focussed our attention on the more reactive but equally readily accessible  $\alpha,\beta$ -unsaturated thioesters<sup>40</sup>. The addition of MeMgBr to a series of unsaturated thioesters revealed the success of this approach<sup>41</sup>. The complex prepared *in situ* from CuBr•SMe<sub>2</sub> (1.0 mol%) and Josiphos (1.1 mol%) catalyzed the conjugate addition of MeMgBr providing the corresponding  $\beta$ -methyl-substituted thioesters with complete regioselectivity and excellent enantioselectivities (95–96% ee) (Table 8). The drastically higher yields obtained for the methyl adducts from  $\alpha,\beta$ -unsaturated thioesters, compared to the oxoester analogs, are most probably due to their inherent electronic properties, which are closer to those of enones.

TABLE 8. Enantioselective conjugate addition of MeMgBr to  $\alpha,\beta$ -unsaturated thioesters<sup>a</sup>

$\text{R}^1\text{-CH=CH-C(=O)SR}^2 \xrightarrow[\text{Josiphos, } t\text{-BuOMe, } -75^\circ\text{C}]{\text{MeMgBr, CuBr}\cdot\text{SMe}_2} \text{R}^1\text{-CH(Me)-CH}_2\text{-C(=O)SR}^2$			
R <sup>1</sup>	R <sup>2</sup>	Yield (%)	ee (%)
<i>n</i> -Pent	Et	90	96
<i>n</i> -Pent	Me	93	96
<i>n</i> -Pr	Et	92	96
BnO(CH <sub>2</sub> ) <sub>3</sub>	Et	94	95
Ph	Et	88	95

<sup>a</sup> MeMgBr, CuBr•SMe<sub>2</sub> (1.0 mol%), Josiphos (1.2 mol%), *t*-BuOMe, −75 °C.

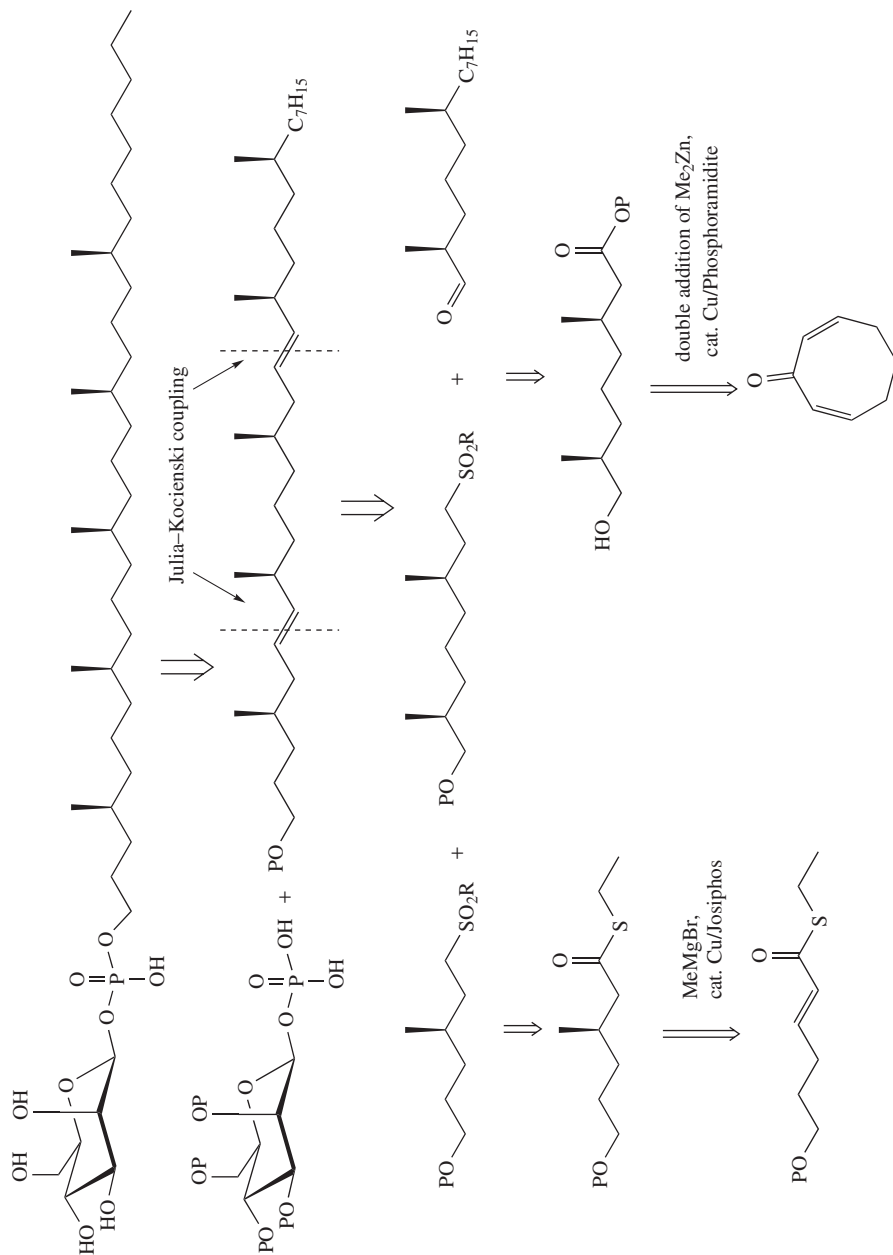
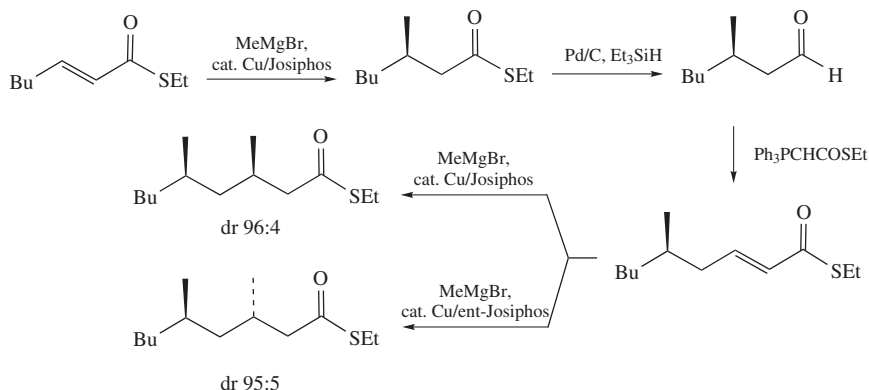


FIGURE 5. A  $\beta$ -D-mannosyl phosphomycoketide from *Mycobacterium tuberculosis*

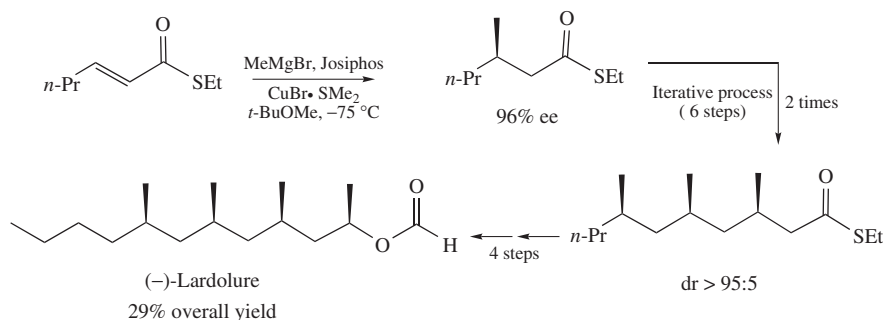
## V. APPLICATION OF THE CONJUGATE ADDITION OF GRIGNARD REAGENTS TO $\alpha,\beta$ -UNSATURATED THIOESTERS IN THE SYNTHESIS OF NATURAL PRODUCTS

An illustration of the use of  $\beta$ -methyl-substituted thioesters in the synthesis of natural products is present in the total synthesis of a  $\beta$ -D-mannosyl phosphomycoketide from *Mycobacterium tuberculosis* (Figure 5)<sup>42</sup>. Addition of MeMgBr to ethyl 6-benzzyloxy-2-hexene thioate catalyzed by Cu/Josiphos (92% yield, 93% ee) furnished one of the building blocks. The other four methyl groups were introduced using copper/phosphoramidite-catalyzed dimethylzinc addition.

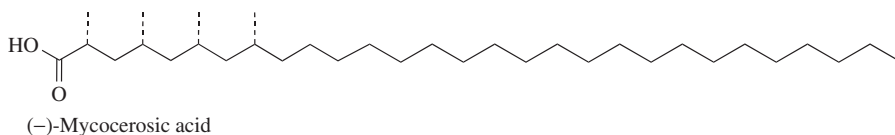
Moreover, the enantioselective conjugate addition of Grignard reagents to  $\alpha,\beta$ -unsaturated thioesters allows access to enantiopure *syn*- and *anti*-1,3-dimethyl arrays by way of an iterative procedure<sup>41,43</sup>. The approach relies on sequential enantioselective conjugate additions, the protocol of which is shown in Scheme 7. The first stereogenic center is created by the addition of MeMgBr, using Josiphos (95% ee). The resulting thioester is converted in one step into the corresponding aldehyde, which subsequently undergoes a



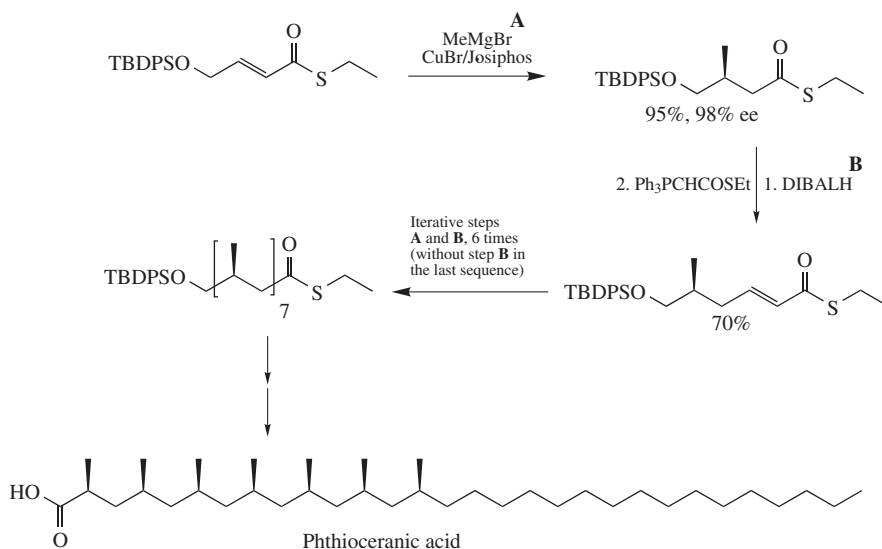
SCHEME 7. An iterative catalytic route to enantiopure *syn*- and *anti*-1,3-dimethyl arrays. Adapted with permission from *Acc. Chem. Res.*, **40**, 179–188 (2007). Copyright 2007 American Chemical Society



SCHEME 8. Application of the iterative conjugate addition in the synthesis of (-)-Lardolure. Adapted with permission from *Acc. Chem. Res.*, **40**, 179–188 (2007). Copyright 2007 American Chemical Society

FIGURE 6. Mycocerosic acid from *M. tuberculosis*

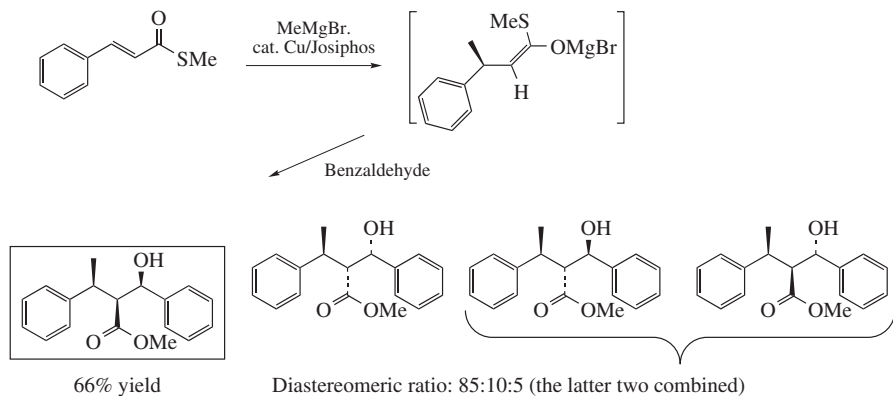
Wittig reaction to give the desired Michael acceptor. A second catalytic conjugate addition using Josiphos or its enantiomer affords with excellent diastereoselectivities the *syn*- or *anti*-1,3-dimethyl derivative.



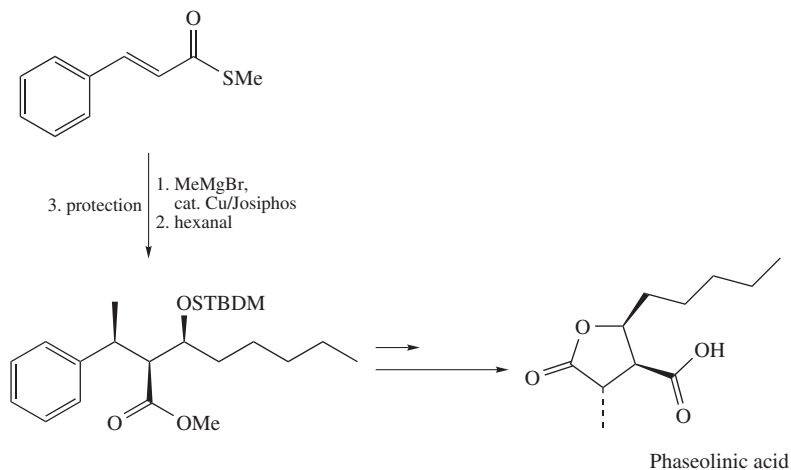
SCHEME 9. Catalytic asymmetric synthesis of Phthioceranic acid

The synthetic utility of this iterative catalytic protocol is especially apparent in the preparation of natural products containing so-called deoxypropionate units<sup>44</sup>. This was demonstrated in the asymmetric total synthesis of (-)-Lardolure, the aggregation pheromone of the acarid mite *Lardoglyphus konoi* (Scheme 8)<sup>41</sup>. Furthermore, as a convincing illustration of the high efficiency of this iterative protocol, this strategy has been applied in the synthesis of Mycocerosic acid<sup>45</sup> (Figure 6) and Phthioceranic acid<sup>46</sup>, lipids present in the cell wall of *M. tuberculosis* (Scheme 9).

As the product of the conjugate addition of a Grignard reagent is a magnesium enolate, it is tempting to use this species in a subsequent diastereoselective reaction. The development of a tandem conjugate addition–aldol reaction, starting with the Cu/Josiphos-catalyzed addition of methylmagnesium bromide to unsaturated thioesters, turned out to be very successful<sup>47</sup>. A fast reaction of the magnesium enolate at low temperature with a suitable aldehyde afforded the corresponding *syn,syn* aldol product predominantly. The excellent diastereoselectivity of this acyclic three-component reaction is remarkable as exemplified in Scheme 10. This strategy was used for an efficient synthesis of Phaseolinic acid (Scheme 11).



SCHEME 10. A tandem conjugate addition-aldol reaction



SCHEME 11. Total synthesis of Phaseolinic acid

## VI. MECHANISTIC STUDIES

An extensive spectroscopic and mechanistic study on the enantioselective Cu/ferrocenyl bisphosphine-catalyzed conjugate addition has been performed<sup>48</sup>. Several parameters such as solvent, nature of the halide present in the Grignard reagent and Cu(I) source, and additives (i.e. dioxane and crown ethers) were identified. These factors directly affect the formation and nature of the intermediate active species, and therefore the selectivity, rate and overall outcome of the reaction. Importantly, the presence of  $\text{Mg}^{2+}$  and  $\text{Br}^-$  ions in the reaction are essential in order to achieve high selectivity and efficiency.

Kinetic studies carried out on a model reaction, the addition of  $\text{EtMgBr}$  to methyl crotonate catalyzed by Cu/Josiphos, indicated that the rate of the conjugate addition reaction is dependent on catalyst, Grignard reagent and substrate. Although the determination of the reaction order in methyl crotonate and Grignard reagent was impeded due to side reactions and inhomogeneity, the observation that the reaction rate increases with their



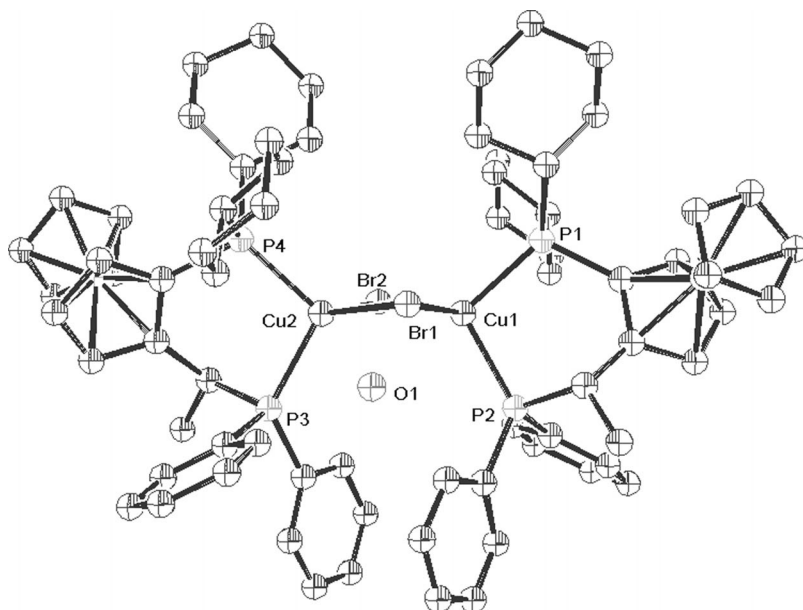


FIGURE 7. The X-ray structure of **13** (hydrogen atoms are omitted for clarity). Adapted with permission from *Acc. Chem. Res.*, **40**, 179–188 (2007). Copyright 2007 American Chemical Society

concentrations suggests that both reactants are involved in the rate-determining step. On the other hand, the order of the reaction (1.10) with respect to the catalyst suggests that a mononuclear species is involved. This was also supported by the observation that the ee of the product shows a linear dependency on the ee of the catalyst. The structure of the initial dinuclear Cu–Josiphos complex **13** was established by X-ray analysis (Figure 7).

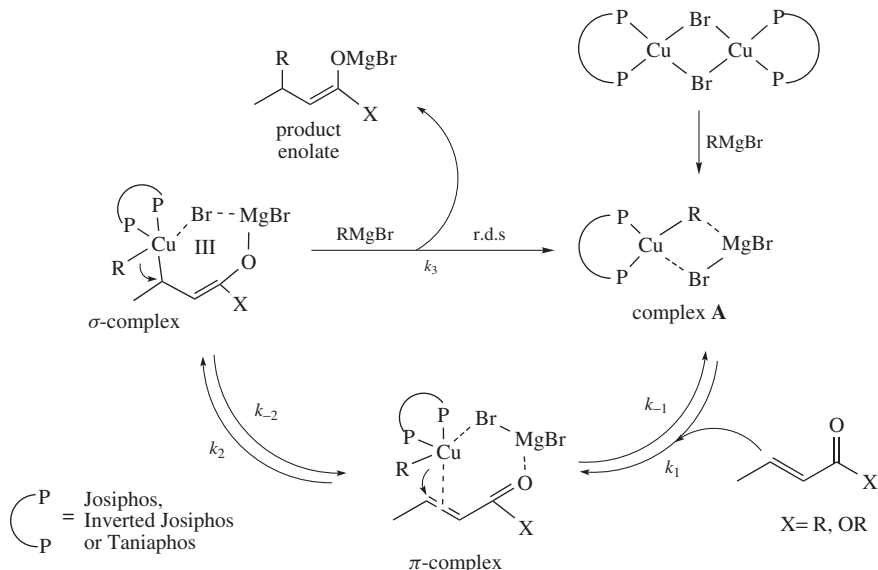
A reaction pathway which is consistent with the experimental, kinetic and spectroscopic results is proposed in Scheme 12.

Alkyl transfer from the magnesium halide to the chiral Cu complexes generates the Cu complex **A**, as deduced from NMR experiments. Very likely, this complex functions in a similar manner as previously postulated for organocuprate additions<sup>49</sup>.

The second intermediate proposed is a Cu–olefin  $\pi$ -complex with an additional interaction of  $\text{Mg}^{2+}$  with the carbonyl oxygen of the enone (enoate). The formation of a  $\pi$ -complex is presumably followed by intramolecular rearrangement to a Cu(III) intermediate, where Cu forms a  $\sigma$ -bond with the  $\beta$ -carbon of the enone (enoate), in fast equilibrium with the  $\pi$ -complex.

This catalytic cycle gives an explanation for the observed isomerization of *Z*-enoates to their *E*-isomers, which occurs within the time scale of the reaction. Indeed, these isomerization experiments provide evidence for the presence of a fast equilibrium between a  $\pi$ -complex and a Cu(III) species ( $\sigma$ -complex), which should be followed by the rate limiting, reductive elimination step and the formation of complex **A** again.

The proposed catalytic cycle is in accordance with the results of the kinetic studies. The dependence of the reaction rate on the substrate and Grignard reagent indicates that both reactants are involved in the rate-limiting step. This step is preceded by fast equilibria between complexes, for example, a substrate-bound  $\sigma$ -complex and  $\pi$ -complex and substrate-unbound complex **A**.



SCHEME 12. Proposed catalytic cycle. Adapted with permission from *Acc. Chem. Res.*, **40**, 179–188 (2007). Copyright 2007 American Chemical Society.

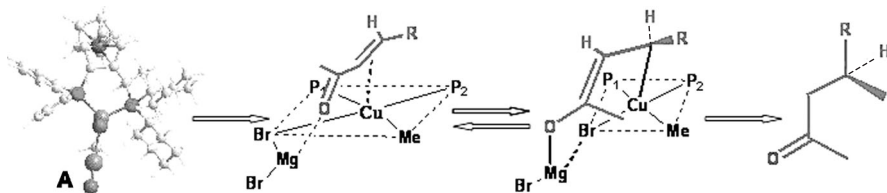


FIGURE 8. Model for the enantioselective conjugate addition of Grignard reagents ( $\text{P}_1$ :  $\text{PPh}_2$  moiety  $\text{P}_2$ :-  $\text{PCy}_2$ ). Adapted with permission from *Acc. Chem. Res.*, **40**, 179–188 (2007). Copyright 2007 American Chemical Society

Semiempirical  $[\text{PM3}(\text{tm})]$  calculations indicated that Cu complex **A** adopts a distorted tetrahedral structure with the positioning of the Grignard reagent at the bottom face of the complex (Figure 8).

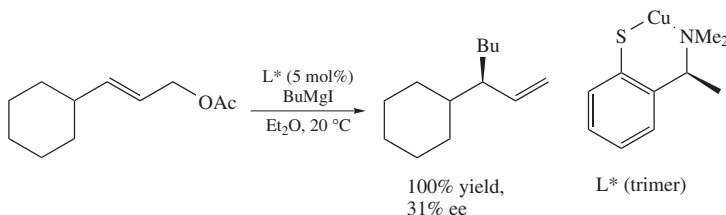
In the proposed model it can be envisioned that the enone approaches the alkylcopper complex **A** from the least hindered side and binds to the top apical position. This forces the complex to adopt a square pyramidal geometry, which is stabilized via  $\pi$ -complexation of the alkene moiety to the Cu and, importantly, through the interactions between Mg and the carbonyl moiety of the skewed enone. Formation of a transition structure with the chair-like seven-membered ring conformation is proposed in the next step, where Cu forms a  $\sigma$ -bond approaching from the bottom side of the  $\beta$ -carbon leading to the Cu(III) intermediate with the absolute configuration shown (Figure 8). Up to this stage in the catalytic cycle, complex formation is reversible, but in the subsequent rate-determining step, the alkyl transfer step, the product stereochemistry is established. To avoid steric interactions with the dicyclohexyl moieties at the nearby phosphorus, the final transfer

of the alkyl group occurs as shown in Figure 8. Although this model predicts the correct sense of asymmetric induction, it is nevertheless a model and further mechanistic studies and DFT calculations need to be performed to shed light on the factors that determine the origin of the enantioselectivity.

## VII. ENANTIOSELECTIVE ALLYLIC ALKYLATION WITH GRIGNARD REAGENTS

As recently highlighted by Woodward, enantioselective  $S_N2'$  allylic substitution reactions are mechanistically related to conjugate addition reactions<sup>50</sup>. Theoretical studies carried out by Nakamura and coworkers for the conjugate addition and allylic alkylation using Gilman's cuprates revealed profound mechanistic similarities between these two processes<sup>49, 51</sup>.

Compared to the enantioselective allylic alkylation using soft nucleophiles<sup>52</sup>, the reaction with Grignard reagents has received much less attention. The first enantioselective copper-catalyzed allylic alkylation with alkylmagnesium reagents was reported in 1995 by the groups of Bäckvall, van Koten and coworkers (Scheme 13)<sup>53</sup>.



SCHEME 13. Copper-catalyzed allylic substitution using an arenethiolate ligand

In contrast, the first highly enantioselective version of this reaction used bulky dialkylzincs and was reported a few years later by Dübner and Knochel<sup>54</sup>. For linear dialkylzincs, highly efficient catalysts were reported soon after this disclosure by Hoveyda and coworkers<sup>55</sup> and Feringa and coworkers<sup>56</sup>. As in the field of conjugate addition reactions, organozinc reagents dominated the field until recently<sup>50</sup>. Grignard reagents regained attention, however, after two reports of the Alexakis group on the highly enantioselective allylic substitution of cinnamyl chlorides catalyzed by a Cu/phosphoramidite (Table 9)<sup>57</sup>.

In a subsequent report, the scope of this method was expanded to cyclic and linear  $\beta$ -substituted allyl chlorides using a slightly different ligand (Table 10)<sup>58</sup>.

Similar to Hoveyda's work, which describes NHC ligands for the allylic alkylation with dialkylzinc reagents<sup>59</sup>, Okamoto and coworkers reported the enantioselective allylic alkylation with Grignard reagents using an  $\alpha$ -methyl naphthylamine-based NHC complex (Scheme 14)<sup>60</sup>.

Surprisingly, also the use of *N*-heterocyclic carbenes as such, e.g. without copper, is a valuable approach for the allylic alkylation using Grignard reagents. The NHC acts as a Lewis base that activates the reagent and modifies its reactivity. This was used in a versatile preparation of esters containing quaternary stereocenters (Table 11)<sup>61</sup>. The formation of the corresponding cyclopropyl-containing side product, which is formed in the absence of ligand, could rather effectively be suppressed, although reaction times were rather long (24–60 h).

Next to the successful conjugate addition of Grignard reagents, the catalyst generated from Josiphos and  $\text{CuBr} \cdot \text{SMe}_2$  also effectively promotes the allylic alkylation of cinnamyl bromide with  $\text{MeMgBr}$ , affording the corresponding products with good regioselectivity (85:15) and high ee (85% ee)<sup>62</sup>. Under the same conditions, the allylic alkylation of

TABLE 9. Asymmetric allylic substitution using a Cu/phosphoramidite ligand

$\text{Cu(I)thiophene-2-carboxylate (1 mol\%)}$   
 $\text{L}^* (1.1 \text{ mol\%})$   
 $\text{RMgBr (1.2 eq.)}$   
 $\text{CH}_2\text{Cl}_2, -78^\circ\text{C}$

$\text{L}^*$

Substrate	R	Product	Yield (%)	$S_N2'/S_N2$	ee (%)
	Et		86	99/1	96 ( <i>R</i> )
	Me		100 (conv.)	89/11	96
	Me		90 (conv.)	90/10	95
	Me		100 (conv.)	84/16	93
	Butenyl		83	96/4	92 ( <i>R</i> )
	Pentenyl		81	91/1	96 ( <i>R</i> )
	Et		85	99/1	96 ( <i>R</i> )
	Butenyl		83	97/3	93 ( <i>R</i> )
	Pentenyl		86	91/1	94 ( <i>R</i> )
	Et		82	99/1	91 (–)

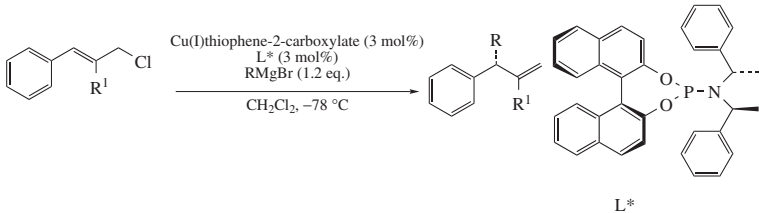
TABLE 10. Asymmetric allylic substitution of disubstituted allylic chlorides using a Cu/phosphoramidite ligand

$\text{Cu(I)thiophene-2-carboxylate (3 mol\%)}$   
 $\text{L}^* \text{ (3 mol\%)}$   
 $\text{RMgBr (1.2 eq.)}$   
 $\text{CH}_2\text{Cl}_2, -78^\circ\text{C}$

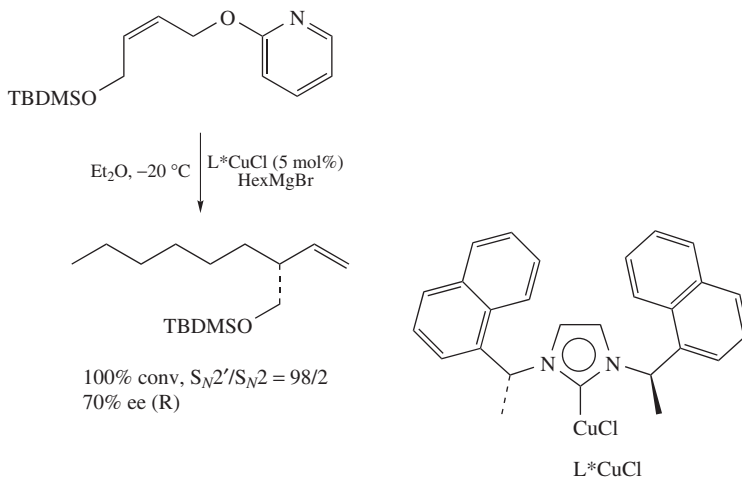
$\text{L}^*$

Substrate	R	Product	Yield (%)	$S_N2'/S_N2$	ee (%)
	Et		87	92/8	98 (+)
	Pr		85	84/16	97 (+)
	Pent		83	83/17	96 (+)
	Butenyl		84	89/11	97 (+)
	Pentenyl		87	87/13	96 (+)
	Et		87	92/8	96 (+)
	Et		85	84/16	96 (+)
	Et		83	83/17	92 (+)

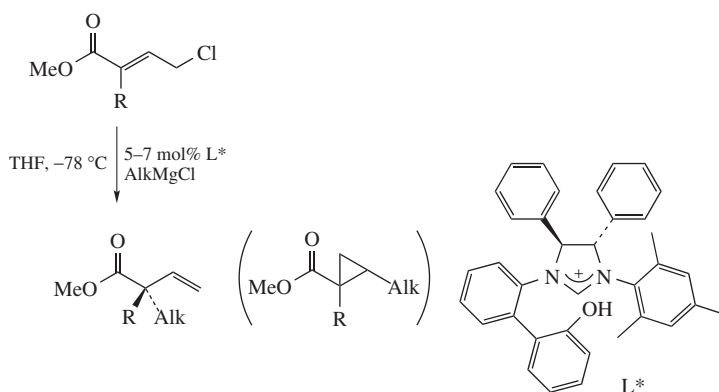
TABLE 10. (continued)


  
 $\text{Cu(I)thiophene-2-carboxylate (3 mol\%)}$   
 $\text{L}^* \text{ (3 mol\%)}$   
 $\text{RMgBr (1.2 eq.)}$   
 $\text{CH}_2\text{Cl}_2, -78\text{ }^\circ\text{C}$

Substrate	R	Product	Yield (%)	$S_N2'/S_N2$	ee (%)
	Bu		99 (conv)	96/4	98
	Hex		91	98/2	98
	phenethyl		99 (conv)	97/3	98
	<i>t</i> -BuO		60	98/2	98
	Bu		73	81/19	98
	Butenyl		83	97/3	99
	Hex		67	97/3	98
	phenethyl		78	85/15	99
	<i>t</i> -BuO		99 (conv)	91/9	99



SCHEME 14. Synthesis of secondary allylic alcohols by Cu/NHC-catalyzed allylic substitution

TABLE 11. Allylic alkylation of  $\gamma$ -chloro- $\alpha,\beta$ -unsaturated esters

R	Alkyl	$S_N2'/S_N2$	Cyclopropyl product (%)	$S_N2'$ Yield (%)	ee (%)
Me	<i>i</i> -Pr	90/10	9	80	97
Me	<i>c</i> -Pent	81/19	12	57	75
Me	<i>c</i> -Hex	92/8	27	63	94
Me	<i>n</i> -Bu	86/14	28	34	63
Et	<i>i</i> -Pr	91/9	7	73	97
Bu	<i>i</i> -Pr	91/9	7	75	98
Et	<i>c</i> -Pent	88/12	8	66	90
Bu	<i>c</i> -Pent	78/22	13	59	85
Et	<i>c</i> -Hex	93/7	19	60	96
Bu	<i>c</i> -Hex	92/8	13	57	96
Et	<i>n</i> -Bu	88/12	26	35	79

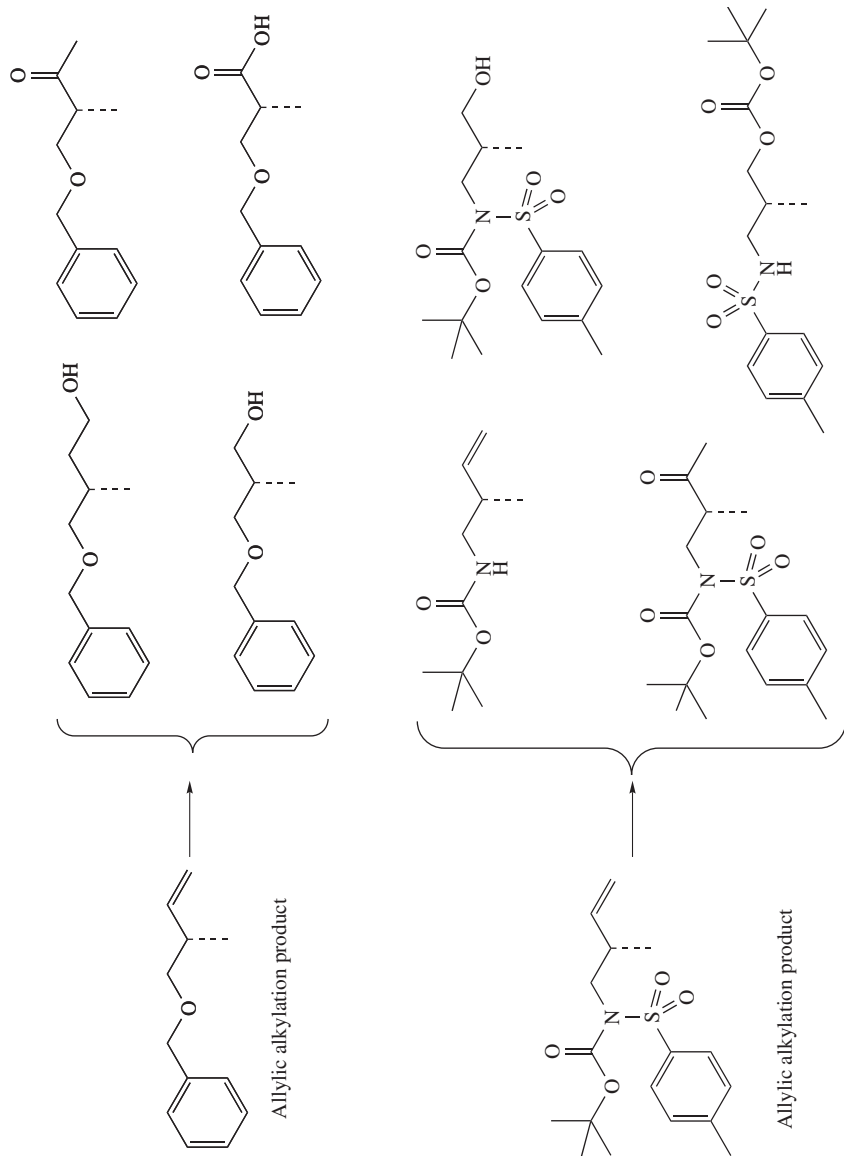
cinnamyl bromide with EtMgBr provided a modest regioselectivity (38:62) and a disappointing 56% ee. However, a dramatic improvement was observed using Taniaphos as the ligand and CH<sub>2</sub>Cl<sub>2</sub> instead of *t*-BuOMe as the solvent. The desired product was obtained with a good regioselectivity (82:18) and an excellent ee (96%).

The scope of the method turned out to be particularly broad (Table 12). The allylic substitution of cinnamyl bromide could also be performed with other linear alkyl Grignard

TABLE 12. Cu/Taniaphos-catalysed enantioselective allylic alkylation with Grignard reagents

$  \begin{array}{c}  \text{CuBr}\cdot\text{SMe}_2 \text{ (1 mol\%)} \\  \text{L}^* \text{ (1.1 mol\%)} \\  \text{R}^2\text{MgBr} \\  \text{CH}_2\text{Cl}_2, -75^\circ\text{C}  \end{array}  \xrightarrow{\quad}  \begin{array}{c}  \text{R}^1\text{---}\text{CH}(\text{R}^2)\text{---CH=CH}_2 + \text{R}^1\text{---CH=CH---CH}_2\text{R}^2  \end{array}  $					
R <sup>1</sup>	R <sup>2</sup>	S <sub>N</sub> 2'/S <sub>N</sub> 2	Product	Yield (%)	ee (%)
Ph	Et	82/18		92	95
Ph	Bu	87/13		92	94
Ph	Butenyl	91/9		93	95
Ph	Me	97/3		91	98
1-Naph	Me	100/0		87	96
<i>p</i> -ClC <sub>6</sub> H <sub>4</sub>	Me	99/1		95	97
<i>p</i> -MeOOC <sub>6</sub> H <sub>4</sub>	Me	98/2		94	97
BnOCH <sub>2</sub>	Me	100/0		93	92
Bu	Me	100/0		99	92



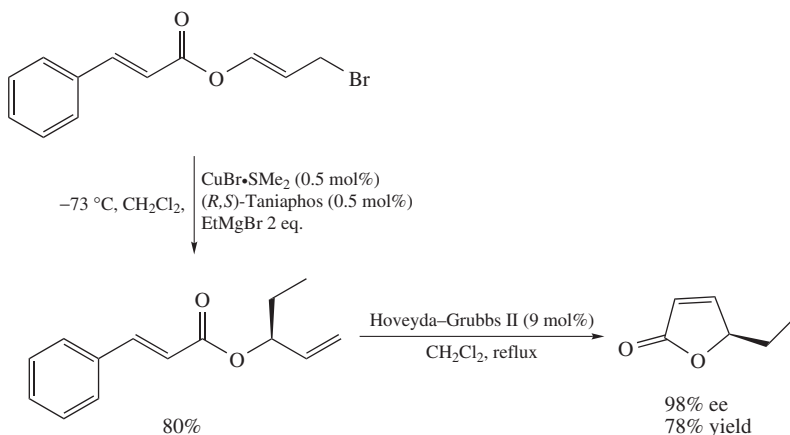


SCHEME 15. Synthesis of bifunctional building blocks through copper/Taniaphos-catalyzed allylic alkylation

reagents. Most important, the alkylations with MeMgBr afforded the products with almost complete control of regioselectivity and enantioselectivity ( $\geq 96\%$ ) and also linear allylic bromides turned out to be excellent substrates.

The utility of the copper/Taniaphos-catalyzed allylic alkylation was further illustrated in two subsequent reports. The application of aliphatic allylic bromides containing protected alcohols and amines leads to the efficient synthesis of bifunctional building blocks (Scheme 15)<sup>63</sup>.

A recent and entirely novel application of this reaction to readily available 3-bromopropenyl esters, leads to virtually enantiopure allylic esters, e.g. alcohols<sup>64</sup>. The reaction is chemo-, regio- and enantioselective as illustrated in Scheme 16, which also shows an application of this method for the synthesis of a naturally occurring butenolide. Known catalytic methods for the preparation of allylic alcohol derivatives involve metal-catalyzed allylic substitution using oxygen nucleophiles. Most of these methods provide ethers<sup>65</sup>, although the use of carboxylic acids<sup>66</sup> and the preparation of amines<sup>67</sup> have also been reported. The synthesis of allylic esters using catalytic enantioselective carbon–carbon bond formation is therefore a new and versatile addition. In addition, the reaction is a nice complement to the kinetic resolution of allylic alcohols using Sharpless' asymmetric epoxidation. The scope of the method is large as shown in Table 13.



SCHEME 16. Copper-catalyzed asymmetric synthesis of chiral allylic esters; synthesis of a natural butenolide using allylic alkylation followed by ring-closing metathesis

## VIII. CONCLUSIONS

Although already studied for a long time, the development of efficient and versatile catalysts for the conjugate addition and allylic alkylation using Grignard reagents is a recent development. In the conjugate addition reactions, the high enantiomeric excesses, the versatile asymmetric conjugate addition to  $\alpha,\beta$ -unsaturated esters and thioesters and the formation of quaternary stereocenters are particularly noteworthy features. In addition, an iterative and catalytic approach to deoxypropionate subunits has been developed and applied to the synthesis of multimethyl branched natural products. In the allylic alkylation, the different substitution patterns of the substrate and the alkylation of 3-bromopropenyl esters have strongly broadened the synthetic utility of the reaction.

TABLE 13. The allylic substitution of 3-bromopropenyl esters using Cu/Taniaphos

$  \begin{array}{c}  \text{CuBr}\cdot\text{SMe}_2 \text{ (5 mol\%)} \\  (R,S)\text{-Taniaphos (5 mol\%)} \\  \text{R}^2\text{MgBr (2 eq)} \\  \text{CH}_2\text{Cl}_2, -75^\circ\text{C}  \end{array}  $				
R <sup>1</sup>	R <sup>2</sup>	Product	Yield (%)	ee (%)
H	Et		87	(+ )98
H	Pent		99	(- )97 <sup>a</sup>
H	<i>i</i> -Bu		—	—
H	Butenyl		96	(+ )97
H	Phenethyl		93	(+ )93
H	Octadecyl		93	(+ )95
Me	Et		97 <sup>b</sup>	97
Me	Pent		96 <sup>b</sup>	98

<sup>a</sup> The enantiomer of the ligand was used.<sup>b</sup> A mixture of regioisomers was isolated.

In view of this, it is evident that in the coming years, expansion of the catalytic toolbox for the conjugate addition and allylic substitution of these readily accessible organometallic reagents will be reported.

## IX. REFERENCES AND NOTES

- (a) P. Perlmutter, *Conjugate Addition Reactions in Organic Synthesis*, Tetrahedron Organic Chemistry Series 9, Pergamon, Oxford, 1992.  
(b) V. Caprio, 'Recent Advances in Organocopper Chemistry', *Lett. Org. Chem.*, **3**, 339 (2006).
- (a) K. Tomioka and Y. Nagaoka, in *Comprehensive Asymmetric Catalysis* (Eds. E. N. Jacobsen, A. Pfaltz and H. Yamamoto), Vol. 3, Springer-Verlag, New York, 1999, pp. 1105–1120.  
(b) B. L. Feringa and A. H. M. de Vries, in *Advances in Catalytic Processes* (Ed. M. Doyle), Vol. 1, JAI Press, Connecticut, 1995, pp. 151–192.
- (a) T. Kogure and E. L. Eliel, *J. Org. Chem.*, **49**, 578 (1984).  
(b) T. Mukaiyama and N. Iwasawa, *Chem. Lett.*, 913 (1981).
- B. E. Rossiter and N. M. Swingle, *Chem. Rev.*, **92**, 771 (1992).
- E. J. Corey, R. Naef and F. J. Hannon, *J. Am. Chem. Soc.*, **108**, 7114 (1986).
- Y. Asano, A. Iida and K. Tomioka, *Tetrahedron Lett.*, **38**, 8973 (1997) and references cited therein.
- (a) G. M. Villacorta, C. P. Rao and S. J. Lippard, *J. Am. Chem. Soc.*, **110**, 3175 (1988).  
(b) K.-H. Ahn, B. Klassen and S. J. Lippard, *Organometallics*, **9**, 3178 (1990).
- (a) M. Spescha and G. Rihs, *Helv. Chim. Acta*, **76**, 1219 (1993).  
(b) Q.-L. Zhou and A. Pfaltz, *Tetrahedron*, **50**, 4467 (1994).  
(c) M. van Klaveren, F. Lambert, D. J. F. M. Eijkelkamp, D. M. Grove and G. van Koten, *Tetrahedron Lett.*, **35**, 6135 (1994).  
(d) D. Seebach, G. Jaeschke, A. Pichota and L. Audergon, *Helv. Chim. Acta*, **80**, 2515 (1997).
- (a) E. L. Stangeland and T. Sammakia, *Tetrahedron*, **53**, 16503 (1997).  
(b) M. Kanai and K. Tomioka, *Tetrahedron Lett.*, **36**, 4275 (1995).
- J. F. G. A. Jansen and B. L. Feringa, *J. Org. Chem.*, **55**, 4168 (1990).
- K. Soai, T. Hayasaka and S. Ugajin, *J. Chem. Soc., Chem. Commun.*, 516 (1989).
- A. Alexakis, J. Frutos and P. Mangeney, *Tetrahedron: Asymmetry*, **4**, 2427 (1993).
- A. H. M. de Vries, A. Meetsma and B. L. Feringa, *Angew. Chem., Int. Ed. Engl.*, **35**, 2374 (1996).
- B. L. Feringa, M. Pineschi, L. A. Arnold, R. Imbos and A. H. M. de Vries, *Angew. Chem., Int. Ed. Engl.*, **36**, 2620 (1997).
- L. A. Arnold, R. Naasz, A. J. Minnaard and B. L. Feringa, *J. Am. Chem. Soc.*, **123**, 5841 (2001).
- B. L. Feringa, R. Naasz, R. Imbos and L. A. Arnold, in *Modern Organocopper Chemistry* (Ed. N. Krause), Wiley-VCH, Weinheim, 2002, pp. 224.
- N. Krause and A. Hoffmann-Röder, *Synthesis*, 171 (2001).
- A. H. Hoveyda, A. W. Hird and M. A. Kacprzynski, *Chem. Commun.*, 1779 (2004).
- (a) A. Alexakis and C. Benhaim, *Eur. J. Org. Chem.*, 3221 (2002).  
(b) M. P. Sibi and S. Manyem, *Tetrahedron*, **56**, 8033 (2000).
- For relevant recent examples, see:  
(a) M. Shi, C.-J. Wang and W. Zhang, *Chem. Eur. J.*, **10**, 5507 (2004).  
(b) A. P. Duncan, and J. L. Leighton, *Org. Lett.*, **6**, 4117 (2004).
- (a) Y. Takaya, M. Ogasawara, T. Hayashi, M. Sakai and N. Miyaara, *J. Am. Chem. Soc.*, **120**, 5579 (1998).  
(b) T. Hayashi and K. Yamasaki, *Chem. Rev.*, **103**, 2829 (2003).  
(c) J. G. Boiteau, A. J. Minnaard and B. L. Feringa, *Org. Lett.*, **5**, 681 (2003).
- K. Tomioka, in *Comprehensive Asymmetric Catalysis, Suppl. 2* (Eds. E. N. Jacobsen, A. Pfaltz and H. Yamamoto), Springer-Verlag, New York, 2004, pp. 109–124.
- W. W. Lin, O. Baron and P. Knochel, *Org. Lett.*, **8**, 5673 (2006) and references cited therein.
- For an exception to the rule, see: K. Yoshida, M. Ogasawara and T. Hayashi *J. Org. Chem.*, **68**, 1901 (2003).
- (a) D. M. Knotter, D. M. Grove, W. J. J. Smeets, A. L. Spek and G. van Koten, *J. Am. Chem. Soc.*, **114**, 3400 (1992).

- (b) A. L. Braga, S. J. N. Silva, D. S. Lüdtke, R. L. Drekenner, C. C. Silveira, J. B. T. Rocha and L. A. Wessjohann, *Tetrahedron Lett.*, **43**, 7329 (2002).
- (c) M. Kanai, Y. Nakagawa and K. Tomioka, *Tetrahedron*, **55**, 3843 (1999) and references cited therein.
26. R. Noyori, *Asymmetric Catalysis in Organic Synthesis*, Wiley, New York, 1994.
27. (a) T. J. Colacot, *Chem. Rev.*, **103**, 3101 (2003).  
(b) A. Togni, C. Breutel, A. Schnyder, F. Spindler, H. Landert and A. Tijani, *J. Am. Chem. Soc.*, **116**, 4062 (1994).
28. T. Ireland, G. Grossheimann, C. Wieser-Jeunesse and P. Knochel, *Angew. Chem., Int. Ed.*, **38**, 3212 (1999).
29. B. L. Feringa, R. Badorrey, D. Peña, S. R. Harutyunyan and A. J. Minnaard, *Proc. Natl. Acad. Sci. U.S.A.*, **101**, 5834 (2004).
30. K.S. Lee, M. K. Brown, A. W. Hird and A. H. Hoveyda, *J. Am. Chem. Soc.*, **128**, 7182 (2006).
31. D. Martin, S. Kehrli, M. d'Augustin, H. Clavier, M. Mauduit and A. Alexakis, *J. Am. Chem. Soc.*, **128**, 8416 (2006).
32. F. López, S. R. Harutyunyan, A. J. Minnaard and B. L. Feringa, *J. Am. Chem. Soc.*, **126**, 12784 (2004).
33. For selected examples, see:  
(a) H. Mizutani, S. J. Degrado and A. H. Hoveyda, *J. Am. Chem. Soc.*, **124**, 779 (2002).  
(b) B. H. Lipshutz and J. M. Servesko, *Angew. Chem., Int. Ed.*, **42**, 4789 (2003).  
(c) T. Hayashi, K. Ueyama, N. Tokunaga and K. A. Yoshida, *J. Am. Chem. Soc.*, **125**, 11508 (2003).  
(d) P. K. Fraser and S. Woodward, *Chem. Eur. J.*, **9**, 776 (2003).
34. With 1 mol% of catalyst the products were obtained with equal enantioselectivity and slightly lower regioselectivity.
35. For a Rh-catalyzed asymmetric conjugate addition of arylboronic reagents to  $\alpha,\beta$ -unsaturated esters, see: S. Sakuma, M. Sakai, R. Itooka and N. Miyaura, *J. Org. Chem.*, **65**, 5951 (2000) and references cited therein.
36. A. W. Hird and A. H. Hoveyda, *Angew. Chem., Int. Ed.*, **42**, 1276 (2003).
37. For an alternative strategy, see: J. Schuppan, A. J. Minnaard and B. L. Feringa, *Chem. Commun.*, 792 (2004).
38. F. López, S. R. Harutyunyan, A. Meetsma, A. J. Minnaard and B. L. Feringa, *Angew. Chem., Int. Ed.*, **44**, 2752 (2005).
39. S.-Y. Wang, S.-J. Ji and T.-P. Loh, *J. Am. Chem. Soc.*, **129**, 276 (2007).
40. The reduced electron delocalization in the thioester moiety, compared to oxoesters, results in a higher reactivity towards conjugate addition reactions; see Reference 41.
41. R. Des Mazery, M. Pullez, F. López, S. R. Harutyunyan, A. J. Minnaard and B. L. Feringa, *J. Am. Chem. Soc.*, **127**, 9966 (2005).
42. R. P. Van Summeren, D. B. Moody, B. L. Feringa and A. J. Minnaard, *J. Am. Chem. Soc.*, **128**, 4546 (2006).
43. The occurrence of polydeoxypropionate chains in numerous biologically relevant compounds and the paucity of iterative catalytic asymmetric procedures is a stimulus for the development of new methodologies.
44. For alternative iterative approaches, see:  
(a) B. Liang, T. Novak, Z. Tan and E. Negishi, *J. Am. Chem. Soc.*, **128**, 2770 (2006).  
(b) T. Novak, Z. Tan, B. Liang and E. Negishi, *J. Am. Chem. Soc.*, **127**, 2838 (2005) and references cited therein.
45. B. ter Horst, B. L. Feringa and A. J. Minnaard, *Chem. Commun.*, 489 (2007).
46. B. ter Horst, B. L. Feringa and A. J. Minnaard, *Org. Lett.*, **9**, 3013 (2007).
47. G. P. Howell, S. P. Fletcher, K. Geurts, B. ter Horst and B. L. Feringa, *J. Am. Chem. Soc.*, **128**, 14977 (2006).
48. S. R. Harutyunyan, F. López, W. R. Browne, A. Correa, D. Peña, R. Badorrey, A. Meetsma, A. J. Minnaard and B. L. Feringa, *J. Am. Chem. Soc.*, **128**, 9103 (2006).
49. E. Nakamura and S. Mori, *Angew. Chem., Int. Ed.*, **39**, 3751 (2000).
50. (a) S. Woodward, *Angew. Chem., Int. Ed.*, **44**, 5560 (2005).  
For recent reviews on copper-catalyzed asymmetric allylic substitution, see:  
(b) H. Yorimitsu and K. Oshima, *Angew. Chem., Int. Ed.*, **44**, 4435 (2005).

- (c) A. Alexakis, C. Malan, L. Lea, K. Tissot-Croset, D. Polet and C. Falciola, *Chimia*, **60**, 124 (2006).
51. M. Yamanaka, S. Kato and E. Nakamura, *J. Am. Chem. Soc.*, **126**, 6287 (2004).
52. B. M. Trost and M. L. Crawley, *Chem. Rev.*, **103**, 2921 (2003).
53. (a) M. van Klaveren, E. S. M. Persson, A. del Villar, D. M. Grove, J. E. Bäckvall and G. van Koten, *Tetrahedron Lett.*, **36**, 3059 (1995).  
(b) J. Meuzelaar, A. S. E. Karlström, M. Van Klaveren, E. S. M. Persson, A. del Villar, G. Van Koten and J. E. Bäckvall, *Tetrahedron*, **56**, 2895 (2000).  
(c) A. S. E. Karlström, F. F. Huerta, G. J. Meuzelaar and J. E. Bäckvall, *Synlett*, 923 (2001).  
(d) H. K. Cotton, J. Norinder and J. E. Bäckvall, *Tetrahedron*, **62**, 5632 (2006).  
Although not enantioselective but stereospecific, the related copper-mediated and diphenylphosphanylbenzoyl-directed *syn*-allylic substitution with Grignard reagents is mentioned here:  
(e) C. Herber and B. Breit, *Angew. Chem., Int. Ed.*, **44**, 5267 (2005).
54. (a) F. Dübner and P. Knochel, *Angew. Chem., Int. Ed.*, **38**, 379 (1999).  
(b) F. Dübner and P. Knochel, *Tetrahedron Lett.*, **41**, 9233 (2000).
55. C. A. Luchaco-Cullis, H. Mizutani, K. E. Murphy and A. H. Hoveyda, *Angew. Chem., Int. Ed.*, **40**, 1456 (2001).
56. H. Malda, A. W. van Zijl, L. A. Arnold and B. L. Feringa, *Org. Lett.*, **3**, 1169 (2001).
57. (a) K. Tissot-Croset, D. Polet and A. Alexakis, *Angew. Chem., Int. Ed.*, **43**, 2426 (2004).  
(b) K. Tissot-Croset and A. Alexakis, *Tetrahedron Lett.*, **45**, 7375 (2004).  
(c) A. Alexakis, C. Malan, L. Lea, C. Benhaim and X. Fournieux, *Synlett*, 927 (2001).  
(d) A. Alexakis and K. Croset, *Org. Lett.*, **4**, 4147 (2002).  
(e) K. Tissot-Croset, D. Polet, S. Gille, C. Hawner and A. Alexakis, *Synthesis*, 2586 (2004).
58. C. A. Falciola, K. Tissot-Croset and A. Alexakis, *Angew. Chem., Int. Ed.*, **45**, 5995 (2006).
59. (a) A. O. Larsen, W. Leu, C. N. Oberhuber, J. E. Campbell and A. H. Hoveyda, *J. Am. Chem. Soc.*, **126**, 11130 (2004).  
(b) J. J. van Veldhuizen, J. E. Campbell, R. E. Giudici and A. H. Hoveyda, *J. Am. Chem. Soc.*, **127**, 6877 (2005).
60. (a) S. Tominaga, Y. Oi, T. Kato, D. K. An and S. Okamoto, *Tetrahedron Lett.*, **45**, 5585 (2004).  
(b) S. Okamoto, S. Tominaga, N. Saino, K. Kase and K. Shimoda, *J. Organomet. Chem.*, **690**, 6001 (2005). Note that due to a drawing error in a Table it erroneously looks as if silyl enol ethers are used as substrates.
61. Y. Lee and A. H. Hoveyda, *J. Am. Chem. Soc.*, **128**, 15604 (2006).
62. F. López, A. W. van Zijl, A. J. Minnaard and B. L. Feringa, *Chem. Commun.*, 409 (2006).
63. A. W. Van Zijl, F. López, A. J. Minnaard and B. L. Feringa, *J. Org. Chem.*, **72**, 2558 (2007).
64. K. Geurts, S. P. Fletcher and B. L. Feringa, *J. Am. Chem. Soc.*, **128**, 15572 (2006).
65. (a) B. M. Trost and A. Aponick, *J. Am. Chem. Soc.*, **128**, 3931 (2006) and references cited therein.  
(b) C. Shu and J. F. Hartwig, *Angew. Chem., Int. Ed.*, **43**, 4794 (2004) and references cited therein.
66. S. F. Kirsch and L. E. Overman, *J. Am. Chem. Soc.*, **127**, 2866 (2005).
67. C. E. Anderson and L. E. Overman, *J. Am. Chem. Soc.*, **125**, 12412 (2003).

# Author Index

This author index is designed to enable the reader to locate an author's name and work with the aid of the reference numbers appearing in the text. The page numbers are printed in normal type in ascending numerical order, followed by the reference numbers in parentheses. The numbers in *italics* refer to the pages on which the references are actually listed.

- Aavula, B. R. 289 (264), *311*  
 Abarbri, M. 518 (44, 46), 519 (51), 525 (41), 585  
 Abarca, A. 278 (208), *310*  
 Abarca, B. 689 (26, 27), 713 (24), *714*, *715*  
 Abate, Y. 171 (92), *186*  
 Abbondondola, J. A. 171 (103), *186*  
 Abd El-Hady, D. 277 (200), *310*  
 Abd El-Hamid, M. 277 (200), *310*  
 Abdel-Fattah, A. A. 559 (232), *590*  
 Abdel-Hadi, M. 550 (167), *589*  
 Abegg, R. 2 (10), 92, 107 (25), *127*  
 Abel, E. W. 58 (3, 4), 92, 512 (4), *583*, *657* (90), *678*  
 Abeles, R. H. 348 (245), *364*  
 Abeln, D. 50 (166), *96*  
 Abo El-Maali, N. 277 (200), *310*  
 Abraham, W. D. 760 (49), *769*  
 Abrahams, J. P. 329 (94, 102), *361*  
 Abrams, S. 288 (257), *311*  
 Abreu, J. B. 172 (108), *186*  
 Acar, O. 277 (206), *310*  
 Ackermann, L. 550 (171, 172), *589*  
 Adamo, C. 384 (30), *402*  
 Adamowicz, L. 323 (55), *360*  
 Adams, F. C. 302 (340, 341), 304 (319), *313*  
 Adams, J. A. 347 (233), 348 (221, 234, 240, 243), *364*, 560 (234), *590*, 673 (148, 149), *679*  
 Adderley, C. J. R. 476 (91), *508*  
 Adhikari, R. 495 (111), *509*  
 Adzuma, K. 355 (311), *366*  
 Afeefy, H. Y. 113 (56), *128*  
 Afghan, B. K. 300 (320), *313*  
 Aggarwal, S. K. 303 (344, 350), 304 (354), *313*, *314*  
 Agostiano, A. 212 (115), *217*  
 Agrawal, Y. K. 282 (233), *311*  
 Agus, Z. S. 268 (87), *307*  
 Ahmadi, M. A. 246 (91), *262*  
 Ahmed, H. M. 280 (220), *310*  
 Ahmed, S. 305 (364), *314*  
 Ahn, K-H. 772 (7), *800*  
 Ahn, N. G. 347 (228), *364*  
 Ahr, M. 554 (191), *589*, 626 (76), *630*  
 Aimetti, J. A. 499 (117), *509*  
 Ainai, T. 558 (217), *590*  
 Akamine, P. 348 (241), *364*  
 Akao, A. 524 (63), *585*, 699 (31), 702 (39), *715*  
 Akihiro, Y. 538 (105), *587*  
 Akishin, P. A. 183 (154), 184 (152), *187*, 391 (15), *402*  
 Akiyama, M. 194 (29), 213 (119), *215*, *217*  
 Akkerman, O. S. 3 (15), 34 (106, 116), 35 (117, 118), 38 (83), 40 (140), 43 (146), 44 (142), 61 (198), 66 (213–216), 86 (269), 92, 94, 95, 97, 99, 116 (58), 120 (67), 121 (71), *128*, 183 (140), *187*, 318 (22), *359*  
 Akola, J. 331 (120), *362*  
 Akutagawa, S. 657 (88), *678*  
 Alam, H. 318 (21), *359*  
 Alami, M. 555 (195–198), *589*, 607 (48), 608 (51), *629*  
 Albachi, R. 516 (29), *584*  
 Alberti, A. 259 (144), 263, 580 (313), *593*  
 Alcaraz, M. 302 (337), 304 (331), *313*  
 Aleandri, L. E. 610 (60), *630*  
 Aleksniuk, O. 471 (93), *508*

- Alemparte, C. 583 (319), 593  
 Alexakis, A. 558 (219, 220), 564 (255), 565 (257), 590, 591, 633 (1), 635 (16), 676, 774 (12), 775 (31), 779 (19), 791 (50, 57, 58), 800–802  
 Alexopoulos, E. 74 (245), 98, 413 (43), 435  
 Al-Fekri, D. M. 103 (7), 126, 519 (53), 585  
 Alhambra, C. 350 (263), 365  
 Ali, A. M. M. 276 (198), 310  
 Al-Juaid, S. S. 23 (77, 78), 63 (112, 206, 208), 94, 97  
 Al-Laham, M. A. 384 (30), 402  
 Allan, A. 391 (16), 402  
 Allan, J. F. 422 (59), 424 (61), 435, 469 (79), 508  
 Allan, J. R. 425 (70), 436  
 Allan, L. M. 302 (338), 313  
 Allen, A. 303 (345), 313  
 Almo, S. C. 357 (342), 366  
 Alonso de Diego, S. A. 727 (24), 768  
 Alonso, T. 46 (158), 96, 123 (89), 129  
 Alonso-Rodríguez, E. 271 (164), 309  
 Alpaugh, H. B. 268 (13), 306  
 Altarejos, J. 440 (7), 506  
 Althammer, A. 550 (171), 589  
 Altink, R. M. 34 (106), 94  
 Altman, R. B. 270 (160), 309  
 Altman, S. 335 (150), 362  
 Altura, B. M. 268 (20, 97, 98), 270 (153), 306, 307, 309  
 Altura, B. T. 268 (19, 20, 97, 98), 270 (153), 276 (18), 306, 307, 309  
 Alvarez, E. 608 (54, 55), 629  
 Alves, J. 355 (320), 366  
 Amao, Y. 214 (135), 218  
 Ammann, D. 276 (14), 306  
 Armstrong, D. R. 18 (67), 93  
 Amzel, L. M. 329 (93), 361  
 An, D. K. 791 (60), 802  
 An, X. 356 (326), 366  
 Ananvoranich, S. 336 (160), 362  
 Anastassopoulou, J. 334 (142), 362  
 Anctil, E. J.-G. 537 (102), 586  
 Andersen, A. 124 (97), 125 (105), 129, 161 (56), 185  
 Andersen, R. A. 26 (94), 29 (102), 91 (277), 94, 99, 123 (85), 125 (102), 129, 183 (147, 149), 187  
 Anderson, C. E. 798 (67), 802  
 Anderson, J. D. 424 (66), 436, 473 (85), 508  
 Anderson, R. A. 23 (75), 93, 150 (12), 153  
 Anderson, V. E. 348 (238), 364  
 Andersson, I. 357 (343), 359 (354), 366, 367  
 Andersson, P. 519 (53), 585  
 Andersson, P. G. 564 (252), 591  
 Ando, K. 749 (42), 769  
 André, I. 323 (54, 57), 360  
 Andrés, J. 357 (347), 359 (356, 357), 366, 367, 393 (25), 402  
 Andres, J. L. 369 (2), 384 (30), 401, 402  
 Andrews, L. 157 (20), 158 (28, 31), 159 (33, 34), 184, 185  
 Andrews, P. C. 19 (68), 64 (209), 93, 97  
 Andrews, T. J. 358 (348–350), 359 (339, 351, 353), 366, 367  
 Andrikopoulos, P. C. 9 (52), 17 (66), 20 (70), 22 (72, 74), 93, 419 (50), 435  
 Androulakis, G. 278 (207), 310  
 Angermund, K. 33 (114), 45 (157), 86 (266), 94, 96, 99  
 Anisimov, A. V. 299 (306), 312  
 Anteunis, M. 292 (282), 312  
 Antolini, F. 62 (201), 97  
 Antonucci, V. 293 (267), 311  
 Aoyama, T. 556 (207), 590  
 Apeloig, Y. 156 (1), 184  
 Aponick, A. 798 (65), 802  
 Appleby, I. C. 103 (6), 126  
 Arai, M. 107 (21), 126  
 Araki, S. 285 (237), 311  
 Araki, Y. 201 (41, 42, 70), 216  
 Arayama, K. 572 (287), 592  
 Arduengo, A. J. 53 (175), 96  
 Argade, N. P. 557 (209), 590  
 Ariese, F. 269 (151), 309  
 Arkhangelsky, S. E. 330 (106, 107), 361  
 Armentrout, P. B. 124 (97), 125 (105), 129, 160 (39), 161 (56), 185  
 Armstrong, D. R. 9 (52), 17 (66), 20 (70), 22 (72, 74), 57 (186), 93, 96, 124 (91), 129, 413 (42), 419 (50), 435  
 Arnaud, M. J. 288 (254, 255), 311  
 Arnold, J. J. 352 (301), 365  
 Arnold, L. A. 774 (14–16), 791 (56), 800, 802  
 Arpe, H. J. 214 (124), 218  
 Arrayás, R. G. 659 (95), 678  
 Arrebola, F. J. 302 (335), 313  
 Arruda, M. A. Z. 271 (167), 309  
 Arsenian, M. A. 268 (103), 308  
 Arseniyadis, S. 468 (83), 469 (84), 508, 528 (85), 586  
 Artacho, R. 271 (168), 309  
 Asahi, T. 194 (30), 201 (76), 215, 216  
 Asai, F. 579 (311), 592  
 Asakawa, N. 760 (50), 764 (52), 769  
 Asano, Y. 426 (71), 436, 498 (41), 507, 772 (6), 800  
 Asaoko, M. 563 (248), 591  
 Ashby, E. C. 23 (76), 58 (11), 92, 93, 103 (4, 7), 107 (29), 108 (31, 32, 40), 126, 127, 132 (1, 2), 134 (18), 138 (21), 139 (9), 140 (5), 146 (40), 147 (42), 153, 154, 183 (148), 187, 389 (3), 391 (8, 10), 401, 411 (40), 424 (68), 428 (83), 435, 436, 513 (14), 519 (53), 584, 585, 683 (16), 714



- Ashkenazi, V. 248 (113), 262  
 Ashley-Facey, A. 172 (108), 186  
 Aso, Y. 290 (274), 312  
 Atas, M. 278 (214), 310  
 Athar, T. 16 (63), 93  
 Atsmon, J. 268 (144), 308  
 Atwood, J. L. 28 (100), 47 (47), 93, 94  
 Audergon, L. 774 (8), 800  
 Audrain, H. 646 (37), 677  
 Ault, B. S. 157 (23), 185, 391 (17), 402  
 Aultman, J. F. 512 (7), 583  
 Aurbach, D. 247 (106, 108), 248 (96, 107, 113), 250 (115), 251 (112), 252 (114, 116), 253 (117–119), 258 (109–111), 262  
 Avedissian, H. 555 (198), 589, 626 (29), 629  
 Avent, A. G. 62 (120), 63 (112), 94, 95  
 Avola, S. 550 (167), 589  
 Avolio, S. 534 (81), 586, 767 (58), 769  
 Awad, H. 44 (44), 93, 689 (26–28), 713 (24, 25), 714, 715  
 Axten, J. 391 (22), 402  
 Ayala, P. Y. 384 (30), 402  
 Baal-Zedaka, I. 211 (110), 217  
 Baba, T. 341 (201), 363  
 Babcock, G. T. 201 (72), 216  
 Babu, C. S. 322 (44), 360  
 Bac, P. 267 (1), 268 (50, 54), 306, 307  
 Baccolini, G. 674 (151), 679  
 Bach, T. 525 (65), 585  
 Bachain, P. 301 (358), 314  
 Bachand, C. 500 (118), 509  
 Bachert, D. 103 (8), 126, 519 (52), 585  
 Bäckvall, J. E. 791 (53), 802  
 Bäckvall, J.-E. 544 (131), 555 (201, 204), 557 (210), 558 (218), 588, 590  
 Baddeley, G. V. 476 (91), 508  
 Badham, N. F. 760 (46), 769  
 Badorrey, R. 775 (29), 788 (48), 801  
 Baer, R. 347 (237), 364  
 Baev, A. K. 122 (77), 128  
 Baeyer, A. 2 (6), 92, 107 (24), 127  
 Bai, Y. 277 (205), 310  
 Bailey, P. J. 74 (124, 243, 244), 76 (249), 95, 98, 150 (43), 154, 406 (19), 407 (21, 22), 414 (45), 422 (15, 20), 423 (17), 434, 435  
 Bailey, S. M. 113 (2), 126  
 Bailey, W. F. 395 (4), 401, 527 (28), 584  
 Baily, P. J. 81 (255, 256), 98  
 Baird, M. S. 528 (82), 586  
 Baizer, M. M. 219 (8), 233 (2), 238 (6), 239 (78), 260, 261  
 Bajaj, A. V. 3 (24), 92  
 Bakale, R. P. 395 (35), 402  
 Baker, D. C. 478 (65), 508  
 Baker, J. 369 (2), 401  
 Baker, T. A. 352 (275), 365  
 Bakhtina, M. 352 (290), 365  
 Bakos, J. T. 339 (178), 363  
 Balaban, T. S. 356 (330), 366  
 Baldwin, J. E. 547 (149), 588  
 Balenkova, E. S. 547 (148), 588  
 Balkovec, J. M. 443 (13), 506  
 Ballard, S. G. 193 (17), 215  
 Ballem, K. H. D. 74 (246), 98  
 Ballesteros, R. 689 (26, 27), 713 (24), 714, 715  
 Baltzer, G. 268 (39), 306  
 Baluja-Santos, C. 268 (36), 306  
 Ban, N. 336 (161), 362  
 Banas, K. 299 (311), 312  
 Banatao, D. R. 270 (160), 309  
 Banon-Tenne, D. 633 (1), 676  
 Bara, M. 267 (1), 268 (50, 54, 102), 306–308  
 Baranov, V. 124 (96), 129, 180 (134), 187  
 Baranov, V. I. 180 (135), 187  
 Barber, J. 355 (321), 366  
 Barber, J. J. 259 (149), 263  
 Barbier, P. 2 (1), 92  
 Barbot, F. 657 (89), 678  
 Barbour, H. 268 (86), 307  
 Barbour, H. M. 282 (158), 309  
 Bard, A. J. 219 (3, 5), 260  
 Bare, W. D. 158 (28, 31), 185  
 Barford, D. 347 (226), 364  
 Barish, R. A. 268 (83), 307  
 Barkovskii, G. B. 171 (5), 184  
 Barley, H. R. L. 419 (50), 435  
 Barlow, S. E. 118 (61), 128  
 Barmasov, A. V. 198 (59), 216  
 Barnes, K. 219 (1), 260  
 Barnett, N. D. R. 15 (62), 38 (126), 93, 95, 149 (47), 154  
 Baron, O. 268 (10, 11), 306, 525 (66), 534 (99), 540 (114), 585–587, 774 (23), 800  
 Barone, R. 260 (147), 263  
 Barone, V. 384 (30), 402  
 Barran, P. E. 175 (122), 187, 318 (23), 359  
 Barrett, J. 208 (88), 217  
 Barrientos, C. 106 (16), 126  
 Barth, I. 357 (336), 366  
 Barthelat, J. C. 331 (114–116), 361, 362  
 Bartmann, E. 45 (154), 95  
 Bartoli, G. 566 (263), 591, 674 (151), 679  
 Barton, T. L. 268 (59), 307  
 Baruah, M. 548 (161), 588  
 Bassindale, M. J. 424 (64), 436, 473 (86), 508  
 Batey, R. T. 334 (140), 362  
 Batra, V. K. 352 (299), 365  
 Bätting, K. 656 (84), 678  
 Battioni, P. 634 (12), 676  
 Bau, R. 86 (268), 99  
 Bauer, C. E. 193 (28), 214 (139), 215, 218  
 Bäuerle, W. 287 (253), 311  
 Baum, E. 26 (97), 94  
 Baumann, F. 52 (173), 53 (174), 96  
 Baumeister, D. 301 (359), 314

- Baumgartner, J. 38 (130), 95  
 Baxter, D. C. 304 (351), 313  
 Baxter, J. T. 512 (5), 583  
 Bayh, O. 44 (44), 93, 689 (26–28), 715  
 Bazureau, J. P. 44 (44), 93, 689 (28), 715  
 Beale, S. I. 208 (90–92), 217  
 Beals, B. J. 259 (146), 263  
 Beard, W. A. 352 (288, 299), 365  
 Beardah, M. S. 184 (156), 187  
 Beattie, T. 499 (116), 509  
 Bebenek, K. 355 (315), 366  
 Beceiro-González, E. 271 (164), 309  
 Becerra, E. 283 (236), 311  
 Beck, K. R. 141 (28), 153  
 Becke, A. D. 384 (28), 402  
 Becker, J. S. 287 (251), 311  
 Becker, W. E. 107 (29), 127, 389 (3), 401  
 Becker, W. F. 108 (33, 34, 38), 127  
 Beckmann, J. 514 (24), 584  
 Bedford, R. B. 546 (144), 588, 615 (68–70), 630  
 Beeby, A. 196 (43), 216  
 Beese, L. S. 354 (310), 366  
 Begtrup, M. 517 (38), 518 (49), 525 (64), 574 (297), 584, 585, 592  
 Begum, S. A. 545 (136), 588  
 Begun, G. M. 124 (92), 129  
 Behrend, C. 285 (156), 309  
 Behrens, U. 10 (54), 42 (144), 48 (163), 93, 95, 96, 122 (81), 128  
 Beigelman, L. 340 (187), 341 (188), 363  
 Bejun, G. M. 182 (4), 184  
 Belchior, J. C. 270 (152), 309  
 Beletskaya, I. P. 171 (5, 100), 175 (101), 184, 186, 268 (5), 306  
 Belfiore, F. 268 (49), 307  
 Bell, C. E. 351 (284), 365  
 Bell, L. 673 (140, 141), 679  
 Bell, S. P. 352 (275), 365  
 Beller, M. 544 (129, 130), 588, 596 (27), 629  
 Bello, Z. I. 259 (146), 263  
 Belmonte Vega, A. 302 (335), 313  
 Belov, S. A. 65 (211), 97  
 Benafoux, D. 539 (111), 587  
 Benaglia, M. 259 (144), 263  
 Bencze, L. 653 (69, 70), 677  
 Bendicho, C. 272 (170), 309  
 Benech, H. 268 (43), 306  
 Benhaim, C. 558 (219), 564 (255), 590, 591, 779 (19), 791 (57), 800, 802  
 Benjamini, E. 347 (230), 364  
 Benkeser, R. A. 141 (28), 153  
 Benkovic, S. J. 355 (274), 365  
 Benn, R. 71 (227), 97, 123 (80, 86), 128, 129, 143 (32, 37), 151 (15), 152 (50, 51), 153, 154  
 Bension, R. M. 659 (97), 678  
 Berdinsky, V. L. 330 (109), 361  
 Berezin, B. D. 214 (138), 218  
 Berezin, M. B. 214 (138), 218  
 Berg, A. 206 (78), 217  
 Bergauer, M. 518 (49), 585  
 Bergbreiter, D. E. 289 (265), 311  
 Bergenhem, N. C. H. 344 (217), 364  
 Berger, I. 335 (31), 360  
 Bergkamp, M. A. 198 (57), 216  
 Bergman, R. G. 91 (277), 99  
 BergStresser, G. L. 44 (147), 95  
 Bérillon, L. 518 (43), 525 (41, 67), 534 (81, 98), 585, 586  
 Bermejo-Martínez, F. 268 (36), 306  
 Bernard, D. 517 (34), 584  
 Bernardi, A. 484 (101), 509  
 Bernardi, P. 580 (313), 593  
 Berner, H. J. 419 (55), 435  
 Bernhard, L. 289 (271), 312  
 Bertagnolli, H. 3 (16), 92  
 Berthelot, J. 125 (101), 129, 182 (138), 187  
 Bertini, F. 258 (133), 263  
 Bertrand, G. 718 (2), 767  
 Bertrand, J. 458 (50), 478 (97), 507, 508  
 Bestman, H. J. 537 (104), 586  
 Betham, M. 615 (70), 630  
 Bhagi, A. K. 428 (86), 436  
 Bhakat, K. K. 353 (307), 366  
 Bhatia, A. V. 559 (227), 590  
 Bhatt, R. K. 558 (218), 590  
 Bhattacharya, A. 595 (8), 628  
 Bhupathy, M. 760 (49), 769  
 Biali, S. E. 471 (93), 508  
 Bianchet, M. A. 329 (93), 361  
 Bianciotto, M. 331 (114), 361  
 Bica, K. 618 (74), 630  
 Bickelhaupt, F. 3 (15, 28), 34 (106, 116), 35 (117, 118), 38 (83), 39 (135), 40 (137, 138, 140), 43 (146), 44 (142), 58 (187), 61 (136, 198), 62 (199), 66 (213–216), 86 (269), 92, 94–97, 99, 116 (58), 120 (66–68), 121 (69, 71), 128, 145 (27), 153, 183 (140), 187, 268 (3, 4), 306, 318 (22), 359, 384 (31), 402, 512 (6), 583  
 Bicker, G. R. 293 (266), 311  
 Bierbaum, V. M. 118 (61), 128  
 Billing, D. G. 538 (109), 587  
 Bilodeau, M. T. 503 (123), 509  
 Bindels, R. J. M. 268 (66), 307  
 Bindra, R. 634 (12), 676  
 Binkley, J. S. 369 (1, 2), 401  
 Biran, C. 467 (77), 472 (76), 473 (74), 508, 539 (111), 587  
 Bischoff, L. 689 (27), 715  
 Bivens, L. 144 (29), 153  
 Bjerregaard, T. 518 (49), 585  
 Björklund, E. 304 (351), 313  
 Black, C. B. 320 (7), 359  
 Blackmore, I. J. 71 (231), 98, 411 (33), 435

- Blackwell, H. E. 707 (48), 715  
 Blades, A. T. 175 (115, 123), 186, 187  
 Blagouev, B. 503 (121), 509  
 Blair, S. 84 (265), 99, 298 (304), 312, 427 (73), 436  
 Blakemore, P. R. 722 (13), 768  
 Blanco, F. 689 (26, 27), 713 (24), 714, 715  
 Blankenship, R. E. 193 (28), 214 (139), 215, 218, 356 (327), 366  
 Blart, E. 198 (66), 216  
 Bläser, D. 71 (230), 98, 405 (12), 434  
 Blau, W. J. 212 (113), 217  
 Blessing, R. H. 328 (82), 361  
 Bloch, R. 571 (285), 592  
 Blom, R. 29 (102), 94, 123 (85), 129, 183 (147, 149), 187  
 Blomberg, C. 3 (18), 40 (137, 138), 62 (199), 92, 95, 97, 107 (30), 120 (66, 68), 127, 128, 145 (27), 153, 258 (132), 263, 384 (31), 402  
 Blount, K. F. 341 (180), 363  
 Bobbio, C. 702 (38), 715  
 Bobkowski, W. 268 (110), 308  
 Bobrovskii, A. P. 196 (51), 216  
 Boche, G. 59 (192), 62 (204), 97, 395 (34), 402, 516 (32), 584  
 Bochkarev, A. 327 (67), 360  
 Bochman, M. 74 (247), 98  
 Bochmann, M. 421 (18), 434  
 Bocian, D. F. 201 (38, 39, 45, 46), 215, 216  
 Bock, C. W. 319 (25), 324 (35), 360, 391 (22), 402  
 Bock, H. 62 (203), 97  
 Boero, M. 341 (204), 363  
 Boersma, J. 69 (29), 77 (251), 92, 98  
 Boese, R. 71 (230), 98, 405 (12), 434  
 Boff, J. M. 211 (111), 217  
 Bogdanović, B. 33 (114, 115), 44 (113, 149, 150, 152, 153), 45 (154, 156), 47 (159), 94–96, 513 (17), 514 (22), 540 (118), 584, 587, 610 (60), 621 (79), 630  
 Böhländ, H. 419 (55), 435  
 Böhm, H.-J. 300 (317), 313  
 Böhm, V. P. W. 135 (11), 153, 550 (166, 168), 589, 720 (6), 768  
 Bohme, D. K. 124 (94, 96), 125 (95), 129, 156 (13), 160 (54), 161 (55), 180 (46, 134, 135), 184, 185, 187  
 Böhner, C. 711 (49), 715  
 Bohr, V. A. 353 (305), 366  
 Boiteau, J. G. 774 (21), 800  
 Boldea, A. 285 (242), 311  
 Bolesov, I. G. 528 (82), 586  
 Bollewein, T. 81 (261), 98  
 Bollwein, T. 302 (302), 312, 409 (30), 410 (37), 435  
 Bolm, C. 517 (34), 584, 596 (30), 629, 722 (15), 768  
 Bols, M. 548 (161), 588  
 Boman, X. 268 (138), 308  
 Bommer, J. C. 193 (21), 214 (133), 215, 218  
 Bonafoux, D. 467 (77), 472 (76), 508  
 Boncella, J. M. 183 (147), 187  
 Bonde, S. E. 604 (46), 629  
 Bongini, A. 564 (253), 591  
 Bonini, B. F. 259 (144), 263, 559 (228), 590  
 Bonne, F. 574 (295), 592  
 Bonnekessel, M. 554 (189), 589, 608 (57), 629  
 Bonnet, V. 524 (60), 525 (41), 537 (103), 553 (186), 585, 586, 589  
 Bonnett, R. 214 (134), 218  
 Bons, P. 540 (118), 587, 610 (60), 630  
 Bordeau, M. 467 (77), 472 (76), 473 (74), 508, 539 (111), 587  
 Borg, D. C. 196 (47), 216  
 Born, R. 550 (172), 589  
 Borodin, V. A. 121 (70), 128  
 Borzak, S. 268 (106), 308  
 Borzov, M. V. 65 (211), 97  
 Bosco, M. 566 (263), 591, 674 (151), 679  
 Boudet, N. 524 (62), 585  
 Boudier, A. 525 (41), 585  
 Boukherroub, R. 243 (85), 262  
 Boulain, J. C. 344 (215), 364  
 Boutevin, B. 711 (50), 715  
 Bowen, B. P. 356 (327), 366  
 Bowen, M. E. 289 (264), 311  
 Bowyer, W. J. 259 (146), 263, 513 (12), 583  
 Boyd, W. A. 144 (29), 153  
 Boyer, P. D. 329 (91), 361  
 Boyles, H. B. 391 (7), 401  
 Boymond, L. 517 (35), 534 (81, 100), 584, 586, 619 (45), 629, 690 (30), 715  
 Brade, K. 576 (301), 592  
 Braga, A. L. 774 (25), 801  
 Braithwaite, D. 233 (22), 234 (23), 244 (21), 260  
 Braithwaite, D. G. 239 (70), 240 (64–69), 261  
 Brancaleoni, D. 580 (313), 593  
 Brand, R. A. 610 (60), 630  
 Brändén, C. I. 359 (355), 367  
 Bräse, S. 531 (93), 586  
 Brasuel, M. 285 (156), 309  
 Braun, M. 718 (2), 768  
 Brautigam, C. A. 352 (295), 365  
 Breaker, R. R. 336 (153), 362  
 Breckenridge, W. H. 157 (16, 19), 159 (18), 184  
 Brehon, B. 555 (195), 589  
 Breit, B. 455 (42), 507, 557 (213), 590, 791 (53), 802  
 Bremer, T. H. 235 (50), 261  
 Brenek, S. J. 103 (10), 126  
 Breneman, C. M. 113 (56), 128  
 Brenner, A. 246 (99), 262  
 Brereton, R. G. 211 (109), 217  
 Breton, G. 524 (60), 585

- Brettreich, M. 675 (154), 679  
 Breutel, C. 775 (27), 801  
 Brewer, J. M. 320 (26), 349 (249, 251, 254, 256–258), 360, 364, 365  
 Brian, C. 539 (111), 587  
 Brick, P. 351 (286), 365  
 Brintzinger, H. H. 125 (102), 129  
 Brintzinger, H.-H. 48 (164), 49 (165), 96  
 Brion, J.-D. 555 (197, 198), 589, 607 (48), 608 (51), 629  
 Britt, R. D. 341 (198), 363  
 Brochette, P. 198 (60), 216  
 Brockhoff, H. 301 (356), 314  
 Brodbelt, J. S. 178 (130), 187  
 Brodilova, J. 193 (20), 215  
 Broeke, J. 519 (53), 585  
 Brombrun, A. 557 (210), 590  
 Bronstrup, M. 135 (11), 153, 720 (6), 768  
 Brookings, D. C. 673 (141), 679  
 Brosche, T. 537 (104), 586  
 Brown, J. D. 514 (19), 584  
 Brown, M. 302 (324), 313  
 Brown, M. K. 775 (30), 801  
 Brown, R. F. C. 540 (115), 587  
 Brown, S. B. 208 (97), 210 (100), 211 (108), 217  
 Brown, S. N. 469 (78), 508  
 Brown, T. L. 4 (35, 36), 92, 682 (2), 714  
 Browne, W. R. 788 (48), 801  
 Bruce, D. W. 546 (144), 588, 615 (68–70), 630  
 Bruening, G. 339 (178), 363  
 Bruhn, C. 38 (127), 42 (143), 95, 136 (16), 153  
 Bruice, T. C. 341 (202), 363  
 Brunschwig, B. S. 196 (48), 216, 259 (143), 263  
 Brunvoll, J. 183 (146), 187  
 Bruzzoniti, M. C. 273 (182), 309  
 Bryce-Smith, D. 674 (150), 679  
 Brym, M. 64 (209), 97  
 Bučević-Popović, V. 345 (218), 364  
 Buchachenko, A. L. 330 (106–110), 331 (104, 111), 361  
 Bucher, A. 44 (44), 93, 689 (28), 715  
 Buchwald, S. L. 550 (170), 589  
 Buck, P. 576 (303), 592  
 Buckingham, M. J. 286 (246), 311  
 Budzelaar, P. H. M. 77 (251), 98  
 Buechler, J. A. 347 (231), 364  
 Buell, G. R. 661 (105), 678  
 Bugg, C. E. 318 (16), 359  
 Bühler, R. 517 (39), 585  
 Buhlmayer, P. 443 (13), 506  
 Bulgakov, O. V. 344 (215), 364  
 Bulgakov, R. G. 235 (51), 261  
 Bullock, T. H. 51 (51), 93  
 Bulska, E. 287 (192), 310  
 Bulygin, V. V. 329 (92), 361  
 Bumagin, N. A. 553 (187), 589  
 Bünder, W. 25 (90), 94  
 Bunlaksananusorn, T. 525 (41), 585  
 Bunnage, M. E. 454 (40), 507  
 Burack, J. L. 268 (19), 306  
 Burant, J. C. 384 (30), 402  
 Burdon, J. 654 (77), 678  
 Bures, F. 559 (223), 590, 601 (44), 629  
 Burke, D. H. 341 (193), 363  
 Burke, J. M. 341 (195, 197), 363  
 Burke, S. D. 718 (2), 768  
 Burla, M. C. 328 (83), 361  
 Burns, C. J. 183 (147), 187  
 Burns, D. H. 545 (134), 588  
 Buron, F. 702 (40), 715  
 Burt, S. K. 158 (27), 185, 331 (117, 118), 362  
 Burton, A. 720 (5), 768  
 Burton, D. J. 516 (30), 517 (34), 584  
 Burton, R. F. 287 (250), 311  
 Busacca, C. A. 555 (203), 590  
 Busch, D. H. 342 (207), 363  
 Busch, F. R. 499 (115), 509  
 Bush, J. E. 283 (234), 311  
 Bushnell, D. A. 355 (313), 366  
 Bustamante, C. 336 (163), 362  
 Buttrus, N. H. 63 (207), 97  
 Butts, C. P. 556 (206), 590  
 Buzayan, J. M. 339 (178), 363  
 Cabrol, N. 478 (97), 508  
 Cachau, R. E. 331 (118), 362  
 Cadman, M. L. F. 493 (106), 509  
 Cahiez, G. 517 (34, 35), 518 (43), 519 (51), 534 (81, 98, 100), 544 (133), 545 (137), 546 (143), 552 (176), 554 (191), 555 (195, 196, 198), 559 (223), 563 (245), 584–586, 588–591, 601 (43, 44), 607 (47), 618 (72), 619 (45), 626 (29, 76), 629, 630, 635 (16), 676, 690 (30), 715  
 Cai, M. 540 (121, 122), 587  
 Calabrese, G. 268 (91), 307  
 Calabrese, J. C. 527 (28), 584  
 Calaza, M. I. 525 (41), 585  
 Caldecott, K. W. 351 (283), 365  
 Calderon, R. L. 268 (130), 308  
 Cali, P. 517 (38), 574 (297), 584, 592  
 Calingaert, G. 238 (77), 261  
 Calvin, M. 207 (85–87), 217  
 Cameron, C. E. 352 (301), 365  
 Cameron, I. L. 268 (12), 306  
 Camici, L. 475 (81), 508  
 Caminiti, R. 318 (17), 359  
 Cammi, R. 384 (30), 402  
 Campbell, J. E. 791 (59), 802  
 Campbell, M. J. 579 (310), 592  
 Campos Pedrosa, L. de F. 268 (96), 307  
 Camus, C. 348 (246), 350 (261), 364, 365  
 Canè, F. 580 (313), 593

- Canfranc, E. 278 (208), 310  
 Cannon, K. C. 55 (178), 96, 225 (40), 261  
 Cannone, J. J. 337 (169), 363  
 Cao, Z. 275 (193), 310  
 Capelo, J. L. 272 (170), 309  
 Capozzi, M. A. M. 583 (318), 593  
 Caprio, V. 774 (1), 800  
 Carda, M. 391 (26), 393 (25), 402  
 Cardani, S. 484 (101), 509  
 Cardellicchio, C. 583 (317, 318), 593, 601 (41, 42), 629  
 Cardillo, G. 564 (253), 591  
 Carey, F. A. 387 (32), 402  
 Carmichael, I. 206 (77), 217  
 Caro, C. F. 32 (111), 37 (121), 62 (120), 94, 95, 416 (49), 435  
 Caro, Y. 301 (358), 314  
 Carpentier, J.-F. 69 (223), 97  
 Carreira, L. A. 349 (258), 365  
 Carrera, A. 303 (348), 313  
 Carrera, S. 659 (95), 678  
 Carretero, J. C. 518 (48), 585, 659 (95), 678  
 Carroll, G. L. 253 (124), 263  
 Carroll, J. D. 293 (266), 311  
 Carson, A. S. 109 (46, 47), 127  
 Carswell, E. L. 424 (63), 435, 473 (89), 508  
 Carter, J. P. 323 (57), 360  
 Carvalho, S. 270 (152), 309  
 Carver, J. P. 323 (54), 360  
 Casareno, R. 322 (44), 360  
 Casarini, A. 580 (313), 592  
 Casellato, U. 268 (148), 308  
 Casey, W. H. 257 (129), 263  
 Cason, J. 600 (37), 601 (38, 39), 629  
 Castedo, L. 540 (115), 587  
 Castellato, U. 64 (210), 97  
 Castillo, A. 268 (119), 308  
 Castillo, R. 393 (25), 402  
 Castro, A. M. M. 727 (24), 768  
 Castro, B. 442 (10), 484 (100), 506, 508  
 Castro, C. 352 (301), 365  
 Castro, J. M. 440 (7), 506  
 Cazeau, P. 472 (76), 473 (74), 508, 539 (111), 587  
 Ceccarelli, S. M. 625 (93), 630  
 Cech, T. R. 320 (29), 335 (149), 337 (154, 170, 171), 360, 362, 363  
 Cerdà, V. 283 (236), 311  
 Cernak, I. 268 (145), 308  
 Černohorský, T. 279 (217), 310  
 Ceulemans, M. 302 (340, 341), 313  
 Cevette, M. J. 268 (73), 307  
 Chaboche, C. 544 (133), 554 (191), 588, 589, 626 (76), 630  
 Chacon, D. R. 82 (162), 96, 417 (13), 434  
 Chai, G. 349 (251), 364  
 Challacombe, M. 384 (30), 402  
 Chamberlin, S. A. 559 (227), 590  
 Chambers, R. D. 516 (30), 517 (34), 584  
 Champ, M. A. 302 (330), 313  
 Chan, H.-K. 545 (134), 588  
 Chan, T. H. 515 (26), 584  
 Chandler, D. 329 (90), 361  
 Chandra, T. 196 (44), 216  
 Chang, C.-C. 81 (228), 98, 149 (46), 154, 422 (25), 435  
 Chang, C. H. 270 (159), 309  
 Chang, C. K. 198 (57), 201 (71–73), 216  
 Chang, J. 272 (177), 309  
 Chang, W. 356 (326), 366  
 Chanon, M. 157 (15), 184, 260 (147), 263, 391 (20), 402, 513 (15), 584  
 Chao, L.-C. 411 (40), 435, 683 (16), 714  
 Chapdelaine, M. J. 451 (33), 507  
 Chapleur, Y. 484 (100), 508  
 Chasid, O. 253 (119), 262  
 Chau, A. S. Y. 300 (320), 313  
 Chau, Y. K. 300 (320, 321), 302 (324, 338), 303 (318), 313  
 Chazalviel, J.-N. 241 (79, 80), 243 (81–83, 85), 262  
 Chechik-Lankin, H. 642 (29), 643 (31), 677  
 Cheeseman, J. R. 384 (30), 402  
 Chemla, F. 516 (32), 584  
 Chen, A. 244 (89), 262  
 Chen, B. 213 (118), 217  
 Chen, C. 547 (154), 588  
 Chen, C.-D. 547 (155), 588  
 Chen, G. 540 (121, 122), 587  
 Chen, J. 162 (59, 60), 163 (62), 164 (63), 171 (105), 185, 186  
 Chen, K. 123 (90), 129  
 Chen, M. 159 (36), 185  
 Chen, M. L. 277 (205), 310  
 Chen, S. J. 335 (11), 359  
 Chen, T.-A. 514 (19), 584  
 Chen, W. 384 (30), 402  
 Chen, W.-C. 566 (262), 591  
 Chen, X. 162 (61), 185  
 Chen, Y. 291 (280), 312, 325 (73), 361  
 Chen, Y.-H. 547 (154), 588  
 Chenal, T. 69 (223), 97  
 Cheney, M. C. 277 (201), 310  
 Cheng, D. 514 (23), 584, 619 (78), 630  
 Cheng, F.-C. 278 (209, 211, 212), 310  
 Cheng, W.-L. 547 (154), 588  
 Cheng, Y. 348 (244), 364  
 Cheng, Y. C. 162 (60), 163 (62), 171 (105), 185, 186  
 Chérest, M. 666 (114), 678  
 Chernomorsky, S. 214 (131), 218  
 Chernow, B. 268 (81), 307  
 Chernyh, I. N. 219 (7), 260  
 Cherry, D. A. 667 (118), 678  
 Chevrot, C. 236 (60), 258 (38, 130), 261, 263, 291 (279), 312

- Chiang, M. Y. 81 (228), 98, 149 (46), 154, 422 (25), 435
- Chiavarini, S. 302 (323), 313
- Chiba, N. 563 (248), 591
- Chiba, S. 579 (309), 592
- Chickos, J. 121 (70), 128
- Chiechi, R. C. 531 (94), 586
- Childs, B. J. 479 (82), 508
- Chinkov, N. 563 (249), 591, 633 (1), 676
- Chipperfield, J. R. 122 (76), 128
- Chisholm, M. H. 73 (240), 98, 418 (11), 434
- Chittleborough, G. 268 (35), 306
- Chiu, T. K. 335 (144), 362
- Chivers, T. 78 (253), 98, 244 (89), 262, 421 (34), 435
- Cho, C.-H. 553 (178), 589
- Cho, D.-G. 557 (215), 590
- Cho, Y.-H. 554 (194), 589
- Chong, J. M. 54 (177), 83 (176), 96, 426 (31), 435
- Choplin, A. 174 (114), 186
- Chou, S. K. 621 (80), 630
- Chowdhury, F. A. 560 (235), 590
- Chrisman, W. 554 (193), 589
- Christensen, B. G. 499 (116), 509
- Christensen, C. 576 (303), 592
- Christian, E. L. 337 (173), 363
- Christian, G. D. 280 (223), 310
- Christian, W. 348 (247), 364
- Christiansen, T. F. 283 (234), 311
- Christophersen, C. 525 (64), 585
- Chrost, A. 25 (82), 94, 299 (307), 312
- Chu, B. 305 (362, 363), 314
- Chu, C.-M. 566 (262), 591
- Chuang, M.-C. 566 (262), 591
- Chubanov, V. 268 (56), 307
- Chubb, J. E. 713 (52), 715
- Chung, K.-G. 558 (219), 590
- Churakov, A. V. 65 (211), 97
- Churney, K. L. 113 (2), 126
- Chusid, O. 247 (106), 248 (113), 251 (112), 252 (114, 116), 258 (111), 262
- Cini, R. 328 (83), 361
- Cioslowski, J. 384 (30), 402
- Citra, A. 158 (31), 185
- Cittadini, A. 268 (58), 307, 317 (2), 359
- Citterio, D. 285 (237), 311
- Cladera, A. 283 (236), 311
- Clark, D. R. 395 (4), 401
- Clausen, T. 268 (125), 308
- Clavier, H. 565 (257), 591, 775 (31), 801
- Clay, M. D. 647 (41), 677
- Clayden, J. 553 (179), 589, 730 (28), 768
- Clegg, W. 15 (62), 20 (70), 38 (126), 83 (263), 84 (265), 93, 95, 98, 99, 149 (47), 154, 298 (304), 312, 413 (42), 419 (50), 422 (41, 59), 427 (73), 435, 436
- Cleland, W. W. 319 (24), 349 (250), 359 (339), 359, 364, 366
- Clemens, M. R. 214 (130), 218
- Clifford, P. J. 103 (10), 126
- Clifford, S. 384 (30), 402
- Cloke, F. G. N. 51 (168), 96
- Cloutier, R. 285 (241), 311
- Coates, G. E. 4 (34), 92, 410 (39), 428 (87), 435, 436, 682 (12), 714
- Cobb, M. H. 347 (237), 364
- Coburn, E. R. 398 (39), 402
- Coelho, L. M. 271 (167), 309
- Cogan, D. A. 575 (298, 299), 592, 673 (145), 679
- Cogdell, R. J. 324 (58), 356 (325, 331), 360, 366
- Cohen, H. 250 (115), 262
- Cohen, T. 514 (23), 584, 760 (49), 769
- Cohen, Y. 248 (96, 113), 251 (112), 258 (109, 110), 262
- Cohn, M. 329 (89), 331 (112), 361
- Cola, S. Y. 303 (343), 313
- Colacot, T. J. 53 (174), 96, 775 (27), 801
- Colasson, B. 576 (303), 592
- Cole, P. E. 335 (143), 362
- Cole, S. C. 70 (225), 97, 430 (77), 436
- Coleman, G. H. 578 (307), 592
- Coles, M. P. 70 (225), 97, 430 (77), 436
- Colin, C. L. 190 (1), 214
- Collett, J. R. 337 (169), 363
- Collins, J. D. 52 (173), 53 (174), 96
- Collman, J. P. 438 (2), 506
- Colombo, L. 484 (101), 509
- Colonge, J. 439 (3), 506
- Combellas, C. 513 (15), 584
- Comes-Franchini, M. 559 (228), 590
- Commeyras, A. 516 (29), 584
- Compton, R. N. 124 (92), 129, 182 (4), 184
- Compton, T. R. 288 (259), 311
- Conlon, D. A. 648 (47), 677
- Conn, R. S. E. 640 (25, 26), 677
- Conroski, K. 119 (64), 128
- Conway, B. 81 (224), 97, 414 (35), 430 (80), 435, 436
- Cook, N. C. 599 (36), 629
- Cook, P. F. 347 (236), 364
- Cooney, J. J. A. 553 (179), 589
- Cooper, G. D. 112 (52), 127
- Corbel, B. 462 (59), 507
- Corbet, J. P. 596 (23), 629
- Corchado, J. C. 350 (263), 365
- Cordray, K. 214 (136), 218
- Corey, E. J. 484 (102), 509, 582 (316), 593, 772 (5), 800
- Corich, M. 500 (55), 507
- Cornejo, J. 208 (90–92), 217
- Cornelis, R. 269 (151), 309
- Correa, A. 788 (48), 801

- Correll, C. C. 335 (147), 362  
 Corriu, R. 661 (105), 678  
 Cosma, P. 212 (115), 217  
 Cossi, M. 384 (30), 402  
 Costello, R. B. 268 (136), 308  
 Cotterell, C. 148 (48), 154  
 Cottet, F. 702 (38), 715  
 Cotton, F. 25 (87), 94  
 Cotton, H. K. 791 (53), 802  
 Coudray, C. 288 (256–258), 311  
 Coutrot, P. 489 (8, 9), 491 (105), 506, 509  
 Cowan, J. A. 268 (51), 307, 318 (4), 320 (7, 8), 321 (37), 322 (44), 328 (1), 347 (6), 354 (27), 359, 360  
 Cowan, P. J. 462 (58), 494 (109), 507, 509  
 Cowden, C. J. 648 (47), 677  
 Cox, J. D. 110 (50), 127  
 Coxall, R. A. 74 (124, 243), 81 (255), 95, 98, 406 (19), 407 (21), 423 (17), 434  
 Coxhall, R. A. 150 (43), 154  
 Crabtree, R. H. 58 (5), 92, 633 (1), 676  
 Cracco, R. Q. 268 (130), 306  
 Cram, D. J. 395 (5), 401  
 Cramer, R. E. 68 (219), 97  
 Crandall, J. K. 634 (12), 676  
 Craun, F. F. 268 (130), 308  
 Crauste, C. 491 (105), 509  
 Crawford, H. M. 653 (6), 676  
 Crawford, J. J. 424 (64), 436, 473 (86), 508  
 Crawford, K. S. K. 113 (55), 127  
 Crawley, M. L. 791 (52), 802  
 Creighton, J. R. 122 (78), 128  
 Crimmins, M. T. 468 (83), 508  
 Crombie, L. 462 (57), 493 (106, 107), 494 (108), 507, 509  
 Croset, K. 791 (57), 802  
 Cross, R. L. 329 (92), 361  
 Crossland, I. 3 (17), 92, 391 (9), 401  
 Crossland, L. 451 (30), 507  
 Croteau, D. L. 351 (280), 365  
 Crothers, D. M. 335 (143), 362  
 Cuddihy, K. P. 259 (146), 263  
 Cudzilo, S. 103 (5), 126  
 Cui, C. 74 (248), 98, 424 (16), 434  
 Cui, Q. 384 (30), 402  
 Cui, X.-L. 547 (158), 588  
 Cukier, R. I. 201 (73), 216  
 Cundy, D. J. 495 (111), 509  
 Cunniff, P. 283 (166), 309  
 Čurdová, E. 279 (217), 310  
 Curran, D. J. 277 (201), 310  
 Curri, M. L. 212 (115), 217  
 Cutshall, N. S. 667 (120), 678  
 Cuvigny, T. 608 (54, 55), 629  
 Cvetovich, R. 103 (8), 126, 519 (52), 585  
 Czako, B. 742 (14), 768  
 D'Augustin, M. 565 (257), 591, 775 (31), 801  
 D'Hollander, R. 292 (282), 312  
 D' Sa, B. 472 (94), 508  
 D'Souza, F. 201 (41, 42), 216  
 D'Souza, L. M. 337 (169), 363  
 Daasbjerg, K. 256 (28), 259 (136, 137), 260, 263  
 Dakternieks, D. 514 (24), 550 (164), 584, 588  
 Dalai, S. 452 (36), 507  
 Dale, S. H. 419 (50), 435  
 Dalton, J. 198 (57), 216  
 Damen, H. 655 (64), 677  
 Damin, A. 125 (108), 129  
 Damrau, H.-R. 49 (165), 96  
 Damrauer, R. 118 (61), 128  
 Daniels, A. D. 384 (30), 402  
 Danielson, N. D. 305 (364), 314  
 Danielsson, L.-G. 269 (151), 309  
 Dankwardt, J. W. 433 (90), 436, 553 (182), 589  
 Danly, D. E. 239 (78), 261  
 Danopoulos, A. A. 615 (70), 630  
 Dapprich, S. 384 (30), 402  
 Daris, J. P. 500 (118), 509  
 Darki, A. 144 (29), 153  
 Daskapan, T. 579 (309), 592  
 Datta, A. 571 (282), 592  
 Daugaard, G. 268 (141), 308  
 Davanzo, C. U. 295 (288), 312  
 Davidson, F. 53 (175), 96  
 Davidson, W. 282 (158), 309  
 Davidsson, Ö. 59 (145), 95  
 Davies, I. W. 5 (43), 93  
 Davies, S. G. 454 (40), 507  
 Davis, D. A. 559 (227), 590  
 Davis, F. A. 575 (299), 592  
 Davis, I. W. 703 (41), 715  
 Davis, S. R. 158 (26), 185, 391 (18, 19), 402  
 Dawson, G. J. 673 (141), 679  
 de Armas, G. 283 (236), 311  
 de Armas, J. 561 (240), 591  
 de Diego, J. E. 518 (48), 585  
 de Groot, A. 474 (47), 507  
 de Groot, H. J. M. 356 (332), 366  
 de Jong, J. C. 268 (66), 307  
 de Kanter, F. J. J. 86 (269), 99  
 De, L. 331 (119), 362  
 de la Calle-Gutiñas, M. B. 302 (323), 304 (319), 313  
 de la Fuente Blanco, J. A. 482 (6), 506  
 de la Peña, M. 341 (191), 363  
 De Luca, L. 559 (226), 590  
 de Meijere, A. 452 (36), 507, 531 (93), 547 (153), 550 (126), 582 (315), 586–588, 593, 596 (28), 629, 633 (1), 676  
 de Pablos, F. 302 (334), 313  
 de Valk, H. W. 268 (95), 307  
 de Vries, A. H. M. 774 (2, 13, 14), 800  
 Deakyne, C. A. 107 (20), 126  
 DeAntonis, D. M. 103 (10), 126

- Debal, A. 487 (22), 506  
 Decambox, P. 275 (189), 310  
 Dechert, S. 54 (95), 94  
 Deelman, B.-J. 519 (53), 585  
 Defrees, D. J. 369 (1, 2), 401  
 Degrado, S. J. 779 (33), 801  
 Deguchi, J. 206 (82), 217  
 Dehmel, F. 518 (46), 519 (51), 525 (41), 585  
 DeHoff, B. S. 645 (34), 677  
 Dei Cas, L. 268 (105), 308  
 Deiderich, F. 633 (1), 676  
 Dekker, J. 77 (251), 98  
 del Amo, V. 557 (208), 580 (314), 590, 593  
 del Prado, M. 518 (48), 585  
 del Rosario, J. D. 395 (36), 402  
 Del Villar, A. 558 (218), 590, 791 (53), 802  
 Delacroix, T. 534 (98), 586  
 Delagoutte, E. 351 (270, 271), 365  
 Delaney, M. O. 545 (134), 588  
 Delbaere, L. T. J. 332 (125), 362  
 Demay, S. 525 (41), 585  
 Dembech, P. 475 (81), 508, 580 (313), 592, 593  
 Demel, P. 455 (42), 507, 557 (213), 590  
 Demiroglu, A. 278 (215), 310  
 Demissie, T. 53 (174), 96  
 Demtschuk, J. 54 (95), 94  
 Denisko, O. V. 547 (156), 588  
 Denmark, S. E. 571 (284, 286), 592  
 DePuy, C. H. 118 (61), 128  
 Derkacheva, V. M. 213 (120, 122), 217  
 DeRose, V. J. 336 (168), 341 (198), 363  
 Des Mazery, R. 457 (45), 507, 787 (41), 801  
 Desai, H. 144 (29), 153  
 Dessy, R. E. 107 (28), 127, 244 (89), 258 (36, 88), 261, 262, 633 (10), 676  
 Dettwiler, J. E. 563 (246), 591  
 DeWald, H. A. 633 (3), 676  
 DeWolfe, R. H. 141 (33), 154  
 Dhupa, N. 268 (85), 307  
 Di Carro, M. 302 (332), 313  
 Di Furia, F. 500 (55), 507  
 Di Ninno, F. 499 (116), 509  
 Diaz, N. 348 (242), 364  
 Dick, C. M. 74 (124, 243), 81 (255, 256), 95, 98, 150 (43), 154, 406 (19), 407 (21, 22), 422 (15), 423 (17), 434  
 Dick, C. M. E. 74 (244), 98  
 Dickerson, R. E. 335 (144), 362  
 Dickey, J. B. 289 (270), 312  
 Didierjean, C. 491 (105), 509  
 Didiluk, M. T. 672 (137), 679  
 Didiuk, M. T. 557 (212), 590, 673 (143, 144), 679  
 Die, M. 555 (202), 590  
 Diebler, H. M. 318 (18), 359  
 Dieckmann, R. 345 (218), 364  
 Diederich, F. 550 (126), 587, 633 (1), 676  
 Diers, J. R. 201 (39), 215  
 Dieter, R. K. 474 (95), 508, 559 (222), 590  
 Dieterich, F. 325 (68), 360  
 Dietze, H.-J. 287 (251), 311  
 Dietzek, B. 357 (337), 366  
 Digeser, M. H. 427 (72), 436  
 Digiovanni, S. 295 (286), 312  
 Dilsiz, N. 278 (214), 310  
 Ding, L. N. 162 (60), 185  
 Ding, Y. 74 (248), 98, 424 (16), 434  
 Dinsmore, A. 538 (109), 587  
 Dirx, W. M. R. 302 (341), 313  
 Dirnbach, E. 344 (216), 364  
 Dismukes, G. C. 322 (42), 360  
 Dix, D. T. 138 (13), 153  
 Dobrovetsky, E. 327 (67), 360  
 Dobson, M. P. 175 (122), 176 (119–121), 186, 187, 318 (23), 359  
 Dohle, W. 268 (8), 306, 518 (36, 42, 47), 519 (51), 525 (41, 68), 555 (198), 577 (305), 584, 585, 589, 592, 607 (47), 629  
 Dohmeier, C. 68 (218), 97  
 Dol, I. 278 (213), 310  
 Dolev, E. 268 (144), 308  
 Dolling, U. 103 (8), 126, 519 (52), 585  
 Dolling, U.-H. 648 (47), 677  
 Dolman, S. J. 703 (41), 715  
 Dolphin, D. 193 (14), 196 (47), 215, 216  
 Dombovári, J. 287 (251), 311  
 Domcke, W. 332 (131), 362  
 Donato, F. 268 (130), 308  
 Dong, C.-G. 550 (165), 588  
 Dong, F. 184 (160), 187  
 Donkervoort, J. G. 545 (137), 588  
 Donohoe, T. J. 485 (24), 507  
 Dooley, C. A. 303 (343), 313  
 Dorea, J. G. 268 (127), 308  
 Dorigo, A. E. 422 (47), 435  
 Dorough, G. D. 207 (85), 217  
 Dorup, I. 268 (125), 308  
 Dorwald, F. Z. 718 (2), 767  
 Dorziotis, I. 654 (72), 678, 699 (31), 715  
 Dos Santos, M. 555 (198), 589, 608 (51), 629  
 Dotson, L. 268 (44), 306  
 Doublíé, S. 352 (298), 365  
 Doudna, J. A. 334 (140), 337 (154), 362  
 Douglas, R. H. 191 (9), 215  
 Dove, A. P. 76 (242), 77 (250), 98, 424 (44), 435, 484 (99), 508  
 Dowd, P. 760 (47), 769  
 Downs, A. J. 157 (17, 20), 184  
 Doyle, D. A. 327 (67), 360  
 Doyle, M. 774 (2), 800  
 Draeger, M. 514 (24), 584  
 Drane, M. 238 (63), 261  
 Dranka, M. 410 (36), 435  
 Draper, D. E. 334 (139), 335 (10), 336 (164, 166), 359, 362, 363



- Drekener, R. L. 774 (25), 801  
 Dreosti, I. E. 268 (123), 308  
 Driessens, F. C. 268 (68, 69), 307  
 Dror, Y. 211 (110), 217  
 Du, Y. 337 (169), 363  
 Dubbaka, S. R. 576 (301), 580 (314), 592, 593  
 Dube, H. 531 (92), 586  
 Dübner, F. 791 (54), 802  
 Dubois, J. E. 458 (51), 507, 482 (98), 508  
 Dubois, L. H. 172 (109), 186  
 Dubois, T. 241 (79), 262  
 Duboudin, J.-G. 635 (13–15), 648 (49, 50), 676, 677  
 Ducros, V. 288 (257), 311  
 Dudek, J. 268 (107), 308  
 Dudev, M. 321 (39), 360  
 Dudev, T. 320 (28), 321 (37–39), 322 (43, 44), 360  
 Dufford, R. T. 235 (49), 261  
 Duke, R. B. 391 (8), 401  
 Dulai, K. 191 (9), 215  
 Dumouchel, S. 700 (33, 34), 715  
 Dunbar, R. C. 125 (99, 106), 129, 156 (11, 14), 160 (48, 52), 162 (53), 184, 185  
 Duncan, A. P. 779 (20), 800  
 Duncan, J. L. 391 (16), 402  
 Duncan, M. A. 124 (98), 129, 168 (75), 184 (158, 159), 186, 187  
 Duncan, T. M. 329 (92), 361  
 Dunn, K. 550 (164), 588  
 Dunogues, J. 467 (77), 472 (76), 508, 539 (111), 587  
 Duplais, C. 546 (143), 559 (223), 588, 590, 601 (44), 618 (72), 629, 630  
 Duquerroy, S. 348 (246), 350 (261), 364, 365  
 Durlach, J. 267 (1), 268 (33, 50, 54, 102, 110), 306–308  
 Durlach, V. 268 (33, 102), 306, 308  
 Dürr, C. 610 (60), 630  
 Duthie, A. 514 (24), 584  
 Dvorak, D. 518 (45), 585  
 Dvoráková, H. 611 (61, 62), 630  
 Dykstra, C. E. 171 (99), 186  
 Dyrda, G. 196 (49), 216  
 Dzhemilev, U. M. 123 (87), 129, 421 (53), 435, 671 (131–133, 135), 679  
 Eaborn, C. 23 (77, 78), 32 (110), 63 (112, 206, 208), 94, 97  
 Eaborn, C. A. 63 (207), 97  
 Eastham, J. F. 288 (261), 311, 682 (15), 714  
 Eaton, P. E. 419 (54, 56, 57), 435, 466 (66), 508, 538 (105, 106), 587  
 Ebdrup, S. 525 (64), 585  
 Ebel, G. E. 513 (13), 583  
 Ebersole, M. H. 196 (50), 216  
 Ebersson, L. 258 (56), 259 (61), 261  
 Eckert, J. 246 (92), 262  
 Edmondson, D. L. 358 (348), 367  
 Edwards, A. M. 327 (67), 360  
 Edwards, G. L. 479 (82), 508  
 Edwards, P. G. 86 (268), 99  
 Efthimiou, E. 282 (232), 311  
 Egekeze, J. O. 293 (266), 311  
 Egli, M. 335 (9, 31, 145, 146), 359, 360, 362  
 Egorov, A. M. 299 (306), 312  
 Eguchi, K. 300 (314), 313  
 Eicher, T. 451 (29), 507  
 Eigen, G. 318 (18), 359  
 Eijkelkamp, D. J. F. M. 774 (8), 800  
 Eilerts, N. W. 73 (240), 98, 418 (11), 434  
 Einspahr, H. 318 (16), 359  
 Eisch, J. J. 268 (2), 306, 664 (110–113), 678  
 Ek, F. 611 (64), 630  
 Ekane, S. 268 (117), 308  
 Eklov, B. M. 300 (300), 312  
 El-Demerdash, S. H. 176 (124), 187  
 El-Hamruni, S. M. 63 (112), 94  
 El-Kaderi, H. M. 78 (252), 98, 122 (77), 128, 422 (28, 29), 435  
 El-Kaderi, M. 72 (234), 98  
 El-Kheli, M. N. A. 63 (207), 97  
 El-Khouly, M. E. 201 (41, 42), 216  
 Elhanine, M. 169 (81), 186  
 Eliel, E. L. 395 (4), 401, 772 (3), 800  
 Elin, R. J. 268 (41, 135), 270 (29, 77), 275 (193), 306–308, 310  
 Ellenberger, T. 352 (298), 355 (316), 365, 366  
 Eller, K. 160 (40, 41), 185  
 Ellerd, M. G. 742 (14), 768  
 Ellis, A. M. 123 (84), 129, 184 (156, 157), 187  
 Ellison, J. J. 62 (202), 97  
 Ellman, J. A. 575 (298–300), 592  
 El-Nahas, A. M. 176 (124), 187  
 El-Shereefy, E.-S. E. 176 (124), 187  
 Elving, P. J. 300 (315), 313  
 Emanuel', V. L. 268 (118), 308  
 Emel'ianov, A. B. 268 (118), 308  
 Emerson, K. 699 (31), 715  
 Emteborg, H. 304 (351), 313  
 Ende, D. J. 103 (10), 126  
 Engel, N. 210 (102), 217  
 Engelbrecht, S. 329 (95), 361  
 Engelhardt, F. C. 648 (47), 677  
 Engelhardt, L. M. 58 (155), 81 (260), 96, 98, 405 (5), 427 (74), 434, 436  
 Englert, U. 29 (103), 94  
 Englisch, U. 71 (229), 98, 407 (23), 434  
 Erdik, E. 579 (309), 592  
 Erickson, W. E. 667 (54), 677  
 Eriksson, M. C. 555 (203), 590  
 Erikson, H. 38 (129), 95  
 Eriksson, J. 59 (61), 60 (185), 93, 96  
 Erkelens, C. 356 (332), 366  
 Ermini, G. 512 (10), 583  
 Ershov, V. V. 330 (108), 361  
 Ertel, T. S. 3 (16), 92

- Eshaghi, S. 325 (70), 361  
 Esipov, S. E. 171 (5), 175 (101), 184, 186  
 Eskins, M. 493 (107), 509  
 Estela, J. M. 283 (236), 311  
 Etcheberry, A. 243 (83), 262  
 Etkin, N. 419 (26), 435  
 Evans, D. A. 503 (62, 123, 124), 504 (90), 505 (61), 508, 509, 539 (112), 587  
 Evans, D. E. 108 (41), 127  
 Evans, D. F. 139 (26), 140 (19), 150 (45), 153, 154  
 Evans, M. C. W. 356 (329), 366  
 Evans, S. 124 (93), 129  
 Evans, W. H. 113 (2), 126  
 Evans, W. V. 220 (12), 228 (16), 231 (20), 233 (22), 234 (23), 235 (18), 238 (17), 244 (19, 21), 258 (15), 260  
 Evers, E. A. I. M. 116 (58), 128  
 Evstigneev, V. B. 198 (58), 216  
 Evstigneeva, E. V. 110 (48), 127  
 Ewbank, P. C. 286 (244), 311  
 Ezhov, Y. S. 183 (153), 184 (155), 187  
 Ezhova, M. B. 52 (173), 53 (174), 96  
 Fabbri, G. 580 (313), 593  
 Faber, T. 661 (104), 678  
 Fabre, J. L. 608 (52, 53), 629  
 Fabre, S. 74 (124, 243, 244), 81 (255, 256), 95, 98, 150 (43), 154, 406 (19), 407 (21, 22), 422 (15), 423 (17), 434  
 Fahey, D. W. 156 (8), 160 (45), 184, 185  
 Faid, K. 285 (238, 241), 311  
 Fajer, J. 196 (47), 216  
 Fajert, J. 201 (71), 216  
 Fakhfakh, M. A. 608 (49, 50), 629  
 Falciola, C. 791 (50), 802  
 Falciola, C. A. 558 (220), 590, 791 (58), 802  
 Falck, J. R. 558 (218), 590  
 Faller, L. D. 329 (101), 361  
 Fallis, A. G. 567 (268), 591, 633 (1), 646 (37, 38), 647 (41–43), 648 (44, 45, 48), 676, 677  
 Fang, Q. K. 583 (319), 593  
 Fantucci, P. 331 (119), 362  
 Farády, L. 653 (69–71), 677, 678  
 Farghaly, O. A. 276 (198, 199), 310  
 Farias, P. A. M. 276 (197), 310  
 Farkas, J. 684 (18), 713 (53), 714, 715  
 Farkas, O. 384 (30), 402  
 Farnham, W. B. 527 (28), 584  
 Farquhar, G. D. 359 (353), 367  
 Farrar, J. M. 166 (76), 186  
 Farrell, R. P. 552 (175), 589  
 Farthing, C. N. 547 (149), 588  
 Farwell, J. D. 305 (305), 312  
 Fatiadi, A. J. 528 (86), 586  
 Fau, S. 137 (10), 153, 720 (7), 768  
 Faust, R. 196 (43), 216  
 Fauvarque, J. F. 258 (130), 263  
 Favaloro, F. G. 742 (14), 768  
 Fazakerley, G. V. 108 (41), 127, 140 (19), 153  
 Fazekas, M. 212 (113), 217  
 Fedorchuk, C. 78 (253), 98, 421 (34), 435  
 Fedorov, A. A. 357 (342), 366  
 Fedorov, E. V. 357 (342), 366  
 Fedoseev, G. B. 268 (118), 308  
 Fedushkin, I. L. 79 (254), 98, 414 (32), 426 (48), 435  
 Fehsenfeld, F. C. 156 (8), 160 (45), 184, 185  
 Feillet-Coudray, C. 288 (256–258), 311  
 Feitelson, J. 198 (55), 216  
 Fejfarová, K. 86 (270), 99  
 Feldberg, S. W. 196 (48), 216  
 Felding, J. 518 (49), 585  
 Feldman, A. K. 576 (303), 592  
 Felkin, H. 656 (83), 665 (115), 666 (114), 678  
 Fellah, S. 243 (81–83, 85), 262  
 Fellmann, P. 458 (51), 482 (98), 507, 508  
 Felton, R. H. 196 (47), 216  
 Fendler, J. H. 206 (79), 217  
 Feng, B. 337 (169), 363  
 Feng, Z. 253 (120), 262  
 Ferguson, E. E. 156 (8), 160 (45), 184, 185  
 Ferguson, H. D. 103 (10), 126  
 Feringa, B. L. 457 (44, 45), 500 (46), 507, 558 (220, 221), 563 (244), 564 (255), 590, 591, 774 (2, 10, 13–16, 21), 775 (29), 779 (32), 780 (37, 38), 786 (42), 787 (41, 45–47), 788 (48), 791 (56, 62), 798 (63, 64), 800–802  
 Ferment, O. 268 (40), 306  
 Fernandez-Lazaro, F. 201 (40), 216  
 Fernholt, L. 23 (76), 93, 183 (148), 187  
 Ferracutti, N. 442 (10), 506  
 Ferrão, M. F. 295 (288), 312  
 Fiammengio, R. 336 (162), 362  
 Fiandanesi, V. 601 (40–42), 629  
 Fiaschisi, R. 555 (203), 590  
 Fidélis, A. 241 (80), 243 (82), 262  
 Field, E. 231 (20), 233 (22), 239 (74), 244 (19), 260, 261  
 Field, M. J. 348 (242), 364  
 Fields, E. K. 595 (3), 628  
 Figadère, B. 554, 555 (190, 197, 198), 589, 607 (48), 608 (49–51), 614 (65), 629, 630  
 Filgueiras, A. V. 272 (170), 309  
 Fillebeen, T. 73 (239), 98, 424 (10), 434  
 Finch, J. T. 340 (186), 363  
 Findl, E. 246 (91), 262  
 Finkbeiner, H. L. 112 (52), 127  
 Fischer, A. K. 30 (108), 94, 243 (86), 262  
 Fischer, E. O. 88 (88), 89 (89), 94  
 Fischer, M. 540 (116), 566 (266), 587, 591  
 Fischer, R. 39 (133), 95  
 Fishel, W. P. 289 (269), 312  
 Fitzgerald, R. 303 (344), 313  
 FitzGerald, S. 196 (43), 216  
 Fjellvaag, H. 107 (19), 126

- Flaherty, K. M. 340 (181), 363  
 Flatman, P. W. 268 (60), 307  
 Fleck, O. 355 (317), 366  
 Fleischmann, M. 241 (37), 261  
 Fleming, F. F. 432 (88), 436, 528 (85, 87), 563 (250), 565 (258–261), 586, 591, 647 (39, 40), 667 (121, 122), 670 (123–125), 671 (126–130), 677–679  
 Fleming, I. 439 (5), 485 (4), 506, 540 (115), 587  
 Fleming, M. J. 547 (151), 588  
 Fletcher, K. S. 277 (201), 310  
 Fletcher, S. P. 500 (46), 507, 558 (221), 590, 787 (47), 798 (64), 801, 802  
 Florencio, M. H. 302 (322), 313  
 Florer, J. B. 325 (69), 361  
 Flores, R. 341 (191), 363  
 Florián, J. 352 (300), 365  
 Fochi, M. 259 (144), 263, 559 (228), 576 (301), 590, 592  
 Focia, P. J. 318 (21), 359  
 Fogh-Andersen, N. 276 (16), 306  
 Fokin, V. V. 576 (303), 592  
 Folest, J. C. 236 (60), 258 (38), 261, 291 (279), 312  
 Fondekari, K. P. 473 (85), 508  
 Fontani, M. 30 (108), 94, 243 (86), 262  
 Forbes, G. C. 17 (65), 93  
 Ford, W. T. 140 (14), 153  
 Foresman, J. B. 369 (2), 384 (30), 401, 402  
 Forgione, P. 567 (268), 591, 633 (1), 646 (38), 647 (43), 648 (44), 676, 677  
 Forman, A. 196 (47), 216  
 Forster, A. C. 339 (179), 363  
 Foster, W. E. 653 (57), 677  
 Fournier, A. 608 (50), 629  
 Fournioux, X. 558 (219), 590, 791 (57), 802  
 Fox, D. J. 369 (2), 384 (30), 401, 402  
 Fox, J. M. 560 (233), 590, 659 (98, 99, 100), 678  
 Fraenkel, G. 116 (59), 128, 138 (13), 148 (48), 153, 154  
 Frajerman, C. 666 (114), 678  
 France, M. R. 168 (75), 186  
 Francis, C. L. 495 (111), 509  
 Franck, X. 554 (190), 555 (197, 198), 589, 607 (48), 608 (49–51), 614 (65), 629, 630  
 Frandt, J. 653 (62), 677  
 Franks, M. A. 648 (46), 677  
 Franz, K. 268 (73), 307  
 Franz, T. 573 (290), 592  
 Franzen, R. G. 534 (101), 586  
 Franzini, E. 331 (119), 362  
 Franzke, C. 301 (357), 314  
 Fraser, P. K. 779 (33), 801  
 Frash, M. V. 124 (94), 129, 180 (46), 185  
 Frech, W. 304 (351), 313  
 Frederiksen, M. U. 707 (47), 715  
 Fredj, A. B. 357 (335), 366  
 Freeborn, B. 335 (147), 362  
 Freiser, S. 493 (106), 509  
 Freer, A. A. 324 (58), 356 (325, 331), 360, 366  
 Freijee, F. J. M. 120 (67), 121 (71), 128  
 Freiser, B. S. 160 (43), 162 (42, 57), 185  
 French, H. E. 238 (63), 246 (14), 260, 261  
 Frenzen, G. 516 (32), 584  
 Freycon, M. T. 268 (116), 308  
 Freyer, W. 196 (54), 216  
 Freymann, D. M. 318 (21), 359  
 Friedberg, E. C. 355 (316), 366  
 Friedman, H. 235 (50), 261  
 Friedrichsen, W. 517 (40), 585  
 Friesner, R. A. 350 (265), 365  
 Frisch, A. C. 544 (129, 130), 588, 596 (27), 629  
 Frisch, M. J. 369 (2), 384 (30), 401, 402  
 Fromme, P. 356 (36, 322, 324, 330), 360, 366  
 Froschauer, E. M. 325 (68), 360  
 Frost, R. M. 546 (144), 588, 615 (68–70), 630  
 Fruchier, A. 491 (105), 509  
 Frutos, J. 774 (12), 800  
 Fry, A. J. 255 (127, 128), 263  
 Frydman, B. 211 (103), 217  
 Frydman, L. 328 (84), 361  
 Frydman, V. 328 (84), 361  
 Frye, S. V. 395 (4), 401  
 Fu, G. C. 571 (283), 592, 618 (66), 630  
 Fu, Q. 169 (80), 186  
 Fuchimoto, Y. 468 (80), 508  
 Fuchs, C. F. 604 (7), 628  
 Fuhrhop, J.-H. 208 (93–95), 217  
 Fuji, K. 480 (92), 508  
 Fujihara, H. 517 (34), 584  
 Fujii, T. 767 (57), 769  
 Fujii, Y. 561 (239), 591  
 Fujikura, S. 661 (103), 678  
 Fujimori, K. 701 (36), 715  
 Fujino, O. 279 (218), 310  
 Fujisawa, H. 484 (28), 507  
 Fujisawa, T. 486 (25), 507  
 Fujita, H. 329 (99), 361  
 Fujita, K. 737 (32), 768  
 Fujita, M. 767 (55), 769  
 Fujiwara, K. 303 (349), 313  
 Fujiwara, Y. 513 (14), 583  
 Fujiyoshi, Y. 356 (328), 366  
 Fukaya, F. 193 (27), 215  
 Fukin, G. K. 426 (48), 435  
 Fukuhara, K. 625 (91), 630, 700 (32), 715  
 Fukui, H. 279 (218), 310  
 Fukumoto, H. 123 (73), 128  
 Fukuzumi, S. 200 (69), 201 (40, 70), 216  
 Funabashi, Y. 570 (280), 591  
 Funseth-Smotzer, J. 323 (51), 360  
 Furcola, N. C. 289 (271), 312

- Furois, J. M. 198 (60), 216  
 Fürstner, A. 514 (19), 546 (145), 554 (188, 189), 559 (231), 584, 588–590, 596 (32), 608 (57), 614 (58, 59), 616 (73), 624 (35), 626 (83, 94–96), 629, 630  
 Furukawa, N. 517 (34), 584  
 Furuya, A. 163 (66, 67), 185  
 Furuyama, T. 419 (51), 435  
 Fuson, R. C. 299 (309), 312, 633 (2–5), 676  
 Futai, M. 329 (97), 361  
 Fuxreiter, M. 355 (319), 366  
 Gaboyard, M. 711 (50), 715  
 Gabrielsson, A. 200 (67), 216  
 Gadde, S. 201 (41, 42), 216  
 Gaddum, L. W. 235 (49), 246 (14), 260, 261  
 Gaderbauer, W. 38 (130), 95  
 Gaertner, P. 618 (74), 630  
 Gaertner, R. 633 (3), 676  
 Gafni, A. 344 (216, 217), 364  
 Gagas, D. 119 (64), 128  
 Gago, S. 341 (191), 363  
 Gahan, L. R. 343 (210), 364  
 Gaidies, A. 610 (60), 630  
 Gait, M. J. 339 (184), 363  
 Gajda, T. 547 (147), 588  
 Gaje, J. R. 503 (124), 509  
 Gal, J.-Y. 290 (273), 292 (281), 312  
 Galili, T. 201 (71), 206 (78), 216, 217  
 Galimov, E. M. 330 (108), 361  
 Galizzi, A. 327 (77), 361  
 Gallagher, D. J. 22 (71), 93  
 Galland, L. 268 (19), 306  
 Galle, J. E. 664 (113), 678  
 Galli, C. 198 (56), 216  
 Gallucci, J. C. 50 (98), 94, 123 (83), 129  
 Games, D. E. 493 (107), 509  
 Games, D. F. 462 (57), 507  
 Gan, Z. 357 (333), 366  
 Gao, H.-W. 282 (228), 310  
 Gao, J. 350 (263), 365  
 Gao, K. 163 (69), 186  
 Gao, Y. 540 (120), 587  
 Gapeev, A. 125 (99), 129  
 Garavaglia, S. 327 (77), 361  
 García Alonso, J. I. 273 (181), 309, 303 (346), 313  
 García, F. 51 (51), 93  
 García-Fernández, R. 273 (181), 309  
 García García, P. 424 (66), 436473 (85) 508,  
 García Ruano, J. L. 583 (319), 593  
 Gardiner, K. 335 (150), 362  
 Gardiner, M. G. 26 (92), 51 (168), 94, 96  
 Gardner, P. D. 735 (31), 768  
 Garland, H. O. 268 (92), 307  
 Garrido Frenich, A. 302 (335), 313  
 Garst, J. F. 55 (180, 182), 96, 172 (106–108), 186, 512 (5), 513 (11, 14), 583  
 Gasser, R. 268 (26), 306  
 Gasyna, Z. 196 (52), 216  
 Gaucheron, F. 268 (129), 308  
 Gauld, J. W. 336 (160), 362  
 Gault, Y. 173 (110–113), 174 (114), 186  
 Gautheron, B. 50 (98), 94, 123 (83), 129  
 Gavrilova, V. A. 198 (58), 216  
 Gavryushin, A. 633 (1), 676  
 Gawaz, M. 268 (62), 307  
 Gawley, R. E. 395 (37), 402  
 Gebara-Coghlan, M. 495 (111), 509  
 Geetha, V. 576 (303), 592  
 Geissler, M. 682 (10), 714  
 Gellene, G. I. 159 (38), 185  
 Genchel, V. G. 110 (48), 127  
 Genders, J. D. 246 (98), 262  
 Genet, J.-P. 559 (224), 590  
 Gengyo, K. 760 (50), 769  
 Gennari, C. 625 (93), 630  
 Gentemann, S. 201 (46), 216  
 Gentil, S. 50 (98), 94, 123 (83), 129  
 George, P. 319 (25), 360  
 Gerber, B. 276 (195, 196), 310  
 Gerbhardt, P. 39 (133), 95  
 Gerlt, J. A. 357 (342), 366  
 Geurts, K. 500 (46), 507, 558 (221), 590, 787 (47), 798 (64), 801, 802  
 Geven, W. B. 287 (248), 311  
 Geyer, A. 49 (165), 96  
 Ghahramani, M. 268 (34), 306  
 Ghandour, M. A. 276 (198), 310  
 Ghosland, F. 458 (50), 507  
 Giacomelli, G. 559 (226), 590  
 Giannotti, C. 198 (62), 216  
 Gianopoulos, J. G. 268 (135), 308  
 Gibbs, C. S. 347 (235), 364  
 Gibson, V. C. 71 (231), 74 (241), 76 (242), 77 (250), 98, 411 (33), 418 (14), 424 (44), 434, 435, 484 (99), 508  
 Gilardi, R. 419 (57), 435, 538 (105), 587  
 Gilbert, T. M. 91 (278), 99  
 Gilfillan, C. J. 20 (70), 93  
 Gilje, J. W. 68 (219), 97  
 Gill, P. M. W. 369 (2), 384 (30), 401, 402  
 Gille, S. 791 (57), 802  
 Gillespie, S. E. 328 (85), 361  
 Gilman, H. 289 (269, 270), 295 (289–295), 296 (296, 298), 297 (297), 312, 619 (75), 630, 633 (7), 653 (6, 8), 676  
 Giraitis, A. P. 228 (43, 44), 261  
 Girard, J. E. 157 (22), 185  
 Girgis, S. I. 282 (232), 311  
 Girjavallabhan, V. M. 574 (296), 592  
 Giudici, R. E. 791 (59), 802  
 Gizbar, C. 253 (118, 119), 262  
 Gizbar, H. 247 (106), 248 (96, 113), 251 (112), 252 (114, 116), 262  
 Glanz, M. 54 (95), 94  
 Glaus, T. M. 276 (195, 196), 310

- Gless, R. D. 451 (34), 507  
 Glover, C. V. C. 349 (257), 364  
 Glusker, J. P. 319 (25), 324 (35), 360  
 Gmeiner, P. 518 (49), 585  
 Gneupel, K. 246 (92), 262  
 Gobley, O. 50 (98), 94, 123 (83), 129  
 Godlewska-Żyłkiewicz, B. 273 (184), 309  
 Goedheer, J. C. 208 (98, 99), 217  
 Goel, A. B. 138 (21), 139 (9), 153  
 Goel, B. 147 (42), 154  
 Gofar, Y. 247 (106), 248 (96, 113), 250 (115),  
     251 (112), 252 (114, 116), 253 (117–119),  
     258 (111), 262  
 Goff, J. P. 268 (126), 308  
 Göhr, H. 246 (97), 262  
 Gokel, G. W. 121 (70), 128  
 Gold, H. 513 (18), 584  
 Gold, M. G. 347 (226), 364  
 Goldberg, I. 252 (114), 262  
 Goldberg, N. 156 (1), 184  
 Golden, J. T. 91 (277), 99  
 Goldie, H. 332 (125), 362  
 Gol'dshleger, U. I. 125 (103), 129  
 Goldsmith, E. J. 347 (237), 364  
 Golen, J. A. 659 (99), 678  
 Gomez, J. 198 (66), 216  
 Gommernann, N. 268 (8), 306, 518 (42), 548  
     (160), 550 (126), 585, 587, 588  
 Gomperts, R. 369 (2), 384 (30), 401, 402  
 Goncharova, V. A. 268 (118), 308  
 Gonella, M. 268 (91), 307  
 Gong, Z. 123 (90), 129  
 Gonzalez, C. 369 (2), 384 (30), 401, 402  
 González, F. 391 (26), 393 (25), 402  
 Gonzalez-Portal, A. 268 (36), 306  
 González-Rodríguez, M. J. 302 (335), 313  
 González-Soto, E. 271 (164), 309  
 Good, M. C. 347 (229), 364  
 Goodby, J. W. 546 (144), 588, 615 (68), 630  
 Goodman, M. F. 352 (300), 365  
 Goodwin, C. J. 454 (40), 507  
 Görbing, M. 517 (34), 584  
 Goris, J. 268 (37), 306  
 Görls, H. 39 (133), 95  
 Görög, S. 292 (283), 312  
 Gorrichon-Guigon, L. 458 (50), 478 (97), 507,  
     508  
 Gosh, P. 335 (148), 362  
 Gossage, R. A. 545 (137), 588  
 Gossauer, A. 210 (102), 217  
 Gosselin, F. 703 (41), 715  
 Goto, H. 675 (158), 679  
 Götte, M. 352 (301), 365  
 Gottfriedsen, J. 54 (95), 94  
 Gottlieb, H. E. 252 (114, 116), 262  
 Gottschling, D. E. 335 (149), 362  
 Gouin, L. 652 (55), 653 (56), 677  
 Goursoot, A. 157 (15), 184, 391 (20), 402  
 Gouterman, M. 193 (14), 215  
 Gozzi, C. 596 (26), 629  
 Grabowski, P. J. 335 (149), 362  
 Graening, T. 517 (40), 585  
 Graham, D. V. 13 (59), 22 (72), 93  
 Graille, J. 301 (355, 358, 361), 314  
 Grant, B. 347 (233), 364  
 Grant, C. V. 328 (84), 361  
 Graves, D. J. 347 (230), 364  
 Gray, T. C. 52 (173), 53 (174), 96  
 Gray, T. G. 51 (171, 172), 96  
 Gready, J. E. 359 (351), 367  
 Greaves, J. 302 (330), 313  
 Green, L. G. 576 (303), 592  
 Green, M. L. H. 124 (93), 129  
 Greenbaum, E. 214 (136), 218  
 Greenberg, A. 113 (56), 128  
 Greene, T. M. 157 (17, 20), 184  
 Gregory, T. D. 247 (100, 101), 262  
 Greiser, T. 6 (48), 38 (122), 42 (49), 93, 95  
 Grenet, S. 439 (3), 506  
 Gretsova, N. S. 213 (120), 217  
 Gribov, E. 125 (108), 129  
 Grieco, P. A. 718 (2), 768  
 Griesser, R. 332 (123), 362  
 Griffioen, S. 66 (213), 97  
 Grignard, V. 2 (2, 7), 92, 107 (23), 127, 268  
     (2), 306, 389 (3), 401, 512 (1), 583  
 Grigorenko, B. L. 331 (117, 118), 362  
 Grigsby, W. J. 82 (162), 96, 417 (13), 434  
 Grilley, D. 336 (164), 362  
 Grimes, R. N. 51 (169), 96  
 Grimm, B. 191 (8), 215  
 Grison, C. 489 (8, 9), 491 (105), 506, 509  
 Gritz, H. 48 (164), 96  
 Grizard, D. 288 (256), 311  
 Grognet, J. M. 268 (43), 306  
 Gromada, J. 69 (223), 97  
 Gromek, J. M. 65 (212), 97, 395 (37), 402  
 Gronert, S. 118 (61), 128  
 Grosche, M. 519 (53), 550 (168), 585, 589  
 Gröser, T. 675 (156), 679  
 Grossheimann, G. 775 (28), 801  
 Grossie, D. A. 458 (49), 507  
 Grove, D. M. 774 (8, 25), 791 (53), 800, 802  
 Grover, P. 583 (319), 593  
 Grubbs, R. D. 268 (52), 307, 325 (61), 328  
     (5), 359, 360  
 Gruber, P. R. 191 (7), 215  
 Grulich, P. F. 325 (74), 361  
 Gruter, G.-J. M. 66 (215), 97  
 Grutzner, J. B. 140 (14), 141 (28), 153  
 Gryko, D. T. 201 (45), 216  
 Gstöttmayr, C. W. K. 550 (166, 168), 589  
 Guallar, V. 350 (265), 365  
 Guay-Woodford, L. M. 268 (64), 307  
 Güçer, Ş. 271 (161), 309  
 Guddat, L. W. 343 (210), 364

- Gudermann, T. 268 (55, 56), 307  
 Gudipati, V. 432 (88), 436, 565 (259), 591, 647 (39, 40), 677  
 Guenter, F. 574 (296), 592  
 Guerin, C. 661 (105), 678  
 Guerrier-Takada, C. 335 (150), 362  
 Gueux, E. 288 (256–258), 311  
 Guggenberger, L. J. 58 (20, 190), 92, 96, 391 (14), 402  
 Gui, L. 356 (326), 366  
 Guida-Pietrasanta, F. 711 (50), 715  
 Guiet-Bara, A. 267 (1), 268 (50, 54, 102), 306–308  
 Guijarro, A. 514 (20), 584  
 Guijarro, D. 519 (53), 585  
 Guillard, R. 193 (11, 13, 15), 194 (32), 195 (16), 215  
 Guillamet, B. 550 (173), 589  
 Guillaume, T. 268 (138), 308  
 Guitian, E. 540 (115), 587  
 Gunther, T. 268 (63), 307  
 Guo, H. 554 (192), 589  
 Guo, J. 667 (121), 678  
 Guo, W. 162 (61), 163 (71), 166 (77), 167 (82–85), 168 (73, 86), 169 (80, 87), 185, 186  
 Gupta, P. 268 (24), 306  
 Gupta, R. K. 268 (24), 306  
 Gupta, S. 286 (247), 311, 428 (85), 436  
 Gurinovich, V. V. 211 (107), 217  
 Guss, J. M. 30 (105), 94  
 Gust, D. 194 (35), 195 (16), 215  
 Gustafsson, B. 59 (145), 95  
 Gutell, R. R. 337 (169), 363  
 Gutierrez, A. M. 201 (40), 216  
 Gutman, E. L. 289 (271), 312  
 Gutmann, V. 226 (41), 261  
 Gutteridge, S. 357 (338, 346), 359 (339), 366  
 Gyepes, R. 86 (270), 89 (273), 99  
 Haaland, A. 23 (76), 26 (91), 29 (102), 93, 94, 123 (85), 129, 183 (139, 146, 148, 149), 187  
 Haas, O. 246 (95), 262  
 Habiak, V. 546 (143), 588, 618 (72), 630  
 Hackmann, C. 142 (30), 154  
 Hadei, N. 550 (167), 589  
 Haelters, J. P. 462 (59), 507  
 Hafner, W. 88 (88), 94  
 Haga, M. 675 (158), 679  
 Hagaman, E. 656 (83), 678  
 Hagopian, R. A. 579 (309), 592  
 Hahn, R. C. 723 (16), 768  
 Hairault, L. 711 (50), 715  
 Håkansson, M. 38 (129), 59 (61, 145), 60 (185), 93, 95, 96  
 Halasa, A. F. 19 (46), 93  
 Haley, M. M. 531 (93, 94), 586  
 Halford, S. E. 355 (311), 366  
 Halow, I. 113 (2), 126  
 Hamada, Y. 370 (112), 458 (52), 507, 509  
 Hamdouchi, C. 259 (145), 260 (150), 263, 512 (5), 518 (48), 583, 585  
 Hamilton, C. L. 119 (62), 128, 654 (76), 678  
 Hamlin, R. 351 (286), 365  
 Hamman, C. 340 (183), 363  
 Hammann, C. 341 (190), 363  
 Hammerich, O. 219 (9), 253 (122, 123), 260, 263  
 Hammes, W. 517 (39), 585  
 Hampton, E. M. 268 (84), 307  
 Han, C. 282 (229), 310  
 Han, J. 341 (197), 363  
 Han, K.-L. 169 (94, 95), 170 (97, 98), 186  
 Han, R. 73 (235–238), 98, 148 (17), 153, 418 (7), 419 (6, 52), 422 (60), 423 (8, 9), 434, 435  
 Han, W. 193 (19), 215  
 Han, Z. 395 (35), 402, 583 (319), 593  
 Hanafusa, T. 259 (134), 263, 391 (11), 402  
 Hanawalt, E. M. 711 (51), 713 (53), 715  
 Hanay, W. 419 (55), 435  
 Hand, E. S. 478 (65), 508  
 Handler, G. S. 107 (28), 127, 258 (88), 262  
 Handwerker, S. M. 268 (19), 306  
 Handy, S. T. 515 (25), 584  
 Hanks, S. K. 347 (224), 364  
 Hannon, F. J. 772 (5), 800  
 Hansen, J. 65 (212), 97, 336 (161), 362, 395 (37), 402  
 Hansen, M. U. 514 (19), 584  
 Hansford, K. A. 563 (246), 591  
 Hanson, E. M. 719 (3), 768  
 Hanson, M. V. 514 (19), 584  
 Hanusa, T. P. 58 (5), 92  
 Hao, H. 74 (248), 98, 424 (16), 434  
 Hao, W. 540 (122), 587  
 Hara, M. 194 (29), 213 (119), 215, 217  
 Harada, T. 718 (2), 768  
 Harding, M. M. 321 (33, 34), 360  
 Hardy, J. A. 344 (211), 364  
 Hargittai, I. 183 (142), 187  
 Hargittai, M. 183 (143–145, 150, 151), 187  
 Harino, H. 302 (333), 313  
 Harkins, P. C. 347 (237), 364  
 Harmat, N. 180 (137), 187, 425 (69), 436  
 Harms, K. 59 (192), 62 (204), 97, 395 (34), 402, 516 (32), 527 (75), 584, 586, 725 (20), 768  
 Harriman, A. 198 (63), 216  
 Harrington, D. J. 320 (29), 360  
 Harrington, P. E. 707 (47), 715  
 Harrington, R. W. 84 (265), 99, 298 (304), 312, 427 (73), 436  
 Harris, M. E. 348 (238), 364  
 Harris, R. K. 151 (49), 154  
 Harrison, R. M. 303 (345), 313  
 Harritty, J. P. A. 673 (147), 679

- Hartig, J. R. 68 (220), 97  
 Hartl, F. 200 (67), 216  
 Hartl, F. T. 347 (236), 364  
 Hartley, F. R. 156 (2), 184  
 Hartman, F. C. 359 (339), 366  
 Hartman, R. J. 398 (39), 402  
 Hartmann, N. 540 (117), 587  
 Hartwich, G. 193 (28), 215  
 Hartwig, A. 351 (278), 365  
 Hartwig, J. F. 553 (178, 180), 589, 798 (65), 802  
 Hartwig, T. 610 (60), 630  
 Harutyunyan, S. R. 457 (44, 45), 507, 564 (255), 591, 775 (29), 779 (32), 780 (38), 787 (41), 788 (48), 801  
 Harvey, J. N. 333 (133), 362  
 Harvey, P. C. 190 (1), 214  
 Harvey, S. 46 (158), 58 (155), 96, 123 (89), 129  
 Hascall, T. 73 (239), 82 (162), 96, 98, 417 (13), 424 (10), 434  
 Hase, T. A. 288 (263), 311  
 Hasegawa, T. 214 (132), 218  
 Hashimoto, W. 327 (78), 361  
 Hasobe, T. 201 (70), 216  
 Hassan, J. 596 (26), 629  
 Hässig, M. 276 (195, 196), 310  
 Hassner, A. 742 (14), 768  
 Hatada, M. 349 (256), 364  
 Hatano, M. 19 (45), 93, 569 (274), 570 (278, 279), 591, 684 (19), 714  
 Hauk, D. 520 (56), 585, 682 (9), 714  
 Hawkes, S. A. 63 (112), 94  
 Hawner, C. 791 (57), 802  
 Hawthornthwaite-Lawless, A. M. 324 (58), 356 (325, 331), 360, 366  
 Hayasaka, T. 774 (11), 800  
 Hayashi, K. 458 (52), 468 (80), 507, 508  
 Hayashi, T. 546 (143), 547 (146), 553 (185), 554 (191, 194), 568 (272), 588, 589, 591, 615 (67), 619 (77), 622 (88), 623 (89), 630, 637 (23), 639 (24), 677, 774 (21, 24), 779 (33), 800, 801  
 Hayashi, Y. 623 (90), 630, 743 (38), 769  
 Haycock, J. W. 347 (237), 364  
 Hayes, D. 424 (63, 66), 435, 436, 473 (85, 89), 508  
 Hayes, P. C. 224 (29), 260  
 Hayes, T. K. 559 (227), 590  
 Hazell, T. 268 (121), 308  
 Hazimeh, H. 260 (147), 263, 513 (15), 584  
 Hazra, T. K. 353 (307), 366  
 He, X. 469 (78, 79), 508  
 Head-Gordon, M. 369 (2), 384 (30), 401, 402  
 Healy, E. M. 259 (146), 263  
 Heathcock, C. H. 468 (83), 469 (84), 478 (65), 484 (103), 485 (4), 506, 508, 509  
 Heathcote, P. 356 (329), 366  
 Heck, L. L. 295 (293–295), 296 (296), 312  
 Heckman, J. E. 341 (195), 363  
 Heckmann, B. 558 (218), 590  
 Heckmann, G. 525 (65), 585  
 Heeg, J. 50 (101), 94  
 Heeg, M. J. 47 (160, 161), 72 (234), 78 (252), 83 (233), 84 (264), 96, 98, 122 (77, 79), 128, 303 (303), 312, 419 (27), 422 (28, 29), 433 (89), 435, 436  
 Hefter, G. 322 (47), 360  
 Hegedus, L. S. 563 (251), 591  
 Hein, J. W. 214 (128), 218  
 Hein, M. 573 (290), 592  
 Heinemann, F. W. 136 (16), 153  
 Heinemann, W. 42 (143), 95  
 Helfert, S. C. 51 (171, 172), 52 (173), 53 (174), 96  
 Helmy, R. 291 (280), 312  
 Henderson, K. W. 17 (64), 19 (69), 69 (222), 83 (263), 93, 97, 98, 150 (41), 154, 413 (42), 422 (41, 47, 59), 424 (61–67), 425 (70), 429 (76), 435, 436, 460 (56), 469 (78, 79), 473 (85–89), 507, 508, 539 (110), 587  
 Henderson, L. C. 74 (124), 95, 150 (43), 154, 423 (17), 434  
 Henderson, M. J. 31 (109), 94  
 Hendersson, K. W. 539 (112), 587  
 Hendriks, C. J. 474 (47), 507  
 Hendry, G. A. 210 (100), 217  
 Hendry, L. 625 (92), 630  
 Hengge, A. C. 319 (24), 359  
 Henneberg, D. 653 (66), 655 (63–65), 677  
 Henningsen, I. 351 (287), 365  
 Hennion, G. F. 621 (80), 630  
 Henrotte, J. G. 268 (61), 307  
 Henry, D. J. 550 (164), 588  
 Herber, C. 74 (124), 95, 150 (43), 154, 423 (17), 434, 791 (53), 802  
 Herberich, G. E. 29 (103), 94  
 Herbst-Imer, R. 57 (186), 96, 124 (91), 129  
 Hermann, G. 357 (337), 366  
 Hermes Sales, C. 268 (96), 307  
 Hernandez, D. 457 (48), 507  
 Herndon, D. N. 268 (134), 308  
 Herold, D. A. 303 (344, 350), 304 (354), 313, 314  
 Heron, N. M. 560 (234), 590, 673 (148, 149), 679  
 Herrmann, W. A. 519 (53), 550 (166, 168), 585, 589  
 Herschlag, D. 338 (176), 341 (188), 363  
 Hervé du Penhoat, C. 608 (54, 55), 629  
 Herzog, R. 59 (132), 95, 149 (6), 153  
 Heslop, J. A. 4 (34), 92, 428 (87), 436, 682 (12), 714  
 Hesse, M. 760 (47), 769  
 Hettinger, W. P. 240 (72), 261

- Hevia, E. 9 (52), 13 (59), 17 (64), 20 (70), 22 (71, 72, 74), 73 (73), 81 (224, 259), 93, 97, 98, 414 (35, 46), 419 (50), 430 (80), 431 (82), 435, 436, 460 (56), 507
- Hewgill, F. R. 476 (91), 508
- Hey, E. 427 (74), 436
- Heyn, A. S. 667 (54), 677
- Hibbert, H. 300 (313), 313
- Hideki, Y. 545 (139), 588
- Hideyuki, H. 544 (128), 588
- Higashi, S. 555 (199), 589, 608 (56), 629
- Higashiyama, K. 547 (159), 588
- Higuchi, T. 707 (46), 715
- Hilbers, C. W. 287 (248), 311
- Hill, C. L. 513 (14), 583, 584
- Hill, E. A. 119 (63, 64), 128, 144 (29), 153, 654 (73, 75), 678
- Hill, M. S. 63 (112, 208), 94, 97
- Hiller, J. 87 (271), 99
- Hills, I. D. 618 (66), 630
- Himeshima, N. 214 (135), 218
- Himmel, H.-J. 157 (17), 184
- Himo, F. 341 (202), 363
- Hingorani, M. M. 353 (272), 365
- Hinkley, W. 667 (117), 678
- Hino, N. 559 (225), 590
- Hioki, T. 452 (37), 502 (119, 120), 507, 509
- Hirai, A. 622 (86), 630, 658 (92), 678
- Hiraishi, A. 193 (22–26), 215
- Hirano, T. 107 (22), 127
- Hird, A. W. 774 (18), 775 (30), 780 (36), 800, 801
- Hird, M. 546 (144), 588, 615 (68–70), 630
- Hirsch, A. 675 (154–156), 679
- Hisamoto, H. 285 (237), 311
- Hitchcock, P. B. 23 (77, 78), 24 (80), 32 (110, 111), 37 (121), 51 (168), 62 (120, 201), 63 (112, 206–208), 70 (225), 71 (231), 94–98, 411 (33), 416 (49), 430 (77), 435, 436
- Hitomi, K. 353 (306), 366
- Hiyama, T. 285 (243), 311, 487 (68, 104), 508, 509
- Hoang, T. 699 (31), 715
- Hoarau, C. 689 (26, 27), 715
- Hocek, M. 611 (61–63), 630
- Hochstrasser, R. M. 198 (56), 216
- Hocková, D. 611 (62), 630
- Hocquemiller, R. 554 (190), 555 (197, 198), 589, 607 (48), 608 (49–51), 614 (65), 629, 630
- Hodgson, D. M. 547 (151), 588
- Hodoscek, M. J. 125 (104), 129
- Hoeijmakers, J. H. J. 351 (279), 365
- Hoelzer, B. 550 (163), 588
- Hoffman, R. 86 (86), 94
- Hoffman, R. J. 247 (100, 101), 262
- Hoffmann, R. W. 135 (11), 137 (10), 153, 516 (32), 527 (75, 76, 78, 79), 528 (80), 534 (81), 540 (115), 550 (163), 584, 586–588, 661 (104), 678, 719 (4), 720 (5–7), 721 (12), 724 (17), 725 (20, 22), 727 (21), 734 (30), 768
- Hoffmann-Röder, A. 774 (17), 800
- Hofmann, F. R. 419 (55), 435
- Hogenbirk, M. 61 (198), 86 (269), 97, 99
- Holland, M. J. 349 (257), 364
- Holland, P. L. 91 (277), 99
- Hollingsworth, C. 107 (28), 127
- Holloway, C. E. 3 (26), 25 (25), 92
- Hollstein, E. 301 (357), 314
- Holm, T. 3 (17), 92, 108 (36), 109 (37, 42, 43), 115 (45), 116 (13), 119 (14), 126, 127, 235 (54, 55), 258 (52, 53), 259 (135), 261, 263, 389 (3), 391 (9), 398 (39), 401, 402, 451 (30), 507
- Holmes, A. B. 537 (104), 586
- Holmes, R. R. 30 (107), 94
- Holten, D. 201 (38, 39, 45, 46), 215, 216
- Holtkamp, H. C. 40 (137, 138), 95, 120 (66, 68), 128
- Holton, R. A. 473 (75), 508, 597 (33), 598 (34), 629
- Holzer, B. 527 (75), 586, 725 (20), 727 (21), 768
- Holzwarth, A. R. 356 (330), 366
- Honda, K. 270 (157), 309
- Honeyman, G. W. 69 (222), 73 (73), 93, 97, 150 (41), 154, 419 (50), 435
- Honeymoon, G. W. 429 (76), 436
- Hong, Q. 572 (288), 592
- Hong, S. 330 (103), 361
- Hoogstraten, C. G. 341 (198), 363
- Hope, G. A. 107 (20), 126
- Hopkinson, A. C. 124 (94, 96), 125 (95), 129, 160 (54), 176 (129), 180 (46, 134, 135), 185, 187
- Hopman, M. 63 (112), 94
- Horáček, M. 86 (270), 87 (271), 88 (272), 89 (273), 99
- Horan, N. R. 672 (137), 679
- Hordyewska, A. 268 (109), 308
- Horibe, H. 556 (207), 590
- Horiguchi, K. 767 (56), 769
- Hormnirum, P. 424 (44), 435
- Hormnirun, P. 76 (242), 98
- Horn, E. 40 (140), 95
- Horrobin, D. F. 301 (360), 314
- Horsburgh, L. 422 (59), 435
- Hosmane, N. S. 51 (170–172), 52 (173), 53 (174), 96
- Hosmane, S. N. 53 (174), 96
- Hou, X. 279 (216), 310
- Houghton, J. D. 210 (100), 217
- Houk, K. N. 391 (24), 402
- Houpis, I. N. 654 (72), 678, 699 (31), 715
- Hour, A. F. 672 (137–139), 673 (145), 679



- House, D. 485 (24), 507  
 House, H. O. 137 (7), 153, 156 (3), 184, 295 (287), 312  
 Housecroft, C. E. 512 (4), 583  
 Houte, H. 268 (7), 306  
 Hoveyda, A. H. 557 (212), 560 (234), 561 (240), 590, 591, 671 (136), 672 (137–139), 673 (142–149), 679, 774 (18), 775 (30), 779 (33), 780 (36), 791 (55, 59, 61), 800–802  
 Howard, J. A. K. 24 (80), 65 (211), 94, 97  
 Howden, M. E. H. 654 (77), 678  
 Howell, G. P. 500 (46), 507, 787 (47), 801  
 Howson, W. 547 (147), 588  
 Hoye, T. R. 300 (300), 312  
 Hoylaerts, M. F. 345 (220), 364  
 Hruby, V. J. 455 (43), 507  
 Hsieh, K. 119 (64), 128  
 Hsieh, Y.-T. 547 (154), 588  
 Hsu, S.-F. 16 (63), 93  
 Hsueh, M.-L. 16 (63), 93  
 Hu, G. G. 335 (30), 360  
 Hu, Q.-S. 550 (165), 588  
 Hu, S. 167 (84), 186  
 Hu, Y. 163 (65), 164 (64), 167 (83), 169 (79, 80, 93, 96), 170 (98), 185, 186  
 Huang, C.-H. 547 (153), 588  
 Huang, H. W. 320 (7), 359  
 Huang, J. 550 (166), 588  
 Huang, J.-W. 547 (155), 588  
 Huang, J.-Y. 81 (228), 98, 149 (46), 154, 422 (25), 435  
 Huang, L.-F. 547 (153), 588  
 Huang, P.-Y. 398 (39), 402  
 Huang, Q. 107 (18), 126  
 Huang, W. 213 (118), 217  
 Huang, X. 644 (32), 677  
 Huang, Y.-L. 278 (209, 211, 212), 310  
 Huang, Z. 159 (36), 185  
 Hockett, S. C. 610 (60), 630  
 Huennekens, F. M. 207 (86, 87), 217  
 Huerta, F. F. 791 (53), 802  
 Huffman, J. C. 73 (240), 98, 196 (44), 216, 418 (11), 434  
 Huffman, J. L. 353 (303), 365  
 Huffman, M. 293 (267), 311  
 Hug, G. 206 (77), 217  
 Hug, G. L. 190 (2, 3), 214  
 Hugerat, M. 201 (71), 216  
 Huggett, R. J. 302 (330), 313  
 Hughes, D. L. 74 (247), 98, 421 (18), 434  
 Hughes, G. 5 (43), 93  
 Hughes, T. R. 329 (89), 361  
 Huijgen, H. J. 268 (88), 307  
 Huisgen, R. 540 (115), 587  
 Hulanicki, A. 273 (184), 309  
 Hulce, M. 451 (33), 507  
 Hull, H. S. 122 (75), 128  
 Hullihen, J. 329 (93), 361  
 Hulsbergen, F. B. 356 (332), 366  
 Hummert, M. 79 (254), 98, 414 (32), 435  
 Humphrey, S. M. 51 (51), 74 (247), 93, 98, 421 (18), 434  
 Hung, I. 152 (52), 154  
 Hunt, D. 191 (9), 215  
 Hunt, J. C. A. 574 (294), 592  
 Hunter, T. 347 (222, 224), 364  
 Huong Giang, L. T. 302 (333), 313  
 Hupe, E. 268 (7), 306, 525 (41), 585  
 Hurd, P. W. 458 (49), 507  
 Hurley, P. T. 259 (143), 263  
 Hurry, W. H. 599 (5), 628  
 Husk, G. R. 664 (110), 678  
 Hutcheon, M. L. 329 (92), 361  
 Hutchins, C. J. 339 (179), 363  
 Hutchison, D. A. 141 (28), 153  
 Huth, A. 538 (107), 587  
 Huth, J. A. 305 (364), 314  
 Hutjgen, H. J. 275 (191), 310  
 Hwang, C.-S. 59 (191), 97  
 Hynninen, P. H. 191 (9), 211 (106), 214 (112), 215, 217  
 Iacuone, A. 583 (317), 593  
 Iannello, S. 268 (49), 307  
 Ibragimov, A. A. 123 (87), 129  
 Iché-Tarrat, N. 331 (115, 116), 362  
 Ichikawa, K. 145 (39), 154  
 Ichikawa, T. 579 (309), 592  
 Ichimura, A. 259 (138), 263  
 Ida, R. 357 (333), 366  
 Ide, M. 686 (22), 688 (23), 714  
 Idriss, K. A. 280 (220), 310  
 Ieawsuwan, W. 552 (177), 589, 725 (19), 768  
 Iida, A. 772 (6), 800  
 Iida, H. 767 (55), 769  
 Iida, T. 524 (63), 585, 699 (31), 702 (39), 715  
 Iitsuka, D. 466 (71), 508  
 Iizuka, T. 90 (276), 99  
 Ijare, O. B. 286 (247), 311  
 Ikeda, H. 335 (31), 360  
 Ikeda, T. 285 (237, 243), 311  
 Iko, Y. 329 (97), 361  
 Ikonomou, M. G. 175 (115), 186  
 Ikumi, A. 544 (128), 545 (135), 588  
 Ila, H. 268 (10, 11), 306, 525 (66), 585  
 Ilani, A. 206 (80), 217  
 Ilgen, F. 540 (116), 587  
 Ilgenfritz, G. 318 (18), 359  
 Ilim, M. 277 (206), 310  
 Imahori, H. 200 (68, 69), 201 (70), 216  
 Imamoto, T. 63 (60), 93, 182 (6), 184, 570 (280), 591  
 Imanishi, M. 270 (157), 309  
 Imbos, R. 774 (14, 16), 800  
 Imhof, R. 246 (95), 262  
 Imi, K. 661 (103), 678  
 Imizu, Y. 171 (24), 185

- Imker, H. J. 357 (342), 366  
 Inagaki, K. 193 (27), 215  
 Inagaki, S. 125 (109), 129  
 Inganäs, O. 285 (240), 311  
 Ingrosso, C. 212 (115), 217  
 Inhoffen, H. H. 211 (104), 217  
 Inoue, A. 5 (42), 41 (41), 93, 341 (199–201), 363, 523 (59), 528 (77, 83), 585, 586, 633 (1), 676, 690 (29), 699 (11), 703 (43), 706 (42, 44), 714, 715  
 Inoue, K. 194 (29), 208 (96), 213 (119), 215, 217  
 Inoue, R. 567 (270), 591, 636 (18), 676  
 Inoue, S. 196 (37), 215, 274 (186, 187), 309, 310  
 Inoue, T. 214 (137), 218, 622 (84), 630, 658 (93), 678  
 Ireland, R. E. 494 (110), 509  
 Ireland, T. 775 (28), 801  
 Irisa, S. 767 (56), 769  
 Isaacs, N. W. 324 (58), 356 (325, 331), 360, 366  
 Isago, H. 192 (12), 215  
 Isaka, K. 517 (34), 519 (54), 584, 585  
 Iseki, Y. 196 (37), 215  
 Iseri, L. T. 268 (100), 307  
 Ishifune, M. 254 (121), 263  
 Ishihara, K. 19 (45), 93, 569 (274), 570 (278, 279), 591, 684 (19), 714  
 Ishii, D. 300 (312), 313  
 Ishii, T. 463 (63), 508  
 Isoyama, N. 193 (25), 215  
 Itagaki, M. 284 (178), 309  
 Itami, K. 544 (131), 555 (199, 204), 588–590, 608 (56), 629, 641 (27, 28), 662 (109), 664 (108), 677, 678  
 Ito, M. 193 (26), 215, 558 (217), 590  
 Ito, O. 201 (41, 42, 70), 216  
 Ito, S. 546 (142), 588, 616 (71), 630, 701 (36), 715  
 Itoh, H. 329 (100), 361  
 Itoh, K. 517 (34), 519 (54), 584, 585, 675 (157, 158), 679  
 Itoh, N. 479 (14, 16), 506, 760 (50), 769  
 Itoh, S. 193 (24, 25), 215  
 Itoh, T. 699 (31), 715  
 Itono, S. 107 (22), 127  
 Itooka, R. 780 (35), 801  
 Iturraspe, J. 211 (103), 217  
 Ivanov, D. 503 (53, 121), 507, 509  
 Iwahara, T. 662 (106), 678  
 Iwai, S. 353 (306), 366  
 Iwaki, M. 193 (24), 215  
 Iwaki, S. 193 (25), 215  
 Iwamoto-Kihara, A. 329 (97), 361  
 Iwasawa, N. 772 (3), 800  
 Iyer, S. S. 73 (240), 98, 418 (11), 434  
 Izatt, R. M. 328 (85, 86), 361  
 Izod, K. 84 (265), 99, 298 (304), 312, 427 (73), 436  
 Izumi, T. 353 (307), 366  
 Jablonski, A. 295 (288), 312  
 Jackson, P. R. 268 (142), 308  
 Jacob, A. P. 182 (133), 187  
 Jacob, K. 30 (108), 94, 243 (86), 262  
 Jacob Morris, J. 469 (78), 508  
 Jacobsen, E. N. 774 (2), 779 (22), 800  
 Jaenschke, A. 48 (163), 96, 122 (81), 128  
 Jaeschke, G. 774 (8), 800  
 Jäger, V. 573 (290), 592  
 Jaggarr, A. J. 63 (206), 97  
 Jaidane, N. 357 (335), 366  
 Jain, N. 421 (58), 435, 700 (35), 715  
 Jaiswal, A. 353 (307), 366  
 James, A. W. G. 462 (57), 507  
 James, P. F. 181 (131), 182 (133), 187  
 Jamison, W. C. L. 667 (118), 678  
 Janin, J. 348 (246), 350 (261), 364, 365  
 Janke, N. 44 (152), 45 (154, 156), 47 (159), 95, 96  
 Jansen, B. J. M. 474 (47), 507  
 Jansen, J. F. G. A. 774 (10), 800  
 Jaramillo, C. 518 (48), 585  
 Jarvis, J. A. J. 30 (104), 94  
 Jäschke, A. 336 (162), 362  
 Jasien, P. G. 171 (99, 103), 186  
 Jastrzebski, J. T. B. H. 69 (29), 79 (257), 92, 98, 545 (137), 588  
 Jayasena, S. D. 341 (192, 194), 363  
 Jayaweera, P. 175 (115), 186  
 Jeltsch, A. 355 (318, 320), 366  
 Jenkins, H. D. B. 106 (15), 126  
 Jensen, A. 270 (154), 309  
 Jensen, A. E. 518 (36), 519 (51), 584, 585  
 Jensen, C. M. 71 (232), 98  
 Jewitt, B. 124 (93), 129  
 Jezequel, M. 544 (133), 588  
 Ji, S. 565 (256), 591  
 Ji, S.-J. 782 (39), 801  
 Jia, J. 293 (285), 312  
 Jiang, G. 302 (327), 313  
 Jiang, G.-b. 302 (336), 313  
 Jiang, H. 123 (90), 129  
 Jiang, L. 272 (176), 309, 329 (87), 361  
 Jiang, P. 391 (22), 402  
 Jiwoua Ngounou, C. 283 (162), 309  
 Joachimiak, A. 327 (67), 360  
 Job, A. 653 (68), 677  
 Jockusch, R. A. 318 (19, 20), 359  
 Johansen, T. N. 519 (50), 585  
 John, N. B. St. 295 (293), 312  
 Johnson, B. G. 369 (2), 384 (30), 401, 402  
 Johnson, C. 67 (217), 97  
 Johnson, F. B. 268 (13), 306  
 Johnson, J. S. 579 (310), 592  
 Johnson, K. A. 352 (289, 291, 292), 365

- Johnson, L. N. 348 (239), 364  
 Johnson, S. C. 478 (65), 508  
 Jolibois, P. 107 (27), 127, 220 (10, 11), 260  
 Jolly, B. S. 81 (260), 98, 405 (5), 434  
 Jońca, Z. 277 (203, 204), 310  
 Jones, B. T. 279 (216), 310  
 Jones, C. 64 (209), 97  
 Jones, E. G. 290 (275), 312  
 Jones, M. C. 519 (53), 585  
 Jones, P. 534 (96), 586  
 Jones, R. 133 (4), 153, 301 (301), 312  
 Jones, R. G. 295 (291), 312  
 Jones, R. O. 331 (120), 362  
 Jones, R. V. H. 673 (140, 141), 679  
 Joordens, J. J. M. 287 (248), 311  
 Jordan, K. D. 391 (12), 402  
 Jordan, P. 356 (36, 322), 360, 366  
 Jousseau, B. 635 (13–15), 648 (49, 50), 676, 677  
 Joyce, C. M. 352 (297), 355 (274), 365  
 Joyce, G. F. 336 (151), 362  
 Juan, D. 268 (76), 307  
 Julia, M. 553 (179), 589, 608 (52–55), 629, 727 (23), 730 (28), 768  
 Julius, M. 516 (32), 584  
 Juneau, K. 320 (29), 360  
 Junge, W. 329 (95), 361  
 Jungreis, E. 280 (221), 310  
 Jungwirth, P. 322 (47), 360  
 Junk, C. L. 190 (1), 214  
 Junk, P. C. 46 (158), 64 (209), 81 (260), 96–98, 123 (89), 129, 405 (5), 434  
 Justyniak, I. 410 (36), 435  
 Jutzi, P. 67 (93), 68 (221), 94, 97  
 Kabeláč, M. 323 (50), 360  
 Kacprzynski, M. A. 774 (18), 800  
 Kadish, K. M. 193 (11, 13, 15), 194 (32), 195 (16), 215  
 Kaeseberg, C. 665 (115), 678  
 Kageyama, H. 60 (194–196), 61 (197), 97  
 Kahn, L. R. 369 (1), 401  
 Kai, Y. 51 (167), 60 (194, 196), 61 (197), 96, 97, 121 (74), 128, 254 (126), 263, 540 (119), 587  
 Kaim, W. 52 (173), 53 (174), 79 (258), 96, 98  
 Kalia, O. L. 213 (120, 122), 217  
 Kalojanoff, A. 214 (126, 127), 218  
 Kalsbeck, W. A. 201 (46), 216  
 Kalscheuer, R. 301 (359), 314  
 Kambe, N. 544 (127, 128), 545 (135, 136), 560 (235), 561 (239, 241, 242), 588, 590, 591  
 Kamei, K. 699 (31), 715  
 Kamei, T. 641 (27, 28), 677  
 Kamikawa, T. 553 (185), 589  
 Kamiya, N. 356 (323), 366  
 Kamm, B. 191 (7), 215  
 Kamm, M. 191 (7), 215  
 Kamm, O. 2 (9), 92  
 Kanai, M. 564 (254), 591, 774 (9, 25), 800, 801  
 Kanakamma, P. P. 547 (154), 588  
 Kanatani, R. 661 (101, 107), 662 (106), 678  
 Kanazawa, A. 285 (243), 311  
 Kandil, S. A. 633 (10), 676  
 Kane, H. J. 358 (348), 367  
 Kanegisa, N. 540 (119), 587  
 Kanehisa, N. 51 (167), 96, 121 (74), 128, 254 (126), 263  
 Kanemasa, S. 452 (35), 474 (96), 507, 508  
 Kang, S.-K. 557 (215), 590  
 Kanno, K.-I. 554 (192), 589  
 Kanoufi, F. 513 (15), 584  
 Kao, K.-H. 566 (262), 591  
 Kaplan, F. 138 (22), 153  
 Kapoor, P. N. 428 (86), 436  
 Kapoor, R. N. 428 (86), 436  
 Kapur, G. N. 395 (4), 401  
 Kar, A. 557 (209), 590  
 Karaghiosoff, K. 27 (99), 94  
 Karakyriakos, E. 159 (35), 185  
 Karam, J. D. 352 (294), 365  
 Karbstein, K. 341 (188), 363  
 Karen, P. 107 (18, 19), 126  
 Karen, V. L. 107 (18), 126  
 Karfunkel, H. R. 675 (155), 679  
 Kargin, Yu. M. 219 (7), 260  
 Karlson, L. 304 (351), 313  
 Karlsson, R. 347 (232), 364  
 Karlström, A. S. E. 555 (201, 204), 590, 558 (218), 590, 791 (53), 802  
 Karlström, E. 544 (131), 588  
 Karnachi, T. 214 (137), 218  
 Karpeisky, A. 340 (187), 363  
 Karplus, M. 341 (203), 363  
 Karpov, A. S. 547 (148), 588  
 Karppanen, H. 268 (21), 270 (155), 306, 309  
 Karr, P. A. 201 (41, 42), 216  
 Karras, M. 640 (25, 26), 677  
 Kasai, N. 51 (167), 60 (194–196), 61 (197), 96, 97, 121 (74), 128, 254 (126), 263, 540 (119), 587  
 Kasai, Y. 341 (199, 201), 363  
 Kaschube, W. 86 (266), 99  
 Kase, K. 791 (60), 802  
 Kashimura, S. 254 (121), 263  
 Kasho, V. N. 329 (101), 361  
 Kasparov, V. V. 183 (153), 184 (155), 187  
 Kasper, B. 213 (123), 217  
 Kasting, J. F. 355 (13), 359  
 Katagiri, T. 389 (3), 401  
 Katayama, Y. 193 (23), 215  
 Kathuria, P. 268 (44), 306  
 Kato, S. 198 (64), 216, 531 (90), 586, 699 (31), 715, 791 (51), 802  
 Kato, T. 791 (60), 802

- Kato, Y. 675 (158), 679, 699 (31), 715  
 Kato-Yamada, Y. 329 (99), 361  
 Katritzky, A. R. 547 (156–158), 559 (232), 572 (288, 289), 588, 590, 592, 729 (26), 768  
 Kattnig, E. 626 (96), 630  
 Katz, A. K. 324 (35), 360  
 Katz, J. J. 211 (105), 217  
 Kauffman, S. L. 289 (271), 312  
 Kaul, F. A. R. 519 (53), 585  
 Kaupp, M. 79 (258), 98  
 Kawabata, T. 480 (92), 508  
 Kawai, R. 348 (243), 364  
 Kawai, S. 327 (78), 361  
 Kawamura, S.-I. 452 (37), 507  
 Kawasaki, M. 699 (31), 715  
 Kawashima, T. 766 (53), 769  
 Kazakov, V. P. 235 (51), 261  
 Kazantsev, A. V. 336 (157), 362  
 Kazmaier, U. 487 (19), 237, 506, 507  
 Kazuta, K. 556 (207), 590  
 Kealy, T. J. 25 (84), 94  
 Kebarle, P. 175 (115, 123), 186, 187  
 Kehres, D. G. 325 (3), 359  
 Kehrli, S. 565 (257), 591, 775 (31), 801  
 Keith, T. 384 (30), 402  
 Keizer, S. P. 193 (19), 215  
 Kellog, M. S. 499 (117), 509  
 Kelly, J. 293 (267), 311  
 Kemp, B. E. 347 (230), 364  
 Kennard, C. H. L. 26 (92), 94  
 Kennedy, A. L. 9 (52), 93  
 Kennedy, A. R. 13 (59), 15 (62), 17 (64–66), 18 (67), 19 (68, 69), 20 (70), 22 (71, 72, 74), 69 (222), 73 (73), 81 (224, 259), 93, 97, 98, 150 (41), 154, 414 (35, 46), 419 (50), 422 (59), 424 (61), 425 (70), 429 (76), 430 (80), 431 (82), 435, 436, 460 (56), 469 (79), 507, 508  
 Kephart, J. C. 214 (125), 218  
 Kern, D. 344 (212), 364  
 Kern, J. 356 (324), 366  
 Kerr, W. J. 424 (63–67), 435, 436, 473 (85–89), 508, 539 (110, 112), 587  
 Kerwin, S. M. 478 (65), 508  
 Kessar, S. V. 540 (115), 587, 729 (26), 768  
 Keyes, W. R. 288 (254), 311  
 Khairallah, G. N. 181 (132), 187  
 Khalilov, A. M. 671 (132), 679  
 Khalilov, L. M. 123 (87), 129  
 Kham, K. 258 (130), 263, 291 (279), 312  
 Khan, M. A. 81 (81), 94  
 Khan, M. S. 139 (26), 150 (45), 153, 154  
 Khan, S. I. 86 (268), 99  
 Kharasch, M. S. 288 (146), 308, 389 (3), 401, 512 (3), 583, 595 (1, 3, 8), 599 (5), 604 (7), 624 (4), 625 (2, 6), 628, 653 (67), 677  
 Khawaja, J. A. 268 (21), 270 (155), 306, 309  
 Khetrapala, C. L. 286 (247), 311  
 Kholmogorov, V. E. 196 (51), 216  
 Kholmogorov, V. Ye. 198 (59), 216  
 Khutoreskaya, G. 327 (67), 360  
 Khvoinova, N. M. 426 (48), 435  
 Khvorova, A. 341 (192, 194), 363  
 Kibune, N. 302 (326), 313  
 Kiefer, W. 357 (337), 366  
 Kienle, M. 576 (301), 580 (314), 592, 593  
 Kii, S. 524 (63), 585, 702 (39), 715  
 Kikuchi, M. 563 (248), 591  
 Kikuchi, W. 549 (162), 588  
 Kilbourn, B. T. 30 (104), 94  
 Kilic, E. 278 (215), 310  
 Kiliç, Z. 277 (206), 310  
 Kiljunen, H. 288 (263), 311  
 Kim, C.-B. 553 (178), 589  
 Kim, C. G. 70 (226), 97, 432 (79), 436  
 Kim, D. 196 (53), 216  
 Kim, E. E. 354 (309), 366  
 Kim, J. 70 (226), 97, 432 (79), 436  
 Kim, J.-H. 270 (159), 309  
 Kim, K. M. 268 (13), 306  
 Kim, T.-S. 667 (120), 678  
 Kim, Y. 70 (226), 97, 432 (79), 436  
 Kimball, D. B. 531 (93), 586  
 Kimura, E. 675 (157), 679  
 Kimura, M. 270 (157), 309, 395 (38), 402, 558 (218), 590  
 Kimura, T. 622 (88), 630, 637 (23), 677  
 Kina, A. 554 (194), 589  
 King, A. O. 293 (266), 311  
 King, B. A. 11 (56), 93, 686 (17), 714  
 King, W. A. 359 (351), 367  
 Kinoshita, K. 329 (96, 100), 361  
 Kinter, M. 303 (350), 304 (354), 313, 314  
 Kintopf, S. 123 (88), 129  
 Kinugasa, H. 254 (121), 263  
 Kinzelmann, H.-G. 44 (152), 95  
 Kirby, S. P. 116 (1), 126  
 Kirchner, F. 578 (307), 592  
 Kirmse, W. 718 (2), 767  
 Kirsch, S. F. 798 (66), 802  
 Kirschleger, B. 288 (262), 311, 516 (31), 584  
 Kisanga, P. 472 (94), 508  
 Kise, H. 193 (25), 194 (29), 213 (119), 215, 217  
 Kishimoto, N. 193 (27), 215  
 Kisker, C. 351 (280), 365  
 Kisko, J. L. 73 (239), 98, 424 (10), 434  
 Kitagawa, K. 5 (42), 41 (41), 93, 523 (59), 585, 699 (11), 714  
 Kitagawa, T. 259 (138), 263  
 Kitamura, M. 579 (309), 592  
 Kitamura, T. 453 (38, 39), 507  
 Kitamura, Y. 285 (237), 311  
 Kitazume, T. 558 (218), 590  
 Kitching, W. 244 (89), 262  
 Kitoh, Y. 479 (16), 485 (15, 17), 506

- Kitsunai, T. 285 (243), *311*  
 Kjekshus, Å. 107 (18), *126*  
 Klabunde, K. J. 171 (24, 25), *185*  
 Klabunde, T. 322 (49), *360*  
 Klages, F. 578 (307), *592*  
 Klassen, B. 772 (7), *800*  
 Kleiber, P. D. 162 (59, 60), 163 (62), 164 (63), 169 (88–91), 171 (92, 105), *185, 186*  
 Kleiger, S. C. 595 (1), *628*  
 Kleimeier, J. 68 (221), *97*  
 Klein, D. J. 334 (141), *362*  
 Klein, G. L. 268 (134), *308*  
 Klein, T. E. 270 (160), *309*  
 Klein, W. R. 514 (19), *584*  
 Kleinrock, N. S. 159 (38), *185*  
 Klenow, H. 351 (287), *365*  
 Klix, R. C. 559 (227), *590*  
 Kloth, M. 64 (209), *97*  
 Klug, A. 340 (186), *363*  
 Kluge, S. 332 (14), 350 (268), *359, 365*  
 Kluger, R. 331 (113), *361*  
 Klukas, O. 356 (36), *360*  
 Knauf, W. 537 (104), *586*  
 Kneisel, F. F. 268 (8), *306, 518 (42), 534 (96), 585, 586*  
 Knighton, D. R. 347 (232), *364*  
 Knizek, J. 27 (99), *94*  
 Knochel, P. 268 (7, 8, 10, 11), 291 (276, 277), *306, 312, 517 (35), 518 (36, 42–44, 46, 47), 519 (51), 520 (55), 524 (61, 62), 525 (41, 66–69), 526 (72), 527 (28), 528 (83, 84, 87), 529 (88), 531 (57, 89, 92), 533 (95), 534 (81, 96–99, 100), 539 (113), 540 (114, 116), 543 (125), 545 (138), 548 (160), 550 (126), 553 (186), 555 (198), 557 (208), 559 (223), 563 (245), 566 (266), 569 (277), 576 (301, 304), 577 (305, 306), 578 (308), 580 (314), 584–593, 601 (44), 607 (47), 619 (45), 629, 633 (1), 676, 690 (29, 30), 714 (7, 8), 714, 715, 738 (33), 739 (34), 748 (40), 767 (58), 768, 769, 774 (23), 775 (28), 791 (54), 800–802*  
 Knochen, M. 278 (213), *310*  
 Knoers, N. V. 268 (65), *307*  
 Knoers, N. V. A. M. 268 (66), *307*  
 Knopff, O. 527 (75, 78, 79), *586, 661 (104), 678, 724 (17), 725 (20), 734 (30), 768*  
 Knotter, D. M. 774 (25), *800*  
 Knox, J. E. 47 (161), 96, 122 (79), *128*  
 Ko, B.-T. 16 (63), *93*  
 Ko, K.-Y. 395 (4), *401*  
 Ko, Y. H. 330 (103), *361*  
 Kobayashi, F. 201 (76), *216*  
 Kobayashi, H. 474 (96), *508*  
 Kobayashi, K. 107 (21), *126, 453 (38, 39), 466 (71), 468 (80), 487 (67, 68, 72, 104), 507–509*  
 Kobayashi, M. 193 (24, 25), 194 (29), 213 (119), *215, 217*  
 Kobayashi, S. 767 (56), *769*  
 Kobayashi, T. 198 (64), *216*  
 Kobayashi, Y. 480 (11, 12), *506, 558 (217), 590*  
 Kobe, K. A. 231 (45), *261*  
 Kober, R. 517 (39), *585*  
 Kobetz, P. 222 (26), *260*  
 Kobrich, G. 718 (2), *767*  
 Kobyshev, G. I. 198 (65), *216*  
 Koch, E.-C. 103 (5), *126*  
 Kochi, J. K. 258 (133), 263, 596 (11, 17), 604 (9, 10, 13–15), 615 (12, 16), 628, *629*  
 Kocienski, P. 666 (116), *678*  
 Koebrich, G. 576 (303), *592*  
 Kofink, C. 531 (89), *586*  
 Kofink, C. C. 545 (138), *588*  
 Koga, N. 387 (33), *402*  
 Kogure, T. 772 (3), *800*  
 Kohl, A. 325 (70), *361*  
 Kohler, E. P. 299 (309, 310), *312*  
 Koide, N. 285 (243), *311*  
 Koizumi, M. 339 (185), *363*  
 Kojima, C. 341 (199), *363*  
 Kojima, K. 157 (21), *185*  
 Kok, G. L. 219 (5), *260*  
 Kok, W. T. 275 (191), *310*  
 Kolisek, M. 325 (66, 68), *360*  
 Kolodner, R. D. 351 (282), *365*  
 Kolonits, M. 183 (151), *187*  
 Kolotuchin, S. V. 566 (264), *591*  
 Kolthoff, I. M. 300 (315), *313*  
 Komander, D. 347 (226), *364*  
 Komaromi, I. 384 (30), *402*  
 Komatsu, H. 285 (237), *311*  
 Komatsu, K. 125 (100), *129*  
 Komiya, N. 419 (57), *435, 538 (105), 587*  
 Kondo, A. 527 (74), *586, 727 (18), 728 (25), 730 (27), 768*  
 Kondo, J. 528 (77, 83), *586, 703 (43), 706 (42, 44), 715*  
 Kondo, K. 556 (207), *590*  
 Kondo, Y. 341 (199), *363, 404 (2), 434, 538 (105, 108), 587, 713 (55), 715*  
 Kondyrew, N. W. 224 (31, 32), 244 (87), 246 (13, 30), *260–262*  
 Kongsaree, P. 725 (19), *768*  
 Konigsberg, W. 352 (301), *365*  
 Konigsberg, W. H. 352 (294), *365*  
 Konishi, H. 453 (38, 39), 466 (71), 468 (80), *487 (72), 507, 508*  
 Konrad, M. 268 (67), *307*  
 Konstantinović, S. 540 (118), *587*  
 Koo, W. W. 268 (70), *307*  
 Kooijman, H. 40 (140), 66 (215), 86 (269), *95, 97, 99*  
 Koon-Church, S. E. 259 (146), *263*

- Koop, U. 505 (26), 507  
 Koops, R. W. 559 (227), 590  
 Kooriyama, Y. 486 (25), 507  
 Kopecky, K. R. 395 (5), 401  
 Kopelman, R. 285 (156), 309  
 Kopf, J. 6 (48), 38 (122), 42 (49), 93, 95, 682 (10), 714  
 Kopnyshev, S. B. 121 (70), 128  
 Kopp, F. 268 (8), 291 (277), 306, 312, 525 (41), 528 (84), 531 (57), 555 (198), 569 (277), 576 (304), 585, 586, 589, 591, 592, 607 (47), 629, 739 (34), 768  
 Koppel, H. 268 (26), 306, 332 (131), 362  
 Koppetsch, G. 33 (114, 115), 94  
 Koradin, C. 548 (160), 588  
 Korn, T. 268 (8), 306, 518 (42), 585  
 Korn, T. J. 559 (223), 590, 601 (44), 629  
 Kornberg, A. 327 (76), 361  
 Kornberg, R. D. 355 (313), 366  
 Korneeva, V. S. 352 (301), 365  
 Korotkov, V. I. 198 (59), 216  
 Korpics, C. J. 398 (39), 402  
 Korppi-Tommola, J. 357 (334), 366  
 Kosar, W. 258 (131), 263  
 Koschatzky, K. H. 537 (104), 586  
 Koss, A.-M. 673 (149), 679  
 Kossa, W. C. 654 (80), 678  
 Kost, G. J. 276 (15), 306  
 Kostas, I. D. 66 (215), 97  
 Koth, C. M. 327 (67), 360  
 Kotoku, M. 556 (207), 590  
 Koudsi, Y. 458 (50), 507  
 Kouznetsov, D. A. 330 (106, 107), 361  
 Kowalewska, A. 32 (110), 94  
 Koyama, M. 526 (70), 586, 746 (39), 769  
 Koyanagi, G. K. 161 (55), 185  
 Kozhushkov, S. I. 582 (315), 593  
 Krafczyk, R. 53 (175), 96  
 Krafft, M. E. 473 (75), 508, 597 (33), 598 (34), 629  
 Kraft, B. J. 196 (44), 216  
 Kramer, J. G. 289 (271), 312  
 Krasovskaya, V. 539 (113), 587  
 Krasovskiy, A. 291 (276, 277), 312, 520 (55), 526 (72), 527 (28), 529 (88), 531 (57), 539 (113), 543 (125), 557 (208), 569 (277), 580 (314), 584–587, 590, 591, 593, 633 (1), 676, 690 (29), 714 (7, 8), 714, 715  
 Kraszewska, I. 410 (36), 435  
 Kraus, K. W. 600 (37), 601 (39), 629  
 Krause, H. 554 (189), 589, 608 (57), 614 (59), 624 (35), 629  
 Krause, N. 455 (42), 474 (95), 505 (26), 507, 508, 596 (21), 629, 633 (9), 676, 774 (16, 17), 800  
 Kräutler, B. 210 (101), 217  
 Krauß, N. 356 (36, 322, 324, 330), 360, 366  
 Kravchuk, A. V. 338 (176), 363  
 Krebs, B. 322 (49), 360  
 Krebs, E. G. 347 (230), 364  
 Krejčová, A. 279 (217), 310  
 Krisanov, R. S. 65 (211), 97  
 Krishnamurthy, D. 521 (58), 583 (319), 585, 593  
 Krishnan, R. 369 (1), 401  
 Krishnan, S. 707 (48), 715  
 Kristensen, J. 518 (49), 585  
 Krivan, V. 287 (253), 311  
 Krogh, S. C. 283 (234), 311  
 Krogsgaard-Larsen, P. 370 (113), 509, 519 (50), 585  
 Kroll, J. 301 (357), 314  
 Kromann, H. 519 (50), 585  
 Kromov, V. I. 212 (117), 217  
 Kropf, H. 213 (123), 217  
 Kroth, H. J. 26 (96), 94  
 Krow, G. R. 55 (178), 96, 225 (40), 261, 760 (47), 769  
 Krueger, C. 123 (80), 128  
 Kruger, C. 152 (51), 154  
 Krüger, C. 33 (114, 115), 45 (156, 157), 47 (159), 67 (93), 71 (227), 86 (266), 94, 96, 97, 99  
 Kruger, K. 335 (149), 362  
 Krumpe, K. E. 718 (2), 768  
 Krut'ko, D. P. 65 (211), 97  
 Krysan, D. J. 497 (60), 507  
 Krywult, B. 495 (111), 509  
 Krzesinski, J. M. 268 (138), 308  
 Kuang, T. 356 (326), 366  
 Kubišta, J. 86 (270), 89 (273), 99  
 Kubo, T. 701 (36), 715  
 Kubota, K. 566 (265), 591  
 Kubota, T. 285 (237), 311, 558 (218), 590  
 Kucharski, L. M. 325 (74, 75), 361  
 Kudin, K. N. 384 (30), 402  
 Kühlbrandt, W. 356 (328), 366  
 Kuhn, A. 57 (186), 96, 124 (91), 129  
 Kuhn, N. 71 (230), 98, 405 (12), 434  
 Kuimelis, R. G. 337 (159), 362  
 Kukovinets, A. G. 671 (132), 679  
 Kulinkovich, O. 582 (315), 593  
 Kulinkovich, O. G. 268 (6), 306, 582 (315), 593  
 Kulpmann, W. R. 268 (30), 306  
 Kumada, M. 661 (101, 107), 662 (106), 678  
 Kumamaru, T. 303 (349), 304 (352, 353), 313, 314  
 Kumar, S. N. 214 (137), 218  
 Kumazawa, K. 484 (69), 508  
 Kundu, K. 23 (78), 94  
 Kundu, S. 201 (70), 216  
 Kuniyasu, H. 544 (127, 128), 545 (135, 136), 561 (239), 588, 591  
 Kunkel, T. A. 351 (273), 355 (315), 365, 366  
 Küntzel, H. 237 (62), 261

- Kunz, W. 322 (47), 360  
 Kupfer, V. 88 (272), 99  
 Kurihara, T. 737 (32), 768  
 Kuriyan, J. 347 (227), 364  
 Kuroda, A. 480 (92), 508  
 Kurti, L. 742 (14), 768  
 Kusche, A. 527 (78), 534 (81), 586, 719 (4), 724 (17), 768  
 Kushlan, D. M. 682 (5), 714  
 Kuwabara, T. 341 (189), 363  
 Kuwahara, Y. 206 (81), 217  
 Kuwata, K. 212 (114), 217  
 Kuyper, J. 291 (278), 312  
 Kuznetsov, D. A. 331 (104), 361  
 Kuznetsova, N. A. 213 (120, 122), 217  
 Kuznetsova, S. V. 299 (306), 312  
 Kwan, C. L. 604 (15), 629  
 Kyler, K. S. 528 (85), 586  
 Laaziri, H. 534 (81), 586  
 Labbauf, A. 120 (65), 128  
 Labeeuw, M. 268 (114), 308  
 Labeeuw, O. 559 (224), 590  
 LaBelle, J. T. 356 (327), 366  
 Ladbury, J. E. 300 (317), 313  
 Ladlow, M. 711 (49), 715  
 Laemmle, J. 108 (32), 127, 389 (3), 401, 683 (16), 714  
 Lagarden, M. 610 (60), 630  
 Lahiri, S. 341 (198), 363  
 Lai, J.-J. 208 (97), 217  
 Lajer, H. 268 (141), 308  
 Lajeunesse, E. 344 (215), 364  
 Lakhdar, Z. B. 357 (335), 366  
 Lakowicz, J. R. 283 (235), 311  
 Lamarche, B. J. 352 (290), 365  
 Lamberet, G. 301 (355), 314  
 Lambert, D. 341 (195), 363  
 Lambert, F. 774 (8), 800  
 Lambert, R. L. 517 (34), 584, 719 (3), 768  
 Lamm, G. 320 (32), 323 (52), 360  
 Lammi, R. K. 201 (39, 45), 215, 216  
 Lamoure, C. 344 (215), 364  
 Lan, X. 547 (156), 588  
 Lander, E. S. 347 (223), 364  
 Lander, P. A. 563 (251), 591  
 Landert, H. 775 (27), 801  
 Lang, F. 699 (31), 715  
 Lang, K. 193 (20), 215  
 Lang, S. 520 (56), 585, 682 (9), 714  
 Lange, G. 4 (31), 92, 686 (1), 714  
 Lanzisera, D. V. 157 (20), 159 (34), 184, 185  
 Lappert, M. F. 24 (80), 30 (104), 31 (109), 32 (111), 37 (121), 40 (139), 62 (120, 201), 94, 95, 97, 305 (305), 312, 416 (49), 435  
 Lapsker, I. 211 (110), 217  
 Larchevêque, M. 487 (22), 506  
 Largo, A. 106 (16), 126  
 Larhed, M. 513 (18), 584  
 Larsen, A. O. 791 (59), 802  
 Larsen, C. D. 328 (86), 361  
 Larsen, R. D. 293 (266), 311  
 Larsen, T. M. 349 (252, 255, 259), 364, 365  
 Larson, G. L. 457 (48), 507  
 Laszlo, P. 86 (86), 94  
 Latham, R. A. 156 (3), 184  
 Latham, R. L. 137 (7), 153  
 Lau, S. Y. W. 5 (43), 93  
 Laurent, A. 647 (42), 677  
 Laurich, D. 554 (189), 589, 626 (95), 630  
 Lautens, M. 658 (94), 678  
 Laux, M. 505 (26), 507  
 Lavilla, I. 272 (170), 309  
 Law, M. C. 515 (26), 584  
 Lawler, R. G. 138 (20), 153  
 Lawrence, L. M. 513 (14), 584  
 Lay, J. O. 176 (125), 187  
 Laye, P. G. 109 (47), 127  
 Layfield, R. A. 51 (51), 93  
 Layh, M. 37 (121), 95  
 Lazzari, D. 580 (313), 592, 593  
 Le Du, M. H. 344 (215), 364  
 Le Paith, J. 596 (30), 629  
 Lea, L. 558 (219), 590, 791 (50, 57), 802  
 Leach, C. S. 268 (93), 307  
 Leader, G. R. 300 (316), 313  
 Leal-Granadillo, I. A. 303 (346), 313  
 Leazer, J. L. 103 (8), 126, 519 (52), 585  
 Lebioda, L. 349 (251, 256–258), 364, 365  
 Lebret, B. 711 (50), 715  
 Leclerc, F. 341 (203), 363  
 Leclerc, M. 285 (238, 239, 241, 242), 311  
 Lecomte, C. 328 (82), 361  
 LeCours, S. M. 198 (56), 216  
 Lee, C. 384 (28), 402  
 Lee, C.-F. 559 (230), 590  
 Lee, C. H. 235 (18), 260, 466 (66), 508, 538 (105), 587  
 Lee, C.-H. 419 (54), 435  
 Lee, C.-P. 278 (211), 310  
 Lee, F. H. 228 (16), 235 (18), 238 (17), 260  
 Lee, G.-H. 81 (228), 98, 149 (46), 154, 422 (25), 435, 547 (154), 588  
 Lee, H. 103 (9), 126, 517 (37), 584  
 Lee, J. 514 (20), 584, 654 (72), 678, 699 (31), 715  
 Lee, J.-B. 278 (209, 212), 310  
 Lee, J. I. 166 (76), 186  
 Lee, J. Y. 355 (312), 366  
 Lee, K.-S. 268 (135), 308  
 Lee, K.S. 775 (30), 801  
 Lee, Y. 791 (61), 802  
 Lefrancois, M. 173 (111), 186  
 Legros, J. 596 (30), 629  
 Lehmann, C. W. 624 (35), 629  
 Lehmkuhl, H. 45 (17), 71 (227), 96, 97, 123 (80, 86, 88), 128, 129, 143 (37), 154, 221

- (24, 25), 222 (27), 233 (2), 260, 653 (62, 66), 655 (59–61, 63–65, 81), 656 (87), 677, 678
- Lehmkuhl, H. 151 (15), 152 (51), 153, 154
- Lehner, R. S. 499 (115), 509
- Leibfritz, D. 136 (8), 153
- Leiboda, L. 320 (26), 349 (248, 254), 360, 364
- Leier, C. V. 268 (105), 308
- Leighton, J. L. 779 (20), 800
- Leinweber, C. M. 289 (271), 312
- Leising, F. 69 (223), 97
- Leitner, A. 554 (189), 589, 614 (58, 59), 626 (94), 629, 630
- Lemaire, M. 596 (26), 629
- Lentz, D. 26 (96), 94
- Leontis, N. B. 335 (148), 362
- Leotta, G. J. 563 (247), 591
- Lepage, O. 626 (96), 630
- Lepifre, F. 552 (176), 589
- Leprêtre, A. 518 (43), 534 (81), 585, 586
- Leroi, G. E. 201 (73), 216
- Lesar, A. 125 (104), 129
- Lescoute, A. 341 (192), 363
- Lesley, S. A. 325 (70), 361
- Leslie, A. G. W. 329 (94, 102), 361
- Leśniewska, B. 273 (184), 309
- Lessène, G. 473 (74), 508
- Lesseue, G. 539 (111), 587
- Leu, W. 791 (59), 802
- Leung, M.-K. 547 (155), 588
- Leung, W.-P. 24 (80), 94
- Leupold, D. 196 (54), 216
- Leuser, H. 633 (1), 676
- Levanon, H. 201 (71), 206 (78), 216, 217
- Lever, O. W. 760 (46), 769
- Levesque, I. 285 (242), 311
- Levi, E. 247 (106), 248 (96, 113), 262
- Levi, M. D. 253 (117), 262
- Lewandowski, W. 277 (203, 204), 310
- Lewenstam, A. 268 (21), 270 (155), 306, 309
- Lewiński, J. 25 (82), 94, 299 (307), 312, 410 (36), 435
- Lewinski, K. 320 (26), 360
- Lewis, L. D. 268 (112), 308
- Lewis, N. S. 243 (84), 259 (143), 262, 263
- Lewis, R. 531 (92), 586
- Lex, J. 517 (40), 585
- L'Hostis-Kervella, I. 462 (59), 507
- Li, F. 201 (46), 216
- Li, G. 455 (43), 507
- Li, G. Y. 550 (171, 174), 589
- Li, L. 107 (20), 126, 272 (176), 309
- Li, N. 395 (35), 402
- Li, P. 272 (169), 309
- Li, W. 484 (102), 509
- Li, X. 293 (285), 312
- Li, Y. 272 (169), 309
- Li, Z. 62 (120), 95
- Liang, B. 787 (44), 801
- Liang, Y.-J. 278 (212), 310
- Liao, J. C. 329 (90), 361
- Liao, L.-a. 659 (98, 99), 678
- Liao, S. 44 (113, 153), 45 (154), 94, 95
- Liashenko, A. 384 (30), 402
- Licheri, G. 318 (17), 359
- Lichtenwalter, M. 619 (75), 630
- Licini, G. 500 (55), 507
- Liddle, S. T. 74 (124), 76 (249), 95, 98, 150 (43), 154, 422 (20), 423 (17), 434
- Liebenow, C. 247 (35, 102–105), 261, 262, 305 (365), 314
- Liebman, J. F. 107 (20), 110 (49), 111 (51), 113 (55, 56), 126–128
- Liebscher, D.-E. 268 (90), 307
- Liebscher, D.-H. 268 (90), 307
- Lieff, M. 300 (313), 313
- Lilley, D. M. 340 (183), 363
- Lilley, D. M. J. 341 (194), 363
- Lim, C. 320 (28), 321 (37–39), 322 (43, 44), 360
- Lim, W. A. 347 (229), 364
- Lima, C. D. 727 (23), 768
- Limbach, M. 452 (36), 507
- Lin, C.-C. 16 (63), 81 (228), 93, 98, 149 (46), 154, 422 (25), 435
- Lin, L. 272 (174), 309
- Lin, M.-C. 278 (209, 211, 212), 310
- Lin, N. 337 (169), 363
- Lin, P. 352 (299), 365
- Lin, T. 272 (176), 309
- Lin, W. 540 (114, 116), 566 (266), 587, 591
- Lin, W. W. 774 (23), 800
- Lin, W.-W. 566 (262), 591
- Lin, X. 301 (360), 314
- Lin, Y. L. 321 (39), 360
- Lin, Y.-M. 566 (262), 591
- Linares-Palomino, P. J. 440 (7), 506
- Lindahl, T. 353 (302), 365
- Lindqvist, O. 271 (165), 309
- Lindqvist, Y. 359 (355), 367
- Lindsay, D. M. 518 (36), 525 (41), 531 (89), 584–586
- Lindsay Smith, J. R. 200 (67), 216
- Lindsell, W. E. 58 (3, 4), 92, 512 (4), 513 (13), 583
- Lindsey, J. S. 201 (38, 39, 45, 46), 215, 216
- Linnanto, J. 357 (334), 366
- Linsk, J. 239 (73, 74), 240 (42, 75), 261
- Linstrom, P. J. 116 (3), 126
- Lion, C. 666 (114), 678
- Liotta, D. C. 667 (117–119), 678
- Liparini, A. 270 (152), 309
- Lipkowski, J. 25 (82), 94, 299 (307), 312
- Lippard, S. J. 322 (41), 360, 772 (7), 800
- Lipscomb, W. N. 53 (174), 96, 322 (49), 360



- Lipshutz, B. H. 142 (30), 154, 512 (2), 554 (193), 583, 589, 596 (20), 629, 779 (33), 801
- Little, B. F. 4 (37), 92
- Little, R. D. 253 (124), 263
- Liu, C. 282 (229), 310
- Liu, C.-Y. 533 (95), 534 (97), 586
- Liu, D.-K. 162 (60), 185
- Liu, G. 293 (285), 312, 384 (30), 402, 575 (298, 299), 592
- Liu, H. 163 (68, 69), 166 (77), 167 (82, 83, 85), 168 (73, 86), 169 (78–80, 87, 93–96), 170 (97, 98), 185, 186, 336 (160), 350 (262), 362, 365
- Liu, H.-C. 163 (70, 71), 168 (72, 74), 186
- Liu, H.-J. 572 (276), 591
- Liu, H.-W. 278 (209, 211, 212), 310
- Liu, J.-Y. 566 (262), 591
- Liu, L. 272 (169), 309, 391 (19), 402, 644 (33), 677
- Liu, Q. 159 (36), 185
- Liu, T.-J. 566 (262), 591
- Liu, W. 528 (87), 586
- Liu, X. 560 (233), 590
- Liu, X.-K. 463 (63), 508
- Liu, Y. 268 (72), 302 (337), 304 (331), 307, 313
- Liu, Z. 356 (326), 366
- Livshin, S. 642 (29), 677
- Llewellyn, C. A. 211 (109), 217
- Lloyd, C. 574 (294), 592
- Lloyd-Jones, G. C. 556 (206), 590
- Loader, C. 493 (107), 509
- Łobiński, R. 269 (151), 302 (341), 309, 313
- Lobitz, P. 247 (35, 103), 261, 262
- LoBrutto, R. 291 (280), 312
- Locos, O. B. 212 (113), 217
- Loeb, L. A. 332 (128), 351 (276, 277), 362, 365
- Loewe, R. S. 286 (244), 311
- Loh, T. 565 (256), 591
- Loh, T.-P. 782 (39), 801
- Lohrenz, J. C. W. 516 (32), 584
- London, R. E. 268 (25), 306
- Lone, S. 352 (293), 365
- Long, A. M. 352 (298), 365
- Lonnerdal, B. 268 (124), 308
- Looney, A. 73 (235), 98, 419 (6), 434
- Loos, D. 68 (218), 97
- Lopez-Avila, V. 302 (337), 304 (331), 313
- López, C. 271 (168), 309
- López, F. 457 (44, 45), 507, 563 (244), 564 (255), 591, 779 (32), 780 (38), 787 (41), 788 (48), 791 (62), 798 (63), 801, 802
- López-Mahía, P. 271 (164), 309
- Lopez, X. 322 (45), 360
- Lorimer, G. H. 357 (344, 345), 358 (352), 359 (339), 366, 367
- Loroño-González, D. 74 (124), 95, 150 (43), 154, 414 (45), 423 (17), 434, 435
- Lou, B.-S. 455 (43), 507
- Love, B. E. 290 (275), 312
- Love, C. 666 (116), 678
- Loveland, L. L. 349 (251), 364
- Lovell, T. 341 (202), 363
- Lovey, R. G. 574 (296), 592
- Lowe, E. D. 348 (239), 364
- Lowe, G. 348 (239), 364
- Lowe, R. 137 (10), 153, 720 (7), 768
- Lowther, W. T. 343 (209), 364
- Lu, B. Z. 395 (35), 402
- Lu, G. 277 (202), 310
- Lu, K.-J. 52 (173), 53 (174), 96
- Lu, T. 318 (21), 359
- Lu, W. Y. 169 (88–91), 186
- Lu, X. 162 (61), 167 (83, 84), 185, 186
- Lu, Z. 248 (96, 107, 113), 262, 567 (271), 591, 648 (51, 52), 677
- Lu, Z.-H. 583 (319), 593
- Lu, Z.-R. 32 (110), 94
- Lubbe, W. J. 325 (75), 361
- Lubell, W. D. 563 (246), 591
- Lubin, C. 495 (111), 509
- Lucast, L. 334 (140), 362
- Luchaco-Cullis, C. A. 791 (55), 802
- Lüdtke, D. S. 774 (25), 801
- Luftmann, H. 301 (359), 314
- Luh, T.-Y. 547 (152–154), 559 (230), 588, 590
- Lui, K. 246 (91), 262
- Lui, C. 659 (100), 678
- Lukaski, H. C. 268 (57), 307
- Lukyanets, E. A. 213 (120, 122), 217
- Lukzen, N. N. 331 (111), 361
- Luna, A. 125 (101), 129, 182 (138), 187
- Lund, H. 219 (5, 8, 9), 238 (6), 239 (78), 253 (122, 123), 256 (28), 259 (136, 137), 260, 261, 263
- Lund, T. 259 (136, 137), 263
- Lung, F.-D. 455 (43), 507
- Lunin, V. V. 327 (67), 360
- Luo, Q. 213 (118), 217
- Luo, X. 123 (90), 129
- Luszytki, J. 26 (91), 94, 183 (146), 187
- Lutter, R. 329 (94, 102), 361
- Lutz, H. 276 (195), 310
- Lutz, M. 36 (119), 95
- Luzikova, E. V. 553 (187), 589
- Lyalin, G. N. 198 (65), 216
- Lynch, J. 699 (31), 715
- Ma, S. 567 (271), 591, 648 (51, 52), 658 (94), 677, 678
- Maass, G. 318 (18), 355 (320), 359, 366
- Macaev, F. Z. 474 (47), 507
- Macciantelli, D. 259 (144), 263
- MacGregor, M. 413 (42), 435

- Mach, K. 86 (270), 87 (271), 88 (272), 89 (273–275), 99
- Mack, J. 193 (15, 18), 215
- Mackey, O. N. D. 428 (84), 436
- Macklin, T. K. 553 (184), 589
- MacMahon, T. J. 162 (57), 185
- Madabusi, L. V. 337 (169), 363
- Madigan, M. T. 193 (28), 214 (139), 215, 218
- Maeda, H. 559 (225), 590
- Maekawa, Y. 302 (326), 313
- Maercker, A. 654 (77, 78), 678
- Magerlein, B. J. 289 (268), 311
- Magi, E. 302 (332), 313
- Magiera, D. 583 (319), 593
- Magnuson, V. R. 83 (262), 98, 417 (4), 434
- Maguire, J. A. 51 (170–172), 52 (173), 53 (174), 96
- Maguire, M. E. 268 (51, 53), 307, 325 (3, 61, 64, 69, 74, 75), 326 (60), 327 (67, 72), 328 (1), 359–361
- Maguire, R. J. 302 (338), 313
- Mahiuddin, S. 322 (47), 360
- Mahmoud, J. S. 276 (197), 310
- Mahrwald, R. 180 (137), 187, 425 (69), 436
- Mahuteau-Betzer, F. 554 (191), 589, 626 (76), 630
- Maibaum, J. 370 (114), 509
- Maier, S. 487 (19), 506
- Mair, J. H. 539 (112), 587
- Mairanovskii, S. G. 219 (4), 260
- Maj-Zurawska, M. 287 (249), 311
- Maj-Żurawska, M. 275 (190), 310
- Maj-Żurawska, M. 287 (192), 310
- Makropoulos, N. 27 (99), 81 (261), 94, 98, 302 (302), 312, 409 (30), 410 (37), 435
- Maksimchuk, K. R. 352 (301), 365
- Maksimenka, R. 357 (337), 366
- Malakauskas, K. K. 268 (118), 308
- Malan, C. 534 (81), 558 (219), 586, 590, 767 (58), 769, 791 (50, 57), 802
- Malda, H. 791 (56), 802
- Malick, D. K. 384 (30), 402
- Maligres, P. 699 (31), 715
- Mallard, W. G. 116 (3), 126
- Mallory, J. 253 (124), 263
- Malmgren, S. M. 438 (1), 506
- Malon, A. 287 (192, 249), 310, 311
- Maloney, L. 340 (187), 363
- Malpass, D. B. 682 (15), 714
- Manabe, Y. 145 (38), 154
- Manas, M. 268 (48), 307
- Mandy, K. 538 (109), 587
- Manes, T. 345 (220), 364
- Mangeney, P. 574 (293), 592, 774 (12), 800
- Mann, B. E. 151 (49), 154
- Mann, C. K. 219 (1), 260
- Manning, G. S. 334 (137), 362
- Mano, M. 468 (80), 487 (72), 508
- Manojew, D. P. 246 (30), 261
- Mansoorabadi, S. O. 349 (252), 364
- Mantoura, R. F. C. 211 (109), 217
- Manyem, S. 779 (19), 800
- Manz, J. 357 (336), 366
- Mao, M. K. T. 443 (13), 506
- Mao, X. A. 329 (87), 361
- Maqanda, W. 213 (121), 217
- Marcaccio, M. 259 (144), 263
- Marcantoni, E. 566 (263), 591
- Marchese, G. 601 (40–42), 629
- Marchi-Delapierre, C. 260 (147), 263, 513 (15), 584
- Marciniak, B. 190 (2, 3), 214
- Marco, J. A. 391 (26), 402
- Marder, L. 295 (288), 312
- Maree, M. D. 213 (121), 217
- Marek, I. 41 (141), 69 (29), 92, 95, 110 (49), 127, 196 (4), 215, 297 (260), 311, 525 (69), 528 (83, 84), 534 (81), 560 (233), 563 (249), 566 (265), 585, 586, 590, 591, 633 (1), 642 (29), 643 (31), 676, 677, 738 (33), 739 (34), 748 (40), 767 (58), 768, 769
- Marier, J. R. 268 (122), 308
- Marina, M. L. 278 (208), 310
- Marini, E. 580 (313), 592
- Markarian, A. A. 330 (106, 107), 361
- Markell, M. S. 268 (19), 306
- Markham, G. D. 319 (25), 324 (35), 360
- Markies, P. R. 3 (15), 34 (106, 116), 35 (117, 118), 38 (83), 43 (146), 44 (142), 66 (213, 214, 216), 92, 94, 95, 97, 183 (140), 187, 318 (22), 359
- Markó, L. 653 (69–71), 677, 678
- Marks, V. 252 (116), 262
- Maroni-Barnaud, Y. 458 (50), 478 (97), 507, 508
- Maroni, P. 458 (50), 507
- Marquez, V. E. 335 (31), 360
- Marr, I. L. 302 (334), 313
- Marsais, F. 524 (60), 585, 689 (26, 27), 702 (40), 713 (24, 25), 714, 715
- Marsch, M. 59 (192), 62 (204), 97, 395 (34), 402, 516 (32), 584
- Marschner, C. 38 (130), 95, 305 (305), 312
- Marsden, C. J. 183 (150), 187
- Marsden, S. P. 722 (13), 768
- Marsh, T. 335 (150), 362
- Marshall, J. A. 645 (34), 677
- Marshall, E. L. 76 (242), 77 (250), 98, 424 (44), 435, 484 (99), 508
- Marshall, G. D. 280 (222), 310
- Marshall, J. A. 494 (110), 509
- Marshall, W. J. 53 (175), 96, 550 (174), 589
- Marsischky, G. T. 351 (282), 365
- Marsoner, H. J. 268 (34), 306
- Martel, A. 500 (118), 509
- Marti, T. M. 355 (317), 366

- Martick, M. 341 (196), 363  
 Martin, D. 565 (257), 591, 775 (31), 801  
 Martin, J. A. 595 (1), 628  
 Martin-Landa, I. 302 (334), 313  
 Martin, M. R. 727 (24), 768  
 Martin, R. 550 (170), 554 (188), 589, 596 (32), 616 (73), 629, 630  
 Martin, R. L. 369 (2), 384 (30), 401, 402  
 Martin, R. M. 538 (105), 587  
 Martin, S. F. 760 (46), 769  
 Martin, T. R. 40 (139), 95  
 Martina, V. 601 (40), 629  
 Martinek, R. G. 269 (149), 308  
 Martínez-Isla, A. 282 (232), 311  
 Martínez Vidal, J. L. 302 (335), 313  
 Martinho Simões, J. A. 111 (51), 127  
 Martinot, L. 246 (46, 59), 261  
 Marumo, S. 201 (74, 75), 216  
 Maruoka, K. 580 (312), 592  
 Maruyama, K. 194 (30), 201 (75, 76), 215, 216, 389 (3), 391 (10), 401  
 Maruyama, T. 285 (243), 311  
 Marvi, M. 512 (8), 583  
 Maryanoff, C. A. 667 (117–119), 678  
 Marzi, E. 702 (38), 715  
 Marzilli, T. A. 138 (20), 153  
 Masalov, N. 474 (47), 507  
 Mase, T. 524 (63), 531 (90), 585, 586, 699 (31), 702 (39), 715  
 Mash, E. A. 289 (264), 311  
 Mashima, H. 550 (169), 555 (200), 589  
 Mashima, K. 51 (167), 96, 121 (74), 123 (73), 128, 254 (126), 263, 540 (119), 587  
 Masironi, R. 268 (120), 308  
 Mason, R. 30 (105), 94  
 Mason, R. S. 302 (328), 313  
 Mason, S. A. 24 (80), 94  
 Massa, W. 62 (204), 97, 395 (34), 402  
 Massey, L. K. 268 (128), 308  
 Masson, E. 702 (38), 715  
 Mataga, N. 194 (30), 201 (74–76), 215, 216  
 Mateos, A. F. 482 (6), 506  
 Mathers, F. C. 246 (90), 262  
 Mathiasson, L. 304 (351), 313  
 Matile, P. 210 (101), 217  
 Matoba, T. 302 (333), 313  
 Matsubara, K. 90 (276), 99  
 Matsuda, K. 526 (70), 586, 746 (39), 769  
 Matsue, R. 767 (57), 769  
 Matsui, S. 485 (20), 506  
 Matsui, Y. 701 (36), 715  
 Matsukawa, S. 570 (280), 591  
 Matsumoto, K. 517 (34), 519 (54), 584, 585  
 Matsumoto, T. 475 (73), 508  
 Matsumoto, Y. 419 (51), 435, 686 (22), 714  
 Matsumura, T. 19 (45), 93, 570 (279), 591, 684 (19), 714  
 Matsuo, K. 259 (139–142), 263, 546 (142), 588, 616 (71), 622 (84), 630, 658 (93), 678  
 Matsuo, T. 212 (114), 217  
 Matsuo, Y. 123 (73), 128  
 Matsuumi, M. 558 (217), 590  
 Matsuura, K. 193 (23), 215  
 Matsuura, T. 208 (96), 217  
 Matsuyama, T. 259 (134), 263, 391 (11), 402  
 Mattalia, J.-M. 260 (147), 263, 513 (15), 584  
 Matte, A. 332 (125), 362  
 Matthews, B. W. 343 (209), 364  
 Mauduit, M. 565 (257), 591, 775 (31), 801  
 Mauser, H. 359 (351), 367  
 Mauskop, A. 268 (19), 306  
 Mauzerall, D. 193 (17), 206 (80), 208 (89, 93), 215, 217  
 Mauzerall, D. C. 198 (55), 216  
 Mayer, A. 246 (93, 94), 262  
 Mayer, P. 409 (30), 435  
 Mayer, V. A. 289 (271), 312  
 Mayerle, E. A. 240 (42), 261  
 Mayo, F. R. 595 (1), 628  
 Mayr, H. 557 (208), 590  
 Mazur, A. 288 (257, 258), 311  
 Mbofung, C. M. F. 283 (162), 309  
 McBee, E. T. 516 (29), 584  
 McCaffrey, J. G. 157 (19), 184  
 McCammon, J. A. 348 (244), 364  
 McCarthy, W. J. 323 (55), 360  
 McCarty, A. L. 201 (41, 42), 216  
 McCord, J. 268 (106), 308  
 McCormick, M. 667 (118), 678  
 McCoull, W. 575 (299), 592  
 McCullough, R. D. 286 (244), 311  
 McDermott, G. 324 (58), 356 (325, 331), 360, 366  
 McDonald, J. E. 51 (171, 172), 96  
 McDonald, J. H. 395 (4), 401  
 McFail-Isom, L. 335 (30), 360  
 McGarvey, G. J. 395 (38), 402  
 McGeary, C. A. 23 (77, 78), 94  
 McKay, D. B. 340 (181), 363  
 McKean, D. C. 391 (16), 402  
 McKinley, A. J. 159 (35), 185  
 McLaughlin, L. W. 337 (159), 362  
 McLeod, D. 472 (94), 508  
 McMahon, J. P. 575 (300), 592  
 McMahon, R. J. 106 (17), 126  
 McNamara, J. M. 648 (47), 677  
 McTyre, R. B. 268 (107), 308  
 Meetsma, A. 774 (13), 780 (38), 788 (48), 800, 801  
 Mehler, K. 45 (157), 71 (227), 96, 97, 123 (80, 86, 88), 128, 129, 143 (37), 151 (15), 152 (51), 153, 154  
 Mehrotra, R. 268 (44), 306  
 Meij, I. C. 268 (65, 66), 307  
 Meijer, E. W. 718 (2), 768

- Meiners, A. F. 516 (29), 584  
 Meinwald, J. 625 (92), 630  
 Mekelburger, H. B. 485 (4), 506  
 Meldal, M. 576 (303), 592  
 Melnik, M. 3 (26), 25 (25), 92  
 Memon, Z. S. 268 (19), 306  
 Menard, M. 500 (118), 509  
 Méndez, M. 554 (189), 559 (231), 589, 590, 614 (59), 626 (83), 629, 630  
 Mendler, B. 487 (23), 507  
 Menefee, A. L. 349 (252), 364  
 Ménez, A. 344 (215), 364  
 Mennucci, B. 384 (30), 402  
 Mentasti, E. 273 (182), 309  
 Menunier, L. 404 (3), 434  
 Mercero, J. M. 322 (45), 360  
 Mergelsberg, I. 574 (296), 592  
 Merkley, J. H. 664 (111–113), 678  
 Merlevede, W. 268 (37), 306  
 Mertinat-Perrier, O. 292 (281), 312  
 Mervaaala, E. 268 (21), 270 (155), 306, 309  
 Mesquita, R. B. R. 280 (225), 310  
 Metra, M. 268 (105), 308  
 Meulemans, T. M. 474 (47), 507  
 Meunier, P. 50 (98), 94, 123 (83), 129  
 Meuzelaar, G. J. 558 (218), 590, 791 (53), 802  
 Meuzelaar, J. 791 (53), 802  
 Meyer, D. 550 (172), 589  
 Meyer, F. J. 4 (31), 92, 686 (1), 714  
 Meyer, R. 458 (50), 507  
 Meyers, A. I. 566 (264), 591  
 Meyers, C. H. 289 (269), 312  
 Meyers, R. A. 280 (221), 310  
 Michael, J. P. 538 (109), 587  
 Michaelis, K. 537 (104), 586  
 Michrin, N. 211 (110), 217  
 Miginiac, P. 657 (89), 678  
 Mignani, G. 596 (23), 629  
 Mihalios, D. 519 (53), 585  
 Miki, H. 527 (73), 540 (122), 586, 587  
 Miki, K. 51 (167), 60 (194–196), 61 (197), 96, 97, 121 (74), 128, 254 (126), 263, 540 (119), 587  
 Milburn, R. K. 124 (94, 96), 125 (95), 129, 160 (54), 180 (46, 134, 135), 185, 187  
 Milburn, R. R. 553 (183), 589  
 Mildvan, A. S. 328 (88), 361  
 Miles, W. H. 395 (36), 402  
 Millam, J. M. 384 (30), 402  
 Millán, J. L. 345 (220), 364  
 Millart, H. 268 (33), 306  
 Miller, C. G. 325 (69), 361  
 Miller, J. 552 (175), 589  
 Miller, J. A. 433 (90), 436, 544 (132), 553 (181), 555 (205), 588–590  
 Miller, J. D. 545 (134), 588  
 Miller, M. A. 201 (38, 39), 215  
 Miller, M. J. 659 (96), 678  
 Miller, R. B. 257 (129), 263  
 Miller, R. E. 184 (160–162), 187  
 Miller, S. A. 25 (85), 94  
 Miller, T. A. 123 (84), 129  
 Milligan, W. O. 458 (49), 507  
 Mills, J. E. 667 (118), 678  
 Mimouni, F. 268 (133), 308  
 Min, D. B. 211 (111), 217  
 Minaard, A. J. 564 (255), 591  
 Minasov, G. 335 (145, 146), 362  
 Mineno, M. 555 (199), 589, 608 (56), 629  
 Mingardi, A. 564 (253), 591  
 Mingos, D. M. P. 633 (1), 676  
 Mingos, M. D. P. 58 (5), 92  
 Minnaard, A. J. 457 (44, 45), 507, 563 (244), 591, 774 (15, 21), 775 (29), 779 (32), 780 (37, 38), 786 (42), 787 (41, 45, 46), 788 (48), 791 (62), 798 (63), 800–802  
 Minofar, B. 322 (47), 360  
 Minor, W. 349 (258), 365  
 Mioskowski, C. 558 (218), 590  
 Misaizu, F. 163 (66, 67), 185  
 Mishima, M. 466 (70), 508  
 Misra, V. K. 334 (139), 336 (166), 362, 363  
 Mistry, J. 493 (106), 509  
 Mitchell, H. L. 259 (148), 263, 513 (14), 583  
 Miti, N. 343 (210), 364  
 Mitra, S. 353 (307), 366  
 Mitsudo, K. 664 (108), 678  
 Mitsuhashi, S. 475 (73), 508  
 Mittendorf, R. 268 (135), 308  
 Mityaev, V. I. 212 (117), 217  
 Mitzel, F. 196 (43), 216  
 Miura, M. 741 (36), 769  
 Miura, T. 475 (73), 508  
 Miwa, T. 274 (186, 187), 309, 310, 463 (63), 508  
 Miyake, Y. 558 (219), 590  
 Miyamoto, T. 569 (274), 591  
 Miyashita, K. 480 (18), 506, 761 (51), 769  
 Miyaura, N. 596 (22), 629, 774 (21), 780 (35), 800, 801  
 Mizu, Y. 766 (53), 769  
 Mizumoto, A. 212 (116), 217  
 Mizutani, H. 779 (33), 791 (55), 801, 802  
 Mizutani, K. 557 (216), 560 (236), 590  
 Mizuuchi, K. 355 (311), 366  
 Mo, X. 357 (333), 366  
 Mochida, K. 157 (21), 185  
 Mochizuki, H. 285 (243), 311  
 Mochizuki, S. 341 (199), 363  
 Modena, G. 500 (55), 507  
 Moeder, C. W. 293 (266), 311  
 Mogano, D. 538 (109), 587  
 Moir, J. H. 424 (65–67), 436, 473 (85, 87, 88), 508  
 Mojovic, L. 550 (173), 589

- Mokhallalati, M. K. 574 (292), 592, 674 (152), 153), 679
- Molander, G. A. 604 (46), 629
- Molina, A. 654 (72), 678, 699 (31), 715
- Molina, D. M. 325 (70), 361
- Moliner, V. 393 (25), 402
- Mollenhauer, D. 350 (269), 365
- Molnar, J. 183 (150), 187
- Monarca, S. 268 (130), 308
- Moncrieff, D. 57 (186), 96, 124 (91), 129
- Mongin, F. 44 (44), 93, 404 (2), 434, 524 (60), 537 (103), 550 (173), 553 (186), 585, 586, 589, 689 (26–28), 700 (33, 34), 713 (24, 25), 714, 715
- Monnens, L. A. H. 287 (248), 311
- Monnereau, C. 198 (66), 216
- Montaño, G. A. 356 (327), 366
- Montes de Lopez-Cepero, I. 457 (48), 507
- Montet, D. 301 (355), 314
- Montgomery, J. A. 384 (30), 402
- Montreux, A. 69 (223), 97
- Moody, C. J. 574 (294), 592
- Moody, D. B. 786 (42), 801
- Moore, A. L. 194 (35), 215
- Moore, D. T. 184 (161, 162), 187
- Moore, G. J. 516 (33), 584
- Moore, P. B. 334 (141), 335 (147, 148), 336 (161), 362
- Moore, R. D. 268 (24), 306
- Moore, T. A. 194 (35), 195 (16), 215
- Morabito, R. 302 (323), 313
- Morales-Morales, D. 71 (232), 98
- Morales Sánchez, M. C. 302 (335), 313
- Moreau, P. 516 (29), 584
- Moreda-Piñeiro, J. 271 (164), 309
- Moreno-Torres, R. 271 (168), 309
- Morgat, J. L. 235 (47, 48), 261
- Mori, S. 327 (78), 361, 791 (49), 801
- Morikawa, O. 453 (38, 39), 466 (71), 468 (80), 487 (72), 507, 508
- Morikawa, S. 767 (57), 769
- Morita, E. H. 341 (199), 363
- Morita, K. 214 (132), 218
- Morita, N. 701 (36), 715
- Moritani, T. 305 (362, 363), 314
- Morken, J. P. 557 (212), 590, 672 (138, 139), 673 (142–144), 679
- Morlender-Vais, N. 563 (249), 591
- Morley, C. P. 67 (93), 94, 428 (84), 436
- Mornet, R. 652 (55), 653 (56), 677
- Morokuma, K. 384 (30), 387 (33), 402, 419 (51), 435
- Morris, J. J. 424 (62), 435
- Morris, M. D. 219 (3, 5), 260
- Morris, M. E. 268 (71), 307
- Morris, M. L. 268 (112), 308
- Morrison, C. A. 76 (249), 98, 422 (20), 434
- Morrison, J. D. 486 (54), 507
- Morrison, R. T. 599 (5), 628
- Moryganov, A. P. 214 (138), 218
- Moser-Veillon, P. B. 268 (136), 308
- Mosher, H. S. 108 (39), 127
- Moshkovich, M. 247 (108), 248 (96, 107, 113), 251 (112), 258 (109, 110), 262
- Most, K. 74 (245), 98, 413 (43), 435
- Motellier, S. 275 (189), 310
- Mountokalakis, T. D. 268 (115), 308
- Moyano, N. 211 (103), 217
- Moyeux, A. 546 (143), 588, 618 (72), 630
- Mozzanti, G. 559 (228), 590
- Mukai, T. 327 (78), 361
- Mukaiyama, T. 484 (28), 507, 549 (162), 588, 772 (3), 800
- Mulholland, A. J. 333 (133), 362
- Müller, A. 59 (192), 97, 516 (32), 584
- Muller, B. H. 344 (215), 364
- Müller, G. 36 (119), 95
- Müller, I. 74 (245), 98, 413 (43), 435
- Müller, K. M. 337 (169), 363
- Muller, M. 135 (11), 153
- Müller, M. D. 302 (325), 313
- Mullica, D. F. 458 (49), 507
- Mullineaux, C. W. 191 (9), 215
- Mulvey, R. E. 9 (52), 13 (59), 15 (62), 17 (64–66), 18 (67), 19 (68, 69), 20 (70), 22 (71, 72, 74), 38 (126), 39 (39), 40 (40), 69 (222), 73 (73), 81 (224, 259), 83 (263), 93, 95, 97, 98, 149 (47), 150 (41), 154, 404 (1, 2), 413 (42), 414 (35, 46), 419 (50), 422 (41, 47), 429 (76), 430 (80), 431 (82), 434–436, 460 (56), 507, 682 (6), 713 (54), 714, 715
- Mulvihill, M. J. 659 (96), 678
- Mulzer, J. 538 (107), 587
- Mumford, F. E. 633 (4), 676
- Munch-Petersen, J. 398 (39), 402
- Mundy, B. P. 742 (14), 768
- Muniategui-Lorenzo, S. 271 (164), 309
- Munoz, R. 268 (81), 307
- Muntau, H. 269 (151), 309
- Muntean, F. 124 (97), 125 (105), 129, 161 (56), 185
- Münzel, E. 287 (253), 311
- Murafuji, T. 701 (36), 715
- Murai, T. 579 (311), 592
- Murakami, K. 568 (273), 591, 636 (22), 677
- Murakami, Y. 556 (207), 590
- Muralidharan, K. R. 574 (292), 592, 674 (153), 679
- Murata, K. 327 (78), 361
- Murayama, T. 475 (73), 508
- Murdoch, J. R. 579 (309), 592
- Murov, S. 206 (77), 217
- Murphy, E. 268 (32), 306
- Murphy, K. E. 791 (55), 802
- Murray, J. B. 340 (187), 363

- Murray, P. T. 268 (89), 307  
 Murray, R. K. 765 (48), 769  
 Murrell, J. N. 175 (122), 187, 318 (23), 359  
 Murso, A. 520 (56), 585, 682 (9), 714  
 Murthy, K. V. S. 272 (173), 309  
 Muruges, M. G. 558 (217), 590  
 Musashi, J. 527 (74), 586, 727 (18), 730 (27), 768  
 Musgrave, W. K. R. 516 (30), 517 (34), 584  
 Muslukhov, R. R. 123 (87), 129  
 Myers, A. G. 559 (229), 590  
 Mynott, R. 33 (114, 115), 44 (153), 45 (156), 94–96  
 Naasz, R. 774 (15, 16), 800  
 Nabeshima, Y. 285 (243), 311  
 Nackashi, J. 103 (4), 126, 146 (40), 154, 428 (83), 436  
 Naef, R. 772 (5), 800  
 Nagana Gowda, G. A. 286 (247), 311  
 Nagano, T. 546 (143), 547 (146), 554 (191), 588, 589, 615 (67), 619 (77), 630  
 Nagao, Y. 463 (63), 508  
 Nagaoka, Y. 774 (2), 800  
 Nagase, H. 517 (34), 519 (54), 584, 585  
 Nagase, S. 391 (23), 402  
 Nagashima, H. 675 (157), 679  
 Nagashima, K. V. P. 193 (23), 215  
 Nagashima, U. 107 (22), 127  
 Nagel, U. 39 (131), 95  
 Nair, S. K. 547 (157), 588  
 Naitoh, Y. 544 (127), 588  
 Nakagawa, J. 285 (237), 311  
 Nakagawa, Y. 774 (25), 801  
 Nakahashi, R. 453 (39), 507  
 Nakajama, N. 571 (284), 592  
 Nakajima, H. 675 (158), 679  
 Nakajima, K. 675 (157), 679  
 Nakajima, S. 194 (30), 215  
 Nakamura, A. 51 (167), 96, 121 (74), 123 (73), 128, 254 (126), 263, 540 (119), 560 (235), 587, 590  
 Nakamura, E. 387 (33), 402, 546 (142), 550 (169), 555 (200), 566 (265), 588, 589, 591, 616 (71), 622 (84, 86), 630, 658 (92, 93), 678, 791 (49, 51), 801, 802  
 Nakamura, M. 302 (326), 313, 387 (33), 402, 526 (71), 546 (142), 586, 588, 616 (71), 622 (84, 86), 630, 658 (92, 93), 678, 749 (42), 758 (44), 769  
 Nakamura, T. 707 (45), 715  
 Nakanishi, S. 767 (56), 769  
 Nakashima, T. 329 (99), 361, 487 (72), 508  
 Nakata, K. 558 (217), 590  
 Nakata, M. 555 (202), 590, 686 (22), 688 (23), 714  
 Namkoong, E.-Y. 557 (215), 590  
 Nanayakkara, A. 384 (30), 402  
 Napieraj, A. 547 (147), 588  
 Narasaka, K. 579 (309), 592  
 Narayana, M. 735 (31), 768  
 Narula, A. K. 428 (85), 436  
 Nasielski, J. 550 (167), 589  
 Naso, F. 583 (317, 318), 593  
 Nassar, R. 424 (62), 435  
 Nasser, D. 282 (233), 311  
 Näther, C. 62 (203), 97  
 Naumov, V. A. 183 (154), 187  
 Navarro, M. 271 (168), 309  
 Naylor, R. D. 116 (1), 126  
 Ndjouenkeu, R. 283 (162), 309  
 Neber, G. 578 (307), 592  
 Nedden, G. 39 (131), 95  
 Negishi, E. 671 (134), 679, 787 (44), 801  
 Négrel, J.-C. 391 (20), 402  
 Negrel, J.-C. 157 (15), 184  
 Nell, P. G. 527 (76), 586, 720 (5), 721 (12), 768  
 Nelson, B. 325 (63), 360  
 Nelson, J. M. 220 (12), 260  
 Nelson, S. G. 504 (90), 508, 539 (112), 547 (150), 587, 588  
 Nemanick, E. J. 259 (143), 263  
 Nemoto, T. 699 (31), 715  
 Nemukhin, A. V. 121 (72), 128, 158 (27), 160 (32), 185, 268 (147), 308, 331 (117, 118), 362  
 Nemutlu, E. 274 (188), 310  
 Nenajdenko, V. G. 547 (148), 588  
 Nerín, C. 303 (348), 313  
 Nesterova, T. N. 122 (82), 128  
 Netherton, N. R. 618 (66), 630  
 Netzel, T. L. 198 (57), 216  
 Neumann, B. 68 (221), 97  
 Neumann, H. M. 108 (32), 127, 391 (8), 401, 411 (40), 435  
 Neumann, S. M. 596 (11), 604 (13), 628, 629  
 Neves, A. 343 (210), 364  
 Neville, M. E. 347 (236), 364  
 Newman, J. 357 (346), 366  
 Newman, K. 302 (328), 313  
 Newmann, H. M. 389 (3), 401  
 Nguyen, B. T. 512 (9), 583  
 Nguyen, N. 647 (41), 677  
 Ni, H.-R. 119 (63), 128  
 Ni Mhuircheartaigh, E. M. 212 (113), 217  
 Nicaise, O. J.-C. 571 (284, 286), 592  
 Nichols, G. 121 (70), 128  
 Nicholson, J. 304 (354), 314  
 Nicholson, J. K. 286 (246), 311  
 Nicoloff, N. 503 (53), 507  
 Nie, L.-H. 273 (183), 309  
 Niegowski, D. 325 (70), 361  
 Nielsen, F. H. 268 (57), 307  
 Nielsen, M. F. 253 (123), 263  
 Niemczyk, M. P. 194 (31), 215  
 Niemeyer, M. 540 (117), 587

- Nightingale, D. 235 (49), 261  
 Nii, S. 560 (235), 561 (241), 590, 591  
 Niikura, S. 563 (248), 591  
 Nikiforov, G. A. 330 (108), 361  
 Nikolaev, E. N. 171 (5), 184  
 Nikolaev, S. A. 175 (101), 186  
 Nilsson, P. 513 (18), 584  
 Nilsson, R. 285 (240), 311  
 Ninomiya, Y. 452 (35), 507  
 Nishi, S. 502 (119), 509  
 Nishide, K. 487 (104), 509  
 Nishii, Y. 622 (85), 630  
 Nishikawa, T. 636 (20, 21), 677  
 Nishimae, S. 567 (270), 591, 636 (18), 676  
 Nishimura, Y. 194 (30), 201 (75, 76), 215, 216  
 Nishiyama, H. 517 (34), 519 (54), 584, 585  
 Nissen, P. 336 (161), 362  
 Niwaki, K. 259 (140), 263  
 Nizovtsev, A. V. 528 (82), 586  
 Njock, M. G. K. 357 (335), 366  
 Nobbs, T. J. 355 (311), 366  
 Noble, M. E. M. 348 (239), 364  
 Nobuto, D. 419 (51), 435  
 Nocera, D. G. 201 (73), 216  
 Noe, M. C. 582 (316), 593  
 Nogueira, J. M. F. 302 (322), 313  
 Nogueras, M. 440 (7), 506  
 Noji, H. 329 (96, 98, 99, 100), 361  
 Nolan, S. P. 550 (166), 588  
 Noll, B. C. 469 (78, 79), 508  
 Nolph, K. D. 268 (44), 306  
 Noltemeyer, M. 74 (248), 98, 424 (16), 434  
 Noltes, J. G. 30 (105), 94  
 Nomoto, T. 35 (117, 118), 43 (146), 95  
 Nomura, N. 557 (211), 590, 621 (81, 82), 630  
 Nonoyama, N. 531 (90), 586  
 Noodleman, L. 341 (202), 363  
 Nordahl Larsen, A. L. 370 (113), 509  
 Nordlander, J. E. 141 (34), 142 (35), 154, 654 (74), 678  
 Nordlund, P. 325 (70), 361  
 Norinder, J. 791 (53), 802  
 Normant, J. 633 (1), 676  
 Normant, J. F. 517 (34), 584, 633 (1), 635 (16), 676, 765 (48), 769  
 Normant, J.-F. 566 (265), 591  
 Noske, H. J. 301 (357), 314  
 Notaras, E. G. A. 212 (113), 217  
 Nöth, H. 27 (99), 94, 409 (30), 427 (72), 435, 436  
 Noubi, L. 283 (162), 309  
 Novak, D. P. 26 (91), 94, 183 (146), 187  
 Novák, P. 246 (95), 262  
 Novak, T. 293 (267), 311, 787 (44), 801  
 Novoderezhkin, V. I. 194 (34), 215  
 Nowak, A. 268 (110), 308  
 Nowak, T. 350 (260), 365  
 Nowotny, M. 355 (312), 366  
 Noyori, R. 775 (26), 801  
 Nozaki, H. 484 (69), 508, 661 (103), 678, 765 (48), 769  
 Nozaki, K. 194 (30), 215  
 Nsango, M. 357 (335), 366  
 Nudelman, N. S. 260 (147), 263  
 Nudenberg, W. 595 (8), 628  
 Nugent, W. A. 258 (133), 263, 615 (16), 629  
 NuLi, Y. 253 (120), 262  
 Nummy, L. 517 (37), 584  
 Nummy, L. J. 103 (9), 126  
 Nunzi, A. 328 (83), 361  
 Nuske, H. 531 (93), 586  
 Nuttall, R. L. 113 (2), 126  
 Nuzzo, R. G. 172 (109), 186  
 Nyman, E. S. 214 (112), 217  
 Nyokong, T. 192 (12), 213 (121), 215, 217  
 Oae, S. 720 (8), 768  
 Oberhuber, C. N. 791 (59), 802  
 O'Brian, P. J. 354 (285), 365  
 O'Brien, C. 550 (167), 589  
 O'Hair, R. A. J. 156 (2), 180 (136), 181 (131, 132), 182 (133), 184, 187  
 O'Hara, C. T. 9 (52), 13 (59), 17 (66), 19 (69), 20 (70), 22 (71, 72), 93  
 O'Hare, P. A. G. 107 (20), 126  
 Occhialini, D. 259 (136), 263  
 Ochterski, J. 384 (30), 402  
 Oda, R. 767 (54), 769  
 Ödman, F. 304 (351), 313  
 Odobel, F. 198 (66), 216  
 O'Donnel, M. 353 (272), 365  
 Oei, T. O. 268 (79), 307  
 Oesch, U. 276 (14), 306  
 Oesterlund, K. 564 (252), 591  
 Ogasawara, M. 774 (21, 24), 800  
 Ogata, M. 214 (132), 218  
 Ogata, S. 734 (29), 768  
 Ogino, Y. 749 (42), 756 (43), 769  
 Ogura, F. 290 (274), 312  
 Ogura, K. 767 (55), 769  
 Ohashi, M. 90 (276), 99  
 Ohbayashi, T. 728 (25), 768  
 Ohkohchi, M. 201 (75), 216  
 Ohkubo, K. 201 (40), 216  
 Ohmiya, H. 545 (139, 140), 546 (141), 560 (237, 238), 568 (273), 588, 591, 636 (22), 677  
 Ohmori, H. 559 (225), 590  
 Ohmori, K. 707 (46), 715  
 Ohno, K. 163 (66, 67), 185, 517 (34), 519 (54), 584, 585  
 Ohno, M. 303 (349), 313  
 Ohno, T. 194 (30), 215  
 Ohta, A. 701 (36), 715  
 Ohtani, H. 198 (64), 216  
 Ohtsuka, E. 339 (185), 363  
 Oi, Y. 791 (60), 802

- Oikonomakos, N. G. 348 (239), 364  
 Ok, E. 278 (215), 310  
 Oka, K. 285 (237), 311  
 Okada, K. 567 (269), 591, 636 (17, 19), 676  
 Okada, S. 699 (31), 715  
 Okada, T. 201 (70, 74–76), 216, 284 (178), 309  
 Okamoto, K. 125 (100), 129  
 Okamoto, S. 791 (60), 802  
 Okamoto, Y. 60 (194–196), 61 (197), 97, 303 (349), 304 (353), 313, 314  
 Oku, A. 718 (2), 768  
 Okubo, M. 259 (138–142), 263, 391 (10), 401  
 Okunchikov, V. V. 213 (122), 217  
 Okuno, H. 556 (207), 590  
 Okura, I. 214 (137), 218  
 Olbrysch, O. 653 (66), 677  
 Olcucu, A. 278 (214), 310  
 Olerich, M. A. 276 (17), 306  
 Oliva, M. 357 (347), 359 (356, 357), 366, 367, 393 (25), 402  
 Oliveira, C. C. 280 (224), 310  
 Ollis, D. L. 351 (286), 365  
 Olmstead, M. M. 82 (162), 96, 417 (13), 434  
 Olsson, R. 611 (64), 630  
 Olszewski, T. K. 491 (105), 509  
 Omote, H. 329 (97), 361  
 Onan, K. D. 485 (21), 506  
 Onda, K.-I. 479 (14, 16), 485 (15, 17), 506  
 O'Neil, B. T. 499 (115), 509  
 O'Neil, P. 83 (263), 98  
 O'Neil, P. A. 38 (126), 95, 149 (47), 154, 413 (42), 422 (41), 435  
 Ong, C. M. 419 (26), 435  
 Onishi, S. 268 (139), 308  
 Ono, A. 576 (302), 592  
 Ono, N. 531 (91), 586  
 Ono, T. 198 (64), 216  
 Onsager, L. 384 (29), 402  
 Oohara, T. 721 (11), 768  
 Operti, L. 162 (44, 57), 185  
 Oppolzer, W. 656 (82, 84–86), 678  
 Orchard, A. F. 124 (93), 129  
 Ordóñez, L. A. 268 (119), 308  
 Orf, J. 121 (70), 128  
 Organ, M. G. 550 (167), 589  
 Orhanović, S. 344 (219), 364  
 Orita, M. 341 (189), 363  
 Orlov, M. A. 330 (107), 361  
 Orlova, M. A. 330 (106), 361  
 Orr, M. 214 (136), 218  
 Ortega-Blake, I. 323 (55, 56), 360  
 Örtendahl, M. 38 (129), 95  
 Orth, P. 356 (324), 366  
 Ortiz, J. 201 (40), 216  
 Ortiz, J. V. 384 (30), 402  
 Os, C. W. v. 287 (248), 311  
 Osada, Y. 212 (116), 217  
 Osawa, A. 728 (25), 768  
 Osawa, E. 675 (158), 679  
 Osborn, H. M. I. 547 (147), 588  
 Osborne, C. G. 268 (107), 308  
 Oscarson, J. L. 328 (85, 86), 361  
 O'Shea, P. D. 5 (43), 93, 703 (41), 715  
 Oshima, K. 5 (42), 41 (41), 93, 276 (9), 306, 523 (59), 527 (73), 528 (77, 83), 540 (122), 545 (139, 140), 546 (141), 557 (216), 560 (236–238), 561 (243), 567 (269, 270), 568 (273), 585–588, 590, 591, 596 (31), 623 (90), 629, 630, 633 (1), 636 (17–22), 643 (30), 676, 677, 690 (29), 699 (11), 703 (43), 706 (42, 44), 707 (45), 714, 715, 791 (50), 801  
 Oshima, Koichiro 675 (158), 714  
 Oshiyama, A. 341 (204), 363  
 Osman, A. 224 (29), 260  
 Osowska-Pacewicka, K. 547 (147), 588  
 Ossola, F. 64 (210), 97, 268 (148), 308  
 Oster, G. 327 (81), 329 (90), 361  
 Osuka, A. 194 (30), 201 (74–76), 215, 216  
 Oswald, J. 513 (14), 584  
 Ota, H. 526 (70), 586, 746 (39), 769  
 Otsubo, T. 290 (274), 312  
 Otsuka, S. 657 (88), 678  
 Ottesen, L. K. 611 (64), 630  
 Ottow, E. 538 (107), 587  
 Ou, X. 272 (176), 309  
 Ough, E. 196 (52), 216  
 Ouyang, J. M. 277 (205), 310  
 Overcash, D. M. 246 (90), 262  
 Overman, L. E. 563 (247), 591, 798 (66, 67), 802  
 Owen, D. J. 348 (239), 364  
 Owens, J. M. 259 (146), 263  
 Owens, T. D. 575 (298), 592  
 Özaltın, N. 274 (188), 310  
 Ozanam, F. 241 (79, 80), 243 (81–83, 85), 262  
 Ozenne, C. 301 (355), 314  
 Ozin, G. A. 157 (19), 184  
 Paap, J. 48 (163), 96, 122 (81), 128  
 Pace, N. 335 (150), 362  
 Pace, N. R. 336 (157), 362  
 Pack, G. R. 320 (32), 323 (51, 52), 360  
 Pacold, M. 73 (240), 98, 418 (11), 434  
 Padwa, A. 718 (2), 768  
 Pages, N. 267 (1), 268 (50, 54), 306, 307  
 Pahlira, J. J. 268 (113), 308  
 Pai, E. F. 327 (71), 361  
 Pai Fondecarr, K. 424 (66), 436  
 Pajerski, A. D. 39 (134), 44 (147), 56 (57), 69 (183), 93, 95, 96, 410 (38), 429 (78), 435, 436, 682 (5, 14), 713 (53), 714, 715  
 Pallaud, R. 235 (47, 48), 261  
 Pan, J. 337 (172), 363  
 Pan, T. 336 (167), 363  
 Panasenکو, A. A. 123 (87), 129



- Pande, N. 337 (169), 363  
 Panov, D. 512 (8, 9), 583  
 Paolucci, F. 259 (144), 263  
 Papageorgiou, T. 278 (207), 310  
 Papasergio, R. I. 31 (109), 94  
 Papazachariou, I. M. 282 (232), 311  
 Pape, A. 36 (119), 95  
 Papillon, J. P. N. 707 (47), 715  
 Papiz, M. Z. 324 (58), 356 (325, 331), 360, 366  
 Paquette, L. A. 50 (98), 94, 123 (83), 129  
 Paradies, H. H. 517 (34), 584  
 Paris, G. 134 (18), 153  
 Paris, G. E. 140 (5), 153, 428 (83), 436  
 Park, C.-H. 557 (215), 590  
 Park, E. J. 285 (156), 309  
 Park, K. 553 (178), 589  
 Parker, R. D. 289 (272), 292 (284), 312  
 Parker, V. B. 113 (2), 126  
 Parkin, A. 74 (124), 95, 150 (43), 154, 423 (17), 434  
 Parkin, G. 73 (235–239), 98, 148 (17), 153, 344 (213), 364, 418 (7), 419 (6, 52), 422 (60), 423 (8, 9), 424 (10), 434, 435  
 Parkinson, J. A. 20 (70), 69 (222), 93, 97, 150 (41), 154, 429 (76), 436  
 Parnis, J. M. 157 (19), 184  
 Parr, R. G. 384 (28), 402  
 Parris, G. E. 108 (40), 127, 146 (40), 154  
 Parrish, J. D. 253 (124), 263  
 Parsons, S. 74 (124, 243, 244), 76 (249), 81 (255, 256), 95, 98, 150 (43), 154, 406 (19), 407 (21, 22), 414 (45), 422 (15, 20), 423 (17), 434, 435  
 Partridge, J. C. 191 (9), 215  
 Parts, E. O. 116 (57), 128  
 Parves, M. 44 (147), 95  
 Parvez, M. 39 (134), 56 (57, 184), 69 (183), 78 (253), 93, 95, 96, 98, 421 (34), 429 (78), 435, 436, 682 (5, 14), 714  
 Pasquinet, E. 711 (50), 715  
 Pasternak, K. 268 (109), 308  
 Pasto, D. J. 621 (80), 630  
 Patai, S. 113 (55), 127, 451 (29), 507, 528 (86), 586  
 Patel, D. J. 119 (62), 128, 654 (76), 678  
 Patel, P. H. 332 (128), 362  
 Patel, S. S. 352 (289, 292, 296), 365  
 Patil, S. 538 (109), 587  
 Patricia, J. J. 527 (28), 584  
 Patrick, B. O. 74 (246), 98  
 Patterson, D. B. 19 (46), 93  
 Patterson, E. V. 106 (17), 126  
 Paul, A. 196 (54), 216  
 Paul, A. G. 478 (65), 508  
 Paunier, L. 268 (42), 306  
 Pauson, P. L. 25 (84), 94  
 Pavela-Vrancić, M. 345 (218), 364  
 Pavela-Vrani, M. 344 (219), 364  
 Paver, M. A. 57 (186), 96, 124 (91), 129  
 Pavlenko, S. A. 333 (132), 362  
 Payandeh, J. 327 (71), 361  
 Pearce, F. G. 357 (340), 358 (349, 350), 366, 367  
 Pearce, R. 30 (104), 94  
 Pearson, R. 234 (23), 258 (15), 260  
 Pearson, T. H. 228 (43), 261  
 Pearson, W. H. 729 (26), 768  
 Pedersen, E. B. 701 (37), 715  
 Pedersen, J. B. 331 (111), 361  
 Pedersen, L. C. 352 (299), 365  
 Pedersen, L. G. 352 (299), 365  
 Pedersen, P. L. 329 (93), 330 (103), 361  
 Pedersen, S. U. 256 (28), 259 (136, 137), 260, 263  
 Pedley, J. B. 109 (47), 116 (1), 126, 127  
 Pedrares, A. S. 324 (59), 360  
 Pei, W. 619 (78), 630  
 Peled, A. 211 (110), 217  
 Pelissier, H. 540 (115), 587  
 Pellicena, P. 347 (227), 364  
 Peña, D. 775 (29), 788 (48), 801  
 Pendergrass, E. 289 (265), 311  
 Penedo, J. C. 341 (194), 363  
 Peng, C. Y. 384 (30), 402  
 Pennella, D. R. 648 (46), 677  
 Pentikäinen, U. 333 (133), 362  
 Penwell, A. J. 567 (268), 591, 648 (48), 677  
 Peracchi, A. 341 (188), 363  
 Pérez, E. 157 (15), 184, 391 (20), 402  
 Percival, W. C. 599 (36), 629  
 Pereira-Filho, E. R. 271 (167), 309  
 Périchon, J. 236 (60), 258 (38, 130), 261, 263, 291 (279), 312  
 Perlmutter, P. 774 (1), 800  
 Perpall, H. J. 293 (266), 311  
 Perrier, O. 290 (273), 312  
 Perriot, P. 765 (48), 769  
 Pershin, A. P. 330 (108), 361  
 Persson, E. 558 (218), 590  
 Persson, E. S. M. 557 (210), 590, 791 (53), 802  
 Perutz, R. N. 200 (67), 216  
 Peschek, G. A. 193 (24), 215  
 Peschke, M. 175 (123), 187  
 Petek, S. 489 (8, 9), 506  
 Peter, K. 285 (240), 311  
 Peters, E.-M. 573 (290), 592  
 Peters, K. 573 (290), 592  
 Petersen, H. 525 (64), 585  
 Peterson, J. M. 653 (8), 676  
 Peterson, T. H. 91 (277), 99  
 Petersson, G. A. 384 (30), 402  
 Petit, S. 275 (189), 310  
 Petrella, A. 212 (115), 217

- Petrie, S. 125 (106, 107), 129, 156 (9–14), 160 (52), 162 (53), 184, 185
- Petrov, A. S. 320 (32), 323 (51, 52), 360
- Petrova, N. V. 110 (48), 127
- Petrusová, L. 88 (272), 89 (273), 99
- Peyrat, J. F. 607 (48), 608 (51), 629
- Peyrat, J.-F. 555 (197, 198), 589
- Pfaltz, A. 774 (2, 8), 779 (22), 800
- Pfitzer, A. 409 (30), 427 (72, 75), 435, 436
- Phansavath, P. 559 (224), 590
- Philbert, M. A. 285 (156), 309
- Phillips, N. H. 527 (28), 584
- Phomphrai, K. 73 (240), 98, 418 (11), 434
- Piarulli, U. 625 (93), 630
- Piccaluga, G. 318 (17), 359
- Piccirilli, J. A. 338 (176), 363
- Pichota, A. 774 (8), 800
- Pierce, J. 357 (338, 345), 366
- Pierce, O. R. 516 (29), 584
- Pietsch, E. C. 648 (46), 677
- Pietzsch, C. 30 (108), 94, 243 (86), 262
- Pilard, J.-F. 253 (122), 263
- Pilcher, G. 110 (50), 127
- Pileni, M. P. 198 (60), 216
- Pillai, C. K. S. 323 (53), 360
- Pimerzin, A. A. 122 (82), 128
- Pina, M. 301 (355, 358, 361), 314
- Pineschi, M. 774 (14), 800
- Pingoud, A. 355 (318–320), 366
- Pinho, P. 519 (53), 585
- Pinkerton, R. C. 222 (26), 228 (43), 260, 261
- Pinkus, A. G. 458 (32, 49), 507
- Pinna, G. 318 (17), 359
- Piotroski, H. 81 (261), 98
- Piotrowski, H. 302 (302), 312, 409 (30), 410 (37), 435
- Pipik, B. 648 (47), 677
- Piskorz, P. 384 (30), 402
- Pistón, M. 278 (213), 310
- Pitteloud, R. 656 (85, 86), 678
- Pizziconi, V. B. 356 (327), 366
- Platz, H. 537 (104), 586
- Plé, N. 518 (43), 585, 702 (40), 715
- Pletcher, D. 241 (37), 246 (98), 261, 262
- Pley, H. W. 340 (181), 363
- Plieninger, H. 517 (39), 585
- Ploch, D. 301 (361), 314
- Ploom, L. R. 116 (57), 128
- Po, P. L. 159 (37), 185
- Podall, H. E. 653 (57), 677
- Podell, E. 320 (29), 360
- Podkovyrov, A. I. 122 (77), 128
- Poerwono, H. 547 (159), 588
- Poh, J. 357 (333), 366
- Pohl, R. 611 (63), 630
- Pohmakotr, M. 725 (19), 768
- Polášek, M. 87 (271), 99
- Polborn, K. 409 (30), 435, 528 (84), 586, 738 (33), 739 (34), 768
- Polet, D. 558 (220), 590, 791 (50, 57), 802
- Poli, G. 484 (101), 509
- Polidori, G. P. 328 (83), 361
- Polikarpov, E. V. 121 (72), 128, 160 (32), 185
- Polyakova, E. V. 279 (219), 310
- Pomelli, C. 384 (30), 402
- Poncini, L. 537 (104), 587
- Pons, B. 303 (348), 313
- Pont, F. 288 (254, 255), 311
- Poonia, N. S. 3 (24), 92
- Pople, J. A. 369 (1, 2), 384 (30), 401, 402
- Popp, J. 357 (337), 366
- Porat, A. 211 (110), 217
- Porcheddu, A. 559 (226), 590
- Poretz, R. D. 214 (131), 218
- Porra, R. J. 191 (8), 215
- Pörschke, K.-R. 86 (266), 99
- Porsev, V. V. 158 (30), 171 (104), 185, 186
- Porter, H. D. 633 (2), 676
- Porter, R. F. 159 (37, 38), 185
- Posner, G. H. 596 (18, 19), 629, 633 (9), 676
- Potapov, D. A. 171 (102), 175 (101), 186
- Poter, G. 198 (63), 216
- Powell, L. A. 272 (175), 309
- Power, P. P. 58 (58), 59 (191), 62 (202), 79 (79), 82 (162), 93, 94, 96, 97, 417 (13), 434, 682 (4), 714
- Poyner, R. R. 349 (250, 253, 259), 364, 365
- Pozet, N. 268 (114), 308
- Pozniak, B. P. 160 (48), 185
- Prabpai, S. 725 (19), 768
- Prada-Rodríguez, D. 271 (164), 309
- Prathapan, S. 201 (38, 39), 215
- Prebil, S. 125 (104), 129
- Preis, C. 411 (24), 434
- Premo, J. G. 240 (71), 261
- Preuss, H. 79 (258), 98
- Prévost, C. 515 (27), 584
- Price, S. M. 356 (325), 366
- Pridgen, L. N. 574 (292), 592, 674 (152, 153), 679
- Prince, S. M. 324 (58), 356 (331), 360, 366
- Procter, G. 503 (122), 509
- Prody, G. A. 339 (178), 363
- Prokhorenko, V. I. 356 (330), 366
- Prosenc, M.-H. 49 (165), 96
- Proulx, J. 268 (85), 307
- Prout, F. S. 398 (39), 402
- Provot, O. 555 (197, 198), 589, 607 (48), 608 (51), 629
- Prust, J. 74 (245), 98, 413 (43), 435
- Pryde, P. G. 268 (135), 308
- Przybilski, R. 341 (190), 363
- Psarras, T. 244 (89), 258 (36), 261, 262
- Puar, M. S. 574 (296), 592
- Puchta, G. T. 519 (53), 585

- Puga, Y. M. 103 (10), 126  
 Pullez, M. 457 (45), 507, 787 (41), 801  
 Pullins, S. H. 168 (75), 186  
 Pupowicz, D. 517 (34), 584, 722 (15), 768  
 Pygall, C. F. 124 (93), 129  
 Pyle, A. M. 334 (136), 337 (12), 359, 362  
 Qi, D. 302 (327), 313  
 Qi, M. 729 (26), 768  
 Qin, J. 349 (251), 355 (311), 364, 366  
 Qiu, G. 547 (157), 588  
 Quamme, G. A. 268 (31, 74, 75), 288 (252), 306, 307, 311  
 Quéguiner, G. 518 (43), 524 (60), 525 (41), 534 (81), 537 (103), 586, 550 (173), 553 (186), 585, 586, 589, 689 (26, 27), 700 (33, 34), 713 (24, 25), 714, 715  
 Quevauviller, P. 302 (323), 313  
 Quintin, J. 554 (190), 589, 614 (65), 630  
 Rabezzana, R. 162 (44), 185  
 Rabinowitch, E. 207 (83, 84), 217  
 Rabuck, A. D. 384 (30), 402  
 Rachamim, M. 206 (78), 217  
 Rachtan, M. 299 (311), 312  
 Radojević, M. 303 (345), 313  
 Radzio-Andezelm, E. 347 (225), 364  
 Rafailovich, M. 305 (362), 314  
 Raghavachari, K. 369 (2), 384 (30), 401, 402  
 Raghavendra, A. S. 194 (33), 215  
 Ragsdale, S. W. 342 (208), 363  
 Rague, B. 484 (100), 508  
 Rahman, A. U. 540 (115), 587  
 Rahn, B. J. 604 (46), 629  
 Rakita, P. E. 3 (18, 27), 55 (178), 58 (13), 92, 96, 225 (40), 258 (131, 132), 259 (145), 261, 263, 389 (3), 401, 512 (3, 5–7), 583  
 Ralph, W. C. 239 (74), 261  
 Rambaud, M. 288 (262), 311, 516 (31), 584  
 Rambidi, N. G. 183 (153), 184 (155), 187  
 Rambo, R. P. 334 (140), 362  
 Ramesh, V. 286 (247), 311  
 Ramiandrasoa, P. 552 (176), 555 (195, 196), 589  
 Ramírez-Solís, A. 323 (56), 360  
 Ramirez, U. D. 318 (21), 359  
 Ramsay, L. E. 268 (142), 308  
 Ramsden, H. E. 44 (148), 95  
 Ranade, C. R. 208 (96), 217  
 Rangel, A. O. S. S. 280 (225), 310  
 Rankin, D. W. H. 183 (141), 187  
 Rao, C. P. 772 (7), 800  
 Rao, J. K. 272 (172), 309  
 Rao, S. A. 582 (316), 593  
 Rapoport, H. 451 (34), 507  
 Rapoport, Z. 41 (141), 69 (29), 92, 95, 110 (49), 113 (55), 118 (60), 127, 128, 156 (1), 184, 196 (4), 215, 297 (260), 311, 471 (93), 508, 528 (86), 586  
 Rapsomanikis, S. 303 (345), 313  
 Rardin, R. L. 322 (41), 360  
 Rasmussen, H. S. 268 (104), 308  
 Raston, C. L. 19 (68), 26 (92), 31 (109), 40 (139), 44 (151), 46 (158), 51 (168), 58 (155), 81 (260), 93–96, 98, 123 (89), 129, 405 (5), 427 (74), 434, 436  
 Rataboul, F. 544 (130), 588  
 Rathjen, P. D. 339 (179), 363  
 Rathke, M. W. 462 (58), 494 (109), 507, 509  
 Ravi Kumar, G. 272 (172, 173), 309  
 Ray, J. 148 (48), 154  
 Rayment, I. 349 (253, 255, 259), 364, 365  
 Rayssiguier, Y. 268 (102), 288 (256–258), 308, 311  
 Ready, J. M. 622 (87), 630, 652 (53), 677  
 Reamer, B. 654 (72), 678  
 Reamer, R. 699 (31), 715  
 Record, M. R. 334 (138), 362  
 Redden, P. R. 301 (360), 314  
 Reddinger, J. 286 (244), 311  
 Reddy, C. K. 534 (96), 586  
 Reddy, G. S. 357 (345), 366  
 Redeker, T. 68 (221), 97  
 Redondo, P. 106 (16), 126  
 Redwood, M. E. 428 (87), 436  
 Reed, D. 38 (126), 95, 149 (47), 154  
 Reed, D. P. 395 (4), 401  
 Reed, G. H. 349 (250, 252, 253, 255, 259), 364, 365  
 Rees, C. W. 71 (231), 98, 411 (33), 435  
 Rees, T. C. 654 (75, 79, 80), 678  
 Reetz, M. F. 425 (69), 436  
 Reetz, M. T. 180 (137), 187  
 Reeves, J. T. 517 (37), 584  
 Reeves, T. 103 (9), 126  
 Reffy, B. 183 (151), 187  
 Regev, A. 201 (71), 216  
 Reginato, G. 580 (313), 592  
 Reich, H. J. 527 (28), 584  
 Reich, I. L. 527 (28), 584  
 Reich, R. 653 (68), 677  
 Reichard, G. A. 484 (102), 509  
 Reid, A. F. 122 (75), 128  
 Reider, P. J. 654 (72), 678, 699 (31), 715  
 Reimuth, O. 288 (146), 308  
 Reinehr, D. 653 (62, 66), 655 (59–61, 63–65), 656 (87), 677, 678  
 Reinhart, R. A. 268 (38), 306  
 Reinmuth, O. 389 (3), 401, 512 (3), 583  
 Reisinger, C.-P. 550 (168), 589  
 Reist, E. J. 601 (38), 629  
 Reiter, S. M. 121 (70), 128  
 Reményi, A. 347 (229), 364  
 Ren, H. 524 (61), 526 (72), 534 (97), 585, 586  
 Replogle, E. S. 369 (2), 384 (30), 401, 402  
 Resing, K. A. 347 (228), 364  
 Resnick, L. M. 268 (19, 101), 306, 308  
 Respress, W. L. 295 (287), 312

- Reusch, C. E. 276 (195, 196), 310  
 Reutrakul, V. 725 (19), 768  
 Rezabal, E. 322 (45), 360  
 Rha, R. 334 (140), 362  
 Riber, E. 270 (154), 309  
 Ricchiardi, G. 125 (108), 129  
 Ricci, A. 475 (81), 508, 519 (51), 531 (89),  
     534 (81), 559 (228), 563 (245), 576 (301),  
     580 (313), 585, 586, 590–593  
 Rich, D. H. 370 (114), 509  
 Richard, O. 268 (116), 308  
 Richardson, C. C. 352 (298), 365  
 Richey, G. H. 172 (107), 186  
 Richey, H. G. 3 (16, 17, 28), 11 (56), 39 (134),  
     44 (147, 151), 55 (182), 56 (55, 57, 184),  
     58 (14), 69 (183), 92, 93, 95, 96, 268 (4, 5),  
     306, 389 (3), 401, 410 (38), 429 (78), 431  
     (81), 435, 436, 451 (30), 507, 512 (3, 5, 6),  
     543 (124), 583, 587, 634 (11), 645 (35, 36),  
     654 (75, 79, 80), 657 (91), 659 (97), 667  
     (54), 676–678, 682 (5, 14), 684 (13, 18),  
     686 (17), 711 (51), 713 (52, 53), 714, 715  
 Richmann, P. N. 68 (219), 97  
 Richoux, M.-C. 198 (63), 216  
 Richter, J. 191 (7), 215  
 Richtmyer, N. K. 299 (310), 312  
 Ridley, D. 410 (39), 428 (87), 435, 436  
 Riech, I. 247 (106), 262  
 Rieger, D. L. 503 (123), 509  
 Rieke, R. D. 254 (125), 263, 514 (19, 20), 540  
     (119), 584, 587  
 Rihs, G. 774 (8), 800  
 Rijksen, G. 287 (248), 311  
 Rinaldi, R. 331 (115), 362  
 Ritter, C. 268 (34), 306  
 Rivaro, P. 302 (332), 313  
 Rivera, S. L. 395 (36), 402  
 Rizzi, M. 327 (77), 361  
 Robb, M. A. 369 (2), 384 (30), 401, 402  
 Robbins, D. L. 124 (98), 129  
 Roberts, B. A. 19 (68), 93  
 Roberts, C. W. 516 (29), 584  
 Roberts, D. A. 666 (116), 678  
 Roberts, J. D. 119 (62), 128, 136 (8), 138  
     (22–25), 141 (34), 142 (35, 36), 153, 154,  
     654 (74, 76–78), 678  
 Robertson, H. E. 183 (141), 187  
 Robinet, J. J. 336 (160), 362  
 Robinson, G. C. 240 (76), 261  
 Robinson, M. J. 347 (237), 364  
 Robl, C. 68 (218), 97  
 Robles, E. S. J. 123 (84), 129  
 Rocha, J. B. T. 774 (25), 801  
 Roche, K. E. 268 (107), 308  
 Rock, P. A. 257 (129), 263  
 Rodger, P. J. A. 17 (65), 93  
 Rodgers, J. D. 667 (118), 678  
 Rodigari, F. 303 (342), 313  
 Rodriguez-Cruz, S. E. 318 (19, 20), 359  
 Rodríguez, S. 391 (26), 402  
 Roenn, M. 555 (201), 590  
 Roesky, H. 74 (245), 98  
 Roesky, H. W. 74 (248), 98, 413 (43), 424  
     (16), 434, 435  
 Roffia, S. 259 (144), 263  
 Rogers, H. R. 259 (148), 263, 513 (14), 583  
 Rogers, R. D. 50 (98), 94, 123 (83), 129  
 Rogers, R. J. 259 (148), 263, 513 (14), 583  
 Roithova, J. 162 (58), 185  
 Rojas, F. G. 559 (227), 590  
 Roland, S. 574 (293), 592  
 Roldán, J. L. 518 (48), 585  
 Rollick, K. L. 615 (16), 629  
 Romani, A. M. 268 (47), 307  
 Romani, A. M. P. 268 (53), 307, 325 (64, 65),  
     342 (62), 360  
 Romano, L. J. 352 (293), 365  
 Rondelez, Y. 329 (99), 361  
 Ronzini, L. 601 (40–42), 629  
 Root, K. S. 513 (14), 584  
 Rosenplänter, J. 29 (103), 94  
 Rosito, V. 583 (318), 593  
 Roskoski, J. R. 347 (236), 364  
 Ross, M. J. 413 (42), 435  
 Rossana, D. M. 485 (21), 506  
 Rossini, F. D. 120 (65), 128  
 Rossiter, B. E. 772 (4), 800  
 Rostovtsev, V. V. 576 (303), 592  
 Roth, K. 537 (104), 586  
 Rothman, A. M. 634 (11), 676  
 Rottländer, M. 517 (35), 525 (41), 534 (81,  
     100), 584–586, 690 (30), 701 (37), 715  
 Röttländer, M. 619 (45), 629  
 Rousset, C. J. 671 (134), 679  
 Roussi, G. 666 (114), 678  
 Rowe, B. R. 156 (8), 160 (45), 184, 185  
 Rowlings, R. B. 17 (65, 66), 18 (67), 19 (68,  
     69), 93  
 Roy, A. H. 553 (178), 589  
 Roy, A. M. 553 (180), 589  
 Roy, G. 353 (307), 366  
 Roy, R. 353 (307), 366  
 Roychowdhury-Saha, M. 341 (193), 363  
 Rozhnov, A. M. 122 (82), 128  
 Ruano, J. L. G. 727 (24), 768  
 Ruben, M. 546 (145), 588  
 Rüchardt, C. 654 (74), 678  
 Rude, R. K. 268 (78), 276 (17), 306, 307  
 Rüdiger, W. 191 (8), 215  
 Rue, C. 124 (97), 125 (105), 129, 161 (56),  
     185  
 Rueping, M. 552 (177), 589  
 Rüffer, T. 38 (127), 136 (16), 42 (143), 59  
     (132), 95, 149 (6)153  
 Ruffner, D. E. 339 (182), 363

- Rufińska, A. 71 (227), 97, 123 (80, 86), 128, 129, 143 (32, 37), 151 (15), 152 (50, 51), 153, 154
- Ruhland, T. 516 (32), 584
- Ruhlandt-Senge, K. 71 (229), 98, 324 (59), 360, 407 (23), 434
- Ruiz-Lopez, M. 331 (116), 362
- Ruiz-López, M. D. 271 (168), 309
- Ruiz-Vicent, L. E. 323 (56), 360
- Rumyantseva, S. V. 214 (138), 218
- Rundle, R. E. 58 (19, 20, 188, 190), 92, 96, 391 (14), 402
- Russel, C. A. 124 (91), 129
- Russell, A. T. 547 (149), 588
- Russell, C. A. 57 (186), 96
- Russell, C. J. 424 (63), 435, 473 (89), 508
- Russell, J. 148 (48), 154
- Ruszczycky, M. W. 348 (238), 364
- Ruzicka, J. 280 (222), 310
- Ryan, M. F. 268 (82, 86), 307
- Ryan, M. P. 268 (140), 308
- Ryan, R. R. 91 (278), 99
- Ryde, K. W. 268 (79), 307
- Ryde, U. 322 (40), 360
- Rylander, R. 268 (111), 308
- Ryppa, C. 191 (8), 215
- Ryzen, E. 268 (78), 307
- Ryznar, J. W. 240 (71), 261
- Sabatier, M. 288 (254, 255), 311
- Sabbert, D. 329 (95), 361
- Sachdev, H. 411 (24), 434
- Sadler, P. J. 286 (246), 311
- Saenger, W. 356 (36, 324), 360, 366
- Safont, V. S. 357 (347), 359 (356, 357), 366, 367, 393 (25), 402
- Sahni, J. 325 (63), 360
- Sahrawat, K. L. 272 (172, 173), 309
- Saino, N. 791 (60), 802
- Saint-Martin, H. 323 (55, 56), 360
- Saito, I. 208 (96), 217
- Saito, M. 675 (158), 679
- Saito, N. 285 (237), 311
- Saito, S. 739 (35), 769
- Sakabe, Y. 145 (39), 154
- Sakai, K. 741 (36), 769
- Sakai, M. 774 (21), 780 (35), 800, 801
- Sakai, S. 125 (109), 129, 391 (12), 402
- Sakamoto, F. 302 (329), 313
- Sakamoto, K. 720 (9), 768
- Sakamoto, S. 63 (60), 93, 182 (6), 184
- Sakamoto, T. 538 (105, 108), 587, 713 (55), 715, 748 (41), 769
- Sakata, G. 566 (265), 591
- Sakata, Y. 201 (70), 216
- Saksena, A. K. 574 (296), 592
- Sakuma, S. 780 (35), 801
- Sakurada, J. 756 (43), 769
- Sakurai, Y. 193 (25, 26), 215
- Salem, G. 190 (1), 214
- Salem, M. 268 (81), 307
- Sales, Z. S. 424 (62), 435
- Salido, S. 440 (7), 506
- Salih, B. 303 (347), 313
- Salinger, R. 244 (89), 262
- Salinger, R. M. 108 (39), 127
- Salkeld, A. A. 268 (107), 308
- Salvucci, M. E. 358 (341), 366
- Samaj, J. 325 (66), 360
- Sambongi, Y. 329 (97), 361
- Sammakia, T. 774 (9), 800
- Sancar, A. 351 (281), 365
- Sánchez, A. 440 (7), 506
- Sánchez-Barbara, L. F. 74 (247), 98, L. F., 421 (18)434
- Sánchez-Martínez, C. 518 (48), 585
- Sander, L. 518 (49), 585
- Sander, W. 540 (115), 587
- Sanders, G. T. 268 (88), 307
- Sanders, G. T. B. 275 (191), 310
- Sanders, R. 268 (88), 307
- Sands, J. 335 (149), 362
- Sane, D. C. 279 (216), 310
- Sano, S. 463 (63), 508
- Santabarbara, S. 356 (329), 366
- SantaMaria, C. 103 (10), 126
- Santelli, M. 540 (115), 587
- Sanz-Medel, A. 273 (181), 303 (346), 309, 313
- Sapountzis, I. 268 (8), 306, 518 (36, 42), 525 (41, 68), 531 (92), 540 (116), 543 (125), 550 (126), 559 (223), 566 (266), 576 (301, 304), 577 (306), 584–587, 590–592, 601 (44), 629, 690 (29), 714 (8), 714, 715
- Saraymen, R. 278 (215), 310
- Saris, N. E. 268 (21), 306
- Saris, N.-E. L. 270 (155), 309
- Sartini, R. P. 280 (224), 310
- Sarvestani, M. 103 (9), 126, 517 (37), 584
- Sarzanini, C. 273 (182), 309
- Sasahara, T. 145 (39), 154
- Sasaki, C. 302 (329), 313
- Sasaki, H. 576 (302), 592
- Sasaki, Y. 484 (28), 507
- Sassian, M. 512 (8), 583
- Sastre-Santos, A. 201 (40), 216
- Satar, A. K. M. A. 352 (294), 365
- Sato, F. 540 (120), 543 (124), 587, 700 (32), 715
- Sato, T. 572 (287), 592
- Satoh, T. 479 (14, 16), 480 (18), 485 (15, 17), 506, 526 (70, 71), 527 (74), 586, 720 (10), 721 (11), 727 (18), 728 (25), 730 (27), 734 (29), 737 (32), 739 (35), 741 (36), 743 (38), 746 (39), 748 (41), 749 (42), 756 (43), 758 (44), 760 (45, 50), 761 (51), 764 (52), 766 (53), 767 (56, 57, 59), 768, 769
- Satomi, H. 452 (37), 507

- Sattelberger, A. P. 91 (278), 99  
 Sauer, A. 540 (115), 587  
 Sauv  , G. 286 (244), 311  
 Savchenko, A. I. 582 (315), 593  
 Sav  ant, J. M. 235 (57), 259 (58), 261  
 Savory, J. 516 (30), 517 (34), 584  
 Sayles, D. C. 624 (4), 628  
 Scarpa, A. 268 (47), 307, 342 (62), 360  
 Scerbo, R. 302 (323), 313  
 Schaefer, H. F. 718 (2), 768  
 Sch  fer, H. 237 (62), 261  
 Schaper, F. 48 (164), 49 (165), 96  
 Scharenberg, A. M. 325 (63), 360  
 Schat, G. 34 (116), 35 (118), 38 (83), 40 (138), 140, 61 (198), 62 (199), 66 (213), 86 (269), 94, 95, 97, 99, 116 (58), 120 (66–68), 121 (71), 128, 384 (31), 402  
 Schechter, A. 247 (108), 248 (96, 107, 113), 251 (112), 252 (114), 253 (118), 258 (110), 262  
 Scheer, H. 191 (5, 8), 193 (28), 211 (105, 106), 214 (133), 215, 217, 218  
 Scheinman, S. J. 268 (64), 307  
 Scheiper, B. 554 (189), 589, 608 (57), 629  
 Schenk, G. 343 (210), 364  
 Scheuplein, R. 268 (107), 308  
 Schiesser, C. H. 550 (164), 588  
 Schilling, B. E. R. 29 (102), 94, 123 (85), 129, 183 (149), 187  
 Schimeczek, M. 720 (6), 768  
 Schimperna, G. 484 (101), 509  
 Schink, H. E. 564 (252), 591  
 Schlecker, W. 538 (107), 587  
 Schlegel, H. 122 (79), 128  
 Schlegel, H. B. 47 (161), 96, 369 (1, 2), 384 (30), 401, 402  
 Schlenk, W. 3 (12), 92, 107 (26), 127, 132 (3), 153, 225 (39), 261, 391 (21), 402  
 Schlichte, K. 44 (153), 45 (154, 156), 47 (159), 95, 96  
 Schlingmann, K. P. 268 (55, 56, 67), 307  
 Schloss, J. D. 50 (98), 94, 123 (83), 129  
 Schloss, J. V. 358 (352), 367  
 Schlosser, M. 142 (31), 154, 702 (38), 715  
 Schmalz, H.-G. 517 (40), 585  
 Schmid, G. 89 (274, 275), 99  
 Schmidt, E. 201 (72), 216  
 Schmidt, H. 59 (132), 95, 149 (6), 153  
 Schmidt, H.-G. 74 (248), 98, 424 (16), 434  
 Schmidt, M. 357 (337), 366  
 Schnare, M. N. 337 (169), 363  
 Schneider, B. 323 (50), 360  
 Schneider, G. 300 (317), 313, 359 (355), 367  
 Schneider, H. 519 (53), 585  
 Schneider, I. R. 339 (178), 363  
 Schneider, W. P. 289 (268), 311  
 Schneiderbauer, S. 409 (30), 435  
 Schn  ckel, H. 26 (97), 68 (218, 220), 94, 97  
 Schnyder, A. 775 (27), 801  
 Schofield, C. J. 547 (149), 588  
 Schomburg, G. 653 (66), 655 (64, 65), 677  
 Schormann, M. 74 (248), 98, 424 (16), 434  
 Schrader, E. A. 648 (46), 677  
 Schrader, U. 208 (95), 217  
 Schreiber, S. L. 707 (48), 715  
 Schr  der, F. A. 69 (189), 96  
 Schroeder, D. 162 (58), 185  
 Schroth, G. 653 (62), 655 (63–65), 677  
 Schubert, B. 14 (50), 42 (144), 93, 95  
 Schuessler, H. A. 160 (50, 51), 185  
 Sch  ler, P. 51 (51), 93  
 Schulman, C. C. 268 (117), 308  
 Schulten, M. 71 (230), 98, 405 (12), 434  
 Schultz, E. 596 (26), 629  
 Schultz, M. 26 (94), 94, 125 (102), 129  
 Schultz, R. A. 355 (316), 366  
 Schulz, C. P. 169 (81), 186  
 Schulze, F. 295 (289, 290), 312  
 Schulze, V. 135 (11), 137 (10), 153, 720 (5–7), 768  
 Schumann, H. 26 (96), 54 (95), 79 (254), 94, 98, 414 (32), 435  
 Schumm, R. H. 113 (2), 126  
 Schuppan, J. 780 (37), 801  
 Schurko, R. W. 152 (52), 154  
 Schutte, S. 26 (96), 94  
 Schwarz, H. 156 (1), 160 (40), 184, 185  
 Schweigel, M. 325 (66, 68), 360  
 Schwenk-Kircher, H. 27 (99), 94  
 Schwenke, D. C. 279 (216), 310  
 Schwerdtfeger, P. 720 (6), 768  
 Schweyen, R. J. 325 (66, 68), 360  
 Schwickardi, M. 33 (114), 44 (113), 94, 513 (17), 540 (118), 584, 587, 621 (79), 630  
 Scolastico, C. 484 (101), 509  
 Scott, W. G. 340 (186, 187), 341 (196), 363  
 Scuseria, G. E. 384 (30), 402  
 Seburg, R. A. 106 (17), 126  
 Seck, M. 555 (197), 589, 607 (48), 629  
 Seconi, G. 475 (81), 508, 580 (313), 592, 593  
 Sedaira, H. 280 (220), 310  
 Seebach, D. 65 (212), 97, 395 (37), 402, 571 (281), 591, 774 (8), 800  
 Seeger, R. 369 (1), 401  
 Seelig, M. S. 268 (131), 308  
 Segal, J. A. 74 (241), 76 (242), 98, 418 (14), 424 (44), 434, 435  
 Segelmann, A. 214 (131), 218  
 Seidel, G. 554 (189), 589, 626 (95), 630  
 Seidel, N. 30 (108), 94, 243 (86), 262, 525 (41), 585  
 Seifert, F. 227 (34), 261  
 Seifert, T. 27 (99), 94, 427 (72), 436  
 Seiler, A. 246 (97), 262  
 Seiler, H. G. 269 (150), 308  
 Seiler, P. 65 (212), 97, 395 (37), 402

- Seip, R. 23 (76), 93, 183 (148), 187  
 Seitz, L. M. 4 (35–37), 92, 682 (2), 714  
 Selg, P. 125 (102), 129  
 Seliem, M. M. 277 (200), 310  
 Seligman, P. F. 302 (330), 313  
 Sell, M. S. 514 (19), 584  
 Semba, F. 720 (9), 768  
 Sembri, L. 566 (263), 591  
 Semmelhack, H. F. 540 (115), 587  
 Senanayake, C. 395 (35), 402  
 Senanayake, C. H. 103 (9), 126, 517 (37), 521 (58), 583 (319), 584, 585, 593  
 Senge, M. O. 191 (6–8), 192 (10), 196 (4), 212 (113), 214 (139), 215, 217, 218  
 Sengupta, S. 512 (2), 583, 596 (20), 629  
 Senior, A. E. 330 (105), 361  
 Senn, H. M. 350 (264), 365  
 Seo, Y.-S. 553 (178), 589  
 Štěpnička, P. 86 (270), 99  
 Sergeev, G. B. 121 (72), 128, 158 (27), 160 (32), 185  
 Sergeeva, N. N. 196 (4), 215  
 Seriaga, M. P. 513 (11), 583  
 Servesko, J. M. 779 (33), 801  
 Servis, K. L. 268 (78), 307  
 Seth, J. 201 (38, 39, 46), 215, 216  
 Seudeal, N. 224 (29), 260  
 Sévignon, M. 596 (26), 629  
 Sevvana, M. 452 (36), 507  
 Seyberth, H. W. 268 (67), 307  
 Seyferth, D. 517 (34), 584, 661 (102), 678, 719 (3), 768  
 Shadrina, M. S. 331 (117), 362  
 Shafer, P. R. 654 (74), 678  
 Shafirovich, E. Ya. 125 (103), 129  
 Shah, R. D. 667 (118), 678  
 Shaikh, N. 544 (129), 588  
 Shakoor, A. 45 (157), 96  
 Shan, S. 338 (176), 363  
 Shang, X. 572 (276), 591  
 Shang, Z. 337 (169), 363  
 Shaper., A. G. 268 (120), 308  
 Shapiro, H. 238 (77), 261  
 Sharma, H. K. 428 (86), 436  
 Sharma, S. 428 (85), 436  
 Sharpless, K. B. 576 (303), 592  
 Shaw, J. T. 503 (62), 505 (61), 508  
 Shaw, Y.-J. 547 (154), 588  
 Shen, H. 123 (90), 129  
 Shen, J. R. 356 (323), 366  
 Shen, Y. 567 (267), 591  
 Sheng, Y. 169 (88, 89), 186  
 Shepherd, L. H. 653 (58), 677  
 Sherrington, D. C. 69 (222), 73 (73), 93, 97, 150 (41), 154, 429 (76), 436  
 Shi, L. 325 (74), 361  
 Shi, M. 779 (20), 800  
 Shi, T. 176 (129), 187  
 Shi, Y.-J. 648 (47), 677  
 Shi, Z. 347 (228), 364  
 Shia, K.-S. 572 (276), 591  
 Shiba, T. 193 (26), 215  
 Shibutani, T. 517 (34), 584  
 Shieu, J.-C. 547 (154), 588  
 Shigeru, K. 514 (21), 584  
 Shigeta, Y. 357 (336), 366  
 Shikanai, D. 572 (287), 592  
 Shilai, M. 538 (105), 587  
 Shimada, K. 193 (22–25), 215  
 Shimada, T. 554 (194), 589  
 Shimizu, A. 453 (39), 507  
 Shimizu, H. 767 (59), 769  
 Shimizu, M. 466 (70), 486 (25), 507, 508  
 Shimoda, K. 791 (60), 802  
 Shimokubo, H. 567 (270), 591  
 Shimomura, A. 201 (70), 216  
 Shin, C. S. 270 (159), 309  
 Shin, H. 667 (120), 678  
 Shin, J.-S. 557 (215), 590  
 Shin, S. 707 (47), 715  
 Shingu, H. 125 (100), 129  
 Shinokubo, H. 5 (42), 41 (41), 93, 276 (9), 306, 523 (59), 527 (73), 528 (77, 83), 540 (122), 560 (236), 561 (243), 567 (269), 585–587, 590, 591, 596 (31), 623 (90), 629, 630, 636 (17, 18, 20, 21), 676, 677, 699 (11), 703 (43), 706 (42, 44), 707 (45), 714, 715  
 Shintani, R. 571 (283), 592, 623 (89), 630, 639 (24), 677  
 Shintou, T. 549 (162), 588  
 Shioiri, T. 370 (112), 458 (52), 507, 509  
 Shioji, H. 302 (333), 313  
 Shiono, T. 285 (243), 311  
 Shiragami, H. 661 (103), 678  
 Shirai, M. 713 (55), 715  
 Shirakawa, E. 568 (272), 591, 622 (88), 623 (89), 630, 637 (23), 639 (24), 677  
 Shiraki, R. 259 (141), 263  
 Shirazi, A. R. 271 (165), 309  
 Shireman, B. T. 707 (47), 715  
 Shirey, T. L. 268 (108), 308  
 Shiro, M. 463 (63), 508  
 Shiue, J.-L. 566 (262), 591  
 Shkel, I. A. 334 (138), 362  
 Shono, T. 254 (121), 263  
 Shook, B. C. 528 (85), 586  
 Showalter, A. K. 352 (290), 365  
 Shu, C. 798 (65), 802  
 Shubert, D. C. 604 (46), 629  
 Shui, X. 335 (30), 360  
 Shults, R. H. 621 (80), 630  
 Shumaker, J. B. 633 (7), 676  
 Shuman, H. 268 (22), 306  
 Shumov, Y. S. 212 (117), 217  
 Shuvaeva, O. V. 279 (219), 310

- Shvartsburg, A. A. 176 (125–128), 187  
 Sibi, M. P. 426 (71), 436, 498 (41), 507, 779 (19), 800  
 Sidoriskikh, P. F. 212 (117), 217  
 Siede, W. 355 (316), 366  
 Siefert, J. L. 355 (13), 359  
 Siero, J. P. J. 208 (98), 217  
 Sierra, I. 278 (208), 310  
 Sigel, H. 327 (79), 331 (121), 332 (122–124, 126), 361, 362  
 Sigel, R. K. O. 334 (136), 336 (156), 362  
 Siggaard-Andersen, O. 276 (16), 306  
 Sikorsky, P. 44 (113), 94  
 Sillen, L. G. 286 (245), 311  
 Silva, S. J. N. 774 (25), 801  
 Silveira, C. C. 774 (25), 801  
 Silver, B. B. 268 (27), 306  
 Silver, M. S. 654 (74), 678  
 Silverman, G. S. 3 (18, 27), 55 (178), 58 (13), 92, 96, 225 (40), 258 (131, 132), 259 (145), 261, 263, 512 (3, 5, 6), 583  
 Silvermann, G. S. 389 (3), 401  
 Silverstein, B. 268 (107), 308  
 Simaan, S. 560 (233), 590  
 Simon, J. 268 (117), 308  
 Simon, W. 276 (14), 306  
 Simonet, J. 253 (122), 263  
 Simpson, G. W. 495 (111), 509  
 Sims, P. A. 349 (252), 364  
 Simuste, H. 512 (9), 583  
 Singh, J. 268 (48), 307  
 Singh, P. 729 (26), 768  
 Singh, S. K. 572 (289), 592  
 Sinha, P. 577 (306), 578 (308), 592  
 Sinitsyna, T. M. 268 (118), 308  
 Sirover, M. A. 351 (276, 277), 365  
 Sisido, K. 484 (69), 508  
 Sitzmann, H. 26 (94), 94  
 Siu, K. W. M. 176 (125, 129), 187  
 Skaltitzky, D. 119 (64), 128  
 Skamnaki, V. T. 348 (239), 364  
 Skatova, A. A. 79 (254), 98, 414 (32), 426 (48), 435  
 Skell, P. S. 157 (22), 185  
 Skelton, B. 123 (89), 129  
 Skelton, B. W. 40 (139), 46 (158), 81 (260), 95, 96, 98, 405 (5), 434  
 Skiebe, A. 675 (156), 679  
 Skinner, H. A. 109 (46), 127  
 Sklute, G. 528 (84), 586, 739 (34), 768  
 Skov, K. 259 (137), 263  
 Slawin, A. M. Z. 574 (294), 592  
 Slayden, S. W. 110 (49), 111 (51), 113 (55, 56), 127, 128  
 Slim, G. 339 (184), 363  
 Sliwiński, W. 410 (36), 435  
 Slok, F. A. 519 (50), 585  
 Slota, R. 196 (49), 216  
 Smalley, J. F. 196 (48), 216  
 Smeets, W. J. J. 3 (15), 34 (106, 116), 35 (117, 118), 38 (83), 40 (140), 95, 43 (146), 44 (142), 66 (213–216), 79 (258), 92, 94, 95, 97, 98, 183 (140), 187, 318 (22), 359, 774 (25), 800  
 Smeets, W. J. J. ,  
 Smidansky, E. 352 (301), 365  
 Smil, D. V. 648 (45), 677  
 Smirnov, V. V. 171 (5, 100, 102), 175 (101), 184, 186, 268 (5), 306  
 Smirnova, I. N. 329 (101), 361  
 Smith, D. M. A. 323 (55), 360  
 Smith, J. D. 23 (77, 78), 32 (110), 63 (112, 206–208), 94, 97  
 Smith, K. D. 28 (100), 94  
 Smith, K. M. 74 (246), 98, 193 (11, 13, 15), 194 (32), 195 (16), 208 (97), 211 (108), 214 (139), 215, 217, 218  
 Smith, M. B. 108 (33, 34, 38), 127  
 Smith, N. K. 268 (12), 306  
 Smith, R. S. 23 (76), 93, 183 (148), 187, 391 (10), 401, 604 (14), 629  
 Smith, S. G. 108 (35), 127, 389 (3), 401  
 Smith, S. J. 343 (210), 364  
 Smith, W. B. 108 (31), 127  
 Smitrovich, J. H. 557 (214), 590  
 Snavely, M. D. 325 (69), 361  
 Sneyd, J. C. R. 122 (76), 128  
 Snider, B. B. 640 (25, 26), 677  
 Snieckus, V. 537 (102), 553 (183, 184), 586, 589  
 Soai, K. 774 (11), 800  
 Sobolev, G. A. 183 (154), 187  
 Soep, B. 169 (81), 186  
 Sofia, A. 544 (131), 588  
 Sofield, C. D. 26 (94), 94  
 Sofoniou, M. C. 281 (227), 310  
 Soi, A. 675 (155, 156), 679  
 Sokolov, V. V. 452 (36), 507  
 Sölch, O. 278 (210), 310  
 Soler-López, M. 334 (135), 362  
 Solladié-Cavallo, A. 574 (295), 592  
 Solladié, G. 486 (54), 507  
 Solomon, M. 667 (118), 678  
 Solov'ev, V. N. 121 (72), 128, 158 (27), 160 (32), 185  
 Somashekar, B. S. 286 (247), 311  
 Someya, H. 526 (70), 560 (238), 586, 591, 746 (39), 769  
 Somlyo, A. P. 268 (22), 306  
 Song, J. J. 103 (9), 126, 517 (37), 584  
 Song, J. Z. 699 (31), 715  
 Sonnentag, H. 119 (64), 128  
 Soriaga, M. P. 172 (106, 108), 186, 512 (5), 583  
 Sosnick, T. R. 336 (167), 363  
 Sosnicki, J. G. 686 (20, 21), 714



- Soto, A. M. 336 (164), 362  
 Soto, J. E. 172 (108), 186  
 S  tofte, I. 30 (105), 94  
 Souhassou, M. 328 (82), 361  
 Souza, F. E. S. 567 (268), 591, 648 (45, 48), 677  
 Sowadski, J. M. 347 (232), 348 (234), 364  
 Spatling, L. 268 (132), 308  
 Spatz, J. H. 550 (172), 589  
 Spek, A. L. 3 (15), 34 (106, 116), 35 (117, 118), 38 (83), 40 (138, 140), 43 (146), 44 (142), 62 (199), 66 (213–216), 77 (251), 79 (258), 86 (269), 92, 94, 95, 97–99, 120 (68), 128, 183 (140), 187, 318 (22), 359, 384 (31), 402, 774 (25), 800  
 Spero, D. M. 573 (291), 592  
 Sperry, D. C. 166 (76), 186  
 Spescha, M. 774 (8), 800  
 Spialter, L. 661 (105), 678  
 Spichiger, U. 268 (26), 306  
 Spiess, A. 525 (65), 585  
 Spikes, J. D. 193 (21), 214 (133), 215, 218  
 Spina, G. 583 (318), 593  
 Spindler, F. 775 (27), 801  
 Spiridonov, V. P. 183 (154), 184 (152), 187, 391 (15), 402  
 Spivey, A. C. 547 (149), 588  
 Spliethoff, B. 44 (113), 45 (154), 94, 95, 554 (193), 589  
 Sporikou, C. N. 537 (104), 586  
 Spoto, G. 125 (108), 129  
 Spreitzer, R. J. 358 (341), 366  
 Spring, D. R. 707 (48), 711 (49), 715  
 Squiller, E. P. 56 (55), 69 (183), 93, 96, 410 (38), 429 (78), 431 (81), 435, 436, 684 (13), 714  
 Sreedhara, A. 320 (8), 359  
 Ssusi, A. K. 224 (31), 261  
 Stace, A. 175 (117), 186  
 Stace, A. J. 175 (116, 118, 122), 176 (119–121), 186, 187, 318 (23), 359  
 Stadnikov, G. L. 2 (8), 92  
 Stahl, T. 79 (258), 98  
 Stahle, M. 142 (31), 154  
 Stahley, M. R. 339 (174, 177), 363  
 Staley, R. H. 160 (47), 185  
 Stalke, D. 41 (141), 57 (186), 95, 96, 124 (91), 129  
 Stallard, M. O. 303 (343), 313  
 Stammler, H.-G. 68 (221), 97  
 Stan, M. A. 547 (150), 588  
 Sta  czyk, W. A. 32 (110), 94  
 Standen, M. C. H. 673 (140, 141), 679  
 Stanford, S. 596 (25), 629  
 Stang, P. J. 596 (28), 629, 633 (1), 676, 718 (2), 742 (37), 768, 769  
 Stangeland, E. L. 774 (9), 800  
 Stanton, J. F. 106 (17), 126  
 Stanway, S. J. 547 (151), 588  
 Stapleton, L. 512 (7), 583  
 Starowieyski, K. B. 25 (82), 94, 183 (146), 187, 299 (307), 312  
 Stasch, A. 74 (245), 98, 413 (43), 435  
 Staubitz, A. 518 (47), 577 (305), 585, 592  
 Stec, B. 349 (248, 254), 364  
 Steel, D. G. 344 (216, 217), 364  
 Steel, P. J. 547 (158), 588  
 Steele, I. 419 (57), 435, 538 (105), 587  
 Stefan, R. I. 280 (226), 310  
 Stefanov, B. B. 384 (30), 402  
 Steglich, W. 517 (39), 585  
 Stegmann, W. 288 (252), 311  
 Steichen, J. J. 268 (70), 307  
 Steinborn, D. 38 (127), 42 (143), 59 (132), 95, 136 (16), 149 (6), 153  
 Steinb  chel, A. 301 (359), 314  
 Steiner, A. 57 (186), 96, 124 (91), 129  
 Steinig, A. G. 573 (291), 592  
 Steitz, J. A. 355 (175), 363  
 Steitz, T. A. 334 (141), 335 (147), 336 (161), 351 (286), 352 (127, 297), 354 (310), 355 (175, 314), 362, 363, 365, 366  
 Steitz, T. J. 352 (294, 295), 365  
 Stengelin, M. 329 (101), 361  
 Stephan, D. W. 419 (26), 435  
 Stephenson, N. A. 342 (207), 363  
 Stergiades, I. A. 450 (27), 507  
 Sternbach, D. D. 485 (21), 506  
 Steward, O. W. 432 (88), 436, 563 (250), 565 (259–261), 591, 647 (39, 40), 667 (122), 670 (123, 125), 671 (126–130), 677, 679  
 Stewart, J. J. P. 369 (2), 401  
 Stey, T. 41 (141), 95  
 Stiasny, C. 734 (30), 768  
 Stiasny, H. C. 527 (79), 586  
 Stickney, J. L. 172 (108), 186  
 Stiel, H. 196 (54), 216  
 Stile, M. 476 (64), 508  
 Stiles, P. L. 184 (162), 187  
 Still, W. C. 395 (4), 401  
 Stillman, M. J. 193 (15, 18, 19), 196 (52), 215, 216  
 Stivers, J. T. 353 (308), 366  
 St  ckl, D. 273 (180), 309  
 Stoll, A. H. 529 (88), 586  
 Stoll, H. 79 (258), 98  
 Stone, F. G. A. 58 (3, 4), 92, 512 (4), 583, 657 (90), 678  
 Stone, F. G. S. 513 (13), 583  
 Stone, J. F. 299 (309), 312  
 Stork, G. A. 474 (47), 507  
 Stormo, G. D. 339 (182), 363  
 Stoudt, S. J. 713 (53), 715  
 Stowasser, R. 342 (205), 363  
 Stowell, J. C. 760 (46), 769  
 Stoy, P. 729 (26), 768

- Strain, M. C. 384 (30), 402  
 Sträter, N. 322 (49), 360  
 Stratmann, R. E. 384 (30), 402  
 Straub, B. F. 527 (28), 584, 714 (7), 714  
 Strauss, H. F. 656 (85), 678  
 Strell, M. 214 (126, 127), 218  
 Striccoli, M. 212 (115), 217  
 Strissel, C. 305 (305), 312  
 Strobel, S. A. 339 (174, 177), 363  
 Strohmeier, W. 226 (33), 227 (34), 261  
 Stryer, L. 327 (80), 361  
 Stubbe, J. 348 (245), 364  
 Stuckey, G. D. 38 (128), 95  
 Stucky, D. 62 (200), 97  
 Stucky, G. 58 (188), 96  
 Stucky, G. D. 47 (47), 58 (19), 62 (205), 67 (217), 83 (262), 92, 93, 97, 98, 384 (31), 402, 417 (4), 434  
 Studte, C. 557 (213), 590  
 Stulgies, B. 531 (93), 547 (153), 586, 588  
 Stumer, C. 742 (14), 768  
 Su, G. 108 (35), 127, 389 (3), 401  
 Su, M. I. 352 (290), 365  
 Su, X. 583 (319), 593  
 Subba Reddy, B. V. 576 (303), 592  
 Subirana, J. A. 334 (135), 362  
 Subramaniam, V. 344 (217), 364  
 Subramanian, J. 208 (95), 217  
 Subramanian, S. 337 (169), 363  
 Sudakin, D. L. 214 (129), 218  
 Suess, J. 537 (104), 586  
 Suga, S. 219 (9), 260  
 Suga, T. 579 (309), 592  
 Sugihara, Y. 701 (36), 715  
 Sugimoto, F. 272 (171), 309  
 Sugimoto, O. 514 (21), 584  
 Suginome, H. 487 (67), 508  
 Sugio, T. 193 (27), 215  
 Sugita, T. 145 (39), 154  
 Sugiyama, S. 767 (59), 769  
 Sui, S. F. 325 (73), 361  
 Sui, Z. 421 (58), 435, 700 (35), 715  
 Sullivan, A. C. 63 (207), 97  
 Sultanov, R. M. 671 (131, 132), 679  
 Sun, J. 169 (78), 186  
 Sun, J.-L. 169 (94, 95), 170 (97, 98), 186  
 Sun, L. 272 (169), 309  
 Sun, M. 553 (178), 589  
 Sun, S. 329 (90), 361  
 Sun, W. 293 (285), 312  
 Sun, X. 521 (58), 585  
 Sun, Z. H. 325 (73), 361  
 Sundaresan, N. 323 (53), 360  
 Sundberg, R. J. 387 (32), 402  
 Sundheim, O. 353 (303), 365  
 Sung, M. M. 70 (226), 97, 432 (79), 436  
 Suresh, C. H. 323 (53), 360  
 Surman, M. D. 659 (96), 678  
 Suter, M. 409 (30), 435  
 Suzmura, K. 341 (189), 363  
 Suzuki, A. 596 (22), 629  
 Suzuki, H. 90 (276), 99, 720 (9), 768  
 Suzuki, K. 285 (237), 311, 707 (46), 715  
 Suzuki, N. 671 (134), 679  
 Suzuki, S. 327 (78), 361, 570 (278), 591  
 Suzuki, Y. 285 (237), 311  
 Sviridov, S. V. 582 (315), 593  
 Svith, H. 256 (28), 260  
 Swain, C. G. 391 (7), 401  
 Sweeney, J. B. 547 (147), 588  
 Sweeney, O. R. 296 (296), 312  
 Swierczewski, G. 666 (114), 678  
 Swingle, N. M. 772 (4), 800  
 Swiss, J. 297 (297), 312  
 Swiss, K. A. 667 (117, 119), 678  
 Syfrig, M. A. 395 (37), 402  
 Sykes, P. 391 (6), 401  
 Symons, R. H. 336 (158), 339 (179), 362, 363  
 Szepesi, G. 292 (283), 312  
 Szmecinski, H. 283 (235), 311  
 Szulbinski, W. S. 198 (61), 216  
 Tabor, S. 352 (298), 365  
 Tabushi, I. 767 (54), 769  
 Taddei, M. 475 (81), 508  
 Taguchi, H. 765 (48), 769  
 Tainer, J. A. 353 (303, 306), 365, 366  
 Taira, K. 337 (152), 341 (189, 199–201), 362, 363  
 Tajiri, A. 701 (36), 715  
 Takabatake, H. 453 (38), 507  
 Takada, S. 760 (50), 769  
 Takafumi, K. 568 (272), 591  
 Takagi, K. 767 (54), 769  
 Takagi, Y. 341 (199–201), 363  
 Takahashi, H. 547 (159), 588  
 Takahashi, K. 559 (225), 590, 767 (55), 769  
 Takahashi, T. 554 (192), 589, 671 (134), 679  
 Takai, K. 484 (103), 509  
 Takaichi, S. 193 (23–25), 194 (29), 213 (119), 215, 217  
 Takano, K. 107 (22), 127, 485 (17), 506, 526 (70), 586, 720 (10), 746 (39), 748 (41), 768, 769  
 Takaya, Y. 774 (21), 800  
 Takayama, Y. 700 (32), 715  
 Takeda, A. 270 (157), 309  
 Takeda, T. 270 (157), 309  
 Takehisa, T. 463 (63), 508  
 Takeuchi, S. 329 (99), 361  
 Takeuchi, T. 274 (186, 187), 309, 310  
 Taki, M. 341 (199), 363  
 Takle, A. K. 574 (294), 592  
 Talmard, C. 13 (59), 22 (71, 72), 93  
 Tamaki, K. 201 (70), 216  
 Tamao, K. 661 (101, 107), 662 (106), 678  
 Tamaru, Y. 452 (37), 507, 596 (24), 629

- Tamborski, C. 516 (33), 584  
 Tamm, M. 53 (175), 96, 452 (36), 507  
 Tamura, M. 206 (81, 82), 217, 604 (9, 10), 628  
 Tamura, Y. 502 (119, 120), 509  
 Tan, Z. 103 (9), 126, 517 (37), 584, 787 (44), 801  
 Tan, Z. J. 335 (11), 359  
 Tanabe, M. 329 (97), 361  
 Tanabe, Y. 622 (85), 630  
 Tanaka, H. 193 (27), 215, 300 (314), 313  
 Tanaka, J. 452 (35), 474 (96), 507, 508  
 Tanaka, M. 259 (140), 263, 302 (333), 313  
 Tanaka, N. 60 (195), 97  
 Tanaka, R. 572 (287), 592  
 Tanaka, S. 764 (52), 769  
 Tanaka, Y. 341 (189, 199), 363  
 Tang, H. 56 (184), 96  
 Tang, J. 567 (269), 591, 636 (17), 676  
 Tang, K. H. 352 (290), 365  
 Tang, T. P. 575 (298), 592  
 Tani, K. 123 (73), 128  
 Taniguchi, S. 201 (74, 75), 216  
 Tanji, K. 514 (21), 584  
 Tanmatsu, M. 468 (80), 508  
 Tanno, T. 198 (64), 216  
 Tano, T. 193 (27), 215  
 Tao, S. 304 (352, 353), 314  
 Tapia, O. 357 (347), 359 (356, 357), 366, 367  
 Targrove, M. A. 305 (364), 314  
 Tarhouni, R. 516 (31), 584  
 Tari, L. W. 332 (125), 362  
 Tasaka, T. 720 (9), 768  
 Tasler, S. 554 (193), 589  
 Tateno, M. 341 (204), 363  
 Tauber, A. Y. 191 (9), 215  
 Tavakkoli, K. 63 (207), 97  
 Tawney, P. O. 625 (2, 6), 628  
 Taylor, N. J. 83 (176), 96  
 Taylor, S. S. 347 (225, 231, 232), 348 (234, 241), 364  
 Taylor, T. C. 357 (343), 359 (354), 366, 367  
 Tcherkez, G. G. B. 359 (353), 367  
 Teager, D. S. 765 (48), 769  
 Tease, R. L. 272 (175), 309  
 Teat, S. J. 424 (61), 435  
 Tebbboth, J. A. 25 (85), 94  
 Tedrow, J. S. 503 (62), 505 (61), 508  
 Teerlinck, C. E. 259 (146), 263, 513 (12), 583  
 Teixeira, P. 302 (322), 313  
 Templeton, D. M. 269 (151), 309  
 Ten Eyck, L. F. 347 (232), 348 (234), 364  
 Teng, W. 324 (59), 360  
 ter Horst, B. 500 (46), 507, 787 (45–47), 801  
 Terakura, K. 341 (204), 363  
 Terao, J. 544 (127, 128), 545 (135, 136), 560 (235), 561 (239, 241, 242), 588, 590, 591  
 Terasaki, H. 675 (157), 679  
 Terauchi, N. 563 (248), 591  
 Terenin, A. N. 198 (65), 216  
 Teresa Aranda, M. 583 (319), 593  
 Tereshldko, V. 335 (31, 145, 146), 360, 362  
 Terpstra, R. A. 268 (69), 307  
 Terwey, D. P. 340 (187), 363  
 Tesche, B. 554 (193), 589  
 Tesfaldet, Z. O. 280 (226), 310  
 Tessier, P. E. 567 (268), 591, 647 (41), 648 (48), 677  
 Teuchner, K. 196 (54), 216  
 Tews, E. C. 162 (57), 185  
 Teyssot, A. 243 (82, 83), 262  
 Thakker, R. V. 268 (64), 307  
 Thatcher, G. R. J. 331 (113), 361  
 Themelis, D. G. 281 (227), 310  
 Therien, M. J. 198 (56), 216, 579 (309), 592  
 Therkelsen, F. D. 701 (37), 715  
 Thewalt, U. 88 (272), 89 (274, 275), 99  
 Thewalt, Y. 87 (271), 99  
 Thibonnet, J. 525 (41, 67), 585  
 Thiel, W. 350 (264), 365  
 Thienpont, L. M. 273 (180), 309  
 Thirumalai, D. 337 (172), 363  
 Thivet, A. 555 (195), 589  
 Thoenes, D. 6 (48), 9 (53), 38 (122, 123), 93, 95, 682 (3), 714  
 Thomas, C. J. 52 (173), 96  
 Thomas, G. L. 711 (49), 715  
 Thomas, M. J. 279 (216), 310  
 Thompson, C. A. 159 (33), 185  
 Thompson, R. I. 160 (49–51), 185  
 Thorarensen, A. 555 (201), 590  
 Thorp, L. 2 (9), 92  
 Thorup, N. 701 (37), 715  
 Thurston, C. E. 231 (45), 261  
 Thyssen, K. 370 (113), 509  
 Tian, H. 213 (118), 217  
 Tichelaar, G. R. 398 (39), 402  
 Tiekink, E. R. 550 (164), 588  
 Tijani, A. 775 (27), 801  
 Tilley, T. D. 38 (130), 95, 305 (305), 312  
 Tilstam, U. 513 (16), 584  
 Tinga, M. A. G. M. 40 (140), 95  
 Tinoco, I. 336 (163), 362  
 Tishkov, A. 557 (208), 590  
 Tissot-Croset, K. 558 (220), 590, 791 (50, 57, 58), 802  
 Tius, M. A. 450 (27), 507  
 Tjepkema, M. W. 646 (37), 677  
 Tjurina, L. A. 171 (5, 100, 102), 175 (101), 184, 186, 268 (5), 306  
 Tobrman, T. 518 (45), 585  
 Tochtermann, W. 4 (33), 92  
 Todo, H. 545 (136), 588  
 Togni, A. 775 (27), 801  
 Tohdo, K. 370 (112), 509  
 Tokoro, N. 300 (312), 313  
 Tokunaga, N. 779 (33), 801

- Tolmann, W. B. 322 (41), 360  
 Tolstikov, G. A. 235 (51), 261  
 Tomasi, J. 384 (30), 402  
 Tomasini, C. 564 (253), 591  
 Tomaszewicz, I. 107 (20), 126  
 Tomedi, P. 295 (288), 312  
 Tomilov, A. P. 219 (7), 260  
 Tomimoto, K. 531 (90), 586, 699 (31), 715  
 Tominaga, S. 791 (60), 802  
 Tomioka, K. 564 (254), 591, 772 (6), 774 (2, 9, 25), 779 (22), 800, 801  
 Tompkins, J. 723 (16), 768  
 Tonami, K. 302 (329), 313  
 Toney, J. 38 (128), 62 (200, 205), 67 (217), 95, 97, 384 (31), 402  
 Tongate, C. 275 (193), 310  
 Tooke, D. M. 20 (70), 93  
 Topf, J. M. 268 (89), 307  
 Topiol, S. 369 (1), 401  
 Topol, I. A. 158 (27), 185, 268 (147), 308, 331 (117, 118), 362  
 Topolski, M. 513 (12), 583  
 Tornøe, C. W. 576 (303), 592  
 Torrente, E. 727 (24), 768  
 Torres, L. E. 457 (48), 507  
 Torres, R. A. 341 (202), 363  
 Tortajada, J. 125 (101), 129, 182 (138), 187  
 Torti, S. V. 648 (46), 677  
 Tortorella, P. 583 (317, 318), 593  
 Tosello, L. 268 (94), 307  
 Touitou, Y. 268 (40), 306  
 Touster, J. 255 (127, 128), 263  
 Towrie, M. 200 (67), 216  
 Toyozawa, A. 341 (199), 363  
 Trachtman, M. 319 (25), 360, 391 (22), 402  
 Trafny, E. A. 348 (234), 364  
 Traxler, M. D. 503 (53), 507  
 Treber, J. 45 (154), 47 (159), 95, 96  
 Trécourt, F. 44 (44), 93, 524 (60), 537 (103), 550 (173), 553 (186), 585, 586, 589, 689 (26–28), 700 (33, 34), 713 (24, 25), 714, 715  
 Trellopoulos, A. V. 281 (227), 310  
 Tremaine, J. F. 25 (85), 94  
 Tresset, G. 329 (99), 361  
 Tressol, J. C. 288 (256), 311  
 Tribolet, R. 332 (126), 362  
 Trindle, C. 158 (31), 185  
 Tripoli, R. 473 (74), 508, 539 (111), 587  
 Trost, B. M. 439 (5), 443 (13), 485 (4), 506, 540 (115), 587, 707 (47), 715, 791 (52), 798 (65), 802  
 Troupel, M. 236 (60), 258 (38), 261, 291 (279), 312  
 Troxler, R. E. 208 (97), 217  
 Troxler, R. F. 211 (108), 217  
 Troy, J. 391 (22), 402  
 Trucks, G. W. 369 (2), 384 (30), 401, 402  
 Truglio, J. J. 351 (280), 365  
 Truhlar, D. G. 350 (263), 365  
 Trzcinski, W. A. 103 (5), 126  
 Tsai, M. D. 352 (290, 296), 365  
 Tsang, R. C. 268 (133), 308  
 Tsay, F.-R. 103 (8), 126, 519 (52), 585  
 Tsay, Y.-H. 33 (114), 45 (157), 94, 96  
 Tschaen, D. 699 (31), 715  
 Tschelintzeff, W. 104 (11, 12), 126  
 Tseng, H.-R. 559 (230), 590  
 Tshelintsev, V. 104 (12), 126  
 Tsien, R. Y. 268 (23), 306  
 Tso, E. L. 268 (83), 307  
 Tsodikov, O. V. 334 (138), 362  
 Tsuda, T. 300 (312), 313  
 Tsuge, O. 452 (35), 474 (96), 507, 508  
 Tsuji, M. 274 (187), 310  
 Tsuji, T. 545 (139), 546 (141), 588, 707 (45), 715  
 Tsukada, M. 145 (39), 154  
 Tsunoi, S. 302 (333), 313  
 Tsurusaki, N. 259 (140), 263  
 Tsuruta, H. 212 (116), 217  
 Tsutsui, H. 579 (309), 592  
 Tsutsumi, T. 259 (138, 139), 263  
 Tsvirko, M. P. 211 (107), 217  
 Tuchinda, P. 725 (19), 768  
 Tuck, D. G. 224 (29), 260  
 Tucker, B. J. 336 (153), 362  
 Tulub, A. A. 158 (29, 30), 185, 332 (130), 333 (129, 134), 362  
 Tulub, A. V. 158 (30), 171 (104), 185, 186  
 Tunuli, S. 206 (79), 217  
 Turck, A. 518 (43), 585, 702 (40), 715  
 Turgeman, R. 247 (108), 248 (96, 113), 250 (115), 251 (112), 258 (111), 262  
 Turnbull, A. G. 122 (75), 128  
 Turnlund, J. R. 288 (254, 255), 311  
 Turon, F. 301 (358), 314  
 Tuulmets, A. 512 (8, 9), 583  
 Tuulmets, A. V. 116 (57), 128  
 Tvaroska, I. 323 (54, 57), 360  
 Twamley, B. 81 (81), 94  
 Tzanavaras, P. D. 281 (227), 310  
 Uchibori, Y. 391 (23), 402  
 Uchida, M. 304 (353), 314  
 Uchiyama, M. 404 (2), 419 (51), 434, 435, 713 (55), 715  
 Ueda, I. 329 (97), 361  
 Ueda, Y. 721 (11), 768  
 Uemura, S. 558 (219), 590  
 Ueyama, K. 779 (33), 801  
 Ugajin, S. 774 (11), 800  
 Ugalde, J. M. 322 (45), 360  
 Uhlenbeck, O. C. 339 (182), 341 (180), 363  
 Uhm, H. L. 3 (27), 92, 512 (6), 583  
 Ulaşan, M. 277 (206), 310  
 Umemoto, H. 159 (18), 184

- Umetani, S. 279 (218), 310  
 Umland, F. 279 (185), 309  
 Umpleby, J. D. 656 (83), 678  
 Unger, M. A. 302 (330), 313  
 Ungváry, F. 55 (182), 96, 512 (5), , 583, 172 (107), 186, 512 (5), 583  
 Uno, H. 720 (9), 768  
 Unterer, S. 276 (195, 196), 310  
 Uppal, J. S. 160 (47), 185  
 Urabe, H. 572 (287), 592, 625 (91), 630  
 Urpi, F. J. 503 (123), 509  
 Usher, D. A. 342 (205), 363  
 Usman, N. 340 (187), 363  
 Usón, I. 74 (245), 98, 413 (43), 435  
 Utimoto, K. 527 (73), 540 (122), 586, 587, 636 (19), 661 (103), 676, 678  
 Utley, J. H. P. 253 (123), 263  
 Uzal Barbeito, L. A. 302 (339), 313  
 Valente, C. 550 (167), 589  
 Valiev, M. 348 (243), 364  
 Vallino, M. 59 (193), 97  
 van den Heuvel, L. P. 268 (65), 307  
 van den Heuvel, L. P. W. J. 268 (66), 307  
 van der Kerk, G. J. M. 77 (251), 98  
 van der Sluis, P. 38 (83), 94  
 van der Wal, G. 116 (44), 121 (71), 127, 128  
 Van Draanen, N. A. 468 (83), 508  
 van Gammeren, A. J. 356 (332), 366  
 van Grondelle, R. 194 (34), 215  
 Van Hook, J. W. 268 (80), 307  
 Van Houten, B. 351 (280), 365  
 van Ingen, H. E. 275 (191), 310  
 Van Klaveren, M. 558 (218), 590, 774 (8), 791 (53), 800, 802  
 van Koten, G. 30 (105), 69 (29), 79 (257, 258), 92, 94, 98, 519 (53), 545 (137), 558 (218), 585, 588, 590, 774 (8, 25), 791 (53), 800, 802  
 van Leeuwen, H. P. 269 (151), 309  
 van Lier, J. E. 193 (21), 215  
 Van Nuwenborg, J. E. 273 (180), 309  
 van Staden, J. F. 280 (226), 310  
 Van Summeren, R. P. 786 (42), 801  
 van Veldhuizen, J. J. 791 (59), 802  
 van Willigen, H. 196 (50), 216  
 van Zijl, A. W. 791 (56, 62), 798 (63), 802  
 Vance, C. J. 241 (37), 261  
 Vandenheede, J. R. 268 (37), 306  
 Vander, R. J. 295 (292), 312  
 Vaquero, M. P. 268 (137), 308  
 Varchi, G. 519 (51), 531 (89), 534 (81), 559 (228), 563 (245), 585, 586, 590, 591  
 Varga, V. 89 (274, 275), 99  
 Vargas, W. 71 (229), 98, 407 (23), 434  
 Vasil'ev, V. P. 121 (70), 128  
 Vasilevski, D. A. 582 (315), 593  
 Vater, H. D. 722 (13), 768  
 Vedsø, P. 518 (49), 525 (64), 585  
 Veenstra, A. 325 (74), 361  
 Veith, U. 573 (290), 592  
 Velarde-Ortiz, R. 514 (20), 584  
 Verkade, J. 472 (94), 508  
 Verma, D. K. 302 (338), 313  
 Verpeaux, J.-N. 727 (23), 768  
 Verpeaux, J. N. 608 (52, 53), 629  
 Verresha, G. 571 (282), 592  
 Vestergren, M. 59 (61, 145), 60 (185), 93, 95, 96  
 Vestfrid, Y. 247 (106), 252 (116), 262  
 Vicario, J. L. 545 (137), 588  
 Vicens, Q. 337 (171), 363  
 Vickery, T. 103 (8), 126, 519 (52), 585  
 Victorov, N. B. 540 (123), 587  
 Viebrock, H. 10 (54), 41 (125), 50 (166), 93, 95, 96  
 Vierling, W. 268 (46), 307  
 Viestfrid, Yu. 253 (117), 262  
 Vigneron, J. 243 (83), 262  
 Vigroux, A. 331 (114–116), 361, 362  
 Villà, J. 350 (263), 365  
 Villacorta, G. M. 772 (7), 800  
 Villalva-Servín, N. P. 647 (42), 677  
 Villena, A. 34 (106, 116), 66 (213, 216), 94, 95, 97  
 Villieras, J. 288 (262), 311, 442 (10), 506, 765 (48), 769  
 Villiérás, J. 516 (31), 584  
 Villiger, V. 2 (6), 92, 107 (24), 127  
 Vinarov, D. A. 350 (260), 365  
 Vink, R. 268 (145), 308  
 Visser, M. S. 673 (144, 146, 147), 679  
 Vlcek, A. 200 (67), 216  
 Vlismas, T. 289 (272), 292 (284), 312  
 Vogels-Mentink, G. M. 287 (248), 311  
 Vogt, M. 341 (198), 363  
 Voitjuk, A. A. 333 (132), 362  
 Volante, R. P. 654 (72), 678, 699 (31), 715  
 Volden, H. 29 (102), 94, 123 (85), 129  
 Volden, H. V. 183 (147, 149), 187  
 Vollet, J. 26 (97), 68 (220), 94, 97  
 Voloshin, M. 300 (300), 312  
 von der Brück, D. 517 (39), 585  
 von Hippel, P. H. 351 (270, 271), 365  
 Von Rein, F. W. 645 (35, 36), 677  
 von Schnering, H. G. 573 (290), 592  
 von Zezschwitz, P. 531 (93), 586  
 Voorbergen, P. 62 (199), 97, 384 (31), 402  
 Vormann, J. 268 (73), 307  
 Vostrikova, O. S. 421 (53), 435, 671 (131–133), 679  
 Vostrowsky, O. 537 (104), 586  
 Vrade, H. 543 (124), 587  
 Vrana, K. E. 347 (236), 364  
 Vreugdenhill, A. D. 107 (30), 127  
 Vrieze, C. 79 (257), 98  
 Vrieze, K. 291 (278), 312

- Vrkic, A. K. 181 (131), 187  
 Vu, V. A. 268 (8), 306, 518 (36, 42), 525 (41, 67, 69), 528 (83), 584–586, 738 (33), 748 (40), 768, 769  
 Wacker, W. E. 268 (28), 306  
 Wada, T. 661 (102), 678, 699 (31), 715  
 Wada, Y. 329 (97), 361  
 Wade Downey, C. 503 (62), 505 (61), 508  
 Waggoner, K. M. 58 (58), 93, 682 (4), 714  
 Wagman, D. D. 113 (2), 126  
 Wagner, A. J. 268 (10, 11), 306, 525 (66), 585  
 Wagner, B. 287 (192), 310  
 Wagner, B. O. 136 (8), 153  
 Wagner, C. 59 (132), 95, 149 (6), 153  
 Wagner, I. 350 (267), 365  
 Wagner, R. C. 599 (36), 629  
 Wagnerova, D. M. 193 (20), 215  
 Wahab, A. 322 (47), 360  
 Wakabayashi, K. 560 (237), 591  
 Wakao, N. 193 (23–26), 194 (29), 213 (119), 215, 217  
 Wakasugi, D. 734 (29), 768  
 Wakasugi, K. 622 (85), 630  
 Wakefield, B. J. 389 (3), 401, 451 (31), 507, 512 (3), 583, 633 (1), 657 (90), 674 (150), 676, 678, 679, 690 (29), 715, 720 (8), 768  
 Wakisaka, A. 341 (199), 363  
 Waladkhani, A. R. 214 (130), 218  
 Walborsky, H. M. 55 (179), 96, 259 (145), 260 (150), 263, 512 (5), 513 (12, 14), 583  
 Wald, S. A. 395 (35), 402  
 Walder, L. 219 (8), 260  
 Walfort, B. 59 (132), 95, 149 (6), 153  
 Walker, F. 134 (18), 153  
 Walker, G. C. 355 (316), 366  
 Walker, J. E. 329 (94, 102), 361  
 Walker, N. 175 (122), 187, 318 (23), 359  
 Walker, N. R. 184 (159), 187  
 Walling, C. 55 (181), 96, 513 (14), 583  
 Wallis, J. M. 67 (93), 94  
 Walter, D. 124 (97), 125 (105), 129, 161 (56), 185  
 Wälfertmann, M. 301 (359), 314  
 Walters, I. A. S. 454 (40), 507  
 Walters, R. S. 184 (159), 187  
 Walther, D. 39 (133), 95  
 Walther, H. 160 (49–51), 185  
 Walther, L. E. 278 (210), 310  
 Wan, W. B. 531 (94), 586  
 Wan, Z. 547 (150), 588  
 Wang, C.-J. 779 (20), 800  
 Wang, C. 168 (73, 74), 186  
 Wang, C. C. 352 (294), 365  
 Wang, C.-S. 163 (71), 186  
 Wang, D. N. 356 (328), 366  
 Wang, G. T. 122 (78), 128  
 Wang, H. 574 (296), 592  
 Wang, H.-M. 170 (97), 186  
 Wang, J. 253 (120), 262, 276 (197), 310, 352 (294), 365, 644 (33), 677  
 Wang, J.-Q. 51 (170), 96  
 Wang, K. 356 (326), 366  
 Wang, L. 169 (80), 186, 277 (202), 310  
 Wang, L. Y. 322 (46), 360  
 Wang, M. 559 (232), 590  
 Wang, P. 272 (176), 309, 328 (85, 86), 361  
 Wang, Q. 565 (258–261), 591, 667 (121, 122), 670 (123–125), 671 (126, 127), 678, 679  
 Wang, S. 341 (188), 363, 565 (256), 591, 644 (33), 677  
 Wang, S.-Y. 782 (39), 801  
 Wang, S. Z. 325 (73), 361  
 Wang, T. 291 (280), 312, 595 (8), 628  
 Wang, X.-J. 521 (58), 585  
 Wang, Y. 52 (173), 53 (174), 81 (228), 96, 98, 149 (46), 154, 293 (285), 312, 422 (25), 435, 547 (154), 566 (262), 588, 591  
 Wanklyn, J. A. 4 (30), 92  
 Warashina, M. 341 (189), 363  
 Warburg, O. 348 (247), 364  
 Ward, H. D. 765 (48), 769  
 Ward, H. R. 138 (20), 153  
 Wardell, J. L. 302 (339), 313  
 Warnock, D. G. 268 (64), 307  
 Warren, M. A. 325 (74), 361  
 Warshel, A. 352 (300), 365  
 Wasielewski, M. R. 194 (31), 195 (36), 215  
 Wasser, P. K. W. 208 (95), 217  
 Watabe, H. 561 (242), 591  
 Watanabe, K. 284 (178), 309  
 Watanabe, M. 526 (71), 586, 748 (41), 758 (44), 769  
 Watanabe, T. 194 (29), 213 (119), 215, 217, 701 (36), 715  
 Waterhouse, A. 621 (80), 630  
 Watkins, E. K. 657 (91), 678  
 Watson, S. C. 288 (261), 311  
 Watt, D. S. 528 (85), 586  
 Watt, G. D. 328 (86), 361  
 Weakley, T. J. R. 531 (94), 586  
 Weare, J. H. 348 (243), 364  
 Weatherstone, S. 15 (62), 17 (66), 81 (224, 259), 93, 97, 98, 414 (35, 46), 430 (80), 431 (82), 435, 436  
 Weaver, D. 667 (121), 678  
 Webb, L. J. 243 (84), 262  
 Weber, B. 571 (281), 591  
 Weber, F. 26 (94), 94  
 Weber, G. 349 (249), 364  
 Weber, J. 330 (105), 361  
 Webster, D. E. 122 (76), 128  
 Wedekind, J. E. 349 (253, 255, 259), 364, 365  
 Weeber, A. 49 (165), 96  
 Weghuber, J. 325 (66), 360  
 Wehlacz, J. T. 634 (12), 676  
 Wehmschulte, R. J. 79 (79), 81 (81), 94

- Wei, G. 563 (250), 591, 671 (128–130), 679  
 Wei, X.-H. 62 (120, 201), 95, 97  
 Weigmann, R. 579 (309), 592  
 Weinberg, M. S. 268 (107), 308  
 Weiner, M. 595 (8), 628  
 Weingarten, M. D. 718 (2), 768  
 Weinhold, F. 268 (147), 308  
 Weinmann, H. 513 (16), 584  
 Weiss, E. 5 (38), 6 (48), 9 (53), 10 (54), 14 (50), 25 (21, 22, 90), 38 (122, 123), 41 (125), 42 (49, 144), 50 (166), 89 (89), 92–96, 682 (3, 10), 714  
 Weiss, F. T. 300 (315), 313  
 Weiss, J. 207 (83, 84), 217  
 Welker, M. E. 648 (46), 677  
 Weller, D. D. 451 (34), 507  
 Welling, M. 160 (49–51), 185  
 Wells, J. A. 344 (211), 364  
 Welmaker, G. S. 563 (247), 591  
 Welsby, A. M. 109 (47), 127  
 Wende, W. 355 (319), 366  
 Wenkert, E. 656 (83), 678  
 Weskamp, T. 550 (166, 168), 589  
 Wessjohann, L. A. 774 (25), 801  
 Westeppe, U. 44 (152, 153), 45 (154, 156), 95, 96, 540 (118), 587  
 Westera, G. 145 (27), 153  
 Westerhausen, M. 27 (99), 81 (261), 94, 98, 302 (302), 312, 409 (30), 410 (37), 427 (72, 75), 435, 436  
 Westhof, E. 341 (192), 363  
 Weston, J. 332 (14), 344 (214), 350 (266), 359, 364, 365  
 Westover, K. D. 355 (313), 366  
 Whang, D. D. 268 (79, 84), 307  
 Whang, R. 268 (45, 79, 84, 99), 306, 307  
 Whetten, A. 171 (25), 185  
 Whitby, R. J. 673 (140, 141), 679  
 White, A. H. 31 (109), 40 (139), 46 (158), 58 (155), 81 (260), 94–96, 98, 123 (89), 129, 405 (5), 427 (74), 434, 436  
 White, A. J. P. 71 (231), 74 (241), 76 (242), 77 (250), 98, 411 (33), 418 (14), 424 (44), 434, 435, 484 (99), 508  
 White, D. A. 238 (6), 260  
 White, J. D. 667 (120), 678  
 Whiteside, R. A. 369 (1), 401  
 Whitesides, G. M. 137 (7), 138 (22–24), 141 (34), 153, 154, 156 (3), 184, 259 (148, 149), 263, 513 (14), 583, 584  
 Whittle, R. R. 56 (55), 69 (183), 93, 96, 410 (38), 429 (78), 431 (81), 435, 436, 684 (13), 714  
 Wiederhold, L. R. 353 (307), 366  
 Wiehe, A. 191 (8), 215  
 Wieneke, B. 27 (99), 94  
 Wieser-Jeunesse, C. 775 (28), 801  
 Wilcox, C. S. 485 (4), 506  
 Wilcox, D. E. 343 (48), 360  
 Wilczok, U. 45 (154), 95, 610 (60), 630  
 Wildschutz, T. 268 (117), 308  
 Wilke, G. 86 (266, 267), 99  
 Wilkes, J. G. 176 (125, 126, 128), 187  
 Wilkinson, G. 23 (75), 25 (87), 58 (3, 4), 92–94, 150 (12), 153, 512 (4), 513 (13), 583, 657 (90), 678  
 Wilkinson, H. S. 583 (319), 593  
 Wilkinson, P. D. 289 (269), 312  
 Willard, G. F. 424 (68), 436  
 Willems, J. L. 287 (248), 311  
 Willey, K. F. 124 (98), 129  
 William, A. D. 480 (11, 12), 506  
 Williams, D. J. 71 (231), 74 (241), 76 (242), 77 (250), 98, 411 (33), 418 (14), 424 (44), 434, 435, 484 (99), 508  
 Williams, E. R. 318 (19, 20), 359  
 Williams, L. D. 335 (30), 360  
 Williams, M. A. 300 (317), 313  
 Williamson, R. C. N. 282 (232), 311  
 Williard, P. G. 439 (5), 506  
 Wilson, D. M. 353 (305), 366  
 Wilson, P. D. 646 (37), 647 (43), 648 (44), 677  
 Wilson, S. H. 352 (288, 299), 365  
 Wilson, T. J. 341 (194), 363  
 Winkler, R. 318 (18), 359  
 Winnefeld, K. 278 (210), 310  
 Winter, C. H. 47 (160, 161), 50 (101), 72 (234), 78 (252), 83 (233), 84 (264), 94, 96, 98, 122 (77, 79), 128, 303 (303), 312, 419 (27), 422 (28, 29), 433 (89), 435, 436  
 Winterton, R. C. 247 (100, 101), 262  
 Wiss, J. 512 (10), 583  
 Wissing, E. 79 (258), 98  
 Witanowski, M. 138 (23, 25), 153  
 Witt, H. T. 356 (36, 324), 360, 366  
 Wittig, G. 4 (31, 32), 92, 686 (1), 714  
 Woerpel, K. A. 557 (214), 590  
 Wolf, F. I. 268 (58), 307, 317 (2), 359  
 Wolfes, H. 355 (320), 366  
 Wong, A. 357 (333), 366  
 Wong, I. 352 (289, 292), 365  
 Wong, K.-Y. 515 (26), 584  
 Wong, M. W. 369 (2), 384 (30), 401, 402  
 Wong, P. T. S. 300 (320), 313  
 Wong, T. 646 (37), 677  
 Wong, T. H. 162 (60), 164 (63), 169 (88, 89), 185, 186  
 Wood, R. D. 353 (304), 355 (316), 365, 366  
 Woodbury, N. W. 356 (327), 366  
 Woodle, M. 206 (80), 217  
 Woods, K. L. 268 (143), 308  
 Woods, L. A. 296 (298), 312  
 Woodson, S. A. 336 (155, 165), 337 (172), 362, 363  
 Woodward, C. A. 176 (120, 121), 186

- Woodward, J. 214 (136), 218  
 Woodward, S. 779 (33), 791 (50), 801  
 Woon, D. E. 107 (22), 126  
 Wotiz, H. 107 (28), 127  
 Wowk, A. 295 (286), 312  
 Wozniak, R. 25 (82), 94, 299 (307), 312  
 Wright, D. S. 57 (186), 96, 124 (91), 129  
 Wright, G. F. 300 (313), 313  
 Wright, L. 293 (267), 311  
 Wright, R. R. 175 (122), 187, 318 (23), 359  
 Wu, A-B. 458 (32), 507  
 Wu, G. 357 (333), 366  
 Wu, H.-F. 178 (130), 187  
 Wu, M.-J. 674 (152), 679  
 Wu, S. 162 (61), 185  
 Wu, T.-M. 16 (63), 93  
 Wu, W. 201 (72, 73), 216  
 Wu, Y. 168 (73), 186  
 Wu, Y.-D. 163 (70, 71), 168 (72, 74), 186, 391 (24), 402  
 Wurst, J. R. 514 (20), 584  
 Würthwein, E.-U. 579 (309), 592  
 Wyckoff, H. W. 354 (309), 366  
 Wynberg, H. 718 (2), 768  
 Wynne, K. 198 (56), 216  
 Xenos, D. 278 (207), 310  
 Xia, A. 47 (160, 161), 50 (101), 72 (234), 78 (252), 83 (233), 84 (264), 94, 96, 98, 122 (77, 79), 128, 303 (303), 312, 419 (27), 422 (28, 29), 433 (89), 435, 436  
 Xia, J. 540 (121, 122), 587  
 Xie, M. 644 (32, 33), 677  
 Xing, X. 351 (284), 365  
 Xiong, H. 254 (125), 263, 540 (119), 587  
 Xiong, Y. 419 (54), 435, 466 (66), 508, 538 (105), 587  
 Xu, D. 107 (20), 126  
 Xu, J. 421 (58), 435, 700 (35), 715  
 Xu, X. 619 (78), 630  
 Xu, Y. 521 (58), 585  
 Xu, Z. 671 (136), 672 (137–139), 673 (145), 679  
 Xuong, N. G. 351 (286), 365  
 Xuong, N. H. 347 (232), 348 (234, 241), 364  
 Yadav, J. S. 576 (303), 592  
 Yagi, K. 357 (336), 366  
 Yaginuma, F. 576 (302), 592  
 Yago, M. D. 268 (48), 307  
 Yahara, K. 194 (29), 213 (119), 215, 217  
 Yamabe, S. 384 (27), 402, 569 (275), 591  
 Yamada, A. 198 (64), 216  
 Yamada, S. 212 (114), 217, 514 (21), 584  
 Yamada, T. 327 (78), 361  
 Yamagami, T. 568 (272), 591, 622 (88), 623 (89), 630, 637 (23), 639 (24), 677  
 Yamaguchi, K. 63 (60), 93, 156 (7), 182 (6), 184, 419 (51), 435  
 Yamaguchi, S. 568 (272), 591, 622 (88), 630, 637 (23), 677  
 Yamakawa, K. 479 (14, 16), 485 (15, 17), 506, 721 (11), 743 (38), 760 (50), 766 (53), 768, 769  
 Yamamoto, C. 302 (326), 313  
 Yamamoto, H. 557 (211), 580 (312), 590, 592, 621 (81, 82), 630, 633 (1), 676, 690 (29), 715, 765 (48), 769, 774 (2), 779 (22), 800  
 Yamamoto, M. 274 (187), 310  
 Yamamoto, T. 285 (243), 311  
 Yamamura, M. 194 (29), 213 (119), 215, 217  
 Yamanaka, M. 791 (51), 802  
 Yamani, Y. 760 (50), 769  
 Yamasaki, K. 341 (199), 363, 774 (21), 800  
 Yamashita, H. 290 (274), 312  
 Yamataka, H. 259 (134), 263, 391 (11), 402, 466 (70), 471 (93), 508  
 Yamauchi, Y. 559 (225), 590  
 Yamazaki, I. 194 (30), 201 (75, 76), 206 (81, 82), 215–217  
 Yamazaki, S. 384 (27), 402, 569 (275), 591  
 Yamazaki, T. 558 (218), 590  
 Yan, H. 356 (326), 366  
 Yan, M.-C. 566 (262), 591  
 Yan, N. 659 (99), 678  
 Yanagida, T. 329 (97), 361  
 Yanagisawa, A. 557 (211), 590, 621 (81, 82), 630  
 Yang, B. 547 (158), 588  
 Yang, C. G. 419 (57), 435  
 Yang, C.-G. 538 (105), 587  
 Yang, D.-Y. 278 (209, 211, 212), 310  
 Yang, F. 302 (324, 338), 303 (318), 313  
 Yang, H. 572 (289), 592  
 Yang, J. 253 (120), 262  
 Yang, J.-X. 282 (228), 310  
 Yang, J. Z. 547 (156), 588  
 Yang, K.-C. 81 (228), 98, 149 (46), 154, 422 (25), 435  
 Yang, L.-L. 278 (211), 310  
 Yang, L.-M. 559 (230), 590  
 Yang, N. C. 595 (8), 628  
 Yang, Qi 495 (111), 509  
 Yang, S. 163 (65, 68–71), 164 (64), 166 (77), 167 (82–85), 168 (72–74, 86), 169 (78–80, 87, 93–96), 170 (97, 98), 185, 186  
 Yang, S. D. 268 (37), 306  
 Yang, S. I. 201 (38, 39), 215  
 Yang, S. K. 335 (143), 362  
 Yang, W. 350 (262), 355 (312), 365, 366, 384 (28), 402  
 Yang, X. 163 (65, 68, 69), 164 (64), 185, 186  
 Yang, Y. L. 353 (308), 366  
 Yang, Z. 247 (35, 103), 261, 262, 279 (216), 310, 572 (288), 592  
 Yang, Z. Y. 516 (30), 517 (34), 584  
 Yao, C.-F. 566 (262), 591



- Yao, J. 567 (267), 591  
 Yao, S.-Z. 273 (183), 309  
 Yap, G. P. A. 647 (42, 43), 677  
 Yarkony, D. 332 (131), 362  
 Yarus, M. 337 (173), 363  
 Yasar, S. B. 271 (161), 309  
 Yasuda, H. 51 (167), 96, 121 (74), 123 (73), 128, 254 (126), 263, 540 (119), 587  
 Yasuda, M. 686 (22), 688 (23), 714  
 Yasuda, N. 524 (63), 585, 702 (39), 715  
 Yasuda, R. 329 (96, 100), 361  
 Yasui, H. 557 (216), 590, 643 (30), 677  
 Yazawa, T. 300 (314), 313  
 Yee, N. K. 103 (9), 126, 517 (37), 584  
 Yee, R. 253 (124), 263  
 Yeh, C. S. 124 (98), 129  
 Yeh, S.-M. 547 (154), 588  
 Yellowlees, L. J. 81 (255, 256), 98, 407 (21, 22), 434  
 Yeo, W. W. 268 (142), 308  
 Yiin, S.-J. 547 (154), 588  
 Yin, H.-M. 169 (95), 186  
 Yin, Y. W. 355 (314), 366  
 Yokoi, N. 193 (25), 215  
 Yokoo, T. 527 (73), 540 (122), 586, 587  
 Yokoyama, Y. 741 (36), 769  
 Yonemoto, W. 347 (231), 364  
 Yonemura, H. 212 (114), 217  
 Yong, K. H. 54 (177), 83 (176), 96, 426 (31), 435  
 Yoon, K. 305 (362, 363), 314  
 Yoon, T. 559 (229), 590  
 Yorimitsu, H. 545 (139, 140), 546 (141), 557 (216), 560 (237, 238), 567 (269), 568 (273), 588, 590, 591, 636 (17, 22), 643 (30), 676, 677, 707 (45), 715, 791 (50), 801  
 Yorimitsu, Hideki 675 (158), 714  
 York, O. 633 (5), 676  
 Yoshida, A. 538 (108), 587  
 Yoshida, J. 219 (9), 260, 608 (56), 629, 641 (27, 28), 662 (109), 664 (108), 677, 678  
 Yoshida, J.-I. 555 (199), 589  
 Yoshida, K. 774 (24), 800  
 Yoshida, K. A. 779 (33), 801  
 Yoshida, M. 329 (96, 98, 100), 361  
 Yoshida, Y. 157 (21), 185  
 Yoshida, Z. I. 502 (119, 120), 509  
 Yoshida, Z.-I. 452 (37), 507  
 Yoshikai, N. 550 (169), 555 (200), 589  
 Yoshinari, K. 341 (189), 363  
 Yoshino, S. 268 (139), 308  
 Yoshino, T. 145 (38), 154  
 Yoshiwara, H. 517 (34), 519 (54), 584, 585  
 Young, M. A. 171 (105), 186  
 Young, W. G. 141 (33), 154  
 Youngblood, W. J. 201 (45), 216  
 Yousef, R. I. 59 (132), 95, 149 (6), 153  
 Yu, B.-S. 273 (183), 309  
 Yu, C. 293 (285), 312  
 Yu, N. 337 (169), 363  
 Yu, S. 103 (4), 126  
 Yu, S. H. 116 (59), 128  
 Yu, Z. 514 (23), 584  
 Yuan, H. S. H. 86 (268), 99  
 Yuan, Q.-G. 273 (183), 309  
 Yuan, T. 162 (61), 185  
 Yuan, T.-M. 547 (154), 588  
 Yuki, H. 60 (194–196), 61 (197), 97  
 Yun, H.-S. 553 (178), 589  
 Yurkowski, M. 301 (356), 314  
 Yvernault, T. 290 (273), 292 (281), 312  
 Zabicky, J. 297 (260), 311  
 Zacharoulis, D. 278 (207), 310  
 Zagatto, E. A. G. 280 (224), 310  
 Zakrzewski, J. 198 (62), 216  
 Zakrzewski, V. G. 384 (30), 402  
 Zaleski, J. M. 196 (44), 201 (73), 216  
 Zanzizzi, P. F. 328 (83), 361  
 Zandler, M. E. 201 (41, 42), 216  
 Zanello, P. 30 (108), 94, 243 (86), 262  
 Zani, L. 596 (30), 629  
 Zapf, A. 544 (129, 130), 588  
 Zarzuelo, M. M. 583 (319), 593  
 Zaug, A. J. 335 (149), 362  
 Zawadzka, M. 212 (113), 217  
 Zawadzki, S. 547 (147), 588  
 Zecchina, A. 125 (108), 129  
 Žemva, B. 74 (248), 98, 424 (16), 434  
 Zeng, Y. 277 (202), 310  
 Zerbini, I. 268 (130), 308  
 Zerevitinov, T. 299 (308), 312  
 Zewge, D. 699 (31), 715  
 Zhai, L. 286 (244), 311  
 Zhang, D. 622 (87), 630, 652 (53), 677  
 Zhang, E. 320 (26), 349 (256, 258), 360, 364, 365  
 Zhang, F. 659 (99), 678  
 Zhang, H. 51 (171, 172), 52 (173), 53 (174), 96, 200 (67), 201 (72), 216  
 Zhang, J. 268 (72), 307, 347 (237), 356 (326), 364, 366  
 Zhang, L. 521 (58), 585  
 Zhang, M.-X. 419 (56, 57), 435, 538 (105, 106), 587  
 Zhang, P. 395 (37), 402  
 Zhang, R. 327 (67), 360  
 Zhang, W. 760 (47), 769, 779 (20), 800  
 Zhang, X. 168 (73), 186  
 Zhang, X.-H. 163 (70), 168 (72, 74), 186  
 Zhang, Y. 348 (244), 350 (262), 364, 365  
 Zhang, Y. H. 322 (46), 360  
 Zhang, Z. 528 (87), 563 (250), 565 (260, 261), 586, 591, 670 (123, 125), 671 (127–130), 679  
 Zhao, H. 540 (122), 587  
 Zhao, J.-F. 282 (228), 310

- Zhao, L. 162 (61), 167 (83), 185, 186, 452 (36), 507  
 Zhao, L. J. 322 (46), 360  
 Zhao, X. 161 (55), 185  
 Zhel'vis, A. I. 224 (32), 261  
 Zhen, P. 277 (202), 310  
 Zheng, C. 51 (170), 96  
 Zheng, J. 347 (232), 364  
 Zheng, W. 107 (20), 126  
 Zheng, X. 29 (103), 94  
 Zhong, X. 352 (296), 365  
 Zhonghua, L. 253 (118), 262  
 Zhou, D. M. 337 (152), 341 (201), 362, 363  
 Zhou, G. 648 (47), 677  
 Zhou, G. X. 291 (280), 312  
 Zhou, J. 348 (240), 364  
 Zhou, J. M. 341 (201), 363  
 Zhou, M. 159 (36), 185  
 Zhou, Q-L. 774 (8), 800  
 Zhou, Q. 302 (327), 313, 325 (73), 361  
 Zhou, Q.-f. 302 (336), 313  
 Zhou, X. 277 (202), 310  
 Zhou, Y. 329 (92), 361  
 Zhou, Z.-Z. 282 (228), 310  
 Zhu, B.-Y. 572 (276), 591  
 Zhu, D. 51 (171, 172), 53 (174), 96  
 Zhu, L. 272 (174), 309  
 Zhu, S. 514 (23), 584  
 Zhu, W. 123 (90), 129  
 Zieger, H. E. 142 (36), 154  
 Ziegler, K. 221 (24, 25), 222 (27), 260  
 Ziemer, K. 62 (203), 97  
 Ziller, J. W. 69 (223), 97  
 Zimmerman, H. E. 503 (53), 507  
 Zirngast, M. 38 (130), 95  
 Zisbrod, Z. 268 (19), 306  
 Zoellner, E. A. 289 (270), 312  
 Zoller, M. J. 347 (235), 364  
 Zouni, A. 356 (324), 366  
 Zsurka, G. 325 (66), 360  
 Zubritskii, L. M. 540 (123), 587  
 Zuiderweg, E. R. P. 344 (212), 364  
 Zureck, J. 333 (133), 362  
 Zuther, F. 214 (126, 127), 218  
 Zwierzak, A. 547 (147), 588

# Subject Index

Entries are in letter-by-letter alphabetical order ignoring spaces and punctuation marks. Page numbers in *italic* refer to Figures and Tables not included in the relevant page ranges.

- AAS *see* Atomic absorption spectrometry  
*Ab initio* calculations, modified Schlenk equilibrium, 378–380  
 Absorption spectra, tetrapyrroles, 192–193  
 Acetaldehyde, Mg cation complex, 169  
 Acetamide, Mg cation fragmentation, 176, 177  
 Acetates, aldol stereochemistry, 447  
 Acetic acid  
   Mg cation complex, 169  
   organomagnesate anion decarboxylation, 181  
 Acetolysis, enthalpies of reaction, 120  
 Acetone  
   enthalpy of formation, 115  
   Mg cation binding energy, 175  
 Acetonitrile, Mg cation fragmentation, 176, 177  
 Acetophenone  
   butylation, 684–685  
   potentiometric titration, 292  
 Acetylenes  
   halogen–Mg exchange, 526  
   hydromagnesiation, 540, 543  
 Acetylenic fragments, PET, 196, 197  
 Acetylenic organomagnesium amides, structures, 81–82  
 Acetylides, donor–acceptor complexes, 42–43  
 Acid–base reactions, organomagnesium anions, 180  
 Acid Chrome Blue K, UV–visible spectrophotometry, 282  
 L-Acosamine, aminosugar, 487, 488  
 Active hydrogen compounds  
   gas chromatography, 295  
   Grignard analytical reagents, 299–300  
 Acyclic enones, enantioselective conjugate addition, 774, 779, 780  
  
 $\alpha$ -Acyl aminoesters, preparation, 462, 497–498  
 Acylation, Fe-catalyzed, 559, 599–603  
 C-Acylation, dialkyl malonate, 462, 494–496  
 Acyl chlorides, organometallic compound acylation, 559  
 N-Acyloxazolidinones  
   aldol-type reaction, 503  
   amination, 504  
   preparation, 462, 463  
 Acyl silanes,  $\alpha,\beta$ -unsaturated, 450  
 N-Acylthiazolidinethiones  
   aldol-type reaction, 503  
   preparation, 462, 463  
 Addition reactions  
   1,2-addition, 17, 450–451, 569  
   1,4-addition, 4–5, 450–451, 478, 543, 547, 563–565  
     asymmetric, 454–457, 564  
   addition–elimination, 471  
   conjugated unsaturated carbonyl compounds, 624–625, 626, 628  
   enantioselective addition, 571  
     conjugate addition, 771–791  
   functionalized Grignard reagents, 543, 559–575  
 Grignard carbonyl additions  
   experimental background, 370–374  
   polar mechanisms, 370, 387–388, 389, 391, 394, 396, 400–401  
   theoretical studies, 369–370, 374–401  
   transition-state structures, 375–376, 377, 380–382, 388–389, 391, 393, 394–396  
   without solvent molecules, 384–389, 390, 391

- Addition reactions (*continued*)  
    with solvent molecules, 389, 391, 392, 393, 401  
    nucleophilic, 256–257, 683–686  
    organomagnesiates  
        1,2-addition, 17  
        1,4-addition, 4–5  
    oxidative, 512–515  
    *see also* Carbomagnesiation; Conjugate addition  
Adduct-forming reactions  
    Mg cations, 160  
    radiative associative, 160  
Adenosine diphosphate *see* ADP  
Adenosine monophosphate *see* AMP  
Adenosine triphosphate *see* ATP  
ADP, glycolytic cycle, 345, 346  
AES *see* Atomic emission spectrometry  
Agostic interactions  
    diorganomagnesium compounds, 24  
    heteroleptic organomagnesiates, 18  
Air exclusion, calorimetry, 104  
Alcohols  
    active hydrogen determination, 299  
    Mg cation reactions, 161, 165–166  
Aldehydes  
    one-carbon ring expansion, 763–764  
    organomagnesium amide reactions, 423–426  
Aldol-type reactions  
     $\alpha$ -bromoketones, 440, 482  
    diketones, 493–495  
     $\beta$ -hydroxyacid synthesis, 486  
     $\beta$ -lactam, 499–500  
    lactone synthesis, 486  
    magnesium enolate preparation, 447–450, 463  
    oxazolidinones, 503  
    silyl enol ether, 472–473, 484, 486  
     $\alpha$ -sulfinyl magnesium carbanion enolates, 459, 486, 487, 500  
    sulfoxides, 486, 487  
    tandem conjugate addition, 453, 788, 789  
    thioamides, 500–501, 502  
Alkali-activated PTFE tube, UV–visible fluorometry, 283  
Alkali alkoxides, heteroleptic organomagnesiates production, 15–16  
Alkaline phosphatase (AP), allosteric behavior, 344  
Alkalinity, hydrolysis, 289  
Alkanes  
    Mg atom reactions, 157  
    Mg cation reactions, 160, 162–163, 180  
Alkenes  
    carbomagnesiation reactions, 633, 653–674  
    allyl/homoallyl alcohols, 664–671  
    allylmagnesiation, 655–657  
    intermolecular, 655–656, 662, 663, 665–666, 671–674  
    intramolecular, 654–655, 656, 661–662, 665–666  
    simple alkenes, 653–655  
    strained alkenes, 657–661  
    vinylsilanes, 661–664  
    Zr-catalyzed ethylmagnesiation, 671–674  
    Mg cation reactions, 160  
ortho-Alkenylated products, formation, 749, 750–751  
Alkenylation  
    arylamines, 748–749, 750–751  
    Fe-catalyzed, 604–608, 626  
    magnesium alkylidene carbenoids, 748  
Alkenylboron reagents, Rh-catalyzed conjugate addition, 774  
Alkenyl bromides  
    Br<sub>2</sub>–Mg exchange, 527  
    Fe-catalyzed cross-coupling, 604–605, 606, 607–608  
Alkenyl chlorides, Fe-catalyzed cross-coupling, 605, 606, 607–608  
Alkenyl derivatives, Fe-catalyzed cross-coupling, 608–610  
Alkenyl halides  
    Fe-catalyzed cross-coupling, 605–608  
    halogen–Mg exchange, 525–526  
Alkenyl iodides, I<sub>2</sub>–Mg exchange, 526–527  
Alkenyl sulfides, trisubstituted, 758–760  
Alkoxides  
    cubane structure, 70–71, 145, 146  
    heteroleptic monoorganomagnesium compounds, 69–71  
    NMR spectra, 145–147  
    organomagnesium-group 16-bonded complexes, 428–432  
    solution-state species, 132, 133  
Alkoxydialkylmagnesate, addition reactions, 711, 713  
Alkoxymagnesium bromides, enthalpies of formation, 114–115, 116  
Alkylation  
    enantioselective allylic, 792–799  
    enolate intermediate, 762, 763  
    Fe-catalyzed, 615–618  
Alkyl bromides  
    cross-coupling reactions  
        Fe-catalyzed, 617  
        transition-metal-catalyzed, 544–546  
    *n*-Alkyl bromides, transition-metal-catalyzed cross-coupling, 544  
Alkyl chlorides, primary, 544  
Alkyl fluorides, transition-metal-catalyzed cross-coupling, 545  
Alkyl Grignard reagents

- Fe-catalyzed arylation and heteroarylation, 610–614  
oxidation at inert electrodes, 232–233  
distribution of anodic products, 232
- Alkyl halides  
halogen–Mg exchange, 528  
Mg atom reactions, 157–158  
Mg cation reactions, 160–161  
Mg cluster reactivity, 157  
multi-carbon homologation, 723–724  
Schlenk equilibrium, 108–109, 134
- Alkylidene carbenoids *see* Magnesium alkylidene carbenoids
- Alkylidene cyclopropanes, synthesis, 739–740
- Alkylmagnesium amides, weak acid deprotonation, 419
- Alkylmagnesium bromides, methylene increment, 110–111
- Alkylmagnesium chlorides  
lithium chloride complexes, 682  
Schlenk equilibrium, 107  
transition-metal-catalyzed cross-coupling, 545
- Alkylmagnesium compounds, NMR spectra, 133–138, 141
- Alkylmagnesium fluorides, Schlenk equilibrium, 107
- Alkylphosphonium ylides, addition, 567
- Alkyl transfer, catalytic enantioselective conjugate addition, 790
- Alkyl trihaloacetate, halogen–metal exchange, 442
- Alkynes  
carbomagnesiation reactions, 633–653  
alkynylsilanes, 639–641, 642  
intermolecular, 635–639  
intramolecular, 633–635  
N-, O- and S-attached alkynes, 641–644  
propargyl alcohols, 645–652  
propargyl amines, 652–653  
Mg film self-hydrogenation, 173  
unactivated, 567, 568
- Alkynylsilanes, carbomagnesiation, 639–641, 642
- All-carbon quaternary chiral centers, 565
- Allenes  
Doering–LaFlamme synthesis intermediates, 735–738  
magnesium alkylidene carbenoid alkenylation, 748
- 2,-Allenols, synthesis by substitution, 559, 560
- $\beta$ -Allenyl ester magnesium enolates, asymmetric synthesis, 449, 450, 506
- Allenyl iodides,  $I_2$ –Mg exchange, 527, 528
- Allenyl ketones,  $\alpha,\beta$ -enone formation, 563
- Allosteric enzymes, protein-based, 343–345
- Allyl alcohols  
carbomagnesiation, 664–671  
cyclopropanation, 722  
substitution, 557
- Allyl amines, functionalized Grignard reactions, 548, 549
- Allyl carbamates, substitution, 557
- Allyl ethers, substitution, 557
- Allylic alkylation, enantioselective, 792–799
- Allylic isomers, allylmagnesium compounds, 142–143, 144
- Allylic *N*-protected aminoesters, magnesium chelate, 446
- Allylic substitutions, functionalized Grignard reagents, 543, 557–558
- Allylmagnesiation, alkenes, 655–657
- Allylmagnesium bromide, DME complex, 59
- Allylmagnesium chloride  
di-Grignard reagents, 62  
tetraorganomagnesiates production, 7
- Allylmagnesium compounds  
allylic exchange, 142, 143  
dynamic equilibria, 143, 144  
 $^nJ_{HH}$  spin coupling constants, 143–144, 145  
NMR spectra, 141–145, 151  
Schlenk equilibrium, 107, 140, 142, 144–145
- Allylmagnesium  $\beta$ -diketiminates, structure, 76, 77
- Allylmagnesium halides,  
transition-metal-catalyzed cross-coupling, 545–546
- Allylsilanes, catalyzed addition to C=C bonds, 561
- Aluminum compounds, organic derivatives, 103
- Amide enolates, reactions with electrophiles, 499–500
- Amides  
heteroleptic monoorganomagnesium compounds, 54, 71–83  
mixed Mg/Li, 539  
secondary, 81, 82  
Weinreb, 559  
*also* Organomagnesium amides
- Amidocuprates, oxidative coupling, 580–581
- Amination  
*N*-acyloxazolidinones, 504  
electrophilic, 575–580
- Amines  
active hydrogen determination, 299  
carbomagnesiation, 641–642, 652–653, 667  
Mg cation complexes, 167–169  
sterically hindered, 457, 464, 538
- $\alpha$ -Amino acids  
electrophilic reactions, 729, 730  
functionalized Grignard reagent synthesis, 517–518
- $\beta$ -Amino acids, chiral derivatives, 454

- $\beta$ -Amino- $\alpha,\beta$ -diesters, Michael addition preparation, 489
- Aminoester enolates, 487, 489
- Aminoesters, allylic *N*-protected, 446
- $\gamma$ -Amino- $\beta$ -ketoester derivatives, ethyl hydrogen malonate, 497
- $\alpha$ -Amino-substituted carbanions, non-stabilized, 728–729
- $\alpha$ -Amino-substituted cyclopropylmagnesium, 740, 741–742
- Aminosugar, L-acosamine, 487, 488
- Ammonia, organomagnesium ion reactivity, 180
- AMP, cAMP, 347–348
- Analytical aspects, 265–314
- acronyms, 266–267
  - elemental analysis of Mg, 268, 269–288
  - Grignard analytical reagents, 269, 299–305
  - speciation analysis, 268, 269, 288–299
- Angle strain, magnesacycloalkanes, 120–121
- Anhydrides, enantioselective desymmetrization, 571
- Aniline, potentiometric titration, 291
- Anilines, functionalized Grignard reagent protection, 530–531
- Anion abstraction, Mg cation–organohalogen complexes, 163
- Anionic ligands, Mg cation fragmentation, 176–178
- Anions
- anthracene radical anions, 45, 46
  - bimolecular reactions, 180–182
  - bis-anions, 15
  - chiral oxazolidinones, 503–505
  - $\beta$ -diketiminates, 74
  - indenyl, 29
  - magnesium complex fragmentation, 178–179
  - speciation analysis of Mg, 269
  - tris[aryl]magnesiates, 35
- ANN (artificial neural networks), 269–270
- Anodic oxidation, 227–244
- diorganomagnesium compounds, 227–228
  - Grignard reagents, 228–243
    - addition to olefins, 237
    - inert electrodes, 229–236
    - reactivity, 235–236, 258–260
    - sacrificial anodes, 237–241
    - semiconductor anodes, 241–243
- Antenna pigments, chlorophylls, 191
- Anthracene, magnesium compounds, 44–47, 514
- 9-Anthraldehyde, liquid chromatography, 293
- Anti*-carbomagnesiation
- alkenes, 672–673
  - alkynes, 644, 645–651
- AP (alkaline phosphatase), 342
- Arene metalation, heteroleptic organomagnesiates production, 22
- Aromatic compounds, carbomagnesiation reactions, 674–675, 676
- Aromatic Grignard reagents, Fe-catalyzed homocoupling, 619–621
- Arrays, porphyrins, 201, 204–205
- Arsenic compounds, derivatization, 303
- Artificial neural networks (ANN), speciation analysis, 269–270
- Aryl acetic acids, Ivanov reaction, 458, 502, 503
- Aryl amidocuprates, oxidative coupling, 580–581
- Aryl amines, direct alkenylation, 748–749
- Arylation, Fe-catalyzed, 610–614
- Arylazo tosylates, electrophilic amination, 577–578
- Arylboron reagents, Rh-catalyzed conjugate addition, 774
- Aryl chlorides
- dechlorination, 554
  - Fe-catalyzed cross-coupling, 611, 612
  - functionalized Grignard reagent preparation, 513
  - Kumada–Tamao–Corriu reactions, 550
- Aryl fluorides, transition-metal-catalyzed cross-coupling, 550, 551
- Aryl glycines, synthesis, 574–575
- Aryl Grignard reagents
- Fe-catalyzed reactions
    - addition, 624–625
    - alkylation, 615–618
    - heteroarylation, 614–615
    - homocoupling, 619–621
    - functionalized, 601, 603
    - oxidation at inert electrodes, 233–235
    - distribution of anodic products, 233
- Arylmagnesium compounds
- dynamic equilibria, 140
  - NMR spectra, 134, 138–140, 151
- Aryloxides
- NMR spectra, 146, 147
  - organomagnesium-group 16-bonded complexes, 428–432
  - solution-state species, 132, 133
- Aryl sulfoxide, halogen–Mg exchange, 526
- Aryl tosylates, Fe-catalyzed cross-coupling, 611, 612
- Aryl triflates, Fe-catalyzed cross-coupling, 611, 612
- Arynes, functionalized Grignard reagent synthesis, 540, 542
- Association, Grignard reagents, 108
- Asymmetric 1,4-addition
- magnesium enolate preparation, 454–457
  - Michael acceptors, 564
- Asymmetric aldol-type reactions,  $\alpha$ -sulfinyl magnesium carbanion enolates, 459, 486, 487, 500

- Asymmetric homologation, chiral magnesium carbenoids, 722
- Asymmetric synthesis  
cyclopropane derivatives, 734  
magnesium enolates, 454–457  
     $\beta$ -allenyl ester magnesium enolates, 449, 450, 506  
     $\beta$ -sulfinyl ester magnesium enolates, 448, 449
- Ate complexes, 681–715
- Atomic absorption spectrometry (AAS)  
elemental analysis, 272, 277–278  
Mg in body fluids, 270
- Atomic emission spectrometry (AES)  
elemental analysis, 278–279  
ICP–AES, 279, 284  
Mg in body fluids, 270
- Atomization *see* Enthalpies of atomization
- ATP  
biosynthesis, 329–331  
hydrolysis, 331–333  
isotope effect, 330  
MgATP, 328–329  
Mg<sup>2+</sup> binding, 317, 331–332  
NMR spectroscopy, 286–287
- ATP synthases  
biosynthesis of ATP, 329–330  
PET, 194–195
- Aza-allyl type bonding, diorganomagnesium compounds, 32
- Aza-crowns, monoorganomagnesium cations, 56
- Aziridines, ring opening, 547
- Bacteria, photosynthesis, 194
- Bacteriochlorins, photosynthesis, 192–193
- Bacteriochlorophylls, photosynthesis, 191
- Barbier conditions, functionalized Grignard reagent synthesis, 514
- Base excision repair, DNA, 353–354
- Bases, acid–base reactions, 180
- Benzalacetomesitylene, Michael addition, 451
- Benzene complexes, photodissociation spectra, 163
- Benzimidazoles, synthesis, 577
- Benzophenone, potentiometric titration, 292
- Benzotriazole, substitution leaving group, 547, 548
- O*-Benzoyl-*N,N*-dialkylhydroxylamines, electrophilic amination, 579
- Benzyl-*n*-chloroamines, electrophilic amination, 578–579
- Benzyllic magnesium reagents, S–Mg exchange, 529–530
- Benzyne, radical cations, 163–164
- Biaryl compounds, transition-metal-catalyzed cross-coupling, 554
- Bicyclo[*n*.1.0]alkanes, 1,3-C–H insertion of magnesium carbenoids, 732, 733–734
- Bidentate coordination  
Mg cation–alcohol complexes, 166  
Mg<sup>2+</sup>, 322, 324
- Bifunctional organomagnesium compounds, structure, 39–40
- 1,1-Bimetallic species, addition reactions, 566–567
- Bimolecular reactions, gas-phase organomagnesium ions, 179–182
- BINAP ligand, catalytic enantioselective conjugate addition, 775, 776, 782–784
- Binary magnesium salts, enthalpies of atomization, 115
- Binding energies, Mg cations, 175
- Binding mechanisms, Mg, 320–324, 331–332
- Biochemistry, Mg, 315–367
- Biochromism, polythiophene, 285
- Biological issues, Mg analysis, 268–269, 270, 275–276, 278–279, 282, 287–288
- Biomedical issues, Mg analysis, 268–269, 278
- Biosynthesis, ATP, 329–331
- 2,2'-Biquinoline, indicator, 288, 289
- Bis(allyl)magnesium compounds, NMR spectra, 143, 144–145, 151
- Bis(amide) species  
deprotonation of arenes, 419, 421  
disproportionation reactions, 422  
formation, 412
- 1,2-Bis(2-aminophenoxy)ethane-*N,N,N',N'*-tetraacetic acid, UV–visible spectrophotometry, 282, 283
- Bis-anions, heteroleptic organomagnesiates, 15
- Bis(*ortho*-anisyl)magnesium, structure, 34, 35
- Bis(benzene)chromium, heteroleptic organomagnesiates production, 22
- Bis[1,3-bis((dimethoxy)methyl)phenyl]magnesium, structure, 34, 35
- Bis[1,3-bis((dimethylphosphino)methyl)phenyl]magnesium, structure, 36
- Bis *tert*-butylmagnesium, structure, 24–25
- Bis(4-*tert*-butylphenyl)magnesium, donor–acceptor complexes, 41–42
- Bis(cyclopentadienyl)magnesium *see* Magnesocene
- Bis-deprotonation, ethyl hydrogen malonate, 458
- Bis[3-(dialkyl)aminobutyl]magnesium, structure, 32–33
- Bis[4-(dialkylamino)butyl]magnesium, structure, 32–33
- 1,5-Bis(3,5-dichloro-2-hydroxy)-3-cyanoformazan, UV–visible spectrophotometry, 282
- Bis[2,6-diethylphenyl]magnesium, structure, 24, 25

- 1,2-Bis[(2,6-diisopropylphenyl)imino]acene-  
phenanthrene, radical anion, 79, 80
- Bis[2-(*N,N*-dimethylamino)ethyl]ether,  
halogen–Mg exchange, 521, 523
- Bis[(2-(dimethylamino)methyl)ferrocenyl]  
magnesium, structure, 30, 31
- 2,6-Bis(imino)pyridines, dialkylmagnesium  
compound reactions, 71–72
- Bis(indenyl)magnesium, structure, 28–29, 48
- exo,exo*-Bis(iso-dicyclopentadienyl)magnesium,  
structure, 27
- Bis(1-methylboratabenzene)magnesium,  
structure, 29
- Bis(2-methylbutyl)magnesium, sparteine  
complex, 148
- Bis(neopentyl)magnesium, structure, 23
- Bis(pentamethylcyclopentadienyl)magnesium,  
carbene complex, 53–54
- 1,4-Bis(phenyl)-2-butene-1,4-diylmagnesium  
tris-THF complex, structure, 51, 52
- Bis[ $\alpha$ -(2-pyridyl)- $\alpha,\alpha$ -bis(trimethylsilyl)  
methyl]magnesium, structure, 31–32
- N,N'*-Bis(salicylidene)2,3-diaminobenzofuran,  
UV–visible fluorometry, 283, 284
- Bis(2-thienyl)magnesium, donor–acceptor  
complexes, 43
- Bis(thiomethyl)magnesium compounds,  
structure, 42, 43
- Bis(toluene)chromium, heteroleptic  
organomagnesium production, 22
- Bis(*p*-tolyl)magnesium, structure, 37–39
- Bis[2,4,6-tri-*t*-butylphenyl]magnesium,  
structure, 23–24
- 9,10-Bis(trimethylsilyl)anthracene magnesium,  
structure, 45–46
- 1,4-Bis(trimethylsilyl)-2-butene-1,4-  
diylmagnesium, TMEDA complex, 51,  
52
- Bis[(trimethylsilyl)methyl]magnesium,  
structure, 23–24
- Bis(trimethylsilyl)peroxide, hydroxycarbonyl  
compound synthesis, 475
- Blood  
AAS, 278  
AES, 279  
electrolyte determination, 275–276  
mass spectrometry, 288
- BMDA (bromomagnesium diisopropylamide),  
472, 473
- Boc-protected 2-substituted pyrroles,  
magnesium enolate, 447, 449
- Body fluids, elemental analysis, 270, 278–279
- Bond dissociation energies, 102  
magnesium cationic sandwiches, 124
- Bond energies  
cyclopentadienyl magnesium, 123  
heteroatom organomagnesium bromides,  
115  
magnesium cationic sandwiches, 124–125
- Bonds  
C=C addition, 471, 559–568  
C–halogen bond strength, 516  
C–H bond activation, 158  
C=N addition, 571–575  
C–O bond activation, 159, 161, 167  
C=O addition, 569–571  
C–X bond activation, 48, 156, 158, 159  
electron-deficient, 5  
Mg–F, 103
- Bone, mass spectrometry, 288
- Boronic acids, conjugate addition, 774
- Boron reagents, conjugate addition, 774
- Borosilicate glass, silanol groups, 300
- Breast cancer, elemental analysis in hair, 278
- Bridge bidentate coordination,  $\text{Mg}^{2+}$ , 322
- Bridging amide nitrogen atoms, heteroleptic  
organomagnesiums, 21
- Britton–Robinson buffer, UV–visible  
spectrophotometry, 282
- Bromine–magnesium exchange  
functionalized Grignard reagent synthesis,  
515, 519–526, 527, 528, 529  
lithium magnesates, 692–694, 696–700,  
702, 703–707, 711, 712–713
- o*-Bromoaryl magnesium, functionalized  
Grignard reagent synthesis, 520, 521
- 9-Bromo-9-[(bromomagnesium)methylene]  
fluorene, THF complex, 59
- Bromocresol Green, UV–visible  
spectrophotometry, 280, 281
- $\alpha$ -Bromoketones  
Mg-mediated aldol-type reaction, 440, 482  
permutational halogen/metal  
interconversions, 437–440, 482  
Polysantol preparation, 440
- 2-(Bromomagnesium)-1,3-phenylene-16-crown-5,  
66, 67
- 2-(Bromomagnesium)-1,3-xylyl-15-crown-4, 66,  
67
- 2-(Bromomagnesium)-1,3-xylyl-18-crown-5, 66,  
67
- Bromomagnesium diisopropylamide (BMDA),  
472, 473
- Bromomagnesium enolates, 438–440, 449
- 3-Bromopropenyl esters, enantioselective  
allylic alkylation, 799
- Bromopyrogallol Red, elemental analysis of  
Mg, 277
- Bromothiophenes,  $\text{Br}_2$ –Mg exchange, 525
- Bronsted acids, magnesium bromide salts, 113,  
115
- Bruceantin tetrahydrofuran ring, 478
- 1,3-Butadiene, transition-metal-catalyzed  
cross-coupling, 544
- Butanol  
gas chromatography, 295



- titration, 288, 291, 293
- Butenolide, enantioselectic allylic alkylation/chela, 799
- Buttenberg, Fritsch–Buttenberg–Wiechell rearrangement, 742–744
- t*-Butyl acetate, metalation, 457, 466
- tert*-Butylallylmagnesium chloride, Schlenk equilibrium, 145
- Butylmagnesium, nucleophilic addition, 684–685
- t*-Butylmagnesium chloride, sparteine complex, 60
- 2-[(4-*tert*-Butylphenyl)magnesium]-1,3-xylene-18-crown-5, 35–36
- C<sub>2</sub>-symmetric ligand, catalytic enantioselective conjugate addition, 782–784
- Cadmium compounds, derivatization, 304
- Calmagite, UV–visible spectrophotometry, 282
- Calorimeters, 104–105
- Calorimetry, 104–106
- cAMP, protein kinase interactions, 347–348
- Cancer, pathogenesis indicators, 278
- Capillary electrophoresis, tube coating, 301, 305
- Carbanions
- cycloalkylmagnesium halides, 118
  - non-stabilized  $\alpha$ -amino-substituted, 728–729
  - $\alpha$ -sulfinyl lithium, 760–766
  - $\alpha$ -sulfinyl magnesium enolates, 459, 486, 487, 500
  - $\alpha$ -sulfonyl lithium, 727–728, 748
- Carbazoles, functionalized, 533, 534
- Carbenacyclopropanes *see* Magnesium cyclopropylidenes
- Carbenes
- bis(pentamethylcyclopentadienyl)magnesium complexes, 53–54
  - synthesis intermediates, 718, 735
- Carbenoids *see* Magnesium carbenoids
- Carbocations, Mg atom reactions, 159
- Carbocyclic compounds, thermochemistry, 117
- Carbomagnesiation reactions, 631–679
- alkenes, 633, 653–674
  - alkynes, 633–653
  - anti*-carbomagnesiation, 644, 645–651
  - aromatic compounds, 674–675, 676
  - functionalized Grignard reagents, 543
- Carbometalation, Fe-catalyzed, 622–623
- Carbon, Mg compounds, 106–107
- Carbon–carbon bonds
- C=C addition, 471, 559–568
  - 1,4-addition to Michael acceptors, 563–565
  - activated alkenes, 565–567
  - catalyzed, 559–562
  - triple C–C bonds, 567–568
- Carbon dioxide
- liquid chromatography, 293
  - organomagnesium ion reactivity, 180
- Carbon dioxide fixing, rubisco enzyme, 357–359
- Carbon–halogen bonds
- reactivity order, 516
  - reductive metal insertion, 438–441
- Carbon–hydrogen bond activation, 158
- 1,2-Carbon–hydrogen insertion reactions, 732
- 1,3-Carbon–hydrogen insertion reactions, 729–734
- 1,5-Carbon–hydrogen insertion reactions, 734
- Carbon–magnesium bonds, reactivity, 517
- Carbon monoxide
- Mg complexes, 125
  - organomagnesium ion reactivity, 180
- Carbon–nitrogen bonds, C=N addition, 571–575
- Carbon–oxygen bonds
- C–O activation, 159, 161, 167
  - C=O addition, 569–571
- Carbon tetrachloride, titration, 289
- Carbon–X bond activation, 156, 158, 159, 162
- Carbonyl compounds
- conjugated unsaturated, 624–625, 626, 628
  - Grignard additions
    - experimental background, 370–374
    - rare-earth metal salts, 569–570
    - theoretical studies, 369–370, 374–401, 569  - one-carbon homologation, 760–766
  - synthesis by substitution, 559
- Carboxylate ligands, magnesate anions, 178–179
- Carboxylates, Mg<sup>2+</sup> coordination, 321–322
- Carboxylic acid derivatives,  $\alpha,\beta$ -unsaturated, 451
- Carboxylic acid dianions, 503
- Carboxylic esters, magnesium enolate, 446
- Catalysts
- addition to C=C bonds, 559–562
  - carbomagnesiation
    - alkenes, 657–660, 662, 663, 664–665, 671–674
    - alkynes, 634–644, 648, 651–652  - cooperative, 567, 568
  - cross-coupling reactions, 543–547, 550–556
  - enantioselective conjugate addition, 771–791
- Catalyzed Claisen rearrangement, 444
- Catalyzed Mukaiyama reaction, 456, 457, 474
- Cathodic reduction, 244–253
- general mechanism, 244–245

- Cathodic reduction, (*continued*)  
Mg deposition and reverse process,  
245–253  
kinetics, 252–253  
organomagnesium cations, 246  
Cationic sandwiches, thermochemistry,  
124–125  
Cations  
dimagnesium, 10  
heteroleptic monoorganomagnesium, 56–57  
Mg biochemistry, 316–327  
organic substrate reactions, 160–170  
Cellulose, matrix obliteration, 272  
Chalcogenides, heavy group 15 complexes,  
433–434  
Chalcone, 1,4-addition, 478  
Charcoal, Ni catalyst immobilization, 554  
Charge reduction, ligated Mg cations, 175  
Charge transfer  
carbocation–Mg atom reactions, 159  
Mg cation complexes, 163  
Chelation  
allylic *N*-protected aminoesters, 446  
carbomagnesiatio, 636, 642, 647, 667–670,  
671–672  
 $\beta$ -diketones, 461, 463, 493–494  
Grignard addition calculations, 380–384,  
391, 393–396, 397  
 $\beta$ -ketoesters, 445, 493–494  
stereoselectivity, 440, 441, 491, 492, 493  
Chemical shifts  
alkylmagnesium compounds, 134, 135–137,  
138–139, 141  
 $^{25}\text{Mg}$  NMR spectroscopy, 151–152, 153  
Chemical vapor deposition, organomagnesium  
alkoxides, 432  
Chemisorption, Mg(0001) single-crystal  
surface, 172, 173  
Chiral acetates, aldol stereochemistry, 447  
Chiral additives, Grignard reagents, 60–61  
Chiral  $\beta$ -amino acid derivatives, 454  
Chiral auxiliaries, 1,4-addition to Michael  
acceptors, 563–564  
Chiral centers, all-carbon quaternary, 565  
Chiral dioxolones, aldol stereochemistry, 448  
Chiral enolates, 505–506  
Chiral ferrocenyl-based diphosphines,  
asymmetric 1,4-addition, 456  
Chiral Grignard reagents, synthesis, 514–515,  
527–528, 725–727  
Chiral magnesium amides, 454, 498  
Chiral magnesium carbenoids, asymmetric  
homologation, 722  
Chiral magnesium enolates, 500  
Chiral oxazolidinone anions, 503–505  
Chiral oxime ethers, addition to C=N bonds,  
574  
Chiral sulfinimines, addition to C=N bonds,  
575  
Chiral sulfoxides, synthesis, 582–583  
Chloranil, oxidative coupling of  
amidocuprates, 580, 581  
Chlorins  
photooxidation, 207, 210–211  
photosynthetic pigments, 125, 191–193  
 $\alpha$ -Chloroalkyl aryl sulfoxides, preparation, 721  
Chloroaluminate complexes, cathodic  
reduction, 248–249  
2-Chloro-4,6-dimethoxy-1,3,5-triazine,  
carbonyl compound synthesis, 559  
 $\alpha$ -Chloroesters, preparation, 444  
 $\alpha$ -Chloroglycidic ester, 440, 441  
 $\alpha$ -Chloro- $\beta$ -hydroxy sulfoxides,  
desulfinylation, 444  
Chlorophyll-bound magnesium, speciation  
analysis, 270  
Chlorophyllin, 213–214  
Chlorophylls  
applied photochemistry, 213–214  
 $\text{Mg}^{2+}$  coordination, 324  
photochemical reactions, 209–212  
photosynthesis, 191, 356–357  
1-Chlorovinyl *p*-tolyl sulfoxide  
geometrical isomers, 749, 751, 752  
magnesium alkylidene carbenoid formation,  
744, 745, 746–747  
Chromatic chemosensors, elemental analysis  
of Mg, 285–286  
Chromatography  
elemental analysis of Mg, 273–274  
speciation analysis, 292–295  
Chromism, polythiophene, 285  
Chromium-catalyzed reactions  
addition to triple C–C bonds, 567, 568  
carbomagnesiatio, 636–637, 638  
Chromophores, absorption spectra, 193  
CID *see* Collision-induced dissociation  
Claisen rearrangement  
ester enolates, 446, 487, 491  
magnesium dihalide, 444  
Clerodane, synthesis, 456, 457, 474  
Cluster Grignard reagents, 171, 172  
Clusters *see* Magnesium clusters  
CND (conductivity measurement), 273  
 $^{13}\text{C}$  NMR spectroscopy  
alkoxides, 145, 146–147, 147  
alkylmagnesium compounds, 134, 135–137  
alkylmagnesium compounds, 141, 142, 143,  
151  
bis(cyclopentadienyl) magnesium, 152, 153  
co-ordination complexes, 149–150  
Evans-type 4-phenyloxazolidinone auxiliary,  
455  
magnesium carbenoids, 720  
speciation analysis, 297

- Cobalt-*bis*-(1,3-diphenylphosphino)propane complex, 545–546
- Cobalt-catalyzed reactions  
addition to C=C bonds, 560–561  
cross-coupling reactions, 545–546
- Cobalt chloride, cyclization reactions, 545–546
- Coldspray ionization, 156
- Collision-induced dissociation (CID)  
Mg cation reactions, 161, 182  
magnesium cationic sandwiches, 124
- Colorimetry, elemental analysis of Mg, 279–283
- Color tests, speciation analysis, 295–296
- Column separation methods, elemental analysis of Mg, 273–275
- Complexation energies, 102
- Complexes  
ate complexes, 681–715  
electrochemistry, 248–252  
Grignard reagents, 58–66, 108  
ligated Mg cation photoactivation, 162–170  
Mg–CO thermochemistry, 125  
NMR spectra, 148, 149–150  
organomagnesium-group 15-bonded, 403–427, 428  
organomagnesium-group 16-bonded, 427–434  
*see also* Donor–acceptor complexes
- Complexometric titration  
elemental analysis, 282–283  
Mg in body fluids, 270
- Concentration, NMR solutions, 132–133
- Condensation reactions, Mg cation–alcohols, 161
- Conductivity measurement (CND), ion chromatography, 273
- Configurational stability  
functionalized Grignard reagents, 514–515  
magnesium alkylidene carbenoids, 745, 751
- Conglomerates, monoorganomagnesium cations, 57
- Conjugate addition  
asymmetric, 454–457, 565  
carbomagnesiation, 654, 667–671, 674–675, 676  
magnesium enolate preparation, 450–457  
*see also* Enantioselectivity, conjugate addition
- Conjugated unsaturated carbonyl compounds, Fe-catalyzed addition, 624–625, 626, 628
- Cooperative catalysis, addition to triple C–C bonds, 567, 568
- Coordination  
intramolecularly coordinating substituents, 30–36  
Mg, 318–324  
bidentate, 322, 324  
binding modes, 320–324, 331–332  
bridge bidentate, 322  
coordination sphere, 318–324  
inner sphere, 320–321, 323–324  
mixed sphere, 320–321  
monodentate, 322, 324  
outer sphere, 320–321, 324  
template effect, 342  
NMR spectra, 148, 149–150
- Copper, amidocuprate oxidative coupling, 580–581
- Copper(I) salts, catalysts, 557–558
- Copper(II) chloride lithium chloride, 544
- Copper-catalyzed reactions  
addition to triple C–C bonds, 567, 568  
allylic substitution, 557–558  
carbomagnesiation, 634–635, 636, 637–639, 641–644, 648, 651–652, 659, 660, 662, 663  
conjugate addition, 455, 457, 772–791  
cross-coupling reactions, 544–545  
enantioselective  
allylic alkylation, 792–799  
conjugate addition, 772–791  
olefin  $\pi$ -complex, 790  
semiempirical [PM3(tm)] calculations, 790–791
- Copper–magnesium cluster compound, structure, 86, 87
- Corriu, Kumada–Tamao–Corriu reactions, 550
- Coumarin 343, UV–visible fluorometry, 285
- Coupling reactions  
Kumada coupling reaction, 513  
oxidative, 580–581  
homocoupling, 547  
*see also* Cross-coupling reactions
- Covalency, ferrocene, 122
- Covalently bound magnesium, speciation analysis, 270
- o*-Cresolphthalein, UV–visible spectrophotometry, 280, 281
- Cross-coupling reactions  
Fe-catalyzed, 604–618, 626–628  
alkenylation, 604–608, 626  
alkylation, 615–618  
arylation and heteroarylation, 610–615, 626, 627–628  
lithium tripyridylmagnesate, 688  
transition-metal-catalyzed, 543–547, 550–556  
transition-metal-free, 556–557
- Crown ethers  
12-Crown-4, 178  
donor–acceptor complexes, 34–36, 42, 44  
Grignard reagents, 66–67  
Mg cation fragmentation, 178  
organomagnesiate production, 11–12, 14
- Cryoscopy, speciation analysis, 299

- 2,1,1-Cryptand, triorganomagnesate production, 12–13
- Cryptands, disproportionation reactions, 11, 12–13
- Crystallography, magnesium carbides, 107
- CSD database, organomagnesium compounds, 3
- Cubane structure  
alkoxides, 70–71, 145, 146  
diorganomagnesium compounds, 29, 50, 51  
*see also* Heterocubane structure
- Cumene, Grignard reagent coupling, 295
- Cumulene, 106
- Cyanoacetylene  
Mg cation reactions, 160  
magnesium cationic sandwiches, 125
- Cyanohydrins, functionalized Grignard reagent protection, 534, 535–536
- Cyanopolyenes, Mg cation reactions, 160
- Cyclic compounds  
cAMP, 347–348  
ring-opening of small cycles, 543, 547, 548  
thermochemistry, 117–121
- Cyclic dodecamers, ethylmagnesium amides, 82, 83
- Cyclic enones, enantioselective conjugate addition, 774–779
- Cyclization, radical, 623–624
- Cycloalkanes, enthalpies of formation, 117–118
- Cycloalkylmagnesium halides, thermochemistry, 110, 117–120
- Cyclobutanes, substituted, 547
- Cyclobutyl Grignard reagents, thermochemistry, 118–119
- Cycloheptanones, 2,2,7-trisubstituted, 765
- 2-Cyclohexen-1-one, diethylmagnesium reactions, 684, 685
- 1,5-Cyclooctadiene, NMR spectroscopy, 296
- Cyclooctene, NMR spectroscopy, 296
- Cyclopentadienyl anion, formation, 182
- Cyclopentadienylmagnesium, lowest excited electronic state, 123
- Cyclopentadienylmagnesium amides, 83, 84
- Cyclopentadienylmagnesium amidinate complex, 72–73
- Cyclopentadienylmagnesium bromide(tetraethylethylenediamine), 67
- Cyclopentadienylmagnesium *tert*-butylthiolate, 84, 85
- Cyclopentadienylmagnesium chloride, dimer, 67–68
- Cyclopentadienylmagnesium  $\beta$ -diketiminato, 78
- Cyclopentadienylmagnesium ethoxide, 70, 71
- Cyclopentadienylmagnesium halide complexes, 67–69
- Cyclopentadienyl(neopentyl)magnesium, 29
- Cyclopropanation  
allylic alcohols, 722  
Simmons–Smith-type, 722
- Cyclopropanes  
magnesium carbenoid reactions, 730–731, 734, 735  
substituted, 547  
synthesis, 582
- Cyclopropanols, synthesis, 582
- Cyclopropenes, addition to C=C bonds, 560
- Cyclopropenyl derivatives, magnesium cationic sandwiches, 125
- Cyclopropylamines, synthesis, 582
- Cyclopropyl  $\alpha$ -amino acid, synthesis, 742
- Cyclopropyl bromides, Br<sub>2</sub>–Mg exchange, 528
- Cyclopropyl Grignard reagents, thermochemistry, 118–119
- Cyclopropylidenes *see* Magnesium cyclopropylidenes
- Cyclopropyl iodides, I<sub>2</sub>–Mg exchange, 528
- Cyclopropylmagnesium,  $\alpha$ -amino-substituted, 740, 741–742
- Cyclopropyne, 106
- Cytosine, Mg cation complex, 170
- DABCO  
donor–acceptor complexes, 39, 40  
tetraorganomagnesiate production, 9
- Danofloxacin, 499
- DCTA, ion chromatography, 273
- Decarboxylation, magnesate anions, 178–179, 180, 181
- Dechlorination, aryl chlorides, 554
- Decomposition, organomagnesium films, 173
- Dehydration, Mg cation–acetic acid complex, 169
- Dehydrogenation, Mg film reactions, 173–174
- Dehydropyridine, radical cation formation, 164–165
- Density functional theory (DFT), Grignard carbonyl additions, 369–370, 376
- Deoxypropionate units, enantioselective conjugate addition, 786, 788, 799
- Deposition–dissolution of magnesium  
cathodic reduction, 245–253  
kinetics, 252–253
- Deprotonation  
bis-deprotonation, 458  
1,1'-di-deprotonation, 19  
enantioselective, 424, 469–470, 473  
epoxides, 547  
hindered Hauser bases, 464, 465  
ketones, 424, 425, 596–599  
toluene, 19  
triorganomagnesates, 686–690, 713  
*see also* Protonation

- Deprotonative metalation, heteroleptic organomagnesiates production, 18–22
- Derivatization reagents, Grignard reagents, 300–301, 302–304
- Desulfinylation  
   $\alpha$ -chloro- $\beta$ -hydroxy sulfoxides, 444  
   $\alpha,\alpha$ -disulfonylated lactones, 443–444  
   $\alpha$ -halo- $\beta$ -ketosulfoxide, 444, 479  
  isopropylmagnesium chloride, 445  
   $\beta$ -keto-sulfinylcarboxylic acid derivatives, 444–445  
   $\beta$ -keto-sulfoxide, 444, 479
- Desymmetrization, enantioselective, 571
- Deuteration, magnesium enolates, 441, 479, 489
- Deuterium oxide, Mg film desorption, 173
- DFT (density functional theory), 369–370
- $\alpha,\beta$ -Diacylglycerols, derivatization, 301
- Dialkylmagnesium compounds  
  2,6-bis(imino)pyridine reactions, 71–72  
   $\beta$ -diketimine reactions, 73–78  
  enthalpies of formation, 116–117  
  sparteine complexes, 148, 150
- Dialkyl malonate C-acylation, 462, 494–496
- N,N*-Dialkyl- $\alpha$ -methacrylthioamides, Michael addition, 452
- Dialkylphosphine oxides,  
  transition-metal-catalyzed cross-coupling, 550, 552
- N,N*-Dialkyl sulfamate, *ortho*-directing group, 553
- Dialkylzinc reagents, conjugate addition, 774
- Diaminocarbenes, catalytic enantioselective conjugate addition, 775, 777, 778
- Dianions  
  carboxylic acid, 503  
  tetraorganomagnesium, 8–9
- 1,4-Diarylbutadienes, functionalized Grignard reagent synthesis, 540, 543
- Diarylmagnesium compounds, <sup>1</sup>H NMR spectra, 138
- Diarylmagnesium reagents, Br<sub>2</sub>–Mg exchange, 521, 522, 523
- Diastereoselectivity, carbomagnesiation, 671–672
- Diazines, transition-metal-catalyzed cross-coupling, 553
- DIBAH (diisobutylaluminum hydride), 513
- Dibenzofuran derivatives, 476, 477
- Dibromo- $\beta$ -lactam, halogen–metal exchange, 443, 446
- Dibutylmagnesium,  
  2,2'-ethylidenebis(2,4-di-*tert*-butylphenol) reaction, 16
- Dicarbonyl enolates, reactions with electrophiles, 489–499
- Dichloromethyl phenyl sulfoxide, one-carbon homologation, 765–766
- Dickerson–Drew dodecamer, 335
- Dicyclopentadienyl titanium dichloride, functionalized Grignard reagent synthesis, 540, 543
- 1,1'-Di-deprotonation, heteroleptic organomagnesiates production, 19
- Dienes, Mg film self-hydrogenation, 173
- 1,3-Dienyl triflates, transition-metal-catalyzed cross-coupling, 555
- Diethyl *N*-Boc-iminomalonate, functionalized Grignard reagent synthesis, 517–518
- Diethyl ether, chemisorbed film solubility, 173
- Diethylmagnesium  
  18-crown-6 complex, 44  
  nucleophilic addition, 684, 685  
  structure, 25
- Diffuse reflectance infrared Fourier transform spectroscopy (DRIFTS), 295
- Diffusively bound magnesium(II) ions, in RNA, 270
- Diglyme, donor–acceptor complexes, 41–42
- 1,1-Di-Grignard reagents, structure, 61–62
- 1,1-Dihalocyclopropanes, Doering–LaFlamme allene synthesis, 735–738
- Dihydroquinoline-2*H*-3-carboxylic acid derivatives, 453
- Diisobutylaluminum hydride (DIBAH), Mg activation, 513
- Diisopropylamine, Mg cation complex, 168
- $\beta$ -Diketiminates  
  anion chelation, 74  
  enolization, 424  
  metalation, 419, 421  
  O<sub>2</sub> reactions, 422–423  
  structure, 417–418  
  synthesis, 411
- $\beta$ -Diketimines, dialkylmagnesium compound reactions, 73–78
- $\beta$ -Diketones  
  aldol-type reactions, 493–495  
  chelated magnesium enolate, 461, 463
- Dilithium tetrabutylmagnesate, deprotonation, 689–690
- Dilution *see* Enthalpies of dilution
- Dimagnesacycloalkanes, thermochemistry, 120–121
- 1,7-Dimagnesiocyclododecane tetra THF complex, 40
- Dimagnesium cations, tetraorganomagnesiates, 10
- Dimerization  
  alkoxy- and aryloxymagnesium hydrides, 147  
  PET, 206  
  *see also* Enthalpies of dimerization
- Dimethoxyethane *see* DME complexes
- 1,2-Dimethoxyethane, Mg cation complex photofragmentation, 166

- 1,3-Dimethylallylmagnesium chloride, Schlenk equilibrium, 145
- Dimethylamine, Mg cation complex, 168
- (Dimethylamino)dimethylmagnesium chloride, structure, 64
- 1-[2-(Dimethylamino)ethyl]-2,3,4,5-tetramethylcyclopentadienylmagnesium bromide, 68–69
- 2-[(Dimethylamino)methyl]ferrocenyl groups, 30, 31
- Dimethyl ether, chemisorption, 172
- N,N*-Dimethylformamide, Mg cation complex, 169
- Dimethylmagnesium  
donor–acceptor complexes, 39, 40  
structure, 25, 26
- Dimethylsilyl chloride, Grignard reagent coupling, 295
- Dimethyl sulfoxide, Mg cation fragmentation, 176
- Diorganomagnesium compounds  
anodic oxidation, 227–228  
dioxane complexes, 39, 40  
disproportionation reactions, 11  
electrochemical synthesis, 221–224, 253–256  
nucleophilic addition, 256–257  
heteroleptic organomagnesiates production, 15–16  
structural chemistry, 23–54  
donor–acceptor complexes, 36–44, 47–54  
donor–base-free compounds, 23–25  
intramolecularly coordinating substituents, 30–36  
magnesium anthracene compounds, 44–47  
multi-hapto-bonded groups, 25–29, 47–54  
 $\sigma$ -bonded compounds, 36–44  
thermochemistry, 116–117
- Dioxanate, Schlenk equilibrium, 107
- Dioxane, diorganomagnesium complexes, 39, 40
- Dioxolones, aldol stereochemistry, 448
- Diphenyl ditelluride, titration, 290
- 2,2-Diphenylethyl-2,4,6-trimethylphenyl ketone (Kohler's ketone), 457, 458
- Diphenylmagnesium  
donor–acceptor complexes, 43–44  
structure, 25, 26
- cis*-Diphenylvinylmagnesium THF complex, 40–41
- Diphosphine ligands  
asymmetric 1,4-addition, 456  
conjugate addition of Grignard reagents, 775
- Dipole moments, Grignard reagent calculations, 375
- Dipropylamine, Mg cation complex, 168
- Direct alkenylation, arylamines, 748–749
- Direct oxidative addition, Mg to organic halides, 512–515
- Displacement reactions, Mg cation–alkyl halides, 160–161
- Disproportionation reactions  
cryptands, 11, 12–13  
Lewis base donor solvent effects, 412  
organomagnesium amide complexes, 422
- Dissolution, electrochemical  
deposition–dissolution of Mg, 245–253
- $\alpha,\alpha$ -Disulfonylated lactones, desulfonylation, 443–444
- Dithioacetals, ring opening, 547, 548
- 1,3,16,18-Dixylylene-30-crown-8,  
donor–acceptor complexes, 42
- DME complexes, Grignard reagents, 59–60
- DNA  
capillary electrophoresis, 305  
Mg<sup>2+</sup> interactions, 320–321, 333–342  
ribozymes, 335–342  
replication and repair, 350–355  
base excision repair, 353–354  
DNA replicases, 351–353  
generic two-ion mechanism, 354–355
- DNA replicases, 351–353
- Doering–LaFlamme allene synthesis,  
magnesium cyclopropylidene intermediates, 735–738
- Donor–acceptor complexes  
multi-hapto-bonded groups, 47–54  
 $\sigma$ -bonded diorganomagnesium compounds, 36–44  
*see also* Complexes
- Donor–acceptor transfer compounds,  
photochemistry, 196–201
- Donor–base-free diorganomagnesium compounds, structures, 23–25
- Double bonds, addition reactions, 11, 35, 559–567
- Double titration, organolithium compounds, 289
- DRIFTS (diffuse reflectance infrared Fourier transform spectroscopy), 295
- Dry ashing, matrix obliteration, 271, 272
- DuPHOS ligand, catalytic enantioselective conjugate addition, 775, 776
- Dynamic equilibria  
allylmagnesium compounds, 143, 144  
arylmagnesium compounds, 140
- Eclipsed structure, magnesocene, 183
- EDTA  
AAS, 278  
complexometric analysis, 282–283

- ion chromatography, 273
- NMR spectroscopy, 286
- EGTA, UV-visible spectrophotometry, 280, 281
- Electric conductivity
  - organomagnesium solutions, 224–227
  - solvent effects, 226–227
- Electroanalytical determination, elemental analysis of Mg, 276–277
- Electrochemistry, 219–263
  - anodic oxidation, 227–244
    - diorganomagnesium compounds, 227–228
    - Grignard reagents, 228–243
    - methyl group grafting, 241–243
  - cathodic reduction, 244–253
    - general mechanism, 244–245
    - Mg deposition and reverse process, 245–253
  - diorganomagnesium compound synthesis, 221–224, 253–256
    - nucleophilic addition, 256–257
  - elemental analysis of Mg, 275–277
  - Grignard reagents, 305
  - organomagnesium intermediates, 253–257
  - solution conductivity, 224–227
- Electrochromism, polythiophene, 285
- Electrodes
  - inert, 229–236
  - ion-selective, 275–276
- Electrolytes, blood/plasma/serum, 275–276
- Electron-deficient bonds, organomagnesiates structures, 5
- Electron diffraction, gas-phase, 183–184
- Electron donor–acceptor transfer compounds, 196–201
- Electronegativity, methyl deviation correlation, 111–112, 118
- Electronic absorption spectra, tetrapyrroles, 192–193
- Electron impact, ligated Mg cations, 175
- Electron spin resonance (ESR) spectroscopy
  - monomethyl magnesium radical, 159
  - speciation analysis, 299
- Electron transfer
  - ligated Mg cations, 175–176
  - Mg cation–amine complexes, 168
  - magnesium anthracene compounds, 45
  - photochemistry, 191, 194–206
    - donor–acceptor compounds, 196–201
    - heteroligand systems, 201, 204–206
  - see also* Single-electron transfer
- Electrooxidation
  - Grignard reagents, 237–241
  - organoelemental compounds, 240
- Electrophilic reactions
  - amination, 575–580
  - carboxylic acid dianions, 503
  - chiral oxazolidinone anions, 503–505
  - magnesium alkylidene carbenoids
    - alkenylation, 748
    - N*-lithio arylamines, 748–755
    - N*-lithio nitrogen-containing heterocycles, 755–757
  - lithium acetylides, 758
  - lithium thiolates, 758–760
  - tetrasubstituted olefin one-pot synthesis, 746–748
- magnesium amide enolates, 499–500
- magnesium carbenoids
  - 1,3-C–H insertion reaction, 729–734
  - Grignard reactions, 723–725
  - N*-lithio arylamine reactions, 728–729, 730
  - secondary chiral Grignard reagent synthesis, 725–727
  - $\alpha$ -sulfonyl lithium carbanion reactions, 727–728, 748
- magnesium cyclopropylidenes, 739–742
- magnesium dicarbonyl enolates, 489–499
- magnesium ester enolates, 484–489
- magnesium ketone enolates, 472–484
- magnesium lactam enolates, 499–500
- magnesium lactone enolates, 484–489
- magnesium thioamide enolates, 500–502
- magnesium thioesters, 500–502
- Electrophoresis
  - capillary, 301, 305
  - elemental analysis of Mg, 273–274
- Electropositivity, Mg, 102–103, 125
- Electrospray ionization (ESI), gas-phase Mg ion fragmentation, 174–175, 178
- Electrothermal atomic absorption spectrometry (ETAAS), 278
- Elemental analysis of magnesium, 268, 269–288
  - column separation methods, 273–275
  - electrochemical methods, 275–277
  - sample preparation, 271–273
  - spectral methods, 277–288
- Elimination reactions
  - addition–elimination, 471
  - $\beta$ -hydride, 544
  - Mg cation–organic substrates, 160–161
- Emission spectroscopy, tetraphenylporphyrins, 199
- Enamides, 1,4-addition to Michael acceptors, 563–564
- Enantioselectivity
  - carbomagnesiatio, 659–661, 673, 674
  - conjugate addition, 771–791
    - acyclic enones, 774, 779, 780
    - cyclic enones, 774–779
  - magnesium enolate preparation, 454
  - mechanistic studies, 789–791
  - organomagnesium amides, 426

- Enantioselectivity (*continued*)  
  polar mechanism, 370  
  tandem aldol reaction, 788, 789  
   $\alpha,\beta$ -unsaturated esters, 779–784  
   $\alpha,\beta$ -unsaturated thioesters, 784  
  natural product synthesis, 785, 786–789  
deprotonation, 424, 425, 469–470, 473  
desymmetrization of anhydrides, 571  
Grignard reagents  
  addition to ketones, 571  
  allylic alkylation, 792–799  
  chiral additives, 60–61  
  ketone deprotonation, 424, 425  
  protonation, 480, 481  
Endocyclic compounds, thermochemistry, 117  
Energy currency of life, Mg biochemistry, 327–333  
Energy thresholds, magnesium cationic sandwiches, 124  
Enolases, metabolic enzymes, 348–350  
Enolate intermediate, alkylation, 762, 763–765  
Enolates *see* Magnesium enolates  
Enolization  
  hindered ketones, 478  
  organomagnesate anions, 180–181  
  solvent-free Grignard reagents, 157  
Enol phosphates  
  magnesium enolate reactions, 480, 481, 489–491  
  transition-metal-catalyzed cross-coupling, 544  
Enol triflates, transition-metal-catalyzed cross-coupling, 555  
Enones  
  acyclic, 774, 779  
  cyclic, 774–779  
 $\alpha,\beta$ -Enones, 1,4-addition, 563  
Enthalpies of atomization, binary magnesium salts, 115  
Enthalpies of dilution, Grignard reagents, 107–108  
Enthalpies of dimerization, magnesacycloalkanes, 120  
Enthalpies of formation  
  acetone, 115  
  alkoxymagnesium bromides, 114–115, 116  
  cycloalkanes, 117–118  
  cycloalkylmagnesium halides, 110, 117–120  
  dialkylmagnesium compounds, 116–117  
  difference, 112, 114, 119  
  Grignard reagents, 115–116  
  hydrocarbylmagnesium bromides, 109, 110, 114  
  magnesium sandwich species  
  magnesocene, 122  
  neutral magnesium half-sandwiches, 123  
  Mg–fluorocarbon reactions, 103  
  organomagnesium bromides, 111, 112, 113–114, 115  
  parent hydrocarbons, 112  
  *see also* Molar standard enthalpies of formation  
Enthalpies of hydrogenation, unsaturated organomagnesium bromides, 113, 119  
Enthalpies of hydrolysis  
  butylmagnesium chloride, 110  
  calorimetry, 104  
  magnesacycles, 121  
Enthalpies of protonation, unsaturated organomagnesium halides, 112  
Enthalpies of reaction  
  acetolysis, 120  
  Bronsted acids, 113, 115  
  calorimetry, 105–106  
  Grignard reagents, 116  
  hydrocarbylmagnesium bromides, 109, 110  
  magnesium sandwich species  
    cationic sandwiches, 124  
    neutral magnesium half-sandwiches, 123  
  organomagnesium bromides, 111  
  phenylethynylmagnesium bromide, 112  
  *see also* Molar standard enthalpies of reaction  
Enthalpies of solution, enthalpy of formation calculation, 116  
Enthalpies of solvation, Schlenk equilibrium, 109, 117  
Enthalpies of vaporization, calorimetry, 105–106  
Entropy  
  cycloalkylmagnesium halides, 120  
  magnesacycloalkanes, 120  
Environmental aspects, Mg metal, 102–103  
Environmental pollution control, organometallic compounds, 300  
Enzymes (protein-based), 342–359  
  allosteric systems, 343–345  
  DNA replication and repair, 350–355  
  enzymatic modes of action, 342–345  
  metabolic enzymes, 345–350  
  photosynthesis, 355–359  
  sequential systems, 343, 348–350  
  template enzymes, 342–343  
  *see also* ATP synthases  
Epimers, functionalized Grignard reagents, 514–515  
Epoxides, deprotonation, 547  
Equilibrium constant, Schlenk equilibrium, 108  
ESI (electrospray ionization), 174–175, 178  
Esophageal cancer, elemental analysis in hair, 278  
ESR spectroscopy *see* Electron spin resonance spectroscopy



- Ester enolates  
  Claisen rearrangement, 446, 487, 491  
  reactions with electrophiles, 484–489
- Esters  
  quaternary stereocenters, 792, 796  
   $\alpha,\beta$ -unsaturated, 779–784
- Ether-functionalization, diorganomagnesium compounds, 33
- Ethyl hydrogen malonate  
   $\gamma$ -amino- $\beta$ -ketoester derivatives, 497  
  bis-deprotonation, 458
- 2,2'-Ethylidenebis(2,4-di-*tert*-butylphenol), 16
- Ethyl isocyanate, Mg cation complex, 169
- Ethyl isothiocyanate, Mg cation complex, 169
- Ethylmagnesium, Zr-catalyzed, 671–674
- Ethylmagnesium amides, cyclic dodecamer, 82, 83
- Ethylmagnesium bromide  
  ethoxide structure, 58–59  
  sparteine complexes, 60–61
- Ethylmagnesium tris(3-*tert*-butylpyrazolyl)phenylborate, 73, 74
- O*-Ethyl *S*-(tetrahydro-2-oxo-3-furanyl) dithiocarbonate, magnesium enolate, 447
- Evans-type 4-phenyloxazolidinone auxiliary, NMR spectroscopy, 447
- Evaporation, solvent, 15
- Evening primrose oil, analysis, 301
- Exchange reactions  
  alkyl–halide, 108–109, 134  
  allylmagnesium compounds, 142, 143  
  halogen–metal, 439, 442, 443, 446, 718  
  halogen–Mg, 515–537, 690–711, 712–713, 718–720  
  H–metal, 742–743  
  *see also* Ligand exchange
- Excited states  
  cyclopentadienyl magnesium, 123  
  Mg atoms, 157, 158, 159
- Exo,exo*-bis(iso-dicyclopentadienyl)magnesium, structure, 27
- Exothermic reactions, Mg fluorocarbon reactions, 103
- FAAS (flame atomic absorption spectrometry), 271–272, 277–278, 288
- FAES (flame atomic emission spectrometry), 278
- Fecal endogenous excretion (FEE), mass spectrometry, 288
- FEE (fecal endogenous excretion), 288
- Ferrocene  
  nomenclature, 122  
  structure, 25
- Ferrocenylacetylene, NMR spectroscopy, 297
- Ferrocenyl-based diphosphines  
  asymmetric 1,4-addition, 456  
  conjugate addition of Grignard reagents, 775
- Ferrocenyl dianions, heteroleptic organomagnesiates production, 20, 21
- Fertilizers, complexometric analysis, 283
- FIA (flow injection analysis) systems, 280
- Films, formation of organomagnesium species, 172–174
- Flame atomic absorption spectrometry (FAAS), 271–272, 277–278, 288
- Flame atomic emission spectrometry (FAES), 278
- Flow injection analysis (FIA) systems, UV–visible spectrophotometry, 280
- Fluorescence, Mg(II) tetrapyrroles, 193
- Fluoroaryl magnesium compounds,  $^{19}\text{F}$  NMR spectra, 139–140
- Fluorocarbons, pyrolants, 103
- Fluorometry, elemental analysis of Mg, 270, 283–285, 288
- 2-Fluoropyridine, photodissociation spectra, 164
- 3-Fluoropyridine, deprotonation, 688
- $^{19}\text{F}$  NMR spectroscopy, fluoroaryl magnesium compounds, 139–140
- Food additives, chlorophyll, 213–214
- Force constants, cyclopentadienyl magnesium, 123
- Forensic analysis, organometallic compounds, 300
- Formaldehyde, Mg cation complex, 169
- Formation  
  Grignard reagent calculations, 376, 378  
  solvent-free environments, 156–179  
  ligated Mg ion fragmentation, 166, 174–179  
  Mg atom reactions, 157–159  
  Mg cation reactions, 160–170  
  Mg cluster reactions, 171–172  
  Mg surfaces and films, 172–174  
  *see also* Enthalpies of formation; Molar standard enthalpies of formation
- Fragmentation of organomagnesium ions  
  ligated, 166, 174–179  
  unimolecular reactions, 182
- Free energy, universal energy currency of life, 327–333
- Free-energy difference, cycloalkylmagnesium halides, 119
- Free hydrated magnesium ions, speciation analysis, 269
- Free radicals *see* Radicals
- Fritsch–Buttenberg–Wiechell rearrangement, alkylidene carbenoids, 742–744
- FT–ICR (Fourier transform–ion cyclotron resonance), 160
- Fullerenes  
  carbomagnesium, 674–675, 676  
  PET, 196, 200–201

- Fulvenes, cyclopentadienylmagnesium compounds, 27–28
- Functionalized Grignard reagents
- acylation, 559, 601, 603
  - addition, 543
    - 1,4-addition, 543, 547, 563–565
    - C=C bonds, 559–568
    - C=N bonds, 571–575
    - C=O bonds, 569–571
    - multiple bonds, 559–575
  - amination, 575–581
    - electrophilic, 575–580
    - oxidative coupling, 580–581
  - chiral sulfoxide synthesis, 582–583
  - cyclopropane synthesis, 582
  - reactivity, 543–583
  - substitution
    - Sp-center, 559
    - Sp<sup>2</sup>-center, 544, 550–559
    - Sp<sup>3</sup>-center, 543–550
  - synthesis, 512–543
    - direct oxidative addition, 512–515
    - functional group tolerance, 530–537
    - halogen–Mg exchange, 515–537
    - metalation, 537–540, 541
- Gallium compounds, derivatization, 304
- Gas chromatography
- organometallic compounds, 300–301, 302–304
  - speciation analysis, 293, 295
- Gas phase
- ligated Mg ion fragmentation, 174–179
  - Mg atoms, 157–159
  - organomagnesium ions
    - bimolecular reactions, 179–182
    - unimolecular reactions, 182
  - structure determination, 183–184
- Gas-phase electron diffraction, structure determination, 183–184
- Geometries
- Grignard reagent calculations, 374–375, 376, 377, 380, 381
  - magnesium alkylidene carbenoids, 751, 753–754, 755
- GFAAS (graphite furnace atomic absorption spectroscopy), 272, 273, 277–278
- Gibbs energies, 102
- cycloalkylmagnesium halides, 119
- Gilman's color tests, speciation analysis, 295–296
- Gilman's cuprates, enantioselective allylic alkylation, 792
- Glaucyrene,  $\beta$ -ketoester reactions, 494
- Glucidic  $\alpha$ -ketoacids, 492
- Glucidic phosphoenolpyruvic acid derivatives, 491
- Glycerides, analysis, 301
- Glycol ethers, oxidative addition solvents, 512
- Glycolytic cycle, metabolic enzymes, 345, 346
- Glymes, Mg cation fragmentation, 178
- Glyoxal, 1,2-bismimine addition reaction, 574
- Grafting, semiconductor anodes, 241–243
- Graphite furnace atomic absorption spectroscopy (GFAAS), 272, 273, 277–278
- Grignard, Victor, 2, 268
- Grignard reactions
- chemisorption, 173
  - computational studies, 384–399
    - carbonyl addition without solvent molecules, 384–389, 390, 391
    - carbonyl addition with solvent molecules, 389, 391, 392, 393, 401
    - chelation-controlled addition, 380–384, 391, 393–396, 397
    - computational methods, 384
    - Grignard reagent structures, 384–387
    - polar mechanisms, 370, 387–388, 389, 391, 394, 396, 400–401
    - single-electron transfer, 370, 372, 396–399
    - transition-state structures, 375–376, 377, 380–382, 388–389, 391, 393, 394–396
  - model reactions, 380–384
  - organomagnesate anions, 180–181
  - photochemistry, 190
- Grignard reagents
- addition–elimination, 471
  - alkyl, 232–233
  - analytical reagents and aids, 269, 299–305
    - active hydrogen determination, 299–300
    - derivatization reagents, 300–301, 302–304
  - anodic oxidation, 228–243
    - addition to olefins, 237
    - inert electrodes, 229–236
    - reactivity, 235–236, 258–260
    - sacrificial anodes, 237–241
    - semiconductor anodes, 241–243
  - aryl, 601, 603
  - association, 108
  - benzylic, 529–530
  - calculations, 374–380
    - computational studies, 384–399
    - model Grignard reactions, 380–384
  - carbonyl additions
    - experimental background, 370–374
    - Fe-catalyzed reactions, 624–625, 626, 628
    - theoretical studies, 369–370, 374–401
  - cathodic reduction
    - general mechanism, 244–245

- Mg deposition and reverse process,  
245–248  
chiral synthesis, 514–515, 527–528,  
725–727  
cluster, 171  
complexation, 108  
conjugate addition, 450–452, 772–791  
crown ethers, 66–67  
derivatization reagents, 300–301, 302–304  
diaryl, 521, 522, 523  
1,1-di-Grignard reagents, 61  
DME complexes, 59–60  
electric conductivity, 224–227  
electrochemical behavior, 305  
electrophilic amination, 575–581  
enantioselectivity  
  allylic alkylation, 792–799  
  chiral additives, 60–61  
  conjugate addition, 772–791  
enthalpies of dilution, 107–108  
enthalpies of reaction, 115–116  
Fe-catalyzed reactions, 595–630  
  acylation, 559, 599–603  
  addition to conjugated unsaturated  
    carbonyls, 624–625, 626, 628  
  alkenylation, 604–608, 626  
  alkylation, 615–618  
  arylation and heteroarylation, 610–615  
  carbometalation, 622–623  
  cross-coupling reactions, 604–618, 626,  
    627–628  
  deprotonation of ketones, 596–599  
  homocoupling, 619–621, 626, 627  
  organic synthesis, 625–628  
  radical cyclization, 623–624  
  substitution, 621–622  
formation  
  mechanisms, 55–56, 376, 378  
  Mg surfaces and films, 1974  
fragmentation reactions, 182  
functionalized  
  aryl, 601, 603  
  reactivity, 543–583  
  synthesis, 512–543  
 $\alpha$ -heteroatom-substituted, 767  
history, 2–3  
magnesium carbenoid electrophilic  
  reactions, 723–725  
NMR spectra, 131–132, 144–145  
  optically enriched, 721  
  oxonium structure, 107  
  perfluorinated synthesis, 516  
  rate constant–oxidation potential  
    correlations, 258–260  
  reactive halide coupling, 295  
  Schlenk equilibrium, 132, 140–141,  
    144–145, 151  
  secondary chiral, 725–727  
  solvent-free, 157  
  structural chemistry, 58–69, 384–387  
   $\alpha$ -sulfur-stabilized, 725, 726  
  surface conditioning, 301, 305  
  thermochemistry, 103  
  *see also* Alkyl Grignard reagents; Aryl  
  Grignard reagents; Methyl Grignard reagents  
Group 1 introns, self-splicing, 337–339  
Group 15, organomagnesium complexes,  
  403–427, 428  
Group 16, organomagnesium complexes,  
  427–434  
  
Haber–Weiss process, photooxidation, 207  
Hair analysis, pathogenesis indicators for  
  cancer, 278  
Half-sandwiches, thermochemistry, 123, 124  
Halides  
  exchange reactions, 108–109, 134  
  gas chromatography, 295  
Halobenzene complexes, photodissociation  
  spectra, 163  
Halogen compounds  
  heteroleptic monoorganomagnesium  
    compounds, 58–69  
  *see also* Grignard reagents  
Halogen–lithium exchange  
  functionalized Grignard reagent synthesis,  
    530, 532  
  mechanism, 516  
Halogen–magnesium exchange  
  carbenoid generation, 718–720  
  functionalized Grignard reagent synthesis,  
    515–537  
  magnesium enolate preparation, 442–443  
  triorganomagnesates, 690–711, 712–713  
Halogen–metal exchange reactions, 439, 442,  
  443, 446, 718  
 $\alpha$ -Haloketones, preparation, 444, 479  
 $\alpha$ -Halo- $\beta$ -ketosulfoxide, desulfinylation, 444,  
  479  
Hammerhead ribozymes, 339–342  
Hapticity, magnesocene, 122  
Heat of formation, 102  
Heat of reaction, 102  
Heteroanionic enolates, 460  
Heteroaryl amidocuprates, oxidative coupling,  
  580–581  
Heteroarylation  
  alkyl Grignard reagents, 610–614, 626,  
    627–628  
  aryl Grignard reagents, 614–615  
Heteroaryl bromides, Br<sub>2</sub>–Mg exchange, 524,  
  525  
Heteroaryl chlorides  
  Fe-catalyzed cross-coupling, 611, 612  
  Kumada–Tamao–Corriu reactions, 550

- Heteroaryl Grignard reagents, Fe-catalyzed homocoupling, 619–621
- Heteroaryl iodides, functionalized Grignard reagent synthesis, 518–519
- Heteroatoms
- $\alpha$ -heteroatom-substituted Grignard reagents, 767
  - monoorganomagnesium compounds, 54–85
  - organomagnesium bromides, 113–116
  - permutational heteroatom/metal enolate preparation, 441–445
- Heterocubane structure
- cyclopentadienylmagnesium *tert*-butylthiolate, 84, 85
  - cyclopentadienylmagnesium ethoxide, 70, 71
  - diorganomagnesium compounds, 29, 50, 51
  - methylmagnesium *tert*-butoxide, 70
  - see also* Cubane structure
- Heterocycles, *N*-lithio nitrogen-containing, 755–757
- N*-Heterocyclic carbenes (NHCs)
- catalytic enantioselective reactions
    - allylic alkylation, 792, 796
    - conjugate addition, 775, 777, 778  - transition-metal-catalyzed cross-coupling, 550, 551
- Heterogeneous processes, Grignard reagent formation, 172
- Heteroleptic compounds
- diorganomagnesium compounds, 29
  - monoorganomagnesium compounds, 54–85
  - organomagnesiates, 5, 14–22
  - bis-anions, 15
- Heteroligand systems, PET, 201, 204–206
- Hexaaquomagnesium ion, coordination, 318–320
- Hexamethylenetetramine (HMTA),
- Fe-catalyzed alkylation, 617
- High-performance liquid chromatography (HPLC), elemental analysis of Mg, 274
- Hindered amines, 457, 464, 538
- Hindered Hauser bases
- deprotonation
    - regioselectivity, 464
    - stereoselectivity, 465  - metalation, 464
- Hindered ketones, enolization, 478
- Hindered magnesium amides, metalation, 464–469
- <sup>1</sup>H NMR spectroscopy
- alkoxides, 145, 146–147
  - alkylmagnesium compounds, 134–138, 141
  - allylmagnesium compounds, 141–142, 143, 144–145, 151
  - arylmagnesium compounds, 138–139
  - co-ordination complexes, 148, 149–150
  - elemental analysis of Mg, 286
  - Evans-type 4-phenyloxazolidinone auxiliary, 455
  - peroxides, 147
  - speciation analysis, 296–298
  - No-D NMR spectroscopy, 296
- Homoallyl alcohols, carbomagnesiation, 664–671
- Homocoupling
- Fe-catalyzed, 554, 619–621, 626, 627
  - oxidative, 547
  - transition-metal-free, 557
- Homoleptic iron carbonyls, 125
- Homoleptic organomagnesiates
- structural chemistry, 5
  - thermochemistry, 103
- Homologation
- alkyl halides, 723–724
  - asymmetric, 722
  - one-carbon, 760–766
- Homologous series, organomagnesium halides, 110–112, 117
- Homopropargylic alcohols, I<sub>2</sub>–Mg exchange, 527, 528
- Horseradish peroxidases, porphyrin photooxidation, 206–207
- HPLC (high-performance liquid chromatography), 274
- $\beta$ -Hydride elimination,
- transition-metal-catalyzed cross-coupling, 544
- $\beta$ -Hydride transfer, ketone reduction, 425–426
- Hydrocarbyllithium compounds, 103
- Hydrocarbylmagnesium bromides, enthalpies of formation, 109, 110, 114
- Hydrocarbylmagnesiums, 103
- Hydrogen
- C–H bond activation, 158
  - organomagnesium ion reactivity, 180
  - see also* Active hydrogen compounds
- Hydrogenation
- self-hydrogenation, 173
  - see also* Enthalpies of hydrogenation
- Hydrogen atom abstraction
- Mg–alkane reactions, 157
  - Mg cation–formaldehyde complex, 169
- Hydrogen compounds
- gas chromatography, 295
  - Grignard analytical reagents, 299–300
- Hydrogen–metal exchange, magnesium alkylidene carbenoids, 742–743
- Hydrolysis
- alkalinity titration, 289
  - ATP, 331–333
  - pancreatic lipase, 301
  - see also* Enthalpies of hydrolysis
- Hydromagnesiation, acetylenes, 540, 543
- $\beta$ -Hydroxyacids, aldol-type reactions, 486

- Hydroxycarbonyl compounds,  
  bis(trimethylsilyl)peroxide synthesis, 475
- Hydroxyl-assisted carbomagnesiation, 665,  
  666, 667–671
- IC (ion chromatography), 273
- ICP–AES (inductively coupled plasma–atomic  
  emission spectrometry), 279, 284
- ICP–MS (inductively coupled plasma–mass  
  spectrometry), 287–288
- IE (ionization energy), 174–175
- Imines, addition to C=N bonds, 571–572,  
  573–574
- Iminium triflates, functionalized Grignard  
  reactions, 548, 549
- Immonium ion, Mg cation–amine complex,  
  168
- Indenyl anions, bis(indenyl)magnesium, 29
- Indicators, speciation analysis, 288, 289, 290
- Indoles, magnesiation, 538
- Induction period, oxidative addition, 513
- Inductive effects, hydrocarbylmagnesium  
  bromides, 114
- Inductively coupled plasma  
  AES, 279, 284  
  mass spectrometry, 287–288
- Inert electrodes  
  anodic oxidation of Grignard reagents,  
    229–236  
  distribution of anodic products, 230, 232,  
    233
- Infrared (IR) spectroscopy  
  Mg atom reactions, 157, 158  
  magnesium enolate, 451  
  near-IR spectroscopy, 512  
  speciation analysis, 295
- Insertion reactions  
  C–halogen bonds, 438–441  
  Mg atoms with organic substrates, 157, 158,  
    159  
  magnesium carbenoids  
    1,2-C–H insertion, 732  
    1,3-C–H insertion, 729–734  
    1,5-C–H insertion, 734  
  Mg cation complexes, 166–167, 168
- Interconversion  
  permutation of H<sub>2</sub>/metal, 457–470  
  permutation of metal/metal salts, 445–450
- Interfacial chemistry, Grignard reagent  
  formation, 172–174
- Intermediate compounds  
  chiral sulfoxides, 582–583  
  electrode reactions, 253–257
- Intermolecular agostic interactions,  
  diorganomagnesium compounds, 24
- Intermolecular carbomagnesiation  
  alkenes, 655–656, 662, 663, 665–666,  
    671–674  
  alkynes, 635–639
- Intramolecular carbomagnesiation  
  alkenes, 654–655, 656, 661–662, 665–666  
  alkynes, 633–635, 654–655
- Intramolecular coordination  
  diorganomagnesium compounds  
    substituents, 30–36  
  oxygen atom, 66
- Inverse crown structures, heteroleptic  
  organomagnesiates, 5, 14, 19, 20–21
- Inversion, pyramidal, 738
- Iodine, titration, 290–291
- Iodine–lithium exchange, carbenoid  
  generation, 718
- Iodine–magnesium exchange  
  carbenoid generation, 719–720  
  functionalized Grignard reagent synthesis,  
    517–519, 526–527, 528, 531, 532  
  lithium tributylmagnesate, 690–692, 694,  
    695, 697, 700–703, 707, 708–710
- $\beta$ -Iodo- $\alpha$ -ketoester magnesium enolate, 440,  
  441, 491, 492
- Iodoketones  
  enol phosphate preparation, 480, 481  
  halogen–metal exchange, 439
- Iodomagnesium enolates, 438–441, 449, 491,  
  492
- Ion chromatography (IC), elemental analysis  
  of Mg, 273
- Ionic liquids, functionalized Grignard reagent  
  synthesis, 515
- Ionic ring–metal interactions, magnesocene,  
  122
- Ionization energy (IE), ligated Mg ions,  
  174–175
- Ionization reactions, conductivity  
  measurements, 225–227
- Ionochromism, polythiophene, 285
- Ion-selective electrodes (ISE), elemental  
  analysis of Mg, 275–276, 283
- Iridium, organomagnesium compounds, 90, 91
- Iron, CO complexes, 125
- Iron(III) catalysts  
  acetylacetonate, 546, 601–603, 605–609,  
    615–617, 621–622, 623  
  chloride, 546, 596, 599–601, 604, 615–617,  
    619–620, 623  
  cross-coupling reactions, 546
- Iron-catalyzed reactions  
  carbomagnesiation, 637–639, 652, 657–659  
  Grignard reagents, 595–630  
    acylation, 559, 599–603  
    addition to conjugated unsaturated  
      carbonyl compounds, 624–625,  
      626, 628  
    addition to triple C–C bonds, 567, 568

- Iron-catalyzed reactions (*continued*)  
 alkenylation, 604–608, 626  
 alkylation, 615–618  
 allylic substitution, 557  
 arylation and heteroarylation, 610–615  
 carbometalation, 622–623  
 cross-coupling reactions, 553–554,  
 604–618, 626, 627–628  
 deprotonation of ketones, 596–599  
 homocoupling, 554, 619–621, 626, 627  
 organic synthesis, 625–628  
 radical cyclization, 623–624  
 substitution, 621–622
- IR spectroscopy *see* Infrared spectroscopy
- ISE (ion-selective electrodes), 275–276, 283
- (Isodicyclopentadienyl)(butyl)magnesium,  
 TMEDA complex, 50, 51
- Isomers, allylmagnesium compounds,  
 142–143, 144
- Isopropylamine, Mg cation complex, 168
- Isopropylmagnesium chloride  
 desulfinylation, 445  
 halogen–metal exchange, 442  
 I<sub>2</sub>–Mg exchange, 531, 532  
 lithium chloride reagent, 531, 533–537, 714
- Isopropylmagnesium  $\beta$ -diketiminate, structure,  
 77
- Isopropylmagnesium  
 tris(3-*tert*-butylpyrazolyl)hydroborate, 73,  
 74
- Isotopically labelled magnesium  
 biosynthesis of ATP, 330  
 reverse isotope dilution technique, 287–288  
 Schlenk equilibrium, 107
- Isovanillin, active hydrogen determination, 300
- Ivanov reaction, arylacetic acids, 458, 502, 503
- Jojoba wax, analysis, 301
- Josiphos ligand  
 catalytic enantioselective conjugate addition,  
 775, 776, 777, 780, 781, 786, 788–789  
 catalyzed 1,4-addition, 564  
 magnesium thioester reactions, 501
- <sup>N</sup>J<sub>HH</sub> spin coupling constants, allylmagnesium  
 compounds, 143–144, 145
- Ketenes  
 Grignard reagents, 471  
 Mg cation–acetic acid dehydration, 169
- $\beta$ -Ketoesters  
 glaucyrene, 494  
 magnesium chelate reactions, 445, 493–494  
 transition-metal-catalyzed cross-coupling,  
 555  
 xanthryone, 494
- Ketone enolates, reactions with electrophiles,  
 472–484
- Ketones  
 deprotonation, 424, 425, 596–599  
 enantioselective addition, 571  
 hindered, 478  
 Kohler's ketone, 457, 458  
 Michler's ketone, 295, 296  
 one-carbon ring expansion, 762, 763,  
 764–765  
 organomagnesium amide reactions, 423–426  
 tetrasubstituted, 457
- $\beta$ -Ketophosphonates, preparation, 462
- $\beta$ -Ketosilanes, preparation, 457
- $\beta$ -Keto-sulfinylamides, magnesium enolate  
 preparation, 444
- $\beta$ -Keto-sulfinylcarboxylic acid derivatives,  
 desulfinylation, 444–445
- $\beta$ -Keto-sulfoxide, desulfinylation, 444, 479
- Kinetics  
 electrochemical Mg deposition, 252–253  
 ligated Mg cation fragmentation, 176
- Klenow fragment, DNA replicase, 351–352
- KMG-20-AM/27-AM, UV–visible  
 fluorometry, 285
- Kohler's ketone, metalation, 457, 458
- Krasnovskii reduction, chlorophyll, 211, 212
- Kumada coupling reaction, microwave  
 activation, 513
- Kumada–Tamao–Corriu reactions, aryl  
 electrophiles, 550
- $\beta$ -Lactam  
 aldol-type reactions, 499–500  
 halogen–metal exchange, 442, 443  
 synthesis, 475, 476
- Lactones  
 aldol-type reactions, 486  
 magnesium enolate, 484–489
- LaFlamme, Doering–LaFlamme allene  
 synthesis intermediates, 735–738
- Lanthanum(III), FAAS analysis, 272
- Lanthanum chloride lithium chloride, addition  
 to multiple bonds, 569, 572
- (–)-Lardolure, enantioselective conjugate  
 addition, 786, 788
- Large-angle X-ray scattering, structural  
 studies, 3
- Laser ablation, Mg atom formation, 157, 159
- Lewis bases, titration, 288
- Ligand exchange  
 Mg<sup>2+</sup>, 318–321  
 cationic sandwiches, 124  
 sulfoxides, 444, 720
- Ligand loss, Mg cation–alcohol reactions, 161
- Ligand redistribution, organomagnesium  
 amides, 411
- Ligands  
 anionic, 176–178

- carboxylate, 178–179
- enantioselective conjugate addition, 774–777, 780–784
- Mg<sup>2+</sup> coordination
  - carboxylates, 321–322
  - nitrogen compounds, 324
  - phosphate functionalities, 322–324
  - water, 318–320
- organomagnesium cation reactivity, 180
- Ligand switching, Mg cation–alcohol reactions, 161
- Ligated magnesium ions
  - adduct-forming reactions, 160
  - electron impact, 175
  - gas-phase fragmentation, 174–179
  - ligands, 174–175
  - photoactivation reactions, 162–170
- Linear sweep cathodic stripping voltammetry (LSCSV), sodium pentothal, 276
- Liquid chromatography
  - high-performance, 274
  - speciation analysis, 292–293
- N-Lithio amines, magnesium carbenoid reactions, 741
- N-Lithio arylamines
  - magnesium alkylidene carbenoid reactions, 748–755
  - magnesium carbenoid reactions, 728–729, 730
- N-Lithio nitrogen-containing heterocycles, 755–757
- Lithium acetylides, magnesium alkylidene carbenoid reactions, 526, 758
- Lithium aluminum hydride, titration, 288, 290
- Lithium butyldimethylmagnesium, I<sub>2</sub>–Mg exchange, 692, 695
- Lithium chloride
  - addition to multiple bonds, 569–570, 572
  - alkylmagnesium chloride complexes, 682, 714
  - Cu(II) chloride, 544
  - functionalized Grignard reagent synthesis, 519–521, 531, 533–537
  - lanthanum chloride, 569
  - 2,2,6,6-tetramethylpiperidine magnesium chloride, 539–540, 541
  - transition-metal-free homocoupling, 556, 557
- Lithium dialkylamides, metalation, 537
- Lithium dibutylisopropylmagnesate,
  - halogen–Mg exchange, 692, 694, 697, 699, 700
- Lithium magnesiates, halogen–Mg exchange reagents, 523
- Lithium tetramethylpiperidide, epoxide deprotonation, 547
- Lithium thiolates, magnesium alkylidene carbenoid reactions, 758–760
- Lithium tributylmagnesate
  - deprotonation, 688
  - halogen–Mg exchange, 690–692, 693, 696–698, 707
- Lithium trimethylmagnesate, 681, 683–684, 706, 707
- Lithium triorganomagnesates, 682
- Lithium triphenylmagnesate, 681, 683
- Lithium tris(*sec*-butyl)magnesate, Br<sub>2</sub>–Mg exchange, 706, 707
- Lithium tris(2,2,6,6-tetramethylpiperidino)magnesate, 713
- Lithospermic acid, liquid chromatography, 293, 294
- Lowest excited electronic state, cyclopentadienyl magnesium, 123
- Low-temperature ashing (LTA), matrix obliteration, 271
- LSCSV (linear sweep cathodic stripping voltammetry), 276
- LTA (low-temperature ashing), 271
- Lung cancer, elemental analysis in hair, 278
- Lymphoblastic leukemia, elemental analysis in hair, 278
- Lymphoma, elemental analysis in hair, 278
- Mag-fura-2/5/Red, UV–visible fluorometry, 283, 284, 288
- Mag-indo-1, UV–visible fluorometry, 283, 284
- Magnesacarboranes, molecular geometry, 51–53
- Magnesacycles
  - magnesium anthracene compounds, 46–47
  - thermochemistry, 117, 120–121
- Magnesacycloalkanes, thermochemistry, 120–121
- Magnesacyclohexane, structure, 39–40
- Magnesate anions
  - bimolecular reactions, 180–182
  - fragmentation, 178–179
- Magnesiation
  - hydromagnesiation of acetylenes, 540, 543
  - magnesium amide bases, 537–540
  - see also* Carbomagnesiation; Metalation
- Magnesium
  - activation, 513
  - in adult human body, 270
  - biochemistry, 315–367
  - cation transporters, 324–327
  - DNA and RNA interactions, 320–321, 333–342
  - isotope effect, 330
  - protein-based enzymes, 342–359
  - universal energy currency of life, 327–333
  - bound to DNA, 270
  - CO complexes, thermochemistry, 125

- Magnesium (*continued*)  
coordination, 318–324  
binding modes, 320–324, 331–332  
carboxylate ligands, 321–322  
hexaaquamagnesium ion, 318–320  
nitrogen ligands, 324  
phosphate functionalities, 322–324  
direct oxidative addition to organic halides, 512–515  
electrochemical deposition, 245–253  
kinetics, 252–253  
electropositivity, 102–103, 125  
elemental analysis, 268, 269–288  
films, 172–174  
free hydrated ions, 269  
isotopically labelled, 107  
properties, 102–103  
Rieke magnesium, 514  
second ionization energy, 175  
surfaces, 172–174  
vaporization, 157  
<sup>24,25,26</sup>Magnesium, reverse isotope dilution technique, 287–288  
Magnesium acetylides, structure, 42–43  
Magnesium–adenosine triphosphate (MgATP), 328–329  
Magnesium alcoholates, solubility, 521  
Magnesium alkoxide, metalation, 461, 493  
Magnesium alkylidene carbenoids  
electrophilic reactions  
alkenylation, 748  
*N*-lithio arylamines, 748–755  
*N*-lithio nitrogen-containing heterocycles, 755–757  
lithium acetylides, 758  
lithium thiolates, 758–760  
tetrasubstituted olefin one-pot synthesis, 746–748  
generation, 742–745  
nucleophilic property, 744–746  
structure, 751, 753–754, 755  
Magnesium allenyl enolates, 449, 450, 506  
Magnesium amide bases  
chiral, 470  
magnesium enolate preparation, 464–465, 466–469  
metalation agents, 537–543  
Magnesium amide enolates, 499–500  
Magnesium amides  
chiral, 454, 498  
hindered, 464–469  
Magnesium  $\beta$ -aminoenolate, 454  
Magnesium aminoester enolates, 487, 489, 497  
Magnesium–anthracene compounds  
functionalized Grignard reagent synthesis, 514  
structural chemistry, 44–47  
Magnesium atoms  
excited state, 157, 158, 159  
formation, 157  
organic substrate reactions, 157–159  
alkanes, 157  
alkyl halides, 157–158  
unsaturated substrates, 158–159  
reactivity, 171  
triplet states, 158  
Magnesium bicarbonate, as-received Mg surfaces, 172  
Magnesium bisamides, metalation, 539  
Magnesium carbenoids, 717–769  
chiral, 722  
cyclopropanation of allylic alcohols, 722  
electrophilic reactions  
1,3-C–H insertion reaction, 729–734  
Grignard reagent reactions, 723–725  
*N*-lithio arylamine reactions, 728–729, 730  
secondary chiral Grignard reagent synthesis, 725–727  
 $\alpha$ -sulfonyl lithium carbanion reactions, 727–728, 748  
generation, 718–722  
halogen–Mg exchange, 718–720  
sulfoxide–Mg exchange, 718, 720–722  
halogen–Mg exchange, 516  
 $\alpha$ -heteroatom-substituted Grignard reagents, 767  
magnesium alkylidene carbenoids, 742–760  
magnesium cyclopropylidenes, 735–742  
magnesium  $\beta$ -oxido carbenoids, 479, 760–766  
Magnesium carbides, 106–107  
Magnesium cations  
bimolecular reactions, 179–180  
organic substrate reactions, 160–170  
adduct-forming reactions, 160  
alcohols, 161, 165–166  
alkane complexes, 162–163  
alkyl halides, 160–161  
amine complexes, 167–169  
C=X bonds, 169–170  
ether complexes, 166–167  
MgX<sup>+</sup>, 162  
organohalogen complexes, 163–165  
photoactivation, 162–170  
radicals, 160–170  
reactivity, 160  
speciation analysis, 271  
Magnesium chiral enolates, 505–506  
Magnesium chloride, cation reactions, 162  
Magnesium clusters  
Cu–Mg cluster structure, 86, 87  
solvent-free environments  
alkyl halide reactivity, 157  
Mg cation–ether complexes, 167



- organic substrate reactions, 171–172
- reactivity, 171
- Magnesium cyclopropylidenes
  - electrophilic reactions, 739–742
  - intermediates in Doering–LaFlamme allene synthesis, 735–738
  - nucleophilic reactions, 738–739
  - pyramidal inversion, 738
- Magnesium dialkylmalonate, 462, 494–499
- Magnesium dicarbonyl enolates, 489–499
- Magnesium dihalide
  - catalyzed Claisen rearrangement, 444
  - transmetalation, 491, 492
- Magnesium enolates
  - chiral, 500
  - deuteration, 441, 479, 489
  - enantioselective conjugate addition, 789
  - IR spectroscopy, 451
  - one-carbon ring expansion, 762, 763–765
  - preparation, 438–472
    - conjugate addition, 450–457, 789
    - permutational H<sub>2</sub>/metal interconversions, 457–470
    - permutational metal/metal salts interconversion, 445–450
    - permutation of heteroatom/metal, 441–445
  - reductive metal insertion, 438–441
- reactivity, 472–506
  - carboxylic acid dianions, 503
  - chiral oxazolidinone anions, 503–505
  - electrophiles, 472–505
  - magnesium amide enolates, 499–500
  - magnesium dicarbonyl enolates, 489–499
  - magnesium ester enolates, 484–489
  - magnesium ketone enolates, 472–484
  - magnesium lactam enolates, 499–500
  - magnesium lactone enolates, 484–489
  - magnesium thioamide enolates, 500–502
  - magnesium thioesters, 500–502
- Magnesium ester enolates, 484–489
- Magnesium ethyl carbonate (MMC, Stile's reagent), 463, 476
- Magnesium–fluorine bonds, 103
- Magnesium Green, UV–visible fluorometry, 283, 284, 285
- Magnesium halides, gas-phase structures, 3084
- Magnesium hydride
  - functionalized Grignard reagent synthesis, 540, 543
  - titanocene hydride–magnesium hydride complex, 88–89
- Magnesium hydrogen alkylmalonate, 494–499
- Magnesium hydroxide, as-received Mg surfaces, 172
- Magnesium ionophores, ion-selective electrodes, 275
- Magnesium  $\alpha$ -ketoester enolates, 489–493
- Magnesium ketone enolates, 472–484
- Magnesium lactam enolates, 442, 443, 499–500
- Magnesium lactone enolates, 484–489
- Magnesium lithospermate, liquid chromatography, 293, 294
- Magnesium Orange, UV–visible fluorometry, 283, 284
- Magnesium organohaloaluminate salts, cathodic reduction, 248–251
- Magnesium oxide, cation reactions, 162
- Magnesium  $\beta$ -oxido carbenoids, 479, 760–766
- Magnesium phthalocyanine, PET, 198
- Magnesium sandwich species
  - cationic sandwiches, 124–125
  - half-sandwiches, 123, 124
  - thermochemistry, 115, 122–125
  - triple decker (club) sandwiches, 123–124
- Magnesium(II)-selective fluorophores, UV–visible fluorometry, 283–284
- Magnesium thioamide enolates, 500–502
- Magnesium thioesters, 500–502
- Magnesocene
  - <sup>25</sup>Mg NMR spectra, 152, 153
  - multi-hapto-bonded complexes, 25–26, 47–50
  - organomagnesium cation formation, 180, 182
  - structure, 183
  - thermochemistry, 122–123
- ansa*-Magnesocene complexes, structure, 48–50
- Magon, UV–visible spectrophotometry, 282, 283
- Mag-quin-1/2, UV–visible fluorometry, 283, 284
- MALDI (matrix assisted laser desorption ionization), 156, 171
- Mandiphos ligand, catalytic enantioselective conjugate addition, 775, 776
- Manganese, catalyzed carbomagnesiation, 636, 637
- Manganese salts, transmetalation, 552
- Mass spectrometers, EI sources, 156
- Mass spectrometry
  - elemental analysis of Mg, 287–288
  - FT-ICR, 160
  - ICP-MS, 287–288
  - solvent-free environments, 156, 159, 160, 162
- Matrix assisted laser desorption ionization (MALDI), 156, 171
- Matrix isolation, Mg atom reactions, 157–159, 171
- Matrix obliteration, elemental analysis sample preparation, 271–272

- Mechanisms  
  enantioselective conjugate addition,  
    789–791  
    semiempirical [PM3(tm)] calculations,  
      790–791
- Medicinal applications, chlorophyll, 191, 211, 214
- Metabolic enzymes (protein-based), 345–350  
  enolases, 348–350  
  glycolytic cycle, 345, 346  
  protein kinases, 345, 347–348
- $\alpha$ -Metalated nitriles, functionalized Grignard reagent synthesis, 528, 529
- Metalation  
  arene, 22  
  deprotonative, 18–22  
  Fe-catalyzed carbometalation, 622–623  
  hindered Hauser bases, 464  
  hindered magnesium amides, 464–469  
  Kohler's ketone, 457, 458  
  magnesium alkoxide, 461, 493  
  magnesium enolate preparation, 457–470  
  organomagnesium amides, 419–421, 537–540, 541  
  thioamides, 452  
  see also Transmetalation
- Metal-bonded butyl groups, heteroleptic organomagnesiates, 22
- Metal carbonyls, 125
- Metal insertion, C–halogen bonds, 438–441
- Metalla-cyclobutane, Grignard reaction, 86
- Metalloclusters, 106
- Metalloids, CO complexes, 125
- Metallo-olefins, 106
- Metalloproteins, speciation analysis, 269
- Metallopyrroles, photochemistry, 212–213
- Metal powders, water determination, 299
- Metastable conditions, organomagnesium cation fragmentation, 182
- Methane, active hydrogen determination, 299–300
- Methanol, Mg cation fragmentation, 176
- 2-Methoxyethanol, Mg cation complex photofragmentation, 166
- 2-(Methoxymethyl)phenylmagnesium bromide, 65, 66
- N*-Methylacetamide, Mg cation binding energy, 175
- (2-Methylallyl)magnesium, allylic exchange, 143
- Methylamine, Mg cation complex, 168
- N*-Methylation, enthalpies of formation, 113–114
- Methyl bromide, enthalpy of reaction, 105–106
- Methyl crotonate, enantioselective conjugate addition, 781, 789
- Methyl deviations, alkylmagnesium bromides, 111
- Methylene increment, organomagnesium bromides, 110–111, 113–114
- 9-Methylfluorene, titration, 288, 289
- Methyl Grignard reagents  
  oxidation at inert electrodes, 229–231  
  distribution of anodic products, 230
- Methyl groups, electrochemical grafting, 241–243
- Methyl halide, Mg atom reactions, 158
- Methyl 2-halogeno-2-cyclopropylideneacetate, Michael addition, 452
- Methyl 4-iodobenzoate, functionalized Grignard reagent synthesis, 517
- Methylmagnesium alkoxides, <sup>1</sup>H NMR spectra, 145
- Methylmagnesium *tert*-butoxide, 70
- Methylmagnesium  
  tris(3-*tert*-butylpyrazolyl)hydroborate, 73, 74
- Methylmagnesium  
  tris(3-*tert*-butylpyrazolyl)phenylborate, 73, 74
- Methyl methacrylate, polymerization, 16, 484
- N*-Methylpyrrolidinone (NMP)  
  alkenylation, 604–605  
  functionalized Grignard reagent synthesis, 534, 535
- Methylthymol Blue, UV–visible spectrophotometry, 280, 281
- Methyl 2-(trimethylsilyl)propenoate, Michael addition, 452
- MgATP (Mg–adenosine triphosphate), 328–329
- <sup>25</sup>Mg NMR spectroscopy, 143, 151–152, 153
- Michael addition  
   $\beta$ -amino- $\alpha,\beta$ -diester preparation, 489  
  benzalacetomesitylene, 451  
  C=C bonds, 563–565  
  *N,N*-dialkyl- $\alpha$ -methacrylthioamides, 452  
  magnesium aminoester enolates, 497  
  magnesium enolate preparation, 451–454  
  methyl  
    2-halogeno-2-cyclopropylideneacetate, 452  
    methyl 2-(trimethylsilyl)propenoate, 452  
     $\alpha,\beta$ -unsaturated carboxylic acid derivatives, 451  
     $\alpha,\beta$ -unsaturated thioesters, 501
- Michler's ketone, Gilman's color test, 295, 296
- Microfluorimetry, elemental analysis of Mg, 288
- Microwave-aided extraction, elemental analysis of Mg, 271
- Microwave digestion, FAAS analysis, 272
- Microwave irradiation, aryl chloride/bromide activation, 513

- Microwave spectroscopy, Mg film reactions, 174
- Milk  
  complexometric analysis, 283  
  mineralization, 271, 279
- Mineralization, matrix obliteration, 271
- Mixed magnesate reagents, nucleophilic addition, 685–686
- Mixed magnesium/lithium amides, metalation, 539
- Mixed metal alkyl–amido base, triorganomagnesate production, 13–14
- Mixed organomagnesium transition-metal compounds, 85–91
- MMC (magnesium ethyl carbonate (Stile's reagent)), 463, 476
- Model reactions, Grignard calculations, 380–384
- Modified Schlenk equilibrium, *ab initio* calculations, 378–380
- Moisture exclusion, calorimetry, 104
- Molar standard enthalpies of formation, 102  
  *see also* Enthalpies of formation
- Molar standard enthalpies of reaction, 102  
  *see also* Enthalpies of reaction
- Molecular geometry  
  slipped geometry, 53–54  
  *see also* Structural chemistry
- Monensin, synthesis, 482, 483
- $\beta$ -Monoacylglycerols, derivatization, 301
- Monodentate coordination,  $\text{Mg}^{2+}$ , 322, 324
- Monoorganomagnesium  $\beta$ -diketiminates, 73–78
- Monoorganomagnesium heteroleptic compounds, 54–85  
  amides, 71–83  
  cations, 56–57  
  halogen compounds, 58–69  
  oxygen compounds, 69–71  
  phosphorus compounds, 84–85  
  sulfur compounds, 84, 85
- Mukaiyama reaction, 450, 456, 457, 474
- Multi-carbon homologation, alkyl halides, 723–724
- Multi-hapto-bonded groups, diorganomagnesium compounds, 25–29, 47–54
- Multiple bonds, organomagnesium reagent addition, 471, 559–575
- Multivariate PLS regression, IR spectroscopy, 295
- Mycocerosic acid, enantioselective conjugate addition, 787, 788
- 1,8-Naphthalene diylmagnesium THF complex, 40–41
- Nasopharyngeal cancer, elemental analysis in hair, 278
- Natural products  
  catalytic enantioselective synthesis, 786–789, 799  
  Fe-catalyzed Grignard reactions, 625–628
- Near-IR spectroscopy, concentration monitoring, 512
- Neodymium trichloride, addition to C=O bonds, 570
- Neopentylmagnesium bromide, functionalized Grignard reagent synthesis, 534, 535
- NHCs *see* *N*-Heterocyclic carbenes
- Nickel  
  catalyst immobilization on charcoal, 554  
  organomagnesium compounds, 86
- Nickel-catalyzed reactions  
  addition to C=C bonds, 560  
  carbomagnesiation, 635, 640, 653–654, 664–665  
  cross-coupling reactions, 543–544, 550–552, 554
- Nitriles  
   $\alpha$ -metalated, 528, 529  
   $\alpha,\beta$ -unsaturated, 565–566
- Nitroalkenes, addition, 566
- Nitroarenes, electrophilic amination, 576
- Nitro compounds,  $\text{I}_2$ –Mg exchange, 531, 533
- Nitrogen, organomagnesium ion reactivity, 180
- Nitrogen compounds  
  carbomagnesiation, 641–642  
  *N*-lithio nitrogen-containing heterocycles, 755–757  
   $\text{Mg}^{2+}$  coordination, 324
- Nitrogen oxides, organomagnesium ion reactivity, 180
- Nitrosoarenes, electrophilic amination, 576–577
- NMP (*N*-methylpyrrolidinone), 534, 535, 604–605
- NMR spectroscopy, 131–153  
  alkoxides, 145–147  
  alkylmagnesium compounds, 133–138, 141  
  allylmagnesium compounds, 141–145  
  arylmagnesium compounds, 134, 138–140  
  aryloxides, 146, 147  
  co-ordination complexes, 148, 149–150  
  elemental analysis of Mg, 286–287  
  peroxides, 147–148  
  solution concentration, 132–133  
  speciation analysis, 296–298  
  vinylmagnesium compounds, 145  
  *see also*  $^{13}\text{C}$  NMR spectroscopy;  $^{19}\text{F}$  NMR spectroscopy;  $^1\text{H}$  NMR spectroscopy;  $^{25}\text{Mg}$  NMR spectroscopy;  $^{17}\text{O}$  NMR spectroscopy
- No-D NMR spectroscopy, speciation analysis, 296

- Non-stabilized  $\alpha$ -amino-substituted carbanions, 728–729
- Nuclear magnetic resonance spectroscopy *see* NMR spectroscopy
- Nucleobases, tautomeric forms, 170
- Nucleophilicity, magnesium alkylidene carbenoids, 744–746
- Nucleophilic reactions
- diorganomagnesium compounds, 256–257
  - magnesium cyclopropylidenes, 738–739
  - triorganomagnesiates, 683–686, 711, 713
- Olefination, Peterson, 474–475, 487, 488
- Olefins
- anodic addition of Grignard reagents, 237
  - Cu–olefin  $\pi$ -complex, 790
  - tetrasubstituted, 746–748
- One-carbon homologation, magnesium  $\beta$ -oxido carbenoids, 760–766
- One-pot synthesis, tetrasubstituted olefins, 746–748
- $^{17}\text{O}$  NMR spectroscopy, peroxides, 147–148
- Optically active compounds
- chloroalkyl aryl sulfoxides, 721, 725–727
  - magnesium carbenoid generation, 721–722
- Organic alkali compounds, stability, 103
- Organic chromophores, absorption spectra, 193
- Organic halides
- direct oxidative addition of Mg, 512–515
  - Mg cation reactions, 162
- Organic substrates
- Mg atom reactions, 157–159
  - unsaturated substrates, 158–159
- Organoaluminum compounds, 103
- Organoantimony compounds, derivatization, 300, 304
- Organoelemental compounds, electrooxidation of Grignard reagents, 228, 237–241
- Organohaloaluminate salts, cathodic reduction, 248–251
- Organohalogens, Mg cation complexes, 163–165
- Organolanthanides, titration with  $\text{I}_2$ , 290–291
- Organolead compounds, derivatization, 300, 303
- Organolithium compounds, titration, 288, 289
- Organolithium reagents, lithium magnesiate preparation, 523
- Organomagnesiates, 681–715
- anion reactivity, 178–179, 180
- Organomagnesia and rings, thermochemistry, 117–121
- Organomagnesiates
- structural chemistry, 4–22
  - heteroleptic, 5, 14–22
  - homoleptic, 5
  - tetraorganomagnesiates, 5–12
  - triorganomagnesiates, 12–14
- Organomagnesium alkoxides, 428–432
- Organomagnesium amides
- metalation, 537–540, 541
  - reactivity, 419–426
  - structure, 71–83, 405–410, 412–419
  - synthesis, 54, 71–83, 403, 404–412, 413–416
- Organomagnesium aryloxides, 428–432
- Organomagnesium ate complexes, 681–715
- Organomagnesium bromides
- heteroatoms, 113–116
  - methylene increment, 110–111
  - unsaturated
    - enthalpies of hydrogenation, 113, 119
    - formal protonation reactions, 112
- Organomagnesium cations *see* Magnesium cations
- Organomagnesium chloroaluminate complexes, cathodic reduction, 248–249
- Organomagnesium compounds
- analytical aspects, 265–314
  - speciation analysis, 268, 269, 288–299
  - bifunctional, 39–40
  - film decomposition, 173
  - functionalized
    - reactivity, 543–583
    - synthesis, 512–543  - gas-phase structures, 183–184
  - solvent-free environments, 155–187
- Organomagnesium fluorides, 103
- Organomagnesium-group 15-bonded complexes, 403–427, 428
- Organomagnesium-group 16-bonded complexes, 427–434
- Organomagnesium halides
- homologous series, 110–112, 117
  - thermochemistry, 109–116
  - unsaturated compounds, 112–113
- Organomagnesium ions
- gas-phase bimolecular reactions, 179–182
  - gas-phase unimolecular reactions, 182
  - insertion reactions, 168
  - ligated Mg ion fragmentation, 174–179
- Organomagnesium phosphanide, 427, 428
- Organomagnesium sulfides, 433–434
- Organomagnesium transition-metal compounds, structures, 85–91
- Organomercury compounds, derivatization, 304
- Organometallic compounds
- derivatization, 300–301, 302–304
  - electrooxidation of Grignard reagents, 228, 237–241
- Organotin compounds, gas chromatography, 300, 302–303, 304
- Organozinc compounds, titration with  $\text{I}_2$ , 290–291

- Osmometric measurements, Schlenk equilibrium, 107
- Oxazolidinones  
1,4-addition to Michael acceptors, 563–564  
chiral, 503–505
- Oxidation  
Mg cation reactions, 160–161, 163  
photoinduced ring-opening, 207–209, 210, 211  
*see also* Anodic oxidation
- Oxidation potentials, Grignard reagent correlations, 258–260
- Oxidative addition  
induction period, 513  
Mg to organic halides, 512–515
- Oxidative coupling  
polyfunctional aryl/heteroaryl amidocuprates, 580–581  
silver tosylate homocoupling, 547
- $\beta$ -Oxido carbenoids, 479, 760–766
- Oxime ethers, chiral, 574
- Oxine  
high-performance liquid chromatography, 274  
UV–visible spectrophotometry, 279, 280–281
- Oxonium structure, Grignard reagents, 107
- Oxonium ions, stability, 104
- Oxygen  
organomagnesium amide reactions, 422–423  
organomagnesium ion reactivity, 180
- Oxygen compounds  
carbomagnesiation, 643  
C–O bond activation, 159, 161, 167  
heteroleptic monoorganomagnesium compounds, 69–71  
intramolecular coordination, 66
- Palladium-catalyzed reactions  
addition to C=C bonds, 561  
carbomagnesiation, 641, 642  
cross-coupling reactions, 543–544, 550, 552, 553
- Pancreatic lipase hydrolysis, glyceride analysis, 301
- Particulate matter, Mg speciation analysis, 270–271
- Pathogenesis indicators for cancer, AAS, 278
- PDT (photodynamic therapy), 191, 211, 214
- Pearl, ICP–AES Mg analysis, 279
- PEBBLES, UV–visible fluorometry, 285
- PEPPSI, transition-metal-catalyzed cross-coupling, 550, 551
- Perfluorinated Grignard reagents, synthesis, 516
- Perfluoroalkylmagnesium halides, halogen–Mg exchange synthesis, 516
- Perfluorophenylmagnesium bromide, synthesis, 516
- Periodic table, bond energies, 115
- Permutational hydrogen/metal interconversions, 437–440, 457–470, 482
- Permutational metal/metal salts interconversions, 445–450
- Permutation of heteroatom/metal, 441–445
- Peroxides, NMR spectra, 147–148
- Perturbative quantum chromodynamics (PQCD), ion chromatography, 273
- Perylene-linked systems, PET, 201, 202–203
- PET (photoinduced electron transfer), 191, 194–206
- Peterson olefination, 474–475, 487, 488
- Pharmacological issues, Mg analysis, 268–269
- (–)-Phaseolinic acid, synthesis, 500, 501
- 1,10-Phenanthroline, indicator, 288, 289
- Phenylacetylene, NMR spectroscopy, 297
- 4-(Phenylazo)diphenylamine, indicator, 289
- 1,2-Phenylene magnesium THF complex, structure, 40–41
- Phenylethynylmagnesium bromide, enthalpy of reaction, 112
- 2-(Phenylmagnesium)-1,3-xylene-15-crown-4, 34–36
- Phenylmagnesium bromide ethoxide, structure, 58
- N*-Phenyl-1-naphthylamine, titration, 288, 289
- 4-Phenylpicnic acid, preparation, 451
- 4-Phenylloxazolidinone, Evans-type auxiliary, 447
- 1-Phenylpropyne, transition-metal-catalyzed cross-coupling, 545
- Pheophytinization, porphyrins, 194
- Phosphates,  $Mg^{2+}$  coordination, 322–324
- Phosphines, monomagnesium compounds, 84–85
- Phosphomycoketides, enantioselective conjugate addition, 785, 786
- Phosphoramidites  
allylic substitution, 558  
Cu-catalyzed enantioselective reactions  
allylic alkylation, 792, 793, 794  
conjugate addition, 774, 792, 793
- Phosphorus compounds, heteroleptic monoorganomagnesium compounds, 84–85
- Photoactivation  
excited-state Mg atoms, 157  
ligated Mg cation complexes  
alcohols, 165–166  
alkanes, 162–163  
amines, 167–169  
C=X bonds, 169–170  
ethers, 166–167  
organohalogens, 163–165

- Photochemical reactions  
  chlorophyll, 209–212, 213–214  
  porphyrins, 206–209  
  ring-opening reactions, 207–209, 210, 211
- Photochemistry, 189–218  
  applied, 212–214  
  electron transfer, 191, 194–206  
  Mg cation–alkane complexes, 163  
  phthalocyanines, 190–191, 198  
    applied photochemistry, 213  
    electron transfer systems, 196, 198  
    porphyrin dyads, 196  
  porphyrins, 190–191, 192–194  
    applied photochemistry, 212–214  
    reactions, 206–209  
    stability, 193–194
- Photochromism, polythiophene, 285
- Photodissociation spectroscopy, Mg cation complexes, 162–164, 165–166, 168–169, 171
- Photodynamic therapy (PDT), chlorophylls, 191, 211, 214
- Photofragmentation, Mg cation complexes, 166–170
- Photoinduced electron transfer (PET), 191, 194–206
- Photoionization, Mg cation–ether clusters, 167
- Photooxidation  
  phthalocyanines, 213  
  ring-opening reactions, 207–209, 210, 211
- Photooxygenation, chlorophylls, 211, 212
- Photopigments, porphyrins, 193–194
- Photosensitizers, chemical transformations, 206, 211
- Photosynthesis, 191–196  
  chlorophylls, 191, 356–357  
  photochemical reaction center, 194, 195  
  photosystems I and II, 355–356  
  protein-based enzymes, 355–359  
  rubisco, 357–359  
  Z-scheme, 194, 195
- Photosystems I and II, photosynthesis, 355–356
- Phthalocyanines  
  photochemistry, 190–191, 198  
  applied photochemistry, 213  
  electron transfer systems, 196, 198  
  porphyrin dyads, 196
- Phthioceranic acid, enantioselective conjugate addition, 788
- Phytochlorin, photosynthesis, 192
- Piezochromism, polythiophene, 285
- Piezoelectric detection, ion chromatography, 273
- Pigments, photosynthesis, 191–192
- Pinacolborates, functionalized synthesis, 534, 537
- Plasma  
  AAS, 278  
  electrolyte determination, 275–276  
  electrophoresis, 274  
  mass spectrometry, 288  
  speciation analysis, 269–270
- Platinum terpyridine acetylide complex, PET, 198
- PLS (partial least squares) regression, IR spectroscopy, 295
- Pnictogenides, heavy group 15 complexes, 427
- <sup>31</sup>P NMR spectroscopy  
  elemental analysis of Mg, 286–287  
  speciation analysis, 297–298
- Polar bonds, Mg, 103, 118
- Polar mechanisms, Grignard carbonyl additions, 370, 387–388, 389, 391, 394, 396, 400–401
- Polycenter electron-deficient bonds, magnesium carbides, 107
- Poly(chlorotrifluoroethylene), surface conditioning, 305
- Polycyclic aromatic hydrocarbons, Mg cation reactions, 160
- Polyenes, Mg cation reactions, 160
- Polyfluorinated pyridines, Mg cation complexes, 164
- Polyfunctional aryl/heteroaryl amidocuprates, oxidative coupling, 580–581
- Polymerization  
  methyl methacrylate, 16, 484  
  organomagnesium-group 15-bonded complex catalysts, 421
- Polymers, chromatic chemosensors, 285
- Polymetallic host, deprotonative metalation, 19
- Polyphenol-bound magnesium, speciation analysis, 271
- Polysaccharide-bound magnesium, speciation analysis, 271
- Polysantol, preparation, 440
- Polythiophene, chromatic chemosensors, 285
- Polyvinyl alcohol, surface conditioning, 305
- Porphyrin photochemistry, 125, 190–191, 192–194  
  applied photochemistry, 212–214  
  arrays, 201, 204–205  
  dimerization, 206  
  electron transfer systems, 196–206  
  photochemical reactions, 206–209  
  phthalocyanine dyads, 196  
  stability, 193–194
- Portland cement, voltametric analysis, 277
- Potassium triiodide, potentiometric titration, 291–292
- Potential energy profile, Grignard reagent calculations, 376, 377, 381
- Potentiometric titration, speciation analysis, 291–292

- PQCD (perturbative quantum chromodynamics), 273
- Preconcentration, elemental analysis sample preparation, 272–273
- Primary alkyl chlorides, transition-metal-catalyzed cross-coupling, 544
- Proazaphosphatane, magnesium enolate, 472
- Probe encapsulated by biologically localized embedding (PEBBLE), 285
- Propargyl alcohols  
  carbomagnesiation, 645–652  
  Fritsch–Buttenberg–Wittich rearrangement, 744
- Propargyl amines  
  carbomagnesiation, 652–653  
  functionalized Grignard reactions, 548, 549
- $\beta$ -Propiolactones, ring opening, 547
- Propylamine, Mg cation complex, 168
- Propylmagnesium bromide, DME complexes, 59
- Prostatic carcinoma, elemental analysis in hair, 278
- Protecting groups, functionalized Grignard reagents, 530–531, 534
- Protein-based enzymes  
  Mg biochemistry, 342–359  
  allosteric systems, 343–345  
  DNA replication and repair, 350–355  
  enzymatic modes of action, 342–345  
  metabolic enzymes, 345–350  
  photosynthesis, 355–359  
  sequential systems, 343, 348–350  
  template enzymes, 342–343
- Protein kinases, 345, 347–348
- Proteins, speciation analysis, 269
- Protonation  
  enantioselective, 480, 481  
  *see also* Deprotonation; Enthalpies of protonation
- Proton transfer  
  carbocation–Mg atom reactions, 159  
  Mg cation reactions, 162, 175
- Protoporphyrins, photooxidation, 207–208
- PTFE, alkali-activated, 283
- Pulsed photoacoustic spectroscopy, PET, 198
- Purpurin, UV–visible spectrophotometry, 279–280
- Pyramidal inversion, magnesium cyclopropylidenes, 738
- 1-Pyreneacetic acid, titration, 288, 289
- 1-Pyrenemethanol, titration, 288, 289
- Pyridine-enhanced precatalyst preparation  
  stabilization and initiation (PEPPSI), 550, 551
- Pyridines  
  diethylmagnesium reactions, 684  
  Mg cation complex, 168  
  metalation, 537  
  transition-metal-catalyzed cross-coupling, 553
- Pyridylmagnesium,  $\text{Br}_2$ –Mg exchange, 524
- 2-Pyridylmagnesium bromide, THF complex, 65
- 2-Pyridylsilylmethyl  
  tris(trimethylsilyl)methylmagnesium bromide, THF complex, 63, 64
- Pyroangelensolide, preparation, 482, 483
- Pyrolants, fluorocarbons, 103
- Pyrophosphates,  $\text{Mg}^{2+}$  coordination, 323–324
- Pyrroles  
  Boc-protected 2-substituted, 447, 449  
  magnesiation, 538, 539
- Quadrupole ion trap mass spectrometers, organomagnesium ions, 180
- Quality control, organometallic compounds, 300
- Quaternary chiral centers, all-carbon, 565
- Quaternary stereocenters  
  allylic alkylation of esters, 792, 796  
  one-carbon expanded ketone, 762, 763
- Quinalizarin, UV–visible spectrophotometry, 279–280, 282
- Quinolines, transition-metal-catalyzed cross-coupling, 553
- Quinones, PET, 194–196, 197–198, 207
- Racemic magnesium carbenoids, generation, 720–721
- Radiative association kinetics, bond dissociation energies, 124
- Radiative associative adduct formation, Mg cation reactions, 160
- Radical anions  
  anthracene, 45, 46  
  1,2-bis[(2,6-diisopropylphenyl)imino]acenaphthene, 79, 80
- Radical cations, 160–170
- Radical cyclization, Fe-catalyzed, 623–624
- Radicals  
  anodic oxidation of Grignard reagents, 229–237, 238, 258–259  
  2-thenyl, 299
- Rare-earth metal salts, addition to C=O bonds, 569–570
- Rate constants, Grignard reagent correlations, 258–260
- Reaction *see* Enthalpies of reaction; Molar standard enthalpies of reaction
- Reactive halides, gas chromatography, 295
- Reactivity  
  Grignard reagents, 235–236, 258–260  
  functionalized, 543–583

- Reactivity (*continued*)  
Mg cations, 160–170  
magnesium enolates, 472–506  
organomagnesium amides, 419–426
- Rearrangement reactions  
Claisen, 444, 446, 487, 491  
Fritsch–Buttenberg–Wiechell, 742–744
- Redistribution reactions  
heteroleptic monoorganomagnesium compounds, 55  
ligand redistribution, 411
- Reduction  
Krasnovskii reduction, 211, 212  
*see also* Cathodic reduction
- Reductive metal insertion, C–halogen bonds, 438–441
- Reflectance, IR spectroscopy, 295
- Reformatski reagent, enolate bridge-bonding, 77
- Regioselectivity  
carbomagnesiation, 636–638, 641–644, 652–653, 675  
hindered Hauser base deprotonation, 464
- Resonance effects, hydrocarbylmagnesium bromides, 114
- Resorcinol, formation, 493, 505
- Retro-Ritter reactions, Mg cation fragmentation, 177
- Reverse isotope dilution technique, elemental analysis of Mg, 287–288
- Rharasch reaction, natural product synthesis, 625–626
- Rhenium complexes, tetraphenylporphyrins, 199–200
- Ribozymes  
Mg<sup>2+</sup> DNA/RNA interactions, 335–342  
group 1 introns, 337–339  
hammerhead ribozymes, 339–342
- Rieke magnesium, functionalized Grignard reagent synthesis, 514
- Ring contraction, cyclohexane, 476
- Ring expansion, one-carbon, 760–766
- Ring opening  
photoinduced, 207–209, 210, 211  
small cycles, 543, 547, 548
- Ring strain  
cycloalkylmagnesium halides, 117  
magnesacycloalkanes, 120–121
- Ritter reactions, retro-Ritter, 177
- RMSEP parameter, IR spectroscopy, 295
- RNA  
Mg<sup>2+</sup> interactions, 333–342  
5S rRNA domain, 335  
Loop E motif, 335  
ribozymes, 335–342  
speciation analysis of bound Mg, 270
- Root mean square error of prediction (RMSEP), IR spectroscopy, 295
- Rosmarinic acid, liquid chromatography, 293, 294
- Rotaxane structure, donor–acceptor complexes, 43–44
- Rubisco, CO<sub>2</sub> fixing enzyme, 357–359
- Ruthenium, organomagnesium compounds, 90–91
- $\sigma$ -bonded diorganomagnesium compounds, donor–acceptor complexes, 36–44
- Sacrificial anodes, electrooxidation of  
Grignard reagents, 237–241
- Salicylaldehyde phenylhydrazones, titration, 290
- Sample preparation  
elemental analysis of Mg, 271–273  
matrix obliteration, 271–272  
preconcentration, 272–273
- Sandwich species *see* Magnesium sandwich species
- Scaffold effect, template enzymes, 342
- Schlenck dimer, chelation-controlled addition, 393–395
- Schlenk equilibrium, 2, 422  
*ab initio* calculations, 378–380  
alkylmagnesium compounds, 107, 134, 137  
allylmagnesium compounds, 140, 142, 144–145
- Grignard reagents  
solutions, 132, 140–141, 144–145, 151  
structures, 384–387  
heteroleptic monoorganomagnesium compounds, 55  
thermochemistry, 107–109, 116
- Scymmol, synthesis, 495, 496
- Secondary amides, organomagnesium amide structures, 81, 82
- Secondary chiral Grignard reagents, synthesis, 725–727
- Second ionization energy, Mg, 175
- SEFT (spin-echo Fourier transform), 286
- Selected ion flow tube (SIFT), Mg cation reactions, 160
- Self-assembly processes, heteroleptic organomagnesium production, 18–19
- Self-hydrogenation, alkyne/diene Mg films, 173
- Semiconductor anodes, electrochemical oxidation of Grignard reagents, 241–243
- Semiempirical calculations  
magnesium chelates, 504  
[PM3(tm)] calculations, 790–791
- Sensitizers, PET, 206, 211
- Sequential enzymes, protein-based, 343, 348–350
- Sequential injection analysis (SIA) systems, UV–visible spectrophotometry, 280



- Serines,  $\alpha$ -substituted, 463, 505
- Serum
- electrolyte determination, 275–276
  - liquid chromatography, 293
  - Mg speciation, 273
  - UV–visible spectrophotometry, 282
- SET *see* Single-electron transfer
- Shell/shellfish, ICP–AES Mg analysis, 279
- SIA (sequential injection analysis) systems, 280
- SIFT (selected ion flow tube), 160
- Silanol groups
- borosilicate glass, 300
  - fused silica capillary tubes, 301, 305
- Silicon anodes, electrochemical oxidation of
- Grignard reagents, 241–243
- Silicon–magnesium exchange, silylenol ethers, 450
- Silver perchlorate, potentiometric titration, 291
- Silver tosylate, oxidative homocoupling, 547
- Silyl dienol ethers, preparation, 597–599
- Silyl enol ethers
- aldol-type reactions, 472–473, 484, 486
  - preparation, 472–474
  - Si–Mg exchange, 450
  - transmetalation, 450
- Simmons–Smith-type cyclopropanation, magnesium carbenoids, 722
- Single-electron transfer (SET)
- Grignard carbonyl additions, 370, 372, 396–399, 400–401
  - magnesium anthracene compounds, 45
- Site-bound magnesium(II) ions, in RNA, 270
- Small cycles, ring opening, 543, 547, 548
- $S_N2'$ -substitution, Cu(I) catalyst, 557
- Sodium bis(2-methoxyethoxy)aluminum hydride, titration, 290
- Solubility, lithium chloride effects, 521
- Solutions
- Grignard reagent formation, 172–174
  - NMR spectroscopy, 131–133
  - see also* Enthalpies of solution
- Solvation *see* Enthalpies of solvation
- Solvation energies, 104
- Solvent effects
- electric conductivity, 226–227
  - Grignard carbonyl additions, 387–391, 392, 393, 401
- Solvent evaporation, Mg cation–amine complexes, 15
- Solvent-free environments, 155–187
- bimolecular reactions, 179–182
  - formation of organomagnesium species, 156–179
  - Grignard reagents, 157, 384–389, 390, 391
  - structures of organomagnesiums/magnesium halides, 183–184
  - unimolecular reactions, 182
- Sparteine complexes
- dialkylmagnesium compounds, 148, 150
  - Grignard reagents, 60–61
- Sp-centers
- Sp<sup>2</sup>-center, 544, 550–559
  - Sp<sup>3</sup>-center, 543–550
  - substitution, 543–559
- Speciation analysis, 268, 269, 288–299
- chromatographic methods, 273, 292–295
  - cryoscopy, 299
  - free hydrated Mg ions, 269, 271
  - Mg bound to low molecular mass anions, 269
  - Mg strongly bound in metalloproteins, 269
  - Mg weakly bound to proteins, 269
  - spectral methods, 295–299
  - titation methods, 288–292
  - total Mg, 269, 270
- Spectral methods
- elemental analysis of Mg, 277–288
  - speciation analysis, 295–299
- Spectrophotometry, Mg in body fluids, 270
- Spin coupling constants, allylmagnesium compounds, 143–144, 145
- Spin-echo Fourier transform (SEFT), NMR spectroscopy, 286
- Spiro-organomagnesium compound, Tebbe-type, 86, 87
- Square wave adsorptive stripping voltammetry (SWAdSV), elemental analysis of Mg, 276
- Stability
- functionalized Grignard reagents, 514–515
  - magnesium alkylidene carbenoids, 744–745, 751
  - Mg<sup>2+</sup>–DNA/RNA interactions, 320–321, 334–335
  - organic alkali compounds, 103
  - oxonium ions, 104
  - porphyrin photochemistry, 193–194
- Staggered structure, magnesocene, 183
- Statine, enantioselective addition, 571
- Stereoselectivity
- carbomagnesiation, 636–638, 641–644, 652–653, 670, 671–672, 675
  - Grignard addition calculations, 380, 381
  - hindered Hauser base deprotonation, 465
  - magnesium chelate, 440, 441, 491, 492, 493, 504
  - magnesium enolate preparation, 446–450, 455–456, 457
- Sterically hindered amines
- magnesium amide formation, 538
  - magnesium enolate preparation, 457, 464
- Sterically hindered Hauser bases
- deprotonation
  - regioselectivity, 464

- Sterically hindered Hauser bases (*continued*)  
  stereoselectivity, 465  
  metalation, 464
- Sterically hindered ketones, enolization, 478
- Sterically hindered magnesium amides,  
  metalation, 464–469
- Stile's reagent (magnesium ethyl carbonate),  
  463, 476
- Strained alkenes, carbomagnesiation, 657–661
- Strain energies, magnesacycloalkanes, 121
- Strong Lewis bases, titration, 288
- Structural chemistry, 1–99  
  cubane structure, 29, 50, 51, 145, 146  
  diorganomagnesium compounds, 23–54  
  gas phase, 183–184  
  heteroleptic monoorganomagnesium  
    compounds, 54–85  
  magnesium alkylidene carbenoids, 751,  
    753–754, 755  
  organomagnesiates, 4–22  
  organomagnesium alkoxides/aryloxides,  
    428–432  
  organomagnesium amides, 71–83, 405–410,  
    412–419  
  rotaxane structure, 43–44  
  slipped geometry, 53–54
- Substitution  
   $\alpha$ -substituted serine preparation, 463, 505  
  allylic, 543, 557–558  
  Boc-protected 2-substituted pyrroles, 447,  
    449  
  Fe-catalyzed, 621–622  
   $\alpha$ -heteroatom-substituted Grignard reagents,  
    767  
   $S_N2'$ -substitution, 557  
  Sp-centers, 543–559  
     $Sp^2$ -center, 544, 550–559  
     $Sp^3$ -center, 543–550  
  tetrasubstitution  
    ketone preparation, 457  
    olefin synthesis, 746–748  
  trisubstitution  
    alkenyl sulfides, 758–760  
    2,2,7-trisubstituted cycloheptanones, 765
- Sulfinimines, chiral, 575
- $\beta$ -Sulfinyl ester magnesium enolates,  
  asymmetric synthesis, 448, 449
- $\alpha$ -Sulfinyl lithium carbanions, magnesium  
   $\beta$ -oxido carbenoids, 760–766
- $\alpha$ -Sulfinyl magnesium carbanion enolates,  
  asymmetric aldol-type addition, 459, 486,  
    487, 500
- Sulfonamides, substitution leaving groups, 553
- Sulfonates, substitution leaving groups, 553
- Sulfones, substitution leaving groups, 553
- $\alpha$ -Sulfonyl lithium carbanions  
  magnesium alkylidene carbenoid  
    alkenylation, 748  
  magnesium carbenoid reactions, 727–728
- Sulfoxide–magnesium exchange  
  magnesium carbenoids  
    generation, 718, 720–722  
    Grignard reagent reactions, 725  
    optically active, 721–722  
    racemic, 720–721  
  magnesium enolate preparation, 444
- Sulfoxide–metal exchange reactions, 720–721
- Sulfoxides  
  aldol-type reactions, 486, 487  
  chiral intermediates, 582–583  
   $I_2$ –Mg exchange, 527, 528
- Sulfur compounds  
  carbomagnesiation, 642–643, 644  
  heteroleptic monoorganomagnesium  
    compounds, 84, 85  
  magnesium enolate preparation, 443–444
- Sulfur–magnesium exchange, benzylic  
  magnesium reagent synthesis, 529–530
- $\alpha$ -Sulfur-stabilized Grignard reagent, 725, 726
- Surface chemistry  
  Grignard reagent formation, 172–174  
  Mg(0001) single-crystal chemisorption, 172,  
    173  
  surface modification, 172
- Surface conditioning, Grignard reagents, 301,  
  305
- SWAdSV (square wave adsorptive stripping  
  voltammetry), 276
- TAEN (N,N',N''-trimethyltriazacyclononane),  
  9–11
- TAG (triacylglycerols), 301
- Tamao, Kumada–Tamao–Corriu reactions, 550
- Tandem reactions, conjugate addition–aldol,  
  453, 457, 788, 789
- Taniaphos ligand  
  catalytic enantioselective reactions  
    allylic alkylation, 792, 797–798  
    conjugate addition, 775, 776, 777
- Tautomeric forms, nucleobases, 170
- Tautomerization, Mg cation–acetamide  
  complex, 177
- Tebbe-type spiro-organomagnesium  
  compound, 86, 87
- Tellurium compounds, derivatization, 304
- 3,3',5,5'-Tetra-*tert*-butyldiphenylquinone,  
  transition-metal-free homocoupling, 556,  
    557
- 1,3,5,7-Tetracyanocyclooctatetraene,  
  magnesium cationic sandwiches, 125
- Tetrahydrocannabinols, preparation, 481
- Tetrahydrofuran (THF) complexes  
  diorganomagnesium compounds, 40–41,  
    48–53  
  donor–acceptor, 39–43

- Grignard reagents, 58, 59, 63–66  
Mg cation fragmentation, 176  
4,4,5,5-Tetramethyl-1,3-dioxolan-2-one  
  *O*-phenylsulfoxime, electrophilic  
  amination, 579  
2,2,6,6-Tetramethylpiperidine magnesium  
  chloride, lithium chloride complex,  
  539–540, 541  
Tetraorganomagnesiates  
  dianions, 8–9  
  structural chemistry, 5–12  
Tetraphenylporphyrins, PET, 199–200  
Tetrapyrroles, photochemistry, 192–193,  
  212–213  
Tetrasubstituted compounds  
  ketone preparation, 457  
  olefin synthesis, 746–748  
Texas Red–dextran, UV–visible fluorometry,  
  285  
Thallocene, magnesocene reactions, 123  
Thenyl bromide, ESR spectroscopy, 299  
2-Thenyl free radical, ESR spectroscopy,  
  299  
Theoretical calculations  
  Grignard carbonyl additions, 369–370,  
  374–401  
  magnesium alkylidene carbenoid structure,  
  751, 753–754, 755  
  Mg–organic substrate reactions, 157–158  
Thermochemistry, 101–130  
  calorimetry, 104–106  
  cyclic compounds, 117–121  
  diorganomagnesium compounds, 116–117  
  magnesium carbides, 106–107  
  Mg–CO complexes, 125  
  magnesium sandwich species, 115,  
  122–125  
  organomagnesia and rings, 117–121  
  organomagnesium halides, 109–116  
  Schlenk equilibrium, 107–109, 116  
Thermochromism, polythiophene, 285  
Thermometric titration, speciation analysis,  
  292  
THF *see* Tetrahydrofuran complexes  
Thiazoles, Br<sub>2</sub>–Mg exchange, 525  
Thienamycin, preparation, 442  
(2-Thenyl)magnesium bromide, DME  
  complex, 59  
Thioamide enolates, reactions with  
  electrophiles, 500–502  
Thioamides  
  aldol-type reaction, 500–501, 502  
  metalation, 452  
Thioesters  
  reactions with electrophiles, 500–502  
   $\alpha,\beta$ -unsaturated, 501, 784  
  natural product synthesis, 785, 786–789  
Thioformamides, electrophilic amination, 579,  
  580  
Thorium, organomagnesium compounds, 90,  
  91  
Thymine, Mg cation complex, 170  
Tight ion pairs, thermochemistry, 123  
Titanium, organomagnesium compounds,  
  87–90  
Titanocene dichlorides, catalyzed addition to  
  C=C bonds, 561, 562  
Titanocene hydride–magnesium hydride  
  complex, 88–89  
Titration  
  complexometric, 270, 282–283  
  speciation analysis, 288–292  
  indicators, 288, 289, 290  
  potentiometric titration, 291–292  
  thermometric titration, 292  
  visual endpoint, 288–291  
TMEDA complexes  
  Grignard reagents, 59, 62  
  Fe-catalyzed reactions, 615–618, 622  
  multi-hapto-bonded groups, 50–52  
Tol-BINAP ligand, catalytic enantioselective  
  conjugate addition, 782–784  
Toluene, deprotonation, 19  
*p*-Tolylmagnesium bromide, DME complex,  
  60  
Tosylates, transition-metal-catalyzed  
  cross-coupling, 544  
Transition metal carbonyls, 125  
Transition-metal-catalyzed reactions  
  addition to C=C bonds, 559–562  
  allylic substitution, 557–558  
  cross-coupling, 543–547, 550–556  
Transition metal compounds,  
  organomagnesium moieties, 85–91  
Transition-state structures, Grignard reagent  
  calculations, 375–376, 377, 380–382,  
  388–389, 391, 393, 394–396  
Transmetalation  
  cluster Grignard reagents, 171  
  functionalized Grignard reagents, 550, 552,  
  557  
  magnesium dihalide, 491, 492  
  magnesium enolate preparation, 445–450  
  silyl enol ethers, 450  
  *see also* Metalation  
Triacylglycerols (TAG), derivatization, 301  
Trialkylphosphines, transition-metal-catalyzed  
  cross-coupling, 550  
Trialkyltin halides, transmetalation, 550  
Triaryl magnesiates, structural chemistry, 13  
Triazenes, halogen–Mg exchange, 531, 533,  
  534  
Triethylamine, Mg cation complex, 168  
Triisopropylsilylamine, NMR spectroscopy,  
  297

- Trimethylsilyl dienol ethers, preparation, 598, 599
- Trimethylsilyl enol ether, preparation, 597
- Trimethylsilylmethylmagnesium  
tris(3,5-dimethylpyrazolyl)hydroborate,  
73, 74
- 3-(Trimethylsilyl)propionic acid-*d*<sub>4</sub>, NMR  
spectroscopy, 286
- N,N',N''-Trimethyltriazacyclononane (TAEN),  
tetraorganomagnesiates production, 9–11
- Triorganomagnesiates  
deprotonation, 686–690, 713  
halogen–Mg exchange, 690–711,  
712–713  
nucleophilic addition, 683–686, 711, 713  
preparation, 682  
structural chemistry, 12–14
- Triple bonds, C–C bond addition reactions,  
567–568
- Triple decker (club) sandwiches,  
thermochemistry, 123–124
- Triplet states  
Mg atoms, 158  
Mg(II) tetrapyrroles, 193
- Tris[aryl]magnesiates anions,  
diorganomagnesium compounds, 35
- Tris(ethylene)nickel(0), diorganomagnesium  
compounds, 86
- Tris(pyrazolyl)borato alkylmagnesium  
derivatives, 73–74
- ( $\eta^3$ -Tris(pyrazolyl)borato) derivatives, 411,  
417–418
- $\eta^3$ -Tris(pyrazolyl)-hydroborate  
ketone reactions, 424, 425  
metalation, 419, 420
- Tris(trimethylsilyl)methylmagnesium bromide,  
THF complex, 63, 64
- Trisubstituted compounds  
alkenyl sulfides, 758–760  
2,2,7-trisubstituted cycloheptanones, 765
- Tropylium salts, magnesium cationic  
sandwiches, 125
- Trost ligand, catalytic enantioselective  
conjugate addition, 775
- Ultrasonic extraction, FAAS analysis, 272
- Ultraviolet–visible fluorometry, elemental  
analysis of Mg, 283–285
- Ultraviolet–visible spectrophotometry,  
elemental analysis of Mg, 279–283
- Ultraviolet–visible spectroscopy  
Mg–organic substrate reactions, 171  
unsaturated substrates, 158
- Unactivated alkynes, addition to triple C–C  
bonds, 567, 568
- Unimolecular reactions, gas-phase  
organomagnesium ions, 182
- Universal energy currency of life,  
327–333
- Universal methylene increment, 110–111
- Unsaturated compounds  
conjugated carbonyls, 624–625, 626, 628  
Mg cation reactions, 160  
organomagnesium halides  
enthalpies of hydrogenation, 113, 119  
formal protonation reactions, 112
- $\alpha,\beta$ -Unsaturated compounds  
acyl silanes, 450  
enantioselective conjugate addition  
esters, 779–784  
natural product synthesis, 785,  
786–789  
thioesters, 784  
Michael addition, 451, 501  
nitrile addition, 565–566
- Unsaturated organic substrates, Mg atom  
reactions, 158–159
- Uracil  
Br<sub>2</sub>–Mg exchange, 524  
Mg cation complex, 170
- Urine, mass spectrometry, 288
- Vacuum tight equipment, calorimetry, 104
- Vanillin, active hydrogen determination,  
300
- Vaporization *see* Enthalpies of vaporization
- Vetraldehyde, active hydrogen determination,  
300
- Vibrational frequencies, Grignard reagent  
calculations, 375
- Vinylmagnesium bromide  
DME complex, 59  
surface conditioning, 301, 305
- Vinylmagnesium compounds, NMR spectra,  
145
- Vinylsilanes, carbomagnesiation, 661–664
- Vinyl sulfides, magnesium alkylidene  
carbenoid reactions, 759, 760
- Viologen, PET, 198, 199
- Visible spectroscopy *see* Ultraviolet–visible  
fluorometry; Ultraviolet–visible  
spectrophotometry; Ultraviolet–visible  
spectroscopy
- Visual endpoint, titrations, 288–291
- Voltametric methods, elemental analysis of  
Mg, 276
- Walphos ligand, catalytic enantioselective  
conjugate addition, 775, 776
- Water  
determination in metal powders, 299  
gas chromatography, 295  
Mg cation binding energy, 175

- organomagnesium ion reactivity, 180  
titrations, 290  
Waxes, analysis, 301  
Weinreb amides, acylation reagents, 559  
Wet digestion, mineralization of milk, 271, 279  
Wiechell, Fritsch–Buttenberg–Wiechell rearrangement, 742–744
- Xanthyrone,  $\beta$ -ketoester reactions, 494  
X-ray absorption spectroscopy, structural studies, 3  
X-ray photoelectron spectroscopy, Mg surfaces, 172  
X-ray powder diffraction, diorganomagnesium compounds, 25  
X-ray scattering, large-angle, 3  
*o*-Xylylenemagnesium bis THF complex, 40
- Yeast enolase, sequential behavior, 348–350  
Yttrium trichloride, addition to C=O bonds, 570
- Zerevitinov's method, active hydrogen determination, 299  
Zinc chloride lithium chloride, addition to C=O bonds, 570  
Zinc reagents, conjugate addition, 774  
Zirconium  
  catalyzed alkene ethylmagnesium, 671–674  
  organomagnesium compounds, 86–87  
Zirconium-catalyzed reactions, addition to C=C bonds, 560, 561, 562  
Zirconocene dichlorides, catalyzed addition to C=C bonds, 561, 562  
Z-scheme, photosynthesis, 194, 195

*With kind thanks to Caroline Barlow for the creation of the Subject Index.*